POLITECNICO DI TORINO
Repository ISTITUZIONALE

Phenomenology of two-gap superconductor hydrogen-intercalated titanium diselenide explained in the framework of Eliashberg theory

Original
Phenomenology of two-gap superconductor hydrogen-intercalated titanium diselenide explained in the framework of Eliashberg theory / Ummarino, G.A.. - ELETTRONICO. - (2026). (ICSM-ICQMT2026 Oludeniz-Fethiye, Mugla, Turkey April 19-26,2026).

Availability:
This version is available at: 11583/3015071 since: 2026-09-01T17:21:46Z

Publisher:
icsmforever.org

Published
DOI:

Terms of use:

This article is made available under terms and conditions as specified in the corresponding bibliographic description in the repository

Publisher copyright

(Article begins on next page)

26 November 2026

ICSM 2026 ICQMT 2026

11th INTERNATIONAL CONFERENCE on SUPERCONDUCTIVITY and MAGNETISM

&

4th INTERNATIONAL CONFERENCE on QUANTUM MATERIALS and TECHNOLOGIES

April 19th to 26th 2026

Liberty Hotels Lykia / Ölüdeniz-Fethiye/TÜRKİYE



Abstract Book

The bridge between east and west in scientific and technological excellence of quality

www.icsm2014.org
www.icsm2016.org
www.icsm2018.org
www.icsm2020.org
www.icsm2023.org
www.icsmforever.org

organizers@icsmforever.org • www.icsmforever.org

CONTENTS

CONTENTS 2

1 - PUBLIC OUTREACH AND PLENARY SESSION 53

THE GLOBAL NEED FOR CLEAN ENERGY VIA COMPACT NUCLEAR REACTORS IN VIEW OF SUPERCONDUCTING AND CONVENTIONAL TECHNOLOGIES 54
A. Gencer[1,2] 54

ADVANCEMENT OF COATED CONDUCTORS 55
A. Goyal 55

INTERPLAY OF SUPERCONDUCTIVITY AND MAGNETISM 56
Z. Guguchia 56

A LIFETIME FASCINATION WITH HIGH-TEMPERATURE SUPERCONDUCTIVITY 57
I. Božović 57

THE INVENTION AND INDUSTRIALIZATION OF NEODYMIUM IRON BORON MAGNETS 59
M. Sagawa 59

EPITAXIALLY ENGINEERED HYBRID MATERIALS FOR QUANTUM TECHNOLOGIES 60
N. Samarth 60

VISUALIZING EMERGENT PROPERTIES OF QUANTUM MATERIALS WITH MILLIKELVIN STM 61
H. Suderow 61

2 - PLENARY 62

ENHANCED MAGNETIC PROPERTIES IN BI-MAGNETIC CORE/SHELL NANOPARTICLES 63
J. Nogués[1,2] 63

MAGNETISM AND SUPERCONDUCTIVITY WITH HIGH-BRILLIANCE X-RAYS: RECENT HIGHLIGHTS FROM THE ESRF 64
G. Martínez-Criado 64

SUPERCONDUCTIVITY UNDER EXTREME CONDITIONS 65
J. Wosnitza 65

THE APPLICATION OF SUPERCONDUCTOR FOR CARBON-NEUTRALITY-DRIVEN ENERGY & POWER IN CHINA 66
L. Xiao 66

CURRENT STATUS AND FUTURE PROSPECTS OF ROTATING MACHINERY SYSTEMS THAT COMBINE SUPERCONDUCTING TECHNOLOGY AND LIQUEFIED HYDROGEN 67
T. Nakamura 67

TOPOLOGICAL i-WAVE SUPERCONDUCTIVITY IN $PtBi_2$ 68
B. Buechner[1,2,3] 68

PRESENT STATUS AND LATEST DEVELOPMENTS IN REBCO-BASED HTS WIRES FOR LARGE-SCALE HTS APPLICATIONS 69
A. Goyal 69

3D NANOMAGNETISM - ADVANCES, CHALLENGES AND OPPORTUNITIES FOR MAGNETIC SOFT X-RAY MICROSPECTROSCOPIES 70
P. Fischer[1,2] 70

DISCOVERY MAGNETIC MATERIALS WITH MACHINE LEARNING AND AI 71
S. Sanvito 71

THE STRONG INTERPLAY BETWEEN THE MAGNETIC AND ELECTRONIC STRUCTURE OF CUPRATES AND NICKELATE SUPERCONDUCTORS 72
G. Sawatzky[1], K. Foyevstova[3], M. Jiang[3], I. Elfimov[1] 72

SPIN-TRIPLET SUPERCONDUCTIVITY AND FIELD INDUCED PHENOMENA OF UTe2 73
D. Aoki 73

THE NATIONAL HIGH MAGNETIC FIELD LABORATORY: PUSHING THE FRONTIERS OF SCIENCE WITH EXTREME FIELDS 74
K. M. Amm 74

SIX NEW PIECES OF THE HIGH-T_c PUZZLE 75
I. Božović 75

SUPERCONDUCTIVITY FOR FUTURE ACCELERATORS 77
A. Ballarino 77

3 - HALF-PLENARY 78

PRESSURE EFFECTS ON TYPE-I SUPERCONDUCTIVITY 79
R. Khasanov[1], G. A. Ummarino[2], I. I. Mazin[3], R. Vocaturo[4], J. van den Brink[4], E. Svanidze[5] 79

MOLECULAR QUBIT ASSEMBLIES 80
J. van Slageren[1], J. Wischnat[1], L. Tesi,[1] P. Thielert[2], J. Werner[3], A.-N. Unterreiner[3], S. Richert[2] 80

ON SPIN TRANSPORT IN SOLIDS AND ALTERMAGNETISM 81
H. Reichlova 81

SPIN TEXTURES AND SPIN WAVES AS SEEN BY X-RAY IMAGING 82
S. Wintz 82

EFFECTS OF QUANTUM INTERFERENCE IN QUANTUM RINGS AND 3D NANOPRINTED STRUCTURES 83
V. M. Fomin[1,2] 83

HOW TO CREATE MAGNONIC NETWORKS 84
P. Pirro 84

HIGH-T_c CUPRATES AND IRON PNICTIDES – COHERENCE, INCOHERENCE, AND LOCALIZATION 85
N. Barišić[1,2] 85

CURVILINEAR AND 3D NANOMAGNETISM: FROM RECONFIGURABLE TETRAPODS TO SKYRMION NUCLEATION AND VORTEX DYNAMICS 86

S. Koraltan *86*

THE ROLE OF SUPERCONDUCTING ELECTRONICS IN SCALING QUANTUM COMPUTERS BEYOND THE WIRING/THERMAL BOTTLENECK **87**
A. Bozbey[1,2] *87*

RARE EARTH ELEMENT RESOURCES IN TÜRKIYE: GEOLOGICAL CONTROLS, EXPLORATION STRATEGIES, AND THEIR CRITICAL ROLE IN ADVANCED TECHNOLOGIES. **88**
Y. K. Kadioğlu[1,2] *88*

4 - 2D GRAPHENE FUNDAMENTALS, MATERIALS AND THEIR APPLICATIONS .**89**

DIMENSIONAL TRANSFORMATION OF BOROPHENE: FROM HYDROGENATED 2D SHEETS TO 0D BORON QUANTUM DOTS **90**
O. G. Yildiz[1,2], U. Aydemir[2,3] *90*

OPTICAL HIGH-ORDER HARMONIC GENERATION IN DIRAC MATERIALS **91**
S. Rakhmanov[1], K. Matchonov[2], H. Yusupov[3], K. Nasriddinov[1], D. Matrasulov[4,5] *91*

GAUGE-INVARIANT NONCOMMUTATIVE LANDAU PROBLEM IN GRAPHENE: EMERGENT MAGNETIC RESPONSE IN A DIRAC MATERIAL **92**
A. Halder *92*

REDUCED GRAPHENE OXIDE NANOCOMPOSITES FOR LITHIUM AND SODIUM BATTERIES ANODES **93**
S. Karamat *93*

HIGH-FIDELITY SPIN TRANSPORT IN GRAPHENE-BASED SPIN VALVES **94**
A. Avsar[1,2] *94*

5 - ADVANCED REBCO-BASED CONDUCTORS FOR LARGE-SCALE HTS APPLICATIONS IN ENERGY GENERATION, TRANSMISSION, STORAGE AND USE IN ENERGY-EFFICIENT DEVICES **95**

INCREASING THE CRITICAL CURRENT DENSITY OF GdBCO COATED CONDUCTORS AND YBCO FILMS DEPOSITED ON STO SUBSTRATES BY HIGH-PRESSURE- HIGH TEMPERATURE OXYGENATION **96**
T. Prikhna[1,2,3], R. Vlad[2], A. Kethamkuzhi[2], R. Kluge3, B. Büchner[3], M. Karpets[1,4], S. Ponomaryov[5], V. Moshchil[1], X. Obradors[2], J. Gutierrez[2], T. Puig[2] *96*

THE TRANSIENT LIQUID ASSISTED GROWTH (TLAG) METHOD FOR ULTRAFAST GROWTH OF REBCO COATED CONDUCTORS **97**
T. Puig[1], R. Vlad[1], X. Obradors[1], J. Gutierrez[1], E. Pach[1,5], C. Pop[1], K. Gupta[1,2], S. Rasi[1], C. Torres[1], A. Kethamkuzhi[1], O. Mola[1], E. Ghiara[1], V. Bertini[1], M. Voulhoux[1], L. Salterilli[1], D. Garcia[1,3], S. Ricart[1], R. Yanez[3], D. Sanchez[4], J. Farjas[4], E. Solano[5], L. Simonelli[5] *97*

2G-HTS TAPE DEVELOPMENT AT HIGH TEMPERATURE SUPERCONDUCTORS, INC. **98**
I. Wyrsta, J. Weiss, R. Karam *98*

DEVELOPMENT AND SCALE UP OF HIGH-PERFORMANCE REBCO TAPES **99**
V. Selvamanickam[1,2] *99*

PROGRESS IN R&D AND INDUSTRIALIZATION OF SECOND-GENERATION HIGH-TEMPERATURE SUPERCONDUCTING TAPE AT SUPERMAG TECHNOLOGY.....100
Y. Zhao[1,2], G. Jiang[1], S. Xu[1].....100

MASS PRODUCTION AND PERFORMANCE OF SST REBCO TAPE.....101
J. Zhu, S. Chen, Z. Gao, C. Zhang, S. Zhen, X. Lin, P. Bai, B. Song, X. Wang.....101

LATEST ADVANCE IN MOD-YBCO COATED CONDUCTORS WITH THICK HTS LAYER AND STRONG FLUX PINNING 102
C. Cai, R. Huang, J. Chen, N. Zhang, Y. Li, Z. Liu.....102

NANOSTRUCTURE AND STRAIN IN YBCO LAYER OF HIGH-PERFORMANCE 2G HTS WIRES FOR LOW-TEMPERATURE MAGNET APPLICATIONS 103
V. A. Amelichev[1], P. N. Degtyarenko[1], A. A. Kamenev[1], A. L. Vasiliev[2], M. V. Lovygin[3], I. G. Maryasev[3] 103

SCALE-UP AND APPLICATION-DRIVEN R&D OF FFJ REBCO CONDUCTORS FOR FUSION MAGNETS, CABLES, AND AIRCRAFT MOTORS.....104
V. Petrykin, S. Samoilenkov, R. Valikov, M. Gaifullin, M. Okube, A. Borisov, H. Dao, K. Begic, H. Hirose, V. Vyatkin, K. Vereshchagin, N. Khozhempo, I. Veschunov, A. Molodyk, S. Lee.....104

BMO-DOPED REBCO COATED CONDUCTOR WITH HIGH PERFORMANCE AND PRODUCTIVITY BY USING HOT-WALL PLD ON IBAD TEMPLATED SUBSTRATE 105
Y. Iijima, M. Ohsugi, K. Kakimoto, S. Muto, S. Fujita, W. Hirata, N. Nakamura, M. Daibo.....105

TOWARD THE PRACTICAL APPLICATION OF REBCO HIGH-TEMPERATURE SUPERCONDUCTING WIRE - BEYOND CRITICAL CURRENT 106
T. Kiss[1, 2], Z. Wu[2], S. Sera[2], S. Shiotani[2], R. Iwanaga[2], K. Higashikawa[1,2], V. Petrykin[3], S. Lee[3], X. Obradors[4], T. Puig[4] 106

6 - ADVANCES AND CHALLENGES IN THE COMMERCIALIZATION OF SUPERCONDUCTIVITY APPLICATIONS.....107

ADVANCES AND CHALLENGES IN COMMERCIALIZATION OF SUPERCONDUCTING MAGNETS FOR MEDICAL APPLICATIONS 108
J. V. Minervini 108

OVERVIEW OF SMES FOR COMMERCIAL POWER APPLICATIONS 109
K. Higashikawa[1], T. Kiss[1], K. Shiohara[2] 109

SUPERCONDUCTING MAGNETIC CORE REACTOR: A CONTRIBUTION TO EFFICIENT POWER FLOW CONTROL IN TRANSMISSION GRIDS 110
J. Murta-Pina[1,2,3], L. Miúdo[1,2], N. Amaro[1,2,3], A. Pronto[1,2,3], R. Pastor[4].....110

A SELECTIVE METAL LAYER REMOVAL METHOD FOR REBCO-COATED CONDUCTORS BASED ON ELECTROCHEMICAL TECHNIQUES AND INVESTIGATION OF PERFORMANCE DEGRADATION MECHANISMS 111
Z. Wang, S. Gao, F. Liu.....111

NET ZERO BY 2050 IS POSSIBLE 112
G. J. Levermore 112

THE SUPERCONDUCTING GLOBAL ALLIANCE (ScGA) AND THE COMMERCIALISATION OF SUPERCONDUCTIVITY.....113
Z. Melhem[1,2] 113

ROLE OF HTS MATERIALS IN DEVELOPING COMMERCIAL COMPACT PARTICLE THERAPY SOLUTIONS 114
A. Godeke[1,2] 114

TECHNO-ECONOMIC ASSESSMENT OF A SUPERCONDUCTING DC TRACTION SUBSTATION 115
L. Ferreira[1,2], Y. Baazizi[1,2], S. Meunier[1,2], T. Phulpin[1,2], L. Quéval[1,2] 115

7 - ADVANCES IN MAGNETIC SENSOR TECHNOLOGIES 116

DESIGN, MANUFACTURING, AND EXPERIMENTAL CHARACTERIZATION OF A LOW NOISE FLUXGATE SENSOR WITH Co-BASED MAGNETIC CORE 117
B. Tuncay[1,2], F.Inanır[2], P. Švec[3], I. Škorvánek[4], U.Topal[1] 117

DEVELOPMENT OF AMORPHOUS MICROWIRES FOR SENSOR APPLICATIONS 118
A. Zhukov[1,2,3], P. Corte-León[3,4,5], A. Gonzalez[1,2,3], V. Zhukova[1,2,3] 118

MAGNETIC SENSING AT BOSCH 119
P. Mather[1], Bosch Sensortec TMR Team[1,2], Bosch Quantum Sensing[3] 119

SENSING SPIN PRECESSION WITH TRANSMISSION ELECTRON MICROSCOPY 120
A. Jaroš, M. S. Seifner, J. Toyfl, B. Czasch, S. B. Romero, I. C. Bicket, P. Haslinger 120

QUANTUM SENSING OF MAGNETIC PHENOMENA WITH CRYOGENIC SCANNING NV MAGNETOMETRY 121
M. Bacani[1], A. Sharma[1], C. Kelvin von Grundherr[1], D. Andres[1], J. Rhensius[2], G. Puebla-Hellmann[2], A. Morales[2], C. Schäfermeier[1] 121

THE DETECTION OF NUCLEAR QUADRUPOLE RESONANCE SIGNALS INSIDE OBJECTS 122
G. Mozzhukhin[1], P. Kupriyanov[1], S. Kazan[1], B. Çolak[1], G. Kupriyanova[2], B. Rameev[1,3,4] 122

8 - ADVANCES IN NICKELATE SUPERCONDUCTORS 123

SPIN DENSITY WAVE ORDER IN LAYERED NICKELATES $La_3Ni_2O_7$ AND $La_2PrNi_2O_7$ VIA NEUTRON DIFFRACTION 124
I. Plokhikh[1,2] 124

ELEMENTARY EXCITATIONS IN SUPERCONDUCTING $Nd_{1-x}Eu_xNiO_2$ AND COMPARISON WITH THE CUPRATES 125
J. Pelliciari 125

UNIVERSAL ELECTRONIC STRUCTURE OF LAYERED NICKELATES VIA OXYGEN-CENTERED PLANAR ORBITALS 126
A. Damascelli[1,2] 126

AMBIENT PRESSURE GROWTH OF NICKELATE SINGLE CRYSTALS WITH SUPERCONDUCTIVITY UP TO 96 K UNDER HIGH PRESSURE 127
J. Zhang 127

SPIN AND ORBITAL EXCITATIONS OF TRILAYER NICKELATES 128
Q. Wang 128

TRIPLON-MEDIATED COOPER PAIRING IN BILAYER NICKELATES 129

G. Khaliullin 129

OXYGEN-DRIVEN ELECTRONIC AND LATTICE INSTABILITIES IN $La_3Ni_2O_7$ **130**
Y. Lu[1,2] 130

UNCONVENTIONAL SUPERCONDUCTIVITY IN INFINITE-LAYER SAMARIUM NICKELATES **131**
D. Li 131

UNDERSTANDING THE PAIRING MECHANISM OF BILAYER NICKELATES **132**
F. Yang 132

BILAYER NICKELATE AS A POLAR METAL WITH CHECKERBOARD CHARGE ORDER **133**
R. Misawa, M. Hirschberger 133

THEORY OF SUPERCONDUCTIVITY IN PRESSURIZED BILAYER NICKELATE $La_3Ni_2O_7$ **134**
G. Su[1,2] 134

9 - ADVANCES IN SUPERCONDUCTOR TECHNOLOGIES FOR HIGH FIELD MAGNETS 135

NOVEL AND SUSTAINABLE COOLING STRATEGIES FOR HIGH TEMPERATURE SUPERCONDUCTING MAGNET SYSTEMS **136**
S. V. Pamidi 136

REVIEW OF THE DEVELOPMENT OF A ROUND CABLE WITH SMALL MAGNETIZATION / LOW AC LOSS **137**
N. Amemiya 137

PROGRESS ON QUENCH RESEARCH OF HIGH-FIELD REBCO MAGNETS AT ASIPP: **138**

FROM FAILURE ANALYSIS TO 35.1 T **138**
S. Gao[1], W. Hong[1], X. Zhang[1], S. Hu[1], H. Liu[1,2], F. Liu[1] 138

10 - ADVANCES IN THIN FILMS, MULTI-LAYERS AND PATTERNED NANOSTRUCTURES 139

ENGINEERING MAGNETIC ANISOTROPY IN PERMALLOY FILMS VIA ATOMIC FORCE NANOLITHOGRAPHY **140**
A. Naik[1], C. Delforge[1], N. Lejeune[1], D. Stoffels[1], J. V. Vondel[2], K. Temst[2, 3], A. V. Silhanek[1], E. Fourneau[1] .. 140

^{77}Se NMR STUDY OF $TlInSe_2$ **141**
G. S. Kupriyanova[1], A. Sönmez[2], M. H. Yu. Seyidov[2], I. G. Mershiev[3], G. V. Mozzhukhin[2] 141

OPTICAL PROPERTIES OF MnTe THIN-FILM POLYMORPHS GROWN BY MBE **142**
O. Yastrubchak[1], S. Mamykin[1], V. Romanyuk[1], L. Borkovska[1], Y. Smortsova[3], A. Kaleta[2] 142

HIGH-PERFORMANCE HUMIDITY SENSOR BASED ON SCHIFF BASE COMPOUND WITH FAST RESPONSE, HIGH SENSITIVITY, AND STABILITY FOR HUMIDITY SENSING APPLICATION **143**
M. U. Rahman 143

11 - AI-DRIVEN DISCOVERY OF NOVEL QUANTUM MATERIALS.....144

POLYCRYSTALLINE INFORMATICS FOR DATA-DRIVEN DESIGN OF HIGH-FUNCTIONALITY POLYCRYSTALLINE MATERIALS 145
N. Usami 145

DEEP LEARNING APPROACH FOR FLAT-BAND 2D QUANTUM MATERIALS 146
Q. Yang, A. Bhattacharya, X. Wang, H. Pentz, Y. Wei, A. Mishchenko 146

DIRECT ATOMIC LAYER PROCESSING (DALP®): SPATIALLY LOCALIZED, MULTI-MATERIAL FABRICATION FOR NEXT-GENERATION DEVICES FROM DISCOVERY TO MANUFACTURING 147
M. Plakhotnyuk 147

AI-GUIDED DISCOVERY OF NOVEL OPTICAL MATERIALS FOR SMART ELECTRONIC DEVICES 148
V. Volkov[1], I. Kruglov[1], L. Klimova[1], I. Trofimov[1], A. Arsenin[1], K. Novoselov[2] 148

VAE-BASED INTERPRETATION OF SHAPE VARIABILITY IN MULTI-QUANTUM WELL MICRORING LASERS.....149
M. R. Athavale[1,2], S. Church[3], W. W. Wong[4], A. K. Low[2,5], H. H. Tan[4], K. Hippalgaonkar[2,5], P. Parkinson[1] . 149

HARNESSING NONLINEAR ANTIFERROMAGNETISM: $L1_2$–PHASE $IrMn_3$ FOR NEXT-GENERATION HIGH-PERFORMANCE SPIN-TORQUE DEVICES 150
O. Ozatay[1,2], U. Sasun[1], S. Ari[1], M. Kocyigit[1], A. Iskesen[1], E. K. Taga[1], K. Akin[1], B. Kocaman[1], H. Piskin[1], I. Goksal[1], V. Karakas[1] 150

CHIRAL DUAL SPIN CURRENTS FIELD-FREE PERPENDICULAR SWITCHING BY ALTERMAGNET RuO_2 151
G. Meng[1,2], Q. Sun[3], Y. Yang[1,2], Y. Zhang[1,4], N. Lei[3], D. Wei[1,2] 151

ROOM-TEMPERATURE HIGH-ORDER NONLINEAR HALL EFFECT IN A TOPOLOGICAL WEYL ANTIFERROMAGNET 152
L. Yang[1], W. H. Niu[1], Y. M. Yang[2], D. H. Wei[2], N. Lei[1,3] 152

ALTERMAGNETIC MAGNON TRANSPORT IN d-WAVE ORTHOFERRITE INSULATORS.....153
E. Galindez-Ruales[1], W. Yang[2], T. Dannegger[3], M. Kundu[3], J. Köhler[1], C. Schmitt[1], F. Fuhrmann[1], A. Akashdeep[1], D. M. Tran[1], X. Ma[2], G. Jakob[1], S. Cao[2], U. Nowak[3], M. Kläui[1] 153

SPIN HALL MAGNETORESISTANCE AT THE ALTERMAGNETIC INSULATOR/Pt INTERFACE 154
M. Leiviskä[1], R. Firouzmandi[2], K. Ahn[1], P. Kubaščik[3], Z. Soban[1], S. Bommanaboyena[1], C. Müller[1], D. Kriegner[1], D. Reustlen[4], S. Sailler[4], M. Lammel[4], K. Bestha[2,5], M. Hyvl[1], L. Šmejkal[6,7,1], J. Zelezny[1], A. U. B. Wolter[2], M. Scheufele[8,9], J. Fischer[10], M. Opel[8], S. Geprägs[8], M. Althammer[8], B. Büchner[2,11,12], T. Jungwirth[1,13], L. Nádvorník[3], S. T. B. Goennenwein[4], V. Kocsis[2], H. Reichlova[1] 154

FRAGILITY OF THE MAGNETIC ORDER IN THE PROTOTYPICAL ALTERMAGNET RuO_2 155
A. Smolyanyuk[1], I. I. Mazin[2], L. Garcia-Gassull[3], L. Šmejkal[4,5,6], R. Valentí[3] 155

T-SYMMETRY BREAKING PHENOMENA IN ALTERMAGNETIC MnTe.....156
A. Dal Din, O. J. Amin, K. W. Edmonds, R. P. Campion, P. Wadley..... 156

PHASE STABILITY AND TUNABILITY IN THE NON-COLLINEAR ANTIFERROMAGNET $Mn_{3+x}Sn_{1-x}$.....157
K. Gas[1,2,3] 157

MAGNETIC PROPERTIES OF HEXAGONAL MnTe AND THEIR IMPLICATIONS FOR TRANSPORT PHENOMENA 158
M. Sawicki 158

NON-RELATIVISTIC SPIN CURRENTS AND TORQUES IN ANTIFERROMAGNETS 159
J. Železný 159

SHIELDING THE STRAY MAGNETIC FIELD OF A LARGE SUPERCONDUCTING COIL FROM A ROTATING MACHINE: EXPERIMENTAL DEMONSTRATION OF SCALABLE SCREENS COMBINING BULK SUPERCONDUCTORS AND COATED CONDUCTORS 160
N. Rotheudt[1], J.-F. Fagnard[1], F. Antoncik[2,3], T. Hlasek[2,3], J. Plechacek[2], P. Vanderbemden[1], A. B. Abrahamsen[4] 160

EXPERIMENTAL ANALYSIS AND 3D MODELLING OF DC MAGNETIC SHIELDING USING A Bi-2223 VESSEL AND Bi-2223/Fe HYBRID LAYOUTS 161
M. Fracasso[1,2], R. Gerbaldo[1,2], G. Ghigo[1,2], J.F. Fagnard[3], P. Vanderbemden[3], L. Gozzelino[1,2] 161

HIGH-PRESSURE SYNTHESIS AND SUPERCONDUCTING PROPERTIES OF F-DOPED SmFeAsO BULKS: COMPARATIVE STUDY OF HIGH-GAS PRESSURE, CUBIC-ANVIL, AND SPARK-PLASMA SINTERING 162
S. J. Singh 162

HIGH PERFORMANCE RE123 BULKS BY TOP SEEDED MELT-GROWTH 163
X. Yao 163

SYNTHESIS, STRUCTURE AND PHYSICAL PROPERTIES OF THE RHOMBOHEDRAL RIr_3 BINARY COMPOUNDS 164
K. Górnicka, T. Klimczuk 164

STRUCTURALLY DEPENDENT SUPERCONDUCTING PROPERTIES OF Ti-RICH HIGH-ENTROPY ALLOYS: COMPOSITION AND AFTERTREATMENT EFFECT ON CRITICAL CURRENT DENSITY 165
P. Sobota, W. Idziak, R. Idczak 165

SUPERCONDUCTIVITY IN NEW HIGH ENTROPY ALLOYS DOPED WITH ELEMENTS FROM GROUP 3 AND 13 166
P. Olejnik[1,2], D. Gnida[2], P. Sobota[1] 166

NEW Ti-RICH YTTRIUM-CONTAINING SUPERCONDUCTING HIGH-ENTROPY ALLOY WITH HIGH UPPER CRITICAL FIELD 167
B. Rusin[1], W. Nowak[1], R. Idczak[1], M. Babij[2] 167

MAGNETIC LEVITATION OF A SUPERCONDUCTING HOLLOW CYLINDER FOR QUANTUM MAGNETOMECHANICS 168
N. Bort-Soldevila, J. Cunill-Subiranas, D. Sarrat, N. Del-Valle, C. Navau 168

PAST AND FUTURE PERSPECTIVE OF Tl-1212 SUPERCONDUCTOR 169
E. Yusrianto[1], Y. Lizar[2] 169

BULK $GdBa_2Cu_3O_7$ SUPERCONDUCTORS PREPARED BY SINGLE DIRECTION MELT GROWTH (SDMG): KEY POINTS TO UNDERSTAND THEIR BEHAVIOUR UNDER A TIME-DEPENDENT MAGNETIC FIELD 170
N. Rotheudt[1], D. Szewczyk[2], P. Stachowiak[2], J. F. Fagnard[1], T. Hlasek[3,4], J. Plechacek[3], P. Vanderbemden[1] 170

REBCO BULK SUPERCONDUCTORS BASED ON Y, Gd, Eu AND Dy PREPARED BY TSMG AND SDMG PROCESS 171
P. Diko[1], M. Radušovská[1], D. Volochová[1], L. Vojtková[1], K. Zmorayová[1], V. Kuchárová[1], R. Smolko[1], M. Rajnak[1], B. Guner[2,3], T. Motoki[4] 171

REVEALING FILAMENT MICROSTRUCTURE IN ADVANCED MgB_2 MULTIFILAMENTARY WIRES BY DEEP LEARNING SEGMENTATION 172
A. Yamamoto[1], M. Ito[1], K. Ogi[1], D. Fukui[1], K. Ando[1], Y. Shimada[2], M. Kodama[3], H. Tanaka[3] 172

IN-PLANE MAGNETIC ANISOTROPY AND LOCAL CHEMICAL CORRELATIONS IN $Ba_{1-x}Na_xFe_2As_2$ 173
O. Chmaissem 173

PROGRESS IN THE FABRICATION OF HIGH-PERFORMANCE IRON-BASED SUPERCONDUCTING WIRES 174
X. Zhang[1,2], Y. Ma[1,2] 174

CRITICAL CURRENT DENSITY IN VARIOUS EPITAXIAL FILMS OF A HYDROGEN-SUBSTITUTED 1111-TYPE IRON-BASED SUPERCONDUCTOR 175
K. Hanzawa[1], K. Mitsui[2], Y. Takahara[1], J. Matsumoto[1], M. Miura[3], H. Hosono[2,4], H. Hiramatsu[1,2] 175

COMPLETE ELECTRONIC PHASE DIAGRAM AND SUPERCONDUCTING PROPERTIES OF $PrFeAsO_{1-x}F_x$ ACROSS THE FULL DOPING RANGE ($0 \le x \le 1$) 176
P. Singh[1], K. Kwatek[2], T. Zajarniuk[3], A. Szewczyk[3], S. J. Singh[1] 176

UNCONVENTIONAL SIGNATURES OF A QUANTUM GRIFFITHS PHASE IN THE VICINITY OF A QUENCHED NEMATIC QUANTUM CRITICAL POINT 177
P. Reiss[1,2], D. E. Graf[3], A. A. Haghighirad[4,2], M. Bristow[2], Z. Zajicek[2], W. Knafo[5], A. J. Schofield[6], T. Vojta[7], A. I. Coldea[2] 177

MICROWAVE PROPERTIES of Fe(Se,Te) IN A DC MAGNETIC FIELD: TWO-BAND VORTEX PHYSICS AND POTENTIAL APPLICATIONS TO LARGE-SCALE PHYSICS EXPERIMENTS 178
A. Alimenti[1,2], V. Braccini[3], M. Cialone[3,4], A. Magalotti[1,2], P. Manfrinetti[5], N. Pompeo[1,2], E. Silva[1,2], K. Torokhtii[1] 178

GIANT PINNING EFFICIENCY IN AN IRON-BASED SUPERCONDUCTOR WITH SELF-ASSEMBLED INCLINED NANORODS 179
D. Gong, X. Xia, Z. Xu, Y. Ma 179

RESEARCH ON THE DELAMINATION BEHAVIOR OF METER-LENGTH FeSeTe-COATED CONDUCTOR TAPES 180
Y. Han 180

15 - CURVILINEAR AND 3D NANOARCHITECTURES FOR SUPERCONDUCTIVITY AND MAGNETISM 181

SPIN DYNAMICS AND MAGNON EXCITATIONS IN QUASI-2D VAN DER WAALS COMPOUNDS 182
V. Kataev 182

ROLE OF CURVATURE ON THE CURRENT-DRIVEN TRANSPORT OF MAGNETIC TEXTURES 183
J. I. Costilla[1], G. H. R. Bittencourt[2], D. Altbir[3], V. P. Kravchuk[4,5], V. L. Carvalho-Santos[1] 183

Co/Ni-BASED FLEXIBLE PMA SPIN-VALVE HETEROSTRUCTURES FOR SUSTAINABLE SPINTRONICS.....184
M. Hassan[1,2], S. Laureti[1], C. Rinaldi[3], G. Barucca[4], A. Ullrich[2], M. Albrecht[2], G. Varvaro[1] 184

MAPPING MAGNETIC FIELDS AND CURRENTS IN SUPERCONDUCTING RESONATORS ...185
J. Baumgarten[1], N. Lejeune[1], L. Nulens[2], J. Van de Vondel[2], A. V. Silhanek[1]..... 185

TUNNEL MAGNETIC JOSEPHSON JUNCTIONS: FROM FUNDAMENTAL PHYSICS TO SUPERCONDUCTING QUANTUM ARCHITECTURES 186
R. Satariano[1], R. Ferraiuolo[2], H. G. Ahmad[1], E. Raja[1], D. Gatta[1], G. Serpico[1], D. Montemurro[1], A. Vettoliere[3], G. Ausanio[1], L. Parlato[1], G.P. Pepe[1], C. Granata[1], A. Bruno[2], F. Tafuri[1], D. Massarotti[4]..... 186

ARTIFICIAL SPIN ICE ON THE CaVO LATTICE: A BRIDGE FROM SQUARE TO KAGOME 187
F. Museur[1,2], G. M. Macauley[1,2], S. Nilsson[1,2], L. Berchialla[1,2], P. M. Derlet[2,3], V. Scagnoli[1,2], L. J. Heyderman[1,2]..... 187

TOPOLOGICAL INVARIANTS AND POLYMORPHISM OF MAGNETIC HOPFIONS.....188
F. N. Rybakov..... 188

STRAIGHT AND CURVED SINGLE CRYSTALLINE IRON NANOWIRES EXPOSED TO LARGE MAGNETIC FIELD GRADIENTS 189
F. Sandbaumhüter[1], A. S. Prasad[1], R. Ravishankar[1], D. Wolf[1], O. Volkov[2], V. Neu[1], D. Makarov[3], T. Mühl[1]189

MICRO-FOCUSED BLS FOR CURVILINEAR MAGNETISM 190
O. Wojewoda[1,2], M. Urbánek[2] 190

MODELING STRAIN INDUCED CURVATURE WITH FULLY COUPLED MAGNETO-MECHANICAL FEM MODEL.....191
S. Chiroli[1,2] 191

SCANNING SQUID-ON-CANTILEVER MICROSCOPY OF NANOSCALE MAGNETISM IN LOW-DIMENSIONAL MATERIALS.....192
B. Gross[1], M. Poggio[1,2]..... 192

FLEXOMAGNETISM AND THE LINEAR FLEXOMAGNETIC EFFECT IN 2D MAGNETS 193
A. Edström[1], S. Picozzi[2,3], P. Barone[3], M. Stengel[4] 193

CHALLENGES TOWARDS THE LASER FABRICATION OF CURVILINEAR SUPERCONDUCTOR ARCHITECTURES 194
L. Porta-Velilla[1], A. Badía[1], J. Frechilla[1], N. Lejeune[2], J. Baumgarten[2], C. Delforge[2], E. Martinez[1], A. Silhanek[2], L.A. Angurel[1], G.F. de la Fuente[1] 194

SKYRMIONS INDUCED AND SUPPRESSED BY CURVILINEAR DEFECTS OBSERVED BY MFM 195
H. J. Hug[1,2], E. Darwin[1], D. Rothhardt[1,2], R. Peremadathil-Pradeep[1,2], L. Berchialla[1,3], A. Hrabec[3]..... 195

MAGNETISM UNDER MECHANICAL LOADING: FRAGMENTATION, GEOMETRY, AND MAGNETOELASTIC EFFECTS IN FERROMAGNETIC THIN FILMS.....196
F. Zighem[1], H. Ben Mahmoud[1], P.-O. Renault[1], P. Godard[1], D. Thiaudière[1], D. Faurie[1]..... 196

SUPERCONDUCTING NANO/MICROSTRIP SINGLE PHOTON DETECTORS FOR QUANTUM APPLICATIONS.....197
L. Parlato[1], P. Ercolano[1], C. Bruscino[1], M. Peluso[1], C. Cirillo[2], C. J. Zhang[1], F. Avitabile[2], Z. M. Kakhaki[3], C. Attanasio[3], G.P. Pepe[1] 197

INERTIAL SPIN-WAVE DYNAMICS IN TWISTED MAGNETIC NANOSTRIPS 198

M. d'Aquino 198

GEOMETRICALLY ENGINEERED QUANTUM PHASES: SUPERCONDUCTIVITY, TOPOLOGY AND ANTIFERROMAGNETISM **199**
P. Gentile 199

FLEXIBLE MAGNETORESISITVE SENSORS ENABLING NOVEL CAPABILITIES IN NON-DESTRUCTIVE TESTING **200**
A. Nicolicea, M. Melzer, M. Pelkner 200

COHERENT FLUXON–MAGNON INTERACTION FOR CRYOGENIC MAGNONICS **201**
O. V. Dobrovolskiy 201

CUSTOM-BUILT ANISOTROPIC SUPERCONDUCTING FILMS VIA ULTRASHORT LASER PULSES **202**
A. Badía-Majós[1], J. Frechilla[1], A. Ajayan[1], S. Martín[1], E. Martínez[1], L.A. Angurel[1], G.F. de la Fuente[1], N. Lejeune[2], E. Fourneau[2], A.V. Silhanek[2], L.R. Cadorim[3,4], M.V. Milosevic[4] 202

16 - DEVICE PHYSICS OF JOSEPHSON JUNCTIONS AND THEIR FUNDAMENTAL TECHNOLOGIES **203**

GENERALIZED NOISE MODELLING IN SUPERCONDUCTING CIRCUITS: FROM THERMAL TO 1/f AND FLUX NOISE **204**
J. A. Delport 204

EMERGENT NETWORK OF JOSEPHSON JUNCTIONS IN A KAGOME SUPERCONDUCTOR 205
T. J. Blom[1], M. Rog[1], M. Altena[2], A. N. Capa Salinas[3], R. Q. Regter[1], S. D. Wilson[3], M. P. Allan[1,4,5,6,7], C. Li[2], K. Lahabi[1,7] 205

TAPPING-MODE SQUID-ON-TIP MICROSCOPY WITH PROXIMITY JOSEPHSON JUNCTIONS **206**
M. Rog[1], T. J. Blom[1], D. B. Boltje[2], J. D. de Haan[2], R. Fermin[1,3], J. Niu[1,4,6], Y. C. Doedes[1], M. P. Allan[1,2,4,5,6], K. Lahabi[1,2] 206

BALLISTIC TRANSPORT IN NANOCRYSTALS OF $Bi_2(Te_xSe_{1-x})_3$ TOPOLOGICAL INSULATOR **207**
D. S. Yakovlev, S. K. Kozlov, D. Roditchev, V. S. Stolyarov, C. Feuillet-Palma 207

CLOSING THE DESIGN LOOP FOR NONLINEAR JOSEPHSON METAMATERIALS **208**
E. Palumbo[1,2], A. Alocco[1,2], C. Celotto[1,2], L. Fasolo[2], B. Galvano[3], P. Livreri[3, 4], E. Enrico[2] 208

THERMAL CONTROL OF NON-EQUILIBRIUM TRANSPORT IN A MICROWAVE-DRIVEN SUPERCONDUCTING JUNCTION **209**
M. Kumar 209

MODELING QUASIPARTICLE DISSIPATION IN $Bi_2Sr_2CaCu_2O_{8+x}$ INTRINSIC JOSEPHSON JUNCTION STACKS **210**
O. Kizilaslan[1,2], R. Wieland[1], E. Dorsch[1], D. Koelle[1], R. Kleiner[1] 210

RELATIVISISTIC DESCRIPTION OF CANONICAL QUANTIZATION OF JOSEPHSON EFFECT FOR THE CASE OF SUPERCONDUCTOR INTERFACED TO SEMICONDUCTOR QUANTUM DOTS **211**
K. Pomorski[1], L. Stepien[2], A. Bednorz[3] 211

TUNABLE JOSEPHSON GENERATOR FOR QUBIT EXCITATION AND TWO-TONE SPECTROSCOPY 212
M. M. Khrenov[1,2], I. A. Nazhestkin[1], I. I. Soloviev[2], D. S. Yakovlev[3] 212

INTERPLAY OF SUPERCONDUCTIVITY AND ALTERMAGNETISM IN HYBRID SYSTEMS 213
A. S. Mel'nikov[1,2], M. M. Vasiakin [1,3] 213

EFFECTS OF LOW-TEMPERATURE ANNEALING AND ELECTRON-BEAM IRRADIATION ON INTRINSIC JOSEPHSON JUNCTIONS IN $Bi_2Sr_2CaCu_2O_{8+\delta}$ 214
Y. Simsek[1,2] 214

INTRINSIC NON-LINEARITY OF JOSEPHSON JUNCTIONS AS AN ALTERNATIVE ORIGIN OF THE MISSING FIRST SHAPIRO STEP 215
L. Xu, P. L. Li, G. T. Liu, F. M. Qu, L. Lu 215

ENERGY-EFFICIENT HYBRID SUPERCONDUCTOR–SEMICONDUCTOR MILLIKELVIN ELECTRONICS FOR SCALABLE QUANTUM INFORMATION PROCESSING 216
K. Delfanazari 216

17 - DYNAMICAL CONTROL OF ELECTRONIC PROPERTIES IN FUNCTIONAL MATERIALS 217

OBSERVING DIFFERENTIAL SPIN CURRENTS BY RESONANT INELASTIC X-RAY SCATTERING 218
Y. Gu[1], J. Barker[2,3], J. Pelliciari[4], G. E. W. Bauer[3,5], V. Bisogni[4] 218

STRAIN AND ELECTRIC FIELD CONTROL OF NEEL VECTORS AND MAGNONS IN MULTIFERROIC $BiFeO_3$ 219
T. Kim[1], Y. Liu[2], N. Zheng[2], S. Fan[1], V. Bhartiya[1], J. Li[1], Y. Gu[1], K. Kisslinger[3], F. Camino[3], S. Lee[4], J.-G. Park[5], S.-W. Cheong[6], P. Stevenson[7], P.R. Raghuvanshi[8], V. Cooper[8], C.-Y. Kuo[9], M.P.M. Dean[10], Y. Nie[2], J. Pelliciari[1], V. Bisogni[1] 219

IN-PLANE ANOMALOUS HALL EFFECT IN QUANTUM MATERIALS 220
M. Uchida[1,2] 220

MUELLER MATRIX MAGNETO ELLIPSOMETRY AND VORTEX BEAM SPECTROSCOPY OF MAGNETIC AND CHIRAL MATERIALS 221
A. Sirenko 221

STRANGE METALS STUDIED BY EELS AND RIXS 222
J. Fink 222

CIRCULAR DICHROISM IN RESONANT INELASTIC X-RAY SCATTERING AS A PROBE OF ALTERMAGNETIC DOMAINS 223
H. Suzuki 223

RECENT ADVANCES IN THE OPTICAL CONTROL OF SUPERCONDUCTIVITY 224
M. Buzzi 224

DIMENSIONALITY-DRIVEN ANTIFERROMAGNETIC DOMAIN DYNAMICS IN NICKELATE HETEROSTRUCTURES 225
S. Lee[1], J. Jiang[1], G. Fabbris[2], A. S. Disa[3], M. P. M. Dean[2], S. Ismail-Beigi[1], Y. Wang[4], F. J. Walker[1], C. Mazzoli[5], C. H. Ahn[1] 225

MAGNETIC TEXTURES, PHASE TRANSITIONS AND DOMAIN EVOLUTION UNDER DYNAMICAL CONTROL.....226
A. Bombardi.....226

SPIN, ORBITAL, AND CHARGE DYNAMICS ACROSS THE STRAIN-INDUCED INSULATOR-METAL TRANSITION IN Ca_2RuO_4.....227
B. Zager[1,2], C. Occhialini[1,3], T. Kim[1], R. Fittipaldi[4], J. Pelliciari[1], A. Vecchione[4], M. Cuocco[4], M. P. M. Dean[2], V. Bisogni[1].....227

MAGNETO-OPTICAL KERR EFFECT IN PUMP-PROBE SETUPS 228
A. Eskadari-asl[1], A. Avella[1,2,3].....228

THEORETICAL AND EXPERIMENTAL STUDIES OF INTER- AND INTRA- ELEMENTARY EXCITATION CORRELATIONS 229
G. Sawatzky.....229

ELUCIDATING MICROSCOPIC INTERACTIONS IN SKYRMION HOSTS FROM SPATIOTEMPORAL LATTICE DYNAMICS 230
A. M. Barbour[1], M. G. Han[2], C. Liu[1], F. Camino[3], F. Forte[4], F. Gabriele[4], J. Seidel[3], M. Cuoco[4], Y. Zhu[2], C. Mazzoli[1].....230

STRAIN TUNING MATERIALS AND UNRAVELLING THEIR MAGNETIC PROPERTIES USING NEUTRON DIFFRACTION 231
P. Manuel 231

18 - ELECTRICAL CONTROL OF MAGNETISM 232

TUNABLE MAGNETO-IONIC STATES IN NANOSCALE DOT ARRAYS FOR SELF-PROTECTED, REPROGRAMMABLE AND LOW-POWER DEVICES 233
I. Spasojević[1], F. Celegato[2], A. Magni[2], A. Barrera[3], Z. Ma[1], S. Ruiz-Gómez[4], M. Foerster[4], A. Palau[3], K. S. Buchanan[5], P. Tiberto[2], J. Sort[1,6].....233

SPIN-CHARGE INTERCONVERSION IN 2D VAN DER WAAL MATERIALS.....234
C. K. Safeer 234

UNIVERSAL HALL TORQUES 235
E. A. Montoya.....235

CHIRAL SPINTRONICS DEVICE.....236
S. Miwa.....236

ZEEMAN SPIN TEXTURES WITHOUT MAGNETISM.....237
B. Kilic[1], S. Alvarruiz[1], E. Barts[1], B.v. Dijk[1], P. Barone[2], J. Sławińska[1].....237

LARGE-SCALE DIRECT-WRITE NANOSCALE CONTROL OF HIGH-T_C SUPERCONDUCTIVITY AND MAGNETISM VIA PHASE NANOENGINEERING 238
I. Biancardi[1], V. Levati[1], M. Panzeri[1], J. Alcalà[2], D. Girardi[1], N. Pellizzi[1], M. Vitali[1], P. Florio[1], O. Boulle[3], T.Günkel[2], N. Mestres[2], D. Petti[1], A. Palau[2], E. Albisetti[1].....238

LIGHT-CONTROLLED MAGNETISM IN MAGNETOSTRICTIVE THIN FILMS VIA LIQUID CRYSTALLINE NETWORKS 239
G. Barrera[1], D. Martella [2,3], F. Celegato[1], A. Magni[1], M. Coïsson[1], C. Parmeggiani[3,4], D. S. Wiersma[2,4], P. Tiberto[1].....239

VOLTAGE-CONTROLLED MAGNETOIONIC DEVICES AS CANDIDATES FOR IN-MEMORY COMPUTING.....240
M. Ameziane[1,2], K. Skailand[1,2], S. Nilsson[1,2], A. Hrabec[1,2], L. J. Heyderman[1,2] 240

3D NANOSCALE CONTROL OF MAGNETISM IN CRYSTALLINE YTTRIUM IRON GARNET VIA DIRECT LASER WRITING.....241
M. Vitali[1], P. Florio[1], V. Levati[1], A. D. Giacco[1], N. Pellizzi[1], R. Silvani[2], L. C. Mavilla[2], M. Madami[2], S. Genoni[1], I. Biancardi[1], D. Girardi[1], M. Panzeri[1], M. Cocconcelli[1], D. Breitbach[3], P. Pirro[3], L. Rovatti[4], N. Lecis[4], F. Maspero[1], R. Bertacco[1], G. Corrielli[5], R. Osellame[5], V. Russo6, A. L. Bassi[6], S. Tacchi[7], D. Petti[1], E. Albisetti[1] 241

SPIN HALL MAGNETORESISTANCE AND SPIN SEEBECK EFFECT IN NONCOLLIENAR MAGNETIC INSULATORS.....242
A. Aqeel 242

MAGNETO-IONIC CONTROL OF ANTIFERROMAGNET-FERROMAGNET SYSTEMS 243
E. Niapos[1], M. Staňo[1], J. A. Arregi[1], M. Otýpka[2], V. Uhlíř[1,2] 243

VOLTAGE-DRIVEN CONTROL OF EXCHANGE BIAS FIELD IN Pt/Co/CoO THIN FILMS VIA MAGNETO-IONIC EFFECTS 244
A. Klimeczek[1], M. De-Santis[1], F. Gay[1], L. Ranno[1], J. Vogel[1], A. Masseboeuf[2], A. Lamirand[3], S. Pizzini[1] 244

SPIN – FLOP TRANSITION AND MAGNETOGALVANIC EFFECT IN TETRAGONAL ANTIFERROMAGNETS: CuMnAs, Mn_2Au.....245
Z. V. Gareeva[1,2], A. K. Zvezdin[3] 245

EFFICIENT SPIN-CHARGE CONVERSION AT ROOM TEMPERATURE WITH FERROELECTRICS: ENABLING FESO.....246
S. Chiroli[1], R. Tomar[1], T. Buttiens[1,2], A. S. Goossens[1], E. Vazquez[3], M. Martemucci[3], Y. B. Fazlioglu[4], A. Raj[5], P. Sgarro[3], V. Giannone[3], S. Mallik[1,6], E. Gradauskaite[1], L. M. Vicente-Arche[1], W. Savero-Torres[7], T. Maroutian[2], A. Barthélémy[1], J. Varignon[8], A. Gloter[5], L. Iglesias[1], I. Boventer[1], J.-P. Attané[7], A. Charvier[7], L. Vila[7], R. Engel-Herbert[4,9], M. Bibes[12] 246

EXCHANGE BIAS AT ROOM TEMPERATURE IN ANTIFERROMAGNET NiCoO SINGLE LAYER BY MAGNETO-IONICS.....247
S. Privitera[1,2], Z. Ma[1], H. Gómez-Torres[1,2], A. Arredondo-López[1], M. O. Liedke[3], E. Hirschmann[3], A. Wagner[3], H. Tan[1], A. Quintana[1], T. Dias[4], D. Gouéré[5], E. Monteblanco[5], D. Ravelosona[5,6], A. Lopeandia[1,2], J. Sort[1,7], E. Menéndez[1] 247

LIGHT-CONTROLLED OF MAGNETISM IN MULTIFERROIC HETEROSTRUCTURES 248
H. Tan[1,2], Z. Ma[1], C. B. Karroum[3], M. Liparo[3], J.-P. Jay[3], D. Spenato[3], D. T. Dekadjevi[3], L. M. Armesto[1,2], A. Quintana[1,2], J. Sort[1,2,4] 248

MAGNETIC-FIELD-FREE MAGNETO-IONICS IN CoFeN for NEUROMORPHIC FUNCTIONALITY 249
L. M. Armesto[1], H. Tan[1,2], Z. Ma[1], I. Spasojevic[1,2], E. Pellicer[1], J. Sort[1,2,3] 249

HIGH HARMONICS CARRIER PUMPING FROM ALTERMAGNETS 250
O. Ly 250

INVESTIGATION OF THE EFFECTS OF SOLVENT TYPE AND Al/Cu DOPING ON THE CRYSTAL STRUCTURE AND ELECTRICAL PROPERTIES OF ZnO-BASED THERMISTORS SYNTHESIZED BY SOL-GEL METHOD 251
T. Seydioğlu 251

SOLID-STATE LITHIUM-ION BATTERY AND SUPERCAPACITOR STRUCTURES FOR VOLTAGE CONTROL OF MAGNETISM 252
S. van Dijken 252

MERGING VOLTAGE-IONTRONICS WITH MAGNETISM FOR ADVANCED MEMORY APPLICATIONS 253
J. Sort[1,2,3], N. López-Pintó[1], I. Spasojević[1], Z. Ma[1], Z. Tan[1], M. Peda[1], A. Quintana[1], E. Pellicer[1], J. Nogués[2,3], E. Menéndez[1] 253

19 - EMERGENT PHENOMENA AND TOPOLOGY IN MAGNET-SUPERCONDUCTOR HYBRIDS 254

RARE-EARTH MAGNETISM AND YU–SHIBA–RUSINOV STATES IN SUPERCONDUCTING Nb-BASED NANOSTRUCTURES 255
A. Odobesko 255

UNCONVENTIONAL SUPERCURRENT PHASE IN ISING SUPERCONDUCTOR JOSEPHSON JUNCTION WITH ATOMICALLY THIN MAGNETIC INSULATOR 256
F. Pientka 256

USING QUANTUM CORRALS TO NON-LOCALLY DETECT MAGNET-SUPERCONDUCTOR HYBRID STATES 257
J. Wiebe[1,2] 257

MAGNETIC AND SPIN-PUMPING PROPERTIES OF MgB_2-BASED AND NbN-BASED MULTILAYERS 258
L. Peridon, T. Courtois, K. Dumesnil, S. Mangin, T. Hauet 258

INTERFACE-DRIVEN TRIPLET PROXIMITY EFFECTS AND ELECTRONIC TRANSPORT IN SPIN-ORBIT COUPLED SUPERCONDUCTOR/FERROMAGNET HYBRIDS 259
N. Banerjee 259

CRITICAL SLOWING-DOWN IN LASER-INDUCED PICOSECOND SUPERCONDUCTING PHASE TRANSITION 260
G. N. Antonio[1], T. Courtois[2], C. Pfaff[2], K. M. S. Shukla[1], A. Sudbø[3], S. Mangin[2], T. Hauet[2], C. Ciccarelli[1, 3] . 260

TOPOLOGY AND ENERGY DEPENDENCE OF MAJORANA BOUND STATES IN A CAVITY ..261
A. Kobialka [1], A. K. Ghosh[1], R. Arouca[1,2], A. M. Black-Schaffer[1] 261

INTERPLAY OF SUPERCONDUCTIVITY, FERROMAGNETISM AND HALF-METALLICITY IN GATED SINGLE-LAYER g-C3N4 262
P. N. Brangi, F. Martini, P. Cudazzo, M. Calandra 262

20 - EMERGING PHENOMENA AND APPLICATIONS IN MOLECULAR AND METAL-ORGANIC MAGNETIC MATERIALS 263

ENGINEERING TRITYL RADICAL-SURFACE HYBRIDS FOR MOLECULAR SPINTRONIC AND OPTOELECTRONIC APPLICATIONS 264
J. A. de Sousa[1,4], D. Schäfter[2], S. Settele[3], L. Tesi[2], M. Mas-Torrent[1], J. Veciana[1], J. Zaumseil[3], J. van Slageren[2], S. Cambré[4], N. Crivillers[1] 264

TAILORING MULTIFUNCTIONALITY IN MULTIMETALLIC CARBORANE METAL-ORGANIC FRAMEWORKS VIA CONTROLLED METAL COMPOSITION AND SEQUENCING 265
E. Bartolomé[1], X. Liu[1], X.-B. Li[1], A. Arauzo[2], J. Luzón[2], E. Ruiz[3], S. Gómez-Coca[3], J. G. Planas[1] 265

2D MAGNETIC MATERIALS FROM SILANE-BRIDGED DICARBOXYLATES: MULTIFUNCTIONALITY AND DIMENSIONALITY EFFECTS 266
Ana Arauzo[1], Mirela-Fernanda Zaltariov[2], Cristina Piquer[1], Elena Bartolomé[3], Sara Fuertes[4], Ionut-Radu Tigoianu[2], Sergiu Shova[2], Maria Cazacu[2] 266

PHOTORESPONSIVE DYSPROSIUM-ANTHRACENE COMPLEXES: EFFECTS OF TEMPERATURE AND IRRADIATION TIME ON THE REVERSIBLE PHOTOCYCLOADDITION REACTION OF ANTHRACENE 267
L.-M. Zheng..... 267

ELEMENT SELECTIVE PROBE FOR MOLECULAR MAGNETISM: XMCD OF 5D PARAMAGNETIC COMPLEXES 268
A. A. Rogalev[1], K.S. Pedersen[2], F. Wilhelm[1], R. Clérac[3] 268

SPIN-ELECTRIC EFFECT IN A Co(II)-BASED ANTIFERROMAGNETIC SPIN TRIANGLE 269
T. Guidi[1,2], M. Albanesi[3,4], E. Garlatti[5], S. Carretta[5], M. Fittipaldi[6], R. Sessoli[3], B. Kintzel[7], W. Plass[7] 269

TUNING CHARGE AND SPIN INTERACTIONS AT SURFACES WITH MOLECULAR STRATEGIES.....270
A. Mugarza[1,2]..... 270

QUANTUM AND EXOTIC EFFECTS IN MOLECULE-BASED MAGNETIC MATERIALS - QUIXOTICS 271
A. K. Powell..... 271

GENERALIZED QUANTUM GEOMETRY DRIVEN TRANSPORT IN UNCONVENTIONAL MAGNETS.....272
S. Nandy[1], N. Chakraborty[2], S. K. Ghosh[2]..... 272

BREAKING PERFORMANCE LIMITS IN TWO-DIMENSIONAL METAL-ORGANIC MAGNETS THROUGH CHEMICAL DESIGN 273
A. Adak[1], R. Diego[1], V. L. Nadurata[1], P. Perlepe[1,2], I. Oyarzabal[1,3,4], N. Yutronkie[1], D. Lou[1], A. Zabala-Lekuona[5], A. Mailman[6], M. Gonidec[2], M. Rouzieres [1], E. A. Suturina[7], S. Giri[8], S. Bonhommeau[9], G. Clermont[9], F. Wilhelm[10], A. Rogalev[10], C. Mathonière[1], R. Clérac[1] 273

THE INFLUENCE OF SUPERCONDUCTIVITY ON THE SPIN STATES OF Er^{3+} COMPLEXES IN COMPOSITE STRUCTURES 274
E. I. Kunitsyna, R.B. Morgunov 274

21 - FERROMAGNETIC SHAPE MEMORY ALLOYS AND MAGNETOCALORICS .275

STRUCTURAL, MAGNETIC, AND MAGNETOCALORIC PROPERTIES OF TEXTURED DyNiAl INTERMETALLIC COMPOUND.....276
J. Ćwik[1], Y. Koshkid`ko[1], D. Gajda[1], M. Małecka[1], D. Szymański[1], E. Tereshina-Chitrova[2], A. Czernuszewicz[3] 276

RECENT DEVELOPMENTS IN PARTICULATE HEUSLER TYPE MAGNETIC SHAPE MEMORY HYBRID MATERIALS FOR ACTUATION AND ENERGY 277
V. Chernenko[1,2], V. Lvov[3], H. Hosoda[4], S. Lanceros-Mendes[1,2]..... 277

ROLE OF Fe, Co AND Cu ADDITION IN THE STRUCTURAL AND MAGNETIC PROPERTIES OF Ni-Mn-Ga MAGNETIC SHAPE MEMORY ALLOYS 278
N. A. Río-López [1,+], P. Lázpita [1,2], A. Pérez-Checa [3], J. Feuchtwanger [1,4], J. A. Rodríguez-Velamazán [5], I. Zabala [1], V. Chernenko [1,2,4], F. Plazaola[1], C. Seguí [6], J. M. Porro[2,4] 278

THERMOELECTRIC PROPERTIES OF HALF- AND DOUBLE HALF-HEUSLER ALLOYS: A THEORETICAL STUDY 279
V. Buchelnikov, V. Sokolovskiy, A. Enenko, M. Matyunina 279

BEYOND GGA: THE QUEST FOR AN ACCURATE GROUND STATE DESCRIPTION OF Ni_2MnTi HEUSLER ALLOY 280
V. Sokolovskiy[1], K. Erager[1], D. Baigutlin[1], D. Novokreshenov[1], M. Matyunina[1], O. Miroshkina[2], V. Buchelnikov[1] 280

MARTENSITIC MICROSTRUCTURE ENGINEERING: A VERSATILE APPROACH FOR MAGNETIC MANIPULATION OF MULTIFERROIC HEUSLER FILMS AND SPATIALLY CONFINED STRUCTURES 281
M. Takhsha 281

FATIQUE PROPERTIES OF Ni-Mn-Ga-BASED RIBBONS PRODUCED BY RAPID CRYSTALLIZATION 282
M. J. Szczerba, M. Dudziński, M. Kowalska, P. Czaja, Ł. Rogal 282

THE EFFECT OF BORON ADDITION ON THE STRUCTURAL AND MECHANICAL PROPERTIES OF Ni-Mn-Co-Ti 283
M. Matyunina, V. Sokolovskiy, V. Buchelnikov 283

IMPACT OF DISORDER ON MAGNETIC AND VIBRATIONAL PROPERTIES OF Ni-Mn-Sn HEUSLER ALLOYS 284
O. Miroshkina, M. E. Gruner 284

DIRECT MEASUREMENTS OF ADIABATIC TEMPERATURE CHANGE IN La-Fe-Si ALLOYS IN CYCLIC MAGNETIC FIELDS: FREQUENCY EFFECTS AND LONG-TERM STABILITY 285
A. Gamzatov[1], N. Z. Abdulkadirova[1], A. M. Aliev[1], Y. Lin[2], J. Wang[2], F.-X.a Hu[2] 285

MARTENSITIC TRANSFORMATION WITH SMALL HYSTERESIS AND MAGNETIC-FIELD-INDUCED STRAIN IN Mn_3Ga ALLOYS 286
X. Xu[1,2], D. Imatomi[1], Y. Kinoshita[3], M. Gen[3], Y. Kohama[3], Y. Ishii[3], Y. H. Matsuda[3], Y. Kubota[4], Y. Inubushi[4,5], M. Yabashi[4,5], A. Ikeda[6], K. Noda[6], K. Seki[6], Y. Urabe[6], T. Kihara[7], Y. Hokuse[7], Y. Hirose[7], T. Omori[1], Masashi Tokunaga[3], R. Kainuma[1] 286

22 - HIGH TEMPERATURE SUPERCONDUCTORS FOR FUSION APPLICATIONS 287

PROGRESS AND CHALLENGES IN DEVELOPING HTS MAGNETS FOR THE STEP FUSION PLANT 288
S. C. Wimbush 288

MANUFACTURING PROGRESS OF THE WINDING PACK FOR CFEDR TF PROTOTYPE COIL 289
J. He[1,2], W. Wen[1,2], Y. Wu[1], CRAFT TF Team[1] 289

HTS WIRE REQUIREMENTS FOR FUSION MAGNETS AND PRODUCTION OF HTS MAGNETS AT RENAISSANCE FUSION 290
D. Longo 290

GENERATING ANY MAGNETOSTATIC FIELD FROM A SINGLE SOURCE 291
J. Cunill-Subiranas[1], N. Bort-Soldevila[1], F. Resare[2], N. Del-Valle[1], W. Wieczorek[2], C. Navau[1] 291

A COMPLETE NOVEL MULTIPHYSICS SOFTWARE FOR MODELING QUENCH IN NON-INSULATED HTS COILS FOR HIGH FIELD MAGNETS 292
A. Dadhich, E.Pardo 292

EFFECT OF SILANE COUPLING AGENT MODIFICATION ON THE PROPERTIES OF ALUMINA-SILICATE FIBER REINFORCED COMPOSITES FOR Bi-2212 CICC 293
J. Sun[1,2], Z. Liu[1,2], Z. Yan[3],W. Wen[1,2], J. He[1,2], J. Wu[1] 293

DESIGN, SIMULATION, AND EXPERIMENTAL VALIDATION OF A HEAT TREATMENT SYSTEM FOR CRAFT TF COIL: A CRITICAL STEP TOWARDS CFETR TF 294
Y. Wu, W. Wang, Y. Wu, J. Qin 294

EARLY OPERATIONAL RESULTS FROM DEMO4 295
R. Bateman, B. van Nugteren 295

CONTROLLING OXYGEN MIGRATION IN $YBa_2Cu_3O_{7-\delta}$ WITH SHORT CURRENT PULSES AND DEVICE GEOMETRY 296
D. Stoffels[1], C. C. Quaglio-Gomes[1,2], F. Egyenes[3], B. Aichner[4], A. Palau[5], W. Lang[4], M. Motta[2], A. V. Silhanek[1] 296

LOW-ENERGY CHARGE EXCITATIONS IN CUPRATE SUPERCONDUCTORS VIA RESONANT INELASTIC X-RAY SCATTERING 297
T. Tohyama 297

CRITICAL PHOTOINDUCED REFLECTIVITY RELAXATION DYNAMICS IN SINGLE-LAYER Bi-BASED CUPRATES 298
T. Shimizu[1], R. Tobise[1], T. Kurosawa[1], S. Tsuchiya[1], Y. Toda[1], M. Oda[2], V. V. Kabanov[3], D. Mihailovic[3], T. Mertelj[3] 298

CHARGE, SPIN AND LATTICE DEGREES OF FREEDOM IN $YBa_2Cu_3O_x$ STUDIED BY ELECTRON PARAMAGNETIC RESONANCE 299
A. Shengelaya[1,2], A. Maisuradze[1], E. Pomjakushina[3], K. Conder[3], H. Keller[4] 299

24 - HYDROGEN ENABLING TECHNOLOGY FOR SUPERCONDUCTORS 300

AC INDUCTIVE ENERGIZATION TESTS OF HTS ASSEMBLED CONDUCTORS FOR LH2-COOLED HTS GENERATORS 301
M. Ohya, T. Gotomyo, T. Obuchi 301

RESEARCH AND DEVELOPMENT OF LIQUID HYDROGEN PUMPS DRIVEN BY HTS MOTORS 302
K. Kajikawa[1], T. Nakamura[2], H. Kobayashi[3], A. Kikuchi[4], T. Miura[5] 302

CRYOGENIC HELIUM GAS CIRCULATION SYSTEM FOR INDIRECT LH_2 COOLING OF SUPERCONDUCTING DEVICES 303
B. A. Glowacki[1,2] 303

LIQUID HYDROGEN-ENABLED COOLING OF SUPERCONDUCTING DEVICES FOR VARIOUS APPLICATIONS 304
S. V. Pamidi 304

25 - KAGOME MATERIALS FROM FUNDAMENTALS TO THEIR POTENTIAL APPLICATIONS.....305

TOPOLOGICAL HALL EFFECT ANISOTROPY IN KAGOME BILAYER METAL Fe_3Sn_2.....306
C. Petrovic.....306

MICROSCOPIC MUON SPIN ROTATION INSIGHTS INTO THE DISTINCT SUPERCONDUCTING REGIONS OF THE PHASE DIAGRAM IN Ti-DOPED CsV_3Sb_5.....307
P. Král[1], S. S. Islam[1], A. C. Salinas[2], J. Graham[1], O. Gerguri[1], H. Luetkens[1], R. Khasanov[1], S. Wilson[2], Z. Guguchia[1].....307

REAL MATERIALS CONTAINING KAGOME LATTICE: LATTICE DYNAMICS PERSPECTIVE..308
A. Ptok.....308

NMR INVESTIGATION OF THE CDW TRANSITION IN KAGOME METAL ScV_6Sn_6.....309
C. N. Kuo[1,2,3], W. S. Tian[2], G. T. Chen[2], C. S. Lue[1,2,3].....309

BREAKING THE KAGOME LATTICE: MAGNETIC FRUSTRATION AND SPIN REORIENTATION IN $Fe_{32+\delta}Ge_{35-x}Si_x$.....310
R. A. Khalaniya[1], V. Yu. Verchenko[1], A. V. Mironov[1], A. N. Samarin[2], A. V. Bogach[2], A. N. Kulchu[1], A. O. Polevik[1], Z. Wei[3], E. V. Dikarev[3], R. Stern[4], A. V. Shevelkov[1].....310

KAGOME ANTIFERROMAGNETS AS MULTIFUNCTIONAL SPIN-ORBIT PLATFORMS: FROM LARGE AHE TO TUNABLE SPIN PUMPING.....311
S. Sachin[1], I. Sinha[1], B. K. Kuanr[2], S. Manna[1].....311

26 - LARGE SCALE APPLICATIONS OF SUPERCONDUCTORS AND THEIR FUNDAMENTAL TECHNOLOGIES.....312

PERFORMANCE AND DEGRADATION MECHANISMS OF HIGH-J_c Nb_3Sn CICC FOR HIGH-FIELD APPLICATIONS.....313
Y. Liu[1], C. Dai[1],Y. Wu[1], A. Nijhuis[2], A. Devred[3], J. Qin[1].....313

MAGNET TECHNOLOGY FOR MRI AT SIEMENS HEALTHINEERS.....314
A. Johnstone.....314

CRYOGEN-FREE MAGNETS FOR MAGNETIC RESONANCE.....315
J. Good.....315

HTS CONDUCTORS AND COILS WITH Bi2212 FOR FAST-RAMP AND HIGH FIELD USAGE 316
A. Otto[1], A. Bouthillette[1], B. Bouchard[1], A. Croteau[1], J. Voccio[1,2].....316

HTS MAGNET DEVELOPMENT AT TOKAMAK ENERGY.....317
R. Bateman.....317

SUPERCONDUCTING MAGNET DEVELOPMENT AND PRODUCTION AT TESLA ENGINEERING LIMITED.....319
A. Davidson, all the Tesla Engineering Limited Team.....319

ELECTROMAGNETIC DESIGN OF 3 T NbTi SPLIT SUPERCONDUCTING MAGNET FOR BLANKET MULTI-PHYSICAL FIELD INTEGRATED TEST PLATFORM.....320
J. Li[1,2], Z. Lin[1,2], L. Gao[1,2], S. Wei[1,2].....320

UPDATE ON PARTICLE THERAPY SOLUTIONS AT MEVION MEDICAL SYSTEMS.....321

M. Jones 321

FUTURE DIRECTIONS IN ACCELERATOR MAGNET TECHNOLOGY 322
L. Rossi 322

MRI STARTS TO FALL IN LOVE WITH HTS: FUTURE PERSPECTIVES OF CLINICAL MRI 323
D. W. J. Klomp[1,2] 323

THE DYNAMIC 14T: WHAT HTS-BASED MRI CAN DO FOR COGNITIVE NEUROIMAGING 324
M. A. Cloos 324

27 - MACHINE LEARNING AND DATA-DRIVEN APPROACHES IN SUPERCONDUCTIVITY 325

EFFICIENT ONLINE QUANTUM CIRCUIT LEARNING WITH NO UPFRONT TRAINING 326
T. O'Leary[1,2], P. Czarnik[3,4], E. Pelofske[5], A. T. Sornborger[6,7], M. McKerns[6,8], L. Cincio[1,7]* 326

VOLTAGE RISE PREDICTION OF REBCO COILS WITH MACHINE LEARNING FOR QUENCH PROTECTION 327
S. Noguchi[1], R. Sakakibara[2], T. Mato[1] 327

VISUAL FEEDBACK CONTROL USING A PLUME SHAPE MAP FOR REPRODUCIBLE SUPERCONDUCTOR THIN FILM DEPOSITION 328
K. Horio[1,5], T. Hachiya[1,5], S. Nakao[1,5], K. Kawabata[2,5], Y. Ichino[3,5], A. Ichinose[4,5], T. Horide[2,5], K. Matsumoto[2,5], T. Yoshida[2,5] 328

DIFFERENTIABLE PHYSICS AS THE ENGINE FOR GENERATIVE DISCOVERY: ACCELERATING SUPERCONDUCTOR DATA ACQUISITION WITH RIEMANNIAN DIRECT OPTIMIZATION 329
A. Chatterjee[1,2], J. Burton[1] 329

DATA DRIVEN AND NUMERICAL BASED OPTIMIZATION OF MAGNETIC LEVITATION SYSTEMS: FROM MULTI-SURFACE HTS MAGLEV TO HALBACH-ARRAY ELECTRODYNAMIC LEVITATION 330
U. K. Ozturk[1], E. C. Ozkat[2], M. Abdioglu[3] 330

MACHINE LEARNING PERSPECTIVES ON SUPERCONDUCTING MAGNETIC LEVITATION SYSTEMS: ENERGY EFFICIENCY TRENDS AND EMERGING DESIGN STRATEGIES 331
E. C. Özkat[1,2], U. K. Öztürk[2] 331

EXTENDING ALTERMAGNETIC MATERIAL BASE BY MAGNETRON SPUTTERING 332
D. Kriegner 332

HALL EFFECT AND NONRECIPROCAL CURRENT IN CLEAN CHIRAL MAGNETS: ASYMMETRIC SCATTERING AND QUANTUM FLUCTUATIONS 333
H. Ishizuka 333

UNUSUAL CO-PLANAR MAGNETIC ORDER IN $In_2Ir_2O_7$ 334
A. Yaresko[1], A. Krajewska[1], T. Takayama[1,2], H. Takagi[1] 334

SPIN-SELECTIVE ELECTRON TRANSPORT IN CHIRAL DIRUTHENIUM PADDLEWHEEL MONOLAYERS 335
I. Coloma[1], E. A. Hillard[1], N. Giaconi[2], S. Herrero[3], P. Rosa[1], L. Poggini[2], M. Mannini[2], M. Cortijo[3], T. Buffeteau[4], M. Gonidec[1] 335

CHIRALITY-DEPENDENT SPIN POLARIZATION IN METALS: LINEAR AND QUADRATIC RESPONSES 336
Y. Kato 336

POLARIZED NEUTRON SCATTERING IN MAGNETISM 337
A. Goukassov 337

CRYSTALLOGRAPHIC FRUSTRATION AS A MEANS TO INDUCE COMPLEX SPIN TEXTURES TOWARD NEW QUANTUM MATERIALS 338
Y.-X. Wang[1,2], I. Campbell[1], X. Wang[3], M. Shatruk[1,4] 338

EMERGENT FUNCTIONALITY OF SPIN SPIRALS: FROM P-WAVE MAGNETS TO TOPOLOGICAL TEXTURES 339
S. Okumura[1,2] 339

DECIPHERING INTRIGUING ISSUES OF THE MAGNETOELASTIC PHASE TRANSITION IN Fe-Rh ALLOYS AROUND EQUIATOMIC COMPOSITION 340
K. Padrón-Aleman[1,2], P. Álvarez-Alonso[1,3], M. L. Arreguín-Hernández[4], G. J. Cuello[2], J. A. Blanco[1], J. L. S. Llamazares[5], P. Gorria[1,3] 340

X-RAY DIRECTIONAL DICHROISM – AN ELEMENT SELECTIVE PROBE OF MAGNETOELECTRICITY 341
A. Rogalev 341

CONICAL STATES IN A COMPOSITE CHIRAL MAGNET 342
V. Laliena[1], J. Campo[2] 342

29 - MAGNETIC MATERIALS PROCESSING AND PHYSICAL PROPERTIES 343

THERMAL HISTORY-DEPENDENT CHARACTERISTICS IN VAN DER WAALS FERROMAGNET $Fe_{5-x}GeTe_2$ (x ~ 0.16) 344
R. L. Yadav[1], P. Bag[1], C.-C. Lai[1], Y.-K. Kuo[1], C.-N.g Kuo[2], C. S. Lue[2] 344

SPINEL FERRITES AS EVOLVING MATERIALS FOR Re-RAM: CORRELATION OF THERMOPHYSICAL PROPERTIES WITH SWITCHING PHENOMENA 345
M. Anis-ur-Rehman 345

ARTIFICIAL SURFACE CORRUGATION OF PERMALLOY FILMS THROUGH FEMTOSECOND LASER IRRADIATION 346
C. Delforge[1], J. Frechilla[2], N. Lejeune[1], A. Naik[1], A. Frechilla[2], A. Badía-Majós[2], M. Ciria[2], L. A. Angurel[2], E. Martínez[2], G. F. de la Fuente[2], E. Fourneau[1], A. V. Silhanek[1] 346

TAILORING THE ELECTRICAL PROPERTIES OF LITHIUM FERRITES THROUGH COBALT DOPING FOR RESISTIVE MEMORY DEVICES 347
K. Naheed[1,2], W. Mehmood[2], M. Anis-ur-Rehman[1] 347

INVESTIGATION OF HTS COIL-PM MAGNETIC FIELD PROFILE WITH DIFFERENT COIL PARAMETERS 348
H. Mollahasanoglu[1], U. K. Ozturk[2], M. Abdioglu[3] 348

NEW MONOCLINIC MODIFICATIONS OF $MFeTe_2$ (M = Nb, Ta) LAYERED VAN DER WAALS TELLURIDES 349
A. V. Stepanova[1], A. N. Azarevich[2], A. V. Bogach[2], A. V. Mironov[1], M. A. Kirsanova[3], A. V. Sobolev[1], I. A. Presniakov[1], A. V. Shevelkov[1], V. Yu. Verchenko[1] 349

30 - MAGNETISM OF NANOPARTICLES, NANO-WIRES AND NANO-STRUCTURES 350

SOLUTION-PROCESSED METAL OXIDE NANOCOMPOSITES FOR ENHANCED MAGNETISM AND SPIN TRANSPORT 351
A. Shahid 351

31 - MAGNONICS AND MAGNETIZATION DYNAMICS 352

REAL-SPACE IMAGING OF MAGNONS INTERACTING WITH NONCOLLINEAR MAGNETIC TEXTURES 353
P. Che 353

TEMPERATURE DEPENDENCE OF VOLUME AND INTERFACE CONTRIBUTIONS TO THE MAGNETIC DAMPING OF PERMALLOY THIN FILMS 354
V. Ney[1], K. Lenz[2], R. Hübner[2], F. Ganss[2], J. Lindner[2], A. Ney[1] 354

SPIN-PUMPING AND INDUCED MAGNETIC POLARIZATION IN PERMALLOY/PLATINUM HETEROSTRUCTURES 355
V. Ney[1], K. Lenz[2], F. Wilhelm[3], R. Hübner[2], F. Ganss[2], A. Rogalev[3], J. Lindner[2], A. Ney[1] 355

HIGHLY EFFICIENT COHERENT AMPLIFICATION OF ZERO-FIELD SPIN WAVES IN YIG NANO-WAVEGUIDES 356
K. O. Nikolaev[1], S. R. Lake[2], B. Das Mohapatra[2], G. Schmidt[2,3], S. O. Demokritov[1], V. E. Demidov[1] 356

OPTIMIZING SPINWAVE TRANSDUCER FOR 5G APPLICATIONS 357
F. Bruckner, K. Davídková, I. Douveas, C.Abert, A. Chumak, D.Suess 357

NONRECIPROCAL MAGNON PHASE SHIFTS FROM ELECTRIC FIELDS: THE AHARONOV–CASHER MECHANISM 358
A. A. Serga 358

ADVANCED GARNET HETEROSTRUCTURES BY LATERAL CRYSTALLIZATION 359
C. Holzmann[1], S. Glamsch[1], D. Stein[1], M. Mihm[1], A. Ullrich[1], R.Schlitz[2], M. Lammel[2], J. Boneberg[2], M. Albrecht[1] 359

ONE- AND TWO-DIMENSIONAL YIG MAGNONIC NANOCRYSTALS 360
K. O. Levchenko 360

ULTRA-LONG-LIVING MAGNONS IN YIG FOR QUANTUM MAGNONICS 361
R. O. Serha 361

ADVANCES IN MICRO-FOCUSED BRILLOUIN LIGHT SCATTERING: MIE RESONANCES AND POLARIZATION ANALYSIS OF THE SCATTERED LIGHT 362
M. Urbánek 362

A TIME-MULTIPLEXED SPINWAVE ISING MACHINE 363
A. Litvinenko[1], R. Khymyn[2], R. Ovcharov[2], V. Tyberkevych[1], J. Åkerman[2,3,4], A. Slavin[2] 363

THEORY OF NONLINEAR INTERACTIONS OF PARAMETRICALLY-EXCITED SPIN-WAVE MODES IN CONFINED MICROMAGNETIC SYSTEMS 364
M. d'Aquino 364

RESONANT DOMAIN WALL DYNAMICS IN A THREE-DIMENSIONAL MAGNETIC NANO DOUBLE HELIX 365
P. Morales-Fernández[1,2], I. Konstantinos-Douveas[3], C. Abert[3], E. Zhakina[1], S. Ruiz-Gómez[1,4], C. Fernández-González[1,4], L. A. Turnbull[1,5], S. Wintz[6], M. König[1], S. Finizio[6,7], M. Weigand[6], N. Leo[8], D. Suess[3,9], A. Hierro-Rodríguez[10], A. Fernández-Pacheco[2], C. Donnelly[1,5] 365

NANOSCALED SPIN-WAVE DEVICES FOR 5G TECHNOLOGY OPERATING AT FR2 366
K. Davídková[1], K. Levchenko[1], F. Bruckner[1], R. Verba[2], R. Serha[1], F. Majcen1, Q. Wang[3], M. Lindner[4], C. Dubs[4], V. Vlaminck[5], J. Klíma[6], M. Urbánek[6], D. Suess[1], A. Chumak[1,3] 366

VERTICAL CONTROL IN MAGNONICS FOR EITHER TUNABLE MAGNON-MAGNON INTERACTION OR MAGNONIC METAL-TO-INSULATOR TRANSITION 367
F. Montoncello[1], P. Micaletti[1], R. Sultana[2], M. T. Kaffash[2], G. Gubbiotti[3], Y. Ji[2], M. B. Jungfleisch[2] 367

ENHANCEMENT OF COHERENT FREQUENCY COMBS IN STACKED MAGNET-SUPERCONDUCTOR HYBRID LAYERS 368
A. Ghirri[2], M. Cavani[1], C. Bonizzoni[1,2], M. Affronte[1,2] 368

QUANTUM STATE PREPARATION OF FERROMAGNETIC MAGNONS BY EXTERNAL CLASSICAL DRIVES 369
C. G. Ballestero 369

TOMOGRAPHY OF PARAMETRIC TRANSITION AND THERMAL SQUEEZING IN A MAGNET 370
T. Hioki[1,2,3] 370

COHERENT AND INCOHERENT MAGNONS IN NANOSTRUCTURED 3D TUBULAR FERROMAGNETS 371
D. Grundler[1,2] 371

32 - METASTABILITY, DISORDER, AND HIDDEN ORDERS IN 2D QUANTUM MATERIALS 372

HIDDEN STATES IN IRON-CHALCOGENIDE SUPERCONDUCTORS AND THEIR POTENTIALS FOR TOPOLOGICAL QUANTUM COMPUTING 373
Q. Li[1,2] 373

EMERGENT DIMENSIONALITY REDUCTION DRIVEN BY NANOSCALE SYMMETRY BREAKING IN SnSe 374
E. S. Bozin 374

FLUCTUATION-ENHANCED ELECTRON–PHONON COUPLING IN FeSe 375
B. Višić[1,2], J. Blagojević[1], A. Milosavljević[1], T. Belojica[1], M. Opačić[1], A. Šolajić[1], J. Pešić[1], E. Bozin[1], C. Petrovic[3,4,5], R. Hackl[6,7], N. Lazarević[1] 375

HIDDEN ORDER AND FLUCTUATING PHASES IN VAN DER WAALS TELLURIDES 376
J. Pešić[1], T. Belojica[1], J. Blagojević[1], A. Šolajić[1], B. Višić[1], E. S. Božin[1], S. D. Mijin[1], C. Petrović[2,3,4], Z. V. Popović[5], R. Hackl[6,7], A. Milosavljević[1], N. Lazarević[1] 376

PHASE COEXISTENCE AND ELECTRONIC ORDERING IN 1T-TaS_2 377
N. Lazarević[1], S. Djurdjić Mijin[1,9], A. Baum[2], J. Bekaert[3], J. Pešić[1], Y. Liu[4], G. He[2], M. V. Milošević[3], C. Petrovic[4,5,6], Z. V. Popović[7], R. Hackl[10] 377

DECIPHERING THE SEQUENCE OF PHASE TRANSITIONS IN $KNiCl_3$ 378
M. J. Gutmann[1], K. Wang[2], S.-W. Kim[2], B. Monserrat[2], G. L. Pascut[3] 378

ELECTRONIC-STRUCTURAL INTERPLAY IN THE PARAMAGNETIC STATE OF LOW DIMENSIONAL SYSTEMS 379
Q. Zhang[1], S.-W. Kim[2], K. Wang[2], M. Gutmann[3], A. Devashibhai[3,4], B. Monserrat[2], K. Haule[5], G. L. Pascut[6] 379

DETERMINATION OF LOCAL ORDER FROM DIFFUSE SCATTERING BY HIGH ENERGY X-RAYS 380
M. v. Zimmermann 380

NON-EQUILIBRIUM ELECTRON DYNAMICS ON THE SURFACE OF 1T-TaS_2 381
Y. Vaskivskyi 381

HIGH-PRESSURE SYMMETRY EVOLUTION AND FERROELECTRIC SUPPRESSION IN LAYERED PEROVSKITE-LIKE TITANATES 382
A. G. Asadov[1,2], A. I. Mammadov[1], D. P. Kozlenko[2], R. Z. Mehdiyeva[1], E. V. Lukin[2], S. E. Kichanov[2] 382

33 - MGB2 – MATERIALS AND APPLICATIONS 383

INFLUENCE OF Dy_2O_3 ADMIXTURES ON THE CRITICAL CURRENT DENSITY AT 20 K AND 30 K IN MgB_2 WIRES 384
D. Gajda[1], M. Babij[1], A. Zaleski[1], D. Avci[2], F. Karaboga[3], H. Yetis[4], I. Belenli[4], D. Szymanski[1], M. Małecka[1], D. Zasada[5], T. Czujko[5] 384

COMPOSITES OF MgB_2 PROCESSED BY SPARK PLASMA SINTERING: POWDER-IN-TUBE TAPES AND BULKS WITH SELECTED ADDITIVES 385
P. Badica 385

THE STORY OF MgB_2 DISCOVERY 386
J. Nagamatsu 386

PROTOTYPE MgB_2 SUPERCONDUCTING COIL USING ULTRA-FINE WIRES 387
T. Nakayama[1], J. Nagamatsu[2], K. Kikuchi[3], A. Kikuchi[4], M. Otsubo[1] 387

DEVELOPMENT ON UNIFORM, HIGH-PERFORMANCE MgB_2 MULTI-FILAMENT IMD LONG WIRES 388
C. Guo[1], D. Wang[1,2,3], Y. Ma[1,2,3] 388

THE EFFECTS OF STABLE MATRIX ON THE ELECTROMAGNETIC PROPERTIES FOR MULTI-FILAMENTS MgB_2 WIRES 389
M. Wang[1], Q. Guo[1], W. Yuan[1], W. Xie[1], Q. Yu[1], Y. Zhu[1], B. Wu[1], Y. Shi[1], J. Li[2], X. Liu[1], Y. Feng[1], P. Zhang[1,2] 389

TUNING OF TRANSPORT PROPERTIES OF MgB_2 THIN FILMS VIA X-RAY NANOPATTERNING 390
A. Alessio[1], S. Singh[1], M. Fretto[2], V. Bonino[3], A. Agostino[4], B. Vitale[4], E. Di Francia[1], M. Belogolovskii[5], M. Truccato[1] 390

INDUSTRIAL PRODUCTION OF MgB_2 WIRES FOR MAGNET SYSTEMS AND HIGH-CURRENT CABLES AT ASG SUPERCONDUCTORS 391
A. Tumino, M. Tropeano, A. Ansaldo, A. Traverso, T. Spina, F. Mazzei, G. Grasso 391

MgB_2 SUPERCONDUCTING WIRES FABRICATED BY INTERNAL MAGNESIUM DIFFUSION (IMD) METHOD: INTERFACE ENGINEERING AND MULTI-FILAMENTARY DESIGN 392
S. Safran[1,2], A.Gencer[1,2], C. Guo[3], F. Almokdad[4], F. Ervüz[1], H. Koralay[5], Y. Oznal[1,8], S. Salahi[6], A. Seçkin[7], K. Sönmez[1,4], S. C. Taşkın[1], D. Wang[3], Y. Ma[3] 392

COMPARATIVE ANALYSIS OF J_c AND J_e IN MgB_2 POWDER-IN-TUBE AND THIN-FILM CONDUCTORS FOR LIQUID HYDROGEN CRYOMAGNETIC APPLICATIONS (15–20 K) 393
B. A. Glowacki[1,2] 393

34 - MICROMAGNETICS, MODELING, AND SCIENTIFIC MACHINE LEARNING 394

SELF-MODULATION INSTABILITY IN HIGH POWER FERROMAGNETIC RESONANCE OF BiYIG NANODISKS.....395
I. Ngouagnia Yemeli[1], S. Perna[2], D. Goueré[3], A. Kolli[1], M.Munoz[4], A. Anane[3], M.d'Aquino[2], H. Merbouche[1], C. Serpico[2], G. de Loubens[1] 395

VOLTAGE GENERATION BY FERROMAGNETIC RESONANCE IN Fe/Co BILAYER WITH PERPENDICULAR MAGNETIC ANISOTROPY.....396
N. Leśniewski[1], A. K. Dhiman[2], P. Graczyk[2] 396

GRAPH NEURAL NETWORKS TO PREDICT PROPERTIES OF HARD MAGNETIC MICROSTRUCTURES.....397
H. Moustafa[1], A. Kovacs[1], J. Fischbacher, M. Gusenbauer[1], Q. Ali[1,2], L. Breth[1], T. Schrefl[1,2], H. Oezelt[1] 397

HIGHER ORDER STRAY FIELD COMPUTATION ON TENSOR PRODUCT DOMAINS.....398
L. Exl[1,2,3], S. Schaffer[1,2] 398

LEVEL-SET PARAMETRIZATION APPROACH FOR INVERSE-DESIGN MAGNONICS.....399
A. Voronov[1], M. C. Santos[2,3], F. Bruckner[1], D. Suess[1], A. Chumak[1], C. Abert[1] 399

MODELING OF THE MAGNETOCALORIC EFFECT DURING MAGNETOSTRUCTURAL PHASE TRANSITIONS 400
A. Kosogor[1,2,3], V. A. L'vov[3], D. Böhm[1], T. Schrefl[1] 400

SIMULATING STRONGLY NONLINEAR DYNAMICS OF QUANTUM SYSTEMS WITH MACHINE LEARNING – OVERCOMING INSTABILITIES.....401
H. Vrcan, J. H. Mentink 401

BEYOND MONOLITHIC SIMULATIONS: A FEDERATED COMPUTING PLATFORM FOR RESILIENT MICROMAGNETIC WORKFLOWS.....402
M. Ender[1], P. Pirro[2,1] 402

NON-RECIPROCAL SPIN WAVE DYNAMICS IN MÖBIUS-SHAPED NANOMAGNETS.....403
R. Hertel 403

35 - MOLECULAR SPIN QUBITS AND MOLECULAR SPINTRONICS BASED ON MOLECULAR MAGNETS 404

TOPOLOGICAL QUENCHING OF QUANTUM TUNNELLING OF THE MAGNETISATION IN A SINGLE MOLECULE MAGNET 405
E. Moreno-Pineda[1,2], S. Paul[1], C. Molina-Jirón[1,2], A. Sunil[1], M. Ruben[1], A. Garg[3], W. Wernsdorfer[1] 405

REVISITING LANTERN COMPLEXES AS MOLECULAR SPIN QUBITS.....406
A. Cornia[1], O. Mironova[1], M. Borsari[1], M. Briganti[2], M. Chiesa[3], R. Clérac[4], M. Imperato[1,5], Y.-K. Liao[3], A. Nicolini[1], M. C. Pagliero[3], A. Ranieri[6], A. Raza[2], M. Rouzières[4], E. Salvadori[3], L. Sorace[2] 406

STUDY AND CONTROL OF MANY-BODY EFFECTS IN MOLECULAR SPIN CRYSTALS BY MEANS OF CIRCUIT QUANTUM ELECTRODYNAMICS 407

F. Luis 407

KONDO RESONANCE OF $LnPc_2$ SINGLE-MOLECULE MAGNETS **408**
M. Yamashita[1,2] 408

MOLECULAR SPIN QUBIT BEHAVIOR IN MULTIFUNCTIONAL SPIN CROSSOVER SYSTEMS **409**
S. Hayami 409

ORBIT-ORBIT INTERACTION-ENABLED OPTICALLY INDUCED MAGNETIZATION IN HYBRID ORGANIC-INORGANIC PEROVSKITE FILM **410**
B. Hu 410

ENLARGING QUANTUM COHERENCE OF MOLECULAR SPIN QUBITS IN ZIRCONIUM PORPHYRINIC MOFs **411**
D. Žilić[1], L. Vujević[1], B. Karadeniz[1], K. Užarević[1], A. A. Popov[2] 411

SELF-COOLING MOLECULAR SPIN QUDITS **412**
G. Aromí[1], F. Luis[2], L.A Barrios[1], S. Carretta[3], O. Roubeau[2], V. Novikov[1] 412

ADDRESSING MOLECULAR SPIN QUBITS BY SUPERCONDUCTING CIRCUITS **413**
M. Affronte[1,2], C. Bonizzoni[1,2], M. Lanza[1,2], A. Ghirri[2] 413

HOW ENCAPSULATION ENHANCES THE QUANTUM COHERENCE OF A SOLID-STATE MOLECULAR SPIN QUBIT **414**
L. A Barrios[1], A. Swain[1], Y. Nelyubina[2], S. J. Teat[3], O. Roubeau[4], G. Aromí[1], V. Novikov[1] 414

36 - MULTICOMPONENT SUPERCONDUCTIVITY AND RELATED PHENOMENA **415**

ELECTRONIC STRUCTURE AND MAGNETIC FLUCTUATIONS IN UTe_2 UNDER PRESSURE **416**
M. Shimizu, Y. Yanase 416

COMPETING AND COOPERATING ORDERS IN UTe_2 ..... **417**
D. Braithwaite[1], T. Vasina[1], G. Knebel[1], J.-P. Brison[1], G. Lapertot[1], G. Seyfarth[2] 417

QUASIPARTICLE SCATTERING INTERFERENCE IMAGING OF TOPOLOGICAL SUPERCONDUCTIVITY IN UTe_2 ..... **418**
S. Wang 418

THERMODYNAMIC EVIDENCE FOR MULTIPHASE SUPERCONDUCTIVITY AND MAGNETIC QUANTUM CRITICALITY IN UTe_2 ..... **419**
T. I. Weinberger[1], A. Cabala[2], V. Sechovsky[2], M. Valiska[2], A. G. Eaton[1], F. M. Grosche[1] 419

THE HIGH PRESSURE HIGH FIELD PHASE LANDSCAPE OF UTe_2 ..... **420**
A. G. Eaton 420

MULTIPLE NODAL SUPERCONDUCTING PHASES AND ORDER PARAMETER EVOLUTION IN PRESSURIZED UTe_2 ..... **421**
S. Zou[1], W. Huang[2], X. Lu[3], H. Yuan[3], Y. Luo[1] 421

37 - NEW DEVELOPMENTS IN QUANTUM MAGNETISM **422**

SOLITON EXCITATIONS IN THE SPIN-1/2 METAL-ORGANIC FRAMEWORK MATERIAL $[(C_2H_5)_3NH]_2Cu_2(C_2O_4)_3$ 423
S.A. Zvyagin[1], J. Wosnitza[1], C. Dissanayake[2,], M. Tomlinson[2], AKM A. Rahman[2], K. Kumarasinghe[2], Y. Nakajima[2] 423*

CLASSICAL FRACTON ISING SPIN LIQUID ON THE OCTOCHLORE LATTICE 424
M. Stern[1], M. D. Burke[2], M. J. P. Gingras[2], J. Romhanyi[1], K. T. K. Chung[3] 424

DEMYSTIFYING QUANTUM ESCAPISM ON THE HONEYCOMB LATTICE 425
A. L. Chernyshev 425

HYBRID MAGNON MODES 426
A. Hoffmann 426

OBSERVING ALTERMAGNETISM USING POLARIZED NEUTRONS 427
P. A. McClarty[1], A. Gukasov[1], J. G. Rau[2] 427

ANOMALOUS PHONON NONRECIPROCITY IN THE PARAMAGNETIC PHASE OF MULTIFERROIC $CoTe_6O_{13}$ 428
S. Fan[1], X. Xu[2], Y. Q. Cai[1] 428

SPIN–ORBIT COUPLING AND MAGNETIC EXCITATIONS IN THE XY-LIKE S = 1/2 CHAIN SYSTEM Li_2CoCl_4 429
M. Ozerov 429

QUANTUM MAGNETISM WITH NEURAL NETWORK QUANTUM STATES 430
A. E. Feiguin 430

PHONON DYNAMICS AND MAGNON-PHONON COUPLING IN THE VAN DER WAALS MAGNET $FePS_3$ 431
S. Kim[1], S. Fan[1], A. Alatas[2], A. Said[2], C. Nelson[1], Y. Q. Cai[1] 431

QUANTUM SENSING OF MAGNETIC PHASE TRANSITION VIA ON-CHIP SUPERCONDUCTING RESONATOR 432
P. Li 432

Fe-BASED VAN DER WAALS TELLURIDES: INTERPLAY BETWEEN ELECTRONIC AND MAGNETIC STATES IN LOW DIMENSIONS 433
V. Yu. Verchenko[1], A. V. Stepanova[1], A. N. Azarevich[2], A. V. Bogach[2], S. V. Zhurenko[3], A. V. Tkachev[3], A. A. Gippius[4], I. S. Soboleva[1], A. V. Sobolev[1], I. A. Presniakov[1], A. V. Shevelkov[1] 433

THE VAN DER WAALS CHALCOGENIDES WITH $MgAl_2Se_4$- AND $Mg_2Al_2Se_5$-TYPE STRUCTURE: SYNTHESIS, EXFOLIATION, AND MAGNETIC PROPERTIES 434
I.V. Chernoukhov[1], A.V. Bogach[2], K.A. Cherednichenko[3], A.V. Shevelkov[1], V.Yu. Verchenko[1] 434

ENHANCED DYNAMICS IN DISORDERED NON-KRAMERS SPIN ICE $Ho_2(Ti_{1-x}$-$Hf_x)_2O_7$: TOWARD THE COULOMB QUANTUM SPIN LIQUID STATE 435
N. Bujault[1], V. Porée[2,4], F. Morineau[1], E. Riordan[1], P. Falus[3], T. Fennell[4], V. Pomjakushin[4], R. Sibille[4], E. Lhotel[1] 435

ANISOTROPIC TRANSVERSE QUANTUM MAGNETORESISTANCE IN Fe DOPED $TlInTe_2$ ONE-DIMENSIONAL CHAIN-LIKE SEMICONDUCTOR 436
S. Gökçe[1], A. K. Fedotov[2], F. Mikailzade[3], J. Fedotova[2] 436

MAGNETISM ON THE SHASTRY-SUTHERLAND LATTICE 437
F. Mila 437

QUANTUM SPIN ICE PHYSICS AND THE DIPOLE-OCTUPOLE Ce-BASED PYROCHLORES ..438
B. D. Gaulin[1,2,3]..... 438

38 - NEW DEVELOPMENTS IN SUPERCONDUCTIVITY OF ATOMICALLY THIN SUPERCONDUCTORS 439

DETECTING INDIVIDUAL PEARL VORTICES WITH A TWISTED-GRAPHENE JOSEPHSON JUNCTION 440
M. Perego[1], C. G. Agero[1], P. Koopmann[1], A. Mestre-Torà[1], A. O. Denisov[1], T. Taniguchi[2], K. Watanabe[3], F. Gaggioli[4,5], V. Geshkenbein[4], G. Blatter[4,6], T. Ihn[1,6], K. Ensslin[1,6]..... 440

SUPERFLUID STIFFNESS OF TWISTED BILAYER GRAPHENE 441
M. Tanaka[1,2], J. I-J. Wang[1], T. Dinh[1], D. Rodan-Legrain[1], S. Zaman[1], M. Hays[1], K. Watanabe[3], T. Taniguchi[3], P. Jarillo-Herrero[1], W. D. Oliver[1] 441

ELECTRICALLY TUNABLE SUPERCONDUCTING DIODE VIA MOIRÉ PHONONS IN TWISTED $NbSe_2$ 442
J. Zhao[1,2], Z. Chen[1,2], F. Gaggioli[3], S. Grebenchuk[1,4], Z. Qiu[1], Y. Han[5], J. Hu[6], K. Watanabe[7], T. Taniguchi[8], A. H. C. Neto[1,4,9], J. Lu[1,5], M. Wu[10], V. B. Geshkenbein[3], K. S. Novoselov[1,4] 442

ABRIKOSOV VORTICES SWITCHING JOSEPHSON CURRENT IN MAGIC ANGLE GRAPHENE 443
G. Blatter[1], M. Perego[2], … , V. B. Geshkenbein[1]..... 443

INTERPLAY OF FERROELECTRICITY AND INTERLAYER SUPERCONDUCTIVITY IN VAN DER WAALS BILAYERS.....444
A. S. Mel'nikov[1,2], A. A. Kopasov[2,3], D. Annenkov[1,4] 444

39 - NONRECIPROCAL TRANSPORT PHENOMENA AND THE DIODE EFFECT IN SUPERCONDUCTORS 445

SUPERCONDUCTING PHASE DIAGRAM AND DIODE EFFECT IN A MISFIT LAYERED SUPERCONDUCTORS 446
Y. Itahashi, Y. Iwasa..... 446

NONLOCAL JOSEPHSON DIODE EFFECT IN MINIMAL KITAEV CHAINS 447
J. Cayao[1], M. Sato[2] 447

AC FLUX-DRIVEN DIODE EFFECT AS A PROBE OF FRACTIONAL CPRS IN DC SQUIDS.....448
Y. Yerin[1,2], I. Askerzade[2,3,4], A. Gencer[3] 448

NONRECIPROCAL JOSEPHSON TRANSPORT IN FRACTAL SUPERCONDUCTORS: A FRACTIONAL GINZBURG–LANDAU PERSPECTIVE 449
Y. Yerin[1,2], I. Askerzade[2,3] 449

GATE-TUNABLE POLARITY INVERSIONS OF THE SUPERCONDUCTING DIODE EFFECT FOR TOPOLOGICAL SUPERCONDUCTIVITY 450
J. Shabani..... 450

JOSEPHSON EFFECTS IN DIRAC SEMIMETAL Cd_3As_2.....451
W. Pan 451

TOWARDS ENERGY-TIME PTYCHOGRAPHY OF X-RAY SCATTERING FOR MICROMAGNETICS 452
G. Meier[1], A. Negi[2,3], L. M. Lohse[2,3], S. Velten[2], I. Sergeev[2], O. Leupold[2], S. Sadashivaiah[4,5], D. Bessas[6], A. Chumakhov[6], C. Brandt[7], L. Bocklage[2,3], R. Röhlsberger[2,3,4,5,8] 452

CONTROLLING AND SENSING SPIN SYSTEMS WITH FREE SPACE ELECTRONS 453
P. Haslinger 453

PATTERNING TWO-DIMENSIONAL GRADIENTS IN STRUCTURAL AND MAGNETIC PROPERTIES FOR SPINTRONICS APPLICATIONS 454
A. Hrabec[1,2] 454

SKYRMIONS AND ANTISKYRMIONS IN ROOM-TEMPERATURE NONCENTROSYMMETRIC MAGNETS 455
K. Karube[1], L. C. Peng[1,2], Y. L. Chiew[1], X. Z. Yu[1], J. Masell[1,3], L. Keller[4], J. S. White[4], V. Ukleev[4,5], M. Hemmida[6], H.-A. Krug von Nidda[6], I. Kézsmárki[6], M.-C. Jiang[1,7,8], G.-Y. Guo[7,8], R. Arita[1,9], F. Kagawa[1,10], Y. Tokura[1,11,12], Y. Taguchi[1] 455

FORMATION MECHANISMS OF SQUARE SKYRMION LATTICES IN MULTI-ORBITAL ELECTRON SYSTEMS 456
Y. S. Zha, S. Hayami 456

COUPLED VORTEX-SKYRMION 3-DIMENSIONAL HETEROSTRUCTURES: STABILITY AND MAGNETIC FIELD-INDUCED MOTION 457
J. Sunny[1], S. Koraltan[2], T. Gokita[2], T. Schmidt[1], S. Wintz[4], D. Suess[3], M. Albrecht[1] 457

CRYOGENIC REAL SPACE MEASUREMENTS OF NONTRIVIAL TOPOLOGICAL SPIN TEXTURES 458
F. S. Yasin[1], M. El Gazzah[2,3], Y.-H. Kim[1], N. Y. Kim[1], S. Jamaluddin[2,3], H. Bhandari[2,3,4], R. B. Regmi[2,3], A. Kikkawa[5], Y. Taguchi[5], J. Yan[6], M. Birch[5], X. Yu[5,7], N. J. Ghimire[2,3], M. Chi[1] 458

PROBING ULTRAFAST MAGNETISM AT THE NANOSCALE WITH COHERENT XUV SCATTERING AND MICROSCOPY 459
S. Zayko[1], H-T. Chang[1], O. Kfir[2], T. Schmidt[3], M. Sivis[1], M. Albrecht[3], C. Ropers[1] 459

LOCALIZED SPIN TEXTURES STABILIZED BY GEOMETRY-INDUCED STRAIN IN 2D MAGNET Fe_3GeTe_2 460
Y. Sun[1], M. T. Birch[2], S. Finizio[3,4], L. Powalla[1], S. Satheesh[1], T. Priessnitz[1], E. Goering[1], E. Knöckl[5], C. Kastl[5], A. Holleitner[5], K. Kern[1], M. Weigand[4], S.Wintz[4], M. Burghard[1] 460

PHYSICS-INFORMED MAGNETIZATION RECONSTRUCTION FROM NV MAGNETOMETRY 461
C. Abert 461

CHIRAL MAGNETIC PHENOMENA AT FERRIMAGNETIC INSULATOR/METAL INTERFACES 462
C. O. Avci 462

41 - NOVEL FUNCTIONAL MAGNETIC MATERIALS- BASIC APPROACH AND APPLICATIONS 463

ENGINEERING SHAPE-MEMORY CHARACTERISTICS IN Ni-Fe-Ga MICROWIRES 464
M. Elias[1,2,3], S. Sakthivel[1], T. Ryba[1], M. Vavrga[1], O. Milkovic[1,4], L. Straka[3], O. Heczko[3], R. Varga.[1,3,5] 464

MAGNETO-OPTICAL OBSERVATIONS OF MICROWIRES AND THEIR RELEVANCE TO PRACTICAL APPLICATIONS 465
M. Kozachok[2], K. Richter[1,2,3] 465

STRUCTURE AND MAGNETIC PROPERTIES OF FeCoNiAlMn HIGH-ENTROPY ALLOY FROM MICRO TO ATOMIC SCALE 466
P. Švec[1,2], O. Roik[3], I. Gejdoš Janotová[1], D. Janičkovič[1], M. Jakubčin[4], B. Kunca[4], J. Marcin[4], I. Škorvánek[4], Yu. Plevachuk[1,5], P. Švec Sr[1] 466

CRYSTALLIZATION BEHAVIOR AND SOFT MAGNETIC PROPERTIES OF ULTRA-RAPIDLY ANNEALED HIGH-Bs Fe-Co-B-Si-Cu NANOCRYSTALLINE ALLOYS 467
I. Škorvánek[1], B. Kunca[1], J. Marcin[1], F. Romer[2], P. Ramasamy[3], P. Švec sr.[4], P. Švec[4] 467

OPTIMIZED MAGNETOELASTIC SENSOR FOR APPLICATIONS IN HARSH ENVIRONMENTS 468
A. Lasheras[1], A.C. Lopes[2,3] 468

ENGINEERING SPIN TEXTURES IN FE NANODISKS FOR CELL MANIPULATION 469
I. Solozabal[1], R. Zurbano[1], C. Redondo[1], L.M. Alvárez-Prado[2], A. Benedicto[3], M. Vélez[2,4], R. Morales[5,6] 469

NANOSCALE-RESOLVED EPITAXY, MISFIT DISLOCATIONS AND SPIN PUMPING IN Fe/Rh BILAYERS 470
J. Wiemeler[1], H. Ali[2], A. Kovacs[2], I. Tarasov[1], F. Wilhelm[3], A. Rogalev[3], R. Dunin-Borkowski[2], M. Farle[1], A. Semisalova[1] 470

UNUSUAL PHASE SHIFT BETWEEN QUANTUM OSCILLATIONS IN Sr_2RuO_4 MEASURED SIMULTANEOUSLY WITH ORGANIC BILAYER TORQUE MAGNETOMETER 471
D. Krstovska[1], E. Steven[2,3], E. S. Choi[3], D. Suarez[3], E. Jobiliong[4] 471

MAGNETIC PROPERTIES AND ELECTRONIC STRUCTURE OF $FeRhGa_{1-x}Z_x$ (Z=As, Sb, Sn, Ge) ALLOYS: ab INITIO STUDY 472
O. Pavlukhina, V. Buchelnikov, V. Sokolovskiy 472

MAGNETOSTRICTION OF Fe-Ga ALLOYS FROM FIRST PRINCIPLES AND MONTE CARLO CALCULATIONS 473
M. Matyunina, M. Zagrebin, V. Sokolovskiy, V. Buchelnikov 473

42 - NOVEL MAGNETORESISTANCE AND SPIN-CHARGE INTERCONVERSION 474

UNUSUAL ANISOTROPIC MAGNETORESISTANCES IN VAN DER WAALS MAGNETIC INTERFACES 475
Q. Chen[1,2], Y. Zhai[1], X. Wang[3,4], K. Xia[1] 475

ON THE ANGULAR DEPENDENCE OF ANOMALOUS HALL CURRENT 476
K. Xia 476

CLASSIFY PURE SPIN CURRENT ORIGIN WITH SYMMETRY ANALYSIS 477
H. Ding 477

EVIDENCE FOR STRONG LOCALIZATION OF ORBITAL POLARIZATION 478
L. Zhu[1,2] 478

SPIN-CHARGE INTERCONVERSION AND ITS APPLICATIONS IN 1D TO 3D MAGNETIC FIELD SENSING 479

Y. Wu 479

TENSOR ANALYSIS, CHARGE-SPIN INTERCONVERSION, AND MAGNETORESISTANCE....480
X. Wang 480

UNCONVENTIONAL SPIN CURRENT AND SPIN TORQUE ARISING FROM MAGNETIC STRUCTURES 481
H. Wu[1,2] 481

43 - ORBITRONICS 482

CURRENT INDUCED SPIN DYNAMICS MEDIATED BY ORBITAL EXCHANGE INTERACTION 483
G.-H. Lee 483

NONLOCAL AND DYNAMICAL ORBITAL TRANSPORT IN OXIDIZED Cu 484
L. Liao[1,2], Y. Otani[2] 484

X-RAY DETECTION OF CURRENT-INDUCED ORBITAL ANGULAR MOMENTUM ACCUMULATION AT Cu/OXIDE INTERFACES 485
P. Pradeep[1], P. Olleros[2,3], A. Gudin[2], G. Orero-Gámez[1], H. Madathil[1], A. Guedeja-Marrón[4], M. A. Niño[5], M. Varela[4], F. Ajejas[2], M. Foerster[5], P. Perna[2], S. Vélez[1] 485

ORBITRONICS WITH ORBITAL MAGNETS: MAGNETORESISTANCE, PUMPING AND BEYOND 486
S. Krishnia[1], C. Schmitt[1], O. Ledesma[1], D. Kumar[1], A. Do[1], E. Saitoh[2], O. Gomonay[1], G. Jakob[1], Y. Mokrousov[1], M. Kläui[1,3] 486

PHONON-DRIVEN MANIPULATION OF ORBITAL CURRENTS IN LIGHT TRANSITION METALS.....487
M. Rovirola[1,2], J. Òdena[1,2], A. Castellví[1,2], Q. Badosa[1,2], J. M. Hernàndez[1,2], B. Casals[2,3], S. Vélez[4,5], F. Macià[1,2] 487

WHY ORBITAL CURRENTS APPEAR SHORT- OR LONG-RANGED: GENERALIZED ORBITAL DIFFUSION WITH MULTIPLE LENGTH SCALES.....488
J. Sohn, S. Han, H.-W. Lee 488

EFFICIENT MAGNETIC MANIPULATION VIA SUPERCONDUCTOR-ENHANCED SPIN-ORBIT TORQUES 489
R. Zhang[1], P. Li[2] 489

MAGNETIC ENGINEERING AND SPIN/ORBITAL TORQUE SWITCHING IN FERRIMAGNETIC GARNETS.....490
C. O. Avci 490

44 - QUANTUM EMISSION AND DEFECTS IN SOLID STATE MATERIALS.....491

DEFECT ENGINEERING IN HEXAGONAL BORON NITRIDE FOR STABLE SINGLE-PHOTON EMISSION.....492
H. Moon[1,2] 492

THE BORON VACANCY IN hBN: FROM ELECTRONIC STRUCTURE THROUGH DECOHERENCE TO COHERENT NUCLEAR SPIN CONTROL 493

V. Ivády[1,2] 493

ENGINEERING SINGLE SPIN DEFECTS IN HEXAGONAL BORON NITRIDE 494
M. Kianinia[1,2] 494

QUANTUM EMISSION FROM COUPLED SPIN PAIRS IN HEXAGONAL BORON NITRIDE ... 495
S. Li[1], A. Pershin[1,2], A. Gali[1,2,3] 495

ENHANCING SPIN-PHOTON INTERFACE SENSITIVITY THROUGH vdW ENGINEERING 496
E. Mayner[1], A. Radenovic[2] 496

HYBRID QUANTUM DEFECTS IN HEXAGONAL BORON NITRIDE AND THEIR ROLE IN SINGLE-PHOTON EMISSION 497
S. Amin[1], A. Jimenez[1], E. Mejia[1], Y. Cao[2], M. Silvetti[3], A. Biondini[3], M. Govoni[3], J. Pelliciari[2], G. Grosso[1] ... 497

UNDERSTANDING THE ORIGIN OF DEFECT-BASED SINGLE-PHOTON EMISSION IN NITRIDE MATERIALS 498
A. Biondini[1], M. Silvetti[1], S. Amin[2], A. Jimenez[2], Y. Cao[3], J. Pelliciari[3], G. Grosso[2], M. Govoni[1] 498

QUANTUM EMISSION IN N-BASED MATERIALS: IMPORTANCE OF MOLECULAR-LIKE DEFECTS 499
J. Pelliciari 499

45 - QUANTUM FUNCTIONAL MATERIALS AND THEIR EMERGING TECHNOLOGIES 500

PEROVSKITE PHOTONICS – HARNESSING NONLINEARITIES USING A FIBERIZED PLATFORM 501
N. Healy[1], L. Cording[1], C. Johnson-Richards[1], H.C.L. Tsui[1], P. Docampo[2] 501

PHOTON PAIRS, SQUEEZED LIGHT AND THE QUANTUM WAVE MIXING EFFECT IN A CASCADED QUBIT SYSTEM 502
R. D. Ivanovskikh[1], W. V. Pogosov[1,2,3], A. A. Elistratov[1], S. V. Remizov[1,4,5] 502

TOPOLOGICAL FUNCTIONALITY MEETS MODULAR GROWTH: A BOTTOM-UP APPROACH TO TI HETEROSTRUCTURES 503
K. Bandopadhyay, K. Markus, A. Materna, D. A. Pawlak 503

SYNERGISTIC SILVER DOPING AND HALIDE PASSIVATION FOR STABLE, EFFICIENT $CsPbI_3$ QUANTUM DOTS FOR LED APPLICATIONS 504
P. Naziri[1,2], U. Aydemir[2,3] 504

FAST-FORWARD ADIABATIC DYNAMICS: PRACTICAL ROUTES TO HIGH-FIDELITY STATE CONTROL 505
S. Ashirbekov, S. Matniyazov, A. Abdullayev, J. Matrasulov 505

MICROWAVE-TO-OPTICAL QUANTUM TRANSDUCTION WITH Er^{3+} IONS AND YIG 506
B. Rameev[1,2,3], M. Maksutoğlu[4], E. Demirci[1], S. Kazan[1], H. Pişkin[5] 506

GEOMAGNETIC ANOMALY MAPPING USING FLUXGATE MAGNETOMETERS 507
M. Maksutoğlu[1], N. G. Saribas[1], A. Demirtaş[1], H. Piskin[2], B. Rameev[3,4,5] 507

46 - QUANTUM INFORMATION TECHNOLOGY AND APPLICATIONS 508

QUANTUM WAVE MIXING ON A SUPERCONDUCTING QUBIT AS A TOOL FOR STUDYING PHOTON STATISTICS 509
A. V. Vasenin[1,2], S. A. Gunin[1,2], A. Yu. Dmitriev[1], A. A. Elistratov[3], R. D. Ivanovskikh[3], S. V. Remizov[3,4], T. R. Sabirov[1,2], W. V. Pogosov[3,6,1], O. V. Astafiev[2,1] 509

BOSE CONDENSATION AND BOGOLIUBOV EXCITATION IN RESONATOR-EMBEDDED SUPERCONDUCTING QUBIT NETWORK 510
P. Navez[1], V. Di Meo[2], B. Ruggiero[3], C. Gatti[4], F. Chiarello[5], A. D'Elia[4], A.Rettaroli[4], G. Brida[6], E. Enrico[6], L. Fasolo[6], M. Fistul[7], A. Zagoskin[8], P. Silvestrini[9], P. Vanacore[3], M. Lisitskiy[2] 510

QUANTUM IMPLICIT NEURAL REPRESENTED AUTOENCODER AND VARIATIONAL AUTOENCODER WITH MULTI-OBSERVABLE READOUTS 511
S. M. Eren 511

REAL-TIME DYNAMICS OF DOUBLE QUANTUM DOT ANDREEV MOLECULE 512
K. Wrześniewski, I. Weymann 512

COMPARATIVE ANALYSIS OF QUANTUM ERROR CORRECTION APPROACHES WITH RANDOMLY COMPILED CIRCUITS 513
M. N. Akarsubaşı[1], M. Çolak[1], A. Bozbey[1], M. Ünlü[1], F. B. Atalay[2], B. Tavli 513

COMPARATIVE BENCHMARKING OF LEARNING BASED ERROR MITIGATION TECHNIQUES FOR NOISY QUANTUM COMPUTATION 514
M. Çolak[1], M. N. Akarsubaşı[1], A. Bozbey[1], M. Ünlü[1], F. B. Atalay[2], B. Tavlı[1] 514

47 - QUANTUM TRANSPORT AND NOVEL BROKEN SYMMETRY GROUND STATES 515

UNIFIED THEORY OF INTERACTING TWO-DIMENSIONAL DIRAC FERMIONS 516
I. F. Herbut 516

MODELING CHARGE DENSITY WAVE PHASE DIAGRAM AND ULTRAFAST DYNAMICS IN TRANSITION METAL DICHALCOGENIDES USING MACHINE-LEARNED ELECTRONIC FREE ENERGY 517
I. Lončarić 517

AN IMPURITY IN A HETERONUCLEAR TWO-COMPONENT BOSE MIXTURE 518
G. Bighin[1], A. Burchianti[2,3], F. Minardi[2,3,4], T. Macrì 518

NONRECIPROCAL TRANSPORT IN QUANTUM MATTER 519
R. Wang, B. Liu, W. Tian, P. Song 519

TOPOLOGY, NON-HERMITICITY, AND TOMOGRAPHY IN MULTI-TERMINAL ANDREEV CONTACTS 520
W. Belzig 520

TRION STATE TRANSITIONS AND HYBRID BOUND STATES OF ELECTRON CHANNEL-QUANTUM DOT-TYPE STRUCTURE AT QUANTIZED MAGNETIC FIELDS 521
Z.-N. Wang[1], Y. Wang[1], F.-L. Song[1], S.-Y. Zheng[2], L. Lu[2], J. Zhang[1], C. Zhang[1] 521

GATE-TUNABLE POLARITY REVERSAL IN A SPIN-ORBIT JOSEPHSON DIODE 522
J. Shin[1], J.-H. Han[2,3], A. Rathore[4], J. S. Lee[4], S.-B. Shim[5], J. Cha[5], S. Park[3], J. Suh[1] 522

MAGNETOTRANSPORT PROPERTIES AND GROUND STATE OF A TWO-DIMENSIONAL CONDUCTOR WITH THE ISOTROPIC FERMI SURFACE SUBJECTED TO THE BIAXIAL CHARGE DENSITY WAVE 523
B. Keran[1], A. M. Kadigrobov[1,2] D. Radić[1], Z. Rukelj[1] 523

DYNAMICAL CONDUCTIVITY OF A 3D DIRAC SYSTEM WITH HOLSTEIN-LIKE ELECTRON-PHONON COUPLING 524
P. Papac 524

CHARGE DENSITY WAVE GROUND STATE IN THE INTERCALATED GRAPHITE CaC_6 AND ITS MAGNETOCONDUCTIVITY IN MAGNETIC BREAKDOWN CONDITIONS 525
P. Đ. Grozić[1], Z. Rukelj[1], B. Keran[1], A. M. Kadigrobov[2], D. Radić[1] 525

48 - RECENT ADVANCES IN THERMOELECTRIC MATERIALS AND APPLICATIONS 526

THERMOELECTRIC AND CHIRALITY DEPENDENT PROPERTIES OF *R*RhC_2 (R=La, Ce) 527
V. Levytskyi[1], U. Burkhardt[2], M. König[2], E. Svanidze[2], Yu. Grin[2], R. Gumeniuk[1] 527

EFFECTIVE MASS MODEL FOR THERMOELECTRICS 528
M. Heo[1,2], H.-S. Kim[2], G. J. Snyder[1] 528

ESSENTIAL ROLE OF TEMPERATURE-DEPENDENT BAND GAPS IN (p × n)-TYPE TRANSVERSE THERMOELECTRICS 529
Q. Shao[1], J. Li[1], X. Yan[1], B. Cui[1], X. Li[2], C. J. Zeman IV[1], M. A. Mosquera[1], L. O. Jones[1], G. C. Schatz[1], J. Yang[2], M. A. Grayson[1] 529

ACCELERATING DOUBLE HALF-HEUSLER THERMOELECTRIC SEARCH WITH MULTI-TASK ML 530
D. R. Baigutlin, V. V. Sokolovskiy, S. V. Taskaev 530

ENHANCING THE THERMOELECTRIC PERFORMANCE OF $Mg_3(Sb,Bi)_2$ VIA QUANTUM-DOT BOROPHENE INCORPORATION 531
S. S. Shahgoli[1,2], U. Aydemir[2,3] 531

BENCHTOP ROOM-TEMPERATURE SYNTHESIS OF HIGH PERFORMANCE THERMOELECTRICS 532
K. Kovnir[1,2] 532

49 - SPECIAL PANELS 533

SPINAL EPIDURAL MAGNETIC FIELD CONTROLLED NANOPARTICLE SYSTEM FOR FERRITIN REGULATION: A NOVEL BIOPHYSICAL APPROACH FOR NEURODEGENERATIVE DISEASES 534
T. Yazar 534

50 - SUPERCONDUCTING BASE ELEMENTS FOR SPINTRONICS AND NEURAL NETWORKS 535

USING SPIN-ORBIT COUPLING TO GENERATE TRIPLET PAIRS IN HALFMETALLIC $La_{0.7}Sr_{0.3}MnO_3$ 536

Y. Jungxiang[1], M. Cabero[2], J. Aarts[1] 536

FEATURES OF COHERENT TRANSPORT IN PLANAR JOSEPHSON SNS STRUCTURES WITH SPIN POLARIZATION IN THE BARRIER **537**
T. E. Golikova[1], V. V. Ryazanov[2,1], I. A. Nazhestkin[2] 537

SUPERCONDUCTING BASE ELEMENTS FOR BRAIN-INSPIRED NEURAL NETWORKS: SPINTRONIC INNOVATIONS FOR NEUROMORPHIC COMPUTER **538**
A. Sidorenko[1,2] 538

CONTROLLING PROPERTIES OF PEROVSKITE THIN FILMS VIA STRAIN ENGINEERING (RESULTS OF THE PROJECT "INTERNATIONAL ACADEMIC COOPERATION" OF HSE UNIVERSITY) **539**
M. R. Samatov, D. Liu, A. S. Vasenko 539

JOSEPHSON EFFECT IN JUNCTIONS WITH BARRIERS BASED ON TOPOLOGICAL MATERIALS: THEORY AND EXPERIMENT **540**
A. A. Golubov[1,2] 540

MULTIFUNCTIONAL LOGIC GATES FOR COMPACT SUPERCONDUCTING PROCESSORS **541**
A. A. Maksimovskaya[1,2], V. I. Ruzhickiy[2], I. I. Soloviev[2], M. Yu. Kupriyanov[3], N. V. Klenov[1], S. V. Bakurskiy[3] 541

IMPURITY-ENHANCED DETECTION OF MAJORANA ZERO MODES IN VORTEX CORES **542**
A. Vagov[1], V. D. Neverov[1], T. Karabassov[1], A. V. Krasavin[1], D. Roditchev[2], V. S. Stolyarov[2] 542

PHOTOGALVANIC PHENOMENA, VORTEX INTERACTION AND MAGNETOELECTRIC EFFECT IN SUPERCONDUCTORS SUPPORTING INTRINSIC DIODE EFFECT **543**
A. Buzdin[1], S. Mironov[2], A. Melnikov[2], V. Plastovets[3] , A. Putilov[2] 543

A FOUNDRY-READY TOP-DOWN EDA FLOW FOR ADIABATIC QUANTUM-FLUX-PARAMETRON LOGIC: FROM RTL TO GDSII **544**
O. Chen 544

REINFORCEMENT LEARNING WITH SUPERCONDUCTING CIRCUITS **545**
M. L. Schneider 545

REVISED RCLSJ MODEL WITH IMPROVED MODEL-TO-HARDWARE CORRELATION FOR SUPERCONDUCTING DIGITAL CIRCUIT SIMULATION **546**
J. Ren[1,2], S. Wang[3], X. Gao[1,2] 546

SCANNED SQUID MICROSCOPY OF SUPERCONDUCTING DIGITAL LOGIC **547**
I. W. Haygood[1], B. Xu[2,3], M. L. Schneider[1] 547

DEVELOPMENT OF FABRICATION PROCESSES FOR HIGH-PERFORMANCE SUPERCONDUCTING ELECTRONIC DEVICES AND INTEGRATED DIGITAL CIRCUITS AT SIMIT **548**
L. Ying, G. He, L. Ma, H. Xie, W. Shi, H. Li, J. Ren, Z. Lin, W. Peng, L. You, Z. Wang 548

THE INFLUENCE OF FLUX ON AQFP CIRCUITS FOR A DOUBLE-ACTIVE-LAYERED NIOBIUM FABRICATION PROCESS **549**
L. Schindler[1,2], K. Jackman[1,2], N. Yoshikawa[3], C. J. Fourie[1,2] 549

THE EFFECT OF LAYOUT ON THE SENSITIVITY OF DIGITAL AQFP CIRCUIT MARGINS TO TRAPPED FLUX **550**

C. J. Fourie[1,2] 550

LOW-POWER SUPERCONDUCTING CIRCUITS USING FERROMAGNETIC π-JUNCTIONS...551
M. Tanaka, S. Deguchi, K. Inagaki, K. Toyama, K. Suzuki, F. Li, A. Fujimaki 551

RECENT PROGRESS IN DUAL-RAIL DIRECT-COUPLED ADIABATIC QUANTUM-FLUX-PARAMETRON (D^2AQFP) INTEGRATED CIRCUITS 552
N. Yoshikawa[1,2], Y. Hasegawa[2], Y, Hoshika[2], C. Ayala[1] 552

THREE-DIMENSIONAL EXTRACTION OF PARASITIC INDUCTANCE AND CAPACITANCE IN LARGE SHUNT CAPACITORS FOR SUPERCONDUCTING QUBITS 553
K. Jackman[1], C. J. Fourie[1,2] 553

SFQ CONTROL OF A TRANSMON 554
A. Kirichenko, K. T. Tsai, A. Somoroff, C. Jordan, N. Shumiya, A. Weis, I. Vernik, R. Albu, S. J. Han 554

SUPERCONDUCTING QUANTUM CIRCUITS BASED ON NITRIDE SUPERCONDUCTORS ...555
H. Terai[1], S. Kim[2], T. Fuse[2], S. Mima[1], D. Pham[1], S. Ashhab[2], K. Semba[2,3], T. Yamashita[4] 555

VORTEX MITIGATION STRATEGIES IN SUPERCONDUCTING MICROELECTRONIC DEVICES USING LARGE-SCALE SIMULATIONS 556
A. Glatz[1], D. Joseph[1], Z. Zhao[1], L. Cadorim[2], M. Milosevic[2] A. Koshelev[3], B. Janko[3]..... 556

A SUPERCONDUCTING ISING MACHINE BASED ON JOSEPHSON PARAMETRIC OSCILLATOR NETWORKS.....557
B. Z. Ucpinar, S. Razmkhah, M. Pedram 557

ADVANCING THE FRONTIERS OF ADIABATIC SUPERCONDUCTOR DIGITAL ELECTRONICS 558
C. L. Ayala 558

INTEGRATED DIGITAL SYSTEM SOLUTION FOR SUPERCONDUCTING QUANTUM COMPUTING BASED ON mK-GENERATED SINGLE FLUX QUANTUM PULSE PATTERNS FOR MULTI-QUBIT CONTROL 559
Th. Ortlepp [1,2], A. Reinhardt[1], T. Haddad[1], M. Schmelz[3], N. Yoshikawa[2] 559

SFQ-BASED TDCS FOR SNSPDS 560
T. V. Filippov, D. E. Kirichenko 560

SPATIALLY RESOLVED PHOTODOPING OF OXYGEN-DEFICIENT $YBa_2Cu_3O_{7-\delta}$ RESONATORS 561
N. Lejeune[1], L. Nulens[2], H. Li[3], T. Günkel[3], L. Fabrega[3], A. Palau[3], J. Van de Vondel[2], A. V. Silhanek[1]..... 561

THE FLUXONICS MIXED-SIGNAL FABRICATION PROCESS BASED ON SUB-µm Nb/AlO_x/Nb CROSS-TYPE JOSEPHSON JUNCTIONS 562
M. Schmelz[1], J. Kunert[1,2], K. Peiselt[1,3], G. Oelsner[1], T. Ortlepp[4], R. Stolz[1,2,5]..... 562

PROGRAMMABLE SUPERCONDUCTING NEURON WITH INTRINSIC IN-MEMORY SPIKING COMPUTATION AND DUAL-TIMESCALE PLASTICITY FOR ULTRA-EFFICIENT NEUROMORPHIC COMPUTING 563
M. Wang[1,2], S. Yang[1,2], J. Ren[1,2] 563

NOISE CHARACTERISTICS OF MgB_2 THERMAL KINETIC INDUCTANCE DETECTORS 564
T. Jabbari[1], A. Hawkins[2], A. Wandui[1], C. Frez[1], J. Greenfield[1,3], C. Roberson[3], M. J. Lee[3], P. Mauskopf[2,3], D. Cunnane[1] 564

ANALYSIS OF SQUIDS BASED ON NANO-JUNCTIONS.....565
P. Febvre[1], U. Yilmaz[2], K. Jackman[3], C. Fourie[3] 565

EXPERIMENTAL STUDY OF SUPERCONDUCTING SPIN VALVES.....566
A. A. Kamashev[1], N. N. Garif'yanov[1], A. A. Validov[1], D. A. Arbuzov[1,2], V. Kataev[3], Ya. V. Fominov[4,5], A. S. Osin[4,5], I. A. Garifullin[1] 566

52 - SUPERCONDUCTING MOTORS AND APPLICATIONS IN ELECTRICAL ENGINEERING.....567

STRATEGIES OF MODELING SUPERCONDUCTING MACHINES BY USING VOLUME INTEGRAL EQUATIONS.....568
H. Menana 568

CHARACTERIZATION OF HTS COILS FOR SUPERCONDUCTING MOTOR APPLICATION....569
B. Douine 569

BASIC OPERATIONAL CHARACTERISTICS OF A PARTIAL SUPERCONDUCTING SYNCHRONOUS MOTOR IMPREGNATED BY SOLID-NITROGEN REFRIGERANT 570
Y. Terao, T. Nakamura 570

AC LOSS AND ELECTROTHERMAL STABILITY OF HIGH-TEMPERATURE SUPERCONDUCTING MOTORS FOR HYDROGEN-ELECTRIC AIRCRAFT PROPULSION 571
E. Pardo[1], A. Dadhich[1], A. Hussain[1], J. Šouc[1], J. Kováč[1], A. Colle[2], R. Dorget[2], M. E. Ahmed[2] 571

ELECTRO-THERMAL MODEL OF STATOR COILS IN SUPERCONDUCTING MOTORS UNDER AC AND DC VOLTAGES: PARALLEL TAPES AND INHOMOGENEITY.....572
A. Hussain, A. Dadhich, E. Pardo 572

DESIGN STUDY OF DIRECT DRIVE MULTI-MW HTS GENERATORS FOR OFFSHORE WIND USING THE MODULAR AIR-CORED SUPERMACHINE TOPOLOGY 573
O. Keysan[1,2], S. You[1], A. Shah[1], H. Zhang[1], M. Mueller[1] 573

53 - SUPERCONDUCTING POWER APPLICATIONS FOR ENHANCED DATA CENTER EFFICIENCY 574

SUPERCONDUCTING SOLUTIONS AS ENABLERS FOR HIGH POWER DENSITY DC DATA CENTERS.....575
P. Corsaro[1,2], T. Botto[1], U. Melaccio[1] 575

REVOLUTIONIZING DATA CENTER POWER DELIVERY WITH HIGH TEMPERATURE SUPERCONDUCTING CABLES.....576
P. Feldman 576

MAGNETIZATION LOSSES AND NON-REDUCED THREE-DIMENSIONAL MODELLING OF HYBRID CORC-TSTC SUPERCONDUCTING CABLES 577
H. Alssalih[1], M. Clegg[1,3], A. Badia[2], H. S. Ruiz[1] 577

54 - SUPERCONDUCTING THIN FILMS AND INTERFACE SUPERCONDUCTIVITY 578

ELECTRON-PLASMON SCATTERING IN DOPED GRAPHENE 579
J. Jakovac 579

PHENOMENOLOGY OF TWO-GAP SUPERCONDUCTOR HYDROGEN-INTERCALATED TITANIUM DISELENIDE EXPLAINED IN THE FRAMEWORK OF ELIASHBERG THEORY 580
G. A. Ummarino[1,2] 580

LASER STRATEGIES FOR THE FABRICATION OF Nb NITRIDES AND NbTi ALLOYS FOR SUPERCONDUCTING APPLICATIONS.....581
J. Frechilla[1], A. Frechilla[1], G.F. de la Fuente[1], A. Larrea[1], C. Barreneche[2], S. Dosta[2], L.A. Angurel[1], E. Martinez[1] 581

55 - SUPERCONDUCTIVITY AND MAGNETISM IN HEAVY FERMION SYSTEMS 582

QUANTUM ASPECTS OF HYPERBOLIC LATTICES 583
B. Roy 583

PROSPECTING FOR UNCONVENTIONAL SUPERCONDUCTING STATES IN HEAVY FERMION MATERIALS 584
F. M. Grosche 584

SCREENED SUPEREXCHANGE MECHANISM FORSUPERCONDUCTIVITY APPLIED TO CUPRATES 585
P. Navez 585

STRONGLY CORRELATION AND TOPOLOGY IN KONDO LATTICE SYSTEMS 586
S. Ran 586

INTERPLAY OF NAGAOKA FERROMAGNETISM, SUPERCONDUCTIVITY AND KONDO CORRELATIONS IN QUADRUPLE QUANTUM DOT ARRAY 587
E. Siuda, I. Weymann 587

HEAVY-FERMION QUANTUM CRITICALITY IN CeNiAsO: BEYOND LANDAU'S SCOPE.....588
F. Lu, Z. Wang, Y. Luo 588

56 - SUPERCONDUCTIVITY AND MAGNETISM UNDER PRESSURE AND STRAIN 589

$LaCrGe_3$ UNDER PRESSURE: FROM FERROMAGNET WITH UNUSUAL COERCIVITY TO AVOIDED QUANTUM CRITICALITY.....590
Sergey L. Bud'ko 590

DOPING AND PRESSURE EFFECTS ON THE SUPERCONDUCTING STATE OF CsV_3Sb_5 KAGOME 591
S. Sanna[1], A. Kataria[2], I. J. Onuorah [2], P. Bonfà[3], A. Capa Salinas[4], V. Mitrović[5], Z. Guguchia[6], R. Khasanov[6], S. D. Wilson[5] 591

PRESSURE CONTROL OF INTERTWINED QUANTUM ORDERS IN 6R-TaS_2.....592
Z. Guguchia[1], V. Sazgari[1], J. Graham[1], S.S. Islam[1], P. Kral[1], A. Achari[2], O. Gerguri[1], J. Tangermann[3], G. Simutis[1], R. Khasanov[1], H. Luetkens[1], M. Janoschek[1], J. Yin[4], F.v. Rohr[3], R. Nair[2] 592

ADVANCEMENTS IN HIGH-PRESSURE INSTRUMENTATION FOR STUDYING MAGNETIC PROPERTIES OF MATERIALS 593
K. V. Kamenev 593

HIGH TEMPERATURE SUPERCONDUCTIVITY WITH GIANT PRESSURE EFFECT IN 3D NETWORKS OF BORON DOPED ULTRA-THIN CARBON NANOTUBES IN THE PORES OF ZSM-5 ZEOLITE 594
T. H. Koo[1], Y. Wang[1], R. Huang[1], Y. H. Ng[1], T. T. Lortz[1], T. Zhang[1], W. M. Chan[1], Y. Hou[1], J. Pan[1], R. Lortz[2], N. Wang[1], P. Sheng[1,3] 594

57 - SUPERCONDUCTIVITY AND TOPOLOGY IN PTBI2 595

QUASIPARTICLE INTERACTION IN 2H-TaS_2 REFLECTED BY POINT-CONTACT SPECTROSCOPY 596
O. Kvitnitskaya[1,2], M. Behnami[1], B. Büchner[1,3], Yu. Naidyuk[2] 596

MECHANISM FOR NODAL TOPOLOGICAL SUPERCONDUCTIVITY ON PtB_{i2} SURFACE 597
K. Mæland, G. Sangiovanni, B. Trauzettel 597

TOPOLOGICAL SUPERCONDUCTIVITY ON THE SURFACE OF $PtBi_2$ 598
C. Fulga 598

SURFACE-EXTENDED ANDREEV BOUND STATES EMERGING FROM INTRINSIC SURFACE SUPERCONDUCTIVITY OF $PtBi_2$ 599
X. Huang[1], L. Zhao[2], S. Schimmel[3,4], J. Besproswanny[3,4], P. Härtl[1], C. Hess[3,4], B. Büchner[4,5], M. Bode[1,6] 599

UNCONVENTIONAL SURFACE SUPERCONDUCTIVITY OF t-$PtBi_2$ 600
S. Schimmel[1,2], Julia Besproswanny[1,2], Y. Fasano[1,3], G. Shipunov[2], S. Aswartham[2], D. Baumann[2], B. Büchner[2], C. Hess[1,2] 600

GINZBURG–LANDAU THEORY FOR UNCONVENTIONAL SURFACE SUPERCONDUCTIVITY IN $PtBi_2$ 601
H. Waje[1], F. Jakubczyk[1,2], J. van den Brink[1,2,3], C. Timm[1,2] 601

ARPES EVIDENCE FOR UNCONVENTIONAL TOPOLOGICAL SUPERCONDUCTIVITY IN THE FERMI ARC STATES OF t-$PtBi_2$ 602
S. Borisenko 602

58 - THE SPINTRONIC REVOLUTION IN NEUROMORPHIC COMPUTING 603

PROBABILISTIC COMPUTING WITH DIGITAL CMOS INTEGRATED CIRCUITS AND 604

VOLTAGE-CONTROLLED MAGNETIC TUNNEL JUNCTIONS 604
P. Khalili[1,2] 604

TOPOLOGICAL SPINTRONICS 605
Y. Zhou 605

PROBABILISTIC COMPUTING WITH p-BITS: HARDWARE, OPTIMIZATION, AND GenAI ..606
K. Y. Çamsarı 606

STOCHASTIC MAGNETIC TUNNEL JUNCTIONS FOR PROBABILISTIC COMPUTING AND SOLVING COMBINATORIAL OPTIMIZATION PROBLEMS 607

A. D. Kent 607

ION-ENGINEERED MAGNETIC TUNNEL JUNCTIONS FOR MRAM, MAGNETIC SENSORS, AND NEUROMORPHIC COMPUTING 608
D. Ravelosona[1,2] 608

59 - THEORY OF MAGNETISM 609

A LANDAU PARADIGM FOR QUANTUM SPIN LIQUIDS: BEYOND GAUGE THEORY 610
Y. Zhou 610

MOLECULAR SPIN–ELECTRIC COUPLING IN NON-CENTROSYMMETRIC LANTHANIDE COMPLEXES: A COMPUTATIONAL STUDY 611
C. Bigelli[1], D. Sartini[1], L. Tacconi[1], M. Gakiya Teruya[2], A.Cini, L. Passerini, G. K. Gransbury[1], M. Fittipaldi[3], L. Sorace[1], M. Shatruk[2,3], M. Briganti[1], M. Perfetti[1] 611

QUANTUM MONTE CARLO STUDY OF THE CYLINDRICAL BOUNDARY CONDITIONS IN THE TWO-DIMENSIONAL HUBBARD MODEL 612
N. Bulut 612

EFFECT OF THE CRYSTAL LATTICE PARAMETER ON THE CRITICAL SUPERCONDUCTING TRANSITION TEMPERATURE IN Pd_2YSn: ab INITIO CALCULATIONS 613
M. Matyunina, V. Sokolovskiy, V. Buchelnikov 613

60 - THEORY OF SUPERCONDUCTIVITY 614

PHASE-SPACE THEORY FOR FRACTIONAL ORBITALS AND FLAT BAND SUPERCONDUCTIVITY 615
T. Das, R. O. Sharma, Y. B. Yogendra 615

SUPERCONDUCTIVITY ON THE BRINK OF PHASE SEPARATION 616
A. Sinha, A. W. Max 616

CHARGE-ENTROPY-STABILIZED SUPERCONDUCTOR (Ag,Sn)Se 617
M. Oudah 617

HOURGLASS STRUCTURE OF THE SPECTRAL WEIGHT OF THE MAGNON IN THE FL* APPROACH TO HOLE-DOPED CUPRATES 618
P.A. Marchetti[1,2] 618

MASS OF POLARON IN Hg-1201 CUPRATE 619
G. G. Saburova, B. Ya. Yavidov 619

A TWO-SCALE POLARONIC FRAMEWORK FOR THE MAGNETIC FIELD-DOPING PHASE DIAGRAM OF CUPRATES 620
O. K. Ganiev[1,2] 620

A NEW VISION FOR THE THEORY OF SUPERCONDUCTIVITY (SC) AND PHASE DIAGRAM (PD) IN HTSC LBCO AND YBCO 621
Bassam M. Mustafa 621

EXACT SOLUTION TO THE LINEAR GINZBURG--LANDAU EQUATION FOR A SINGLE-BAND TYPE-II SUPERCONDUCTOR CONFINED INTO THE THIN FILM STRUCTURE 622

E. I. Jafarov[1,2], A. M. Jafarova[1], I. N. Askerzade[1,3,4] 622

EXACT SOLUTION TO THE GINZBURG-LANDAU EQUATION FOR A SINGLE-BAND SUPERCONDUCTOR FULLY CONFINED INTO THE CYLINDRICAL THIN FILM STRUCTURE .623
A. M. Jafarova[1], E. I. Jafarov[1,2], I. N. Askerzade[1,3,4] 623

61 - TOPOLOGICAL QUANTUM PHYSICS AND MATERIALS.....624

ANALYTICAL APPROACHES TO TIGHT-BINDING POLARONS IN FINITE-WIDTH CONDUCTION BANDS 625
S. N. Klimin[1], J. Tempere[1], M. Houtput[1], S. Ragni[2], T. Hahn[2], C. Franchini[2], A. S. Mishchenko[3] 625

SUPERINSULATION, A NEW STATE OF MATTER REALIZING CONFINEMENT IN CONDENSED MATTER SYSTEMS 626
C. A. Trugenberger[1,2] 626

CONTROLLING AND SCALING-UP THE ENERGIES IN CUPRATE SUPERCONDUCTING QUANTUM TECHNOLOGIES 627
N. Poccia 627

PHOTOCURRENT AND PHOTOCONDUCTIVITY IN SUPERINSULATORS 628
A.Y. Mironov 628

TYPE-III SUPERCONDUCTIVITY: VORTICES, TOPOLOGY AND QUANTUM MATTER.....629
M. C. Diamantini[1], C. A. Trugenberger[2], V. M. Vinokur[3] 629

62 - UNCONVENTIONAL SUPERCONDUCTIVITY AND TUNABLE QUANTUM STATES 630

FROM MONOLAYERS TO BULK: ISING SUPERCONDUCTIVITY IN LAYERED SYSTEMS 631
T. Samuely[1], M. Gmitra[1,2], P. Samuely[2] 631

DISCOVERY OF NODAL-LINE SUPERCONDUCTIVITY IN CHIRAL CRYSTALS 632
T. Shiroka[1,2], J. Zhao[3], L.-H. Hu[4], K. Xia[5], M. O. Ajeesh[6], M. Nicklas[6], Y. Xu[5], Q. Zhan[5], D. J. Gawryluk[2], M. Shi[4], T. Shang[5] 632

IMPACT OF LOW-ENERGY SPIN FLUCTUATIONS ON THE STRANGE METAL IN A CUPRATE SUPERCONDUCTOR 633
D. J. Campbell[1], M. Frachet[1], V. Oliviero[1], T. Kurosawa[2], N. Momono[3], M. Oda[2], J. Chang[4], D. Vignolles[1], C. Proust[1], D. LeBoeuf[1] 633

63 - UNCONVENTIONAL SUPERCONDUCTORS AND MAGNETS BASED ON LIGHT ELEMENTS.....634

PRESSURE SYNTHESIS OF NEW IMMISCIBLE MATERIALS.....635
E. Svanidze 635

CONTROL OF SUPERCONDUCTIVITY IN UBe_{13} BY ATOMIC-SCALE IMPERFECTIONS 636
M. König 636

ODD-PARITY-WAVE SPIN-POLARIZED MULTIFERROICS 637
J. Priessnitz[1], L. Šmejkal[1,2,3] 637

RECORD HIGH-TEMPERATURE SUPERCONDUCTIVITY IN HYDRIDES 638
S. Friedemann 638

UNIAXIAL-STRAIN TUNING OF THE METAL-INSULATOR TRANSITION IN κ-(BEDT-TTF)$_2$Cu[N(CN)$_2$]Br 639
P. Doležal[1,2], T. Pinter[1], K. Boniecki[1], A. Chen[1], R. Saito[3], A. Kawamoto[3], A. Pustogow[1] 639

HYDROGEN ABSORPTION IN URANIUM: ACCESSING MAGNETISM VIA THIN-FILM SYNTHESIS 640
E. Tereshina-Chitrova[1], M. Paukov[2], L. Havela[3], L. Horak[3], F. Wilhelm[4], A. Rogalev[4], T. Gouder[5] 640

NODAL SUPERCONDUCTIVITY IN KAGOME FLAKES OBSERVED WITH HYBRID MICROWAVE CIRCUITS 641
U. Vool 641

MAGNETIC AND STRUCTURAL PROPERTIES OF $Ce_5Fe_{18}B_{18}$: A PARAMAGNETIC RARE-EARTH IRON BORIDE WITH NON-MAGNETIC Fe 642
A. A. Aydın[1,2], Ö. Evren[3], M. Krnel[3], Y. Prots[3], E. Svanidze[3], G. J. Snyder[5], U. Aydemir[2,4] 642

SYNTHESIS-ENABLED SEARCH FOR NOVEL BORIDE ALTERMAGNETS 643
K. Kovnir[1,2] 643

WIDE-FIELD KERR MICROSCOPY AND MAGNETOMETRY: FROM MAGNETIC IMAGING TO LOCAL HYSTERESIS ANALYSIS 644
I. Soldatov 644

64 - VORTEX MATTER, DYNAMICS AND PINNING 645

VORTEX DYNAMICS IN SUPERCONDUCTING MICROWAVE COPLANAR RESONATORS: ROLE OF NATIVE AND ARTIFICIAL PINNING CENTERS 646
G. Ghigo[1,2], M. Fracasso[1,2], R. Gerbaldo[1,2], L. Gozzelino[1,2], D. Torsello[1,2], C. Pira[3], M. Scuderi[4] 646

IRREVERSIBILITY FIELD REVISITED: WHEN STRUCTURAL INHOMOGENEITY, NOT VORTEX MELTING, SETS THE LIMIT 647
V. V. Guryev, S. V. Shavkin 647

QUANTUM PRINTING AND OPTICALLY INDUCED VORTICITY IN SUPERCONDUCTORS 648
T.-T. Yeh[1], H. Yerzhakov[2], L. Bishop-Van Horn[3], S. Raghu[3], E. Wilson[1], M. Fogelström[2,4], A. Balatsky[1,2] 648

VORTEX PHYSICS IN FeSe EXPLORED BY MEASUREMENTS OF THE MICROWAVE SURFACE IMPEDANCE, AND PERSPECTIVES FOR FeSe-COATED HALOSCOPES 649
A. Alimenti[1,2], G. Celentano[3], A. Magalotti[1,2], A. Mancini[3], A. Masi[3], N. Pompeo[1,2], E. Silva[1,2], K. Torokhtii[1], A. Vannozzi[3] 649

ANGULAR-DEPENDENT INTERTYPE DOMAIN IN ANISOTROPIC SUPERCONDUCTORS: FROM SCALING TRANSFORMATIONS TO EXPERIMENTAL SIGNATURES IN ZrB_{12} 650
T. T. Saraiva 650

65 - POSTER SESSION 651

TAILORING THE CONDUCTIVITY OF PARTICLE EMBEDDED NANOFIBERS FOR ENERGY STORAGE DEVICES 652
U. Fatima, W. Mehmood, M. Anis-ur-Rehman 652

NEW Ti-RICH HIGH-ENTROPY SUPERCONDUCTOR $Ti_{0.4}Zr_{0.2}(NbTaHf)_{0.4}$ WITH HIGH CRITICAL PARAMETERS 653
W. Idziak, P. Sobota 653

DESIGN AND CHARACTERIZATION OF A HIGH-PERFORMANCE MAGNETIC TORQUE ROD WITH AN ANNEALED Ni-Fe ALLOY CORE 654
B. Tuncay[1,2], M. D. Topal[3], Y. E. Duran[4], Y. S. Çalışkan[4], Y. M. Demiral[4], K. A. Kardaş[4], M. A. Yiğit[4], F. Hıraman[4] 654

SINGLE CRYSTAL GROWTH, MAGNETIC AND ELECTRIC PROPERTIES OF $Eu_5Sn_2As_6$ 655
D. Kumar[1], R. Kalaivanan[2], R. Sankar[2], I. P. Muthuselvam[1,3] 655

HALL EFFECT IN $(MnSe)_{1-x}(Tm_{0.76}Se)_x$ 656
A. M. Kharkov, D. A. Shakhbazian, R. V. Runov 656

ENHANCING LEGAL INTERPRETATION THROUGH QUANTUM-INSPIRED PROBABILITY MODELING: A HYBRID LLM APPROACH 657
C. Aydın 657

TUNING OF SECOND ORDER PHASE TRANSITION OF NiMnGa HEUSLER-TYPE GLASS-COATED MICROWIRES 658
C. Garcia[1], V. Zhukova[2], P. Corte-Leon[2], S. Shevyrtalov[3], A. Zhukov[4,5] 658

INFLUENCE OF ORGANIC COMPOUND ($C_{15}H_{12}O$) INCORPORATION ON THE MICROSTRUCTURAL AND SUPERCONDUCTING PROPERTIES OF IN-SITU SPS-PROCESSED MgB_2 BULK SUPERCONDUCTORS 659
H. Ağıl[1], A. A. Agil[1], E. Ayas[2] 659

MAPPING IN-PLANE MAGNETIZATION DYNAMICS WITH A HIGH RESOLUTION LASER SCANNING MOKE SYSTEM 660
B. Bozkurt[1], C. Rogenbuke[1], U. Topal[2] 660

3D MICROFLUIDIC SYNTHESIS OF MAGNETIC AEROGEL COMPOSITES: OPTIMIZATION, MORPHOSTRUCTURAL CONTROL, BIOEVALUATION, AND WATER DECONTAMINATION EVALUATION 661
D.-I. Tudorache (Trifa)[1], A. C. Bîrcă[1], A.-G. Niculescu[1,2], E.-T. Moldoveanu[1], A. Hudiță[2,3], M. S. Stan[3], A. C. Burdușel[1], B. Purcăreanu[1], T. Hadibarata[1,4], D. E. Mihaiescu[1], A. M. Grumezescu[1,2] 661

ENGINEERED MAGNETIC AEROGELS VIA MICROFLUIDIC PROCESSING - BRIDGING LABORATORY PERFORMANCE AND REAL-WORLD WATER REMEDIATION APPLICATIONS 662
E. C. Florea[1], D.-I. Tudorache (Trifa)[1], E.-T. Moldoveanu[1], A.-G. Niculescu[1,2], A. C. Bîrcă[1], D. A. Florea[1], A. C. Burdușel[1], R. D. Trușcă[1], T. Hadibarata[1,3], O. C. Pârvulescu[1], D. E. Mihaiescu[1], A. M. Grumezescu[1,2] 662

EVALUATING MAGNETIC AEROGELS IN A LABORATORY AQUATIC MODEL: WATER, FISH, AND PLANT RESPONSES TO DECONTAMINATION TREATMENTS 663
A.-G. Niculescu[1,2], A. C. Bîrcă[1], D.-I. Tudorache (Trifa)[1], E.-T. Moldoveanu[1], A. C. Burdușel[1], A. M. Croitoru[1], R. D. Trușcă[1], T. Hadibarata[1,3], A. Hudiță[2,4], M. S. Stan[4], D. E. Mihaiescu[1], A. M. Grumezescu[1,2] 663

RESISTIVITY, DENSITY OF ELECTRONIC STATES, AND SUPERCONDUCTING TRANSITION TEMPERATURE IN DENSITY WAVE COMPOUNDS WITH IMPERFECT NESTING 664
A. V. Tsvetkova[1], Ya. I. Rodionov[2], P. D. Grigoriev[3] 664

MAGNETIC LANDSCAPE OF NbTiN SUPERCONDUCTING RESONATORS UNDER RADIO-FREQUENCY EXCITATION 665
J. Baumgarten[1], N. Lejeune[1], L. Nulens[2] , J. Van de Vondel[2], A. V. Silhanek[1] 665

STATUS AND ON-SITE MAINTENANCE OF SCL2 CRYOGENIC PLANT FOR SUPERCONDUCTING LINAC OF RAON 666
H. C. Jo[1], M. K. Lee[1], I. Park[1], S. Kim[1], J. Kim[1], G. Lee[1], J. Han[1], Y. T. Choi[2], J. H. Shin[1] 666

Ab INITIAL AUTOMATED PACKAGE FOR THERMOELECTRIC PROPERTIES ASSESSMENT AND CALCULATION 667
V. Buchelnikov, A. Enenko, V. Sokolovskiy 667

A REVIEW OF HIGH-PRESSURE GROWTH EFFECTS ON HIGH-T_c IRON-BASED SUPERCONDUCTORS 668
P. Singh, M. Azam, M. Manasa, S. J. Singh 668

BIAS-PRESERVING ENTANGLEMENT OF KERR-CAT QUBITS WITH AN ATS COUPLER 669
K. Yurtseven[1,2], S. R. Jha[3,4], A. Limaye[5], R. Pokhrel[6], M. M. Kamelabad[7], M. W. Amin[8] 669

SYNTHESIS OF CURVED SUPERCONDUCTING NbN 3D STRUCTURES BY ATOMIC LAYER DEPOSITION 670
M. C. Mihaescu[1], D. Grundler[1,2] 670

SUPERCURRENT IN A LATERAL S/F/S JOSEPHSON JUNCTION INCORPORATING NbTiN AND Ni GROWN BY ATOMIC LAYER DEPOSITION 671
F. Posva[1], D. Grundler[1,2] 671

DEVELOPMENT OF SEARCH COIL MAGNETOMETER FOR DETECTION OF ULTRA LOW FREQUENCY (ULF) MAGNETIC FIELD VARIATIONS 672
A. E. Yıldırım[1], H. Can[1], U. Topal[1], M. A. Aksan[2], H. Sözeri[1] 672

BIOLOGICAL SOLITONS IN BIOMEMBRANES: ANALYTICAL SOLUTIONS OF A BOUSSINESQ-TYPE EQUATION WITH AMPLITUDE-DEPENDENT NONLINEARITY 673
S. A. Baloch 673

RAMAN SCATTERING FEATURES IN $MnSb_2Te_4$ MAGNETIC SEMICONDUCTORS 674
N. A. Abdullayev[1,2], Z. A. Jahangirli[1,2], Z. S. Aliev[2,1], I. R. Amiraslanov[1,2], N. T. Mamedov[1,2] 674

PHOTOLUMINESCENCE AND MAGNETIC PROPERTIES OF Nd-DOPED $ZnGa_2Se_4$ 675
Z. A. Jahangirli[1,2], S. G. Asadullayeva[1,3,4] 675

EFFECT OF TWISTED SQUARE-LATTICE PINNING ARRAYS ON THE CRITICAL CURRENT DENSITY OF SUPERCONDUCTOR TAPES 676
Z. Owjifard, M. Hosseini 676

THE SURFACE TE-MAGNON-POLARITONS AT THE JUNCTION OF TWO MAGNONIC CRYSTALS WITH GRAPHENE SHEETS AT THE EACH INTERFACES 677
R. T. Askerbeyli[1,2], H. Elharkati[1], U. Kanbur[1] 677

SINGLE-GAP VS TWO-GAP SCENARIOS IN UNCONVENTIONAL SUPERCONDUCTORS: AN ELECTRONIC SPECIFIC HEAT ANALYSIS 678
O. Ganiev[1,2], Z. Rakhmonov[3] 678

CRYSTAL SYMMETRY EFFECT ON SUPERCONDUCTIVITY AND PHASE DIAGRAM IN 2212 679

B. M. Mustafa 679

INVESTIGATION OF STRUCTURE-RELATED CHANGES IN THE MAGNETIC PROPERTIES OF $SrFe_{12-x}Ni_xO_{19}$ (x = 0–0.3) **680**
A. S. Abiyev, V. A. Turchenko 680

EXPERIMENTAL TESTING OF A 10 kW-CLASS SCALED-DOWN HTS-ISM WITH SINUSOIDALLY DISTRIBUTED STATOR WINDING FOR PROPULSION MOTORS OF ELECTRIC AIRCRAFT SYSTEMS **681**
M. Yamamoto, T. Nakamura 681

TAILORING THE ELECTROCHEMICAL PERFORMANCE OF COBALT–MANGANESE PHOSPHATE ELECTRODES THROUGH SUBSTRATE ENGINEERING **682**
H. Ali, M. Anis-ur-Rehman 682

DIELECTRIC BEHAVIOR OF RE-DOPED COBALT FERRITE ELECTROSPUN FIBERS **683**
S. Gul-e-Rana, M. Anis-Ur-Rehman 683

ROLE OF ELECTROLYTE SELECTION IN GOVERNING THE ELECTROCHEMICAL RESPONSE OF COBALT PHOSPHATE ELECTRODES **684**
H. Ali, M. Anis-ur-Rehman 684

CRITERION FOR SOFTENING THE PHONON SPECTRUM OF A CRYSTALLINE FILM WITH A TWO-DIMENSIONAL COATING **685**
V. N. Kushnir[1,2], S. L. Prischepa[1] 685

CONTROLLED SPIKING BEHAVIOR OF A SUPERCONDUCTING NbTiN NEURON **686**
Z. Alzoubi[1], K. Harrabi[1,2], L. R. Cadorim[3,4], A. Mekki[1,5], A. M. Aljalal[1], M. V. Milosevic[4] 686

SYNTHESIS AND CHARACTERIZATION OF (Mg-Co-Fe-O) PARTICLES FOR MEMORY DEVICE APPLICATIONS **687**
M. Ammar Bin Masood, M. Anis-ur-Rehman 687

EFFICIENT ELECTRONIC STRUCTURE PREDICTION IN CARBON MATERIALS USING DFT-CALIBRATED EXTENDED HÜCKEL THEORY **688**
G. S. Kupriyanova, I. G. Mershiev, V. V. Savin 688

ELECTROCHEMICAL STUDIES OF $NiMn_2O_4$–$NiFe_2O_4$/CNT COMPOSITES FOR ENERGY STORAGE APPLICATIONS **689**
H. Sultan, H. Ali, M. Anis-ur-Rehman 689

THE PINNING ENERGY OF $Bi_2Sr_2Ca_{0.6}Zn_{0.4}Cu_2O_x$ **690**
S.S. Ragimov[1,2], I. N. Askerzade[3,4] 690

EFFECT OF RARE EARTH DOPING ON ZINC COBALT FERRITE FOR RESISTIVE RANDOM ACCESS MEMORY **691**
H. Mazhar, M. Anis-ur-Rehman 691

TAILORING THE ELECTRICAL PROPERTIES OF COBALT FERRITES THROUGH LITHIUM DOPING FOR RESISTIVE MEMORY DEVICES **692**
Y. Iqbal, H. Mazhar, K. Naheed, M. Anis-ur-Rehman 692

DEVELOPMENT OF FOLATE RECEPTOR TARGETED AND LIPOIC ACID LOADED THERANOSTIC NANOPARTICLES **693**
O. Gok[1,2], S. N. Ozkan[2], E. Ozkul[2], M. N. Atilmis[1], P. S. Unlu[1] 693

A BRIEF STUDY OF THE ENHANCED STRUCTURAL AND ELECTRICAL PROPERTIES OF SAMARIUM-DOPED COBALT FERRITE NANOPARTICLES FOR POTENTIAL RESISTIVE RAM APPLICATIONS 694
H. Ramzan, A. Saif, M. Anis-ur-Rehman 694

CONTINUOUS AND TOPOLOGICAL PHASE TRANSITIONS IN THE JOSEPHSON MEDIUM OF GRANULAR HIGH-TEMPERATURE SUPERCONDUCTOR $DyBa_2Cu_3O_{7-\delta}$ 695
T. V. Sukhareva 695

THE PREPARATION OF HIGH CURRENT PERFORMANCE MgB_2 WIRES WITH CARBON COATED BORON 696
W. Yuan[1], Q. Guo[1], M. Wang[1], W. Xie[1], Q. Yu[1], Y. Zhu[1], B. Wu[1], Y. Shi[1], J. Li[2], X. Liu[1], Y. Feng[1], P. Zhang[1]. 696

IMPACT OF LARGE-RADIUS IMPURITIES ON METAL/SUPERCONDUCTOR- INSULATOR TRANSITIONS AND SUPERCONDUCTIVITY ENHANCEMENT IN DOPED CUPRATES 697
S. Dzhumanov[1], U.T. Kurbanov[1,2] 697

THEORETICAL STUDY OF THE SEEBECK EFFECT IN DOPED HIGH-T_c CUPRATE SUPERCONDUCTORS USING THE HUBBARD MODEL 698
I. Sh. Kabulov[1], D. G'. Khajibaev[2], S. Dzhumanov[3], B. Ya. Yavidov[2], E. X. Karimbaev[1,3] 698

RESEARCH ON PREPARATION OF HIGH CRITICAL CURRENT AND HIGH THERMAL STABILITY CABLE-IN-CHANNEL (CIC) SUPERCONDUCTING WIRES 699
J. Hu[1], Q. Guo[1,2], R. Wang[1,2], X. Liu[2], W. B. Jia[2], Y. W. Yang[1], Y. K. Fang[1] 699

FORMATION OF MATTER-WAVE MODES IN BOSE-EINSTEIN CONDENSATES 700
O. Y. Otajonov[1], T. Iskandarov[2], E. X. Karimbaev[3,4] 700

INVESTIGATION OF ELECTRICAL TRANSPORT AND DIELECTRIC RESPONSE IN Zn–Mn–Co SPINEL FERRITES AS A FUNCTION OF TEMPERATURE 701
H. Mazhar, S. Kousar, M. Anis-ur-Rehman 701

FREQUENCY AND ELECTRIC FIELD-DEPENDENT CAPACITANCE BEHAVIOR IN BENZOIC ACID MODIFIED POLYURETHANE COMPOSITES 702
G. Sayın[1], S. Kurnaz[2], T. Seydioğlu[3], E. Aşıkuzun Tokeşer[4], Ö. Öztürk[1] 702

THE EFFECT OF EFFECT OF Co ON PARTICLE SIZE, MAGNETIC PROPERTIES AND MICROWAVE ABSORBANCE PROPERTIES OF Fe-25%Ni-5%Si-x%Co (x=0, 10, 15) NANO ALLOYS 703
H. Gungunes, S. Delice 703

INFLUENCE OF A LOW-TEMPERATURE SN ACTIVATOR AND SINTERING CONDITIONS ON IMD-PROCESSED MgB_2 SUPERCONDUCTING WIRES 704
Y. Oznal[1,2], C. Guo[3], F. Almokdad[4], F. Ervüz[1], H. Koralay[5], S. Safran[1,6], S. Salahi[7], A. Seçkin[8], K. Sönmez[1,4], S. C. Taşkın[1], D. Wang[3], A. Gencer[1,6], Y. Ma[3] 704

SUPERCONDUCTING AND STRUCTURAL PROPERTIES OF Ag-COATED MgB_2 WIRES PRODUCED BY IMD METHOD 705
F. Ervüz[1], S. C. Taşkın[1], C. Guo[3], F. Almokdad[4], H. Koralay[5], Y. Oznal[1,8], S. Safran[1,2], S. Salahi[6], A. Seçkin[7], K. Sönmez[1,4], D. Wang[3], A.Gencer[1,2], Y. Ma[3] 705

THE INFLUENCE OF Cu, Sn, AND Ag ACTIVATOR COATINGS ON THE SUPERCONDUCTING PERFORMANCE OF MgB_2 WIRES 706
S. Salahi[1], C. Guo[2], F. Almokdad[3], F. Ervüz[4], H. Koralay[5], S. Safran[4,6], Y. Oznal[4,7], A. Seçkin[8], K. Sönmez[3,4], S. C. Taşkın[4], A.Gencer[4,6], D. Wang[2], Y. Ma[2] 706

Cu-COATED IMD FABRICATION OF MULTIFILAMENT MgB_2 WIRES WITH ENHANCED SUPERCONDUCTING PROPERTIES 707
F. Al-Mokdad[1], K. Sönmez[1,2], C. Guo[3], F. Ervüz[2], S. Safran[2,4], H. Koralay[5], S. Salahi[6], S. C. Taşkın[2], A. Seçkin[7],Y. Oznal[2,8], D. Wang[3], A.Gencer[2,4], Y. Ma[3] 707

OVERVIEW OF MAGNETIC LEVITATION AND LATERAL FORCES IN MgB_2 BULKS WITH VARIOUS FABRICATION TECHNIQUES 708
B. Savaşkan[1], P. Badica[2], S. B. Güner[3] 708

ECO-FRIENDLY MAGNETIC SILICA NANOCOMPOSITES: FROM RICE HUSK WASTE TO RAPID RECOVERY OF BRILLIANT BLUE R DYE 709
B. Akmeşe[1], Ç. Dönmez Güngüneş[2], V. Aliyev[3], İ. Tosun Satır[4] 709

EFFECT OF Cu COATING THICKNESS ON MAGNESIUM DIFFUSION AND SUPERCONDUCTING PROPERTIES OF IMD-PROCESSED MgB_2 WIRES 710
K. Sönmez[1,4], C. Guo[3], F. Almokdad[4], F. Ervüz[1], H. Koralay[5], Y. Oznal[1,8], S. Safran[1,2], S. Salahi[6], A. Seçkin[7], S. C. Taşkın[1], D. Wang[3], A.Gencer[1,2], Y. Ma[3] 710

DETERMINATION OF THE OPTIMUM LEVITATION FORCE OF BULK YBCO USING IRON BLOCKS AND PMS OF DIFFERENT SIZES IN PMG THROUGH NUMERICAL MODELLING 711
İ. E. Gumrukcuoglu[1], U. K. Ozturk[1], O. Uzun[1], H. Mollahasanoglu[2] 711

SURFACTANT-FREE SYNTHESIS OF MULTIFUNCTIONAL SPINEL FERRITE NANOPARTICLES: FROM FUNDAMENTAL TO PHOTOCATALYTIC PROPERTIES AND BIOMEDICAL APPLICATIONS 712
N. T. Mliki 712

HIGH T_c OF $Tl_2Ba_2CaCu_2O_8$ SUPERCONDUCTOR 713
E. Yusrianto 713

INFLUENCE OF MAGNETIC CORRELATIONS ON SCATTERING OF CARRIERS IN IRON ARSENIDES 714
D. E. Zhelezniakova, I. I. Gimazov, Y. I. Talanov 714

ORIENTATION-DEPENDENT UPPER CRITICAL MAGNETIC FIELD AND DENSITY OF STATE FOR URANIUM DITELLURIDE 715
H. A. Muluneh 715

FABRICATION OF 10-KILOMETER-CLASS MgB_2 WIRES BY THE INTERNAL-MAGNESIUM-DIFFUSION METHOD IN WST 716
W. Xie[1,2], Q. Yu[2], Q. Guo[1,2], M.-Wang[1], W. Yuan[1], Y. Zhu[1], B. Wu[2], Y. Shi[1,2], G. Yan[2], X. Liu[3], Y. Feng[1,2], J. Li[3], P. Zhang[3] 716

K-MAPPING: ADVANCED PHOTOLUMINESCENCE IMAGING METHOD FOR CHARACTERIZATION OF PEROVSKITE FILM QUALITY 717
M. Çoban 717

CYLINDRICAL VORTEX-TYPE MICROFLUIDIC DEVICE FOR ON-CHIP NANOMATERIAL SYNTHESIS TOWARD ADVANCED WATER TREATMENT TECHNOLOGIES 718
E.-T. Moldoveanu[1], D.-I. Tudorache (Trifa)[1], A.-G. Niculescu[1,2], A. C. Bîrcă[1], A. M. Croitoru[1], A. C. Burduşel[1], A. Hudiţă[2,3], T. Hadibarata[1,4], D. E. Mihaiescu[1], A. M. Grumezescu[1,2] 718

MAGNETIC PROPERTIES OF MAGNETIC NANOPARTICLE (Fe_3O_4)-FILLED POLYVINYLIDENE FLUORIDE NANOFIBERS 719
A. Demirtaş, M. Maksutoğlu 719

THE ONSET OF BULK SUPERCONDUCTIVITY AT + 39°C IN OXYGEN DOPED DELAFOSSITE $CuYO_{2.33}$ 720
D. Djurek 720

DECOUPLING BROWNIAN ALIGNMENT AND NEEL ROTATION IN SPIO TRACERS TO IMPROVE BIOMEDICAL MAGNETIC PARTICLE IMAGING PERFORMANCE 721
S. A. Shah[1,2], D. B. Reeves[1], R. M. Fergosun[1], K. M. Krishnan[1] 721

TIGHT BINDING MODEL AND BEYOND IN MODELING INTEGRATED SEMICONDUCTOR SINGLE AND FEW-ELECTRON DEVICES 722
K. Pomorski[1], E. Hałubek[2], D. Górniak[3], F. Buchcic[4], M. Dolecki[5], A. Michalak[3], W. Nowakowski[5], P. Imiński[5], A. Żak[6] 722

Cr-DRIVEN ELECTRONIC CONTROL OF MARTENSITIC TRANSFORMATION AND EXCHANGE BIAS IN Ni–Mn–Sb HEUSLER ALLOYS 723
M. Ayyıldız[1], G. Kırat[2], M. A. Aksan[1] 723

SYMMETRY-DRIVEN Nb-Sn STRUCTURAL MODELS WITH LONG-RANGE ORDER: PREDICTIVE DESIGN THROUGH THE INTERPLAY OF THEORETICAL MODELING AND ATOMIC SIMULATIONS 724
T. Priinits, A. Vargunin, A. Liivand 724

PREPARATION OF THE hBN NANOCRYSTALS USING GREEN ROUTE 725
L. Bazgir[1], A. Bakoue[1], M. Sasani Ghamsari[2] 725

MXene-BASED COMPOSITES FOR RENEWABLE ENERGY AND WASTE WATER TREATMENT 726
Z. N. Kayani, K. Javed 726

ELECTRON SPIN RESONANCE AND MAGNETIC PROPERTIES OF COBALT SUBSTITUTED CHROMIUM NANOFERRITES 727
M. Sethosa[1], L. Kotsedi[2], T. Mokoena[3], T. Mokhena[4], A. Nhlapo[5] 727

INTERDISCIPLINARY INTEGRATION OF QUANTUM PHENOMENA FOR ADVANCING THE NEXT QUANTUM REVOLUTION 728
I. Ahmad[1,2] 728

EFFECTS OF DOPANT ON THE OPTOELECTRONICS PROPERTIES OF DOPED $LaAl_{1-x}Ga_xO_3$ NANO-PARTICLES 729
W. H. Shah 729

DEFECT-MEDIATED ROOM-TEMPERATURE FERROMAGNETISM IN Er-DOPED TiO_2 NANOSTRUCTURED THIN FILMS 730
S. Iram, Z. N. Kayani 730

CRITICAL CURRENT IN HIGH-T_c SUPERCONDUCTORS VIA HTS-PM INTERACTION USING THE BEAN MODEL 731
J. Rojas, A. Mariño 731

EFFECT OF ALKALI-METAL SUBSTITUTION IN TUNING BiCuSeO FOR HIGH-PERFORMANCE THERMOELECTRIC APPLICATIONS 732
T. Khalid, M. A. Rehman 732

INFLUENCE OF Fe INTERLAYERS ON PHONON AND CHARGE CARRIER DYNAMICS IN Bi_2Te_3 TOPOLOGICAL INSULATOR 733

Kh. V. Aliguliyeva[1], N. A. Abdullayev[2,3], S. Sh. Gahramanov[2] 733

INVESTIGATION OF THE DEPENDENCE OF THE SPIN HALL ANGLE ON THE CONCENTRATION IN THE $L1_0$-Mn_xPt_{1-x} SYSTEM **734**
A. Kh. Kadikova[1], I. V. Yanilkin[1], A. I. Gumarov[1], B. F. Gabbasov[1], D. G. Zverev[1], L. R. Tagirov[1,2], R. V. Yusupov[1] 734

RAPID ADIABATIC CONTROL OF HEAT FLOW IN TRANSPARENT THERMAL NETWORKS **735**
Y. Sattorov, M. Salohiddinov, D. Mardonov, J. Matrasulov 735

NEUTRON DIFFRACTION STUDY OF CRYSTALLINE AND MAGNETIC STRUCTURE OF $Sr_2FeMo_{1-x}V_xO_6$ (x= 0-0.25) AT ROOM TEMPERATURE **736**
K. M. Hasanov[1,2], S. V. Sumnikov[2], V.G. Kostishin[3], M. Čebela[4], V. A. Turchenko[2,3] 736

A MULTI-SENSOR FLUXGATE SYSTEM WITH INTEGRATED DATA PROCESSING TECHNIQUES FOR HIGH-RESOLUTION MAGNETIC ANOMALY DETECTION **737**
N. G. Saribas, A. Demirtaş, M. Maksutoğlu 737

FIELD-DEPLOYABLE MAGNETIC ANOMALY DETECTION SYSTEM USING ORTHONORMAL BASIS FUNCTIONS DECOMPOSITION **738**
E. Kaya[1], A. Demirtaş[2], N. G. Saribas[2], M. Maksutoğlu[2] 738

A COMPARISON BETWEEN THE NANOSTRUCTURE OF Y-123 AND Y-358 HIGH-TEMPERATURE SUPERCONDUCTOR **739**
E. K. Al-Shakarchi[1], M. B. Abood[2] 739

MAGNETOCALORIC CHARACTERISTICS OF NiFeMnSnB SHAPE-MEMORY RIBBONS IN THE MARTENSITIC PHASE TRANSITION REGION **740**

HIGH ENTROPY RARE-EARTH BORIDES: SYNTHESIS, CHARACTERIZATION AND POTENTIAL EVALUATION FOR SUPERCONDUCTORS **741**
B. Boztemur, C. F. Arısoy, D. Ağaoğulları 741

LEVITATION FORCE RELAXATION ANALYSIS OF FLUX PINNING IN SINGLE-GRAIN YBCO **742**
S. B. Guner[1,2,3], Z. Bekiryazıcı[4] 742

THE IMPACT OF Mn SUBSTITUTION ON THE STRUCTURAL AND MAGNETIC PROPERTIES OF HIGH-LAYER (m ≥ 5) AURIVILLIUS-PHASE MULTIFERROIC THIN FILMS **743**
Y. Demirolmez[1], S. Conroy[2], L. Keeney[1] 743

INDEXES **744**

SPONSORS **761**

..... **772**

11th ICSM 2026

&

4th ICQMT 2026

1 - PUBLIC OUTREACH AND PLENARY SESSION

Abstract ID: 30822

THE GLOBAL NEED FOR CLEAN ENERGY VIA COMPACT NUCLEAR REACTORS IN VIEW OF SUPERCONDUCTING AND CONVENTIONAL TECHNOLOGIES

A. Gencer[1,2]

[1] *Ankara University, Center of Excellence for Superconductivity Research, CESUR, Göblaşı-Ankara, TURKIYE*
[2] *Ankara University, Faculty of Sciences, Physics Department, 06100, Beşevler, Ankara, TURKIYE*

The growing global demand for clean energy, the accelerating impacts of climate change, and the 2050 net-zero emissions target have significantly increased interest in reliable, low-carbon, and high-energy-density technologies. In this context, compact nuclear reactors have emerged as a strategic option due to their ability to deliver high power density within limited space, enable continuous baseload power generation, and contribute to energy security. In particular, compact fusion reactors based on magnetic confinement attract considerable attention because of their no long-lived radioactive waste, the absence of meltdown risk in the conventional fission sense, and their potential to support both high-temperature process heat and electricity production.

This study evaluates the global need for clean energy within the framework of compact nuclear reactors and compares the fundamental differences between superconducting technologies and conventional conductor-based systems. Superconducting magnets, particularly those based on REBCO high-temperature superconductors, make it possible to achieve higher magnetic fields in smaller volumes and with lower ohmic losses; thus, they contribute to improved plasma confinement and strengthen the engineering feasibility of compact reactor designs. In contrast, conventional resistive magnet systems exhibit clear limitations in compact reactor architectures because of their higher ohmic losses, increased cooling and power requirements, and larger structural volume demands. As a result, superconducting-based compact nuclear reactors can be regarded as a highly promising, technically robust, and strategically important technological pathway in the clean energy transition.

In this inaugural talk, world-wide efforts of compact reactor projects will be summarized together with their advances and challenges.

Abstract ID: 30767

ADVANCEMENT OF COATED CONDUCTORS

A. Goyal

State University of New York (SUNY) at Buffalo, 14260, New York, USA

Abstract ID: 30798

INTERPLAY OF SUPERCONDUCTIVITY AND MAGNETISM

Z. Guguchia

Laboratory for Muon Spin Spectroscopy, Paul Scherrer Institute, Villigen SWITZERLAND

Abstract ID: 30818

A LIFETIME FASCINATION WITH HIGH-TEMPERATURE SUPERCONDUCTIVITY

I. Božović

Shanghai Advanced Research in Physical Sciences (SHARPS), Shanghai 201203, CHINA

I have been beguiled by high-temperature superconductivity (HTS) ever since I stumbled upon Ginzburg's list of the most important open problems in physics [1] in 1971. HTS was his topic #2. However, experimental physics was almost nonexistent in Belgrade, so for my PhD thesis (1972-1975), I invented the theory of the symmetry of solid (3D) objects periodic in one direction, such as polymers and quasi-1D metals. I called these the line groups, and the name stuck. One of the prophecies was that nonsymmorphic symmetry elements (glide planes or screw axes) dictate topologically invariant crossings of electron energy bands, with linear dispersion [2]. Decades later, these were rediscovered and dubbed Dirac crossings, to much acclaim. Another was a discussion of whether polyacenes, polyacenacenes, etc., should be metallic [3]. These are now called graphene nanoribbons. I also predicted that Li:BeH2 should feature a very strong (nonadiabatic) electron-phonon coupling and HTS. [4]

I got the chance to run my own experiments in 1986 at Stanford, when Ted Geballe hired me to run the optics spectroscopy lab. Before long, I figured out how to determine spectral functions much more accurately than the standard at the time [5]. I published a bunch of optics and Raman papers, but eventually realized that what these spectra conclusively inform about HTS is limited. Moreover, the key hurdle is in synthesis. Cuprates have complex phase diagrams containing dozens of stable compounds, and the phase control is tedious yet critical. My focus thus shifted to atomic-layer-by-layer molecular beam epitaxy (ALL-MBE), first at Varian, then at Oxxel, and eventually at BNL and Yale.

ALL-MBE synthesis yields the highest-quality HTS films, heterostructures, and superlattices. The crux is in detailed material characterization, in real time, or at least in situ. So, I coupled ALL-MBE systems to TOF-ISARS, ARPES, STM, LEEM/LEED/PEEM, in situ transport and magnetization measurements, etc. My group also found a way to measure the London penetration depth with 1% absolute accuracy [6], introduced angle-resolved transverse resistivity (ARTR) and magnetoresistance (ARTMR) techniques [7], and achieved ±1 mK thermal stabilization of closed-cycle cryocoolers.

Our grand aspiration was to produce the best samples anywhere and make the most accurate measurements of the physical properties most relevant for HTS — and then use that to test the most important HTS theories. These included the excitonic pairing scenarios proposed by Bardeen, Ginzburg, and Little [8], the Marginal Fermi Liquid theory [9], the SO(5) theory of S-C. Zhang [10] and, more recently, the dirty BCS-FL models of the demise of HTS with overdoping in cuprates [11]. Next, we showed that in cuprates the insulating states behave like a quantum charge-cluster glass [12]. The "normal" metallic state is nematic [7] and (at some doping) shows T- and B-linear resistivity, unexpected in a gas of charged (quasi)particles [13]. We also showed that Tc scales with the superfluid density, rather than with the interaction strength [6]. These experimental results were so incisive and restrictive that they ruled out almost the entire corpus of HTS theories, models, and scenarios.

On the positive side, we discovered, at BNL, interface HTS [14,15] confined to a single CuO2 layer – the thinnest known superconductor, yet with Tc equal to, or higher than in bulk LSCO. We also discovered, at Yale, two new 2D quantum materials, borophene and beryllene, new allotropes of B and Be [16,17].

Now, I am at SHARPS, starting a new chapter, and trying to develop some new techniques. But the grand goal remains the same — HTS, in all its glory.

References

[1] V. L. Ginzburg, Usp. Fiz. Nauk **103**, 87 (1971); Sov. Phys. Usp. **14**, 21 (1971).
[2] I. Božović, Phys. Rev. B **32**, 8136 (1985).
[3] I. Božović, Phys. Rev. B **29**, 6586 (1984).
[4] I. Božović and J. Delhalle, Phys. Rev. B **29**, 4733 (1984).
[5] I. Božović, Phys. Rev. B **42**, 1969 (1990).
[6] I. Božović, J. Wu, X. He and A. T. Bollinger, Nature **536**, 309 (2016).
[7] J. Wu, A. T. Bollinger, X. He and I. Božović, Nature **547**, 432 (2017).
[8] I. Božović, *et al.*, Phys. Rev. Lett. **59**, 2219 (1987).
[9] I. Božović, *et al.*, Phys. Rev. Lett. **73**, 1436 (1994).

[10] I. Božović, *et al.*, Nature **422**, 873 (2003).
[11] R. Caruso, X. He, A. T. Bollinger and I. Božović, Phys. Rev. Lett. **136**, 076003 (2026).
[12] J. Wu, A. T. Bollinger, Y.-J. Sun and I. Božović, PNAS **113**, 4284 (2016).
[13] P. Giraldo-Gallo, *et al.*, Science **361**, 479 (2018).
[14] A. Gozar, *et al.*, Nature **455**, 782 (2008).
[15] G. Logvenov, A. Gozar and I. Božović, Science **326**, 699 (2009).
[16] R. Wu, *et al.*, Nature Nanotech. **14**, 44 (2019).
[17] R. Wu, *et al.*, Nature Chemistry **14**, 377 (2022).

Abstract ID: 30839

THE INVENTION AND INDUSTRIALIZATION OF NEODYMIUM IRON BORON MAGNETS

M. Sagawa

Tohoku University, 980-8577, Sendai, Miyagi, JAPAN

In the late 1970s, while researching ways to improve the mechanical strength of Sm-Co magnets, I wondered why rare-earth iron magnets didn't exist. At a rare-earth magnet symposium I attended around that time, I heard an explanation that the reason rare-earth iron magnets couldn't be made was because the interatomic spacing between iron atoms in rare-earth iron compounds was too small. This gave me the idea that perhaps alloying the compounds with atoms of small atomic radii, such as B or C, would solve the problem. Based on this idea, I continued my research as a side project, and four years later, after joining Sumitomo Special Metals, a company that fully supported my research, I achieved the world's strongest magnet: the Nd-Fe-B sintered magnet.

I, along with researchers at Sumitomo Special Metals, successfully completed the fundamental research and industrialization research for Nd-Fe-B sintered magnets in a short period. Sumitomo Special Metals then licensed Nd-Fe-B sintered magnets to numerous magnet manufacturers not only in Japan but also in the United States, Europe, and China. Alongside my research on Nd-Fe-B sintered magnets, John Croat and others at GM were also conducting research on Nd-Fe-B magnets made from rapidly cooled alloys. Now, Nd-Fe-B sintered magnets and Nd-Fe-B magnets made from rapidly cooled alloys are supporting the miniaturization and performance improvement of hard disk devices, air conditioners, EV main motors, and wind power generation, making a significant contribution to preventing global warming.

As one of the inventors of this Nd-Fe-B magnet, I sincerely hope that this magnet will continue to benefit people around the world.

Abstract ID: 30428

EPITAXIALLY ENGINEERED HYBRID MATERIALS FOR QUANTUM TECHNOLOGIES

N. Samarth

Penn State University, Pa 16802, Pennsylvania, USA

The synthesis of complex epitaxial quantum materials allows the exploration of emergent phenomena arising from the interplay between factors such as electron-electron correlations, broken symmetry, spin-orbit coupling, electron-phonon coupling, and topological order. This provides exciting opportunities for engineering quantum materials that can be potentially exploited for quantum technologies, including quantum computing, quantum sensing, and quantum communications. We provide an overview of a program centered on the epitaxial synthesis of hybrid quantum materials that interface superconductivity, magnetism, and quantum states in semiconductors with an eye on applications in quantum technologies. We first focus on emergent superconductivity in van der Waals (vdW) heterostructures grown by molecular beam epitaxy. These epitaxial heterostructures reveal a surprising concurrence of superconductivity, ferromagnetism, and topological states [1,2], providing attractive wafer-scale vdW platforms for developing non-reciprocal devices for superconducting electronics and, potentially, serving as topological quantum computation platforms. Second, we discuss pathways for engineering materials wherein superconducting Josephson junction qubits can be integrated with quantum defect spin qubits [3]. This approach exploits the emergence of superconductivity in heavily B-doped diamond films grown by microwave plasma chemical vapor deposition with superconducting transition temperature around 3 K. Transport measurements of these superconducting films reveal signatures of an emergent hidden anisotropic order, a fundamental understanding of which may be important for exploiting superconducting diamond for quantum technologies [4].

Supported by the Penn State 2DCC-MIP (NSF Grant No. DMR-2039351), the National Science Foundation (DMR-2407130), the Penn State Center for Nanoscale Science/MRSEC (NSF Grant No. DMR-2011839) and the U.S. Department of Energy Office of Science National Quantum Information Science Research Centers (Q-NEXT).

References

[1] H. Yi, *et al.*, *Interface-induced superconductivity in magnetic topological insulators*, Science **383**, 634-639 (2024).
[2] S. Islam, *et al., Emergent superconductivity and non-reciprocal transport in a van der Waals Dirac semimetal/antiferromagnet heterostructure*, arXiv: 2504.20393.
[3] J. Dwivedi, *et al., Boron-Doped Diamond: A superconducting semiconductor for hybrid quantum integration*, submitted.
[4] J. Dwivedi, *et al., Emergent anisotropic three-phase order in critically doped superconducting diamond films*, arXiv:2506.09925.

Abstract ID: 30591

VISUALIZING EMERGENT PROPERTIES OF QUANTUM MATERIALS WITH MILLIKELVIN STM

H. Suderow

Laboratorio de Bajas Temperaturas y Altos Campos Magnéticos, Unidad Asociada UAM-CSIC, Departamento de Física de la Materia Condensada and Instituto Nicolás Cabrera, Universidad Autónoma de Madrid,, E-28049, Madrid, SPAIN

Scanning Tunneling Microscopy (STM) offers a direct method to characterize the ground state of quantum materials. We have used millikelvin STM to directly measure the superconducting Cooper pair wavefunction at atomic scale through the Josephson effect [1]. Scanning Josephson STM represents the ultimate spatial limit for Josephson junctions, as the junction is restricted to a single atom. The Josephson coupling in such small junctions is highly sensitive to thermal fluctuations. I will discuss how a delayed feedback element induces a novel Josephson regime, characterized by spontaneous oscillations between DC and AC Josephson tunneling, and provides an improved route for mapping the Cooper pair wavefunction at atomic scale. Furthermore, I will present experiments in heavy fermion systems, describing novel forms correlated states occurring at the surface of quantum materials as quantum well states [2]. A further focus will be on efforts allowing to visualize with precision the electronic properties of a novel charge density wave (CDW). CDWs are often observed in dichalcogenides, cuprates, and pnictides and arise from features in the lattice that facilitate electronic charge ordering but compete with Kondo screening and are rare in heavy fermion metals. The heavy fermion topological superconductor candidate UTe2 presents a notable exception, exhibiting a heavy fermion surface CDW [3]. I will also briefly present efforts on the properties and vortex lattices of purely two-dimensional superconductors [4], on Shiba states in disordered superconductors [5], on vortex lattice melting [6] and present the status of recent advances towards experiments at very high magnetic fields [7] and rotatable STM [8].

References

[1] S.D. Escribano, *et al.*, *The feedback driven atomic scale Josephson microscope*, Nat Com **16**, 5842 (2025).
[2] E. Herrera, *et al.*, *Quantum well states at the surface of a heavy fermion superconductor*, Nature **616**, 465 (2023).
[3] P. García, *et al.*, Surface charge density wave in UTe_2, arXiv:2504.12505.
[4] J.A. Moreno, *et al.*, *Gapless superconductivity from extremely dilute magnetic disorder in 2H-$NbSe_{2-x}S_x$*, arxiv 2508.00435.
[5] J.A. Moreno, *et al.*, *Robust surface superconductivity and vortex lattice in the Weyl semimetal g-$PtBi_2$*, arxiv 2508.04867.
[6] O. Bou, *et al.*, *Direct observation of vortex liquid droplets in the iron pnictide superconductor $CaKAs_4Fe_4$ at 0.5T_c*,
[7] B. Wu, *et al.*, *Conductance of atomic size contacts of Ag and Au at high magnetic fields*, Phys. Rev. Research (2026), https://doi.org/10.1103/cmh2-frmf.
[8] J Rumeu, *et al.*, *Scanning Tunneling Microscopy in high vectorial magnetic fields*,

2 - PLENARY

Abstract ID: 30086

ENHANCED MAGNETIC PROPERTIES IN BI-MAGNETIC CORE/SHELL NANOPARTICLES

J. Nogués[1,2]

[1] *Catalan Institute of Nanoscience and Nanotechnology (ICN2), Bellaterra, SPAIN*
[2] *ICREA, Barcelona, SPAIN*

Traditionally, shells in magnetic core/shell nanoparticles have only played a rather passive role, e.g., to protect against oxidation or to reduce dipolar interactions. However, when the shell is also magnetic, forming bi-magnetic core-shell nanoparticles, new and enhanced properties emerge. Consequently, bi-magnetic core-shell nanoparticles have had a sustained interest during the last decades owing to their unique magnetic properties and the wide range of potential applications [1],[2]. Actually, many different combinations of ferromagnetic, ferrimagnetic and antiferromagnetic materials have been combined to form bi-magnetic core/shell nanoparticles with very diverse properties, like exchange bias or spring magnet effects. The morphology (such as core diameter, shell thickness, and shape), the constituent materials, and their interface are key in determining the final properties, thus, precise determination of these parameters is essential for understanding and adapting their functionalities. Here, we will present an overview of diverse core/shell structures: ferromagnetic/antiferromagnetic (e.g., Co/CoO [3]), antiferromagnetic/ferrimagnetic (e.g., MnO/Mn_3O_4 [4] or FeO/Fe_3O_4 [5]) or ferrimagnetic/ferrimagnetic (Fe_3O_4/Mn_3O_4 [6]). We will also discuss some structural, morphological and magnetic experimental techniques which are particularly interesting to obtain unique information on core/shell nanoparticles (e.g., x-ray magnetic circular dichroism, electron energy loss spectroscopy, polarized neutron powder diffraction, electron magnetic circular dichroism or anomalous small angle x-ray scattering [4]-[9]). Interestingly, depending on the system novel phenomena arise, such us tuneable exchange bias (Co/CoO [3], MnO/Mn_3O_4 [4] or FeO/Fe_3O_4 [5]), graded interfaces (FeO/Fe_3O_4 [8]), antiferromagnetic interface coupling (Fe_3O_4/Mn_3O_4 [6]) or magnetic proximity effects (MnO/Mn_3O_4 [10] and Fe_3O_4/Mn_3O_4 [11]).

References

[1] J. Nogués, *et al.*, Phys. Rep. **422**, 65 (2005).

[2] A. López-Ortega, *et al.*, Phys. Rep. **553**, 1 (2015).

[3] V. Skumryev, *et al.*, Nature **423**, 850 (2003).

[4] G. Salazar-Alvarez, *et al.*, J. Am. Chem. Soc. **129**, 9102 (2007).

[5] M. Estrader, *et al.*, Nanoscale **7**, 3002 (2015).

[6] M. Estrader, *et al.*, Nat. Commun. **4**, 2960 (2013).

[7] I. V. Golosovsky, *et al.*, Small Methods **7**, 201725 (2023).

[8] D. del-Pozo-Bueno, *et al.*, Nano Lett. **21**, 6923 (2021).

[9] K.L. Krycka, *et al.*, ACS Nano **7**, 921 (2013).

[10] I. V. Golosovsky, *et al.*, Phys. Rev. Lett. **102**, 247201 (2009).

[11] A.G. Roca, *et al.*, unpublished (2025).

Abstract ID: 30097

MAGNETISM AND SUPERCONDUCTIVITY WITH HIGH-BRILLIANCE X-RAYS: RECENT HIGHLIGHTS FROM THE ESRF

G. Martínez-Criado

European Synchrotron Radiation Facility, ESRF, 38000, Grenoble, FRANCE

High brilliance synchrotron X-rays at the ESRF are offering unprecedented insights into the intertwined phenomena of magnetism and superconductivity. Exploiting the ESRF's new Extremely Brilliant Source (EBS) and advanced beamlines using high-pressure X-ray diffraction has resolved complex structural transformations linked to superconductivity, from tuning charge-density waves in high-Tc cuprates under uniaxial strain to discovering unexpected hydrogen-rich "superhydride" phases under extreme conditions. Meanwhile, element-specific X-ray absorption and magnetic circular dichroism, under simultaneous high field, low temperature and high pressure conditions, have shed light on the magnetic properties of unconventional superconductors, exemplified by new insight into the uranium 5f electron magnetism in UTe2. In parallel, resonant X-ray scattering techniques, notably high-resolution RIXS, are uncovering electronic and spin correlations in novel materials. For instance, Ni L-edge RIXS on infinite-layer nickelate films revealed a charge order that vanishes with Sr-doping as superconductivity emerges, highlighting a competition between charge order, magnetism and superconductivity. Together, these highlights demonstrate how advanced synchrotron methods (high-pressure diffraction, XMCD, RIXS) at the ESRF beamlines are enabling a deeper understanding of the structural and electronic mechanisms driving magnetism and high-temperature superconductivity.

Abstract ID: 30098

SUPERCONDUCTIVITY UNDER EXTREME CONDITIONS

J. Wosnitza

Dresden High Magnetic Field Laboratory (HLD-EMFL), Helmholtz-Zentrum Dresden-Rossendorf, 01328 Dresden, GERMANY

High magnetic fields and superconductivity are usually incompatible. The magnetic field favors parallel electron spins, while superconductivity requires Cooper pairs with antiparallel spins. There exist, however, some superconductors, in which superconductivity survives to extraordinary high magnetic fields as we found in studies using static and pulsed magnetic fields up to 70 T provided at the Dresden High Magnetic Field Laboratory.

As a first example, I will present our robust evidence for the existence of the so-called Fulde-Ferrell-Larkin-Ovchinnikov (FFLO) state in quasi-two-dimensional organic superconductors. Besides specific-heat and magnetization results, NMR studies give strong microscopic evidence for the realization of the FFLO state. A one-dimensional sinusoidal order-parameter modulation can favorably explain the NMR spectra in this high-field low-temperature phase. I will further discuss the recently discovered heavy-fermion superconductor UTe_2. This material shows multiple unconventional superconducting phases under field and pressure with unusually large upper critical fields. For certain field orientations, superconductivity even reappears at very high fields and survives to a record-breaking upper critical field of about 73 T. The Jaccarino-Peter effect is a likely mechanism for the appearance of this reentrant superconductivity.

Abstract ID: 30285

THE APPLICATION OF SUPERCONDUCTOR FOR CARBON-NEUTRALITY-DRIVEN ENERGY & POWER IN CHINA

L. Xiao

Chinese Academy of Sciences, Institute of Electrical Engineering, 100190, Beijing, CHINA

In order to establish a carbon-neutrality energy system, many countries in the world are making efforts to develop new energies such as renewable energy and fusion energy. For renewable energy, its large-scale replacement of traditional fossil energy will bring a series of major challenges, and Superconducting technology has many potential applications to deal with these challenges. For fusion energy, magnetic confinement is a promising technology, and superconducting magnets are the key equipment of the fusion facility.

China has set the goal of achieving carbon neutrality by 2060, and all kinds of new energy technologies including superconductor technology have been supported by Chinese government and industries. Recently, superconductor technology for energy and power haas been well developed in China. In this talk, an overview of the progress of superconductor in China would be also presented, including the progress of HTS superconducting materials, superconducting power cable, energy pipeline, DC fault current limiter, electric machines and synchronous condenser, fusion magnets for EAST and BEST projects. Besides, the maglev projects by superconductor will be reviewed, too.

Abstract ID: 30330

CURRENT STATUS AND FUTURE PROSPECTS OF ROTATING MACHINERY SYSTEMS THAT COMBINE SUPERCONDUCTING TECHNOLOGY AND LIQUEFIED HYDROGEN

T. Nakamura

Kyoto University, Department of Electrical Engineering, 6158245, Kyoto, JAPAN

Hydrogen, which is an environmentally friendly and clean energy source, is expected to become one of the main players supporting the next generation energy society. In order to realize a hydrogen society, activities are being promoted to build a supply chain [1,2].

Meanwhile, liquefied hydrogen is being considered as a storage and transportation medium for hydrogen energy. The boiling point of liquid hydrogen at atmospheric pressure is 20 K, and by placing a High Temperature Superconductor (HTS) in this environment, it is possible to take advantage of its characteristics, such as zero DC electrical resistance. In other words, the synergy between the cryogenic environment of liquid hydrogen and superconducting equipment is expected to lead to the realization of a rational and efficient system.

Various research and development efforts are underway regarding liquid hydrogen-cooled HTS motor systems. The research group from Torishima Pump Mfg. Co., Ltd. and Kyoto University has successfully developed an HTS liquid hydrogen submerged pump for the hydrogen supply chain (Fig. 1) [3]. The Airbus group is conducting research and development into HTS motors for aircraft that are cooled indirectly using liquid hydrogen [4]. Furthermore, Toyota Motor Corporation, together with Kyoto University, developed a liquid hydrogen booster submerged pump equipped with an HTS motor and successfully conducted demonstration run on a hydrogen engine racing car [5]. That is, the liquid hydrogen-cooled HTS motors are now at the stage of practical application.

In this presentation, the details of the research and development status of liquid hydrogen-cooled HTS motors will be introduced and future prospects are to be discussed.



Fig. 1: *Liquid hydrogen circulation test of an HTS submerged pump at JAXA Noshiro Rocket Facility (Japan) [3].*

References

[1] (IEA website) https://iea.blob.core.windows.net/assets/9e3a3493-b9a6-4b7d-b499-7ca48e357561/The_Future_of_Hydrogen.pdf.
[2] (NEDO website) https://green-innovation.nedo.go.jp/en/about/#anchor04.
[3] (Torishima website) https://www.torishima.co.jp/common/uploads/sites/2/2024/03/20240314a-.pdf.
[4] (Airbus website) https://www.airbus.com/en/newsroom/press-releases/2024-10-airbus-and-toshiba-to-partner-on-superconductivity-research.
[5] (Toyota Times website) https://toyotatimes.jp/en/newscast/157.html.

Abstract ID: 30365

TOPOLOGICAL i-WAVE SUPERCONDUCTIVITY IN $PtBi_2$

B. Buechner[1,2,3]

[1] *IFW Dresden, GERMANY*
[2] *The Institute for Solid State Research (IFF), GERMANY*
[3] *Experimental Condensed Matter Physics, TU Dresden, GERMANY*

Unconventional superconductivity with nodal gap structures is rare and of particular interest in the context of topological phases. In this talk, I will present angle-resolved photoemission spectroscopy (ARPES) results demonstrating that the non-centrosymmetric Weyl semimetal $PtBi_2$ hosts an unconventional, topological i-wave superconducting state at its surface. Below about 20 K, superconductivity selectively gaps the topological Fermi-arc surface states, while the bulk electronic states remain normal. High-resolution ARPES reveals nodes in the superconducting gap located precisely at the centre of the Fermi arcs, providing direct evidence for i-wave pairing symmetry. The nodal structure implies the presence of topologically protected Majorana cones in momentum space and establishes $PtBi_2$ as an intrinsic topological surface superconductor. Complementary scanning tunnelling spectroscopy shows a pronounced spatial inhomogeneity of the superconducting gap and, in some cases, very large gap values reminiscent of high-temperature superconductors, indicating strong surface superconducting correlations. In addition, AC susceptibility and magnetotransport measurements reveal superconducting fluctuations extending to elevated temperatures, consistent with a surface-confined superconducting state of small effective volume fraction. Together, these results highlight $PtBi_2$ as a unique platform for studying the interplay of topology, unconventional pairing and strong superconducting correlations, and for exploring new routes towards Majorana-based quantum states.

References

[1] A. Kuibarov et al., Nature (2024).
[2] A. Kuibarov et al., Phys. Rev. B (2025).
[3] S. Changdar et al., Nature (2025).
[4] S. Schimmel et al., Nat. Commun. (2024).
[5] X. Huang et al., arXiv:2507.13843v1
[6] J. Besproswanny et al., arXiv:2507.10187v1

Abstract ID: 30425

PRESENT STATUS AND LATEST DEVELOPMENTS IN REBCO-BASED HTS WIRES FOR LARGE-SCALE HTS APPLICATIONS

A. Goyal

State University of New York (SUNY) at Buffalo, 14260, New York, USA

An overview as well as the current status related to commercialization of three platform technologies – (1) Rolling-Assisted-Biaxially-Textured Substrates; (2) LMOe-enabled IBAD MgO Substrate technology, for fabrication of kilometer-long HTS wires and (3) Phase Separation and Strain-driven Self-Assembly technology for creating nanocolumnar insulating defects in kilometer-long wires, will be presented. Most companies world-wide, fabricating long-lengths of coated conductors or REBCO-based HTS wires, use one or more of these platform technologies for fabricating high-performance, single-crystal-like HTS wires. These kilometer-long, coated conductor-based, HTS wires are now enabling many large-scale applications such as commercial nuclear fusion for energy generation as well as numerous other large-scale applications in the electric power industry. This overview talk will summarize the present status and latest developments in coated conductor fabrication world-wide.

Abstract ID: 30426

3D NANOMAGNETISM - ADVANCES, CHALLENGES AND OPPORTUNITIES FOR MAGNETIC SOFT X-RAY MICROSPECTROSCOPIES

P. Fischer[1,2]

[1] *Materials Sciences Division, Lawrence Berkeley National Lab, Berkeley CA 94720, USA*
[2] *Physics Department, University of California Santa Cruz, Santa Cruz CA 95064, USA*

The study of three-dimensional magnetic nanostructures is a rapidly evolving field, offering a wealth of new physical phenomena stemming from the increased complexity of spin textures, topology, and frustration in three dimensions [1,2]. By designing tailored three-dimensional nanomagnetic structures, including artificial spin ice systems or magnonics, one can unlock novel applications in magnetic sensor and information processing technologies, leading to improved energy efficiency, processing speed, and miniaturization of future spintronic devices.

Another key approach in exploring and harnessing the full three-dimensional space is the use of curvature as a design parameter, where the local curvature impacts physical properties across multiple length scales, ranging from the macroscopic to the nanoscale at interfaces and inhomogeneities in materials with structural, chemical, electronic, and magnetic short-range order. This is particularly relevant in quantum materials, where correlations, entanglement, and topology dominate play a dominant role. The local curvature opens the path to novel phenomena that have recently emerged and could have a dramatic impact on future fundamental and applied studies of materials. Magnetic systems, in particular, hosting non-collinear and topological states, as well as artificial 3D magnetic nanostructures strongly benefit from treating curvature as a new design parameter to explore prospective applications in magnetic field and stress sensing, micro-robotics, and information processing and storage.

To fully realize the potential of 3d nanomagnetism advances are needed in modelling/theory, synthesis/fabrication, and state-of-the-art nanoscale characterization techniques to understand, realize and control the properties, behavior, and functionalities of these novel magnetic nanostructures.

I will summarize and review the challenges but also the opportunities ahead of us in the future exploration of nanomagnetism in three dimensions with particular emphasis on 3D topological spin textures. As examples, I will present our recent studies on the statics and dynamics of magnetic Hopfions [3,4], the deconvolution of the 3D spin texture in a single magnetic skyrmion using advanced magnetic soft x-ray laminography [5], and curvature induced modifications of chirality and magnetic configuration in perpendicular magnetized films [6].

This work was supported by the U.S. Department of Energy, Office of Science, Office of Basic Energy Sciences, Materials Sciences and Engineering Division under Contract No. DE-AC02-05-CH11231 within the Non-equilibrium Magnetic Materials Program (MSMAG).

References

[1] 2024 Roadmap on 3D Nano-magnetism, G Gubbiotti, A. Barman eds, J. Phys.: Condens. Matter **37**, 143502 (2025).
[2] A. Fernández-Pacheco, *et al.*, Nature Comm. **8**, 15756 (2017).
[3] D. Raftrey, P. Fischer, Phys. Rev. Lett. **127**, 257201 (2021).
[4] N. Kent, *et al.*, Nature Comm. **12**, 1562 (2021).
[5] D. Raftrey, *et al.*, Science Advances **10**, eadp8615 (2024).
[6] D. Raftrey, *et al.*, ACS Nano (2025).

Abstract ID: 30427

DISCOVERY MAGNETIC MATERIALS WITH MACHINE LEARNING AND AI

S. Sanvito

School of Physics, AMBER and CRANN Institute, Trinity College, Dublin 2, IRELAND

The process of finding new materials, optimal for a given application, is lengthy, often unpredictable, and has a low throughput. Here, I will describe a collection of numerical methods, merging advanced electronic structure theory and machine learning, for the discovery of novel compounds, which demonstrates an unprecedented throughput and discovery speed. This is applied to magnetism, but it can be used for any materials class and potential application.

Firstly, I will discuss a machine-learning scheme for predicting the Curie temperature of ferromagnets, which uses solely the chemical composition of a compound as feature and experimental data as target [1]. In particular, I will discuss how to develop meaningful feature attributes for magnetism and how these can be informed by experimental and theoretical results. Furthermore, I will show how the experimental data can be mined from published scientific literature with the help of natural language processing tools [2].

Then, I will describe how an accurate description of the structure of materials, which is amenable to be used with machine learning, can offer a quantum-chemistry-accurate description of local properties at virtually no computational costs. This is based on a newly developed cluster expansion formulated in terms of Jacobi-Legendre polynomials. Such general framework allows us to construct, on the same footing, extremely accurate force fields [3] as well as converged DFT charge densities [4]. These can both be integrated in material-discovery workflows generating unprecedented speedup.

Finally, I will present a novel rotationally invariant representation for generic vector fields. This can be used to generate linear and non-linear machine-learning models, where the total energy depends both on the atomic position and the vector field direction [5]. The scheme will be put to the test against a hierarchy of simple spin models, demonstrating an impressive ability to extrapolate away from the training region of the data. Application to complex potential energy surfaces, as those extracted from DFT are then shown.

References

[1] J. Nelson and S. Sanvito, *Predicting the Curie temperature of ferromagnets using machine learning*, Phys. Rev. Mat. **3**, 104405 (2019).

[2] L. P. J. Gilligan, M. Cobelli, V. Taufour and S. Sanvito, *A rule-free workflow for the automated generation of databases from scientific literature*, npj Comp. Mater. **9**, 222 (2023).

[3] M. Domina, U. Patil, M. Cobelli and S. Sanvito, *Cluster expansion constructed over Jacobi-Legendre polynomials for accurate force fields*, Phys. Rev. B **108**, 094102 (2023).

[4] B. Focassio, M. Domina, U. Patil, A. Fazzio and Stefano Sanvito, *Linear Jacobi-Legendre expansion of the charge density for machine learning-accelerated electronic structure calculations*, npj Comp. Mater. **9**, 87 (2023).

[5] M. Domina, M. Cobelli and S. Sanvito, *Spectral neighbor representation for vector fields: Machine learning potentials including spin*, Phys. Rev. B **105**, 214439 (2022).

Abstract ID: 30590

THE STRONG INTERPLAY BETWEEN THE MAGNETIC AND ELECTRONIC STRUCTURE OF CUPRATES AND NICKELATE SUPERCONDUCTORS

G. Sawatzky[1], K. Foyevstova[3], M. Jiang[3], I. Elfimov[1]

[1] Quantum Matter Institute University of British Columbia, BC V6T 1Z4, Vancouver, CANADA
[2] Physics department University of Notre Dame, 46556, Indiana, USA
[3] School of Physical Science and Technology, Soochow University, 215006, Suzhou, CHINA

3d transition metal compounds are a continued source of new discoveries of exotic physical properties impacting our everyday life. Emerging properties like; high temperature superconductivity, hard magnets, large thermoelectric effects, potential dissipation less spin transport, altermagnets, and topological insulators to mention a few. I will address the question as to why these elements are unique and retain much of there atomic characteristics in the solids leading to the diversity in physical properties forcing us to address the problem of strong electron correlations in describing the electronic, magnetic and crystallographic structures. As special examples we concentrate on the Cu and Ni transition metal oxides some of which exhibit high temperature superconductivity. I will describe both the many body exact diagonalization of small clusters and hybrid density functional band theory methods in attempts to understand their physical properties. We demonstrate the strong interplay between the spin, charge, and lattice degrees of freedom leading to diversity in physical properties. This will also lead into a new type of electron boson coupling where the bosons are represented by local singlet triplet excitations distinct from more conventional magnons.

Abstract ID: 30658

SPIN-TRIPLET SUPERCONDUCTIVITY AND FIELD INDUCED PHENOMENA OF UTe2

D. Aoki

IMR, Tohoku University, Ibaraki 311-1313, JAPAN

Unconventional superconductivity in the heavy fermion paramagnet UTe_2 has emerged as one of the most compelling topics in the field of strongly correlated electron systems [1]. Superconductivity sets in below T_c = 1.5–2.1 K, accompanied by a large specific heat jump indicative of a strong-coupling regime. The system exhibits a highly anisotropic and exceptionally large upper critical field H_{c2}, reminiscent of that found in ferromagnetic superconductors such as URhGe and UCoGe. Although ferromagnetic fluctuations in UTe_2 have not yet been confirmed, inelastic neutron scattering has revealed the presence of antiferromagnetic fluctuations with an incommensurate q-vector.

A striking feature of UTe_2 is its field-reentrant superconductivity, which persists up to the metamagnetic transition field, $H_m \approx 35$ T, when the magnetic field is applied along the b-axis of the orthorhombic crystal structure. In addition, multiple superconducting phases emerge at high fields and at high pressure, implying the realization of distinct superconducting order parameters. These experimental findings collectively support a spin-triplet superconducting state, which arises from the spin and orbital degrees of freedom.

A key ongoing challenge is elucidating the Fermi surface topology via quantum oscillation measurements below and above H_m, as well as in the antiferromagnetic state above P_c, using ultraclean single crystals [2]. In this talk, I will present our latest results on UTe_2, focusing on Fermi surface properties [3,4], the nature of multiple superconducting phases, and the intriguing regime of field-reentrant superconductivity [5,6].

References

[1] See a review paper, for example, D. Aoki, J. P. Brison, J. Flouquet, K. Ishida, G. Knebel, Y. Tokunaga, and Y. Yanase, J. Phys.: Condens. Matter **34**, 243002 (2022).
[2] D. Aoki, J. Phys. Soc. Jpn. **93**, 043703 (2024).
[3] D. Aoki, H. Sakai, P. Opletal, Y. Tokiwa, J. Ishizuka, Y. Yanase, H. Harima, A. Nakamura, D. Li, Y. Homma, Y. Shimizu, G. Knebel, J. Flouquet, and Y. Haga, J .Phys. Soc. Jpn. **91**, 083704 (2022).
[4] D. Aoki, I. Sheikin, A. McCollam, J. Ishizuka, Y. Yanase, G. Lapertot, J. Flouquet, and G. Knebel, J. Phys. Soc. Jpn. **92**, 065002 (2023).
[5] D. Aoki, I. Sheikin, N. Marquardt, G. Lapertot, J. Flouquet, and G. Knebel, J. Phys. Soc. Jpn., **93**, 123702 (2024).
[6] T. Vasina, D. Aoki, A. Miyake, G. Seyfarth, A. Pourret, C. Marcenat, M. Amano Patino, G. Lapertot, J. Flouquet, J.-P. Brison, D. Braithwaite, and G. Knebel, Phys. Rev. Lett. **134**, 096501 (2025).

Abstract ID: 30702

THE NATIONAL HIGH MAGNETIC FIELD LABORATORY: PUSHING THE FRONTIERS OF SCIENCE WITH EXTREME FIELDS

K. M. Amm

National High Magnetic Field Laboratory, Florida State University, 32310, Tallahassee, Florida, USA

The National High Magnetic Field Laboratory (MagLab) is the world's premier user facility for research in high magnetic fields, enabling transformative science across physics, chemistry, materials science, biology, and engineering. By providing unparalleled continuous and pulsed magnetic fields, advanced instrumentation, and deep technical expertise, the MagLab serves as a critical engine for discovery and innovation.

In this plenary talk, I will highlight how extreme magnetic fields open unique windows into quantum matter, emergent phenomena, and complex systems that are inaccessible by other means. I will discuss recent scientific advances enabled by the MagLab's facilities, including breakthroughs in quantum materials, superconductivity, energy relevant materials, and biomolecular structure and dynamics. These examples illustrate how high field research not only deepens fundamental understanding but also informs technologies with long term societal impact.

I will also describe the MagLab' s role as a national and international hub for the scientific community, emphasizing its user driven model, interdisciplinary reach, and commitment to training the next generation of researchers. Finally, I will outline future directions for high magnetic field science and technology, including emerging experimental capabilities and strategic priorities that will shape the field in the coming decade. Together, these efforts position the MagLab to continue advancing the frontiers of science and sustaining U.S. leadership in high magnetic field research.

Abstract ID: 30817

SIX NEW PIECES OF THE HIGH-T_c PUZZLE

I. Božović

Shanghai Advanced Research in Physical Sciences, Shanghai, CHINA

This talk will describe several incisive new experiments addressing the burning questions about the physics of HTS in cuprates and nickelates. The results are so unexpected that they may reset the field. They refute most of the theoretical models and "scenarios" proposed so far and impose very tight constraints on the correct theory yet to be formulated.

(Ir)relevance of disorder. The prevailing dogma in the HTS field is that overdoped cuprates are Fermi Liquid metals and BCS superconductors. However, we demonstrated that in $La_{2-x}Sr_xCuO_4$, as the doping is increased, the superfluid density N_{s0} decreases and vanishes, tracking the decrease in T_c. [1] Moreover, $N_s(T)$ is linear in T. [1] Neither is expected from the standard BCS theory. Several theoretical models were proposed to explain this 'paradox' away. The common postulate is that with increased dopant density and disorder, pair breaking proliferates, causing the demise of T_c and N_{s0}.

Now, we tuned T_c in overdoped LSCO films by electrolyte gating and protonation. We found that as the disorder increases, T_c and N_{s0} *increase* – the opposite of what is predicted by the dirty-BCS scenario [2].

Very strange magnetoresistance. In an FL metal, in a field B perpendicular to the current, the Lorentz force bends the quasiparticle trajectories, causing magnetoresistance $\propto B^2$. But in some cuprates, we found MR $\propto B$ [3]. This is incompatible with FL theory, and even with the more general picture of gas of charged particles, be they fermions, bosons, or classical.

Now, we show an unusual scaling of MR with the direct sum of thermal and magnetic energies, implying the predominance of energy relaxation. Moreover, we demonstrate that the B-linear term comes from spin (Zeeman) in both cuprates and nickelates., while the orbital MR is not detected.

Electronic nematicity. Another major puzzle is that the transport in a tetragonal single-crystal LSCO films is anisotropic. [4] It was proposed that this is due uniaxial CDW or charge order, but the nematicity amplitude is almost T-independent (below 300 K), rather than mean-field like. Moreover, it is macroscopic, while one would expect a CDW to form nanometer-scale domains.

Now, we measured Faraday rotation and dichroism, from sub-THz to eV scale, confirmed the dc results, and showed that nematicity persists to the mid-infrared energy range. Hence, nematicity cannot originate from low-energy orders such as CDW, SDW, SC fluctuations, vortices, etc.

Electron pairing. In cuprates, by shot-noise experiments, we showed the existence of pairs in the normal state — at temperatures well above T_c and voltages above the SC gap. [5] We also found that the metal-to-insulator transition occurs near $R\square = R_Q = h/(2e)^2 = 6.5$ KW, indicating that electrons are paired in the insulating state, as well. [6]. Now we show the same is true in nickelates.

Electron-lattice interaction. Tunneling spectra of LSCO junctions with in-plane current outlined the phonon DOS exactly, implying that phonons are strongly coupled to quasiparticle excitations. [7] Colossal photo-induced lattice expansion along the c-axis showed that the same is true for out-of-plane phonons. [8] Now, we show that the out-of-plane tunneling spectra of cuprates and nickelates host vibronic progressions — multiple phonon emissions following an electron tunneling event. Such progressions are seen very rarely and testify to ultra-strong (non-adiabatic) electron-lattice interaction.

Dependence of R(T) on n in $La_{n+1}Ni_nO_{3n+1}$. All Riddlesden-Popper nickelate phases are predicted to be metallic, with similar $r(T)$. Experimentally, we show that $r(T)$ decreases exponentially with n, spanning over five orders of magnitude in r, and crossing over from insulating to metallic behavior. This also indicates a strong coupling of electrons to specific lattice distortions.

References

[1] I. Božović, *et al.*, Nature **536**, 309 (2016).
[2] R. Caruso, *et al.*, Phys. Rev. Lett. **136**, 076003 (2026).
[3] P. Giraldo-Gallo, *et al.*, Science **361**, 479 (2018).
[4] J. Wu, *et al.*, Nature **547**, 432 (2017).
[5] P. Zhou, *et al.*, Nature **572**, 493 (2019).

[6] A. T. Bollinger, *et al.*, Nature **472**, 458 (2011).
[7] H. Shim, *et al.*, Phys. Rev. Letters **101**, 247004 (2008).
[8] N. Gedik, *et al.*, Science **316**, 425 (2007).

Abstract ID: 30838

SUPERCONDUCTIVITY FOR FUTURE ACCELERATORS

A. Ballarino

Centre Europeen de Recherche Nucleaire (CERN), 1211, Geneva 23, SWITZERLAND

While the Large Hadron Collider (LHC) continues operation, the High Luminosity Large Hadron Collider is driving the next generation of superconducting technologies for particle accelerators. Nb3Sn high-field quadrupole magnets, MgB2 and REBCO superconducting transmission lines, and Nb-Ti crab cavities will be installed in the LHC underground during Long Shutdown 3 (LS3) and are expected to become operational in 2030. These developments will significantly increase the achievable LHC luminosity, thereby enhancing the potential for new discoveries in high-energy physics.

In the meantime, studies of new accelerators for the post-LHC era continue. Both circular and linear collider concepts are being explored, with Higgs factories playing a central role as candidate future facilities, enabling precision Higgs boson studies. Following a review of superconducting technologies for the HL-LHC, the role of superconductivity in next- generation accelerator concepts is discussed, with particular emphasis on its contribution to higher magnetic fields and improved energy efficiency.

3 - HALF-PLENARY

Abstract ID: 30001

PRESSURE EFFECTS ON TYPE-I SUPERCONDUCTIVITY

R. Khasanov[1], G. A. Ummarino[2], I. I. Mazin[3], R. Vocaturo[4], J. van den Brink[4], E. Svanidze[5]

[1] *PSI Center for Neutron and Muon Sciences CNM, PSI 5232 Villigen, SWITZERLAND*
[2] *Istituto di Ingegneria e Fisica dei Materiali, Dipartimento di Scienza Applicata e Tecnologia, Politecnico di Torino, 10129 Torino, ITALY*
[3] *Department of Physics and Astronomy, George Mason University, Fairfax, Virginia 22030, USA*
[4] *Leibniz Institute for Solid State and Materials Research (IFW) Dresden, Helmholtzstrasse 20, 01069 Dresden, GERMANY*
[5] *Max-Planck-Institut für Chemische Physik fester Stoffe, Nöthnitzer Straße 40, 01187 Dresden, GERMANY*

Pressure is one of the most powerful parameters in superconductivity research. It enables the discovery of new superconducting materials that either do not superconduct — or may not even exist — under ambient conditions, yet display substantially enhanced critical temperatures when subjected to external pressure [1–3].

In this talk, I will present results from muon-spin rotation/relaxation experiments investigating the thermodynamic critical field (B_c) in type-I superconductors, including elemental metals such as In, Sn, and Al [4,5], as well as the binary compound BeAu [6]. Applying pressure enhances the deviation of $B_c(T)$ from the parabolic temperature dependence expected for a conventional type-I superconductor, indicating a progressive weakening of the coupling strength. This coupling strength is characterized by $\alpha = \Delta/k_B T_c$, where Δ denotes the superconducting energy gap and T_c the critical temperature.

As pressure (p) increases from ambient conditions to approximately 3.0 GPa, α decreases linearly, approaching the weak-coupling BCS limit $\alpha_{BCS} = 1.764$ in elemental Sn and In. In Al, α decreases even further, reaching $\alpha = 1.61$ at $p = 2.0$ GPa. In the multigap type-I superconductor BeAu, pressure induces distinct evolutions of the coupling strengths associated with the bands hosting the weaker and stronger superconducting gaps.

Analysis within the Eliashberg theoretical framework shows that only part of the pressure-induced reduction in α can be attributed to phonon-spectrum hardening, which leads to a decrease in the electron-phonon coupling constant. Remarkably, in In and Sn, nearly 40% of the observed change originates from an enhanced anisotropy of the superconducting energy gap, while in elemental Al, the entire pressure dependence of α is governed by changes in gap anisotropy.

References

[1] B. Lorenz and C. W. Chu, *Frontiers in Superconducting Materials*, Springer, Berlin, Heidelberg (2005).

[2] J. S. Schilling, in *Handbook of High-Temperature Superconductivity*, Springer, New York, NY (2007).

[3] J. S. Schilling and J. J. Hamlin, J. Phys.: Conf. Ser. **121**, 052006 (2008).

[4] R. Khasanov and G. A. Ummarino, Phys. Rev. B **110**, 214515 (2024).

[5] R. Khasanov and I. I. Mazin, Phys. Rev. B 10**3**, L060502 (2021).

[6] R. Khasanov, *et al.*, Phys. Rev. B **111**, 104507 (2025).

Abstract ID: 30021

MOLECULAR QUBIT ASSEMBLIES

J. van Slageren[1], J. Wischnat[1], L. Tesi,[1] P. Thielert[2], J. Werner[3], A.-N. Unterreiner[3], S. Richert[2]

[1] *Institute of Physical Chemistry, University of Stuttgart, Stuttgart, GERMANY*
[2] *Institute of Surface Chemistry and Catalysis, Ulm University, Ulm, GERMANY*
[3] *Institute of Physical Chemistry, Karlsruhe Institute of Technology (KIT), Karlsruhe, GERMANY*

Paramagnetic molecules that may be employed as molecular qubits have been shown to possess long coherence times in the three digit microsecond regime, in nuclear-spin-poor and dilute matrices, such as doped solids and frozen solutions [1]. To make progress toward implementing quantum technologies with such molecules, a long road lies ahead.

A first step is the preparation of two- and other few-qubit assemblies [2]. This is essential for the implementation of two-qubit gate operations. Ideally, the interaction between the two qubits should be switchable, e.g., by light excitation. To this end, we have prepared dimers of the TEMPO radical which are bridged by anthracene moieties, using different coupling strategies [3]. Time-resolved absorption measurements reveal different intersystem crossing efficiencies. The coupled nature of the photoexcited three-spin system was unambiguously demonstrated by time-resolved EPR measurements.

For quantum computing and quantum simulation, extended two-dimensional arrays of qubits are required. As a first step in this direction, we have prepared self-assembled monolayers (SAMs) of TEMPO-molecules using a modular approach [4]. Careful analysis demonstrated clean SAM formation. EPR measurements on intact SAMs revealed sizable coherence times. Recent investigations with other radicals substantiated and enhanced on these findings [5].

References

[1] D. Schäfter, J. Wischnat, L. Tesi, J.A. De Sousa, E. Little, J. McGuire, M. Mas-Torrent, C. Rovira, J. Veciana, F. Tuna, N. Crivillers, J. van Slageren, Adv. Mater., **35**, 2302114 (2023); K. Bader, D. Dengler, S. Lenz, B. Endeward, S.D. Jiang, P. Neugebauer, J. van Slageren, Nat. Commun., **5**, 5304 (2014); J. M. Zadrozny, J. Niklas, O. G. Poluektov, D. E. Freedman, ACS Cent. Sci., **1**, 488 (2015).

[2] S. Gorgon, K. Lv, J. Grüne, B. H. Drummond, W. K. Myers, G. Londi, G. Ricci, D. Valverde, C. Tonnelé, P. Murto, A. S. Romanov, D. Casanova, V. Dyakonov, A. Sperlich, D. Beljonne, Y. Olivier, F. Li, R. H. Friend, E. W. Evans, Nature, **620**, 538, (2023).

[3] J. Wischnat, L. Tesi, P. Thielert, J. Werner, A.N. Unterreiner, S. Richert, J. van Slageren, to be published.

[4] L. Tesi, F. Stemmler, M. Winkler, S.S.Y. Liu, S. Das, X. Sun, M. Zharnikov, S. Ludwigs, J. van Slageren, Adv. Mater., **35**, 2208998 (2023).

[5] J. Wischnat, L. Tesi, J. van Slageren, to be published.

Abstract ID: 30395

ON SPIN TRANSPORT IN SOLIDS AND ALTERMAGNETISM

H. Reichlova

Technische Universität Dresden,01062 ,Dresden, GERMANY

Altermagnets represent a newly emerging class of magnetic materials that combine the favorable properties of ferromagnets and antiferromagnets, offering remarkable potential for future spintronic applications. Numerous theoretical studies have highlighted their unique electronic structures and the resulting implications for spin transport in solids. In this talk, I will first summarize the potential of altermagnets, providing an overview of known material systems and the current experimental evidence supporting altermagnetic behavior. In the second part, I will focus on our spin transport experiments in altermagnets. In single layers of altermagnets special attention will be given to the anomalous Hall and anomalous Nernst effects, which are symmetry-forbidden in conventional collinear antiferromagnets but can emerge in altermagnets due to time-reversal symmetry breaking in their electronic band structures. Finally, I will discuss our ongoing spin transport studies in multilayer structures incorporating altermagnets.

References

[1] Song, *et al.*, Nature Reviews Materials (2025).
[2] Jungwirth, *et al.,* Altermagnetic Spintronics, arXiv:2508.09748.
[3] R. D. Gonzalez Betancourt, *et al.,* Phys. Rev. Lett. **130**, 036702 (2023).
[4] H. Reichlová, *et al.,* Nat. Commun. **15**, 4961 (2024).

Abstract ID: 30479

SPIN TEXTURES AND SPIN WAVES AS SEEN BY X-RAY IMAGING

S. Wintz

Helmholtz-Zentrum Berlin, 14109, Berlin, GERMANY

The investigation of spin-wave phenomena—magnonics—plays an increasingly central role in modern condensed-matter research [1]. Spin waves are considered promising signal carriers for next-generation spintronic information-processing devices, with the potential to surpass charge-based technologies in both energy efficiency and device miniaturization. A key challenge on this path is the generation, control, and detection of spin waves with nanoscale wavelengths.

In this talk, I will show how time-resolved x-ray microscopy enables direct imaging of nanoscale spin dynamics. Using this technique, it has been demonstrated that ferromagnetic spin textures—particularly vortex cores and domain walls—can act as nanoscale spin-wave emitters and non-reciprocal waveguides [2–7]. I will further discuss recent advances in x-ray imaging of spin-wave dynamics in ferrimagnetic and antiferromagnetic materials, as well as emerging approaches for probing three-dimensional magnetic systems [8].

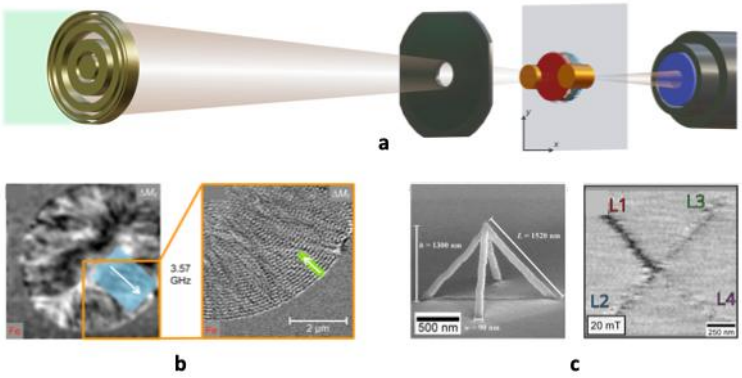

Fig. 1: *(a) X-ray imaging (schematic) [7], (b) TR-STXM images of non-reciprocal spin waves [5], (c) SEM and STXM images of 3D magnetic structure [8].*

References

[1] A. V. Chumak, *et al.*, IEEE Trans. Magn. **56**, 0800172 (2022).
[2] S. Wintz, *et al.*, Nat. Nanotech. **11**, 948 (2016).
[3] G. Dieterle, *et al.,* Phys. Rev. Lett. **122**, 117202 (2019).
[4] V. Sluka, *et al.*, Nat. Nanotech. **14**, 328 (2019).
[5] R. A. Gallardo, *et al.*, ACS nano **18**, 5249 (2024).
[6] S. Mayr, *et al.*, Appl. Phys. Rev. **11**, 041411 (2024).
[7] S. Koraltan, *et al.*, Sci. Adv. **10**, eado 8635 (2024).
[8] S. Koraltan, *et al.*, Adv. Funct. Mater. e15338 (2025).

Abstract ID: 30579

EFFECTS OF QUANTUM INTERFERENCE IN QUANTUM RINGS AND 3D NANOPRINTED STRUCTURES

V. M. Fomin[1,2]

[1] *Institute for Emerging Electronic Technologies, Leibniz Institute for Solid State and Materials Research (IFW) Dresden, D-01069 Dresden, GERMANY*
[2] *Department of Physics and Engineering, Moldova State University, MD-2009 Chişinău, REPUBLIC OF MOLDOVA*

Quantum rings are a special class of modern high-tech nanostructures, which provide a unique playground for the quantum-mechanical paradigm and topological physics [1]. I will represent their formation by molecular beam epitaxy and droplet epitaxy of semiconductors as well as their topology-driven electronic, optical, and magnetic properties. Highly complex theoretical models will be discussed which have been developed to adequately explain the specific features of quantum rings. I will provide an ample presentation of the recent advancements in the physics of quantum rings related to spin dynamics and the spin-orbit interaction (spin interference in Rashba rings, tunable exciton topology on type II InAs/GaAsSb quantum nanostructures), the electron-phonon interaction in ring-like structures, quantum-interference manifestations in novel materials (e.g., graphene cylinders, cyclocarbons, MoS_2), effects of electric field and THz radiation on optical properties of quantum rings and quantum-ring molecules. Special emphasis will be made on fascinating novel effects emerging due to double-connectedness in various physical systems, embracing the occurrence of the continuous geometric phase provoking formation of non-integer mode numbers in Möbius microring light cavities, the inverse Faraday effect on the generation of current states in an array of superconductor nanorings, and the emergence of lightning-like magnetic flux bursts into a macroscopic superconductor ring. The frontline methods of fabrication and characterization of quantum rings together with the sophisticated cutting-edge theoretical research and numerical simulations have allowed for accumulation of a significant thesaurus of fundamental information on their behavior. This highly diversified knowledge underpins numerous suggestions for prospective applications of nanostructures with nontrivial topology, like quantum rings and 3D nanoprinted arrays, as a highly tunable elemental base for future device design and optimization in optoelectronics, spintronics, information storage and processing, as magnetic memory elements as well as photonic sources and detectors. Recently, in a densely packed W–C nanoarray fabricated via 3D nanoprinting using He^+ focused-ion-beam-induced deposition, the well-defined magnetoresistance minima have been detected over a wide temperature range. They are associated with vortex pinning, exhibiting matching conditions between the vortex lattice and the square nanoarray geometry [2]. In addition to vortex pinning phenomena, periodic magnetoresistance oscillations may be associated with magnetic flux quantization effects and interference of circulating supercurrents within the periodic structure. The interplay between vortex dynamics and quantum interference could point to the emergence of a collective quantum regime. These findings highlight the potential of 3D nanoprinted structures as a tunable platform to study quantum transport phenomena and engineer novel superconducting devices.

References

[1] V. M. Fomin (Ed.), Physics of Quantum Rings, 3rd edition (Springer International Switzerland, Cham, 2025).
[2] A. Arroyo-Fructuoso, G. Hlawacek, V. M. Fomin and R. Córdoba, APL Quantum **3**, in print (2026).

Abstract ID: 30645

HOW TO CREATE MAGNONIC NETWORKS

P. Pirro

Fachbereich Physik and Landesforschungszentrum OPTIMAS, Rheinland-Pfälzische Technische Universität Kaiserslautern-Landau, 67663 Kaiserslautern, GERMANY

Magnonics addresses the dynamic excitations of a magnetically ordered material. These excitations, referred to as spin waves and their quanta, magnons, are a powerful tool forinformation transport and processing on the microscale and nanoscale. In recent years, there has been a dramatic increase in the conceptual development and experimental demonstration of magnonic devices [1]. In particular, the development of robust amplification and normalization methods, new materials and fabrication techiques have made the realisation of extended magnonic networks feasible [2].

In my presentation, I will introduce various methods of generating and amplifying spin waves, such as parametric processes and spin-orbit torque-driven magnonic elements, and discuss their potential in terms of scalability and energy efficiency. The coherent wave interference phenomena and the influence of nonlinear magnon processes on different building blocks will be given particular focus. I will compare approaches to encoding information (e.g. in wave phase [3], intensity [4], or frequency) in terms of scalability, robustness, and potential information density and discuss which building blocks can be used for the different encoding schemes. Finally, I will discuss the new opportunities that will be unlocked by the development of 3D magnonic systems [5].

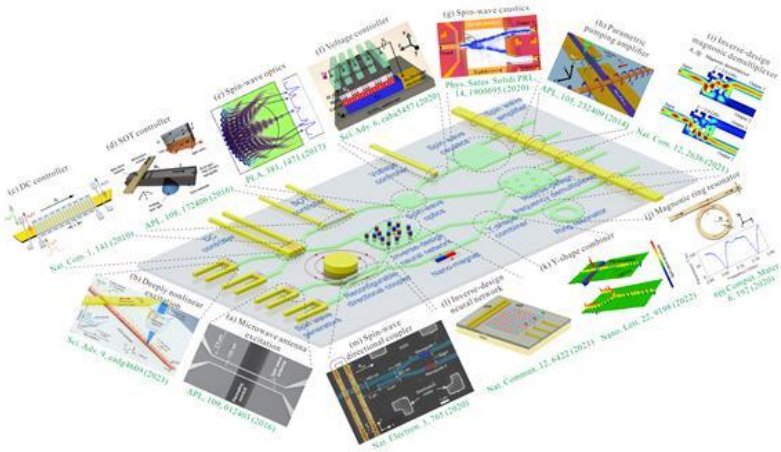

Fig. 1: *Schematic of a nanoscale integrated magnonic network, including spin-wave generators, connectors, modulators, and amplifiers [2].*

References

[1] P. Pirro, V. I. Vasyuchka, A. A. Serga, and B. Hillebrands, Nat Rev Mater **6**, 1114 (2021).
[2] Q. Wang, G. Csaba, R. Verba, A. V. Chumak, and P. Pirro, Phys. Rev. Appl. **21**, 040503 (2024).
[3] G. Talmelli, *et al.*, Sci Adv **6**, (2020).
[4] Q. Wang, *et al.*, Nat Electron **3**, 765 (2020).
[5] G. Gubbiotti, *et al.*, J. Phys.: Condens. Matter **37**, 143502 (2025).

Abstract ID: 30664

HIGH-T_c CUPRATES AND IRON PNICTIDES – COHERENCE, INCOHERENCE, AND LOCALIZATION

N. Barišić[1,2]

[1] *Institute of Solid State Physics, TU Wien, Wiedner Hauptstraße 8, 1040 Wien AUSTRIA*
[2] *Department of Physics, University of Zagreb, Bijenička c. 32, 10000 Zagreb, CROATIA*

In high-T_c cuprates, we have identified a set of surprisingly simple and universal behaviors (1-7). Building on these findings, we show [8,9] that the phenomenology of cuprates across the phase diagram can be captured by two simple relations:

$$1 + p = n_{loc} + n_{eff} \quad (1)$$

$$\rho_s = n_{eff} \,.\, (O_s \,.\, n_{loc}) \quad (2)$$

where p denotes the hole doping, n_{eff} is the density of Fermi-liquid carriers, n_{loc} is the density of (Mott-like) localized charge, and ρ_S is the superfluid density. Here, O_S is a compound-dependent constant set by the local crystal structure [9], which provides key insights into the microscopic superconducting mechanism [9,10]. Importantly, all quantities can be determined directly from experiment.

Another scenario has been proposed, related at first glance [11,12]. Focusing on the overdoped regime, transport measurements in high magnetic fields have been interpreted to suggest that n_{loc} is an incoherent ("Planckian") component (n_{incoh}) rather than localized charge, and that this incoherent component is the one that becomes superconducting. We use iron pnictides [7] to elucidate the essential distinctions between coherence, incoherence and localization, which in turn critically shape our understanding of the superconducting mechanism in cuprates and, potentially, other materials.

References

[1] N. Barišić, *et al.*, New J. Phys. **21**, 113007 (2019) (see also arXiv:1507.07885 (2015)).
[2] Y. Li, *et al.*, Sci. Adv. **5**, eaap7349 (2019).
[3] N. Barišić, *et al.*, Proc. Natl. Acad. Sci. U.S.A. **110**, 12235 (2013).
[4] S. I. Mirzaei, *et al.*, Proc. Natl. Acad. Sci. U.S.A.**110**, 5774 (2013).
[5] M. K. Chan, *et al.*, Phys. Rev. Lett. **113**, 177005(2014).
[6] P. Popčević, *et al.*, npj Quantum Mater. **3**, 42 (2018).
[7] C. M. N. Kumar, *et al.*, Phys. Rev. B **107**, 144515 (2023).
[8] D. Pelc, *et al.*, Sci. Adv. **5**, eaau4538 (2019).
[9] N. Barišić, D. K. Sunko, J Supercond. Nov. Magn. **35**, 1781 (2022).
[10] N. Barišić, D. K. Sunko, Arxiv:2512.20530 (2025).
[11] J. Ayres, *et al.*, Nature **595**, 661 (2021).
[12] G. Grissonnanche, *et al.*, Nature **595**, 667 (2021).

Abstract ID: 30698

CURVILINEAR AND 3D NANOMAGNETISM: FROM RECONFIGURABLE TETRAPODS TO SKYRMION NUCLEATION AND VORTEX DYNAMICS

S. Koraltan

Institute of Applied Physics, TU Wien, Vienna, AUSTRIA

The extension of nanomagnetism into three dimensions and curvilinear geometries opens new frontiers for spintronic applications, offering additional degrees of freedom beyond conventional planar thin films [1]. This talk presents recent advances in understanding and controlling magnetic states in 3D nanoarchitectures and curved surfaces, covering three interconnected topics: reconfigurable magnetization in 3D tetrapods, skyrmion nucleation on curvilinear surfaces, and direct-observation of spin-wave modes of magetic vortices on spherical geometries.

First, we demonstrate the magnetic reconfigurability of Co3Fe tetrapod nanostructures fabricated using focused electron beam-induced deposition (FEBID) [2]. Using scanning transmission X-ray microscopy (STXM) combined with finite element micromagnetic simulations, we show that the magnetization of individual tetrapod legs can be reversed sequentially, and the switching order can be controlled by tuning the direction of the applied magnetic field.

Second, we investigate skyrmion formation on self-assembled polystyrene particles coated with Pt/Co/Ta multilayers [3]. Using magnetic force microscopy (MFM), we demonstrate that the confinded spiraling stripe states can be transformed into metastable skyrmions at the apex of spherical particles through local magnetic field stimuli from the MFM tip.

Third, we present the direct experimental observation of vortex core gyration and azimuthal spin-wave modes on curvilinear surfaces [4]. NiFe-coated polystyrene spheres hosting magnetic vortices are excited using a stripline antenna, and time-resolved STXM captures real-space dynamics with sub-nanosecond resolution.

References

[1] A. Fernández-Pacheco, *et al.*, Nature Communications **8**, 15756 (2017).
[2] S. Koraltan, *et al.*, Advanced Functional Materials **35**, 2515338 (2025).
[3] S. Koraltan, *et al.*, arXiv:2511.22557 (2025).
[4] S. Koraltan, *et al.*, In Preparation (2026).
[5] S. Koraltan, *et al.*, Science Advances 10, eado8635 (2024).

Abstract ID: 30768

THE ROLE OF SUPERCONDUCTING ELECTRONICS IN SCALING QUANTUM COMPUTERS BEYOND THE WIRING/THERMAL BOTTLENECK

A. Bozbey[1,2]

[1] *Phi0 Quantum Technologies, Ankara, TÜRKIYE*
[2] *TOBB University of Economics and Technology, Ankara, TÜRKIYE*

The rapid progress in superconducting quantum processors over the past decade has exposed a critical but often overlooked challenge: the interface between quantum hardware and its classical control infrastructure. Today's architectures rely on dedicated coaxial cables to deliver microwave pulses from room-temperature electronics to qubits operating at millikelvin temperatures. While this approach has served systems with tens to hundreds of qubits, it introduces thermal load, signal integrity constraints, and physical wiring complexity that present a fundamental scalability barrier as qubit counts approach and exceed one thousand. The severity of this challenge is now widely recognized across the industry. Major quantum hardware manufacturers have begun developing in-house cryogenic control solutions, and startups focused exclusively on superconducting electronics have attracted valuations in the hundreds of millions of dollars, reflecting a clear shift from research interest to commercial investment.

Several strategies are being explored to address this bottleneck. Cryo-CMOS approaches aim to bring conventional transistor-based electronics closer to the quantum plane; while superconducting digital electronics offers an alternative path: control and readout circuits that operate natively at cryogenic temperatures with near-zero power dissipation. This talk reviews the current landscape of cryogenic control and readout architecture, examines the relative merits and limitations of each approach, and discusses the system-level integration challenges that must be resolved for any solution to become practical.

A critical gap in the superconducting electronics ecosystem is the lack of mature design automation infrastructure. Unlike the semiconductor industry, where decades of EDA tool development have enabled billion-transistor designs, superconducting circuit design has historically relied on manual workflows and adapted CMOS tools that do not capture the unique physics of the domain. Over the past decade, several government-funded research initiatives have produced open-source tools targeting various stages of superconducting design flow. While these efforts have expanded the available tooling, the resulting tools remain largely fragmented and do not yet constitute an integrated, production-ready ecosystem comparable to commercial semiconductor EDA platforms. We discuss ongoing efforts to develop native design automation for superconducting circuits.

Finally, we assess where the field stands today, what milestones remain on the path from laboratory prototypes to deployable cryogenic control platforms, and what role the superconducting electronics community can play in enabling the next generation of quantum computers.

Abstract ID: 30840

RARE EARTH ELEMENT RESOURCES IN TÜRKIYE: GEOLOGICAL CONTROLS, EXPLORATION STRATEGIES, AND THEIR CRITICAL ROLE IN ADVANCED TECHNOLOGIES

Y. K. Kadioğlu[1,2]

[1] *Ankara University Geol.Eng.Department, TÜRKIYE*
[2] *Earth Science Application and Research Center (YEBIM) of Ankara University, TÜRKIYE*

Rare Earth Elements (REEs) have emerged as indispensable components of modern advanced technologies due to their unique electronic, magnetic, and physicochemical properties. Their strategic importance stems from their critical role in high-performance permanent magnets, low-resistance conductive systems, energy-efficient devices, and renewable energy technologies. Among these elements, neodymium (Nd) stands out due to its exceptional magnetic anisotropy, high coercivity, and ability to form Nd–Fe–B permanent magnets, which exhibit superior energy density and thermal stability compared to conventional magnetic materials. These properties make REEs fundamental to applications ranging from electric vehicles and wind turbines to defense systems and high-frequency electronics.

Türkiye, located within the Alpine–Himalayan orogenic belt, represents a geodynamically complex region shaped by subduction, collision, and post-collisional extensional tectonics. Following the closure of Neotethys and subsequent slab break-off processes, widespread alkaline and peralkaline magmatism developed, particularly in extensional regimes. These tectonomagmatic conditions are highly favorable for REE enrichment, especially in association with foid-bearing alkaline rocks, carbonatites, and related magmatic-hydrothermal systems.

Significant REE exploration targets in Türkiye are associated with such alkaline complexes, notably in Eastern Anatolia (Malatya–Kuluncak, Elazığ–Keban), Central Anatolia (Kırşehir Bayındır, Tatarilyas, Kayseri–Özvatan), and Western Anatolia (Afyon–Çiçektepe, Uşak, Manisa–Kula). These regions host REE-bearing mineral assemblages including bastnasite (Ce), monazite-(Ce), xenotime-(Y), fluorite-associated REE phases, and other fluorocarbonates, which are typically concentrated within magmatic differentiation zones and structurally controlled hydrothermal alteration systems.

The genesis of REE mineralization in these settings is closely linked to magma evolution processes such as fractional crystallization, volatile enrichment (F–CO_2-rich fluids), and late stage fluid–rock interactions. Structural features, particularly fault-controlled fracture systems, play a crucial role in localizing REE mineralization and enhancing fluid mobility, thereby increasing the potential for economic concentrations.

Exploration strategies for REEs require an integrated, multidisciplinary approach combining geological mapping, petrography, whole-rock geochemistry, trace element analysis (including LIBS, ICP-MS and LA-ICP-MS), and advanced mineralogical techniques such as Raman spectroscopy, FTIR, and electron microscopy. In addition, geophysical methods (e.g., resistivity and radiometric surveys) provide valuable insights into subsurface alteration zones and structural controls. Particular attention must be given to identifying indicator lithologies such as peralkaline syenites, foid-bearing rocks, and carbonatitic systems, which are key hosts for REE mineralization.

From a beneficiation perspective, REE-bearing minerals require specialized processing techniques, including physical separation (gravity, magnetic, flotation) and hydrometallurgical methods, to achieve economic extraction. The complex mineralogy and fine-grained nature of REE ores often necessitate advanced processing technologies to optimize recovery rates.

In conclusion, Türkiye possesses significant potential for REE resources within its post collisional extensional tectonic framework. The integration of geological, geochemical, and geophysical data is essential for effective exploration and resource development. Given their critical role in modern technology particularly in low-resistance conductive systems and high efficiency permanent magnets REEs represent not only a scientific and economic opportunity but also a strategic asset for sustainable technological advancement and energy transition.

4 - 2D GRAPHENE FUNDAMENTALS, MATERIALS AND THEIR APPLICATIONS

Abstract ID: 30654

DIMENSIONAL TRANSFORMATION OF BOROPHENE: FROM HYDROGENATED 2D SHEETS TO 0D BORON QUANTUM DOTS

O. G. Yildiz[1,2], U. Aydemir[2,3]

[1] *Graduate School of Sciences and Engineering, Koç University, Istanbul 34450, TÜRKIYE*
[2] *Koç University Boron and Advanced Materials Application and Research Center, Istanbul 34450, TÜRKIYE*
[3] *Department of Chemistry, Koç University, Sariyer, Istanbul 34450, TÜRKIYE*

Following its first experimental realization in 2015, borophene has attracted considerable attention as a mono-elemental two-dimensional (2D) boron sheet [1]. Since then, a variety of borophene polymorphs, comprising triangular, hexagonal, and mixed arrangements of boron atoms with different concentrations of atomic vacancies, have been theoretically predicted and experimentally observed, revealing boron's remarkable structural diversity [2,3]. Unlike the well-established 2D hexagonal boron nitride (h-BN), whose strong σ covalent B-N bonds provide excellent structural stability, elemental boron's electron deficiency favors icosahedral or cluster-like configurations [2,4]. This unique bonding nature renders the synthesis of free-standing, structurally stable borophene intrinsically challenging.

In this study, we introduce a solid-state route that enables the transformation of hydrogenated borophene into either two-dimensional borophene or zero-dimensional boron quantum dots (BQDs) via thermal dehydrogenation. This approach exploits intrinsic gas evolution from B-H bond cleavage to generate self-induced internal pressure that drives dimensional transformation. Under open conditions, gas release favors the formation of extended borophene sheets, whereas in confined environments, accumulated pressure induces fragmentation into QDs. This solvent-free, bottom-up process converts a functionalized 2D boron framework into tunable low-dimensional architectures using only heat and atmospheric confinement. Beyond the morphological transition, the resulting materials exhibit different photoluminescence behavior relative to hydrogenated borophene, consistent with quantum confinement and reduced surface chemistry. The method provides a clean and versatile platform for pressure-assisted dimensional engineering of 2D borophene, with broad implications for boron-based optoelectronics, quantum devices, and energy applications.

References

[1] Science (1979) 2015, 350 (6267), 1513–1516. https://doi.org/10.1126/science.aad1080.
[2] Materials Science and Engineering: R: Reports, **163**, 100913 (2025). https://doi.org/https://doi.org/10.1016/j.mser.2024.100913.
[3] Small Struct, **2500186** (2025). https://doi.org/https://doi.org/10.1002/sstr.202500186.
[4] Advanced Materials, **33 (44)**, 2101589 (2021). https://doi.org/https://doi.org/10.1002/adma.202101589.

Abstract ID: 30445

OPTICAL HIGH-ORDER HARMONIC GENERATION IN DIRAC MATERIALS

S. Rakhmanov[1], K. Matchonov[2], H. Yusupov[3], K. Nasriddinov[1], D. Matrasulov[4,5]

[1] Chirchik State Pedagogical University, 104 Amur Temur Str., 111700 Chirchik, UZBEKISTAN
[2] National University of Uzbekistan, 4 University Str., 100174 Tashkent, UZBEKISTAN
[3] Kimyo International University in Tashkent, 156 Usman Nasyr Str., 100121 Tashkent, UZBEKISTAN
[4] Turin Polytechnic University in Tashkent, 17 Niyazov Str., 100095 Tashkent, UZBEKISTAN
[5] Tashkent University of Architecture and Civil Engineering, Yangishahar Str. 9A, 100095 Tashkent, UZBEKISTAN

We study high-order harmonic generation by optically driven one- and two-dimensional hydrogen-like atoms formed by Coulomb impurities in graphene. The time-dependent Dirac equations with Coulomb plus time-periodic monochromatic field potentials are solved for both cases. Such characteristics of the optical high harmonic generation, as average dipole moment and high harmonic generation spectra, are computed. It is found that in one-dimensional case the HHG intensity has narrow plateau, while for 2D atom only narrow peaks without plateau are observed. A remarkable feature of the above models is caused by the fact that the strength of the external field needed for high harmonic generation is rather small (few MV/m), which is (approximately) by two orders smaller than that of atomic nucleus field strength. Such a feature makes possible experimental realization of the models at table-top level. A sketch for table-top experimental realization of the considered models is proposed.

References

[1] C. A. Downing, M. E. Portnoi, Phys. Rev. A **90**, 052166 (2014).
[2] D. Novikov, Phys. Rev. B **76**, 245435 (2007).
[3] X. Tong, Sh. Chu, Chem. Phys. B **217(2–3)**, 119 (1997).

Abstract ID: 30607

GAUGE-INVARIANT NONCOMMUTATIVE LANDAU PROBLEM IN GRAPHENE: EMERGENT MAGNETIC RESPONSE IN A DIRAC MATERIAL

A. Halder

West Bengal State Universty, Barasat, Kolkata, INDIA

Graphene provides a unique platform where relativistic quantum dynamics, geometry, and magnetism intersect. In this work, we investigate the Landau problem for massless Dirac fermions in graphene within a noncommutative (NC) phase-space framework, with particular emphasis on gauge consistency and physically observable magnetic responses. Using the Seiberg–Witten map, we construct a fully gauge-invariant effective theory that systematically incorporates noncommutativity while preserving the correct commutative limit.

We derive the modified Landau level spectrum and the corresponding density of states, carefully accounting for the relativistic nature of charge carriers. Based on this formulation, we compute the thermodynamic potential and analyze magnetization and magnetic susceptibility as experimentally relevant observables. A key result of our analysis is the emergence of a finite magnetic response induced by the NC geometry, including signatures of spontaneous magnetization, while ensuring that standard graphene behavior is smoothly recovered in the commutative limit.

Our results demonstrate that noncommutative geometry can be interpreted as an effective description of emergent gauge structures influencing magnetic properties in Dirac materials. The predicted modifications to magnetization provide clear qualitative trends that may be relevant for high-field graphene systems and engineered quantum materials with emergent geometric or topological features. This work highlights the role of gauge-invariant geometric effects as a potential source of novel magnetic phenomena in quantum materials.

Abstract ID: 30772

REDUCED GRAPHENE OXIDE NANOCOMPOSITES FOR LITHIUM AND SODIUM BATTERIES ANODES

S. Karamat

Physics department, COMSATS University Islamabad, PAKISTAN

Commercially available lithium-ion batteries (LIBs) utilize graphitic anodes, which have a lower energy density of approximately 300 mAh/g. Reduced capacity retention and low power density are problems shared by both LIBs and SIBs. In this work, the main focus is to change the chemistry of anode material by reaction mechanisms (insertion/intercalation, conversion, and alloying) occurring during the storage of Li+1/Na+1. For this purpose, doping of binary composites (oxide/sulfide-based transition metal-carbonaceous (graphene oxide, graphene, carbon nanotubes, etc.) materials) such as MoO3/rGO, MoS2/rGO, MoO3/MoS2/rGO, Fe2O3/rGO would be used, because they are intercalation materials which have high cyclic stability and less volume fluctuations, to further enhance the electrochemical properties such as energy density and cyclic stability of the battery.

Owing to the enhanced theoretical specific capacity of 1117 mAh/g, MoO3 is the utmost desirable anode material used in lithium-ion batteries (LIBs). Due to the volume expansion problem, a composite of MoO3/reduced graphene oxide (rGO) was synthesized for efficient cyclic stability. Doping of nickel (Ni+2) into the composite optimizes the reaction kinetics of the LIB coin cell. Charge/discharge analysis has been done with the excellent discharge specific capacity measured near 1380 mAh/g at 0.3 A/g, which dramatically left behind the undoped composite with its highest discharge specific capacity at 771 mAh/g. Electrochemical impedance spectroscopy (EIS) finds the higher Li+1 ion diffusion rate with Warburg constant (Wz) value of 0.208 kΩ. Lowest charge transfer resistance (Rct) value of 43.15 Ω showed by 2% Ni-MoO3/rGO along with a lowest charge transfer time measured with the value of 0.0013 ms. Furthermore, doped MoO3/rGO composite exhibits outstanding capacity retention of 90.8% after 300 cycles as compared to the undoped MoO3/rGO composite with capacity retention of 80.4% after 164 cycles. Additionally, the ZnO/rGO anode exhibits a discharge capacity of 445 mAh/g at 100 mA g−1 that was significantly enhanced to 463 mAh/g after doping ZnO with 2 % Mg. By further increasing the concentration of Mg to 4 %, the Mg-ZnO/rGO anode achieves a higher discharge capacity of 520 mAh g−1 with better rate capability than its counterpart electrodes.

The synergistic effects between Mg-ZnO and carbon-based nanomaterials are ascribed to the creation of additional contact sites to penetrate electrolyte ions into the electrode, thus resulting in the fast lithium-ion diffusion rate. The same effect has been observed for the Co doping in the Fe2O3 with rGO composites. Doping offers an extra redox active site due to the formation of oxygen vacancies, which are responsible for increasing charge storage phenomenon and speeding up the reaction kinetics during lithiation/de-lithiation process. Overall, doping of transition metals in carbonaceous material exhibits optimum electrochemical performances and proving the improved composite as an anode material for the LIBs and SIBs.

Abstract ID: 30312

HIGH-FIDELITY SPIN TRANSPORT IN GRAPHENE-BASED SPIN VALVES

A. Avsar[1,2]

[1] *Department of Materials Science and Engineering, National University of Singapore, Singapore 117575, SINGAPORE*
[2] *Department of Physics, National University of Singapore, Singapore 117542, SINGAPORE*

Graphene's exceptional electronic and spin transport properties make it a compelling platform for next-generation spintronic devices [1, 2]. Realizing its full potential, however, critically depends on interfacial engineering, as spin transport and spin proximity effects are highly sensitive to disorder and contamination. Here, we employ an all-van der Waals assembly strategy performed entirely in an inert environment to fabricate clean graphene/hBN heterostructures with controlled crystallographic alignment. This approach yields devices with atomically sharp and nearly residue-free interfaces that preserve the intrinsic spin coherence of graphene.

Using these high-quality heterostructures, we explore two regimes of spin physics. In monolayer graphene, we demonstrate highly efficient spin injection and detection through crystalline tunnel barriers, achieving near-unity spin polarization and revealing spin transport governed by intrinsic relaxation mechanisms. In bilayer graphene, we access gate-tunable spin proximity effects arising from interfacial exchange coupling, evidenced by the reversal of spin polarization near the charge neutrality point and at moiré-induced satellite peaks. Together, these results underscore the critical role of interfacial cleanliness and crystallographic control in realizing coherent spin phenomena in two-dimensional materials. Our observation of large nonlocal spin signals highlights the promise of van der Waals spintronics for scalable, energy-efficient spin-based logic and information processing.

References

[1] A. Avsar, *et al.*, Rev. Mod. Phys. **92**, 021003 (2020).

[2] J. F. Sierra, *et al.*, Nature Nanotechnology **16 (8)**, 856-868 (2021).

5 - ADVANCED REBCO-BASED CONDUCTORS FOR LARGE-SCALE HTS APPLICATIONS IN ENERGY GENERATION, TRANSMISSION, STORAGE AND USE IN ENERGY-EFFICIENT DEVICES

Abstract ID: 30064

INCREASING THE CRITICAL CURRENT DENSITY OF GdBCO COATED CONDUCTORS AND YBCO FILMS DEPOSITED ON STO SUBSTRATES BY HIGH-PRESSURE- HIGH TEMPERATURE OXYGENATION

T. Prikhna[1,2,3], R. Vlad[2], A. Kethamkuzhi[2], R. Kluge3, B. Büchner[3], M. Karpets[1,4], S. Ponomaryov[5], V. Moshchil[1], X. Obradors[2], J. Gutierrez[2], T. Puig[2]

[1] *V. Bakul Institute for Superhard Materials of the National Academy of Sciences of Ukraine, 2, Avtozavodska Str., Kyiv 07074, UKRAINE*

[2] *Institut de Ciencia de Materials de Barcelona, CSIC, Campus UAB, 08193 Bellaterra, SPAIN*

[3] *Leibniz-Institut für Festkörper- und Werkstoffforschung Dresden e. V., Helmholtzstrasse 20 01069 Dresden, GERMANY*

[4] *National Technical University of Ukraine «Igor Sikorsky Kyiv Polytechnic Institute", Peremogy Avenue 37, 03056 Kyiv, UKRAINE*

[5] *V.E. Lashkaryov Institute of Semiconductor Physics of the National Academy of Sciences of Ukraine, 41, Nauky Ave., Kyiv 03028, UKRAINE*

High pressure-high temperature oxygenation allows for an increase increase in the critical current density of melt-textured YBCO ceramics due to a smoother oxygen incorporation into the $YBa_2Cu_3O_{7-\delta}$ structure compared to lower-temperature oxygenation under 1 bar oxygen pressure [1, 2]. Our previous studies of REBCO (RE=Gd, Eu) coated conductors (CC) oxygenation at high pressure and high temperature [3, 4] showed that the superconducting layer structure does not deteriorate even after heating to 800°C under a pressure of 160 bar of oxygen, and the charge carrier density n_H(100 K) can be significantly increased due to oxygen overdoping. The present study revealed that after treatment at 160 bar O_2 at 800 °C for 3 h J_C(77K,0T) of GdBCO_CC was increased for 21.5 % from 2.12 to 2.70 MA/cm², (n_H (100 K) = 7.3×10^{21} cm^{-3}, *c*-parameter decreased to 1.1727(1) nm), while heating for 6 h under same pressure-temperature conditions leaded to J_C(77K,0T) increase for 18 % only. It has been shown that J_c as a result of oxygenation of tetragonal $YBa_2Cu_3O_{7-d}$ film (250±7% nm thick) deposited on $SrTiO_3$ (STO) singlecrystaline substrate by spin coating method after treatment under 100 bar oxygen pressure at 600 °C for 8h was increased by 61 % (at 77 K) and 74% (at 5K) compared to the values after standard oxygen saturation at 1 bar, 450 °C, 3.5 h: J_c(77 K, 0 T)=3.74 MA/cm², J_c(5 K, 0 T)=33.34 MA/cm² versus J_c(77 K, 0 T)=2.28 MA/cm² J_c(5 K, 0 T)=24.83 MA/cm². The n_H(100 K), estimated from Hall effect increased from 3.2×10^{21} cm^{-3} up to 10.78×10^{21} cm^{-3}.

References

[1] T. A. Prikhna, J. Rabier, A. Proult, X. Chaud, W. Gawalek, A.V. Vlasenko, J.-L. Soubeyroux, R. Tournier, F. Sandiumenge, Ya. M. Savchuk, V. E. Moshchil .A. Nagorny, N. V. Sergienko, V. S. Melnikov, S. Kraĉunovska, D. Litzkendorf, S. N. Dub, Supercond. Sci. Tecnol. **17**, S515-S519 (2004).

[2] T. A. Prikhna, V. E. Moshchil, S. N. Dub, V. B. Sverdun, A. Joulain, J. Rabier, X. Chaud, W. Gawalek, Litzkendorf, D., T. Habisreuther, Journal of Superhard Materials **34(5)**, 283-298. (2012).

[3] T. Prikhna, A. Kethamkuzhi, R. Vlad, M. Karpets, R. Kluge, S. Ponomaryov, V. Moshchil, X. Obradors, B. Büchner, J. Gutierrez, S. Wurmehl, T. Puig, IEEE Transactions on Applied Superconductivity **35**, **no. 5**, 1-5., Art no. 6601505 (2025). DOI:10.1109/TASC.2024.3511544.

[4] T. Prikhna, A Kethamkuzhi, R. Vlad, R. Kluge, M. Karpets, S. Ponomaryov, V.Moshchil, B. Büchner, S. Wurmehl, J. Gutierrez, X. Obradors, T. Puig, IOP Conf. Ser.: Mater. Sci. Eng. **1327**, 012200 (2025). DOI 10.1088/1757-899X/1327/1/012200.

Abstract ID: 30501

THE TRANSIENT LIQUID ASSISTED GROWTH (TLAG) METHOD FOR ULTRAFAST GROWTH OF REBCO COATED CONDUCTORS

T. Puig[1], R. Vlad[1], X. Obradors[1], J. Gutierrez[1], E. Pach[1,5], C. Pop[1], K. Gupta[1,2], S. Rasi[1], C. Torres[1], A. Kethamkuzhi[1], O. Mola[1], E. Ghiara[1], V. Bertini[1], M. Voulhoux[1], L. Salterilli[1], D. Garcia[1,3], S. Ricart[1], R. Yanez[3], D. Sanchez[4], J. Farjas[4], E. Solano[5], L. Simonelli[5]

[1] *Institut de Ciència de Materials de Barcelona, ICMAB-CSIC, Campus UAB; 08193 Bellaterra, SPAIN*
[2] *Institut de Nanociencia i Nanotecnologia, ICN2, Campus UAB, 08193 Bellaterra, SPAIN*
[3] *Departament de Química, Universitat Autonoma de Barcelona, Campus UAB, 08193 Bellaterra, SPAIN*
[4] *GRMT, Department of Physics, University of Girona, E17071-Girona, SPAIN*
[5] *ALBA Synchrotron, 08290 Bellaterra, SPAIN*

The remarkable potential of $REBa_2Cu_3O_7$-coated conductors (REBCO CCs) has finally become a tangible reality by unlocking new technological opportunities like compact fusion, hybrid electric aviation, DC transmission lines or complex magnets in accelerator physics. However, the market perspectives advices to invest in high throughput manufacturing processes of reduced cost-to-performance ratio to compile with the large demands and foster initiatives to improve performance ensuring robustness. To address these challenges, at ICMAB we are developing a scalable, high-throughput growth process known as *Transient Liquid Assisted Growth* (TLAG) [1]. This method achieves ultra-high growth rates exceeding 1000 nm/s while maintaining high critical current densities [2] by using nanocrystalline precursor films that can be prepared from chemical solution deposition (CSD) [3,4] or low temperature physical deposition (like Pulsed Laser Deposition) [5]. In the CSD case, the use of multifunctional colloidal inks enables the fabrication of nanocomposites CC for high-magnetic field applications.

TLAG is a highly non-equilibrium liquid-solid growth process in which nucleation and growth are kinetically controlled. For that reason, we have developed advanced in situ techniques to elucidate the underlying growth mechanisms and establish correlations between process parameters, epitaxy, growth rate and performance. This includes, an in-situ growth installation at ALBA synchrotron with fast acquisition XRD and XAS coupled with mass spectrometry and in-situ electrical resistance. Results show that TLAG can operate at a very wide P_{O2}-Temperature window, where nucleation density and growth rate can be tuned by liquid composition, RE ion and process parameters. Moreover, the CSD approach enables us to employ high-throughput experimentation by developing inkjet-printed combinatorial compositional gradient films for fast process screening and data driving science. Besides, in order to improve performance in a robust manner, we are investigating the modification of the electronic structure by increasing the charge carrier density up to the overdoped state, where the vortex pinning centres improve their effectiveness by the increase of the condensation energy [6,7]. The combination of advanced transmission electron microscopy and high field angular transport measurements permits the understanding of the vortex physics of these complex materials grown at these high rates [8].

In this presentation, I will report on the progress of the above mentioned challenges with the aim of designing a robust, high throughput and flexible growth method for the manufacturing of Coated Conductors at competitive cost-performance ratio.

We acknowledge funding from EU-ERC_AdG-2014-669504 ULTRASUPERTAPE, EU-ERC-PoC-2020-IMPACT, EU-ERC-PoC-2022-SMS-INKS, CSIC-TRANSENER-PTI+, MICIN-SUPERENERTECH and SEVERO OCHOA MATRANS42 (CEX2023-001263-S).

References

[1] L. Soler, *et al.*, Nature Communications (2020).
[2] S. Rasi, *et al.*, Advance Science (2022).
[3] L. Saltarelli, *et al.*, ACS Appl Materials and Interfaces (2022).
[4] L. Saltarelli, *et al.*, ACS Appl Materials and Interfaces (2024).
[5] A. Queralto, *et al.*, SUST (2023).
[6] A. Stangl, *et al.*, Sci. Rep (2021).
[7] X. Obradors, *et al.*, Nat Mat N&V (2024).
[8] T. Puig, *et al.*, Nat Phys Rev. (2024).

Abstract ID: 30530

2G-HTS TAPE DEVELOPMENT AT HIGH TEMPERATURE SUPERCONDUCTORS, INC.

I. Wyrsta, J. Weiss, R. Karam

High Temperature Superconductors, Inc., CA-93103, Santa Barbara, USA

The recent surge in AI data centers is calling for High Temperature Superconductors (HTS) as a transformative solution to meet the escalating power and thermal management challenges pushing traditional copper-based power infrastructure beyond its limits. In parallel, the demand for second generation (2G) high temperature superconducting wire in the magnetic-confinement fusion sector is skyrocketing as private investment has surpassed $10 billion globally. With global supply chains becoming increasingly challenging, HTSI is uniquely positioned to become a leading tape manufacturer addressing this unmet HTS wire demand in the U.S. Employing Pulsed Laser Deposition (PLD) as the HTS deposition method ensures superior high-magnetic field performance suitable for fusion magnets (20 K, 20 Tesla) as well as power transmission. We believe the key to providing HTS wire at a competitive price is to increase the production line speed beyond state-of-the art, and together with our wholly owned subsidiary, PVD Products, Inc., we are set out to develop a 500 m/hr production line. At ICSM, we will share the most recent status of our development towards long-length, large-scale production.

Abstract ID: 30535

DEVELOPMENT AND SCALE UP OF HIGH-PERFORMANCE REBCO TAPES

V. Selvamanickam[1,2]

[1] *Department of Mechanical Engineering, Advanced Manufacturing Institute, Texas Center for Superconductivity University of Houston, 77204, Texas, USA*
[2] *AMPeers Houston, 77059-3733, Texas, USA*

There is an immense need for low-cost, high quality, abundantly available REBCO tapes that meet a wide range of specifications for many applications. High throughput manufacturing methods that yield uniform, long tapes with a high critical current are essential. Additionally, the tapes need to exhibit high delamination strength and preferably quench resilience and tolerance to neutron irradiation in the case of fusion magnets. We have been developing advanced REBCO conductors to address these challenges, with very high critical currents especially in high magnetic fields, large-area deposition techniques, quench-resilient architectures, and compositions/architectures with better resistance to delamination and irradiation, as well as excellent flexibility. Recent advances in the development and scale up of our high-performance REBCO tapes will be presented.

This work was supported by awards from the U.S. Department of Energy and the U.S. Navy.

Abstract ID: 30537

PROGRESS IN R&D AND INDUSTRIALIZATION OF SECOND-GENERATION HIGH-TEMPERATURE SUPERCONDUCTING TAPE AT SUPERMAG TECHNOLOGY

Y. Zhao[1,2], G. Jiang[1], S. Xu[1]

[1] *SuperMag Technology (Shanghai) Ltd, Shanghai, CHINA*
[2] *Shanghai Jiao Tong University, Shanghai, CHINA*

SuperMag Technology Ltd., a nascent enterprise spun off from Shanghai Jiao Tong University, has demonstrated remarkable progress in both R&D and manufacturing capabilities despite its recent inception in late 2022. In just one year, the company has successfully set up a production line based on an IBAD+PLD process route. This paper reports the latest progress in high-performance 2G-HTS tape production at SuperMag. We developed an ultra-fast pulsed laser deposition (PLD) technique with a peak growth rate of 200 nm/s. By combining REBCO formula optimization and deposition process improvements, REBCO films achieve excellent pinning performance, i.e., Ic values of over 245 A/4 mm-w @ 50 K, 5 T, and 340 A/4 mm-w @20 K, 20 T. The new-generation products synergistically deliver strong low-temperature/high-field performance and excellent electromechanical properties. This product offers both improved cost-effectiveness and increased manufacturing throughput, providing an optimized solution for high-field magnets, particularly in fusion applications. Parallelly, SuperMag has established in-depth collaborations with clients and is actively advancing research in areas such as filamentization and joining technologies.

Abstract ID: 30565

MASS PRODUCTION AND PERFORMANCE OF SST REBCO TAPE

J. Zhu, S. Chen, Z. Gao, C. Zhang, S. Zhen, X. Lin, P. Bai, B. Song, X. Wang

Shanghai Superconductor Technology Co., Ltd., 201315, Shanghai, CHINA

With the beneficial characteristics of high irreversible field, high superconducting transition temperature and high critical current density, REBCO material has reached the stage of mass commercial production. Meanwhile a large number of superconducting power transmission projects and superconducting magnets have been developed using REBCO tapes. Recently, due to the significant demand for REBCO tapes by compact fusion industry, Shanghai Superconductor Technology Co., Ltd. (SST) has kicked off a new round of production expansion. Through independent design and manufacturing, SST has swiftly built a large number of vacuum coating equipment and post-processing equipment, including MS, IBAD, PLD, slitting, copper-plating, lamination and so on. This production expansion targets to further reduce the fabrication cost and improve the performance of REBCO tapes, providing a consistent supply of high performance tapes for downstream applications. By the end of 2023, the SST's annual REBCO supply has reached 2000 km/12 mm, and will be further expanded to 4000 km/12 mm in 2025. Along with the production expansion, SST also carries out researches extensively on tape customization and problem solving for specific application scenarios, covering laser slitting, stainless steel lamination, insulation coating, low resistance joints, continuous online thickness measurement techniques, and superconducting coil winding technologies, to help customers meet their technical requirements and achieve a successful project using SST's REBCO products. This paper will focus on the industrialization and R&D progress that SST has recently achieved.

Abstract ID: 30581

LATEST ADVANCE IN MOD-YBCO COATED CONDUCTORS WITH THICK HTS LAYER AND STRONG FLUX PINNING

C. Cai, R. Huang, J. Chen, N. Zhang, Y. Li, Z. Liu

[1] *Department of Physics, Shanghai Key Laboratory of High Temperature Superconductors, Shanghai University, Shanghai, CHINA*
[2] *Shanghai Creative Superconductor Technologies Co. Ltd., Shanghai, CHINA*

For the practical application of $REBa_2Cu_3O_{7-\delta}$ (REBCO, RE=rare earth elements) high-temperature superconducting tapes, enhancing current-carrying capacity through thicker superconducting layers and introducing controllable flux pinning centers, alongside boosting industrial batch production capabilities, represent key drivers for future development. Shanghai Creative Superconductor Technologies Co., Ltd. (SCSC) has established a complete industrial manufacturing line based on the IBAD+MOD technology route. MOD technology achieves nearly 100% raw material utilization, offering significant advantages in producing thicker, wider, and longer high-temperature superconducting tapes. Currently, SCSC can mass-produce hundreds-meter-long REBCO tapes with a superconducting layer thickness of 3.5 μm [1, 2]. Combined with pre-prepared nanocrystal addition/ion irradiation techniques, the in-field performance of MOD-REBCO thick-film tapes can be effectively enhanced, achieving I_c (4.2 K, 10 T) of 870 A/4 mm-w.

References

[1] R. Huang, *et al.*, Advanced Functional Materials, 2401251 (2024).
[2] R. Huang, *et al.*, Advanced Materials, 0:e09630 (2025).

Abstract ID: 30756

NANOSTRUCTURE AND STRAIN IN YBCO LAYER OF HIGH-PERFORMANCE 2G HTS WIRES FOR LOW-TEMPERATURE MAGNET APPLICATIONS

V. A. Amelichev[1], P. N. Degtyarenko[1], A. A. Kamenev[1], A. L. Vasiliev[2], M. V. Lovygin[3], I. G. Maryasev[3]

[1] *S-Innovations LLC, Moscow, RUSSIA*
[2] *Institute of Crystallography, Russian Academy of Science, Moscow, RUSSIA*
[3] *Skolkovo Microanalysis Systems, Moscow, RUSSIA*

Since industrially produced REBCO-based 2G HTS wires met the Je(20 K, 20T) = 700 A/mm^2 criterion formulated by magnet designers for compact fusion devices operating at T ≤ 20 K, further technological developments are largely governed by the demands of fusion community [1]. The type of defects that dominate the pinning of flux lines in this temperature and magnetic field range is still unclear. The 5 to 10 nm large nanoparticles intentionally precipitated in the HTS matrix are more than an order of magnitude larger than the anisotropic superconducting coherence lengths [2], so that it is reasonable to assume that smaller defects created by the strain fields around nanoprecipitates are the dominant pinning centers [3]. Therefore, in addition to the TEM studies, we develop XRD methods for assessing the strain fields in the HTS layer of our YBCO based 2G HTS wires [4, 5]. In this contribution, we will present the advances in performance as well as the progress in understanding the nanostructure and strain fields in the HTS layer of our production wires.

The major advance was optimization of PLD processing that makes possible a 30 to 50% improvement in Ic(20K, 8 T) values, which can be related to variation in morphology and particle size distribution of Y_2O_3 nanoprecipitates in the Y123 matrix, which in turn causes a strong variation of average strain values.

Correlations between performance, nanoparticle size (TEM and XRD data), and strain characteristics derived from XRD measurements will be presented. We also discuss possible effects of the strain fields on the twin domain structure and formation of Y124 intergrowth defects formed during oxygenation of Y123.

References

[1] A. Molodyk and D. Larbalestier, Science, **386**, **no. 6651**, pp. 1220-1222 (2023).
[2] B. Oh, K. Char, A. D. Kent *et al.*, Phys. Rev. B **37**, 7861 (1988).
[3] A. Xu J. Jaroszynski, F. Kametani and D. Larbalestier, Appl. Phys. Lett. **106**, 052603 (2015).
[4] M. O. Rikel, V. A. Amelichev, A. V. Markelov *et al.*, IEEE Trans. Appl. Supercond., **34**, 6601205 (2024)
[5] M. O. Rikel, V. A. Amelichev, A. V. Markelov *et al.*, ICSM presentation (2025)

Abstract ID: 30492

SCALE-UP AND APPLICATION-DRIVEN R&D OF FFJ REBCO CONDUCTORS FOR FUSION MAGNETS, CABLES, AND AIRCRAFT MOTORS

V. Petrykin, S. Samoilenkov, R. Valikov, M. Gaifullin, M. Okube, A. Borisov, H. Dao, K. Begic, H. Hirose, V. Vyatkin, K. Vereshchagin, N. Khozhempo, I. Veschunov, A. Molodyk, S. Lee

Faraday Factory Japan, Hibarigaoka 5-12-15, Zama-shi, Kanagawa, 252-0003, JAPAN

The second-generation REBCO coated conductors (2G-HTS tapes) are now key enabling technology for large-scale HTS applications in compact fusion magnets, power cables, and high-efficiency rotating machinery. Faraday Factory Japan (FFJ) has expanded its reel-to-reel manufacturing platform and reached an annual production capacity of 3,000 km/year of standard YBCO-based ***Hermes*** tape in 2025, while maintaining a strong R&D focus on application-driven 2G-HTS tapes design and performance under corresponding operating conditions.

In this presentation we will make an overview of FFJ current manufacturing profile and the main R&D directions that support further scale-up and performance improvement of FFJ 2G-HTS tapes. For high-field applications, we summarize the present status of ***Mirai*** conductors with Ic(20K, 20T) ≈ 300A/4mm and a LF(20K, 20T) ~1.5, corresponding to Je > 1,200 A/cm² under these conditions. For cable-oriented 2G-HTS conductors, we report progress on REBCO-based ***Electra*** tapes achieving Ic(77K, s.f.) ≈ 1,200 A/12mm (or ≈ 350A/4mm). For different types of tapes we will demonstrate measured large datasets describing their functional properties in statistically valid manner. We will also discuss recent advances in filamentized wires produced by laser scribing, having 10–15 filaments per 4 mm, with the goal of reducing AC losses.

In addition, we will highlight selected R&D results on buffer-layer and 2G-HTS manufacturing improvements and on oxygenation/annealing strategies aimed at studying and controlling hole doping in the REBCO material. To characterize such samples, we applied advanced spectroscopy methods including Cu-K and O-K XANES and Raman spectroscopy to link local electronic structure and oxygen content to in-field transport performance. Finally, we outline our "big-data" project targeting two practical outcomes: automatic processing of production datasets, and inline process control during both buffer and REBCO fabrication. The talk will conclude with FFJ's near-term roadmap for next-generation REBCO conductors for fusion magnets, cables, and aircraft motor technologies.

Abstract ID: 30511

BMO-DOPED REBCO COATED CONDUCTOR WITH HIGH PERFORMANCE AND PRODUCTIVITY BY USING HOT-WALL PLD ON IBAD TEMPLATED SUBSTRATE

Y. Iijima, M. Ohsugi, K. Kakimoto, S. Muto, S. Fujita, W. Hirata, N. Nakamura, M. Daibo

Fujikura Ltd., 1440, Mutsuzaki, Sakura-shi, Chiba, 285-8550, JAPAN

Recent compact fusion programs have brought big demand of REBCO wires and mass production lines have rapidly been set up worldwide, employing manufacturing methods that reliably deliver high enough pinning performance and large enough tensile strength under strong magnetic fields around 20 T. Most of them are produced on thin metallic alloy substrates by using peculiar physical vapor deposition processes as combination of textured buffer films by ion-beam-assisted deposition (IBAD), and REBCO films by pulsed-laser deposition (PLD), both used from the earliest days of REBCO coated conductor [1].

PLD is characterized to be much supersaturated high-rate growth, resulting from fine and rapid evaporation by UV pulsed laser, creating blast wave that can reach far beyond mean free path in high enough oxygen pressure suitable for REBCO growth [2]. It allows to control high density dislocations and small-size secondary phase particles including BMO nanorods, dispersed inside uniformly textured REBCO films growing at extremely high rates. It brings about high production throughput and good homogeneity assisted by Hot-Wall architecture and resulting excellent production yield and capacity, which could shrink the equipment cost of high-power UV lasers per production length effectively.

We succeeded in commercialization of long length and uniform REBCO wires including scattered short length $BaHfO_3$ nano-rods, which have less angular dependent, but higher J_c compared to non-doped samples [3]. Both longitudinal and lot-to-lot uniformity of in-field I_c are quite good, and mechanical strengths are strictly examined with varied tape width, thickness, and protection layers. Though the RE elemental dependence of J_c in high field at 20 K was better where RE=Y [4], the one of crystalline growth stability was better where RE=Eu, Gd, for c-axis aligned thick film, which should come from better lattice stability [5,6]. We had chosen Eu for better growth stability promising better uniformity and productivity, but the trade-off relationships could suggest other approaches to cope with higher performance.

Fujikura group has now been increasing production capacity by using IBAD/Hot-wall PLD processes, for REBCO wires of good uniformity which should also be important to establish reliable quench protection or lower AC loss, even in large-scale magnets using NI technology or not, and assembled, or striated conductors.

References

[1] Y. Iijima, *et al.*, Appl. Phys. Lett., **vol. 60**, 769 (1992).
[2] A.V. Bulgakov, *et al.*, J. Phys. D: Appl. Phys., **vol. 28**, 1220 (1995).
[3] S. Fujita, *et al.*, IEEE Trans. Appl. Supercond., **vol. 29**, 8001505 (2019).
[4] A. Molodyk, *et al.*, Nature Scientific Reports, **11** 2084 (2021).
[5] M. Murakami, *et al.*,, Supercond. Sci. Tech., **9**(12), 1015 (1996).
[6] H. Su, *et al.*, Phys. Rev. B, **70**, 054517 (2004).

Abstract ID: 30678

TOWARD THE PRACTICAL APPLICATION OF REBCO HIGH-TEMPERATURE SUPERCONDUCTING WIRE - BEYOND CRITICAL CURRENT

T. Kiss[1, 2], Z. Wu[2], S. Sera[2], S. Shiotani[2], R. Iwanaga[2], K. Higashikawa[1,2], V. Petrykin[3], S. Lee[3], X. Obradors[4], T. Puig[4]

[1] *Res. Inst. of Superconductor Science and Systems, Kyushu Univ., Fukuoka 819-0395, JAPAN*
[2] *Dept. of Electrical Engineering, Kyushu Univ., Fukuoka 819-0395, JAPAN*
[3] *Faraday Factory Japan LLC, Kanagawa 252-0132, JAPAN*
[4] *ICMAB-CSIC, Barcelona 08193, SPAIN*

REBCO high-temperature superconducting wire is expected to be applied to a wide range of innovative devices, such as compact fusion reactors, NMRs, and motors, due to its excellent critical current (I_c). On the other hand, further sophistication of process conditions is required, such as optimizing production conditions according to the usage environment, and mass production techniques for low-cost wires. Moreover, to realize superconducting applications with distinct low loss and high current capacity, it is essential to establish low-resistance joining technology of REBCO wires that excels in reproducibility and high reliability. In other words, for the practical application of REBCO wire, establishing its surrounding technologies as an engineering material, beyond just critical current, is an urgent issue. This talk introduces the advanced technologies the authors are working on toward the practical application of REBCO high-temperature superconducting wire. To obtain high-quality REBCO layers quickly and with high reproducibility, a precise understanding of the impact of complex manufacturing conditions on superconducting properties and the phase diagram during synthesis is required. However, the optimization of manufacturing conditions and the determination of phase diagrams have not yet fully moved beyond the realm of try and error. Our research aims to establish a new methodology for understanding the relationship between process conditions and wire characteristics by developing a magnetic measurement method that is non-destructive, non-contact, and high-speed, measuring characteristics in low temperature and magnetic fields which are the actual application environments of the wires. Based on examples of high-speed measurement of the relationship between process conditions during continuous PLD film formation and Ic and n-values, and the relationship between sample composition and process conditions and Ic under various conditions using the TLAG method, we introduce a data-driven approach to elucidating the effects of process conditions during wire manufacturing. Furthermore, regarding the joining between REBCO wires, as a technique that joins the outermost surface between Cu stabilization layers with low resistance and good reproducibility, we proposed a solder-free joining technique using only acoustic energy, along with its physical model, discussing the controllability of resistance values, selection of process parameters according to the target sample, evaluation of integrity of the joint, and considerations on the mechanism of degradation occurrence. This method enables joining with a joint resistivity of less than 20 $n\Omega cm^2$ within process times of less than one second, achieving a connection without degrading superconducting properties while also being excellent in mechanical strength.

Acknowledgements

This work is supported by Moonshot R&D - MILLENNIA Program Grant Number JPMJMS24A2 and JSPS KAKENHI Grant Number JP24H00320.

6 - ADVANCES AND CHALLENGES IN THE COMMERCIALIZATION OF SUPERCONDUCTIVITY APPLICATIONS

Abstract ID: 30413

ADVANCES AND CHALLENGES IN COMMERCIALIZATION OF SUPERCONDUCTING MAGNETS FOR MEDICAL APPLICATIONS

J. V. Minervini

Novum Industria LLC, Harvard, MA 01451, USA

Superconductivity plays a pivotal role in modern healthcare, enabling significant advances in medical diagnostics and cancer therapy. There are two primary medical applications of superconductivity, each with unique functions and requirements: MRI and particle beam radiotherapy. The most widespread and impactful application of superconductivity in medicine is in imaging and diagnostics, specifically in Magnetic Resonance Imaging (MRI). MRI scanners utilize superconducting magnets to generate strong, stable magnetic fields, enabling high-resolution images of internal body structures without invasive procedures. This technology provides patients with safer, more accurate diagnostic options. The second major application of superconductivity in medicine is found in particle beam radiotherapy used for cancer treatment. Although the use of superconducting magnets in this area is smaller compared to MRI applications, particle beam radiotherapy has become a critical, growing method for treating certain types of cancer. This approach offers targeted radiation therapy, improving outcomes for patients with specific medical needs. The integration of superconducting magnets into healthcare diagnostics and therapeutic treatments has led to substantial improvements in patient care, providing fewer invasive procedures, enhanced accuracy, and safer alternatives. Ongoing development of superconducting technologies continues to expand the capabilities of these essential diagnostic and treatment tools. While both MRI and hadron radiotherapy rely on superconducting magnets, their roles and technical demands differ, leading to distinct requirements for further commercialization. As such, each application is considered separately in this discussion, highlighting their unique contributions to medical science and patient health.

Abstract ID: 30546

OVERVIEW OF SMES FOR COMMERCIAL POWER APPLICATIONS

K. Higashikawa[1], T. Kiss[1], K. Shiohara[2]

[1] *Kyushu University, JAPAN*
[2] *SWCC Corporation, JAPAN*

Superconducting Magnetic Energy Storage (SMES) offers extremely fast response times and high round-trip efficiency, making it well suited for short-duration energy compensation in commercial power systems and industrial facilities. This talk provides an overview of SMES applications in the commercial power sector, organizing candidate use cases and associated performance requirements, and outlining both current status and future perspectives. Existing and demonstrated application areas include voltage sag mitigation, power quality enhancement, frequency support, short-cycle fluctuation compensation in fast control systems, and stability support during renewable energy grid integration. In addition, anticipated future use cases driven by increasing power electronics penetration and emerging electricity markets will be introduced, such as fast ancillary services, dynamic stabilization of DC links, short-duration support for power electronics-intensive loads, data centers as high-reliability power consumers, and provision of virtual inertia functions. The aim is to illustrate the scope of applications in which SMES may offer value and to provide a broad perspective on its potential role in future commercial power systems.

This work was partly supported by grants from Power Academy and JSPS KAKENHI Grant Number JP 25K01219.

Abstract ID: 30601

SUPERCONDUCTING MAGNETIC CORE REACTOR: A CONTRIBUTION TO EFFICIENT POWER FLOW CONTROL IN TRANSMISSION GRIDS

J. Murta-Pina[1,2,3], L. Miúdo[1,2], N. Amaro[1,2,3], A. Pronto[1,2,3], R. Pastor[4]

[1] *Centre of Technology and Systems, CTS-UNINOVA, 2829-516, Caparica, PORTUGAL*
[2] *NOVA School of Science and Technology, 2829-516, Caparica, PORTUGAL*
[3] *Intelligent Systems Associate Laboratory (LASI), 2829-516, Caparica, PORTUGAL*
[4] *R&D NESTER, 2685-038, Sacavém, PORTUGAL*

The integration of superconducting technologies into power grids has long been envisaged for its potential to minimize energy losses and enhance grid reliability. Among these technologies, superconducting magnetic core reactors present a novel approach to controlling power flow in transmission or even distribution networks. This is an old concept, but, unlike conventional reactors, which suffer from unreasonable resistive losses, superconducting magnetic core reactors leverage the unique properties of superconductors to enable highly efficient grid management.

This contribution will present the working principles and advantages of superconducting magnetic core reactors compared to conventional power flow control devices, emphasizing their role in improving grid flexibility and stability, particularly in the context of high renewable energy penetration. A comparative analysis will highlight technical and economic factors, including operational efficiency, footprint, and long-term cost-effectiveness. Furthermore, insights from the Portuguese transmission system operator will provide a practical perspective on the challenges that hinder the widespread adoption of superconducting technologies. Key concerns, such as high production costs, cooling infrastructure requirements, and regulatory uncertainties, will be discussed, shedding light on the barriers to commercialization. Despite these challenges, superconducting power flow control devices represent a paradigm-shifting solution for future power grids, particularly as energy systems transition toward higher shares of renewable generation.

Abstract ID: 30725

A SELECTIVE METAL LAYER REMOVAL METHOD FOR REBCO-COATED CONDUCTORS BASED ON ELECTROCHEMICAL TECHNIQUES AND INVESTIGATION OF PERFORMANCE DEGRADATION MECHANISMS

Z. Wang, S. Gao, F. Liu

Institute of Plasma Physics Chinese Academy Of Sciences, CHINA

Research on superconducting joint technology for REBa2Cu3O7-x (REBCO) coated conductors (CCs) contributes to kilometer-scale applications of REBCO tapes and to the development of nuclear magnetic resonance (NMR) magnets. The metal layer etching is a necessary step in the preparation of superconducting joints for REBCO tapes and can contribute to the direct application of many surface characterization techniques to the superconducting layer. The metal layer needs to be completely removed from the specified area and retain excellent performance and microstructure.

Since REBCO CCs are sensitive to most inorganic solutions, etching conditions can severely affect their performance and microstructure when using wet etching processes. Since purely chemical methods may cause irreversible damage to the performance and microstructure of superconducting layers and are not easy to control, we propose an etching method based on electrochemical methods, which removes two metal layers using only one solution and is easy to operate. We systematically investigated the effects of parameters such as solution concentration, temperature, time and voltage on the superconducting performance and microstructure, and obtained very stable etching parameters. SEM, XRD, Raman, XPS, and TEM analyses revealed that the underlying cause of performance degradation is the electrolytic dissolution of the edge superconducting layer due to tip effects.

Abstract ID: 30456

NET ZERO BY 2050 IS POSSIBLE

G. J. Levermore

The University of Manchester, Dept. of Mechanical Aerospace and Civil Engineering, M13 9PL, England, UK

This paper discusses whether Net Zero is possible by 2050, especially considering new technology and suitable infrastructure plans and suitable energy contracts for low-cost renewable energy.

A number of countries' governments, although they signed up to the Paris Agreement to try to keep the world's air temperature below 1.5C and so achieve net zero by 2050 are turning away from the 2050 net zero ambition. This is primarily due to cost and other pressures caused by the Ukraine war causing fossil fuel prices to rise substantially and also Trump's tariff and America first policy. There is also some scepticism about climate change itself by some populist politicians and this paper challenges this, briefly discussing the climate change science.

The paper also considers the ethics of climate change especially around the Golden Rule, part of most religions and many successful societies.

Abstract ID: 30567

THE SUPERCONDUCTING GLOBAL ALLIANCE (ScGA) AND THE COMMERCIALISATION OF SUPERCONDUCTIVITY

Z. Melhem[1,2]

[1] *Oxford Quantum Solutions Ltd., Oxford, OX2 9SB, UK*
[2] *Lancaster University, Department of Physics, Lancaster LA1 4YB, UK*

There have been significant advancements in superconducting technologies, particularly in the performance and supply of low- and high-temperature superconductors, as well as cryogenics and system integration. These developments are now prepared for scaling up and deployment in a variety of applications beyond their current uses, including MRI, NMR, and other fields in the physical sciences and research.

To fully unlock the potential of superconductors, it is crucial to establish new partnerships and alliances, as well as to explore innovative business models for investment and funding. This strategy will accelerate the development of commercial superconducting technologies and solutions across various sectors, ultimately transforming these innovations into successful commercial applications.

This presentation will review the progress of the Superconducting Global Alliance (ScGA) initiative [1] in tackling the challenges and opportunities related to the commercialization of superconductivity. The goal of this initiative is to promote a greener, healthier, more prosperous, and sustainable future. We will present the key challenges identified and the proposed strategic roadmaps aimed at accelerating the development of a commercial superconductivity ecosystem.

References

[1] Superconductivity Global Alliance (ScGA) ScGA – Superconductivity Global Alliance

Abstract ID: 30578

ROLE OF HTS MATERIALS IN DEVELOPING COMMERCIAL COMPACT PARTICLE THERAPY SOLUTIONS

A. Godeke[1,2]

[1] *Senior Consulting for Superconductivity, Hengelo, NETHERLANDS*
[2] *Compact PT: The Compact Particle Therapy Development Initiative, Hengelo, NETHERLANDS*

High Temperature Superconductors (HTS) that combine small, well-separated and twisted filaments with very high current-density (J_E) have recently become available. Since such superconductors enable compact, cryogen-free, fast-ramping magnets with high field-quality, they are ideally suited to trigger revolutionary advances in medical applications in general, and in Particle Therapy specifically. Despite the clinical advantages of Particle Therapy over X-ray treatment, leading to improved quality-of-life after treatment, and a dramatically reduced occurrence of secondary tumors in patients, accessibility to Particle Therapy is highly limited due to the huge installation cost of Particle Therapy compared to X-ray facilities.

In this presentation, it is demonstrated how recent HTS materials can be utilized to conceptually design Particle Therapy systems that are about 25% of the volume, and about 1/3rd of the price, of the current status-of-art, without compromising on clinical performance. It is shown how such reductions in system-volume and -price make Particle Therapy cost-competitive with X-ray facilities, and how such compact Particle Therapy systems can possibly even be retro-fitted in existing X-ray bunkers. However, despite this huge potential, and the readiness of the superconducting technologies, it is extremely difficult to entice the industry to invest in the development and marketing of such game-changing next generation Particle Therapy systems. The presentation will therefore conclude with a discussion on the difficulties in commercializing such concepts.

11th International Conference on Superconductivity and Magnetism ICSM2026
4th International Conference on Quantum Materials and Technologies ICQMT2026
19th April to 26th April, 2026, Ölüdeniz – Fethiye/Muğla, Türkiye
https://icsmforever.org/

Abstract ID: 30638

TECHNO-ECONOMIC ASSESSMENT OF A SUPERCONDUCTING DC TRACTION SUBSTATION

L. Ferreira[1,2], Y. Baazizi[1,2], S. Meunier[1,2], T. Phulpin[1,2], L. Quéval[1,2]

[1] *Université Paris-Saclay, CentraleSupélec, CNRS, GeePs, 91192 Gif-sur-Yvette, FRANCE*
[2] *Sorbonne Université, CNRS, GeePs, 75252 Paris, FRANCE*

Strengthening electric rail traction is a major lever for reducing greenhouse gas emissions in the transport sector. This work investigates the techno-economic feasibility of a 6.6 MW superconducting DC traction substation, in which the conventional transformer, diode rectifier, and copper cables are replaced by a partially superconducting transformer, a cryogenic diode rectifier, and superconducting cables (see Fig. 1). This approach could enable a more efficient use of limited space while meeting increasing power demands.

The techno-economic assessment follows a clearly structured methodology to ensure reproducibility and considers the uncertainty associated with the technology readiness level (TRL) of the various components. Sensitivity studies were performed, highlighting the key parameters influencing economic competitiveness. In addition, the analysis is based on data from two different prototypes. The first is a 3 kW superconducting DC traction substation prototype, which was characterized and compared with its conventional counterpart. The second prototype is a 100 kW three-phase diode rectifier with RC snubbers, cooled by liquid nitrogen cooling plates, which achieved efficiencies greater than 99%.

The results of the techno-economic assessment suggest that superconducting traction substations could be economically competitive with conventional alternatives, depending on civil engineering costs, cable length, cryogenic rectifier efficiency, and the cost of cryogenic refrigeration systems. The study confirms the relevance of superconducting and cryogenic components for next-generation railway systems.

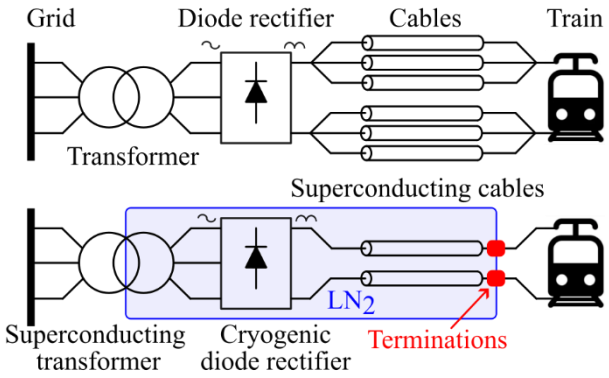

Fig. 1: *Conventional and superconducting DC traction substation architectures.*

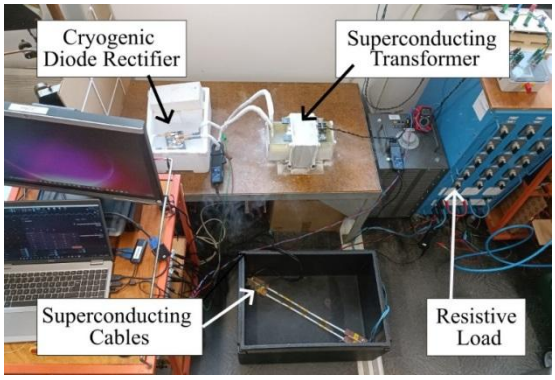

Fig. 2: *Superconducting DC traction substation prototype.*

References

[1] L. Ferreira, *Towards superconducting railway traction substations*, PhD thesis, University Paris-Saclay, France, Nov. (2025).

[2] Y. Baazizi, *Contribution to the development of cryo-converters for power electronics*, PhD thesis, University Paris-Saclay, France, Nov. (2025).

7 - ADVANCES IN MAGNETIC SENSOR TECHNOLOGIES

Abstract ID: 30038

DESIGN, MANUFACTURING, AND EXPERIMENTAL CHARACTERIZATION OF A LOW NOISE FLUXGATE SENSOR WITH Co-BASED MAGNETIC CORE

B. Tuncay[1,2], F.Inanır[2], P. Švec[3], I. Škorvánek[4], U.Topal[1]

[1] *TÜBİTAK National Metrology Institute (UME), 41470, Kocaeli, TURKIYE*
[2] *Yıldız Technical University, Dept. of Physics, 34220, Istanbul, TURKIYE*
[3] *Institute of Physics, Slovak Academy of Sciences, 84511, Bratislava, SLOVAKIA*
[4] *Institute of Experimental Physics, Slovak Academy of Sciences, 04001, Kosice, SLOVAKIA*

Fluxgate magnetometers are essential sensors utilized in applications requiring the precise measurement of low-amplitude magnetic fields, such as in geophysical surveys and attitude control systems [1, 2]. For systems where high resolution is essential, the intrinsic noise floor of the sensor has critical importance. This study presents the design, manufacturing, and experimental characterization of a low noise fluxgate sensor with a specific focus on performance optimization. In the design process, a high-permeability cobalt-based amorphous alloy was fabricated as the core material to achieve the goals of high sensitivity and low magnetic hysteresis [3, 4]. The fabricated cores were annealed at 250°C and 320°C under argon atmosphere to optimize the sensing properties. Geometry of the excitation and the pick-up coils were improved by matching with designed electronics. Experimental results demonstrate that the prototype sensor successfully achieves an optimum noise floor of 38 pT/√Hz at 1 Hz under nominal operating conditions.

References

[1] C. Lei, S. Zhi and Y. Zhou, Sensors, **21**, 2492 (2021).

[2] M. Butta and B. P. Schutte, IEEE Trans. Magn., **55**, 8638829 (2019).

[3] N. Murata, R. Nomura, and A. Matsuoka, J. Magn. Magn. Mater., **484**, 497 (2019).

[4] M. Dressler, M. Janosek, and M. Butta, AIP Adv. **11**, 015347 (2021).

11th International Conference on Superconductivity and Magnetism ICSM2026
4th International Conference on Quantum Materials and Technologies ICQMT2026
19th April to 26th April, 2026, Ölüdeniz – Fethiye/Muğla, Türkiye
https://icsmforever.org/

Abstract ID: 30068

DEVELOPMENT OF AMORPHOUS MICROWIRES FOR SENSOR APPLICATIONS

A. Zhukov[1,2,3], P. Corte-León[3,4,5], A. Gonzalez[1,2,3], V. Zhukova[1,2,3]

[1] Dept. Appl. Phys., EIG, Univ.Basque Country, UPV/EHU, 20018, San Sebastian, SPAIN
[2] IKERBASQUE, Basque Foundation for Science, 48011 Bilbao, SPAIN
[3] EHU Quantum Center, University of the Basque Country, UPV/EHU, SPAIN
[4] Dept. Polym.Adv. Mater., Univ. Basque Country, UPV/EHU San Sebastián 20018, SPAIN
[5] Department of Materials Science & Metallurgy, University of Cambridge, UK

Amorphous magnetic wires have attracted great attention owing to their excellent soft magnetic, mechanical and corrosion properties. Rather unusual magnetic properties such as magnetic bistability or Giant Magnetoimpedance (GMI) effect are suitable for various sensor applications [1]. Recent tendency in devices miniaturization stimulated development of thin (few μm diameters) microwires. Generally, better magnetic softness and higher GMI effect have been observed in Co-rich amorphous microwires (Fig1b), while Fe-rich amorphous microwires present spontaneous magnetic bistability related to remagnetization process through fast domain wall propagation (see Fig.1a). Less expensive Fe-rich microwires are preferable for the applications, but exhibit rather high magnetostriction coefficient, λ_s, and hence present quite low GMI effect. We designed the post- processing allowing remarkable improvement of soft magnetic properties of Fe- and Fe-Co based glass-coated microwires [1,2]. Stress annealing of Fe-rich microwires allows considerable magnetic softening (Fig.1c), GMI effect enhancement and remarkable improvement of domain wall (DW) dynamics. In Co-rich microwires stress-annealing allows better magnetic softness (Fig.1d), GMI effect improvement due to induction of transverse magnetic anisotropy at high enough annealing temperature. On the other hand, conventional annealing allows to obtain Co-rich microwires with magnetic bistability (Fig.1d) and rather fast DW dynamics [1].

Observed versatile properties of properly processed glass-coated amorphous microwires with enhanced and tuneable soft magnetic properties make them suitable for various sensor applications.

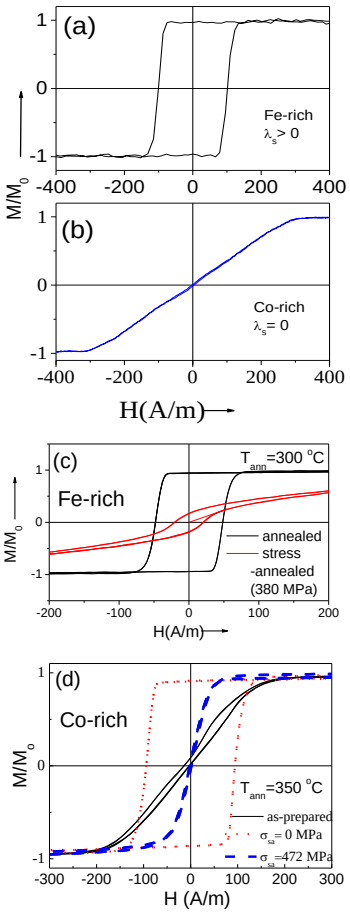

Fig.1: *Typical hysteresis loops of as-prepared (a,b) and processed (c,d) Fe- and Co-rich amorphous microwires.*

References

[1] A. Zhukov, P. Corte-Leon, L. Gonzalez-Legarreta, M. Ipatov, J. M. Blanco, A. Gonzalez and V. Zhukova, J. Phys. D: Appl. Phys. **55**, 253003 (2022).

[2] V. Zhukova, J. M. Blanco, M. Ipatov, M.Churyukanova, S. Taskaev and A. Zhukov, Sci. Reports, **8**, 3202 (2018).

Abstract ID: 30548

MAGNETIC SENSING AT BOSCH

P. Mather[1], Bosch Sensortec TMR Team[1,2], Bosch Quantum Sensing[3]

[1] Robert Bosch LLC, 960 W. Elliot Rd. Tempe, AZ 85284 GERMANY
[2] Bosch Sensortec, GmbH, Gerhard-Kindler-Straße 9, 72127 Reutlingen, GERMANY
[3] Bosch Quantum Sensing GmbH Grönerstraße 9, 71636 Ludwigsburg, GERMANY

The rapidly expanding field of magnetic sensors touches upon our everyday lives in myriad ways. Magnetic sensors ensure our safety through detection of wheel speed rotation in antilock braking systems, and by enabling precise and reliable measurement of steering wheel angular position. They improve the efficiencies of electrical power delivered to high current electrical motors and generated in solar arrays. Magnetic sensors are an integral part of the sensing system suite forming the intuitive human - machine interface present in game controllers, cell phones, and virtual and augmented reality devices. Furthermore, with enhanced detectivity afforded by recent advances in quantum sensing, applications are rapidly expanding into human machine interfaces (HMI) and medical imaging of heart and brain waves.

The recent acceleration in magnetometry arose from the virtuous cycle of an expanding application field ushered in by innovations and technological advancements, which lead to new market opportunities. Reducing noise and power consumption while simultaneously delivering higher accuracy required a shift away from the prior generations of Hall and Anisotropic Magneto Resistance technologies and incorporation of novel designs and process technologies. Tunneling Magneto Resistance (TMR) technology is showing the highest growth rate among the magnetic sensing technologies as it affords new degrees of freedom in transducer design: Decoupling magnetic and electrical performances and allowing independent control of each. Adjustable device impedance allows a fully optimized read path to be tailored for the integration with the Application Specific Integrated Circuitry (ASIC). Simultaneously, the high output signal of the technology can be utilized to both extend the sensing field range and the signal strength. The drive to smaller form factors enabled but such integration opens up unique mounting locations and assembly solutions, such as brushless DC motor rotor sensing, ultra-low current, compact switches and countless other space sensitive positioning applications. A compact magnetometer that is monolithically integrated with CMOS, offering the flexibility of in plane and out of plane field sensitivity, can be tuned to address these applications.

Essential elements of a high-performance wafer level chip scale three axis monolithically integrated TMR magnetometer will be described. The TMR layers and interconnects are deposited directly on top of a mixed signal CMOS process technology. A high throughput lot-level wafer batch processing step is performed to create two orthogonal pinned reference layer directions for orthogonal in plane response directions. Integrated flux guides steer the out of plane magnetic field into the in-plane sense elements allowing detection of the magnetic fields in all three directions with no additional thickness added to the overall chip height [1].

At Bosch Quantum Sensing, advances in miniaturization of quantum sensors have enabled a cell phone sized magnetometer based on nitrogen vacancies in diamond. This enables unprecedented detectivity and precise vectorial measurements in such a compact form factor. The goal is to achieve an IC sized footprint while preserving detectivity and robustness, opening up new applications and markets. Recent advances in this technology will be discussed. With global leadership in the motion sensing marketplace, achieved through pioneering technology developments across a wide portfolio of MEMS sensors, Bosch produces over 4 million motion sensors a day. Bosch Sensortec is a wholly owned subsidiary which develops products tuned to the consumer electronics market. Bosch Sensortec has been the world leading supplier of consumer MEMS and electronic compass modules and is developing the next generation of magnetic sensing solutions.

References

[1] https://www.bosch-sensortec.com/products/motion-sensors/
[2] https://www.bosch-sensortec.com/products/motion-sensors/magnetometers/bmm350/
[3] https://www.bosch-quantumsensing.com/

Abstract ID: 30072

SENSING SPIN PRECESSION WITH TRANSMISSION ELECTRON MICROSCOPY

A. Jaroš, M. S. Seifner, J. Toyfl, B. Czasch, S. B. Romero, I. C. Bicket, P. Haslinger

Vienna Center for Quantum Science and Technology, Atominstitut, USTEM, Technische Universität Wien, Stadionallee 2, Vienna, 1020, AUSTRIA

Transmission Electron Microscopy (TEM) offers sub-ångström spatial resolution and provides an exceptionally versatile platform for materials characterization [1]. We have developed a novel spectroscopic technique that enables the detection of microwave (MW)-driven spin precession within a TEM (Fig. 1a) [2, 3]. This method offers a powerful and cost-effective route to probe magnetization dynamics with spatial resolution far beyond the limits of conventional Brillouin light scattering (BLS) and even large-scale synchrotron facilities. As a result, it has the potential to reveal dynamic magnetic phenomena that have remained inaccessible to existing techniques.

We present proof-of-concept measurements in which the free-space electron probe of a TEM serves as a nanoscale signal receiver (Fig. 1b) [3]. The strong objective-lens field of the TEM is employed both to align the spins and to focus and shape the electron probe, while a microcoil resonator drives the specimen. We demonstrate that both electron spin resonance (ESR, Fig. 1c) and ferromagnetic resonance (FMR) spectra can be detected through picoradian-scale deflections of the electron probe.

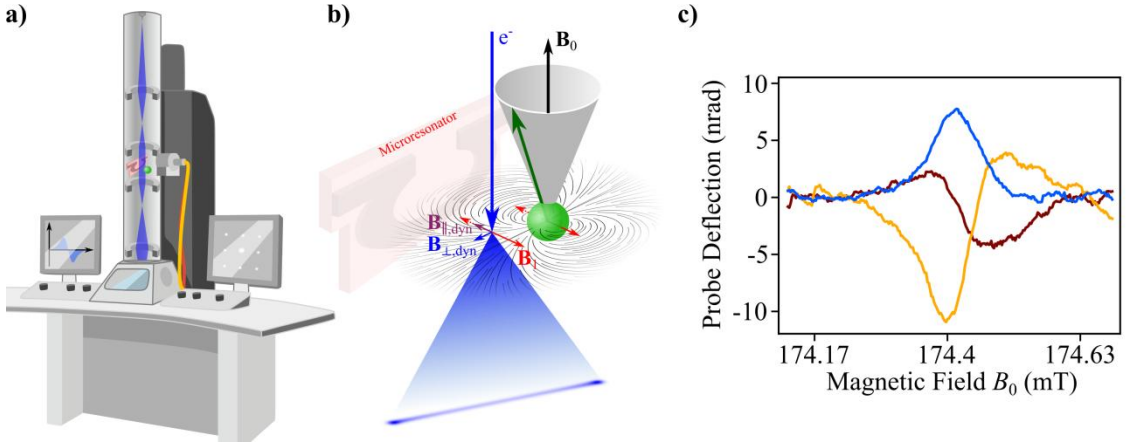

Fig. 1: *(a) Schematic of the TEM equipped with a custom-built MW sample holder that enables sensing of spin precession using a free-space electron probe. (b) Detailed view of the sample-holder region, where spins are aligned by the B_0 field of the TEM objective lens while a microresonator provides continuous MW excitation. The electron probe is deflected by both the driving B_1 field and the specimen's dynamic magnetic field B_{dyn}, enabling phase-locked signal detection from deflection patterns averaged over billions of precession cycles. (c) Spatially resolved ESR spectra via the electron probe deflection.*

References

[1] Y. Kohno, *et al.*, Nature **602**, 234-239 (2022).

[2] A. Jaroš, *et al.*, Ultramicroscopy **278**, 114224 (2025).

[3] A. Jaroš, *et al.*, arXiv:2503.06761 (2025).

Abstract ID: 30110

QUANTUM SENSING OF MAGNETIC PHENOMENA WITH CRYOGENIC SCANNING NV MAGNETOMETRY

M. Bacani[1], A. Sharma[1], C. Kelvin von Grundherr[1], D. Andres[1], J. Rhensius[2], G. Puebla-Hellmann[2], A. Morales[2], C. Schäfermeier[1]

[1] *attocube systems GmbH, 85540 Haar, GERMANY*
[2] *QZabre AG, 8050 Zurich, SWITZERLAND*

Emerging technologies increasingly rely on precise control and understanding of magnetic phenomena at the nanoscale and cryogenic temperatures. NV magnetometry offers a unique approach, combining quantum sensing with scanning probe precision to achieve magnetic field mapping at resolutions and sensitivities beyond conventional limits. We present cw-ODMR imaging of materials hosting emergent quantum and topological magnetic phenomena, including Abrikosov vortices in BSCCO and YBCO, interlayer domain textures in twisted bilayer CrSBr, magnetic domains in skyrmions-hosting Ir/Fe/Co/Pt multilayers, and meronic spin textures in synthetic antiferromagnets. The imaging was performed by the cryogenic scanning NV magnetometer integrated into a closed-cycle cryostat with turnkey operation from 2–300 K. The system reaches the sensitivity of ≤3 μT/√Hz for quantitative stray-field mapping [1]. These results exemplify the versatility of cryogenic NV magnetometry as a tool for probing superconductivity, correlated magnetism, and emergent spin textures in quantum materials.

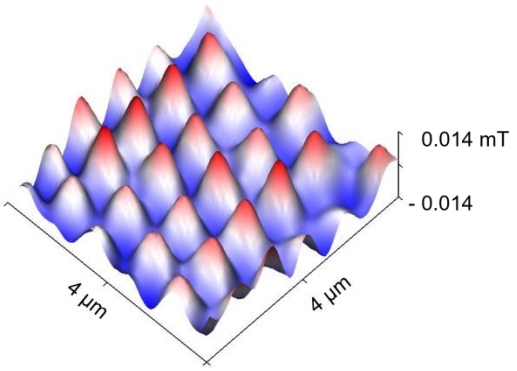

Fig. 1: *Magnetic vortices in BSCCO-2212 sample acquired by cw-ODMR at T=71 K, measured in tip-sample contact. The sample was field-cooled at B_z=3.7 mT and measured in bias field of B=7 mT projected along the NV axis.*

References

[1] C. Schäfermeier, *et al.*, e-print arXiv:2502.16599 (2025).

Abstract ID: 30483

THE DETECTION OF NUCLEAR QUADRUPOLE RESONANCE SIGNALS INSIDE OBJECTS

G. Mozzhukhin[1], P. Kupriyanov[1], S. Kazan[1], B. Çolak[1], G. Kupriyanova[2], B. Rameev[1,3,4]

[1] Physics Department, Gebze Technical University, Gebze, Kocaeli, TURKEY
[2] Baltic Federal University, Kaliningrad, RUSSIAN FEDERATION
[3] Kazan State Power Engineering University, Kazan/Tatarstan, RUSSIAN FEDERATION
[4] Zavoisky Physical-Technical Institute – Subdivision of the FRC "Kazan Scientific Center of Russian Academy of Sciences", Kazan/Tatarstan, RUSSIAN FEDERATION

The application of nuclear quadrupole resonance (NQR) for the detection of hazardous and harmful objects is a promising approach in civil security in transport [1-3]. In some cases, the type of container may influence the remote NQR detection of nitrogen-based explosives and narcotic substances. Plastic, wood and glass containers do not affect the NQR signal, while metal or metal- layered containers will partially or completely screen the signal. Not only containers, but the presence of other conducting objects may affect remote detection.

In this work, we study the influence of metals and liquids on the detection of NQR signals of illicit substances. The influence of different objects in a scanned volume, as well as the effect of shielding, has been studied and discussed. We have also shown the feasibility of NQR detection of nitrogen-based substances inside small electronic devices (e.g., mobile phones).

Acknowledgements

The current research was supported by the Technology Transfer Office (TTO) of Gebze Technical University.

References

[1] A. N. Garroway, M. L. Buess, J. B. Miller, B. H. Suits, A. D. Hibbs, G.y A. Barrall, R. Matthews, and L. J. Burnett, *Remote Sensing by Nuclear Quadrupole Resonance*, IEEE Trans. Geosci. Remote Sens. **39(6)**, 1108-1118 (2001).

[2] B. Rameev, G. Mozzhukhin, B. Aktaş, *Magnetic Resonance Detection of Explosives and Illicit Materials*, Appl. Magn. Reson. 43, 463–467 (2012).

[3] Magnetic Resonance Detection of Explosives and Illicit Materials. Eds: T. Apih, B. Rameev, G. Mozzhukhin, J. Barras, NATO Science for Peace and Security Series B: Physics and Biophysics, Springer (2014).

8 - ADVANCES IN NICKELATE SUPERCONDUCTORS

Abstract ID: 30227

SPIN DENSITY WAVE ORDER IN LAYERED NICKELATEs $La_3Ni_2O_7$ AND $La_2PrNi_2O_7$ VIA NEUTRON DIFFRACTION

I. Plokhikh[1,2]

[1] *TU Dortmund, 44227, Dortmund, GERMANY*
[2] *Recearch Center Future Energy Materials and Systems, 44227, Dortmund, GERMANY*

Layered nickelates, particularly $La_3Ni_2O_7$ and its derivatives, have emerged as a compelling platform for exploring unconventional superconductivity [1, 2]. These materials exhibit high-temperature superconductivity under pressure, placing them among the few transition-metal oxides with such properties alongside cuprates and iron-based superconductors. The intricate interplay of spin density waves (SDWs) [3], charge density waves (CDWs), and electronic correlations in these systems highlight their potential as key candidates for elucidating the mechanisms of unconventional superconductivity.

In this study, I present direct evidence of long-range SDW order in bilayer nickelates $La_3Ni_2O_7$ and $La_2PrNi_2O_7$ using high-intensity neutron powder diffraction (NPD) [4]. Magnetic Bragg reflections were observed below 150 K at propagation vectors $q_1 = (0, ½, 0)$ for both compounds and an additional vector $q_2 = (½, ½, 0)$ exclusively in undoped $La_3Ni_2O_7$. Representation and magnetic symmetry-guided analysis revealed spin-structures with alternating low- (0.05–0.075 μ_B) and high-moment (~0.66 μ_B) stripes within single Ni layers, forming bilayers through antiferromagnetic stacking along the *c*-axis. The proposed models are substantiated by the muon spectroscopy data. The coexistence of two distinct magnetic stacking polymorphs corresponding to q_1 and q_2 in $La_3Ni_2O_7$ further underscores the quasi-2D nature of its magnetic order.

These findings provide critical insights into the magnetic ground state of layered nickelates and establish a foundation for understanding their role as precursor states to superconductivity. Future studies will be important to unravelling the connection between SDW suppression and superconducting onset, potentially confirming SDWs as competing or complementary instabilities in these systems. This work advances our understanding of nickelate physics while channelling the way for targeted exploration of superconductivity mechanisms in transition-metal oxides.

References

[1] M. Wang, H.-H. Wen, T. Wu, *et al.*, Chinese Physics Letters, **41**, 077402 (2024).

[2] N. Wang, G. Wang, X. Shen, *et al.*, Nature, **634**, 579–584 (2024).

[3] R. Khasanov, T. J. Hicken, D. J. Gawryluk, *et al.*, Nature Physics, **21**, 430–436 (2025).

[4] I. Plokhikh, T. J. Hicken, L. Keller et al. arXiv:2503.05287 [cond-mat.supr-con] (2025).

Abstract ID: 30272

ELEMENTARY EXCITATIONS IN SUPERCONDUCTING $Nd_{1-x}Eu_xNiO_2$ AND COMPARISON WITH THE CUPRATES

J. Pelliciari

NSLS-II, Brookhaven National Laboratory, 11772, Upton, USA

The discovery of superconductivity in infinite layer of nickelates offers the possibility of studying a new class of $3d^9$ system where the phase diagram displays an interplay of magnetism and superconductivity [1]. The detailed investigation of the microscopic and spectroscopic characteristics of these systems requires high quality samples to perform advanced spectroscopy. In this respect $Nd_{1-x}Eu_xNiO_2$ represents one of the best candidate sfor high quality samples thanks to the flexibility of Europium to assume different oxidation states such as 2+ and 3+ enabling the synthesis of high-quality perovskites films and the topotatic reduction [2]. In this talk I will present x-ray absorption spectroscopy at the Ni and Europium edges to clarify the oxidations states of these materials. From this absorption we can observe an intermixing of oxidation states of europium in the infinite layer and confirm the actual doping of holes into the Ni states. Building on this we perform Resonant Inelastic X-ray Scattering (RIXS) studies on multiple samples uncovering the orbital configuration and the energy of the spin excitations. We observe persistent long-range correlations across the superconducting dome as well as a renormalization to lower energies of the spin excitations. This effect is similar to $Nd_{1-x}Sr_xNiO_2$ but different than what observed in other cuprates. I will proceed by making comparisons between the spectroscopy/scattering signals observed in nickelates and cuprates highlining commonalities and differences.

References

[1] D. Li, *et al.*, Nature **572**, pages 624–627 (2019).

[2] W. Wei, *et al.*, Science Advances, **9(27)**, eadh3327 (2023).

Abstract ID: 30275

UNIVERSAL ELECTRONIC STRUCTURE OF LAYERED NICKELATES VIA OXYGEN-CENTERED PLANAR ORBITALS

A. Damascelli[1,2]

[1] *Quantum Matter Institute, UBC, Vancouver, CANADA*
[2] *Physics & Astronomy Department, UBC, Vancouver, CANADA*

In a series of ground-breaking discoveries, superconductivity has been demonstrated in the family of multi-layered nickelates $La_3Ni_2O_7$ and $La_4Ni_3O_{10}$, with Tc as high as 91 and 30K respectively under moderate pressure. Key questions remain open regarding the low-energy electronic states that support superconductivity in these compounds. Here we take advantage of the natural polymorphism between bilayer (2222) and alternating monolayer-trilayer (1313) stacking sequences that arises in bulk $La_3Ni_2O_7$ crystals, and by employing angle-resolved photoemission spectroscopy (ARPES) we identify a universal low-energy electronic structure in this family of materials. We observe the fingerprint of a doping-dependent spin-density wave (SDW) instability – strong and coherent enough to reconstruct the Fermi surface, both by gapping out regions of the low-energy electronic structure as well as translating the β pocket by a vector Qtβ consistent with the results of previous neutron and x-ray scattering experiments. This demonstrates a universal connection between magnetism and fermiology in these materials [1]. Using an effective tight-binding model, we simulate the spectral weight distribution observed in our ARPES dichroism experiments and establish that the low-energy electronic phenomenology is dominated by oxygen-centered planar orbitals, which – upon moving along the Fermi surface away from the Ni-O-Ni bond directions – evolve from the $d3x^2-r^2$ and $d3y^2-r^2$ symmetry characteristic of 3-spin polarons (3SP) to the familiar dx^2-y^2 Zhang-Rice singlets (ZRS) that support high-temperature superconductivity in cuprates. By inclusion of magnetic moments on plaquettes of oxygen orbitals in our model, we show that ZRS-like states mediate the SDW. Combined with the observation that oxygen annealing is required to induce superconductivity in both thin films and bulk $La_3Ni_2O_7$, this demonstrates that the ZRS population dictates whether the ground state favors density-wave order or superconductivity – with hole doping suppressing the former and stabilizing the latter, as in the cuprates. Despite the multiorbital nature of the nickelates, our work thus establishes an empirical correspondence between their low-energy electronic structure and that of the cuprates, suggesting a common origin for unconventional superconductivity in both families [1].

References

[1] C. C. Au-Yeung, X. Chen, S. Smit, M. Bluschke, *et al.*, arXiv:2502.20450 (2025).

Abstract ID: 30276

AMBIENT PRESSURE GROWTH OF NICKELATE SINGLE CRYSTALS WITH SUPERCONDUCTIVITY UP TO 96 K UNDER HIGH PRESSURE

J. Zhang

State Key Laboratory of Crystal Materials, Institute of Crystal Materials, Shandong University, Jinan 250100, Shandong, CHINA

Recently, the Ruddlesden-Popper bilayer nickelate $La_3Ni_2O_7$ has emerged as a superconductor with a transition temperature (T_c) of ~80 K above 14 GPa. Achieving higher T_c in nickelate superconductors, along with the synthesis of reproducible high-quality single crystals without relying on high oxygen-pressure growth conditions, remains a significant challenge. Here we report superconductivity up to 96 K under high pressure in bilayer nickelate single crystals synthesized at ambient pressure. Energy dispersive spectroscopy, single crystal X-ray diffraction, nuclear quadrupole resonance, and scanning transmission electron microscopy evidenced high crystal quality of $La_2SmNi_2O_{7-\delta}$ single crystals. $La_2SmNi_2O_7$ exhibits clear bulk superconductivity, including zero resistivity ($T_{c,\,max}^{onset}$ = 92 K and $T_{c,\,max}^{zero}$ = 73 K at 21.6 GPa) and Meissner effect (T_c = 60 K at 20.6 GPa). Our low-temperature high-pressure structural study indicates that both monoclinic and tetragonal structures can support superconductivity in this bilayer nickelate. Furthermore, we established a correlation between Tc under high pressures and in-plane lattice distortion at ambient conditions, corroborated by observing even higher T_c onset of 96 K in $La_{1.57}Sm_{1.43}Ni_2O_{7-\delta}$. This study overcomes key limitations in nickelate superconductor crystal growth, resolves the crystal structure in the superconducting state, and demonstrates an effective pathway towards achieving higher T_c.

In collaboration with Feiyu Li, Zhenfang Xing, Di Peng,* Jie Dou, Ning Guo, Liang Ma, Yulin Zhang, Lingzhen Wang, Jun Luo, Jie Yang, Jian Zhang, Tieyan Chang, Yu-Sheng Chen, Weizhao Cai, Jinguang Cheng, Yuzhu Wang, Yuxin Liu, Tao Luo, Naohisa Hirao, Takahiro Matsuoka, Hirokazu Kadobayashi, Zhidan Zeng, Qiang Zheng, Rui Zhou, Qiaoshi Zeng,* and Xutang Tao*

References

[1] F. Li, *et al.*, *Bulk superconductivity up to 96 K in pressurized nickelate single crystals*, Nature (2025).

Abstract ID: 30277

SPIN AND ORBITAL EXCITATIONS OF TRILAYER NICKELATES

Q. Wang

Department of Physics, The Chinese University of Hong Kong, CHINA

The recent discovery of superconducting nickelates has inspired extensive efforts to understand their low-energy properties [1, 2]. A Ni L-edge resonant inelastic x-ray scattering (RIXS) and an inelastic neutron scattering studies on bilayer $La_3Ni_2O_7$ have revealed dispersive spin excitations indicating a dominant inter-layer exchange coupling of $J_z \sim 70$ meV [3, 4]. While recent RIXS studies of trilayer nickelates have reported signatures of spin excitations [5, 6], their dispersions are yet to be determined. It thus remains unclear whether bilayer and trilayer nickelates share common magnetic interactions that may underpin the superconducting pairing mechanism. In this talk, I will present our recent RIXS study of trilayer nickelate single crystals $La_4Ni_3O_{10}$ and $Pr_4Ni_3O_{10}$ at Ni L-edge and O K-edge resonances. While the orbital excitations exhibit similarities to those in $La_3Ni_2O_7$, distinct low-energy excitations are observed in $La_4Ni_3O_{10}$. We identify two localized magnetic excitation modes at around 0.1 eV and 0.2 eV. Additional excitations were observed around 50 meV, originating from collective spin excitations. Our results highlight the distinct magnetism of trilayer nickelates, and suggest that magnetic interactions may serve as a common pairing strength in the nickelates.

References

[1] H. Sun, *et al.*, Nature **621**, 493 (2023).

[2] Y. Zhu, *et al.*, Nature **631**, 51 (2024).

[3] X. Chen, *et al.*, Nat. Commun. **15**, 9597 (2024).

[4] T. Xie, *et al.*, Sci. Bull. **69**, 3221 (2024).

[5] S. TenHuisen, *et al.*, Phys. Rev. B **111**, 165145 (2025).

[6] S. Zhang, *et al.*, arXiv:2509.20727.

Abstract ID: 30290

TRIPLON-MEDIATED COOPER PAIRING IN BILAYER NICKELATES

G. Khaliullin

Max Planck Institute for Solid State Research, Heisenbergstr. 1, 70569 Stuttgart, GERMANY

We propose a microscopic model [1] for the high-temperature superconductivity in bilayer nickelates. The model reveals the physical mechanism by which the in-plane compressive strain stabilizes the superconductivity over charge- and magnetically-ordered states. The Cooper pairing is mediated by a weakly dispersive singlet-to-triplet excitations ("triplons") of the interlayer spin dimers. The calculated momentum dependence of the gap function [2] well reproduces the experimental data. A general phase behavior of the model is discussed.

References

[1] G. Khaliullin and J. Chaloupka, arXiv:2506.16360.

[2] H. Liu and G. Khaliullin, unpublished.

Abstract ID: 30296

OXYGEN-DRIVEN ELECTRONIC AND LATTICE INSTABILITIES IN $La_3Ni_2O_7$

Y. Lu[1,2]

[1] *National Laboratory of Solid State Microstructures and School of Physics, Nanjing University, Nanjing 210093, CHINA*

[2] *Collaborative Innovation Center of Advanced Microstructures, Nanjing University, Nanjing 210093, CHINA*

The Ruddlesden-Popper nickelate $La_3Ni_2O_7$ exhibits high-temperature superconductivity under pressure, while at ambient conditions it hosts pronounced competing electronic and structural instabilities. In this talk, I discuss how oxygen plays a central role in shaping these phenomena through distinct electronic and lattice mechanisms. From the electronic perspective, the mixed-valence nature of nickel places $La_3Ni_2O_7$ in a small or negative charge-transfer regime, where ligand oxygen holes become active low-energy degrees of freedom. These ligand holes naturally promote coupled charge, spin, and lattice instabilities, which can be suppressed by pressure or carrier doping [1]. From the structural perspective, oxygen defects such as vacancies and interstitials induce lattice distortions and strongly modify local coordination and electronic coherence, suppressing superconductivity through reduced coherence or the stabilization of weakly correlated metallic states [2]. These theoretical results find support in recent experiments, including direct imaging of ligand holes, optical evidence for orbital-selective instabilities, spectroscopic evidence for spin-density-wave order and interlayer-superexchange-dominated magnetic excitations, as well as observations of oxygen defects suppressing superconductivity [3-5]. Together, these studies highlight oxygen, through its dual electronic and structural roles, as a key element governing instabilities and superconductivity in $La_3Ni_2O_7$.

References

[1] X. Chen, *et al.*, arXiv:2307.07154; Phys. Rev. B **111**, 014515 (2025).

[2] P. Jiang, *et al.*, arXiv:2512.00301.

[3] Z. Dong, *et al.*, Nature **630**, 847 (2024).

[4] Z. Liu, *et al.*, Nat. Commun. **15**, 7570 (2024).

[5] X. Chen, *et al.*, Nat. Commun. **15**, 9597 (2024).

Abstract ID: 30305

UNCONVENTIONAL SUPERCONDUCTIVITY IN INFINITE-LAYER SAMARIUM NICKELATES

D. Li

Department of Physics, City University of Hong Kong, Kowloon, Hong Kong SAR, CHINA

Infinite-layer nickelates have emerged as a frontier platform for studying unconventional superconductivity beyond the cuprates. In this talk, I will present our recent advances on samarium-based infinite-layer nickelate thin films, which exhibit enhanced superconductivity and a mixed two- and three-dimensional superconducting character arising from strong coupling between rare-earth 5*d* and Ni 3*d* orbitals. I will further highlight our discovery of robust field-induced re-entrant superconductivity in heavily Eu-doped $Sm_{0.95-x}Ca_{0.05}Eu_xNiO_2$, where superconductivity suppressed at low fields re-emerges above 6 T and persists to 45 T. This exotic high-field state results from the interplay between NiO-plane superconductivity and Eu^{2+}-sublattice magnetism, revealing a unique coexistence of magnetism and superconductivity within a single material system. These findings demonstrate how rare-earth-site engineering and magnetic-field tuning provide powerful routes for realising and manipulating magnetically enabled high-field superconductivity.

References

[1] M. Yang, H. Wang, J. Tang, J. Luo, *et al.*, *Enhanced Superconductivity and Mixed-dimensional Behaviour in Infinite-layer Samarium Nickelate Thin Films*, arXiv:2503.18346 (2025).

[2] M. Yang, J. Tang, X. Wu, H. Wang, *et al.*, *Robust Field Re-entrant Superconductivity in Ferromagnetic Infinite-layer Rare-Earth Nickelates*, arXiv:2508.14666 (2025).

Abstract ID: 30543

UNDERSTANDING THE PAIRING MECHANISM OF BILAYER NICKELATES

F. Yang

School of Physics, Beijing Institute of Technology, Beijing 100081, CHINA

The discovery of high-temperature superconductivity (HTSC) in bulk $La_3Ni_2O_7$ under high pressure (HP) and its film at ambient pressure (AP) has become an emergent hot-spot frontier. Based on our series of work, we proposed the minimal model regarding the pairing mechanism of this material, as shown in Fig. 1. Fig.1(a) shows that each nickel atom hosts the nearly half-filled d_{z2} orbital and the nearly 1/4-filled d_{x2-y2} orbital. Under strong Hubbard-repulsion, the d_{z2} orbital is nearly a localized spin with interlayer spin exchange, and the charge carriers reside on the d_{x2-y2} orbitals. Fig. 1(b) shows the effective AFM interlayer superexchange interaction $J_\perp$ between the $3d_{x2-y2}$ orbitals transmitted from that between the $3d_{z2}$ orbitals via the on-site Hund's rule coupling J_H. These considerations lead to the single d_{x2-y2} orbital bilayer t-J-$J_\perp$ model [1]. With this model, we can naturally understand why HTSC arises under HP or in the film at AP [2]. Using this model, we predicted that the substitution of the element La with Sm or Nd will prominently enhance the Tc [3], which has been verified by recent experiments. We also proposed that an imposed perpendicular electric field can strongly enhance the T_c of $La_3Ni_2O_7$ film at AP [4], which is ready for experimental verification. Very recently, using the model, we have provided a unified understanding toward the experimental parameters dependence of T_c, establishing this model as the minimal model regarding the pairing mechanism in the bilayer nickelates.

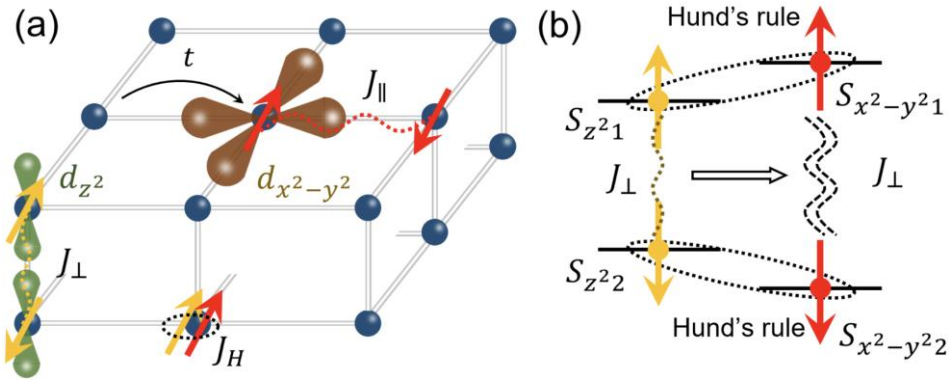

Fig. 1: *(a) Schematic diagram for the two-orbital bilayer t-J-J_H model. The charge carriers reside on the $3d_{x2-y2}$ orbitals. The $3d_{z2}$ orbital is a localized spin with interlayer spin exchange $J_\perp$. (b) Schematic diagram showing the effective AFM interlayer superexchange interaction $J_\perp$ between the $3d_{x2-y2}$ orbitals transmitted from that between the $3d_{z2}$ orbitals via the on site Hund's rule coupling J_H.*

References

[1] C. Lu, Z. Pan, F. Yang, and C. Wu, Phys. Rev. Lett. **132**, 146002 (2024).
[2] C. Lu, M. Zhang, Z. Pan, C. Wu, and F. Yang, Commun. Phys. **8**, 354 (2005).
[3] Z. Pan, C. Lu, F. Yang, and C. Wu, Chin. Phys. Lett. **41**, 087401 (2024).
[4] Z.-Y. Shao, J.-H. Ji, C. Wu, D.-X. Yao, and F. Yang, arXiv: 2411.13554 (Nat. Commun. in press, with DOI:10.1038/s41467-025-67880-5).

Abstract ID: 30841

BILAYER NICKELATE AS A POLAR METAL WITH CHECKERBOARD CHARGE ORDER

R. Misawa, M. Hirschberger

Department of Applied Physics, The University of Tokyo, Bunkyo, Tokyo 113-8656, JAPAN

The Ruddlesden-Popper (RP) family of layered transition metal oxides is a platform for strongly correlated electron physics, including charge ordering, multiferroics, and superconductivity. Here we present our recent study that reveals the charge order in the bilayer nickelate $La_3Ni_2O_7$ under ambient conditions [1]. Using synchrotron X-ray diffraction on a high-quality single crystal, we resolve faint reflections, nearly four orders of magnitude weaker than the main Bragg reflections, that were overlooked in prior studies. The existence of these reflections evidences a polar crystal structure, rather than the widely employed centrosymmetric structure model. The polarity is induced by checkerboard charge order on nickel sites in combination with octahedral tilting. Our results connect $La_3Ni_2O_7$ to the broader field of RP phases with broken inversion symmetry and charge order, proposing the polar charge order as a competing phase of its superconducting state. Finally, we present our recent experiments on bond orders in kagome metals [2,3] and on multipoles in altermagnets [4].

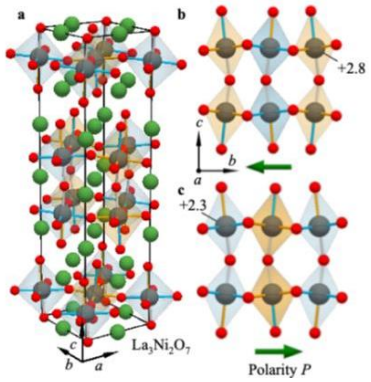

Fig. 1: *Polar, checkerboard charge order in $La_3Ni_2O_7$ under ambient conditions.* ***a****, Revised crystal structure of $La_3Ni_2O_7$ with two inequivalent Ni sites.* ***b,c****, Inversion-paired domains with polarity P. The polarity arises from the combination of charge and bond alternations.*

References

[1] R. Misawa, *et al.*, arXiv:2603.25119 (2026).
[2] R. Misawa, *et al.*, Advanced Materials **38**, e13015 (2026).
[3] R. Misawa, *et al.*, arXiv:2604.01691 (2026).
[4] R. Misawa, *et al.*, submitted.

Abstract ID: 30379

THEORY OF SUPERCONDUCTIVITY IN PRESSURIZED BILAYER NICKELATE $La_3Ni_2O_7$

G. Su[1,2]

[1] *Institute of Theoretical Physics, Chinese Academy of Sciences, Beijing 100190 CHINA*
[2] *Kavli Institute for Theoretical Sciences, University of Chinese Academy of Sciences, Beijing 100190 CHINA*

Since its landmark discovery in 1986, high-temperature superconductivity above liquid nitrogen temperature has remained one of the most perplexing puzzles in modern physics that is widely regarded as a "century-long challenge" and the "holy grail" of condensed matter physics. In 2023, superconductivity with a transition temperature T_c ~ 80 K was experimentally observed in bilayer nickelate $La_3Ni_2O_7$ under high pressures exceeding 14 GPa. Subsequently, in 2025, ambient-pressure superconductivity with T_c ~ 40 K was demonstrated in epitaxial $La_3Ni_2O_7$ thin films grown on $SrLaAlO_4$ substrates. In this talk, I will outline a theoretical framework based on two complementary models — a bilayer single-orbital t-J-$J_\perp$ model and a bilayer two-orbital model — to elucidate the superconducting mechanisms underlying both the high-pressure bulk $La_3Ni_2O_7$ and ambient-pressure thin-film systems. Our analysis reveals that the bilayer single-orbital t-J-$J_\perp$model captures the core physical essence governing the superconducting behavior of $La_3Ni_2O_7$. Specifically, we identify that high-T_c superconductivity in both bulk and thin-film bilayer nickelates is dominated by $d_{x^2-y^2}$ orbital electron pairing, with interlayer magnetically mediated interactions serving as the primary pairing glue; notably, Hund's coupling plays a pivotal role in this process. We further show that interlayer antiferromagnetic coupling acts as the key driving force for Cooper pair formation, and its strength directly tracks the evolution of T_c under external pressure or epitaxial strain. Enhanced strain is found to elevate T_c by effectively suppressing competing charge-density-wave (CDW) and spin-density-wave (SDW) instabilities. We propose that high-symmetry cubic or tetragonal substrates — such as $NdAlO_3$, $SrGd_2Al_2O_7$ and $AlAsO_4$—hold great promise for realizing higher T_c in ambient-pressure thin-film superconductors. Additionally, our calculations indicate that strong Fermi surface nesting favors the emergence of CDW phases in these nickelate systems. Finally, a finite-temperature phase diagram, derived from our theoretical model, is presented to contextualize the interplay between superconductivity, magnetic order, and competing ordered phases.

References

[1] X.Z. Qu, D. W. Qu, J. Chen, C. Wu, F. Yang, W. Li, G. Su, Phys. Rev. Lett. **132**, 036502 (2024).
[2] X.-W. Yi, Y. Meng, J.-W. Li, Z.-W. Liao, W. Li, J.-Y. You, B. Gu, G. Su, Phys. Rev. B **110**, L140508 (2024).
[3] X.-Z. Qu, D.-W. Qu, X.-W. Yi, W. Li, G. Su, Phys. Rev. B **112**, L161101 (2025).
[4] X.-W. Yi, W. Li, J.-Y. You, B. Gu, G. Su, Phys. Rev. B **112**, L140504 (2025).

9 - ADVANCES IN SUPERCONDUCTOR TECHNOLOGIES FOR HIGH FIELD MAGNETS

Abstract ID: 30726

NOVEL AND SUSTAINABLE COOLING STRATEGIES FOR HIGH TEMPERATURE SUPERCONDUCTING MAGNET SYSTEMS

S. V. Pamidi

The Center for Advanced Power Systems & FAMU-FSU College of Engineering, Florida State University, Tallahassee, Florida 32310, UNITED STATES OF AMERICA

REBCO and MgB2 superconductors are being used for magnet systems for various applications. In addition to large magnet systems for research and high-energy physics, large HTS magnet systems or coils are being developed for fusion power plants, superconducting magnetic energy storage systems, wind generators, and rotating machines for aviation and marine transportation. Economic and sustainable cooling strategies are necessary for these applications. The target temperature of some of these applications is 20 K or higher, providing an opportunity to eliminate the need for liquid helium and reduce the cryogenic cooling costs.

Cryogenic gaseous helium circulation has been effectively used for superconducting prototype fusion magnet systems, large ship propulsion motors, multi-megawatt power cables, and precool MRI magnet systems [1-4]. Closed-loop cryogenic helium circulation systems require small amounts of helium without the need for recovery systems.

Cryogenic helium circulation systems currently in operation use cryocoolers. To enable large-scale market penetration, low-cost, low-maintenance cryogenic cooling strategies are necessary. The ongoing development of green hydrogen technologies and the potential use of liquid hydrogen for large-scale energy storage can support cooling HTS magnet systems. Liquid hydrogen serving as an integrated energy storage and cryogenic heat sink would be an excellent solution for cooling HTS magnet systems.

Distributed renewable power generation and microgrids are attracting attention to achieve sustainable, resilient power and energy systems. Liquid hydrogen is being considered as a grid-level bulk long-duration energy storage option. Liquid hydrogen storage provides the synergy needed to reduce the complexity of HTS magnet systems, as liquid hydrogen at 20 K can serve as a cryogenic heat sink. However, the liquefaction of is energy intensive. Hence, the cooling power of 20 K liquid hydrogen must be exploited to offset the cost of liquefaction. Using liquid hydrogen as a cryogenic heat sink as part of the cooling strategies for HTS magnet systems eliminates the need for large mechanical cryocoolers and the corresponding capital and operating expenditures.

The paper will discuss the opportunities and challenges of using cryogenic helium circulation in conjunction with liquid hydrogen in cryogenic cooling strategies of HTS magnet systems.

References

[1] C. Michael, *et al.*, *A 20-K, 600-W, Cryocooler-Based, Supercritical Helium Circulation System for the SPARC Toroidal Field Model Coil Program*, IEEE Transactions on Applied Superconductivity, **vol. 34**, 1-13, (2024).

[2] T. Golfinopoulos, *et al.*, *Building the Runway: A New Superconducting Magnet Test Facility Made for the SPARC Toroidal Field Model Coil*, IEEE Transactions on Applied Superconductivity, **vol. 34**, **no. 2**, Art no. 0600416, pp. 1-16, (2024).

[3] B. B. Gamble, G. L. Snitchler, T. MacDonald, *Full Power Test of a 36.5 MW HTS Propulsion Motor*, IEEE Transactions on Applied Superconductivity, **21**, 1083-1088 (2011).

[4] S. Pamidi, C.H. Kim, L. Graber, High-Temperature Superconducting (HTS) Power Cables Cooled by Helium Gas, published in *Superconductors in the Power Grid: Materials and Applications,* Editor(s): Christopher Rey, Woodhead Publishing (2015), Pages 225-260, ISBN 9781782420293.

Abstract ID: 30737

REVIEW OF THE DEVELOPMENT OF A ROUND CABLE WITH SMALL MAGNETIZATION / LOW AC LOSS

N. Amemiya

Kyoto University, 6158510, Kyoto, JAPAN

Although nothing compares to REBCO coated conductors in terms of current transport properties in high magnetic fields, their tape shape leads to their intrinsic drawbacks: they cannot be cabled like round low T_c superconductors to attain high current carrying capacity; they can be bent almost flat-wise only; they generate large magnetization and AC losses. We have been developing the SCSC cable and its variant, the SCSC-IFB cable. In these cables, the copper-plated striated (multifilament) conductors are wound helically around round cores. Their filament geometries are similar to those of low T_c superconductors, and thus the filaments are electromagnetically decoupled in transverse time-dependent magnetic fields.

Multifilament coated conductors with inter-filament bridges (IFBs) are used in SCSC-IFB cables, in which inter-filament bridges allow superconducting current transfer between filaments to improve robustness against local defects in filaments. In this talk, the development of the SCSC-IFB cable and the SCSC cable, which is supported by multiple funding programs in Japan, is reviewed, and their prospects are presented.

This work was supported in part by the NEDO Frontier Program (JPNP14004), in part by the JSPS KAKENHI Grant Number JP22H00142, and in part by the JST-ALCA-Next Program Grant Number JPMJAN24G1.

Abstract ID: 30721

PROGRESS ON QUENCH RESEARCH OF HIGH-FIELD REBCO MAGNETS AT ASIPP: FROM FAILURE ANALYSIS TO 35.1 T

S. Gao[1], W. Hong[1], X. Zhang[1], S. Hu[1], H. Liu[1,2], F. Liu[1]

[1] *Institute of Plasma Physics, Chinese Academy of Science, Hefei 230031, PEOPLE'S REPUBLIC OF CHINA*
[2] *Hefei International Applied Superconductivity Center, Hefei 230601, PEOPLE'S REPUBLIC OF CHINA*

REBCO superconducting tapes have successfully pushed all-superconducting DC steady-state fields to 35.1 T, enabling new frontiers in science and fusion. However, despite the self-protecting characteristics of No-Insulation (NI) magnets, there are quench risks due to complex current bypassing mechanisms during high-field operations. Drawing on operational data and failure analysis of the 32.4 T, 26.86 T, and 35.1 T magnets at the Institute of Plasma Physics, Chinese Academy of Sciences (ASIPP) (2023–2025), this report comprehensively reviews quench behavior, failure modes, stability designs, and advanced prediction models. First, we compare failure modes in hybrid and all-REBCO configurations. The analysis of the 32.4T hybrid magnet reveals a key problem in the LTS-HTS coupling: the rapid discharge of the external LTS magnet induces a large number of "Induction Shocks" in the HTS inserting magnet through mutual inductance. This phenomenon generates damaging hoop stress milliseconds before thermal diffusion occurs, causing irreversible degradation. Recent tests on 19T and other nested HTS magnets have further confirmed that the quench of high-inductance external magnets will bring fatal inductive coupling risks. Second, studies of the 26.86 T all-REBCO magnet reveal a novel high-field instability: Turn-to-turn Separation. Extreme Lorentz forces drive radial expansion, physically separating turns and causing a surge in contact resistance that disables the magnet's self-protection capability. This finding shifts the safety design focus from suppressing thermal runaway to maintaining the mechanical integrity of contact surfaces. To quantify these behaviors, we developed a bidirectional coupled multi-physics framework integrating external protection circuits. This approach accurately captures dynamic current redistribution, screening current effects, and the non-linear mechanics of winding separation under various quench scenarios. Finally, we discuss the evolution from passive protection to active prediction. Validated by the successful 35.1 T record in 2025, we demonstrate the efficacy of high mechanical safety margin design and anti-separation winding techniques. The report concludes with an outlook on Deep Learning-based quench prediction and distributed fiber optic sensing as key monitoring technologies for future ultra-high-field magnet safety.

References

[1] S. Gao, Supercond. Sci. Technol., **38**, 035001 (2025).
[2] X. Zhang, L. Shao, Supercond. Sci. Technol.,**37**, 125003 (2024).
[3] X. Zhang, Supercond. Sci. Technol., **37**, 085003 (2024).
[4] H. Liu, S. Hu, X. Zhang, Innovation, 0 (2025).
[5] L. Shao, IEEE Trans. Appl. Supercond., **33**, 1–6 (2023).

10 - ADVANCES IN THIN FILMS, MULTI-LAYERS AND PATTERNED NANOSTRUCTURES

Abstract ID: 30161

ENGINEERING MAGNETIC ANISOTROPY IN PERMALLOY FILMS VIA ATOMIC FORCE NANOLITHOGRAPHY

A. Naik[1], C. Delforge[1], N. Lejeune[1], D. Stoffels[1], J. V. Vondel[2], K. Temst[2, 3], A. V. Silhanek[1], E. Fourneau[1]

[1] *Experimental Physics of Nanostructured Materials, Department of Physics, Université de Liège, B-4000 Sart-Tilman, BELGIUM*
[2] *Quantum Solid-State Physics, Department of Physics and Astronomy, KU Leuven, Celestijnenlaan 200D, Leuven, B-3001, BELGIUM*
[3] *Imec, Kapeldreef 75, 3001 Leuven, BELGIUM*

In this work, we investigate the induction of in-plane uniaxial magnetic anisotropy in permalloy thin films through Surface Artificial Grooving and Engraving (SAGE), a technique that involves the controlled nanoscale scratching of the film surface using atomic force nanolithography. This process generates a well-ordered groove array resulting in a strong uniaxial anisotropy with the easy axis aligned along the groove direction. The strength of this anisotropy is found to increase for small period and deep engraving. This approach is applied to patterned Py structures, enabling the mastering of domain arrangement and domain-wall motion. In particular, we demonstrate the design of a magnetic chessboard in ferromagnetic thin-film and the zero-field of spin wave propagation in corrugated permalloy waveguides.

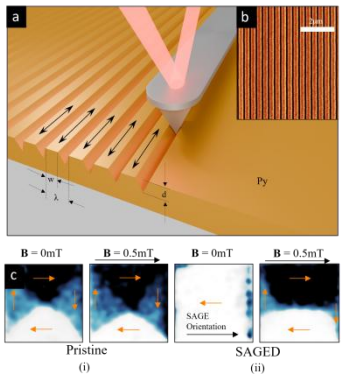

Fig. 1: *(a) Schematic representation of the SAGE technique via atomic force nanolithography. (b) Atomic Force Microscopy image of a SAGE-patterned region. (c)-(i) MOKE images of a pristine 30 nm thick Py square in the remanent state (left) and under a 0.5 mT applied field (right). (ii) MOKE images of a SAGED Py square (with SAGE orientation along the indicated direction) in the remanent state (left) and under a 0.5 mT field (right) highlighting the emergence of uniaxial anisotropy. The orange arrows in the samples indicate the direction of magnetization (**M**).*

References

[1] M. O. Liedke, *et al.*, Phys. Rev. B **87**, 024424 (2013).

[2] M. Y. Im, *et al.*, Nat. Commun. **5**, 5620 (2014).

[3] I. Turčan, *et al.*, Appl. Phys. Lett. **118**, 092405 (2021).

[4] J. Klíma, *et al.*, Appl. Phys. Lett. **124**, 112404 (2024).

Abstract ID: 30470

^{77}Se NMR STUDY OF $TlInSe_2$

G. S. Kupriyanova[1], A. Sönmez [2], M. H. Yu. Seyidov[2], I. G. Mershiev[3], G. V. Mozzhukhin[2]

[1] *Immanul Kant Baltic University, Institute of High Technology, 236041, Kaliningrad, RUSSIA*
[2] *Gebze Technical University, 41400, Gebze/Kocaeli, TURKEY*

The quasi-one-dimensional of $TlInSe_2$ single crystal exhibits semiconducting feature, including *p*-type conductivity and narrow bandgap size at ambient conditions. In also exhibits a large Seebeck coefficient, low thermal conductivity, and diverse electrical and nonlinear phenomena [1,2]. To provide complementary information about the crystal structure, crystalline symmetry and atomic spacing, a magic angle spinning (MAS) nuclear magnetic resonance (NMR) spectroscopy using the selenium -77 (^{77}Se) nuclei as a probe was used. In particular, it is very difficult to investigate a local geometry and chemical environment of the Se environment $TlInSe_2$ single crystal. To address these issues, we performed ^{77}Se NMR studies on $TlInSe_2$ single crystals and powders. Static and MAS NMR spectra were acquired using a Varian 400 spectrometer (B_0 = 9.35 T, ν = 76.2579 MHz) with a Hahn echo sequence ($\pi/2$ = 3.5 μs; 80,000 scans). In static measurements, two intense signals appeared when the crystal was aligned with the magnetic field, with the positions and widths of the lines strongly dependent on orientation, reflecting pronounced magnetic anisotropy corresponding to $InSe_4$ chains along the *c*-axis bridged by Tl chains. MAS NMR spectra (spinning rate: 16 kHz; magic angle: 54.74°) revealed four distinct lines. Line width measurements as a function of temperature (213–368 K, ±0.5 °C accuracy, spinning stability ±1 Hz) did not show sharp changes. However, the line widths exhibited two distinct behaviors: resonances at –90 ppm and –290 ppm varied only slightly (8.2–8.8 kHz), indicating a rigid Se environment, while the resonances at 329 ppm and 117 ppm fluctuated significantly (7.0–9.2 kHz). These dynamic lines have been tentatively assigned to Se sites that are highly sensitive to local fields from mobile Tl ions, which may themselves undergo angular displacements.

References

[1] M. Hanias, A.N. Anagnostopoulos, K. Kambas, and J. Spyridelis. Phys. Rev. B **43**, 4135–4140 (1991).
[2] C. Karakotsou and A.N. Anagnostopoulos. Physica D **93**, 157–164 (1996).

Abstract ID: 30542

OPTICAL PROPERTIES OF MnTe THIN-FILM POLYMORPHS GROWN BY MBE

O. Yastrubchak[1], S. Mamykin[1], V. Romanyuk[1], L. Borkovska[1], Y. Smortsova[3], A. Kaleta[2]

[1] *V.E. Lashkaryov Institute of Semiconductor Physics, National Academy of Sciences of Ukraine, 41 pr. Nauky, 03028, Kyiv, UKRAINE*
[2] *Institute of Physics, Polish Academy of Sciences, 32/46 Al. Lotników, 02-668, Warsaw, POLAND*
[3] *Deutsches Elektronen-Synchrotron DESY, Notkestr. 85, 22607 Hamburg, GERMANY*

Manganese telluride (MnTe) is a polymorphic magnetic semiconductor that has recently attracted **significant renewed attention due to the rapid development of altermagnetic spintronics based on α-phase** [1]. **Altermagnetism (AM) in α-MnTe represents a newly identified class of magnetic order that combines the vanishing net magnetization characteristic of antiferromagnets with the breaking of time-reversal symmetry typical of ferromagnets**. The thermodynamically stable **NiAs-type *α*-MnTe**, with a bandgap of $E_g \approx 1.3$ eV, has therefore been **extensively revisited in light of its unconventional magnetic symmetry and strong potential for spintronic applications**. In contrast, the **metastable *β*-MnTe** has received comparatively limited attention and is mentioned mainly in the context of **low-energy phase-change memory concepts** [2].

While the spin splitting and domain structure of AM have been recently confirmed by photoemission spectroscopy (ARPES) and X-ray magnetic circular dichroism (XMCD) imaging [3], the macroscopic *optical* signatures of the phase transition remain underexplored. This gap hinders the development of accessible, tabletop metrology for altermagnetic devices, currently reliant on complex synchrotron facilities.

We present a comprehensive study of the optical properties of high-quality epitaxial *α*- and *β*-MnTe thin films grown by molecular beam epitaxy (MBE) on different substrates. The investigation spans a broad temperature range (80–400 K), encompassing the Néel temperature ($T_N \approx 310$ K) associated with the altermagnetic phase transition in α-MnTe. A critical challenge in MnTe characterization is its susceptibility to surface oxidation, which can obscure intrinsic bulk properties. Temperature-dependent spectroscopic ellipsometry in the 0.6–5.0 eV range was used to extract the complex dielectric function [4, 5] and to quantify the exchange-mediated "magnetic blue shift" of the optical band gap [6].

Additional low-temperature (≈12 K) photoluminescence measurements were performed at the Deutsches Elektronen-Synchrotron (DESY). The structural characterization of the films were performed using the high resolution X-ray diffractometry (HRXRD) and in transmission electron microscopy (TEM).

OY acknowledge financial support from Polish Academy of Science and V. Volobuev for sample growth and XRD characterization. This work was also partially sponsored by the CRDF foundation (G-202506-73640) and the IEEE program "Magnetism for Ukraine 2025", supported by the IEEE Magnetic Society under the Science and Technology Center in Ukraine (STCU) framework.

References

[1] L. Šmejkal, *et al.*, Phys. Rev. X **12**, 040501 (2022). https://doi.org/10.1103/PhysRevX.12.040501
[2] M. Kim, *et al.*, Phys. Status Solidi RRL **16**, 2100641 (2022). https://doi.org/10.1002/pssr.202100641
[3] O. J. Amin, *et al.*, Nature **636**, 348–353 (2024). https://doi.org/10.1038/s41586-024-08234-x
[4] L. Gluba, *et al.*, Applied Physics Letters **105**, 032408 (2014). https://doi.org/10.1063/1.4891329
[5] N. L. Dmitruk, *et al.*, Thin Solid Films **364**, 280-283 (2000). https://doi.org/10.1016/S0040-6090(99)00945-1
[6] D. Bossini, *et al.*, New J. Phys. **22**, 083029 (2020). https://doi.org/10.1088/1367-2630/aba0e7

Abstract ID: 30705

HIGH-PERFORMANCE HUMIDITY SENSOR BASED ON SCHIFF BASE COMPOUND WITH FAST RESPONSE, HIGH SENSITIVITY, AND STABILITY FOR HUMIDITY SENSING APPLICATION

M. U. Rahman

Islamia College Peshawar, Department of Physics, 25120, KP, PAKISTAN

In this study, the Schiff base compound, 2-((2,4-dichlorophenylimino)methyl)-5-(diethylamino)phenol (hereafter L2 compound), synthesis has been carried out and then implemented to fabricate three different humidity sensors with different concentrations of L2 compound i.e. 3 wt%, 6 wt%, and 9 wt%. These sensors were checked at altered levels of humidity and at various frequencies. The surface morphologies of the L2 compound with different concentrations are shown in the SEM images. Filled and empty grooves, voids, solid flakes, and flowery structures can be seen in SEM images, which played a sumptuous role in the accommodation of H 2 O molecules and the sensing mechanism. The phototropic mobility is based on the Grotthuss mechanism. When the humidity level was increased from 32 %RH to 96 %RH, the capacitance of the sensor was enhanced from 9.5 pF to 16.7 pF, from 8.95 pF to 11.3 pF, and from 8.7 pF to 10.6 pF at different frequencies of 500 Hz and 10 kHz, and 1 MHz, correspondingly. The response/recovery time of the sensor was 1.7/2.62 s which are better than the reported results [1-3]. The goodness of fit (R 2 values) 0.87 and 0.96 were noted for the chemisorbed and multi-physisorbed layers and were near to unity and hence considered as the best linear fit. The sensitivity of the sensors was high at 500 Hz. The L2-based sensor's high sensitivity, rapid response/recovery time, and reliable performance make it a good choice for real-time humidity monitoring in environmental control, healthcare, food storage, and industrial applications.

References

[1] K. Ullah, M.U. Rahman, Hina, R. Khan, H. Ali, S. Al Otaibi, K. Althubeiti, S. Abdullaev, N. A. Elboughdiri, *High-performance humidity sensor based on Schiff base compound with fast response, high sensitivity, and stability for humidity sensing application*, Materials Science in Semiconductor Processing **198**, 109794 (2025).
https://doi.org/10.1016/j.mssp.2025.109794

[2] S. Begum, M.U. Rahman, S. Al Otaibi, K. Althubeiti, N. Nazarova, B. U. Zulfiqar, R. Khan, *High sensitivity and low hysteresis of humidity sensor based on imidazole derivative*, J. Mater. Sci. Mater. Electron. **34**, 920 (2023).
https://doi.org/10.1007/s10854-023-10349-2.

[3] M.U. Rahman, G. Shah, A. Ullah, Z.U. Rahman, A. Mehwish, R. Khan, B. Ullah Zulfiqar, I. Ahmad, *Resistive-and capacitive-type humidity and temperature sensors based on a novel caged nickel sulfide for environmental monitoring*, J. Mater. Sci. Mater. Electron. **31**, 3557–3563 (2020).
https://doi.org/10.1007/s10854-020-02904-y

11 - AI-DRIVEN DISCOVERY OF NOVEL QUANTUM MATERIALS

Abstract ID: 30415

POLYCRYSTALLINE INFORMATICS FOR DATA-DRIVEN DESIGN OF HIGH-FUNCTIONALITY POLYCRYSTALLINE MATERIALS

N. Usami

Nagoya University, 464-8603, Nagoya, JAPAN

Polycrystalline materials constitute the backbone of a wide range of materials systems, spanning structural materials, energy-conversion devices, and electronic materials. In such systems, macroscopic performance is not determined solely by composition, but is critically governed by complex microstructural features, including grain size distributions, crystallographic orientations, and grain boundary networks. Understanding and controlling these heterogeneous microstructures are therefore essential for the rational design of high-functionality polycrystalline materials.

Traditionally, the development of polycrystalline materials has relied heavily on empirical knowledge and trial-and-error approaches, reflecting the complexity and high dimensionality of microstructural descriptors. In recent years, however, data-driven approaches have emerged that aim to predict macroscopic properties from microstructural information, thereby enabling inverse design of both microstructures and processing conditions based on targeted material functions.

In this presentation, we review our recent efforts toward establishing polycrystalline informatics, an integrated research framework that combines experimental characterization, theoretical analysis, computational modeling, and data science. Our goal is to predict the properties of polycrystalline materials from microstructural information and to enable inverse analysis of microstructures and process conditions required to achieve desired properties.

We first describe the construction of three-dimensional polycrystalline models by combining visualization of crystal defect distributions [1] with machine-learning-based prediction of crystallographic orientation distributions [2]. We then discuss the coupling of three-dimensional microstructural models with stress analysis and crystal growth simulations, as well as the integration of multiscale structural analyses. Through these approaches, we elucidate key aspects of the mechanisms underlying dislocation cluster formation in complex polycrystals [3]. In addition, we introduce a graph-based representation of polycrystalline microstructures and explore the use of graph neural networks to predict macroscopic properties of polycrystalline materials [4].

Furthermore, we demonstrate that generative image models trained on real three-dimensional polycrystalline microstructural data can generate diverse microstructures that faithfully capture essential characteristics of actual polycrystals [5]. If microstructure generation from process parameters via physics-based models can be fully integrated into this framework, it will become possible to evaluate the performance of a wide variety of polycrystalline microstructures in cyberspace, enabling inverse identification of optimal microstructures and fabrication pathways for targeted functionalities.

References

[1] Y. Hayama, *et al.*, Sol. Energy Mat. Sol. Cells **189**, 239 (2019).
[2] K. Hara, *et al.*, APL Machine Learning **1**, 026113 (2023).
[3] K. Yamakoshi, *et al.*, Adv. Mater. **36**, 2308599 (2024).
[4] K. Torii, *et al.*, Sci Technol Adv Mater. **26**, 2512703 (2025).
[5] T. Deshimaru, *et al.*, Adv. Intell. Discov. **1**, 2500012 (2025).

Abstract ID: 30689

DEEP LEARNING APPROACH FOR FLAT-BAND 2D QUANTUM MATERIALS

Q. Yang, A. Bhattacharya, X. Wang, H. Pentz, Y. Wei, A. Mishchenko

Department of Physics and Astronomy, University of Manchester, Manchester, UK

Flat electronic bands underpin a wide range of correlated quantum phenomena, yet their discovery remains challenging due to the vastness of structural and chemical design spaces. In this talk, we present our AI-driven framework for the systematic discovery of flat-band two-dimensional (2D) materials that bypasses conventional trial-and-error and brute-force first-principles screening.

We introduce structure-informed deep learning models, a scalable multi-modal learning paradigm that directly ingests atomic structures to predict complex electronic features such as flat electronic bands without precomputed band structures, enabling unprecedented throughput in materials screening across vast compositional spaces [1]. Complementing this, unsupervised learning techniques are used to construct low-dimensional electronic fingerprints that reveal hidden structure–property relationships and autonomously cluster flat-band motifs across large materials databases [2]. Together, these approaches form a scalable "materials genome" for flat-band systems, linking local geometry, orbital connectivity, and emergent electronic flatness [3,4].

Our results demonstrate that AI can not only accelerate the discovery of flat-band materials across diverse chemical families, but also provide interpretable insights into the structural principles governing flat-band formation. Our works establish practical pathways toward data-driven design of correlated quantum materials and lays the foundation for closed-loop discovery integrating theory, machine learning, and experiment.

References

[1] X. Wang, *et al.*, arXiv:2506.07518 (2025).
[2] H. K. Pentz, *et al.*, Communications Physics, **8**, 25 (2025).
[3] A. Bhattacharya, *et al.*, npj Computational Materials, **9**, 101 (2023).
[4] A. Mishchenko, *et al.*, Digital Discovery, **5**, 28-63 (2026).

Abstract ID: 30700

DIRECT ATOMIC LAYER PROCESSING (DALP®): SPATIALLY LOCALIZED, MULTI-MATERIAL FABRICATION FOR NEXT-GENERATION DEVICES FROM DISCOVERY TO MANUFACTURING

M. Plakhotnyuk

ATLANT 3D, Mårkærvej 2B, 2630, Taastrup, DENMARK

Progress in next-generation advanced electronic and functional devices, based on complex heterostructures and advanced materials integration, is increasingly constrained by the rigidity of conventional thin-film processing and patterning workflows. While these approaches deliver high material quality and uniformity, they offer limited flexibility for spatially localized, multi-material fabrication, three-dimensional thickness engineering, and rapid experimentation at the nanoscale within a single process flow.

ATLANT 3D introduces Direct Atomic Layer Processing (DALP®), a nanofabrication technology enabling digitally controlled, spatially localized deposition of multiple materials with atomic-scale precision [1, 2]. DALP® allows different materials to be deposited sequentially and locally in a unified workflow, enabling manufacturing of complex material stacks, heterostructures, interfaces, and thickness gradients without intermediate lithographic patterning steps. This presentation describes the DALP® process architecture and its role in both combinatorial materials discovery [3] and targeted device manufacturing for next-generation devices [4, 5]. By enabling programmable material placement, controlled thickness variation, and repeatable execution within a single platform, DALP® supports accelerated materials exploration while also enabling the direct production of device-ready structures as part of broader manufacturing flows. Representative examples include multi-material nanoscale structures for advanced semiconductor and functional material applications, where precise interface control, spatial selectivity, repeatability, and manufacturability are critical. DALP® expands the accessible design space of nanoscale fabrication and provides a direct pathway from materials discovery to device-ready, manufacturable structures.



Fig. 1: *a) Microfluidic precursor delivery concept: schematic view of the delivery nozzle in frontal view (top) and in cross-section (lower panel). b) Demonstration of direct pattern generation: Pt-printed ATLANT logo featuring letters from A to T obtained with 140, 150, 170, 190, 200 and 210 individual passes, respectively [1] .*

References

[1] I. Kundrata, *et al.*, Small Methods, **6.5**, 2101546 (2022).
[2] M. K. S. Barr, *et al.*, The Electrochemical Society, **240**, 29, (2021).
[3] S. Kürten, *et al.*, Materials Advances (2025).
[4] M. Plakhotnyuk, *et al.*, The Electrochemical, Society, **244**, 29, (2023).
[5] B. Hudec, *et al.*, The Electrochemical Society, **240**, 55, (2021).

Abstract ID: 30738

AI-GUIDED DISCOVERY OF NOVEL OPTICAL MATERIALS FOR SMART ELECTRONIC DEVICES

V. Volkov[1], I. Kruglov[1], L. Klimova[1], I. Trofimov[1], A. Arsenin[1], K. Novoselov[2]

[1] *Emerging Technologies Research Center, XPANCEO, Dubai Investment Park First, Dubai, UNITED ARAB EMIRATES*

[2] *Department of Materials Science and Engineering, National University of Singapore, Singapore, 03-09 EA, SINGAPORE*

In recent years, the demand for novel materials with targeted properties has grown rapidly, driven by increasing industrial performance requirements and the high cost and limited throughput of experimental discovery. Traditional trial-and-error approaches, relying on expert intuition and extensive experimentation, are time-consuming and resource-intensive. Advances in computational materials science and materials informatics have enabled accurate prediction of material structures and properties prior to synthesis. The integration of artificial intelligence has further accelerated this shift: large materials databases, machine-learning models, and generative algorithms now enable systematic, data-driven materials discovery, significantly improving its efficiency and scope.

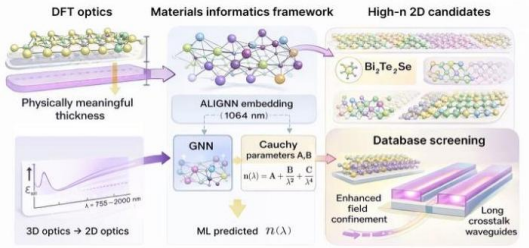

Fig. 1: *Physically informed ML model for the search of novel 2D materials with target optical properties.*

In this talk, we demonstrate how AI-driven methodologies transform the design of smart electronic devices, with a focus on data-driven discovery of functional materials for next-generation smart contact lenses. Van der Waals (vdW) materials, known for their unique optical properties and strong anisotropy, are promising platforms for advanced photonics. However, manual screening of vdW materials with extreme optical anisotropy is impractical. We constructed a database of vdW materials and their optical properties [1–3] and trained a graph neural network to predict birefringence with near ab initio accuracy.

Experimental validation using 2H-$MoTe_2$ and $CdPS_3$ confirms the predictions, highlighting the potential of machine learning for discovering vdW materials with exceptional optical performance [4]. To bridge theory and experiment, we developed a physics-guided ML framework combining DFT, graph neural networks, experimental data, and Cauchy-model corrections. Using a dataset of over 1000 two-dimensional materials, this approach enables reliable prediction of near-infrared refractive indices and introduces a physically meaningful definition of 2D thickness. The resulting models capture structure–property relationships with high fidelity and enable rapid screening of monolayers with tailored optical functionalities, identifying high-index candidates such as Bi_2Te_2Se for enhanced field confinement in photonic devices (Fig. 1) [5]. We further present an AI-driven framework for predicting substrate-stabilized 2D structures that integrate evolutionary optimization, lattice matching, machine-learning interatomic potentials, and ab initio thermodynamics. Applied to the Mo–S system on c-cut sapphire, this approach reveals multiple stable and metastable phases, including 1H-MoS_2 and previously unknown compounds, providing a pathway for computational substrate engineering and guided experimental synthesis [6]. Overall, these results demonstrate how physics-informed AI enables a transition from empirical trial-and-error to predictive, data-driven materials design, unifying ab initio modeling, machine learning, and experiment to accelerate the discovery of functional materials for next-generation photonic and electronic technologies.

References

[1] G. A. Ermolaev, *et al.*, Nat. Commun. **12(1)**, 854 (2021).
[2] G. A. Ermolaev, *et al.*, Nat. Commun. **15(1)**, 1552 (2024).
[3] A. S. Slavich, *et al.*, Light Sci. Appl. **13(1)**, 68 (2024).
[4] L. A. Bereznikova, *et al.*, Mater. Horiz. (2025).
[5] L. A. Klimova, *et al.*, ACS Nano (2026).
[6] A. Mazitov, *et al.*, npj Comput. Mater. **11(1)**, 270 (2025).

Abstract ID: 30503

VAE-BASED INTERPRETATION OF SHAPE VARIABILITY IN MULTI-QUANTUM WELL MICRORING LASERS

M. R. Athavale[1,2], S. Church[3], W. W. Wong[4], A. K. Low[2,5], H. H. Tan[4], K. Hippalgaonkar[2,5], P. Parkinson[1]

[1] *Department of Physics and Astronomy and The Photon Science Institute, University of Manchester, Oxford Road, Manchester, M13 9PL, UNITED KINGDOM*

[2] *Institute of Materials Research and Engineering (IMRE), Agency for Science, Technology and Research (A*STAR), 2 Fusionopolis Way, Innovis #08-03, Singapore, 138634, REPUBLIC OF SINGAPORE*

[3] *Centre for Engineering the Future, School of Science, Engineering and Environment, University of Salford, Manchester, Salford, M5 4QJ, UNITED KINGDOM*

[4] *ARC Centre of Excellence for Transformative Meta-Optical Systems, Department of Electronic Materials Engineering, Australian National University, Mills Road, Canberra, ACT 2601, AUSTRALIA*

[5] *School of Materials Science and Engineering, Nanyang Technological University, Singapore, 639798, SINGAPORE*

Bottom-up InP/InAsP multi-quantum-well microring lasers grown by selective-area epitaxy offer compact, integrable light sources, yet growth-induced variability still hinders reproducible performance [1]. We conducted two sequential multi-objective to efficiently improve lasing performance while minimizing costly trial growths. The first campaign achieved a 1.6× threshold reduction and tuned emission to 1268 nm (O-band) with 100% lasing yield [2]. The second campaign targeted a lower threshold, longer wavelength, and reduced variance; two independent growth sets were fabricated under identical parameters to assess reproducibility. We achieved a further 2× reduction in median threshold (15.9 μJ cm^{-2}), reduced variance by 73%, and shifted the median emission to 1333 nm toward the C-band. Both sets showed consistent improvements, yet measurable differences between them indicated persistent morphology-driven variability. Variational autoencoder analysis revealed distinct shape distributions and linked subtle morphological differences to threshold and variance, indicating shape-induced stochasticity and motivating morphology-aware routes to more reproducible, high-yield photonic integration.

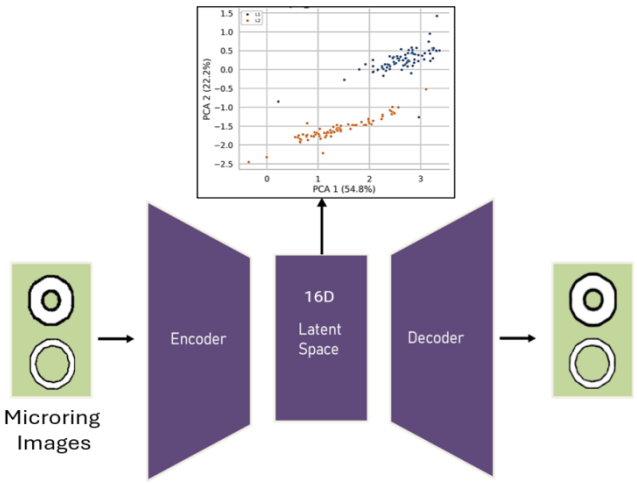

Fig. 1: *Overview of the Variational Autoencoder (VAE) used to quantify shape distributions across device subsets.*

References

[1] W. W. Wong, *et al.*, ACS Nano **17**, **15**, 15065-15076 (2023).
[2] M. R. Athavale, *et al.*, ACS Photonics, **12**, **8**, 4260-4268 (2025).

Abstract ID: 30081

HARNESSING NONLINEAR ANTIFERROMAGNETISM: $L1_2$–PHASE $IrMn_3$ FOR NEXT-GENERATION HIGH-PERFORMANCE SPIN-TORQUE DEVICES

O. Ozatay[1,2], U. Sasun[1], S. Ari[1], M. Kocyigit[1], A. Iskesen[1], E. K. Taga[1], K. Akin[1], B. Kocaman[1], H. Piskin[1], I. Goksal[1], V. Karakas[1]

[1] *Bogazici University, Dept. of Physics, 34342, Istanbul, TURKIYE*
[2] *SUNUM, Sabanci University Nanotechnology Research and Application Center, 34956 Istanbul, TÜRKIYE*

Non-collinear antiferromagnets (AFMs) are emerging as highly promising materials for next-generation spintronic devices, such as spin orbit torque – magnetic random access memory (SOT-MRAM) and neuromorphic computing, owing to their ultrafast spin dynamics and robust magnetic properties. The $L1_2$-phase of $IrMn_3$, in particular, has garnered significant attention due to its unique non-collinear triangular spin structure and strong spin-orbit coupling, which are predicted to generate large, unconventional spin-orbit torques (SOTs). However, the production of high-quality, single-crystal $L1_2$-$IrMn_3$ thin films remains a critical material science challenge [1].

Here we report our comprehensive investigation into the production and characterization of epitaxial $L1_2$-$IrMn_3$ thin films. While focusing on optimizing the film growth process via DC magnetron sputtering [2] in an Ultra-High Vacuum (UHV) system, we have systematically tuned key deposition parameters, including substrate temperature (up to 825°C), substrate choice (e.g., MgO, Al_2O_3), Ar pressure, and DC power, to achieve precise control over crystallographic orientation and phase purity.

Structural analysis using X-Ray Diffraction (XRD) confirms the successful growth of highly-textured, phase-pure $L1_2$-$IrMn_3$ films. Atomic Force Microscopy (AFM) was employed to characterize the surface morphology, revealing smooth, high-quality surfaces suitable for subsequent device fabrication. Magnetic characterization was performed using a Vibrating Sample Magnetometer (VSM) allowing for the determination of magnetic ordering and the Néel temperature of the films.

These foundational results demonstrate the successful fabrication of high-quality $L1_2$-$IrMn_3$ films, which is the essential first step for investigating their spin transport properties. Current work is focused on fabricating Hall bar devices from these films to perform electrical characterization of SOT efficiencies in $IrMn_3$-based heterostructures (e.g., with Pt and W). This research provides a critical pathway for understanding SOT mechanisms in non-collinear AFMs and unlocking their potential for high-performance, energy-efficient spintronic technologies.

We acknowledge support from TUBITAK under project numbers 118F116 and 118F431 and Bogazici University Research Fund BAP under project number 20379.

References

[1] W. Zhang, *et al.*, Sci. Adv., **2**, e1600759, (2016).

[2] A. A. Jara, *et al.*, IEEE Magn. Lett., **v7**, (2016).

Abstract ID: 30126

CHIRAL DUAL SPIN CURRENTS FIELD-FREE PERPENDICULAR SWITCHING BY ALTERMAGNET RuO_2

G. Meng[1,2], Q. Sun[3], Y. Yang[1,2], Y. Zhang[1,4], N. Lei[3], D. Wei[1,2]

[1] *State Key Laboratory of Semiconductor Physics and Chip Technologies, Institute of Semiconductors, Chinese Academy of Sciences, 100083, Beijing, CHINA*
[2] *Center of Materials Science and Optoelectronics Engineering, University of Chinese Academy of Sciences, 100190, Beijing, CHINA*
[3] *Fert Beijing Institute, MIIT Key Laboratory of Spintronics, School of Integrated Circuit Science and Engineering, Beihang University, 100191, Beijing, CHINA*
[4] *School of Industry-education Integration, University of Chinese Academy of Sciences, 100049, Beijing, CHINA*

Conventional spintronic mechanisms, such as spin-transfer and spin-orbit torques (STT&SOT) based on the spin current, rely on breaking time-reversal symmetry to manipulate magnetic moments. In contrast, for spatially separated dual spin currents, the time-reversal-invariant vector chirality emerges as a critical factor governing magnetization dynamics. Here, we investigate field-free perpendicular magnetization switching in an altermagnet RuO_2/ferromagnet/heavy metal Pt trilayer, driven by chiral dual spin currents (CDSC). We demonstrate that the chirality of these dual spin currents acts as the deterministic role in breaking out-of-plane symmetry. Leveraging the intrinsic spin-splitting effect (SSE) [1,2] of the d-wave altermagnet [3] to generate an x-polarized spin component, the interplay of non-collinear spin currents from two adjacent layers induces a helical magnetic texture within the intermediate layer. The resulting intralayer exchange coupling manifests as an effective in-plane magnetic field, facilitating deterministic switching. This distinct physical picture, validated by switching measurements and micromagnetic simulations, reveals that the switching polarity is dictated by chirality rather than charge current polarity. Characterized by the novel symmetry and low power consumption, CDSC offers a promising paradigm for next-generation high-performance spintronic architectures.

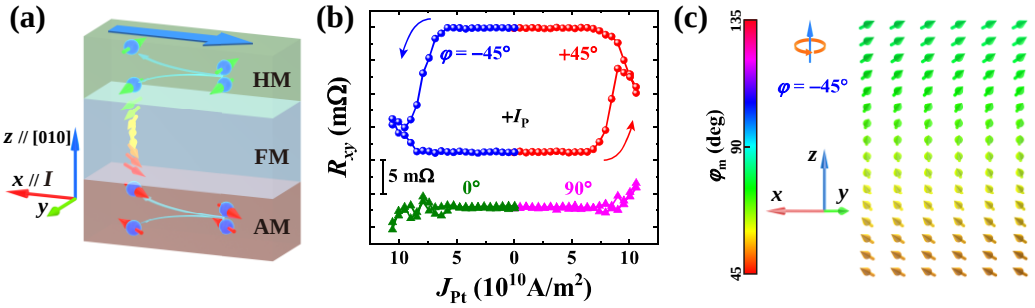

Fig. 1: *(a) Sample structure, CDSC and magnetic moments. (b) Field-free switching loops for different current directions. (c) CDSC induced helical magnetic structure.*

References

[1] L. Šmejkal, *et al.*, Phys. Rev. X **12**, 040501 (2022).

[2] S. Karube, *et al.*, Phys. Rev. Lett. **129**, 137201 (2022).

[3] Z. Feng, *et al.*, , Nature Electronics **5**, 735 (2022).

Abstract ID: 30198

ROOM-TEMPERATURE HIGH-ORDER NONLINEAR HALL EFFECT IN A TOPOLOGICAL WEYL ANTIFERROMAGNET

L. Yang[1], W. H. Niu[1], Y. M. Yang[2], D. H. Wei[2], N. Lei[1,3]

[1] *Fert Beijing Institute, MIIT Key Laboratory of Spintronics, School of Integrated Circuit Science and Engineering, Beihang University, Beijing 100191, CHINA*

[2] *State Key Laboratory for Superlattices and Microstructures, Institute of Semiconductors, Chinese Academy of Sciences, Beijing 100083, CHINA*

[3] *National Key Lab of Spintronics, Institute of International Innovation, Beihang University, Yuhang District, Hangzhou, 311115, CHINA*

The Hall effect refers to the generation of a transverse voltage in response to a longitudinal driving current injected into the sample [1]. While the conventional linear Hall effect is a well-known indicator of time-reversal symmetry breaking, nonlinear Hall transport provides a powerful tool for probing topological physics in solids governed by distinct symmetry requirements [2]. In this study, we report a high-order nonlinear Hall effect in topological Weyl antiferromagnet $D0_{19}$-Mn_3Sn at room temperature. Through angle-resolved transport measurements, we demonstrate that the nonlinear Hall response exhibits a clear rotational dependence on the current direction that reflects the underlying distinct symmetry breaking. Moreover, the response has a complicated temperature dependence and is tunable by external magnetic field, reflecting the underlying evolution of the magnetic texture. Our results pave the way for nonlinear device design based on antiferromagnet operating at room temperature.

References

[1] Z. Z. Du, H. Z. Lu, and X. C. Xie. Nat. Rev. Phys. **3(11)**, 744-752 (2021).

[2] R. Y. Chu, L. Han, Z. H. Gong, X.Z. Fu, H. Bai, S.X. Liang, C. Chen, S-W. Cheong, Y.Y. Zhang, J. W. Liu, Y. Y. Wang, F. Pan, H. Z. Lu, and C. Song. Phys. Rev. Lett. **135(21)**, 216703 (2025).

Abstract ID: 30224

ALTERMAGNETIC MAGNON TRANSPORT IN d-WAVE ORTHOFERRITE INSULATORS

E. Galindez-Ruales[1], W. Yang[2], T. Dannegger[3], M. Kundu[3], J. Köhler[1], C. Schmitt[1], F. Fuhrmann[1], A. Akashdeep[1], D. M. Tran[1], X. Ma[2], G. Jakob[1], S. Cao[2], U. Nowak[3], M. Kläui[1]

[1] *Institute of Physics, Johannes Gutenberg University Mainz, 55128 Mainz, GERMANY*
[2] *Materials Genome Institute, Shanghai University, 200444 Shanghai, CHINA*
[3] *Fachbereich Physik, Universität Konstanz, D-78457 Konstanz, GERMANY*

Altermagnets are collinear magnets with symmetry-enforced spin-split bands despite zero net magnetization, offering a route to field-free spin transport in both electronic and magnonic channels [1]. While electronic altermagnetism has recently been demonstrated, most altermagnets are insulating, and their *magnon* transport properties remain largely unexplored.

In this work, we performed non-local spin transport experiments on the *d*-wave orthoferrite altermagnets $LuFeO_3$ and $YFeO_3$ [2]. Using Pt|orthoferrite devices, we detect both thermally driven (spin Seebeck) and spin-bias-driven magnon currents via the inverse spin Hall effect. Two key altermagnetic fingerprints emerge: (i) a robust sign inversion of the non-local signal between distinct altermagnetic crystallographic directions, and (ii) a second sign inversion of the thermal signal as a function of injector–detector distance.

These effects are absent when transport is aligned along or perpendicular to the easy axis, where our atomistic spin-dynamics and linear spin-wave calculations predict vanishing net magnon magnetization. The excellent agreement between experiment and theory shows that the observed signals originate from altermagnetic magnon band splitting, not from weak ferromagnetism or conventional antiferromagnetic transport. In particular, the anisotropic magnon lifetimes and group velocities in the *d*-wave altermagnetic directions give rise to direction- and distance-dependent magnon spin accumulation, including the observed sign reversals. Our results establish orthoferrite altermagnets as a versatile platform for field-free, anisotropic magnon transport and point toward altermagnetic magnonics as a promising route for low-power spintronic devices.

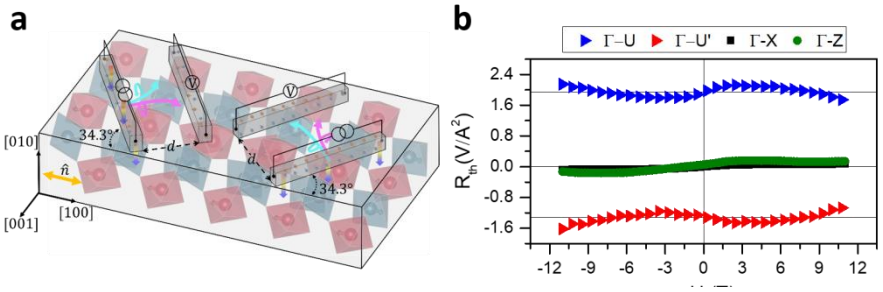

Fig. 1: *Schematic of the non-local Pt|orthoferrite device and representative non-local signals showing sign inversion with crystallographic direction and injector–detector distance.*

References

[1] L. Šmejkal, *et al.*, Phys. Rev. Lett. **131**, 256702 (2023).

[2] E. Galindez-Ruales, *et al.,* arXiv:2508.14569 [cond-mat.mtrl-sci] (2025).

Abstract ID: 30230

SPIN HALL MAGNETORESISTANCE AT THE ALTERMAGNETIC INSULATOR/Pt INTERFACE

M. Leiviskä[1], R. Firouzmandi[2], K. Ahn[1], P. Kubaščik[3], Z. Soban[1], S. Bommanaboyena[1], C. Müller[1], D. Kriegner[1], D. Reustlen[4], S. Sailler[4], M. Lammel[4], K. Bestha[2,5], M. Hyvl[1], L. Šmejkal[6,7,1], J. Zelezny[1], A. U. B. Wolter[2], M. Scheufele[8,9], J. Fischer[10], M. Opel[8], S. Geprägs[8], M. Althammer[8], B. Büchner[2,11,12], T. Jungwirth[1,13], L. Nádvorník[3], S. T. B. Goennenwein[4], V. Kocsis[2], H. Reichlova[1]

[1] *Institute of Physics, Czech Academy of Sciences, CZECHIA*
[2] *Institut für Festkörperforschung, Leibniz IFW Dresden, GERMANY*
[3] *Faculty of Mathematics and Physics, Charles University, CZECHIA*
[4] *Department of Physics, University of Konstanz, GERMANY*
[5] *Institute of Solid State and Materials Physics, TU Dresden, GERMANY*
[6] *Max Planck Institute for the Physics of Complex Systems, GERMANY*
[7] *Max Planck Institute for Chemical Physics of Solids, GERMANY*
[8] *Walther-Meißner-Institut, Bayerische Akademie der Wissenschaften, GERMANY*
[9] *Technical University of Munich, TUM School of Natural Sciences, GERMANY*
[10] *Universite Grenoble Alpes, CEA, CNRS, Spintec, FRANCE*
[11] *Institute of Solid State and Materials Physics and Würzburg-Dresden Cluster of Excellence ct.qmat, Technische Universität Dresden, GERMANY*
[12] *Center for Transport and Devices, Technische Universität Dresden, GERMANY*
[13] *School of Physics and Astronomy, University of Nottingham, UK*

Spin Hall magnetoresistance (SMR) is a magnetoresistive effect present in bilayers comprising of a magnet (here insulating) and a heavy metal [1]. It relies on the concerted action of spin Hall effect, inverse spin Hall effect, and dissipation of spin accumulation at the interface. The dissipation of the spin accumulation occurs via various channels, including spin-transfer torque and magnon-mediated spin current transfer. Altermagnets are a new class of collinear compensated magnets with a unique anisotropic spin ordering with characteristic spin-degenerate nodes and alternating even-parity spin polarization that breaks the time-reversal symmetry [2]. In this work, we present a set of SMR measurements in heterostructures of Pt and an insulating and ferroelectric altermagnet candidates $Ba_2CoGe_2O_7$ [3] and $Sr_2CoSi_2O_7$. We will first detail the fabrication of devices for SMR experiments on bulk crystals and then discuss characteristic SMR features of the systems under study. We show that in both systems the SMR ratio is unexpectedly large and shows anisotropy depending on in which crystal direction the current is applied. We systematically rule out device-to-device variations, magnetic domains, and magnetocrystalline anisotropy as the main origin of this current-direction anisotropy of the SMR ratio, and also address the possible effects of ferroelectric polarization on the SMR. Finally, we will suggest mechanisms through which the crystal symmetries that characterize the altermagnetic phase of $Ba_2CoGe_2O_7$ and $Sr_2CoSi_2O_7$ could give rise to the observed anisotropy.

References

[1] H. Nakayama, M. Althammer, Y.-T. Chen, *et al.*, Phys. Rev. Lett. **110**, 206601 (2013).

[2] L. Šmejkal, J. Sinova, and T. Jungwirth. Phys. Rev. X **12**, 031042 (2022).

[3] M. Leiviskä, R. Firouzmandi, K. Ahn, *et al.*, Phys. Rev. Mat. **9**, 084403 (2025).

Abstract ID: 30338

FRAGILITY OF THE MAGNETIC ORDER IN THE PROTOTYPICAL ALTERMAGNET RuO_2

A. Smolyanyuk[1], I. I. Mazin[2], L. Garcia-Gassull[3], L. Šmejkal[4,5,6], R. Valentí[3]

[1] *Institute of Solid State Physics, TU Wien, 1040 Vienna, AUSTRIA*
[2] *George Mason University, Department of Physics & Astronomy and Center for Quantum Science and Engineering, Fairfax, Virginia 22030, USA*
[3] *Institut für Theoretische Physik, Goethe-Universität Frankfurt, 60438 Frankfurt am Main, GERMANY*
[4] *Max Planck Institute for the Physics of Complex Systems, Dresden, GERMANY*
[5] *Max Planck Institute for Chemical Physics of Solids, Dresden, GERMANY*
[6] *Institute of Physics, Czech Academy of Sciences, Praha 6, CZECH REPUBLIC*

Altermagnetism is a topic that has lately been gaining attention and the RuO_2 compound is among one of the most studied altermagnetic candidates. However, the survey of available literature on RuO_2 properties suggests that there is no consensus about the magnetism of this material. By performing density functional theory (DFT) calculations, we show that the electronic properties of stoichiometric RuO_2 are described in terms of a Hubbard U, within DFT+U, smaller than the value required to have magnetism. We further argue that Ru vacancies can actually aid the formation of a magnetic state in RuO_2. This in turn suggests that a characterization of the amount of Ru vacancies in experimental samples might help the resolution of the controversy between the different experimental results [1].

The electronic structure of RuO_2 hints at a possibility of realizing a magnetically ordered state upon hole doping, and such a possibility was explored experimentally in Cr-doped RuO_2, where it was suggested that this system exhibits the anomalous Hall effect (AHE) due to altermagnetism. Based on our density functional calculations, we revise the results obtained for this system and propose a different interpretation of experimental results. Our calculations

suggest that extra holes are bound to Cr impurity and do not dope Ru bands, which remain nonmagnetic. Thus, the observed AHE is not due to the altermagnetism but stems entirely from magnetic Cr ions [2].

References

[1] A. Smolyanyuk, I. I. Mazin, L. Garcia-Gassull, R. Valentí, Phys. Rev. B **109**, 134424 (2024).
[2] A. Smolyanyuk, L. Šmejkal, I. I. Mazin, Phys. Rev. B **111**, 064406 (2025).

Abstract ID: 30343

T-SYMMETRY BREAKING PHENOMENA IN ALTERMAGNETIC MnTe

A. Dal Din, O. J. Amin, K. W. Edmonds, R. P. Campion, P. Wadley

School of Physics and Astronomy, University of Nottingham, University Park Campus, Nottingham, NG72RD, UNITED KINGDOM

One of the most characteristic features of altermagnets is their non-relativistic alternating spin-split band structures. Though these bands give rise to previously unexpected behavior in altermagnets of a certain symmetry, such as spin-polarized currents, it is the relativistic spin-orbit coupled bands that are the origin of many of the other T-reversal symmetry breaking phenomena of altermagnets, such as the anomalous Hall effect and X-ray magnetic circular dichroism. By combining both cutting-edge and well-established techniques, newly predicted properties of this class may be observed. Here I will present recent experimental development and results highlighting how to measure some of these phenomena, along with ways in which altermagnetic domains can be controlled and manipulated to aid in their detection. In this talk the anomalous Hall effect, X-ray magnetic circular dichroism, and photoemission electron microscopy domain imaging will be shown, with discussion of device fabrication and spin-resolved ARPES measurements that demonstrate the full success and application of this unique control.

References

[1] O.J. Amin, A. Dal Din, *et al.*, *Nanoscale imaging and control of altermagnetism in MnTe*, Nature **636**, 348–353 (2024).

[2] A. Hariki, A. Dal Din, *X-ray magnetic circular dichroism in altermagnetic α-Mn*Te, Physical Review Letters, **132(17)**, 176701 (2024).

[3] A. Dal Din, *et al.*, *Unconventional relativistic spin polarization of electronic bands in an altermagnet*, arXiv preprint arXiv:2511.01690 (2025).

Abstract ID: 30351

PHASE STABILITY AND TUNABILITY IN THE NON-COLLINEAR ANTIFERROMAGNET $Mn_{3+x}Sn_{1-x}$

K. Gas[1,2,3]

[1] *Center for Science and Innovation in Spintronics, Tohoku University, 2-1-1 Katahira, Aoba-ku, Sendai 980-8577, JAPAN*
[2] *Laboratory for Nanoelectronics and Spintronics, Research Institute of Electrical Communication, Tohoku University, 2-1-1 Katahira, Aoba-ku, Sendai 980-8577, JAPAN*
[3] *Institute of Physics, Polish Academy of Sciences, 2-1-1 Katahira, Aoba-ku, Sendai 980-8577, POLAND*

Non-collinear antiferromagnets provide a unique platform where magnetic order, symmetry, and electronic structure are intimately intertwined, giving rise to unconventional transport phenomena such as the anomalous Hall effect in the absence of net magnetization. Understanding the stability and tunability of magnetic phases in these systems is essential, both from a fundamental perspective and for potential spintronic applications.

In this talk, we present a systematic investigation of magnetic phase stability in epitaxial thin films of the chiral antiferromagnet $Mn_{3+x}Sn_{1-x}$ [1]. By combining temperature-dependent magnetic and transport measurements with controlled variation of composition, and by carefully accounting for substrate-related magnetic contributions inherent to thin-film magnetometry [2], we construct a magnetic phase diagram that delineates the paramagnetic, inverse triangular antiferromagnetic, and incommensurate spin phases, as summarized in the magnetic phase diagram presented in Fig. 1. We show that intrinsic alloying provides a robust route to continuously tune the phase boundaries, allowing the transition from the inverse triangular antiferromagnetic phase to the incommensurate state to be shifted and ultimately suppressed. As a result, the inverse triangular phase responsible for the anomalous Hall effect can be stabilized down to low temperatures.

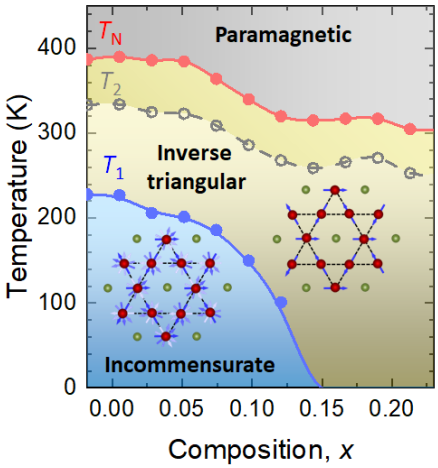

Fig. 1: *Magnetic phase diagram of epitaxial $Mn_{3+x}Sn_{1-x}$ thin films as a function of temperature and composition.*

The resulting magnetic phase diagram reveals clear deviations from bulk behavior and highlights the role of lattice effects and reduced dimensionality. Our work broadens the understanding of the correlation between structural and magnetic properties in $Mn_{3+x}Sn_{1-x}$ thin films, providing a solid basis for future studies and device-oriented investigations.

References

[1] K. Gas, J.-Y. Yoon, Y. Sato, H. Kubota, P. Dłużewski, S. Kret, J.Z. Domagala, Y. K. Edathumkandy, Y. Takeuchi, S. Kanai, H. Ohno, M. Sawicki, and S. Fukami, Appl. Phys. Lett. Mater. **13**, 041105 (2025).

[2] K. Gas, and M. Sawicki, Phys. Rev. Appl. Accepted, e-print arXiv:2507.01385 (2025).

Abstract ID: 30352

MAGNETIC PROPERTIES OF HEXAGONAL MnTe AND THEIR IMPLICATIONS FOR TRANSPORT PHENOMENA

M. Sawicki

Institute of Physics, Polish Academy of Sciences, Warsaw, POLAND

Hexagonal MnTe has recently been identified as a promising altermagnet candidate [1-3], in which a unique spin arrangement combines collinear, fully compensated antiferromagnetic ordering in real space with non-relativistic, alternating spin splitting in momentum space. This unconventional magnetic symmetry enables large time-reversal-symmetry-breaking responses without net magnetization, supports terahertz spin dynamics, and has been proposed to host a spontaneous anomalous Hall effect (AHE).

To shed further light on the origin of the AHE in hexagonal MnTe, we perform a comprehensive experimental and theoretical investigation [4]. Using bulk, substrate-free samples, we eliminate background contributions and demonstrate that the AHE in MnTe [5] is accompanied by a weak ferromagnetic (FM) signal, most clearly observed in the remnant state. This magnetization is strictly aligned along the hexagonal c axis, perpendicular to the Neel vector, and vanishes precisely at the Neel temperature.

To account for the emergence of this weak FM component in zero field, we introduce a macrospin toy model incorporating a phenomenological energy term inspired by the Dzyaloshinskii-Moriya interaction. In parallel, Berry curvature calculations confirm that the AHE persists even in the absence of net magnetization. These results indicate that both the AHE and the weak FM signal originate from the same underlying symmetry properties of the magnetic structure, revealing a significantly richer magnetic landscape of hexagonal MnTe than expected for a simple collinear antiferromagnet.

References

[1] L. Šmejkal, J. Sinova, T. Jungwirth, *Emerging research landscape of altermagnetism*, Phys. Rev. X **12**, 040501 (2022).

[2] I. Mazin, *Editorial: Altermagnetism—A new punch line of fundamental magnetism*, Phys. Rev. X **12**, 040002 (2022).

[3] O. J. Amin, *et al.*, *Nanoscale imaging and control of altermagnetism in MnTe*, Nature **636**, 348–353 (2024).

[4] K. P. Kluczyk, K. Gas, M. J. Grzybowski, P. Skupiński, M. A. Borysiewicz, T. Fąs, J. Suffczyński, J. Z. Domagala, K. Grasza, A. Mycielski, M. Baj, K. H. Ahn, K. Výborný, M. Sawicki, M. Gryglas-Borysiewicz, *Coexistence of anomalous hall effect and weak net magnetization in collinear antiferromagnet MnTe*, Phys. Rev. B **110**, 155201 (2024)

[5] M. Gryglas-Borysiewicz, *Anomalous Hall effect and magnetoresistance study of bulk MnTe*, this conference.

Abstract ID: 30706

NON-RELATIVISTIC SPIN CURRENTS AND TORQUES IN ANTIFERROMAGNETS

J. Železný

Institute of Physics of the Czech Academy of Sciences, 162 00 Prague, CZECH REPUBLIC

Contrary to the early understanding of antiferromagnets as limited compared to ferromagnets, a rich landscape of phenomena in antiferromagnets has been demonstrated that could be utilized for various spintronics functionalities. Here, we discuss recent advances in understanding of how electrical current can induce spin currents or spin torques in antiferromagnetic systems, focusing primarily on non-collinear antiferromagnets and on phenomena that originate from the non-collinear order without requiring the relativistic spin-orbit coupling. We show that antiferromagnets can host spin-polarized currents and that these can be utilized for magnetic junctions, that antiferromagnets can be used for spin-charge conversion, potentially even without any spin loss, and that a non-relativistic current-induced torque analogous to the spin-orbit torque can exist in antiferromagnets.

Abstract ID: 30140

SHIELDING THE STRAY MAGNETIC FIELD OF A LARGE SUPERCONDUCTING COIL FROM A ROTATING MACHINE: EXPERIMENTAL DEMONSTRATION OF SCALABLE SCREENS COMBINING BULK SUPERCONDUCTORS AND COATED CONDUCTORS

N. Rotheudt[1], J.-F. Fagnard[1], F. Antoncik[2,3], T. Hlasek[2,3], J. Plechacek[2], P. Vanderbemden[1], A. B. Abrahamsen[4]

[1] *Department of Electrical Engineering & Computer Science, University of Liège, BELGIUM*
[2] *CAN SUPERCONDUCTORS, s.r.o., Ringhofferova 66, 251 68 Kamenice, CZECH REPUBLIC*
[3] *Department of Inorganic Chemistry, University of Chemistry and Technology Prague, Technická 5, 166 28 Prague 6, CZECH REPUBLIC*
[4] *Department of Wind and Energy Systems, Technical University of Denmark, 4000 Roskilde, DENMARK*

Conventional rotating machines use a ferromagnetic structure to enclose the magnetic field lines and protect sensitive equipment and human operators. However, next-generation, superconductor-based rotating machines aim to increase the power density in several applications (e.g., electric aircraft or floating offshore wind turbine) [1,2], thereby reducing the weight and/or enabling operation at higher fields and, consequently, removing or reducing the ferromagnetic structure. New ways must therefore be found to attenuate the high, low-frequency, inhomogeneous stray magnetic field over wide surface areas.

In our previous works, we demonstrated that closed-loop coated conductors can be placed around a bulk superconductor to improve its magnetic screening/shielding properties [3,4]. In this work, we introduce a new topology made of four 60 mm-diameter disk-shaped bulks arranged side-by-side. Closed-loop coated conductors are interleaved around them and short stack tape segments are added. The resulting structure is subjected (at 77 K) to the inhomogeneous stray magnetic field (up to ~150 mT) of a large superconducting coil designed to demonstrate a rotating machine pole of a direct-drive wind turbine. The key findings are as follows. First, adding the loops around the bulks is a lightweight and effective way to mitigate the presence of the gaps between the bulks (one of the main problems in building large screens). The role of these loops is also confirmed by trapped field measurements. Second, the screened surface area is, consequently, substantially increased and suitable field attenuations are obtained at low fields over at least 138 mm. Third, analysing the measurements in terms of axial and transverse components of the field help us explain the influence of the inhomogeneity of the applied field on the screening properties.

Acknowledgments

N. Rotheudt is recipient of a research grant from F.R.S-FNRS. This work is supported by F.R.S.-FNRS grant CDR J.0184.23. The work of Tomas Hlasek was supported by the Czech Science Foundation (project 24-10171S).

References

[1] A. B. Abrahamsen, *et al.*, Supercond. Sci. Technol., **23**, 034019 (2010).

[2] Y. Terao, *et al.*, IEEE Trans. Appl. Supercond., **29(5)**, 5202305 (2019).

[3] N. Rotheudt, *et al.*, Supercond. Sci. Technol., **37,** 065008 (2024).

[4] N. Rotheudt, *et al.*, Supercond. Sci. Technol., **38**, 025012 (2025).

Abstract ID: 30199

EXPERIMENTAL ANALYSIS AND 3D MODELLING OF DC MAGNETIC SHIELDING USING A Bi-2223 VESSEL AND Bi-2223/Fe HYBRID LAYOUTS

M. Fracasso[1,2], R. Gerbaldo[1,2], G. Ghigo[1,2], J.F. Fagnard[3], P. Vanderbemden[3], L. Gozzelino[1,2]

[1] Department of Applied Science and Technology, Politecnico di Torino, 10129 Torino, ITALY
[2] INFN - National Institute for Nuclear Physics, Sezione di Torino, 10125 Torino, ITALY
[3] Department of Electrical Engineering and Computer Science Montefiore Institute, Universite de Liège, Liège, BELGIUM

High-quality magnetic shielding is essential for achieving the highly stable, low-noise magnetic environments required by sensitive scientific instrumentation, advanced medical diagnostics, and high-precision industrial applications. Superconducting (SC) bulk materials have consequently attracted significant interest as high-efficiency DC shielding solutions, leveraging their ability to sustain large persistent currents and to be manufactured in tailored geometries [1]. Among these, $Bi_2Sr_2Ca_{n-1}Cu_nO_{2n+4+x}$ (Bi-2223) is particularly attractive thanks to its favorable processing routes, which allow the fabrication of large, closed-shape structures [2], making it a strong candidate for practical shielding devices.

In this work, we present a comprehensive experimental characterization of the magnetic shielding performance of a commercial Pb-doped polycrystalline Bi-2223 vessel (CAN Superconductor, CSV-12). The shielding efficiency was assessed under both axial (AF) and transverse (TF) applied magnetic field orientations. Since the superimposition of a ferromagnetic (FM) layer can significantly improve the effectiveness of SC shields [3], we also investigated a hybrid SC/FM configuration obtained placing a coaxial soft iron shield around the SC vessel. The results demonstrate a significant improvement in shielding capabilities for this hybrid structure in both AF and TF orientations, highlighting a functioning strategy for designing compact and highly efficient magnetic shields.

Moreover to consider realistic working conditions, where the direction of the applied magnetic field is not necessarily well defined, we further investigated complex crossed-field conditions by measuring the axial shielding capability after a pre-magnetization process in a transverse field, and vice versa.

Finally, to accurately elucidate these coupling behaviors, we developed a full 3D finite-element model using COMSOL Multiphysics® [4], employing a magnetic vector potential-based formulation. The numerical outputs support the experimental evidences and provide crucial insights into the interplay between SC and FM shielding mechanisms underscoring the critical role of magnetic history in determining the overall system's performance.

Acknowledgements

This study was partially carried out within the Space It Up project funded by the Italian Space Agency, ASI, and the Ministry of University and Research, MUR, under contract n. 2024-5-E.0 - CUP n. I53D24000060005.

References

[1] N. Rotheudt, M. Fracasso, *et al.*, Supercond. Sci. Technol., **38**, 043002, (2025).

[2] CAN Superconductor, https://www.can-superconductors.com.

[3] J.H. Durrell, *et al.*, Supercond. Sci. Technol., **31**, 103501, (2018).

[4] L. Gozzelino, *et al.*, Supercond. Sci. Technol., **35**, 044002, (2022).

[5] M. Solovyov and F. Gömöry, Supercond. Sci. Technol., **32**, 115001 (2019).

Abstract ID: 30206

HIGH-PRESSURE SYNTHESIS AND SUPERCONDUCTING PROPERTIES OF F-DOPED SmFeAsO BULKS: COMPARATIVE STUDY OF HIGH-GAS PRESSURE, CUBIC-ANVIL, AND SPARK-PLASMA SINTERING

S. J. Singh

Institute of High Pressure Physics (IHPP), Polish Academy of Sciences, Sokołowska 29/37, 01-142 Warsaw, POLAND

The high-pressure (HP) growth technique serves as an essential method, enabling the stabilization of new phases and the precise control of structural parameters that play a crucial role in influencing electronic and magnetic properties [1, 2]. In this presentation, we review our recent studies based on the optimization of the growth condition of $SmFeAsO_{0.8}F_{0.2}$ (Sm1111) bulks prepared by three different high-pressure techniques: the high-gas pressure and high-temperature synthesis (HP-HTS) [1-3], cubic anvil high pressure (CA-HP) [4] and spark plasma sintering (SPS) [5] techniques using *in-situ* and *ex-situ* processes together with the conventional synthesis process at ambient pressure (CSP-AP) and compared their superconducting properties. These methods employ high growth pressure, reaching up to 4 GPa, alongside varying heating temperatures (up to 1600°C) and durations to optimize the best conditions for achieving both high superconducting properties and sample quality [1-5]. Multiple samples are prepared by these techniques under different conditions and analyzed through various characterizations to reach the conclusions and identify the optimal growth conditions [3-5]. Our studies suggest that high-pressure growth could be an effective method for producing iron-based superconductors (FBS) to improve their superconducting properties, including the transition temperature (T_c), critical current density, and pinning force [3-5], but only under optimized growth conditions. In addition, the quality of the samples and their density are enhanced by the HP growth process through the improvement of intergrain connections and homogeneity of the samples [3-5]. Furthermore, the comprehensive evaluations and investigations indicate that the *in-situ* process of Sm1111 needs high growth pressure and temperature (4 GPa, 1400°C, 1 h) to complete the Sm1111 phase formation and enhance the transition temperature by 3 K, whereas the *ex-situ* process can be completed at the low growth pressure of 0.5 GPa and enhance the critical current density by one order of magnitude by keeping almost the same T_c (~53 K) as that by the CSP-AP process. These studies are briefly compared and discussed alongside CSP-AP to understand the three different HP synthesis effects on Sm1111 bulks [3-5], which may significantly influence the future development of FBS.

Acknowledgement

This research was supported by the National Science Centre (NCN), Poland through the SONATA-BIS 11 project (2021/42/E/ST5/00262) and the Weave-UNISONO project (2025/07/Y/ST5/00116). SJS acknowledges financial support from NCN Poland through Project numbers 2021/42/E/ST5/00262 and 2025/07/Y/ST5/00116.

References

[1] S. J. Singh and M. I. Sturza, Crystals, **Vol 12**, pp 20 (2022).

[2] Priya Singh and Shiv J. Singh et al., Cryogenics (Elsevier), **Vol 147**, pp 104028 (2025).

[3] M. Azam and Shiv J. Singh et. al., Crystals, Vol 13 (10), pp 1525 (2023); Ceramics International, **Vol 51**, pp. 13734-13751 (2025).

[4] M. Azam, T. Zajarniuk H. Ogino and Shiv J. Singh, Materials Research Express, **Vol 12**, pp 116001 (2025).

[5] M. Azam, T. Zajarniuk, K. Kwatek, Paolo Mele and Shiv J. Singh, Cryogenic, **Vol 150**, pp 104125, (2025).

Abstract ID: 30450

HIGH PERFORMANCE RE123 BULKS BY TOP SEEDED MELT-GROWTH

X. Yao

School of Physics and Astronomy, Shanghai Jiao Tong University, Shanghai 200240, CHINA

We are interested in understanding and controlling the process-microstructure-property of REBCO bulk superconductors**.** For high-performance and reliable-fabrication, a variety of approaches have been newly developed in our lab, such as

1) Cooling-rate-control melt-growth was conducted for LRE123 bulks with high superconducting performance The underlying mechanism correlated with superconducting properties are comprehensively elucidated.

2) Aiming to refined and uniform RE211, a novel TSMG approach was developed, in which instead of RE211+RE123, modified precursor powders (MPP, RE_2O_3, and $Ba_xCu_yO_z$) were employed. As a result, massive numbers of small-sized RE211 were in-situ derived from the homogeneous nucleation. Furthermore, MPP is used to combine with a compositional graded structure, effectively suppressing the inherent enlargement and segregation of RE211 particles.

Two novel seeding strategies for creating incomplete crystallographic shapes of REBCO crystals were developed, which possess self-repairing capability, leading to rapid surface growth for sizable bulks. One is in situ self-assembly seeding, by which self-reparability promotes REBCO growth, while the other is vertically-connected seeding, by which self-reparability triggers REBCO nucleation.

Abstract ID: 30745

SYNTHESIS, STRUCTURE AND PHYSICAL PROPERTIES OF THE RHOMBOHEDRAL RIr_3 BINARY COMPOUNDS

K. Górnicka, T. Klimczuk

Faculty of Applied Physics and Mathematics, Gdansk University of Technology, Narutowicza 11/12, 80-952 Gdansk, POLAND
and
Advanced Materials Centre, Gdansk University of Technology, ul. Narutowicza 11/12, 80-233 Gdańsk, POLAND

The family of compounds characterized by the general formula $R_{2m+n}T_{4m+5n}$, where R is the rare earth or actinide metal and T is a transition metal, is of significance due to its structural complexity and wide range of observed physical properties. The m and n parameters determine the number of $MgCu_2$-type and $CaCu_5$-type structural blocks, respectively, thereby providing a systematic framework for understanding structural variations and their influence on the properties.

The RIr_3 system (m = 1 and n = 1) is known to form in different crystal structure types, depending on the choice of the R metal and the post-synthesize annealing temperature. In this lecture we will present synthesis, structural and physical studies of the rhombohedral ($PuNi_3$ type) $CeIr_3$, $PrIr_3$, $NdIr_3$ and $ThIr_3$. The key element in this family, which affects the physical properties, is the rare earth or actinide metal (R). While $LaIr_3$, $CeIr_3$ and $ThIr_3$ are superconductors with T_c = 3.5 K [1], 2.5 K [2,3] and 4.4K [4], respectively. In contrast, the remaining two are are classified as ferromagnets, with the Curie temperature T_{Curie} = 7.5 K ($PrIr_3$) [5] and 10.6 K ($NdIr_3$) [6]. Interestingly, at around 70 K, the both magnetic compounds reveal a structural phase transition. The rhombohedral R-3m crystal structure undergoes a transformation to a monoclinic C2/m structure upon cooling, and further cooling reveals temperature-independent behaviour of the unit cell volume.

The preliminary data on $NpIr_3$ and $PuIr_3$ will also be presented. These binary transuranic compounds have been synthesized and studied at JRC-KA (Germany). While $PuIr_3$ appears to be a paramagnet, $NpIr_3$ is likely to be an itinerant antiferromagnet with T_N = 17 K.

References

[1] N. Haldolaarachchige, L. Schoop, M. A. Khan,W. Huang, H. Ji, Kalani Hettiarachchilage, and D. P. Young, J. Phys.: Condens. Matter **29**, 475602 (2017).
[2] Y. J. Sato, A. Nakamura, Y. Shimizu, A. Maurya, Y. Homma, D. Li, . Honda, and D. Aoki, Journal of the Physical Society of Japan, **87**, 053704 (2018).
[3] K. Górnicka, E. M. Carnicom, S. Goląb, M. Łapiński, B. Wiendlocha, W. Xie, D. Kaczorowski, R. J. Cava, and T. Klimczuk, Supercond. Sci. Technol. **32**, 025008 (2019).
[4] K. Górnicka, D. Das, S. Gutowska, B. Wiendlocha, M. J. Winiarski, T. Klimczuk, and D. Kaczorowski, Phys. Rev. B **100**, 214514 (2019).
[5] K. Górnicka, M. J. Winiarski, R. J. Cava, M. A. McGuire, and T. Klimczuk, Phys. Rev. B **110**, 064431 (2024).
[6] K. Górnicka, W. Xie, E. M. Carnicom, R. J. Cava, and T. Klimczuk, Phys. Rev. B **99**, 14430 (2019).

11th International Conference on Superconductivity and Magnetism ICSM2026
4th International Conference on Quantum Materials and Technologies ICQMT2026
19th April to 26th April, 2026, Ölüdeniz – Fethiye/Muğla, Türkiye
https://icsmforever.org/

Abstract ID: 30005

STRUCTURALLY DEPENDENT SUPERCONDUCTING PROPERTIES OF Ti-RICH HIGH-ENTROPY ALLOYS: COMPOSITION AND AFTERTREATMENT EFFECT ON CRITICAL CURRENT DENSITY

P. Sobota, W. Idziak, R. Idczak

Institute of Experimental Physics, University of Wrocław, pl. M. Borna, 9 50-204 Wrocław, POLAND

Superconducting high-entropy alloys (HEAs) are the new category of disordered superconductors. They are solid solutions of five or more elements mixed in non-negligible proportions (more than 5 at.% of each element). These materials exhibit excellent mechanical properties, great stability in extreme temperatures, and significant robustness to high pressure. Such properties make them a perfect candidate for high-field magnets in LHC, ITER, or NMR applications. In particular, the titanium rich family of HEA superconductors seems interesting with their exceptionally high upper critical field parameters close to the ones of commercial Nb-Ti [1,2].

The present study investigates the structure-dependent superconductivity in titanium-rich high-entropy alloys, focusing on the interplay between composition, crystal structure, and superconducting properties. Two routes were considered: (1) A series of HEAs with systematically varied titanium concentrations were synthesized to explore how Ti enrichment influences the emergence and characteristics of superconductivity. (2) A promising alloy underwent systematic mechanical deformation and thermal treatment. Comprehensive characterization was carried out using X-ray diffraction (XRD) to determine crystal structure, scanning electron microscopy combined with energy-dispersive X-ray spectroscopy (SEM-EDXS) for microstructural and compositional analysis, magnetization measurements to probe superconducting transitions, and specific heat measurements to gain insight into the thermodynamic properties of the superconducting state.

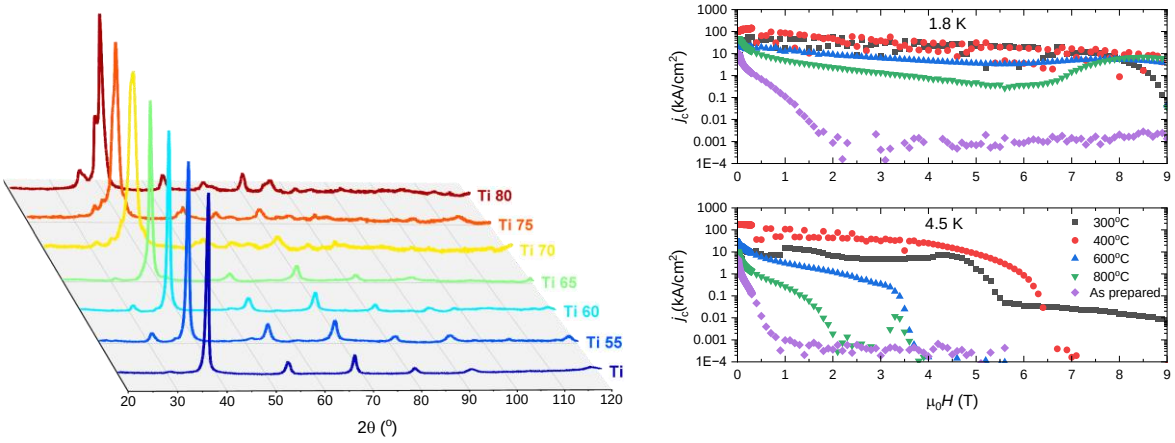

Fig. 1: *(left) Structural evolution of high-entropy alloy with increasing Ti concentration. (right) Change of critical current densities in the alloy with different annealing temperatures.*

References

[1] P. Sobota, *et al.*, Acta Materialia **285(2)**, 120666 (2024).

[2] R. Idczak, *et al.*, Materials **16(17)**, 5814 (2023).

Abstract ID: 30015

SUPERCONDUCTIVITY IN NEW HIGH ENTROPY ALLOYS DOPED WITH ELEMENTS FROM GROUP 3 AND 13

P. Olejnik[1,2], D. Gnida[2], P. Sobota[1]

[1] *Institute of Experimental Physics, University of Wrocław, pl. M. Borna 9, Wrocław, 50-204, POLAND*
[2] *Institute of Low Temperature and Structure Research, Polish Academy of Sciences, ul. Okólna 2, Wrocław, 50-422, POLAND*

High-entropy alloys (HEA) are solid solutions of 5 to 20 elements mixed with at least 5% of each element. Their distinguishable feature is that they do not form multiple binary or ternary intermetallic compounds, instead high-entropy mixing stabilizes simple HEA phases (body centered cubic, face centered cubic or hexagonal), while the phases themselves exhibit high order of chemical disorder. Due to those features HEAs may possess superior chemical, mechanical and physical properties such as high strength, thermal stability or corrosion resistance. Additionally, in recent years the growing group of HEAs was revealed to exhibit superconductivity [1], which combined with properties mentioned above points at their great potential in applications such as high-field magnets.

$Ti_{0.5}(ZrNbHfTa)_{0.5}$ [2] were doped with elements from group 3 and 13. Samples were synthesized by conventional arc melting and examined using powder X-ray diffraction, scanning electron microscopy (SEM) and their properties were characterized using PPMS platform (magnetic susceptibility, specific heat and electrical resistivity measurements). The effect of the additional sixth elements where discussed. New compositions show significantly different superconducting properties from the parent compound.

References

[1] P. Koželj, *et al.*, Physical Review Letters, **113**, 107001 (2014).

[2] P.Sobota, *et al.*, Acta Materialia Vol. **285**, 120666 (2025).

Abstract ID: 30017

NEW Ti-RICH YTTRIUM-CONTAINING SUPERCONDUCTING HIGH-ENTROPY ALLOY WITH HIGH UPPER CRITICAL FIELD

B. Rusin[1], W. Nowak[1], R. Idczak[1], M. Babij[2]

[1] *University of Wrocław, Institute of Experimental Physics, pl. Maxa Borna 9, 50-204 Wrocław, POLAND*
[2] *Polish Academy of Sciences, Institute of Low Temperature and Structure Research, ul. Okólna 2, Wrocław, 50-422, POLAND*

High-Entropy Alloys (HEAs) are solid solutions of five or more elements mixed in non-negligible proportions. Their unique and tunable physical properties have attracted significant attention since their discovery in 2004 [1]. HEAs typically form well-defined, close-packed structures (BCC, FCC, HCP). Due to their structural features, HEAs are known for exceptional mechanical properties, thermal stability, and corrosion resistance. These materials have enormous potential for various applications, especially if their high durability is combined with more sophisticated phenomena, such as magnetic ordering and superconductivity. Superconductivity in HEAs was discovered in 2014 [2]. Superconducting HEAs represent a novel class of disordered superconductors that exhibit substantial robustness against environmental perturbations, i.e., great stability in high pressures and at extreme temperatures. Such remarkable properties make them a perfect candidate for high-field magnets in Large Hadron Collider (LHC), nuclear fusion reactors such as ITER, or nuclear magnetic resonance (NMR) systems. Our recent research has shown that the upper critical fields of BCC HEA superconductors can be significantly enhanced by synthesizing Ti-rich compositions [3]. Building upon these findings, the present study focuses on the synthesis and characterization of a new Ti-rich HEA superconductor.

In this work, we report the first results of the synthesis, structural and physical characterization of a new refractory Ti-rich HEA superconductor $Ti_{50}(YNbTaHf)_{50}$, which exhibits a high upper critical field $\mu_0 H_{c2}$. The alloy was prepared by the arc melting method. Structure of the alloy was characterized by X-ray diffraction (XRD), scanning electron microscopy (SEM), and energy-dispersive X-ray spectroscopy (EDXS). Superconductivity was investigated via electrical resistivity, AC susceptibility, DC magnetization, and specific heat measurements. The upper critical field was determined using Werthamer-Helfand-Hohenberg (WHH) model. The effect of yttrium on microstructure and superconducting properties was examined. The results obtained showed that alloy crystallizes in BCC structure. The determined superconducting transition temperature T_c for $Ti_{50}(YNbTaHf)_{50}$ is 6.3 K and the upper critical field $\mu_0 H_{c2}$ reaches 14.65 T – the highest reported value among BCC HEA superconductors verified within the WHH framework. The high $\mu_0 H_{c2}$, comparable to that of commercial NbTi superconductor, highlights $Ti_{50}(YNbTaHf)_{50}$ as a promising candidate for high-field magnet applications.

References

[1] J. -W. Yeh, *et al.*, Adv. Eng. Mater. **6**, 299–303 (2004).

[2] P. Koželj, *et al.*, Phys. Rev. Lett. 113, (2014).

[3] P. Sobota, *et al.*, Acta Mater. **285**, 120666 (2025).

Abstract ID: 30148

MAGNETIC LEVITATION OF A SUPERCONDUCTING HOLLOW CYLINDER FOR QUANTUM MAGNETOMECHANICS

N. Bort-Soldevila, J. Cunill-Subiranas, D. Sarrat, N. Del-Valle, C. Navau

Departament de Física, Universitat Autònoma de Barcelona, 08193 Bellaterra, Barcelona, SPAIN

We investigate a superconducting levitation architecture based on a hollow finite cylinder threaded by a current-carrying wire, aimed at applications in quantum magnetomechanics. The system consists of a superconducting cylindrical shell with inner radius R_1, outer radius R_2 and length L together with an infinite straight wire that runs along its axis or is slightly displaced from it. The resulting screening currents generate repulsive forces that enable stable magnetic levitation of the cylinder.

Within London theory, we derive a semi-analytical solution for the equilibrium coaxial configuration, obtaining the azimuthal magnetic field as a series of cosine axial modes and modified Bessel radial modes, and validate this description against finite-element simulations. A 3D numerical model of the London equation is then used to evaluate the restoring magnetic forces arising from small lateral displacements. From the linear response of these forces we extract the effective stiffness and the corresponding vibrational frequencies of the levitated mechanical modes, and perform a parametric study as a function of penetration depth, shell thickness and cylinder length.

We identify regimes with strong restoring forces and well-defined translational modes, indicating that this and related geometries are promising superconducting magnetomechanical resonators. We also outline how the same modelling strategy can be extended to alternative levitated superconducting oscillators for future quantum magnetomechanical and magnetic sensing experiments.

References

[1] N. Bort-Soldevila, *et al.*, *Modeling magnetically levitated superconducting ellipsoids, cylinders, and cuboids for quantum magnetomechanics*, Physical Review Research, **vol. 6**, **no 4**, p. 043046 (2024).

[2] J. Cunill-Subiranas, *et al.*, *Magnetic flux threading a planar holed superconductor*, Physical Review B, **vol. 111**, **no 17**, p. 174530 (2025).

[3] A. Sanchez, N. Bort-Soldevila, *Shaping magnetic fields with zero-magnetic-permeability media*, Journal of Applied Physics, **vol. 130**, **no 16** (2021).

Abstract ID: 30711

PAST AND FUTURE PERSPECTIVE OF Tl-1212 SUPERCONDUCTOR

E. Yusrianto[1], Y. Lizar[2]

[1] *Faculty of Education Sciences, Universitas Islam Negeri Imam Bonjol Padang, 25153 Padang, West Sumatera, INDONESIA*

[2] *Faculty of of Science & Technology, Universitas Islam Negeri Imam Bonjol Padang, 25153 Padang, West Sumatera, INDONESIA*

Thirty years after the discovery of superconductivity above 90 K in Tl-Ba-Cu-O system, several elemental substitutions in this system may lead to higher-temperature superconductivity [1]. Sheng and Hermann used $BaCu_3O_4$ as a starting material because it has the lowest melting point among the Ba-Cu oxides.

In Tl-cuprate, most of chemical substitutions are concerned with Tl-2223 for its high superconducting transition temperature and Tl-1223 for its potential use in industry. The chemical substitution in Tl-1212 is rare which may be due to its lower T_c and J_c [2]. But the Tl-1212 type phase is of interest due to its simple preparation, high quality and sharp superconducting transition [3].

In this report, we reviewed many rare-earth elements substituted in Tl-system especially Tl-1212 superconductors. Many new superconducting phases have been reported including $TlSr_2CaCu_2O_7$. The Tl-1212 type phase such as $TlBa_2CaCu_2O_7$ and $TlSr_2CaCu_2O_7$ has similar structure with $YBa_2Cu_3O_7$ [4]. Previous works also showed that partial substitution of Cr, Pb and Bi at Tl site can stabilize the Tl-1212 phase [5-7].

Most of high-temperature superconductors in Tl-1212 have led to the formation of the Tl-1223 and 1201 type as a minor phase. The elements substitution and addition which give benefits in 1212 phase study and higher-temperature superconductors are discussed.

Abstract ID: 30311

BULK $GdBa_2Cu_3O_7$ SUPERCONDUCTORS PREPARED BY SINGLE DIRECTION MELT GROWTH (SDMG): KEY POINTS TO UNDERSTAND THEIR BEHAVIOUR UNDER A TIME-DEPENDENT MAGNETIC FIELD

N. Rotheudt[1], D. Szewczyk[2], P. Stachowiak[2], J. F. Fagnard[1], T. Hlasek[3,4], J. Plechacek[3], P. Vanderbemden[1]

[1] Montefiore Research Unit B28, University of Liège, Liège B-4000, BELGIUM
[2] Institute for Low Temperature and Structure Research, 50-422 Wroclaw, POLAND
[3] CAN SUPERCONDUCTORS, s.r.o., Ringhofferova 66, 251 68 Kamenice, CZECH REPUBLIC
[4] Department of Inorganic Chemistry, University of Chemistry and Technology Prague, Technická 5, Prague 6 166 28, CZECH REPUBLIC

Bulk, large grain $GdBa_2Cu_3O_7$ superconductors prepared by the 'Single-Direction Melt Growth' (SDMG) process [1,2] are known to exhibit an unprecedented homogeneity of their superconducting properties [3]. Hence, they offer great ability as trapped field superconducting magnets or magnetic shields and screens [4]. In most engineering applications, however, the superconductor is subjected to several cycles of the applied field. Examples include a bulk magnet in a rotating machine or a superconducting magnetic screen subjected to a changing stray field. The goal of this communication, therefore, is to highlight key parameters required to predict and study the change of properties of an SDMG bulk superconductor when it is subjected to repeated cycles of applied field. For low-frequency magnetic fields, we study the magnetic screening properties of a disk-shaped superconducting bulk. Experimentally, the screening factor SF that we obtain after up to 30 cycles of low-frequency applied field is the same (at the maximum field) as the SF after the first ramp from zero field to its maximum. Numerically, we show that the relative decay of SF between successive occurrences of the maximum field is smaller than the decay that would be obtained if the maximal field was maintained. Hence, the key parameters are the magnetic relaxation and the penetration depth in the bulk, since a higher penetration depth leads to a smaller SF and a faster magnetic relaxation. At higher frequencies of applied field, the hysteresis losses may yield a temperature increase which, in turn, affects the magnetic properties. To predict this self-heating, we provide experimental data on the thermal properties of SDMG bulk samples ($GdBa_2Cu_3O_7$ + 0.4 mol Gd_2BaCuO_5 + 10% Ag_2O) and compare them to those of other bulk samples ($YBa_2Cu_3O_7$ and $Bi_2Sr_2CaCu_2O_8$). Among others, we investigate the anisotropy of both the thermal conductivity and the electrical resistivity, the peaks appearing in the temperature-dependent specific heat and the temperature dependence of the irreversibility line ($H||ab$ and $H||c$). Practical implications for engineering applications are discussed.

This work is partially funded by a collaboration programme between the FRS-FNRS (Belgium) and the PAN (Poland) under reference PINT-BILAT-M R.M002.24. Nicolas Rotheudt is recipient of an FRS-FNRS Research Fellow Grant.

References

[1] T. Motoki, *et al.*, Appl. Phys. Express **13**, 093002 (2020).

[2] F. Antoncik, *et al.*, IEEE Trans. Appl. Supercond. **35**, 6800205 (2025).

[3] T. Motoki, *et al.*, Supercond. Sci. Technol. **35**, 094003 (2022).

[4] N. Rotheudt, *et al.*, Supercond. Sci. Technol. **38**, 025012 (2025).

Abstract ID: 30566

REBCO BULK SUPERCONDUCTORS BASED ON Y, Gd, Eu AND Dy PREPARED BY TSMG AND SDMG PROCESS

P. Diko[1], M. Radušovská[1], D. Volochová[1], L. Vojtková[1], K. Zmorayová[1], V. Kuchárová[1], R. Smolko[1], M. Rajnak[1], B. Guner[2,3], T. Motoki[4]

[1] *Institute of Experimental Physics SAS, Watsonova 47, 04001 Košice SLOVAKIA*
[2] *Department of Physics, Faculty of Arts and Sciences, Recep Tayyip Erdogan University, 53100 Rize, TURKEY*
[3] *Center of Excellence for Superconductivity Research, 50. Year Campus, Ankara University, Golbasi, 06830 Ankara, TURKEY*
[4] *Department of Physical Sciences, Aoyama Gakuin University, 5-10-1 Fuchinobe, Chuo-ku, Sagamihara, Kanagawa 252-5258, JAPAN*

The microstructure and superconducting properties of REBCO bulk single-grain superconductors (BSS) based on Y, Gd, Eu and Dy prepared by TSMG and SDMG processes were studied. The microstructure was analysed by optical and electron microscopy, and XRD to characterize the size and volume fraction of RE211 particles, subgrain structure, oxygenation microcracks, and their sintering during high-temperature post-annealing. Macroscopic superconducting properties (levitation force and trapped magnetic field) were measured at 77 K and below 77 K on laboratory-fabricated devices, and the effective critical current density of the prepared REBCO BSS was determined from the trapped magnetic field measurements. The transition temperature to the superconducting state and the dependence of the critical current density on the magnetic field at 77 K and their dependence on the distance from the seed were measured on small samples separated from bulk crystals. Our analyses demonstrate the advantages of the newly developed method of preparing REBCO BSS by a single-directional melt-growth process [1-4]. They also point to the possibility of increasing the effective cross-section of the sample by partially sintering oxygenation cracks during high-temperature post-annealing [5] and maintaining open porosity (Fig. 1) for oxygen flow into the sample during subsequent oxygenation.

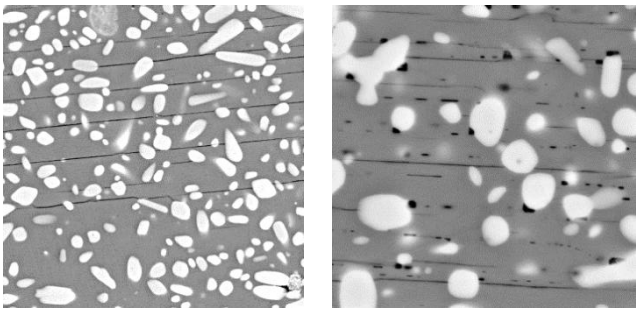

Fig. 1: *Microstructure of the DyBCO sample grown by SDMG process. Left: a/b-oxygenation cracks after standard oxygenation seen on a/c-surface, right: parially sintered a/b-oxygenation cracks after high temperature annealing at 900 °C seen on a/c-surface.*

References

[1] T. Motoki and J. Shimoyama, Supercond. Sci. Technol. **37**, 115019 (2024).
[2] P. Diko, K. Zmorayová, T. Motoki and J. Shimoyama, Ceram. Int. **49** 39280-39288 (2023).
[3] F. Antoncik, M. Lojka, T. Hlasek, O. Jankovsky and D. Semidubsky, IEEE T. Appl. Supercon. **35**, 6800205 (2025).
[4] M. Radusovská, P. Diko, D. Volochová, R. Smolko, V. Kuchárová and J. Bednarčík, Ceramics International, **51**, pp.24699-24706 (2025).
[5] T. Motoki, M. Miwa, M. Semba and J. Shimoyama, IEEE Trans. Appl. Supercond. **33**, 6800205 (2023).

Abstract ID: 30667

REVEALING FILAMENT MICROSTRUCTURE IN ADVANCED MgB_2 MULTIFILAMENTARY WIRES BY DEEP LEARNING SEGMENTATION

A. Yamamoto[1], M. Ito[1], K. Ogi[1], D. Fukui[1], K. Ando[1], Y. Shimada[2], M. Kodama[3], H. Tanaka[3]

[1] *Department of Biomedical Engineering, Tokyo University of Agriculture and Technology, 2-24-16 Naka, Koganei, Tokyo, JAPAN*
[2] *Department of Advanced Materials Science and Engineering, Kyushu University, 6-1 Kasuga-koen, Kasuga, Fukuoka, JAPAN*
[3] *Research & Development Group, Hitachi, Ltd., 7-1-1 Omika, Hitachi, Ibaraki, JAPAN*

Magnesium diboride (MgB_2) has a high critical temperature, making it a promising superconducting material for applications at cryo-cooling and liquid hydrogen temperatures. MgB_2 long-length wires can be fabricated by the powder-in-tube (PIT) method. In recent years, research on multifilamentary long-length wires for various magnet applications has been conducted [1]. A challenge toward multifilamentation of MgB_2 wires is that degradation of J_c appears in some cases when the number of filaments is greatly increased. On the other hand, we have focused on semantic segmentation, a deep learning technique also applied to medical image processing [2], and have succeeded in the prediction of constituent phases with high accuracy for polycrystalline materials with complex microstructures [3]. In this study, we quantified the microstructure using deep learning on an observation dataset obtained with a 3D-SEM to analyze the 3D filament structure of a MgB_2 superconducting wire. The analyzed sample was a superconducting multifilamentary wire under research and development [4], consisting of 51 superconducting filaments of approximately 10 μm in diameter arranged in a circular pattern. 3D-SEM observations were performed on the area where several filaments exist. Secondary electron images obtained with the 3D-SEM and manually segmented images were used as a training and testing dataset for a deep learning model. Based on the 1232 observed images, the application of deep learning for semantic segmentation and subsequent 3D reconstruction successfully quantified and visualized the internal filament structure.

References

[1] H. Tanaka and M. Kodama, J. Cryo. Super. Soc. Jpn. **56**, 327 (2021).
[2] O. Ronneberger, P. Fischer and T. Brox, Proc. MICCAI **9351** (2015).
[3] Y. Hirabayashi, H. Iga, H. Ogawa, S. Tokuta, Y. Shimada and A. Yamamoto, npj Comput. Mater. **10**, 46 (2024).
[4] M. Kodama, H. Kotaki, T. Suzuki and H. Tanaka, Supercond. Sci. Technol. **34**, 025018 (2021).

Abstract ID: 30013

IN-PLANE MAGNETIC ANISOTROPY AND LOCAL CHEMICAL CORRELATIONS IN $Ba_{1-x}Na_xFe_2As_2$

O. Chmaissem

Department of Physics, Northern Illinois University, DeKalb, IL 60115, USA

A comprehensive understanding of nematicity, magnetic anisotropy, and their relation to superconductivity in hole-doped 122-type pnictides requires both high-quality crystals with well-controlled compositions and measurements capable of resolving subtle short-range correlations. This work presents a detailed investigation of $Ba_{1-x}Na_xFe_2As_2$ single crystals combining precise stoichiometry control with high-field structural and diffuse-scattering studies.

High-quality crystals were synthesized over a wide composition range, and a quantitative correlation was established between the superconducting transition temperature and sodium content. This empirical relationship provides a reliable means to determine the actual Na stoichiometry, revealing that the effective substitution level in the best crystals is about 50–60% of the nominal value. Pulsed-field x-ray diffraction experiments up to 31.4 T applied along the c-axis show that the stripe-type spin-density-wave order remains strictly confined to the *ab* plane, with no evidence of detwinning or spin reorientation. These results demonstrate the pronounced in-plane magnetic anisotropy and the stability of the orthorhombic order against strong out-of-plane fields.

Diffuse x-ray scattering and three-dimensional ΔPDF analyses further identify two-dimensional short-range chemical correlations between Ba and Na atoms within the *ab* plane, accompanied by local atomic displacements due to their size mismatch. The observed local correlations reproduce structural features often attributed to intrinsic nematic fluctuations. Together, these findings delineate the intrinsic magnetic anisotropy of $Ba_{1-x}Na_xFe_2As_2$ and establish how local compositional order can influence the interpretation of nematic behavior in iron-based superconductors.

Abstract ID: 30095

PROGRESS IN THE FABRICATION OF HIGH-PERFORMANCE IRON-BASED SUPERCONDUCTING WIRES

X. Zhang[1,2], Y. Ma[1,2]

[1] *Institute of Electrical Engineering, Chinese Academy of Sciences, Beijing 100190, CHINA*
[2] *University of Chinese Academy of Sciences, Beijing 100049, CHINA*

Iron-based superconductor (IBS) has significant application potential in high magnetic field region due to their high upper critical field and low anisotropy [1]. To meet the requirements of strong current applications, systematic research has been carried out to improve the critical current density (J_c) of IBS wires. Currently, the Jc of the IBS wires has exceeded 4.5×10^5 A/cm^2 (4.2 K, 10 T), and the Jc of hundred-meter length wires have also reached 10^5 A/cm^2 (4.2 K, 10 T). Based on the IBS wires, insert coils, racetrack coils, and balloon type coils have been successfully fabricated. For example, one insert coil has generated 1 T under 20 T background field [2]. Even more, transposition cables with critical currents up to 7200 A have been developed for future large-scale magnet requirements. The above applications further verify the feasibility of high field applications of iron-based superconducting wires.

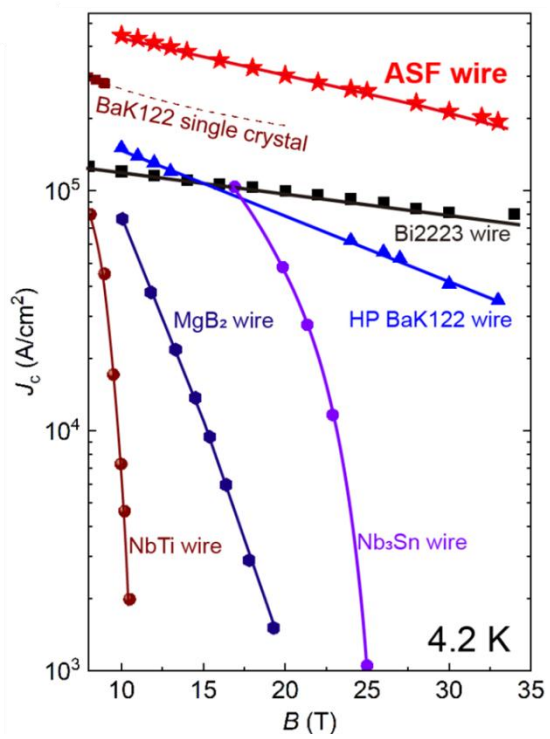

Fig. 1: The J_c-B data of Ba122 tape fabricated extrusion deforming technology.

References

[1] Y. Kmihara, T. Watanabe, M. Hirano, *et al.*, J. Am. Chem. Soc. **130**, 3296–3297 (2008).

[2] H. W. Ding, H. Zhao, P. C. Huang, *et al.*, Supercond. Sci. Technol. **36**, 11LT01 (2023).

Abstract ID: 30171

CRITICAL CURRENT DENSITY IN VARIOUS EPITAXIAL FILMS OF A HYDROGEN-SUBSTITUTED 1111-TYPE IRON-BASED SUPERCONDUCTOR

K. Hanzawa[1], K. Mitsui[2], Y. Takahara[1], J. Matsumoto[1], M. Miura[3], H. Hosono[2,4], H. Hiramatsu[1,2]

[1] *Materials and Structures Laboratory, Institute of Integrated Research, Institute of Science Tokyo, 226-8501, Yokohama, JAPAN*
[2] *MDX Research Center for Element Strategy, Institute of Integrated Research, Institute of Science Tokyo, 226-8501, Yokohama, JAPAN*
[3] *Graduate School of Science and Technology, Seikei University, 180-8633, Tokyo, JAPAN*
[4] *National Institute for Materials Science, 305-0044, Tsukuba, JAPAN*

1111-type iron-based superconductors (IBSCs) exhibit the highest critical temperature (T_c) in the bulk state among IBSCs. Although this high-T_c superconductivity is typically induced through electron doping with F or H, the H-substituted 1111-type IBSCs possess distinct advantages for wire/tape applications due to the insensitivity of T_c to the H concentration [1]. Nevertheless, the difficulty in epitaxial thin-film growth, mainly caused by the high vapor pressure of H, previously hindered advanced research on the H-substituted IBSCs.

In this context, we developed a topotactic H-substitution process for 1111-type IBSC epitaxial films using alkaline-earth metal (AE) hydrides (AEH_2) as the hydrogen source [2, 3]. The obtained H-substituted SmFeAsO, denoted as SmFeAs(O,H), not only exhibited a high T_c but also demonstrated a high upper critical field reaching 120 T, the highest value experimentally confirmed among all IBSCs [4]. Furthermore, it was recently revealed that the SmFeAs(O,H) epitaxial film records extremely high critical current density (J_c) and depairing current density (J_d) of >10 MA/cm^2 and >400 MA/cm^2, respectively [5]. These values are the highest among IBSCs, and notably, the J_d closely approaches that of cuprates, suggesting the high potential of SmFeAs(O,H) for practical wire applications.

Even though for instance the quality of pristine films and the H concentration/distribution likely affect the J_c of SmFeAs(O,H), their contributions still remain largely unclear. Therefore, gaining insights into the factors governing J_c is crucial for understanding the origin of the high J_c and achieving even higher J_c, advancing research toward the applications.

In this study, we investigate the relationship between J_c and the H-substitution process, including annealing conditions and the choice of H sources (i.e., the type of AEH_2). Furthermore, we also examine how the initial state of the pristine film, including its crystallinity and structural parameters, affects J_c. By combining the results obtained above, we discuss the J_c properties in SmFeAs(O,H).

References

[1] T Hanna, Y Muraba, S Matsuishi, N Igawa, K Kodama, S Shamoto, and H Hosono, Phys. Rev. B **84**, 024521 (2011).

[2] J. Matsumoto, K. Hanzawa, M. Sasase, S. Haindl, T. Katase, H. Hiramatsu, and H. Hosono, Phys. Rev. Materials **3**, 103401 (2019).

[3] H. Hiramatsu, J. Matsumoto, and H. Hosono, Appl. Phys. Express **13**, 073002 (2020).

[4] K. Hanzawa, J. Matsumoto, S. Iimura, Y. Kohama, H. Hiramatsu, and H. Hosono, Phys. Rev. Materials **6**, L111801 (2022).

[5] M. Miura, S. Eley, K. Iida, K. Hanzawa, J. Matsumoto, H. Hiramatsu, Y. Ogimoto, T. Suzuki, T. Kobayashi, T. Ozaki, H. Kurokawa, N. Sekiya, R. Yoshida, T. Kato, T. Okada, H. Okazaki, T. Yamaki, J. Hänisch, S. Awaji, A. Maeda, B. Maiorov, and H. Hosono, Nat. Mater. **23**, 1370–1378 (2024).

Abstract ID: 30184

COMPLETE ELECTRONIC PHASE DIAGRAM AND SUPERCONDUCTING PROPERTIES OF $PrFeAsO_{1-x}F_x$ ACROSS THE FULL DOPING RANGE ($0 \leq x \leq 1$)

P. Singh[1], K. Kwatek[2], T. Zajarniuk[3], A. Szewczyk[3], S. J. Singh[1]

[1] *Institute of High Pressure Physics (IHPP), Polish Academy of Sciences, Sokołowska 29/37, 01-142 Warsaw, POLAND*
[2] *Faculty of Physics, Warsaw University of Technology, Koszykowa 75, 00-662 Warsaw, POLAND*
[3] *Institute of Physics, Polish Academy of Sciences, Aleja Lotnikow 32/46, 02-668 Warsaw, POLAND*

The full electronic phase diagram of fluorine-doped $PrFeAsO_{1-x}F_x$ has remained largely unexplored, as previous studies were restricted to a narrow doping range ($0 \leq x \leq 0.23$). In this work, we address this longstanding gap by constructing, for the first time, a comprehensive electronic phase diagram spanning the entire fluorine substitution range ($0 \leq x \leq 1$). A systematic series of $PrFeAsO_{1-x}F_x$ samples was synthesized via a conventional solid-state route and thoroughly characterized using structural, microstructural, transport, magnetization, magnetotransport, and specific heat measurements. Superconductivity is observed over an extended doping interval, $0.15 \leq x \leq 0.7$, forming a well-defined superconducting dome. The optimally doped composition ($x = 0.3$) exhibits a transition temperature $T_c \approx 48$ K, while the highest $T_c \approx 52.3$ K is obtained in the overdoped regime at $x = 0.6$-0.7, exceeding previously reported values for $PrFeAsO_{1-x}F_x$ [1] by 5-6 K. The normal-state resistivity shows pronounced non-Fermi-liquid behaviour, following a power-law $T^{0.8}$-$T^{1.3}$ for $0.2 \leq x \leq 0.5$. Analysis of the upper critical field using the Werthamer–Helfand–Hohenberg model yields $H_{c2}(0) \approx 200$ T for $x = 0.3$–0.35, accompanied by a Maki parameter $\alpha > 1$, highlighting the dominant role of spin-paramagnetic pair breaking over the orbital pair-breaking mechanism. Under applied magnetic fields, the resistive broadening follows Arrhenius behaviour, and thermally activated flux flow analysis reveals a crossover from single-vortex to collective bulk pinning. Specific heat measurements show a reduced normalized jump $\Delta C/\gamma T_c < 1.43$, below the BCS weak-coupling limit [2], consistent with strong thermal fluctuations associated with a large Ginzburg number G_i. These results establish the first complete electronic phase diagram of $PrFeAsO_{1-x}F_x$, ($0 \leq x \leq 1$), elucidating the evolution from the nonsuperconducting parent compound to the fluorine-rich limit and mapping the full superconducting dome [3]. This comprehensive dataset provides new insights into the interplay among doping and electronic correlations in iron-based superconductors.

Acknowledgement

This research was supported by the National Science Centre (NCN), Poland through the SONATA-BIS 11 project (2021/42/E/ST5/00262). SJS acknowledges financial support from NCN Poland through Project number 2021/42/E/ST5/00262.

References

[1] C. R. Rotundu, D. T. Keane, B. Freelon, *et al.*, Phys. Rev. B **80**, 144517 (2009).

[2] N. Nakai, H. Nakamura, Y. Ota, *et al.*, Physica C **470**, S368–S369 (2010).

[3] Priya Singh, *et al.*, Submitted to Physical Review Materials (Sept 2025) (Under review).

Abstract ID: 30213

UNCONVENTIONAL SIGNATURES OF A QUANTUM GRIFFITHS PHASE IN THE VICINITY OF A QUENCHED NEMATIC QUANTUM CRITICAL POINT

P. Reiss[1,2], D. E. Graf[3], A. A. Haghighirad[4,2], M. Bristow[2], Z. Zajicek[2], W. Knafo[5], A. J. Schofield[6], T. Vojta[7], A. I. Coldea[2]

[1] *Max Planck Institute for Solid State Research, 70569 Stuttgart, GERMANY*
[2] *Clarendon Laboratory, University of Oxford, Oxford OX1 3PU, UK*
[3] *National High Magnetic Field Laboratory, Tallahassee, Florida 32310, USA*
[4] *Institute for Quantum Materials and Technologies, KIT, 76021 Karlsruhe, GERMANY*
[5] *Laboratoire National des Champs Magnétiques Intenses–EMFL, F-31400 Toulouse, FRANCE*
[6] *Department of Physics, Lancaster University, Lancaster LA1 4YB, UK*
[7] *Department of Physics, Missouri University of Science and Technology, Rolla, Missouri 65409, USA*

Upon suppression of a continuous electronic phase transition towards 0K, for example through hydrostatic pressure as an external tuning parameter, a quantum critical point (QCP) occurs in many different material classes. These points constitute a fascinating research area as the diverging quantum fluctuations and electronic correlations could be linked to many unconventional and exciting quantum phases, including the emergence of high-T_c superconductivity. Nevertheless, even more exotic phase may be expected if the symmetry of the electronic order parameter allows for a bilinear coupling to the structural degrees of freedom. The electronic nematic order, ubiquitous in the iron-based superconductors, is one such candidate, where long-range interactions can be mediated through the lattices shear modes [1].

In this talk, we will first review the unique nature of the isolated nematic QCP in $FeSe_{0.89}S_{0.11}$ under hydrostatic pressure, in the absence of any competing electronic order. At this point, the nematoelastic coupling quenches the quantum critical fluctuations and hence, superconductivity is weakened instead of enhanced [2]. We will then demonstrate that the magnetoresistivity close to the QCP obeys a scaling relation over two decades in temperature with diverging critical exponents at low temperatures. Such divergences are in a stark contrast to the usual ansatz using fixed exponents and the notion of universality classes. We will discuss our findings in the context of an unusual quantum Griffiths phase [3], emerging from disconnected static and dynamic quantum fluctuations. Moreover, the coupling between the electronic and phononic modes and a possible topological change of the Fermi surface lead to the emergence of an atypical non-zero energy scale at the QCP, consistent with the observation of finite electronic correlations.

References

[1] I. Paul and M. Garst, Phys. Rev. Lett. **118**, 227601 (2017).

[2] P. Reiss, *et al.*, Nat. Phys. **16**, 89-94 (2020).

[3] P. Reiss, *et al.*, Phys. Rev. Lett. **127**, 246402 (2021).

Abstract ID: 30541

MICROWAVE PROPERTIES of Fe(Se,Te) IN A DC MAGNETIC FIELD: TWO-BAND VORTEX PHYSICS AND POTENTIAL APPLICATIONS TO LARGE-SCALE PHYSICS EXPERIMENTS

A. Alimenti[1,2], V. Braccini[3], M. Cialone[3,4], A. Magalotti[1,2], P. Manfrinetti[5], N. Pompeo[1,2], E. Silva[1,2], K. Torokhtii[1]

[1] *Dept. of Industrial, Electronic, Mechanical Engineering, University Roma Tre, Roma, ITALY*
[2] *INFN Sezione di Roma Tre, Roma, ITALY*
[3] *CNR-SPIN, Genoa, ITALY*
[4] *Dept. of Physics, University of Genoa, Genoa, ITALY*
[5] *Dept. of Chemistry and Industrial Chemistry, University of Genoa, Genoa, ITALY*

The microwave surface impedance $Z = R+iX$ is a powerful tool to study vortex dynamics in superconductors: by simultaneous measurements of the surface resistance R and reactance X for each measuring frequency, we derive the flux-flow resistivity ρ_{ff}, the pinning constant (Labusch parameter) k, the creep factor χ, and the characteristic frequency ν_c in $FeSe_xTe_{1-x}$ (x = 0.5, FeSeTe) epitaxial thin films as a function of the temperature T (6 K – T_c), the applied magnetic field $\mu_0 H \leq 12$ T, and its orientation ϑ with respect to the c-axis.

Multifrequency microwave measurements were performed with dielectric loaded resonators at frequencies ~ {14, 16, 24, 26} GHz [1]. FeSeTe [2] films of thickness 200-400 nm were grown by pulsed laser deposition on CaF_2 substrates. Structure was checked with X-ray diffraction.

From ρ_{ff} (H,T) we extract the vortex core quasiparticle scattering time, whence we find that our samples are at the edge between clean and dirty regimes. Using a scaling approach, we obtain the T dependence of the orbital upper critical field, which is masked in direct measurements by the Pauli limit. Clear indications for multiband superconductivity are obtained [3]. Pinning was studied up to our maximum field $\mu_0 H \leq 12$ T exploiting k [4]. It is shown that a crossover from single-to-collective behaviour exists at a temperature-dependent $H^{\times}$ of several tesla. The intrinsic anisotropy was evaluated from the angular dependence of the flux-flow resistivity at low fields, $\mu_0 H \leq 1.2$ T. We find an anisotropy ratio $\gamma \sim 2$ [5] without a pronounced temperature dependence.

With the measured vortex parameters, we can assess the response of a potential microwave haloscope for dark matter search, in terms of its figures of merit (scan rate, power, signal-to-noise ratio) [7]. By comparing the numerical results obtained with Fe-based and more conventional superconductors (YBCO, Nb_3Sn, NbTi) we conclude that Fe-based superconductors could, in principle, give better performances in specific (H, T) ranges.

Work partially supported by MIUR-PRIN project IronMOON, Grant No.2022BPJL2L, and INFN-CSN5 project "SuperMAD.

References

[1] A. Alimenti, *et al.*, Meas. Sci. Technol. **30** 065601 (2019).
[2] A. Palenzona, *et al.*, Supercond. Sci. Technol. **25** 115018 (2012).
[3] A. Magalotti, *et al.*, arXiv:2509.04912 [cond-mat.supr-con] (2025).
[4] N. Pompeo, *et al.*, Supercond. Sci. Technol. **33** 114006 (2020)
[5] N. Pompeo, *et al.*, IEEE Trans. Appl. Supercond. **31** 800805 (2021)

Abstract ID: 30620

GIANT PINNING EFFICIENCY IN AN IRON-BASED SUPERCONDUCTOR WITH SELF-ASSEMBLED INCLINED NANORODS

D. Gong, X. Xia, Z. Xu, Y. Ma

Key Laboratory of Applied Superconductivity, Institute of Electrical Engineering, Chinese Academy of Sciences, Beijing 100190, CHINA

High dissipation-free current densities are essential for energy-efficient technologies and ultrahigh magnetic-field applications. Superconductors provide an ideal platform for lossless electrical transport, while the critical current density J_c is fundamentally limited by vortex motion. Although conventional defect engineering enhances vortex pinning, the maximum attainable J_c generally remains below the theoretically predicted limit of 32.4% of the depairing current density J_d. Here, we introduce a self-assembled inclined-nanorod strategy that enables J_c to surpass this conventional limit, providing insights beyond established theoretical frameworks. The inclined nanorods intersect to form splayed defect planes, which promote vortex entanglement and generate distinctive zigzag pinning paths, significantly increasing the flux-hopping energy barrier. We demonstrate this concept using $FeSe_{0.6}Te_{0.4}$ thin films containing MnTe inclusions, which self-assemble into inclined nanorods governed by symmetry constraints. The resulting films exhibit record-high J_c values among 11-type iron-based superconductors of comparable thickness, along with an exceptionally high pinning efficiency J_c/J_d that exceeds the theoretical limit for well-studied type-II superconductors. These results underscore the effectiveness of inclined nanorods for vortex pinning and establish a viable roadmap for engineering large-scale, high-performance superconductors.

Abstract ID: 30742

RESEARCH ON THE DELAMINATION BEHAVIOR OF METER-LENGTH FeSeTe-COATED CONDUCTOR TAPES

Y. Han

Institute Of Plasma Physics, Chinese Academy of Sciences, Hefei, CHINA

FeSeTe-coated conductor tapes have garnered significant attention due to their simple crystal structure, ease of fabrication, elimination of the need for heat treatment, and absence of the toxic element arsenic. With the successful preparation of meter-length tapes, the development of this material has progressed smoothly. To facilitate its broader application, this study investigated the transverse delamination strength of FeSeTe-coated conductor tapes, with a particular focus on the influence of temperature on delamination strength and the location where delamination occurs. Mechanical delamination tests were conducted using the anvil pull method, while the microstructure of the fracture surfaces was analyzed using Transmission Electron Microscopy (TEM). The results revealed that the average transverse delamination strength of copper-plated tapes was 1.77 MPa at room temperature, but it dropped significantly to 0.74 MPa at 77 K, indicating that low temperatures affect the mechanical properties of copper-plated tapes. TEM analysis demonstrated that the majority of delamination occurred in the superconducting layer. These findings provide reliable experimental evidence for optimizing the mechanical properties of FeSeTe-coated conductor tapes in practical applications.

15 - CURVILINEAR AND 3D NANOARCHITECTURES FOR SUPERCONDUCTIVITY AND MAGNETISM

Abstract ID: 30027

SPIN DYNAMICS AND MAGNON EXCITATIONS IN QUASI-2D VAN DER WAALS COMPOUNDS

V. Kataev

Leibniz Institute for Solid State and Materials Research Dresden, 01069 Dresden, GERMANY

Layered van der Waals (vdW) magnetic compounds attract currently large attention as they may display an intrinsically low-dimensional magnetic behavior and as such offer an extensive materials base for exploring fundamental magnetic properties of strongly correlated two-dimensional (2D) electron systems [1-4]. Moreover, the structural and compositional variety of these class of materials offers a possibility to realize magnetic ground states with desired types of order and intrinsic anisotropy essential for their application in next-generation spintronic devices [4]. In particular, many of vdW compounds are low-damping antiferromagnetic (AFM) dielectrics, and as such they become promising materials in the new rapidly developing field of AFM spintronics that leverages AFM magnons for transmitting of spin currents instead of electric current to transport and process information [5-7].

In this talk, we will discuss the spin dynamics in the paramagnetic state and the AFM magnon excitations in the magnetically ordered state of two representative vdW antiferromagnets $Mn_2P_2S_6$ (T_N = 78 K) and $CuCrP_2S_6$ (T_N = 30 K), as revealed by electron spin resonance (ESR) and AFM resonance (AFMR) spectroscopies [8-10]. Remarkably, according to the ESR data, above the ordering temperature T_N both compounds demonstrate an inherent 2D correlated spin dynamics characterized by the diffusive long-time decay of the in-plane spin correlation function evidencing the weakness of the interlayer magnetic coupling in bulk singe crystals. Below T_N, $Mn_2P_2S_6$ and $CuCrP_2S_6$ feature anisotropic 3D AFM order of the easy-axis and easy-plane type, respectively. Due to distinct anisotropies, the low-energy magnon excitations, the so-called a- and b-AFMR modes, show different behavior in these compounds. The two modes in $Mn_2P_2S_6$ are quasi-degenerate at zero magnetic field (H = 0) with the magnon excitation energy gaps $D_{a,b}$ ~ 100 GHz at the wave-vector q = 0. Application of magnetic field removes their degeneracy and, very interestingly, the spin wave dynamics can be tuned from the 3D mean field type at small fields to the 2D XY type in strong fields. In contrast, the a- and b-AFMR modes in $CuCrP_2S_6$ are substantially non-degenerate already at H = 0 with excitation energies D_a = 84 GHz and D_b = 13 GHz. Remarkably, these AFM magnon modes can be tuned to the FM type of collective spin excitations with increasing H. Based on these interesting findings we discuss the perspectives for the use of $Mn_2P_2S_6$ and $CuCrP_2S_6$ as transmitting medium for spin currents in prototype magnonic devices.

References

[1] C. Gong, *et al.*, Nature **546**, 265 (2017).

[2] B. Huang, *et al.*, Nature **546**, 270 (2017).

[3] M. M.Otrokov, *et al.*, Nature **576**, 416 (2019).

[4] S. Yang, *et al.*, Adv. Sci. **8**, 2002488 (2021).

[5] A V. Chumak, *et al.*, Nature Phys. **11**, 453 (2011).

[6] B. Flebus, *et al.*, J. Appl. Phys. **133**, 160401 (2023).

[7] S. M. nas Valero, *et al.*, Newton **1**, 100018 (2025).

[8] Y. Senyk, et al., Phys. Rev. Mater. **7**, 014003 (2023).

[9] J. J. Abraham, *et al.*, Phys. Rev. B **107**, 165141 (2023).

[10] J. J. Abraham, *et al.*, Adv. Funct. Mater., e11057 (2025).

Abstract ID: 30028

ROLE OF CURVATURE ON THE CURRENT-DRIVEN TRANSPORT OF MAGNETIC TEXTURES

J. I. Costilla[1], G. H. R. Bittencourt[2], D. Altbir[3], V. P. Kravchuk[4,5], V. L. Carvalho-Santos[1]

[1] *Departamento de Física, Universidade Federal de Viçosa, 36572-116, Viçosa, BRAZIL*
[2] *Instituto Federal de Santa Catarina, Campus São Carlos, 89885-000, São Carlos, BRAZIL*
[3] *Facultad de Ingeniería y Ciencias, Universidad Diego Portales,* ***8360024****, Santiago, CHILE,*
[4] *Leibniz-Institut für Festkörper- und Werkstoffforschung, D-01069 Dresden, GERMANY*
[5] *LBogolyubov Institute for Theoretical Physics of the National Academy of Sciences of Ukraine, 03143 Kyiv, UKRAINE*

The shape of magnetic nanoparticles has been known to fundamentally govern their magnetic properties. Recent advances in nanofabrication, enabling a plethora of complex geometries, combined with new theoretical frameworks for curved magnetism, have propelled the field of curvilinear micromagnetism a cornerstone in condensed matter researches. In this talk, we explore how curvature influences the current-driven dynamics of magnetic textures, such as domain walls and skyrmions. We demonstrate that in nanostripes with curvature gradients, the transport of domain walls exhibits a chiral character. This chirality arises from the interplay between the spin-polarized current direction and the direction for which the domain wall center points (DW phase), leading to a preferential propagation direction. The critical current required to traverse regions of maximum curvature is shown to be DW phase-dependent, a phenomenon we describe as a chiral spin-transfer torque [1]. Furthermore, in two-dimensional systems, curvature fundamentally modifies the dynamics of topological textures like skyrmions. It induces a shift in the gyrotropic vector and the dissipative tensor of the Thiele equation. This interplay between current and curvature can generate a skyrmion Hall effect in geometries where it is otherwise absent in flat systems. Therefore, the curvature-current interplay emerges as a fundamental design parameter for engineering next-generation spintronic nanodevices.

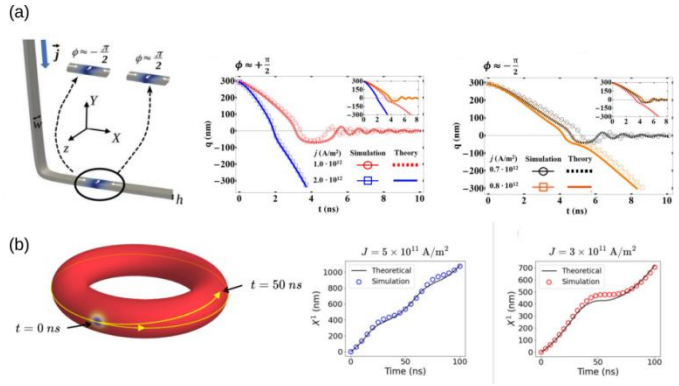

Fig. 1: *Schematic representation of propagation of domain walls and skyrmions in curved substracts. (a) Domanin wall position as a function of time or dinstinct DW phases. (b) Skyrmion position as a function o time in a magnetic nanotube for dinstinct current values.*

References

[1] G. H. R. Bittencourt, M. Castro, A. S. Nunez, D. Altbir, S. Allende, and V. L. Carvalho-Santos, Nanoscale **16**, 16844 (2024).

Abstract ID: 30047

Co/Ni-BASED FLEXIBLE PMA SPIN-VALVE HETEROSTRUCTURES FOR SUSTAINABLE SPINTRONICS

M. Hassan[1,2], S. Laureti[1], C. Rinaldi[3], G. Barucca[4], A. Ullrich[2], M. Albrecht[2], G. Varvaro[1]

[1] *CNR-ISM, nM2-Lab, Area della Ricerca Roma 1, Monterotondo Scalo (Roma), 00015, ITALY*
[2] *Institute of Physics, Un. Augsburg, Universitätsstraße 1 Nord, D-86159 Augsburg, GERMANY*
[3] *Department of Physics, Politecnico di Milano, c/o via G. Colombo 81, 20133 Milano, ITALY*
[4] *Università Politecnica delle Marche, Dept. SIMAU, Via Brecce Bianche, Ancona, ITALY*

Flexible spin-valve (SV) heterostructures with perpendicular magnetic anisotropy (PMA) have recently emerged, expanding the family of magneto-resistive elements suitable for flexible electronics [1–3]. Early studies relied on Pt- and Pd-based multilayers to achieve excellent performance but raising sustainability concerns due to the critical nature of these elements [4]. In this work [5], we propose Co/Ni-based PMA-SV heterostructures with reduced content of critical Pt-group elements as a more sustainable alternative, while offering additional advantages such as lower magnetic damping and higher spin polarization. The stacks comprise a $[Co/Ni]_n$ free layer and a $[Co/Ni]_n$ /Ru/$[Co/Ni]_n$ synthetic antiferromagnet reference layer, while various metallic seed and capping layers are used (Pt, Pd, Cu/Ta). The best performance is achieved using Pt and Cu as the seed and capping layers, with the structures showing MR ratios comparable to rigid counterparts and maintaining excellent functionality under bending up to 180° (Fig. 1a,b), all while using a reduced amount of critical elements, thus demonstrating their strong potential for sustainable flexible spintronic devices. Furthermore, preliminary investigations demonstrate that such complex architectures can also be realized as rolled microtube powders that preserve their magnetic properties despite curvature (Fig. 1c,d), thereby opening new prospects for the development of advanced printable inks for low-energy manufacturing of flexible spintronic components.

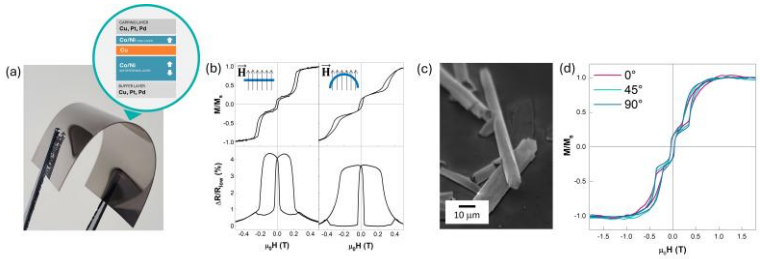

Fig. 1: *(a) Representative image of a flexible PMA Co/Ni-based SV deposited on PEN tapes and (b) corresponding out-of-plane hysteresis loop and magnetoresistance response (bending angle: 180°). (c) Micrograph of Co/Ni-based SV rolled microtubes and (d) corresponding out-of-plane hysteresis loops measured at different angles, showing the isotropic magnetic behavior of the powder.*

References

[1] H. Hassan, *et al.*, Applied Surface Science **635**, 157740 (2023).

[2] P. Makushko, *et al.*, Adv. Funct. Mat. **31**, 2101089 (2021).

[3] M. Hassan, *et al.*, Nanoscale Advances **3**, 3076 (2021).

[4] A. Palomino, *et at.*, Sustainable Materials and Technologies **28**, e00270 (2021).

[5] M. Hassan, *et al.*, ACS Appl. Mater. Interfaces **14**, 51496 (2022).

Abstract ID: 30051

MAPPING MAGNETIC FIELDS AND CURRENTS IN SUPERCONDUCTING RESONATORS

J. Baumgarten[1], N. Lejeune[1], L. Nulens[2], J. Van de Vondel[2], A. V. Silhanek[1]

[1] *Experimental Physics of nanostructured Materials (EPNM), QMAT, Université de Liège, Liège, BELGIUM*
[2] *Quantum Solid-State Physics, Department of Physics and Astronomy, KU Leuven, Celestijnenlaan 200D, Leuven, B-3001, BELGIUM*

Superconducting radio-frequency (RF) resonators are essential in quantum circuits and ultra-sensitive sensors. Yet, their performance can degrade due to magnetic flux penetration, as flux quanta interacting with RF currents in the superconducting thin film lead to significant energy loss. This issue becomes even more pronounced at low temperatures, where thermomagnetic instabilities can cause sudden magnetic flux avalanches [1]. A pressing question is whether the RF signal, necessary for excitation or readout, itself initiates the nucleation and spread of these flux avalanches. The existing literature offers no clear answer, partly due to limited direct evidence. In this work, we present a groundbreaking visualization of magnetic flux penetration via Faraday rotation imaging during simultaneous RF excitation. We observe that avalanche activity is only weakly dependent on RF intensity, but magnetic flux bursts visibly impact the device's resonance frequency. Importantly, we establish a direct link between a particular avalanche event and a shift in resonance frequency, allowing us to identify the most damaging sites and differentiate the origins of upward and downward frequency shifts. Electromagnetic simulations support our findings, showing that local changes in kinetic inductance replicate flux avalanches. These insights aim to deepen the understanding of magnetic instabilities in superconducting resonators and will be instrumental for designing resonators with improved efficiency and reliability.

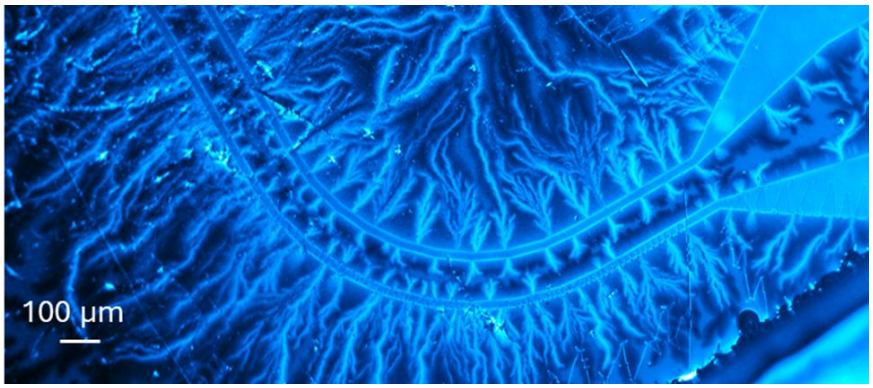

Fig. 1: *Magneto-optical images of a NbTiN resonator depicting magnetic flux avalanches.*

References

[1] L. Nulens, N. Lejeune, *et al.*, Commun. Phys. **6**, 267 (2023).

Abstract ID: 30154

TUNNEL MAGNETIC JOSEPHSON JUNCTIONS: FROM FUNDAMENTAL PHYSICS TO SUPERCONDUCTING QUANTUM ARCHITECTURES

R. Satariano[1], R. Ferraiuolo[2], H. G. Ahmad[1], E. Raja[1], D. Gatta[1], G. Serpico[1], D. Montemurro[1], A. Vettoliere[3], G. Ausanio[1], L. Parlato[1], G.P. Pepe[1], C. Granata[1], A. Bruno[2], F. Tafuri[1], D. Massarotti[4]

[1] *Dipartimento di Fisica Ettore Pancini, Università degli Studi di Napoli Federico II, c/o Complesso Monte Sant'Angelo, via Cinthia 26, I-80126 Napoli, ITALY*
[2] *QuantWare, Elektronicaweg 10, 2628 XG Delft, THE NETHERLANDS*
[3] *Consiglio Nazionale delle Ricerche—ISASI, Via Campi Flegrei 31, I-80078 Pozzuoli, ITALY*
[4] *Dipartimento di Ingegneria Elettrica e delle Tecnologie dell'Informazione, Università degli Studi di Napoli Federico II, I-80125 Napoli, ITALY*

Magnetic Josephson junctions (MJJs) provide an intriguing playground to explore the interplay between superconductivity and ferromagnetism [1]. A series of fascinating experiments have revealed striking phenomena at the Superconductor/ Ferromagnet (S/F) interface, e.g., 0-π phase transition and the generation of spin-triplet correlations, thus paving the way for advances in a wide range of applications from spintronics to superconducting digital electronics [2]. For what concerns the use of MJJs in quantum architectures, because of their intrinsic high dissipation resulting from the metallic nature of standard ferromagnetic barriers, they have been mainly suggested as π -phase shifters [3]. Advances in realizing MJJs by coupling ferromagnetic layers with insulating barriers [4] and by exploiting intrinsic insulating ferromagnetic materials [5] have allowed engineering MJJs with very low damping, even accessing the macroscopic tunneling quantum regime [6]. The integration of MJJs as active components in quantum circuits has thus gained attention. In Ref. [7], we have proposed a proof-of-concept of a hybrid ferromagnetic transmon qubit, namely the ferro-transmon. The main idea of the ferro-trasmon consists in the use of tunnel MJJs that allows an alternative control of the qubit frequency by means of magnetic field pulses with a significant potential impact on the scalability of superconducting quantum circuits. In this talk, we will present the recent advances in realizing a tunnel MJJs compatible with the circuit outlined above, with also special focus on its magnetic properties [8] and dissipation phenomena [9,10].

References

[1] A. I. Buzdin, *Proximity effects in superconductor-ferromagnet heterostructures*, Rev. Mod. Phys., **vol. 77**, **no. 3**, pp. 935–976, (2005). doi: 10.1103/RevModPhys.77.935.

[2] I. I. Soloviev, *et al.*, *Beyond Moore's technologies: operation principles of a superconductor alternative*, Beilstein Journal of Nanotechnology, **vol. 8**, pp. 2689–2710 (2017). doi: 10.3762/bjnano.8.269.

[3] S. Kim, *et al.*, *Superconducting flux qubit with ferromagnetic Josephson π-junction operating at zero magnetic field*, Commun. Mater., **vol. 5**, **no. 1**, p. 216 (2024). doi: 10.1038/s43246-024-00659-1.

[4] A. Vettoliere, *et al.*, *Aluminum-ferromagnetic Josephson tunnel junctions for high quality magnetic switching devices*, Appl. Phys. Lett., **vol. 120**, **no. 26**, p. 262601 (2022). doi: 10.1063/5.0101686.

[5] H. G. Ahmad, *et al.*, *Electrodynamics of highly spin-polarized tunnel Josephson junctions*, Phys. Rev. Appl., **vol. 13**, **no. 1**, p. 14017 (2020). doi: 10.1103/PhysRevApplied.13.014017.

[6] D. Massarotti, *et al.*, *Macroscopic quantum tunnelling in spin filter ferromagnetic Josephson junctions*, Nat. Commun., **vol. 6**, **no. 1**, p. 7376 (2015). doi: 10.1038/ncomms8376.

[7] H. G. Ahmad, *et al.*, *Hybrid ferromagnetic transmon qubit: Circuit design, feasibility, and detection protocols for magnetic fluctuations*, Phys. Rev. B, **vol. 105**, **no. 21**, p. 214522 (2022). doi: 10.1103/PhysRevB.105.214522.

[8] R. Satariano, *et al.*, *Nanoscale spin ordering and spin screening effects in tunnel ferromagnetic Josephson junctions*, Commun. Mater., **vol. 5**, **no. 1**, p. 67 (2024). doi: 10.1038/s43246-024-00497-1.

[9] H. G. Ahmad, *et al.*, *Phase dynamics of tunnel Al-based ferromagnetic Josephson junctions*, Appl. Phys. Lett., **vol. 124**, **no. 23**, p. 232601 (2024). doi: 10.1063/5.0211006.

[10] R. Satariano, *et al.*, *Submicrometer tunnel ferromagnetic Josephson junctions with transmon energy scale*, Appl. Phys. Lett., accepted for publication (2025).

Abstract ID: 30177

ARTIFICIAL SPIN ICE ON THE CaVO LATTICE: A BRIDGE FROM SQUARE TO KAGOME

F. Museur[1,2], G. M. Macauley[1,2], S. Nilsson[1,2], L. Berchialla[1,2], P. M. Derlet[2,3], V. Scagnoli[1,2], L. J. Heyderman[1,2]

[1] *Laboratory for Mesoscopic Systems, Department of Materials, ETH Zurich, SWITZERLAND*
[2] *PSI Center for Neutron and Muon Sciences, 5232 Villigen PSI, SWITZERLAND*
[3] *PSI Center for Scientific Computing, Theory and Data, 5232 Villigen PSI, SWITZERLAND*

Artificial spin ices are arrangements of dipolar-coupled nanomagnets, with magnetic moments that behave like Ising spins as a result of shape anisotropy. They have been successfully implemented as platforms for imaging and controlling phase transitions in systems with long-range interactions [1]. However, the exploration of thermally-activated phase transitions has been mostly focused on two lattices: the square and the kagome. Artificial square ice orders readily into an antiferromagnetic, two-in/two-out ground state, with a transition belonging to the Ising 2D universality class [2]. In contrast, artificial kagome ice is highly frustrated and the predicted phase diagram is richer [3, 4]. Upon lowering the temperature, the system first experiences a crossover from a paramagnetic to a spin liquid state with no long range order, then transitions into a Coulomb phase with charge crystallization. This is an example of magnetic moment fragmentation [5, 6], in which each magnetic moment can be decomposed into the sum of a long-range ordered, divergence-full fragment and a fluctuating, divergence-free fragment which can be elegantly mapped to a dimer model.

We have carried out a comprehensive characterization of the thermodynamics of an artificial spin ice based on the CaVO (also called the square-octagon) lattice, part of the family of Archimedean lattices [7]. We show that the magnetic interactions on the vertex level can be significantly tuned by changing the relative sizes of square and octagonal plaquettes, while preserving the lattice constant and symmetries. This results in a complex phase diagram, with two very different ground states and ordering processes separated by a multicritical region. Each bears strong similarities with either the square or kagome phenomenologies. We map out this phase diagram with Monte-Carlo simulations and magnetic force microscopy of as-grown configurations. Different spin liquid states can be observed, as well as moment fragmentation for some geometries. Finally, we perform temperature and field-dependant magnetometry measurements on a series of lattice geometries, making it possible to detect thermally-active correlated phases without using large-scale instrumentation. Our work paves the way for engineering exotic magnetic properties at the mesoscale. By tuning frustration within a single lattice geometry, we can design artificial systems that exhibit spin liquid and multicritical behaviours - something that, in natural magnetic systems, typically requires extremes of either pressure, field or temperature.

References

[1] S. H. Skjærvø, *et al.*, Nature Reviews Physics **2**, 13–28 (2019).

[2] O. Sendetskyi, *et al.*, Physical Review B **99**, 214430 (2019).

[3] G. Möller and R. Moessner, Physical Review B **80**, 140409 (2009).

[4] G.-W. Chern, *et al.*, Physical Review Letters **106**, 207202 (2011).

[5] M. E. Brooks-Bartlett, *et al.*, Physical Review X **4**, 011007 (2014).

[6] B. Canals, *et al.*, Nature Communications **7**, 11446 (2016).

[7] O. A. Starykh, *et al.*, Physical Review Letters **77**, 2558–2561 (1996).

Abstract ID: 30189

TOPOLOGICAL INVARIANTS AND POLYMORPHISM OF MAGNETIC HOPFIONS

F. N. Rybakov

Uppsala University, SE-75120 Uppsala, SWEDEN

The term "hopfion", after Heinz Hopf, comes from topology. Objects with this name are characterized by a topological invariant connected with the fact that continuous maps of a three-dimensional sphere into a two-dimensional one are non-trivial. Recent studies have experimentally confirmed the existence of hopfions in magnetic crystals [1]. Moreover, the diversity of hopfions and their topological properties turned out to be much richer than previously thought. In this talk, I will highlight the current progress in this field [1,2]. We will discuss homotopy constructions, their groups, and formulas allowing calculation of topological invariants for micromagnetic textures containing hopfions.

References

[1] F. Zheng, *et al.*, Nature **623**, 718 (2023).

[2] X. Chen, *et al.*, e-print Research Square: rs.3.rs-7435743 (2025).

Abstract ID: 30254

STRAIGHT AND CURVED SINGLE CRYSTALLINE IRON NANOWIRES EXPOSED TO LARGE MAGNETIC FIELD GRADIENTS

F. Sandbaumhüter[1], A. S. Prasad[1], R. Ravishankar[1], D. Wolf[1], O. Volkov[2], V. Neu[1], D. Makarov[3], T. Mühl[1]

[1] *IFW Dresden, 01069 Dresden, GERMANY*
[2] *Goethe University Frankfurt, 60438 Frankfurt, GERMANY*
[3] *Helmholtz-Zentrum Dresden-Rossendorf, 01328 Dresden, GERMANY*

The talk will cover (i) our development and preparation of nanosized electromagnets [1]—capable of generating static and pulsed magnetic fields and field gradients exceeding 1 T and 10^6 T/m, respectively—and (ii) nanomagnetic samples and devices based on straight or curved single crystalline iron nanowires with diameters below 50 nm. We employ advanced imaging techniques, including differential magnetic force microscopy (MFM) and transmission electron microscopy (TEM)-based electron holography, to study domain wall pinning site locations and domain wall motion in relation to curvature and strain distributions within our magnetic nanowire systems.

The magnetization reversal of straight FeCNTs exposed to a homogeneous external field occurs abruptly in a single step. However, at short time scales, at least two consecutive processes are involved, i.e. the nucleation of a reversed magnetic domain and a subsequent domain wall propagation through the entire iron nanowire [2]. By applying highly inhomogeneous magnetic field distributions provided by the above-mentioned nano-electromagnets (see Fig. 1), we can separate both processes. A localized peak field is used to introduce a reversed magnetic domain at one of the nanowire's ends creating a metastable two-domain state. Afterwards, depinning fields can be probed.

Furthermore, we show that nanowire-based MFM probes attached to our nano-electromagnets form the basis for a novel integrated differential MFM approach.

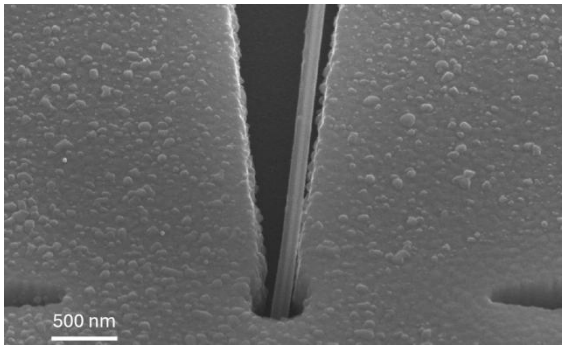

Fig. 1: *FeCNT attached to the bore of a nano-electromagnet (i.e., a half-turn planar coil).*

References

[1] A. S. Prasad, R. Ravishankar, B. Büchner, V. Neu, and T. Mühl, Communications Materials **6**, 164 (2025).

[2] P. Banerjee, F. Wolny, D. V. Pelekhov, M. R. Herman, K. C. Fong, U. Weissker, T. Mühl, Y. Obukhov, A. Leonhardt, B. Büchner, and P. C. Hammel, Applied Physics Letters **96**, 252505 (2010).

Abstract ID: 30293

MICRO-FOCUSED BLS FOR CURVILINEAR MAGNETISM

O. Wojewoda[1,2], M. Urbánek[2]

[1] *Department of Materials Science and Engineering, Massachusetts Institute of Technology, Cambridge, Massachusetts 02139, USA*
[2] *CEITEC BUT, Brno University of Technology, Purkyňova 123, 621 00 Brno, CZECH REPUBLIC*

Curvilinear magnetism has come to the forefront of research interest [1, 2]. However, the effects induced by the curvilinear geometry are usually very subtle and hard to measure by investigating the static magnetization configuration [3]. On the other hand, in the dynamic response these effects can demonstrate themself in a much more pronounced manner. Here, I will introduce the possibilities of utilization of the micro-focused Brillouin light scattering (BLS) for such investigations. By modeling the shape of the measured spectra and performing precise analysis of the acquired spectra the micro-focused BLS can be used to reveal the static magnetization configuration or fit the exact energy contribution originating from various sources [4, 5].

We demonstrate these capabilities on the case study focused towards pyramid-shaped matrix made out of the permalloy. We have observed field-dependent change of the spin wave band structure, with opening of a complete two-dimensional band gap. Moreover, together with finite-element method, we modelled obtained micro-focused BLS spectra and identified strong localization of the low-frequency modes. This case study proves that, the micro-focused BLS enhanced by modeling can be a valuable tool in the curvilinear magnetism research.

References

[1] D. Sheka, Appl. Phys. Lett. **118**, 230502 (2021).

[2] D. Makarov, *et al.*, Adv. Matter. **34**, 3 (2022).

[3] O. Volkov, *et al.*, Nat. Commun. **15**, 2193 (2024).

[4] O. Wojewoda, *et al.*, Phys. Rev. B **110**, 224428 (2024).

[5] J. Krčma, O. Wojewoda, *et al.*, Sci. Adv. **11**, 44 (2025).

Abstract ID: 30316

MODELING STRAIN INDUCED CURVATURE WITH FULLY COUPLED MAGNETO-MECHANICAL FEM MODEL

S. Chiroli[1,2]

[1] *Laboratoire Albert Fert, CNRS, Thales, Université Paris-Saclay, Palaiseau, FRANCE*
[2] *Laboratoire des Sciences des Procédés et des Matériaux, CNRS, Université Sorbonne Paris Nord, Villetaneuse, FRANCE*

Curvilinear magnetism has recently emerged as a distinct paradigm in magnetism, revealing how curvature and geometry fundamentally alter magnetic interactions and ground states beyond planar systems. Curvature-induced effects such as effective anisotropies, chiral interactions, and topological frustration enable novel magnetic configurations and functionalities [1]. However, most numerical approaches employed to study curvilinear magnetism rely on prescribed or static geometries, neglecting the physical mechanisms by which curvature is generated and dynamically coupled to the magnetic state. As a result, the role of mechanical deformation, elastic relaxation, and magneto-mechanical feedback remains largely unexplored within existing modeling. In our past work, we developed a model based on finite element method in which magnetic and mechanical phenomena are fully coupled. This model enables one to describe precisely the static and dynamic response of the magnetization in presence of complex strain field. This model open ways to study both shape effects and strain effects on the magnetization behaviour. Here we propose to present our recent studies performed on periodic nanostructures and on finite nano objects where the shape, the strain, and the material parameters play an important role on the magnetization state [2,3].

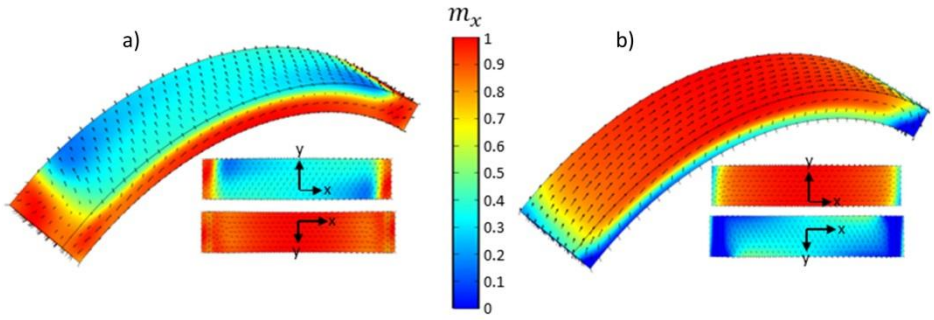

Fig. 1: *Strain induced curvature applied on a magnetic nanobar. The colormap shows the m_x component of the magnetization for a) a negative magnetoelastic constant λ=-100ppm and b) a positive magnetoelastic constant λ=-100ppm. The figure shows the apparition of a domain wall with two separated perpendicular domains on both sides of the neutral axis [3].*

References

[1] D. Makarov, O. M. Volkov, A. Kákay, O. V. Pylypovskyi, B. Budinská, and O. V. Dobrovolskiy, Advanced Materials **34**, 2101758 (2022).

[2] G. Gubbiotti, O. Bezsmertna, O. V. Pylypovskyi, R. Xu, S. Chiroli, F. Zighem, *et al.*, arXiv:2512.11663 (2025).

[3] M. Khelif, S. Chiroli, N. Challab, D. Faurie, M. Haboussi, and F. Zighem, J. Phys. D: Appl. Phys. **58**, 475001 (2025).

Abstract ID: 30350

SCANNING SQUID-ON-CANTILEVER MICROSCOPY OF NANOSCALE MAGNETISM IN LOW-DIMENSIONAL MATERIALS

B. Gross[1], M. Poggio[1,2]

[1] *Department of Physics, University of Basel, SWITZERLAND*
[2] *Swiss Nanoscience Institute, University of Basel, SWITZERLAND*

Global magnetization and transport measurements can mask the local nature of magnetism, for instance when competing magnetic configurations coexist within the same device or flake. To access these spatially inhomogeneous magnetic textures, we develop and employ non-invasive scanning SQUID-on-cantilever probes—nanometer-scale superconducting quantum interference devices integrated onto cantilevers—that enable quantitative mapping of magnetic stray fields with high sensitivity and spatial resolution.

I will discuss recent efforts in our group aimed at applying these probes to low-dimensional magnetic material systems. In particular, our measurements target representative systems such as the atomically thin antiferromagnet $CrPS_4$, as well as magnetic thin films based on V-doped $(Bi,Sb)_2Te_3$, a platform for the quantum anomalous Hall effect. These experiments illustrate how stray-field imaging can reveal the evolution of magnetic configurations across individual flakes and devices under variation of external parameters.

Abstract ID: 30360

FLEXOMAGNETISM AND THE LINEAR FLEXOMAGNETIC EFFECT IN 2D MAGNETS

A. Edström[1], S. Picozzi[2,3], P. Barone[3], M. Stengel[4]

[1] *Department of Applied Physics, School of Engineering Sciences, KTH Royal Institute of Technology, AlbaNova University Center, 10691 Stockholm, SWEDEN*
[2] *Department of Materials Science, University of Milan-Bicocca, Milan, ITALY*
[3] *Consiglio Nazionale delle Ricerche CNR-SPIN, ITALY*
[4] *Institut de Ciència de Materials de Barcelona (ICMAB-CSIC), Campus UAB, 08193 Bellaterra, Spain, 08010 Barcelona, SPAIN*

Curvature has emerged as a powerful tool to engineer and control rich magnetic phase diagrams, including chiral or topological spin states [1,2]. Intriguing insights from micromagnetic modeling have been followed by notable experimental advances. However, a realistic and materials specific microscopic description, using first principles theory, was hindered by challenges related to breaking of translational symmetry. Overcoming this difficulty is particularly important when going to the nano- or atomic scale, as encountered in 2D magnetic Van der Waal's monolayers, such as CrI_3 or $MnPX_3$, which exhibit high mechanical flexibility and a natural tendency to ripple.

In previous work, we employed relativistic density-functional theory (DFT) to investigate the flexomagnetic coupling in ferromagnetic monolayers, and demonstrated that curvature-induced Dzyaloshinskii–Moriya interactions (DMI) stabilize non-collinear states, such as spin cycloids [3]. While these interactions have intriguingly been shown to appear as purely geometric, non-relativistic effects, our results revealed that spin-orbit coupling (SOC) significantly alters their curvature dependence, leading to qualitatively new magnetic behavior.

Expanding this framework to Néel antiferromagnets, in the same important class of monolayer magnets with crystallographic D_{3d} point group, we investigate the linear flexomagnetic effect, where a magnetization is induced linearly with curvature. In this work, we present a first-principles methodology to compute the linear flexomagnetic tensor for monolayer magnets, using $MnP(S/Se)_3$ as prototypical examples. With the flexomagnetic tensor fully determined, we demonstrate how complex spin states can be induced and manipulated with a combination of curvature and external magnetic fields.

Acknowledgements

We acknowledge support from the Swedish Research Council (2018-06807 and 2022-04720), ÅForsk, the Göran Gustafsson foundation, and the Wallenberg foundations (KAW) through WISE. Calculations were done on resources provided by the National Academic Infrastructure for Supercomputing in Sweden (NAISS).

References

[1] D. Sheka, *A Perspective on Curvilinear Magnetism*, Applied Physics Letters **118**, 230502 (2021).
[2] R. Hertel, *Curvature Induced Magnetochirality*, SPIN **3**, 1340009 (2013).
[3] A. Edström, D. Amoroso, S. Picozzi, P. Barone, M. Stengel, *Curved Magnetism in CrI_3*, Physical Review Letters **128**, 177202 (2022).

Abstract ID: 30363

CHALLENGES TOWARDS THE LASER FABRICATION OF CURVILINEAR SUPERCONDUCTOR ARCHITECTURES

L. Porta-Velilla[1], A. Badía[1], J. Frechilla[1], N. Lejeune[2], J. Baumgarten[2], C. Delforge[2], E. Martinez[1], A. Silhanek[2], L.A. Angurel[1], G.F. de la Fuente[1]

[1] *Instituto de Nanociencia y Materiales de Aragón (INMA), CSIC-Universidad de Zaragoza, Zaragoza, SPAIN*
[2] *Experimental Physics of Nanostructured Materials (EPNM), Q-MAT, Université de Liége, Liège, BELGIUM*

Lasers emitting ultra-short (fs) pulses are convenient tools for the fabrication of complex surface nanostructures. They are, furthermore, ideal for the generation of curvilinear arquitectures in materials with attractive electromagnetic properties. Moreover, lasers are non-contact surface modification tools, and as thus they provide important advantages which, combined with their spatial and temporal flexibility and unlimited capabilities, provide conditions for a plethora of engineered nanostructures with non-restricted geometries. Among the latter architectures, a number of circular figures based on the generation of structures with different inter-related distances, radii and size, were prepared to explore how these differences affect their physical properties, particularly in high-critical-temperature superconductor samples.

An important challenge here is related to the fact that laser beam spots are typically in the order of several to tens of micrometers in diameter. In principle, this poses a hurdle on the attempt to fabricate nanometer size features. This work explores potential solutions to the latter problem.

Although not exclusively, emission wavelength, pulse duration, irradiance/intensity level, beam scanning procedure (geometry and raster speed), along with process atmosphere, are most relevant parameters guiding the fabrication of desired curvilinear nanostructures. These will be overviewed with examples produced by using different laser wavelengths and additional processing parameters. Correlation of the latter with the microstructural and nanostructure features observed, along with their influence on physical properties, will be presented and overviewed.

Acknowledgments

The authors are grateful for funding from project PID2023-146041OB-C21 (funded by MICIU/AEI/10.13039/501100011033 and ERDF/EU) and from Gobierno de Aragón (Research Group T54_23R). J. Frechilla acknowledges support from Gobierno de Aragón through a predoctoral contract.

11th International Conference on Superconductivity and Magnetism ICSM2026
4th International Conference on Quantum Materials and Technologies ICQMT2026
19th April to 26th April, 2026, Ölüdeniz – Fethiye/Muğla, Türkiye
https://icsmforever.org/

Abstract ID: 30390

SKYRMIONS INDUCED AND SUPPRESSED BY CURVILINEAR DEFECTS OBSERVED BY MFM

H. J. Hug[1,2], E. Darwin[1], D. Rothhardt[1,2], R. Peremadathil-Pradeep[1,2], L. Berchialla[1,3], A. Hrabec[3]

[1] *Empa, 8600 Dübendorf, SWITZERLAND*
[2] *Department of Physics, University of Basel, 4056 Basel, SWITZERLAND*
[3] *Paul Scherrer Institut PSI, 5232 Villigen, SWITZERLAND*

Curvilinear substrates provide a promising route for tailoring the magnetic properties of multilayer systems and may enable the stabilization of topologically non-trivial spin textures such as skyrmions [1]. Here, we deposit Ta(3)/Pt(10)/[Pt(0.7)/Co(1.7)/Ru(1.3)]$_6$/Pt(3) multilayers with perpendicular magnetic anisotropy (PMA) and interfacial Dzyaloshinskii–Moriya interaction (iDMI) onto PMA substrates featuring microfabricated convex and concave curvilinear defects with radii between 100 and 600 nm. We investigate the resulting magnetic configurations using in-vacuum high-sensitivity magnetic force microscopy (MFM) [2] operated with capacitive, frequency-modulated tip–sample distance control [3], enabling simultaneous mapping of topography, contact potential difference (CPD), and magnetic contrast.

For larger defects, stripe domains formed on concave bumps are disconnected from those in the surrounding flat regions. Upon application of sufficiently strong magnetic fields, these stripes evolve into multiple skyrmions both inside and outside the defects, indicating no clear signature of curvature-induced DMI effects. In contrast, for defects with diameters around 200 nm, a pronounced asymmetry between concave bumps and convex dips emerges when reducing the applied field from near saturation. While the magnetization on the bumps remains aligned with the saturation field direction, a robust, ultra-small skyrmion consistently nucleates inside all convex dips. In agreement with theoretical predictions [1], the radius of these curvature-induced skyrmions is significantly smaller than that of sparse, conventional skyrmions appearing outside the defects at comparable fields. In addition, we observe curvature-dependent variations in CPD, possibly indicating the presence of electric fields associated with non-collinear magnetization textures.

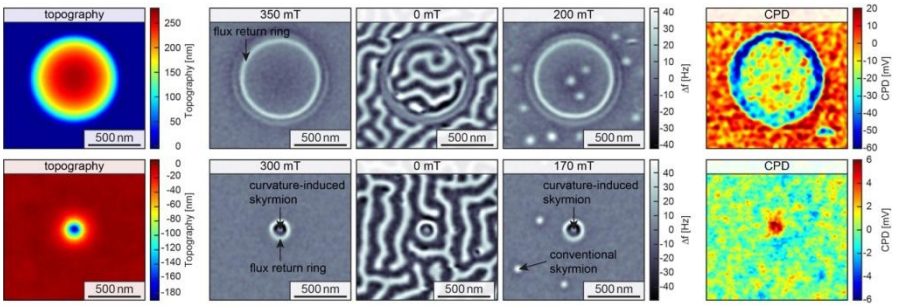

Fig. 1: *Topography, magnetic and CPD signals obtained on a 800nm diameter bump (top row) and 200nm diameter dip. A curvature-induced skyrmion appears at the center of the dip.*

References

[1] V. P. Kravchuk, *et al.*, Phys. Rev. Lett. **120**, 067201 (2018).
[2] Y. Feng, *et al.*, J Magn Magn Mater **551**, 169073 (2022).
[3] X. Zhao, *et al.*, New Journal of Physics **20**, 013018 (2018).

Abstract ID: 30401

MAGNETISM UNDER MECHANICAL LOADING: FRAGMENTATION, GEOMETRY, AND MAGNETOELASTIC EFFECTS IN FERROMAGNETIC THIN FILMS

F. Zighem[1], H. Ben Mahmoud[1], P.-O. Renault[1], P. Godard[1], D. Thiaudière[1], D. Faurie[1]

[1] LSPM CNRS UPR 3407, Université Sorbonne Paris Nord, Villetaneuse, FRANCE
[2] Institut Pprime, CNRS - Université de Poitiers - ENSMA, Poitiers, FRANCE
[3] Synchrotron SOLEIL, Saint-Aubin, FRANCE

Magnetoelastic coupling plays a central role in magnetic thin films operating under mechanical deformation, particularly in the context of flexible and stretchable substrates. When ferromagnetic films are deposited on polymer supports and subjected to mechanical loading, the combination of elastic strain and mechanical damage can strongly modify their magnetic behavior. In this contribution, we investigate the impact of mechanical loading on the magnetic properties of ferromagnetic thin films, with a particular focus on fragmentation phenomena and strain heterogeneity.

Under uniaxial and biaxial tensile loading, thin metallic films undergo progressive fragmentation, leading to the formation of uniaxial or two-dimensional crack networks. These crack patterns induce strong spatial variations of strain and geometry, which in turn affect effective magnetic anisotropies and magnetization reversal mechanisms. To address these effects, we combine in situ X-ray diffraction under mechanical loading with magneto-optical Kerr effect (MOKE) magnetometry, allowing simultaneous access to lattice strain evolution and magnetic response during deformation.

The evolution of crack density and crack orientation is analyzed as a function of the applied mechanical strain, providing a quantitative description of the fragmentation process. Correlations between crack morphology, strain redistribution, and magnetic response are discussed, highlighting the role of mechanically induced geometric structuring on the observed magnetic behavior. This analysis enables a clear separation between intrinsic magnetoelastic effects and geometry-driven contributions.

This approach enables the investigation of magnetoelastic effects from the linear elastic regime to advanced multi-cracking states. In addition, we show that, beyond intrinsic magnetoelastic contributions, crack-induced geometrical structuring plays a major role in shaping the magnetic response, especially in materials with low or vanishing magnetostriction. These results highlight the importance of accounting for mechanical damage and strain heterogeneity when analyzing and interpreting the magnetic behavior of ferromagnetic thin films subjected to complex mechanical loading.

Abstract ID: 30406

SUPERCONDUCTING NANO/MICROSTRIP SINGLE PHOTON DETECTORS FOR QUANTUM APPLICATIONS

L. Parlato[1], P. Ercolano[1], C. Bruscino[1], M. Peluso[1], C. Cirillo[2], C. J. Zhang[1], F. Avitabile[2], Z. M. Kakhaki[3], C. Attanasio[3], G.P. Pepe[1]

[1] Dip. di Fisica "E. Pancini", Università degli Studi di Napoli Federico II, I-80125 Napoli, ITALY
[2] CNR-SPIN, Via Campi Flegrei, 34, 80078 Pozzuoli NA, ITALY
[3] Dip. Di Fisica "E. R. Caianiello", Università degli Studi di Salerno, I-84084, Fisciano, Salerno, ITALY

In the last decades the advancing of quantum information science concerning quantum computation, quantum communication and sensing have largely pushed the development of single-photon detectors (SPDs). With respect to conventional semiconducting SPDs, e.g. photomultipliers and avalanche photodiodes, superconducting materials with an energy gap of a few meV could allow to detect single photons with high efficiency in a wide range of wavelengths, from ultraviolet to mid-infrared range [1]. In recent years significant developments in Superconducting Nanowire Single Photon Detector (SNSPD) technology have been achieved by producing detectors characterized by >95% detection efficiency, picosecond time resolution, milli-Hz dark count rates, and nanosecond recovery time [1-3]. High-performance commercial products based on NbN or NbTiN SNSPDs in customized cryostats are now available both for quantum and interdisciplinary technologies for operation up to 1550 nm wavelengths. However, many challenges are still open to optimize the performance of these devices for specific applications such as the large area coverage. Superconducting Microstrip Single Photon Detectors (SMSPDs) are increasingly attracting the interest of the scientific community as a new platform for large area detectors with large advantages in terms of fabrication. Moreover, there is an increasing demand of devices capable of detecting low-energy photons, as in free space communications, due to a reduced solar background, or space-ground integrated quantum network. We present our research activity regarding the impact of SNSPDs and SMSPDs in different applications including Quantum Key Distribution [4,5].

References

[1] I. Zadeh, *et al.*, *Superconducting nanowire single-photon detectors: A perspective on evolution, state-of-the-art, future developments and applications*, APL **118**, 190502 (2021).
[2] L. You, *Superconducting nanowire single-photon detectors for quantum information*, Nanophot. **9**, 2673 (2020).
[3] F. P. Venza, M. Colangelo, *Research trends in single-photon detectors based on superconducting wires*, APL Photonics, **10 (4)**, 040901 (2025).
[4] C. Cirillo, *et al.*, *Single photon detection up to 2 μm in pair of parallel microstrips based on NbRe ultrathin films*, Scientific Rep., **14(1)**, 20345 (2024).
[5] G. Guarda, *et al.*, *BB84 decoy-state QKD protocol over long-distance optical fiber*, 2023 23rd International Conference on Transparent Optical Networks (ICTON), Bucharest, Romania, pp. 1-4 (2023).

Abstract ID: 30467

INERTIAL SPIN-WAVE DYNAMICS IN TWISTED MAGNETIC NANOSTRIPS

M. d'Aquino

Dept. of Electrical Eng. and ICTs, University of Naples Federico II, 80125 Naples, ITALY

The growing ability to exploit the third dimension in the fabrication of magnetic nanoscale systems has allowed overcoming the constraints imposed by traditional flat structures[1]. While thin-film magnetic systems have established the foundation for spintronics and magnonics[2], the transition to three-dimensional (3D) nanomagnetism reveals profound effects arising from curvature, torsion, and topology[3]. In this context, the study of spin-wave propagation in geometrically complex nanostructures—such as twisted magnetic strips—has attracted increasing attention. In addition to exhibiting intricate magnetization textures, these systems enable fundamentally novel dynamical phenomena as a consequence of their inherent spatial asymmetry. Concurrently, the experimental observation of terahertz (THz) nutation arising from magnetic inertia[4], predicted over a decade ago for ferromagnets[5], has opened new avenues in ultrafast magnetism and stimulated extensive research into inertial spin-wave dynamics, following pioneering experiments on planar magnetic nanostructures.

In this presentation, we outline novel dynamical phenomena produced by the excitation of inertial spin-wave dynamics in 3D twisted soft-magnetic nanostrips, where curvature and torsion couple with magnetic inertia to produce THz magnetic oscillations. We show that these inertial effects, enhanced by the underlying 3D geometry, lead to a pronounced nonreciprocal behavior in the spin-wave spectrum[6]. The combination of geometric chirality and inertial dynamics introduces an effective symmetry breaking, positioning these twisted architectures as promising candidates that pave the way to the field of curvilinear THz magnonics.

We present a theoretical treatment[6] that allows quantitative understanding for the onset of geometric (Berry) phase in inertial spin wave dynamics, which is responsible for the aforementioned symmetry breaking. Analytical formulas for dispersion relations and spectral linewidths are derived both in the precessional (GHz) and in the nutational (THz) regimes and offer a complete picture of the influence of each single parameter on the propagation of inertial spin waves. Application to nanostrips with different nontrivial topology such as Möbius and helical strips reveals different wave number quantization rules, enlightening the role of topology in spin-wave dynamics.

References

[1] G. Gubbiotti Ed., Three-Dimensional Magnonics: Layered, Micro- and Nanostructures, Jenny Stanford Publishing, New York (2019).
[2] V. V. Kruglyak, S. O. Demokritov, and D. Grundler J. Phys. D **43**, 264001 (2010).
[3] D. D. Sheka, O. V. Pylypovskyi, O. M. Volkov, K. V. Yershov, V. P. Kravchuk, and D. Makarov, Small **18**, 2105219 (2022).
[4] K. Neeraj, N. Awari, S. Kovalev, D. Polley, N. Z. Hagström, S. S. P. K. Arekapudi, A. Semisalova, K. Lenz, B. Green, J.-C. Deinert, I. Ilyakov, M. Chen, M. Bawatna, V. Scalera, M. d'Aquino, C. Serpico, O. Hellwig, J.-E. Wegrowe, M. Gensch, and S. Bonetti, Nat. Phys. **17**, 245 (2020).
[5] M.-C. Ciornei, J. M. Rubí, and J.-E. Wegrowe, Phys. Rev. B **83**, 020410(R) (2011).
[6] M. d'Aquino, R. Hertel, Phys. Rev. Lett. **135** (2025), 216705.

Abstract ID: 30779

GEOMETRICALLY ENGINEERED QUANTUM PHASES: SUPERCONDUCTIVITY, TOPOLOGY AND ANTIFERROMAGNETISM

P. Gentile

CNR-SPIN, I-84084 Fisciano (Salerno), ITALY
c/o Università di Salerno, I-84084 Fisciano (Salerno), ITALY

Geometry offers a powerful and versatile handle to shape quantum matter in low-dimensional systems [1]. Electrons confined to curved or buckled structures experience a spatially varying local geometry such that, in the presence of spin–orbit coupling, it generates position-dependent effective spin–orbit fields. In systems with structural inversion asymmetry, nanoscale deformations intertwined with Rashba spin–orbit coupling establish a direct link between spin textures, spin transport, and device geometry [2], and may give rise to geometrically driven topological phases [3–5].

In superconducting systems, the curvature-driven modulation of spin-texture influences the structure of the pair correlations, enabling singlet–triplet mixing and spatial variations of the superconducting order parameter [6]. As a result, geometry can modify the topological properties of the superconducting state and the Josephson effect of weak links [7], providing a route to engineer unconventional superconducting phases through structural design.

Magnetic order is equally sensitive to geometric structure. A buckled zigzag chain [8] constitutes a minimal one-dimensional platform in which lattice buckling cooperates with antiferromagnetic order to generate a crystalline topological phase characterized by strong Z2 invariants. In this setting, topology emerges from the interplay between geometry and magnetic symmetry and encodes a quantized response at the one-dimensional level. When embedded in higher-dimensional Dirac systems, this structure provides the microscopic origin of a (quasi)-topological magnetoelectric polarizability, linking the response of two-dimensional Dirac semimetals to the topology of their one-dimensional crystalline building blocks.

References

[1] P. Gentile, M. Cuoco, O. M. Volkov, Z.-J. Ying, I. J. Vera-Marun, D. Makarov and C. Ortix, Nature Electronics **5**, 551–563 (2022).
[2] Z.-J. Ying, P. Gentile, C. Ortix and M. Cuoco, Phys. Rev. B **94**, 081406(R) (2016).
[3] P. Gentile, M. Cuoco and C. Ortix, Phys. Rev. Lett. **115**, 256801 (2015).
[4] P. Gentile, V. Benvenuto, C. Ortix, C. Noce and M. Cuoco, Condens. Matter **4(1)**, 25 (2019).
[5] S. Pandey, N. Scopigno, P. Gentile, M. Cuoco and C. Ortix, Phys. Rev. B **97**, 241103(R) (2018).
[6] Z.-J. Ying, M. Cuoco, C. Ortix and P. Gentile, Phys. Rev. B **96**, 100506(R) (2017).
[7] G. Francica, M. Cuoco and P. Gentile, Phys. Rev. B **101**, 094504 (2020).
[8] J. W. F. Venderbos, P. Gentile and C. Ortix, arXiv:2512.05862.

Abstract ID: 30826

FLEXIBLE MAGNETORESISITVE SENSORS ENABLING NOVEL CAPABILITIES IN NON-DESTRUCTIVE TESTING

A. Nicolicea, M. Melzer, M. Pelkner

Bundesanstalt für Materialforschung und –prüfung (BAM), Dept. of Non-destructive Testing, 12205, Berlin, GERMANY

The detection of local magnetic stray fields near the surface of metallic parts can be used to identify material defects, fatigue or emerging cracks in critical infrastructure [1]. Classical non-destructive testing (NDT) methods use magnetic particles, coils or rigid magnetic sensors to localize those defect-induced stray fields. They may be directly detected in ferromagnetic materials via flux-leakage testing or electrically induced in conductive materials via eddy-current testing. None of these methods is able to measure surface stray fields at axle and narrow spots on complex-shaped parts, due to the bulky nature of sensing heads, although this is where defects typically tend to occur. The lift-off distance (LO) from the sensor to the surface is the most critical parameter for a reliable measurement in magnetic NDT. In order to avoid collision damage or wear on both, test specimen and sensing head, the LO is typically several hundreds of micrometer, even on smooth and planar metal surfaces, which results in low stray-field strengths to be acquired.

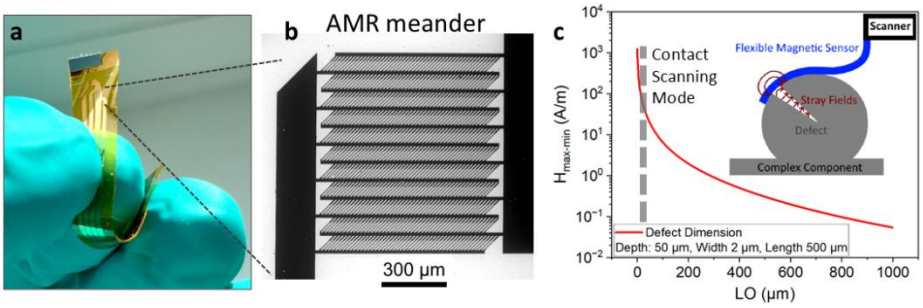

Fig. 1: *Flexible AMR sensors enable non-destructive contact scanning of curvilinear parts for defect detection. a) photography of single flexible sensor; b) micrographic image of AMR element on capton foil; c) dependence of local stray field strength from the lift-off distance from surface to sensor highlighting the signal gain for contact scanning mode, inset: conceptual illustration of contact scanning of curvilinear parts using flexible magnetic sensors.*

This contribution introduces novel magnetic NDT methods using flexible magnetic sensors [2], that enable stray field measurement in direct contact with the specimen, also on curvilinear surfaces and complex shaped parts (Fig. 1). Due to the flexible substrate thickness being the only limiting LO-factor, dynamic imaging measurements of curved magnetic stray field reference landscapes in 20 µm proximity to the surface could be demonstrated for both, flux-leakage [3] and eddy-current [4] testing.

References

[1] D.C. Jiles, NDT International, **23**, 2, 83-92 (1990).
[2] D. Makarov, *et al.*, Applied Physics Reviews **3**, 011101 (2016).
[3] A. Nicolicea, *et al.*, NDT&E International **146**, 103160 (2024).
[4] A. Nicolicea, *et al.*, Measurement **253**, 117340 (2025).

Abstract ID: 30118

COHERENT FLUXON–MAGNON INTERACTION FOR CRYOGENIC MAGNONICS

O. V. Dobrovolskiy

Cryogenic Quantum Electronics, EMG and LENA, Technische Universität Braunschweig, 38106 Braunschweig, GERMANY

Ferromagnetism and superconductivity are fundamental states in condensed-matter physics. Recent discoveries in these topical areas enable the exploration of new physical phenomena at their interfaces. In this regard, interactions between the fundamental quasiparticles – magnetic flux quanta (fluxons) in superconductors and quanta of spin waves (magnons) in magnets – are especially fascinating. Nanoscale 2D and 3D hybrid systems offer unique platforms for studies of such interactions, and coherent spin waves are promising information carriers in magnonic devices for wave-based computing and quantum information technology [1]. While short-wavelength magnons are indispensable building blocks for magnonic nanodevices it is challenging to excite them coherently. Previous efforts have combined magnetic nanogratings [2] or spin textures [3] with microwave induction to push the limit of the shortest wavelength down to about 50 nm. But it was not possible to go beyond this value in the past several years.

In our recent work [4], coherent excitation of exchange magnons has been demonstrated experimentally, with a wavelength down to 36 nm by driving fast-moving fluxons in a superconductor. The successful generation of monochromatic magnons at a record short wavelength of 36 nm represents a milestone in coherent magnonics [5]. It provides an alternative means for coherent magnon excitation beyond conventional inductive microwave methods by leveraging magnetic flux quanta moving at a speed beyond 1 km/s. Once the velocity of the vortices in the superconductor reaches the phase velocity of magnons in the ferromagnetic CoFe film, the condition for coherent coupling is met, see Fig. 1. The dynamic stray fields of the vortices, which vary both in time and space, excite magnons unidirectionally along the direction of vortex motion. The generated magnons are monochromatic and the period of the vortex lattice, which can be tuned by varying the external magnetic field, defines the magnon wavelength.

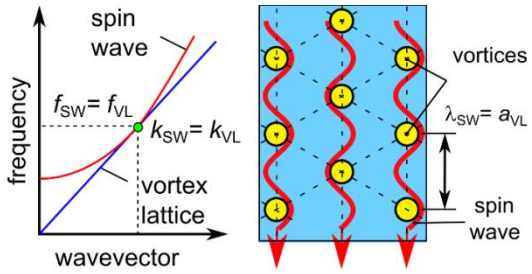

Fig. 1: *The left panel shows the schematic dispersion relations of magnons (red parabola) and fluxons (blue straigh line). The magnons are excited by fast-moving fluxons when their frequency (energy) and wavevector (momentum) match. The right panel shows a schematic of the correspondence of the wavelength of the excited spin wave with the parameter of the vortex lattice. Experimentally, this regime is realized in [4] for vortices moving in a NbC superconductor film and magnons propagating in an adjacent CoFe magnonic conduit.*

References

[1] P. Pirro, *et al.*, Nat. Rev. Mater. **6**, 1114 (2021).

[2] C. Liu, *et al.*, Nat. Commun. **9**, 738 (2018).

[3] V. Sluka, *et al.*, Nat. Nanotechnol. **14**, 328 (2019).

[4] O. Dobrovolskiy, *et al.*, Nat. Nanotechnol. https://doi.org/10.1038/s41565-025-02024-w, (2025).

[5] H. Yu, Nat. Nanotechnol. https://doi.org/10.1038/s41565-025-02023-x, (2025).

Abstract ID: 30304

CUSTOM-BUILT ANISOTROPIC SUPERCONDUCTING FILMS VIA ULTRASHORT LASER PULSES

A. Badía-Majós[1], J. Frechilla[1], A. Ajayan[1], S. Martín[1], E. Martínez[1], L.A. Angurel[1], G.F. de la Fuente[1], N. Lejeune[2], E. Fourneau[2], A.V. Silhanek[2], L.R. Cadorim[3,4], M.V. Milosevic[4]

[1] *Instituto de Nanociencia y Materiales de Aragón (INMA), CSIC-Universidad de Zaragoza, Zaragoza, SPAIN*
[2] *Experimental Physics of Nanostructured Materials, Q-MAT, Université de Liège, Liège, BELGIUM*
[3] *Departamento de Física, Universidade Estadual Paulista, Sao Paulo, BRASIL*
[4] *Department of Physics, University of Antwerp, Antwerp, BELGIUM*

Ultrashort-pulse laser irradiation allows to fabricate anisotropic superconducting layers *à la carte* as demanded by flux manipulation technologies. In particular, the possibility of modifying the surface of thin films with control on the mesoscopic scale has been used to demonstrate flux guiding effects via dedicated surface motifs of characteristic undulating dimensions in the range of the superconducting characteristic lengths ξ, λ. Specifically, by using a UV laser beam, we obtain film corrugations (Laser Induced Periodic Surfaces Structures, LIPSS in brief) with repetition period in the range of 250 nm and controllable depth, with undisputed influence on the physical properties. The main experimental facts (magneto-optical imaging, anisotropic resistivity) are well explained on the basis of the flux dynamics in a variable thickness scenario. In fact, by resorting to time-depedent Ginzburg-Landau (TDGL) simulations of the vortex lattice dynamics, we corroborate the topographical origin of the customized anisotropy. According to both the experimental observations and the simulations, the presence of thickness variations of depth $\lesssim 100$ nm in our films, with original thickness of 200 nm, produces an effective flux pinning effect that multiplies the critical current density along the channels by a factor of ≈ 2. This relates to the preference of vortices to settle in the lower thickness region. Some features of the complex behavior of the macroscopic critical current density have been explained within the TDGL framework. In particular, the non-monotonous dependence of the undulation-related critical current density along the "easy axis" aligns with the theoretical observation of the stabilization of the vortex lattice with increasing densities in the vortex chains within the channels defined by the LIPSS.

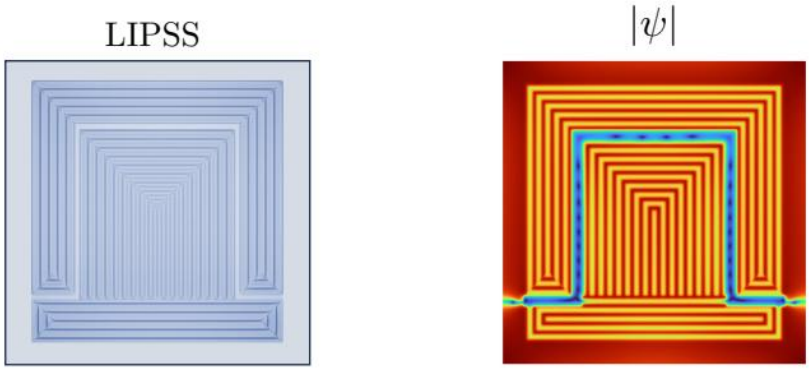

Fig. 1: *Left: sketch of the laser induced local corrugation of a Nb film surface. Anisotropy domains as well as a top-hat path are marked. Right: Ginburg-Landau order parameter simulation for increasing applied field, with vortices penetrating along the path.*

16 - DEVICE PHYSICS OF JOSEPHSON JUNCTIONS AND THEIR FUNDAMENTAL TECHNOLOGIES

Abstract ID: 30142

GENERALIZED NOISE MODELLING IN SUPERCONDUCTING CIRCUITS: FROM THERMAL TO 1/f AND FLUX NOISE

J. A. Delport

SUN Magnetics (RF) (Pty) Ltd, 7600, Stellenbosch, SOUTH AFRICA

Noise and fluctuations play a central role in the performance of superconducting devices, from SQUIDs and resonators to qubit-like circuits, yet circuit-level simulations often remain restricted to simple white-thermal noise models. In this work we introduce a generalized noise framework for a superconducting circuit simulator based on modified nodal/phase analysis, enabling time-domain studies of thermal, 1/f, flux, and critical-current noise in realistic Josephson circuits [1]. Starting from standard Johnson–Nyquist noise in the resistive branches, we implement additional stochastic sources via numerically generated, spectrally shaped random processes. Low-frequency 1/f noise and flux noise are modelled using filtered pseudo-random sequences with adjustable spectral exponents and correlation times [1], while slow critical-current fluctuations are represented as stochastic modulation of the junction critical current [3]. The approach remains compatible with arbitrary circuit topologies, non-sinusoidal current–phase relations, and multi-junction loops. We illustrate the method on several canonical systems: (i) superconducting resonators, where different noise spectra produce distinct signatures in frequency jitter and linewidth broadening [2]; (ii) DC and RF SQUIDs, where thermal and flux noise alter switching current distributions, effective sensitivity, and phase noise [3,4]; and (iii) simple qubit-like nonlinear oscillator circuits, where low-frequency noise leads to dephasing-like phase diffusion in the time domain [1]. In each case we compare simulated observables—such as switching histograms, noise spectra, and effective quality factors—with analytical expectations where available. The results demonstrate how microscopic noise mechanisms map onto macroscopic, circuit-level observables and provide a flexible numerical platform for testing noise hypotheses in existing and emerging superconducting devices. This framework is directly applicable to the analysis and design of analog, RF, and quantum superconducting circuits where noise and fluctuations are performance-limiting.

References

[1] E. Paladino, , Y. M. G. GalperinFalci, B. L. Altshuler, *1/f noise: Implications for solid-state quantum information*, Reviews of Modern Physics, **86(2)**, 361-418 (2014).

[2] B. G. Lakshmi, H. Mukai, T. Yamamoto, J. S. Tsai, *Noise properties of a Josephson parametric oscillator*, Physical Review Applied, **19(1)**, 014065 (2023).

[3] T. Ortlepp, M. H. Volkmann, Y. Yamanashi, *Memory effect in balanced Josephson comparators*, Physica C: Superconductivity, **500**, 20-24 (2014)..

[4] Y. Yamanashi, T. Matsushima, N. Takeuchi, N. Yoshikawa, T. Ortlepp, *Evaluation of current sensitivity of quantum flux parametron*, Superconductor Science and Technology, **30(8)**, 084004 (2017).

Abstract ID: 30509

EMERGENT NETWORK OF JOSEPHSON JUNCTIONS IN A KAGOME SUPERCONDUCTOR

T. J. Blom[1], M. Rog[1], M. Altena[2], A. N. Capa Salinas[3], R. Q. Regter[1], S. D. Wilson[3], M. P. Allan[1,4,5,6,7], C. Li[2], K. Lahabi[1,7]

[1] Huygens-Kamerlingh Onnes Laboratory, Leiden University, 2300 RA, Leiden, THE NETHERLANDS
[2] MESA+ Institute for Nanotechnology, University of Twente, 7500 AE, Enschede, THE NETHERLANDS
[3] Materials Department, University of California Santa Barbara, 93106, Santa Barbara, California, USA
[4] Faculty of Physics, Ludwig-Maximilians-University Munich, 80799, Munich, GERMANY
[5] Center for Nano Science (CeNS), Ludwig-Maximilians-University Munich, 80799, Munich, GERMANY
[6] Munich Center for Quantum Science and Technology (MCQST), Ludwig-Maximilians-University Munich, 80799, Munich, GERMANY
[7] QuantaMap B.V., 2333 CG, Leiden, THE NETHERLANDS

Materials with a Kagome lattice are intensely studied because they host exotic states that combine strong correlations and topology. Recently, critical current oscillations were observed in an unstructured flake of CsV_3Sb_5 [1]. In this work, we show that the origin of these oscillations is a network of Josephs non junctions intrinsic to the flake that emerges below its critical temperature. Under radio-frequency radiation, we observe quantized Shapiro steps. The sensitivity of the step height to the contact placement indicates a complex network of junctions. By performing interference studies along multiple field directions, we demonstrate that the interference effects are a result of small junctions and filamentary supercurrent flow. Upon nanostructuring the flake, prominent features of the interference pattern are preserved, illustrating the localized nature of these junctions and their stability to thermal cycles. These results pave the way for determining the exact nature of superconductivity in the AV_3Sb_5 family.

References

[1] T. Le, *et al.*, Nature **630**, 64-69 (2024).

Abstract ID: 30514

TAPPING-MODE SQUID-ON-TIP MICROSCOPY WITH PROXIMITY JOSEPHSON JUNCTIONS

M. Rog[1], T. J. Blom[1], D. B. Boltje[2], J. D. de Haan[2], R. Fermin[1,3], J. Niu[1,4,6], Y. C. Doedes[1], M. P. Allan[1,2,4,5,6], K. Lahabi[1,2]

[1] *Huygens-Kamerlingh Onnes Laboratory, Leiden University, 2300 RA Leiden, THE NETHERLANDS*
[2] *QuantaMap B.V., Robert Boyleweg 4, 2333 CG Leiden, THE NETHERLANDS*
[3] *Department of Materials Science & Metallurgy, University of Cambridge, 27 Charles Babbage Road, Cambridge CB3 0FS, UNITED KINGDOM*
[4] *Faculty of Physics, Ludwig-Maximilians-University Munich, Munich 80799, GERMANY*
[5] *Center for Nano Science (CeNS), Ludwig-Maximilians-University Munich, Munich 80799, GERMANY*
[6] *Munich Center for Quantum Science and Technology (MCQST), Ludwig-Maximilians-University Munich, Munich 80799, GERMANY*

Describing nanoscale dynamics in strongly correlated quantum systems requires investigating the interplay between dissipation, magnetism and electronic structure. Despite great effort, it remains a major challenge to locally map transport properties such as current flow and its relation to geometry and magnetism. Here, we introduce a hybrid microscope that is uniquely suited for the study of these complex phenomena. By combining SQUID-on-tip imaging with tapping-mode atomic force microscopy, we are able to simultaneously image magnetic flux, electrical currents, local heating and sample topography. Our probes minimize nanoSQUID–sample distance, provide in-plane magnetic sensitivity, and operate even on highly corrugated nanostructures and devices. Our fully electronic readout removes the need for optical elements and external radiation. By using proximity-junction nanoSQUIDs with large voltage output, we resolve nanoscale currents down to 100 nA using a simple four-probe electronic readout that does not require cryogenic amplification.

In addition to demonstrating the technique, we will show the first applications to strongly correlated electron systems, where our microscope offers immediate new insights into the underlying quantum physics. Our approach to SQUID-on-tip offers a powerful route towards the study of dynamic phenomena in exotic materials and delicate quantum circuits.

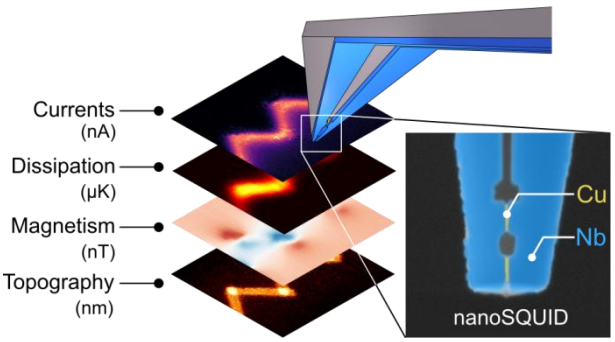

Fig. 1: *Illustration of the tapping-mode SQUID-on-tip technique. [1]*

References

[1] M. Rog, *et al.*, *Tapping-Mode SQUID-on-Tip Microscopy with Proximity Josephson Junctions,* Nano Letters (2026), DOI: 10.1021/acs.nanolett.5c04571

Abstract ID: 30560

BALLISTIC TRANSPORT IN NANOCRYSTALS OF $Bi_2(Te_xSe_{1-x})_3$ TOPOLOGICAL INSULATOR

D. S. Yakovlev, S. K. Kozlov, D. Roditchev, V. S. Stolyarov, C. Feuillet-Palma

Laboratoire de Physique et d''etude des Mat´eriaux, ESPCI Paris, CNRS, PSL University, 75005 Paris, FRANCE

Topological-insulator (TI) nanocrystals provide a compact platform where electronic transport can be driven by quasi-ballistic surface states while the bulk contribution is minimized by thickness control. In this work we summarize a materials-to-devices route for $Bi_2(Te_xSe_{1-x})_3$ nanostructures and demonstrate ballistic transport signatures through proximity-coupled superconducting circuits. Ultrathin, well-faceted TI nanocrystals are grown by Ar-assisted physical vapor deposition with controlled thickness down to a few quintuple layers and tunable composition, enabling reproducible integration into hybrid devices. Nb-TI-Nb Josephson junctions fabricated on individual $Bi_2Te_{2.3}Se_{0.7}$ nanocrystals exhibit a robust proximity supercurrent consistent with a ballistic contribution of topological states, and the junctions can be combined into nanodimensional SQUID-like architectures. In magnetic field, the critical current reveals sharp, resonant oscillations in the ballistic regime, highlighting phase-coherent interference beyond conventional Fraunhofer patterns.

We further address the microwave (ac) response of TI-based Josephson junctions, which have been proposed as a route to Majorana-type bound states and a 4π-periodic current-phase relationship. A frequently discussed experimental consequence is an apparent suppression of odd Shapiro steps under microwave irradiation. By measuring the frequency-dependent Shapiro-step amplitudes in a ballistic junction based on a 23 nm-thick $Bi_2Te_{2.3}Se_{0.7}$ single nanocrystal, we observe a progressive weakening of the first step as the drive frequency is reduced below about 2 GHz. Modeling with a two-channel thermal resistively shunted junction (tRSJ) framework shows that self-heating and non-equilibrium dynamics can account for this behavior even when the junction remains ballistic, emphasizing that a missing first Shapiro step alone is not a definitive signature of topological superconductivity. Finally, we extend the platform to quasi-1D TI nanowires defined by AFM nanopatterning, where ultra-low-temperature magnetotransport confirms phase-coherent, surface-dominated conduction in controlled cross-sections. Together, these results establish TI nanocrystals and nanowires as versatile building blocks for ballistic topological transport and scalable superconducting hybrid circuitry.

References

[1] V. S. Stolyarov, D. S. Yakovlev, *et al.*, *Josephson current mediated by ballistic topological states in $Bi_2Te_{2.3}Se_{0.7}$ single nanocrystals*, Communications Materials **1**, 38 (2020). DOI: 10.1038/s43246-020-0037-y

[2] D. S. Yakovlev, *et al.*, *Physical vapor deposition features of ultrathin nanocrystals of $Bi_2(Te_xSe_{1-x})_3$*, Physical Insights into Quantum Phenomena and Function, **13**, (2022). DOI: 10.1021/acs.jpclett.2c02664

[3] V. S. Stolyarov, *et al.*, *Resonant oscillations of Josephson current in Nb-$Bi_2Te_{2.3}Se_{0.7}$-Nb junctions*, Advanced Quantum Technologies **5(3)**, 2100124 (2022). DOI: 10.1002/qute.202100124

[4] V. Stolyarov, S. Kozlov, D. Yakovlev, *et al.*, *Anomalous microwave response in the dissipative regime of topological superconducting devices based on $Bi_2Te_{2.3}Se_{0.7}$*, arXiv:2309.10897 (2023).

[5] D. S. Yakovlev, *et al.*, *Topological insulator nanowires made by AFM nanopatterning: fabrication process and ultra low-temperature transport properties*, Advanced Physics Research **3(12)**, 2400108 (2024). DOI: 10.1002/apxr.202400108

Abstract ID: 30612

CLOSING THE DESIGN LOOP FOR NONLINEAR JOSEPHSON METAMATERIALS

E. Palumbo[1,2], A. Alocco[1,2], C. Celotto[1,2], L. Fasolo[2], B. Galvano[3], P. Livreri[3,4], E. Enrico[2]

[1] *DISAT, Polytechnic University of Turin, Corso Duca degli Abruzzi 24, 10129 Turin, ITALY*
[2] *INRiM – Istituto Nazionale di Ricerca Metrologica, Strada delle Cacce, 10135 Turin, ITALY*
[3] *Department of Engineering, University of Palermo, 90128 Palermo, ITALY*
[4] *National Inter-University Consortium for Telecommunications (CNIT), Parma, ITALY*

Josephson junction–based metamaterials provide a powerful platform for engineering dispersion, band structure, and nonlinear wave–matter interactions in the microwave regime [1–3]. However, their design remains intrinsically challenging, as nonlinear effects such as Kerr-induced frequency shifts, pump-dependent impedance renormalization, and higher-order mixing feed back onto the effective linear properties of the circuit, often invalidating predictions based solely on linear or weakly nonlinear models [4–6].

In this work, we present an extension of the JosephsonCircuitsOptimizer framework [7], enabling a closed-loop feedback between linear and nonlinear simulations for the automated design of nonlinear Josephson metamaterials. A retroactive correction mechanism is introduced, whereby nonlinear simulation outputs are mapped onto effective linear circuit parameters. These corrected parameters are then reinjected into the linear optimization stage, allowing the circuit geometry and element values to be iteratively modified in order to compensate for nonlinear distortions.
This feedback-assisted methodology enables self-consistent optimization of distributed Josephson junction arrays, in which collective dispersion engineering and nonlinear response emerge from the interplay between unit-cell design and pump-dependent dynamics [2,3]. We show how effective Kerr coefficients, resonance shifts, and impedance variations extracted from nonlinear simulations can be exploited to preserve target linear characteristics—such as matching conditions, band structure, and phase-matching—across realistic operating power levels [4,5]. The proposed workflow provides a systematic and scalable strategy for the robust modeling and design of nonlinear superconducting metamaterials, bridging the gap between small-signal analysis and large-signal operation.

References

[1] M. A. Castellanos-Beltran and K. W. Lehnert, Appl. Phys. Lett. **91**, 083509 (2007).
[2] B. Abdo, *et al.*, Phys. Rev. Lett. **110**, 173902 (2013).
[3] A. B. Zorin, Phys. Rev. Applied **6**, 034006 (2016).
[4] C. Macklin, *et al.*, Science **350**, 307–310 (2015).
[5] N. Bergeal, *et al.*, Nature **465**, 64–68 (2010).
[6] M. Reagor, *et al.*, Appl. Phys. Lett. **102**, 192604 (2013).
[7] E. Palumbo, *et al.*, arXiv:2510.26479 (2025).

Abstract ID: 30640

THERMAL CONTROL OF NON-EQUILIBRIUM TRANSPORT IN A MICROWAVE-DRIVEN SUPERCONDUCTING JUNCTION

M. Kumar

Aalto University, Otakaari 1B, Espoo, FINLAND

Microwave response in superconducting weak links can exhibit complex temperature dependence due to the interplay of critical current, characteristic energy scales, and non-equilibrium transport processes. Inspired by studies showing non-monotonic temperature variations of Shapiro step amplitudes in Josephson grain boundary junctions (see Revin *et al. Beilstein J. Nanotechnol. 2021, 12, 1279–1285*) , we investigate the evolution of microwave-driven conductance features in a superconducting S–S'–S notch junction as a function of temperature at fixed radio-frequency excitation. By mapping differential conductance versus dc bias current and temperature under constant RF frequency and power, we observe a pronounced low-resistance region around zero bias that narrows and collapses upon warming, indicating the thermal suppression of driven subgap bound-state transport. At the lowest temperatures, additional structured patterns reminiscent of interference emerge and are progressively washed out with increasing T. The strong thermal evolution and continuous dispersion of these features with bias and RF power differ qualitatively from conventional phase-locked Shapiro steps, whose voltage positions remain fixed with temperature, and instead point to the temperature-dependent modulation of bound-state dynamics in the weak junction region. These results highlight temperature as a key control parameter for discriminating between equilibrium and driven non-equilibrium transport phenomena in microwave-excited superconducting nanostructures.

Abstract ID: 30810

MODELING QUASIPARTICLE DISSIPATION IN $Bi_2Sr_2CaCu_2O_{8+x}$ INTRINSIC JOSEPHSON JUNCTION STACKS

O. Kizilaslan[1,2], R. Wieland[1], E. Dorsch[1], D. Koelle[1], R. Kleiner[1]

[1] *Physikalisches Institut, Center for Quantum Science and LISA+, Universitat Tübingen, D-72076 Tübingen, GERMANY*

[2] *Department of Biomedical Engineering, Faculty of Engineering, Inonu University, Malatya, TURKEY*

The temperature dependence of the c-axis resistance $R(T)$ in $Bi_2Sr_2CaCu_2O_{8+x}$ (Bi-2212) stacks is analyzed using a phenomenological two-channel transport model that includes normal quasiparticle and superconducting contributions. The normal channel follows a temperature-dependent resistivity with both linear and thermally activated components, while the superconducting channel appears below the doping-dependent critical temperature $T_c(x)$. An additional empirical term accounts for the temperature-dependent contact resistance.

By fitting experimental $R(T)$ data, key parameters such as doping, activation energy, and contact resistance are extracted. Using these parameters, the normal-state conductivity at a probe temperature is calculated and extended to finite frequency via a Drude model to obtain the real part of the conductivity at the plasma frequency. From this, the quasiparticle resistance and the corresponding quality factor Q_{qp} are estimated, providing insight into quasiparticle dissipation in intrinsic Josephson junction stacks.

We gratefully acknowledge financial support by The Scientific and Technological Research Council of Türkiye, TUBİTAK 2219-2020/2-1059B192000817 and the Research Fund of Inonu University, Türkiye under Grant Contract No. FOA-2023-3260.

Abstract ID: 30037

RELATIVISISTIC DESCRIPTION OF CANONICAL QUANTIZATION OF JOSEPHSON EFFECT FOR THE CASE OF SUPERCONDUCTOR INTERFACED TO SEMICONDUCTOR QUANTUM DOTS

K. Pomorski[1], L. Stepien[2], A. Bednorz[3]

[1] *University of New Mexico, Albuquerque, USA & Quantum Hardware Systems, Lodz, POLAND*
[2] *University of the National Education Commission, Cracow, POLAND*
[3] *University of Warsaw, Faculty of Physics, Warsaw, POLAND*

The relativistic relation between the Josephson energy and the transport current has been verified [1-5] and further generalized to include the influence of external charges associated with Wannier-type semiconductor qubits coupled to a Josephson junction [6]. The resulting modification of the Andreev bound states reflects the coupling between the superconducting condensate and the quantum dynamics of the Wannier qubits [7]. Within this framework, a generalized form of the Cooper-pair quasiparticle is introduced. The analysis indicates the emergence of a superposition of effective masses in the generalized superconducting quasiparticle, whose properties can be electrically tuned via the charge states of the nearby Wannier qubits with computational methodology specified in [5-6].

References

[1] G. Schon, V. Ambegaokar, U. Eckern, *Quantum dynamics of a superconducting tunnel junction*, Phys. Rev. B **30**, 6419 (1984).

[2] J.M. Martinis, M.H. Devoret, J. Clarke, *Quantum Josephson junction circuits and the dawn of artificial atoms*, Nat. Phys. **16**, 234–237 (2020).

[3] S. Matsuo, *et al.*, *Phase engineering of anomalous Josephson effect derived from Andreev molecules*, Sci. Adv. **9** (2023).

[4] S. Crowe, S. Evans, A. Smolyaninov, *Analysis of polymerized superconducting circuits*, Arxiv: 2509.1801 (2025).

[5] K. Pomorski, A. Bednorz, *Justification of the canonical quantization of the Josephson effect and its modifications due to high capacitance energy*, J. Phys. A: Math. Theor. **49**, 125002 (2016).

[6] K. Pomorski, P. Peczkowski, R.B. Staszewski, *Analytical solutions for N interacting electron system confined in graph of coupled electrostatic semiconductor and superconducting quantum dots in tight-binding model*, Cryogenics, **Vol.109**, 103117 (2020).

[7] K. Pomorski, *Electrostatically interacting Wannier qubits in curved space*, *Materials, **17*** (2024).

Abstract ID: 30540

TUNABLE JOSEPHSON GENERATOR FOR QUBIT EXCITATION AND TWO-TONE SPECTROSCOPY

M. M. Khrenov[1,2], I. A. Nazhestkin[1], I. I. Soloviev[2], D. S. Yakovlev[3]

[1] *Russian Quantum Center, Skolkovo, 143025 Moscow, RUSSIA*
[2] *Lomonosov Moscow State University, Skobeltsyn Institute of Nuclear Physics, Leninskie gory, GSP-1, Moscow, RUSSIA*
[3] *Laboratoire de Physique et d'Etude des Matériaux, ESPCI-Paris, PSL Research University, 75005 Paris, FRANCE*

The development of quantum computing and thus increasing the number of qubits requires new solutions for qubit control, because conventional qubit control requires a large number of coaxial cables from the room temperature into the cryostat, which becomes impractical due to the heat load and physical space constraints. To eliminate such problem, cryogenic on-chip control systems can be used to prepare signals for qubit control inside the cryostat [1]. In this work, we introduce a tunable Josephson junction-based RF generator for qubit excitation and demonstrate the transmon qubit two-tone spectroscopy using this generator. The capacitively and resistively shunted Nb-AlOx-Nb Josephson junction (JJ) is connected with the spiral resonator [2] having the resonant frequency overlapping the frequency range of the transition frequency $|0\rangle \rightarrow |1\rangle$ of the transmon qubit. The tunable RF emission is due to the Josephson generation with frequency $f=(2e/h)V_{JJ}$ and the resonator widens the emission linewidth down to 820 kHz (FWHM). The voltage V_{JJ} across the JJ can be tuned by tuning the JJ bias current.

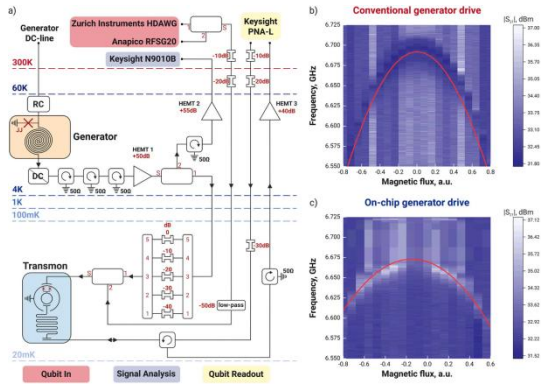

Fig. 1: *(a) Experiment scheme, (b) two-tone spectroscopy of a transmon qubit: using the room-temperature generator and (c) the Josephson on-chip generator.*

We successfully performed the transmon qubit two-tone spectroscopy with our Josephson generator and compared it with the two-tone spectroscopy performed with the room-temperature commercially avaliable generator (Fig. 1) [3].

References

[1] R. McDermott, *et al.*, Quantum Science and Technology **3(2)**, 024004 (2018).
[2] C. Yan, *et al.*, Nature Electronics **4(12)**, 885-892 (2021).
[3] M.M. Khrenov, *et al.*, Advanced Quantum Technologies, e00659 (2025).

Abstract ID: 30661

INTERPLAY OF SUPERCONDUCTIVITY AND ALTERMAGNETISM IN HYBRID SYSTEMS

A. S. Mel'nikov[1,2], M. M. Vasiakin [1,3]

[1] *Moscow Institute of Physics and Technology, Dolgoprudnyi, Moscow Region 141701, RUSSIA*
[2] *Institute for Physics of Microstructures, Russian Academy of Sciences, 603950 Nizhny Novgorod, GSP-105, RUSSIA*
[3] *L. D. Landau Institute for Theoretical Physics, Chernogolovka 142432, RUSSIA*

In this talk we start from an overview of basic properties of the recently discovered new type of magnetic ordering called altermagnetism. For these systems the exchange field acting on the conducting electrons is known to be momentum dependent which can result in rather unusual transport properties. In particular, one can expect strong influence of such exchange field anisotropy on the proximity effect and related interplay between the superconducting and magnetic ordering in different hybrid systems. Here we focus on the effect of disorder on the above interplay and analyze the influence of normal scattering on superconducting phase diagram in superconductor-altermagnet bilayers. Scattering on non-magnetic point impurities is shown to result in a strong enhancement of superconducting critical temperature (T_c) due to the averaging of momentum-dependent exchange field induced by altermagnetic layer.

We derive the Usadel equation for the dirty limit and find out that the joint effect of the altermagnetic exchange field and nonmagnetic potential scattering is similar to the effect of magnetic impurities with an easy axis along the altermagnetic Neel vector. The origin of these phenomena is shown to be related to the Dyakonov-Perel mechanism of spin relaxation. The above analogy leads to a number of curious implications. First of all, using the Abrikosov-Gor'kov approach it is possible to immediately obtain a complete phase diagram and energy dependence of density of states. Depending on impurity concentration, there are three possible phases: normal phase, gapless superconducting phase and gapped superconducting phase. The uniaxial anisotropy determined by the Neel vector of the altermagnet could be detected, e.g., by the Knight shift measurements in NMR experiments.

Similar phenomena of superconducting T_c enhancement reveal itself for superconductivity nucleation near different boundaries and sample edges. We analyze, in particular, the mechanism of stimulation of the edge superconductivity due to the scattering of quasiparticles at the edge which partially suppresses the depairing effect of the exchange field. The inclusion of additional magnetic scattering may lead to the non-monotonic behavior of T_c.

Finally, we focus on the generalization of the Ginzburg-Landau theory caused by the altermagnetic exchange field effects and apply this modified phenomenological theory for the analysis of magnetic properties. The interplay of the Zeeman effect and altermagnetic exchange field results in the magnetic field dependence of the effective mass anisotropy which affects both the structure and dynamics of the vortex matter.

This work was supported by the Russian Science Foundation (Grant No. 25-12-00042).

Abstract ID: 30704

EFFECTS OF LOW-TEMPERATURE ANNEALING AND ELECTRON-BEAM IRRADIATION ON INTRINSIC JOSEPHSON JUNCTIONS IN $Bi_2Sr_2CaCu_2O_{8+\delta}$

Y. Simsek[1,2]

[1] *Sabancı University Nanotechnology Research and Application Center, Istanbul, TURKEY*
[2] *Faculty of Engineering and Natural Sciences, Sabancı University, Tuzla İstanbul, TURKEY*

$Bi_2Sr_2CaCu_2O_{8+\delta}$ (Bi-2212) is a layered high-T_c superconductor that naturally composed of alternating superconducting CuO_2 planes and insulating BiO/SrO layers. The superconducting properties of Bi-2212 are known to be sensitive to external stimuli such as strain, carrier concentration, and pressure. In particular, the hole doping level can be typically modified through heat treatment at high temperatures ($T > 400$ °C) and light irradiation. This study examines the influence of prolonged low-temperature annealing ($T < 200$ °C) and electron-beam exposure on the superconducting properties of Bi-2212. Step-like IJJ stacks of 3×3 μm² in size were fabricated on Bi-2212 single crystals with different initial doping levels. An optimally doped stack was subjected to sequential vacuum annealing at 150 °C, 190 °C, and 204 °C, while an underdoped sample was annealed at 190 °C in an oxygen atmosphere. In a separate experiment, an optimally doped junction structure was exposed to sequential electron-beam irradiations. After each heat treatment and e-beam irradiation, resistance–temperature (R–T) and current–voltage (I–V) measurements were performed to track changes in the critical temperature (T_c) and critical current density (J_c). Both prolonged heating and e-beam exposure were found to significantly alter the superconducting properties of Bi-2212. While the effects of low-temperature annealing can be attributed with changes in oxygen content in microscale IJJ structures, the superconductivity degradation observed after electron-beam exposure likely involves additional mechanisms beyond simple oxygen doping. These results show that common microfabrication processes can strongly influence superconductivity in Bi-2212 IJJs and may provide a route for post-fabrication tuning of device performance.

Abstract ID: 30713

INTRINSIC NON-LINEARITY OF JOSEPHSON JUNCTIONS AS AN ALTERNATIVE ORIGIN OF THE MISSING FIRST SHAPIRO STEP

L. Xu, P. L. Li, G. T. Liu, F. M. Qu, L. Lu

Institute of Physics, Chinese Academy of Sciences, 100190, Beijing, CHINA

The absence of the first Shapiro step in microwave-irradiated Josephson junctions is often interpreted as a hallmark of topological superconductivity mediated by Majorana bound states. However, this signature can also arise from trivial mechanisms, complicating definitive conclusions. Here, we report systematic microwave spectroscopy measurements on Al/WTe_2 Josephson junctions, revealing not only the suppressed first Shapiro step at low frequencies but also a distinct and previously unreported zigzag pattern in the step transitions at intermediate frequencies (~3–5 GHz). These features cannot be explained by conventional models based on junction underdamping or heating alone. We demonstrate that both phenomena emerge naturally from the intrinsic nonlinear current-voltage characteristics of junctions with low-to-moderate transparency. By extending the standard resistively and capacitively shunted junction (RCSJ) model to include a voltage-dependent normal resistance (nonlinear RCSJ model), we successfully reproduce the missing first step, the zigzag transition lines, and the emergence of half-integer steps at higher frequencies. Our findings establish that intrinsic junction nonlinearity—a common property in many semiconductor-superconductor hybrid structures—can mimic key signatures of exotic physics. This work provides a crucial diagnostic framework, emphasizing the necessity of comprehensive frequency-dependent spectroscopy before attributing the missing first Shapiro step to topological origins, thereby guiding the ongoing search for Majorana zero modes in solid-state systems.

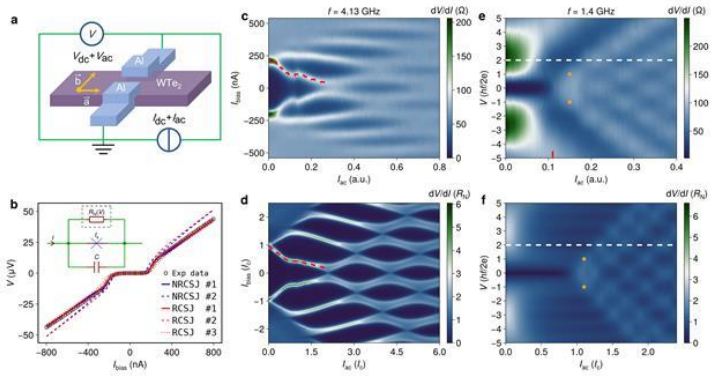

Fig. 1: ***a*** *Schematic of the Josephson junction device.* ***b*** *Fits of voltage-current characteristics.* ***c*** *Zigzag transition lines in the Shapiro spectra.* ***d*** *Simulation of Shapiro spectra with zigzag transition lines corresponding to panel c.* ***e*** *Missing first Shapiro steps in the Shapiro spectra.* ***f*** *Simulation of Shapiro spectra with missing first Shapiro steps corresponding to panel e.*

References

[1] L. Xu, P. L. Li, et al., arXiv:2510.20130.

Abstract ID: 30176

ENERGY-EFFICIENT HYBRID SUPERCONDUCTOR–SEMICONDUCTOR MILLIKELVIN ELECTRONICS FOR SCALABLE QUANTUM INFORMATION PROCESSING

K. Delfanazari

James Watt School of Engineering, University of Glasgow, Glasgow, UK

Scalable quantum computing requires cryogenic electronic platforms that operate efficiently at millikelvin temperatures while overcoming fundamental bottlenecks in chip wiring and cryostat connectivity. The limited number of electrical contact pads and dilution refrigerator wiring restricts the number of quantum devices that can be characterised per cooldown. Architectures enabling the simultaneous measurement of hundreds of devices remove these constraints, reducing experimental overheads in time, cost, and energy while improving device reproducibility and reliability. Hybrid superconductor–semiconductor (S–Sm) electronics offer a promising route to such energy-efficient millikelvin hardware, combining electrostatic tunability with the coherence and low-power operation of superconducting circuits. We present voltage-addressable S–Sm electronics integrated with Nb and NbN platforms, where split-gate-defined electrostatic fields enable nanoscale carrier transport control, switching, and logic functions essential for scalable cryogenic hardware. Large-scale gate-tunable electronic switches are fabricated and experimentally validated using DC and microwave spectroscopy and transport measurements. Robust and reproducible operation in NbN/SiGe microwave circuits over two years confirms their long-term stability and compatibility with semiconductor technology. This work advances the development of scalable, coherent, and energy-efficient cryogenic electronics for next-generation quantum information processing.

References

[1] Nat. Photon. **19, 1163–1177** (2025).

[2] Physical Review Applied **21** (1), 014051 (2024).

[3] Advanced Electronic Materials **10** (2), 2470006 (2023).

[4] Advanced Materials **29** (37), 1701836 (2017).

[5] arXiv:2509.26363

[6] arXiv:2510.25208

17 - DYNAMICAL CONTROL OF ELECTRONIC PROPERTIES IN FUNCTIONAL MATERIALS

Abstract ID: 30062

OBSERVING DIFFERENTIAL SPIN CURRENTS BY RESONANT INELASTIC X-RAY SCATTERING

Y. Gu[1], J. Barker[2,3], J. Pelliciari[4], G. E. W. Bauer[3,5], V. Bisogni[4]

[1] *State Key Laboratory of Low Dimensional Quantum Physics, Beijing Tsinghua Institute for Frontier Interdisciplinary Innovation, Beijing, CHINA*
[2] *Bragg Centre for Materials Research & School of Physics and Astronomy, University of Leeds, Leeds, UK*
[3] *Institute for Materials Research, Tohoku University, Sendai, JAPAN*
[4] *National Synchrotron Light Source II, Brookhaven National Laboratory, Upton, NY, USA*
[5] *WPI Advanced Institute for Materials Research, Tohoku University, Sendai, JAPAN*

Controlling spin currents, that is, the flow of spin angular momentum, in small magnetic devices, is the principal objective of spin electronics, a main contender for future energy-efficient information technologies. A pure spin current has never been measured directly because the associated electric stray fields and/or shifts in the non-equilibrium spin-dependent distribution functions are too small for conventional experimental detection methods optimized for charge transport. In this talk, I will present how resonant inelastic X-ray scattering (RIXS) can bridge this gap by measuring the spin current carried by magnons—the quanta of the spin wave excitations of the magnetic order—in the presence of temperature gradients across a magnetic insulator. we report one of the first direct observations of a spin current with energy and momentum resolution by measuring RIXS spectra of the magnetic insulator yttrium iron garnet $Y_3Fe_5O_{12}$. Our results show that the momentum- and energy-resolved RIXS intensity is sensitive to minute changes in the magnon distribution under non-equilibrium conditions. We use the Boltzmann equation in the relaxation time approximation to extract transport parameters, such as the magnon lifetime at finite momentum, essential for the realization of magnon spintronics. The direct spectroscopic detection-energy and momentum resolved-of the magnon current by RIXS should stimulate the theory and the tomography of material- and momentum-dependent relaxation times in reciprocal space.

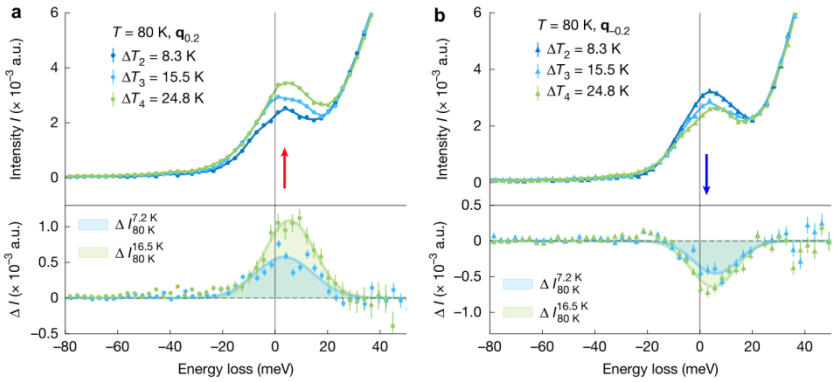

Fig. 1: *RIXS spectra under different temperature gradients.*

References

[1] Y. Gu, J. Barker, J. Li, T. Kikkawa, F. Camino, K. Kisslinger, J. Sinsheimer, L. Lienhard, J. J. Bauer, C. A. Ross, D. N. Basov, E. Saitoh, J. Pelliciari, G.E. W. Bauer and V. Bisogni, Nature **645**, 900–905 (2025).

11th International Conference on Superconductivity and Magnetism ICSM2026
4th International Conference on Quantum Materials and Technologies ICQMT2026
19th April to 26th April, 2026, Ölüdeniz – Fethiye/Muğla, Türkiye
https://icsmforever.org/

Abstract ID: 30119

STRAIN AND ELECTRIC FIELD CONTROL OF NEEL VECTORS AND MAGNONS IN MULTIFERROIC $BiFeO_3$

T. Kim[1], Y. Liu[2], N. Zheng[2], S. Fan[1], V. Bhartiya[1], J. Li[1], Y. Gu[1], K. Kisslinger[3], F. Camino[3], S. Lee[4], J.-G. Park[5], S.-W. Cheong[6], P. Stevenson[7], P.R. Raghuvanshi[8], V. Cooper[8], C.-Y. Kuo[9], M.P.M. Dean[10], Y. Nie[2], J. Pelliciari[1], V. Bisogni[1]

[1] *National Synchrotron Light Source II, Brookhaven National Laboratory, Upton, NY 11973, USA*
[2] *College of Engineering and Applied Sciences, Nanjing University, Nanjing 210093, CHINA*
[3] *Center for Functional Nanomaterials, Brookhaven National Laboratory, Upton, NY 11973, USA*
[4] *Neutron Science Division, HANARO, Korea Atomic Energy Research Institute, Daejeon 305353, REPUBLIC OF KOREA*
[5] *Department of Physics and Astronomy, Seoul National University, Seoul 08826, REPUBLIC OF KOREA*
[6] *Department of Physics and Astronomy, Rutgers University, Piscataway, NJ 08854, USA*
[7] *Department of Physics, Northeastern University, Boston, MA 02115, USA*
[8] *Materials Science and Technology Division, Oak Ridge National Lab, Oak Ridge, TN 37831, USA*
[9] *Department of Electrophysics, National Yang Ming Chiao Tung University (NYCU), 1001 University Road, Hsinchu 30010, TAIWAN*
[10] *Condensed Matter Physics and Materials Science Department, Brookhaven National Laboratory, Upton, NY 11973, USA*

The control of properties in quantum material is important for future applications. $BiFeO_3$, a room-temperature multiferroic, has been considered as a promising candidate in this context, as the manipulation of antiferromagnetic order is possible via switching of ferroelectric polarization. Although various experiments verified this controllability using strain or electric field, the characterization of spin-excitations is little known, and further understanding of how to control them is needed for future spintronics or magnonics.

We performed resonant inelastic X-ray scattering (RIXS) to reveal magnons in $BiFeO_3$ and their evolution under epitaxial strain and electric field. By analyzing linear dichroism of magnons in RIXS spectra combined with crystal-field multiplet theory calculations, we revealed that the Neel vector is systematically rotated as a function of strain, indicating control of magnetic anisotropy in $BiFeO_3$ thin films. We also established the minimal spin Hamiltonian model to explain the observed magnon dispersion and its strain dependence, which provides deeper understanding of modifications in magnetic interactions via strain. In addition, by combining with an in-situ electrical set-up and realizing a capacitor-like device, we observed a robust energy shift in magnon by ferroelectric polarization switching, which represents possible control of magnon energy via electric field. Our results provide unambiguous evidence and insights into strain and electrical control of magnons in $BiFeO_3$.

Abstract ID: 30182

IN-PLANE ANOMALOUS HALL EFFECT IN QUANTUM MATERIALS

M. Uchida[1,2]

[1] *Department of Physics, Institute of Science Tokyo, 152-8551, JAPAN*
[2] *Toyota Physical and Chemical Research Institute, 480-1192, JAPAN*

The Hall effect refers to the generation of a voltage transverse to an electric current on the deflection plane, through diagonal coupling between the out-of-plane Hall vector component and the out-of-plane magnetic field or spin magnetization. However, in recent years, theoretical studies based on various models have suggested that even an in-plane magnetic field can induce an anomalous Hall effect, through off-diagonal coupling between the out-of-plane Hall vector component and the in-plane magnetic field or spin magnetization. Here we present the observation of in-plane anomalous Hall effect in thin films of various quantum materials including Dirac and Weyl semimetals [1-3]. We also introduce recent finding on the unique multipolar nature of the off-diagonal coupling underlying in-plane anomalous Hall effect [4].

References

[1] A. Nakamura, *et al.*, Physical Review Letters **133**, 236602 (2024).

[2] S. Nishihaya, *et al.*, Physical Review Letters **135,** 106603 (2025).

[3] S. Nishihaya, *et al.*, Advanced Materials **37,** e02624 (2025).

[4] A. Nakamura, *et al.*, arXiv:2507.21458 (2025), under review.

Abstract ID: 30220

MUELLER MATRIX MAGNETO ELLIPSOMETRY AND VORTEX BEAM SPECTROSCOPY OF MAGNETIC AND CHIRAL MATERIALS

A. Sirenko

Department of Physics, New Jersey Institute of Technology, Newark, NJ, USA

Coherent synchrotron radiation at the MET beamline at NSLS-II, Brookhaven National Lab enables spectroscopic studies of relatively small single crystals in the far-infrared spectral range using full Mueller matrix magneto-ellipsometer with the sample temperature range between 4 K and 300 K and the magnetic field of ±7 T that can be applied in either the Voight or Faraday geometry with respect to the sample surface. The off-diagonal components of the Mueller matrix allowed for accurate measurements of the resonant Kerr and Faraday rotation at the magnetic resonances. A number of mono-chiral single crystals were measured, where the sign of the chiral handedness was determined. Details of the Mueller matrix data analysis for magneto-rotation of polarization and circular dichroism due to the structural chirality and magnetic resonances will be presented. In addition to full polarization control, the magneto-ellipsometer at MET has the capability to convert coherent synchrotron radiation into vortex beams carrying orbital angular momentum (OAM) L=±1, ±2, ±3, and ±4 in the far-IR spectral range. Thus, spectroscopic measurements using optical beams with a total angular momentum of $J=L\pm S$ are available, where spin angular momentum S=±1 corresponds to right and left-hand circular polarizations. Several examples of the orbital dichroism discovered at the magnetic resonances of (Lu,Sc)FeO_3, $CuOSeO_3$ and $Fe_2Mo_3O_8$ single crystals will be presented. Ni_3TeO_6, $NiCo_2TeO_6$, and *h*-$Lu_{0.6}Sc_{0.4}FeO_3$ single crystals.

References

[1] V.A. Martinez, A.A. Sirenko, L. Bugnon, P. Marsik, C. Bernhard, Q. Zhang, G.L. Pascut, F. Lyzwa, Z. Liu, K. Du, and S.-W. Cheong, Phys. Rev. B accepted (2025). arXiv preprint arXiv:2507.22172

[2] V. A. Martinez, Y. Gao, J. Yang, F. Lyzwa, Z. Liu, C. J. Won, K. Du, V. Kiryukhin, S-W. Cheong, and A. A. Sirenko, Phys. Rev. B **112**, 064411 (2025).

[3] A. A. Sirenko, P. Marsik, L. Bugnon, M. Soulier, C. Bernhard, T. N. Stanislavchuk, X. Xu, and S.-W. Cheong, Phys. Rev. Lett. **126**, 157401 (2021).

Abstract ID: 30250

STRANGE METALS STUDIED BY EELS AND RIXS

J. Fink

Leibniz Institute for Solid State and Materials Research Dresden, Helmholtzstraße 20, 01069 Dresden, GERMANY

Strange metal behavior occurs in the phase diagram of doped cuprates above the dome of unconventional superconductivity. It is characterized by a linear temperature dependence

of the resistivity. This signals a breakdown of the quasiparticle concept used in normal Fermi liquids. There, a quadratic temperature or energy dependence of the scattering rate is detected. In the phenomenological marginal Fermi liquid (MFL) theory, the strange metal behavior is explained by a continuum of low-energy electronic excitations. The latter are possibly related to strong quantum fluctuations which are also supposed to mediate unconventional superconductivity in cuprates and ruthenates. Holographic theories have predicted that this continuum would cause an overdamping of plasmon excitations. These predictions are at variance with our EELS in transmission (T-EELS) and RIXS experiments performed on various doped cuprates [1] and ruthenates [2,3]. In all cases we see well-defined optical plasmons which are overdamped only for large momentum in the range of the classical Lindhard continuum. The dispersion of the optical plasmon can be well described within the RPA without mass renormalization. On the other hand, the low-energy acoustic plasmons, detected by RIXS on p- and n-type doped cuprates [4] show a reduced dispersion which can be related to a mass enhancement also recorded in ARPES experiments on cuprates. These conflicting results can be described by an energy dependent mass renormalization of the charge carriers also detected in optical spectroscopy, being large at low energy due to a coupling to medium-energy excitations and turning small in the energy range of the optical plasmon well above these excitations. Moreover, recent interesting results on the momentum dependence of the plasmon width are presented. Finally, we discuss similar results derived from reflection EELS (R-EELS) which support the holographic theories predicting overdamped plasmons and the appearance of a continuum at momenta well below the Lindhard intra-band continuum [5].

References

[1] N. Nücker, U. Eckern, J. Fink and P. Müller, Phys. Rev. B **44**, 7155 (1991).

[2] M. Knupfer, F. Jerzembeck, N. Kikugawa, F. Roth and J. Fink, Phys. Rev.B **106**, L241103 (2022).

[3] J. Schultz, A. Lubk, F. Jerzembeck, N. Kikugawa, M. Knupfer, D. Wolf, B. Büchner and J. Fink, Nature Comm. **16**, 4287 (2025).

[4] A. Nag, L. Zinni, J. Choi, J. Li, Sijia Tu, A. C. Walters, S. Agrestini, S. M. Hayden, M. Bejas, Z. Lin, H. Yamase, K. Jin, M. García-Fernández, J. Fink, A. Greco and K.-J. Zhou, Phys. Rev. Res. **6**, 043184 (2024).

[5] P. Abbamonte and J. Fink, Annual Rev. Condens. Matter Phys. **16**, 465 (2025).

Abstract ID: 30286

CIRCULAR DICHROISM IN RESONANT INELASTIC X-RAY SCATTERING AS A PROBE OF ALTERMAGNETIC DOMAINS

H. Suzuki

Frontier Research Institute for Interdisciplinary Sciences, Tohoku University, Sendai 980-8578, JAPAN

Altermagnets form a new class of collinear magnets that break time-reversal symmetry without exhibiting net magnetization. Unlike conventional antiferromagnets, altermagnets possess electronic band structures that are split into spin-up and spin-down bands, making them attractive for spintronics applications, particularly when combined with the ultrafast switching capabilities they share with antiferromagnets. While many theoretical proposals implicitly assume a single altermagnetic domain, the absence of magnetization and the presence of crystallographic domains make the experimental identification of altermagnetic domains a central challenge. We have demonstrated that circular dichroism in resonant inelastic X-ray scattering (RIXS-CD) provides a powerful and symmetry-sensitive probe of altermagnetic order [1].

We showed that RIXS-CD does not rely on time-reversal symmetry breaking itself, but instead reflects the breaking of unitary symmetries associated with altermagnetic ordering. By carefully selecting the scattering geometry of the incident and scattered photons, different altermagnetic domains can be distinguished through their characteristic azimuthal-angle dependence of the RIXS-CD signal associated with magnon excitations. These results establish RIXS-CD as a complementary technique to conventional X-ray magnetic circular dichroism, with potential applicability to a broad class of anomalous Hall antiferromagnets.

References

[1] D. Takegami, T. Aoyama, T. Okauchi, T. Yamaguchi, S. Tippireddy, S. Agrestini, M. García-Fernández, T. Mizokawa, K. Ohgushi, Ke-Jin Zhou, J. Chaloupka, J. Kuneš, A. Hariki, and H. Suzuki, Phys. Rev. Lett. **135**, 196502 (2025).

Abstract ID: 30295

RECENT ADVANCES IN THE OPTICAL CONTROL OF SUPERCONDUCTIVITY

M. Buzzi

Max Planck Institute for the Structure and Dynamics of Matter, 22761 Hamburg, GERMANY

Tailored optical excitation in certain high-T_c cuprates has been shown to induce superconducting-like interlayer coherence at temperatures far above T_c, as evidenced by the terahertz-frequency optical properties in the nonequilibrium state [1,2]. In this talk I will discuss our latest experiments in the field of optical control of superconductivity in $YBa_2Cu_3O_{6+x}$, which have led to considerable advances both in optimizing the nonequilibrium state and understanding its nature.

In the first part of the talk, I will discuss how the enhancement of the "superfluid density" $\omega\sigma_2$, and the dissipative response of quasiparticles, σ_1, can be optimized by systematically tuning the duration and energy of the mid-infrared excitation pulse while keeping the peak field fixed [3]. We found that the photoinduced $\omega\sigma_2$ saturates to the zero-temperature equilibrium value for pulses made longer than the phonon dephasing time, while the dissipative component continues to grow with increasing pulse duration. This finding suggests that superfluid and dissipation remain uncoupled as long as the drive is on, enabling the identification of an optimal regime of pump pulse durations for which the superconducting-like response is maximum and dissipation is minimized.

I will then discuss whether these out-of-equilibrium superconducting-like states also show a dynamical diamagnetic response, beyond the documented transient optical conductivities. To this end, we have developed a novel, ultrafast optical magnetometry technique to measure changes in the magnetic field in the vicinity of a $YBa_2Cu_3O_{6.48}$ sample with $\sim 1\ \mu T$ sensitivity and sub-picosecond time resolution (Figure 1). We provide evidence that, under the same excitation conditions that generate a transient superconducting-like state in this material, a prompt expulsion of a statically applied magnetic field ensues, a response indicative of the appearance of an ultrafast Meissner effect [4].

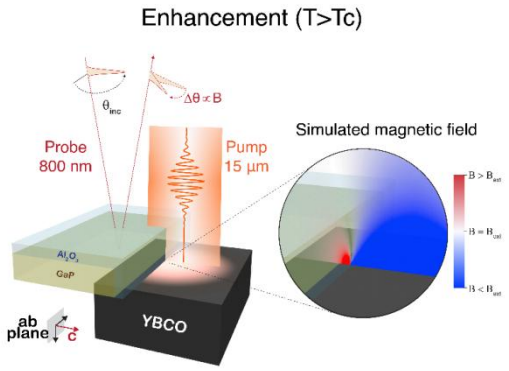

Fig. 1: *Magnetic field expulsion after phonon excitation in $YBa_2Cu_3O_{6.48}$. Schematic of the experiment. A thin Al_2O_3 crystal is placed on top and next to the exposed side of the GaP (100) detection crystal to completely reflect the 15 μm pump and prevent it from generating a spurious non-linear optical response in the GaP (100) crystal. The thin Al_2O_3 crystal also creates a well-defined edge in the mid infrared pump beam, shaping the photo-excited region into a half disc of ~ 375 μm diameter. The expected changes due to magnetic field expulsion upon photo-excitation are shown in the magnified area on the right. The time dependent magnetic field is sampled positioning the probe beam in the vicinity of the edge of the photo-excited region.*

References

[1] W. Hu, S.Kaiser, D. Nicoletti, C. R. Hunt, I. Gierz, M. C. Hoffmann, M. Le Tacon, T. Loew, B. Keimer, A. Cavalleri, Nature Materials **13**, 705 (2014).

[2] B. Liu, M. Först, M. Fechner, D. Nicoletti, J. Porras, B. Keimer, A. Cavalleri, Physical Review X **10**, 011053, (2020).

[3] A. Ribak, M. Buzzi, D. Nicoletti, R. Singla, Y. Liu, S. Nakata, B. Keimer, A. Cavalleri, Physical Review B **107**, 104508, (2023).

[4] S. Fava, G. De Vecchi, G. Jotzu, M. Buzzi, T. Gebert, Y. Liu, B. Keimer, A. Cavalleri, Nature **632**, 75 (2024).

Abstract ID: 30364

DIMENSIONALITY-DRIVEN ANTIFERROMAGNETIC DOMAIN DYNAMICS IN NICKELATE HETEROSTRUCTURES

S. Lee[1], J. Jiang[1], G. Fabbris[2], A. S. Disa[3], M. P. M. Dean[2], S. Ismail-Beigi[1], Y. Wang[4], F. J. Walker[1], C. Mazzoli[5], C. H. Ahn[1]

[1] *Yale University, Department of Applied Physics, New Haven, CT 06520, USA*
[2] *Brookhaven National Laboratory, Condensed Matter Physics and Materials Science Department, Upton, NY 11973, USA*
[3] *Cornell University, School of Engineering and Applied Physics, Ithaca, NY 14853, USA*
[4] *Emory University, Department of Chemistry, Atlanta, GA 30322, USA*
[5] *Brookhaven National Laboratory, National Synchrotron Light Source II, Upton, NY11973, USA*

In strongly correlated crystals, long-range electronic orderings can originate from simple patterns of short-range interactions. Collective excitations are induced by thermal perturbations and modified by quantum fluctuations, and for the specific case of magnetic oxides, dimensional confinement is a controllable and effective knob to modify the exchange patterns. This can deeply modify the magnetic long-range order and its dynamics. We use x-ray photon correlation spectroscopy (XPCS) to assess the dynamics of the nickelate antiferromagnetic domain boundaries in $NdNiO_3/NdAlO_3$ heterostructures. The classical and quantum fluctuations of the collective magnetic excitations can be controlled by tuning the dimensionality of the confined $NdNiO_3$ layers and $NdAlO_3$ insulating space layers, as a consequence of modifications to the intensity and anisotropy of the interfacial exchange interactions. This study demonstrates an approach to characterize dimensional effects on long-range order and the ability to control AF domain configurations in oxide heterostructures. Our results provide a pathway to engineer the phase dynamics and energetics of the spin correlation in magnetic heterostructures, which could lead to a unique design of antiferromagnetic constituents for spintronics application.

Abstract ID: 30385

MAGNETIC TEXTURES, PHASE TRANSITIONS AND DOMAIN EVOLUTION UNDER DYNAMICAL CONTROL

A. Bombardi

Diamond Light Source, STFC Rutherford Appleton Laboratory, Harwell Science and Innovation Campus, Didcot, Oxfordshire, OX11 0QX, UNITED KINGDOM

A characteristic of quantum and functional materials is the emergence of new properties and functionalities resulting from the competition between the energy contributions shaping the landscape of the system. The symmetry of the systems and the possible couplings between the external dynamical variable and the free energy control the evolution of the magnetic, electric and structural properties, with varying responses under electric field, strain, magnetic field and more.

Hard x-ray scattering experiments permits an "easy" introduction of external dynamical variables whilst accessing bulk properties, granting unique access to magnetic, electronic and structural properties through resonant scattering processes.

On the I16 beamline at Diamond, we performed several successful investigations on functional and quantum materials under the effect of magnetic field, electric field, laser induced photostriction, and strain.

In this talk, I will give a brief of what is currently possible on I16 using Bragg Coherent Diffraction Imaging, diffuse multiple scattering, resonant and non-resonant magnetic scattering and what we learned about textures subject to external perturbations in the case of battery materials [1], functional oxides [2-5], and intermetallic systems [6].

References

[1] D. Serban, D.G. Porter, A.H. Mokhtar, *et al.*, Commun Chem **7**, 243 (2024).
[2] M. A. Najeeb, R. Morrison, R., A. H. Mokhtar, *et al.*, Discover Nano **19**, 203 (2024).
[3] A. H. Mokhtar, D. Serban, D. G. Porter, *et al.*, npj Comput Mater **10**, 90 (2024).
[4] C. D. Dashwood, A. H. Walker, M. P. Kwasigroch, *et al.*, Nat Commun **14**, 6197 (2023).
[5] N. Waterfield-Price *et al.*, Phys. Rev. Applied **8**, 014033 (2017).
[6] F. Carneiro, Z. Bacso *et al.*, to be published.

Abstract ID: 30411

SPIN, ORBITAL, AND CHARGE DYNAMICS ACROSS THE STRAIN-INDUCED INSULATOR-METAL TRANSITION IN Ca_2RuO_4

B. Zager[1,2], C. Occhialini[1,3], T. Kim[1], R. Fittipaldi[4], J. Pelliciari[1], A. Vecchione[4], M. Cuocco[4], M. P. M. Dean[2], V. Bisogni[1]

[1] *National Synchrotron Light Source II, Brookhaven National Laboratory, Upton, New York 11973, USA*
[2] *Department of Condensed Matter Physics and Materials Science, Brookhaven National Laboratory, Upton, New York 11973, USA*
[3] *Department of Physics, Columbia University, New York, NY, USA*
[4] *CNR-SPIN, c/o Università di Salerno, I-84084 Fisciano, Salerno, ITALY*

Ca_2RuO_4 (CRO) is a spin-orbit entangled Mott insulator with a rich phenomenology involving the interplay of charge, spin, orbital, and lattice degrees of freedom. This includes an insulator-metal transition (IMT) with a concomitant structural distortion at T_{IMT}=357 K, orbital ordering (OO) at T_{OO}=260 K, and antiferromagnetic (AFM) ordering at T_N=110 K. This complex phase diagram is enabled by competing crystal field (CF), spin-orbit coupling (SOC), lattice distortion, hybridization, and exchange interactions, and results in many proximate ground states. Although the nominal local ground state of the Ru^{4+} ($4d^4$) is a J=0 spin-orbital singlet set by SOC and tetragonal CF, the intersite exchange stabilizes a condensate of ordered J=1 excitons below T_N. The excitonic magnetic order, spin-orbital singlet, and metallic phase, all lie in proximity and can be tuned by doping [1], strain [2,3], and electrical current [4]. Furthermore, the presence of a spin-amplitude or "Higgs" mode suggests that CRO is in the vicinity of a quantum critical point (QCP) separating the ordered condensate from a nonmagnetic spin-orbital singlet ground state [5].

Using resonant inelastic x-ray scattering (RIXS) at the O K-edge, we track the evolution of the spin, orbital, and charge excitations in CRO [6-10] across the strain-induced IMT. Using our homemade voltage-controlled piezoelectric strain device for in-situ strain control within the RIXS sample chamber, we achieved a reversible strain-induced IMT in CRO from 300 K down to 80 K. At low strain, we observe a gradual evolution of the spectrum that can be attributed to phase coexistence of metallic and insulating domains. At sufficiently high strain, we observe a sharp transition to a fully metallic state. The spectrum of the strain-induced metallic phase at all temperatures down to 80 K closely resembles that of the high temperature metallic phase, but we resolve a new mode at 25 meV. These results will guide future momentum dependent RIXS studies on CRO under strain at lower temperatures to observe signatures of quantum critical phenomena [5].

References

[1] D. Pincini, *et al.*, Phys. Rev. B **98**, 014429 (2018).
[2] S. Riccò, *et al.*, Nature Comm. **9**, 4535 (2018).
[3] H. Taniguchi, *et al.*, Phys. Rev. B **88**, 205111 (2013).
[4] F. Nakamura, *et al.*, Sci. Rep. **3**, 2536 (2013).
[5] A. Jain, *et al.*, Nature Phys. **13**, 633-637 (2017).
[6] C. G. Fatuzzo, *et al.*, Phys. Rev. B **91**, 155104 (2015).
[7] L. Das, *et al.*, Phys. Rev. X **8**, 011048 (2018).
[8] K. von Arx, *et al.*, Commun. Phys. **8:210**, 1-7 210 (2025).
[9] V. K. Bhartiya, *et al.*, arXiv:2504.17871 (2025).

Abstract ID: 30439

MAGNETO-OPTICAL KERR EFFECT IN PUMP-PROBE SETUPS

A. Eskadari-asl[1], A. Avella[1,2,3]

[1] *Dipartimento di Fisica "E.R. Caianiello", Università degli Studi di Salerno, I-84084 Fisciano (SA), ITALY*
[2] *CNR-SPIN, Unità di Salerno, I-84084 Fisciano (SA), ITALY*
[3] *CNISM, Unità di Salerno, Università degli Studi di Salerno, I-84084 Fisciano (SA), ITALY*

We develop a general theoretical framework for computing the time-resolved magneto-optical Kerr effect in ultrafast pump–probe setups, formulated within the Dynamical Projective Operatorial Approach (DPOA) [1-3] and its application to the generalized linear-response theory for pumped systems [4]. Furthermore, we exploit this formalism to express the post-pump optical conductivity — and consequently the Kerr rotation — in terms of the time-evolved single-particle density matrix (SPDM), providing a transparent and computationally efficient description of photo-excited multi-band systems. This extension, in addition to its lower computational cost, has the advantage of allowing the inclusion of phenomenological damping. We illustrate the formalism using both (i) a two-band tight-binding model, which captures the essential physics of ultrafast spin–charge dynamics and the Kerr rotation, and (ii) weakly spin-polarized germanium, as a realistic playground with a complex band structure. The results demonstrate that, by exploiting DPOA and/or its SPDM extension, one can reliably reproduce both the short-time features under the pump-pulse envelope and the long-time dynamics after excitation, offering a versatile framework for analyzing time-resolved magneto-optical Kerr effect experiments in complex materials. Moreover, this analysis clearly shows that the Kerr rotation can be used to deduce experimentally the relevant n-photon resonances for a given specific material.

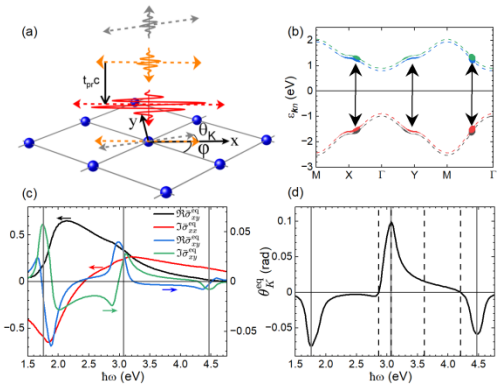

Fig. 1: *(a) The system, the pump pulse, and the time-delayed probe pulse together with its reflected component, showing the Kerr rotation. (b) Band structure of the equilibrium Hamiltonian. (c) Real and imaginary parts of the equilibrium optical conductivities. (d) Equilibrium Kerr rotation angle.*

References

[1] I. Giacomo, L. Adamska, A. Eskandari-asl, …, A. Avella, and M. Lucchini, *Field-driven attosecond charge dynamics in germanium*, Nature Photonics **17**, 1059 (2023).

[2] A. Eskandari-asl, and A. Avella, *TR-ARPES signal in pumped semiconductors within the dynamical projective operatorial approach*, Phys. Rev. B **110**, 094309 (2024).

[3] A. Eskandari-asl, J.I. Facio, O. Janson, A. Avella, and J. van den Brink, *Controlling photoexcited electron spin by light polarization in ultrafast-pumped altermagnets*, Phys. Rev. B **112**, 024401 (2025).

[4] A. Eskandari-asl, and A. Avella, *Generalized linear response theory for pumped systems and its application to transient optical properties*, Phys. Rev. A **110**, 043520 (2024).

Abstract ID: 30476

THEORETICAL AND EXPERIMENTAL STUDIES OF INTER- AND INTRA-ELEMENTARY EXCITATION CORRELATIONS

G. Sawatzky

Quantum Matter Institute University of British Columbia, Vancouver CANADA

The properties of materials are determined by the response to external stimuli which in turn is directly related the elimentary excitations of a solid and the interactions resulting In correlations between them. Many modern applications involve compounds of 3d transition metals or rare earths which are notorious for the strong electron -electron correlations and local magnetic moments resulting in multiferroic behaviour because of the strong interplay between the spin, charge, and lattice degrees of freedom. These are in turn described in terms of the elementary excitations such as electron -hole or excitons, phonons and magnons often resulting in new "quasi" particles involving strong entanglement. So, electrons become dressed with virtual electron hole (excitons), phonons, magnons, --- and combinations of these. In this talk I will discuss especially high energy probe methods to study low energy scale excitations and the (polaronic) nature of these. I include also some pump probe methods and some new ideas about what could be seen and concluded from such measurements. In this development theory of spectroscopic probes is essential to understand what the experiment is trying to tell us.

Abstract ID: 30758

ELUCIDATING MICROSCOPIC INTERACTIONS IN SKYRMION HOSTS FROM SPATIOTEMPORAL LATTICE DYNAMICS

A. M. Barbour[1], M. G. Han[2], C. Liu[1], F. Camino[3], F. Forte[4], F. Gabriele[4], J. Seidel[3], M. Cuoco[4], Y. Zhu[2], C. Mazzoli[1]

[1] *National Synchrotron Light Source II, Brookhaven National Laboratory, 11973, Upton, NY, USA*
[2] *CMPMSD, Brookhaven National Laboratory, 11973, Upton, NY, USA*
[3] *Center for Functional Nanomaterials, Brookhaven National Laboratory, 11973, Upton, NY, USA*
[4] *SPIN-CNR, IT, 84084, Fisciano (SA), ITALY*
[5] *Department of Materials Science and Engineering, The University of New South Wales, 2052, Sydney, AUSTRALIA*

Skyrmions are topological nontrivial spin states in chiral magnets that can be utilized as information carriers. Extensive investigations exist for their potential application in high-density racetrack memories, cache memory, ultra-low energy spintronic switches and skyrmion reshufflers used in probabilistic computing. However, they cannot be truly used as practical information carriers unless they are fully understood, particularly prediction of their manipulated dynamics in reduced dimensions. We report on coherent rotational control of hexagonally close-packed skyrmion lattices (SkL) in a Cu_2OSeO_3 (CSO) host lamella of ~100nm. Utilizing both Lorentz Transmission Electron Microscopy and Resonant Elastic X-ray Scattering, we demonstrate reproducible manipulation of the SkL dynamics as well as provide a phenomenological model that describes the observations by X-ray and electron probes. Such insights help to understand the balance of competing microscopic interactions.

Abstract ID: 30796

STRAIN TUNING MATERIALS AND UNRAVELLING THEIR MAGNETIC PROPERTIES USING NEUTRON DIFFRACTION

P. Manuel

ISIS Neutron and Muon Facility, UKRI-STFC Rutherford Appleton Laboratory, Chilton, OX11 0QX, UNITED KINGDOM

The ability to finely control the properties of quantum materials is a crucial aspect in the development of the next generation of sensors, memories, etc… This has traditionally been achieved via a variety of stimuli such as magnetic field, pressure or doping. Over the past decade, strain has been increasingly used to control materials' properties as it provides an additional as well as clean route (compared to, for instance, doping). Due to its well understood cross sections, Neutron diffraction is the technique of choice to determine magnetic structures of the materials. It is however a flux-limited technique and therefore does not lend itself so well to the study of very small samples which is in direct contradiction with the requirement for very thin samples to apply sufficient strain. In this talk, we will present different setups (including a commonly-used standard commercial solution) available on the high flux cold neutron diffractometer WISH and a selection of experiments from recent publications [1-5] that have been performed on this beamline at the ISIS neutron and muon facility (UK) to determine the magnetic structures of various strain tuned systems.

References

[1] X. Jin, *et al.*, Phys. Rev. Letters **135**, 136701(2025).
[2] C. Dashwood, *et al.*, Nat. Comms **14**, 6197 (2023).
[3] R. Waite, *et al.*, Phys. Rev. B **106**, 224415 (2022).
[4] D. Sun, *et al.*, Phys Rev B **100**, 094414 (2019).
[5] D. Sun, *et al.*, New J. Phys **23**, 123050 (2021).

18 - ELECTRICAL CONTROL OF MAGNETISM

Abstract ID: 30145

TUNABLE MAGNETO-IONIC STATES IN NANOSCALE DOT ARRAYS FOR SELF-PROTECTED, REPROGRAMMABLE AND LOW-POWER DEVICES

I. Spasojević[1], F. Celegato[2], A. Magni[2], A. Barrera[3], Z. Ma[1], S. Ruiz-Gómez[4], M. Foerster[4], A. Palau[3], K. S. Buchanan[5], P. Tiberto[2], J. Sort[1,6]

[1] *Departament de Física, Universitat Autònoma de Barcelona, 08193 Bellaterra, SPAIN*
[2] *Advanced Materials and Life Science Divisions, Istituto Nazionale di Ricerca Metrologica (INRIM), Strada delle Cacce 91, 10135 Turin, ITALY*
[3] *Institut de Ciència de Materials de Barcelona (ICMAB-CSIC), Campus UAB, Bellaterra 08193, Barcelona, SPAIN*
[4] *ALBA Synchrotron Light Facility, Carrer de la llum 2-26, 08290 Cerdanyola del Valles, SPAIN*
[5] *Department of Physics, Colorado State University, Fort Collins, Colorado 80523, USA*
[6] *ICREA, Pg. Lluís Companys 23, 08010 Barcelona, SPAIN*

Control of magnetism through electric-field-induced ion motion (magneto-ionics) is poised to reshape existing voltage actuation approaches aimed at bolstering energy efficiency across a diverse spectrum of spintronics and magnetically driven devices. However, despite the pressing need for strategies to control magnetic states at the nanoscale, most magneto-ionic studies to date have focused on continuous films [1-2].

Here we will demonstrate in-situ probing of ion motion in nanometer-sized dots, revealing the presence of dynamically evolving spin configurations, strongly dependent on the gating duration. More precisely, we will introduce a so far unexplored nanoscale magnetic object: an analog magnetic vortex controlled by electric-field-driven ion motion (*i.e.*, magneto-ionic vortex or, for simplicity, "vortion") [3]. This state is generated from a paramagnetic material (in our case FeCoN) via in-situ voltage application and subsequent gradual extraction of N^{3-} ions within patterned nanodots. What distinguishes vortions from conventional magnetic vortex states is that their key properties, such as amplitude of magnetization, nucleation and annihilation fields, coercivity, remanence and anisotropy, can be controlled and fine-tuned in an analog and reversible manner. Consequently, we demonstrate voltage-mediated transitions between paramagnetic (PM), single-domain (SD), and vortion states. Magneto-ionic states induced within patterned units enable transformative potential for neuromorphic devices, analog computing, multi-state data storage, and adaptive inference protocols implemented directly within magneto-ionic architectures [4]. Moreover, we find that the inherent physical nature of patterned magneto-ionic systems enables robust, self-protected hardware security primitives–crucial as Big Data growth outpaces the reliability of software-based defenses [4].These findings pave the way for a new class of hardware security solutions rooted in emergent magneto-ionic phenomena.

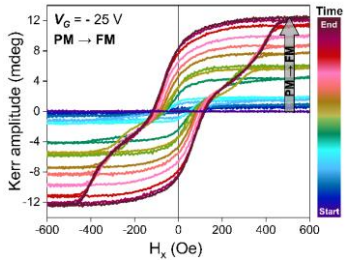

Fig. 1: *MOKE hysteresis loops showing PM↔SD↔magneto-ionic vortex transitions.*

References

[1] U. Bauer, *et al.*, Nat. Mater. **14**, 174-181 (2015).

[2] J. De Rojas, *et al.*, Nat. Commun. **11**, 5871 (2020).

[3] I. Spasojevic, *et al.*, Nat. Commun. **16**, 1990 (2025).

[4] I. Spasojevic, *et al.*, arXiv:2507.14213v1**,**

Abstract ID: 30175

SPIN-CHARGE INTERCONVERSION IN 2D VAN DER WAAL MATERIALS

C. K. Safeer

Clarendon laboratory, Department of Physics, University of Oxford, UK

Graphene has been known as an excellent material for long-distance spin transport due to its weak spin-orbit coupling (SOC). However, the same reason makes graphene an adverse candidate for different spintronics applications in which strong SOC is required, such as the spin-charge interconversion applications. It was predicted theoretically that SOC can be induced in graphene so that spin-orbit phenomena such as spin Hall effect (SHE) or Rashba-Edelstein effect can be obtained. In our work, by using van der Waals heterostructure-based lateral spin valve [1], we experimentally demonstrated the first unambiguous measurement of spin-to-charge conversion (SCC) due to SHE in graphene via spin-orbit proximity with transition metal dichalcogenides (TMD), MoS_2[2] and WSe_2 [3]. We extended similar experiments in graphene combined with an insulator, Bi_2O_3[4] and CuO_x[5]. Then we demonstrated gate tunable SHE in graphene with SCC efficiency larger than in some of the best SCC materials such as topological insulators [3]. Using a similar approach, we performed another set of experiments demonstrating large-efficiency SCC in semi metallic TMDs such as $MoTe_2$ [6-8], $NbSe_2$ [9], and TaS_2 [10]. Also, due to the low symmetry crystal structure of these materials, we detect, along with the conventional SCC, unconventional SCCs where the spin polarization, the spin current and the charge current are not mutually orthogonal to each other. In summary, all these different experiments spread light into the understanding of spin-orbit effects in van der Waal materials opening exciting opportunities in a variety of future spintronics and nanomagnetism applications.

References

[1] C.K. Safeer, F. Herling, WT. Choi, *et al.*, 2D Mater. **9**, 015024 (2021).

[2] C.K. Safeer, J. Ingla-Aynes, F. Herling, *et al.*, Nano Lett. **19**, 1074 (2019).

[3] F. Herling, C.K. Safeer, J. Ingla-Aynes, *et al.*, APL Mater. **8**, 071103 (2020).

[4] C.K. Safeer, J. Ingla-Aynes, N. Ontoso, *et al.*, Nano Lett. **20**, 4573 (2020).

[5] H. Yang, M. Ormaza, Z. Chi, *et al.*, Nano Lett. **23**, 4406 (2023).

[6] C.K. Safeer, N. Ontoso, F. Herling, *et al.*, Nano Lett. **19**, 8758 (2019).

[7] N. Ontoso, C.K. Safeer, F. Herling, *et al.*, Phys. Rev. Appl. **19**, 014053 (2023).

[8] N. Ontoso, C.K. Safeer, J. Ingla-Aynes, *et al.*, Appl. Phys. Lett. **123**, 032401 (2023).

[9] J. Ingla-Aynés, I. Groen, F. Herling, *et al.*, 2D Mater. **9**, 045001 (2022).

[10] Z. Chi, S. Lee, H. Yang, *et al.*, Adv. Mater. **36**, 2310768 (2024).

Abstract ID: 30219

UNIVERSAL HALL TORQUES

E. A. Montoya

University of Utah, Dept. of Physics and Astronomy, 84112, Salt Lake City, UT, USA

Spin–orbit torques provide a powerful means of electrically manipulating magnetization and form the basis of emerging energy-efficient information technologies. Traditionally, giant spin–orbit torques have been generated in ferromagnet/non-magnet bilayers, where broken inversion symmetry gives rise to Rashba and spin Hall torques [1,2]. Recent discoveries, however, reveal that ferromagnetic conductors themselves can generate large spin–orbit torques through their intrinsic Hall transport. The planar Hall and anomalous Hall torques form [3,4], together with the spin Hall torque, a universal triad of Hall torques expected to be present broadly in magnetic conductors. These self-generated torques exhibit distinctive symmetries and offer additional pathways for manipulating magnetic order. In this talk, I will introduce the concept of Universal Hall Torques, discuss their underlying mechanisms, and highlight their potential for enabling next-generation spintronic devices.

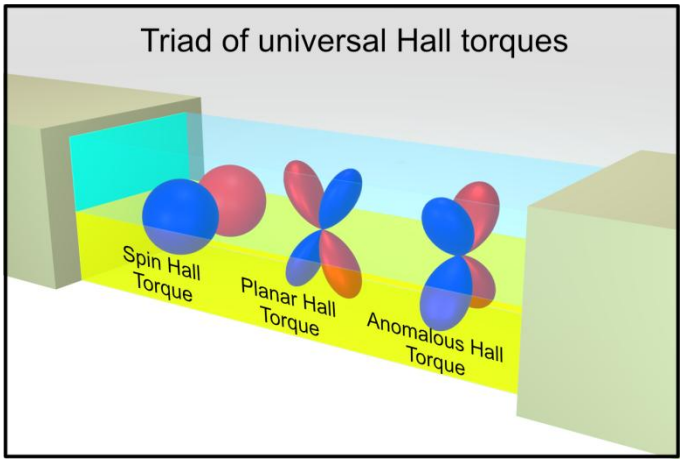

Fig. 1: *The Spin Hall Torque, Planar Hall Torque, and Anomalous Hall Torque form a triad of Universal Hall Torques.*

References

[1] I. M. Miron, *et al.*, Nature Materials **9**, 230–234 (2010).

[2] L. Liu, *et al.*, Science **336**, 555–558 (2012).

[3] C. Safranski, E. A. Montoya, and I. N. Krivorotov, Nature Nanotechnology **14**, 27–30 (2019).

[4] E. A. Montoya, X. Pei, and I. N. Krivorotov, Nature Nanotechnology **20**, 353–359 (2025).

Abstract ID: 30228

CHIRAL SPINTRONICS DEVICE

S. Miwa

The Institute for Solid State Physics (ISSP), The University of Tokyo, Chiba 277-8581, JAPAN

Chirality is recognized as an essential factor in the spintronics devices. For instance, the magnetic domain walls can be effectively controlled using a chiral structure stabilized by the Dzyaloshinskii-Moriya interaction [1]. In this study, we present our recent findings related to chiral spintronics devices.

The first half of this talk is about the chiral antiferromagnet Mn_3Sn. A non-collinear antiferromagnetic spin structure with negative spin chirality induces a ferroic ordering of cluster octupole polarization. This polarization induces a large Berry curvature due to magnetic Weyl points in momentum space. Using molecular beam epitaxy, we have developed epitaxial thin films of Mn_3Sn and achieved full switching of the octupole polarization [2]. In this talk, we demonstrate the efficient coupling of this spin rotation with a microwave current. This coupled dynamics produces a DC anomalous Hall voltage through rectification, which we call the antiferromagnetic spin-torque diode effect. Unlike in ferromagnetic systems, the output voltage shows minimal dependence on frequency due to the stabilization of the precession cone angle by exchange interactions. These results could contribute to developing high-speed microwave devices for next-generation telecommunications applications [3].

Chirality-induced spin selectivity (CISS) is a phenomenon that encompasses magnetoresistance and enantiomer separation using ferromagnets [4]. It has recently received notable attention. Despite this growing interest, the microscopic mechanisms driving CISS remain a subject of intense debate. In this talk, we build upon and expand the prevailing interpretation that attributes CISS primarily to the electric current in chiral molecules. We propose that molecular vibrations drive spin polarization in chiral molecules and play a critical role in CISS. Our results imply that magnetic interactions between chiral molecules and ferromagnets, analogous to interlayer exchange coupling, provide a physically consistent mechanism for the observed selectivity. This finding necessitates reevaluating spin dynamics and expanding its significance beyond traditional solid-state physics to fields such as chemical reactions, molecular biology, and drug discovery. [5, 6].

This is a work in collaboration with S. Sakamoto, M. Shiga, H. Kosaki, W. Gao, S. Nakatsuji, T. Higo, T. Nomoto, R. Arita, Y. Otani, M. Kobayashi of UTokyo, K. Kondou of Osaka U, D. Miyajima of CUHK-shenzhen, Y. Kotani, T. Nakamura of JASRI, T. Nozaki, Y. Hibino, S. Tamaru, H. Kubota, K. Yakushiji of AIST. This work was partially supported by JSPS-KAKENHI, JST-MIRAI Program, JST-ASPIRE, Spin-RNJ, and MEXT-XNICS.

References

[1] S.-H. Yang, *et al.*, Nat. Rev. Phys. **3**, 328 (2021).

[2] T. Higo, S. Miwa, S. Nakatsuji, *et al.*, Nature **607**, 474 (2022).

[3] S. Sakamoto, S. Miwa, *et al.*, Nat. Nanotechnol. **20**, 216 (2025).

[4] R. Naaman, *et al.*, Nat. Rev. Chem. **3**, 250 (2019).

[5] K. Kondou, S. Miwa, *et al.*, J. Am. Chem. Soc. **144**, 7302 (2022).

[6] S. Miwa, *et al.*, Sci. Adv. **11**, eadv5220 (2025).

Abstract ID: 30318

ZEEMAN SPIN TEXTURES WITHOUT MAGNETISM

B. Kilic[1], S. Alvarruiz[1], E. Barts[1], B.v. Dijk[1], P. Barone[2], J. Sławińska[1]

[1] *Zernike Institute for Advanced Materials, University of Groningen, Nijenborgh 3, 9747 AG Groningen, THE NETHERLANDS*

[2] *CNR-SPIN Institute for Superconducting and other Innovative Materials and Devices, Area della Ricerca di Tor Vergata, Via del Fosso del Cavaliere 100, I-00133 Rome, ITALY*

Spin-orbit coupling (SOC) intrinsically links a crystal's spatial symmetry with the electronic spin degree of freedom, producing a rich variety of momentum-space spin textures. The most well known examples are Rashba and Dresselhaus spin textures, which arise under the general condition of surface inversion and bulk inversion symmetry breaking, respectively. These spin textures are further restricted by the additional symmetries of the k-point, ultimately governed by a rich interplay of **unitary crystal symmetries** and **antiunitary symmetries** involving time-reversal. While the conventional Zeeman spin polarization arises from broken time-reversal symmetry due to magnetic order or external fields, *Zeeman-like (persistent) spin textures (PST)* can also emerge **without magnetism**, stabilized purely by SOC and the k-point symmetries [1,3], promising enhanced spin-lifetime via the suppression of spin relaxation mechanisms in materials with significant SOC. [2-4] Here, we generalize this concept using a representation-theory based symmetry analysis of all 230 crystallographic space groups. We show that such spin textures can arise in all nonmagnetic crystals without inversion symmetry. Our analysis identifies the locations and the orientations of PST within the Brillouin zone, which we confirm through first-principles calculations on representative materials. These results provide a unified symmetry framework for realizing Zeeman spin textures without magnetic fields, paving the way for robust and long-lived spintronic states.

References

[1] B.Kilic, *et al.*, Nature Communications **16**, 7999 (2025)
[2] B. A. Bernevig, *et al.*, PRL **97**, 236601 (2006)
[3] L. L. Tao and E. Y. Tsymbal, Nature Communications **9**, 2763 (2018)
[4] J.D. Koralek, *et al.*, Nature **458**, 610-613 (2019)
[5] T. Oguchi and T. Shishidou, J. Phys: Condens. Matter **21**, 092001 (2009).

Abstract ID: 30333

LARGE-SCALE DIRECT-WRITE NANOSCALE CONTROL OF HIGH-T_C SUPERCONDUCTIVITY AND MAGNETISM VIA PHASE NANOENGINEERING

I. Biancardi[1], V. Levati[1], M. Panzeri[1], J. Alcalà[2], D. Girardi[1], N. Pellizzi[1], M. Vitali[1], P. Florio[1], O. Boulle[3], T.Günkel[2], N. Mestres[2], D. Petti[1], A. Palau[2], E. Albisetti[1]

[1] *Department of Physics, Politecnico di Milano, ITALY*
[2] *Institut de Ciència de Materials de Barcelona, ICMAB-CSIC, SPAIN*
[3] *Université Grenoble Alpes, CNRS, CEA, SPINTEC, Grenoble, FRANCE*

Searching for new methodologies for tailoring the physical properties of materials at the nanoscale is of crucial importance both for the discovery of new phenomena, and for harnessing their potential in applications. Here, we discuss the direct control of the physical properties of condensed matter systems using highly localized heating from a nanoscopic probe and focused light [1, 2, 3, 4], for producing controlled phase changes, which in turn lead to finely tunable magnetic, electronic and optical properties. In this framework, we discuss two applications, i.e. the nanoscale grayscale tuning the magnetic anisotropy in perpendicularly magnetized exchange-biased metallic multilayers, and the control of the superconducting properties of YBCO thin films grown by pulsed laser deposition on LAO.

In this second case of YBCO, arbitrarily shaped patterns down to the nanoscale having different optical, structural and conductive properties have been obtained. First, a comprehensive investigation of patterning parameters has been carried out on full films. Arrays of μm-wide laser written lines measured via Conductive Atomic Force Microscopy, reveal an enhanced surface conductivity with respect to the pristine film, while the sample topography remains untouched. These effects are compatible with the thermally-activated migration of oxygen vacancies from the inner film towards the surface - and possibly in the atmosphere. Secondly, cryogenic transport measurements have been performed to assess the superconducting properties of different patterned structures in terms of critical temperature and current density. The modulation of such figures of merit is compatible with oxygen depletion in the bulk material. The behavior of different patterned layouts, as well as the structural characterization will be discussed at the conference. Using this phase nanoengineering approach [1], we demonstrated the feasibility of ranging across the phase diagram of YBCO in a straightforward way, through local oxygen doping. This technique allows for the modification of the physical properties of thin films and direct writing of nanopatterns without causing sizeable structural degradation. The advantages offered by this methodology include further study of the cryogenic transport mechanisms and the realization of superconducting nanostructures with tailored electronic properties or pinning landscapes.

References

[1] V. Levati, *et al.*, Adv. Mater. Technol. **8**, 2300166 (2023).
[2] E. Albisetti, *et al.*, Nat. Rev. Methods Primers **2**, 32 (2022).
[3] E. Albisetti, *et al.*, Nat. Nanotechnol. **11**, 545 (2016).
[4] V. Levati, *et al.*, Nat. Commun. **16**, 9602 (2025).

Abstract ID: 30339

LIGHT-CONTROLLED MAGNETISM IN MAGNETOSTRICTIVE THIN FILMS VIA LIQUID CRYSTALLINE NETWORKS

G. Barrera[1], D. Martella [2,3], F. Celegato[1], A. Magni[1], M. Coïsson[1], C. Parmeggiani[3,4], D. S. Wiersma[2,4], P. Tiberto[1]

[1] *Istituto Nazionale di Ricerca Metrologica (INRiM), 10135 Torino, ITALY*
[2] *European Laboratory for Non Linear Spectroscopy (LENS), 50019 Sesto Fiorentino, Firenze, ITALY*
[3] *Chemistry Dept. "Ugo Schiff", University of Florence, 50019 Sesto Fiorentino, ITALY*
[4] *Physics and Astronomy Dept., University of Florence, 50019 Sesto Fiorentino, Firenze, ITALY*

Composite magnetic materials responsive to environmental stimuli, such as light, are promising for sensing and actuation applications. This work investigates magneto-polymeric composites consisting of magnetostrictive thin films (FeGa and Ni) coupled to photo-responsive liquid crystalline networks (LCNs). This hybrid system enables reversible tuning of thin-film magnetic properties without applying an external magnetic field, relying solely on light irradiation and offering improved energy efficiency compared to conventional magnetic-field-based approaches. UV illumination (λ = 385 nm) induces anisotropic photo-actuation of the LCN, causing contraction along the x-axis and expansion along the y-axis due to dye isomerization. The resulting mechanical stress is transferred to the magnetostrictive thin film, leading to magnetic domain rearrangement governed by uniaxial stress anisotropy and the sign of the magnetostrictive coefficient (positive for FeGa and negative for Ni). Consequently, the magnetic properties depend on the duration and intensity of UV exposure. Green light irradiation (λ = 505 nm) restores the molecular order of the polymer, gradually releasing the stress and recovering the initial magnetic state. Magnetic hysteresis loops were measured with an in-plane applied field along both x- and y-directions after controlled UV and green light irradiation (Figure 1a for the FeGa/LCN sample). Light-induced strain effects on magnetic domain configurations were visualized using magneto-optic Kerr effect microscopy. Additionally, anisotropic magnetoresistance measurements under opto-mechanical control revealed a light-induced magnetic memory effect (see Figure 1b). These results demonstrate effective light-controlled magnetism enabled by opto-mechanical coupling in magnetostrictive thin-film composites.

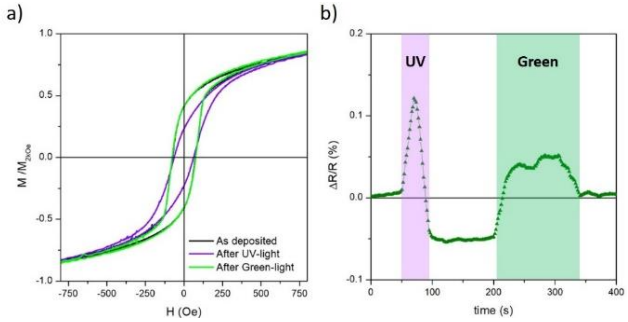

Fig. 1: *a) hysteresis loop of the FeGa/LCN sample in as-deposited state and after UV and green light irradiation time; b) evolution of the* ΔR/R *curve triggered by UV irradiation and green light.*

References

[1] G. Barrera, *et al.*, Advanced Science, **11**, 2408273 (2024).

Abstract ID: 30418

VOLTAGE-CONTROLLED MAGNETOIONIC DEVICES AS CANDIDATES FOR IN-MEMORY COMPUTING

M. Ameziane[1,2], K. Skailand[1,2], S. Nilsson[1,2], A. Hrabec[1,2], L. J. Heyderman[1,2]

[1] *PSI Center for Neutron and Muon Sciences, 5232 Villigen PSI, SWITZERLAND*
[2] *Laboratory for Mesoscopic Systems, Department of Materials, ETH, Zurich, 8093 Zurich, SWITZERLAND*

Von Neumann computing architectures form the basis of most integrated circuits used in modern computers [1]. Thanks to rapid downscaling of transistors, processing power has enormously increased over the past decades. One of the major bottlenecks of such computing architectures, however, is the physical separation of logic and memory units, which causes high losses in processing speed and energy efficiency. Magnetic systems are a natural choice for in-memory computing due to their inherent ability to simultaneously store and process information, enabling energy-efficient, non-volatile operations. A promising avenue for controlling the magnetic state in these systems is through voltage-driven ionic modulation [2]. In this talk, I will discuss magnetoionic devices as potential platforms for spintronics and in-memory computing, with an emphasis on lithium-based systems [2-5]. In particular, I will present a solid-state lithium ion-gated device (Fig. 1a), in which voltage-driven ions modulate the magnetic properties of an in-plane magnetized CoFeB thin film. A two-dimensional map of coercivity (Fig. 1b) reveals distinct, nonlinear dependencies on voltage polarity, amplitude and pulse length, highlighting coupled dynamics between ionic and magnetic processes. Such devices can serve as building blocks for in-memory computing architectures, with relevance for both spintronic implementations and unconventional computing paradigms.

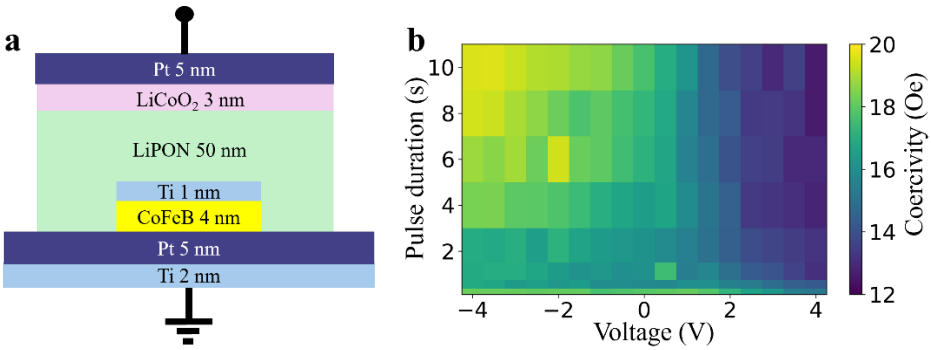

Fig. 1: ***Voltage- and time-dependent magnetic response of a Li ion-gated CoFeB device.*** *(a) Schematic of the cross-section of the magnetoionic device. (b) Two-dimensional map of the magnetic coercivity as a function of applied gate voltage and pulse duration.*

References

[1] D. Kimovski, *et al.*, IEEE Internet Comput **28**, 6-16 (2023).
[2] P. Monalisha, *et al.*, Small Sci. **4**, 2400133 (2024).
[3] M. Ameziane, *et al.*, Adv. Funct. Mater. **32**, 29, 2113118 (2022).
[4] M. Ameziane, *et al.*, Nano Lett. **23**, 8, 3167–3173 (2023).
[5] M. Ameziane, *et al.*, Appl. Phys. Lett. **122**, 232401 (2023).

Abstract ID: 30421

3D NANOSCALE CONTROL OF MAGNETISM IN CRYSTALLINE YTTRIUM IRON GARNET VIA DIRECT LASER WRITING

M. Vitali[1], P. Florio[1], V. Levati[1], A. D. Giacco[1], N. Pellizzi[1], R. Silvani[2], L. C. Mavilla[2], M. Madami[2], S. Genoni[1], I. Biancardi[1], D. Girardi[1], M. Panzeri[1], M. Cocconcelli[1], D. Breitbach[3], P. Pirro[3], L. Rovatti[4], N. Lecis[4], F. Maspero[1], R. Bertacco[1], G. Corrielli[5], R. Osellame[5], V. Russo6, A. L. Bassi[6], S. Tacchi[7], D. Petti[1], E. Albisetti[1]

[1] *Department of Physics, Politecnico di Milano, Milano, ITALY*
[2] *Department of Physics and Geology, Università di Perugia, Perugia, ITALY*
[3] *RPTU University Kaiserslautern-Landau, 67663 Kaiserslautern, GERMANY*
[4] *Department of Mechanical Engineering - Politecnico di Milano, Milano, ITALY*
[5] *Istituto di Fotonica e Nanotecnologie (IFN-CNR), Milano, ITALY*
[6] *Department of Energy - Politecnico di Milano, Milano, ITALY*
[7] *Istituto Officina dei Materiali (CNR-IOM) c/o Department of Physics and Geology, Università di Perugia, Perugia, ITALY*

Ferrimagnetic insulating garnets such as crystalline Yttrium Iron Garnet (YIG, $Y_3Fe_5O_{12}$) are key for spintronics to photonics and phononics, due to their exceptional magnetic, magneto-optical and mechanical properties. Many applications require nanoscale, ideally three-dimensional and grayscale, control of YIG magnetic properties; however, high-quality nanopatterning remains challenging because conventional 2D nanofabrication often degrades the crystalline and functional quality of YIG. Here, we present a large-scale, single-step, maskless nanopatterning approach based on the irradiation with a focused UV laser, following a phase nanoengineering approach [1]. The irradiation induces a stable, giant enhancement of the perpendicular magnetic anisotropy (PMA), while preserving the structural quality of the single crystal YIG [2,3]. In 1 mm-thick films [2], the spatial localization of the anisotropy modulation can be tuned down to the nanoscale and in the third dimension, with a spatial resolution of 100 nm laterally and in depth. In the irradiated areas, above a power threshold, we observe a new magnetic phase in which the magnetic stripe domains reduce their periodicity respect to the pristine material, thanks to the enhanced PMA. In 100 nm-thick films [3], the laser enhanced PMA stabilizes fully out-of-plane magnetization in the nanoscale patterns. In addition, tuning the patterning parameters, amorphous non-magnetic areas can be obtained, which can be recrystallized recovering an out-of-plane magnetic configuration. Exploiting various anisotropy profiles we demonstrate tuning of spin waves (SW) bandstructure and localization, ultimately realizing proof-of-concept magnonic devices, such as magnonic crystals [2], waveguides and filters [3]. Our approach enables non-destructive, rewritable, high-throughput, and continuous greyscale phase nanoengineering of magnetic garnet films under ambient conditions. This capability opens path towards three-dimensional metamaterials and devices based on crystalline magnetic garnets.

References

[1] V. Levati, *et al.*, Adv. Mater. Technol. **8 (16)**, 2300166 (2023).
[2] V. Levati, M. Vitali, *et al.*, Nat. Commun. **16 (1)**, 9602 (2025).
[3] P. Florio, M. Vitali, *et al.*, in preparation.

Abstract ID: 30457

SPIN HALL MAGNETORESISTANCE AND SPIN SEEBECK EFFECT IN NONCOLLIENAR MAGNETIC INSULATORS

A. Aqeel

University of Augsburg, 86135Augsburg, GERMANY

Complex patterns often emerge when simple building blocks interact, and magnetic systems without inversion symmetry are a striking example of this principle. In Cu-based non-collinear oxides, competing interactions give rise to twisted spin textures such as helices, spirals, and skyrmions, whose collective excitations span a broad frequency range [1] and offer new opportunities for spin-based technologies.

In this talk, I will discuss recent progress in understanding spin transport in the chiral magnet Cu_2OSeO_3 and related Cu-based non-collinear oxides using spin Hall magnetoresistance and the spin Seebeck effect [2,3]. These two complementary electrical probes provide access to both interfacial spin transmission and thermally driven magnon currents in insulating magnets. By measuring their temperature and magnetic-field dependence in Pt/Cu-oxide heterostructures, we identify distinct magnetic twists—such as helical, conical, and spiral textures—and demonstrate that spin-current–based transport offers an all-electrical means to detect and distinguish non-collinear magnetic states in magnetic insulators.

References

[1] O. Lee, ...A. Aqeel, *et al.*, Nature Materials **23 (1)**, 79-87 (2024).
[2] A. Aqeel, *et al.*, Science and Technology of Advanced Materials **26 (1)**, 2457320 (2025).
[3] A. Aqeel, *et al.*, Physical Review B **103(10)**, L100410 (2021).

Abstract ID: 30507

MAGNETO-IONIC CONTROL OF ANTIFERROMAGNET-FERROMAGNET SYSTEMS

E. Niapos[1], M. Staňo[1], J. A. Arregi[1], M. Otýpka[2], V. Uhlíř[1,2]

[1] *CEITEC BUT, Brno University of Technology, 612 00, Brno, CZECH REPUBLIC*
[2] *Institute of Physical Engineering, Brno University of Technology, 61669, Brno, CZECH REPUBLIC*

Magneto-ionics, voltage-driven migration of ions, promises low power tuning of magnetic properties. It typically deals with changes in magnetization, coercivity, and anisotropy of ferromagnets [1] and most recently also includes (synthetic) antiferromagnets [2,3]. Here, we focus on material systems combining antiferromagnetic (AF) and ferromagnetic (FM) phases, either in the form of bilayers featuring exchange bias or a single material with an AF to FM phase transition, giving access to emerging interactions at the coexistence of these two phases.

The first material system consists of Co/CoOx with HfOx as oxygen reservoir and Pt electrodes. Voltage-induced oxidation and reduction processes induce reversible changes in the proportion of Co to CoOx. This alters coupling between FM (Co) and AF (CoOx at low temperatures) phases when field-cooled in a cryostat and induces different exchange bias (manifested as magnetic hysteresis loop horizontal offset) [4]. After initial studies with a liquid electrolyte, we adopted purely solid-state geometry. HfOx was prepared in two steps to combine good ionic conductivity and electrical insulation from the top electrode. Solid HfOx electrolyte is more versatile and practical for device miniaturization and CMOS compatibility. Here, the active layer is lithographically-patterned into a micro-cross and the top Pt electrode is permanently attached to the device. This configuration enables in-situ tuning and electrical read-out in one setup.

The second material platform, FeRh, features a first-order phase transition from AF to FM phase around 370 K in bulk. The transition temperature can be tuned by strain, patterning, chemical composition, doping, and by magneto-ionics [5, 6]. Here, devices are patterned from epitaxial FeRh films grown on MgO (001), and the magneto-ionic gate is implemented via HfOx solid electrolyte. All-electric readout using longitudinal resistance or Planar Hall effect is possible due to a large difference in resistivity of the FM and AF phases. For 15-nm-thick FeRh layers we demonstrated non-volatile temperature shift of several K comparable to or better than liquid gating for thicker layers [5]. Better performance is expected for thinner layers [6]. We target this with sub-10-nm-thick continuous FeRh films with phase transition above 300 K.

References

[1] J. de Rojas, *et al.*, Appl. Phys. Lett. **120**, 070501 (2022).
[2] Y. Luo, *et al.*, Crystals **15**, 77 (2025).
[3] Z. Ma, *et al.*, Adv. Mater. **37**, 2415393 (2025).
[4] E. Niapos, *et al.*, In preparation (2026).
[5] M. Jiang, *et al.*, Appl. Phys. Lett. **108**, 202404 (2016).
[6] G. Li, *et al.*, Magnetochemistry **7(4)**, 45 (2019).

Abstract ID: 30552

VOLTAGE-DRIVEN CONTROL OF EXCHANGE BIAS FIELD IN Pt/Co/CoO THIN FILMS VIA MAGNETO-IONIC EFFECTS

A. Klimeczek[1], M. De-Santis[1], F. Gay[1], L. Ranno[1], J. Vogel[1], A. Masseboeuf[2], A. Lamirand[3], S. Pizzini[1]

[1] *Université Grenoble Alpes, CNRS, Institut Néel, 38042 Grenoble, FRANCE*
[2] *Université Grenoble Alpes, CNRS, CEA, SPINTEC, 38054 Grenoble, FRANCE*
[3] *Université Lyon, École Centrale de Lyon, CNRS, INSA Lyon, Université Claude Bernard Lyon, 69130 Écully, FRANCE*

Pt/Co/MO_x thin film heterostructures (where MO_x is a metal oxide, such as AlO_x, MgO, or, in the present work, CoO) with an ultrathin ferromagnetic (FM) Co layer are a model spintronics system. They exhibit strong perpendicular magnetic anisotropy (PMA) and interfacial chiral interactions, such as the Dzyaloshinskii-Moriya interaction (DMI), making them a versatile platform for studying interfacial magnetic phenomena. The PMA in these systems is predominantly interfacial in origin and arises from contributions at both the Pt/Co and Co/oxide (in this work, CoO) interfaces; the latter being dependent on the hybridization of cobalt and oxygen electronic orbitals is observed to bestrongly dependent on the oxidation of the top Co/oxide interface [1-3].

Oxygen magneto-ionics is an electrochemical approach to modify, reversibly, and in a non-volatile manner, the degree of oxidation of a FM/oxide interface. By a controlled movement of O^{2-} ions into, or outside, the magnetic a reduction ($V_g > 0$) or an oxidation ($V_g < 0$) will be observed. This enables direct voltage control of the PMA through a controlled modification of the number of Co – O bonds at the Co/CoO interface. Simultaneously, any changes in the interfacial oxidation of the Co/CoO layers can influence the interface spin structure and exchange coupling, providing a path for voltage-driven engineering of exchange bias (EB).

In this work, we demonstrate a non-volatile and reversible voltage control of magnetic anisotropy and the exchange bias field in Pt/Co/CoO heterostructures using oxygen magneto-ionics. By an electrical manipulation of the interfacial oxidation state, the exchange coupling between the FM Co and AFM CoO can be finely tuned, and recovered by reversing the polarity of the gate voltage. This approach highlights oxygen magneto-ionics as an effective strategy to control electrically exchange bias in FM/AFM systems.

References

[1] P. Bruno, J. Appl. Phys. **64**, 3153 (1988).
[2] N. Nakajima *et al.*, Phys. Rev. Lett. **81**, 5229 (1998).
[3] A. Manchon *et al.*, J. Appl. Phys. **104**, 043914 (2008).
[4] A. Klimeczek *et al.*, Appl. Phys. Lett. **127**, 012408 (2025).

Abstract ID: 30281

SPIN – FLOP TRANSITION AND MAGNETOGALVANIC EFFECT IN TETRAGONAL ANTIFERROMAGNETS: CuMnAs, Mn_2Au

Z. V. Gareeva[1,2], A. K. Zvezdin[3]

[1] *Institute of Molecule and Crystal Physics, Subdivision of the Ufa Federal Research Centre of the Russian Academy of Sciences, 450075, Ufa, RUSSIA*
[2] *National Research University of Electronic Technology - MIET, 124498, Moscow, RUSSIA*
[3] *Prokhorov General Physics Institute of the Russian Academy of Sciences, 119991, Moscow, RUSSIA*

In recent years, antiferromagnets have attracted considerable attention due to their promising potential for spintronic applications. Among conducting antiferromagnets, CuMnAs and Mn_2Au stand out for their high Néel temperatures (~480 *K* and ~1351 *K*, respectively), excellent conductivity, and demonstrated capability for current-induced switching of antiferromagnetic order [1, 2]. The influence of electric currents on spins is most commonly explained through the concept of Néel spin-orbit torques (NSOT), as developed in Ref. [3] and applied to the analysis of magnetization dynamics in these materials [2].

In this report, we consider a mechanism based on symmetry considerations, which enables general exploration of spin dynamics in antiferromagnets. By employing rigorous group - theoretical analysis, we derive invariant combinations of magnetic and electric order parameters and demonstrate that the magnetoelectric effect is intrinsic to tetragonal antiferromagnets such as CuMnAs and Mn_2Au [4]

$$\Phi_{me} = g_1 L_z \left(M_x P_y + M_y P_x\right) + g_2 M_z \left(L_x P_y + L_y P_x\right) + g_3 P_z \left(L_y M_x + L_x M_y\right) \qquad (1)$$

where $\boldsymbol{L}=\boldsymbol{M}_1-\boldsymbol{M}_2$ is antiferromagnetic vector, $\boldsymbol{M}_1$, $\boldsymbol{M}_2$ are the Mn^{3+} ions sublattice magnetizations, $\boldsymbol{P}$ is the magnetically induced electric polarization.

The presence of the magnetoelectric invariant (1) naturally leads to electrically induced torques, including NSOT, which are crucial for understanding various aspects of current-driven spin dynamics.

Another key phenomenon we investigate is the magnetogalvanic effect, which arises in tetragonal antiferromagnets during spin – flop transition under the application of an alternating magnetic field $\boldsymbol{H}(t)$. We explore the generation of electric currents during spin- flop transition induced by an external magnetic fields. By examining the electric response to alternating magnetic fields, we identify key features, including current stabilization and harmonic responses. Through this analysis, we aim to deepen the understanding of the intricate interplay between symmetry, magnetization dynamics, and electric current generation in antiferromagnetic materials, paving the way for future advancements in spintronic technologies.

References

[1] P. Wadley, *et al.*, Science **351**, 587 (2016).

[2] S. Reimers, *et al.*, Phys. Rev. Appl. **21**, 064030(2024).

[3] J. Železný, *et al.*, Phys. Rev. Lett. **113**, 157201 (2014).

[4] A.K. Zvezdin, Z.V. Gareeva, Physics of Solid State **66**, 814 (2024).

Abstract ID: 30447

EFFICIENT SPIN-CHARGE CONVERSION AT ROOM TEMPERATURE WITH FERROELECTRICS: ENABLING FESO

S. Chiroli[1], R. Tomar[1], T. Buttiens[1,2], A. S. Goossens[1], E. Vazquez[3], M. Martemucci[3], Y. B. Fazlioglu[4], A. Raj[5], P. Sgarro[3], V. Giannone[3], S. Mallik[1,6], E. Gradauskaite[1], L. M. Vicente-Arche[1], W. Savero-Torres[7], T. Maroutian[2], A. Barthélémy[1], J. Varignon[8], A. Gloter[5], L. Iglesias[1], I. Boventer[1], J.-P. Attané[7], A. Charvier[7], L. Vila[7], R. Engel-Herbert[4,9], M. Bibes[12]

[1] *Laboratoire Albert Fert, Thales, Université Paris-Saclay, 1 avenue Augustin Fresnel, 91767 Palaiseau, FRANCE*
[2] *Centre de Nanosciences et de Nanotechnologies, CNRS, Université Paris-Saclay, Palaiseau, FRANCE*
[3] *Spintec, CEA, CNRS, Université Grenoble Alpes, 17 Avenue des Martyrs, 38054 Grenoble, FRANCE*
[4] *Pennsylvania State University, University Park, PA 16802, USA*
[5] *Laboratoire de Physique des Solides, Université Paris-Saclay, Orsay, FRANCE*
[6] *Saha Institute of Nuclear Physics, Bidhannagar, Kolkata 700064, INDIA*
[7] *NELLOW, 32 Avenue Alsace-Lorraine, 38000 Grenoble, FRANCE*
[8] *CRISMAT, CNRS UMR 6508, ENSICAEN, Normandie Université, 14050 Caen, FRANCE*
[9] *Paul Drude Institute for Solid State Electronics, Hausvogteiplatz 5–7, 10117 Berlin, GERMANY*

Reducing the energy footprint of information processing requires bringing memory closer to – or ideally into – logic, while suppressing standby power through nonvolatile operation. Ferroelectrics offer this combination, as they couple switchable polarization with nonvolatile functionality and sub-volt operation. Ferroelectric spin-orbit (FESO) devices harness the ferroelectric control of spin-orbit coupling and spin-charge conversion which we previously demonstrated albeit only at low temperature and with bulk $SrTiO_3$ crystals. In this presentation we will provide evidence for spin-charge conversion at room temperature in 2-dimensional electron gases formed within epitaxial ferroelectric $BaTiO_3$ thin films displaying Curie temperatures beyond 300°C, switching voltages in the 100 mV range and endurance beyond 1011 cycles. When interfaced with a ferromagnetic layer, these 2DEGs yield room-temperature spin-charge conversion efficiencies comparable to the best SrTiO3-based systems, corresponding to ~100 mV FESO output voltages and providing matching input/output operation conditions required for device cascading. Circuit-level simulations confirm the potential of FESO devices to surpass CMOS technologies in both energy efficiency and logic density, establishing ferroelectric spin-orbit coupling as a promising route to scalable ultralow-power computing.

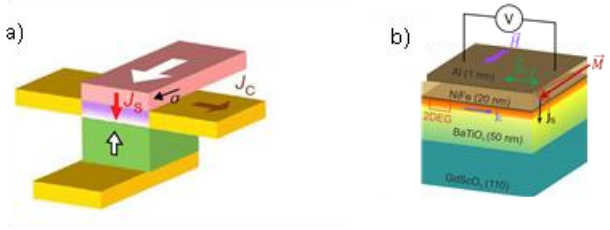

Fig. 1: *a) Scheme of the FESO architecture. b) Schematic representation of the full stack measured experimentally for spin charge conversion.*

References

[1] D. Vaz, *et al.*, *Mapping spin–charge conversion to the band structure in a topological oxide two-dimensional electron gas*, Nature Materials, **18(11)**, 1187-1193.2 (2019).

[2] E. Lesne, Y. Fu, S. Oyarzún, J. C. Rojas-Sánchez, D. C. Vaz, H. Naganuma, ... L. Vila, *Highly efficient and tunable spin-to-charge conversion through Rashba coupling at oxide interfaces*, Nature Materials, **15(12)**, 1261-1266 (2016).

Abstract ID: 30458

EXCHANGE BIAS AT ROOM TEMPERATURE IN ANTIFERROMAGNET NiCoO SINGLE LAYER BY MAGNETO-IONICS

S. Privitera[1,2], Z. Ma[1], H. Gómez-Torres[1,2], A. Arredondo-López[1], M. O. Liedke[3], E. Hirschmann[3], A. Wagner[3], H. Tan[1], A. Quintana[1], T. Dias[4], D. Gouéré[5], E. Monteblanco[5], D. Ravelosona[5,6], A. Lopeandia[1,2], J. Sort[1,7], E. Menéndez[1]

[1] *Department de Física, Universitat Autònoma de Barcelona, 08193 Cerdanyola del Vallès, SPAIN*
[2] *Catalan Institute of Nanoscience and Nanotechnology (ICN2), CSIC and BIST, Campus UAB, 08193 Cerdanyola del Vallès, SPAIN*
[3] *Institute of Radiation Physics, Helmholtz-Zentrum Dresden – Rossendorf, Dresden 01328, GERMANY*
[4] *Universidade Tecnológica Federal do Paraná, Campus Dois Vizinhos, Estrada para Boa Esperança, km 04, 85660-000, Dois Vizinhos PR, BRAZIL*
[5] *Spin-Ion Technologies, 10 Boulevard Thomas Gobert, Palaiseau 91120, FRANCE*
[6] *Centre de Nanosciences et de Nanotechnologies, CNRS, Université Paris-Saclay, 10 Boulevard Thomas Gobert, Palaiseau 91120, FRANCE*
[7] *Institució Catalana de Recerca i Estudis Avançats (ICREA), Pg. Lluís Companys 23, 08010 Barcelona, SPAIN*

Magneto-ionics –as the voltage-driven control of magnetic properties through ionic motion and redox processes– offers a promising route toward energy-efficient spintronic devices. Exchange bias, as the unidirectional anisotropy arising from interfacial coupling between antiferromagnets and ferromagnets, plays a central role in spintronics. Here, we demonstrate reversible, room-temperature magneto-ionic generation, suppression, and modulation of exchange bias in a 50 nm-thick antiferromagnetic NiCoO single-layer. Instead of relying on field cooling to set exchange bias, an applied magnetic field during the growth promotes alignment of the antiferromagnetic spin sublattices, producing a preferential unidirectional orientation. Gating drives oxygen-ion migration along columnar grain boundaries, partially reducing NiCoO and forming ferromagnetic NiCo clusters that couple to the antiferromagnetic matrix. The exchange bias can be controlled by tuning the Ni:Co ratio, which adjusts the Néel temperature, and by varying the actuation time, which controls ferromagnetic cluster size. Micromagnetic simulations reveal that the exchange bias originates from the interfacial uncompensated spins exhibiting partial ferromagnetic-like behavior. This single-layer approach, together with the voltage-controlled formation and tuning of exchange bias without heat treatments, simplifies fabrication and opens a path toward low-power antiferromagnetic spintronic devices.

References

[1] S. Privitera, Z. Ma, H. Gómez-Torres, A. Arredondo-López, M.O. Liedke, E. Hirschmann, A. Wagner, H. Tan, P. Solsona, A. Quintana, T. Dias, D. Gouéré, E. Monteblanco, D. Ravelosona, A. Lopeandia, J. Sort, and E. Menéndez, *Room-temperature programmable exchange bias in a single antiferromagnet by magneto-ionics*, ACS Nano (2026, in peer review).

Abstract ID: 30474

LIGHT-CONTROLLED OF MAGNETISM IN MULTIFERROIC HETEROSTRUCTURES

H. Tan[1,2], Z. Ma[1], C. B. Karroum[3], M. Liparo[3], J.-P. Jay[3], D. Spenato[3], D. T. Dekadjevi[3], L. M. Armesto[1,2], A. Quintana[1,2], J. Sort[1,2,4]

[1] *Departament de Física, Universitat Autònoma de Barcelona, E-08193 Cerdanyola del Vallès, SPAIN*
[2] *Catalan Institute of Nanoscience and Nanotechnology (ICN2), CSIC and BIST, Campus UAB, Bellaterra, 08193 Barcelona, SPAIN*
[3] *Univ. Brest, Laboratoire d'Optique et de Magnétisme (OPTIMAG), UR 938, 29200 Brest, FRANCE*
[4] *Institució Catalana de Recerca i Estudis Avançats (ICREA), Pg. Lluís Companys 23, E-08010 Barcelona, SPAIN*

Spintronic and magnetoelectric systems continue to face intrinsic trade-offs among switching speed, energy consumption, and large-scale integration. Recently studies have shown that optical excitations of antiferromagnetic (AFM)/ferromagnetic (FM) bilayers can modulate exchange bias. While interesting fast magnetization dynamics have already been observed [1], so far, in most cases laser illumination has triggered thermal effects, which is detrimental in terms of energy efficiency. A promising alternative is strain-mediated control via the photovoltaic effect in ferroelectric (FE) substrates, which enables low-power, non-thermal modulation. Additionally, exploring the integration of ferroelectric coupling, optical control, and multi-state functionality has the potential to overcome current performance bottlenecks while enabling new device paradigms for neuromorphic computing, reconfigurable logic architectures, and ultra-low-power wireless data storage.

Here, we present the first demonstration of significant optical control of exchange bias at room temperature in a FE/FM/AFM heterostructure via visible-light-induced photostriction [2]. This effect arises from abnormal strain generated via the photostrictive response of the ferroelectric substrate, which induces compressive stress along both in-plane ferroelectric polarization directions. This strain is transferred to FM layer interfaced with AFM layer, leading to a modulation of magnetic anisotropy and interfacial exchange bias coupling. Unlike conventional electric-field-driven or strain-mediated magnetoelectric coupling, this approach enables non-thermal, reversible, multilevel tuning of magnetic interactions, with programmable states achieved solely by adjusting light intensity as low as 0.1 W cm^{-2}, offering a new pathway toward energy-efficient, wireless opto-magnetic and neuromorphic devices.

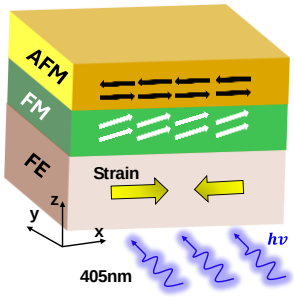

Fig. 1: *Sketch of multiferroic heterostructure under visible illumination.*

References

[1] F. J. F. van Riel, *et al.*, *Understanding field-free single-shot laser-induced reversal of exchange bias*, Communications Materials **6**, 110 (2025).
[2] H. Tan, *et al.*, *Light-modulated exchange bias in multiferroic heterostructures*, Electron (2026), submitted.

Abstract ID: 30486

MAGNETIC-FIELD-FREE MAGNETO-IONICS IN CoFeN for NEUROMORPHIC FUNCTIONALITY

L. M. Armesto[1], H. Tan[1,2], Z. Ma[1], I. Spasojevic[1,2], E. Pellicer[1], J. Sort[1,2,3]

[1] *Autonomous University of Barcelona, Dept. of Physics, 08193, Cerdanyola, SPAIN*
[2] *Catalan Institute of Nanoscience and Nanotechnology, 08193, Cerdanyola, SPAIN*
[3] *Institució Catalana de Recerca i Estudis Avançats, 08010, Barcelona, SPAIN*

Magneto-ionic materials enable non-volatile voltage control of magnetism via ion migration and are promising candidates for neuromorphic computing [1,2]. Compared to conventional memristive devices, magneto-ionic systems offer dual electric and magnetic actuation while operating at low power due to their voltage-driven nature. However, most implementations still require external magnetic fields to establish each magnetic state, limiting their energy efficiency.

Here, we present a CoFeN-based magneto-ionic system in which electric and magnetic field actuation are fully decoupled. By exploiting planar N^{3-} ion migration [3] and ferromagnetic exchange coupling between pre-existing and newly formed CoFe regions, we achieve voltage-only control of remanent magnetization. The device exhibits neuromorphic-inspired functionalities, including synaptic potentiation and depression [4], as well as a cumulative increase in magnetization driven solely by voltage in the absence of any magnetic field [5]. After removal of the magnetic field, the synaptic weight remains determined by the combined electric and magnetic history of the system. Eliminating the need for magnetic-field assistance enables a drastic reduction in energy consumption, highlighting a viable route toward energy-efficient, brain-inspired magneto-ionic devices.

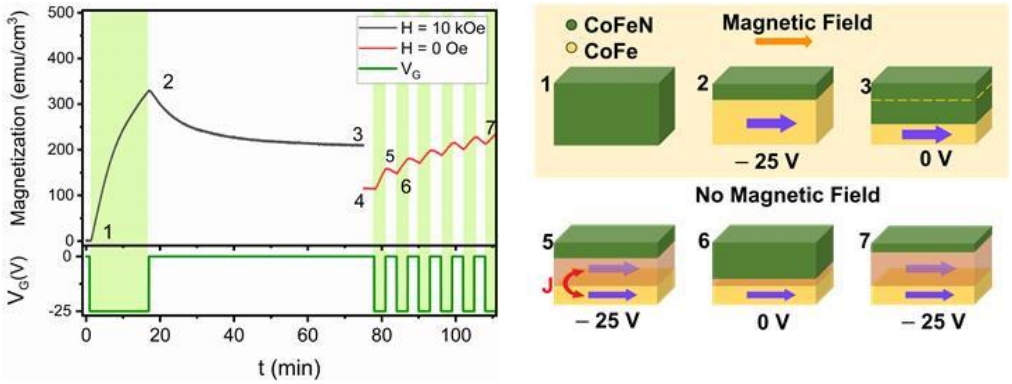

Fig. 1: *Left: Magnetization and Gate Voltage vs time under magnetic field (black curve) and without magnetic field (red curve). Right: schematics of the device at each state.*

References

[1] M. Nichterwitz, *et al.*,APL Mater., **vol. 9**, **no. 3**, p. 030903 (2021).
[2] P. Monalisha, *et al.*, Small Sci., p. 2400133, (2024).
[3] J. De Rojas, *et al.*, Nat. Commun., **vol. 11**, **no. 1**, p. 5871(2020).
[4] D. Marković, A. Mizrahi, D. Querlioz, and J. Grollier, Nat. Rev. Phys., **vol. 2**, **no. 9**, pp. 499–510 (2020).
[5] L. Martínez Armesto, ACS Appl. Mater. Interfaces (2026) in press.

Abstract ID: 30602

HIGH HARMONICS CARRIER PUMPING FROM ALTERMAGNETS

O. Ly

Nouakchott University, Physics Department, Nouakchott, MAURITANIA

We present a theoretical investigation of high-harmonic carrier pumping in altermagnetic systems. A realistic model is introduced to capture nonlinear transport dynamics arising from the time evolution of the electronic band structure. We show that the nonrelativistic spin–momentum locking intrinsic to altermagnets is sufficient to generate a large number of harmonics, extending beyond the hundredth order, without relying on relativistic spin–orbit coupling, in sharp contrast to previously proposed mechanisms [1, 2]. Numerical simulations further reveal that the nonlinear carrier dynamics is accompanied by a strongly non-monotonic dependence of the dc transport responses on the driving frequency. These results establish altermagnets as a promising materials platform for nonlinear spintronics.

References

[1] O. Ly and A. Manchon, Phys. Rev. B **105**, L180415 (2022).
[2] O. Ly, J. Phys.: Condens. Matter, **37**, 465802 (2025).

Abstract ID: 30663

INVESTIGATION OF THE EFFECTS OF SOLVENT TYPE AND Al/Cu DOPING ON THE CRYSTAL STRUCTURE AND ELECTRICAL PROPERTIES OF ZnO-BASED THERMISTORS SYNTHESIZED BY SOL-GEL METHOD

T. Seydioğlu

Kastamonu University, Vocational School, Department of Electronics and Automation, Kastamonu, TÜRKIYE

This study investigated the effects of solvent type and Al/Cu doping on the crystal structure and electrical properties of ZnO-based NTC (Negative Temperature Coefficient) thermistors synthesized using the sol-gel method. In the first stage, undoped ZnO samples were synthesized using methanol, ethanol, and 2-propanol as solvents via the sol-gel method. In the second stage, Al and Cu dopants were added to the ZnO structure in specific ratios. First, the Al ratio was gradually changed while keeping the Cu ratio constant, and then the Cu ratio was changed while keeping the Al ratio constant. Thus, the effects of the dopant elements on the ZnO crystal structure were evaluated comparatively. The crystal structure of the samples was analyzed using X-ray diffraction (XRD). The results showed that the hexagonal wurtzite ZnO phase was preserved in all samples and no secondary phase was formed at the studied doping ratios. With increasing Al doping, slight shifts in the 2θ positions and changes in peak widths were observed in the characteristic ZnO peaks. This situation was attributed to the lattice stress resulting from the incorporation of Al^{+3} ions into the lattice in place of Zn^{+2} ions. In Cu-doped samples, variations in peak intensities and peak widths were observed depending on the doping ratio, but it was determined that the crystal phase integrity was preserved. Structural findings were supported by electrical measurements. Resistance–temperature (R–T) measurements showed that the electrical resistance decreased with increasing temperature in all samples, exhibiting typical NTC thermistor behavior. While a significant decrease in room temperature resistance was observed in Al-doped samples depending on increasing donor density, in Cu-doped samples, although the temperature sensitivity and β doping ratio varied, the variation was observed within a more limited range. These results indicate that the dopant elements affect grain boundary potential barriers and carrier transport mechanisms in different ways. In conclusion, these thermistors synthesized by the sol-gel method are potential candidates for thermistor applications due to their controllable NTC behavior and adjustable electrical parameters.

Abstract ID: 30129

SOLID-STATE LITHIUM-ION BATTERY AND SUPERCAPACITOR STRUCTURES FOR VOLTAGE CONTROL OF MAGNETISM

S. van Dijken

Department of Applied Physics, Aalto University School of Science, Espoo, FINLAND

The ionic control of magnetism enables exceptionally high magnetoelectric coupling efficiencies at low applied voltages [1-3], offering a promising pathway toward energy-efficient magnetic memory and neuromorphic computing technologies. However, existing magneto-ionic platforms often face critical limitations, including slow ionic kinetics, limited cyclability, reliance on liquid electrolytes, and strong sensitivity to ambient conditions.

In this talk, I will present a solid-state approach to voltage-controlled magnetism based on the reversible cycling of Li^+ ions in LiPON-based thin-film batteries and supercapacitors. This architecture overcomes many of the shortcomings of conventional magneto-ionic systems while enabling a versatile range of functionalities. I will demonstrate four key effects:

1. Reversible switching of magnetic anisotropy between in-plane and perpendicular states in ultrathin Co films [4];
2. Voltage-driven nucleation and annihilation of magnetic skyrmions in engineered multilayer stacks [5,6];
3. Li-ion-induced tuning of the Ruderman–Kittel–Kasuya–Yosida (RKKY) exchange interaction in perpendicular Co/Pt heterostructures [7];
4. Dynamic voltage control of propagating spin waves in CoFeB magnonic waveguides.

These results collectively show that Li-ion-based heterostructures enable unusually high magnetoelectric coupling efficiencies, ultrafast (≈60 μs) and fully reversible voltage control at room temperature, and excellent endurance exceeding 750000 operational cycles. Finally, I will discuss how such magneto-ionic platforms can emulate biological synaptic behavior and serve as powerful building blocks for reservoir computing.

Acknowledgements

This work was supported by the European Union's Horizon 2020 research and innovation program under the Marie Skłodowska-Curie Grant Agreement No. 860060 "Magnetism and the effects of Electric Field" (MagnEFi) and was supported by the Research Council of Finland (Grant Nos. 316857 and 359125).

References

[1] M. Nichterwitz, S. Honnali, M. Kutuzau, *et al.*, APL Mater. **9**, 030903 (2021).

[2] Y. Gu, C. Song, Q. Wang, *et al.*, APL Mater. **9**, 040904 (2021).

[3] J. de Rojas, A. Quintana, G. Rius, *et al.*, Appl. Phys. Lett. **120**, 070501 (2022).

[4] M. Ameziane, R. Mansell, V. Havu, P. Rinke, S. van Dijken, Adv. Funct. Mater. **32**, 2113118 (2022).

[5] M. Ameziane, J. Huhtasalo, L. Flajšman, R. Mansell, S. van Dijken, Nano. Lett. **23**, 3167 (2023).

[6] S. Das, R. Mansell, L. Flajšman, M-A. Syskaki, J. Langer, S. van Dijken, Phys. Rev. Appl. **23**, 054043 (2025).

[7] M. Ameziane, R. Rosenkamp, L. Flajšman, S. van Dijken, R. Mansell, Appl. Phys. Lett. **122**, 232401 (2023).

Abstract ID: 30193

MERGING VOLTAGE-IONTRONICS WITH MAGNETISM FOR ADVANCED MEMORY APPLICATIONS

J. Sort[1,2,3], N. López-Pintó[1], I. Spasojević[1], Z. Ma[1], Z. Tan[1], M. Peda[1], A. Quintana[1], E. Pellicer[1], J. Nogués[2,3], E. Menéndez[1]

[1] *Departament de Física, Universitat Autònoma de Barcelona, 08193 Bellaterra, SPAIN*
[2] *ICREA, Pg. Lluís Companys 23, 08010 Barcelona, SPAIN*
[3] *Catalan Institute of Nanoscience and Nanotechnology (ICN2), 08193 Barcelona, SPAIN*

In the same way spintronics revolutionized electronics by introducing spin as a new degree of freedom for device functionality, merging iontronics with magnetism promises a new paradigm for computing technologies. Voltage-driven ion motion coupled to magnetic order (i.e., magneto-ionics) enables energy-efficient, analog, and highly reconfigurable device operation, opening pathways toward neuromorphic architectures and in-memory computing. Many features of neuromorphic materials (non-linearity, multi-level memory, threshold voltage, energy efficiency and actuation in ms or faster) can be achieved via magneto-ionics.

While most reported magneto-ionic systems exploit oxygen, hydrogen, or lithium ion migration, our recent work has established nitrogen magneto-ionics as a powerful complementary approach [1–5]. Voltage-driven nitrogen ion transport can be induced in transition-metal nitride films (e.g., CoN, FeN, CoMnN, FeCoN) at room temperature using either liquid or solid electrolyte gating. A distinguishing feature of nitrogen magneto-ionics is the emergence of a uniform, plane-wave-like N^{3-} migration front, in contrast to clustering or filamentary behavior often observed in oxygen-based systems. This spatially homogeneous transport is particularly advantageous for multilayer memory architectures. Strategies to accelerate magneto-ionic switching and improve device cyclability will be presented.

Voltage-driven nitrogen transport enables modulation of a broad range of neuromorphic behaviors, including potentiation, depression, spike-timing and spike-rate-dependent plasticity, amplitude-dependent plasticity, and multilevel memory states. Cumulative effects arising from pulsed voltage actuation (typically 1–100 Hz) allow emulation of higher-order learning rules, such as learning by maturity or learning under deep sleep. Remarkably, in certain configurations, these responses can be triggered even without direct electrical contacts on the sample, through bipolar electrochemistry (wireless magneto-ionics). At the nanoscale, magneto-ionics gives rise to additional physical phenomena. Patterned arrays of FeCoN sub-micron disks exhibit reversible and voltage-controlled transitions between paramagnetic, coherent-rotation, and vortex states. These behaviors stem from precise control of the planar nitrogen migration front and the locally generated FeCo magnetic layer. In certain conditions, magneto-ionic vortices can act as probabilistic bits offering prospects for probabilistic computing and device authentication. Overall, magneto-ionic systems position as strong candidates for brain-inspired hardware, where dense networks of interconnected synaptic elements hold potential for scalable in-memory computing and secure analog data storage.

References

[1] J. de Rojas, *et al.*, Nat. Commun., **11**, 5871 (2020).

[2] Z. Tan, *et al.*, Mater. Horiz., **10**, 88 (2023).

[3] Z. Ma, *et al.*, Nat. Commun., **14**, 6486 (2023).

[4] N. López-Pintó, *et al.*, Adv. Funct. Mater. 2404487 (2024).

[5] I. Spasojevic, *et al.*, Nat. Commun. **16**, 1990 (2024).

19 - EMERGENT PHENOMENA AND TOPOLOGY IN MAGNET-SUPERCONDUCTOR HYBRIDS

Abstract ID: 30283

RARE-EARTH MAGNETISM AND YU–SHIBA–RUSINOV STATES IN SUPERCONDUCTING Nb-BASED NANOSTRUCTURES

A. Odobesko

Julius Maximilian University of Würzburg, 97074 Würzburg, GERMANY

Rare-earth atoms on superconducting surfaces offer access to a regime where strong localized magnetism, indirect exchange interactions, and superconducting correlations coexist at the atomic scale. Using rare-earth adatoms and atomically assembled chains on Nb(110), Yu–Shiba–Rusinov states induced by 4f-shell magnetic moments are systematically investigated. In contrast to 3d transition-metal impurities, the coupling between 4f moments and the superconducting condensate is mediated by spin-polarized valence states, leading to qualitatively different subgap spectra and magnetic interaction mechanisms. Spectroscopic measurements reveal pronounced orientation-dependent behavior in extended chains, including the appearance of zero-energy end states for specific geometries. Ab initio calculations and spin-dynamics simulations demonstrate that homochiral spin-spiral configurations can be stabilized in rare-earth chains, enabling topological superconductivity without relying on strong spin–orbit coupling. These findings highlight rare-earth–based nanostructures as a promising platform for exploring correlated and topological superconducting states.

Abstract ID: 30353

UNCONVENTIONAL SUPERCURRENT PHASE IN ISING SUPERCONDUCTOR JOSEPHSON JUNCTION WITH ATOMICALLY THIN MAGNETIC INSULATOR

F. Pientka

Institut für Theoretische Physik, Goethe-Universität, Frankfurt am Main, GERMANY

In this talk, I discuss unconventional supercurrents in a van der Waals Josephson junction composed of two $NbSe_2$ superconducting crystals separated by an atomically thin magnetic insulator, $Cr_2Ge_2Te_6$. The interplay between strong spin–orbit coupling in the superconductor and nonuniform magnetization in the insulating barrier gives rise to a rich and unconventional current–phase relationship. The junction hosts a doubly degenerate ground state characterized by a nontrivial Josephson phase, originating from momentum-conserving tunneling of Ising Cooper pairs across magnetic domains in the barrier. This ground-state degeneracy effectively realizes a two-level quantum system, suggesting magnetic-insulator Josephson junctions as a promising new dissipationless building block for superconducting quantum devices.

References

[1] H. Idzuchi, F. Pientka, K. F. Huang, K. Harada, Ö. Gül, Y. J. Shin, L.T. Nguyen, N. H. Jo, D. Shindo, R. J. Cava, P. C. Canfield, P. Kim, Nature Communications **12 (1)**, 5332 (2021).

Abstract ID: 30386

USING QUANTUM CORRALS TO NON-LOCALLY DETECT MAGNET-SUPERCONDUCTOR HYBRID STATES

J. Wiebe[1,2]

[1] *Universität Hamburg, Inst. of Nanostructure and Solid State Physics, Hamburg, GERMANY*
[2] *The Hamburg Centre for Ultrafast Imaging, Luruper Chaussee 149, 22761 Hamburg, GERMANY*

Excitations of spins on surfaces usually can be detected with the STM tip only very locally up to a few Å distance from the spin-carrying atom. When placing this magnetic atom inside a quantum corral, a cage made of many atoms that laterally confines a surface state (see figure 1), the excitation is projected into the eigenmodes of the quantum corral. Thereby, it can still be detected at tens of nanometers distance from the magnetic atom. Here, I will review our work on the long-range detection of excitations in magnet superconductor hybrids [1] using quantum corrals. I will first describe the proximity effects into the surface states [2] and quantum corrals [3] on thin metallic films grown on a superconducting substrate mediated by Andreev reflections. Then, I will describe how a Yu-Shiba-Rusinov state [1] induced by a magnetic atom on such a thin film can be projected into the quantum corral eigenmodes and measured at far distances [4]. Finally, I will show our most recent work on spins in quantum corrals which confine proximitized, strongly Rashba spin-orbit coupled surface states residing in bismuth-based surface alloys [5].

This work was supported by the project WI 3097/4-1 (project No. 543483081) of the Deutsche Forschungsgemeinschaft (DFG) and by the Cluster of Excellence 'Advanced Imaging of Matter' (EXC 2056 – project ID 390715994) of the DFG.

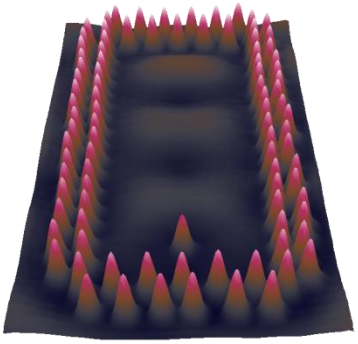

Fig. 1: *The spin of a single magnetic atom is coupled to a quantum corral eigenmode.*

References

[1] R. Lo Conte, J. Wiebe, S. Rachel, D. Morr, and R. Wiesendanger, Riv. Nuovo Cim. (2025).
[2] L. Schneider, C. von Bredow, H. Kim, K. T. Ton, T. Hänke, J. Wiebe, and Roland Wiesendanger, Phys. Rev. B **110**, L100505 (2024).
[3] L. Schneider, K. That Ton, I. Ioannidis, J. Neuhaus-Steinmetz, T. Posske, R. Wiesendan-ger, and J. Wiebe, Nature **621**, 60 (2023).
[4] K. That Ton, C. Xu, I. Ioannidis, L. Schneider, T. Posske, R. Wiesendanger, D. K. Morr, and J. Wiebe, Nat. Phys. (2025). https://doi.org/10.1038/s41567-025-03109-y
[5] H. Jang, D. Crawford, K. T. Ton, L. Schneider, J. Wiebe, M. Shimizu, H. O Jeschke, S. Rachel, and R. Wiesendanger, arXiv:2506.17414 [cond-mat.supr-con] (2025).

Abstract ID: 30399

MAGNETIC AND SPIN-PUMPING PROPERTIES OF MgB_2-BASED AND NbN-BASED MULTILAYERS

L. Peridon, T. Courtois, K. Dumesnil, S. Mangin, T. Hauet

Institut Jean Lamour, Université de Lorraine-CNRS, Nancy, FRANCE

The interplay of magnetism and superconductivity has been heavily studied the past 30 years and recently led to the concept of superconducting spintronic. Proximity effects, Cooper pairs-magnons interactions or injection of polarized quasiparticles at superconductor/ferromagnet (S/F) interfaces have been essentially investigated in niobium or aluminium-based heterostructures with critical temperatures (Tc) of the order of few Kelvin, and in the DC regime. S/F stacks with a higher Tc and carefully tuned interfaces would enable the thorough exploration of new superconducting spintronic features, and would ease the implementation in operating quantum devices. GHz and THz experiments can allow to extend the current knowledge to phenomena occurring at short-time scale. We will present the growth of epitaxial MgB_2-based and NbN-based stacks. Tc reaches 30 K for MgB_2 films as thin as 15 nm and 15 K for NbN films as thin as 10 nm. The original paramagnetic properties of such thin films will first be presented [1] and extended to a broader range of superconducting materials. Then the dependence in temperature of the Gilbert damping of S/F bilayers extracted from FMR measurements will be described as a probe of the spin-transport from F into S. As expected from previous works [1,2], the channel of momentum loss in the S layer is partially suppressed by opening of the superconducting gap below Tc [4]. Here, the role of the interfacial proximity effect on the spin pumping will be especially investigated on the basis of similar FMR measurements performed on NbN/X/F stacks where X is either a Pt or Cu interlayer with thickness from 0 to 50 nm thickness. No signature of spin-triplet Cooper pairs is observed in these two systems when the external magnetic field is applied in-plane. For $T > Tc$, the increase of both Cu and Pt thickness leads to a monotonic increase of the damping due to the spin-pumping enhancement. Interestingly, for $T<Tc$, the damping drop amplitude mostly monotonically decreases with increasing the copper thickness whereas it peaks around 3 nm for Pt thickness. This counter-intuitive result will be linked to the spin-flip length of the interlayer in the normal phase and its superconductive coherence length in its proximitized state. Altogether, these findings shed new light on the parameters governing the magnetic hysteresis loop of thin superconductive films and the spin pumping at superconductor/ferromagnet interface.

References

[1] C. Pfaff, *et al.*, Phys. Rev. B **110**, 094502 (2024).
[2] C. Bell, *et al.*, Phys. Rev. Lett. **100**, 047002 (2008).
[3] M. Müller, *et al.*, Phys. Rev. Lett. **126**, 087201 (2021).
[4] C. Pfaff, *et al.*, Appl. Phys. Lett. **125**, 102601 (2024).

Abstract ID: 30497

INTERFACE-DRIVEN TRIPLET PROXIMITY EFFECTS AND ELECTRONIC TRANSPORT IN SPIN-ORBIT COUPLED SUPERCONDUCTOR/FERROMAGNET HYBRIDS

N. Banerjee

Department of Physics, Blackett Laboratory, Imperial College London, London SW7 2AZ, UNITED KINGDOM

Superconductor/ferromagnet (S/F) hybrids, especially with spin-orbit coupling, provide an excellent platform to study several interesting phenomena ranging from spin triplet to topological superconductivity and the diode effect. These discoveries provide a platform for a wide range of applications in quantum technologies, some of which we have just started to explore [1].

In this talk, I will discuss recent theoretical and experimental progress in S/F structures which incorporate spin-orbit coupling in the context of spin triplet superconductivity. I will highlight our recent work where interface modification leads to a large triplet proximity effect [2] and some results on transport properties of these hybrid structures.

References

[1] M. Amundsen, *et al., Spin-orbit effects in superconducting hybrid structures*, Reviews of Modern Physics **96**, 021003 (2024).

[2] A. T. Bregazzi, *et al.*, *Enhanced controllable triplet proximity effect in superconducting spin–orbit coupled spin valves with modified superconductor/ferromagnet interfaces*, *Appl. Phys. Lett.* **124**, 162602 (2024).

Abstract ID: 30728

CRITICAL SLOWING-DOWN IN LASER-INDUCED PICOSECOND SUPERCONDUCTING PHASE TRANSITION

G. N. Antonio[1], T. Courtois[2], C. Pfaff[2], K. M. S. Shukla[1], A. Sudbø[3], S. Mangin[2], T. Hauet[2], C. Ciccarelli[1, 3]

[1] Cavendish Laboratory, University of Cambridge, Cambridge, UNITED KINGDOM
[2] Institut Jean Lamour, Université de Lorraine, Nancy, FRANCE
[3] Center for Quantum Spintronics, Department of Physics, Norwegian University of Science and Technology, Trondheim, NORWAY

The investigation of the ultrafast response of photo-excited superconductors has provided valuable insight into their low-lying electronic structure and the mechanisms behind Cooper pair formation and breaking. However, up to now, most studies have been confined to the weak-perturbation regime. Here, we advance this line of research by exploring how the condensate evolves after an intense, non-adiabatic perturbation capable of transiently closing the superconducting gap. In particular, via optical pump- THz probe (OPTP) spectroscopy, we study the photo-induced melting of superconductivity in NbN and report a non-equilibrium counterpart to the phenomenon of critical slowing-down in the condensate dynamics.

In this work, we demonstrate that OPTP spectroscopy is an ideally suited technique to characterize superconductivity dynamics driven by extreme perturbations thanks to its resonant sensitivity to the energy gap. This experimental technique allows us to chart the timescale of the superconductivity suppression over a wide range of temperatures and excitation fluences. Our results reveal an elongation of the melting dynamics when the absorbed laser energy is close to the threshold to eradicate the superconducting phase. Supported by time-dependent Ginzburg-Landau simulations, we interpret this as a non-equilibrium analog of critical slowing-down when NbN is dynamically forced into the phase transition boundary.

Previously, critical slowing-down in superconductors close to equilibrium had been indirectly observed, for instance, through its effects on the AC conductivity or magnetic fluctuations. Our work constitutes a novel, direct detection of slowed down superconductivity dynamics arising from pushing the system towards a critical point. Our findings motivate the search of further signatures of universality in strongly out-of-equilibrium systems and pave the way for investigating criticality in real time in other quantum materials.

Abstract ID: 30195

TOPOLOGY AND ENERGY DEPENDENCE OF MAJORANA BOUND STATES IN A CAVITY

A. Kobialka [1], A. K. Ghosh[1], R. Arouca[1,2], A. M. Black-Schaffer[1]

[1] Department of Physics and Astronomy, Uppsala University, Box 516, S-751 20 Uppsala, SWEDEN
[2] Centro Brasileiro de Pesquisas Fisicas, Rua Doutor Xavier Sigaud 150, Rio de Janeiro, 22290-180, BRAZIL

Light-matter interaction plays a crucial role in modifying the properties of quantum materials. Inthis work, we investigate the effect of cavity photon fields on a topological superconductor hosting Majorana bound states (MBS). We model the system using a Peierls substitution of the photonic operator in the kinetic and spin-orbit terms, and utilize an exact diagonalization of a finite number of photon Hamiltonian to investigate the coupled system. The MBS appear at finite energy, in contrast to a usual 1D topological superconductor as the photon energy within the cavity shifts the MBS energy by $\hbar\omega/2$. Interestingly, our results show that the MBS persists even in the presence of a cavity field, but exhibits a pseudo-dispersion as a function of the light-matter coupling strength.

To topologically characterize these finite-energy MBS, we employ the spectral localizer to obtain a space- and energy-resolved topological invariant. We further discuss the limitations of this topological invariant in the case of low photon frequency, where the hybridization between different photon sectors distorts the phase diagram. Our work provides a framework for exploring cavity-modified topological superconductivity and the control of MBS through light–matter coupling.

Abstract ID: 30628

INTERPLAY OF SUPERCONDUCTIVITY, FERROMAGNETISM AND HALF-METALLICITY IN GATED SINGLE-LAYER g-C3N4

P. N. Brangi, F. Martini, P. Cudazzo, M. Calandra

Department of Physics, University of Trento, Via Sommarive 14, 38123 Povo, ITALY

Graphitic carbon nitride (g-C3N4) [1] hosts lone pairs arising from broken carbon-nitrogen bonds in its heptazine structure. These strongly localized and weakly hybridized states form ultraflat bands potentially leading to correlated states when doped. Using first-principles calculations, we show that field-effect hole-doping in single-layer g-C3N4 depletes these lone pairs, unveiling a rich phase diagram (Fig.1) with a complex interplay of superconducting, half-metallic and insulating ferromagnetic phases, even at very low charging and in the absence of transition metal ions. We show that this is a more viable way to obtain a 2D half-metal than some proposed alternatives, such as atomic substitution of a Nitrogen with a Carbon atom (in g-C4N3) as suggested in the pioneering work of Ref. [2], given the difficulty of synthesis of g-C4N3 and the lack of tunability of the magnetization. Our work highlights gated two-dimensional systems hosting lone pairs as a novel platform for strongly correlated states and proposes g-C3N4 as a candidate for transition-metal-free devices.

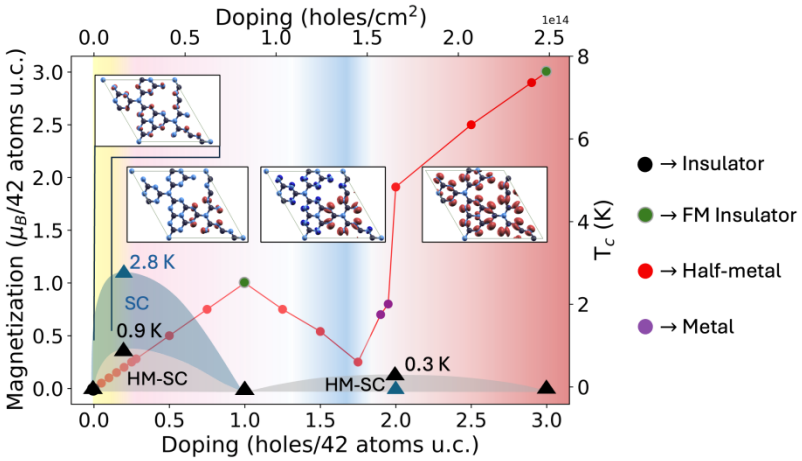

Fig. 1: *Phase diagram of hole doped g-C3N4. We report the magnetization of the 42 atoms u.c. as a function of doping. The color of the dots labels the electronic state of the layer. The background colors correspond to the different character of the magnetization density* $m(r) = \varrho\uparrow(r) - \varrho\downarrow(r)$ *. Black (blue) triangles label the calculated superconducting Tc , in the ferromagnetic half-metallic (non-magnetic) state.*

References

[1] D. Guoping, *et al.*, Journal of Photochemistry and Photobiology C: Photochemistry Reviews **20**, 33-50 (2014).

[2] D. Aijun, S. Sanvito and S. C. Smith. Physical Review Letters **108.19**, 197207 (2012).

20 - EMERGING PHENOMENA AND APPLICATIONS IN MOLECULAR AND METAL-ORGANIC MAGNETIC MATERIALS

Abstract ID: 30039

ENGINEERING TRITYL RADICAL-SURFACE HYBRIDS FOR MOLECULAR SPINTRONIC AND OPTOELECTRONIC APPLICATIONS

J. A. de Sousa[1,4], D. Schäfter[2], S. Settele[3], L. Tesi[2], M. Mas-Torrent[1], J. Veciana[1], J. Zaumseil[3], J. van Slageren[2], S. Cambré[4], N. Crivillers[1]

[1] *Institute of Materials Science of Barcleona (ICMAB-CSIC), Campus UAB, 08193 Bellaterra, SPAIN*
[2] *Institute of Physical Chemistry, University of Stuttgart and Center for Integrated Quantum Science and Technology (IQST), Pfaffenwaldring 55, 70569 Stuttgart, GERMANY*
[3] *Institute for Physical Chemistry, Universität Heidelberg, 69120 Heidelberg, GERMANY*
[4] *Theory and Spectroscopy of Molecules and Materials, Physics Department, University of Antwerp, 2610 Antwerp, BELGIUM*

Polychlorinated triphenylmethyl (PTM) radicals represent a unique class of persistent organic radicals combining paramagnetic, redox, fluorescent, and chiral properties [1]. Their high synthetic versatility enables the preparation of tailored mono- and diradical systems with extraordinarily long spin coherence times, an essential requirement for the implementation of molecular quantum bits (MQBs) and two-qubit gates [2,3]. However, realizing viable molecular quantum devices demands more than long coherence, it requires the reliable integration of these radicals into solid-state architectures.

In this talk, I will present our recent advances in the design and immobilization of PTM radicals on gold and carbon-based substrates. Special emphasis will be given to PTM radicals bearing terminal alkynes, which combine long coherence times with efficient covalent attachment to gold surfaces, offering a promising route toward functional molecular spintronic and quantum devices. I will also discuss the first example of single-walled carbon nanotubes (SWCNTs) covalently modified with PTM radicals via diazonium chemistry. Photoluminescence studies revealed partial quenching of the sp^3-defects emission, attributed to radical-enhanced intersystem crossing leading to triplet-state population, which was recently confirmed by Optically Detected Magnetic Resonance (ODMR) [4].

References

[1] I. Ratera, J. Vidal-Gancedo, D. Maspoch, S. T. Bromley, N. Crivillers, M. Mas-Torrent, J. Mater. Chem. C, **9**, 10610 (2021).
[2] P. Mayorga-Burrezo, F. Bejarano, J. Calbo, X. Zhao, J. A. de Sousa, V. Lloveras, M. R. Bryce, E. Ortí, J. Veciana, C. Rovira, N. Crivillers, J. Phys. Chem. Lett. **12**, 6159 (2021).
[3] D. Schäfter, J. Wischnat, L. Tesi, J. A. Sousa, E. Little, J. McGuire, M. Mas-Torrent, C. Rovira, J. Veciana, F. Tuna, N. Crivillers, J. van Slageren, Adv. Mater. **35**, 2302114 (2023).
[4] J. A. de Sousa, S. Settele, T. Biktagirov, J. Djafari, U. Gerstmann, E. Goovaerts, J. Zaumseil, N. Crivillers, S. Cambré, ACS Nano, **19**, 36384 (2025).

Abstract ID: 30040

TAILORING MULTIFUNCTIONALITY IN MULTIMETALLIC CARBORANE METAL-ORGANIC FRAMEWORKS VIA CONTROLLED METAL COMPOSITION AND SEQUENCING

E. Bartolomé[1], X. Liu[1], X.-B. Li[1], A. Arauzo[2], J. Luzón[2], E. Ruiz[3], S. Gómez-Coca[3], J. G. Planas[1]

[1] *Institut de Ciència de Materials de Barcelona (ICMAB-CSIC), 08193, Barcelona, SPAIN*
[2] *University of Zaragoza, Instituto de Nanociencia y Materiales de Aragón (INMA-CSIC), 50009, Zaragoza, SPAIN*
[4] *Laboratory of Molecular Design, Facultat de Química, Universitat de Barcelona, 08029 Barcelona, SPAIN*

Multimetallic metal–organic frameworks (MOFs) provide a powerful platform to design multifunctional materials with tailored functionalities, and probe how metal composition and sequencing shape emergent magneto-optical, electronic, and quantum phenomena. In this talk, I will highlight our recent advances in multimetallic MOFs built from lanthanide (Ln) or transition-metal (TM) nodes and carborane linkers, endowed with unique hydrophobic, steric, and electronic properties.

We have achieved the unprecedented synthesis of multivariate carborane MOFs incorporating tunable combinations of multiple lanthanides in controlled ratios, opening new directions in the study of complex magnetic materials and in engineering of materials with targeted multifunctionality. This strategy enabled the creation of the first MOF containing eight rare-earth ions [1]; multifunctional {GdLn} (Ln = Tb, Eu, Tb/Eu) MOFs combining magnetocaloric, single-molecule magnet (SMM) and luminescent properties [2, 3]; {Nd/Yb} MOFs with SMM behavior and NIR-emission; and a {Gd_3} quMOF encoding a record 512-level qudit for quantum computing [4].

Carborane linkers have also recently enabled the construction of MOFs embedding well-isolated one-dimensional (1D) antiferromagnetic chains of Co, Ni [5], and alternating Ni/Co ions. Remarkably, modulation of the Co/Ni sequencing along these chains produces distinct magnetic and semiconducting behaviors. These findings pave the way for the rational design of functionally tunable multimetallic frameworks for advanced magnetic, optical and quantum applications.

References

[1] E. Bartolomé, J. G. Planas, *et al.,* Adv. Func. Mat., **vol. 33**, p. 1 (2023).

[2] J. G. Planas, E. Bartolomé, *et al.*, J. Mater. Chem. A, **vol., 12**, p. 21971 (2024).

[3] J. G. Planas, E. Bartolomé, *et al.,* **Dalton Trans., vol., 53**, p. 8969 (2024).

[4] E. Bartolomé, J. G. Planas, *et al.,* ACS Appl. Mater. Interfaces, **29**, 42082 (2025).

[5] E. Bartolomé, J. G. Planas, *et al.*, J. Mater. Chem. C, **13,** 8020 (2025).

Abstract ID: 30069

2D MAGNETIC MATERIALS FROM SILANE-BRIDGED DICARBOXYLATES: MULTIFUNCTIONALITY AND DIMENSIONALITY EFFECTS

Ana Arauzo[1], Mirela-Fernanda Zaltariov[2], Cristina Piquer[1], Elena Bartolomé[3], Sara Fuertes[4], Ionut-Radu Tigoianu[2], Sergiu Shova[2], Maria Cazacu[2]

[1] *Instituto de Nanociencia y Materiales de Aragón (INMA), Departamento de Física de la Materia Condensada, CSIC-Universidad de Zaragoza, 50009, Zaragoza, SPAIN*
[2] *Department of Inorganic Polymers, Petru Poni Institute of Macromolecular Chemistry, 700487, Iasi, ROMANIA*
[3] *Institut de Ciència de Materials de Barcelona (ICMAB-CSIC), 08193 Bellaterra, SPAIN*
[4] *Departamento de Química Inorgánica, Facultad de Ciencias, Instituto de Síntesis Química y Catálisis Homogénea (ISQCH), CSIC – Universidad de Zaragoza, 50009, Zaragoza, SPAIN*

Two-dimensional coordination polymers (2D CPs), which assemble into network-like, sheet-type architectures with relatively weak interlayer interactions, offer a versatile metal–organic counterpart to well-known inorganic 2D materials. Due to surface, interface, and edge effects such complexes can exhibit fascinating properties induced by chemical structure and potentiated by the atomic scale lattice effect. In particular, lanthanide-based 2D CPs serve as an excellent platform for engineering multifunctional materials with tailored functionalities, with emergent magneto-optical, electronic, magneto-caloric and quantum phenomena [1,2].

In this talk, I will report on the synthesis, structural, optical, magnetic and magnetocaloric properties of novel Ln(III) complexes (Ln = Sm, Eu ,Gd, and Dy) built from silicon-centered polycarboxylic ligands. These ligands direct the formation of lanthanide-based coordination polymers (Ln-CPs) with varied network topologies and dimensionalities [3]. The formation of 2D supramolecular networks affords their exfoliation without significant decrease of the functionalities demonstrating the potential of these compounds for integration into two-dimensional and surface-based applications. Our results provide insights into the role of ligand design and dimensionality effects on their physical properties. These results open new possibilities for designing advanced 2D magnetic molecular materials with multifunctional properties relevant to photonics, sensing, and quantum technologies.

References

[1] E. Bartolomé, *et al.*, J. Mater. Chem. C, **13**, 21015-21026 (2025).

[2] E. Bartolomé, E.C. Sañudo, *et al.*, J. Mater. Chem. A, **12**, 6269 (2024).

[3] A. Arauzo, *et al.*, J. Mater. Chem. C, **13**, 18508 (2025).

Abstract ID: 30242

PHOTORESPONSIVE DYSPROSIUM-ANTHRACENE COMPLEXES: EFFECTS OF TEMPERATURE AND IRRADIATION TIME ON THE REVERSIBLE PHOTOCYCLOADDITION REACTION OF ANTHRACENE

L.-M. Zheng

State Key Laboratory of Coordination Chemistry, School of Chemistry and Chemical Engineering, Nanjing University, Nanjing 210023, CHINA

Stimuli-responsive multifunctional molecular materials have potential applications in high-density information storage, information conversion, and molecular devices. By leveraging the rich optical properties of anthracene derivatives and their reversible [4+4] cycloaddition reactions under UV irradiation, we have constructed a series of lanthanide-anthracene complexes, and successfully achieving the synergistic modulation of their single-molecule magnet and luminescent properties. We further investigated the relationship between the stacking mode of anthracene rings and the de-dimerization temperature of in-situ formed dianthracene, identifying key factors influencing the de-dimerization temperature. In addition, we conducted an in-depth study on the impact of temperature and irradiation time on the photocycloaddition reaction of anthracene rings, enabling a rapid and reversible response in optical and magnetic properties based on these findings.

References

[1] X.-D. Huang, X.-F. Ma, L.-M. Zheng, Angew. Chem. Int. Ed., **62**, e202300088 (2023).

[2] L. Wu, X.-D. Huang, W. Li, X. Cao, W.-H. Fang, L.-M. Zheng, M. Dolg, X. Chen, JACS Au, **4**, 3606–3618 (2024).

[3] X.-F. Ma, X. Hou, Y.-H. Qin, Q. Teng, S.-S. Bao, Y. Tian, L.-M. Zheng, Chem. Sci., **16**, 10340-10348 (2025).

[4] Y.-H. Qin, X.-F. Ma, X. Hou, X.-D. Huang, S.-S. Bao, Y. Tian, Y.-Q. Zhang, L.-M. Zheng, Chem. Sci., **16**, 19806-19819 (2025).

Abstract ID: 30248

ELEMENT SELECTIVE PROBE FOR MOLECULAR MAGNETISM: XMCD OF 5D PARAMAGNETIC COMPLEXES

A. A. Rogalev[1], K.S. Pedersen[2], F. Wilhelm[1], R. Clérac[3]

[1] *ESRF-The European Synchrotron, CS 40220, F-38043 Grenoble Cedex 9, FRANCE*
[2] *Department of Chemistry, Technical University of Denmark, DK-2800 Kongens Lyngby, DENMARK*
[3] *Université de Bordeaux, CNRS, Centre de Recherche Paul Pascal, UMR 5031, F-33600 Pessac, FRANCE*

Paramagnetic molecular complexes incorporating 5d transition metals provide new possibilities for molecular magnetism, not paralleled by other elements. These heavy elements offer great advantages, including pronounced magnetic anisotropy driven by strong spin–orbit coupling and the highly diffuse nature of their 5d orbitals which promotes strong covalent hybridization with ligands. The metal-ligand covalency plays a pivotal role in strengthening exchange interactions between metal centers, an essential prerequisite for achieving magnetic ordering at or near room temperature.

The fundamental importance of metal-ligand covalency in magnetic properties of molecular systems was recognized as early as 1953, when Owen and Thornley first demonstrated spin transfer from an Ir(IV) ion to chloride ligands using electron paramagnetic resonance spectroscopy on $(NH_4)_2IrCl_6$ [1]. This pioneering study catalyzed decades of research into the interplay between covalency and magnetism using a large variety of experimental techniques, such as EPR, NMR, and polarized neutron diffraction.

Herein, we revisit this long-standing problem from a new perspective, using element-selective X-ray Magnetic Circular Dichroism (XMCD) to investigate the magnetic properties of paramagnetic 5d transition metal-chlorido complexes, $(PPh_4)_2IrCl_6$ and $(PPh_4)_2ReCl_6$. While XMCD at the $L_{2,3}$-edges of transition metals does not directly measure "covalent bonding", it sensitively reveals its consequences, manifested in changes in orbital and spin magnetic moments, hybridization strength, 5d electron occupation, and charge transfer [2]. Extending XMCD to the chlorine K-edge, we demonstrate that the Cl 3p orbitals become strongly magnetically polarized due to hybridization with the 5d orbitals of the metal centers. The observed XMCD signal provides unambiguous proof for an orbital magnetic moment localized on the ligand, a clear signature of orbital moment delocalization in paramagnetic molecular complexes.

These findings open a promising and largely unchartered territory for probing and quantifying magnetic polarization of ligands and metal-ligand covalency in molecular systems.

References

[1] J. Owen and K.W.H. Stevens, Nature **171**, 836 (1953).

[2] K. Pedersen, J. Bendix, A. Tressaud, *et al.*, Nat Commun **7**, 12195 (2016).

Abstract ID: 30366

SPIN-ELECTRIC EFFECT IN A Co(II)-BASED ANTIFERROMAGNETIC SPIN TRIANGLE

T. Guidi[1,2], M. Albanesi[3,4], E. Garlatti[5], S. Carretta[5], M. Fittipaldi[6], R. Sessoli[3], B. Kintzel[7], W. Plass[7]

[1] *School of Science and Technology-Physics Division, University of Camerino, Camerino, ITALY*
[2] *ISIS Neutron and Muon Source, Rutherford Appleton Laboratory, Didcot, UNITED KINGDOM*
[3] *Synchrotron SOLEIL, Saint-Aubin, FRANCE*
[4] *Department of Chemistry 'Ugo Schiff', University of Florence, Sesto Fiorentino, ITALY*
[5] *Department of Mathematical, Physical and Computer Sciences, University of Parma, Parma, ITALY*
[6] *Department of Physics and Astronomy, University of Florence and INSTM UdR, Sesto Fiorentino, ITALY*
[7] *Institut für Anorganische und Analytische Chemie, Friedrich-Schiller-Universität Jena, Jena, GERMANY*

Magnetic molecules characterized by a doubly-degenerate spin ground state are promising candidates as spin-based qubits, and, among all the possible physical realizations of qubits, they have the unique advantage that their properties can be chemically tuned [1]. The ability to manipulate spin qubits with an electric field (spin-electric coupling) promises to achieve faster and space-confined control of the spin-spin interaction [2]. A sizeable spin-electric coupling has been detected for a Co(II)-based antiferromagnetic triangle (Co3P) (fig.1, left) using EFM-EPR experiments [3]. To shed light on the origin of the observed effect the accurate determination of the microscopic interactions contributing to the energy spectrum of Co3P is necessary. By means of inelastic neutron scattering (INS) the splitting of the low-lying levels, induced both by anisotropy and departures from equilateral exchange topology, was directly measured (fig. 1, right). Moreover, using the LET state-of-the-art spectrometer available at ISIS Neutron and Muon Source we were able to measure the 4D scattering cross-section, which provided the wavevector dependence of the excitations in the cluster. This gives essential information on the eigenvector composition of the system and allows a more selective choice among candidate Hamiltonian models [4]. A promising set of Hamiltonian parameters was derived by modelling the wavevector dependence of the magnetic excitations that best reproduce the experimental data.

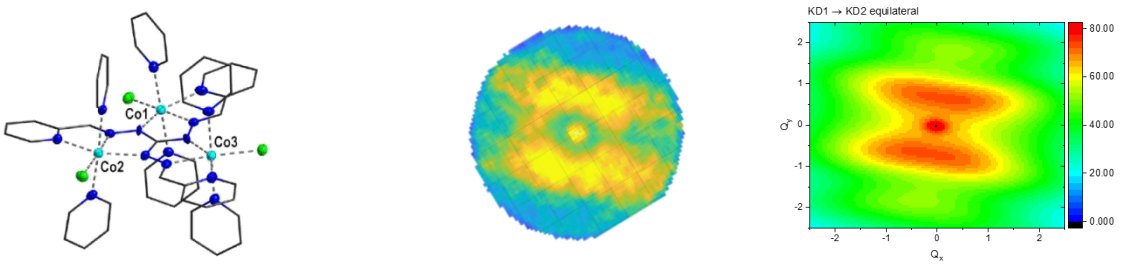

Fig. 1: *The Co(II)-based molecular magnet (left). Experimental (middle) and simulated (right) INS Q-dependence of the low-energy magnetic excitations (right)*

References

[1] E. M. Pineda, *et al.*, Chem. Soc. Rev. **47**, 501-513 (2018).
[2] J. Liu, *et al.*, Phys. Rev. Lett. **122**, 037202 (2019).
[3] B. Kintzel, *et al.*, Angew. Chem. Int. Ed. **60**, 8832-8838 (2021).
[4] E. Garlatti, *et al.*, Eur. J. Inorg. Chem. **9**, 3555-3562 (2018).

Abstract ID: 30371

TUNING CHARGE AND SPIN INTERACTIONS AT SURFACES WITH MOLECULAR STRATEGIES

A. Mugarza[1,2]

[1] *Catalan Institute of Nanoscience and Nanotechnology (ICN2), CSIC and The Barcelona Institute of Science and Technology, Campus UAB, Bellaterra, 08193 Barcelona, SPAIN*
[2] *ICREA Institució Catalana de Recerca i Estudis Avançats, Lluis Companys 23, 08010 Barcelona, SPAIN*

Interfacing materials with different functionalities is an efficient way to manipulate their respective properties and promote the emergence of novel phenomena. Controlling interfacial interactions is however a complicated task in most cases. In that respect, the tunability offered by ligand chemistry in organic materials is an interesting asset that can be exploited at hybrid interfaces. Here I will present two examples where the molecular strategy is employed to tune the interactions of single transition metal ions with underlying spin-degenerated electrons in non-magnetic metals, and with spin-textured electrons in topological insulators. In both cases, we obtain a comprehensive picture of the phenomenology by combining scanning tunnelling microscopy/spectroscopy, atomic manipulation, X-ray absorption and photoelectron spectroscopy, and ab-initio calculations.

On our systematic study of transition metal phthalocyanines on noble metals we show how the interaction with the substrate can be mediated by the metal ion or the organic ligand and how, depending on this, the molecular magnetic moment can either be quenched or enhanced [1,2]. The molecular spin and charge can be further manipulated by doping with alkalis atom by atom [3,4]. By moving from phthalocyanines to porphyrine single molecules, and then to on-surface synthesized covalent networks, we will see that the interaction with substrate can be exquisitely fine-tuned by the conformational differences between the systems [5].

For molecular films on topological insulators, the tunability of ligands is exploited to tune the interaction of Co ions with the underlying topological surface state (TSS), going from the strongly interacting regime where the TSS is quenched in the first quintuple layer [6], to the weakly interacting regime where both the TSS and the Co magnetic moment are preserved [7].

References

[1] A. Mugarza, *et al.*, Phys. Rev. B **85**, 155437 (2012).
[2] A. Mugarza, *et al.*, Nature Comm. **2**, 490 (2011).
[3] C. Krull, *et al.*, Nature Mater. **12**, 337 (2013).
[4] S. Stepanow, *et al.*, J. Am. Chem. Soc. **136**, 5451 (2014).
[5] M.G. Cuxart, *et al.*, unpublished.
[6] M. Caputo, *et al.*, Nano Letters, **16**, 3409 (2016).
[7] M. G. Cuxart, *et al.*, ACS Nano. **14**, 6285–6294 (2020).

Abstract ID: 30662

QUANTUM AND EXOTIC EFFECTS IN MOLECULE-BASED MAGNETIC MATERIALS - QUIXOTICS

A. K. Powell

Karlsruhe Institute of Technology (KIT), Institute of Inorganic Chemistry, D76131 Kaiserstrasse 12, Karlsruhe, GERMANY

As humans we are accustomed to living in both light and darkness. In fact, these days, we mostly live in illuminated situations since we have developed artificial light sources to allow us to see what we are doing for 24 hours a day if needed. However, nearly all of the Universe is hidden to us. We can only observe about 4% of the matter and energy of the Universe – the rest of the matter and energy is hidden in "dark states" and no information content for these states is accessible to us at present.

In the research of my group we have become fascinated by these dark states since our discovery that a molecule – a very small amount of matter in the shape of a Dy3 triangle – can hide its magnetic information (and possibly also its electronic information) by adopting a toroidal spin state. This leads to a propeller topology which ignores the usual principle of molecules with a triangular geometry of becoming spin frustrated.[1] Usually alternating spins on a triangle try to satisfy antiferromagnetic coupling and adopt an alternating up and down pattern. However, on a triangle this leads to one spin always being in a quandary about whether to be up or down and is valid for many 3d transition metal ions, especially Fe(III). For strongly uniaxial anisotropic systems, such as the 4f Dy(III) ion, the alternative solution is to arrange the spins in a cyclic propeller of a "follow my leader" sort, which can be visualized as a three bladed propeller. In this case the ground spin state becomes non-magnetic and this is known as a toroidal state. Given that the magnetic information is now hidden this equates to a "dark state". Not only does this give insights into what happens to matter and energy in the Universe, this is also a promising way of protecting information with applications we are only beginning to imagine.

In our quest to discover such exotic physical properties in coordination compounds we aim to work in a sustainable way. We use Earth abundant metal ions in our synthesis and avoid scarce metals such as platinum and iridium. Our approach can also involve using mixed metal systems and a particularly fruitful strategy is to mix iron centres with lanthanide metal ions. Although the lanthanides belong to the class of metals known as "Rare Earths" they are not rare in the sense of being scarce and are far more abundant than the heavier transition metals such as platinum. The rare here refers to their rare properties, which are now being explored avidly by chemists around the world.

Mixing 3d metal ions, such as Fe(III), with the more exotic anisotropy features of 4f metal ions such as Dy(III) can be understood in terms of the relationship between Sancho Panza and Don Quixote. Sancho represents the calming and donkey riding companion whereas Don Quixote is the crazy horse riding "boss" who liked to tilt his lance (with a significant anisotropic direction) at windmills. This has been substantiated by us in a number of 3d/4f systems which will be discussed in my presentation.

References

[1] J. Tang, I. Hewitt, N. T. Madhu, G. Chastanet, W. Wernsdorfer, C. E. Anson, C. Benelli, R. Sessoli, A. K. Powell Angew. Chem. Int. Ed. Engl., **45**, 1729 (2006).

Abstract ID: 30125

GENERALIZED QUANTUM GEOMETRY DRIVEN TRANSPORT IN UNCONVENTIONAL MAGNETS

S. Nandy[1], N. Chakraborty[2], S. K. Ghosh[2]

[1] *National Institute of Technology Silchar, Dept. of Physics, 788010, Silchar, INDIA*
[2] *Indian Institute of Technology Kanpur, Dept. of Physics, 208016, Kanpur, INDIA*

Unconventional magnets with momentum-dependent spin splitting but zero net magnetization form a recently identified class of collinear magnetic phases that evade detection by traditional probes. We show that such systems can be uniquely identified through *intrinsic gyrotropic magnetic* (IGM) currents arising from Zeeman quantum geometry, which encodes the coupled response of Bloch states to momentum translation and spin rotation. By analyzing prototypical two-dimensional unconventional magnets with Rashba spin–orbit coupling—including a time-reversal-broken *d*-wave altermagnet, a time-reversal-symmetric *p*-wave magnet, and their mixed counterparts, we establish a direct correspondence between crystalline symmetry, spin-split band structure, and gyrotropic transport signatures. The *d*-wave altermagnet hosts both transverse conduction and longitudinal displacement IGM currents, whereas the *p*-wave magnet supports only a transverse conduction current. Remarkably, the mixed *d*-wave state exhibits all four possible IGM responses, including a symmetry-allowed longitudinal conduction current enabled by the symmetric (Zeeman) Berry curvature, which has no analogue in conventional quantum geometry. Extending this framework to general *p*-, *d*-, *f*-, and *g*-wave orders at the interface with a magnetic topological-insulator surface state, we show the transverse displacement response exhibits symmetry-dictated even-fold angular modulations, while longitudinal components display characteristic parity-dependent patterns. Crucially, while conduction currents are largely insensitive to magnetic texture, displacement currents provide a highly sensitive probe of unconventional spin-split orders. Our results position Zeeman quantum geometry as a powerful and experimentally accessible route via Hall transport and optical probes to classify and detect unconventional magnetic phases that remain hidden to conventional symmetry diagnostics.

References

[1] L. Smejkal, *et al.*, Phys. Rev. X **12**, 031042 (2022).

[2] L. Xiang, *et al.*, Phys. Rev. Lett. **134**, 116301 (2025).

[3] N. Chakraborty, *et al.*, e-print arXiv:2508.14745 (2025).

Abstract ID: 30461

BREAKING PERFORMANCE LIMITS IN TWO-DIMENSIONAL METAL-ORGANIC MAGNETS THROUGH CHEMICAL DESIGN

A. Adak[1], R. Diego[1], V. L. Nadurata[1], P. Perlepe[1,2], I. Oyarzabal[1,3,4], N. Yutronkie[1], D. Lou[1], A. Zabala-Lekuona[5], A. Mailman[6], M. Gonidec[2], M. Rouzieres [1], E. A. Suturina[7], S. Giri[8], S. Bonhommeau[9], G. Clermont[9], F. Wilhelm[10], A. Rogalev[10], C. Mathonière[1], R. Clérac[1]

[1] *Univ. Bordeaux, CNRS, Centre de Recherche Paul Pascal, CRPP, UMR 5031, 33600 Pessac, FRANCE*
[2] *Univ. Bordeaux, CNRS, Bordeaux INP, ICMCB, UMR 5026, 33600 Pessac, FRANCE*
3 BCMaterials, Basque Center for Materials, Applications and Nanostructures, 48940 Leioa, SPAIN
[4] *IKERBASQUE, Basque Foundation for Science, 48009 Bilbao, SPAIN*
[5] *Dept. of Applied Chemistry, Faculty of Chemistry, University of the Basque Country, UPV/EHU, 20018 Donostia-San Sebastián, SPAIN*
[6] *Dept. of Chemistry, NanoScience Centre, University of Jyväskylä, 40014 Jyväskylä, FINLAND*
[7] *Dept. of Chemistry, University of Bath, Claverton Down, Bath BA2 7AY, UK*
[8] *Dept. of Quantum Matter Physics, University of Geneva, CH-1211 SWITZERLAND*
[9] *Univ. Bordeaux, CNRS, Bordeaux INP, ISM, UMR 5255, 33400 Talence, FRANCE*
[10] *ESRF - The European Synchrotron, CS40220, 38043 Grenoble Cedex 9, FRANCE*

Two-dimensional (2D) coordination-based materials constitute a versatile platform for designing high-performance molecular magnets [1]. In this contribution, we study a layered molecular network composed of redox-active pyrazine ligands and early 3d transition metal ions, which serves as a platform for post-synthetic modification. [2, 3] Electron injection enabled by post-synthetic reduction enhances magnetic interactions within the layers; however, the reduction process can also lead to the formation of intercalated by-products between adjacent sheets along the c-axis [3]. We describe several approaches to remove these species and show that precise regulation of the interlayer composition leads to marked improvements in both magnetic coercivity (H_C) and magnetic ordering temperature (T_C). In particular, we identify a rational design strategy based on pre-assembled 2D materials that enables the formation of clean, intercalant-free 2D magnetic systems upon reduction, resulting in record performance for molecule-based magnets.

References

[1] J. S. Miller, Chem. Soc. Rev. **40**, 3266–3296 (2011).
[2] K. S. Pedersen, *et al.*, Nat. Chem. **10**, 1056–1061 (2018).
[3] P. Perlepe, *et al.*, Science, **370**, 587–592 (2020).

Abstract ID: 30622

THE INFLUENCE OF SUPERCONDUCTIVITY ON THE SPIN STATES OF Er^{3+} COMPLEXES IN COMPOSITE STRUCTURES

E. I. Kunitsyna, R.B. Morgunov

Federal Research Center of Problems of Chemical Physics and Medical Chemistry RAS, 142432 Chernogolovka, RUSSIA

Molecular magnets based on rare-earth ions are promising candidates for quantum technologies due to their long spin relaxation times and the ability to control quantum states. A significant limitation of their practical application remains the lack of effective methods for reading and controlling spin states in massive structures. One approach to solving this problem is the creation of hybrid composites of molecular magnets with superconductors, in which the interaction of local magnetic moments with Cooper pairs can lead to mutual modification of physical properties. In this work, a composite based on indium microparticles and a molecular magnet with Er^{3+} ions was studied using the AC magnetic susceptibility method in a wide range of frequencies, temperatures and constant magnetic fields. The magnetic dynamics of a pure erbium complex, superconducting indium, and their composite are compared. It is shown that non-additive changes in the magnetic response occur in the hybrid system, indicating interaction between the components. It was found that the presence of molecular magnets leads to a decrease in the critical field of superconducting indium by approximately 1.6 times, while the critical transition temperature remains unchanged. At the same time, the superconducting matrix significantly alters the spin dynamics of erbium complexes: instead of a slowdown in magnetic relaxation with increasing field, characteristic of the suppression of quantum tunneling in free complexes, the composite exhibits an acceleration of relaxation due to the dominance of the direct relaxation mechanism. The obtained results indicate a strong mutual influence between superconductivity and the spin states of molecular magnets, likely related to the modification of the wave functions of Cooper pairs near the magnetic centers.

Hybrid composite structures based on superconductors and molecular magnets can be considered a promising platform for detecting and controlling the quantum states of molecular systems in macroscopic devices.

21 - FERROMAGNETIC SHAPE MEMORY ALLOYS AND MAGNETOCALORICS

Abstract ID: 30052

STRUCTURAL, MAGNETIC, AND MAGNETOCALORIC PROPERTIES OF TEXTURED DyNiAl INTERMETALLIC COMPOUND

J. Ćwik[1], Y. Koshkid`ko[1], D. Gajda[1], M. Małecka[1], D. Szymański[1], E. Tereshina-Chitrova[2], A. Czernuszewicz[3]

[1] *Institute of Low Temperature and Structure Research, PAS, Okólna 2, Wrocław, 50-422, POLAND*
[2] *Institute of Physics CAS, Prague 18221, CZECH REPUBLIC*
[3] *Ames National Laboratory, U.S. Department of Energy, Iowa State University, Ames, IA 50011, USA*

Hydrogen liquefaction requires cooling to cryogenic temperatures below 20 K, which, with the current vapor-compression technology, uses more than 30% of hydrogen energy content [1]. Because of that, there is a great interest in development of more efficient cooling alternative methods. One of the most promising is magnetic refrigeration based on the magnetocaloric effect (MCE). The magnetocaloric effect is defined as the heating (or cooling) of a magnetic material due to the application (or removal) of a magnetic field. Magnetic refrigeration has the potential to be not only more efficient than vapor compression but also more ecologically benign. The selected Laves-phase RNiAl (R-rare earth) intermetallic compounds are promising magnetocaloric material for low-temperature magnetic cooling within the range required for hydrogen liquefaction [2]. Existing literature indicates that these compounds, when in single-crystal form, exhibits superior magnetocaloric properties compared to its polycrystalline counterpart; however, the properties of its textured form have not yet been reported [3]. This work presents the first results for textured Laves-phase DyNiAl intermetallic compound. The material underwent extensive structural, magnetic, and magnetocaloric characterization, confirming properties similar to those of a single crystal. Our textured Laves-phase intermetallic compound demonstrated significant anisotropy in the magnetocaloric effect, showing a much larger response when the magnetic field was applied along the texture axis compared to the response when the field was applied perpendicular to that axis. These findings highlight its potential for applications in both conventional and rotational magnetic cooling systems operating at cryogenic temperatures.

The work was supported by the National Science Center, Poland through the OPUS Program under Grant No. 2023/51/B/ST11/02015.

References

[1] Liquid Hydrogen Delivery, https://www.energy.gov/eere/fuelcells/liquid-hydrogen-delivery. (Accessed: 6 February 2023).

[2] A.M. Tishin, Y.I. Spichkin, *The magnetocaloric effect and its applications*, IOP Publishing (2003).

[3] M. Balli, S. Jandl, P. Fournier, M.M. Gospodinov, *Anisotropy-enhanced giant reversible rotating magnetocaloric effect in $HoMn_2O_5$ single crystals*, Appl Phys Lett 104, (2014).

Abstract ID: 30091

RECENT DEVELOPMENTS IN PARTICULATE HEUSLER TYPE MAGNETIC SHAPE MEMORY HYBRID MATERIALS FOR ACTUATION AND ENERGY

V. Chernenko[1,2], V. Lvov[3], H. Hosoda[4], S. Lanceros-Mendes[1,2]

[1] *BCMaterials, Basque Center for Materials, Applications and Nanostructures, UPV/EHU Science Park, 48940, Leioa, SPAIN*
[2] *IKERBASQUE, Basque Foundation for Science, 48009, Bilbao, SPAIN*
[3] *V.G. Baryakhtar Institute of Magnetism of the NAS of Ukraine, Kyiv,252140, UKRAINE*
[4] *Institute of Integrated Research, Institute of Science Tokyo, Yokohama 226-8503, JAPAN*

Heusler type magnetic shape memory alloys (MSMAs) are multifunctional materials exhibiting "giant" properties in the vicinity of the martensitic phase transition (MT), particularly, magnetic field induced strain and magnetocaloric effect. These materials can be conventionally divided into two groups: ferromagnetic shape memory alloys (FSMAs), such as prototype Ni-Mn-Ga compounds, and the metamagnetic shape memory alloys (MetaMSMAs), such as Mn-rich Ni-Mn-X (X=In, Sn, Sb). Both types of materials are capable to convert effectively the magnetic energy into mechanical (magnetic actuation) or caloric signal (magnetic cooling) and reversely the thermal and/or elastic energy into an electromagnetic signal, which is promising for application in novel transducers and sensors. To prevent the inherent fragility of MSMAs materials, we have created their particulate hybrids with novel characteristics. In contrast to bulk Ni-Mn-Ga microparticles are technologically and costly more efficient. We will showcase the latest developments in MSMA particles containing hybrid materials.

1. We will present the innovative NiMnGa particles/polymer composites that exhibit a remarkable rubber-like response to magnetic fields: under a periodic magnetic field of several kOe the composite can repeatedly deform by 4%. The underlying mechanism of this response has been elucidated through X-ray micro-CT.

2. We found that thin film composites containing NiMnGa particles distributed in the P(VDF-TrFE) piezopolymer exhibit an unprecedented resonance amplification of the magnetoelectric (ME) signal in both martensitic and austenitic states of particles. The physical mechanism of the ME response amplification has been disclosed theoretically.

3. We have elaborated laminated composites comprising a layered ensemble of single crystalline Ni-Mn-Ga particles built-in between Cu foils via thin layers of silicone rubber. Such a robust design enabled a detailed investigation of the simultaneous influence of the magnetic field and compressive opposing stress on a giant magnetic field induced strain and the generated force of the particle layer driving out-of-plane stroke of laminate. A significantly improved magnetostrain response of the laminate composite was achieved after replacing the Cu foils with soft-magnetic Fe foils.

4. A new route for the room-temperature fabrication of the magnetocaloric ink incorporating the polymer binder and Ni(Co)-Mn-Sn MetaMSMA particles was elaborated. The ink was used to print 2D films which do not require a subsequent heat treatment. The field-induced adiabatic temperature measurements reveal that the screen- printed samples displayed the same inverse magnetocaloric effect as the ribbon, which was used to prepare particles.

Abstract ID: 30114

ROLE OF Fe, Co AND Cu ADDITION IN THE STRUCTURAL AND MAGNETIC PROPERTIES OF Ni-Mn-Ga MAGNETIC SHAPE MEMORY ALLOYS

N. A. Río-López [1,+], P. Lázpita [1,2], A. Pérez-Checa [3], J. Feuchtwanger [1,4], J. A. Rodríguez-Velamazán [5], I. Zabala [1], V. Chernenko [1,2,4], F. Plazaola[1], C. Seguí [6], J. M. Porro[2,4]

[1] *Department of Electricity and Electronics, Faculty of Science and Technology, University of the Basque Country, 48080 Bilbao, SPAIN*
[2] *BCMaterials, Basque Center for Materials, Applications & Nanostructures, 48940 Leioa, SPAIN*
[3] *TECNALIA, Basque Research and Technology Alliance (BRTA), Mikeletegi pasealekua 2, 20009 Donostia, SPAIN*
[4] *Ikerbasque, Basque Foundation for Science, 48009 Bilbao, SPAIN*
[5] *Institut Laue-Langevin - 71 avenue des Martyrs, CS 20156, 38042 GRENOBLE Cedex 9 - FRANCE*
[6] *Departament de Física, Universitat de les Illes Balears, E07122 Palma de Mallorca, SPAIN*

Magnetic Shape Memory Alloys (MSMAs) have been attracting attention owing to their interesting magnetocaloric and magnetostrictive effects, which serves as the mechanism governing their applicability in solid state refrigerators, sensors and actuators. These effects arise from a huge magnetostructural coupling allowing the magnetic-field induced martensitic transformation from a low symmetry phase at low temperature (martensitic phase) to a high symmetry one (austenitic phase). Consequently, both the structural and magnetic properties and their transitions play a critical role in these functional responses.

The strong correlation between composition, structure and magnetic properties in magnetic shape memory Heusler alloys is well established. Doped Ni-Mn-Ga alloys are particularly compelling due to their high compositional tunability. Within this context, the present work explores the role of Co, Fe and Cu substitution on the crystal structure and magnetic behaviour of three series of alloys ($Ni_{51}Mn_{29-x}Ga_{20}Co_x$, $Ni_{51}Mn_{29-x}Ga_{20}Fe_x$, $Ni_{50}Mn_{25-x}Ga_{25}Cu_x$). Via Powder Neutron Diffraction (PND), the symmetry and atomic site occupancies of both the austenitic and martensitic phases were disclosed. The structural differences were linked to the observed evolution of martensitic transformation temperature -which increase with Co and Cu substitution but decreases with Fe- and to the atomic distribution, correlated with a change in the predominant type of magnetic exchange interactions, thereby affecting the magnetic coupling. While Fe and Co doping enhance ferromagnetic interactions, Cu atoms provoke the opposite effect, promoting antiferromagnetic ones.

In summary, the results established a clear correlation between dopant concentration, transition temperatures and type of magnetic exchange interactions. Moreover, they underscore the distinct effect associated with each dopant, providing valuable insight into the mechanism behind the finetuning of the actuation temperature range via compositional variations.

Abstract ID: 30131

THERMOELECTRIC PROPERTIES OF HALF- AND DOUBLE HALF-HEUSLER ALLOYS: A THEORETICAL STUDY

V. Buchelnikov, V. Sokolovskiy, A. Enenko, M. Matyunina

Chelyabinsk State University, Dept. of Cond. Matter Physics, 454001, Chelyabinsk, RUSSIA

The main problem of application of thermoelectric (TE) materials is related to their efficiency. The figure of merit ZT of most TE materials at room temperature is small [1]. For example, ZT for SnSe single crystal is 2.6 only at 923 K [2]. At 300 K the ZT of SnSe single crystal is equal to 0.12. So, there is a problem of searching for the TE materials with large ZT at 300 K. The half-Heusler alloys are also promising for TE applications [3]. However, the maximum of ZT for half-Heusler alloys is about 1.5 for high temperatures. At 300 K the ZT of half-Heusler alloys is small. Double half-Heusler compounds are also promising TE materials [4]. However, the high thermal conductivity of the lattice, leading to limited TE efficiency, still prevents their widespread use in practical applications. In this work we suggest new half- and double half-Heusler alloys with low lattice thermal conductivity [5]. The TE properties are investigated within DFT calculations and BoltzTraP2 code. For example, the temperature dependence of ZT for KScX (X=Si, Ge, Sn and Pb) is presented in Figure 1. It is seen that ZT of alloys can achieve the value of about 1 at room temperature.

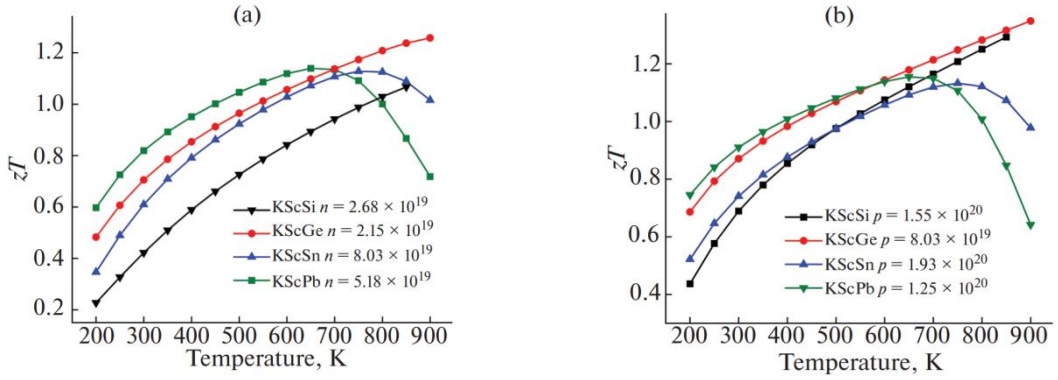

Fig. 1: *Calculated ZT for K_2ScX (X = Si, Ge, Sn, Pb) as a function of temperature at doping level at which the ZT has maximum value for 300 K. (a) n-type and (b) p-type carriers.*

This work was supported by the Russian Science Foundation (project No. 24-12- 20016, https://rscf.ru/project/24-12- 20016/).

References

[1] Liuyijie Huang, *et al.*, Thermal Sci. and Eng. Progress **45,** 102064 (2023).

[2] L.-D. Zhao, *et al.*, Nature **508**, 373 (2014).

[3] G Rogl, PF Rogl: Crystals **13**, 1152 (2023).

[4] S. Anand, *et al.*, Energy Environ. Sci., **11**, 1480 (2018).

[5] V. Buchelnikov, *et al.*, Physics of Metals and Metallography, **126**, 1056 (2025).

Abstract ID: 30165

BEYOND GGA: THE QUEST FOR AN ACCURATE GROUND STATE DESCRIPTION OF Ni_2MnTi HEUSLER ALLOY

V. Sokolovskiy[1], K. Erager[1], D. Baigutlin[1], D. Novokreshenov[1], M. Matyunina[1], O. Miroshkina[2], V. Buchelnikov[1]

[1] *Chelyabinsk State University, 454001, Chelyabinsk, RUSSIA*
[2] *University of Duisburg-Essen, 47057, Duisburg, GERMANY*

The Ni_2MnTi Heusler alloy is s a highly promising material for advanced applications like magnetic cooling (magnetocaloric effect), shape memory devices, due to its strong magneto-structural coupling, large entropy changes, and tunable properties like martensitic transformation (MT) temperatures and mechanical strength [1]. However, a fundamental understanding of its ground state remains elusive and contradictory, posing a significant barrier to its rational design and application. This contradiction is crystallized in the disagreement between experimental observations and standard *ab initio* predictions using the density functional theory (DFT) and generalized gradient approximation (GGA-PBE) for the exchange correlation functional. Experimental data initially reported that Ni_2MnTi crystallize to a cubic B2 phase without MT [2]. However recent advanced characterization [3] reveals a highly complex state: a B2 matrix with $L2_1$-like ordering, nanotwins, and competing spin/strain glass behavior. This suggests a "frustrated" or "smoothed" energy landscape near the phase stability boundary.

The standard computational approach within GGA-PBE consistently predicts a FM $L2_1$ phase as the ground state, which undergoes a spontaneous tetragonal distortion, implying a driving force for MT. This predicted transformation is not observed in the initial experiments, and GGA-PBE often suggests thermodynamic instability against decomposition. This discrepancy indicates that GGA-PBE fails to adequately describe the delicate energy balance between competing structural (cubic $L2_1$ or B2, tetragonal $L1_0$) and magnetic (FM, AFM) configurations in Ni_2MnTi. The very proximity of these states - a "competition on the edge of stability" - is hypothesized to be the microscopic origin of the observed complex, glass-like behavior.

In the given contribution we hypothesize that the root cause of this theory-experiment gap lies in the limitations of the GGA functional. Meta-GGA functionals, such as SCAN and r2SCAN, which incorporate additional electronic density information (the kinetic energy density), possess the necessary accuracy to correctly map the nuanced energy landscape of Ni_2MnTi. We will show that meta-GGA shift the energy balance in favor of the experimentally observed cubic-like phases, correctly predict the compound's thermodynamic stability, and eliminate spurious dynamical instabilities (negative phonon modes) predicted by GGA-PBE. Beyond solving this specific puzzle, our approach provides a critical advance for computationally designing functional materials whose properties depend on fine energy balances.

The research was supported by the RSF Russian Science Foundation Project No. 25-12-20024, https://rscf.ru/project/25-12-20024/.

References

[1] H. L. Yan, *et al.*, Mater. Design **184**, 108180 (2019).

[2] Z.Y. Wei, *et al.*, APL **107**, 022406 (2015).

[3] Q. Ren, *et al.*, Acta Mater. **292**, 121032 (2025).

Abstract ID: 30172

MARTENSITIC MICROSTRUCTURE ENGINEERING: A VERSATILE APPROACH FOR MAGNETIC MANIPULATION OF MULTIFERROIC HEUSLER FILMS AND SPATIALLY CONFINED STRUCTURES

M. Takhsha

Institute of Materials for Electronics and Magnetism (IMEM), National Research Council of Italy (CNR), Parco Area delle Scienze 37/A, 43124, Parma, ITALY

Magnetic shape-memory (MSM) Heuslers are multiferroic materials that show a strong coupling between magnetic, thermal, and mechanical properties. Their multifunctional character arises from a phase transformation between low-temperature martensitic and high-temperature austenitic phase [1]. In particular, epitaxial Ni-Mn-Ga thin film systems are the benchmark also for possible integration in smart micro/nanodevices such as sensors, energy harvesters, and actuators [2].

The ability to control the martensitic microstructure, which rules the magnetic characteristics of these films at different length scales, is the key point for the optimization of their magnetic functional properties. The low-temperature martensite phase of epitaxial Ni-Mn-Ga films, having film(001)//substrate(001) crystallographic relation, evolves either of both or one of the differently oriented hierarchical twinning configurations, where magnetic domain direction is alternatively out of plane and in plane (X-type) or in plane (Y-type). Different arrangements of these twinning configurations give rise to various magnetic properties [3]. The idea of controlling these twinning configurations in Ni-Mn-Ga films was developed in Parma a few years ago. Since then, we have introduced novel methods for martensitic microstructure engineering by including many parameters such as composition, thickness, underlayer/substrate, growth conditions, and post-growth treatments [4-10].

I will present a short introduction to the material functionality and characteristics, then I will continue with an overview of the microstructure engineering methods we have developed, and I will conclude with the recent advancement in this interesting topic.

References

[1] O. Heczko, *et al.*, MRS Bull. **47**, 618 (2022).

[2] L. Fink, *et al.*, Adv. Funct. Mater. **33**, 2305273 (2023).

[3] A. Diestel, *et al.*, J. Phys. Condens. Matter. **25**, 266002 (2013).

[4] P. Ranzieri, *et al.*, Acta Mater. **61**, 263 (2013).

[5] P. Ranzieri, *et al.*, Adv. Mater. **27**, 4760 (2015).

[6] M. Campanini, *et al.*, Small, **14**, 1803027 (2018).

[7] M. Takhsha Ghahfarokhi, *et al.*, Acta Mater. **187**, 135 (2020).

[8] M. Takhsha Ghahfarokhi, *et al.*, Appl. Mater. Today **23**, 101058 (2021).

[9] M. Takhsha Ghahfarokhi, *et al.*, Acta Mater. **221**, 117356 (2021).

[10] M. Takhsha, *et al.*, Small Struct. **6**, 2500284 (2025).

Abstract ID: 30178

FATIQUE PROPERTIES OF Ni-Mn-Ga-BASED RIBBONS PRODUCED BY RAPID CRYSTALLIZATION

M. J. Szczerba, M. Dudziński, M. Kowalska, P. Czaja, Ł. Rogal

Institute of Metallurgy and Materials Science, Polish Academy of Sciences, Krakow, POLAND

In the present study, the fatigue behavior of Ni-Mn-Ga–based Heusler alloys subjected to cyclic bending induced by an external magnetic field was investigated. These alloys attract considerable scientific interest due to their unique magneto-mechanical properties. While earlier research focused primarily on single-crystalline materials, recent attention has shifted towards different polycrystalline forms, which exhibit promising magnetic-field-induced straining and bending effects [1-3].

The aim of this work was therefore to experimentally analyze the response of melt-spun Ni-Mn-Ga ribbons to magnetic-field-induced bending. The materials were produced using different rotation velocity of the copper wheel, which significantly affected both the martensitic transformation temperatures and the magneto-mechanical behavior. These findings are relevant for the design and optimization of functional materials that exploit magnetic-field-induced bending in Ni-Mn-Ga ribbons. Fatigue properties were evaluated over 10 000 cycles. The deflection remained stable in all cases except for the samples annealed at 900 °C, where a slight decrease in deflection was observed during cycling.

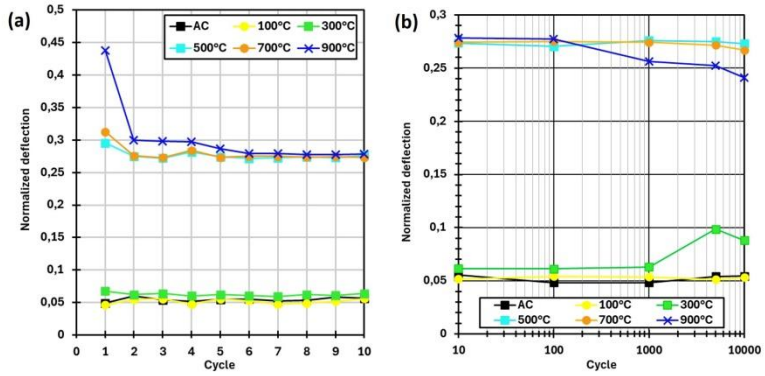

Fig. 1: *Normalized deflection versus cycle number for the studies Ni-Mn-Ga-based ribbos performed for different heat treatment. Data for cycles from 1 to 10 (a) and from 10 to 10 000 (b).*

This work is funded in whole by the National Science Centre, Poland [grant 2021/43/B/ST8/02745], Poland

References

[1] H. Hosoda, J. Lazarczyk, P. Sratong-on, M. Tahara, V. Chernenko, Mater. Lett. **289**, 129427 (2021).

[2] A. Mostafaei, P. Rodriguez De Vecchis, E.L. Stevens, M. Chmielus, Acta Mater., **154**, 355 (2018).

Abstract ID: 30191

THE EFFECT OF BORON ADDITION ON THE STRUCTURAL AND MECHANICAL PROPERTIES OF Ni-Mn-Co-Ti

M. Matyunina, V. Sokolovskiy, V. Buchelnikov

Chelyabinsk State University, 454001, Bratiev Kashirinykh 129, Chelyabinsk, RUSSIA

Ni–Mn–Ti alloys have attracted much attention as cooling materials due to their large volume change (ΔV) during first-order phase transformation, remarkable elastocaloric effect with significant ΔS_{Tra}, and notable $|\Delta T_{\mathrm{ad}}|$ [1]. However, these alloys can only operate under a uniaxial stress field due to their antiferromagnetic austenite, which narrows their operational temperature range for refrigeration. To regulate the magnetic properties of Ni-Mn-Ti alloys and enable them to respond to multi-field control (uniaxial force and magnetic fields), Ni atoms can be substituted with the magnetic element Co. This activates the magnetic-structural coupling of the alloy. The substitution of Co not only reduces the martensitic transformation temperature (T_{M}) but also effectively increases the Curie temperature (T_{C}) of the austenite.

For example, the T_{M} of the $Ni_{35}Co_{15}Mn_{35}Ti_{15}$ alloy is approximately 300 K, which is close to room temperature. This configuration enhances the ferromagnetic exchange interaction between Co and Mn atoms and consequently increases the ferromagnetism of the austenite.

The authors [1] have shown that the addition of 0.2% boron to a directionally solidified $(Ni_{35}Co_{15}Mn_{35}Ti_{15})_{99.8}B_{0.2}$ alloy results in a large, stable elastocaloric effect of 21.3 K over 1013 cycles, while the material simultaneously demonstrates a reversible magnetic entropy change (ΔS_{m}) magnetoelastic coupling enables significant caloric effects across a broad temperature range of 240–340 K, presenting a new strategy for designing high-performance, wide-temperature refrigeration materials.

In this work, the effect of Boron atoms on the structural, mechanical, and magnetic properties of a Ni-Co-Mn-Ti alloy was investigated. A complex approach was employed, combining first-principles calculations and Monte Carlo simulations. Using the VASP [2] package for a 32-atom supercell, the equilibrium parameters of $L2_1$- and $L1_0$ crystal structures were determined, the most energetically stable magnetic configurations were identified, and the elastic tensor constants were calculated. The thermodynamic stability of the phases and the transition temperatures between them were estimated within the framework of the quasi-harmonic Debye approximation. Based on the Heisenberg-BEG model and the Monte Carlo method, the temperature dependence of magnetization was obtained, and thermodynamic characteristics were calculated: magnetic heat capacity, magnetic entropy, isothermal entropy change, and adiabatic temperature change.

The work was supported by Russian Science Foundation, Project No. 25-12-20024, https://rscf.ru/project/25-12-20024/.

References

[1] B. Li, Z. Liu, D. Li, Z. Feng, J. Zhu, H. Zhong, S. Li, Materials Science and Engineering: A **896**, 146260 (2024).

[2] G. Kresse, J. Furthmüller, Phys. Rev. B **54**, 11169 (1996).

Abstract ID: 30194

IMPACT OF DISORDER ON MAGNETIC AND VIBRATIONAL PROPERTIES OF Ni-Mn-Sn HEUSLER ALLOYS

O. Miroshkina, M. E. Gruner

University of Duisburg-Essen, 47057, Duisburg, GERMANY

Mn-rich Ni-Mn-Sn Heusler alloys undergo a first-order magneto-structural phase transition from high-temperature austenite to low-temperature martensite [1-3]. The transformation temperature can be tuned via chemical disorder, making Ni-Mn-Sn an attractive candidate for multi-stimuli caloric cooling applications.

In this work, we investigate the austenitic and martensitic phases near the composition $Ni_{50}Mn_{35}Sn_{15}$ by means of density functional theory and compare our results with the results of magnetometry and nuclear resonant inelastic x-ray scattering (NRIXS). Bain-path calculations reveal strong competition between ferro- (FM) and ferrimagnetic (FiM) states in austenite and a clear preference of FiM configuration in the $L1_0$ martensite. The FiM contribution in the cubic phase is confirmed by comparing the calculated Sn vibrational DOS with that extracted from NRIXS. In martensite, frustrated exchange introduced by Mn excess can prevail in the tetragonally distorted FiM $L1_0$ phases and make nano-twinned arrangements competitive. We find that twins constructed according to the continuum theory of martensite are energetically even more favorable than $L1_0$. A striking outcome is that, independent of the distortion, all Mn/Sn-disordered configurations are energetically more favorable than the ordered ones, with the FiM 4O and 10M phases remaining among the most competitive structures.

This work was performed within the DFG Projects MI 3273/1 and CRC/TRR 270. Large-scale calculations were conducted on the Lichtenberg high performance computer of the TU Darmstadt (Project p0020039).

References

[1] A. Taubel, *et al.*, Phys. Status Solidi B **255**, 1700331 (2018).

[2] F. Cugini, *et al.* Phys. Rev. B **105**, 174434 (2022).

[3] F. Scheibel, *et al.*, Materialia **29** 101783 (2023).

Abstract ID: 30259

DIRECT MEASUREMENTS OF ADIABATIC TEMPERATURE CHANGE IN La-Fe-Si ALLOYS IN CYCLIC MAGNETIC FIELDS: FREQUENCY EFFECTS AND LONG-TERM STABILITY

A. Gamzatov[1], N. Z. Abdulkadirova[1], A. M. Aliev[1], Y. Lin[2], J. Wang[2], F.-X.a Hu[2]

[1] *Amirkhanov Institute of Physics, DFRC, RAS, 367003, Makhachkala, RUSSIA*
[2] *Beijing National Laboratory for Condensed Matter Physics, IOP CAS, Beijing, P. R. CHINA*

In recent years, studies of the magnetocaloric effect (MCE) in cyclic/alternating magnetic fields (under conditions as close as possible to the operating characteristics of magnetic refrigeration devices with operating frequencies of 0.1–20 Hz [1]) have attracted great interest. It has been shown that in materials with giant MCE values, achieving the maximum value of the adiabatic temperature change (ΔT_{ad}) is closely related to the rate of change of the magnetic field due to the kinetics of the phase transition when magnetic fields are close to critical. Recent studies [2–5] have shown that for most magnetocaloric materials, the magnitude of the adiabatic temperature change decreases with an increase in the frequency of the cyclic magnetic field. Moreover, with long-term exposure to cyclic fields, degradation of the effect is observed, which directly hinders their practical application. The attenuation of the magnetocaloric effect with an increase in the frequency of the cyclic magnetic field leads to the fact that the characteristics of magnetocaloric materials in refrigeration units are much less optimistic than theoretically predicted. Possible causes of the strong frequency dependence of the magnetocaloric effect for a number of materials are discussed in the literature [2-5]; however, the nature and underlying mechanisms responsible for MCE instability remain unclear. Therefore, studying and understanding the nature of the frequency-degradation properties of magnetocaloric materials will enable the synthesis of new magnetocaloric materials with controllable properties.

This paper presents the results of direct measurements of ΔT_{ad} in La-Fe-Si alloys in magnetic fields up to 8 T. Direct measurements of ΔT_{ad} were performed using both the classical extraction method (up to 8 T) with single magnetic field applications and magnetic field modulation in cyclic/alternating magnetic fields of 0.62 and 1.2 T with frequencies up to 20 Hz and 1.8 and 8 T at f = 0.2 Hz. It is shown that a number of compositions ($La_{0.8}Pr_{0.2}Fe_{13.7}Si_{1.3}$-$H_\delta$) exhibit strong frequency dependence and degradation of the effect under long-term exposure to cyclic magnetic fields. A number of compositions demonstrate absolute stability of the ΔT_{ad} value both when the frequency of a 1.2 T cyclic magnetic field increases from 1 to 20 Hz (the effect magnitude remains virtually unchanged) and when exposed to a frequency of 10 Hz for over 1 million on/off cycles. An analysis of possible mechanisms for the stability/degradation of ΔT_{ad} in various cyclic magnetic fields is presented.

The study was supported by the Russian Science Foundation, grant No. 24-43-00156, https://rscf.ru/en/project/24-43-00156/.

References

[1] A. Greco, *et al.*, Int. J. Refrig. **106**, 66-88 (2019).

[2] A. G. Gamzatov, *et al.*, Journal of Materials Science, **58**,8503–8514 (2023).

[3] A.M. Aliev, A.G. Gamzatov, JMMM **553**,169300 (2022).

[4] A. Gamzatov, *et al.*, Journal of Alloys and Compounds **1040**, 183453 (2025).

[5] A. Gamzatov, *et al.*, Rare Metals, **44**, 4074–4085 (2025).

[6] Zhengying Tian, *et al.*, Acta Materialia **299**,121472 (2025).

Abstract ID: 30309

MARTENSITIC TRANSFORMATION WITH SMALL HYSTERESIS AND MAGNETIC-FIELD-INDUCED STRAIN IN Mn_3Ga ALLOYS

X. Xu[1,2], D. Imatomi[1], Y. Kinoshita[3], M. Gen[3], Y. Kohama[3], Y. Ishii[3], Y. H. Matsuda[3], Y. Kubota[4], Y. Inubushi[4,5], M. Yabashi[4,5], A. Ikeda[6], K. Noda[6], K. Seki[6], Y. Urabe[6], T. Kihara[7], Y. Hokuse[7], Y. Hirose[7], T. Omori[1], Masashi Tokunaga[3], R. Kainuma[1]

[1] Tohoku Univ., Department of Materials Science, 980-8579, Sendai, JAPAN
[2] Tohoku Univ., Organization for Advanced Studies, 980-8577, Sendai, JAPAN
[3] The Univ. of Tokyo, The Institute for Solid State Physics, 277-8581, Kashiwa, JAPAN
[4] RIKEN SPring-8 Center, 671-5148, Sayo-gun, JAPAN
[5] Japan Synchrotron Radiation Research Institute, 679-5198, Sayo-gun, JAPAN
[6] The Univ. of Electro-Comm., Department of Engineering Science, 182-8585, Chofu, JAPAN
[7] Okayama Univ., Research Institute for Interdisciplinary Science, 700-8530, Okayama, JAPAN

In the family of shape memory alloys, there are two different mechanisms to realize giant magnetic-field-induced strain (MFIS). In Ni-Mn-Ga [1] ferromagnetic shape memory alloys (FMSMA), with the combination of a high magnetic anisotropy and highly flexible twin boundaries in the martensite phase, a phenomenon called variant rearrangement can be realized by the application of magnetic field. In this case, the MFIS can be greater than 10%, but the output stress is usually less than 10 MPa due to the limitation of magnetic anisotropy energy. The other mechanism of MFIS is the use of the first-order martensitic transformation. In the cases where a large magnetization difference exists between the parent and martensite phases, the application of a magnetic field can induce the phase with a stronger magnetization because of the Zeeman energy. These alloys are called metamagnetic shape memory alloys (MMSMA); Ni-Co-Mn-In [2] is a representative for the case of a stronger magnetization in the parent phase, whereas the martensite phase of Fe-Mn-Ga [3, 4] has a stronger magnetism. The MFIS in MMSMAs can be as large as several percent, with a considerable output stress up to 100 MPa. However, the dissipation energy is typically large, thus limits their application possibilities. Recently, we developed a Heusler-type Pd_2MnGa[5] alloy with a dissipation energy almost 1/100 compared to conventional MMSMAs; however, the high cost of Pd is an obvious drawback. In this talk, the martensitic transformation and MFIS in Mn_3Ga alloys will be shown. The Mn_3Ga [6, 7] alloy is known to show a magnetic transition from high-temperature low-magnetic $D0_{19}$ phase to the low-temperature high-magnetic orthorhombic phase with a small thermal hysteresis. We show by both in situ optical microscopy and transmission electron microscopy that this transformation is martensitic. The application of magnetic field can induce the low-temperature orthorhombic martensite phase with MFIS [8]. The change of crystal structure under pulsed high magnetic fields were also investigated using PINK-02 at SACLA[9]. We have found that though the value of MFIS is small, the dissipation energy is extremely small, especially compared with conventional MMSMAs.

References

[1] K. Ullakko, *et al.*, Appl. Phys. Lett., **69**, 1966 (1996).
[2] R. Kainuma, *et al.*, Nature, **439**, 957 (2006).
[3] T. Omori, *et al.*, Appl. Phys. Lett., **95**, 082508 (2009).
[4] W. Zhu, *et al.*, Appl. Phys. Lett., **95**, 222512 (2009).
[5] T. Ito, *et al.*, Adv. Sci., **10**, e2207779 (2023).
[6] H. Niida, *et al.*, J. Phys. Soc. Jpn., **52**, 1512 (1983).
[7] M. F. J. Boeije, *et al.*, J. Magn. Magn. Mater., **433**, 297 (2017).
[8] D. Imatomi, *et al.*, ICOMAT 2025, Prague.
[9] A. Ikeda, *et al.*, Appl. Phys. Lett., **120**, 142403 (2022).

22 - HIGH TEMPERATURE SUPERCONDUCTORS FOR FUSION APPLICATIONS

Abstract ID: 30512

PROGRESS AND CHALLENGES IN DEVELOPING HTS MAGNETS FOR THE STEP FUSION PLANT

S. C. Wimbush

UK Industrial Fusion Solutions Ltd, Culham Campus, Abingdon, Oxfordshire OX14 3DB, UK

The Spherical Tokamak for Energy Production (STEP) is the UK Government's major programme to deliver a prototype fusion powerplant and a path to commercial viability of fusion [1]. To achieve the former goal, HTS technology has been selected for the major (toroidal and poloidal) magnet systems of STEP [2], while to achieve the latter goal a whole-plant design approach focused on remote maintenance and operational lifetime has been adopted from the outset [3]. This creates several unique challenges for the HTS magnets, not least the requirement for the incorporation of remotely remountable joints within the toroidal field coils to allow access to the machine in operation, alongside other presently unrealised challenges for HTS such as high stored energy quench handling (detection and protection), high-current, high-field operation and reliability against cyclic magnetic forces, and manufacturing complexity resulting from the unprecedented scale of the magnets.

In this talk, I will outline our progress to date in tackling each of these challenges, one year into our technology development programme, as well as our plan for the next three years, culminating in the operational testing of our first STEP toroidal field model coil to prove out our technical solutions to each of these challenges. I will also describe our industry-focused approach to partnering on delivery of our major objectives with a view to growing a self-sustaining UK-based HTS industry with the capability to deliver large-scale projects both within the fusion sector and beyond.

References

[1] A. Baker, Phil. Trans. R. Soc. A **382**, 20230401 (2024).
[2] E. Nasr, S. C. Wimbush, P. Noonan, *et al.*, Phil. Trans. R. Soc. A **382**, 20230407 (2024).
[3] A. van Arkel, C. Lamb, H. Robinson, *et al.*, Phil. Trans. R. Soc. A **382**, 20230415 (2024).

Abstract ID: 30688

MANUFACTURING PROGRESS OF THE WINDING PACK FOR CFEDR TF PROTOTYPE COIL

J. He[Hata! Başvuru kaynağı bulunamadı.,Hata! Başvuru kaynağı bulunamadı.], W. Wen[Hata! Başvuru kaynağı bulunamadı.,Hata! Başvuru kaynağı bulunamadı.], Y. Wu[Hata! Başvuru kaynağı bulunamadı.], CRAFT TF Team[Hata! Başvuru kaynağı bulunamadı.]

[1] *Institute of Plasma Physics, Hefei Institutes of Physical Science, Chinese Academy of Sciences, Hefei, 230031, CHINA*
[2] *Anhui Province Key Laboratory of Special Welding Technology, Huainan 232063, CHINA*

The China Fusion Engineering DEMO Reactor (CFEDR) is designed to serve as a key bridge between experimental facilities and fully commercial fusion power plants. The Comprehensive Research Facility for Fusion Technology (CRAFT) project is aimed at addressing both scientific and engineering challenges before constructing CFEDR. One of the core objectives of CRAFT is the manufacturing of a prototype toroidal field (TF) coil for CFEDR, with the aim of validating the D-shape hybrid winding pack (WP) manufacturing process, which has a size of 19.5 m (length) × 11.5 m (width). The WP is composed of low, medium and high field sub-WPs, with the superconducting materials of these sub-WPs being NbTi, ITER-like Nb_3Sn and High-Jc Nb_3Sn. This presentation will introduce the manufacturing progress for CFEDR TF prototype coil, which includes the coil winding, joint manufacturing, heat treatment (for medium and high field sub-WPs), turn insulation wrapping, VPI for sub-WPs, sub-WPs embedding, VPI for WP, and lessons we learnt from the whole process. As demonstrated in Fig. 1, the VPI for the WP after embedding will reach its conclusion by the first week of February 2026. Furthermore, in March 2026, the WP will be inserted into the coil case.



Fig. 1: *Vacuum pressure impregnation for the TF WP.*

Abstract ID: 30831

HTS WIRE REQUIREMENTS FOR FUSION MAGNETS AND PRODUCTION OF HTS MAGNETS AT RENAISSANCE FUSION

D. Longo

Renaissance Fusion, 38600, Fontaine, FRANCE

The development of advanced REBCO conductors is a key enabler for next-generation fusion magnets and large-scale high-temperature superconductor (HTS) applications. Fusion devices, particularly stellarators, impose stringent requirements on conductors in terms of current density, magnetic field strength, scalability, and geometric adaptability. Renaissance Fusion is developing an integrated technological approach to address these challenges, based on two core pillars: liquid metal technologies and simplified HTS-based magnets. In particular, the company focuses on the realization of a stellarator, leveraging innovative design concepts that dramatically simplify magnet complexity. While conventional stellarators rely on intricate three-dimensional coils, Renaissance Fusion proposes a paradigm shift toward effectively two-dimensional magnet architectures using wide (up to 1m), engraved HTS tapes to generate the required magnetic field configurations. A central component of this strategy is the development of wide REBCO tapes, that are then patterned to achieve the required field configurations, enabling high magnetic field performance over large areas. This approach contrasts with conventional narrow-tape technologies and introduces new requirements in terms of width (up to meter scale), homogeneity, and manufacturability. Strong magnetic fields are essential not only for plasma confinement in stellarators, but also for a wide range of applications including medical imaging for research purposes, energy storage systems, and high-energy physics (e.g. particle accelerators). These applications share common requirements in terms of field intensity, homogeneity, and scalability, making advances in HTS conductor technology broadly impactful. To meet industrial-scale demand, Renaissance Fusion is developing a large-scale roll-to-roll deposition platform based on Metal Organic Chemical Vapor Deposition (MOCVD). While MOCVD of REBCO has been extensively studied over the past decades, current commercial tapes are typically limited to widths of 12 mm. The proposed approach targets a step-change increase in width, up to 1 meter, while maintaining high material quality and uniformity over hundreds of meters in length.

Abstract ID: 30144

GENERATING ANY MAGNETOSTATIC FIELD FROM A SINGLE SOURCE

J. Cunill-Subiranas[1], N. Bort-Soldevila[1], F. Resare[2], N. Del-Valle[1], W. Wieczorek[2], C. Navau[1]

[1] Departament de Física, Universitat Autònoma de Barcelona, 08193, Bellaterra, Barcelona, SPAIN
[2] Department of Microtechnology and Nanoscience (MC2), Chalmers University of Technology, SE-41296, Gothenburg, SWEDEN

Precise control of magnetic fields is essential for modern science and engineering, from high-intensity industrial applications to uniform fields for fundamental experiments. We present a theoretical framework enabling the exact generation of arbitrary magnetic fields within a finite region, with a shape entirely independent of the original source. By combining passive media beyond conventional magnetostatic metamaterials [1-5], this method realizes a wide range of 3D fields induced by external sources outside the target region. Using practical materials, we demonstrate this approach with a proof-of-concept experiment, confirming its high accuracy. This framework establishes a new paradigm in magnetic field engineering, with potential applications in MRI [6], fusion confinement [7], particle accelerators [8], and quantum technologies [9,10], providing a universal toolkit for source-independent field design.

References

[1] F. Gömöry, *et al.*, Science **335**, 1466 (2012).

[2] C. Navau, *et al.*, Phys. Rev. Lett. **112**, 253901 (2014).

[3] J. Prat-Camps, C. Navau and A. Sanchez, Sci. Rep. **5**, 12488 (2015).

[4] C. Navau, J. Prat-Camps and A. Sanchez, Phys. Rev. Lett. **109**, 263903 (2012).

[5] N. Bort-Soldevila, J. Cunill-Subiranas, *et al.*, APL Mater. **12**, 021123 (2024).

[6] T. C. Cosmus and M. Parizh, IEEE Trans. Appl. Supercond. **21**, 2104 (2011).

[7] N. Bort-Soldevila, J. Cunill-Subiranas and A. Sanchez, Sci. Rep. **14**, 3653 (2024).

[8] T. Albahri, *et al.*, Phys. Rev. A **103**, 042208 (2021).

[9] O. Romero-Isart, *et al.*, Phys. Rev. Lett. **109**, 147205 (2012).

[10] N. Bort-Soldevila, J. Cunill-Subiranas, *et al.*, Phys. Rev. Research **6**, 043046 (2024).

Abstract ID: 30471

A COMPLETE NOVEL MULTIPHYSICS SOFTWARE FOR MODELING QUENCH IN NON-INSULATED HTS COILS FOR HIGH FIELD MAGNETS

A. Dadhich, E.Pardo

Institute of Electrical Engineering, Slovak Academy of Sciences 84104, Bratislava, SLOVAKIA

High-field REBCO magnets contain several coils with many turns, which can be used in many large scale applications like high field magnets, space propulsion (magneto-plasma dynamic thrusters), and MRI machines. However, these coils are prone to electro-magneto-thermal quench, which can lead to quick thermal runaways [1]. Also, the high fields in such magnets give rise to high Lorentz forces, which can mechanically weaken the system [2], which also include thermal stresses. High temperature superconductors can be modeled using different techniques for electro-magnetic (such as H-formulation, A-V formulation, etc), thermal (finite element method, finite difference), and mechanical (finite element) analysis. However, it takes a lot of time to model the coupled electro-magnetic, electro-thermal, and mechanical behavior of superconductors simultaneously in a commercial software, especially for non-insulated or metal-insulated coils. Thus, there is a need for a fast and accurate software to numerically model the overall performance of full-scale magnets. We have developed a novel and fast model programmed in C++, which performs coupled electro-magnetic, electro-thermal, and mechanical analysis, using variational methods based on Minimum Entropy Production [Minimum Electro-Magnetic Entropy Production (MEMEP)] [3], Finite Differences[1], and Minimum Mechanical Energy, respectively. The developed software is applied to axi-symmetric fullscale magnets of more than 40 T field strength for transient design (thermal quench reliability), taking screening currents into account [4]. The work includes voltage limitation as a fail-safe method to avoid quench, especially in an event of unexpected damage. The software developed can be used by magnet designers for a quick and complete multiphysics quench analysis in various applications.

References

[1] A. Dadhich, P. Fazilleau, E. Pardo, *A novel and fast electromagnetic and electrothermal software for quench analysis of high field magnets*, Supercond. Sci. Technol., **37(9)**, 095024 (2024).

[2] A. K. Srivastava, E. Pardo, *Modelling the mechanics of 32 T REBCO superconductor magnet using numerical simulation*, Supercond. Sci. Technol., **37(7)**, 075014 (2024).

[3] E. Pardo, J. Souc, L. Frolek, *Electromagnetic modelling of superconductors with a smooth current–voltage relation: variational principle and coils from a few turns to large magnets*, Supercond. Sci. Technol., **28(4)**, 044003 (2015).

[4] E. Pardo, A. Dadhich, N. Jerance, P. Fazilleau, *Screening currents increase thermal quench propagation speed in ultra-high-field REBCO magnets*, arXiv preprint arXiv:2509.06621 (2025)..

Abstract ID: 30693

EFFECT OF SILANE COUPLING AGENT MODIFICATION ON THE PROPERTIES OF ALUMINA-SILICATE FIBER REINFORCED COMPOSITES FOR Bi-2212 CICC

J. Sun[1,2], Z. Liu[1,2], Z. Yan[3],W. Wen[1,2], J. He[1,2], J. Wu[1]

[1] *Institute of Plasma Physics, Hefei Institutes of Physical Science, Chinese Academy of Sciences, 230031, Hefei, CHINA*
[2] *Huainan New Energy Research Center, 232063, Huainan, CHINA*
[3] *Institute of Energy, Hefei Comprehensive National Science Center, 230031, Hefei, CHINA*

This study aimed to improve the performance of alumina-silicate fibers by treating them with silane coupling agents, in order to satisfy the insulation requirements for the Bi-2212 CICC superconducting magnet. XPS, SEM, FTIR and contact angle measurement were used to characterize the surface characteristics and morphology of alumina-silicate fibers both before and after silane coupling agent modification. The results show a considerable increase in surface roughness and oxygen-containing functional groups in modified alumina-silicate fibers. With a noticeable decrease in contact angle fluctuation over time, modified fibers demonstrated stronger inter-fiber bonding. Modification of the silane coupling agent KH560 improves the tensile strength and interlaminar shear strength of the alumina-silicate fiber-reinforced resin composites, according to mechanical property studies. The modified composites retained their excellent insulation strength even though their insulation performance slightly declined.

Abstract ID: 30709

DESIGN, SIMULATION, AND EXPERIMENTAL VALIDATION OF A HEAT TREATMENT SYSTEM FOR CRAFT TF COIL: A CRITICAL STEP TOWARDS CFETR TF

Y. Wu, W. Wang, Y. Wu, J. Qin

Hefei Institutes of Physical Science, Chinese Academy of Sciences, Hefei, 230031, PR CHINA

Fusion reactors represent one of the ultimate solutions to humanity's energy challenge. China is accelerating the construction of the China Fusion Engineering Test Reactor (CFETR). In preparation, the Comprehensive Research Facility for Fusion Technology (CRAFT) project was initiated to tackle key engineering and technological challenges anticipated for CFETR. The fabrication of the CRAFT Toroidal Field (TF) magnet is one of the critical steps in developing the CFETR superconducting magnet system. The CRAFT TF coil measures approximately 19.5 m in length, 11.5 m in width, and 1.1 m in height. This design introduces, for the first time, a unique graded winding and nesting structure that integrates superconducting coils of NbTi, ITER-grade Nb_3Sn, and high-performance Nb_3Sn. However, Nb_3Sn must undergo a specific heat treatment (HT) process to form the superconducting A15 phase, and the reacted Nb_3Sn wire is highly sensitive to stress and strain. Consequently, the TF coil fabrication follows the "wind-and-react" (W&R) manufacturing sequence. This paper details the design, simulation, and experimental validation of a full-argon protective atmosphere furnace system for the HT of the CRAFT TF Nb_3Sn coil. The temperature uniformity during all holding stages was maintained within ± 5°C, demonstrating the feasibility of controlled atmosphere HT for TFC in next-generation fusion reactors.

11th International Conference on Superconductivity and Magnetism ICSM2026
4th International Conference on Quantum Materials and Technologies ICQMT2026
19th April to 26th April, 2026, Ölüdeniz – Fethiye/Muğla, Türkiye
https://icsmforever.org/

Abstract ID: 30577

EARLY OPERATIONAL RESULTS FROM DEMO4

R. Bateman, B. van Nugteren

Tokamak Energy, TE Magnetics Dept. 173 Brook Drive, Milton Park, OX14 4SD, UK

This presentation summarizes the build configuration and early operational results of Demo4, our 44 HTS coil tokamak magnet set. Demo4 consists of 14 toroidal field (TF) limbs (28 coils) and 2 poloidal field (PF) coil stacks (16 coils). The Demo4 magnet set (aka cold-mass) is cooled by high-pressure supercritical helium driven by cryofans through temperature-controlled heat exchangers. This enables the cold-mass to be operated at any temperature between 80 K and a base temperature of approximately 15 K. Running the coils at elevated temperatures reduces the critical current, I_c, meaning the operational limits can be explored at lower stored energies. The initial test sequence for the TF coils started at elevated temperatures, energizing the TF coil set with the PF coils at 0 A. The TF coil set current was ramped up until voltage generation was observed from the embedded voltage taps in the TF coils. The TF coil-set was de-energized and the coil-set control temperature was reduced. The coil-set was ramped again. This was a safe and systematic method of characterizing the TF coil-set down to 30 K. Joint resistances, partial insulation (PI) resistances (radial resistances), coil inductances and magnetic field maps were measured at each temperature.

The TF characterization culminated in a quench test of the TF coil-set at 77 K. The coils were driven beyond I_c to drive the HTS tapes into saturation with excess current flowing radially through the ohmic PI resulting in internal coil pack heating. Due to variation in individual tape I_c, one coil reaches saturation first which is observed on the voltage taps. Once this is detected, the power supply current is held at this level. As current flows radially the coil pack warms up, reducing I_c so more current flows radially resulting in greater heating until almost all of the current is flowing radially, the local hall sensor shows the field being generated by that limb drops to almost zero. The magnetic stored energy from the coil is partially converted to thermal energy while some of the energy is inductively coupled into the neighboring coils, driving the current in those coils above the power supply current and driving those coils into quench. The "quench" propagates to neighboring limbs and the quench cascades around all the limbs.

This campaign was followed by energization of the PF coils. Commissioning had revealed a leak on the PF coil cooling circuit which restricts the operation of the PF coils pending a warm-up and repair cycle for Demo4. So, initial characterization of the PF's is limited, but early results are presented.

Abstract ID: 30208

CONTROLLING OXYGEN MIGRATION IN $YBa_2Cu_3O_{7-\delta}$ WITH SHORT CURRENT PULSES AND DEVICE GEOMETRY

D. Stoffels[1], C. C. Quaglio-Gomes[1,2], F. Egyenes[3], B. Aichner[4], A. Palau[5], W. Lang[4], M. Motta[2], A. V. Silhanek[1]

[1] *Q-MAT, Experimental Physics of Nanostructured Materials, Department of Physics, University of Liège, Liège, BELGIUM*
[2] *Departamento de Física, Universidade Federal de São Carlos, São Carlos, SP, BRAZIL*
[3] *Institute of Electrical Engineering, Slovak Academy of Sciences, Bratislava, SLOVAKIA*
[4] *Faculty of Physics, University of Vienna, Vienna, AUSTRIA*
[5] *Institut de Ciència de Materials de Barcelona, ICMAB-CSIC, Bellaterra, SPAIN*

High current densities can induce the directional diffusion of atoms in metallic films. In $YBa_2Cu_3O_{7-\delta}$ (YBCO), this electromigration process selectively acts on oxygen, permitting to vary the oxygen concentration in a targeted volume. This approach has proven successful in mapping the phase diagram of the material as a function of carriers' concentration [1] or as a way to manufacture memristive devices owing to its reversibility under small bipolar excitations [2]. Thus far, most of the investigations have been limited to pulsed excitation with current/voltage pulses on a millisecond or longer scale, for which thermal effects undeniably influence the process. In the present work, we explore the impact of pulse length on the onset current of electromigration of YBCO bridges, covering the range from 100 ns to 1 ms. Then, using Y-shaped three-terminal devices, we demonstrate the possibility to progressively displace oxygen vacancies on a hand-picked terminal without affecting the neighboring ones. The oxygen-rich and oxygen-depleted propagating fronts are directly visualized and are linked to the evolution of the electrical response. Finite element modelling captures these observations and predicts the spatiotemporal evolution of the vacancy fronts by accounting for transient Joule heating and oxygen diffusion due to electromigration. Together, these results establish insight into design rules for programmable, locally-selective oxygen control in YBCO, relevant for memristors and superconducting electronics.

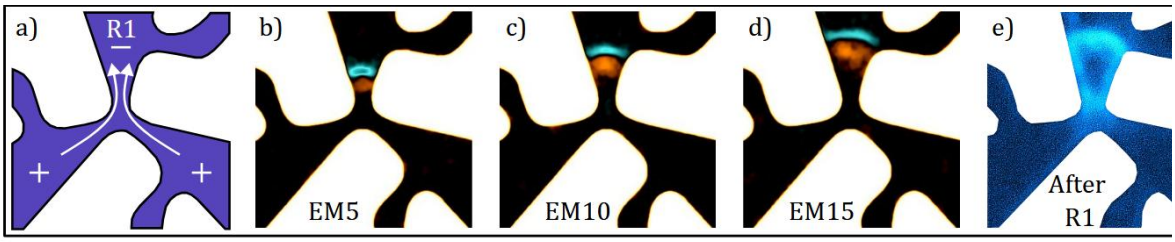

Fig. 1: *Panel (a) illustrates the electrical configuration used to selectively drive electromigration, while panels (b–d) show differential optical images acquired after 5, 10, and 15 runs, respectively. In these images, the oxygen-depleted regions exhibiting higher optical reflectivity are highlighted in light blue. Panel (e) shows the accumulated effect of all 15 EM runs, where overall reflectivity changes are emphasized with a blue scale.*

References

[1] E. Trabaldo, *et al.*, Phys. Rev. Appl. **17**, 024021 (2022).

[2] S. Marinković, *et al.*, Phys. Rev. B **110**, 165157 (2024).

Abstract ID: 30394

LOW-ENERGY CHARGE EXCITATIONS IN CUPRATE SUPERCONDUCTORS VIA RESONANT INELASTIC X-RAY SCATTERING

T. Tohyama

Tokyo University of Science, Department of Applied Physics, 125-8585, Tokyo, JAPAN

Resonant inelastic x-ray scattering (RIXS) has made remarkable progress through studies of strongly correlated electron systems, particularly the cuprate high-temperature superconductors [1]. Improvements in the energy resolution of L-edge RIXS have enabled the observation of momentum-dependent charge excitations across the superconducting gap in cuprates [2]. However, a comprehensive understanding of the full spectrum of charge excitations remains incomplete. While the broadening of single-particle electronic bands in momentum k space arising from electron-electron interactions has been extensively studied using angle-resolved photoemission spectroscopy as a k-dependent anisotropic scattering process, its fingerprints in two-particle excitations in momentum Q space have rarely been considered in RIXS analyses. In this work, we investigate the Q-dependent electron dynamics in optimally doped $Bi_2Sr_2CaCu_2O_{8+\delta}$, expressed through the dynamical charge susceptibility measured by RIXS [3]. In the normal state, the RIXS spectra exhibit a continuum of excitations extending down to 0 meV, whereas in the superconducting state, the spectral weight is suppressed below 80 meV without any corresponding enhancement at higher energies similar to the previous study [2]. To elucidate the observed energy and Q evolution, we introduce a phenomenological form of the dynamical charge susceptibility based on a tight-binding model of the cuprates, incorporating the effects of k-dependent anisotropic electronic scattering. We demonstrate that only the susceptibility model including this anisotropic scattering successfully reproduces the RIXS data, underscoring its essential role in describing the Q dependence of low-energy charge excitations.

References

[1] For example, K. Ishii, T. Tohyama and J. Mizuki, J. Phys. Soc. Jpn. **82**, 021015 (2013); T. Tohyama, J. Elec. Spectro. Related Phenomena **200**, 209 (2015).
[2] H. Suzuki *et al.*, npj Quantum Mater. **3**, 65 (2018).
[3] J. Li, *et al.*, Phys. Rev. Research **7**, 023310 (2025).

Abstract ID: 30556

CRITICAL PHOTOINDUCED REFLECTIVITY RELAXATION DYNAMICS IN SINGLE-LAYER Bi-BASED CUPRATES

T. Shimizu[1], R. Tobise[1], T. Kurosawa[1], S. Tsuchiya[1], Y. Toda[1], M. Oda[2], V. V. Kabanov[3], D. Mihailovic[3], T. Mertelj[3]

[1] *Department of Applied Physics, Hokkaido University, Sapporo 060-8628, JAPAN*
[2] *Department of Physics, Hokkaido University, Sapporo 060-0810, JAPAN*
[3] *Complex Matter Dept., Jozef Stefan Institute, Jamova 39, Ljubljana, SI-1000, SLOVENIA*

Quantum criticality in overdoped superconducting cuprates has remained an unresolved issue despite intensive and systematic research of equilibrium properties. Here we report on nonequilibrium photoinduced transient reflectivity dynamics in heavily overdoped single-layer cuprate $(Bi,Pb)_2Sr_2CuO_{6+\delta}$ (Pb-Bi2201), across the pseudogap and superconducting endpoint dopings. We find that just below the pseudogap endpoint doping the normal-state transient reflectivity dynamics resemble the pseudogap response observed in optimally doped La-Bi2201. Differently from the optimal doping, however, the relaxation time exhibits a power-law divergence, $\tau \sim 10\hbar/k_BT$, signaling a possible quantum critical behavior at the pseudogap end point doping. A similar, but less pronounced, power-law increase in relaxation time is also observed in Pb-Bi2201 just beyond the pseudogap doping end point.

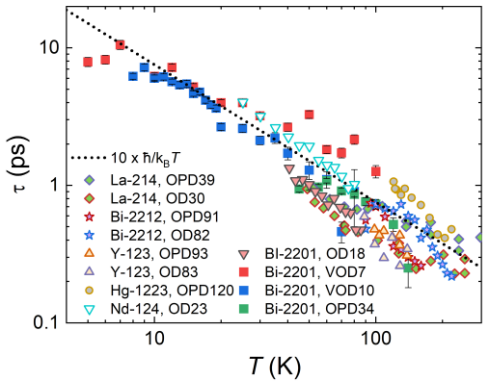

Fig. 1: *Temperature dependence of the normal-state transient-reflectivity relaxation time in various optimally doped (OPDx) and overdoped (ODx) cuprates, where x corresponds to T_c in K. The data for La-124, Bi-2212, Y-123, Hg-1223, Bi-2201 (OD18) and Nd-124 were taken from [1], [2,3], [4], [5], [6] and [7], respectively.*

References

[1] P. Kusar, *et al.*, Phys. Rev. B **72**, 014544 (2005).
[2] Y. Toda, *et al.*, Phys. Rev. B **90**, 094513 (2014).
[3] Y. Toda, *et al.*, Phys. Rev. B **104**, 094507 (2021).
[4] J. Demsar, *et al.*,, Phys. Rev. Lett. **82**, 4918 (1999).
[5] J. Demsar, *et al.*, Phys. Rev. B **63**, 054519 (2001).
[6] M. L. Schneider, *et al.*, EPL **60**, 460 (2002).
[7] J. P. Hinton, *et al.*, Phys. Rev. Lett. **110**, 217002 (2013).

Abstract ID: 30389

CHARGE, SPIN AND LATTICE DEGREES OF FREEDOM IN $YBa_2Cu_3O_x$ STUDIED BY ELECTRON PARAMAGNETIC RESONANCE

A. Shengelaya[1,2], A. Maisuradze[1], E. Pomjakushina[3], K. Conder[3], H. Keller[4]

[1] *Department of Physics, Tbilisi State University, 0179 Tbilisi, GEORGIA*
[2] *Andronikashvili Institute of Physics, Tbilisi State University, 0177 Tbilisi, GEORGIA*
[3] *PSI Center for Neutron and Muon Sciences CNM, 5232 Villigen PSI, SWITZERLAND*
[4] *Physik-Institut der Universität Zürich, 8057 Zürich, SWITZERLAND*

Electron paramagnetic resonance (EPR) of Yb^{3+} ions was used to study fluctuating electric and magnetic fields in $Y_{0.98}Yb_{0.02}Ba_2Cu_3O_x$ across the range from the undoped insulating to optimally doped, superconducting region ($6 < x < 7$). Measurements of the temperature dependence of the EPR linewidth revealed that both electronic and phononic processes contribute to spin relaxation. These contributions were separated, allowing their relative roles to be analyzed as a function of oxygen doping.

Significant changes in the Yb^{3+} EPR spectra, including the emergence of two distinct EPR lines, were observed below an oxygen content of $x = 6.4$. The results indicate the coexistence of fast and slow copper spin fluctuations near the boundary between superconducting and magnetic phases. This behavior is consistent with microscopic electronic phase separation into hole-rich and hole-poor regions. Theoretical analysis relates this phase separation to the formation of charged domain walls (stripes) in the CuO_2 planes.

Our findings demonstrate that Yb^{3+} ions are highly sensitive local spin probes for studying charge, spin, and lattice degrees of freedom in cuprate superconductors.

24 - HYDROGEN ENABLING TECHNOLOGY FOR SUPERCONDUCTORS

Abstract ID: 30170

AC INDUCTIVE ENERGIZATION TESTS OF HTS ASSEMBLED CONDUCTORS FOR LH2-COOLED HTS GENERATORS

M. Ohya, T. Gotomyo, T. Obuchi

Kwansei Gakuin University, School of Engineering, 669-1330, Hyogo, JAPAN

The research and development of high-temperature superconducting (HTS) generators harness the cryogenic energy of liquid hydrogen [1]. A 6 kA-class HTS assembled conductor is required to realize HTS field coils for a 600 MW-class generator. In this study, design experiments were conducted on an assembled conductor with an outer diameter of approximately 6 mm, which could carry 6 kA at 20 K and 5 T, followed by prototyping and verification. To verify the transport current characteristics of the assembled conductor, a 6 kA-class energization test under liquid-hydrogen cooling is necessary. However, the current capacity of the liquid-hydrogen test equipment installed at the Noshiro Rocket Test Center of the Japan Aerospace Exploration Agency is 500 A [2], and modifying it to test equipment with a current capacity of several kiloamperes is challenging. Consequently, alternating current (AC) inductive energization methods have been developed. In this method, the ends of a conductor are short-circuited to form a low-inductance secondary coil. A magnetically coupled high-inductance primary coil is excited by an AC to induce a large current in the secondary coil [3]. Preliminary investigations were conducted using AC inductive energization tests and simulations, employing a secondary coil with a single HTS wire [3]. Subsequently, AC inductive energization tests were performed on a short-circuited secondary coil with a single layer of an assembled conductor. We will present the test results of the experiments conducted under liquid-nitrogen and liquid-hydrogen cooling and discuss the cooling stability of HTS assembled conductors.

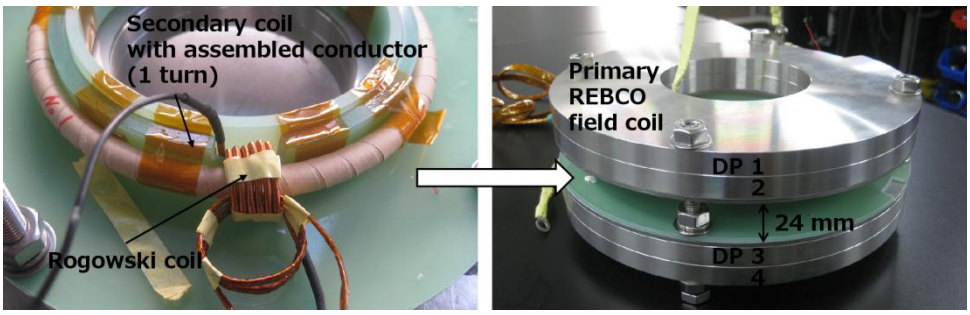

Fig. 1: *AC inductive energization tests of an HTS assembled conductor.*

This work was supported by the New Energy and Industrial Technology Development Organization (NEDO) under Project JPNP20004 and the NIFS Collaboration Research Program (NIFS23KIIA009).

References

[1] M. Ohya, *et al.*, IEEE Trans. Appl. Supercond., **34-3**, 5201507 (2024).

[2] M. Ohya, *et al.*, J. Phys.: Conf. Ser., **3054**, 012010 (2024).

[3] M. Ohya, *et al.*, IEEE Trans. Appl. Supercond., **36-3**, 5000204 (2025).

Abstract ID: 30416

RESEARCH AND DEVELOPMENT OF LIQUID HYDROGEN PUMPS DRIVEN BY HTS MOTORS

K. Kajikawa[1], T. Nakamura[2], H. Kobayashi[3], A. Kikuchi[4], T. Miura[5]

[1] Sanyo-Onoda City University, Dept. of Electrical Engineering, Yamaguchi 756-0884, JAPAN
[2] Kyoto University, Dept. of Electrical Engineering, Kyoto 615-8245, JAPAN
[3] Japan Aerospace Exploration Agency, Sagamihara, Kanagawa 252-5210, JAPAN
[4] National Institute for Materials Science, Tsukuba, Ibaraki 305-0047, JAPAN
[5] Torishima Pump Mfg. Co., Ltd., Takatsuki, Osaka, 569-8660 JAPAN

In the pioneering project, MgB_2 motors are fabricated to drive a centrifugal pump for transferring cryogenic liquids [1,2]. A rotor in the motors is composed of MgB_2 squirrel-cage windings and an iron core. As a result of load test in liquid helium, one of motors combined with a conventional type of armature with copper windings shows a synchronous torque about three times larger than a rated torque in an existing induction motor. By using this MgB_2 motor and separately developed MgB_2 level sensors, a pump system to transfer cryogenic liquids is constructed as shown in Fig. 1. An impeller with an outer casing driven by the MgB_2 motor located inside a metal cryostat pushes out cryogenic liquids into another glass Dewar vessel. A hand-made program code to control the MgB_2 motor and level sensors realizes automatic transfers of not only liquid helium but also liquid hydrogen. The other type of armature is also fabricated using MgB_2 racetrack coils. The fully superconducting motor combined with the MgB_2 rotor is successfully operated in liquid helium.

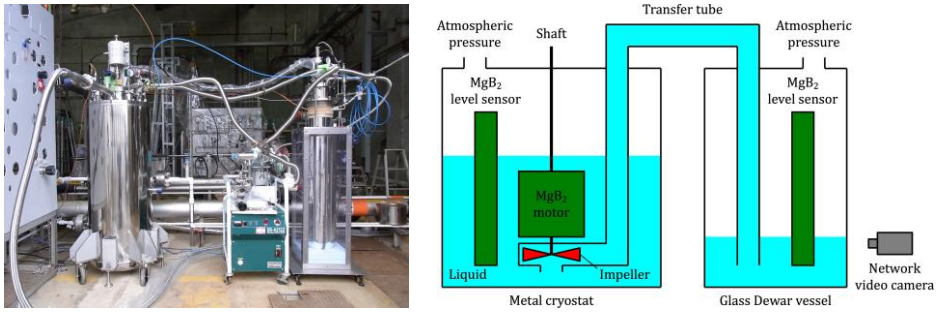

Fig. 1: *Pump system constructed using MgB_2 motor and level sensors.*

In the recent ongoing project, full-scale liquid hydrogen pumps driven by high temperature superconducting (HTS) motors are under development. Squirrel-cage rotor windings are fabricated by soldering HTS wires together. On the other hand, armature windings are consisting of metallic cables [3]. One of pumps is successfully assembled and operated in liquid hydrogen.

This presentation is partly based on results obtained from a project, JPNP23004, subsidized by the New Energy and Industrial Technology Development Organization (NEDO).

References

[1] K. Kajikawa, *et al.*, Cryogenics **52**, 615 (2012).
[2] K. Kajikawa, *et al.*, J. Supercond. Nov. Magn. **26**, 1537 (2013).
[3] K. Kajikawa, *et al.*, J. Supercond. Nov. Magn. **38**, 229 (2025).

Abstract ID: 30681

CRYOGENIC HELIUM GAS CIRCULATION SYSTEM FOR INDIRECT LH_2 COOLING OF SUPERCONDUCTING DEVICES

B. A. Glowacki[1,2]

[1] *Department of Materials Science and Metallurgy, University of Cambridge, 27 Charles Babbage Road, Cambridge CB3 0FS, ENGLAND*
[2] *Institute of Power Engineering, National Research Institute, Warsaw, POLAND*

Hydrogen cryomagnetics opens a practical route to operate superconducting devices in the 15–20 K temperature range using liquid hydrogen as a primary cryogen while avoiding direct contact between LH_2 and superconducting windings [1]. Hydrogen's favourable thermophysical properties and emerging energy infrastructure make it an attractive cold source, but safety, compatibility and integration constraints often demand an indirect interface. In this contribution we present a cryogenic helium gas circulation system, driven by a cryofan [2], that provides indirect cooling of superconducting devices such as DC and AC power cables, magnets and current leads [3]. In the proposed concept, compressed helium gas circulates in a closed loop through compact heat exchangers thermally anchored either to a stand-alone cryocooler or to an external LH_2 reservoir, or to hybrid arrangements combining both. The helium loop delivers uniform 15–20 K operation, decouples the superconducting payload from hydrogen handling when LH_2 is used, and eliminates boiling-cryo instability issues typical of two-phase coolants. We outline the thermodynamic design of the helium circulation loop, including pressure–temperature operating windows, mass-flow optimisation, and integration of low-loss cryofans and heat exchangers tailored to long-length superconducting systems. Building on previous work on hydrogen cryomagnetics, cryofan-based circulation, and indirect cooling of YBCO power cables, we discuss how engineered flow channels and micro-structured substrates can enhance heat-transfer coefficients and improve quench stability at intermediate temperatures. Particular attention is given to application-driven selection between LH_2-anchored systems (where hydrogen infrastructure is available) and purely cryocooler-based systems (for standalone or smaller-scale devices), including options for modular hybridisation. The paper will present example designs for 15–20 K operation of high-temperature superconducting devices, estimate cooling power and exergy efficiency for LH_2- and cryocooler-driven configurations, and compare their expected performance and cost to conventional liquid helium systems. This cryogenic architecture provides a scalable pathway to couple superconducting technologies with both the developing hydrogen economy and mature cryocooler technology, while maintaining robust safety barriers between hydrogen and electrical insulation systems.

References

[1] B. A. Glowacki, Materials, **18**, 3665 (2025).
[2] S. Pamid, *et al.*, Cryogenics **52,** 315–320 (2012).
[3] M. J. Cheadle, *et al.*, AIP Conf. Proc. **1573**, 1685–1693 (2014).

Abstract ID: 30701

LIQUID HYDROGEN-ENABLED COOLING OF SUPERCONDUCTING DEVICES FOR VARIOUS APPLICATIONS

S. V. Pamidi

The Center for Advanced Power Systems & FAMU-FSU College of Engineering, Florida State University, Tallahassee, Florida 32310, UNITED STATES OF AMERICA

There is increased interest in developing high temperature superconducting (HTS) power devices for the electric power grid, data centers, transportation systems, and industrial applications, to benefit from their high power densities and efficiencies. However, the cryogenic systems necessary to operate superconducting power devices add to the cost and complexity. To enable large-scale market penetration, revolutionary simplification of cryogenic cooling strategies is necessary. Fortunately, the ongoing development of green hydrogen technologies and the potential use of liquid hydrogen for large-scale energy storage will provide a solution for cooling HTS power devices. Liquid hydrogen serving as an integrated energy storage and cryogenic heat sink would be an excellent solution for systems that combine hydrogen and HTS devices.

Liquid hydrogen is being considered as an energy carrier for large electric transport platforms, such as electric aircraft and ships, to curb greenhouse gas emissions from the transportation sector. Superconducting technologies will provide the necessary power density to achieve the electrification of large transport platforms. Liquid-hydrogen-fueled platforms provide the synergy needed to reduce the complexity of superconducting technologies, as the liquid hydrogen at 20 K can serve as a cryogenic heat sink.

Hyperscale data centers are contemplating local renewable energy sources for power generation. The variable nature of power generation from solar and wind sources requires large-scale local energy storage to match supply and demand. Hydrogen produced using excess electrical power would serve as energy storage. However, the liquefaction of energy storage is energy-intensive. Hence, the cooling power of the 20 K liquid hydrogen must be exploited to offset the cost of liquefaction. Using liquid hydrogen as a cryogenic heat sink as part of the cooling strategies for HTS power devices eliminated the need for large mechanical cryocoolers and the corresponding capital and operating expenditures.

The integration of liquid hydrogen and HTS power devices will transform the power system of data centers, transportation platforms, and other power-hungry industrial operations. The integration will transform power systems by simultaneously addressing energy storage and efficient power distribution needs, and the solution will facilitate decarbonization across sectors and help achieve Net-Zero targets. The paper will discuss the opportunities and challenges of using liquid hydrogen in cryogenic cooling strategies of superconducting power applications.

25 - KAGOME MATERIALS FROM FUNDAMENTALS TO THEIR POTENTIAL APPLICATIONS

Abstract ID: 30089

TOPOLOGICAL HALL EFFECT ANISOTROPY IN KAGOME BILAYER METAL Fe_3Sn_2

C. Petrovic

SHARPS – Shanghai Advanced Research in Physical Sciences, CHINA

Topologically nontrivial electronic bands intertwined with magnetic order are widely recognized as fundamental source of novel states of matter and technologically important materials properties. Topological Hall effect (THE) arising from the noncollinear spin texture with nonzero spin chirality is a quintessential embodiment of this concept. Kagome lattices exhibit many exotic properties such as quantum spin liquid, Dirac or Weyl fermions and magnetic skyrmions. In Kagome bilayer lattice Fe_3Sn_2 topological spin textures are present at room temperature and over wide temperature and magnetic field regions. They are commonly observed by microscopy techniques in the real space and neutron scattering in the reciprocal space. In my talk I will present first room-temperature thermoelectric signature of skyrmionics textures in a simple thermal gradient [1]. Next, I will present interlayer transport and topological Hall effect anisotropy in mesoscopic Fe_3Sn_2 crystals [2]. For the first time we confirmed the existence of THE and skyrmionics bubbles when the magnetic field is applied in the hexagonal plane for the out-of-plane direction of current. Giant THE is observed in the skyrmion region, down to lower temperature where geometrically frustrated magnet enters the spin-glass state. We also present insight into magnetocrystalline anisotropy and exchange interactions via angular magnetoresistance as well as preliminary high pressure behavior [3].

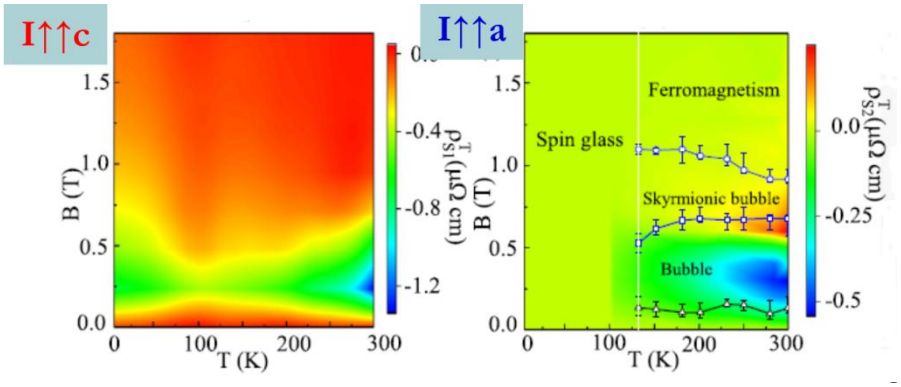

Fig. 1: *Topological Hall resistivity $\varrho^T(xy)_{S1}$ and $\varrho^T(xy)_{S2}$ between 5 and 300 K and B from 0 to 1.8 T. The open symbols represent critical fields of different magnetic phases from Adv. Mater. 29, 1701144 (2017).*

References

[1] Q. Du, M.-G. Han, Y. Liu, W. Ren, Y. Zhu and C. Petrovic, Adv. Quantum Technol. **3**, 2000058 (2020)

[2] Q. Du, Z. Hu, M.-G. Han, F. Camino, Y. Zhu and C. Petrovic, Phys. Rev. Lett. **129**, 236601 (2022).

[3] J. Liu, Z. Hu and C. Petrovic, in preparation (2025).

Abstract ID: 30168

MICROSCOPIC MUON SPIN ROTATION INSIGHTS INTO THE DISTINCT SUPERCONDUCTING REGIONS OF THE PHASE DIAGRAM IN Ti-DOPED CsV_3Sb_5

P. Král[1], S. S. Islam[1], A. C. Salinas[2], J. Graham[1], O. Gerguri[1], H. Luetkens[1], R. Khasanov[1], S. Wilson[2], Z. Guguchia[1]

[1] *PSI Center for Neutron and Muon Sciences CNM, 5232, Villigen PSI, SWITZERLAND*
[2] *Materials Department and California Nanosystems Institute, University of California Santa Barbara, 93106, Santa Barbara, USA*

Kagome materials provide a fertile platform for studying the interplay between unconventional superconductivity and intertwined electronic orders [1,2]. In the AV_3Sb_5 (A = K, Rb, Cs) family, superconductivity (SC) competes with charge order (CO), and chemical doping – such as Nb or Ta substitution in CsV_3Sb_5 – has proven to be an effective tuning method [3-6]. Motivated by these considerations, we turn to hole-doped Ti-CsV_3Sb_5, which hosts two distinct superconducting regimes separated by a critical doping level where charge order has been reported to be suppressed [7,8]. Focusing on two representative compositions – underdoped and optimally doped – we use muon spin spectroscopy to gain microscopic insight into the superconducting states on both sides of the critical doping level. We resolve clear differences in their paring behavior, demonstrating a qualitative change in the SC state. Employing hydrostatic pressure, we reveal a substantial effect on microscopic SC properties. Additionally, both doping levels exhibit the unconventional normal state behavior. All together, these findings demonstrate that Ti substitution and external pressure provide complementary routes to access and control distinct superconducting states in kagome metals.

References

[1] Y. Wang, *et al.*, Nat. Rev. Phys. **5**, 635 (2004).

[2 C. Mielke III, *et al.*, Nature **602**, 245 (2022).

[3] Z. Guguchia, *et al.*, Nat. Commun. **14**, 153 (2023).

[4] Y. Zhong, *et al.*, Nature **617**, 488 (2023).

[5] J. N. Graham, *et al.*, Nat. Commun. **15**, 8978 (2024).

[6] J. N. Graham, *et al.*, Commun. Phys. **8**, 318 (2025).

[7] G. Pokharel, *et al.*, Phys. Rev. Mater. **9**, 094805 (2025).

[8] K. Shtefiienko, *et al.*, Phys. Rev. B **111**, 235135 (2025).

Abstract ID: 30370

REAL MATERIALS CONTAINING KAGOME LATTICE: LATTICE DYNAMICS PERSPECTIVE

A. Ptok

Institute of Nuclear Physics Polish Academy of Sciences, Kraków, POLAND

The ideal two-dimensional kagome lattice has attracted significant attention due to its characteristic electronic band structure features. Unlike the honeycomb lattice, which exhibits Dirac and saddle points, the kagome lattice also hosts an ideal flat band. This unique lattice structure corresponds to rich physics, especially in the context of electronic properties. In several compounds containing the kagome sublattice, the realization of charge density waves (CDW) at low temperatures has been reported.

First, AV_3Sb_5 (A = K, Rb, Cs) compounds are rare examples where CDW coexists with superconductivity. The CDW is realized through atom displacement within the V-kagome sublattice [1]. Second, FeGe exemplifies a case where CDW is induced by correlation-driven phonon softening, resulting in a significant modification of the Ge atom [2]. In both cases, new system symmetries can be identified through phonon spectra analyses.

Lattice dynamics can also lead to intriguing findings. For CoSn-like compounds (P6/mmm symmetry), where both kagome and honeycomb lattices are present, we have discovered chiral phonons [3]. Additionally, in some cases, imaginary soft modes are observed, leading to new symmetries. In our study, we predicted the crystal structure of RhPb with P-62m symmetry (containing a distorted kagome lattice), which was confirmed experimentally [4].

In summary, studies of lattice dynamics can be a valuable tool to confirm [5] or negate [6] the realization of structures containing kagome-like sublattices.

References

[1] A. Ptok, A. Kobiałka, M. Sternik, J. Łazewski, P.T. Jochym, A. M. Oleś, and P. Piekarz, Phys. Rev. B **105**, 235134 (2022).
[2] A. Ptok, S. Basak, A. Kobiałka, M. Sternik, J. Łazewski, P. T. Jochym, A. M. Oleś, and P. Piekarz, Phys. Rev. Materials **8**, L080601 (2024).
[3] A. Ptok, A. Kobiałka, M. Sternik, J. Łazewski, P. T. Jochym, A. M. Oleś, S. Stankov, and P. Piekarz, Phys. Rev. B **104**, 054305 (2021).
[4] A. Ptok, W.R. Meier, A. Kobiałka, S. Basak, M. Sternik, J. Łażewski, P.T. Jochym, M.A. McGuire, B.C. Sales, H. Miao, P. Piekarz, and A.M. Oleś, Phys. Rev. Research **5**, 043231 (2023).
[5] S. Basak, and A. Ptok, Materials **16**, 78 (2023).
[6] A. Ptok, Physical Review B **109**, 216501 (2024).

Abstract ID: 30417

NMR INVESTIGATION OF THE CDW TRANSITION IN KAGOME METAL ScV_6Sn_6

C. N. Kuo[1,2,3], W. S. Tian[2], G. T. Chen[2], C. S. Lue[1,2,3]

[1] *Program on Key Materials, Academy of Innovative Semiconductor and Sustainable Manufacturing, National Cheng Kung University, Tainan 70101, TAIWAN*
[2] *Department of Physics, National Cheng Kung University, Tainan 70101, TAIWAN*
[3] *Taiwan Consortium of Emergent Crystalline Materials, National Science and Technology Council, Taipei 10601, TAIWAN*

Kagome metal of ScV_6Sn_6 has been of current interest as it features unique charge density wave (CDW) ordering accompanied by a structural phase transition, indicating the importance of lattice distortion for the onset of CDW order. To unveil the role of each individual atomic site for the CDW transition, we employed a local probe through the nuclear magnetic resonance (NMR) measurements in which the NMR signals from ^{45}Sc, ^{51}V, and ^{119}Sn nuclei were observed. A noticeable increase in the ^{45}Sc quadrupole frequency across $T_C = 92$ K was identified. The finding can be accounted for by the structural distortion involving the displacement of Sc and Sn atoms along the *c* axis. From the analysis of the NMR shifts, we quantitatively obtained the change in the electronic density of states (DOS) for each atom associated with the transition. We demonstrated a marked reduction in the V 3*d* Fermi-level DOS which can be rationalized as a manifestation of the structural transition. We also resolved three ^{119}Sn NMR resonance lines corresponding to three nonequivalent crystallographic Sn sites and thus estimated the variation in the 5*s* electronic states of each Sn atom in ScV_6Sn_6.

References

[1] C. N. Kuo, W. S. Tian, H. Y. Lee, C. K. Hong, Y. R. Ou, and C. S. Lue Phys. Rev. Res. **7**, 033251 (2025).

Abstract ID: 30169

BREAKING THE KAGOME LATTICE: MAGNETIC FRUSTRATION AND SPIN REORIENTATION IN $Fe_{32+\delta}Ge_{35-x}Si_x$

R. A. Khalaniya[1], V. Yu. Verchenko[1], A. V. Mironov[1], A. N. Samarin[2], A. V. Bogach[2], A. N. Kulchu[1], A. O. Polevik[1], Z. Wei[3], E. V. Dikarev[3], R. Stern[4], A. V. Shevelkov[1]

[1] *Lomonosov Moscow State University, Department of Chemistry, 119991 Moscow, RUSSIA*
[2] *Prokhorov General Physics Institute of the Russian Academy of Sciences, 119991 Moscow, RUSSIA*
[3] *University at Albany, Department of Chemistry, Albany, 12222 New York, UNITED STATES*
[4] *National Institute of Chemical Physics and Biophysics, 12618 Tallinn, ESTONIA*

Recent studies of the intermetallic compounds that contain kagome nets revealed various non-trivial magnetic and transport properties including skyrmion ordering, superconductivity and topological Hall effect [1]. Several other derivative lattices are also known, such as breathing kagome, hyperkagome or square kagome lattices, which conserve frustrated trigonal fragments and thus preserve some features of the pristine kagome lattice compounds. Previously, we have synthesized and studied new ternary intermetallic compounds $Fe_{32+\delta}Ge_{35-x}E_x$ (E = As, P), which present another way to modify the kagome lattice by breaking it into separate hexagrams arranged in a triangular lattice [2-4]. Despite these modifications, the compounds featured high degree of magnetic frustration $f = |\theta_W|/T_N > 3$ coming from relatively low Neel temperatures T_N of around 125 K and Weiss temperatures θ_W below −400 K. Below the transition temperatures, the underlying frustration causes the compounds to exhibit complex non-colinear magnetic structures, which change with the temperature [2-4].

In the present study, we have synthesized the third member of this family of compounds, $Fe_{32+\delta}Ge_{35-x}Si_x$ using solid-state and chemical vapor transport reaction both in powder and single crystalline forms. Structural analysis, showed that the Ge to Si substitution is limited to only of the Ge sites. Magnetic measurements showed antiferromagnetic ordering at $T_N \sim 150$ K, in spite of pronounced antiferromagnetic interactions indicated by strongly negative Weiss temperature θ_W of −500 K. At 80 K, the compound experiences spin reorientation, which can be also achieved above this temperature by applying the magnetic field along the *ab* plane. The detailed discussion of the crystal structure and magnetic properties will be given in the presentation.

This work is supported by the Russian Science Foundation, grant # 24-73-00024.

References

[1] Q. Wang, H. Lei, Y. Qi and C. Felser, Acc. Mater. Res. **5**, 786-796 (2024).

[2] R. A. Khalaniya, A. V. Mironov, V. Y. Verchenko, A. Jesche, A. A. Tsirlin and A. V. Shevelkov, Inorg. Chem. **55**, 12953-12961 (2016).

[3] R. A. Khalaniya, V. Y. Verchenko, Z. Wei, E. V. Dikarev, I. Heinmaa, R. Stern, A. Jesche, A. A. Tsirlin and A. V. Shevelkov, J. Alloys Compd. **779**, 229-236 (2019).

[4] R. A. Khalaniya, A. V. Sobolev, V. Y. Verchenko, A. A. Tsirlin, A. Senyshyn, F. Damay, I A. Presniakov and A. V. Shevelkov, Dalton Trans. **507**, 2210-2220 (2021).

Abstract ID: 30200

KAGOME ANTIFERROMAGNETS AS MULTIFUNCTIONAL SPIN-ORBIT PLATFORMS: FROM LARGE AHE TO TUNABLE SPIN PUMPING

S. Sachin[1], I. Sinha[1], B. K. Kuanr[2], S. Manna[1]

[1] *Department of Physics, Indian Institute of Technology Delhi, 110016, New Delhi, INDIA*
[2] *Special Centre for Nanoscience, Jawaharlal Nehru University, 110067, New Delhi, INDIA*

Kagome antiferromagnets (AFM) are rapidly emerging as playgrounds for unconventional spin physics. In particular, the noncollinear AFMs (Mn_3X family, where X = Pt, Ir, Sn) offer a versatile platform for ultrafast, field-free spintronic technologies owing to their Berry curvature driven topological transport and symmetry-controlled spin textures [1,2]. Among them, Mn_3Pt hosts multiple spin configurations that can be selectively stabilized through lattice and stoichiometric control, enabling access to distinct topological transport regimes. In this work, we grow high-quality Mn_3Pt films using magnetron sputtering and systematically tune the magnetic ground state by varying film stoichiometry ($Mn_{3+x}Pt_{1-x}$) [3]. The strong anomalous Hall response in Mn-rich films confirms the stabilization of a nontrivial Berry curvature driven AFM phase. To probe interfacial spin dynamics, we study ferromagnetic resonance (FMR) in Mn_3Pt interfaced with permalloy (Py). We observe a significant enhancement in Gilbert damping in Mn_3Pt/Py (3.1×10^{-2}) compared to Py (9.8×10^{-3}) driven by efficient spin pumping into the AFM layer. The linear linewidth scaling and effective spin mixing conductance ($g_{eff} \approx 4.8 \times 10^{18}$ m^{-2}) is comparable to other AFM-based systems [4]. Our results establish Mn_3Pt as a promising material platform for next-generation spintronic devices.

References

[1] N. Nagaosa, J. Sinova, S. Onoda, A. H. MacDonald, and N. P. Ong, Reviews of Modern Physics **82**, 1539 (2010).

[2] A. K. Nayak, J. E. Fischer, Y. Sun, B. Yan, J. Karel, A. C. Komarek, C. Shekhar, N. Kumar, W. Schnelle, J. K¨ubler, and C. Felser, Science Advances **2**, e1501870 (2016).

[3] I. Sinha, S. Sachin, S. Sinha, R. Roy, S. Kanungo, and S. Manna, Physical Review Materials **9**, 074202 (2025).

[4] I. Sinha, S. Sachin, P. Kumar, A. Pandey, B. K. Kuanr and S. Manna, arXiv:2508.21014 (2025).

26 - LARGE SCALE APPLICATIONS OF SUPERCONDUCTORS AND THEIR FUNDAMENTAL TECHNOLOGIES

Abstract ID: 30573

PERFORMANCE AND DEGRADATION MECHANISMS OF HIGH-J_c Nb_3Sn CICC FOR HIGH-FIELD APPLICATIONS

Y. Liu[1], C. Dai[1],Y. Wu[1], A. Nijhuis[2], A. Devred[3], J. Qin[1]

[1] *Institute of Plasma Physics, Chinese Academy of Sciences, 230031, Hefei, CHINA*
[2] *University of Twente, Faculty of Science and Technology, 7500AE, Enschede, NETHERLANDS*
[3] *CERN, TE Department, 1 Esplanade des Particules, CH-1211, Geneva, SWITZERLAND*

Burning plasma Experimental Superconducting Tokamak (BEST) targets compact, high-field operation to advance steady-state deuterium–tritium burning plasma research. In the BEST toroidal-field (TF) high-field region, the conductor is required to sustain a peak field of 13.5 T at an operating current of 55 kA, imposing a challenging coupled electromagnetic–thermal–strain environment on Nb_3Sn cable-in-conduit conductors (CICCs). To meet these engineering requirements, we performed a systematic study on several types of high-J_c Nb_3Sn strands, focusing on their coupled electromechanical and thermo-electromagnetic responses and the underlying microscopic degradation mechanisms (e.g., local plastic deformation and filament damage induced by cabling). Based on the strand-level findings, two types of cable pattern were developed and fabricated: a short-twist-pitch (STP) cable and a copper-wound-strand (CWS) cable. Short samples underwent full processing and qualification-style testing in the SULTAN facility, including electromagnetic load cycling, overload tests, warm-up/cool-down thermal cycling, and AC loss measurements, to benchmark current-sharing behavior and temperature sensitivity under representative loads. To identify the drivers of irreversible degradation, post-test conductors were analyzed using (i) an image-recognition workflow (Fiji/Matlab) to quantify cross-sectional geometric features such as local void fraction, centroid migration, strand contact, and ellipticity; and (ii) a magnetic-measurement-based inversion method that reconstructs the evolution of non-uniform internal strain distribution from AC magnetic susceptibility–temperature responses. The combined diagnostics reveal that strand migration and the accumulation of tensile strain during electromagnetic cycling dominate the degradation pathway, and they further demonstrate that the CWS configuration provides higher structural stiffness and improved mechanical stability compared with the STP configuration. These results establish an integrated strand–cable–conductor methodology for designing high-performance Nb_3Sn CICCs for high-field applications.

References

[1] R. Wesche, M. Bagnasco, P. Bruzzone, M. Calvi, F. Cau, R. Herzog, C. Marinucci, and B. Stepanov, *Results of conductor testing in SULTAN: A review*, WAMSDO Workshop Proceedings, CERN (2009).

[2] "Overview and updates of the Burning Plasma Experimental Superconducting Tokamak (BEST)," Ninth DEMO and Fusion Plants Workshop (IAEA), June 11, 2025.

Abstract ID: 30639

MAGNET TECHNOLOGY FOR MRI AT SIEMENS HEALTHINEERS

A. Johnstone

Siemens Magnet Technology, Oxford, UNITED KINGDOM

Superconducting magnet use within Magnetic Resonance Imaging (MRI) systems is a good case study for both the commercialization of superconductivity and the move to more environmentally sustainable superconducting technologies.

Commercialization has brought unique development challenges that need to be addressed within the magnet design. These challenges include design for high volume manufacture, transportation robustness, installation on a customer site, and use on a customer site. This talk will describe these challenges, and the way in which they are addressed in the MRI industry.

Key developments to improve sustainability include the minimization and removal of liquid helium from within MRI magnets, and development of energy saving features within the system. The helium reduction journey within Siemens Healthineers will be presented, and the status of the wider industry highlighted.

It is anticipated that lessons learnt within the MRI industry can be applied to the development of a variety of new large scale superconducting devices.

Abstract ID: 30655

CRYOGEN-FREE MAGNETS FOR MAGNETIC RESONANCE

J. Good

Cryogenic Limited, London, UK

Magnetic Resonance (MR) is a powerful tool with many applications, including Electron Paramagnetic Resonance (EPR), Nuclear Magnetic Resonance (NMR), Magnetic Resonance Imaging (MRI) and Dynamic Nuclear Polarisation (DNP). Growing problems with the cost and availability of liquid helium cause limitations in the use of superconducting magnets for Magnetic Resonance. Cryogen-free technology allows the magnets to work at temperatures around 4K without using liquid helium or liquid nitrogen. A mechanical refrigerator or a cold head is used. A compressor provides helium gas under pressure to the cold head in a closed cycle. The magnetic field can be adjusted and stabilised at will, allowing experiments at different frequencies.

Cryogen-free magnets have additional advantages over counterparts filled with liquid helium. They are much more compact, because they do not require tanks to keep liquid helium or nitrogen. They do not create a dangerous high pressure with the potential risk of suffocation in the event of a magnet quench. Another important innovation in cryogen-free magnets is an integrated cryostat, or Variable Temperature Insert (VTI). When the magnet reaches base temperature, part of the cooling power from the cold head can be used for cooling down the helium gas flow circulating continuously inside the integrated VTI. The temperature of helium gas, which is in thermal contact with a sample inside the VTI, can be stabilised in the range of 1.3K to more than 300K.

A potential disadvantage of cryogen-free magnets is temporal magnetic field variations due to the operation of the refrigerator. This can limit the use of cryogen-free technology in high-resolution NMR. Cryogenic has developed a system to minimise this issue. Examples of the application of cryogen-free magnets in EPR, NMR, MRI and DNP, its advantages and limitations will be discussed.

Abstract ID: 30686

HTS CONDUCTORS AND COILS WITH Bi2212 FOR FAST-RAMP AND HIGH FIELD USAGE

A. Otto[1], A. Bouthillette[1], B. Bouchard[1], A. Croteau[1], J. Voccio[1,2]

[1] *Solid Material Solutions LLC, 55 Middlesex St., North Chelmsford MA 01863 USA*
[2] *Wentworth Institute of Technology, 550 Huntington Ave., Boston MA 02115 USA*

Coils that operate affordably above 10 K in fast ramp and ac modes as well as avoiding trapped / shielding current flux issues require small cross-sectioned, fine-filament, axially twisted wire that is cabled into transposed forms because wide HTS tapes generate excessive losses. In order to address these areas, low loss, high Je Bi2212 wire and cable designs have now been developed with validation of low loss and performance by testing at several facilities coupled with modeling. In our first-generation commercial design, all required loss reducing features are built into nominally 0.14 mm to 0.16 mm diameter round Bi2212 wires, with effectively unmerged, small-sized filaments, short axial twist lengths and increased inter-filament resistances. Process and material science studies as well as a scale-up initiative have also established current density levels required for initial applications and 3 km piece length wire production for cable and wire wound coil feedstock. A baseline 16-strand Rutherford low loss cable has also been developed along with long length production for wind-and-react development of prototype small coils and with react-and-wind development of larger coils. Higher strand count cables are under development to provide optimal operating current ranges along with cable reinforcement techniques for the specific fields and configurations of targeted end user system coils. Applications developments are focused on i) stators with operability in the > 12 K temperature, ~500 Hz frequency and 1T field ranges, ii) fast ramped ion beam cancer treatment magnet systems, iii) scientific instrument magnets and iv) for slow ramp MRI and NMR field boosting coils where trapped flux / uniformity with tape forms can be more problematic. Early-stage prototype coils have been tested for transport properties, loss, stability, cool-ability and quench survivability, with positive results that meet key benchmark requirements. These data set to the stage for establishing commercial coil designs by integrating their development into initiatives that are developing next generation end user systems. Progress on the customization of these conductors and development of specific coil designs for applications in medical, aerospace, energy and instrument end user systems is underway and will also be reviewed.

Abstract ID: 30691

HTS MAGNET DEVELOPMENT AT TOKAMAK ENERGY

R. Bateman

Tokamak Energy, TE Magnetics Dept. 173 Brook Drive, Milton Park, OX14 4SD, UK

This presentation summarizes the high-temperature superconductor (HTS) magnet development program to date, that has been in progress at Tokamak Energy (TE). The program started back in 2015 and focused on the material properties of the 2nd generation HTS conductors, the ReBCO 2G coated conductors. The early objectives were to demonstrate that robust magnet coils could be manufactured and repeatedly operated from these ReBCO tapes.

Initial studies concentrated on non-insulated (NI) coils that were fully solder potted. This provided low-resistance paths to bypass any minor defects that may be present in the ReBCO conductor and also provided high thermal conductivity throughout the winding pack to extract any small heating that may have been present. The team at TE manufactured many of these NI coils from various manufacturers tapes which enabled us to compare the performance of the tapes. These became known as the Quality Assurance (QA) coils.

In parallel with this work, we developed a suite of modelling tools based on Matlab codes, ANSYS models, Dassault OPERA and COMSOL models, to model in detail the electromagnetic, thermal and mechanical behavior of the NI coils. The TE team worked closely with the team at Little Beast Engineering (LBE) to assist with the development and validation of their RAT and RACOON magnet analysis tools. Extensive work was done on ReBCO tape characterization, combining data from the SuperCurrent machine at the Robinson Research Institute (RRI) with data collected from QA coils tested in our Cryogenic Test Rig (CTR). With the solder potted NI coils run in vacuum at controlled temperatures, it was possible to run the coils in excess of their critical current, I_c, limits, defined as "saturation mode", to show that excess current would flow radially through the low-resistance solder path. The power dissipated by current flowing in this path could be determined as we were accurately measuring the power of the heaters required to maintain the coil temperature. As the power dissipated in the radial path increased the power dissipated in the control heaters dropped by and equivalent amount.

The TE team invented Electro-Thermal Interface (ETI) plates as a method of axially stacking QA coils to build larger magnets. The ETI plates have internal structures to inject the current into the correct positions in the coils to maximize the field that can be generated, and to ensure joints of sufficient contact area to avoid localized heating in the winding pack. The ETI plates avoid the need for layer-jump tapes between pancake coils. The NI coil pack terminated with ETI plates forms a versatile magnet building block to create larger magnet coils. This has been demonstrated up to 24 T by our Demo3 magnet. It is possible to make coils with large bore diameters and larger outer diameters, depending on the application.

Whilst the NI coil technology enables the construction of robust magnets, it is not useful for large scale magnets as the turn-to-turn resistance is too low, and therefore the magnet time constant becomes too long. For this reason, the TE team invented wind-in partial insulation (PI). This takes the form of a multi-layer tape which can have a through resistance which can be engineered to a desired value from the design of the layer connections. From our modelling tools developed by TE and LBE, we could precisely model the turn-to-turn resistance required to give a usable time constant for a given magnet size and self-inductance. In addition, we have demonstrated that the PI could be used as a quench protection system. If a hot-spot or voltage signal is detected in the coil, the power supply is switched off (effectively open circuit) forcing the coil current to flow through the radial PI path as the primary return current path. The current through the PI causes heating, which is distributed everywhere in each pancake coil, so through the whole magnet stack. This is a benign method of dissipating the stored energy in the magnet.

Demo2 demonstrated this principle very well, with the quench propagation, measured on the embedded voltage taps, agreeing very well with the simulations.

As part of the spherical tokamak magnet development, the TE team designed and built Demo4. This is covered in detail in another presentation at the conference but briefly it is 14 toroidal field (TF) limbs combined with 2 poloidal field (PF) magnets. Each TF limb consists of 2 ReBCO pancake coils. These are PI coils, 9 tapes per turn, graded down to 7, solder impregnated, each coil pair is terminated with thicker ETI plates which incorporate a supercritical helium cooling loop in each plate. This assembly is clamped in a 316-steel clamshell to support the large forces. The helium circulation is driven through the loops and heat exchangers by cryofans. Each TF limb receives helium at the same pressure, rate and temperature. Each PF magnet consists of a stack of 8 ReBCO coils. These are fully insulated coils with additional copper added into the turns, 8 HTS tapes plus 4 Cu tapes. Solder impregnated and also cooled by supercritical

helium circulation. The heat exchangers for the TF and PF loops have large heaters enabling the ability to control the loop temperatures anywhere between 80 K and 15 K, thus the cold mass of coils, which is in a vacuum, can be run at any of these temperatures. System commissioning is complete, and testing is in progress.

TE have now launched TE Magnetics to develop HTS magnets for other applications. Initial work has focused on fast ramping, fully insulated, but compact magnets. The early prototypes have been repeatedly ramped many times to demonstrate no degradation. Also, a variety of ReBCO racetrack magnets have been developed which look very promising. New winding tables and techniques have been developed for these purposes.

In addition to this, the TE team are developing new winding techniques for larger scale magnets. In this method, termed "Snaky winding", the coil "mandrel" does not rotate but the coil shape is preformed in a Cu channel. The winding table is a track the same size and shape as the coil. The coil is "wound" by trollies moving around the track performing various function to create the coil: tape laying, consolidation, insulation wrapping. Then the populated coil can be fitted with the protection and termination plates and fully potted.

Abstract ID: 30720

SUPERCONDUCTING MAGNET DEVELOPMENT AND PRODUCTION AT TESLA ENGINEERING LIMITED

A. Davidson, all the Tesla Engineering Limited Team

Tesla Engineering Limited, Water Lane, Storrington, Sussex, RH20 3EA, England, UK

Tesla Engineering Limited (Tesla) has a long history in the design and manufacture of electromagnets for scientific, medical and industrial applications. In addition to gradient coils and resistive magnets, Tesla develops complex, first-of-a-kind superconducting magnet systems and has a growing selection of superconducting magnet products. Current projects include high-field MRI magnets, cyclotron magnets, systems for nuclear fusion research, HTS coils and magnets for silicon crystal growth.

This presentation outlines the key stages involved in the design, development and manufacture of superconducting magnet systems at Tesla. The process begins with an initial conceptual design focusing on electromagnetic performance, thermal behaviour and mechanical integrity of the system. At this stage, the conductor, coil design and magnet protection scheme are proposed. Operating temperature calculations are performed in parallel with the development of the cryogenic architecture, while material selection is considered as a function of the system application and force constraints.

During the detailed design phase, the magnet design is iteratively refined and assessed against manufacturability, risk mitigation, cost and QA compliance. As a vertically integrated company, Tesla places emphasis on in-house manufacture. The principal production processes, from conductor winding and magnet assembly through to testing and installation, will also be presented, along with some of the major challenges encountered during manufacture.

Abstract ID: 30643

ELECTROMAGNETIC DESIGN OF 3 T NbTi SPLIT SUPERCONDUCTING MAGNET FOR BLANKET MULTI-PHYSICAL FIELD INTEGRATED TEST PLATFORM

J. Li[1,2], Z. Lin[1,2], L. Gao[1,2], S. Wei[1,2]

[1] *University of Science and Technology of China, Hefei, CHINA*
[2] *Institute of Plasma Physics, Hefei Institutes of Physical Science, Chinese Academy of Sciences, Hefei, CHINA*

Integrated qualification of fusion blanket technologies requires a comprehensive test platform capable of reproducing reactor-relevant coupled environments, including high vacuum, high heat-flux density, and strong magnetic fields. On top of the steady magnetic field, transient electromagnetic perturbations may be superimposed to enable semi-integral/integral-level validation of full-scale blanket components. We are developing a steady-field superconducting magnet system for such a blanket multi-physics integrated test platform.

The key engineering constraint suggests that a large room-temperature bore is required to accommodate the test vacuum vessel (for specimen installation and high heat-flux loading), a pulsed magnet, and associated diagnostic interfaces, while also reserving space for the cryostat wall, thermal shield, and assembly tolerances. Based on a preliminary split-solenoid overall configuration, the end-face distance between the opposed coils is fixed at 1600 mm. The coils are wound using a Rutherford cable (winding pack cell size 3.6 × 2.7 mm) in a split-solenoid arrangement to meet the field requirement under complex geometric and loading constraints while controlling high stresses.

Magnetostatic simulations and parametric analyses are performed using the RAT platform to evaluate the central field, peak field on the conductor, radial field homogeneity within the warm bore, and the effects of DT4 ferromagnetic components (core/yoke/inserts) on field efficiency and homogeneity. On this basis, the focus is shifting toward co-optimization of the split-solenoid coil geometry and DT4 core inserts, with multi-physics trade-offs under coupled electromagnetic–thermal–mechanical conditions to satisfy multiple constraints (field control, stress control, and operating margin).

Under the fixed 1600 mm end-face distance constraint, baseline models and the simulation workflow have been established and verified. Results show that a coil-only baseline design can achieve a 3.0 T central field (current approximately 561 A), but the radial homogeneity over a large working region remains insufficient: along the mid-plane (X direction), the field variation over ±500 mm is about 12.25–14.91%. A comparative assessment with DT4 core/yoke components indicates that, with identical coil geometry and current, ferromagnetic components can increase the central field by about 15%, but the working-region homogeneity may degrade (±500 mm: 12.25% → 13.73%), suggesting that ferromagnetic components need to be jointly optimized with the coil geometry rather than treated as passive add-ons.

Next, parametric sweeps and multi-objective optimization will be carried out for key geometric parameters of the coils and DT4 inserts (aperture, thickness, gaps, and relative positions) to converge on a practical candidate design for blanket multi-physics integrated qualification.

Abstract ID: 30515

UPDATE ON PARTICLE THERAPY SOLUTIONS AT MEVION MEDICAL SYSTEMS

M. Jones

Mevion Medical Systems, Inc., 01460, Littleton, MA, USA

Since the first proton therapy patient was treated in 1954, annual global utilization has grown to approximately 50,000 patients, representing only about 1% of all external beam radiation therapy cases. This remains well below the estimated 20% of patients who could benefit from proton therapy, as recent clinical studies have demonstrated its significant advantages over conventional radiation techniques.

To address this unmet need, Mevion Medical Systems, in collaboration with MIT PSFC, developed the world's smallest proton therapy accelerator, featuring a 9T Nb_3Sn superconducting magnet. This compact design enables mounting the accelerator directly on a rotating gantry, eliminating complex beamlines (DirectBeam™) and gantry bending magnets. First introduced in the S250 and S250i single-room systems, this architecture has successfully reduced facility construction and operational costs, with more than 14,000 patients treated since 2013.

Working with Leo Cancer Care, Mevion has used recent advances in 3D imaging, robotic patient positioning, and treatment planning—alongside its compact superconducting accelerator and DirectBeam™ architecture—to reduce both the size and complexity of its system. These innovations make upright patient treatment possible and eliminate the need for a large rotating gantry making installation into existing radiation therapy treatment rooms possible.

Announced in 2022 and FDA approved in 2025, the new ultracompact S250-FIT system is designed for installation within existing conventional radiation therapy bunkers, expanding access to proton therapy. In addition to its compact form factor, upright treatment introduces new clinical advantages and opportunities for continued innovation in particle therapy. This presentation will review these advancements and outline future development pathways for improving accessibility and clinical impact.

Abstract ID: 30568

FUTURE DIRECTIONS IN ACCELERATOR MAGNET TECHNOLOGY

L. Rossi

University of Milan, Dept. of Physics, and INFN-Division of Milan, LASA Laboratory, via Fratelli Cervi 201, 20054 Segrate (Milan), ITALY

Accelerators—and in particular high-energy colliders—have traditionally been major drivers of superconducting magnet technology. At the same time, they pose some of the most demanding challenges to magnet designers: very high magnetic fields with extreme current densities; exceptionally large stored energy per unit winding volume; stringent field-quality requirements, to be met at the centimetre distance from the winding and in dynamic operation; mechanically non-self-supporting geometries; high reproducibility over many power and thermal cycles; and the need to power hundreds of large magnets in series, with gigajoule-level stored energy. Last but not least, these systems must be highly reliable to cope with the very large number of devices involved (the LHC alone features nearly ten thousand superconducting magnets), while remaining affordable and sustainable.

REBCO conductors offer a potential solution to many of these requirements. However, their form factor—a thin and wide tape—poses intrinsic difficulties for field quality and AC losses, especially during current ramps. This talk will review the state of the art of both LTS and HTS developments for next-generation colliders and other accelerator classes, with particular emphasis on medical applications. It will outline the main lines of technological evolution and the key advances required, highlighting developments that may prove relevant well beyond accelerator science, for a broad range of scientific and societal applications.

Abstract ID: 30584

MRI STARTS TO FALL IN LOVE WITH HTS: FUTURE PERSPECTIVES OF CLINICAL MRI

D. W. J. Klomp[1,2]

[1] *Center for Image Science, University Medical Center Utrecht, THE NETHERLANDS*
[2] *Radiology, Radboud University Medical Center Nijmegen, THE NETHERLANDS*

MRI keeps evolving as recognized by over 6% increased diagnostics every year for the last decades. However, we have come to the stage that we can no longer manage the clinical requests (no staff) and at the same time we see a substantial gap in diagnosing disease at earlier stage or even to improve treatment efficacy with the help of improved MRI systems.

Clinical MRI is traditionally using LTS magnet technologies, which is currently favorable for cylindrical system in terms of financial cost and field stability. While active cooling technologies relax the need for liquid Helium supply and simplify installation of these systems they maintain sensitive to fluctuating fields coming from the fast switching gradient fields required for spatial encoding and contrast weighting. Moreover, when going to higher magnetic fields that meet the requirement for increased spatio-temporal resolution in MRI, the cryogenic conditions become more challenging, and the system consumes a substantial space considering the limited current density. Most of these constraints hinder progress in MRI for increasing field strength and thus performance as well as becoming more accessible.

While other LTS solutions may solve part of the challenges, here we present the direction of using HTS in MRI for two main applications: 1. Realizing a technically derisked 14T MRI system for not only enabling high resolution MRI, but also be able to visualize metabolism throughout the human body as well as neuro feed forward and feedback mechanisms. 2. Utilizing its favorable current density to realize compact and therefore accessible MRI systems that facilitate an MRI selfie (relaxing the requirement for staff).

Although HTS may be considered more expensive to LTS, one needs to realize that the hardware cost an MRI system is often less than 10% of the cost for an MRI diagnose. Moreover, the magnet is no longer the most expensive component of the MRI system, so rethinking MRI system design toward cost per diagnose rather than cost per scanner is favorable for the introduction of HTS in MRI.

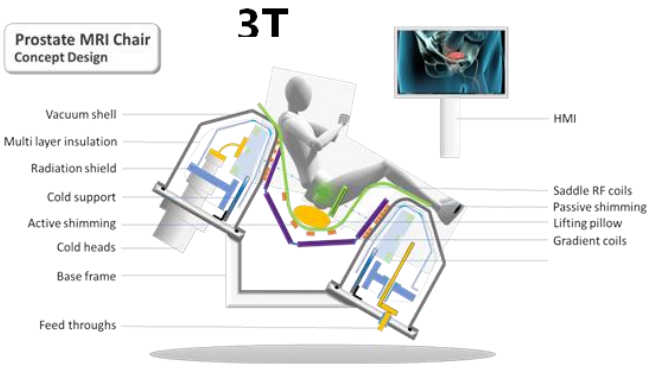

A demonstration of an MRI selfie (i.e. Figure 1) is provided as well as the considerations for realizing the 14T MRI, posing new questions to the HTS field in becoming less sensitive to AC fields (so to provide stronger (switched) gradient fields that may avoid the need for intravenous contrast agents), as well as better understanding of maintain a reproducible uniform field with HTS magnets.

Abstract ID: 30759

THE DYNAMIC 14T: WHAT HTS-BASED MRI CAN DO FOR COGNITIVE NEUROIMAGING

M. A. Cloos

Radboud University, Donders Center for Cognitive Neuroimaging, 6525 EN, Nijmegen, THE NETHERLANDS

The Dutch National 14 Tesla MRI Initiative in Medical Science (DYNAMIC) is reshaping the future of imaging through the development of the world's first 14 T MRI scanner—an instrument powerful enough to probe the human brain and body in fundamentally new ways. Developed in Nijmegen through an ambitious collaboration between academic researchers and industrial partners, DYNAMIC represents a major step forward in ultra-high-field MRI, with particular relevance for cognitive neuroimaging.

The neuroscience community has long been a key driver of advances in MRI magnet technology. Since the discovery of the blood-oxygen-level-dependent (BOLD) contrast mechanism [1], which enables indirect measurements of neuronal activity [2], MRI has become a cornerstone of cognitive neuroimaging [3]. Early functional MRI studies were conducted on clinical scanners operating at approximately 1.5 T, but it was quickly recognized that increasing magnetic field strength not only improves signal-to-noise ratio, but also enhances functional contrast and spatial specificity [4]. As a result, neuroscience researchers have consistently pushed MRI toward higher field strengths. Neuroscientists have therefore consistently pushed MRI toward higher fields. Dedicated research systems operating at 4 T paved the way for the widespread adoption of 3 T clinical scanners in the early 2000s, followed by 7 T systems entering clinical use around 2015.

Today, the state-of-the-art in human brain imaging is 11.7 T [5]. Conventional niobium–titanium (NbTi) superconductors are approaching their upper critical field of approximately 12 T, making further increases increasingly difficult. To overcome this limitation, DYNAMIC has turned to a high-temperature superconductor (HTS) magnet, enabling the leap to 14 T in a practical, unrestricted design [6,7].

In this talk, I will outline the design philosophy behind the DYNAMIC 14 T, trace the evolution of the project from its original concept, and explore how it could inspire a new frontier in MRI magnet technology.

References

[1] S. Ogawa, *et al.*, Magnetic Resonance in Medicine, 14(1), 68–78.2 (1990).
[2] N. Logothetis, *et al.*, Nature, 412(6843), 150–157 (2001).
[3] R.A. Poldrack, *et al.*, Handbook of Functional MRI Data Analysis. Cambridge University Press (2011).
[4] K. Ugurbil, Nature Reviews Neuroscience, 17(8), 456–468 (2016).
[5] N. Boulan, *et al.*, Nature Methods, 21(11), 2013–2016 (2024).
[6] S. Bates, *et al.*, MAGMA. 36(2), 211-225 (2023).
[7] Y. Li, S. Roell, Superconductor Science and Technology, 34(12), 125005 (2021).

27 - MACHINE LEARNING AND DATA-DRIVEN APPROACHES IN SUPERCONDUCTIVITY

Abstract ID: 30505

EFFICIENT ONLINE QUANTUM CIRCUIT LEARNING WITH NO UPFRONT TRAINING

T. O'Leary[1,2], P. Czarnik[3,4*], E. Pelofske[5], A. T. Sornborger[6,7], M. McKerns[6,8], L. Cincio[1,7]

[1] *Theoretical Division, Los Alamos National Laboratory, Los Alamos, NM, USA*
[2] *Department of Physics, Clarendon Laboratory, University of Oxford, Oxford, UK*
[3] *Institute of Theoretical Physics, Jagiellonian University, Krakow, POLAND*
[4] *Mark Kac Center for Complex Systems Research, Jagiellonian University, Krakow, POLAND*
[5] *Information Systems & Modeling, Los Alamos National Laboratory, Los Alamos, NM, USA*
[6] *Information Sciences, Los Alamos National Laboratory, Los Alamos, NM, USA*
[7] *Quantum Science Center, Oak Ridge, TN 37931, USA*
[8] *The Uncertainty Quantification Foundation, Wilmington, DE 19801, USA*

Optimization is a promising candidate for studying the utility of variational quantum algorithms (VQAs). However, evaluating cost functions using quantum hardware introduces runtime overheads that limit exploration. Surrogate-based methods can reduce calls to a quantum computer, yet existing approaches require hyperparameter pre-training and have been tested only on small problems. Here we show surrogate-based methods can enable successful optimization at scale, without pre-training, by using radial basis function interpolation (RBF) to construct an adaptive, hyperparameter-free surrogate. Using the surrogate as an acquisition function drives hardware queries to the vicinity of the true optima. For 16-qubit random 3-regular Max-Cut instances with the Quantum Approximate Optimization Algorithm (QAOA), our method outperforms state-of-the-art approaches, without considering their upfront training costs. Furthermore, we successfully optimize QAOA circuits for 127-qubit random Ising models on an IBM processor using 10^4-10^5 measurements. [1] Strong empirical performance demonstrates the promise of automated surrogate-based learning for large-scale VQA applications.

References

[1] T. O'Leary, P. Czarnik, E. Pelofske, *et al.*, *Efficient online quantum circuit learning with no upfront training*, Commun. Phys. **8**, 514 (2025).

11th International Conference on Superconductivity and Magnetism ICSM2026
4th International Conference on Quantum Materials and Technologies ICQMT2026
19th April to 26th April, 2026, Ölüdeniz – Fethiye/Muğla, Türkiye
https://icsmforever.org/

Abstract ID: 30644

VOLTAGE RISE PREDICTION OF REBCO COILS WITH MACHINE LEARNING FOR QUENCH PROTECTION

S. Noguchi[1], R. Sakakibara[2], T. Mato[1]

[1] *Hokkaido University, Faculty of Information Sci. & Tech., 062-0814, Sapporo, JAPAN*
[2] *Hokkaido University, Grad. School of Information Sci. & Tech., 062-0814, Sapporo, JAPAN*

High-field applications have been developed using Rare-earth Barium Copper Oxide (REBCO) coils. Meanwhile, quench protection of REBCO coils by detecting early voltage rises is difficult because the normal zone propagation is slow due to high heat capacity of REBCO material. When quench detection is failed, REBCO coils are possibly catastrophically destroyed such as burn-out or plastic deformation. Therefore, a new quench protection method must be developed as soon as possible.

We have developed a new detection method of voltage rise, which is followed by quench event, using a machine learning, such as long short-term memory (LSTM) [1] and convolutional neural network (CNN) [2]. The training data were created with electromagnetic partial element equivalent circuit (PEEC) method and thermal finite element method (FEM). The LSTM can predict a voltage rise followed by quench event; however, sufficiently long time cannot be taken to shut down the power supply of REBCO coils [1]. The developed method based on CNN can effectively predict a voltage rise of REBCO pancake coil 2 s prior to the reach to the critical coil voltage [2]. As the next step, the noise robustness of the developed method was investigated to apply it to a measured coil voltage including noises. The noises increase the number of false detections [see Fig. 1(a)]; therefore, we must develop a new voltage rise detection method based on a different machine learning; i.e. the Transformer model is employed to reduce the effect of noises. The false detections of voltage rise, as a quench sign, drastically decrease in number as shown in Fig. 1(a). Fig. 1(b) shows the voltage rise prediction using the Transformer model as a machine learning.

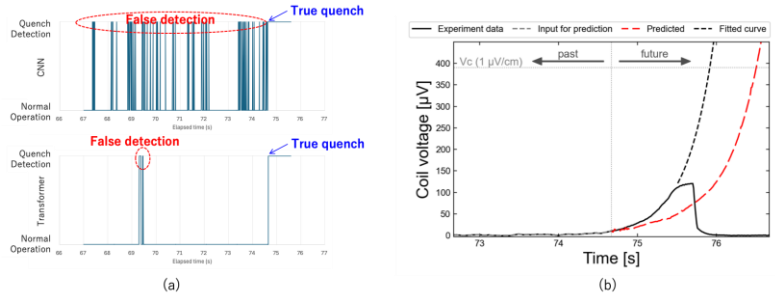

Fig. 1: *(a) Frequency of success and false quench detection by CNN and Transformer and (b) Voltage rise prediction. Noise deteriorates the accuracy of quench detection.*

References

[1] Y. Nakai and S. Noguchi, IEEE Appl. Supercond. **34(5)**, 4703005 (2024).
[2] T. Mato and S. Noguchi, IEEE Appl. Supercond. **35(5)**, 4603405 (2025).

Abstract ID: 30740

VISUAL FEEDBACK CONTROL USING A PLUME SHAPE MAP FOR REPRODUCIBLE SUPERCONDUCTOR THIN FILM DEPOSITION

K. Horio[1,5], T. Hachiya[1,5], S. Nakao[1,5], K. Kawabata[2,5], Y. Ichino[3,5], A. Ichinose[4,5], T. Horide[2,5], K. Matsumoto[2,5], T. Yoshida[2,5]

[1] *Kyushu Institute of Technology, 808-0196, Kitakyushu, JAPAN*
[2] *Nagoya University, 464-8601, Nagoya, JAPAN*
[3] *Aichi Institute of Technology, 470-0392, Toyota, JAPAN*
[4] *Central Research Institute of Electric Power Industry, 240-0196, Yokosuka, JAPAN*
[5] *JST-CREST JAPAN*

We developed a visual feedback control system to stabilize the PLD process for superconductor thin-film deposition. While plume dynamics are difficult to observe and sensitive to chamber conditions, our system achieves the desired plume shape by manipulating laser energy (LE) and oxygen partial pressure (OP).

Fig. 1 shows a conceptual diagram of the system. The core of the system is a "shape map" that represents complex plume shapes, extracted as point sets from binarized images, on a two-dimensional plane. By calculating the difference between the target and observed positions on this map, the system determines optimal LE and OP adjustments.

Fig. 2 shows the change in the shape difference between the observed and target plumes. Experimental results showed that the shape difference converged effectively over time. Remarkably, stable control was achieved using a simple P-control law, despite the inherent nonlinearity and response delays of the PLD process. This result confirms that the shape map effectively captures the complex correlation between plume morphology and operating conditions. Furthermore, this data-driven approach provides a robust framework for automating the PLD process, potentially enhancing the reproducibility of various functional thin films beyond superconductors.

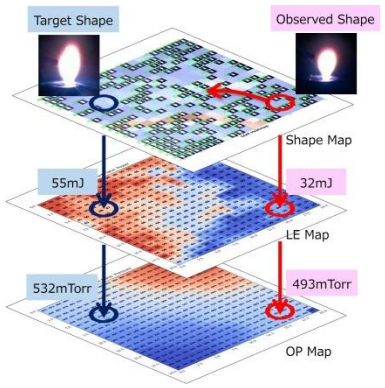

Fig. 1: *Visual feedback control system.*

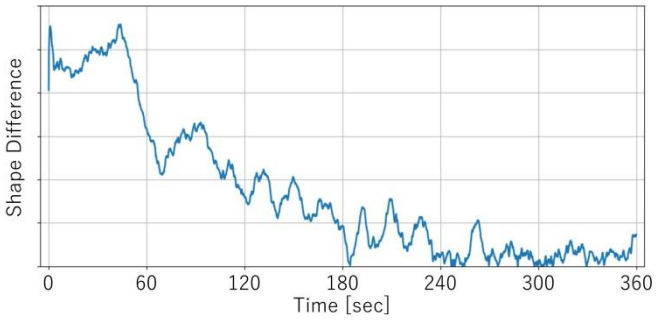

Fig. 2: *Shape distance between target and observed plumes.*

Acknowledgement

This study was supported by the JST-CREST program (JPMJCR2336).

Abstract ID: 30837

DIFFERENTIABLE PHYSICS AS THE ENGINE FOR GENERATIVE DISCOVERY: ACCELERATING SUPERCONDUCTOR DATA ACQUISITION WITH RIEMANNIAN DIRECT OPTIMIZATION

A. Chatterjee[1,2], J. Burton[1]

1 London Superconductors Ltd, London, UK
2 Department of Physics, University of Oxford UK

The development of generative machine learning models for unconventional superconductivity, such as cuprates, nickelates, and iron-based superconductors, is often bottlenecked by the computational cost and stability of simulating underlying electronic structures. Traditional Density Functional Theory (DFT) frameworks, primarily optimized for CPU architectures, can suffer from convergence instabilities like "charge-sloshing" [1] when approaching the complex magnetic phases of these materials.

We present **DiffDFT**, a GPU-native, fully differentiable DFT framework implemented in JAX [2]. At its core, we introduce a **Riemannian Direct Optimization (RDO)** paradigm that bypasses traditional self-consistent field (SCF) iterations by treating electronic structure as a constrained energy minimization problem on the complex Stiefel manifold. This approach enables the use of robust manifold-based optimization routines, ranging from Riemannian Gradient Descent to quasi-first order methods, ensuring stable, monotonic convergence even in pathologically difficult metallic systems. Our implementation natively supports Projector Augmented Wave (PAW) pseudopotentials, explicitly managing the non-trivial overlap metric within the Riemannian framework.

By leveraging automatic differentiation, DiffDFT provides exact gradients for complex functionals and response properties, including complete Pulay forces, with minimal implementation overhead. We discuss how this GPU-accelerated engine facilitates the exploration of large supercells and varied magnetic orderings. By enabling high-throughput data acquisition and supporting mixed-precision experimentation, DiffDFT serves as a differentiable physics engine for the gradient-guided discovery and inverse design of novel superconducting candidates.

References

[1] G. Kresse and J. Furthmüller, Phys. Rev. B **54**, 11169 (1996).
[2] J. Bradbury et al., JAX: composable transformations of Python+NumPy programs (2018). http://github.com/jax-ml/jax

Abstract ID: 30687

DATA DRIVEN AND NUMERICAL BASED OPTIMIZATION OF MAGNETIC LEVITATION SYSTEMS: FROM MULTI-SURFACE HTS MAGLEV TO HALBACH-ARRAY ELECTRODYNAMIC LEVITATION

U. K. Ozturk[1], E. C. Ozkat[2], M. Abdioglu[3]

[1] *Karadeniz Technical University, Dept. of Physics, 61080, Trabzon, TURKEY*
[2] *Recep Tayyip Erdogan University, Dept. of Mechanical Engineering, 53100, Rize, TURKEY*
[3] *Bayburt University, Dept. of. Mathematics and Science Education, 69000, Bayburt, TURKEY*

One part of this study aims to overcome the challenges posed by precise force measurement in high-temperature superconducting (HTS) magnetic levitation (Maglev) systems, including structural constraints, limitations of the stepper motors providing motion, sensor resolutions, and low cooling requirements for superconducting samples. The other part focuses on the use a optimisation based on numerical data to overcome the difficulty in conducting high-speed laboratory experiments in permanent magnet-based electrodynamic levitation (EDL) systems, a type of Maglev system. The results show that, in the static case of the HTS-PMG configuration, the machine learning-based optimization method used successfully determines the optimum magnetic force F_z and F_x depending on different experimental condition parameters such as permanent magnet width, field cooling height, and z-axis travel distance. Furthermore, it is observed that numerical data-based optimization methods can be used to determine the optimum values of parameters such as levitation and drag force of the permanent magnet guide path characteristics that provide the field source of high-speed EDL systems.

Abstract ID: 30761

MACHINE LEARNING PERSPECTIVES ON SUPERCONDUCTING MAGNETIC LEVITATION SYSTEMS: ENERGY EFFICIENCY TRENDS AND EMERGING DESIGN STRATEGIES

E. C. Özkat[1,2], U. K. Öztürk[2]

[1] *Department of Mechanical Engineering, Faculty of Engineering and Architecture, Recep Tayyip Erdogan University, 53100, Rize, TURKEY*
[2] *Electromagnetic Guidance and Acceleration Research Group (EMGA), Department of Physics, Faculty of Science, Karadeniz Technical University, 61080, Trabzon, TURKEY*

Superconducting magnetic levitation (Maglev) systems represent a promising high-efficiency transportation technology due to their reduced mechanical friction, high operational speed, and improved system stability. Recent advances in machine learning (ML) have introduced new opportunities for optimizing superconducting materials, magnetic configurations, and energy-performance characteristics in levitation-based transport systems. This paper presents a comprehensive literature review of data-driven methodologies applied to superconducting Maglev technologies, with particular emphasis on energy efficiency trends and emerging design strategies. The review examines the evolution of ML approaches from descriptor-based predictive models to structure-aware and physics-informed frameworks used in superconducting material optimization and system-level performance analysis. Key developments in uncertainty quantification, feature interpretability, and model generalization are discussed in the context of energy consumption, levitation force stability, and cryogenic efficiency. Furthermore, the integration of ML-assisted design workflows for superconducting magnets and transport infrastructure optimization is analyzed. The study identifies current limitations, including data scarcity, domain transfer challenges, and the need for standardized benchmarking protocols. Finally, future research directions toward sustainable, energy-efficient superconducting Maglev systems are outlined.

References

[1] Z.-J. Guo, , Z.-H. Guo, Z.-W. Chen, G.-Z. Zeng, J.-Q. Xu, *On the active flow control in maglev train safety under crosswinds: Analysis of leeward suction and blowing action*, Physics of Fluids, **36(9)** (2024). https://doi.org/10.1063/5.0224211

[2] L. Hörsting, C. Cleophas, *Scheduling shared passenger and freight transport on a fixed infrastructure*, European Journal of Operational Research, **306(3)**, 1158–1169 (2022). https://doi.org/10.1016/j.ejor.2022.07.043

[3] W. Hu, Y. Zhou, Z. Zhang, H. Fujita, *Model predictive control for hybrid levitation systems of maglev trains with state constraints*, IEEE Transactions on Vehicular Technology, **70(10)**, 9972–9985 (2021). https://doi.org/10.1109/tvt.2021.3110133

[4] M. Janić, *Estimation of direct energy consumption and CO_2 emission by high speed rail, transrapid maglev and hyperloop passenger transport systems*, International Journal of Sustainable Transportation, **15(9)**, 696–717 (2020). https://doi.org/10.1080/15568318.2020.1789780

[5] R. Tang, L. De Donato, N. BeŠInović, F. Flammini, R. M. P. Goverde, Z. Lin, R. Liu, T. Tang, V. Vittorini, Z. Wang, *A literature review of Artificial Intelligence applications in railway systems*, Transportation Research Part C: Emerging Technologies, **140**, 103679 (2022). https://doi.org/10.1016/j.trc.2022.103679

[6] M. Zhai, Z. Long, X. Li, *Fault-tolerant control of magnetic levitation system based on state observer in high speed maglev train*, IEEE Access, **7**, 31624–31633 (2019). https://doi.org/10.1109/access.2019.2898108

[7] Q. Zhu, S.-M. Wang, Y.-Q. Ni, *A review of levitation control methods for low- and medium-speed maglev systems*, Buildings, **14(3)**, 837 (2024). https://doi.org/10.3390/buildings14030837

Abstract ID: 30236

EXTENDING ALTERMAGNETIC MATERIAL BASE BY MAGNETRON SPUTTERING

D. Kriegner

Institute of Physics, Czech Academy of Sciences, 16200 Prague, CZECH REPUBLIC

Altermagnets are compensated collinear magnets in which opposite sublattices are connected by lattice rotations rather than translations [1]. This symmetry causes a spin-split band structure whose sign alternates in momentum space while the net magnetization vanishes. We recently demonstrated such band splitting in hexagonal MnTe [2], where it also enables linear responses, like anomalous Hall effect, and X-ray circular magnetic dichroism traditionally associated with ferromagnets [3-7]. In this talk I will discuss our progress in extending altermagnetism to sputtered thin films and thermoelectric phenomena [8,9]. These films provide a platform to explore spin-split bands and their spin-transport signatures. The results highlight altermagnetism as a promising platform for spintronics [10].

References

[1] L. Smejkal, J. Sinova, and T. Jungwirth, Phys. Rev. X **12**, 031042-040501 (2022).

[2] J. Krempaský, *et al.*, Nature **626**, 517–522 (2024).

[3] R. D. Gonzalez Betancourt, *et al.*, Phys. Rev. Lett. **130**, 036702 (2023).

[4] R. D. Gonzalez Betancourt, *et al.*, npj Spintronics **2**, 45 (2024).

[5] H. Reichlova, *et al.*, Nat. Commun. **15**, 4961 (2024).

[6] A. Hariki, *et al.*, Phys. Rev. Lett. **132**, 176701 (2024).

[7] O. J. Amin, *et al.*, Nature **636**, 348–353 (2024).

[8] S. P. Bommanaboyena, *et al.*, Phys. Rev. Materials **9**, 064402 (2025).

[9] A. Badura, *et al.*, Nat. Commun. **16**, 7111 (2025).

[10] T. Jungwirth, J. Sinova, P. Wadley, D. Kriegner, H. Reichlova, F. Krizek, H. Ohno, L. Smejkal, arXiv:2508.09748 [cond-mat.mtrl-sci]

Abstract ID: 30243

HALL EFFECT AND NONRECIPROCAL CURRENT IN CLEAN CHIRAL MAGNETS: ASYMMETRIC SCATTERING AND QUANTUM FLUCTUATIONS

H. Ishizuka

Institute of Science Tokyo, Dept. of Physics, 142-0041, Tokyo, JAPAN

Chiral spin states give rise to a variety of fascinating transport phenomena, including the anomalous Hall effect (AHE) and nonreciprocal responses. The AHE induced by scalar spin chirality [1–3] has become a popular tool for detecting non-coplanar magnetic textures such as skyrmion crystals, while the electrical magnetochiral effect probes vector spin chirality [4]. Recent experimental advances have enabled detailed studies of these phenomena, revealing rich features such as nonmonotonic temperature dependence and enhanced responses under external pressure—behaviors presumably related to enhanced thermal and quantum fluctuations. However, a theoretical understanding of these behaviors has remained elusive.

In this talk, we present our recent studies on the effects of thermal and quantum fluctuations in chirality-related phenomena in highly conductive metals [5,6]. Using a semiclassical theory, we derive a general formula and analyze the temperature and magnetic-field dependence of the chirality-induced AHE in the regime where skew scattering dominates [5]. The results reveal nonmonotonic temperature dependence and sign reversals originating from competition between short-range and long-range spin correlations, providing a remarkably simple physical picture behind these complicated phenomena.

We also address the role of quantum fluctuations in the AHE and nonreciprocal response [6]. We show that the coexistence of quantum spin fluctuations and vector spin chirality gives rise to a logarithmic temperature enhancement of the electrical magnetochiral effect through a mechanism analogous to the Kondo effect (Fig. 1). This quantum correction can become comparable to the classical contribution near the Kondo temperature; notably, no such enhancement appears in the AHE to leading order. These results demonstrate the distinct roles of classical spin correlations and quantum fluctuations in chirality-related transport phenomena.

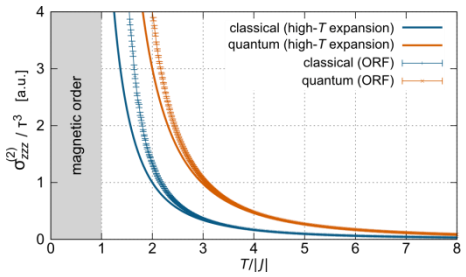

Fig. 1: *Enhanced nonreciprocal response by quantum spin fluctuations (right)*

References

[1] J. Ye, *et al.*, Phys. Rev. Lett. **83**, 3737 (1999).

[2] K. Ohgushi, S. Murakami and N. Nagaosa, Phys. Rev. B **62**, R6065 (2000).

[3] H. Ishizuka and N. Nagaosa, Sci. Adv. **4**, eaap9962 (2018).

[4] H. Ishizuka and N. Nagaosa, Nat. Commun. **11**, 2986 (2020).

[5] R. Terasawa, M. Udagawa and H. Ishizuka, Phys. Rev. Lett. **135**, 256303 (2025).

[6] H. Murata and H. Ishizuka, *submitted.*

Abstract ID: 30340

UNUSUAL CO-PLANAR MAGNETIC ORDER IN $In_2Ir_2O_7$

A. Yaresko[1], A. Krajewska[1], T. Takayama[1,2], H. Takagi[1]

[1] Max Planck Institute for Solid State Research, 70569 Stuttgart, GERMANY
[2] National Institute for Materials Science, Tsukuba, JAPAN

Most of $R_2Ir_2O_7$ iridates with the pyrochlore structure, where R^{3+} is a rare earth ion or Y, undergo a transition to a magnetically ordered state. Neutron diffraction experiments showed that the magnetic order is noncollinear with Ir^{4+} magnetic moments pointing either to or from the center of a tetrahedron. This all-in-all-out (AIAO) order is thought to be stabilized by strong Dzialoshinskii-Moria interaction (DMI) allowed by the symmetry of the pyrochlore lattice.

Recently, a new $In_2Ir_2O_7$ iridate was synthesized in which the trigonal distortion and Ir-O-Ir bond bending is even stronger than in $Lu_2Ir_2O_7$ [1]. Thus, one would expect that also in this compound DMI stabilizes AIAO order.

In order to verify this we performed LDA+*U* calculations for $In_2Ir_2O_7$ and $R_2Ir_2O_7$ (R=Y, Lu, Eu, Nd) assuming different noncollinear magnetic structures. For $R_2Ir_2O_7$, in agreement with neutron diffraction data the lowest energy was obtained for AIAO order. Moreover, the estimated strength of DMI increases with the increase of the trigonal distortion in compounds with a smaller R^{3+} ion. For $In_2Ir_2O_7$, however, noncollinear co-planar Palmer-Chalker order is found to be the most favorable one. This prediction is supported by recent neutron diffraction experiments which exclude AIAO order as a possible ground state. Comparison of exchange parameters estimated from the calculations suggests that the change of the magnetic ground state in $In_2Ir_2O_7$ may be caused by weakening of DMI as a result of strong In–O covalency.

References

[1] A. Krajewska, *et al.*, Phys. Rev. B **101**, 121101 (2020).

Abstract ID: 30374

SPIN-SELECTIVE ELECTRON TRANSPORT IN CHIRAL DIRUTHENIUM PADDLEWHEEL MONOLAYERS

I. Coloma[1], E. A. Hillard[1], N. Giaconi[2], S. Herrero[3], P. Rosa[1], L. Poggini[2], M. Mannini[2], M. Cortijo[3], T. Buffeteau[4], M. Gonidec[1]

[1] *Univ. Bordeaux, CNRS, Bordeaux INP, ICMCB, UMR 5026, F-33600 Pessac, FRANCE*
[2] *Department of Chemistry "Ugo Schiff" (DICUS) & INSTM Research Unit, University of Florence, Sesto Fiorentino 50019, ITALY*
[3] *Dept.of Inorganic Chemistry, Faculty of Chemical Sciences, Complutense University of Madrid, Avda. Complutense s/n, 28040 Madrid, SPAIN*
[4] *Univ. Bordeaux, CNRS, Bordeaux INP, ISM, UMR 5255, F-33405 Talence, FRANCE*

Chirality-induced spin selectivity (CISS) enables spin-polarized charge transport in chiral materials without external magnetic fields, but discrepancies between theory and experiment underscore the need for molecular systems with well-controlled structure, orientation, and electronic properties. Coordination complexes are attractive candidates due to their modular design, metal-centered chirality, and tunable electronic structure.

We developed a reproducible strategy to form electrically stable self-assembled monolayers (SAMs) from a helicoidal diruthenium paddlewheel complex on template-stripped gold [1]. Using a racemic [Ru_2(μ-ap)$_4$(NCS)] system, axial thiocyanate ligands enable covalent attachment, yielding smooth, densely packed monolayers with a preferential alignment of the Ru–Ru axis normal to the surface. AFM, ToF-SIMS, and PM-IRRAS confirm film integrity. Charge transport through Au^{TS}–SAM//Ga_2O_3/EGaIn junctions shows narrow current density distributions and excellent stability, comparable to benchmark alkanethiol SAMs.

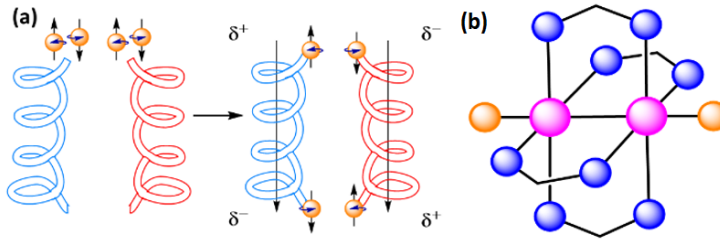

Fig. 1: *(a) Schematic of the CISS effect; (b) Representative paddlewheel compound.*

Building on this platform, enantiopure Ru_2^{5+} paddlewheel complexes incorporating chiral camphorsulfonyl-based ligands were synthesized to access well-defined (R)- and (S)-configurations while retaining the anchoring motif. These complexes form high-quality SAMs on Au and Ni/Au substrates. Magnetoconductive AFM reveals pronounced spin-dependent transport, with spin polarizations up to 81%, demonstrating efficient spin filtering. Together, these results establish chiral diruthenium paddlewheel complexes as a robust molecular materials platform for investigating CISS.

References

[1] I. Coloma, T. Buffeteau, G. Pecastaings, S. Herrero, E. A. Hillard, P. Rosa, M. Cortijo, M. Gonidec, Naoscale **17**, 12065–12071 (2025).

[2] I. Coloma, T. Buffeteau, N. Giaconi, L. Poggini, M. Mannini, S. Herrero, E. A. Hillard, P. Rosa, M. Cortijo, M. Gonidec, *article in preparation*.

Abstract ID: 30398

CHIRALITY-DEPENDENT SPIN POLARIZATION IN METALS: LINEAR AND QUADRATIC RESPONSES

Y. Kato

Department of Basic Science, the University of Tokyo, 3-1-7, Komaba, Tokyo 153-8902, JAPAN

We study spin polarization induced by locally injected electric currents in a metal whose spin--orbit coupling reflects its structural chirality.We reveal both spin polarization in the bulk in the linear response and antiparallel spin polarization near the interface in the quadratic response to electric fields, and reproduce the experimentally observed correlation between the chirality of the metal and the direction of spin polarization.In particular, we elucidate that the sign of the spin polarization in the quadratic response is opposite to that expected from the bulk spin current. This sign discrepancy originates from spin polarization induced by dipole-like charge distribution appearing in the quadratic response.

This presentation is based on a collaboration with Kosuke Yoshimi, Yuta Suzuki, Shuntaro Sumita, Takuro Sato, Hiroshi M. Yamamoto, Yoshihiko Togawa, Hiroaki Kusunose, and Jun-ichiro Kishine.

References

[1] K. Yoshimi, N. P. Author1, Phys. Rev. A **70**, 013603 (2004).

Abstract ID: 30420

POLARIZED NEUTRON SCATTERING IN MAGNETISM

A. Goukassov

Leon Brillouin Laboratory, CEA-CNRS, Gif sur Yvette, FRANCE

Polarized neutrons are crucial to meet the challenges raised by the interplay between magnetism and superconductivity, studies of frustrated systems with emergent and topological states such as magnetic monopoles in spin-ice, chirality of the spin waves and multipoles in altermagnets and other domains of magnetism. In this talk I shall present recent application of polarized neutron powder diffraction in the domain of molecular magnetism[1,2] and nanomagnetism, which allow characterization of the local susceptibility parameters in very complex magnetic compounds and in some cases quantify their local exchange and anisotropy parameters. Recent results of spin waves study of canonical altermagnet MnF_2 using polarized neutron scattering [3,4] will be also presented.

References

[1] I. A. Kibalin and A. Gukasov, *Local magnetic anisotropy by polarized neutron powder diffraction:Application of magnetically induced preferred crystallite orientation*, Phys. Rev. Res. **1**, 033100 (2019).

[2] E. A. Klahn, E. Damgaard-Møller, L. Krause, I. Kibalin, A. Gukasov, S. Tripathi, A. Swain, M. Shanmugam, J. Overgaard, *Quantifying magnetic anisotropy using X-ray and neutron diffraction*, IUCrJ (2021).

[3] P. A. McClarty, A. Gukasov and J. G. Rau, *Observing altermagnetism using polarized neutrons*, Phys. Rev. B **111**, L060405 (2025).

[4] Q. Faure, D. Bounoua, V. Balédent, A. Gukasov, V. O. Garlea, A. Ribeiro, J. G. Rau, S. Petit and P. McClarty, *Altermagnetism revealed by polarized neutrons in MnF2*, ArXiv:2509.07087 (2025).

11th International Conference on Superconductivity and Magnetism ICSM2026
4th International Conference on Quantum Materials and Technologies ICQMT2026
19th April to 26th April, 2026, Ölüdeniz – Fethiye/Muğla, Türkiye
https://icsmforever.org/

Abstract ID: 30438

CRYSTALLOGRAPHIC FRUSTRATION AS A MEANS TO INDUCE COMPLEX SPIN TEXTURES TOWARD NEW QUANTUM MATERIALS

Y.-X. Wang[1,2], I. Campbell[1], X. Wang[3], M. Shatruk[1,4]

[1] *Florida State University, Dept. of Chemistry & Biochemistry, Tallahassee, FL 32306, USA*
[2] *RWTH Aachen University, Institute of Inorganic Chemistry, 52056 Aachen, GERMANY*
[3] *Neutron Scattering Division, Oak Ridge National Laboratory, Oak Ridge, TN 37831, USA*
[4] *Florida State University, FSU Quantum Initiative, Tallahassee, FL 32306, USA*

Materials with intricate spin textures are attractive from both fundamental and practical perspectives [1,2]. The complex patterns of magnetic moments that develop on crystal lattices could enable reliable information storage and processing, including applications in topological quantum computing. In this work, we report the discovery of a complex, skyrmionic-like spin texture in a non-centrosymmetric material, $MnCoGe_{1/3}As_{2/3}$ [3]. This compound arises from structural frustration at the interface between centrosymmetric parent structures of MnCoGe and MnCoAs. Our results demonstrate that this type of structural frustration is a useful indicator for spotting compositional regions where intricate magnetic behavior and associated non-trivial magnetic structures are likely to develop. Specifically, $MnCoGe_{1/3}As_{2/3}$ displays a modulated cycloidal antiferromagnetic arrangement of electron spins on a non-centrosymmetric hexagonal lattice of the ZrNiAl-type structure. This work establishes a novel approach for discovering materials with exotic spin textures for potential applications in advanced spintronic and quantum technologies.

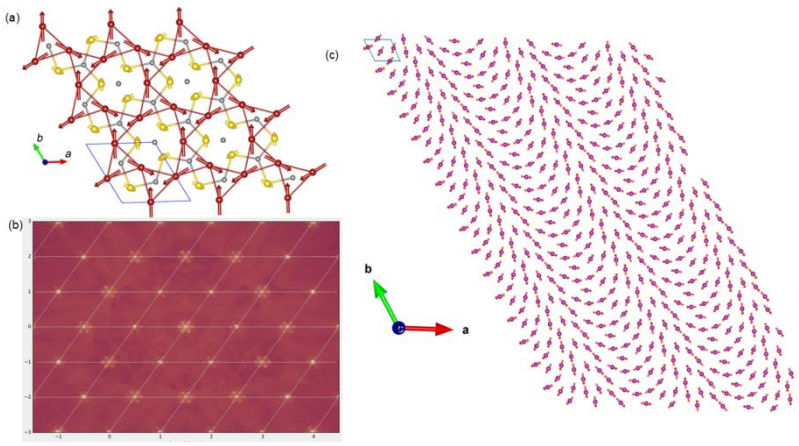

Fig. 1: *The non-collinear magnetic structures of $MnCoGe_{1/3}As_{2/3}$. The commensurate structure (a) observed at higher temperatures is converted to an incommensurate cycloidal structure (b,c) observed at lower temperatures.*

References

[1] L. Balents, Nature **464**, 199-208 (2010).
[2] N. Kanazawa, S. Seki, Y. Tokura, Adv. Mater. **29**, 1603227 (2017).
[3] Y.-X. Wang, I. Campbell, Z. Tener, *et al.*, J. Am. Chem. Soc. **147**, 43550-43559 (2025).

Abstract ID: 30444

EMERGENT FUNCTIONALITY OF SPIN SPIRALS: FROM P-WAVE MAGNETS TO TOPOLOGICAL TEXTURES

S. Okumura[1,2]

[1] *The University of Tokyo, Quantum-Phase Electronics Center, 113-8656, Tokyo, JAPAN*
[2] *RIKEN Center for Emergent Matter Science, 351-0198, Wako, JAPAN*

Spin spiral states have attracted much attention as a class of antiferromagnets that breaks spatial inversion symmetry, which results in odd-parity spin splitting, recently highlighted in the emerging concept of *p*-wave magnetism (Fig. 1). These spin spiral states exhibit a variety of emergent phenomena, such as magnetoelectric effects, spin-dependent transport, and optical responses, which are highly controllable through solitonic or conical modulations of spin spirals.

In this talk, we present our recent findings about the emergent electromagnetic functionalities associated with exotic spin textures in itinerant magnets, based on spin–charge coupled systems. A spin spiral breaks parity due to the chirality and leads to various quantum phenomena. We provide a new insight into the origin of the anomalous Hall effect in a spin spiral [1], which arises from the odd-parity spin splitting and is experimentally observed in a metallic p-wave magnet [2]. Reflecting the asymmetric band dispersion, the spin spiral exhibits nonlinear spin transport [3] and an enormous photovoltaic effect [4] depending on the spin chirality. Furthermore, superpositions of the spin spirals generate various topological spin crystals, such as meron, monopole, and hopfion crystals. We suggest the stabilization mechanisms of such complex topological textures [5, 6], and reveal the characteristic quantum transport, optical responses, and dynamics beyond skyrmion physics.

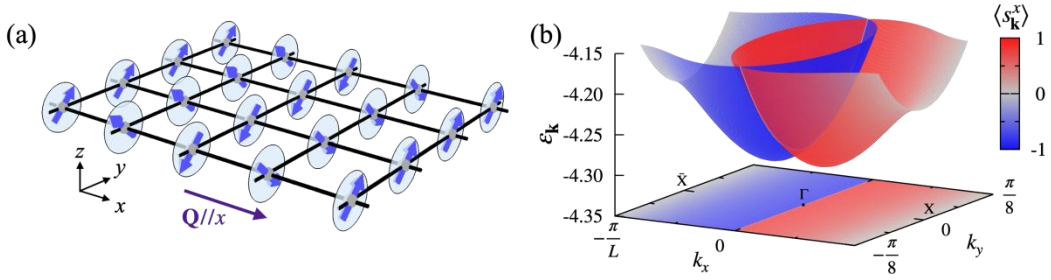

Fig. 1: *(a) A spin spiral state and (b) odd-parity spin splitting in the electronic band structure.*

References

[1] S. Okumura, M. Hirschmann, and Y. Motome, arXiv:2512.14071 (2025).
[2] R. Yamada, M. Birch, P. Baral, S. Okumura, *et al.*, Nature **646**, 837 (2025).
[3] S. Okumura, H. Ishizuka, Y. Kato, J. Ohe, and Y. Motome, Appl. Phys. Lett. **115**, 102401 (2019).
[4] S. Okumura, T. Morimoto, Y. Kato, and Y. Motome, Phys. Rev. B **104**, L180407 (2021).
[5] S. Okumura, S. Hayami, Y. Kato, and Y. Motome, Phys. Rev. B **101**, 144416 (2020).
[6] S. Kasai, K. Shimizu, S. Okumura, Y. Kato, and Y. Motome, Phys. Rev. B **112**, 184424 (2025).

Abstract ID: 30532

DECIPHERING INTRIGUING ISSUES OF THE MAGNETOELASTIC PHASE TRANSITION IN Fe-Rh ALLOYS AROUND EQUIATOMIC COMPOSITION

K. Padrón-Aleman[1,2], P. Álvarez-Alonso[1,3], M. L. Arreguín-Hernández[4], G. J. Cuello[2], J. A. Blanco[1], J. L. S. Llamazares[5], P. Gorria[1,3]

[1] *Departamento de Física, Universidad de Oviedo, Calvo Sotelo 18, 33007 Oviedo, SPAIN*
[2] *Diffraction Group, Institut Laue-Langevin, 71 Ave des Martyrs, CS 20156, 38042 Grenoble cedex 9, FRANCE*
[3] *Instituto Universitario de Tecnología Industrial de Asturias, Universidad de Oviedo, Gijón 33203, SPAIN*
[4] *Centro de Nanociencias y Nanotecnología, Universidad Nacional Autónoma de México, AP 14, Ensenada 22860, Baja California, MEXICO*
[5] *Instituto Potosino de Investigación Científica y Tecnológica A.C., Camino a la presa San José 2055, 78216, San Luis Potosí, MEXICO*

Equiatomic and nearly-equiatomic FeRh alloys exhibit a first-order magnetostructural (FOMPT) transition from antiferromagnetic (AFM) to ferromagnetic (FM) state on heating above room temperature (≈ 320-350 K), and the reverse transformation, FM to AFM on cooling down from high temperature. The simple cubic crystal structure, a B2 CsCl-type, is maintained across the FOMPT, but a drastic change in the unit cell volume, (≈ 1 %) is observed on both heating and cooling processes with a hysteresis that depends on the alloy composition. Although this system has been investigated for decades, the mechanisms governing the transition and the role played by Rh atoms in the magnetism of Fe are still under debate. Moreover, FeRh alloys attract much interest from the applied point of view in areas related to solid-state refrigeration or spintronics, because they display giant caloric effects and magnetoresistance under external stimuli (temperature, pressure, magnetic field).

In this talk we will discuss about some intriguing issues revealed from the joint investigation using conventional magnetic measurements together with neutron thermo-diffraction under applied magnetic field or hydrostatic pressure and polarized neutron imaging.

References

[1] L. H. Lewis, C. H. Marrows and S. Langridge, J. Phys. D: Appl. Phys. **49**, 323002 (2016).
[2] K. Padrón-Alemán, *et al.*, J. Alloys Compd. **1010**, 177876 (2025).
[3] K. Padrón- Alemán, *et al.*, J. Mater. Chem. C **13**, 7017 (2025).
[4] K. Padrón- Alemán, *et al.*, Mat. Chem. Phys. **327**, 129904 (2024).

Abstract ID: 30695

X-RAY DIRECTIONAL DICHROISM – AN ELEMENT SELECTIVE PROBE OF MAGNETOELECTRICITY

A. Rogalev

ESRF - The European Synchrotron, Grenoble, FRANCE

Since the time of Louis Pasteur, the interplay between chirality and magnetism has fascinated successive generations of scientists. The two phenomena appear to be intimately connected in the interaction of light with matter. When a chiral system is also magnetic, it can adsorb unpolarised light in a different way depending on chirality and directions of magnetisation and propagation of light. This effect, known as directional dichroism, was observed for the first time only in 1997 with visible light [1] and soon after with X-rays [2].

The striking features of directional dichroism can be derived from symmetry considerations, i.e. it is observable only in systems where both inversion and time-reversal symmetries are simultaneously broken. These symmetry conditions are satisfied not only for a chiral medium placed in a magnetic field but, more generally, in any system exhibiting linear magnetoelectric effect.

Thus, magneto-chiral dichroism and non-reciprocal linear dichroism in the X-ray range offer a possibility to study the magneto-electric coupling with an element selectivity and orbital specificity inherent to X-ray spectroscopy. The experimental spectra are analyzed with the help of sum rules [3], which gives a unique access to a whole family of magneto-electric operators mixing orbitals of different parities in the ground state. The physical content of these operators is analyzed. For every magnetoelectric group, one can predict which kind of dichroism can be detected with either a single crystal or a powdered sample. Experimental spectra on a polar ferrimagnetic crystal $GaFeO_3$ are presented to illustrate the value of the sum rules and the practical conditions of their application.

References

[1] G.L.J.A. Rikken and E. Raupach, *Nature,* **390**, 493 (1997).
[2] J. Goulon, A. Rogalev, e*t al.*, *Phys. Rev. Lett.,* **88,** 237401 (*2002*).
[3] P. Carra, A. Jerez and I. Marri, Phys. Rev. B, **67**, 045111 (2003).

Abstract ID: 30707

CONICAL STATES IN A COMPOSITE CHIRAL MAGNET

V. Laliena[1], J. Campo[2]

[1] *University of Zaragoza, Dept. of Appl. Mathematics, Zaragoza, SPAIN*
[2] *CSIC, Institut of Noanoscience and Materials of Aragon, Zaragoza, SPAIN*

We present a theoretical study of a composite magnet formed by a monoaxial chiral magnet, with the shape of a rectangular parallelepiped, which has slabs of a uniaxial ferromagnets attached to the sides perpendicular to the chiral axis, as in Fig. 1 (left). It is shown that at low temperature and zero applied magnetic field, this system hosts a large number of metastable helical states that differ by the wave number of the modulation, denoted by p (Fig. 1, right). The application of an external magnetic field in the direction of the chiral axis has a double effect: on the one hand, it introduces a conical deformation of the helical states and, on the other hand, it destabilizes some of them, shrinking the range of p in which they are metastable. Helicity then can be controlled by external means and may be a "degree of freedom" useful as, for instance, information storage. Implications for spintronics and magnonics technologies are discussed.

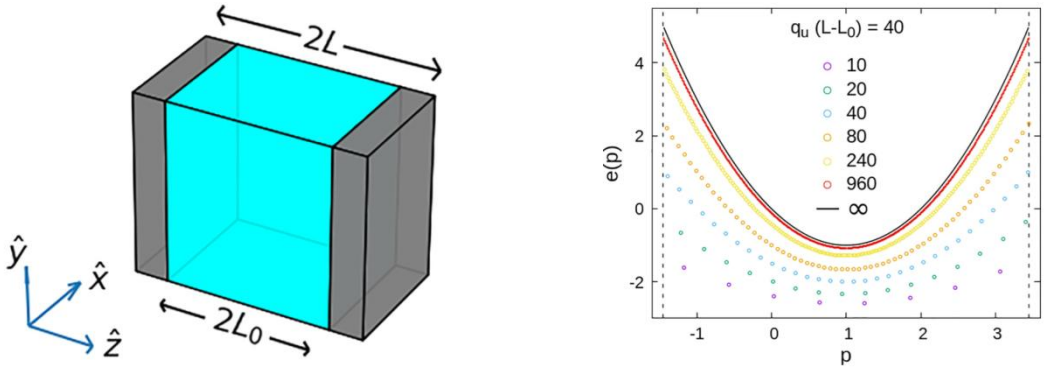

Fig. 1: *A composite chiral magnet (left) and energy of the metastable helical states (right).*

References

[1] V. Laliena, S. Osorio, D. A. Bazo, S. Bustingorry, J. Campo, Phys. Rev. B **108**, 024425 (2023).
[2] V. Laliena, S. Osorio, S. Bustingorry, J. Campo, Phys. Rev. B **109**, 214424 (2024).

29 - MAGNETIC MATERIALS PROCESSING AND PHYSICAL PROPERTIES

Abstract ID: 30419

THERMAL HISTORY-DEPENDENT CHARACTERISTICS IN VAN DER WAALS FERROMAGNET $Fe_{5-x}GeTe_2$ ($x \sim 0.16$)

R. L. Yadav[1], P. Bag[1], C.-C. Lai[1], Y.-K. Kuo[1], C.-N.g Kuo[2], C. S. Lue[2]

[1] *Department of Physics, National Dong Hwa University, Hualien 97401, TAIWAN*
[2] *Department of Physics, National Cheng Kung University, Tainan 70101, TAIWAN*

We investigated the thermal-history dependence of physical properties in a quenched $Fe_{5-x}GeTe_2$ ($x \sim 0.16$) single crystal by measuring magnetization (M), electrical resistivity (ϱ), Seebeck coefficient (S), and thermal conductivity ($\varkappa$) as a function of temperature (T). The results reveal anomalies in these physical quantities around various transition points: ferromagnetic ($T_C \sim 310 - 300$ K), helimagnetic ($T_H \sim 275$ K), charge ordering ($T_{CO} \sim 165$ K), spin-reorientation ($T^* \sim 100 - 120$ K), and a Fermi-liquid (FL) phase below $T_L \sim 35$ K. Using power-law fitting, the $M(T)$ analysis near T_C shows that Fe moments become primarily itinerant after thermal cycling. The $\varrho(T)$ results indicate inherent residual stresses in the crystal that alter with thermal cycling, influencing ferromagnetic domain formations within grain boundaries. The system exhibits strongly correlated FL behavior at low temperatures, which ceases above T_L due to spin fluctuations. In the T-range of $T^* \leq T \leq T_{CO}$, $\varrho(T)$ and $S(T)$ analyses suggest significant electronic band structure modifications with multiband effects. The $\varkappa(T)$ data indicate phonon-dominated heat transport in the crystal, with phonon behavior influenced by inherent lattice strains following initial thermal cycles, as evidenced by the decreased phonon peak height at low temperatures. Additionally, there is evidence of phonon localization and electron-phonon coupling at higher temperatures.

References

[1] Ra. L. Yadav, P. Bag, C.-C. Lai, Y.-K. Kuo, C.-N. Kuo, and C.-S. Lue APL Materials, **12**, 081103 (2024).

Abstract ID: 30547

SPINEL FERRITES AS EVOLVING MATERIALS FOR Re-RAM: CORRELATION OF THERMOPHYSICAL PROPERTIES WITH SWITCHING PHENOMENA

M. Anis-ur-Rehman

Applied Thermal Physics Laboratory, Department of Physics, COMSATS University Islamabad, Islamabad 45550, PAKISTAN

Memories are essential ingredients of modern electronic devices. Resistive Random-Access Memories (Re-RAMs) have emerged as better alternatives for conventional charge-based flash memories due to their distinct features like high speed, ultra-low power consumption, simple structure and long retention [1]. Spinel ferrites are strong potential candidates for Re-RAM applications. In our work, rare earth doped zinc cobalt ferrite, cobalt doped magnesium ferrites, and lithium doped cobalt ferrites elements had been prepared by using wet chemical methods like WOWs sol-gel method and co-precipitation technique. The prepared materials could be employed as resistive switching layers in MIM devices. Structural analysis by X-ray diffraction (XRD) verified that single-phase spinel ferrites have been formed. Various thermophysical characteristics were investigated, such as dielectric tangent loss, dielectric constant, dielectric loss, AC conductivity, AC impedance, DC resistivity and I-V loops. The hysteresis behaviour, as illustrated in Fig. 1 verified the presence of the resistive switching effect in zinc cobalt ferrite samples. For resistive random-access memory, a silver (Ag) top electrode is placed after ferrites are spin-coated over processed Floride Tin Oxide (FTO), which acts as the bottom electrode. The features favourable for resistive switching (RS) characteristics, includes time retention, strong cycling endurance, and comparatively low forming voltage and are studied for the prepared materials. This study illustrates an approach for developing resistive memory devices with improved performance for future non-volatile memory applications and offers a prospective performance enhancement technique to develop resistive memory devices for data storage applications.

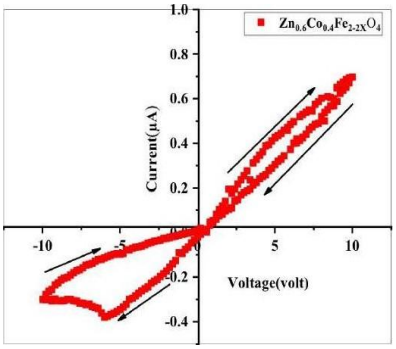

Fig. 1: *I-V response of Zn-Co Ferrite.*

References

[1] A. R. Patil, T. D. Dongale, R. K. Kamat, K. Y. Rajpure, *Binary metal oxide-based resistive switching memory devices: A status review*, Materials Today Communications **34**, 105356 (2023).

Abstract ID: 30210

ARTIFICIAL SURFACE CORRUGATION OF PERMALLOY FILMS THROUGH FEMTOSECOND LASER IRRADIATION

C. Delforge[1], J. Frechilla[2], N. Lejeune[1], A. Naik[1], A. Frechilla[2], A. Badía-Majós[2], M. Ciria[2], L. A. Angurel[2], E. Martínez[2], G. F. de la Fuente[2], E. Fourneau[1], A. V. Silhanek[1]

[1] *Experimental Physics of Nanostructured Materials (EPNM), Q-MAT, Université de Liége, Liège, BELGIUM*
[2] *Instituto de Nanociencia y Materiales de Aragón (INMA), CSIC-Universidad de Zaragoza, Zaragoza, SPAIN*

Magnetic characterization of femtosecond-UV laser-patterned Permalloy (NiFe, Py) reveals that Laser-Induced Periodic Surface Structures (LIPSS) can be directly imprinted into the magnetic film while preserving its ferromagnetic order, as shown in Fig. 1. The patterned Py exhibits an undulated topography with a periodicity of ~280 nm and an amplitude smaller than the overall film thickness, in contrast to most previous studies and departing from the hypothesis of Schlöman's model[1]. Magneto-optical Kerr effect measurements demonstrate the emergence of uniaxial magnetic anisotropy after laser treatment, once the magneto-optical signal is decoupled from the polarizing effect of the LIPSS. Magnetic force microscopy confirms domain organization consistent with the induced anisotropy, while micromagnetic simulations reproduce the observed switching behavior. Magnetodynamic analysis further shows that the excitation and relaxation of spin modes can be tuned by the orientation of the applied magnetic field relative to the LIPSS axis. These results refine our understanding of how direct laser patterning can tailor magnetic properties in Py films, offering a distinctive perspective on anisotropy control and magnetization dynamics in nanostructured magnetic systems. They also reinforce the relevance of magnetic anisotropy for applications such as sensors, filters, and magnetic recording[2].

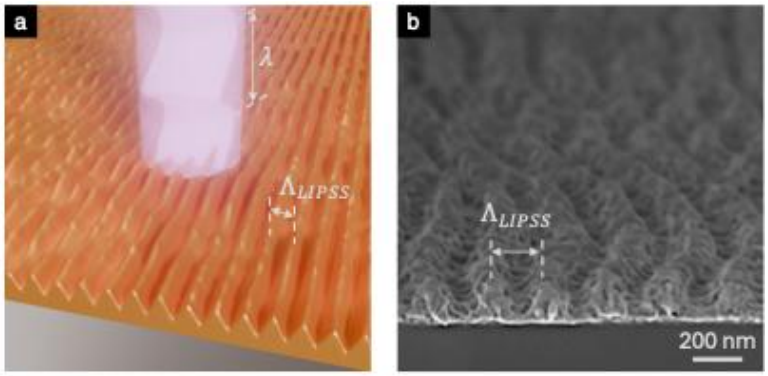

Fig. 1: *(a) Illustration of the LIPSS patterning process, (b) SEM image of the resulting Permalloy (NiFe) film.*

References

[1] E. Schlöman, Jour. Appl. Phys. **41**, 4, 1617 (1970).

[2] V. Belyaev, *et al.*, Jour. Mag. Magn. Mat. **482**, 292 (2019).

11th International Conference on Superconductivity and Magnetism ICSM2026
4th International Conference on Quantum Materials and Technologies ICQMT2026
19th April to 26th April, 2026, Ölüdeniz – Fethiye/Muğla, Türkiye
https://icsmforever.org/

Abstract ID: 30527

TAILORING THE ELECTRICAL PROPERTIES OF LITHIUM FERRITES THROUGH COBALT DOPING FOR RESISTIVE MEMORY DEVICES

K. Naheed[1,2], W. Mehmood[2], M. Anis-ur-Rehman[1]

[1] *Applied Thermal Physics Laboratory, Department of Physics, COMSATS University Islamabad, Islamabad 45550, PAKISTAN*
[2] *Department of Physics, Rawalpindi Women University, Rawalpindi, PAKISTAN*

Spinel ferrites exhibit low conductivity, high magnetic permeability, low coercivity, high Curie temperature, and low eddy current loss. In present work, $Li_{0.5-x}Co_xFe_{2.5}O_4$ (x=0.0, 0.09) ferrites electrical and di-electrical properties have been synthesized by Sol gel method. We have examined the AC electrical properties of our sample. The electrical properties including the di-electric constant(1.0×10^3), di-electric loss(4×10^3), ac conductivity(5.0×10^{-4}) and impedance(3.0×10^6) and when doped with Cobalt ferrite at the concentration of x=0.09 the di-electric constant($2.5x10^3$), di-electric loss(8.0×10^3) ,ac conductivity(4.0×10^{-4}) and impedance (1.8×10^6) have been studied in the frequency range of 20Hz to 3MHz using precision analyzer. For DC electrical measurements, current-voltage (IV) analysis perform using a DC power supply and multimeter to assess the DC conductivity and switching characteristics. For structural analysis, the phase formation and surface morphology were validated using FTIR spectroscopy and SEM and EDX. UV-Visible spectroscopy was used to study the variation of the energy band gap with Cobalt concentration in Lithium Ferrite and the energy bandgap of the material within the range or 2 to 3 eV. Due to this property, Cobalt doped (x=0.09) offers balanced combination of properties for ReRAM application.

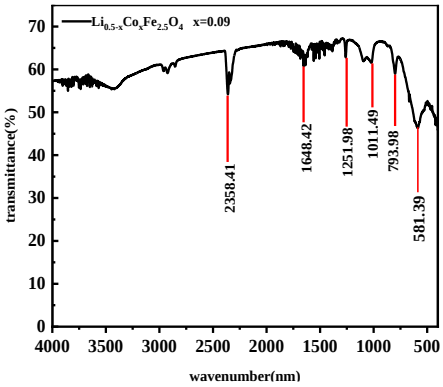

Fig. 1: *FTIR spectrum.*

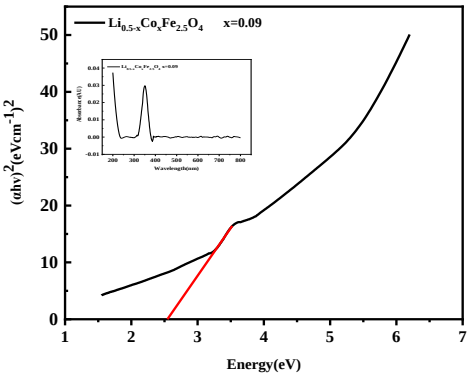

Fig. 2: *UV-Spectrum.*

Abstract ID: 30683

INVESTIGATION OF HTS COIL-PM MAGNETIC FIELD PROFILE WITH DIFFERENT COIL PARAMETERS

H. Mollahasanoglu[1], U. K. Ozturk[2], M. Abdioglu[3]

[1] Recep Tayyip Erdogan University, Dept. of Electrical-Electronics Engineering, 53100, Rize, TURKEY
[2] Karadeniz Technical University, Dept. of Physics, 61080, Trabzon, TURKEY
[3] Bayburt University, Dept. of. Mathematics and Science Education,69000, Bayburt, TURKEY

This study investigates the magnetic field profiles of hybrid systems formed by the integration of High-Temperature Superconducting (HTS) coils and Permanent Magnets (PM). The combination of the high current-carrying capacity provided by HTS coils with the stable magnetic field characteristics of permanent magnets holds significant potential for next-generation electrical machines and precision sensor technologies. Throughout the research process, various topological configurations were developed using different coil geometries and layouts. In this study, the critical design parameters required to achieve the optimum magnetic flux profile for high-efficiency energy applications were determined.

Abstract ID: 30828

NEW MONOCLINIC MODIFICATIONS OF $MFeTe_2$ (M = Nb, Ta) LAYERED VAN DER WAALS TELLURIDES

A. V. Stepanova[1], A. N. Azarevich[2], A. V. Bogach[2], A. V. Mironov[1], M. A. Kirsanova[3], A. V. Sobolev[1], I. A. Presniakov[1], A. V. Shevelkov[1], V. Yu. Verchenko[1]

[1] Lomonosov Moscow State University, Dept. of Chemistry, 119991, Moscow, RUSSIA
[2] Prochorov General Physics Institute of the Russian Academy of Sciences, 199991, Moscow, RUSSIA
[3] Center for Energy Science and Technology, Skolkovo Institute of Science and Technology, 121205, Moscow, RUSSIA

Layered transition metal-based tellurides are of special interest due to their peculiar physical properties and cleavability, which allows to obtain 2D atomically thin materials by simple exfoliation. These ultrathin materials possess tunable properties in contrast to the parent bulk materials. Furthermore, various heterostructures can be constructed by combination of 2D materials with desired properties, which is promising for designing novel spintronic devises, such as new type of magneto resistive random-access memory, which demonstrates outstanding performance in comparison to classic semiconductor-based electronic devises.

$MFeTe_2$ (M = Nb, Ta) are layered van der Waals tellurides with orthorhombic crystal structure [1]. Orthorhombic polymorph of $NbFeTe_2$ demonstrates paramagnetic behavior with low-temperature spin-glass state [2]. At the same time, magnetic properties of $TaFeTe_2$ are not reported.

In this work we successfully synthesized new monoclinic modifications of $NbFeTe_2$ and $TaFeTe_2$ layered tellurides by chemical vapor transport reactions. Their crystal structures were investigated by single-crystal X-ray diffraction and high-resolution transmission electron microscopy. Magnetic properties measurements showed ferromagnetic ordering below 87 and 29 K for $NbFeTe_2$ and $TaFeTe_2$, respectively, with strong perpendicular magnetic anisotropy and itineracy of magnetism. In case of $TaFeTe_2$ ferromagnetic ordering coexists with frozen spin-glass-like state. Analysis of critical behavior demonstrates that 3D Heisenberg model is the most suitable for description of ferromagnetic to paramagnetic phase transition in this compound. Our study shows that the optimization of synthetic conditions is a proper tool to obtain new polymorphic modifications of chalcogenides. $NbFeTe_2$ and $TaFeTe_2$ with the ferromagnetic ground state and layered crystal structure are interesting candidates for constructing next generation spintronic devices.

This work is supported by the Russian Science Foundation, grant No. 24-73-10007.

References

[1] J. Neuhausen, K.-L. Stork, E. Potthoff, W. Tremel, Zeitschrift für Naturforschung B **47(9)**, 1203-1212 (1992).
[2] J. H. Zhang, F. Chen, J. Li, C. J. O'Connor, Journal of Applied Physics **81(8)**, 5283-5285 (1997).

30 - MAGNETISM OF NANOPARTICLES, NANO-WIRES AND NANO-STRUCTURES

Abstract ID: 30373

SOLUTION-PROCESSED METAL OXIDE NANOCOMPOSITES FOR ENHANCED MAGNETISM AND SPIN TRANSPORT

A. Shahid

Department of Physics Lahore College for Women University, Lahore, PAKISTAN

$BiFeO_3$/MXene/Poly(vinylidene fluoride-trifluoroethylene P(VDF-TrFE) multifunctional composites are perfect for complex spintronic, magnetoelectric, and flexible electronic devices because they combine the multiferroic behaviour of $BiFeO_3$, the 2D conductivity of MXene nanosheets, and the ferroelectric polymer physics of P(VDF-TrFE). In order to promote uniform nucleation and reduce secondary phases, a controlled sol-gel method with citric acid chelation was used in this work to produce phase-pure $BiFeO_3$ nanoparticles. Chemical exfoliation was used to create MXene ($Ti_3C_2T_x$) nanosheets, which were then functionalized for better dispersion. To improve ferroelectric β-phase crystallinity, a P(VDF-TrFE) solution in DMF was mixed with a homogeneous suspension of $BiFeO_3$ and MXene. The next steps were solvent casting and thermal poling. Interfacial interactions and structural integrity were confirmed by multidisciplinary characterization. X-ray diffraction (XRD) confirmed the perovskite $BiFeO_3$ phase and dominant P(VDF-TrFE) β-phase peaks with no observable impurity phases. Scanning electron microscopy (SEM) and transmission electron microscopy (TEM) revealed a homogeneous dispersion of approximately 30–60 nm $BiFeO_3$ nanoparticles anchored on few-layer MXene sheets embedded in the polymer matrix. Fourier-Transform Infrared Spectroscopy (FTIR) was used to confirm strong interfacial bonding and high ferroelectricity. BET & BJH analyses demonstrated high specific surface area (>40 m^2/g) and mesoporous networks that are beneficial for interfacial coupling. Energy Dispersive Spectroscopy (EDS) verified the homogeneous distribution of Bi, Fe, Ti, C, F, and O. The composite has improved magnetic properties, with saturation magnetisation (M_s) of approximately 1.2 emu/g and remnant magnetisation (M_r) of approximately 0.15 emu/g under a 15 kOe field, which is significantly higher than pure $BiFeO_3$ nanoparticle films (~0.18 emu/g) prepared under similar conditions, according to Vibrating Sample Magnetometry (VSM) at room temperature. These findings show how interfacial coupling and nanoscale engineering can effectively break the cycloidal spiral structure of $BiFeO_3$ and enable observable ferromagnetic behaviour at room temperature. Stable magnetic ordering at low external fields is further supported by enhanced coercivity (~300 Oe). These composites observed multifunctional coupling creates opportunities for energy-efficient actuators, flexible magnetoelectric memory elements, magnetic field sensors, and spintronic applications. The potential for integration in wearable and flexible electronic systems is highlighted by the flexible polymer matrix and scalable, low-temperature synthesis. Significantly, by advancing next-generation functional materials, this research contributes to SDG 9 (Industry, Innovation, and Infrastructure) and SDG 7 (Affordable and Clean Energy) by enabling materials that can increase energy efficiency in electronic and energy-related systems. The low-cost, scalable synthesis method further highlights the possibility of producing high-performance functional oxides in an environmentally responsible manner.

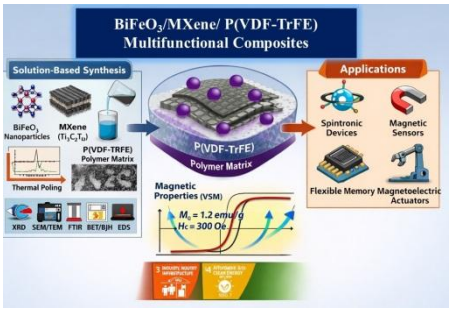

Fig. 1: *Schematic illustration of a solution-processed $BiFeO_3$ / MXene / P(VDF-TrFE) multifunctional composite.*

31 - MAGNONICS AND MAGNETIZATION DYNAMICS

Abstract ID: 30204

REAL-SPACE IMAGING OF MAGNONS INTERACTING WITH NONCOLLINEAR MAGNETIC TEXTURES

P. Che

Laboratoire Albert Fert, CNRS, Thales, Université Paris-Saclay, 91767 Palaiseau, FRANCE

Noncollinear magnetic textures such as skyrmions, bubbles, and domain walls are attracting significant attention in magnonics because they interact with magnons through their internal spin structure, topology, and chirality. These interactions give rise to nontrivial magnon band topology [1], magnon–skyrmion skew scattering [2], multipole magnon modes [3], and edge-localized magnon transport [4], providing new routes to control magnon phase, momentum, and propagation direction. Moreover, such textures can be stabilized without demanding nanofabrication, making them promising building blocks for nanoscale magnonic devices that enable guided and nonreciprocal signal transmission in magnonic circuits. However, experimental verification and real-space imaging of these magnon-noncollinear magnetic textures interactions remain limited. It is challenging to simultaneously realize both low-damping materials that host rich noncollinear magnetic textures at room-temperature, and a microscopy technique capable of resolving both their static configuration and magnon-driven dynamics at the nanoscale.

In this talk, I will present real-space imaging of magnons interacting with magnetic skyrmions, type-II bubbles and domain walls at room temperature using time-resolved scanning transmission X-ray microscope (STXM). In bismuth-dope yttrium iron garnet (Bi-YIG) thin films and Fe/Gd multilayers with interface-induced perpendicular magnetic anisotropy (PMA), the interplay between anisotropy and dipolar energy stabilizes rich magnetic textures including dipolar skyrmions with dimensions of about 200 nm. Time-resolved STXM allows direct visualization of magnon propagation, scattering, and confinement within the textures. We observed that resonantly excited magnons can drive the translational motion of skyrmions and bubbles, reaching a velocity up to 175 m/s. This provides direct experimental evidence that magnons transfer momentum to magnetic textures and move them without electrical current. In addition, we image nonreciprocal magnons confined to deep-sub-100 nm-wide domain walls which is the key to construct chiral edge magnons. These results show that magnons can manipulate noncollinear textures and use them as information transformation channel, enabling energy-efficient and reconfigurable room-temperature magnonic devices.

References

[1] T. Weber, *et al.*, Science **375**, 1025-1030 (2022).

[2] C. Schütte and M. Garst, Phys. Rev. B **90**, 094423 (2014).

[3] P. Che, *et al.*, Commun. Mater. **6**, 139 (2025).

[4] P. Che, *et al.*, Adv. Mater. **37**, e08181 (2025).

Abstract ID: 30205

TEMPERATURE DEPENDENCE OF VOLUME AND INTERFACE CONTRIBUTIONS TO THE MAGNETIC DAMPING OF PERMALLOY THIN FILMS

V. Ney[1], K. Lenz[2], R. Hübner[2], F. Ganss[2], J. Lindner[2], A. Ney[1]

[1] *Solid State Physics Devision, Johannes Kepler University Linz, Linz, AUSTRIA*
[2] *Helmholtz Zentrum Dresden Rossendorf, Dresden, GERMANY*

A thorough understanding of magnetic damping in ferromagnetic materials is of importance in spintronics from both a fundamental and a practical point of view. The phenomenological Gilbert parameter α in the Landau-Lifshitz equation is central to quantify the magnetic damping, which can be measured with ferromagnetic resonance (FMR). Permalloy (Py = $Ni_{80}Fe_{20}$) is one of the model systems with low magnetic damping. Here, we report the outcome of a systematic study of the temperature and frequency dependence of the FMR linewidth of Py, which was grown on typical substrates (silicon and sapphire) and capped with materials commonly used for preventing oxidation (Ta, Al, and SiOx). The resulting frequency and temperature dependence of the FMR linewidth deviates significantly from the expected Gilbert-like behavior. Unwanted non-Gilbert-like contributions appear, especially at low temperatures, and particularly for oxidic interfaces [1]. In contrast, metallic capping layers avoid non-Gilbert-like contributions. Special focus was paid to the influence of the Al spacer thickness which was varied between 1 and 10 nm [2]. In particular, Py sandwiched in between a metallic Al cap and a thin spacer layer exhibits negligible inhomogeneous FMR linewidth broadening and a very small, purely Gilbert-like contribution of α = 0.0068(2) down to the lowest temperature for a fixed Py layer thickness of nominally 20 nm [2]. In addition, the Gilbert damping parameter α was studied as a function of Py layer thickness for Al-sandwiched Py thin films. The full FMR dataset allows to separate the Gilbert-like contributions to the FMR linewidth from non-Gilbert-like ones like two magnon scattering processes for the entire thickness series from 3 nm to 37 nm. We can deconvolute α into its respective bulk and interfacial contributions and their respective temperature dependencies. While the bulk contribution monotonously decreases with temperature from 0.0061(1) down to 0.0054(1), and is thus of purely resistivitylike character [3]. In contrast, the interfacial contribution shows a subsequent increase at low temperature, i.e. it contains both resistivity and conductivity-like contributions [3]. The isolated bulk contribution, which is only of resistivity-like character, can be considered to reflect the intrinsic magnetic damping properties of Py thin films.

References

[1] V. Ney, *et al.*, Phys. Rev. Materials **7**, 124403 (2023).

[2] V. Ney, *et al.*, Phys. Rev. Materials **8**, 124410 (2024).

[3] V. Ney, *et al.*, Phys. Rev. Materials (submitted, 2025).

Abstract ID: 30207

SPIN-PUMPING AND INDUCED MAGNETIC POLARIZATION IN PERMALLOY/PLATINUM HETEROSTRUCTURES

V. Ney[1], K. Lenz[2], F. Wilhelm[3], R. Hübner[2], F. Ganss[2], A. Rogalev[3], J. Lindner[2], A. Ney[1]

[1] *Solid State Physics Devision, Johannes Kepler University (JKU), Linz, AUSTRIA*
[2] *Helmholtz Zentrum Dresden Rossendorf (HZDR), Dresden, GERMANY*
[3] *European Synchrotron Radiation Facility (ESRF), Grenoble, FRANCE*

Spin pumping is the transfer of angular momentum across interfaces into a non-ferromagnetic material driven by the precessing magnetization of an adjacent ferromagnet. Using ferromagnetic resonance (FMR) the presence of spin pumping can be evidenced by an increase of the Gilbert damping parameter α [1]. Here we study Platinum-Permalloy (Pt/Py) heterostructures using temperature-dependent broadband FMR. A clear increase of α is seen in a temperature range from 10-300 K when Pt and Py are in direct contact. The temperature dependence of the spin-pumping contribution can be derived by comparing with an Al-sandwiched Py reference film from [2]. The increase in α depends on the thickness of the Py layer indicating that spin pumping is an interfacial effect as expected. Surprisingly, upon insertion of a thin Al spacer layer between Pt and Py the increase in α is strongly suppressed and the thickness dependence on the Al spacer layer thickness is studied as well [3]. The structural properties of the heterostructures are characterized by a thorough investigation using X-ray reflectivity and transmission electron microscopy as previously done for Al-sandwiched Py in [2]. Here we can demonstrate by X-ray magnetic circular dichroism at the Pt L_3-edge that the presence of spin pumping is associated with a clear magnetic polarization in of the Pt whereas the polarization of Pt is absent when a spacer layer of only 2 nm of Al is inserted [3]. The induced polarization of Pt can therefore be associated with spin pumping, while non-polarized Pt in proximity to Py shows an almost identical (T) behavior as the Py reference sample in [2].

References

[1] Y. Tserkovnyak Phys. Rev. Lett. **88**, 117601 (2002).

[2] V. Ney, *et al.*, Phys. Rev. Materials **8**, 124410 (2024).

[3] V. Ney, *et al.*, (in preparation, 2025)

Abstract ID: 30233

HIGHLY EFFICIENT COHERENT AMPLIFICATION OF ZERO-FIELD SPIN WAVES IN YIG NANO-WAVEGUIDES

K. O. Nikolaev[1], S. R. Lake[2], B. Das Mohapatra[2], G. Schmidt[2,3], S. O. Demokritov[1], V. E. Demidov[1]

[1] *Institute of Applied Physics, University of Muenster, 48149 Muenster, GERMANY*
[2] *Institut für Physik, Martin-Luther-Universität Halle-Wittenberg, 06120 Halle, GERMANY*
[3] *Interdisziplinäres Zentrum für Materialwissenschaften, Martin-Luther-Universität Halle-Wittenberg, 06120 Halle, GERMANY*

Transmission and processing of information at the nanoscale using spin waves and their quanta – magnons, offers numerous advantages and opportunities that make it a promising next-generation technology for integrated electronics. The main challenges that still need to be addressed to ensure high competitiveness of magnonic devices include finding ways to efficiently amplify spin waves in nanostructures and developing nanocircuits that can operate without the need for an external bias magnetic field [1]. Here we demonstrate how these two challenges can be solved using nano-waveguides fabricated from a low-loss magnetic insulator. We show that by using local parametric pumping with a power of only a few milliwatts, one can achieve coherent amplification of spin-wave pulses by more than two orders of magnitude at zero bias magnetic field [2]. Our results provide a simple solution to problems that have long prevented the implementation of efficient integrated magnonic circuits.

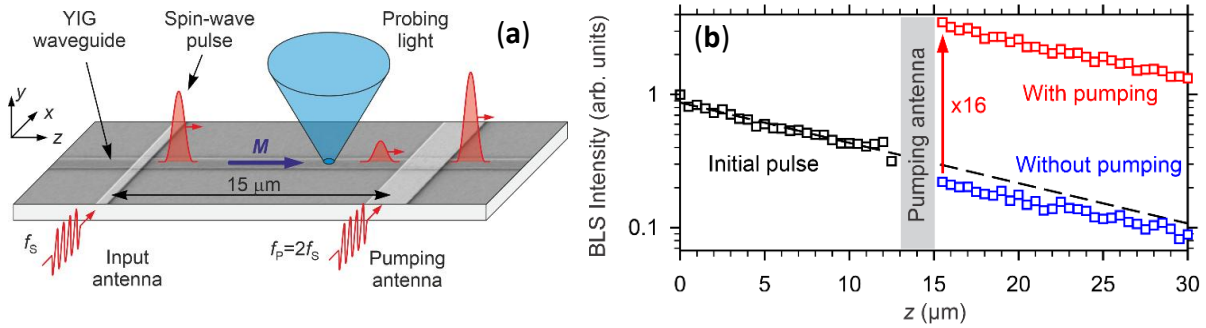

Fig. 1: *(a) Schematics of the experiment. (b) Spatial dependences of the peak intensity of spin-wave pulses with and without pumping.*

References

[1] K. O. Nikolaev, S. R. Lake, G. Schmidt, S. O. Demokritov, V. E. Demidov, Nano Lett. **23**, 8719–8724 (2023).

[2] K. O. Nikolaev, S. R. Lake, B. Das Mohapatra, G. Schmidt, S. O. Demokritov, V. E. Demidov, Sci. Adv. **11**, eadx2018 (2025).

Abstract ID: 30253

OPTIMIZING SPINWAVE TRANSDUCER FOR 5G APPLICATIONS

F. Bruckner, K. Davídková, I. Douveas, C.Abert, A. Chumak, D.Suess

University of Vienna, Faculty of Physics, AUSTRIA

Spin-wave-based devices are promising candidates for compact, low-power signal processing components in future 5G systems, including delay lines [1] and power limiters [2]. In this work, we apply the micromagnetic optimization framework previously introduced in *"Micromagnetic Simulation and Optimization of Spin-Wave Transducers"* [3] to transducer designs tailored for 5G-relevant frequency ranges and device concepts. Using time-domain micromagnetic simulations, we systematically investigate the influence of key design parameters such as YIG film thickness, transducer geometry, and the use of multiple meander structures on spin-wave excitation efficiency and bandwidth. Based on the optimized designs, prototype devices are fabricated, and first experimental measurements are presented. The measurement results show good qualitative agreement with the simulation predictions and demonstrate the potential of optimized spin-wave transducers for practical 5G applications.

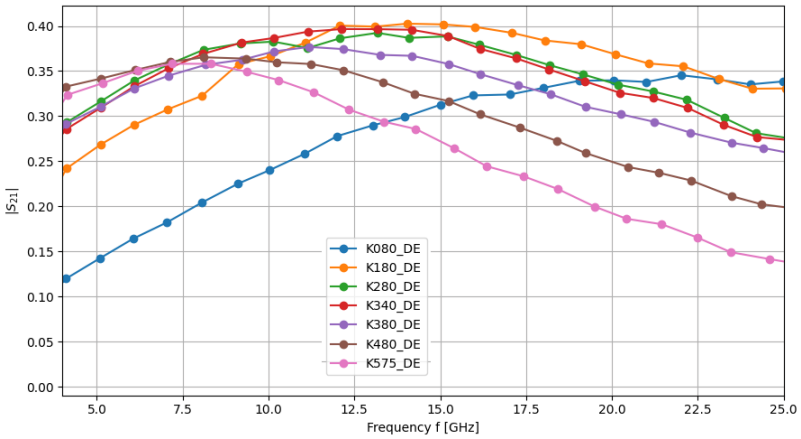

Fig. 1: *Insersion Loss of a Filter consisting of two U-shaped transducers for different transducer lengths. Due to impedance matching the peak of the transmission can be shifted by scaling the transducer length.*

References

[1] K. Davídková, *et al.*, *Nanoscale spin-wave frequency-selective limiter for 5G technology*, Physical Review Applied **23.3**, 034026 (2025).

[2] K. Davídková, *et al.*, *Spin-wave microscale RF delay lines for mid-and high-frequency 5G band,* Journal of Applied Physics **138**, 14 (2025).

[3] F. Bruckner, *et al.*, *Micromagnetic simulation and optimization of spin-wave transducers*, Scientific Reports **15.1**, 19993 (2025).

11th International Conference on Superconductivity and Magnetism ICSM2026
4th International Conference on Quantum Materials and Technologies ICQMT2026
19th April to 26th April, 2026, Ölüdeniz – Fethiye/Muğla, Türkiye
https://icsmforever.org/

Abstract ID: 30326

NONRECIPROCAL MAGNON PHASE SHIFTS FROM ELECTRIC FIELDS: THE AHARONOV–CASHER MECHANISM

A. A. Serga

RPTU University of Kaiserslautern–Landau, Fachbereich Physik and Landesforschungszentrum OPTIMAS, 67663, Kaiserslautern, GERMANY

The Aharonov–Casher (AC) effect [1], which gives rise to an additional phase for neutral particles or quasiparticles carrying a magnetic moment in an electric field, offers a promising route toward full electrical control of short-wavelength magnon transport [2–5]. Its first experimental evidence was obtained by measuring the AC phase of spin waves propagating along and across the magnetization direction in planarly magnetized YIG films subjected to an out-of-plane electric field [6]. This geometry enabled separation of the AC phase from phase shifts caused by magnetoelectric effects. However, the change in magnetization orientation left room for additional contributions associated with the magnetocrystalline anisotropy of YIG.

Here, I present an experimental approach that allows the magnetoelectric contribution and the AC phase to be independently quantified and unambiguously separated by exploiting the intrinsically nonreciprocal nature of the AC effect. By applying an in-plane electric field to a perpendicularly magnetized YIG film, we measure the phase shifts of forward volume magnetostatic spin waves at various frequencies and wavelengths, while systematically varying the applied electric field. The phase shifts differ for waves propagating in opposite directions, providing clear experimental evidence of the contribution of the Aharonov–Casher effect and opening a pathway toward nonreciprocal electric control in magnonic systems.

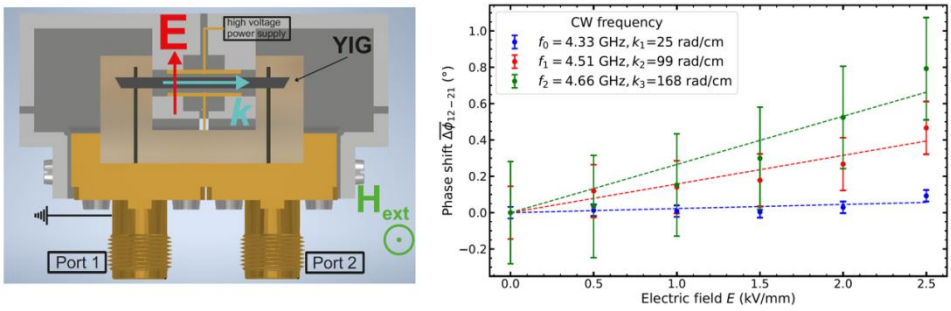

Fig. 1: *Experimental setup and nonreciprocal phase shift.*

This study was funded by the Deutsche Forschungsgemeinschaft (DFG, German Research Foundation) – TRR 173 – Grant No. 268565370 Spin+X (Projects B04 and B13).

References

[1] Y. Aharonov and A. Casher, Phys. Rev. Lett. **53**, 319 (1984).
[2] T. Liu and G. Vignale, Phys. Rev. Lett. **106**, 247203 (2011).
[3] C. Jia, D. Ma, A. F. Schäffer and J. Berakdar, Nat. Commun. **10**, 2077 (2019).
[4] V. N. Krivoruchko and A. S. Savchenko, Phys. Rev. B **109**, 184437 (2024).
[5] Y. Zhu, E. Kleinherbers, L. Levitov and Y. Tserkovnyak, Phys. Rev. B **112**, L100405 (2025).
[6] R. O. Serha, V. I. Vasyuchka, A. A. Serga and B. Hillebrands, Phys. Rev. B **108**, L220404 (2023).

Abstract ID: 30336

ADVANCED GARNET HETEROSTRUCTURES BY LATERAL CRYSTALLIZATION

C. Holzmann[1], S. Glamsch[1], D. Stein[1], M. Mihm[1], A. Ullrich[1], R.Schlitz[2], M. Lammel[2], J. Boneberg[2], M. Albrecht[1]

[1] *Institue of Physics, University of Augsburg, 86159 Augsburg, GERMANY*
[2] *Departement of Physics, University of Konstanz, 78457 Konstanz, GERMANY*

Rare-earth iron garnet thin films are known for their low Gilbert damping, insulating behavior, and tunable magnetic characteristics, such as magnetic anisotropy, compensation points, and spin-reorientation transitions [1]. However, these advantageous properties are typically restricted to single-crystalline films grown on specific substrates like (substituted) GGG (Gd3Ga5O12), which limits their broader use. To overcome this limitation and extend the functionality of garnet thin films, we apply the concept of lateral crystallization [2]. Exemplarily, we crystallize a thulium iron garnet film on a thin Pt interlayer. The Pt layer is sputtered onto a GSGG substrate, followed by garnet growth via Pulsed Laser Deposition. A hole pattern in the Pt layer is formed either naturally through thermal dewetting or intentionally patterned by laser interference patterning and serves as a crystallization seed. Although the as-deposited garnet film is amorphous, crystallization begins in these holes during post-deposition annealing at 700°C and proceeds laterally until the entire Pt layer is covered (Fig. 1). Lateral crystallization rates of about 1µm/min are achieved. The resulting garnet film displays properties comparable to an epitaxially grown film without an interlayer, including a Gilbert damping as low as 0.008 [3]. Thus, lateral crystallization of garnet films offers new opportunities for integrating garnets with metal layers for spintronic devices.

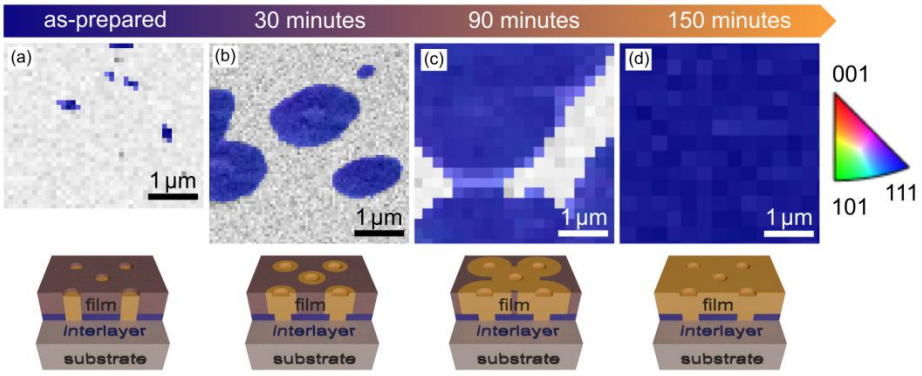

Fig. 1: *(a-d) Inverse pole figure contrast reconstructed from electron backscatter diffraction (EBSD) for a TmIG/Pt bilayer annealed at 700°C, showing the continuous growth of the garnet crystal with a uniform (111) orientation. In addition, the crystallization process in schematically pictured below the EBSD images.*

References

[1] C. Holzmann, M. Albrecht Encyclopedia of Materials: Electronics, 777 (2023).
[2] S. Sailler, *et al.*, Phys. Rev. Mater. **8**, L020402 (2024).
[3] C. Holzmann, *et al.*, Phys. Rev. Mater. **9**, 114416 (2025).

Abstract ID: 30377

ONE- AND TWO-DIMENSIONAL YIG MAGNONIC NANOCRYSTALS

K. O. Levchenko

Faculty of Physics, University of Vienna, Vienna 1090, AUSTRIA

Magnonic crystals (MCs) — artificial magnetic media with periodic modulation — provide a route toward tuneable spin-wave (SW) dynamics [1]. Nanoscaling these systems enhances control by enabling operation in a single SW mode regime [2] and makes nano-MCs attractive for both fundamental research and device applications.

One-dimensional (1D) MCs were fabricated by lithographically patterning 100 nm-thick yttrium iron garnet (YIG) nanowaveguides with periodic holes $d \approx 120$ nm (**Fig. 1(a)**). The resulting structures support SW propagation over several μm and exhibit pronounced Bragg-type band gaps with attenuation up to 26 dB. Clear alternation between transmission (passbands) and periodic band gaps was observed in 7.5–10.5 GHz frequency range (**Fig. 1(b)**, left). Measurements were performed via propagating SW spectroscopy in the Damon–Eshbach geometry. Complementary micro-focused Brillouin light scattering analysis verified these transmission features to originate from the coherent SW propagation rather than the structural defects. TetraX simulations supported the experiment and revealed complex mode interactions with two anticrossings at 3.1 and 18.7 rad/μm (**Fig. 1(b)**, right). Below the first one, a single-mode SW regime was identified within 100 MHz bandwidth, while between the two anticrossings efficient transmission is mostly mediated by the second width mode over a 1 GHz bandwidth.

Furthermore, nanoscale 2D MCs were realised based on a planar nanohole lattice in two designs: (i)"defect-free" and (ii)"defect-ridden" structures featuring e.g., a waveguide formed by a missing row of antidots and a 90-degree magnonic turn. 2D MCs offer a higher density of functional units for the magnonic networks, spatial and frequency (de)multiplexing, and advanced SW routing.

Achieved results explore the applied potential of MCs (e.g., for magnonic RF nanodevices) [3] and establish a pathway toward complex topological 2D magnonic structures [4] — an important scientific challenge that remains experimentally unresolved.

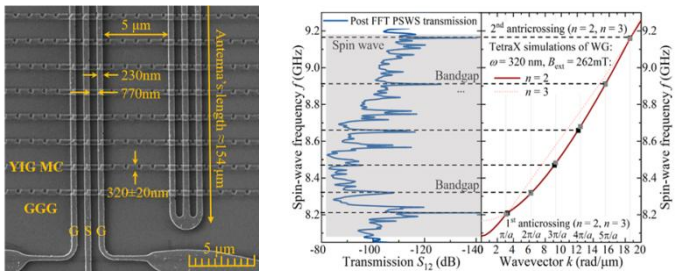

Fig. 1: ***(a)*** *SEM image of a typical 1D MC fabricated from a 100 nm-thick LPE-grown YIG/GGG film;* ***(b)*** *SW transmission signal S_{12} at a bias field ≈ 262 mT (left panel) vs TetraX-simulated dispersion of a uniform waveguide (WG) in Damon–Eshbach configuration (right panel).*

References

[1] A. V. Chumak, A. A. Serga, and B. Hillebrands, Nat. Commun. **5**, 4700 (2014).
[2] B. Heinz, T. Brächer, M. Schneider, *et al.*, Nano Lett. **20**, 4220 (2020)
[3] K. O. Levchenko, K. Davídková, J. Mikkelsen, and A. V. Chumak, arXiv:2411.19212 (2024).
[4] R. Shindou, R. Matsumoto, S. Murakami, and J. Ohe, Phys. Rev. B **87**, 174427 (2013).

Abstract ID: 30378

ULTRA-LONG-LIVING MAGNONS IN YIG FOR QUANTUM MAGNONICS

R. O. Serha

Faculty of Physics, University of Vienna, Vienna 1090, AUSTRIA

Quantum magnonics (QM) investigates magnons — the quanta of spin waves — as information carriers and interconnects in hybrid quantum systems. Yttrium iron garnet (YIG) is the material of choice due to its exceptionally low magnetic damping. Recent experiments have demonstrated single-magnon detection and quantum control in bulk YIG using superconducting qubits [1,2]. However, these studies rely on standing ferromagnetic-resonance magnons, whose lifetimes are typically limited to several hundred nanoseconds, restricting scalability and spatial separation of quantum elements.

Realization of propagating magnons for QM requires YIG films with long lifetimes at millikelvin temperatures (mK). Most high-quality films are grown on paramagnetic gadolinium gallium garnet (GGG) substrates. At mK, GGG increases damping in YIG layer and severely degrade YIG/GGG performance [3]. A viable solution is provided by the recently developed diamagnetic garnet substrate, yttrium scandium gallium aluminum garnet (YSGAG), which is lattice-matched to YIG while remaining magnetically inert down to mK. YIG films grown on YSGAG by liquid-phase epitaxy preserve low damping from room temperature down to 30 mK and outperform YIG/GGG films (Fig. 1(a)), as well as YIG on other diamagnetic substrates [4].

Additionally, progress has been achieved in bulk systems, where ultra-pure YIG crystals exhibit dipolar-exchange magnons with lifetimes exceeding 18 μs at mK (Fig. 1(b)). These record values, extracted from nonlinear threshold measurements of three-magnon splitting, demonstrate that magnon dissipation can be suppressed far beyond previously assumed limits [5]. Together, these advances enable ultra-long-lived magnons in both YIG films and bulk, and support a materials roadmap toward scalable QM circuits integrating propagating magnons with superconducting qubits, photons, and phonons, including access to nonlinear and nonreciprocal magnon dynamics [6].

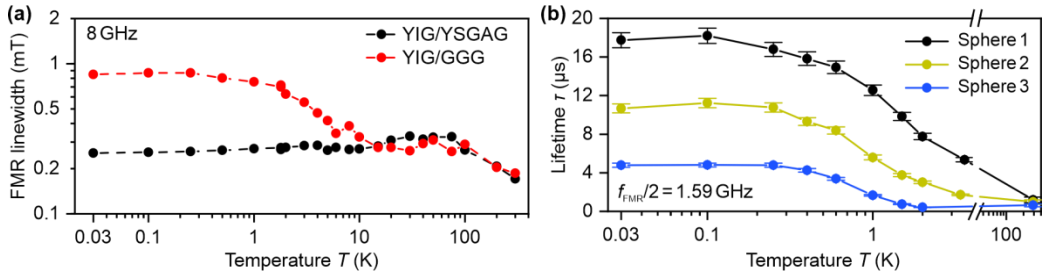

Fig. 1: ***(a)*** *FMR linewidth at 8 GHz YIG films on GGG (red) and YSGAG (black). The GGG substrate causes strong linewidth broadening at mK, while YIG/YSGAG preserves low damping.* ***(b)*** *Dipolar-exchange magnon lifetimes at 1.59 GHz in three YIG spheres with decreasing purity from number 1 to 3.*

References

[1] D. Lachance-Quirion, S. P. Wolski, Y. Tabuchi, *et al.*, Science **367**, 425 (2020).
[2] D. Xu, X.-K. Gu, H.-K. Li, *et al.*, Phys. Rev. Lett. **130**, 193603 (2023).
[3] 3. R. O. Serha, A. A. Voronov, D. Schmoll, *et al.*, npj Spintronics **5**, 100025 (2025).
[4] R. O. Serha, C. Dubs, C. Guguschev, *et al.*, arXiv.2508.19044 (2025).
[5] R. O. Serha, K. H. McAllister, F. Majcen, *et al.*, arXiv.2505.22773 (2025).
[6] R. O. Serha, C. Dubs, A. V. Chumak, arXiv.2510.09331 (2025).

Abstract ID: 30409

ADVANCES IN MICRO-FOCUSED BRILLOUIN LIGHT SCATTERING: MIE RESONANCES AND POLARIZATION ANALYSIS OF THE SCATTERED LIGHT

M. Urbánek

CEITEC Brno University of Technology, Purkyňova 123, 612 00 Brno, CZECHIA

One of the most versatile tools used to investigate dynamic excitations of matter, i.e. phonons and magnons is micro-focused Brillouin light scattering [1] (μ-BLS), see Fig. 1a. This presentation will review recent advances in micro-focused Brillouin light scattering technology and methodology. First, we describe a semi-analytical approach to optics and the microscopic theory of inelastic scattering to model μ-BLS signal [2] (Fig. 1b). Then we will discuss how dielectric nanoresonators supporting Mie resonances can be used (Fig. 1c) to enhance the detection limit to wavelength shorter than 30 nm (larger than 200 rad/μm), which is more than one order of magnitude improvement over standard μ-BLS on the bare film (400 nm, <16 rad/μm), see Fig. 1d [3-5]. In the last part I will discuss, how polarization analysis of the scattered light can be used to extract first- (Voigt) and second-order (Cotton-Mouton) magneto-optical constants of the investigated sample.

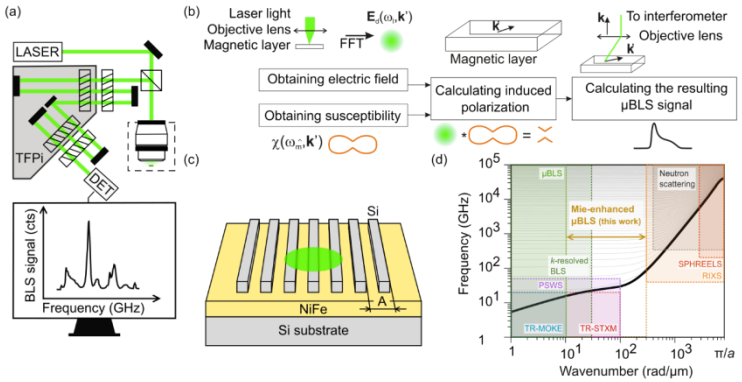

Fig. 1: *Modeling and enhancement of the μ-BLS signal. (a), Schematics of the μ-BLS setup. (b), Schematics of the modeling of the μ-BLS signal using semi-analytical approach and the microscopic theory of inelastic scattering. (c), Periodic nanoscale dielectric resonators for enhancement of the detectable spin-wave wavevectors. (d), Overview of the spin-wave dispersion relation and available methods for its measurement over the whole Brillouin zone.*

References

[1] F. Kargar, A.A. Balandin, Nat. Photon. **15**, 720-731 (2021).
[2] O. Wojewoda, *et al.*, Phys. Rev. B., **110**, 224428 (2024).
[3] J. Krčma, *et al.*, Sci. Adv., **11**, 44 (2025).
[4] O. Wojewoda, *et al.*, Commun. Phys., **6**, 94 (2023).
[5] O. Wojewoda, *et al.*, Appl. Phys. Lett., **122**, 202405 (2023).

Abstract ID: 30440

A TIME-MULTIPLEXED SPINWAVE ISING MACHINE

A. Litvinenko[1], R. Khymyn[2], R. Ovcharov[2], V. Tyberkevych[1], J. Åkerman[2,3,4], A. Slavin[2]

[1] *Department of Physics, Oakland University, 48309, Rochester, Michigan, USA*
[2] *University of Gothenburg, 412 96, Gothenburg, SWEDEN*
[3] *Center for Science and Innovation in Spintronics, Tohoku University, 2-1-1 Katahira, Aoba-ku, Sendai 980-8577, JAPAN*
[4] *Research Institute of Electrical Communication, Tohoku University, 2-1-1 Katahira, Aoba-ku, Sendai 980-8577, JAPAN*

We present a magnonic platform for miniature high-speed Ising machines that supports and rapidly solves large-scale combinatorial problems. The spinwave Ising Machines (SWIM) are a new class of time-multiplexed Ising machines [1] which can be implemented with an arbitrary-interconnected array of spinwave radio frequency (RF) pulses propagating in a ring oscillator with additional measurement and control feedback system realized using an FPGA (Fig. 1). SWIM demonstrates 3-4 orders of magnitude higher thermal stability, as compared to its optical predessor "coherent Ising machine" (CIM). High thermal stability comes from low spinwave propagation speed, which is 5 to 7 orders of magnitude slower than the speed of light. Thus, spin waves can be easily interconverted into RF signals, and can be easily manipulated using off-the-shelf energy-efficient electronic RF components. Altogether, the use of spin waves allows for substantial miniaturization, reduction of power consumption, and significant improvement of frequency stability in time-multiplexed Ising machines.

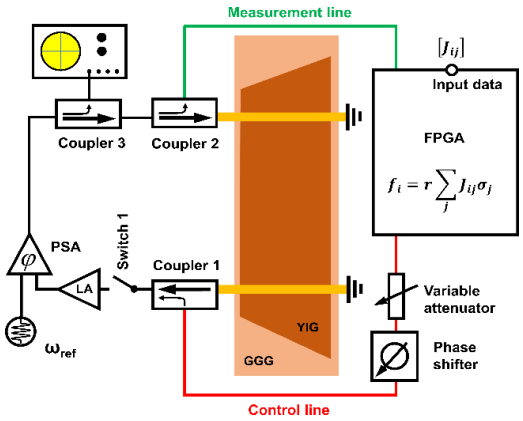

Fig. 1: *Spinwave time-multiplexed Ising machine.*

Below, we discuss the design and potential applications of the SWIM concept. The SWIM main loop (Fig.1) consists of linear and parametric amplifiers, an yttrium-iron garnet (YIG) dispersion-compensated spin wave delay line, where the spin wave RF pulses, playing the role of Ising spins, propagate, and an RF switch that controls the formation of RF pulses inside the ring. The feedback loop consists of an FPGA measurement and control block connected to a variable attenuator and a phase shifter.

Our proposed SWIM design creates a pathway to miniature low-power and commercially feasible Ising machines for solving a wide range of combinatorial optimization problems.

References

[1] A. Litvinenko, R. Khymyn, V. H. Gonzalez, R. Ovcharov, A. A. Awad, V. Tyberkevych, A. Slavin, and J. Åkerman, Communications Physics **6** , 227 (2023).

Abstract ID: 30466

THEORY OF NONLINEAR INTERACTIONS OF PARAMETRICALLY-EXCITED SPIN-WAVE MODES IN CONFINED MICROMAGNETIC SYSTEMS

M. d'Aquino

Dept. of Electrical Eng. and ICTs, University of Naples Federico II, 80125 Naples, ITALY

In this presentation, we address the general theoretical formulation and consequent numerical calculation of magnetization dynamics driven by parallel pumping [1] in arbitrarily shaped confined ferromagnets, achieved using ac external field with one or two tones at appropriate amplitude and frequencies such that parametric instability of one or two normal modes is triggered. The manifestations of such an instability occur in a very complex way due to the highly nonlinear nature of the mode coupling and dynamical interaction between selected modes. To this end, we develop an approach based on magnetization normal modes [2, 3].

The description of micromagnetic dynamics [4] using normal modes [3] has proven to be a powerful tool for the study of magnetization oscillations in ferromagnetic objects [5–7] by means of reduced-order models with few degrees of freedom, i.e. nonlinear coupled oscillators obtained projecting the LLG equation on the linear magnetization eigenmodes, that nevertheless have accuracy comparable with that of much more time-consuming full scale micromagnetic simulations [8].

The main result of this work is a quantitative recipe [9] to determine the phase diagrams of steady-state oscillation regimes for parametrically-excited spin-wave mode pairs that mutually interact in a nonlinear fashion. Despite the multiplicity of regimes achievable changing the excitation conditions, the developed analytical theory shows that such diagrams depend on few parameters, namely appropriate self- and mutual nonlinear frequency shift coefficients and their combinations, which can be quantitatively determined from the knowledge of the eigenmodes profiles and influence the (co-)existence and stability of possible regimes.

The most significant consequences of such complexity include a large number of manifestations of hysteresis and non-commutativity of oscillation regimes as function of external excitation conditions. The diagrams produced by the developed theory can be directly and successfully compared with recent experiments which probe the steady-state regime of parametrically-excited spin-wave mode pairs in a magnetic microdisk [10].

References

[1] A. Gurevich and G. Melkov, Magnetization Oscillations and Waves (CRC Press, 1996).
[2] M. d'Aquino, C. Serpico, G. Miano, and C. Forestiere, Journal of Computational Physics **228**, 6130 (2009).
[3] S. Perna, F. Bruckner, C. Serpico, D. Suess, and M. d'Aquino, Journal of Magnetism and Magnetic Materials **546**, 168683 (2022).
[4] W. F. Brown, Micromagnetics (Interscience Publishers, 1963).
[5] F. Bruckner, M. d'Aquino, C. Serpico, C. Abert, C. Vogler, and D. Suess, Journal of Magnetism and Magnetic Materials **475**, 408 (2019).
[6] S. Perna, F. Bruckner, C. Serpico, D. Suess, and M. d'Aquino, AIP Advances **12** (2022).
[7] I. Ngouagnia Yemeli, S. Perna, D. Gou´er´e, A. Kolli, S. Sangiao, J. M. De Teresa, M. Munoz, A. Anane, M. d'Aquino, H. Merbouche, et al., Phys. Rev. Lett. **135**, 056703 (2025).
[8] C. Abert, The European Physical Journal B **92**, 1 (2019).
[9] M. d'Aquino, S. Perna, H. Merbouche, G. De Loubens, arXiv preprint arXiv:2601.07798 (2026).
[10] G. Soares, R. Lopes Seeger, A. Kolli, M. Massouras, T. Srivastava, J.-V. Kim, N. Beaulieu, J. Ben Youssef, M. Munoz, P. Che, et al., arXiv preprint arXiv:2601.05775 (2026).

Abstract ID: 30502

RESONANT DOMAIN WALL DYNAMICS IN A THREE-DIMENSIONAL MAGNETIC NANO DOUBLE HELIX

P. Morales-Fernández[1,2], I. Konstantinos-Douveas[3], C. Abert[3], E. Zhakina[1], S. Ruiz-Gómez[1,4], C. Fernández-González[1,4], L. A. Turnbull[1,5], S. Wintz[6], M. König[1], S. Finizio[6,7], M. Weigand[6], N. Leo[8], D. Suess[3,9], A. Hierro-Rodríguez[10], A. Fernández-Pacheco[2], C. Donnelly[1,5]

[1] *Max Planck Institute for Chemical Physics of Solids, 01187 Dresden, GERMANY*
[2] *Institute of Applied Physics, TU Wien, Wiedner Hauptstr. 8-10/134,1040 Vienna, AUSTRIA*
[3] *Faculty of Physics, University of Vienna, 1010 Vienna, AUSTRIA*
4 ALBA Synchrotron Light Source, CELLS, Cerdanyola del Valles, 08290, Barcelona, SPAIN
[5] *International Institute for Sustainability with Knotted Chiral Meta Matter (WPI-SKCM2), Hiroshima University, JAPAN*
[6] *Helmholtz-Zentrum Berlin für Materialen und Energie, BESSY II, 12489, Berlin, GERMANY*
[7] *Swiss Light Source, Paul Scherrer Institute, 5232, Villigen, SWITZERLAND*
[8] *Loughborough University, Loughborough LE11 3TU, UNITED KINGDOM*
[9] *Research Platform Mathematics-Magnetism-Materials, University of Vienna, 1010 Vienna, AUSTRIA*
[10] *Depto. Física, Universidad de Oviedo, 33007 Oviedo, SPAIN*

Three-dimensional (3D) magnetic nanostructures promise exciting opportunities beyond the physics of planar systems, with prospects for new topological textures [1], curvilinear effects [2], non-reciprocal dynamics [3] and ultrafast texture motion [4]. Yet, investigating dynamics in complex 3D nanogeometries has remained challenging due to limitations in fabrication and characterization. Our approach combines direct 3D nanoprinting [5] with lab-based magnetic imaging to explore magnetic states and coupling regimes in a cobalt nano double helix [6], and employ time-resolved X-ray microscopy [7] to uncover oscillatory resonant dynamics. Micromagnetic simulations reveal the nature of the observed resonances and further predict higher-frequency excitations that can be systematically tuned via geometric parameters. By precisely engineering the double helix geometry, we directly control the magnetostatic coupling between domain walls, enabling precise tuning of resonant frequencies. These results [8] establish a platform for geometrically programmed magnetization dynamics in complex 3D nanoarchitectures, paving the way toward tunable magnetic functionalities for next-generation computing.

References

[1] S. Castillo-Sepúlveda, *et al.*, *Magnetic hopfions in toroidal nanostructures driven by an Oersted magnetic field*, Phys. Rev. B **104**, (2021).
[2] S. Ruiz-Gómez, *et al.*, *Tailoring the energy landscape of a Bloch point domain wall with curvature*, Nat. Commun. **16**, 7422 (2025).
[3] M. Xu, P. Morales-Fernández, *et al.*, *Geometry-induced spin chirality in a non-chiral ferromagnet at zero field*, Nat. Nanotechnol. (2025).
[4] R. Hertel, *Ultrafast domain wall dynamics in magnetic nanotubes and nanowires*, J. Phys.: Condens. Matter **28**, 483002 (2016).
[5] L. Skoric, *et al.*, *Layer-by-layer growth of complex-shaped three-dimensional nanostructures with focused electron beams*, Nano Lett. **20**, 184 (2020).
[6] C. Donnelly, *et al.*, *Complex free-space magnetic field textures induced by three-dimensional magnetic nanostructures*, Nat. Nanotechnol. **17**, 136 (2022).
[7] M. Weigand, *et al.*, *TimeMaxyne: A shot-noise limited, time-resolved pump-and-probe acquisition system capable of 50 GHz frequencies for synchrotron-based x-ray microscopy*, Crystals **12**, 8 (2022).
[8] P. Morales-Fernández, *et al.*, *Resonant domain wall dynamics in a three-dimensional magnetic nano double helix*, Submitted (2026).

Abstract ID: 30063

NANOSCALED SPIN-WAVE DEVICES FOR 5G TECHNOLOGY OPERATING AT FR2

K. Davídková[1], K. Levchenko[1], F. Bruckner[1], R. Verba[2], R. Serha[1], F. Majcen1, Q. Wang[3], M. Lindner[4], C. Dubs[4], V. Vlaminck[5], J. Klíma[6], M. Urbánek[6], D. Suess[1], A. Chumak[1,3]

[1] *University of Vienna, Faculty of Physics, 1090, Vienna, AUSTRIA*
[2] *V.G. Baryakhtar Institute of Magnetism of the NAS of Ukraine, 03142, Kyiv, UKRAINE*
[3] *School of Physics, Huazhong University of Science and Technology, 430074, Wuhan, CHINA*
[4] *INNOVENT e. V. Technologieentwicklung, 07745, Jena, GERMANY*
[5] *IMT Atlantique, Lab-STICC—UMR 6285 CNRS, 29238, Brest, FRANCE*
[6] *CEITEC BUT, Brno University of Technology, 612 00, Brno, CZECH REPUBLIC*

The ongoing demand for faster and more efficient 5G communication systems requires radio-frequency (RF) devices to adapt from Frequency Range 1 (FR1, sub-6 GHz) to higher operating frequencies of Frequency Range 2 (24.25-71.0 GHz) and proposed Frequency Range 3 (FR3, 7.125-24.25 GHz). However, conventionally used RF devices, such as power limiters (based on PIN diodes), filters and delay lines (based on SAW or BAW) cannot conveniently operate at higher frequency ranges, due to high electronic noise and switching delays (diodes) and increasing damping with higher frequencies (SAW and BAW) [1]. Therefore, spin-wave (SW) based devices are of interest as they maintain their efficiency at high GHz frequencies, although they have only been studied at the macroscale so far [1]. We demonstrate a proof of concept of nanoscale frequency selective limiter (Fig. 1(b)) and delay line based on spin-wave transmission in a 97-nm-thin YIG film. Spin waves are excited and detected using 250 nm wide CPW transducers (Fig. 1(a)). The devices are tested in the frequency range up to 25 GHz for both in-plane fundamental modes, Damon-Eshbach (DE) and Backward Volume (BV), and the key parameters are extracted, such as power threshold Pth (Fig. 1(c)), and delay time T_d (Fig. 1(d)). The SW devices incorporates multifunctionality, thus allowing for more efficient use of space and energy.

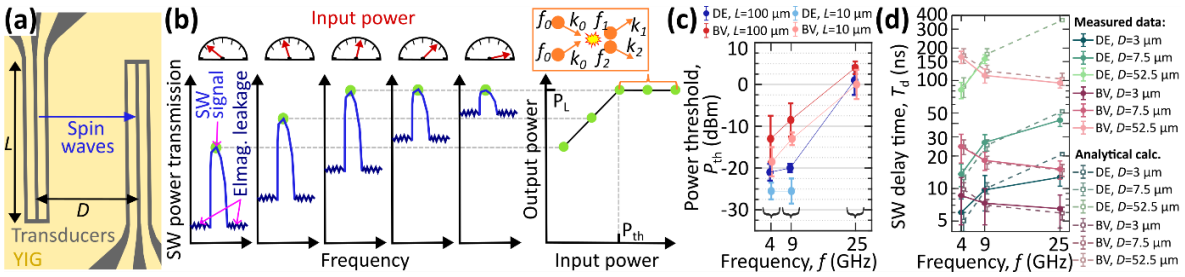

Fig. 1: *(a) The schema of transducers. (b) The schema of the power-limiting effect based on nonlinear spin-wave transmission and multi-magnon scattering. (c) The extracted power threshold Pth for the DE and BV modes measured using the transducers of the length of L=10 μm and 100 μm with the mutual distance of 3 μm; taken from [2]. (d) The extracted delay time for both modes measured using the 100 μm long transducers of the mutual distance of D=3 μm, 7.5 μm and 52.5 μm; taken from [3].*

References

[1] K. O. Levchenko, *et al.*, eprint arXiv:2411.19212, (2024).

[2] K. Davidkova, *et al.*, Physical Review Applied **23.3**, 034026, (2025).

[3] K. Davidkova, *et al.*, Journal of Applied Physics **138**, 14, (2025).

Abstract ID: 30083

VERTICAL CONTROL IN MAGNONICS FOR EITHER TUNABLE MAGNON-MAGNON INTERACTION OR MAGNONIC METAL-TO-INSULATOR TRANSITION

F. Montoncello[1], P. Micaletti[1], R. Sultana[2], M. T. Kaffash[2], G. Gubbiotti[3], Y. Ji[2], M. B. Jungfleisch[2]

[1] *Dipartimento di Fisica e Scienze della Terra, Università di Ferrara, 44121 Ferrara, ITALY*
[2] *Department of Physics and Astronomy, University of Delaware, Newark, DE19716, USA*
[3] *CNR-Istituto Officina dei Materiali (IOM), Unità di Perugia, 06123 Perugia, ITALY*

In Magnonics, the combination of layers with different geometric patterns offers a variety of dynamic degrees of freedom for magnon control at the nanoscale, leading to versatile, miniaturized and extremely low dissipation devices for information transport and manipulation. We show by micromagnetic simulations and experimental evidence how, in coupled artificial spin ice (ASI) and film layers, a frequency selective magnon-magnon interaction arises between the film spin wave and the ASI modes [1]. The ASI modes which are involved (either edge or bulk) can be selected by the choice of the materials, mainly based on the saturation magnetization values [2]. Then, we investigate a straight film layer with an undulated, periodic magnetization distribution determined by the interaction with a likewise undulated magnetic field: this field can be created directly by a meandering conductor, or most interestingly by inverse magnetostriction operated by a coupled ferroelectric layer with a periodic polarization direction [3]. The result is a dynamic magnonic crystal displaying a magnonic band structure, with a frequency gap and a dispersion curvature which can be finely tuned by varying either the magnitude or fan angle of magnetic field created by the meander, or even by the electric field applied on the ferroelectric layer, which we simulate through a variable uniaxial magnetic anisotropy [4]. We discuss the transition between a magnonic metal state, interpreted within the Dirac's magnon picture, and an insulator state, with controllable frequency gap position and width, which is found particularly useful in the context of magnon transfer in directional couplers.

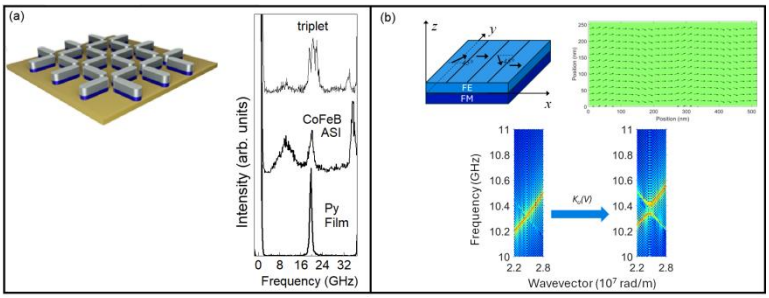

Fig. 1: *(a) Sketch of the system, and Brillouin light scattering spectra where the triplet signals the magnon-magnon interaction in the coupled ASI-film system (b) polarization periodicity in the FE-FM bilayer, resulting undulated magnetization distribution, and magnonic metal-to-insulator transition.*

References

[1] R. Negrello, *et al.*, APL Materials **10**, 091115 (2022).

[2] R. Sultana, *et al.*, https://arxiv.org/abs/2510.06004 (submitted for publication).

[3] P. Micaletti, *et al.*, Journal of Magnetism and Magnetic Materials **6[4]22**, 172959 (2025).

[4] P. Micaletti, *et al.*, Journal of Applied Physics **137**, 153906 (2025).

11th International Conference on Superconductivity and Magnetism ICSM2026
4th International Conference on Quantum Materials and Technologies ICQMT2026
19th April to 26th April, 2026, Ölüdeniz – Fethiye/Muğla, Türkiye
https://icsmforever.org/

Abstract ID: 30179

ENHANCEMENT OF COHERENT FREQUENCY COMBS IN STACKED MAGNET-SUPERCONDUCTOR HYBRID LAYERS

A. Ghirri[2], M. Cavani[1], C. Bonizzoni[1,2], M. Affronte[1,2]

[1] *Università di Modena e Reggio Emilia, Dipartimento di Scienze Fisiche, Informatiche e Matematiche, via G. Campi 213A, 41125 Modena ITALY*
[2] *CNR, Istituto Nanoscienze, via G. Campi 213A, 41125 Modena ITALY*

Frequency combs, i.e. sequences of signals equally spaced in frequency with extremely sharp linewidth, are commonly generated in optics and electronics by nonlinear effects and used in metrology, sensing and also for neuromorphic information processing. In the microwave range, frequency combs can be generated by exploiting the *nonlinearities* in superconductors or in magnetic materials. Here, we report on the generation of microwave/magnonic frequency combs in a stack of high T_c superconducting YBCO and magnetic (Yittrium Iron Garnet) YIG films when static magnetic field drives the latter at ferromagnetic resonance. We show that the interplay between the YIG and YBCO films [1, 2] enhances the generation of frequency combs in terms of number of teeth and by lowering the activation threshold [3]. Moreover the sideband signals preserve phase coherence with respect to the pumps and one to another. We discuss the key intrinsic and extrinsic parameters as well as possible mechanisms at the basis of the *interplay between the magnetic and the superconducting layers* that constitute a challenging theoretical problem but indicate an alternative way for applications in microwave technology.

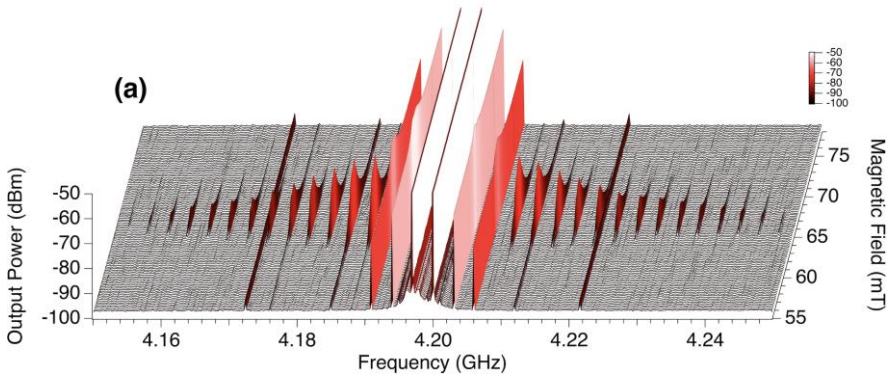

References

[1] A. Ghirri, *et al.*, Phys Rev Appl. **20**, 024039 (2023).

[2] A. Ghirri, *et al.*, Phys. Rev. Applied **22**, 034004 (2024).

[3] A. Ghirri, *et al.*, in preparation (2025).

Abstract ID: 30130

QUANTUM STATE PREPARATION OF FERROMAGNETIC MAGNONS BY EXTERNAL CLASSICAL DRIVES

C. G. Ballestero

Institute for Theoretical Physics, Vienna University of Technology, AUSTRIA

Preparing certifiably quantum states of ferromagnetic magnons represents a central milestone in the emerging field of quantum magnonics. Among these, Gaussian states are particularly attractive, as they can be prepared and manipulated without direct coupling to qubits, thereby allowing a wide range of current solid-state experiments to access the quantum regime. Even more, harnessing magnonic intrinsic nonlinearity allows to prepare such certifiably quantum states using only external classical drives.

In the first part of my talk I will present our recently proposed protocol to generate Gaussian quantum states -- specifically, vacuum-squeezed and entangled states -- in the ferromagnetic resonance mode of anisotropic yttrium iron garnet (YIG) samples using only microwave parametric drive [1]. I will show how these states can be prepared in current cryogenic setups and certified using classical techniques such as FMR resonance or local coil probes.

In the second part of my talk I will present our extension to the preparation of quantum states of *propagating* magnons in continuum structures, which remains an outstanding challenge. One promising route involves spontaneous parametric down-conversion, where intrinsic nonlinear three-magnon processes lead to the splitting of a magnon into an entangled pair. However, when triggered by a microwave drive, these processes are often shadowed by four-magnon interactions which introduce strong dephasing and decoherence. We propose an alternative route that harnesses an *acoustic phonon drive* and the strong nonlinear magnon–phonon coupling in thin film structures. By developing an extensive continuum classical and quantum theoretical framework we quantitatively identify and predict the thresholds for parametric instabilities of all nonlinear processes arising in thin-film geometries [2]. Our analysis reveals that it is possible to increase the efficiency of phonon-to-magnon parametric down-conversion (phonon splitting into two magnons) so that it has a significantly lower threshold than purely magnonic nonlinearities. This result, experimentally validated in the classical regime [3], enables access to quantum magnonic correlations without triggering four-magnon-induced dephasing. We theoretically predict that in the quantum regime the same mechanism allows for the generation of entanglement between propagating magnons at cryogenic temperatures, and propose methods to detect such entanglement in current magnonic experiments.

References

[1] M. Mycroft, R. Serha, A. V. Chumak, C. G. Ballestero, In preparation

[2] M. Brühlmann, Y. Hwang, J. Puebla, C. G. Ballestero, arXiv: 2509.16199 (2025).

[3] Y. Hwang, L. Liao, J. Puebla, M. Brühlmann, C. G. Ballestero, K. Kondou, N. Ogawa, S. Maekawa, Y. Otani, arXiv:2509.19706 (2025).

11th International Conference on Superconductivity and Magnetism ICSM2026
4th International Conference on Quantum Materials and Technologies ICQMT2026
19th April to 26th April, 2026, Ölüdeniz – Fethiye/Muğla, Türkiye
https://icsmforever.org/

Abstract ID: 30157

TOMOGRAPHY OF PARAMETRIC TRANSITION AND THERMAL SQUEEZING IN A MAGNET

T. Hioki[1,2,3]

[1] *Department of Applied Physics, The University of Tokyo, Tokyo 113-8656, JAPAN*
[2] *WPI Advanced Institute for Materials Research, Tohoku University, Sendai 980-8577, JAPAN*
[3] *RIKEN Center for Emergent Matter Science, Riken, Wako 351-0198, JAPAN*

Squeezed states are a key concept underpinning quantum technologies and thermodynamics, widely employed to enhance measurement precision and enable novel information processing methods. While photon-based squeezed states have been extensively studied, magnetic systems remain an underutilized resource for the engineering of squeezed states.

In this study, we excited nonlinear dynamics of magnons and observe magnetization fluctuations by measuring Wigner function, a pseudo-probability distribution of magnons. We achieved thermal squeezing of magnons, creating correlations between magnetization dynamics at different surfaces of the magnetic thin film.

We used a thin film of the ferromagnetic insulator $Y_3Fe_5O_{12}$ (YIG) with a thickness of 1.4 μm, fabricated into a disk shape and coated with platinum. For driving nonlinear dynamics, we employed parametric excitation, where an oscillating magnetic field with twice the ferromagnetic resonance frequency generates magnetization oscillations.

The observed Wigner functions show how parametric excitation process drives magnetization dynamics with temporal resolution, and demonstrate magnon thermal squeezing and its ability to generate correlations between spatially remote magnons. The unconventional magnetization dynamics highlights the promise of magnetic materials as a platform for quantum science in the foreseeable future.

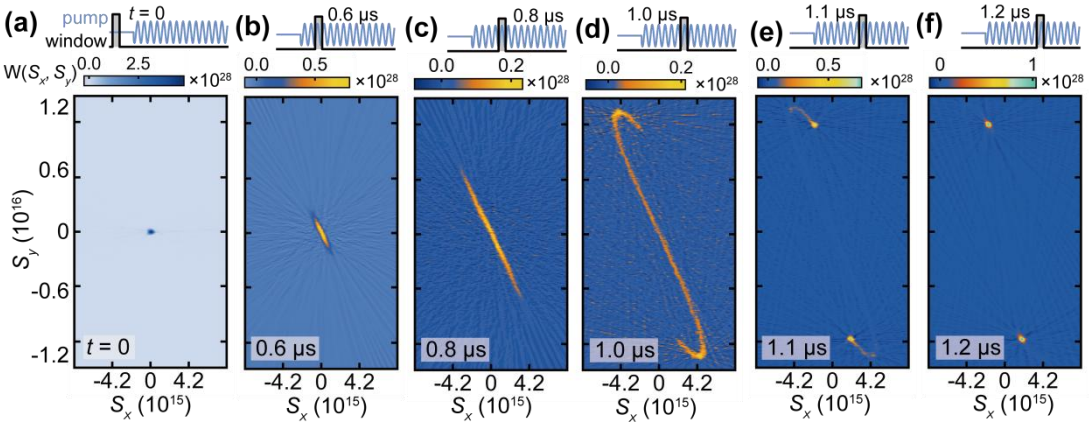

Fig. 1:.*Parametric transition of magnetization dynamics in $Y_3Fe_5O_{12}$.*

References

[1] T. Hioki, H. Shimizu, T. Makiuchi, and E. Saitoh, Phys. Rev. B **104**, L100419 (2021).

[2] T. Makiuchi, T. Hioki, H. Shimizu, *et al.*, Nature Materials, **23**, 627-632 (2024).

[3] H. Shimizu, T. Hioki, S. Takeda, and E. Saitoh, Phys. Rev. Lett., **135**, 106701 (2025).

Abstract ID: 30521

COHERENT AND INCOHERENT MAGNONS IN NANOSTRUCTURED 3D TUBULAR FERROMAGNETS

D. Grundler[1,2]

[1] *Institute of Materials (IMX), Ecole Polytechnique Fédérale de Lausanne (EPFL), 1015, Lausanne, SWITZERLAND*
[2] *Institute of Electrical and Micro Engineering (IEM), Ecole Polytechnique Fédérale de Lausanne (EPFL), 1015, Lausanne, SWITZERLAND*

Three-dimensional (3D) nanomagnetism and magnonics are research directions of great current interest. New functionalities are expected for spin waves (magnons), for instance, in chiral magnets which possess unique 3D spin helices. They give rise to nonreciprocal transport phenomena at zero magnetic field enabling energy efficient data transmission in preferred directions in 3D networks. However experiments are scarce. We report on the creation and exploration of 3D ferromagnetic networks and artificial chiral magnets (ACMs) prepared from Ni. Using atomic layer deposition of high-quality Ni [1] we prepare 3D tubular woodpiles [2] and 3D tubular screws [3], respectively, from thin conformal shells around polymeric nanotemplates. Ferromagnetic Ni shells on 3D woodpile lattices of polymer nanorods have shown incoherent surface magnon modes which exhibited unconventionally high resonance frequencies [2]. In recently performed inductive measurements and micromagnetic simulations in fields up to about 1 T we have identified an unconventional phase evolution of edge magnon modes when coherently excited by a microwave field [4]. Hollow Ni screws exhibited zero-field spin spirals leading to nonreciprocal magnon transport at room temperature studied by means of inelastic light scattering microscopy and micromagnetic simulations. Controlling their toroidal moments and magnetochiral effects via 3D geometrical handedness and field-dependent spin orientation, we obtained ACMs with programmable nonreciprocity at zero magnetic field [3]. Our experiments and findings are a major step in functional 3D nanomagnetism at room temperature and 3D nanomagnonics based on a mass production compatible deposition technology.

Cooperations with M. Xu, A.J.M. Deenen, H. Guo, M. Hamdi, S. Ladak, K. Lenz, M. Golebiewski, R. Narkowicz, J. Lindner, M. Krawczyk, A. Roberts, J Askey, V Lanka, A van den Berg, C. Donelly, P. Morales-Fernández, E. Zhakina, M. Weigand, and S. Wintz are gratefully acknowledged. Our work is funded by SNSF via grant 197360.

References

[1] M.C. Giordano, K. Baumgaertl, S. Escobar Steinvall, *et al.*, ACS Appl. Mater. Interfaces, **Vol. 12**, p. 40443 (2020).
[2] H. Guo, A.J.M. Deenen, M. Xu, *et al.*, Adv. Mater., **Vol. 35**, p. 2303292 (2023).
[3] M. Xu, A.J.M. Deenen, H. Guo, *et al.*, Nature Nanotechnology, (2025). https://rdcu.be/eS7mE
[4] H. Guo, K. Lenz, M. Golebiewski *et al.*, Small, e08983 (2025). http://doi.org/10.1002/smll.202508983
[5]

32 - METASTABILITY, DISORDER, AND HIDDEN ORDERS IN 2D QUANTUM MATERIALS

Abstract ID: 30020

HIDDEN STATES IN IRON-CHALCOGENIDE SUPERCONDUCTORS AND THEIR POTENTIALS FOR TOPOLOGICAL QUANTUM COMPUTING

Q. Li[1,2]

[1] *Condensed Matter Physics and Materials Science Division, Brookhaven National Laboratory, Upton, New York, 11973, USA*
[2] *Department of Physics and Astronomy, Stony Brook University, Stony Brook, New York, 11794 USA*

In the iron-chalcogenide superconductors, a variety of hidden electronic, magnetic, superconducting, and topological states have been uncovered in recent years. By "hidden states," I refer to quantum phases that are not immediately apparent from the crystal structure alone. Remarkably, iron-chalcogenides can be exfoliated into monolayers, which have attracted considerable attention in the field of 2D materials in addition to their unique coexistence of superconductivity, nontrivial electronic topology, and magnetism within a single material system. This convergence opens the door to topological superconductivity, a state that may host Majorana zero modes (MZMs) with potential applications in fault-tolerant quantum computing.

In this presentation, I will discuss our studies of the quantum states in $Fe_{1+\gamma}Te_{1-x}Se_x$ single crystals grown at Brookhaven National Laboratory. These crystals have served as benchmark samples worldwide, enabling extensive investigations into the topological and superconducting properties of iron chalcogenides. Through scanning probe microscopy, angle-resolved photoemission spectroscopy (ARPES), and tunneling transport measurements, we have revealed significant compositional inhomogeneity and variability in the superconducting and topological behaviors. Our findings underscore the importance of precise compositional control and electronic phase tuning for harnessing iron-chalcogenides as viable platforms for quantum technologies.

Abstract ID: 30282

EMERGENT DIMENSIONALITY REDUCTION DRIVEN BY NANOSCALE SYMMETRY BREAKING IN SnSe

E. S. Bozin

Center for Solid State Physics and New Materials, Institute of Physics Belgrade 11080 Belgrade, SERBIA

We reveal how dimensionality reduction arises from nanoscale symmetry breaking in SnSe during its structural phase transition (Fig. 1) [1]. Using advanced X-ray total scattering and pair distribution function analysis, we show that Sn displacement correlations evolve from three-dimensional to quasi-two-dimensional within the SnSe structural bilayers, accompanied by a loss of coherence along their stacking direction. This symmetry-broken nanoscale state (ξ~1nm) persists well above the transition temperature, fundamentally reshaping the local structural landscape. Detailed modeling confirms that ferro-coupling within layers and antiferro-coupling between layers dominate the displacement patterns, while correlations between adjacent bilayers become effectively decoupled. These results demonstrate that the phase transition in SnSe is neither a simple displacive process nor a conventional order–disorder transition, but rather a complex crossover driven by local dipolar distortions and dimensionality reduction.

This intrinsic nanoscale symmetry breaking strongly enhances phonon scattering, giving rise to ultralow lattice thermal conductivity and exceptional thermoelectric performance in SnSe. The persistence of dynamic, short-range correlated Sn displacements above the transition temperature highlights the critical role of local structural fluctuations in governing thermal transport. This provides a complementary mechanism to the nanoscale symmetry-breaking off-centering ("emphanitic") distortions previously observed upon warming from undistorted ground state in PbTe [2], $AgGaTe_2$ [3], and related high-performance thermoelectric materials. By clarifying the interplay between dimensionality reduction and local symmetry breaking, this work establishes a robust framework for understanding and optimizing thermoelectric performance. These insights open new pathways for engineering nanoscale structural features to tailor thermal and electronic properties in complex layered quantum and related materials.

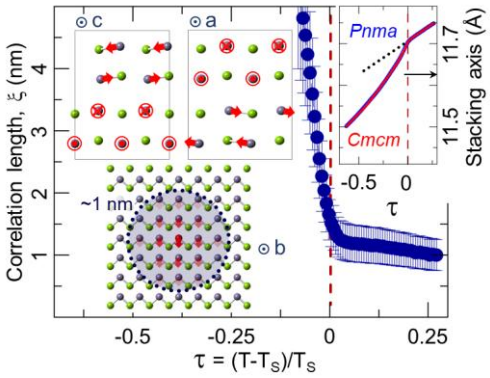

Fig. 1: *Temperature-dependent correlation length and lattice anomalies in SnSe at high temperature*

References

[1] E. S. Bozin, *et al.*, Physical Review Letters **131, 036101 (2023).**

[2] E. S. Bozin, *et al.*, Science **330**, 013603 1660 (2010).

[3] H. Xie, E. S. Bozin, *et al.*, Advanced Materials **34**, e2202255 (2022).

Abstract ID: 30314

FLUCTUATION-ENHANCED ELECTRON–PHONON COUPLING IN FeSe

B. Višić[1,2], J. Blagojević[1], A. Milosavljević[1], T. Belojica[1], M. Opačić[1], A. Šolajić[1], J. Pešić[1], E. Bozin[1], C. Petrovic[3,4,5], R. Hackl[6,7], N. Lazarević[1]

[1] *Institute of Physics Belgrade, University of Belgrade, Pregrevica 118, 11080 Belgrade, SERBIA*
[2] *Department of Condensed Matter Physics, Jozef Stefan Institute, Jamova cesta 39, Ljubljana 1000, SLOVENIA*
[3] *Condensed Matter Physics and Material Science Department, Brookhaven National Laboratory, Upton, NY 11973-5000, USA*
[4] *Shanghai Advanced Research in Physical Sciences (SHARPS), Shanghai 201203, CHINA*
[5] *Department of Nuclear and Plasma Physics, Vinca Institute of Nuclear Sciences, University of Belgrade, Belgrade 11001, SERBIA*
[6] *School of Natural Sciences, Technische Universität München, Garching 85748, GERMANY*
[7] *IFW Dresden, Helmholtzstrasse 20, Dresden 01069, GERMANY*

Unconventional superconductivity often arises in materials with complex interactions, where competing ordered states such as magnetism, nematicity, and superconductivity, interact and sometimes overlap, making their nature elusive. The interactions among lattice, charge, and spin degrees of freedom fundamentally shape material properties.

In FeSe, symmetry-breaking perturbations serve as highly sensitive probes of these couplings. Previous work has shown that defects and isoelectronic substitution can substantially alter these interactions, giving rise to additional phonon modes. In this study, uniaxial strain is employed as a tunable symmetry-breaking control parameter to probe the intrinsic lattice response in the absence of disorder. The temperature evolution of phonon excitations was examined with fine temperature resolution in the vicinity of the nemato-structural transition temperature T_s, under strain applied along the ⟨110⟩ and ⟨100⟩ crystallographic directions. A subtle asymmetry of the A^{ph}_{1g} mode appears in the unstrained crystal within a narrow temperature window around T_s, originating from the emergence of an additional mode in the fully symmetric channel. With applied strain, this feature becomes more distinctly resolved. The anomaly is attributed to modifications of the coupling between lattice and electronic degrees of freedom driven by the ordering fluctuations right above the nematic transition. These fluctuations enhance susceptibility for phonon-electron-phonon coupling in the vicinity of the X and R points of the Brillouin zone and promote two-phonon scattering close to the A^{ph}_{1g} mode. The presence of this two-phonon scattering depends on both the strength and the direction of the applied strain, indicating a high sensitivity of FeSe to local symmetry breaking.

References

[1] J. Blagojević, *et al.*, under review (2025)

Abstract ID: 30324

HIDDEN ORDER AND FLUCTUATING PHASES IN VAN DER WAALS TELLURIDES

J. Pešić[1], T. Belojica[1], J. Blagojević[1], A. Šolajić[1], B. Višić[1], E. S. Božin[1], S. D. Mijin[1], C. Petrović[2,3,4], Z. V. Popović[5], R. Hackl[6,7], A. Milosavljević[1], N. Lazarević[1]

[1] *Center for Solid State Physics and New Materials, Institute of Physics Belgrade, Uni. Of Belgrade, 11000 Belgrade, SERBIA*
[2] *Condensed Matter Physics and Materials Science Department, Brookhaven National Laboratory, Upton, NY 11973-5000, USA*
[3] *Shanghai Advanced Research in Physical Sciences (SHARPS), Shanghai 201203, CHINA*
[4] *Department of Nuclear and Plasma Physics, Vinca Institute of Nuclear Sciences, Uni. of Belgrade, 11001, SERBIA*
[5] *Serbian Academy of Sciences and Arts, Knez Mihailova 35, 11000 Belgrade, SERBIA*
[6] *School of Natural Sciences, Technische Universitat Munchen, Garching 85748, GERMANY*
[7] *IFW Dresden, Helmholtzstrasse 20, Dresden 01069, GERMANY*

Hidden order in quantum materials often manifests as fluctuating phases that modify collective excitations without producing clear structural symmetry breaking. Such behavior has been previously identified in the magnetic van der Waals compound $Mn_3Si_2Te_6$, where temperature-dependent Raman anomalies and phonon self-energy renormalization revealed competing short-range magnetic correlations persisting well above ordering temperature [1]

Here, we demonstrate that an analogous phenomenology arises in the non-magnetic van der Waals telluride $InSiTe_3$, where the hidden order is encoded purely in lattice dynamics [2].

Combining temperature-dependent spectroscopy with first-principles phonon calculations, we identify an isolated high-energy A1g Einstein mode in $InSiTe_3$ that spontaneously forms a phonon frequency comb, signaling a phase-coherent vibrational state stabilized by strong anharmonic interactions. In parallel, pronounced anomalies appear around 200 K in the energies and linewidths of low-energy fully symmetric modes, accompanied by the emergence of multi-phonon excitations within a gap of the phonon density of states. These effects indicate a crossover into a strongly interacting vibrational regime characterized by enhanced fluctuations rather than static ordering.

Viewed together with $Mn_3Si_2Te_6$, where competing short-range magnetic phases strongly renormalize phonon properties, $InSiTe_3$ establishes a broader framework in which hidden order can originate from different microscopic degrees of freedom, magnetic in one case, lattice-anharmonic in the other, yet produce strikingly similar spectroscopic fingerprints. Our results suggest that Raman-visible self-energy anomalies and mode-selective coherence provide a unifying route to identifying hidden and fluctuating phases across van der Waals materials.

References

[1] S. D. Mijin, A. Šolajić, J. Pešić, Y. Liu, C. Petrovic, M. Bockstedte, A. Bonanni, Z. V. Popović, and N. Lazarević, *Spin-phonon interaction and short-range order in $Mn_3Si_2Te_6$*, Phys. Rev. B **107**, 054309 (2023).

[2] T. Belojica, J. Blagojevic, S. Djurdjic Mijin, A. Solajic, J. Pesic, E. S. Bozin, B. Visic, , Y. Liu, C. Petrovic, Z. V. Popovic, Rudi Hackl, Ana Milosavljevic, and Nenad Lazarevic, *Spontaneous phonon frequency combs from an isolated Einstein mode in $InSiTe_3$*, (In press 2026).

Abstract ID: 30325

PHASE COEXISTENCE AND ELECTRONIC ORDERING IN 1T-TaS_2

N. Lazarević[1], S. Djurdjić Mijin[1,9], A. Baum[2], J. Bekaert[3], J. Pešić[1], Y. Liu[4], G. He[2], M. V. Milošević[3], C. Petrovic[4,5,6], Z. V. Popović[7], R. Hackl[10]

[1] *Center for Solid State Physics and New Materials, Institute of Physics Belgrade, University of Belgrade, Pregrevica 118, 11080 Belgrade, SERBIA*
[2] *Walther Meissner Institute, Bavarian Academy of Sciences and Humanities, 85748 Garching, GERMANY*
[3] *Department of Physics & NANOlab Center of Excellence, University of Antwerp, Groenenborgerlaan 171, B-2020 Antwerp, BELGIUM*
[4] *Condensed Matter Physics and Materials Science Department, Brookhaven National Laboratory, Upton, New York 11973-5000, USA*
[5] *Center for Correlated Matter and School of Physics, Zhejiang University, Hangzhou 310058, PEOPLE'S REPUBLIC OF CHINA*
[6] *Department of Nuclear and Plasma Physics, Vinča Institute of Nuclear Sciences, University of Belgrade, Belgrade 11001, SERBIA*
[7] *Serbian Academy of Sciences and Arts, Knez Mihailova 35, 11000 Belgrade, SERBIA*
[8] *Departamento de Física de Materiales, Facultad de Ciencias, Universidad Autónoma de Madrid, 28049 Madrid, SPAIN*
[9] *IFW Dresden, Helmholtzstrasse 20, 01069 Dresden, GERMANY*

Charge-density-wave (CDW) materials are characterized by complex phase diagrams governed by coupled lattice and electronic degrees of freedom. We present a symmetry-resolved Raman scattering study of 1T-TaS_2 across its incommensurate, nearly commensurate, and commensurate CDW regimes. The nearly commensurate phase exhibits clear signatures of phase coexistence, with simultaneous contributions from commensurate and incommensurate domains in the Raman response. In the commensurate CDW phase, polarization-dependent measurements establish trigonal stacking of the Star-of-David clusters. The evolution of the low-energy electronic Raman response reveals a gradual depletion of spectral weight associated with CDW gap formation, followed at lower temperatures by the opening of a correlation-driven Mott gap of approximately 170–190 meV.

Abstract ID: 30423

DECIPHERING THE SEQUENCE OF PHASE TRANSITIONS IN $KNiCl_3$

M. J. Gutmann[1], K. Wang[2], S.-W. Kim[2], B. Monserrat[2], G. L. Pascut[3]

[1] *Rutherford Appleton Laboratory, ISIS spallation neutron source, Chilton Didcot, Oxfordshire OX11 0QX, UNITED KINGDOM*
[2] *Department of Materials Science and Metallurgy, University of Cambridge, Cambridge CB3 0FS, UNITED KINGDOM*
[3] *MANSID Research Center, University Stefan Cel Mare, 720229 Suceava, ROMANIA*

$KNiCl_3$ shows an intriguing series of phase transitions. These occur at 561K, 285K and 274K resulting in a complex evolution of the corresponding diffraction patterns (Fig. 1). The high-temperature phase the compound crystallises in a centrosymmetric hexagonal structure, space group $P6_3/mmc$, characterised by columns of $NiCl_6$ octahedral chains along the crystallographic c-axis with K in-between these columns. A polar structure is found below 561K with a non-vanishing dielectric constant. In the narrow temperature range between 285K and 274K, an intermediate phase characterised by a phase-coexistence of two crystallographic phases and a maximum of the dielectric constant are found. Finally below 274K, the dielectric constant nearly vanishes and the ground-state structure is obtained. I will discuss the resulting crystallographic phases. This study is augmented with first-principles DFT+eDMFT calculations. In particular anharmonic phonons are found to be essential to describe the lattice dynamics in the high-temperature phase [1]. The resulting diffuse scattering from these theory calculations are derived and compared to experiments. Time permitting, I will present results on magnetic diffuse scattering.

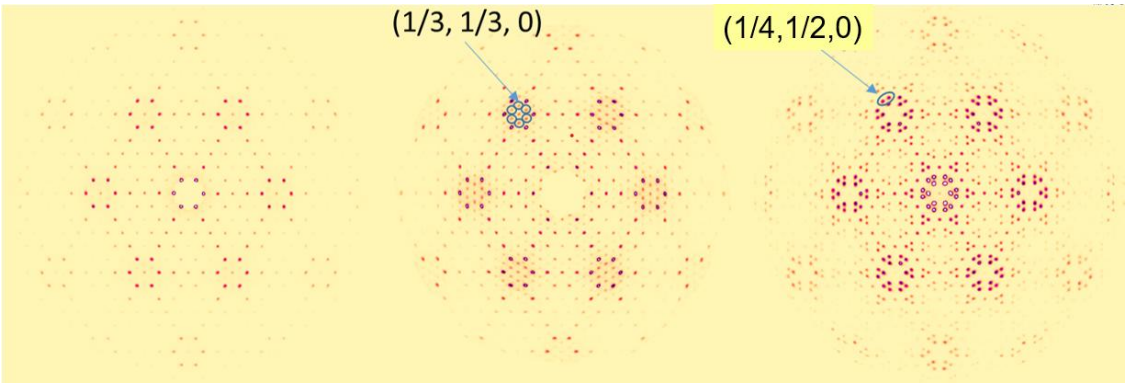

Fig. 1: *Diffraction patterns corresponding to the (h,k,0)-layer at room temperature (left), intermediate (center) and low temperature phase (right), respectively.*

References

[1] M. J. Gutmann, K. Wang, S.-W. Kim, B. Monserrat, and G. L. Pascut, Struct. Dynam. **12**, 054103 (2025).

Abstract ID: 30442

ELECTRONIC-STRUCTURAL INTERPLAY IN THE PARAMAGNETIC STATE OF LOW DIMENSIONAL SYSTEMS

Q. Zhang[1], S.-W. Kim[2], K. Wang[2], M. Gutmann[3], A. Devashibhai[3,4], B. Monserrat[2], K. Haule[5], G. L. Pascut[6]

[1] *School of Physics, Shandong University, Jinan 250100, CHINA*
[2] *Department of Materials Science and Metallurgy, University of Cambridge, Cambridge CB3 0FS, UNITED KINGDOM*
[3] *ISIS Neutron and Muon Source, STFC Rutherford Appleton Laboratory, Harwell Campus, Didcot, Oxfordshire OX11 0QX, UNITED KINGDOM*
[4] *Highly Correlated Matter Research Group, Physics Department, University of Johannesburg, Auckland Park 2006, SOUTH AFRICA*
[5] *Department of Physics, Rutgers University, Piscataway, New Jersey 08854, USA*
[6] *Functional Materials & Sustainability Laboratory (FuMaS Lab), Faculty of Forestry, University Stefan Cel Mare, 720229 Suceava, ROMANIA*

To understand the structure-property relationships in low-dimensional correlated systems, we performed finite-temperature calculations in the paramagnetic state using a first-principles approach. Our results reveal that the charge gap exhibits a mixed Band-Mott character [1, 2, 3]. We discuss this unusual mixing in terms of orbital occupation, character, and hybridization. Furthermore, we unveil these relationships by investigating various metal-substituted systems (M = {Mn, Fe, Ni, Co, Cu, Zn}). By performing structural relaxations at finite temperatures, we demonstrate the predictive power of our method regarding electronic-structural interplay. Finally, we discuss the implications of this mixed Band-Mott nature on the low-energy spin Hamiltonian [4].

References

[1] K. Park, *et al.*, Phys. Rev. B **104**, 195143 (2021).
[2] T. N. Stanislavchuk, *et al.*, Phys. Rev. B **102**, 115139 (2020).
[3] VA Martinez, *et al.*, e-print https://arxiv.org/abs/2507.22172 (2025).
[4] Suheon Lee, *et al.*, e-print https://arxiv.org/abs/2502.04919 (2025).

Abstract ID: 30712

DETERMINATION OF LOCAL ORDER FROM DIFFUSE SCATTERING BY HIGH ENERGY X-RAYS

M. v. Zimmermann

Deutsches Elektronen-Synchrotron DESY, Hamburg, GERMANY

The physical properties of materials are determined by their chemical bonds. In a crystal these can be arranged in long range order, but also very on a local scale due to defects, frustration or other mechanisms. A lack of long range order gives rise to diffuse scattering in a diffraction experiment. The analysis of diffuse scattering in reciprocal space may be tedious, due to the high complexity of these patterns. With the recently developed technique of 3d-ΔPDF, the diffuse scattering of single crystalline materials is transformed into correlations in real space and thus more easily interpretable. In the presentation it is motivated that high energy x-rays are an ideal probe for the detection of diffuse scattering patterns, and recent studies of bulk and thin film samples at the PETRA III high energy x-ray beamlines P21.1 and P07 are presented.

Abstract ID: 30787

NON-EQUILIBRIUM ELECTRON DYNAMICS ON THE SURFACE OF 1T-TaS_2

Y. Vaskivskyi

[1] *Department of Complex Matter, Jozef Stefan Institute, SI-1000, Ljubljana, SLOVENIA*
[2] *CENN Nanocenter, SI-1000, Ljubljana, SLOVENIA*

1T-TaS_2 continues to attract scientific attention due to a variety of non-equilibrium states, which differ significantly from its commensurate charge density wave (CDW) at equilibrium [1]. It can exhibit a long-lived hidden domain state, an electronic amorphous state [2], as well as a range of more exotic CDW states within a single layer [3], all achievable with an ultrafast optical or short electrical excitation. When this material is studied on the nanometre scale, we are limited to either static scanning tunnelling microscopy (STM) experiments or time resolution on the order of minutes between the consecutive STM frames.

In this talk, I will present our latest results obtained using a novel Fast STM method. Using this technique, we can reach millisecond time resolution and observe single-electron and collective charge motion on the surface of 1T-TaS_2, influenced by local CDW configuration and microscopic crystal strains [4].

In addition, I will show how, by synchronising laser excitation with Fast STM scanning, we can force CDW reconfiguration and film it in real time.

References

[1] J. Ravnik, *et al.*, Nat. Commun. **12**, 2323 (2021).
[2] Y. A. Gerasimenko, *et al.*, Nat. Mater. **18**, 1078 (2019).
[3] J. Ravnik, *et al.*, Sci. Rep. **13**, 19622 (2023).
[4] Y. Vaskivskyi, *et al.*, e-print arXiv:2512.02688 (2025).

Abstract ID: 30549

HIGH-PRESSURE SYMMETRY EVOLUTION AND FERROELECTRIC SUPPRESSION IN LAYERED PEROVSKITE-LIKE TITANATES

A. G. Asadov[1,2], A. I. Mammadov[1], D. P. Kozlenko[2], R. Z. Mehdiyeva[1], E. V. Lukin[2], S. E. Kichanov[2]

[1] *Institute of Physics, Ministry of Science and Education of the Republic of Azerbaijan, Baku AZ-1143, AZERBAIJAN*
[2] *Frank Laboratory of Neutron Physics, JINR, 141980 Dubna, RUSSIA*

Layered perovskite-like titanates with the general formula $A_2Ti_2O_7$ (where A = La, Ce, Pr or Nd) attract great interest from researchers due to their outstanding piezoelectric and ferroelectric properties, high Curie temperatures, and excellent permittivity characteristics. High anisotropy of electrical conductivity at low temperatures has also been found in such materials, which makes layered perovskite-like titanates very promising materials as quasi-one-dimensional metals. The anisotropy of the physical properties of $A_2Ti_2O_7$ materials is due to the peculiarities of their crystalline monoclinic structure – the so-called Carpy-Galy phase, in which TiO_6 oxygen octahedra form distorted crystalline layered structures separated by topological distorted layers of rare earth elements. The mutual orientation of distorted oxygen octahedra in the crystal structure of layered perovskite-like materials plays a significant role in the formation of their ferroelectric properties. It is known that a change in the physical properties of materials is possible through variation of the crystal structure parameters in experiments at high pressures. However, the effect of high pressure on the crystal structure of layered perovskite-like titanates has not been studied so far. Therefore, the cycle of works represents the results of a systematic and detailed study of changes in the crystal structure and vibration spectra of layered perovskite-like titanates $Pr_2Ti_2O_7$ [1], $Nd_2Ti_2O_7$ [2], $La_2Ti_2O_7$ [3, 4], and at high pressures up to 30 GPa using X-ray diffraction and Raman spectroscopy. It should be noted that under normal conditions, the parameters of the crystal structures of these complex materials were studied using neutron diffraction method.

It was established for the first time that a structural phase transition is observed in all studied $A_2Ti_2O_7$ compounds at high pressures above 15 GPa [1-5], which is accompanied by anomalies of the baric dependences of both the parameters of the crystal structure and the vibrational modes of these compounds. A detailed analysis of the experimental data indicates a change in the symmetry of the monoclinic crystal structure of perovskite-like titanates from the spatial group $P2_1$ to P2/m [3, 4]. Based on the obtained experimental data, a model of the structural mechanism of the pressure-induced phase transition in perovskite-like layered titanates is proposed [5]. With an increase in pressure above the phase transition point, a change in the mutual tilting of the TiO_6 octahedra is observed, which leads to an increase in the degree of disordering of the titanium layer in the crystal structure. In addition, pressure-induced relative displacements of rare earth ions lead to noticeable changes in the topology of the corresponding crystal layers [2, 4, 5]. The obtained results indicate that an increase in the degree of disordering of the titanium layer in layered perovskite-like titanates leads to suppression of the ferroelectric state at high pressure.

References

[1] A.G. Asadov, *et al.*, *A search for pressure-induced phase transition in the layered perovskite-like $Pr_2Ti_2O_7$*, J. Alloys Compd., **1003**, 175461 (2024). https://doi.org/10.1016/j.jallcom.2024.175461

[2] A.G. Asadov, *et al.*, *The effects of high pressure on the crystal structure and vibration spectra of layered perovskite-like $Nd_2Ti_2O_7$*, Solid State Ionics **406**, 116447 (2024). https://doi.org/10.1016/j.ssi.2023.116447

[3] A.G. Asadov, *et al.*, *The structural mechanisms of pressure-induced phase transitions in the Carpy-Galy phase layered perovskites*, Solid State Sciences **156**, 107676 (2024). https://doi.org/10.1016/j.solidstatesciences.2024.107676

[4] A.G. Asadov, *et al.*, *Vibrational and x-ray measurements of $La_2Ti_2O_7$ under high pressure condition*, Advanced Physical Research **6**, 113-122 (2024). https://doi.org/10.62476/apr62113

[5] A.G. Asadov, *et al.*, *A structural phase transition in $La_2Ti_2O_7$ at high pressure*, Physica B: Condensed Matter **655**, 414753 (2023). https://doi.org/10.1016/j.physb.2023.414753

33 - MGB2 – MATERIALS AND APPLICATIONS

Abstract ID: 30050

INFLUENCE OF Dy_2O_3 ADMIXTURES ON THE CRITICAL CURRENT DENSITY AT 20 K AND 30 K IN MgB_2 WIRES

D. Gajda[1], M. Babij[1], A. Zaleski[1], D. Avci[2], F. Karaboga[3], H. Yetis[4], I. Belenli[4], D. Szymanski[1], M. Malecka[1], D. Zasada[5], T. Czujko[5]

[1] *Institute of Low Temperature and Structure Research, Polish Academy of Sciences (PAS), 50-422 Wroclaw, POLAND*
[2] *Quatum Metrology Laboratory, National Metrology Institute TÜB ITAK, 41470 Kocaeli, TURKEY*
[3] *Mehmet Tanrikulu Vocational School of Health Services, Bolu Abant Izzet Baysal University, 14030 Bolu, TURKEY*
[4] *Department of Physics, Bolu Abant Izzet Baysal University, 14280 Bolu, TURKEY*
[5] *Institute of Materials Science and Engineering, Military University of Technology, 00-908 Warsaw, POLAND*

We will show the microstructure, crystal structure and critical parameters (e.g. critical temperature (T_c), irreversible magnetic field (B_{irr}), transport critical current density (J_c)) of D_2O_3-doped MgB_2 wires. The transmission electron microscope (TEM) images were carried out on the longitudinal section of MgB_2 wires. The results indicated that the Dy_2O_3 admixture significantly influences the microstructure of the MgB_2 material e.g. accelerates the creation of the MgB_2 phase. The measurements performed showed that Dy_2O_3 doping and low annealing temperature allow to obtain high transport critical current density at 25 K and 30 K. XRPD results point out that short-term annealing allowed obtaining a larger amount of MgB_2 phase in MgB_2 wires with Dy_2O_3 doping than undoped MgB_2 wires. Moreover, further results showed that the Dy_2O_3 addition allows to increase B_{irr} especially at higher temperatures. TEM images and analyses indicated that the Dy_2O_3 dopant mainly formed the MgB_2 phase and a high-density MgB_2 material. Further studies performed by using a scanning electron microscope (SEM) showed that the Dy_2O_3 doping significantly influences on the shape and size of MgB_2 grains compared to undoped MgB_2 wire. The conducted studies indicate a very positive effect of the Dy_2O_3 admixture on the microstructure and critical parameters of MgB_2 wires, especially during annealing at Mg in the solid state.

Abstract ID: 30320

COMPOSITES OF MgB_2 PROCESSED BY SPARK PLASMA SINTERING: POWDER-IN-TUBE TAPES AND BULKS WITH SELECTED ADDITIVES

P. Badica

National Institute of Materials Physics, Atomistilor Street 405 A, 077125 Magurele, ROMANIA

Work will present recent results on fabrication and characterization of MgB_2 composites. Samples are processed by ex-situ spark plasma sintering. They are monocore powder-in-tube tapes with stainless steel or Ti sheath and high-density massive bulks. In both types of samples, different additives were introduced. The first part of presentation will be about powder-in tape and the second one will be devoted to bulks.

Use of stainless-steel sheath to fabricate tapes required lower SPS temperatures, of 1050 °C, than for Ti sheath. At higher temperatures the integrity of the tapes is not preserved. On the other hand, tapes with light-weight Ti sheath were successfully processed at 1150°C which is the optimum temperature to sinter high-density bulk samples by SPS. However, we observed a certain level of interdiffusion between MgB_2 core and Ti imposing limitations on the final thickness of the tape. A high purity of Ti is needed to ensure enough deformability for tapes' fabrication. Additions impact on tapes quality and superconducting characteristics measured by magnetometry will be discussed.

As new additives, Ba-based compounds, oxide and carbonate, were introduced into MgB_2 bulk samples to obtain superconducting composites. Comparative analysis of the processes and superconducting properties allows learning on specifics. Namely, depending on the additive-type, formation of BaB_6 as a nano precipitate for an effective vortex pinning effect is strongly influenced.

Acknowledgement

This work is supported by UEFISCDI, Romania, through projects 98PCE/2025 CCOS and 63PED/2025 SYSDELBIO.

Abstract ID: 30545

THE STORY OF MgB_2 DISCOVERY

J. Nagamatsu

YUKI Precision Co., Ltd., Chigasaki, Kanagawa 253-0084, JAPAN

Late at night on October 24, 2000, in an otherwise silent and empty laboratory, a SQUID magnetometer continued its automated measurements when the monitor began to display unmistakable signatures of superconductivity. The inferred transition temperature was 39 K—far beyond expectations for a simple binary compound. This moment constituted the first observation of the superconducting transition of MgB_2.

At that time, the Akimitsu Laboratory at Aoyama Gakuin University comprised approximately 30 students pursuing a remarkably broad spectrum of condensed-matter research, including orbital ordering, Haldane-type systems, mechanisms of ferromagnetism, and systematic exploration of novel superconductors. Professor Akimitsu fostered an environment of exceptional intellectual independence, under which the laboratory had already achieved notable successes, such as the discovery of superconductivity in ladder-structured compounds.

As one of the students in the laboratory, I was engaged in the search for unknown superconductors through persistent trial and error, often guided more by intuition than by established theory. From that period, one remark by Professor Akimitsu remains especially vivid in my memory:

"I have more knowledge and a longer career. However, when it comes to searching for unknown superconductors, we stand on equal ground."

This presentation will provide a detailed retrospective look at the process of discovering and identifying MgB_2 and the scientific atmosphere, decisions, and coincidences that shaped this achievement in the lab.

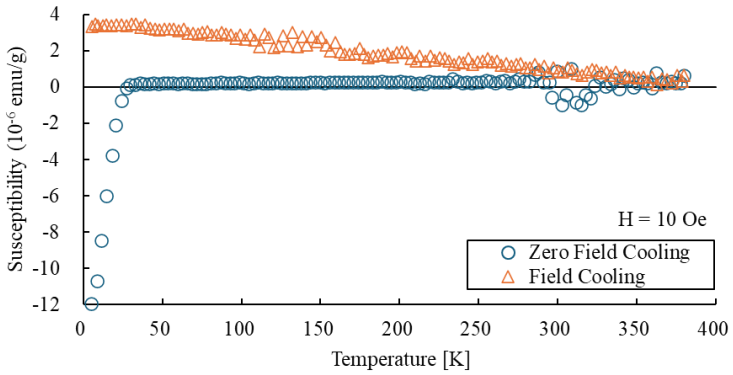

Fig. 1: *First data capturing superconductivity in MgB_2.*

References

[1] J. Nagamatsu, *et. al.*, Nature **410**, pp. 63-64, (2001).

Abstract ID: 30553

PROTOTYPE MgB_2 SUPERCONDUCTING COIL USING ULTRA-FINE WIRES

T. Nakayama[1], J. Nagamatsu[2], K. Kikuchi[3], A. Kikuchi[4], M. Otsubo[1]

[1] *Japan Superconductivity Application Development Inc. JAPAN*
[2] *YUKI Precision Co., Ltd. Chigasaki, Kanagawa 253-0084, JAPAN*
[3] *SOLIZE PARTNERS Corporation, Chiyoda, Tokyo, 102-0075, JAPAN*
[4] *National Institute for Materials Science, Tsukuba, Ibaraki 305-0028, JAPAN*

Japan Superconductivity Application Development Inc. (JSA) was established in 2023 as a carve-out from Meiko Futaba Co., Ltd., a manufacturer with decades of experience in ultra-fine copper wire production [1]. This industrial foundation enables JSA to pursue superconducting wire technologies with a strong emphasis on real-world deployment.

JSA, in collaboration with the National Institute for Materials Science, developed the world's thinnest MgB_2 superconducting wire with a diameter of 15 μm (Fig. 1) [2]. Such an ultra-fine geometry provides exceptional mechanical flexibility and enables stable winding even at very small bending radius.

Experimental evaluations demonstrated markedly reduced AC losses in these wires [3], resulting in suppressed heat generation under time-varying magnetic fields. This characteristic directly addresses a critical limitation in superconducting rotating machinery [4].

The combination of ultra-fine diameter and low AC loss offers new design freedom for compact, lightweight, and high-efficiency superconducting devices with relevance to energy, mobility, and medical systems (Fig. 2). As a practical demonstration, we have fabricated a small-diameter MgB_2 superconducting coil prototype using the developed wire, and the design concept and fabrication details are reported.

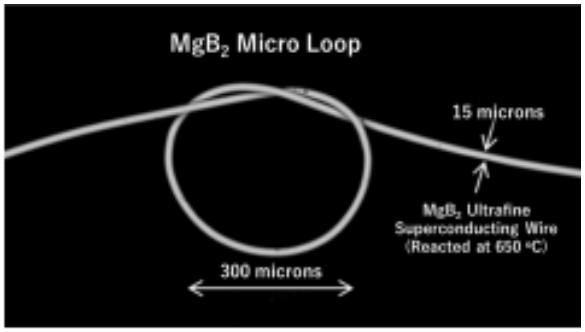

Fig. 1: *Ultra fine wire of MgB_2.*



Fig. 2: *Conceptual vision of future applications.*

References

[1] https://www.cho-dendo.jp/en.
[2] A. Kikuchi, *et al.*, IEEE Trans. Appl. Supercond. **34 (3)**, 6200104 (2024).
[3] J. Kovac, *et al.*, Supercond. Sci. Technol. **38**, 055028 (2025).
[4] K. Kovalev, *et al.*, Proc. ICOECS Ufa Russia, pp. 1-5 (2019).

Abstract ID: 30572

DEVELOPMENT ON UNIFORM, HIGH-PERFORMANCE MgB_2 MULTI-FILAMENT IMD LONG WIRES

C. Guo[1], D. Wang[1,2,3], Y. Ma[1,2,3]

[1] *Chinese Academy of Sciences, Institute of Electrical Engineering, Key Laboratory of Applied Superconductivity, 100190, Beijing, CHINA*
[2] *University of Chinese Academy of Sciences, 100049, Beijing, CHINA*
[3] *Institute of Electrical Engineering and Advanced Electromagnetic Drive Technology, Qilu Zhongke, 250013, Jinan, CHINA*

With a superconducting transition temperature (T_c) as high as 39 K, MgB_2 is regarded as one of the suitable superconductor for application in the liquid-hydrogen temperature range. To date, MgB_2 superconducting wires have already been utilized in various fields, including MRI magnets, superconducting cables, wind turbine generators, etc. As a practical superconductor, the main factor currently limiting the performance of MgB_2 wires is its relatively weak flux-pinning capability, which leads to a significant degradation of critical current under high magnetic fields. At present, the highest short-sample performance reported is from the multi-filament IMD wire by Wan F, achieving a layer J_c exceeding 2×10^5 A/cm^2 at 4.2 K and 10 T, and an engineering J_e of 1.3×10^4 A/cm^2.[1] For long wires, the best performance reported is the 6+1-core hundred-meter IMD wire fabricated by Wang et al., with J_c surpassing 10^5 A/cm^2 at 4.2 K and 8 T.[2] Recently, Chen et al. successfully produced a 600 m-level IMD long wire, which reached a J_c of 7.6×10^5 A/cm^2 at 4.2 K and 4 T, and wound a coil achieving a record central magnetic field of 5.71 T.[3] These advances clearly indicate that high-performance MgB_2 long wires represent the current forefront of research. In this presentation, by optimizing the purification of precursor boron powder, improving processing techniques, and adopting long-wire manufacturing procedures, we have fabricated a 15-meter-long, high-performance seven-core IMD wire. The sample exhibits an average J_c of 9.0×10^4 A/cm^2(4.2 K,10 T), with a maximum J_c of 9.7×10^4 A/cm^2(4.2 K,10 T) and a variation within ±7%. The n-value averages 33.7 with a fluctuation of ±10%, and all wires show n-values above 30. This fabrication approach is scalable to hundred-meter or even kilometer-length IMD wires, offering a feasible route for the production of high-performance MgB_2 long wires.

References

[1] F. Wan, *et al.*, Scripta Materialia **239**, 115784 (2024).
[2] D. L.Wang, *et al.*, Supercond. Sci. Technol. **30**, 064003 (2017).
[3] Z. Y. Chen, *et al.*, Adv. Funct. Mater. **35**, 2413300 (2025).

Abstract ID: 30610

THE EFFECTS OF STABLE MATRIX ON THE ELECTROMAGNETIC PROPERTIES FOR MULTI-FILAMENTS MgB_2 WIRES

M. Wang[1], Q. Guo[1], W. Yuan[1], W. Xie[1], Q. Yu[1], Y. Zhu[1], B. Wu[1], Y. Shi[1], J. Li[2], X. Liu[1], Y. Feng[1], P. Zhang[1,2]

[1] *Western Superconducting Technologies (WST) Co. Ltd., Xi'an 710018, CHINA*
[2] *Superconducting Materials Center, Northwest Institute for Nonferrous Metal Research, Xi'an 710016, CHINA*

Reducing the AC loss of MgB_2 wire is significant for its possible AC engineering applications (generator, motor). In this study, the MgB_2 wire with 102 filaments was fabricated via In-suit PIT (Powder in Tube) method. The effects of stable matrix (Cu, CuNi alloys) on the structure, superconducting properties, magnetic hysteresis loss and thermostability of MgB_2 wires were studied systematically. In order to reduce the coupling loss, the wires were twisted (L_p=20 mm). Compared to Cu matrix, the structure of filaments was more uniform for the MgB_2 wire with CuNi alloys matrix. The critical transition temperature (T_c) of wires was almost consistent with Cu and CuNi alloys. The critical current density (J_c) of MgB_2 wire with CuNi alloys matrix was up to 3000 A/mm^2 (4.2 K, 3 T), which was higher than the Cu matrix wire. The magnetic hysteresis losses (Q_m) of MgB_2 wires were 520 mJ/cm^3 and 580 mJ/cm^3 for CuNi alloys and Cu matrix, respectively. While the thermal conductivity of Cu matrix wire was 1.5 times than that of CuNi alloys matrix wire.

Abstract ID: 30741

TUNING OF TRANSPORT PROPERTIES OF MgB_2 THIN FILMS VIA X-RAY NANOPATTERNING

A. Alessio[1], S. Singh[1], M. Fretto[2], V. Bonino[3], A. Agostino[4], B. Vitale[4], E. Di Francia[1], M. Belogolovskii[5], M. Truccato[1]

[1] *Physics Dept., University of Torino, Via P. Giuria 1, 10135 Torino, ITALY*
[2] *Istituto Nazionale di Ricerca Metrologica (INRiM), Strada delle Cacce 91, 10135 Turin, ITALY*
[3] *ESRF, The European Synchrotron, 71 Avenue des Martyrs, CS40220, 38043 Grenoble Cedex 9, FRANCE*
[4] *Chemistry Dept., University of Torino, Via P. Giuria 7, 10135 Torino, ITALY*
[5] *Centre for Nanotechnology and Advanced Materials, Comenius University Bratislava, Bratislava 84248, SLOVAK REPUBLIC*

Synchrotron nanoprobe induced modifications on MgB_2 superconducting thin films have been investigated. Since X-ray nanopatterning has already been shown to be effective in tuning the electrical properties of high T_c superconductors [1] and functional oxides [2-4], possible application of this technique to MgB_2 has been explored.

MgB_2 thin films have been patterned to obtain micrometer sized bridges, which have been subsequently irradiated by a hard synchrotron X-ray nanobeam. Pristine and irradiated samples have been characterized by SEM-EDX imaging and electrical characterization. Localized increase in room temperature resistivity as well as shifts in T_c values have been interpreted as resulting from irradiation induced defects, namely oxygen incorporation and structural disorder, leading to IV characteristics compatible with SNS Josephson junctions or phase-slip lines. The possibility of fine-tuning the superconducting properties of MgB_2 thin films by means of X-ray nanopatterning could pave the way to a variety of applications ranging from radiation-hard superconducting electronics to ultra-low field MRI machines.

References

[1] M. Truccato, *et al.*, *Direct-Write X-ray Nanopatterning: A Proof of Concept Josephson Device on $Bi_2Sr_2CaCu_2O_{8+\delta}$ Superconducting Oxide*, Nano Lett., **vol. 16**, **no. 3**, pp. 1669–1674, (2016). doi: 10.1021/acs.nanolett.5b04568

[2] A. Alessio, *et al.*, *Functional Modifications Induced via X-ray Nanopatterning in TiO_2 Rutile Single Crystals*, Physica Status Solidi (RRL) – Rapid Research Letters, **vol. 15**, **no. 10**, p. 2100409, (2021). doi: 10.1002/pssr.202100409

[3] L. Mino, *et al.*, *Improving The Control of The Electroforming Process in Oxide-Based Memristive Devices by X-ray Nanopatterning*, J. Mater. Chem. C, 12, 11127 (2024). doi: 10.1039/D4TC01815J

[4] A. Alessio, *et al.*, *Guided Phase Transition from TiO_2 Rutile to Anatase During Electroforming of Memristor-Like Devices*, Journal of the European Ceramic Society, **vol. 45**, **no. 15**, p. 117597, (2025). doi: 10.1016/j.jeurceramsoc.2025.117597

Abstract ID: 30743

INDUSTRIAL PRODUCTION OF MgB_2 WIRES FOR MAGNET SYSTEMS AND HIGH-CURRENT CABLES AT ASG SUPERCONDUCTORS

A. Tumino, M. Tropeano, A. Ansaldo, A. Traverso, T. Spina, F. Mazzei, G. Grasso

ASG Superconductors spa, 16152, Genova, ITALY

ASG Superconductors' production process enables fully reacted MgB_2 wires and tapes up to 5-6 km in length, with customizable layouts tailored to specific applications. These conductors exhibit excellent mechanical properties, making them ideal for react-and-wind techniques in magnet manufacturing and react-and-cable processes for power cables.

Both tapes and round wires are commercialized in various sizes for magnet integration. Ad-hoc doped powders optimize performance up to 4-5 T fields.

Round wires support power cable applications, with production flexibility allowing customization of wire diameter, filament size, twist pitch, and coatings (e.g., copper) to match cable designs.

About 1000 km of wires have been manufactured and fully qualified by CERN for the superconducting link of the HI-LUMI projects, and many projects are now using MgB_2, demonstrating that the technology is reliable and suitable across diverse applications: from power grids for energy transmission to protection and storage systems.

This work presents the characteristics of our commercialized wires, the manufacturing process, the key applications, and ongoing R&D to enhance performance, unlocking new frontiers.

Abstract ID: 30786

MgB_2 SUPERCONDUCTING WIRES FABRICATED BY INTERNAL MAGNESIUM DIFFUSION (IMD) METHOD: INTERFACE ENGINEERING AND MULTI-FILAMENTARY DESIGN

S. Safran[1,2], A.Gencer[1,2], C. Guo[3], F. Almokdad[4], F. Ervüz[1], H. Koralay[5], Y. Oznal[1,8], S. Salahi[6], A. Seçkin[7], K. Sönmez[1,4], S. C. Taşkın[1], D. Wang[3], Y. Ma[3]

[1] *Ankara University, Superconductor Technologies Application and Research Center, Ankara, TURKIYE*
[2] *Ankara University, Science Faculty, Physics Department, Ankara, TURKIYE*
[3] *Chinese Academy of Sciences, Institute of Electrical Engineering, Key Laboratory of Applied Superconductivity, Beijing 100190, Peoples REPUBLIC OF CHINA*
[4] *Ankara University, Graduate School of Natural and Applied Sciences, Ankara, Türkiye*
[5] *Gazi University, Science Faculty, Physics Department, Ankara, TURKIYE*
[6] *Gazi University, Department of Metallurgical and Materials Engineering, Ankara, TURKIYE*
[7] *Gazi University, Basic and Engineering Sciences Central Laboratory Application and Research Center (GUTMAM), Ankara, TURKIYE*
[8] *Ankara University, Elmadag Vocational School, Electronics and Automation Department, Ankara, TURKIYE*

Magnesium diboride (MgB_2) is a promising superconducting material for intermediate-temperature cryogenic applications, distinguished by its low raw material cost and favorable performance. To enhance its in-field performance and critical current density (J_c) for practical applications, the Internal Magnesium Diffusion (IMD) method offers significant potential, as it yields a denser superconducting matrix and superior inter-granular connectivity compared to conventional fabrication techniques. This study presents a comprehensive interface engineering approach to enhance the microstructural and superconducting properties of carbon-doped MgB_2 wires fabricated via the IMD method.

To improve phase formation kinetics, lower the activation energy, and strengthen the magnetic flux pinning mechanisms within the superconducting matrix, the central magnesium rods were coated with various metallic layers (copper, silver, and tin) to serve as low-temperature activators. The thermal reaction behaviors and microstructural evolution of the fabricated wires were thoroughly investigated using Differential Thermal Analysis (DTA) and Scanning Electron Microscopy (SEM). The electrical and magnetic performances were evaluated through Resistance-Temperature (R-T) transition profiles, upper critical field (H_{c2}), irreversibility field (Hirr), and transport critical current density (J_c) measurements under varying applied magnetic fields. The findings demonstrate that the applied metallic coatings effectively modify the magnesium diffusion dynamics, promote a more homogeneous superconducting phase formation, and stabilize the superconducting performance at high magnetic fields.

In the final phase of the study, the optimized parameters obtained from the mono-core wires were utilized to design and fabricate scalable multi-filamentary MgB_2 wires tailored to meet industrial mechanical and stability requirements. Developed with the integration of appropriate barrier and outer sheath materials, these innovative composite structures provide a robust foundation for the integration of MgB_2 superconducting wires into practical, large-scale commercial systems.

This work has been supported by TÜBİTAK and the Chinese Academy of Sciences (CAS) through a Bilateral Cooperation program under Contract No. 123N624.

Abstract ID: 30344

COMPARATIVE ANALYSIS OF J_c AND J_e IN MgB_2 POWDER-IN-TUBE AND THIN-FILM CONDUCTORS FOR LIQUID HYDROGEN CRYOMAGNETIC APPLICATIONS (15–20 K)

B. A. Glowacki[1,2]

[1] *Department of Materials Science and Metallurgy, University of Cambridge, 27 Charles Babbage Road, Cambridge CB3 0FS, UK*

[2] *Institute of Power Engineering, National Research Institute, DZE-2, ul. Mory 8, 01-330 Warsaw, POLAND*

A substantial research effort has been directed toward optimizing Magnesium Diboride (MgB_2) for hydrogen-cooled superconducting systems, yet a direct comparison between established Powder-in-Tube (PIT) wires and emerging Thin-Film Coated Conductors (TFCC) remains complex due to divergent architectural constraints. This study presents a comprehensive comparative analysis of these two technologies at liquid hydrogen temperatures (15–20 K), evaluating how intrinsic critical current density (J_c) translates into practical engineering current density (J_e) when integrated into fully stabilized conductor designs.

We systematically examine the critical parameters of trade-offs between the filament diameter reduction in PIT wires and the coating thickness scaling in thin films. While thin films typically exhibit superior intrinsic flux pinning and J_c, our analysis highlights the significant "dilution" effects imposed by non-superconducting metallic substrates and the necessity for distinct diffusion barriers to prevent poisoning from metal-based supports. Conversely, for PIT conductors, we discuss the limits of increasing the filling factor against the mechanical and chemical constraints of metallic diffusion barriers and sheath materials.

Furthermore, this work quantitatively addresses the often-overlooked penalties of quench protection (copper stabilization) and electrical insulation, which act as volumetric equalizers between the two approaches. By modelling J_e as a function of active superconducting fraction, layer thickness, and operating temperature, we define the specific geometric crossover points (such as film thickness thresholds and filament densification limits) where one technology surpasses the other. The results provide a roadmap for optimizing conductor architecture, suggesting that achieving superior performance at 20 K requires a shift from maximizing intrinsic J_c alone to optimizing the holistic specific current capacity of the finished wire.

34 - MICROMAGNETICS, MODELING, AND SCIENTIFIC MACHINE LEARNING

Abstract ID: 30120

SELF-MODULATION INSTABILITY IN HIGH POWER FERROMAGNETIC RESONANCE OF BiYIG NANODISKS

I. Ngouagnia Yemeli[1], S. Perna[2], D. Goueré[3], A. Kolli[1], M.Munoz[4], A. Anane[3], M.d'Aquino[2], H. Merbouche[1], C. Serpico[2], G. de Loubens[1]

[1] *SPEC, CEA, CNRS, Université Paris-Saclay, Gif-sur-Yvette, FRANCE*
[2] *Department of Electric Engineering and Information Technology, University of Naples Federico II, Naples, ITALY*
[3] *Laboratoire Albert Fert, CNRS, Thales, Université Paris-Saclay, Palaiseau, FRANCE*
[4] *Instituto de Tecnlogías Físicas y de la Información (CSIC), Madrid, SPAIN*

Nonlinear magnetization dynamics in confined nanostructures is a phenomenon that promises the realization of fast and energy efficient ICTs [1]. Ferromagnetic resonance (FMR) is a consolidated investigation technique that uses a uniform RF field oscillating at a frequency close to Kittel's value to bring the magnetization out of the equilibrium. For low RF power, FMR is used to characterize material parameters, while for high power, it brings the magnetization in a deep nonlinear dynamic where foldover and spin wave instability appear [2]. In this work, we investigate the FMR of BiYIG nanodisk uniformly magnetized along the symmetry axis of the disk and subject to a DC field in the same direction, where the out of plane anisotropy almost compensates the shape anisotropy of the sample[3]. Our investigation is based on magnetic resonance force microscope (MRFM), on micromagnetic simulations and normal modes analysis [4]. We find, that the control plane (DC field vs RF field) can be divided in three regions according to the observed regime: the first for very low RF field amplitude, where the magnetization oscillations are synchronous to the RF field (P-mode). The spectrum of the transverse magnetization is single peaked (SP) and then this region is labeled accordingly. The second region for intermediate value of RF field, where there is coexistence between a chaotic attractor and the P-mode. The third region is characterized by high RF fields and the chaotic attractor is the only possible dynamics. The spectrum of the chaotic magnetization dynamics exhibits multiple peaks (MP) equally spaced on the top of a continuous spectrum (C). This region is labeled with MP-C and the region of coexistence is labeled MP-C/SP. In the figure below [3], we show the MRFM data (a), the results of micromagnetic simulations (b), the phase diagram in the control plane (c) and the number of normal modes (NM) significantly excited in a certain dynamic state (d). The possibility to excite such a large number of NM in a deep nonlinear dynamical state suggests the potential use of this phenomenon for novel computation schemes.

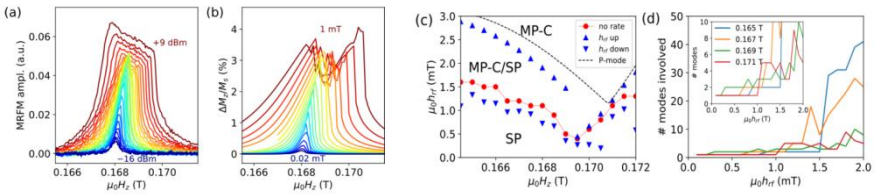

References

[1] A. V. Chumak, *et al.*, IEEE Trans. on Magn., **vol. 58**, **no. 6**, pp. 1-72, (2022).

[2] G. Bertotti, *et al.*, Phys. Rev. Lett. **87**, 217203 (2001).

[3] I. Ngouagnia Yemeli, *et al.*, Phys. Rev. Lett. **135**, 056703 (2025).

[4] S. Perna, *et al.*, J. Magn. Magn. Mater., 546, (2022).

Abstract ID: 30185

VOLTAGE GENERATION BY FERROMAGNETIC RESONANCE IN Fe/Co BILAYER WITH PERPENDICULAR MAGNETIC ANISOTROPY

N. Leśniewski[1], A. K. Dhiman[2], P. Graczyk[2]

[1] *Institute of Spintronics and Quantum Information, Adam Mickiewicz University, Poznań, POLAND*
[2] *Institute of Molecular Physics, Polish Academy of Sciences, Poznań, POLAND*

Magnetoelectric effects, such as the induction of currents or voltages by magnetization dynamics, are key to enabling efficient interconversion between magnetic and electric signals. These mechanisms play an important role in the development of low-power spintronic devices and novel sensing platforms. Understanding and optimizing such coupling is essential for advancing next-generation functional materials and nanoscale technologies.

We performed detailed numerical simulations of the ac and dc voltages generated in an MgO/Fe/Al/Co/MgO structure due to spin pumping and spin-dependent conductivity in ferromagnets (Fig. 1). The study considered the effects of external magnetic fields, the thickness of the Al spacer and Fe layer, the direction, frequency, and amplitude of microwave excitation, as well as the presence of dielectrics in the stack. Our calculations indicate that replacing the aluminum spacer with a low-electronic-conductivity material, such as semiconducting silicon, leads to a significant enhancement of the voltages generated by magnetization precession.

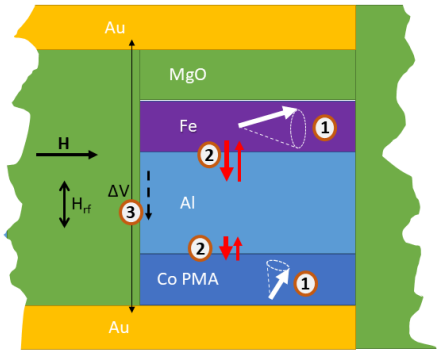

Fig. 1: *Schematic of the simulated system: Fe with in-plane magnetization and Co with perpendicular magnetic anisotropy are separated by a nonmagnetic spacer. The rf field H_{rf} drives magnetization precession (1), which pumps a spin current into the spacer (2). Spin-dependent conductivity in the ferromagnetic layers converts this spin current into a measurable voltage at the outer electrodes (3).*

The study has received financial support from the National Science Centre of Poland under grant 2024/53/B/ST3/02188.

Abstract ID: 30234

GRAPH NEURAL NETWORKS TO PREDICT PROPERTIES OF HARD MAGNETIC MICROSTRUCTURES

H. Moustafa[1], A. Kovacs[1], J. Fischbacher, M. Gusenbauer[1], Q. Ali[1,2], L. Breth[1], T. Schrefl[1,2], H. Oezelt[1]

[1] *Department for Integrated Sensor Systems, University for Continuing Education Krems, Viktor Kaplan-Straße 2, Wiener Neustadt, 2700, AUSTRIA*

[2] *Christian Doppler Laboratory for Magnet Design through Physics-Informed Machine Learning, Viktor Kaplan-Straße 2, Wiener Neustadt, 2700, AUSTRIA*

Due to their structure, graph neural networks (GNN) are a promising tool to predict magnetic properties of large multi-grain microstructures. This can speed up the search for rare-earth free permanent magnets, through micro- and nanostructural design [1]. We use our magnetic simulation data, obtained using our reduced order model (ROM) [2], to train a GNN to predict coercivity of hard magnetic microstructures. We evaluate the performance of the trained GNN and quantify the aleatoric and epistemic uncertainty.

Subsequently, we reuse the GNN architecture and train it again for the prediction of the maximum energy product. Out-of-distribution predictions of coercivity are also performed, specifically in the extrapolated regime of larger structure sizes. To improve these and take into account the complex behavior of the magnetostatic field, we did feature engineering based on the observed logarithmic dependence of coercivity on the system size [3].

In a further development we use the combination of a GNN with an extended long short-term memory architecture (xLSTM) [4] to predict the hysteresis loop of hard magnetic microstructures.

Fig. 1 is showing the results of the proposed GNN evaluated using a five-fold cross- validation on a dataset of 1053 micromagnetic structures. The model explains 93% of the variance. The color-coded predictive uncertainty represents the root-sum-square of the aleatoric and epistemic components.

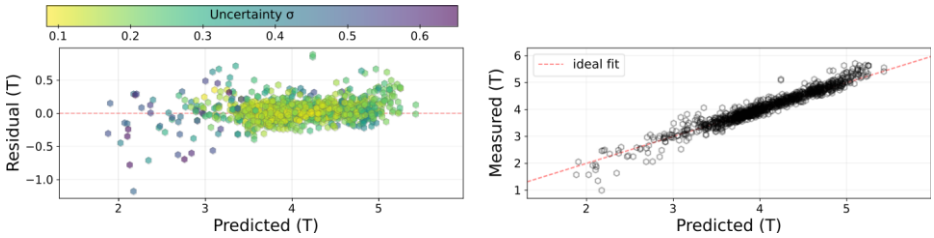

Fig. 1: *GNN Results of five-fold cross validation with R^2=0.93 on the test set. Top: Residual plot, color-coded by predictive uncertainty. Bottom: Measured vs. predicted values.*

Acknowledgements

This work was funded in whole or in part by the Austrian Science Fund (FWF) under porjects [10.55776/I6159] and [10.55776/P35413].

References

[1] Sanchez-Gonzalez, *et al.*, *ICML* (2020).

[2] H. Moustafa, *et al.*, AIP Adv. **14**, 025001 (2004).

[3] H. Moustafa, *et al.*, J. Magn. Magn. Mater., DOI: 10.1016/j.jmmm.2025.173594 (2025).

[4] M. Beck, *et al.*, arXiv:2405.04517v1 [cs.LG] (2024).

Abstract ID: 30263

HIGHER ORDER STRAY FIELD COMPUTATION ON TENSOR PRODUCT DOMAINS

L. Exl[1,2,3], S. Schaffer[1,2]

[1] *Math. AI/ML, Wolfgang Pauli Institute, 1090, Vienna, AUSTRIA*
[2] *Research Platform MMM Mathematics–Magnetism–Materials, University of Vienna, 1090, Vienna, AUSTRIA*
[3] *Department of Mathematics, University of Vienna, 1090, Vienna, AUSTRIA*

We present an extension of the tensor grid method [1] for stray field computation on rectangular domains that incorporates higher-order basis functions [2]. Both the magnetization and the resulting magnetic field are represented as functional Tucker tensors using higher-order tensor product B-spline bases, which allows for continuous field evaluation. Each magnetization component $m^{(\mu)}(\boldsymbol{x}): \Omega \to \mathbb{R}$, $\mu = 1,2,3$ is represented as

$$m^{(\mu)}(\boldsymbol{x}) = \sum_{j_1=1}^{r_1} \sum_{j_2=1}^{r_2} \sum_{j_3=1}^{r_3} \boldsymbol{\mathcal{A}}^{(\mu)}_{j_1,j_2,j_3} \prod_{p=1}^{3} \sigma^{(p)}_{j_p}\left(x^{(p)}\right)$$

where $\boldsymbol{\mathcal{A}}^{(\mu)} = \mathbb{R}^{r_1 \times r_2 \times r_3}$ defines the core tensor of the μ-th magnetization component and $\sigma^{(p)}_{j_p}$ are the 1-dimensional B-spline basis functions of order k>3 defined r_p +k on knots in each direction p of the tensor product domain. This ansatz allows for increased accuracy and smoothness, and further leads to massive compression in terms of degrees of freedom. The method employs a super-potential formulation of the Newton potential, which circumvents the need to convolve with a singular kernel. The super-potential um for the magnetization m is given by

$$\boldsymbol{u_m}(\boldsymbol{x}) = \frac{1}{8\pi} \int_{\Omega} |\boldsymbol{x} - \boldsymbol{y}| \boldsymbol{m}(\boldsymbol{y}) \, \mathrm{dy}$$

and the corresponding stray field h can be evaluated using the relation $\boldsymbol{h}(\boldsymbol{x}) = \nabla\left(\Delta\left(\nabla \cdot \boldsymbol{u_m}(\boldsymbol{x})\right)\right)$, where higher-order derivatives are computed through successive applications of a "differentiate →project" strategy via L^2-projections onto the original basis.

Gaussian sums are used for efficient approximation of the super-potential, leading to a separable expansion on the tensor product domain and a cut-off error of fourth order. In combination with the multilinear tensor product structure inherent in functional Tucker tensors, this results in an efficient and well-conditioned training algorithm for what we refer to as a multilinear tensor product extreme learning machine (ml-tp ELM).

Numerical experiments confirm the accuracy and efficiency of the proposed method, demonstrating exponential convergence of the energy and linear computational scaling with respect to the multilinear expansion rank. The method can significantly enhance both the accuracy and efficiency of micromagnetic field computations and can further be adapted to other types of nonlocal potentials, such as the Coulomb potential [3].

References

[1] L. Exl, W. Auzinger, S. Bance, M. Gusenbauer, F. Reichel and T. Schrefl, *Fast stray field computation on tensor grids*, Journal of Computational Physics, 231(7), 2840–2850 (2012).

[2] L. Exl and S. Schaffer, *Higher order stray field computation on tensor product domains*, arXiv preprint arXiv:2505.19180 (2025).

[3] L. Exl and S. Schaffer, *Near-field-free super-potential FFT method for the three-dimensional free-space Poisson equation*, arXiv preprint arXiv:2506.04489 (2025).

Abstract ID: 30265

LEVEL-SET PARAMETRIZATION APPROACH FOR INVERSE-DESIGN MAGNONICS

A. Voronov[1], M. C. Santos[2,3], F. Bruckner[1], D. Suess[1], A. Chumak[1], C. Abert[1]

[1] *University of Vienna, Faculty of Physics, 1090, Vienna, AUSTRIA*
[2] *University of Vienna, Vienna Doctoral School of Physics, 1090, Vienna, AUSTRIA*
[3] *Faculty of Sciences, University of Oviedo, 33003, Oviedo, SPAIN*

Inverse design in magnonics exploits the wave-based nature of spin excitations together with numerical optimization strategies to realize device functionalities that are difficult to obtain using conventional approaches [1]. However, many existing inverse-design methods are constrained by substantial memory demands, which restrict the attainable geometric complexity of optimized magnonic structures [2, 3]. To overcome these challenges, we present a topology optimization strategy based on a level-set representation coupled to an adjoint-state optimization scheme.

The proposed framework is implemented within the GPU-accelerated micromagnetic simulation package *neuralmag*, which combines a nodal finite-difference formulation with automatic differentiation [4]. The performance of the method is demonstrated using two representative optimization problems. In the first example, we optimize the geometry of a magnetic nanoparticle to engineer its static magnetization response, successfully identifying shapes that closely reproduce a targeted hysteresis behavior. In the second example, we apply the approach to the inverse design of a frequency-selective magnonic demultiplexer realized in a 300-nm-wide yttrium iron garnet waveguide (Fig. 1). Here, the optimized structure enables spatial separation of spin waves at different frequencies by exploiting interference effects, illustrating the suitability of the method for designing functional magnonic devices.

Our results demonstrate that this approach provides a robust and memory-efficient inverse-design tool, opening new ways for the development of advanced magnonic logic elements.

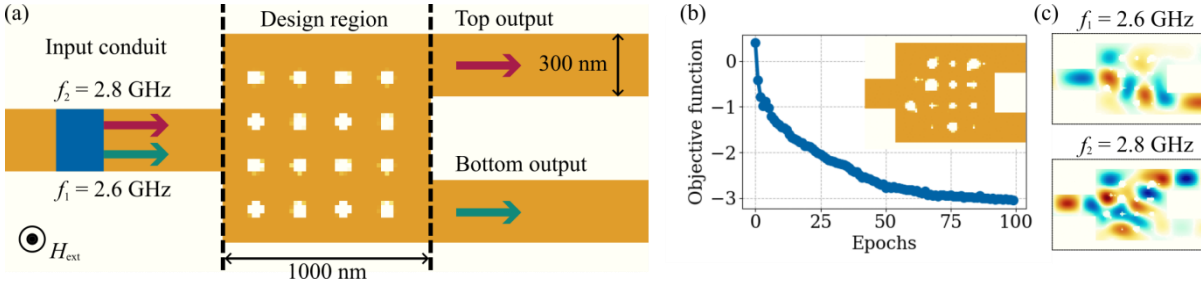

Fig. 1: *(a) Geometry of the magnonic demultiplexer, including the initial distribution of void regions. (b) Convergence of the objective function throughout the optimization process, together with the resulting optimized topology. (c) Simulated spin-wave propagation in the optimized structure for two different excitation frequencies, illustrating frequency-dependent spatial separation of spin-wave signals.*

References

[1] A.V. Chumak, *et al.*, IEEE Transactions on Magnetics **50**, 1 (2022).

[2] Q. Wang, *et al.*, Nature Communications **12**, 2636 (2021).

[3] A. Papp, *et al.*, Nature Communications **12**, 6422 (2021).

[4] C. Abert, *et al.*, npj Computational Materials **11**, 193 (2025).

Abstract ID: 30526

MODELING OF THE MAGNETOCALORIC EFFECT DURING MAGNETOSTRUCTURAL PHASE TRANSITIONS

A. Kosogor[1,2,3], V. A. L'vov[3], D. Böhm[1], T. Schrefl[1]

[1] *University for Continuing Education Krems, 2700, Krems, AUSTRIA*
[2] *University of Vienna, Faculty of Physics, 1090, Vienna, AUSTRIA*
[3] *V.G. Baryakhtar Institute of Magnetism of the NAS of Ukraine, 03127, Kyiv, UKRAINE*

The first-order magnetostructural phase transition from a paramagnetic high-symmetry phase to a ferromagnetic lower-symmetry phase is observed in many magnetic solids and is considered promising for achieving a giant magnetocaloric effect (MCE) [1]. Understanding the thermodynamics of this transition is essential for describing phase stability, the associated hysteresis, and modeling the entropy change across the transition.

A general theoretical framework is presented to describe the magnetostructural phase transition using a Landau-type phenomenological model. The elastic free energy is expanded in terms of order parameters expressed through the strain components [2]. The elastic energy includes contributions from both shear and deviatoric strains, as well as volume changes, with temperature-dependent coefficients determining the stability limits of each phase.

The framework enables computation of heat flow and entropy change associated with the structural transition by relating the evolution of free energy to temperature. Using model functions for the temperature-dependent elastic coefficients, it is possible to simulate the thermal behavior of the system, including latent heat and entropy change [3]. The magnetic subsystem is incorporated by introducing a magnetoelastic coupling and magnetic free energy term for second-order paramagnetic-ferromagnetic transitions [4]. This allows the computation of magnetic-field induced entropy change and adiabatic temperature change during magnetostructural phase transition. Moreover, this approach enables a separation of magnetic and structural contributions to MCE, supporting a deeper understanding of magnetostructural coupling mechanisms.

Acknowledgement

This research was funded by the European Innovation Council, funded by the European Union, through project CoCoMag (Grant No. 101099736) and the Austrian Science Fund (FWF) [10.55776/RIC5537124].

References

[1] N. T. Trung, *et al.*, Appl. Phys. Lett. **96**, 172504 (2010).
[2] V.A. Chernenko, *et al.*, Metals **3**, 237 (2013).
[3] A. Kosogor, *et al.*, Phys. Stat. Sol. (b), **252**, 2758 (2015).
[4] V. A. L'vov, O. Salyuk, A. Kosogor, Sci. Rep. **15**, 31002 (2025).

Abstract ID: 30604

SIMULATING STRONGLY NONLINEAR DYNAMICS OF QUANTUM SYSTEMS WITH MACHINE LEARNING – OVERCOMING INSTABILITIES

H. Vrcan, J. H. Mentink

Institute of Molecules and Materials, Radboud University, Nijmegen, THE NETHERLAND

Classical micromagnetic models successfully capture a vast range of static and dynamic phenomena in magnetically ordered systems. However, as one probes ever shorter length and time scales, set ultimately by the exchange interactions between microscopic spins in the crystal lattice, classical micromagnetic theories are expected to become invalid. Therefore, extending the simulation of magnetism to the smallest length and time scales requires solving a quantum many-body problem.

Recently, important progress in simulating quantum many-body systems has become possible with the application of machine learning methods. Within this approach, known as neural-network quantum states (NQS), the many-body wave function is represented by a neural network as a variational ansatz [1], which resolves the "curse of dimensionality" of the Hilbert space with a controllable number of neural network parameters. However, while this method is effective in representing even very entangled quantum states, obtaining stable dynamics strongly out of equilibrium remains challenging. Beyond this restriction, simulations are plagued by numerical instabilities [2], believed to originate from Monte Carlo sampling noise, nonlinearity, and singularity of equations of motion. The exact cause of instabilities, though, is still not well understood. To address numerical instabilities of NQS, we study a small 2×2 spin lattice, whose wave function is represented by the Restricted Boltzmann Machine (RBM) neural network architecture. To model strongly driven dynamics, the system is prepared in the antiferromagnetic ground state of the Heisenberg model and then quenched out of equilibrium. We find that, even when we eliminate all known sources of numerical instabilities, there is a specific value of the quench strength where the NQS dynamics are drastically different from the exact diagonalization benchmark. This "breakdown" is a property of explicit time integration and could only be resolved using numerically expensive implicit or adaptive integrators [3]. Finally, we present a recipe to repair the numerical instability by forcing the neural network to represent a normalized wave function. With this addition, the neural-network parameters are kept in a stable region even when using simple explicit integration methods. Our results provide a stepping stone to simulate strongly nonlinear quantum spin dynamics of large-scale magnetically ordered systems.

References

[1] G. Carleo, M. Troyer, Science **355**, 602-606 (2017).
[2] D. Hofmann, *et. al.*, SciPost Phys. **12**, 165 (2022).
[3] H. Vrcan, J. Mentink, arXiv:2507.17421 (2025).

11th International Conference on Superconductivity and Magnetism ICSM2026
4th International Conference on Quantum Materials and Technologies ICQMT2026
19th April to 26th April, 2026, Ölüdeniz – Fethiye/Muğla, Türkiye
https://icsmforever.org/

Abstract ID: 30696

BEYOND MONOLITHIC SIMULATIONS: A FEDERATED COMPUTING PLATFORM FOR RESILIENT MICROMAGNETIC WORKFLOWS

M. Ender[1], P. Pirro[2,1]

[1] *Aithericon GmbH, 67663, Kaiserslautern, GERMANY*
[2] *RPTU, 67663, Kaiserslautern, GERMANY*

Modern micromagnetic research is shifting from monolithic simulations toward iterative, branching sequences of thousands of simulations, essential for large-scale parametric sweeps and AI-assisted discovery. However, traditional batch schedulers (e.g., Slurm) are designed for ephemeral, independent jobs, not the persistent coordination required to maintain multi-day inter-dependent studies.

We present a workflow coordinator based on the Petri Net formalism — a mathematical model for concurrent systems where simulation states and data flow as typed tokens through a graph of transitions. Designed as a persistent "guest" across compute resources (Slurm, Nomad), the engine decouples research logic from transient cluster nodes. The architecture provides (1) Automatic Data Lineage, linking every result to its specific parameters; (2) Crash-Proof Execution, ensuring campaigns survive hardware failures by maintaining a persistent event log; and (3) Unified Data Orchestration, which automatically stages required inputs onto compute nodes and archives outputs to long-term storage — eliminating manual data logistics between clusters. We demonstrate the framework via a gradient-free optimization and an online surrogate modelling pipeline. This approach allows researchers to scale from simple sweeps to complex, AI-assisted discovery without writing infrastructure-related code (Fig. 1).

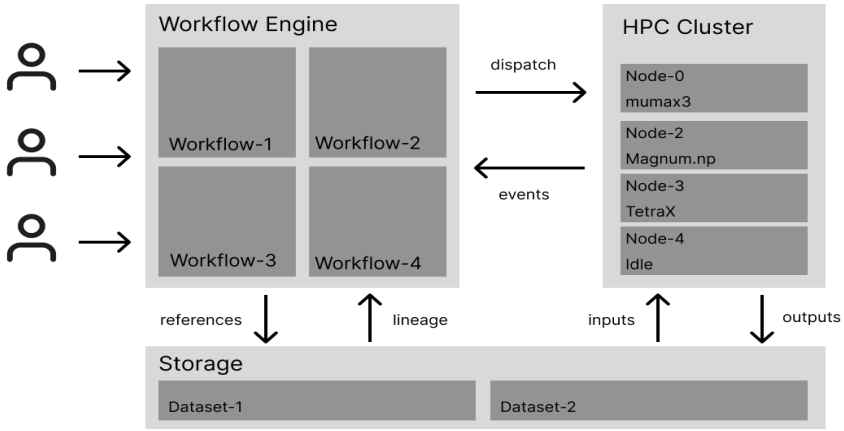

Fig. 1: *Diagram of the federated workflow engine architecture, data and control flow.*

Abstract ID: 30621

NON-RECIPROCAL SPIN WAVE DYNAMICS IN MÖBIUS-SHAPED NANOMAGNETS

R. Hertel

Université de Strasbourg, CNRS, IPCMS, 67000 Strasbourg, Strasbourg, FRANCE

Curved and topologically nontrivial magnetic nanostructures offer new opportunities to control spin-wave dynamics beyond planar systems. In this talk, I will discuss spin-wave modes in nanoscale Möbius-shaped soft-magnetic strips and show how their geometry gives rise to intrinsically nonreciprocal, rotating spin-wave modes that have no analogue in topologically trivial rings.

Using micromagnetic simulations, we compare Möbius strips with different numbers of twists to a twist-compensated bent ring [1]. While the trivial ring supports well-defined standing-wave modes, Möbius nanomagnets exhibit frequency-split mode pairs corresponding to clockwise and counterclockwise rotating spin waves. This splitting originates from a twist-induced geometric (Berry) phase, which lifts the degeneracy between counterpropagating modes and leads to asymmetric dispersion relations, in quantitative agreement with a recently developed analytical theory [2]. The non-orientable topology further imposes antisymmetric boundary conditions, resulting in half-integer wavelength quantization. We also show that localized RF excitation enables selective generation of rotating spin waves with a chosen propagation direction.

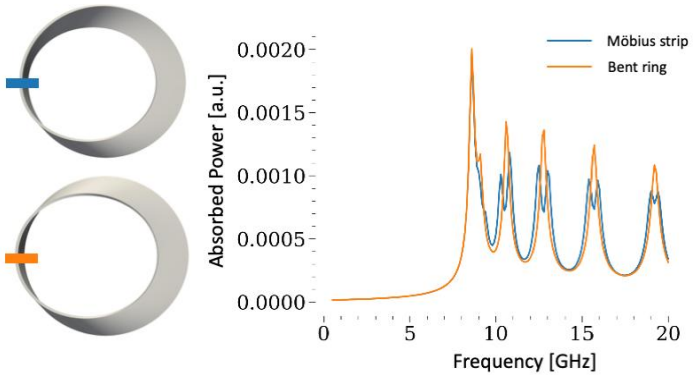

Fig. 1: *Resonant excitation of spin-wave modes by a localized oscillating magnetic field in a Möbius-shaped nanomagnet (top left) and a geometrically similar but topologically trivial "bent" ring (bottom left). Right: The bent ring exhibits distinct resonance frequencies corresponding to standing-wave modes, whereas the Möbius strip displays pairs of nearby resonances—frequency doublets—associated with rotating spin-wave modes of opposite circulation sense [1].*

References

[1] A. Thonikkadavan, M. d'Aquino and R. Hertel, npj Spintronics **4**, 4 (2026).
[2] M. d'Aquino and R. Hertel, Phys. Rev. Lett. **135**, 216705 (2025).

35 - MOLECULAR SPIN QUBITS AND MOLECULAR SPINTRONICS BASED ON MOLECULAR MAGNETS

Abstract ID: 30152

TOPOLOGICAL QUENCHING OF QUANTUM TUNNELLING OF THE MAGNETISATION IN A SINGLE MOLECULE MAGNET

E. Moreno-Pineda[1,2], S. Paul[1], C. Molina-Jirón[1,2], A. Sunil[1], M. Ruben[1], A. Garg[3], W. Wernsdorfer[1]

[1] *Karlsruhe Institute of Technology (KIT), D-76344, Karlsruhe, GERMANY*
[2] *Universidad de Panamá, 0824 Panamá, PANAMÁ*
[3] *Northwestern University, Illinois 60208, UNITED STATES OF AMERICA*

Preserving quantum coherence can be achieved by exploiting a system's topology, where information is encoded in global geometric properties of quantum states that remain resilient to local disturbances. This robustness stems from the fact that certain geometric characteristics depend solely on the trajectory of quantum operations and the curvature of the controlled-parameter space, rather than on microscopic dynamics. Such principles underpin topology-based strategies for fault-tolerant quantum computing. To explore these topological features, geometric phase interference (Berry phase) has been widely investigated in optical systems and condensed matter, including molecular magnets (MMs)[1]. Yet, direct observation in 4f-based MMs—promising qudit platforms—has been hindered by large tunneling gaps and environmental coupling. Here, we introduce a magneto-spectroscopic approach using μSQUID-EPR[2,3] to resolve tunnel splittings in the ^{160}Gd-based MM $[^{160}GdPc_2]^-$ (Pc = phthalocyanine). By applying microwaves under transverse magnetic fields, we map the spin manifold and reveal pronounced oscillations in tunnel splitting, signaling quantum phase interference. These oscillations expose topological quenching of tunneling and emphasize the role of fourth-order transverse anisotropy, unveiling a nontrivial topology that could, in principle, be exploited in advanced holonomic quantum computation.

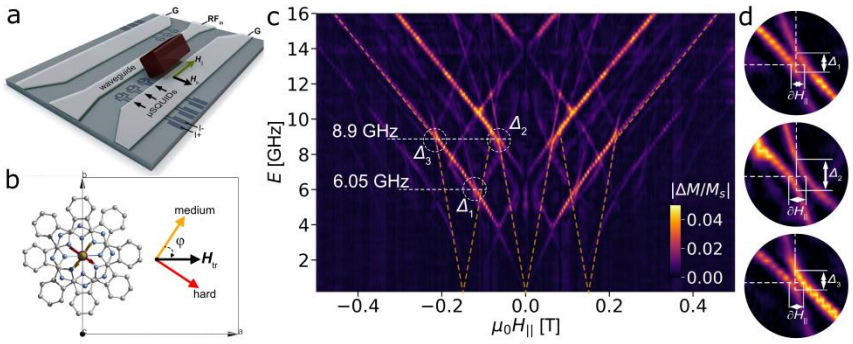

Fig. 1: *(a) Schematic figure of μSQUID-EPR chip comprising the μSQUID loops and the coplanar waveguide for microwave irradiation. (b) Crystallographic orientation of the $[^{160}GdPc_2]^-$ complex. (c) Frequency map ($\angle M(H_{||}, \nu)$) with the field applied along the easy axes of the crystal. (d) Zoomed region for each explored tunnel gap.*

References

[1] E. Moreno-Pineda and W. Wernsdorfer, Adv. QuantumTechnol. **8**, 2300367 (2025).

[2] S. Paul, *et al.*, Inorg. Chem. Front., **12**, 64602 (2025).

[3] G. Taran, E. Moreno-Pineda, M. Schulze, E. Bonet, M. Ruben W. Wernsdorfer, Nat. Commun., **14**, 3361 (2023).

Abstract ID: 30223

REVISITING LANTERN COMPLEXES AS MOLECULAR SPIN QUBITS

A. Cornia[1], O. Mironova[1], M. Borsari[1], M. Briganti[2], M. Chiesa[3], R. Clérac[4], M. Imperato[1,5], Y.-K. Liao[3], A. Nicolini[1], M. C. Pagliero[3], A. Ranieri[6], A. Raza[2], M. Rouzières[4], E. Salvadori[3], L. Sorace[2]

[1] *Dept. of Chemical and Geological Sciences & INSTM, UniMORE, 41125, Modena, ITALY*
[2] *Dept. of Chemistry "Ugo Schiff" & INSTM, UniFI, 50019, Sesto Fiorentino (FI), ITALY*
[3] *Dept. of Chemistry & NIS Centre, UniTO, 10125, Turin, ITALY*
[4] *Univ. Bordeaux, CNRS, CRPP, UMR 5031, 33600, Pessac, FRANCE*
[5] *Dept. of Physics, Informatics and Mathematics, UniMORE, 41125, Modena, ITALY*
[6] *Dept. of Life Sciences, UniMORE, 41125, Modena, ITALY*

Lantern structures are robust and versatile bimetallic complexes with a manifold of applications in metal-organic chemistry. In the few known derivatives containing a vanadyl ion (VO^{2+}) and a diamagnetic Group 10 metal ion (Pd^{2+}, Pt^{2+}), the electronic spin (S = 1/2) is coupled to the nuclear spin of ^{51}V (I = 7/2), yielding an electronuclear spin qudit. We present recent work on four lantern structures $[MVO(SOCR)_4]$ (M = Pd, Pt) with thiocarboxylate ligands (R = Me, Ph; see Fig. 1). In their crystals, these lanterns form antiferromagnetically coupled dimers supported by short M···M or M···S contacts. Metallophilic contacts mediate the strongest magnetic interactions, with triplet-singlet gaps up to 5 cm^{-1} and a slightly more effective coupling in the Pd derivatives. Both M and R significantly affect other electronic properties of the lanterns, like reduction potentials. In a frozen CD_2Cl_2/toluene-d_8 matrix at 10 K, lanterns occur in monomeric form and display coherence times (T_m) ranging from 4.5 to 12 μs (Fig. 1). Thiobenzoate derivatives systematically have longer T_m values, whereas lanterns with M = Pd and Pt show similar coherence lifetimes, despite the quite different magnitude of spin-orbit coupling interactions in the two Group 10 metals. We attribute this effect to the minute spin density delocalized on M, which amounts to ca. 1% and is directly detectable in $[PtVO(SOCR)_4]$ as an additional twofold splitting of EPR lines, arising from superhyperfine coupling with the ^{195}Pt isotope (I = 1/2).

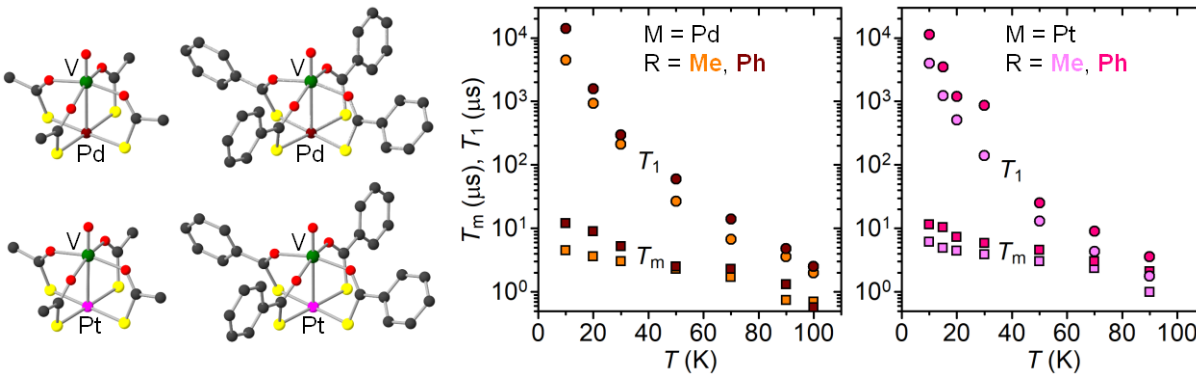

Fig. 1: *Structures and temperature-dependent spin relaxation properties of [MVO(SOCR)4] lanterns.*

References

[1] S. A. Beach, *et al.*, Chem. Commun. **56**, 11062 (2020).

[2] M. Imperato, *et al.*, Inorg. Chem. Front. **11**, 186 (2024).

[3] O. Mironova, *et al.*, Inorg. Chem., in press; DOI: 10.1021/acs.inorgchem.5c04835.

[4] O. Mironova, *et al.*, Chem.-Eur. J., in press; DOI: 10.1002/chem.202503004.

Abstract ID: 30241

STUDY AND CONTROL OF MANY-BODY EFFECTS IN MOLECULAR SPIN CRYSTALS BY MEANS OF CIRCUIT QUANTUM ELECTRODYNAMICS

F. Luis

Instituto de Nanociencia y Materiales de Aragón (INMA), CSIC-Universidad de Zaragoza, Zaragoza, SPAIN

Circuit quantum electrodynamics is considered as a promising platform for wiring up molecular spin qubits into a scalable architecture. The strong, or coherent, coupling of the molecular spins to individual microwave photons gives rise to hybrid light-matter excitations and allows controlling the spin states and reading out the results. Here, I discuss that this interaction can also compete with the long-range equilibrium magnetic state of molecular spin crystals and that it allows detecting such competition in situ by means of microwave transmission experiments [1,2]. The implementation of these theoretical ideas will be illustrated by experiments performed on two model molecular materials. First, we study DPPH $S = ½$ free radicals interacting with a superconducting transmission waveguide [3]. As T decreases below 1 K, the growth of spin correlations along 1-dimensional chains, combined with the anisotropy in the spin-spin exchange constants, tend to suppress the collective spin-photon coupling. In this regime, the microwave transmission also reflects a gradual change in the nature of the dominant spin excitations, from single-spin flips to bosonic magnons. Then, I'll discuss the coupling of $S = 1$ Ni(II)-imdipa monomers to both transmission lines and lumped element superconducting resonators. These molecules provide a simple realization of a zero-field spin clock transition that shields molecular spin qubits against environmental fields [4]. The growth of spin-spin correlations for $T < 0.35$ K increases the photon excitation gap and modifies the coupling to cavity photon modes. The results can be understood on basis of a competition between quantum spin fluctuations and spin-spin interactions, monitored in situ by on-chip microwave spectroscopy.

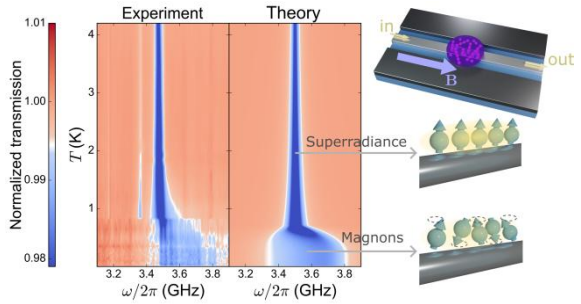

Fig. 1: *Coupling a superconducting line to a 1D magnetic material reveals transitions to collective excitations that evolve as T decreases from superradiant modes to magnons [3].*

References

[1] J. Román-Roche, F. Luis, and D. Zueco, Phys. Rev. Lett. **127**, 167201 (2021).

[2] J. Román-Roche, Á. Gómez-León, F. Luis, and D. Zueco, Nanophotonics **14**, 2053 (2025).

[3] S. Roca-Jerat, M. Rubín-Osanz, M. D. Jenkins, A. Camón, P. J. Alonso, D. Zueco, and F. Luis, Commun. Materials **6**, 172 (2025).

[4] M. Rubín-Osanz, F. Lambert, F. Shao, E. Rivière, R. Guillot, N. Suaud, N. Guihéry, D. Zueco, A.-L. Barra, T. Mallah, and F. Luis, Chem. Sci. **12**, 5123 (2021).

Abstract ID: 30257

KONDO RESONANCE OF $LnPc_2$ SINGLE-MOLECULE MAGNETS

M. Yamashita[1,2]

[1] *Institute for Materials Research, Tohoku University, 2-1-1 Katahira, Aoba-Ku, Sendai 980-8577, JAPAN*
[2] *School of Chemical Science and Engineering, Tongji University, Siping Road 1239, Shanghai 200092, P. R. CHINA*

Spintronics is a key technology in 21st century based on the freedoms of the charge, spin, as well as orbital of the electron. The MRAM systems (magnetic random access memory) by using Giant Magnetoresistance (GMR) or Tunneling Magnetoresitance (TMR) have several advantages such as no volatility of information, the high operation speed of nanoseconds, the high information memory storage density, and the low consuming electric power. Usually in these systems, the conventional or classical magnets composed of the transition metal ions are used, while in our study we will use Single-Molecule Magnets (SMMs), which are usually composed of mono- or multi-nuclear metal complexes, to overcome "Moore`s Limitation". Moreover, SMMs show the slow magnetic relaxations due to the double-well potential. From the beginning of SMMs researches, most researchers have noticed that SMMs will show Kondo resonance because SMMs have unpaired electrons. What is Kondo resonance ? More than 50 years ago, Professor Kondo theoretically explained that if the metallic materials include small amounts of magnetic impurities, the metallic electrons and magnetic impurities make the coupling and then the singlet states with decreasing the temperature, resulting in the metal-insulator transition. However, nobody knows how to detect Kondo resonance on SMMs. We have succeeded in observing Kondo resonance on $LnPc_2$ SMMs by using Scanning Tunnelling Microscopy (STM) and Scanning Tunnelling Spectroscopy (STS).

First, we have tried to input/output one memory into/from double-decker Tb(III) SMM ($TbPc_2$) on Au surface by using STM and STS. In this research, we have observed Kondo resonance for the first time. In this case, the metallic electron is the tunnelling current from STM tips to the Au surface, while the magnetic impurities are not Tb(III) 4f8 but the radical of the Pc ligands. We have succeeded in controlling the appearance and disappearance of Kondo peak by the electron injection using STS, reversibly. This is considered as the first single-molecule memory device.

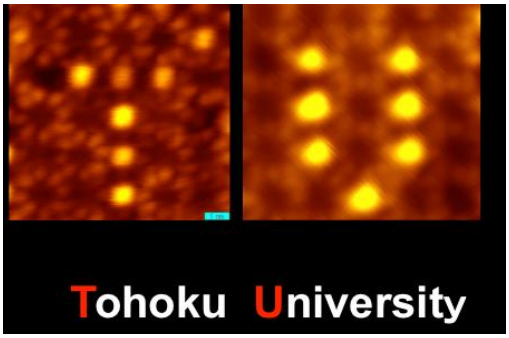

Secondly, we have made doping Cs atoms onto YPc_2, where Kondo peaks have not observed by coupling between the radical of Pc and 6s electron of Cs atom to make a singlet pair, while other YPc_2 sites show Kondo peak due to the radicals of Pc ligands. Thirdly, we have succeeded to write the letters of T and U, which are the initials of Tohoku University as shown in Figure (right). Finally, we have measured STM and STS of $CePc_2$ on Au surface. In the first layer of $CePc_2$, we observed Kondo peaks on both Ce(III)$4f^1$ and radical of Pc ligand. However, on the second layer of $CePc_2$, we have not observed the Kondo peaks on either Ce(IV)$4f^0$ or no radical of Pc ligand. This means that the valence tautomerization occurs between Ce ions and Pc ligands on the first and second layers of $CePc_2$ by Au surface.

References

[1] T. Komeda, M. Yamashita, *et al.*, Nature Commun., **2**, 217(2011).

Abstract ID: 30280

MOLECULAR SPIN QUBIT BEHAVIOR IN MULTIFUNCTIONAL SPIN CROSSOVER SYSTEMS

S. Hayami

Kumamoto University, Dept. of Chemistry, 8608555, Kumamoto, JAPAN

Spin crossover (SCO) systems provide a unique platform for molecular spin qubits because their electronic spin states can be reversibly controlled by external stimuli such as temperature, light, pressure, and electric fields. In addition to bistable spin switching, SCO compounds often exhibit multifunctional properties, including photoresponsivity, thermochromism, conductivity, luminescence, ferroelectricity, and single-molecule magnet behaviour, offering rich opportunities for coherent spin control.

In this presentation, recent progress in coordination metal complex–based SCO materials is discussed with a focus on their potential as molecular spin qubits. Particular attention is paid to how structural dynamics (proton transfer, molecular motion, and lattice flexibility) and electronic dynamics (electron transfer and spin crossover at the metal centre) influence spin coherence and decoherence pathways. Furthermore, synergistic effects arising from the coupling between spin, charge, and lattice degrees of freedom, such as magnetoelectric and spin–phonon coupling, are highlighted.

By integrating spin crossover functionality with qubit-relevant coherence properties, multifunctional SCO systems emerge as promising candidates for stimuli-responsive molecular spin qubits and hybrid quantum materials.

Abstract ID: 30671

ORBIT-ORBIT INTERACTION-ENABLED OPTICALLY INDUCED MAGNETIZATION IN HYBRID ORGANIC-INORGANIC PEROVSKITE FILM

B. Hu

Department of Materials Science and Engineering, University of Tennessee, Knoxville, Tennessee 37996, USA

Realizing the coupling between semiconducting and magnetic properties opens new opportunities for creating the next generation spin-related optoelectronics. Here, we report a fundamentally new phenomenon of optically induced magnetization achieved by coupling photoexcited orbital magnetic dipoles with magnetic spins at perovskite/ferromagnetic interface. The depth-sensitive polarized neutron reflectometry combined with in situ photoexcitation setup, constitutes key evidence of this novel effect. It is demonstrated that a circularly polarized photoexcitation induces a stable magnetization signal within the depth up to 7.5 nm into the surface of high-quality perovskite ($MAPbBr_3$) film underneath a ferromagnetic cobalt layer at room temperature. In contrast, a linearly polarized light does not induce any detectable magnetization in the $MAPbBr_3$. The observation reveals that photoexcited orbital magnetic dipoles at the surface of 2D-superlattice perovskite are coupled with the spins of the ferromagnetic atoms at the interface, leading to an optically induced magnetization within the perovskite's surface. Our finding demonstrates that perovskite semiconductor can be bridged with magnetism through optically controllable method at room temperature in this heterojunction design. This provides the new concept of utilizing spin and orbital degrees of freedom in new-generation spin-related optoelectronic devices.

Abstract ID: 30814

ENLARGING QUANTUM COHERENCE OF MOLECULAR SPIN QUBITS IN ZIRCONIUM PORPHYRINIC MOFs

D. Žilić[1], L. Vujević[1], B. Karadeniz[1], K. Užarević[1], A. A. Popov[2]

[1] *Ruđer Bošković Institute, 10000, Zagreb, CROATIA*
[2] *Leibniz IFW Dresden, 01069, Dresden, GERMANY*

Metal-organic frameworks (MOFs) are porous coordination polymers made of metal centers bridged by organic ligands. Because of their structural and functional tunability, they have wide applications in different fields, including quantum technologies [1, 2, 3]. The quantum coherence of molecular spin qubits hosted in the diamagnetic zirconium MOF PCN-223 was investigated (Fig. 1). The properties of copper- and vanadyl-porphyrin qubits were studied using pulse electron spin resonance (ESR) spectroscopy, which provides electron spin-lattice relaxation time (T_1) and phase memory time (T_m). Enlarging quantum coherence by spin dilution and fullerene encapsulation in MOF pores will be discussed [4, 5].

This work was supported in part by the Croatian Science Foundation under the project number HRZZ-IP-2022-10-9292.

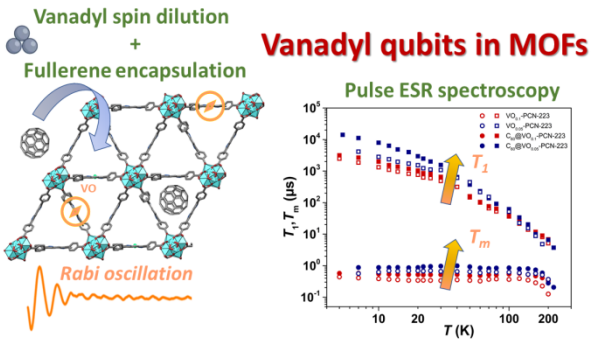

Fig. 1: *Spin dilution within the diamagnetic Zr PCN-223 framework, as well as the encapsulation of fullerenes into the MOF pores, increases both the spin-lattice, T_1, and phase-memory time, T_m, in vanadyl-porphyrin qubits.*

References

[1] A. Gaita-Ariño, F. Luis, S. Hill and E. Coronado, Nat. Chem. **11**, 301 (2019).
[2] T. Yamabayashi, M. Atzori, L. Tesi, G. Cosquer, F. Santanni, M.-E.Boulon, E. Morra, S. Benci, R. Torre, M. Chiesa, L. Sorace, R. Sessoli and M. Yamashita, J. Am. Chem. Soc. **140**, 12090 (2018).
[3] C.-J. Yu, M. D. Krzyaniak, M. S. Fatallah, M. R. Wasielewski and D. E. Freedman, Chem. Sci. **10**, 1702 (2019).
[4] L. Vujević, B. Karadeniz, N. Cindro, A. Krajnc, G. Mali, M. Mazaj, S. M. Avdoshenko, A. A. Popov, D. Žilić, K. Užarević and M. Kveder. Chem. Sci. **14**, 9389 (2023).
[5] L. Vujević, G. Talajić, F. MacMillan, A. A. Popov, M. Kveder, B. Karadeniz, K. Užarević and D. Žilić, (2026) paper in revision.

Abstract ID: 30010

SELF-COOLING MOLECULAR SPIN QUDITS

G. Aromí[1], F. Luis[2], L.A Barrios[1], S. Carretta[3], O. Roubeau[2], V. Novikov[1]

[1] *Universitat de Barcelona, Dept. of Chemistry, 08028, Barcelona, SPAİN*
[2] *Universidad de Zaragoza, Dept. Física de la Materia Condensada, 50009, Zaragoza, SPAIN*
[3] *Università di Parma, Dipt di Scienze Matematiche, Fisiche e Informatiche, I-43124, Parma, ITALY*

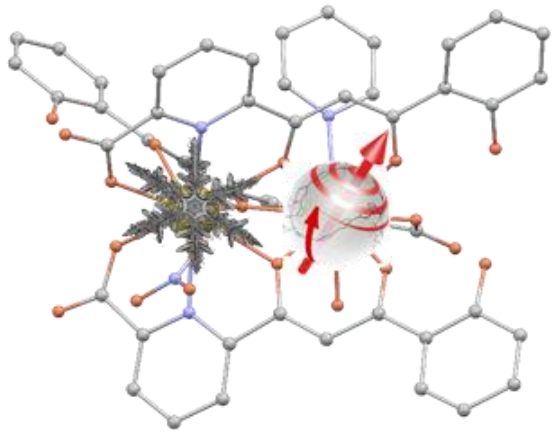

Achieving the coherent control of quantum states of matter for the processing of information and the realization of quantum algorithms fuels the race for finding the optimal technology to reach this goal. Spins within molecules benefit from the atomistic control and reproducibility of synthetic chemistry for the realization of the qubits conforming quantum computers [1,2]. One of the inherent requirements is to operate at very low temperatures. We address this challenge by integrating, in the same molecule, a quantum Bit and magnetic refrigeration component. We exploit the ability to obtain selectively heterolanthanide coordination complexes, used in the past as prototypes of 2-qubit conditional quantum gates [3] to propose a new molecule with these two functions. It consists of a [GdEr] complex, where Er(III) encodes a qubit while Gd(III) provides a large magnetocaloric effect [4]. The properties of each component are separately studied in isostructural [LaEr] and [GdLu] complexes, where each functional ion lies next to a diamagnetic metal otherwise exactly in the same environment as in [GdEr]. We show the magnetic, heat capacity, and EPR measurements for all compounds, emphasizing that the presence of both ions in the same molecule has a synergic effect on both functionalities. Thus, the coupling between Er(III) and Gd(III) leads to a d = 16 set of spin states that, as revealed by pulse EPR measurements, can be coherently manipulated. In turn, Er(III) enhances the magnetocaloric effect compared to [GdLu], extending it to lower temperatures. This is corroborated by direct magnetocaloric measurements, which demonstrates that this material can cool itself, and a device, down to temperatures as low as 0.4 K.

References

[1] G. Aromí, D. Aguilà, P. Gamez, F. Luis, O. Roubeau, Chem. Soc. Rev., **41**, 537-546 (2012).

[2] A. Privitera, A. Chiesa, F. Santanni, A. Carella, D. Ranieri, A. Caneschi, M. D. Krzyaniak, R. M. Young, M. R. Wasielewski, S. Carretta, R. Sessoli, J. Am. Chem. Soc., **147**, 331-341 (2025).

[3] D. Aguilà, L. A. Barrios, V. Velasco, O. Roubeau, A. Repollés, P. J. Alonso, J. Sesé, S. J. Teat, F. Luis, G. Aromí, J. Am. Chem. Soc., **136**, 14215-14222 (2014).

[4] E. Palacios, D. Aguilà, D. Gracia, D. Maniaki, L. A. Barrios, A. Chiesa, J. I. Martínez, V. Novikov, O. Roubeau, S. Carretta, M. Evangelisti, G. Aromí, F. Luis, , Adv. Mater. e11061 (2025).

Abstract ID: 30019

ADDRESSING MOLECULAR SPIN QUBITS BY SUPERCONDUCTING CIRCUITS

M. Affronte[1,2], C. Bonizzoni[1,2], M. Lanza[1,2], A. Ghirri[2]

[1] *Dipartimento di Scienze Fisiche, Informatiche e Matematiche, Università di Modena e Reggio Emilia, via G. Campi 213/A, Modena 41125, ITALY*
[2] *Istituto Nanoscienze—CNR, Centro S3, via G. Campi 213/A, Modena 41125, ITALY*

Coherent manipulation of molecular spin qubits is the prerequisite for applications such as quantum computing [1] or sensing [2] and for advanced Quantum ElectroDynamics (QED) experiments. One route to these goals is to embed molecular spins in superconducting circuits thus allowing to exploit the complementary advantages offered by each system in scalable architectures. To this end, we developed a multifrequency platform based on high-Tc YBCO superconducting planar resonators [3] and home-made heterodyne systems for advanced microwave spectroscopy and arbitrary pulse generation [4, 5].

I first show how to coherently manipulate electron spins in Vanadyl porphyrin derivatives and organic radicals with different coherence times thus demonstrating their functionality as temporary memories for quantum information [5].

We also developed and tested protocols for quantum sensing of magnetic fields and showed that the resulting magnetic field sensitivity can reach values as high as $nT/\sqrt{Hz}$ [6]. We have recently extended these protocols to reconstruct tiny magnetic field signals with different time evolution [7].

Of potential interest for quantum sensing, I shall report on QED experiments we performed at single photon regime at mK temperature. Here I shall discuss some hidden features of molecular spins that we used to control both the spin-photon coupling and the dissipation in order to achieve conditions for *perfect absorption* in a rather unconventional conditions [8].

Finally, we recently implement our setup to separately address electron and nuclear spins in molecular qubits by sequences of alternating RF and MW pulses. Preliminary results depict a viable route to fully exploit both electron and nuclear spins in molecules for quantum technologies.

References

[1] F. Troiani, M. Affronte, Chemical Society Reviews **40**, 3119-3129 (2011).

[2] F. Troiani, *et al.*, J. Magn. Mag. Mat..**491**, 165534 (2019).

[3] C. Bonizzoni, *et al.*, Advances in Physics: X, **3**, 1435305 (2018).

[4] C. Bonizzoni, *et al.*, Appl. Magn. Reson. **54**, 143 (2023).

[5] C. Bonizzoni, et al., npj Quantum Inf., **6**, 68 (2020).

[6] C. Bonizzoni, *et al.*, NPJ Quantum Inf. **10**, 41 (2024).

[7] M. Lanza, *et. al.*, submitted (2025).
https://arxiv.org/abs/2509.17144

[8] C. Bonizzoni, *et al.*, submitted (2025).
https://arxiv.org/abs/2505.05966v2

[9] M. Lanza, *et. al.*, in progress. (2025).

Abstract ID: 30246

HOW ENCAPSULATION ENHANCES THE QUANTUM COHERENCE OF A SOLID-STATE MOLECULAR SPIN QUBIT

L. A Barrios[1], A. Swain[1], Y. Nelyubina[2], S. J. Teat[3], O. Roubeau[4], G. Aromí[1], V. Novikov[1]

[1] *University of Barcelona, Faculty of Chemistry, IN2UB, 08028, Barcelona, SPAIN*
[2] *INEOS, Russian Academy of Sciences, Moscow 119334, RUSSIA*
[3] *Advanced Light Source, Berkeley Laboratory, 1 Cyclotron Road, Berkeley, 94720, USA*
[4] *INMA, University of Zaragoza, 50009, Zaragoza, SPAIN*

Spins within molecules benefit from the atomistic control of synthetic chemistry for the realization of qubits. One advantage is that the quantum superpositions of the spin states encoding the qubit can be coherently manipulated using electromagnetic radiation. The main challenge is the fragility of these superpositions when qubits are to partake of solid-state devices. We address this issue with a supramolecular approach for protecting molecular spin qubits against decoherence. The molecular qubit [Cr(ox)3]3− has been encapsulated inside the diamagnetic triple-stranded helicate $[Zn_2L3]^{4+}$ (L is a bis-pyrazolylpyridine ligand). The quantum coherence of the protected qubit is then analyzed with pulsed EPR spectroscopy and compared with the unprotected qubit, both in solution and in the solid state. Crucially, the spin–spin relaxation in the solid state has been examined within diamagnetic crystal lattices of the isostructural ($[Al(ox)_3]@[Zn_2L3]^{4+}$) or $[Al(ox)_3]^{3-}$ assemblies, respectively, doped with the Cr^{3+} qubit in two different (<10%) concentrations. The study unveils a surprising increase of the phase memory time of the qubit upon encapsulation only in the solid. Spin-lattice relaxation times also exhibit a significant enhancement, as established from inversion recovery pulse sequences and from slow relaxation of the magnetization of the protected qubit, not featured by the free qubit.

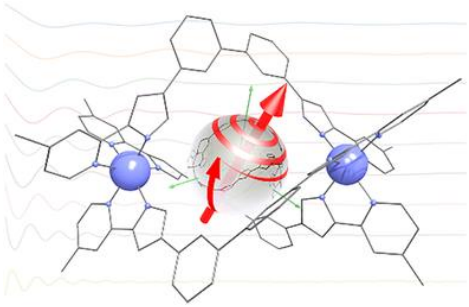

Fig. 1: *A purely synthetic supramolecular chemistry approach enables the protection of the spin-based qubit $[Cr(ox)_3]^{3-}$ from external sources of decoherence in the solid state.*

References

[1] A. Swain, L. A. Barrios, *et al.*, Angew. Chem. Int. Ed., **64**, e202510603 (2025).

36 - MULTICOMPONENT SUPERCONDUCTIVITY AND RELATED PHENOMENA

Abstract ID: 30094

ELECTRONIC STRUCTURE AND MAGNETIC FLUCTUATIONS IN UTe_2 UNDER PRESSURE

M. Shimizu, Y. Yanase

Kyoto University, Graduate School of Science, Dept. of Physics, 606-8502, Kyoto, JAPAN

Pressure-induced changes in the magnetic and superconducting properties of an odd-parity superconductor candidate UTe_2 have attracted considerable interest, underscoring the need for microscopic theoretical insight. In this study, we investigate electronic structure and magnetic fluctuations at ambient pressure and under pressure using density functional theory (DFT) combined with the random phase approximation (RPA). For each pressure, we perform DFT+U calculations for several values of the Coulomb interaction U, construct a 72-orbital periodic Anderson model, and calculate magnetic susceptibilities with use of the RPA.

For U = 2 eV, the Fermi surface have a quasi-two-dimensional shape, antiferromagnetic fluctuations develop with the wave vector $\boldsymbol{Q}_1 \parallel \boldsymbol{a}^*$, and the magnetic anisotropy follows $\chi^b > \chi^a > \chi^c$. The antiferromagnetic fluctuations are suppressed under pressure because of a reduced density of states at the Fermi level, while the magnetic anisotropy is weakened. In contrast, for U = 1 eV, antiferromagnetic fluctuations with $\boldsymbol{Q}_2 \parallel \boldsymbol{b}^*$ appears, accompanied by anisotropy $\chi^a > \chi^c > \chi^b$, consistent with experiments. Under pressure, antiferromagnetic fluctuations around $\boldsymbol{Q}_2$ are enhanced, the magnetic wave vector tilts slightly toward the $\boldsymbol{a}^*$ direction due to Fermi-surface distortion, and the magnetic anisotropy is suppressed. These results demonstrate that the pressure evolution of magnetism in UTe_2 is governed by the momentum-space distribution of U *5f* states and the density of states at the Fermi level, providing a microscopic basis for understanding the magnetic and superconducting properties of UTe_2.

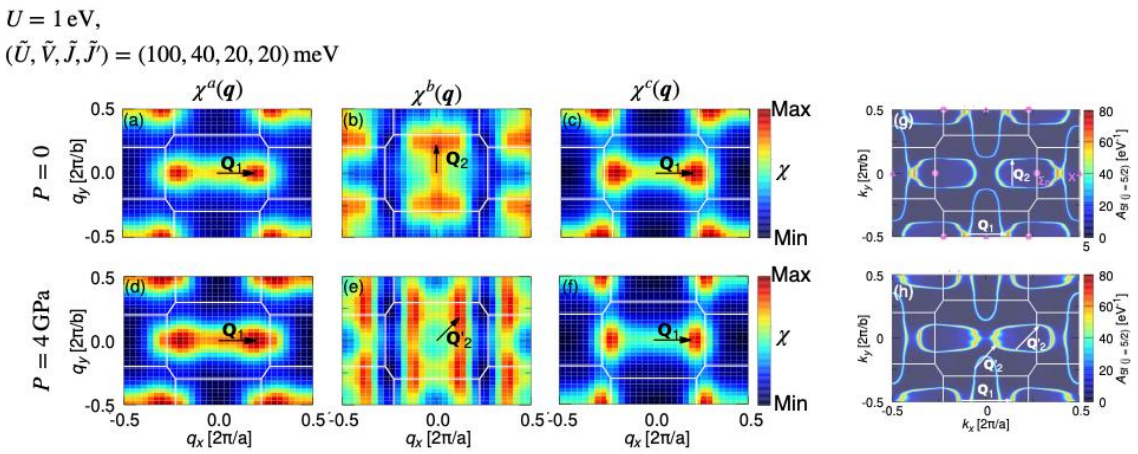

Fig. 1: *(a-f) Magnetic susceptibilities and (g,h) spectral functions obtained for U = 1 eV. Interactions parameters in RPA are* $(\tilde{U}, \tilde{V}, \tilde{J}, \tilde{J}') = (100, 40, 20, 20)$ *meV in these calculations.*

References

[1] M. Shimizu and Y. Yanase, J. Phys. Soc. Jpn. **94**, 124708 (2025).

[2] M. Shimizu and Y. Yanase, arXiv:2510.15322 (2025).

Abstract ID: 30256

COMPETING AND COOPERATING ORDERS IN UTe_2

D. Braithwaite[1], T. Vasina[1], G. Knebel[1], J.-P. Brison[1], G. Lapertot[1], G. Seyfarth[2]

[1] Univ. Grenoble Alpes, Grenoble INP, CEA, IRIG-Pheliqs, F-38000 Grenoble, FRANCE
[2] Univ. Grenoble Alpes, INSA Toulouse, Univ. Toulouse Paul Sabatier, EMFL, CNRS, LNCMI, Grenoble 38042, FRANCE

Superconductivity in UTe_2 has many striking properties, like extremely high and anisotropic critical fields and the existence of multiple superconducting phases induced by either pressure or magnetic field. However perhaps the most unusual feature is the reinforcement of superconductivity in applied magnetic fields. The usual effect of magnetic field on superconductivity is through the effect of the field on the motion or the spin of the carriers. The effect of magnetic field on the pairing mechanism is absent or negligeable. This is not surprising in conventional superconductors where the pairing mechanism stems from the electron-phonon interaction, but it is also the case in most unconventional superconductors, even when the pairing mechanism has a magnetic origin. UTe_2 is one of the few exceptions where an applied magnetic field can enhance the strength of the pairing mechanism and actually reinforce superconductivity. In ambient pressure conditions, this effect is most spectacular when the field is applied along the b-axis of this orthorhombic system, where, above 15T, the superconducting critical temperature increases with increasing field. However, under pressure a reinforcement of superconductivity with magnetic field is found for field applied along the c-axis. In both cases the probable origin is the proximity of a magnetic phase transition line that can be crossed by tuning the field. For H//b this is the metamagnetic transition to a polarized state at about 35T. Under pressure, two further transitions have been detected: a transition to a long-range antiferromagnetic state, and a second transition to a so far unidentified state. We present new results under pressure which help to clarify the role of these different transitions in helping or hindering superconductivity in UTe_2.

Abstract ID: 30359

QUASIPARTICLE SCATTERING INTERFERENCE IMAGING OF TOPOLOGICAL SUPERCONDUCTIVITY IN UTe_2

S. Wang

University of Bristol, UK

Although no known material definitely exhibits intrinsic topological superconductivity, where a spin-triplet electron pairing potential $\Delta(\boldsymbol{k})$ has odd-parity, $\Delta(-\boldsymbol{k}) = -\Delta(\boldsymbol{k})$, UTe_2 is now the leading candidate. Ideally, the parity of $\Delta(k)$ might be established by using Bogoliubov quasiparticle interference (QPI) imaging, a recognized technique for $\Delta(\boldsymbol{k})$ determination in complex superconductors. However, odd-parity superconductors should support a topological quasiparticle surface band (QSB) on crystal termination surfaces only for energies within the superconductive energy gap $|E| \leq \Delta$. The QPI should then be dominated by the QSB electronic structure $k(E)$ and only reveal bulk $\Delta(\boldsymbol{k})$ characteristics excursivly. Here, by using a superconducting scan-tip to achieve $\sim 10\ \mu eV$ energy resolution for UTe_2 studies, we discover and visualize the in-gap quasiparticle interference patterns of its QSB. Specifically, at the UTe_2 (0-11) cleave surface a unique band of Bogoliubov quasiparticles appears only in the superconducting state $T < T_c$ [1]; QPI visualization then yields a characteristic sextet $\boldsymbol{q}_i: i = 1 - 6$ of interference wavevectors from which we establish QSB dispersions $k(E)$, and their existence only for energies $|E| \leq \Delta_{max}$ within the range of Fermi momenta projected onto the (0-11) crystal surface [2]. Quantitative evaluation of this sextet $\boldsymbol{q}_i$ then demonstrates precisely how the QSB is projected from the subtending bulk Fermi surface. Finally, a novel theoretical framework has been developed to predict the QPI signatures of a topological QSB at this (0-11) surface. Its predictions are demonstrably consistent with the experimental results if the bulk $\Delta(\boldsymbol{k})$ exhibits time-reversal conserving, odd-parity, *a*-axis nodal, B_{3u} symmetry. Ultimately, these new techniques adumbrate a novel spectroscopic approach to identification of intrinsic topological superconductors and their superconductive topological surface states.

References

[1] Q. Gu, S. Wang, *et al.*, Science, **388**, 938-944 (2025).
[2] S. Wang, *et al.*, Nature Physics, **21**, 1555-1562 (2025).

Abstract ID: 30361

THERMODYNAMIC EVIDENCE FOR MULTIPHASE SUPERCONDUCTIVITY AND MAGNETIC QUANTUM CRITICALITY IN UTe_2

T. I. Weinberger[1], A. Cabala[2], V. Sechovsky[2], M. Valiska[2], A. G. Eaton[1], F. M. Grosche[1]

[1] Cavendish Laboratory, University of Cambridge, JJ Thomson Avenue, Cambridge, CB3 0HE, UK
[2] Charles University, Faculty of Mathematics and Physics, Department of Condensed Matter Physics, Ke Karlovu 5, Prague 2, 121 16, CZECH REPUBLIC

The triplet superconductor candidate uranium ditelluride (UTe_2) hosts a remarkably rich phase diagram, enabling the investigation of multiphase superconductivity using hydrostatic pressure as a precise, disorder-free probe. While ambient-pressure studies suggest single-component superconductivity, the phase landscape becomes complex under applied pressure. Above 0.3 GPa, the superconducting dome bifurcates into two distinct phases, implying a multicomponent order parameter. This splitting presents a thermodynamic puzzle: the convergence of three second-order phase transition lines at this point appears to challenge standard thermodynamic constraints, necessitating a rigorous examination of the high-pressure landscape. In this talk, we probe this complex phase diagram using semi-quantitative AC calorimetry inside a piston-cylinder cell. This technique allows us to map the low-field evolution of UTe_2 across the bifurcation point and probe the interplay between superconductivity and the pressure-induced antiferromagnetic order onsetting beyond 1.5 GPa. Our thermodynamic measurements reveal a drastic enhancement of quasiparticle effective masses at the border of magnetic order, providing strong evidence for quantum critical behaviour driving the electronic correlations. By integrating these thermodynamic results with transport data, we build a more complete picture of the microscopic physics underpinning the superconducting order parameter, offering essential clues towards a consistent description of the system's evolution under pressure.

Abstract ID: 30587

THE HIGH PRESSURE HIGH FIELD PHASE LANDSCAPE OF UTe_2

A. G. Eaton

Cavendish Laboratory, University of Cambridge, Cambridge, UK

Heavy fermion UTe_2 hosts a rich phase diagram at low temperatures under applied pressure and magnetic fields, with up to six distinct superconducting states having been reported – with several of which exhibiting clear signatures of odd-parity pairing. This talk will examine how the interplay between magnetism and superconductivity unfolds under pressure in this material. Pressure-tuning affects two magnetic instabilities: one is an AFM quantum critical point, while the other is a first-order metamagnetic transition to a field-polarised state. How these instabilities relate to the superconducting phases – and any causal connection to the pairing mechanism(s) – will be critically considered.

Abstract ID: 30680

MULTIPLE NODAL SUPERCONDUCTING PHASES AND ORDER PARAMETER EVOLUTION IN PRESSURIZED UTe_2

S. Zou[1], W. Huang[2], X. Lu[3], H. Yuan[3], Y. Luo[1]

[1] *Huazhong University of Science and Technology, Wuhan 430074, CHINA*
[2] *School of Physical Sciences, Great Bay University, Dongguan 523000, CHINA*
[3] *Zhejiang University, Hangzhou 310058, CHINA*

The recently discovered heavy-fermion superconductor UTe_2 has attracted significant attention as a candidate for spin-triplet superconductivity (SC). Despite extensive studies on its phase diagram, the exact nature of its SC order parameters and their evolution under pressure remains elusive. In this work, we report comprehensive point-contact spectroscopy (PCS) measurements on the (001) surface of UTe_2 under hydrostatic pressure. We observed robust Zero-Bias Conductance Peaks (ZBCP) attributable to surface Andreev bound states, which strongly suggests the presence of a p_z component in the SC gap function. Quantitative analysis utilizing an extended Blonder-Tinkham-Klapwijk model indicates that the pairing symmetry most likely belongs to the B_{2u} or B_{3u} irreducible representations. Furthermore, we find that the multiple pressure-induced SC phases (SC1, SC2, and SC3) can be distinguished by a single parameter: the relative weight between the p_z-wave and $p_{x(y)}$-wave pairing components, denoted as $\perp_z / \perp_{x(y)}$. As illustrated in Fig. 1, this ratio exhibits a distinct evolution across the phase boundaries, with the p_z-wave component becoming dominant in the high-pressure SC3 phase. Our findings provide crucial spectroscopic evidence for the existence of multiple nodal SC phases and impose stringent constraints on the superconducting order parameter in UTe_2 [1].

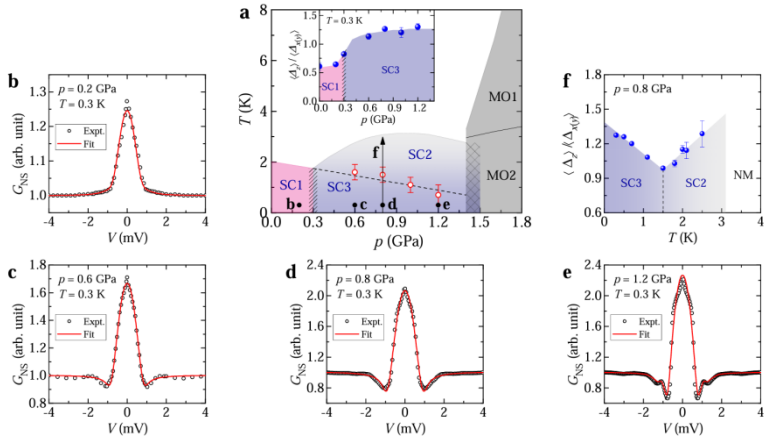

Fig. 1: *(a) Phase diagram of UTe_2 obtained in this work. Inset, the pressure dependent $\perp_z / \perp_{x(y)}$ increases rapidly near $p = 0.3$ GPa, hinting the difference between SC1 and SC3. (b-e) Fitting of PCS data to extended BTK model at selected pressures. (f) The temperature dependent $\Delta_z / \Delta_{x(y)}$ at fixed $p = 0.8$ GPa shows a minimum that is characteristic of the SC2-SC3 transition.*

References

[1] S. Zou, *et al.*, arXiv:2601.01843 (2026).

37 - NEW DEVELOPMENTS IN QUANTUM MAGNETISM

Abstract ID: 30008

SOLITON EXCITATIONS IN THE SPIN-1/2 METAL-ORGANIC FRAMEWORK MATERIAL $[(C_2H_5)_3NH]_2Cu_2(C_2O_4)_3$

S.A. Zvyagin[1], J. Wosnitza[1], C. Dissanayake[2,*], M. Tomlinson[2], AKM A. Rahman[2], K. Kumarasinghe[2], Y. Nakajima[2]

[1] *Dresden High Magnetic Field Laboratory (HLD-EMFL) and Würzburg-Dresden Cluster of Excellence ct.qmat, Helmholtz-Zentrum Dresden-Rossendorf (HZDR), 01328 Dresden, GERMANY*
[2] *Department of Physics, University of Central Florida, Orlando, FL 32816, USA*
** Present address: National High Magnetic Field Laboratory, Florida State University, Tallahassee, FL 32310, USA*

The design flexibility and structural versatility along with the ability to host exotic ground states make metal-organic frameworks (MOFs) one of the most attractive concepts in modern coordination chemistry and material science [1-4]. They can, for instance, manifest a quantum spin liquid, with quantum fluctuations destroying magnetic order down to very low temperatures. The Cu-oxalate material $[(C_2H_5)_3NH]_2Cu_2(C_2O_4)_3$ has been recently proposed as an ideal candidate for a quantum spin liquid on a three-dimensional (3D) hyperhoneycomb lattice [5]. Here, employing electron spin resonance spectroscopy we report on th observation of sine-Gordon soliton and breather excitations, a peculiar feature of a 1D spin liquid realized in a spin-1/2 Heisenberg chain with alternating Dzyaloshinskii-Moriya interaction. Our results motivate systematic studies of magnetic properties of Cu-oxalate and other MOF complexes, establishing them as a perfect playground to investigate novel quantum-mechanical phenomena in strongly correlated electron systems.

Acknowledgment

This work was supported by the Deutsche Forschungsgemeinschaft through the Würzburg-Dresden Cluster of Excellence on Complexity and Topology in Quantum Matter - *ct.qmat* (EXC 2147, project No. 390858490) and SFB 1143 as well as by HLD at HZDR, member of the European Magnetic Field Laboratory (EMFL). C.D., K.K., and Y.N. were supported by an NSF Career DMR-1944975.

References

[1] S. L. James, Chem. Soc. Rev. **32**, 276 (2003).

[2] C. Janiak, Dalt. Trans. **14**, 2781 (2003).

[3] H. Furukawa, K.E. Cordova, M. O'Keeffe and O. M. Yaghi, Science **341**, 6149 (2013).

[4] H. C. Zhou and S. Kitagawa, Chem. Soc. Rev. **43**, 4515 (2014).

[5] B. Zhang, P.J. Baker, Y. Zhang, D. Wang, Z. Wang, S. Su, D. Zhu, and F. L. Pratt, J. Am. Chem. Soc. **140**, 122 (2018).

Abstract ID: 30014

CLASSICAL FRACTON ISING SPIN LIQUID ON THE OCTOCHLORE LATTICE

M. Stern[1], M. D. Burke[2], M. J. P. Gingras[2], J. Romhanyi[1], K. T. K. Chung[3]

[1] *University of California Irvine, Department of Physics and Astronomy, 92697, Irvine, USA*
[2] *University of Waterloo, Department of Physics and Astronomy, N2L 3G1, Waterloo, CANADA*
[3] *Rice University, Department of Physics and Astronomy, TX 77005, Houston, USA*

We consider the lattice of corner-sharing octahedra, dubbed the octochlore lattice and explore the phase diagram of Ising spins including first- and second-neighbor interactions (J1 and J2a, respectively) within each octahedron. In addition to a spin ice classical spin liquid (CSL), we identify a novel fracton CSL with fractonic excitations restricted to move in one dimension and yielding a classical U(1) analog of the celebrated X-cube model of fracton topological order. We characterize this fracton liquid from multiple perspectives; via its flat bands with nodal line touchings, as a condensate of spinon bound states, as a foliated fracton phase of intersecting spin vorticity models, and as a bionic spin liquid of intersecting square ice sheets. This multi-pronged description allows us to achieve a comprehensive understanding of the system's excitations and enables a connection to many recent developments in the understanding of classical spin liquids. This work promotes the realization of fracton CSLs in real materials, provides a constructive method for building classical fracton CSL, and exposes the octochlore geometry as a promising new platform for exploring CSLs in 3D.

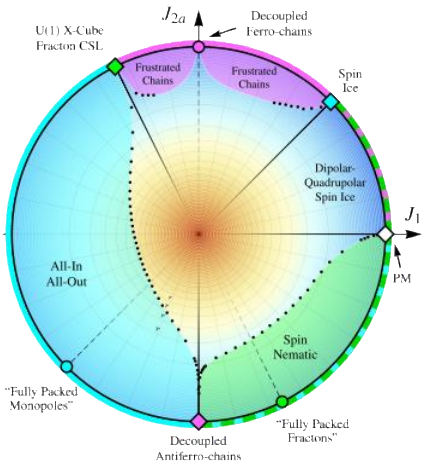

Fig. 1: *Finite-temperature phase diagram as the function of J_1, J_{2a}, and inverse temperature, with zero temperature at the outer edge and infinite temperature at the center. Black dots mark thermal phase transition critical temperatures estimated from Monte Carlo simulation. Near J_1=0 in the Frustrated Chains (magenta) region, numerical determination of the transition temperature is impractical, due to extreme finite size effects from the underlying quasi-1D chains, and the phase boundary is only qualitative.*

Abstract ID: 30042

DEMYSTIFYING QUANTUM ESCAPISM ON THE HONEYCOMB LATTICE

A. L. Chernyshev

Department of Physics and Astronomy, University of California, Irvine, 92697, USA

In recent study [1], we demonstrated the versatility, simplicity, and power of the minimally-augmented spin-wave theory (MAGSWT) in studying phase diagrams of the quantum spin models in which unexpected magnetically ordered phases occur or the existing ones expand beyond their classical stability regions. We use this method to obtain approximate phase diagrams of the two paradigmatic spin-1/2 models on the honeycomb lattice: the J_1-J_3 ferro-antiferromagnetic and J_1-J_2 antiferromagnetic XXZ models. For the J_1-J_3 case, various combinations of the XXZ anisotropies are analyzed; see Figure 1. In a dramatic deviation from their classical phase diagrams, which host significant regions of the noncollinear spiral phases, quantum fluctuations stabilize several unconventional collinear phases and significantly extend conventional ones to completely supersede spiral states. These results are in close agreement with the available density-matrix renormalization group calculations. The applicability of this approach to the other models and its potential extension to different types of orders are discussed.

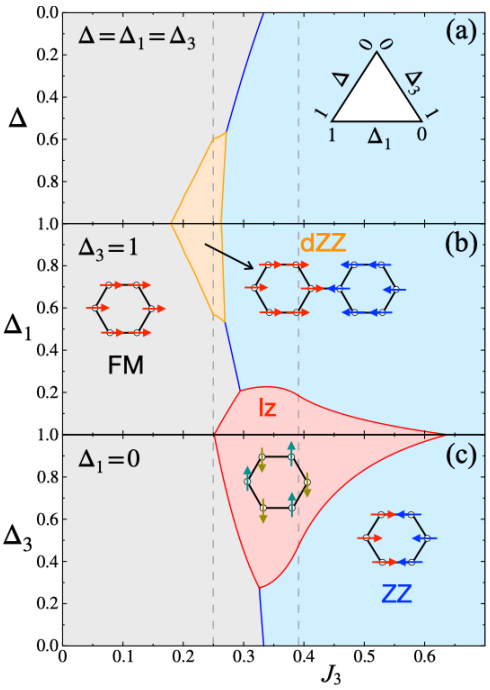

Fig. 1: *MAGSWT phase diagram for the (a) full XXZ, (b) partial XXZ, and (c) Δ_1=0 versions of the J_1-J_3 XXZ model for S= 1/2, with phases and their sketches identified. For details, see [1].*

References

[1] A. L. Chernyshev, *Quantum stabilization of unexpected ordered phases on the honeycomb lattice*, Phys. Rev. B **112**, 174413 (2025).

Abstract ID: 30082

HYBRID MAGNON MODES

A. Hoffmann

University of Illinois Urbana-Champaign, The Grainger College of Engineering, Materials Research Laboratory and Department of Materials Science and Engineering, Urbana, Illinois 61801, U.S.A.

Magnons readily interact with a wide variety of different excitations, including microwave and optical photons, phonons, and other magnons. The resulting hybrid magnon dynamic excitations have recently gained increased interest due to their potential impact on coherent information processing [1]. This in turn opens new pathways for hybrid quantum information systems [2–4]. I will discuss specific examples and strategies, where we developed fully integrated devices that form the essential building blocks for more complex integrated coherent quantum systems. Towards this end, we demonstrated strong magnon-photon coupling in scalable coplanar devices using coplanar superconducting microwave photon resonators [5]. Based on this concept we have shown how two magnon resonators can be coupled over macroscopic distances, and using local time-resolved detection, we demonstrate coherent, Rabi-like, energy exchange between them [6]. Conversely, photons in two separate coplanar waveguides can be transmitted in a directional manner via nonreciprocal coupling to magnons [7]. Lastly, I will show how a superconducting qubit can be used for sensitively detecting magnon populations over a broad dynamic range [8]. These measurements illustrate the potential of using magnons for coherently controlled interactions ultimately even in the single quantum limit.

This work was supported by the U.S. Department of Energy, Office of Science, Materials Sciences and Engineering Division under Contract No. DE-SC0022060.

References

[1] Y. Li, *et al.*, J. Appl. Phys. **128**, 130902 (2020).

[2] D. D. Awschalom, *et al.*, IEEE Quantum Engin. **2**, 5500836 (2021).

[3] Y. Li, *et al.*, 2022 IEEE Intern. Electr. Dev. Meeting, 14.6.1 (2022).

[4] Z. Jiang, *et al.*, Appl. Phys. Lett. **123**, 130501 (2023).

[5] Y. Li, *et al.*, Phys. Rev. Lett. **123**, 107701 (2019).

[6] M. Song, *et al.*, Nat. Commun. **16**, 3649 (2025).

[7] Y. Li, *et al.*, Appl. Phys. Lett. **123,** 022406 (2023).

[8] S. Rani, *et al.*, Phys. Rev. Appl. **23**, 064032 (2025).

Abstract ID: 30085

OBSERVING ALTERMAGNETISM USING POLARIZED NEUTRONS

P. A. McClarty[1], A. Gukasov[1], J. G. Rau[2]

[1] *Laboratoire Léon Brillouin, CEA, CNRS, Université Paris-Saclay, CEA-Saclay, 91191 Gif-sur-Yvette, FRANCE*
[2] *Department of Physics, University of Windsor, 401 Sunset Avenue, Windsor, Ontario N9B 3P4, CANADA*

Altermagnets, a new class of magnetic systems that combine characteristics of both conventional ferromagnets and antiferromagnets, have recently attracted significant attention. These collinear compensated magnets exhibit spin-split bands even in the absence of spin-orbit coupling, offering exciting prospects for applications in antiferromagnetic spintronics due to their lack of stray fields, low damping and fast switching times. In this talk, I will introduce the properties of their magnetic excitations in insulating case. Due an approximate U(1) symmetry the magnons in altermagnets are split into equal and opposite chiral pairs with the anisotropy of the chirality splitting mirroring the splitting of the electronic bands. I will argue that in altermagnets polarized neutrons provide a means to detect the population of time-reversed domains and also allow direct measurement of the magnon chirality anisotropy in momentum space - the central signature of the altermagnetic phase. We demonstrate this response to polarized neutrons theoretically in two candidate materials MnF2 and MnTe and show that the presence of these chiralities is stable to small perturbations that break spin-rotation symmetry. Finally, I will discuss challenges in observing these features experimentally and how to distinguish between altermagnetic and relativistic splittings.

References

[1] P. A. McClarty, A. Gukasov, J. G. Rau, Phys. Rev. B **111**, L060405 (2025).

Abstract ID: 30109

ANOMALOUS PHONON NONRECIPROCITY IN THE PARAMAGNETIC PHASE OF MULTIFERROIC $CoTe_6O_{13}$

S. Fan[1], X. Xu[2], Y. Q. Cai[1]

[1] *National Synchrotron Light Source II, Brookhaven National Laboratory, Upton, New York 11973, USA*
[2] *School of Physics and Astronomy, University of Minnesota, Twin Cities, Minneapolis, Minnesota 55455, USA*

We report the observation of non-reciprocal phonons in the paramagnetic and antiferromagnetic phases of $CoTe_6O_{13}$, a magnetoelectric multiferroic material with a large ferro-toroidic moment[1]. High resolution inelastic x-ray scattering reveals a clear energy splitting of the longitudinal acoustic (LA) branch along Γ→L compared with Γ→−L that persists up to 300 K, with a magnitude of about 0.5 to 1.0 meV [Fig. 1(d,e)]. The effect is strongly anisotropic, appearing only for the *c*-axis longitudinal mode, while the in-plane transverse modes show no detectable asymmetry. Room temperature Raman circular dichroism reveals chiral phonon modes with E_g character, suggesting intrinsic local dynamic lattice chirality. These observations are consistent with the ferro-rotational structural distortion and the associated broken mirror symmetries lifting the degeneracy between phonons propagating along ±L, so that ω(q) and ω(-q) become inequivalent in the paramagnetic state without requiring long range magnetic order. These findings highlight that phonon nonreciprocity can emerge from local structural angular momentum and lattice chirality without necessarily requiring global time reversal symmetry breaking.

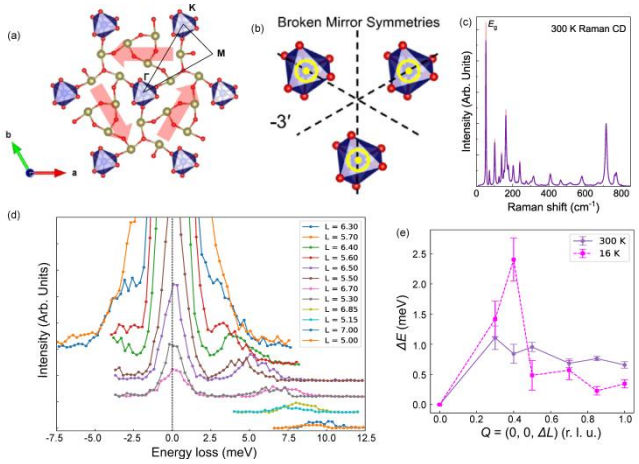

Fig. 1: *(a) Top view of a Co^{2+} triangular layer. The red arrows display the local electric dipoles that form a ferro-rotation structure order. Co,Te, and O atoms are represented by blue, yellow, and red spheres, respectively[1]. High symmetry points are listed. (b) Out-of-plane spins in a triangular lattice with ferro-rotational distortion[1]. (c) Raman circular dichroism spectra of $CoTe_6O_{13}$ at 300 K. The strong dichroism is observed for the E_g mode around ~50 cm^{-1}. (d) IXS spectra of $CoTe_6O_{13}$ at 300 K at different Q points along the (0,0,6 ± ⊿L) direction. The LA mode is measured. (b) Phonon energy difference between the positive and negative branches of the LA mode at 300 and 16 K.*

References

[1] X. Xu, *et al.*, Nat. Commun. **14**, 8034 (2023).

Abstract ID: 30122

SPIN–ORBIT COUPLING AND MAGNETIC EXCITATIONS IN THE XY-LIKE S = 1/2 CHAIN SYSTEM Li_2CoCl_4

M. Ozerov

National High Magnetic Field Laboratory, Florida State University, Tallahassee, 32310, Florida USA

Quantum magnets built from chains of magnetic transition-metal cations provide a powerful platform for exploring spin-1/2 dynamics and quantum-critical behavior. Li_2CoCl_4 contains edge-sharing $CoCl_6$ octahedra that form chains along the crystallographic *c* axis and orders antiferromagnetically at zero field, while exhibiting an intermediate phase between 1.6 T and the saturation field of 3.5 T at T=2K. Using far-infrared magneto-spectroscopy in magnetic fields up to 17.5 T, we reveal the strongly anisotropic nature of the Co^{2+} ion due to strong spin–orbit coupling, which leads to XY-like magnetic behavior ($g\parallel = 2.77$ and $g\perp = 5.23$ shown in Fig.1) and a $J = 1/2$ ground state. Our findings [1] show the strong impact of the Van Vleck contribution on the magnetic response in Li_2CoCl_4 and provide the anisotropic description needed to explore the spin dynamics of the field-driven magnetic phases.

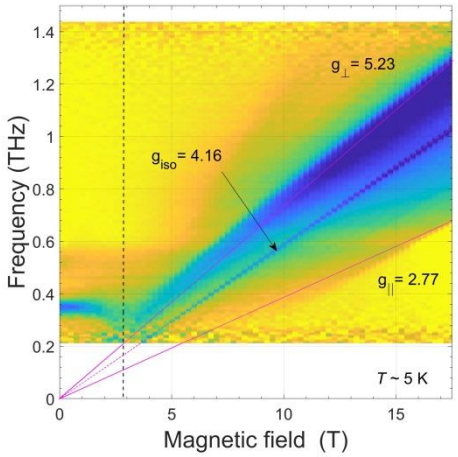

Fig. 1: *The magnetic resonance absorption heat map for Li_2CoCl_4 is shown with magenta lines representing the resonance conditions for different g factors for a noninteracting spin-1/2model. The black dashed line corresponds to the transition to the high-field magnetic phase from magnetic susceptibility data.*

References

[1] Z. Riedel, M. Ozerov, S. Calder, D. Shoemaker, Phys. Rev. B **112**, 104407 (2026).

Abstract ID: 30160

QUANTUM MAGNETISM WITH NEURAL NETWORK QUANTUM STATES

A. E. Feiguin

Northeastern University, Boston, USA

Variational representations of quantum states abound and have successfully been used to guess ground-state properties of quantum many-body systems. Some are based on partial physical insight (Jastrow, Gutzwiller projected, and fractional quantum Hall states, for instance), and others – such as tensor networks and neural network quantum states (NQS)-- operate as black boxes that may contain information about the underlying structure of entanglement and correlations but offering the advantage of a greater representation power. However, using variational approaches to study excited states and calculating the excitation spectrum, remains a challenge.

I will present two variational methods to calculate the dynamical properties and spectral functions of quantum many-body systems in the frequency domain: The first one consists of encoding the Green's function of the problem in the form of a neural network. We introduce a natural gradient descent approach to solve linear systems of equations --the correction vector-- and use Monte Carlo to obtain the dynamical correlation function. The second approach is based on a Chebyshev expansion of the spectral function and a neural network representation for the wave functions. In addition, I will describe how natural gradient descent can be used as a solver to study evolution in imaginary time to reproduce thermodynamic properties of quantum magnets.

References

[1] D. Hendry, H. Chen, P. Weinberg, A. E. Feiguin, *Chebyshev expansion of spectral functions using restricted Boltzmann machines*, Phys. Rev. B **104**, 205130 (2021).

[2] D. Hendry, A. E. Feiguin, *A machine learning approach to dynamical properties of quantum many-body systems*, Phys. Rev. B **100**, 245123 (2019).

[3] H. Chen, D. Hendry, P. Weinberg, A. E. Feiguin, *Systematic improvement of neural network quantum states using a Lanczos recursion*, NeurIPS 2022 (Accepted). arXiv: 2206.14307

[4] D. Hendry, H. Chen, A. Feiguin, N*eural network representation for minimally entangled typical thermal states*, Phys. Rev. B **106**, 165111 (2022).

Abstract ID: 30214

PHONON DYNAMICS AND MAGNON-PHONON COUPLING IN THE VAN DER WAALS MAGNET $FePS_3$

S. Kim[1], S. Fan[1], A. Alatas[2], A. Said[2], C. Nelson[1], Y. Q. Cai[1]

[1] *National Synchrotron Light Source II, Brookhaven National Laboratory, Upton, New York 11973, USA*
[2] *Advanced Photon Source, Argonne National Laboratory, Lemont, Illinois 60439, USA*

$FePS_3$ has garnered significant interest as a two-dimensional magnetic material with the potential for applications in spintronics. Even at a single layer, the material exhibits signs of antiferromagnetic order, evident through changes in Raman spectra across the magnetic transition. Particularly, newly appeared peaks display characteristics of both phonon and magnon. This was attributed to phonon magnon hybridized excitations and highlights the presence of strong spin-lattice coupling in $FePS_3$. Currently, there is limited information available on the influence of spins on phonons away from the Gamma point, and this can be explored through inelastic X-ray scattering. In this work, we mapped out the phonon dispersion across the magnetic transition and find a significant suppression in energy of the longitudinal acoustic phonon mode along the M-direction. The affected mode corresponds to the Raman active hybrid phonon–magnon excitation, which appears at Γ via zone folding only in the magnetically ordered phase. Our momentum-resolved measurements show that this Raman feature originates from a genuine softening of the underlying phonon branch connected to the magnetic ordering vector. This demonstrates that long-range antiferromagnetic order in $FePS_3$ reshapes the phonon dispersion well beyond the zone center, providing evidence of strong, momentum-dependent spin–lattice coupling in a van der Waals magnet.

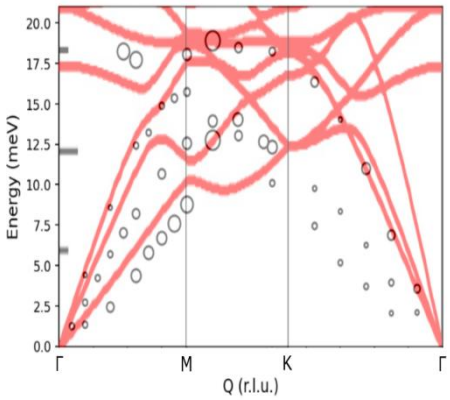

Fig. 1: *Phonon dispersion of $FePS_3$. The circle represents the observed phonon mode measured at T=300K and the size of the circle corresponds to uncertainty. The red curve is the calculated phonon dispersion using DFT. The observed phonon modes at M point are consistent with the Raman measurement.*

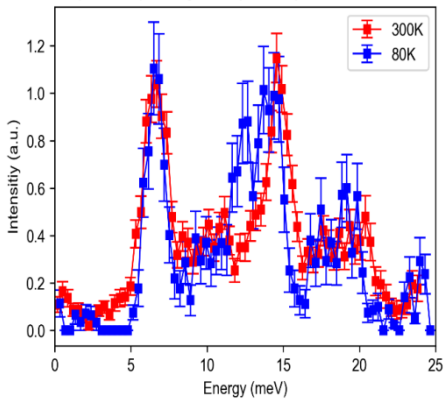

Fig. 2: *Phonon mode at Q=(2,-6.6,-1) compared between above and below the magnetic transition temperature. Significant change is observed longitudinal acoustic phonon mode around E=14meV.*

Abstract ID: 30380

QUANTUM SENSING OF MAGNETIC PHASE TRANSITION VIA ON-CHIP SUPERCONDUCTING RESONATOR

P. Li

University of Science and Technology of China, Hefei, 230026 CHINA

Magnetic phase transitions are central to spintronics and quantum technologies, yet their detection in emerging quantum materials remains challenging[1-4]. Conventional probes are constrained to bulk samples and static measurements, making them unsuitable for 2D flakes with complex spin textures such as chiral or skyrmion states. Here, we report on-chip superconducting resonators with high quality factors (Q) and tunable modes that sensitively probe magnetic dynamics across wide temperature and field ranges. By extracting the cooperativity (C), we establish a highly sensitive and quantitative metric of magnetic order, surpassing conventional approaches and enabling measurements on ultra-thin 2D flakes. Crucially, our platform supports wafer-level, multi-point inspection of magnetic films, using CMOS-compatible resonator arrays. These results position superconducting resonators as a scalable platform for mapping magnetic phase transitions, bridging fundamental physics with technological applications.

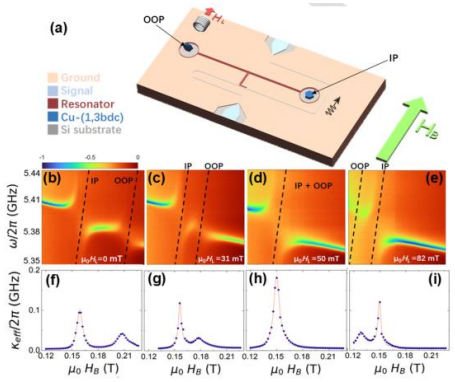

Fig. 1: *Magnetic field tuning of magnon–photon coupling. (a) Schematic of system. (b)–(e) S21 transmission spectra at various magnetic fields. (f)–(i) The relationship between effective loss and magnetic field.*

References

[1] C. Tang, P. Li, *et al.*, Phys. Rep. **1032**, 1 (2023).
[2] L. Alahmed, P. Li, *et al.*, Nano Lett. **22**, 5114 (2022).
[3] C. Li, P. Li, *et al.*, Appl. Phys. Lett. **126**, 092407 (2025).
[4] X. Zhang, P. Li, *et al.*, Adv. Mater. **36**, 2311591 (2024).

Abstract ID: 30105

Fe-BASED VAN DER WAALS TELLURIDES: INTERPLAY BETWEEN ELECTRONIC AND MAGNETIC STATES IN LOW DIMENSIONS

V. Yu. Verchenko[1], A. V. Stepanova[1], A. N. Azarevich[2], A. V. Bogach[2], S. V. Zhurenko[3], A. V. Tkachev[3], A. A. Gippius[4], I. S. Soboleva[1], A. V. Sobolev[1], I. A. Presniakov[1], A. V. Shevelkov[1]

[1] Department of Chemistry, Lomonosov Moscow State University, 119991, Moscow, RUSSIA
[2] Prokhorov General Physics Institute of the Russian Academy of Sciences, 119991, Moscow, RUSSIA
[3] P.N. Lebedev Physics Institute, 119991, Moscow, RUSSIA
[4] Department of Physics, Lomonosov Moscow State University, 119991, Moscow, RUSSIA

Our group is focused on exploratory synthesis of novel complex chalcogenides of transition metals. Chalcogen atoms have the special structural role. They envelop structural fragments and separate them by van der Waals gaps. As a result, the universe of van der Waals materials with naturally low-dimensional crystal structures is formed. Here, the layered compounds are of great importance, because they provide a source of state-of-the-art two-dimensional single crystals with unique electronic and magnetic properties, which cannot be found in the bulk. In this talk, the $NbFe_{1+x}Te_3$ [1], $NbFeTe_2$ [2,3], and $TaFeTe_2$ materials, which combine magnetic Fe and heavy Nb and Ta transition metals sandwiched between Te layers, will be presented. We employ ^{57}Fe Mössbauer and ^{93}Nb nuclear magnetic resonance spectroscopy to study the hyperfine electric and magnetic fields. Furthermore, we carefully investigate their evolution with temperature and magnetic field in line with angle-resolved magnetoresistance and Hall resistance. Combination of these techniques provides unique understanding of nontrivial interplay between electronic and magnetic properties of these low-dimensional Fe-based tellurides.

We thank the Russian Science Foundation for the financial support under grant No. 24-73-10007.

References

[1] V.Yu. Verchenko, A.V. Stepanova, A.V. Bogach, M.A. Kirsanova, A.V. Shevelkov, Dalton Trans. **52**, 5534 (2023).

[2] A.V. Stepanova, A.V. Mironov, A.V. Bogach, A.N. Azarevich, I.A. Presniakov, A.V. Sobolev, D.A. Pankratov, V.A. Zayakhanov, S.S. Starchikov, V.Yu. Verchenko, A.V. Shevelkov, Chem. Commun. **60**, 5518 (2024).

[3] H. Wu, S. Li, Y. Lyu, Y. Guo, W. Liu, J.S. Oh, Y. Zhang, S.-K. Mo, C. Cruz, R.J. Birgeneau, K.M. Taddei, M. Yi, L. Yang, B. Lv, Phys. Rev. B **109**, 174427 (2024).

Abstract ID: 30111

THE VAN DER WAALS CHALCOGENIDES WITH $MgAl_2Se_4$- AND $Mg_2Al_2Se_5$-TYPE STRUCTURE: SYNTHESIS, EXFOLIATION, AND MAGNETIC PROPERTIES

I.V. Chernoukhov[1], A.V. Bogach[2], K.A. Cherednichenko[3], A.V. Shevelkov[1], V.Yu. Verchenko[1]

[1] *Department of Chemistry, Lomonosov Moscow State University, 119991, Moscow, RUSSIA*
[2] *Prokhorov General Phys. Inst. of the Russian Academy of Sciences, 119991, Moscow, RUSSIA*
[3] *Department of Phys. and Colloid Chemistry, Gubkin University, 119991, Moscow, RUSSIA*

Van der Waals materials demonstrate physical properties suitable for various applications, including narrow-band semiconductors, low-dimensional magnetic materials, intercalates for battery technology, and materials for tunnel magnetoresistance. Furthermore, they attract interest as candidate 2D materials with unique magnetic properties. Here, we present the group of layered compounds, including $MnAl_2S_4$, $MnAl_2Se_4$, $Mn_2Al_2S_5$, $Mn_2Al_2Se_5$, $Mn_2Ga_2S_5$, and $Mn_2In_2Se_5$ with the $MgAl_2Se_4$- ("124") and $Mg_2Al_2Se_5$-type ("225") structure, respectively. The magnetic sublattice, which consists of single or double hexagonal layers, is based on the triangular arrangement of Mn atoms, favorable for strong magnetic frustration, spin-glass behavior or specific magnetic orders.

We report synthesis, crystal growth, and crystal structure of several new compounds – $MnAl_2Se_4$, $Mn_2Al_2Se_5$, $Mn_2Al_2S_5$, including new high-temperature polymorph of $Mn_2In_2Se_5$ [1-3]. Refinement of the crystal structures confirms the isomorphism of these compounds (typical cell parameters for "124": *R*-3*m*, a ≈ 3.8 Å, c ≈ 38 Å, and for "225": *P*-3*m1*, a ≈ 3.8 Å, c ≈ 16 Å). We confirm chemical stability in air for some representatives. Exfoliation in non-polar solvents using ultrasonic radiation yields nanomaterials with two types of morphologies: nanosheets and nanoscrolls with typical lateral size of 2 μm and thickness down to few structural layers according to high-resolution transmission electron microscopy and atomic force microscopy. Antiferromagnetic-like transitions were observed at low temperatures (6 K for $Mn_2In_2Se_5$, 13 K for $Mn_2Ga_2S_5$) with noticeable hysteresis below the Neel temperature, which may indicate unconventional antiferromagnetism. Large values of $|\theta|/T_N$ indicate strong exchange interactions and significant frustration.

This research was supported by the Russian Science Foundation, grant no. 24-73-10007.

References

[1] V. Yu. Verchenko, *et al.*, Inorg. Chem., **62.19**, p. 7557-7565 (2023).

[2] I.V. Chernoukhov, *et al.*, Molecules, **29.9**, p. 2026 (2024).

[3] I.V. Chernoukhov, *et al.*, Molecules, **30.9**, p. 1904 (2025).

Abstract ID: 30147

ENHANCED DYNAMICS IN DISORDERED NON-KRAMERS SPIN ICE $Ho_2(Ti_{1-x}\text{-}Hf_x)_2O_7$: TOWARD THE COULOMB QUANTUM SPIN LIQUID STATE

N. Bujault[1], V. Porée[2,4], F. Morineau[1], E. Riordan[1], P. Falus[3], T. Fennell[4], V. Pomjakushin[4], R. Sibille[4], E. Lhotel[1]

[1] *Institut Néel & Université Grenoble-Alpes, Grenoble, FRANCE*
[2] *Synchrotron SOLEIL, Saint-Aubin, FRANCE*
[3] *Institut Laue Langevin, Grenoble, FRANCE*
[4] *Paul Scherrer Institut, Villigen, SWITZERLAND*

$Dy_2Ti_2O_7$ [1] and $Ho_2Ti_2O_7$ [2] classical spin ice compounds are frustrated magnets that do not stabilize an ordered ground state down to the lowest reachable temperature, but instead, enter a correlated but disordered phase called spin-ice. The excitations out of the spin ice state, described as emergent magnetic monopoles, exhibit extremely slow dynamics at low temperature, which manifests by a strong freezing and irreversibility in magnetization [3]. In spin ices such as $Ho_2Ti_2O_7$, where the magnetic element is a non-Kramers ion (integer *J*), the crystal electric field (CEF) ground state is a non-protected doublet. It has been proposed that in that case, quantum fluctuations induced by non-magnetic disorder can push the system toward a Quantum Spin Liquid phase (QSL). This phase is characterized, *inter alia*, by a much faster dynamics [4].

To investigate this potential new QSL phase we performed a comprehensive study on $Ho_2Ti_2O_7$, where non-magnetic disorder is introduced through a controlled substitution of Ti^{4+} ions by Hf^{4+} ions, with substitution rate from 0 to 40%. Conservation of crystal structure and spin ice correlations are confirmed via X-ray and neutron diffraction through the emergence of Frenkel pair defects that locally breaks CEF symmetry around Ho^{3+} ions which is responsible for the stabilization of the magnetic ground state. Low temperature magnetization and specific heat measurements point to a speeding-up of the dynamics. This is confirmed by AC susceptibility and Neutron Spin Echo (NSE) measurements performed down to 50 mK (Figure 1) which reveal that dynamics are accelerated by several orders of magnitude in the spin ice regime and up to 30 K, where quantum tunneling effects are relevant. This strongly suggests that disorder indeed enables quantum fluctuations in the system and opens the way to the stabilization of a Coulomb QSL phase at lower temperature.

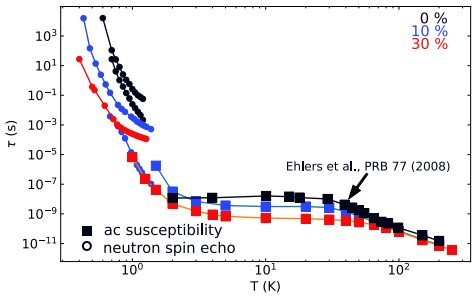

Fig. 1: *Relaxation times obtained from AC susceptibility and NSE (WASP-ILL) measurements for several compositions (% of hafnium introduced).*

References

[1] A. P. Ramirez, *et al.*, Nature **399**, 333-335 (1999).

[2] M. J. Harris, *et al.*, Phys. Rev. Lett. **79**, 2554-2557 (1997).

[3] J. Snyder, *et al.*, Phys. Rev. B **69**, 064414 (2004).

[4] L. Savary, *et al.*, Phys. Rev. Lett. **118**, 087203 (2017).

Abstract ID: 30520

ANISOTROPIC TRANSVERSE QUANTUM MAGNETORESISTANCE IN Fe DOPED $TlInTe_2$ ONE-DIMENSIONAL CHAIN-LIKE SEMICONDUCTOR

S. Gökçe[1], A. K. Fedotov[2], F. Mikailzade[3], J. Fedotova[2]

[1] *Department of Digital Transformation Electronics, Advanced Vocational School, Dogus University, Istanbul, 34775, TÜRKIYE*

[2] *Research Scientific Institute for Nuclear Problems of Belarusian State University, 11, Bobruiskaya Str., 220030 Minsk, BELARUS*

[3] *Department of Physics, Gebze Technical University, Gebze, Kocaeli, 41400, TÜRKIYE*

The results of the study of magnetoresistance in Fe doped narrow-gap semiconductor $TlInTe_2$ having a chain-like structure under the action of external magnetic field up to ~140 kOe are presented. The measurements were performed in heating and cooling regimes in the temperature range of ~ 230 - 270 K in parallel and perpendicular orientations of the magnetic field relative to crystallographic c-axis, coinciding with the directions of chains within the structure of $TlInTe_2$ quasi-one-dimensional host [1].

The experimental results unambiguously revealed the occurrence of anisotropic transverse magnetoresistance in Fe doped $TlInTe_2$ non-magnetic semiconductor arising from the $3d$ iron cations. The magnetoresistance of the sample has been found to be both positive and negative depending on the applied magnetic field direction; it exhibited a negative sign when the external magnetic field was applied along the direction parallel to chains, while it showed a positive sign behavior in perpendicular direction of the applied magnetic field. The experimentally observed oscillations in the positive magnetoresistance curves of Fe doped $TlInTe_2$ chain semiconductors are discussed on the base of Shubnikov-de Haas (SdH) effect [2]. The analysis of the negative magnetoresistance data provides an evidence of quantum localization effects for carriers wave functions in the studied compound.

References

[1] S. Gökçe, T. G. Mammadov, A. I. Najafov, S. Berber, F. Mikailzade, M-H. Yu. Seyidov, *Magnetic resonance and magnetization in Fe doped $TlInTe_2$*, Physica B Condensed Matter **724**, 41814 (2026).

[2] B. M. Askerov, Electron Transport Phenomena in Semiconductors (World Scientific Publishing Co. Pte. Ltd., 1994).

Abstract ID: 30048

MAGNETISM ON THE SHASTRY-SUTHERLAND LATTICE

F. Mila

Institute of Physics, Ecole Polytechnique Fédérale de Lausanne, 1015 Lausanne, SWITZERLAND

The Shastry-Sutherland lattice is an Archimedean lattice that can also be seen as a two-dimensional arrangement of orthogonal dimers. Following the seminal work of Shastry and Sutherland [1], who showed that for not too large inter-dimer coupling the ground state is a product of dimer singlets, a considerable amount of work has been devoted to an almost perfect realization of the Heisenberg model on that lattice, $SrCu_2(BO_3)_2$ [2]. More recently, a new family of insulating Shastry-Sutherland rare-earth compounds with the generic formula $RE_2Be_2GeO_7$ has been synthetized, and the magnetic properties of $Er_2Be_2GeO_7$ have already been fully characterized [3]. The common point of these compounds is to exhibit a puzzling series of fractional magnetization plateaus. In this talk, I will discuss the theoretical solutions to these puzzles. In $SrCu_2(BO_3)_2$, the first plateaus are Wigner crystals of spin-2 bound states [4], and *not* of dimer triplets, as had been naively anticipated early on. For $Er_2Be_2GeO_7$, which is a good realization of the Ising model, the puzzle is the absence of a 1/3 plateau, which is replaced by a 1/4 and a 1/2 plateau, and I will show that this is consistent with a small orthorhombic distortion of the lattice [3].

References

[1] B. Sriram Shastry and Bill Sutherland, Physica B, 108, 1069 (1981).

[2] For an early review, see S. Miyahara and K. Ueda, J. Phys.: Condens. Matter **15**, R327 (2003).

[3] L. Yadav, A. Rufino, R. Bag, M. Ennis, J. A. Koziol, C. dela Cruz, A. I. Kolesnikov, V. O. Garlea, K. M. Taddei, D. Graf, K. P. Schmidt, F. Mila and S. Haravifard, Phys Rev X, in press.

[4] P. Corboz and F. Mila, Phys. Rev. Lett. **112**, 147203 (2014).

Abstract ID: 30121

QUANTUM SPIN ICE PHYSICS AND THE DIPOLE-OCTUPOLE Ce-BASED PYROCHLORES

B. D. Gaulin[1,2,3]

[1] *Department of Physics and Astronomy, McMaster University, Hamilton, ON, CANADA*
[2] *Brockhouse Institute for Materials Research, McMaster University, Hamilton, ON, CANADA*
[3] *Canadian Institute for Advanced Research, 661 University Ave, Toronto, ON, CANADA*

Quantum Spin Ice is a U(1) spin liquid which is known to possess an emergent Quantum Electrodynamics and elementary excitations which correspond to gapped electric and magnetic monopoles as well as gapless emergent photons. The search for real materials that are candidates for such a quantum disordered ground state has recently focussed on Ce-based pyrochlore insulators, such as $Ce_2Zr_2O_7$, $Ce_2Sn_2O_2$ and $Ce_2Hf_2O_7$. The Ce^{3+} ion in this environment possesses a pseudo spin 1/2 degree of freedom which originates from its CEF Kramer's doublet. The wave function for this doublet corresponds to J_z=+/-3/2, which then gives pseudo spin S^z a dipole magnetic moment, but pseudo spin 1/2 S^x and S^y carry octupolar moments. Hence these materials are referred to as dipole-octuple pyrochlores. Theoretical work based on a symmetry-allowed XYZ Hamiltonian predicts ground states that are both ordered and quantum disordered spin ices, each of which can be dominated by either the pseudo spin's dipolar or octupolar components. We and others have been actively characterizing the three Ce-based pyrochlores discussed above, by a variety of techniques including neutron scattering and low temperature thermodynamics. I will review these efforts, as well as the current status of the nature of their ground states [1].

References

[1] E. M. Smith, E. Lhotel, S. Petit and B. D. Gaulin, Annual Review of Condensed Matter Physics **16**, 387 (2025).

38 - NEW DEVELOPMENTS IN SUPERCONDUCTIVITY OF ATOMICALLY THIN SUPERCONDUCTORS

Abstract ID: 30115

DETECTING INDIVIDUAL PEARL VORTICES WITH A TWISTED-GRAPHENE JOSEPHSON JUNCTION

M. Perego[1], C. G. Agero[1], P. Koopmann[1], A. Mestre-Torà[1], A. O. Denisov[1], T. Taniguchi[2], K. Watanabe[3], F. Gaggioli[4,5], V. Geshkenbein[4], G. Blatter[4,6], T. Ihn[1,6], K. Ensslin[1,6]

[1] *Laboratory for Solid State Physics, ETH Zurich, Zurich, SWITZERLAND*
[2] *Research Center for Materials Nanoarchitectonics, National Institute for Materials Science, Tsukuba, JAPAN*
[3] *Research Center for Electronic and Optical Materials, National Institute for Materials Science, Tsukuba, JAPAN*
[4] *Institute for Theoretical Physics, ETH Zurich, Zurich, SWITZERLAND*
[5] *Department of Physics, Massachusetts Institute of Technology, Cambridge, Cambridge, MA, USA*
[6] *Quantum Center, ETH Zurich, Zurich, SWITZERLAND*

Magic-angle twisted multilayer graphene offers an exceptionally tunable platform for exploring two-dimensional superconductivity and its vortex physics. Here, we implement a gate-tuned Josephson junction in a magic-angle twisted four-layer graphene film. We measure the magnetic field-dependence of the junction's critical current and observe a Fraunhofer-like pattern consistent with the film's weak transverse screening properties. The pattern exhibits both an unconventional magnetic field periodicity and a slow decay, which markedly differ from the behavior expected in a standard Josephson junction. In addition, we observe sudden shifts in the measured pattern, which we attribute to Pearl vortices entering and exiting the superconducting leads [1].

By tuning the carrier density of the leads to the edge of the superconducting dome, we uncover rapid switching between superconducting and normal states within a finite current-bias window. We interpret this switching as arising from single-vortex dynamics. At elevated temperatures ($T > 100$ mK), vortices hop over energy barriers via classical thermal activation, whereas at lower temperatures our measurements suggest a crossover to macroscopic quantum tunnelling [2]. Using the junction as a single-vortex sensor, we extract key superconducting parameters—including the superfluid stiffness, Pearl length, and vortex-entry/exit barrier heights of a few kelvin and thickness of order 100 nm.

Our results establish twisted graphene Josephson junctions as powerful probes of vortex dynamics and provide quantitative insight into the fundamental properties governing two-dimensional superconductivity in moiré materials.

References

[1] M. Perego, C. Galante Agero, A. Mestre Torà, *et al.*, *Experimental detection of vortices in magic-angle graphene*, Nat Commun **16**, 10259 (2025).
[2] M. Perego, *et al.*, in preparation.

Abstract ID: 30123

SUPERFLUID STIFFNESS OF TWISTED BILAYER GRAPHENE

M. Tanaka[1,2], J. I-J. Wang[1], T. Dinh[1], D. Rodan-Legrain[1], S. Zaman[1], M. Hays[1], K. Watanabe[3], T. Taniguchi[3], P. Jarillo-Herrero[1], W. D. Oliver[1]

[1] *Research Laboratory of Electronics, Massachusetts Institute of Technology, USA*
[2] *Institute for Solid State Physics, the University of Tokyo, JAPAN*
[3] *Research Center for Functional Materials, National Institute for Materials Science, JAPAN*

One of the most important physical quantities characterizing superconductors is the superfluid stiffness, the proportionality coefficient between the phase gradient and current. While well-established measurement techniques exist for bulk superconductors, such as tunnel diode resonators and three-dimensional microwave cavities, the measurement of atomic-layer superconductors has been challenging. We measured the superfluid stiffness of magic-angle twisted bilayer graphene by coupling an atomic-layer superconductor to a two-dimensional microwave resonator [1]. The superconducting phase of magic-angle twisted bilayer graphene has attracted great interest, with experimental reports suggesting unconventional superconductivity—superconductivity proximate to magnetic phases, large TC/TF, and V-shaped density of states [2–5]. Moreover, it has been pointed out that the observed transition temperature and critical current significantly exceed those expected from superfluid stiffness determined solely by band dispersion [6]. As a possible explanation, theory has proposed the existence of a superfluid stiffness contribution arising from the quantum metric [7], in addition to the conventional band-dispersion contribution, and that this quantum geometric term can be dominant in twisted graphene [8–10]. By directly measuring the superfluid stiffness, we found it to be approximately an order of magnitude larger than the conventional expectation. Furthermore, by examining its temperature dependence and bias current dependence, we obtained evidence suggesting that the superconducting gap is anisotropic.

References

[1] M. Tanaka, *et al.,* Nature **638**, 99 (2025).

[2] Y. Cao, *et al.,* Nature **556**, 43 (2018).

[3] L. Balents, *et al.,* Nat. Phys. **16**, 725 (2020).

[4] E. Andrei, *et al.,* Nat. Mat. **19**, 1265 (2020).

[5] M. Oh, *et al.,* Nature **600**, 240 (2021).

[6] H. Tian, *et al.,* Nature **614**, 440 (2023).

[7] S. Peotta, *et al.,* Nat. Comm. **6**, 8944 (2015).

[8] X. Hu, *et al.,* PRL **123**, 237002 (2019).

[9] A. Julku, *et al.* ,PEB **101**, 060505 (2020).

[10] F. Xie, *et al.,* PRL **124**, 167002 (2020)

Abstract ID: 30128

ELECTRICALLY TUNABLE SUPERCONDUCTING DIODE VIA MOIRÉ PHONONS IN TWISTED $NbSe_2$

J. Zhao[1,2], Z. Chen[1,2], F. Gaggioli[3], S. Grebenchuk[1,4], Z. Qiu[1], Y. Han[5], J. Hu[6], K. Watanabe[7], T. Taniguchi[8], A. H. C. Neto[1,4,9], J. Lu[1,5], M. Wu[10], V. B. Geshkenbein[3], K. S. Novoselov[1,4]

[1] *Institute for Functional Intelligent Materials, National University of Singapore, 117544, SINGAPORE*
[2] *Guangdong Provincial Key Laboratory of Nano-Micro Materials Research, School of Advanced Materials, Peking University Shenzhen Graduate School, Peking University, Shenzhen, 518055, CHINA*
[3] *Institut fur Theoretische Physik, ETH Zurich, CH-8093 Zurich, SWITZERLAND*
[4] *Department of Materials Science and Engineering, National University of Singapore, 117575, SINGAPORE*
[5] *Department of Chemistry, National University of Singapore, Singapore 117543, SINGAPORE*
[6] *Department of Physics, National University of Singapore, 117542 SINGAPORE*
[7] *Research Center for Electronic and Optical Materials, National Institute for Materials Science, 1-1 Namiki, Tsukuba 305-0044, JAPAN*
[8] *Research Center for Materials Nanoarchitectonics, National Institute for Materials Science, 1-1 Namiki, Tsukuba 305-0044, JAPAN*
[9] *Centre for Advanced 2D Materials, National University of Singapore, 117546, SINGAPORE*
[10] *School of Physics, Huazhong University of Science and Technology, Wuhan, Hubei, 430074, CHINA*

Moiré patterns arising from slight rotational misalignment or lattice mismatch between atomically thin layers provide a powerful platform for engineering local crystallographic symmetries through atomic reconstruction. This approach has revealed a range of correlated and topological states in twisted graphene and semiconductors. In contrast, twisted superconductors have received little attention, largely because their high carrier densities make electronic control far more challenging. Here, we demonstrate that a moiré lattice in twisted trilayer $NbSe_2$ imposes a periodic modulation of the superconducting order parameter. This modulation drives a robust superconducting diode effect, with rectification persisting even in the fluctuation regime near the critical temperature. The reconstructed moiré lattice further generates local electric polarizations that couple to moiré phonon modes. Owing to the atomic thinness of the material, this coupling enables a remarkable gate control of superconductivity through modulation of electron–phonon interactions—distinct from conventional electrostatic doping—realizing a superconducting transistor effect. Our findings establish twisted superconductors as a promising platform for creating novel quantum states and tuning many-body interactions, opening new avenues for the design of functional superconducting circuits.

Abstract ID: 30188

ABRIKOSOV VORTICES SWITCHING JOSEPHSON CURRENT IN MAGIC ANGLE GRAPHENE

G. Blatter[1], M. Perego[2], … , V. B. Geshkenbein[1]

[1] *Institut for Theoretical Physics, ETH Zurich, CH-8093 Zurich, SWITZERLAND*
[2] *Laboratory for Solid State Physics, ETH Zurich, Zurich, SWITZERLAND*

Planar Josephson junctions made from atomically thin films exhibit poor transverse screening, causing the magnetic-field dependence of the Josephson current Ic(B) to deviate from the standard Fraunhofer pattern of conventional junctions. Given the weak screening, the junction is highly sensitive to Pearl vortices in the leads. Vortices alter the phase pattern and affect the Josephson current. Thermal fluctuations can cause vortices to jump in and out of the leads, leading to shifts in the Fraunhofer-like pattern, as observed in recent experiment [1]. Our model quantitatively explains these jumps, whose timescale depends on magnetic field, current, temperature, and superfluid stiffness. At elevated temperatures, fast vortex jumps may wash out the Fraunhofer pattern well below Tc. By analyzing the timescale of these jumps, we can determine the superfluid stiffness and the Berezinskii-Kosterlitz-Thouless transition temperature of magic-angle twisted four-layer graphene. These values are in agreement with recent kinetic inductance measurements [2,3|.

References

[1] M. Perego, *et al.,* Nature Communications **16**, 10259 (2025).

[2] A. Banerjee, *et al.*, Nature **638**, 93–98 (2025).

[3] M. Tanaka, *et al.*, Nature **638,** 99–105 (2025).

Abstract ID: 30255

INTERPLAY OF FERROELECTRICITY AND INTERLAYER SUPERCONDUCTIVITY IN VAN DER WAALS BILAYERS

A. S. Mel'nikov[1,2], A. A. Kopasov[2,3], D. Annenkov[1,4]

[1] *Moscow Institute of Physics and Technology, Dolgoprudnyi, Moscow Region 141701, RUSSIA*
[2] *Institute for Physics of Microstructures, Russian Academy of Sciences, 603950 Nizhny Novgorod, GSP-105, RUSSIA*
[3] *National University of Science and Technology "MISIS", Moscow 119049, RUSSIA*
[4] *L. D. Landau Institute for Theoretical Physics, Chernogolovka 142432, RUSSIA*

We study the distinctive features of the interplay between the interlayer superconductivity and ferroelectricity in van der Waals heterostructures. Corresponding analysis is carried out within the framework of the quasiclassical Eilenberger equations for a tunnel coupled bilayer with inhomogeneous relative shift of the conduction bands between the layers, which describes the net charge transfer in sliding ferroelectrics. It is shown that the critical temperature of the interlayer superconductivity can be significantly enhanced for superconducting nuclei localized in the vicinity of ferroelectric domain walls. We demonstrate that the increase in the tunneling amplitude leads to the decrease (increase) in the difference between the critical temperatures for localized and homogeneous superconducting states for the spin-singlet (spin-triplet) interlayer superconductivity. We also perform an extensive analysis of the effects of the in-plane magnetic field on the interlayer superconductivity. It is shown that the orbital effect can result in the suppression of the spin-singlet interlayer superconductivity and to the enhancement of the spin-triplet one. We find that possible manifestations of the paramagnetic effect include the suppression of the interlayer superconductivity by rather weak Zeeman fields, the two-fold anisotropy of the critical magnetic field for the spin-triplet states as well as the appearance of the reentrant superconducting phases. It is shown that the joint influence of the orbital and paramagnetic mechanisms on the spin-triplet interlayer superconductivity can even lead to a nonmonotonic behavior of the superconducting critical temperature as a function of the external magnetic field. The obtained results are discussed in the context of recent experimental data on van der Waals structures with coexisting superconductivity and sliding ferroelectricity.

This work was supported by the Russian Science Foundation (Grant No. 25-12-00042).

39 - NONRECIPROCAL TRANSPORT PHENOMENA AND THE DIODE EFFECT IN SUPERCONDUCTORS

Abstract ID: 30058

SUPERCONDUCTING PHASE DIAGRAM AND DIODE EFFECT IN A MISFIT LAYERED SUPERCONDUCTORS

Y. Itahashi, Y. Iwasa

RIKEN Center for Emergent Matter Science (CEMS), 351-0198, Wako, JAPAN

Two-dimensional (2D) superconductor is a good playground for investigating quantum transport. Recently, bulk 2D superconductors, where superconducting layers are well separated by non-superconducting block layers, has been intensively studied [1,2]. Among them, misfit layered compounds, which consist of alternately stacked layers with incompatible unit cells [3] (Figs. 1a and b), are unique materials, offering a new opportunity for exploring unconventional superconducting phases and symmetry-related physics.

In this work, we report a layer-selective FFLO (Fulde-Ferrell-Larkin-Ovchinnikov) phase, where superconducting order parameters acquire spatial modulation [4] (Fig. 1c), and zero-field superconducting diode effect (Fig. 1d) [5], in misfit layered superconductor $(PbSe)_{1.14}(NbSe_2)_3$. These phenomena are realized by the characteristic crystal structure of the misfit compounds: separation of each superconducting layer, and combination of trigonal and tetragonal crystal symmetry.

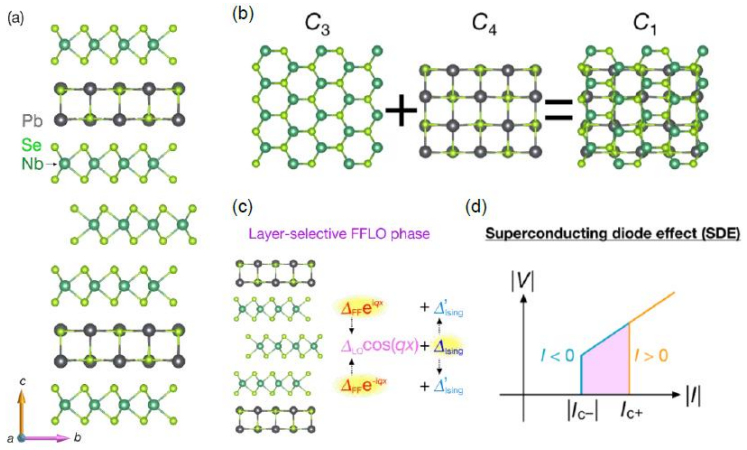

Fig. 1: *(a) Schematic crystal structure of $(PbSe)_{1.14}(NbSe_2)_3$. (b) Combination of trigonal and tetragonal crystral structures in $(PbSe)_{1.14}(NbSe_2)_3$, which kills the rotational symmetry. (c) Schematics of the layer-selective FFLO phase. (d) Schematics of superconducting diode effect.*

References

[1] A. Devarakonda, *et al.,* Science 370, 231 (2020).

[2] P. Samuely, *et al.,* PRB 104, 224507 (2021).

[3] N. Ng and T. M. McQueen, APL Mater. 10, 100901 (2022).

[4] Y. M. Itahashi, *et al.,* Nat. Commun. 16, 7022 (2025).

[5] Y. M. Itahashi, *et al.,* in preparation.

Abstract ID: 30117

NONLOCAL JOSEPHSON DIODE EFFECT IN MINIMAL KITAEV CHAINS

J. Cayao[1], M. Sato[2]

[1] *Department of Physics and Astronomy, Uppsala University, Box 516, S-751 20 Uppsala, SWEDEN*
[2] *Yukawa Institute for Theoretical Physics, Kyoto University, Kyoto 606-8502, JAPAN*

Minimal Kitaev chains have recently attracted great interest due to their potential for Majorana physics [1] and quantum applications [2]. Here, we discuss the emergence of the nonlocal Josephson effect in minimal Kitaev chains and exploit it to realize the nonlocal Josephson diode effect [3]. In particular, we focus on a Josephson setup formed by three laterally coupled minimal Kitaev chains, where the imbalance between crossed Andreev reflections and electron cotunneling in the middle Kitaev chain gives rise to an asymmetric 2π-periodic phase-dependent Andreev spectrum, controlled by the superconducting phases across the left and right junctions. We then demonstrate that this asymmetric Andreev spectrum, formed by hybridized Andreev bound states at the left and right junctions, enables a supercurrent across one junction via the phase difference at the other junction, thereby signaling the nonlocal Josephson effect. These nonlocal Josephson supercurrents develop different positive and negative critical currents, unveiling the realization of the nonlocal Josephson diode effect. We find that this nonlocal Josephson diode possesses a highly tunable polarity and can achieve efficiencies larger than 50%. Furthermore, we show that the nonlocal Josephson diode effect requires breaking local time-reversal and local charge-conjugation symmetries, with the latter being unique to minimal Kitaev chains. Our results establish minimal Kitaev chains as a highly controllable platform for nonreciprocal nonlocal Josephson phenomena.

References

[1] T. Dvir, *et al.*, Nature **614**, 445 (2023).

[2] A. Tsintzis, *et al.*, PRX Quantum **5**, 010323 (2024).

[3] J. Cayao and M. Sato, e-print arXiv:2512.00664 (2025).

Abstract ID: 30174

AC FLUX-DRIVEN DIODE EFFECT AS A PROBE OF FRACTIONAL CPRS IN DC SQUIDS

Y. Yerin[1,2], I. Askerzade[2,3,4], A. Gencer[3]

[1] *Istituto di Struttura della Materia of the National Research Council, via Salaria Km 29.3, I-00016 Monterotondo Stazione, ITALY*
[2] *Department of Computer Engineering, Ankara University, Ankara, 06100, TURKEY*
[3] *Ankara University, Center of Excellence for Superconductivity Research, 06500, Gölbasi, Ankara, TURKEY*
[4] *Institute of Physics, H.Cavid 33, Baku, AZ1143, AZERBAIJAN*

We investigate how AC magnetic flux modulation with tunable amplitude ϕ_{ac} can be employed to reveal and distinguish nontrivial components of the current-phase relation (CPR) in dc SQUIDs. By numerically solving the coupled dynamical equations of a dc SQUID with general CPRs, including harmonic sin(φ), subharmonic sin(φ/2), and second harmonic sin(2φ) terms, we construct two-dimensional phase diagrams of diode efficiency η (ϕ_{ac}, ω) as functions of the AC flux amplitude and frequency. These diagrams exhibit rich structures, whose shape and location are highly sensitive to the specific CPR form. We demonstrate that each type of CPR contribution leaves a distinct "fingerprint" on the phase diagram, thus providing a powerful diagnostic tool for probing the microscopic origin of nonreciprocal superconducting transport. This approach offers a new route to characterize unconventional Josephson junctions and to design superconducting diodes with tunable rectification properties.

Abstract ID: 30202

NONRECIPROCAL JOSEPHSON TRANSPORT IN FRACTAL SUPERCONDUCTORS: A FRACTIONAL GINZBURG–LANDAU PERSPECTIVE

Y. Yerin[1,2], I. Askerzade[2,3]

[1] *Istituto di Struttura della Materia of the National Research Council, via Salaria Km 29.3, I-00016 Monterotondo Stazione, ITALY*
[2] *Department of Computer Engineering and Center of Excellence of Superconductivity Research, Ankara University, Ankara, 06100, TURKEY*
[3] *Institute of Physics, H.Cavid 33, Baku, AZ1143, AZERBAIJAN*

Nonreciprocal superconducting transport, where the critical current differs for opposite current directions, has recently emerged as a key functionality in hybrid Josephson devices and noncentrosymmetric superconductors. In this work, we demonstrate that fractal or nonlocally correlated superconductors provide a natural platform for realizing and controlling the superconducting diode effect. Using a fractional-order Ginzburg-Landau (GL) framework, we show that nonreciprocity arises from the interplay between the Lifshitz invariant and fractional kinetic terms that effectively encode fractal dimensionality, long-range correlations, and memory effects.

Two complementary formulations are developed:

(i) a fractional-integral (measure-weighted) GL functional, capturing transport in media with fractal microstructure;

(ii) a gauge-invariant GL theory using Agrawal variational principle and left/right Caputo fractional derivatives.

Both approaches allow to obtain analytical current-phase relations and diode efficiencies, including exact solutions in terms of generalized Mittag-Leffler (Prabhakar) functions. Fractional kinetics amplifies and reshapes Lifshitz-induced nonreciprocity, enabling nearly ideal diode response without magnetic fields or geometric asymmetry. Our results identify a universal and symmetry-consistent route to engineer superconducting diodes through fractal (fractional-kinetic) transport in Josephson junctions.

Yuriy Yerin acknowledges the funding received from the program TÜBİTAK-2221 Fellowships for Visiting Scientists and Scientists on Sabbatical Leave.

Abstract ID: 30041

GATE-TUNABLE POLARITY INVERSIONS OF THE SUPERCONDUCTING DIODE EFFECT FOR TOPOLOGICAL SUPERCONDUCTIVITY

J. Shabani

Professor of Physics, New York University, USA

Recently it has been suggested Josephson junctions with strong spin orbit coupling can host topological superconductivity [1,2]. While InAs heterostructures are expected to possess strong spin orbit coupling, measuring the type and strength in similar devices is crucial for tuning topological phase. In this work we utilize the superconducting diode effect to understand the role of spin orbit coupling in presence of superconducting proximity effect. The superconducting diode effect is an asymmetry in the critical current with respect to the supercurrent polarity. One impetus driving recent interest in the effect is its dependence on intrinsic or microscopic symmetry breaking mechanisms. Here, we study the superconducting diode effect in gated planar Josephson junctions fabricated on a superconductor--semiconductor heterostructure under an in-plane magnetic field. We observe two gate-driven inversions of the diode polarity in the vicinity of zero field (see Fig. 1), as well as a third-harmonic component in the dependence of the diode efficiency on the in-plane field angle. We analyze the Lifshitz invariant for an arbitrary spin--orbit coupling and show that multiple polarity inversions are possible in the presence of both linear and cubic Dresselhaus terms, where the Rashba parameter varies monotonically with gate voltage (inspired by Fig. 2 data). Numerical calculations of the diode efficiency further reveal the presence of higher harmonics in its field-angle dependence in the presence of spin--orbit coupling [3,4].

References

[1] F. Pientka, *et al.*, Phys. Rev. X, **7**, 021032 (2017).

[2] M. C. Dartiailh, *et al.*, Phys. Rev. Lett., **126**, 036802 (2021).

[3] W. F Schiela, M. Mikalsen, D. Crawford, S. Ilić, W. M Strickland, F. S. Bergeret, J. Shabani, *Gate-tunable polarity inversions and three-fold rotation symmetry of the superconducting diode effect*, preprint available at arXiv:2504.21470 (2025).

[4] W. F. Schiela, M. Mikalsen, W. M. Strickland, J. Shabani, *Geometric dependence of critical current magnitude and nonreciprocity in planar Josephson junctions*, preprint available at arXiv:2502.12400 (2025).

Abstract ID: 30297

JOSEPHSON EFFECTS IN DIRAC SEMIMETAL Cd_3As_2

W. Pan

Sandia National Labs, Livermore, California, USA

Josephson junctions (JJs) made of topological quantum materials have attracted a great deal of current interests due to their non-trivial band topology and the capability of realizing topological superconductivity. Here, I wish to report our recent observations of novel Josephson effects in topological JJs and superconducting quantum interference devices (SQUIDs) mediated by Cd_3As_2, a topological Dirac semimetal [1,2]. First, in aluminum- Cd_3As_2-aluminum JJs, a π periodic supercurrents are observed [3]. Our data analysis suggests that this π period could arise from interference between the induced bulk superconductivity and the induced Fermi-arc surface superconductivity. Moreover, we observe that in Cd_3As_2 SQUIDs [4] this phase coupling between the surface-bulk superconducting channels is responsible for a surprising discovery of the Leggett modes, a collective quantum phenomenon predicted more than 50 years ago [5]. Finally, we show that this phase coupling can further induce time-reversal symmetry breaking [6] and, therefore, can give rise to a zero-field Josephson diode effect in asymmetric Cd_3As_2 SQUIDs [7,8].

Sandia National Laboratories is a multimission laboratory managed and operated by National Technology and Engineering Solutions of Sandia LLC, a wholly owned subsidiary of Honeywell International Inc. for the U.S. DOE's National Nuclear Security Administration under contract DE-NA0003525. This abstract describes objective technical results and analysis. Any subjective views or opinions that might be expressed in the paper do not necessarily represent the views of the U.S. DOE or the United States Government.

References

[1] X. Wan, *et al.*, Phys. Rev. B **83**, 205101 (2011).

[2] Z. Wang, *et al.*, Phys. Rev. B **88**, 125427 (2013).

[3] W Yu, *et al.*, Physical Review Letters **120**, 177704 (2018).

[4] J.J. Cuozzo, *et al.*, Nature Physics **20**, 1118 (2024).

[5] A.J. Leggett, Prog. Theor. Phys. **36**, 901–930 (1966).

[6] Y. Yerin et al., Physical Review B **110**, 054501 (2024).

[7] W Yu et al, Physical Review B **110**, 104510 (2024).

[8] H.C. Travaglini et al., APL Quantum **2**, 026135 (2025).

Abstract ID: 30088

TOWARDS ENERGY-TIME PTYCHOGRAPHY OF X-RAY SCATTERING FOR MICROMAGNETICS

G. Meier[1], A. Negi[2,3], L. M. Lohse[2,3], S. Velten[2], I. Sergeev[2], O. Leupold[2], S. Sadashivaiah[4,5], D. Bessas[6], A. Chumakhov[6], C. Brandt[7], L. Bocklage[2,3], R. Röhlsberger[2,3,4,5,8]

[1] *Max Planck Institute for the Structure and Dynamics of Matter, Luruper Chaussee 149, 22761 Hamburg, GERMANY*
[2] *Department of Photon Science, Deutsches Elektronen-Synchrotron DESY, Notkestr. 85, 22607, Hamburg, GERMANY*
[3] *The Hamburg Centre for Ultrafast Imaging, Luruper Chaussee 149, 22761 Hamburg, GERMANY*
[4] *Helmholtz Institute Jena, Fraunhoferstr. 8, 07743, Jena, GERMANY*
[5] *GSI Helmholtz Centre for Heavy Ion Research, Planckstr. 1, 64291, Darmstadt, GERMANY*
[6] *European Synchrotron Radiation Facility, F-38043 Grenoble, FRANCE*
[7] *Institute for Mathematics and Informatics, Univ. Greifswald, Walther-Rathenau-str. 47, 17489 Greifswald, GERMANY*
[8] *Institute of Optics and Quantum Electronics, University of Jena, Max-Wien-Platz 1, 07743, Jena, GERMANY*

Phase retrieval is at the heart of adaptive optics and modern high-resolution imaging. Without phase information, optical systems are limited to intensity-only measurements, hindering full reconstruction of object structures and wavefront dynamics essential for advanced applications. Here, we address a one-dimensional phase problem in magnetic X-ray scattering linking energy and time, which arises in from ultrasharp nuclear resonances [1]. We leverage the Mössbauer effect, where nuclei scatter radiation without energy loss to the lattice and are sensitive to their magneto-chemical environments [2]. Rather than using traditional spectroscopy with radioactive gamma-ray sources, we measure nuclear forward scattering of synchrotron X-ray pulses in the time domain, providing superior sensitivity and faster data acquisition. Extracting spectral information from a single measurement is challenging due to the missing phase information, typically requiring extensive modeling. Instead, we use multiple energetically overlapping measurements to retrieve both the transmission spectrum and the phase of the scattering response, similar to ptychographic phase retrieval in imaging. Our robust approach can overcome the bandwidth limitations of gamma-ray sources, opening new research directions, to the best of our knowledge, with modern X-ray sources and Mössbauer isotopes.

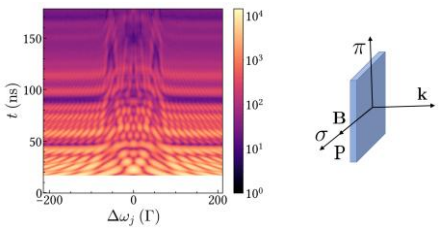

Fig. 2: *Measured ptychogram of a stainless-steel foil as probe and an ^{57}Fe foil as object when the external magnetic field is applied parallel to the direction of polarization of the synchrotron beam (B II σ). P and k denote the polarization and propagation direction of the synchrotron beam, respectively. The relative frequency shift ⊿ω$_j$ is given in units of the natural line width G of ^{57}Fe, which is 4.7 neV.*

References

[1] A. Negi, *et al.*, G.M., *Energy-Time Ptychography for One-Dimensional Phase Retrieval*, Optica **12**, 1529 (2025).

[2] L. Bocklage, *et al.*, G.M., *Coherent Control of Collective Nuclear Quantum States via Transient Magnons*, Science Adv. **7**, eabc3991 (2021); K. P. Heeg, *et al.*, G.M., *Reply to: On Yoctosecond Science*, Nature **608**, E18 (2022).

Abstract ID: 30201

CONTROLLING AND SENSING SPIN SYSTEMS WITH FREE SPACE ELECTRONS

P. Haslinger

Vienna Center for Quantum Science and Technology, Atominstitut, USTEM
TU Wien, Stadionallee 2, 1020 Vienna, AUSTRIA

Coherent control and detection of quantum systems lie at the heart of quantum optics and quantum technologies. While optical and microwave control techniques are well established, the use of free-space electron beams as both manipulator and sensors opens an entirely new regime for spatial resolution and spectroscopic access.

In this talk, I will first outline intuitively our theoretical work [1] showing how the non-radiative near-fields of temporally modulated free-space electron beams can coherently drive spin systems. I show that such manipulation can be performed with only classical control over the electron beam itself and that potential challenges like shot noise and decoherence through back action on the electrons are for certain parameter ranges insignificant for our approach. I will discuss possible implementations and show preliminary data on manipulating spin systems in a sample.

I will then present our recent experimental setup on SPINEM (Spin Electron Microscopy) [2], which integrates continuous-wave electron spin resonance (ESR) spectroscopy directly into a transmission electron microscope. By combining a custom microwave resonator with a free space electron beam [3], we achieve in-situ, phase-locked detection of microwave-driven spin precession with picoradian deflection sensitivity and high spatial mapping capabilities. This approach directly senses the magnetic fields generated by precessing spins in the GHz regime, enabling localized spin spectroscopy in a TEM.

I will conclude with perspectives on pushing SPINEM towards atomic resolution and single-spin sensitivity [4]. These advances could open new frontiers in nanoscale spintronics, magnonics, and quantum materials research, and provide an electron-based analogue to magnetic resonance imaging at the level of individual nanostructures.

References

[1] D. Rätzel, D. Hartley, O. Schwartz, and P. Haslinger, *Controlling Quantum Systems with Modulated Electron Beams*, Phys. Rev. Res. **3**, 023247 (2021).

[2] A. Jaroš, J. Toyfl, A. Pupić, B. Czasch, G. Boero, I. Bicket, P. Haslinger *Sensing Spin Systems with a Transmission Electron Microscope*, arXiv:2503.06761.

[3] A. Jaroš, M. Seifner, J. Toyfl, B. Czasch, I. Bicket, P. Haslinger, *Electron Spin Resonance Spectroscopy in a Transmission Electron Microscope*, arXiv:2408.16492.

[4] P. Haslinger, S. Nimmrichter, D. Rätzel, *Spin Resonance Spectroscopy With an Electron Microscope*, QST, **9**, 035051 (2024).

Abstract ID: 30229

PATTERNING TWO-DIMENSIONAL GRADIENTS IN STRUCTURAL AND MAGNETIC PROPERTIES FOR SPINTRONICS APPLICATIONS

A. Hrabec[1,2]

[1] *Laboratory for Mesoscopic Systems, Department of Materials, ETH Zurich, 8093 Zurich, SWITZERLAND*
[2] *PSI Center for Neutron and Muon Sciences, 5232 Villigen PSI, SWITZERLAND*

Novel spin-based logic architectures are being developed to provide high-performance nonvolatile data retention and processing. Two prominent directions include the development of spin-based in-memory computing and efficient, all-electric control of magnetic order. We have recently showed that spatial patterning of uniaxial anisotropy via selective oxidation can result in strong lateral coupling based on the Dzyaloshinskii–Moriya interaction [1]. The coupling can be incorporated into electrically-controlled devices comprising reconfigurable NAND and NOR logic gates [2]. Despite the limited number of material systems where such in-memory computing can be realized, the capability of patterning magnetic anisotropy opened unprecedented avenues. This discovery highlighted the need to develop new methods for spatial patterning, which could lead to new, disruptive technologies in magnetism and beyond.

To enhance the pool of structural and magnetic properties that can be patterned, we have developed direct-write laser annealing, which is based on local annealing [3]. Here, the underlying magnetic properties are linked to heat-activated processes such as crystallization, interdiffusion or oxidation. We demonstrate the capability of this technique by realization of a spin wave band pass filter and new architectures for passively resetting the position of a magnetic domain wall [3,4]. We also demonstrate that conventional and unconventional spin-orbit torques can be patterned based on the underlying designed structural gradients in tungsten thin films [5].

The laser annealing-based method opens new opportunities to pattern material and magnetic landscapes with high-precision capability, leading to unprecedented applications in spintronics and magnonics, and thin-film based magnetism in general.

References

[1] Z. Luo, *et al.*, Science, 363, 1435 (2019).

[2] Z. Luo, *et al.*, Nature 579, 214-218 (2020).

[3] L. Riddiford, J. A. Brock, *et al.*, Nat. Commun. 16, 10979 (2025).

[4] J. Brock, *et al.*, arXiv: 2508.14252 (2025).

[5] L. Riddiford, *et al.*, manuscript in preparation.

Abstract ID: 30298

SKYRMIONS AND ANTISKYRMIONS IN ROOM-TEMPERATURE NONCENTROSYMMETRIC MAGNETS

K. Karube[1], L. C. Peng[1,2], Y. L. Chiew[1], X. Z. Yu[1], J. Masell[1,3], L. Keller[4], J. S. White[4], V. Ukleev[4,5], M. Hemmida[6], H.-A. Krug von Nidda[6], I. Kézsmárki[6], M.-C. Jiang[1,7,8], G.-Y. Guo[7,8], R. Arita[1,9], F. Kagawa[1,10], Y. Tokura[1,11,12], Y. Taguchi[1]

[1] *RIKEN Center for Emergent Matter Science (CEMS), Wako 351-0198, JAPAN*
[2] *Peking University, Beijing, 100871, CHINA*
[3] *Karlsruhe Institute of Technology, Karlsruhe, 76049, GERMANY*
[4] *Paul Scherrer Institute, Villigen, CH-5232, SWITZERLAND*
[5] *Helmholtz-Zentrum Berlin für Materialien und Energie, D-14109 Berlin, GERMANY*
[6] *University of Augsburg, Augsburg, 86135, GERMANY*
[7] *National Taiwan University, Taipei 10617, TAIWAN*
[8] *National Center for Theoretical Sciences, Taipei 10617, TAIWAN*
[9] *Department of Physics, University of Tokyo, Bunkyo-ku, Tokyo, JAPAN*
[10] *Department of Physics, Institute of Science Tokyo, Meguro-ku, 152-8551, JAPAN*
[11] *Department of Applied Physics, University of Tokyo, Bunkyo-ku, 113-8656, JAPAN*
[12] *Tokyo College, University of Tokyo, Bunkyo-ku, 113-8656, JAPAN*

Magnetic skyrmions and their antiparticles—antiskyrmions—are vortex-like spin textures characterized by integer topological numbers, and they have attracted significant attention in both fundamental physics and spintronics applications. To date, extensive studies of (anti)skyrmions have been carried out in a wide variety of material systems. In particular, the stabilization of these topological spin textures above room temperatures is crucial for accelerating their practical applications. In this presentation, we overview our recent progress on two noncentrosymmetric magnets that host skyrmions and antiskyrmions above room temperature, in which Dzyaloshinskii–Moriya interaction (DMI) and/or magnetic dipolar interactions play dominant roles.

The first material is Pd-doped schreibersite, $(Fe_{0.63}Ni_{0.30}Pd_{0.07})_3P$, which crystallizes in a noncentrosymmetric tetragonal structure with S_4 symmetry. We demonstrated that square antiskyrmions and elliptic skyrmions form in thin plates above room temperature. Furthermore, sawtooth-like anisotropic fractal magnetic domains emerge near the surface of thick bulk crystals. These exotic magnetic textures are attributed to the combined effects of anisotropic DMI and dipolar interactions [1-3].

We also introduce our recent findings on MnRhP, which crystallizes in a noncentrosymmetric hexagonal structure composed of distorted kagome layers of Mn atoms. This material has been identified as a new ferromagnetic topological nodal-line semimetal with a high Curie temperature. We revealed weak easy-axis magnetic anisotropy in this compound and observed a large anomalous Hall conductivity, which is attributed to the Berry curvature associated with the gapped nodal lines. Moreover, stable dipolar skyrmions persisting above room temperature were observed in thin plates [4].

These novel magnetic systems provide a new arena for exploring topological spin textures and large anomalous transport phenomena above room temperature.

References

[1] K. Karube, *et al.*, Nat. Mater. **20**, 335 (2021).
[2] K. Karube, *et al.*, Adv. Mater. **34**, 2108770 (2022).
[3] K. Karube, *et al.*, J. Appl. Crystallogr. **55**, 1392 (2022).
[4] K. Karube, *et al.*, under review

Abstract ID: 30383

FORMATION MECHANISMS OF SQUARE SKYRMION LATTICES IN MULTI-ORBITAL ELECTRON SYSTEMS

Y. S. Zha, S. Hayami

Hokkaido University, Graduate School of Science, Sapporo 060-0810, JAPAN

In condensed matter physics, magnetic skyrmions are topologically protected real-space magnetic-moment textures [1]. Their topological nature ensures stability against weak perturbations. A thermodynamically stable skyrmion lattice (SkL) in a triangular shape was first observed in the noncentrosymmetric B20 compound MnSi (point group: T) in 2009, stabilized by the relativistic Dzyaloshinskii-Moriya interaction (DMI), ferromagnetic exchange interactions, and Zeeman coupling [2]. For nearly a decade, experimental research has focused primarily on such noncentrosymmetric systems that host DMI. In addition, A key theoretical insight is that the triangular SkL (T-SkL) is naturally stabilized by a biquadratic/quartic coupling term, $(S_0 \cdot S_{Q_1})(S_{Q_2} \cdot S_{Q_3})$, among three symmetry-equivalent helices and the uniform magnetization (where $Q_1 + Q_2 + Q_3 = 0$). In contrast, a double-Q superposition (square lattice) lacks this stabilization mechanism because the vector-sum condition $Q_1 + Q_2 \neq 0$ prevents such coupling.

In 2020, a nanometric square skyrmion lattice (S-SkL) driven by frustration rather than DMI was experimentally discovered in the centrosymmetric tetragonal magnet $GdRu_2Si_2$ (point group: D_{4h}) [3]. Subsequent research on S-SkLs in centrosymmetric $4f$-electron systems has been highly active. However, studies have thus far focused on Gd^{3+} and Eu^{2+} ions, which possess quenched orbital angular momentum ($L = 0$). This motivates our search for S-SkLs in centrosymmetric $4f$ systems with unquenched orbital angular momentum ($L \neq 0$).

In this study, we systematically analyze crystal-field effects for S-SkL's formation by considering a plain $4f^1$ electron configuration as a prototype [4,5]. We downfold the full 14-dimensional Hilbert space into a low-energy 4-dimensional subspace to treat the inter-/intra-orbital coupling among two Γ_{t7} Kramers doublets. We construct an effective Hamiltonian and perform iterative self-consistent mean-field calculations to determine the ground state across a wide parameter space, including the superposition coefficient α that controls magnetic anisotropy, crystal-field splitting Δ, and the external magnetic field h.

Furthermore, we address the role of momentum-space frustration. Due to the underlying crystal symmetry, the system exhibits multiple global minima in momentum space. Specifically, when the dominant modulation vectors $Q_{1,2}$ are aligned along the $\langle 110 \rangle$ directions, higher-harmonic terms $Q'_{\pm} \equiv Q_1 \pm Q_2$, which help constitute the relation $Q_1 + Q_2 - Q'_+ = 0$ and stabilize the S-SkL, appear along the $\langle 100 \rangle$ axes. The curvature of the Fourier-transform exchange interaction $\mathfrak{J}(q)$ around these dominant vectors determines the energy cost of the higher-harmonic modes, playing a pivotal role in stabilizing the S-SkL and other double-Q states. In this talk, the impact of this momentum-space frustration mechanism on the formation of the S-SkL will be discussed.

References

[1] N. Nagaosa and Y. Tokura, Nat. Nano. **8**, 899 (2013).
[2] S. Mühlbauer, *et al.*, Science **323**, 915 (2009).
[3] N. D. Khanh, *et al.*, Nat. Nano. **15**, 444 (2020).
[4] Y. Zha and S. Hayami, Phys. Rev. B **111**, 165155 (2025).
[5] Y. S. Zha and S. Hayami, arXiv:2511.05896 [cond-mat.str-el].

Abstract ID: 30422

COUPLED VORTEX-SKYRMION 3-DIMENSIONAL HETEROSTRUCTURES: STABILITY AND MAGNETIC FIELD-INDUCED MOTION

J. Sunny[1], S. Koraltan[2], T. Gokita[2], T. Schmidt[1], S. Wintz[4], D. Suess[3], M. Albrecht[1]

[1] *University of Augsburg, Institute of Physics, 86159, Augsburg, GERMANY*
[2] *TU Wien, Institute of Applied Physics, 1040, Wien, AUSTRIA*
[3] *University of Vienna, Faculty of Physics, 1010, Wien, AUSTRIA*
[4] *Helmholtz-Zentrum Berlin für Materialien und Energie, 14109, Berlin, GERMANY*

Magnetic skyrmions are topologically protected spin textures with nanoscale stability and robustness against external perturbations, making them promising candidates for next-generation spintronic applications. They have been experimentally observed in multilayer thin films even in the absence of Dzyaloshinskii-Moriya interaction (DMI) [1]. However, achieving deterministic control over their nucleation and annihilation remains a key challenge. Recent micromagnetic simulations have proposed coupling skyrmions to magnetic vortices as a potential mechanism for controlled manipulation [2]. In thin films lacking perpendicular magnetic anisotropy, geometric confinement leads to a stable uniform vortex state [3].

In this work, we demonstrate the formation of a coupled vortex-skyrmion three-dimensional spin object in a multilayer system prepared using DC magnetron sputtering and electron-beam lithography. The in-plane spin structure of the coupled object is observed using Lorentz transmission electron microscopy (LTEM), while the out-of-plane (OOP) spin structure is characterized using element-specific scanning transmission X-ray microscopy (STXM). Furthermore, the coupling strength between the vortex and the skyrmion is investigated by introducing Pt spacer layers of varying thickness. The motion of the coupled vortex-skyrmion under in-plane magnetic fields is also studied. The skyrmion is observed to have achieved deterministic nucleation, increased stability, and dynamics acquired through the vortex.

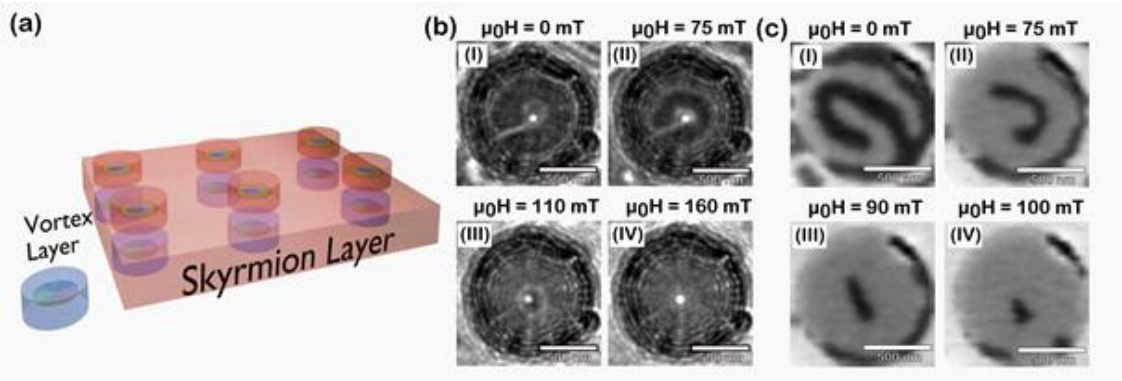

Fig. 1: *(a) Schematic illustration of the 3D heterostructures. (b) LTEM images showing the formation of coupled vortex-skyrmion spin object at different OOP magnetic field. (c) STXM images obtained at Fe L_3 edge for different OOP magnetic fields showing formation of the spin object.*

References

[1] M. Heigl, *et al.*, Nature Commun. **12(1)**, 2611 (2021).
[2] S. Koraltan, *et al.*, Phys. Rev. B **108**, 134401 (2023).
[3] T. Shinjo, *et al.*, Science **289**,930-932 (2000).

Abstract ID: 30434

CRYOGENIC REAL SPACE MEASUREMENTS OF NONTRIVIAL TOPOLOGICAL SPIN TEXTURES

F. S. Yasin[1], M. El Gazzah[2,3], Y.-H. Kim[1], N. Y. Kim[1], S. Jamaluddin[2,3], H. Bhandari[2,3,4], R. B. Regmi[2,3], A. Kikkawa[5], Y. Taguchi[5], J. Yan[6], M. Birch[5], X. Yu[5,7], N. J. Ghimire[2,3], M. Chi[1]

[1] *Center for Nanophase Materials Sciences, Oak Ridge National Laboratory, 1 Bethel Valley Road, Oak Ridge, 37830, USA*
[2] *Department of Physics and Astronomy, University of Notre Dame, Notre Dame, IN 46556, USA*
[3] *Stavropoulos Center For Complex Quantum Matter, University of Notre Dame, Notre Dame, IN 46556, USA*
[4] *Department of Physics and Astronomy, Rice University, Houston, Texas 77005, USA*
[5] *RIKEN Center for Emergent Matter Science, Hirosawa 2-1, Wako, 351-0198, JAPAN*
[6] *Materials Science and Technology Division, Oak Ridge National Laboratory, Oak Ridge, TN 37831, USA*
[7] *The Institute of Science Tokyo, Tokyo 152-8550, JAPAN*

The transmission electron microscope (TEM) offers direct observation of a material's atomic structure and electromagnetic properties and may be configured in a field-free (Lorentz) imaging mode, which was instrumental in acquiring the first real-space images of topological magnetic skyrmions and their antiparticles, antiskyrmions [1,2]. Modern TEM holders provide the opportunity to probe a spin texture's response to various external stimuli such as magnetic fields, heat, and electric/thermal currents. Additionally, the development of highly stable cryogenic TEM holders has facilitated high-resolution real-space mapping of magnetic textures in low-T_C materials.

In this talk, we will review field-free TEM methods [3] and explore the magnetic states that emerge in a metallic ferromagnet with Kagome crystal structure and temperature-dependent magnetocrystalline anisotropy. We will also introduce our recent efforts to perform long time-scale magnetic imaging experiments using a new flow-cryostat TEM holder and demonstrate its thermal performance including a base temperature of base temperature of 4.37 ± 0.004 K measured using a Cernox bare chip sensor located on the holder cradle.

This work was supported by the U.S. Department of Energy, Office of Basic Energy Sciences, Division of Materials Sciences and Engineering. Microscopy technique development (Y.-H.K.) was partially supported by the U.S. BES, Early Career Research Program (KC040304-ERKCZ55). Experiments were performed at the Center for Nanophase Materials Sciences, a U.S. DOE Office of Science User Facility at Oak Ridge National Laboratory (ORNL). Research sponsored by the Laboratory Directed Research and Development Program of ORNL, managed by UT-Battelle, LLC, for the US DOE. X. Z. Y and Y. T acknowledge the support of the Japan Science and Technology Agency (JST) CREST program (# JPMJCR20T1) and the RIKEN TRIP initiative.

References

[1] X. Z. Yu, *et al.*, Nature **465**, 901 (2010).
[2] A. K. Nayak, *et al.*, Nature **548**, 561 (2017).
[3] D. V. Christensen, *et al.*, J. Phys. Mater. **7**, 032501 (2024).

Abstract ID: 30482

PROBING ULTRAFAST MAGNETISM AT THE NANOSCALE WITH COHERENT XUV SCATTERING AND MICROSCOPY

S. Zayko[1], H-T. Chang[1], O. Kfir[2], T. Schmidt[3], M. Sivis[1], M. Albrecht[3], C. Ropers[1]

[1] *Max Planck Institute for Multidisciplinary Sciences, 37077 Göttingen, GERMANY*
[2] *School of Electrical Engineering, Tel Aviv University, Tel Aviv 69978, ISRAEL*
[3] *Institute of Physics, University of Augsburg, 86135 Augsburg, GERMANY*

Understanding ultrafast magnetism at the nanoscale remains a central challenge for spintronics, as key processes—ranging from demagnetization and all-optical switching (AOS) to topological texture dynamics—occur on femtosecond time scales and nanometer length scales. Laboratory-based coherent XUV sources now offer a unique opportunity to access this regime with element specificity and femtosecond pump–probe capability. Here, I will present the development of a complementary toolbox combining coherent XUV scattering and lensless microscopy to probe ultrafast magnetism from both reciprocal and real space perspectives. Our microscopy technique provides unmatched spatio-temporal resolution that allows tracking femtosecond spin dynamics with sub-nm precision, yet within a limited field of view, while time-resolved scattering offers ensemble-averaged sensitivity over large areas, revealing ultrafast redistribution of spin and structural correlations. Together, these approaches enable new insight into the interplay between electronic, spin, and structural degrees of freedom during non-equilibrium excitation. I will discuss ongoing studies on domain wall dynamics, all-optical switching and ultrafast spin dynamics in ferrimagnetic (FeDy, FeGdDy, CoTb) and ferromagnetic (CoPt, CoPd) thin films and multilayers, highlighting the potential of coherent table-top XUV techniques to bridge the gap between ultrafast opto-magnetism and nanoscale spintronic functionality.

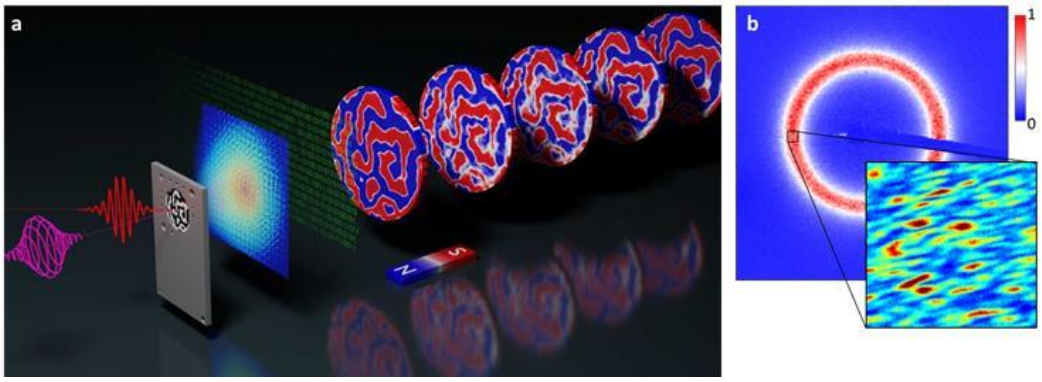

5

Fig. 1: (a) *Schematic of the ultrafast XUV imaging experiment. A diffraction pattern from a nanoscale magnetic sample is recorded and reconstructed numerically using lensless imaging, providing femtosecond snapshots of the transient magnetic state in a stroboscopic fashion.* **(b)** *Small-angle X-ray scattering (SAXS) experiment performed using the same setup without imaging mask, showing the change (pump off minus pump-on image) in ring-like scattering intensity from magnetic domains between relaxed and excited states. The zoom highlights the detailed signal of the typical ring intensity, which carries ensemble magnetic correlations.*

Abstract ID: 30673

LOCALIZED SPIN TEXTURES STABILIZED BY GEOMETRY-INDUCED STRAIN IN 2D MAGNET Fe_3GeTe_2

Y. Sun[1], M. T. Birch[2], S. Finizio[3,4], L. Powalla[1], S. Satheesh[1], T. Priessnitz[1], E. Goering[1], E. Knöckl[5], C. Kastl[5], A. Holleitner[5], K. Kern[1], M. Weigand[4], S.Wintz[4], M. Burghard[1]

[1] *Max Planck Institute for Solid State Research, Heisenbergstrasse 1, 70569 Stuttgart, GERMANY*
[2] *RIKEN Center for Emergent Matter Science, Wako 351-0198, JAPAN*
3 Swiss Light Source, Paul Scherrer Institute, 5232 Villigen PSI, SWITZERLAND
[4] *Helmholtz-Zentrum Berlin für Materialien und Energie GmbH, Institut Nanospektroskopie, 12489 Berlin, GERMANY*
[5] *Walter Schottky Institute and Physics Department, Technical University of Munich, 85748 Garching, GERMANY*

Strain engineering promises to enable manipulation and control of the properties of exfoliated flakes of 2D van der Waals (vdW) ferromagnets for spintronic applications [1,2]. However, while previous studies of strain effects have focused on global properties [3], the impact on local magnetic spin textures remains unexplored. Here, manipulation of magnetism in the 2D ferromagnet Fe_3GeTe_2 (FGT) is demonstrated using geometry-induced strain. Employing scanning transmission X-ray microscopy (STXM), the effects of spatially varying strain profiles on the magnetic order of FGT sheets stamped onto micropillar arrays are directly visualized. It is found that the in-plane strain components, with magnitudes <0.5%, locally elevate the Curie temperature of FGT by 10 K, stabilizing magnetic domains near the pillar corners. These domains include skyrmions and higher-order topological spin textures such as skyrmioniums and skyrmion bags. The possibility to locally seed and control topological spin textures via strain opens new avenues for future spin-based information technologies.

References

[1] Z. Jia, M. Zhao, Q. Chen, Y. Tian, L. Liu, F. Zhang, D. Zhang, Y. Ji, B. Camargo, K. Ye, R. Sun, Z. Wang, Y. Jiang, ACS Nano, **19**, 9452 (2025).
[2] L. Guo, S. Hu, X. Gu, R. Zhang, K. Wang, W. Yan, X. Sun, Adv. Mater., **36**, 2301854 (2024).
[3] Y. Wang, C. Wang, S.-J. Liang, Z. Ma, K. Xu, X. Liu, L. Zhang, A. S. Admasu, S.-W. Cheong, L. Wang, M. Chen, Z. Liu, B. Cheng, W. Ji, F. Miao, Adv. Mater., **32**, 2004533 (2020).

Abstract ID: 30261

PHYSICS-INFORMED MAGNETIZATION RECONSTRUCTION FROM NV MAGNETOMETRY

C. Abert

University of Vienna, Faculty of Physics, 1090 Vienna, AUSTRIA

Magnetic stray-field imaging techniques such as nitrogen-vacancy (NV) magnetometry provide quantitative access to magnetic fields with nanoscale spatial resolution. However, reconstructing the underlying magnetization from such measurements constitutes a fundamentally ill-posed inverse problem: distinct magnetization configurations can give rise to identical stray fields, and the reconstruction is further complicated by experimental noise, finite resolution, and uncertainties in material parameters and sensor–sample distance. Meaningful reconstruction therefore requires the incorporation of physical constraints beyond purely magnetostatic inversion.

In this contribution, we present inverse micromagnetic reconstruction methods that enforce consistency with micromagnetic equilibrium by explicitly incorporating the governing physics into the reconstruction process. We first briefly review a bias-field–constrained micromagnetic relaxation approach, in which an initial magnetization consistent with the measured stray field is stabilized during Landau–Lifshitz–Gilbert relaxation [1]. This strategy resolves ambiguities of purely magnetostatic inversion and enables the extraction of intrinsic material parameters.

The main focus of the talk is a recently developed physics-informed variational reconstruction framework formulated in Fourier space for NV magnetometry. The method embeds the full micromagnetic energy functional directly into the inverse problem and combines an auto-differentiable finite-difference micromagnetic solver with FFT-based stray-field computation and Fourier-space upward extrapolation. This enables efficient gradient-based optimization of the magnetization texture while simultaneously treating the sensor–sample distance as an unknown parameter. As illustrated in Fig. 1, the framework reconstructs physically consistent magnetization textures from stray-field data.

The presented approach provides a transparent and quantitative route to magnetization reconstruction that addresses the inherent non-uniqueness of inverse stray-field problems through physically motivated constraints.

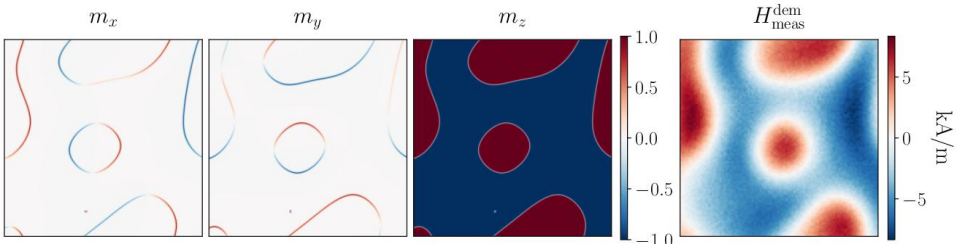

Fig. 1: *Example magnetization configuration and corresponding NV measurement including synthetic noise.*

References

[1] D. Suess, A. Setescak, J. Smith, F. Bruckner, H. J. Hug, C. Abert, Scientific Reports, **15(1)**, 42867 (2025).

Abstract ID: 30669

CHIRAL MAGNETIC PHENOMENA AT FERRIMAGNETIC INSULATOR/METAL INTERFACES

C. O. Avci

Institut de Ciència de Materials de Barcelona, Campus de la UAB, Bellaterra, 08193, SPAIN

The Dzyaloshinskii–Moriya interaction (DMI) is a chiral magnetic exchange interaction that favors the perpendicular alignment of neighboring spins [1,2]. It typically emerges in systems lacking inversion symmetry and exhibiting strong spin–orbit coupling (SOC), such as ferromagnet/non-magnetic metal (FM/NM) interfaces. The microscopic origin of interfacial DMI is commonly described by the three-site Levy–Fert model, where adjacent magnetic moments interact via nearby non-magnetic atoms [3]. This interfacial DMI has been essential for stabilizing chiral spin textures—including Néel domain walls and skyrmions—which underpin a wide range of spintronic device concepts. More recently, a new type of chiral interaction, interlayer DMI, has gained significant attention. It couples two ferromagnetic layers across a high SOC spacer, imposing a preferred orthogonal alignment between their magnetic moments [4]. This interaction enhances device functionality and enables phenomena such as exchange bias and field-free spin–orbit torque (SOT) switching.

This talk is divided into two parts. In the first part, we extend the Levy–Fert framework and provide evidence for substantial DMI arising from long-range interactions with a *nonlocal* interface [5]. We investigate the interfacial DMI in the ferrimagnetic insulator $Tb_3Fe_5O_{12}$ (TbIG) as a function of thickness and for different NM overlayers. By correlating the measured DMI with interfacial spin transport and atomic-resolution electron microscopy, we show that the TbIG/NM interface is the dominant source of DMI in our structures. We further demonstrate that inserting a Cu spacer significantly modifies the interfacial DMI due to a long-range interaction between TbIG and the remote Cu/NM interface. Density functional theory calculations on analogous structures support our experimental findings and reinforce this interpretation.

In the second part, we report interlayer DMI between TbIG and a ferromagnetic layer directly grown on top, without requiring a strong-SOC spacer [6]. This coupling produces a sizable exchange-bias effect, comparable to that of all-metallic heterostructures, and enables new mechanisms for current- and heat-induced magnetization switching in ferrimagnetic insulators. Together, these results deepen our understanding of DMI in magnetic insulators and provide design principles for engineering chiral interactions with potential impact on domain-wall devices, skyrmionics, and probabilistic computing.

References

[1] I. Dzyaloshinsky, Journal of Physics and Chemistry of Solids **4**, 241 (1958).
[2] T. Moriya, Physical Review **120**, 91 (1960).
[3] A. Fert and P. M. Levy, Phys. Rev. Lett. **44**, 1538 (1980); A. R. Fert, Mater. Sci. Forum **5960**, 439 (1990)
[4] C. O. Avci, *et al.*, Phys. Rev. Lett. **127**, 167202 (2021)
[5] S. Fedel, *et al.*, Adv. Funct. Mater. **35** 2418653 (2025)
[6] W. Janus, *et al.*, unpublished (2026)

41 - NOVEL FUNCTIONAL MAGNETIC MATERIALS- BASIC APPROACH AND APPLICATIONS

Abstract ID: 30133

ENGINEERING SHAPE-MEMORY CHARACTERISTICS IN Ni-Fe-Ga MICROWIRES

M. Elias[1,2,3], S. Sakthivel[1], T. Ryba[1], M. Vavrga[1], O. Milkovic[1,4], L. Straka[3], O. Heczko[3], R. Varga.[1,3,5]

[1] *RVmagnetics a.s., Nemcovej 30, 040 01 Kosice, SLOVAKIA*
[2] *Dept. Phys., FEEI, TUKE, Park Komenskeho 2, 042 001 Kosice, SLOVAKIA*
[3] *Institute of Physics, CAS, Na Slovance 2, 18221 Prague, CZECH REPUBLIC*
[4] *Institute of Experimental Physics, Slovak Academy of Sciences, 040 01 Kosice, SLOVAKIA*
[5] *RVactuators s.r.o., Prazska 636, 25241 Dolni Brezany, CZECH REPUBLIC*

Miniaturized actuators are becoming increasingly important for applications in robotics, optics, biomedical devices, and precision engineering, where compact dimensions, high reliability, and large mechanical output are essential. Microwire-based microactuators, particularly those utilizing shape-memory alloys, offer a promising route toward high-performance actuation at the microscale [1,2]. Their advantages include extremely small dimensions, large recoverable strains of up to 12%, tunable transformation temperatures ranging from –170 °C to 400 °C, long-term durability exceeding 9×10^6 cycles, and the ability to generate stresses above 100 MPa. In addition, the Taylor–Ulitovski method enables highly scalable production, yielding approximately 1 km of microwire from just 1 g of alloy.

In this work, we present novel findings in the development of Ni-Fe-Ga–based microwire microactuators. By identifying the key parameters governing both the fabrication process and the resulting functional and mechanical properties, we highlight the critical factors that enable outstanding actuation performance. Several representative examples are provided to demonstrate how optimized processing routes lead to superior shape-memory behavior, high stability, and reliable operation of Ni-Fe-Ga microwire actuators.

References

[1] K. Lal Chaurasiya, A. Sri Harsha, Y. Sinha, B. Bhattacharya, Scientific Reports **12**, 10758 (2022).

[2] A. Zhukov, M. Ipatov, J. J. del Val, V. Zhukova, V. A. Chernenko Scientific Reports **8**, 621 (2018).

[3] M. Hennel, M. Varga, L. Frolova, S. Nalevanko, P. Ibarra-Gaytán, R. Vidyasagar, P. Sarkar, A. Dzubinska, L. Galdun, T. Ryba, Z. Vargova, R. Varga, Phys. Stat. Solidi A, **2100657** (2022)

Abstract ID: 30341

MAGNETO-OPTICAL OBSERVATIONS OF MICROWIRES AND THEIR RELEVANCE TO PRACTICAL APPLICATIONS

M. Kozachok[2], K. Richter[1,2,3]

[1] *Cassovia New Industry Cluster (CNIC), Trieda SNP 457/1, Košice 040 11 SLOVAK REPUBLIC*
[2] *Faculty of Electrical Engineering and Informatics, Technical University of Košice, Kosice, 042 00 SLOVAK REPUBLIC*
[3] *Institute of Experimental Physics, Slovak Academy of Sciences (SAV) Košice, SLOVAK REPUBLIC*

Amorphous glass-coated microwires [1,2] are promising candidates for miniature passive sensors based on single domain wall motion. Although wireless detection of rapid magnetization reversal using induction methods is well established, it is limited by the short distance required between the microwire and the sensing coil. In this contribution, we investigate laser-assisted detection of domain wall motion at larger distances using the magneto-optical Kerr effect (MOKE). A dedicated experimental setup enabling three-dimensional surface mapping of the domain wall inclination is presented [3]. Our results demonstrate that, in addition to the intrinsic properties of the domain wall, local pinning effects play a crucial role. While pinning-free domain wall motion does not affect the surface tilting of the wall, the presence of pinning renders the domain wall motion highly sensitive to external magnetic fields. Finally, our MOKE-based framework [4] is applied to the design and optimization (Fig. 1) of a wireless sensor based on a microwire mounted on a rotating element.

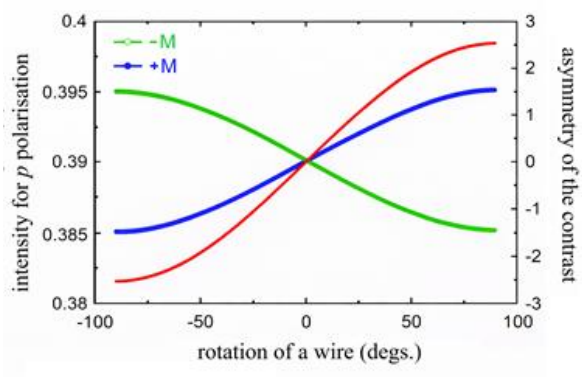

Fig. 1: *Calculation of the magnetooptical contrast for cylindrical microwire under rotation of 45° and incident laser beam with p polarization. The microwire is stuck to the rotation shaft and MOKE response is detected by CCD detector placed at larger distance from rotating element.*

References

[1] A. Zhukov, *et al.*, J. Alloys Compd. **707**, (2017).
[2] M. Vazquez, *et al.*, J. Magn. Magn. Mater. **160**, (1996).
[3] O. Vahovsky, *et al.*, J. Magn. Magn. Mater. **483**, (2019).
[4] K. Richter, *et al.*, J. Magn. Magn. Mater. **562**, (2022).

Abstract ID: 30348

STRUCTURE AND MAGNETIC PROPERTIES OF FeCoNiAlMn HIGH-ENTROPY ALLOY FROM MICRO TO ATOMIC SCALE

P. Švec[1,2], O. Roik[3], I. Gejdoš Janotová[1], D. Janičkovič[1], M. Jakubčin[4], B. Kunca[4], J. Marcin[4], I. Škorvánek[4], Yu. Plevachuk[1,5], P. Švec Sr[1]

[1] *Institute of Physics, Slovak Academy of Sciences, Dúbravská cesta 9, 84511 Bratislava, SLOVAKIA*
[2] *Institute of Materials Research, Slovak Academy of Sciences, Watsonova 47, 040 01 Košice, SLOVAKIA*
[3] *Taras Shevchenko National University of Kyiv, Kyiv 01033, UKRAINE*
[4] *Institute of Experimental Physics, Slovak Academy of Sciences, Watsonova 47, 040 01 Košice, SLOVAKIA*
[5] *Department of Metal Physics, Ivan Franko National University of Lviv, Lviv 79005, UKRAINE*

Among high-entropy alloys, special attention is drawn to multicomponent alloys composed of transition elements, in which the formation of a mixture of solid solutions based on bcc and fcc structures results in a high level of strength and plastic characteristics. In addition, combination of typical "ferromagnetic" atomic species allows to expect control of magnetic properties.

The structure, microstructure, and properties of the equiatomic high-entropy alloy $Fe_{20}Co_{20}Ni_{20}Al_{20}Mn_{20}$ prepared by varying cooling rates, namely conventional die-casting, suction casting, and rapid quenching from the melt, have been studied. The stability of the as-cast phase(s) has been analysed by DTA. Microstructure and distribution of the constituent chemical elements was studied by SEM and STEM techniques combined with energy-dispersive X-ray spectroscopy (EDS). Magnetic thermogravimetry (M-TGA) and VSM were used for the determination of magnetic transitions.

It was shown that the as-prepared alloy structure is morphologically nearly monophase with chemically distinct dendride-like features embedded in the matrix, while the size these morphological features scaled inversely with the quenching rate. All samples contained only cubic B2-type Fe(Al, Mn, Co, Ni) phase. Large scale chemical mapping at the atomic level proved two distinct different occupancy trends, similar as to the initial B2-type structure.. Calorimetric measurements exhibited minimal transformation effect up to 1300 K, however, VSM and M-TGA indicated several magnetic transitions, their temperatures and reversibility differing with the quenching rate used to prepare the samples. Temperature dependence of magnetization and magnetic hysteresis loops of samples annealed conventionally and in external magnetic field were correlated with the evolution of microstructure in the investigated samples.

The results will be discussed with respect to the potential of tailoring the microstructure on atomic scales and magnetic properties using proper preparation routes and post-preparation processing.

Acknowledgements

The work was supported by the projects VEGA 2/0120/25, APVV-23-0281, APVV-20-0124, by joint Slovak Academy of Sciences and TÜBITAK project NOMAGRAD and by the Office of Government of Slovakia project 09I03-03-V01-00047.

Abstract ID: 30357

CRYSTALLIZATION BEHAVIOR AND SOFT MAGNETIC PROPERTIES OF ULTRA-RAPIDLY ANNEALED HIGH-Bs Fe-Co-B-Si-Cu NANOCRYSTALLINE ALLOYS

I. Škorvánek[1], B. Kunca[1], J. Marcin[1], F. Romer[2], P. Ramasamy[3], P. Švec sr.[4], P. Švec[4]

[1] *Institute of Experimental Physics, Slovak Academy of Sciences, 040 01 Košice, SLOVAKIA*
[2] *Department of Materials Science, Montanuniversitat, Leoben, AUSTRIA*
[3] *Erich Schmid Institute of Materials Science, Austrian Academy of Sciences, Leoben, AUSTRIA*
[4] *Institute of Physics, Slovak Academy of Sciences, 842 28 Bratislava, SLOVAKIA*

Rapid thermal processing has proven to be a useful tool for synthesis of Fe-based nanocrystalline soft magnetic alloys with a reduced content of non-magnetic elements, offering an attractive combination of high saturation magnetic flux density (B_s) and low coercivity (H_c) [1,2]. Special attention in this study was given to ultra-rapid annealing (URA), which involves compressing the samples between pre-heated massive copper blocks. A description of the used URA setup is available in a previous publication [3]. The influence of different thermal processing on the structure and soft magnetic properties was investigated of in series of $(Fe_{64}Co_{21}B_{10}Si_5)_{99}Cu_1$ ribbons prepared by planar flow casting. The crystallization behavior at high heating rates was investigated by Flash DSC (FDSC). The heating rates employed in the measurements ranged from 100 K/s to 10 000 K/s, similar to those reported in [4]. The structure of URA annealed samples was investigated by X-ray diffraction, SEM and STEM methods.

Pieces of as-quenched amorphous ribbons were annealed at 510 °C for 0.5 s, which was identified as the optimal ultra-rapid annealing (URA) condition for achieving the best soft magnetic properties. For comparison, the amorphous ribbons were subjected also to conventional annealing (CA) in a vacuum furnace for 30 minutes at 410 °C. Our results revealed that the high heating rate and short processing time associated with URA treatment promoted the formation of finer nanocrystalline grains, typically in the range of 15–17 nm, compared to those obtained by CA. This grain refinement significantly improved magnetic softness, reducing coercivity from 210 A/m in CA samples to 3 A/m in URA samples. The ribbons after URA processing exhibit a saturation magnetic flux density (B_s) close to 1.85 T and maintain excellent coercivity stability from room temperature up to 250 °C, which highlights their strong potential for use in magnetic components operating in high temperature environments.

Acknowledgements

This research was supported by the projects APVV 23-0281, APVV SK-AT-23-0025, VEGA 2/0148/23 and JRP NOMAGRAD.

References

[1] K. Suzuki, *et al.*, Appl. Phys. Lett. **110,** 012407 (2017).
[2] B. Kunca, *et al.*, J. Alloys Compd. **911,** 165033 (2022).
[3] B. Kunca, *et al.*, J. Magn. Magn. Mater. **591**, 171679 (2024).
[4] F. Romer, *et al.*, Materials Today Adv. **25,** 100550 (2025).

Abstract ID: 30407

OPTIMIZED MAGNETOELASTIC SENSOR FOR APPLICATIONS IN HARSH ENVIRONMENTS

A. Lasheras[1], A.C. Lopes[2,3]

[1] *University of the Basque Country (UPV/EHU), Barrio Sarriena s/n, Leioa, 48940, SPAIN*
[2] *IKERBASQUE, Basque Foundation for Science, Plaza Euskadi 5, Bilbao, 48009, SPAIN*

In this work we report the development of an optimized magnetoelastic sensor designed for operation in harsh atmospheric conditions. We studied the effect of incorporating chromium and nickel into the sensor composition to improve its corrosion resistance. We have fabricated a rhombus-shaped sensor and driven the sensor to the crystallization by thermal annealing to maximize its sensitivity. We have achieved an increase of 80% in the resonance frequency value compared to the traditional rectangular and as quenched sensor. The resulting sensor exhibits a sensitivity of 12.6 Hz/μg, representing an improvement over the commonly used magnetoelastic sensor based on the Metglas platform with similar dimensions. In addition, temperature calibration was performed to assess thermal effects on the sensor response. Corrosion tests were also carried out on both crystallized and non-crystallized sensors to evaluate the impact of thermal treatment. The obtained results demonstrate a clear enhancement in the performance, making these sensors promising candidates for applications in adverse environmental conditions.

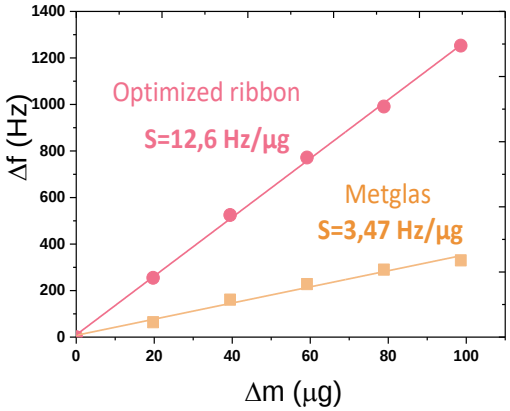

Fig. 1: *Comparison of the sensitivities between the optimized magnetoelastic sensor and the one based on Metglas with similar dimensions.*

Abstract ID: 30539

ENGINEERING SPIN TEXTURES IN FE NANODISKS FOR CELL MANIPULATION

I. Solozabal[1], R. Zurbano[1], C. Redondo[1], L.M. Alvárez-Prado[2], A. Benedicto[3], M. Vélez[2,4], R. Morales[5,6]

[1] *Department of Physical Chemistry, University of the Basque Country UPV/EHU 48940 Leioa, SPAIN*
[2] *Physics Department, University of Oviedo, 33007 Oviedo, SPAIN*
[3] *Department of Cell Biology and Histology, University of the Basque Country UPV/EHU, 48940 Leioa, SPAIN*
[4] *Centro de Investigación en Nanomateriales y Nanotecnología – CINN (CSIC – Univ. de Oviedo – Principado de Asturias), 33940 El Entrego, SPAIN*
[5] *Department of Physical-Chemistry & BCMaterials, University of the Basque Country UPV/EHU, 48940 Leioa, SPAIN*
[6] *IKERBASQUE, Basque Foundation for Science, 48009 Bilbao, SPAIN*

Magnetic nanoparticles continue to gain relevance in biomedical technologies due to their versatile physical and chemical properties. Iron oxide nanoparticles synthesized by wet-chemical routes remain the most widespread because their superparamagnetic behavior ensures zero remanence under physiological conditions. Recent advances in lithographic techniques have enabled a new generation of magnetic micro- and nanostructures with tailored spin architectures, including vortex-state microdisks with highly stable and flux-closed magnetic configurations.[1] While the vortex state has been extensively characterized in soft magnetic alloys such as Permalloy ($Ni_{80}Fe_{20}$),[2] the geometric requirements for stabilizing this spin configuration in single-element Fe nanodisks remain insufficiently understood. Fe nanomagnets are particularly appealing for biomedical applications due to their biocompatibility and high saturation magnetization.

In this work, we systematically investigate the spin textures of Fe nanodisks as a function of their diameter and thickness. The nanodisks were fabricated using top-down lithographic methods,[3] yielding structures with thicknesses from 20 to 150 nm and diameters from 200 to 1000 nm. Magnetic characterization combining magnetometry and magnetic force microscopy (MFM) allowed us to map the morphological boundaries that separate distinct spin states. Two primary magnetic phases were observed: a vortex configuration stabilized in thinner disks and a stripe-domain configuration emerging in thicker nanostructures. Both phases exhibit near-zero remanence, expanding the potential of Fe nanodisks as magnetically reconfigurable platforms for biomedical use. Micromagnetic simulations corroborate the experimentally observed magnetic textures, offering quantitative insight into the geometric factors that govern their stability.

These Fe nanomagnets were incubated *in-vitro* cell cultures to manipulate the growth and motion of living cells. Their low remanence and well-defined spin configurations enable the application of controlled magnetic stimuli, highlighting their potential as minimally invasive tools for cellular manipulation.

This work was supported by grants PID2022-136784NB and PCI2023-143369, funded by MCIN/AEI/10.13039/501100011033 and by the European Union "ERDF A way of making Europe".

References

[1] C. Collier, et *al.*, Adv. Healthc. Mater. **11**, 2101826 (2022).
[2] L. Peixoto, R. Magalhães, D. Navas, S. Moraes, C. Redondo, R. Morales, J. P. Araújo, C. T. Sousa. Appl. Phys. Rev. **7**, 011310 (2020).
[3] B. Mora, A. Perez-Valle, C. Redondo, M.D. Boyano, R. Morales, ACS Appl. Mater. Interfaces **10**, 8165 (2018).

Abstract ID: 30672

NANOSCALE-RESOLVED EPITAXY, MISFIT DISLOCATIONS AND SPIN PUMPING IN Fe/Rh BILAYERS

J. Wiemeler[1], H. Ali[2], A. Kovacs[2], I. Tarasov[1], F. Wilhelm[3], A. Rogalev[3], R. Dunin-Borkowski[2], M. Farle[1], A. Semisalova[1]

[1] *Faculty of Physics and CENIDE, University of Duisburg-Essen, 47057 Duisburg, GERMANY*
[2] *Ernst Ruska Centre for Microscopy and Spectroscopy with Electrons, Forschungszentrum Jülich, 52425, Jülich, GERMANY*
[3] *European Synchrotron Radiation Facility, 38000 Grenoble, FRANCE*

The phenomena of efficient generation, manipulation and detection of spin currents in metallic heterostructures based on metals with strong spin–orbit coupling (SOC) such as Pt (Z=78) and Pd (Z=46) are well-known in spintronics. Among 4d and 5d elements, Rh (Z=45), the direct neighbor of Pd with similar SOC, has been shown to have a high orbital Hall conductivity in addition to spin Hall conductivity, as compared to other 4d and 5d metals [1,2]. However the spin diffusion and spin mixing parameters have not been determined. Here we present a study of Rh-based epitaxial heterostructures for efficient spin-to-charge conversion and investigate the effect of interface quality and Rh polarization on spin pumping parameters. Ultrathin Fe(5,10nm)/Rh(0-15nm) bilayers have been grown on GaAs substrates at room temperature using molecular beam epitaxy in ultrahigh vacuum (5E-10 mbar) and were characterized *in situ* using low energy electron diffraction (LEED) and Auger electron spectroscopy (AES). AES and LEED experiments reveal that Rh grows in a Stranski-Krastanov-like growth mode, forming closed layers within ≈1 nm thickness [3].

We report a significant spin mixing conductance $g^{\uparrow\downarrow}_{mix} = (2.9 \pm 0.2)\cdot 10^{19}$ m^{-2} of Fe/Rh interface evaluated from frequency-dependent magnetic relaxation measured with broadband ferromagnetic resonance. The Fe/Rh bilayers grown epitaxially on GaAs(001) exhibit a large spin mixing conductance comparable to that of Pt while having a spin diffusion length $\lambda_{sd} = 9.0 \pm 1.3$ nm comparable to Pd [3]. Structural characterization performed with cross-sectional high-resolution transmission electron microscopy (HR-TEM), scanning TEM and X-ray diffraction confirmed a high crystallinity of both layers. We find an atomically sharp interface between Rh and Fe. We also find that Fe lattice is tetragonally distorted due to ≈1.4% lattice mismatch with GaAs(001) (c/a≈1.026), while fcc-Rh lattice is cubic and does not exhibit growth-induced distortions and volume strain. Geometric phase analysis (GPA) of HR-TEM images reveals the formation of periodic misfit dislocations at the interface between Rh and Fe which enable a smooth and epitaxial growth despite of the ~6% lattice mismatch between bulk bcc-Fe and fcc-Rh lattice parameters. X-ray magnetic circular dichroism (XMCD) measurements at Rh $L_{2,3}$ edge performed at room temperature showed that the induced polarization of Rh at the interface is negligible. Rougher interfaces on the other hand show a significant interface magnetic moment of Rh at room temperature. This highlights the importance of knowing the exact geometry of the location of elements at the interface for tailoring spin pumping parameters.

This work was supported by the Deutsche Forschungsgemeinschaft (DFG) within CRC/TRR270 (Project ID 405553726) and the project SE 2853/1.

References

[1] H. Kontani, T. Tanaka, D.S. Hirashima, K. Yamada, J. Inoue, PRL **102**, 016601 (2009).
[2] L. Salemi, P.M. Oppeneer, Phys. Rev. Mater. **6**, 095001 (2022).
[3] J. Wiemeler, A.-C. Aktas, M. Farle, A. Semisalova, APL **124**, 212404 (2024).

Abstract ID: 30815

UNUSUAL PHASE SHIFT BETWEEN QUANTUM OSCILLATIONS IN Sr_2RuO_4 MEASURED SIMULTANEOUSLY WITH ORGANIC BILAYER TORQUE MAGNETOMETER

D. Krstovska[1], E. Steven[2,3], E. S. Choi[3], D. Suarez[3], E. Jobiliong[4]

[1] *Faculty of Natural Sciences and Mathematics, Arhimedova str. 3, 1000, Skopje, MACEDONIA*
[2] *Emmerich Research Center, Pluit Karang Permai 12 B9 Barat no 1 and 2, DKI, Jakarta, 14450, INDONESIA*
[3] *National High Magnetic Field Laboratory and Department of Physics, 1800 East Paul Dirac Drive, Tallahassee, 1000, FL, USA*
[4] *Faculty of Science and Technology, Universitas Pelita Harapan, M.H. Thamrin Boulevard 1100 Lippo Village, Tangerang, 15811, INDONESIA*

The layered perovskite superconductor Sr_2RuO_4 is the most disorder-sensitive quantum material known. It has also been a leading candidate for a novel type of quantum computer that would enable calculations to occur over much longer time scales before suffering decoherence. Using a newly developed organic bilayer torque magnetometer [1], we performed simultaneous torque-transport measurements in Sr_2RuO_4 at low temperatures down to 410 mK and high magnetic fields up to 18 T. The measurements performed on the same sample enable determination of the phase shift between magnetic quantum oscillations of the magnetization and magnetoresistance. Below 1 K beatings in the resistance and magnetization are visible while above 1 K they are absent. We find that there is a significant phase shift of $\pi/2$ between the magnetic quantum oscillations (**Fig. 1**) which stabilizes above certain magnetic field but below that field a multiple phase shifts (in-phase, out-of-phase or $\pi/2$, depending on the temperature) between the oscillations are observed. This is a very unusual observation that might give an insight about the pairing mechanism for superconductivity in this material which has been studied for over 30 years but nevertheless, the exact nature of the pairing state still remains unresolved. We discuss the possible reasons behind the unusual phase shift behavior and its implication for superconductivity and density of states.

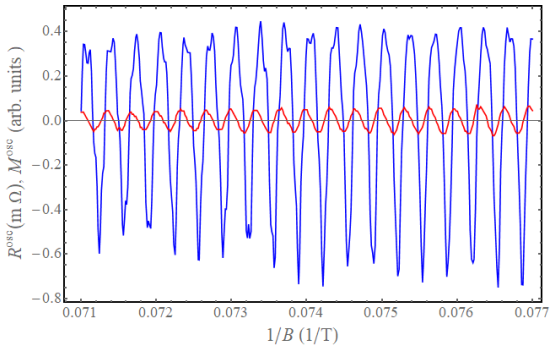

Fig. 1: *A large phase shift of $\pi/2$ between the resistance (blue) and magnetization (red) magnetic quantum oscillations in Sr_2RuO_4 is observed at T=410 mK.*

References

[1] E. Steven, D. Krstovska, D. Suarez, T. Berliani, E. Jobiliong, E. S. Choi, Sens. Actuat. A-Phys. **368**, 115133 (2024).

Abstract ID: 30153

MAGNETIC PROPERTIES AND ELECTRONIC STRUCTURE OF $FeRhGa_{1-x}Z_x$ (Z=As, Sb, Sn, Ge) ALLOYS: ab INITIO STUDY

O. Pavlukhina, V. Buchelnikov, V. Sokolovskiy

Chelyabinsk State University, 454001, Chelyabinsk, RUSSIA

Heusler-based half-metals have attracted significant interest for spintronics applications [1]. The Fe-Rh-based alloy have attracted a lot of attention due to the observation of shape memory effect [2], magnetocaloric effect [3] etc. The properties of $FeRhGa_{1-x}Z_x$ (x = 0, 0.25, 0.5, 0.75, 1) alloys are investigated by using the density functional theory calculations as implemented in the VASP package. The ab initio calculations have been carried out by using the 12-atom supercell approach. The half-Heusler alloys crystallize in non-centrosymmetric cubic structure (space group F-43m). They can crystallize in three possible configurations, namely *a*, *β* and γ phases. It is shown that the γ-phase is energetically favorable in the case of all the alloys, except for the FeRhSi alloy, for which the *β*-phase is the equilibrium one. It has been shown that the addition of a fourth element to a three-component alloy leads to a change in the position of the valence band and conduction band with respect to the Fermi level. For the three-component alloys (FeRhAs and FeRhSb) having a low spin polarization, potentialities have been demonstrated for to provide an increase in spin polarization up to 100% through the addition of a fourth element. Novel half-Heusler alloys having 100% spin polarization are predicted.

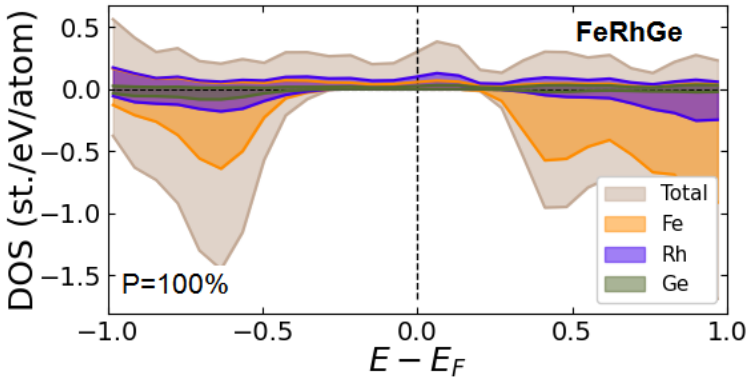

Fig. 1: *The density of electronic states for the FeRhGe alloys. Zero energy indicates the position of the Fermi level.*

References

[1] C. Felser, L. Wollmann, APL Mater. **3**, 041518 (2015).

[2] J. Winterlik, Phys Rev. B. **79**, 064508 (2009).

[3] A. Hirohata and K. Takanashi, J. Phys. D. **47**, 193001 (2014).

Abstract ID: 30611

MAGNETOSTRICTION OF Fe-Ga ALLOYS FROM FIRST PRINCIPLES AND MONTE CARLO CALCULATIONS

M. Matyunina, M. Zagrebin, V. Sokolovskiy, V. Buchelnikov

Chelyabinsk State University, 454001, Chelyabinsk, RUSSIA

Binary alloys based on iron are the focus of experimental and theoretical groups due to their magnetostriction properties [1-4]. The addition of a non-magnetic element such as Ga or Ge leads to a significant increase in the magnitude of magnetostriction [2,5]. The magnetostriction curve of the Fe-Ga alloys demonstrates two peaks of magnetostriction λ_{001} at 19 at.% ($\approx 216\times10^{6}$) and 27 at.% ($\approx 234\times10^{6}$) of Ga content [2,4,5]. Fe-Ge systems exhibit only one peak at 10 at.% ($\approx 54\times10^{6}$) of Ge content [2,6]. Moreover, the magnetostriction of Fe-Ge alloys is negative at a Ge concentration greater than 15 at.% and has a minimum at about 20 at.% ($\approx 96\times10^{6}$) [2,6].

In this study, The magnetic properties of $Fe_{100-x}Ga_x$ alloys ($15.625 \leq x \leq 21.875$ at.%) were investigated using density functional theory and Monte Carlo simulations. In order to investigate the magnetic and structural ground state properties of Fe-Ga alloys, the projector augmented wave method as implemented in VASP (Vienna ab initio simulation program) [7,8] was used. To describe exchange-correlation effects, the generalized gradient approximation according to Perdew-Burke-Ernzerhof parameterization [9] was taken into account. For all compositions, the experimentally observed cubic structures were considered as follows: *A*2 (*Im*-3*m*, α-Fe-type structure) with randomly distributed Fe and Ga atoms; $D0_3$ (*Fm*-3*m*, BiF_3-type structure) with Fe and Ga atoms fully ordered; $L1_2$ (*Pm*-3*m*, Cu_3Au-type structure) with Fe and Ga atoms fully ordered. The coefficient of tetragonal magnetostriction λ_{001} of the cubic structure as well as the magnetocrystalline anisotropy energy were determined from *ab initio* calculations for the most stable structure.

As a result of calculations, it was found that the main contribution to the magnitude of tetragonal magnetostriction is affected by the energetically favorable structures with cubic symmetry. For $Fe_{84.375}Ga_{15.625}$ and $Fe_{81.25}Ga_{18.75}$ the $D0_3$ phase is favorable, while for $Fe_{78.125}Ga_{21.875}$ the $L1_2$ phase is preferable. In general, the obtained results of the alloys considered for tetragonal magnetostriction are qualitatively in agreement with the experimental results.

This work was supported by grant No. 26-12-20023 of the Russian Science Foundation.

References

[1] G. Petculescu, J.B. LeBlanc, M. Wun-Fogle, *et al.*, J. Appl. Phys., **105**, 07A932 (2009).
[2] J.B. Restorff, M. Wun-Fogle, K.B. Hathaway, *et al.*, J. Appl. Phys., **111**, 023905 (2012).
[3] I.S. Golovin, A.M. Balagurov, I.A. Bobrikov, J. Cifrec, J. Alloys Compd., **688**, 310 (2016).
[4] T.A. Lograsso, A.R. Ross, D.L. Schlagel, *et al.*, J. Alloys Compd., **350**, 95 (2003).
[5] A.E. Clark, K.B. Hathaway, M. Wun-Fogle, *et al.*, J. Appl. Phys., **93**, 8621 (2003).
[6] D. Wu, Q. Xing, R.W. McCallum, and T.A. Lograsso, J. Appl. Phys., **10**, 07B307 (2008).
[7] G. Kresse, J. Furthmüller, Phys. Rev. B, **54**, 11169 (1996).
[8] G. Kresse, D. Joubert, Phys. Rev. B, **59**, 1758 (1999).
[9] J.P. Perdew, K. Burke, M. Ernzerhof, Phys. Rev. Lett., **77**, 3865 (1996).

42 - NOVEL MAGNETORESISTANCE AND SPIN-CHARGE INTERCONVERSION

Abstract ID: 30076

UNUSUAL ANISOTROPIC MAGNETORESISTANCES IN VAN DER WAALS MAGNETIC INTERFACES

Q. Chen[1,2], Y. Zhai[1], X. Wang[3,4], K. Xia[1]

[1] *Key Laboratory of Quantum Materials and Devices of Ministry of Education, School of Physics, Southeast University, Nanjing, 211189, CHINA*
[2] *Department of Materials Science and Engineering, National University of Singapore, Singapore 117575, SINGAPORE*
[3] *School of Science and Engineering, Chinese University of Hong Kong, Shenzhen, Shenzhen 518172, CHINA*
[4] *Department of Physics, The Hong Kong University of Science and Technology, Clear Water Bay, Kowloon, Hong Kong, CHINA*

Interfaces have long been used to impart functionalities unattainable in bulk materials. In spintronics, ferromagnet/nonmagnet (FM/NM) interfaces provide the foundation for spin-current-based phenomena. The emergence of two-dimensional (2D) van der Waals (vdW) magnets opens a new frontier in spintronics, where stacked atomic layers with weak interlayer bonding, naturally host ultrasharp interfaces that strongly influence magnetoelectric transport.

In this talk, we will first discuss the unusual anisotropic magnetoresistance (UAMR) in 2D stacked ferromagnetic Fe_3GeTe_2 (FGT) layers [1]. The UAMR exhibits universal behaviors widely observed in various FM/NM bilayers but with distinct features: it shows no thickness dependence up to several hundred nanometers, displays high-order angular oscillations-up to the 8th order-in planes perpendicular to the film, and reaches an out-of-plane magnitude nearly an order of magnitude larger than the in-plane AMR. These characteristics cannot be accounted for by spin-Hall-related mechanisms based on spin/orbital current and charge current interconversion, but align both qualitatively and quantitatively with the predictions of the two-vector magnetoresistance (MR) theory [2], particularly its sum-rule constraints.

We further construct an all-vdW WTe_2/Fe_3GaTe_2 (FGaT) heterostructure where WTe_2 hosts hole-electron resonance, and observe a giant UAMR of up to 289% [3]. This large response originates from sustained carrier-interface interactions enabled by Lorentz-force-driven charge imbalance. This phenomenon lies beyond conventional spin-accumulation-based descriptions developed for electron-dominated systems. Nevertheless, its angular characteristics can still be accommodated within the broader two-vector MR framework, which provides a general mathematical basis for all allowable angular forms of magnetoresistances.

These findings suggest that interfacial engineering can serve as a viable route to tuning magnetoelectric transport in low-dimensional magnetic systems, highlighting the important role of hidden interfacial fields in vdW materials.

References

[1] Q. Chen, *et al.*, Adv. Sci. **12**, e08244 (2025).

[2] X. Wang, *et al.*, Sci. Rep. **13**, 309 (2023).

[3] Q. Chen, *et al.*, submitted (2025).

Abstract ID: 30078

ON THE ANGULAR DEPENDENCE OF ANOMALOUS HALL CURRENT

K. Xia

School of Physics, Southeast University, Nanjing, 211189, CHINA

The transverse current (j_H) due to anomalous Hall effect (AHE) is usually assumed to be perpendicular to the magnetization (m) in ferromagnetic materials, which governs the experiments in spintronics. Generally, this assumption is derived from a continuum model, where the crystal's discrete symmetry is effectively represented by the concept of an effective mass from the band structure.

In this talk, we present a calculation on the spin transport through the nonmagnetic metal (NM) | ferromagnetic metal (FM) interfaces and find that the corresponding Hall current is generally not perpendicular to m with only a few exceptions at high symmetry crystal orientations. The calculation illustrates the breakdown of $j_H = \Theta m \times j_c$, where Θ denotes the anomalous Hall angle and j_c represents the injecting charge current.

We develop an analytical theory based on the discrete symmetry of the solid to describe this effect. In this framework, the leading order corresponds to the conventional anomalous Hall effect (AHE), while higher-order terms account for deviations in the Hall current, which are linked to the multipolar Berry curvature. Additionally, we identify the presence of a chiral anomalous Hall effect (CAHE) in systems with odd rotational symmetry (e.g., C3v). The general existence of multipolar effects in spin-charge conversion is also demonstrated, which highlight the significance of discrete crystal symmetry for spin transport.

References

[1] X. R. Wang, Communications Physics **4**, 55 (2021).

[2] L. Li, J. Sun, L. Wang, X. R. Wang, and K. Xia, Phys. Rev. B **112**, 014403 (2025).

[3] C. Niu, L. Li, Y. Wang, L. Wang and K. Xia, arXiv:2508.19033 submitted (2025).

Abstract ID: 30113

CLASSIFY PURE SPIN CURRENT ORIGIN WITH SYMMETRY ANALYSIS

H. Ding

Department of Physics, Nanjing University, 210093, Nanjing, CHINA

Spin current and the related spin-orbit torque are crucial for spintronic applications, including magnetic random access memory and spin current logic devices. Various methods have been reported to generate pure spin current, including the spin Hall effect, Rashba-Edelstein effect, spin splitting effect etc. These mechanisms induced phenomena are typically similar, making it difficult to distinguish them.

In this talk, I will present systematic methods to distinguish different spin-charge conversion mechanisms based on the symmetry analysis and the reciprocal relation of the spin-charge inter-conversion. We identified the Rashba-Edelstein effect in Ag/Bi-ferromagnetic metal interface and solved the debate about the spin transport picture in Ag/Bi related systems [1], isolated the anisotropic spin Hall effect and spin splitting effect contributions in RuO_2 [2], observed the anamolus spin Hall effect in Py and realized field-free switching of perpendicularly magnetized YIG with the z-polarized spin current [3]. The classification of different mechanisms may provide opportunity to enhance the efficiency of pure spin current generation and related spintronics devices.

References

[1] J. Cheng, *et. al.*, Phys. Rev. Lett. **129**, 097203 (2022).

[2] Z. Q. Wang, *et. al.*, Phys. Rev. Lett. **133**, 046701 (2024).

[3] M. Yang, *et.al.*, Nat. Commun. **15**, 3201 (2024)..

Abstract ID: 30141

EVIDENCE FOR STRONG LOCALIZATION OF ORBITAL POLARIZATION

L. Zhu[1,2]

[1] *State Key Laboratory of Semiconductor Physics and Chip Technologies, Institute of Semiconductors, Chinese Academy of Sciences, Beijing 100083, CHINA*
[2] *Center of Materials Science and Optoelectronics Engineering, University of Chinese Academy of Sciences, Beijing 100049, CHINA*

Whether orbital polarization propagates has become the most essential question of the blooming subject that aims to generate non-local orbital torque and orbital pumping. Recent theories have suggested a strong orbital Hall effect within the several heavy and light metals, providing ideal platforms for experimental verification of possible orbital transport effects. In this talk, I will report robust experimental evidence for the strong localization of orbital polarization [1,2], which are essential advances towards solving the essential orbital torque debate.

References

[1] Q. Liu, L. Zhu, *Absence of orbital current torque in Ta/ferromagnet bilayers*, Nature Communications, **16**, 8660 (2025).

[2] T. Zhang, L. Zhu, Z. Yan, L. Zhu, *Evidence for strong localization of orbital polarization*, arXiv:2512.07102.

Abstract ID: 30158

SPIN-CHARGE INTERCONVERSION AND ITS APPLICATIONS IN 1D TO 3D MAGNETIC FIELD SENSING

Y. Wu

Department of Electrical and Computer Engineering, National University of Singapore, SINGAPORE

Spin–charge interconversion (SCI) lies at the heart of both fundamental studies of the interplay between charge and spin in condensed matter and a wide range of emerging applications, including magnetic memory, sensors, oscillators, energy harvesting, and non-von Neumann computing architectures. Leveraging key SCI phenomena such as spin Hall magnetoresistance and spin–orbit torque, we have conceptualized and developed several 1D, 2D, and 3D magnetic field sensors that overcome key limitations of conventional magnetoresistive sensors, particularly their reliance on complex magnetic biasing schemes to achieve linear response. Despite their remarkably simple structure, these sensors deliver a linear output proportional to the external magnetic field while exhibiting negligible hysteresis, minimal offset drift, and ultra-low noise. The talk will detail the underlying physical mechanisms, scalable fabrication processes, and key performance characteristics of these devices, as well as future prospects for SCI in advanced magnetic sensing [1–4], supported by proof-of-concept demonstrations in real-world applications such as current and position sensing, 3D magnetic field mapping, and biomedical sensing.

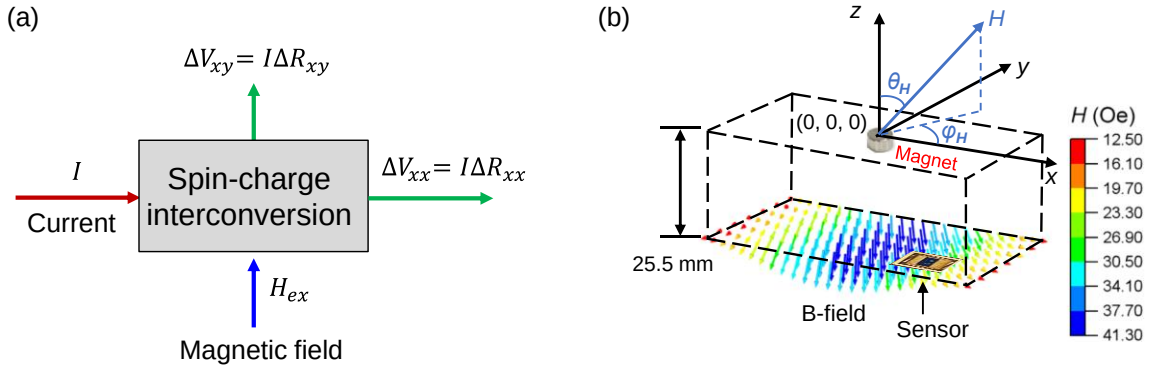

Fig. 1: *(a) SCI-based magnetic sensor; (b) 3D field mapping using spin-orbit torque sensor.*

References

[1] Y. Xu, Y. Yang, M. Zhang, Z. Luo, Y. Wu, *Ultrathin All-in-One Spin Hall Magnetic Sensor with Built-In AC Excitation Enabled by Spin Current*, Adv. Mater. Technol., **3 (8)**, 1800073 (2018).

[2] H. Xie, X. Chen, Z. Luo, Y. Wu, *Spin Torque Gate Magnetic Field Sensor*, Phys. Rev. Appl., **15**, 024041 (2021).

[3] X. Chen, H. Xie, H. Shen, Y. Wu, *Vector Magnetometer Based on a Single Spin-Orbit-Torque Anomalous-Hall Device*, Phys. Rev. Appl., **18**, 024010 (2022).

[4] Y. Wu, Y. Xu, Z. Luo, Y. Yang, H. Xie, Q. Zhang, X. Zhang, *Charge-Spin Interconversion and Its Applications in Magnetic Sensing*, J. Appl. Phys., **129**, 060902 (2021).

Abstract ID: 30232

TENSOR ANALYSIS, CHARGE-SPIN INTERCONVERSION, AND MAGNETORESISTANCE

X. Wang

The Chinese University of Hong Kong (Shenzhen), Shenzhen 51817, CHINA

Two themes in spintronics are the control of electric current by the magnetic states and the control of magnetic state by electric current. Magnetoresistance (MR) is the central concept of the first theme while spin-current generation from charge current is the fundamental concept of the latter. I will show that tensor analysis is a powerful approach to reveal the universal features of these two important concepts in spintronics. Spin-Hall effects (SHE) is one of the most important methods for spin current generation while the widely used to inverse SHE (ISHE) is the only known way for spin current detection. However, spin-polarization and propagation direction of spin current from SHE must both perpendicular to the charge current and mutually perpendicular with each other. This constrains limits greatly the effectiveness of the spin current in their magnetization control, especially for perpendicularly magnetized memory device. Thus, it is desirable to have capabilities of generating spin current of arbitrary form, especially colinear spin current whose spin polarization and propagation direction are parallel to each other. Although such spin current has reported in various materials involve vector parameters such as magnetization, crystalline axis etc., a general understanding of such spin current generation and its underlying physics is still lacking. In this talk, I will use tensor analysis to discuss the most general form of a spin current generated from a charge current when such an interconversion involves vector order parameter [1]. Indeed, the predictions from the vector analysis have been confirmed by various experiments [2-4]. Another surprising discovery in spintronics in recent years is probably all kinds of universal anisotropic MR (UAMR) in nanoscale magnetic/non-magnetic bilayers at lower current density, as well as the universal unidirectional magnetoresistance (UMR) under high current density. Current understanding often involves various mechanisms related to the interconversion of charge current and spin current, giant magnetoresistance, thermal magnonic effects, thermoelectric effects, and diverse spin dependent scattering processes. This raises a fundamental question: do the universal behaviors observed in a wide range of systems stem from underlying general principles? Again, tensor analysis demonstrates that both UMR and unusual anisotropic magnetoresistance (UAMR) [5], another universal phenomenon in magnetic bilayers, arise from electron transport influenced by the magnetization vector present in the magnetic material and the interfacial potential inherent in heterostructures. Specifically, UAMR represents current-independent resistance (resistivity) of bilayers. UMR is the resistance proportional to the current although electron transports of the bilayers are the linear response to high current densities and their induced thermal gradients. Our theory introduces a novel approach that considers the interplay between the magnetization vector, thermal gradients, and the effective internal electric field at the interface [6]. This framework provides a unified explanation for both UMR and UAMR, effectively capturing key experimental features such as dependence on current direction, magnetization orientation, film thickness, and magnetic field strength [7-9]. Furthermore, it offers a universal perspective that bridges UMR and UAMR effects, enhancing our understanding of spin-dependent transport phenomena in bilayers.

References

[1] X. R. Wang, Communications Physics **4**, 55 (2021).

[2] M. Yang, B. Miao, J. Cheng, K. He, X. Yang, Y. Zeng, Z. Wang, L. Sun, X. R. Wang, A. Azevedo, S. Bedanta, H. F. Ding, Phys. Rev. B **105**, 224426 (2022).

[3] M. Yang, L. Sun, Y. Zeng, J. Cheng, K. He, X. Yang, Z. Wang, L. Yu, H. Niu, T. Ji, G. Chen, B. Miao, X. R. Wang, and H. F. Ding, Nature Communications **15**, 3201 (2024).

[4] H. Xie, Z. Mu, Y. Si, J. Wang, X. R. Wang, and Y. Wu, Adv. Mater. 2408340 (2024).

[5] X.R. Wang, C. Wang, X. S. Wang, Sci. Rep. **13**, 309 (2023).

[6] X. R. Wang, Phys. Rev. B **112**, 094451 (2025).

[7] L. Zhu, Q. B. Liu, and X. R. Wang, National Science Review **12**, nwaf240 (2025).

[8 Q. Chen, J. Sun, J. Liang, W. Jiang, Z. Yu, Z. Zeng, Y. Zhai, K. Xia, and X. R. Wang, Advanced Science e08244 (2025).

[9] M. Q. Dong, Zhi-Xin Guo, and X. R. Wang, Phys. Rev. B **108**, L020401 (2023).

Abstract ID: 30260

UNCONVENTIONAL SPIN CURRENT AND SPIN TORQUE ARISING FROM MAGNETIC STRUCTURES

H. Wu[1,2]

[1] *Dongguan Institute of Materials Science and Technology, Chinese Academy of Sciences, Dongguan, Guangdong 523808, CHINA*
[2] *Songshan Lake Materials Laboratory, Dongguan, Guangdong 523808, CHINA*

Spin-orbit torque (SOT) is a novel mechanism for all-electrical control of magnetism, enabling the development of read-write decoupled devices and thereby overcoming the physical limitations of current Magnetic Random-Access Memory (MRAM). In this work, we employ a material-design strategy based on magnetic gradient to induce a non-collinear magnetic intermediate state via SOT. The intrinsic Dzyaloshinsky–Moriya (DM) interaction then breaks the chiral symmetry, enabling deterministic zero-field SOT switching of perpendicular magnetization. Building on this, we further design a dual-magnetic-layer structure as the free layer of a magnetic tunnel junction (MTJ). By exploiting the interlayer DM coupling between the two magnetic layers, we realize zero-field SOT writing for perpendicular-anisotropy MTJs. Beyond collinear magnetic gradients, we design a non-collinear exchange-spring magnetic structure composed of perpendicular-in-plane composite heterostructures. The interaction between the y-spin and the non-collinear exchange-spring texture in the x-z plane induces spin reorientation, generating x- and z-spin polarizations, which in turn enables zero-field SOT manipulation of perpendicular magnetization. Finally, based on the control of the Néel order direction in altermagnetic materials, we utilize the spin-splitting torque to generate a tilted spin polarization collinear with the Néel order, thereby achieving zero-field, all-electrical writing for perpendicular MTJs. The zero-field SOT manipulation mechanisms via magnetic structure regulation provide a material and physical foundation for next-generation SOT-MRAM technology.

References

[1] H. Wu, J. Nance, S. A. Razavi, D. Lujan, B. Dai, Y. Liu, H. He, B. Cui, D. Wu, K. Wong, K. Sobotkiewich, X. Li, G. P. Carman, and K. L. Wang, Nano Lett. **21**, 515 (2021).

[2] C. Wu, S. Cui, Y. Guo, Z. Zhang, J. Zhang, X. Deng, G. Zeng, C. Ren, P. Li, X. Zhou, X. Zhang, J. Li, T. Zhu, X. Han, J. Zhao, H. Wang, Y. Zhang, S. Liang, and H. Wu, Adv. Mater. **137**, 2414139 (2025).

[3] Y. Guo, J. Zhang, Z. Zhu, Y. Jiang, L. Jiang, C. Wu, J. Dong, X. Xu, W. He, B. He, Z. Huang, L. Du, G. Zhang, K. Wu, X. Han, D. Shao, G. Yu, and H. Wu, Adv. Sci. **11**, 2400967 (2024).

[4] Y. Guo, A. Chen, Z. Zeng, T. An, Q. Cui, Y. Ga, D. Zheng, X. Deng, X. Zhang, M. Tang, Z. Zhu, C. Wu, J. Zhang, W. Song, P. Yan, T. Zhu, S. Wang, X. Han, K. L. Wang, G. Yu, X. Zhang, and H. Wu, Nat. Commun. (2025).

43 - ORBITRONICS

Abstract ID: 30167

CURRENT INDUCED SPIN DYNAMICS MEDIATED BY ORBITAL EXCHANGE INTERACTION

G.-H. Lee

Department of Physics, Korea Advanced Institute of Science and Technology (KAIST), Daejeon 34141, REPUBLIC OF KOREA

Spin-orbit torque (SOT) is a key concept in spintronics, enabling crucial applications such as current-induced magnetization switching [1], magnetic soliton dynamics [2], and GHz spin-torque oscillation [3]. Historically, SOT was attributed to spin currents arising from the Rashba effect or the spin Hall effect. However, recent understanding reveals that SOT is a combined effect of spin-orbit interaction (SOI) with either the orbital Rashba effect (ORE) [4] or the orbital Hall effect (OHE) [5].

The underlying mechanism involves the accumulation of orbital density via ORE or OHE. This orbital density is subsequently converted into spin density through SOI, and it is this resulting spin density that ultimately generates SOT. While much research is dedicated to improving the efficiency of SOT or orbital torque [6] by optimizing SOI and discovering materials that produce large orbital density [7, 8], there remains a need to investigate the direct, unique consequences of orbital density itself, independent of SOT.

Our investigation focuses on the orbital exchange interaction [9]. This mechanism provides a direct pathway for interaction between the accumulated orbital density and the orbitals of ferromagnets, unlike the more conventional orbital torque. Our theoretical findings predict that orbital density directly modifies the magneto-crystalline anisotropy, magnetic damping, and the gyromagnetic ratio—effects that are not expected when considering only spin density. We propose two experimental methods to validate these theoretical predictions.

This work illuminates the unique role of orbital current within conventional spin-orbitronic devices. Furthermore, these findings have the potential to be extended to the control or detection of exotic materials, such as altermagnets, where electron orbitals are fundamentally important.

References

[1] I. M. Miron, *et al.*, Nature **476**, 189 (2011).

[2] S. Emori, *et al.*, Nat. Mater. **12**, 611 (2013).

[3] V. E. Demidov, *et al.*, Nat. Mater. **11**, 1028 (2012).

[4] S. R. Park, *et al.*, Phys. Rev. Lett. **107**, 156803 (2011).

[5] D. Go, *et al.*, Phys. Rev. Lett. **121**, 086602 (2018).

[6] D. Go and H. Lee, Phys. Rev. Res. **2**, 013177 (2020).

[7] D. Lee, *et al.*, Nat. Commun. **12**, 6710 (2021).

[8] S. Lee, *et al.*, Commun. Phys. **4**, 234 (2021).

[9] P. Santini, *et al.*, Rev. Mod. Phys. **81**, 807 (2009).

Abstract ID: 30268

NONLOCAL AND DYNAMICAL ORBITAL TRANSPORT IN OXIDIZED Cu

L. Liao[1,2], Y. Otani[2]

[1] *School of Information Science and Technology, ShanghaiTech University, 201210, Shanghai, CHINA*
[2] *Institute for Solid State Physics, University of Tokyo, 277-8581, Kashiwa, JAPAN*

Current-induced nonequilibrium orbital angular momentum (OAM) offers a promising method to manipulate nanomagnets efficiently using light elements. In this talk, I will introduce recent progress on orbital transport in oxidized Cu, utilizing nonlocal transport devices and soft X-ray spectroscopy. We experimentally test the Onsager reciprocity of orbital transport in an orbital Edelstein system by utilizing nonlocal transport (Fig.1). Remarkably, we observe that the direct and inverse orbital-charge conversion processes produce identical electric voltages, confirming Onsager reciprocity in orbital transport. Additionally, we find that the orbital decay length, approximately 100 nm at room temperature, is independent of Cu thickness and decreases with lowering temperature, revealing a distinct contrast to spin transport behavior. The orbital accumulation can also be detected via soft X-ray spectroscopy, with an element-selective energy resolution to clarify the origin of the orbital accumulation. Our findings provide insights into the reciprocity, nonlocal correlation and dynamics of the charge-orbital interconversion in oxidized Cu.

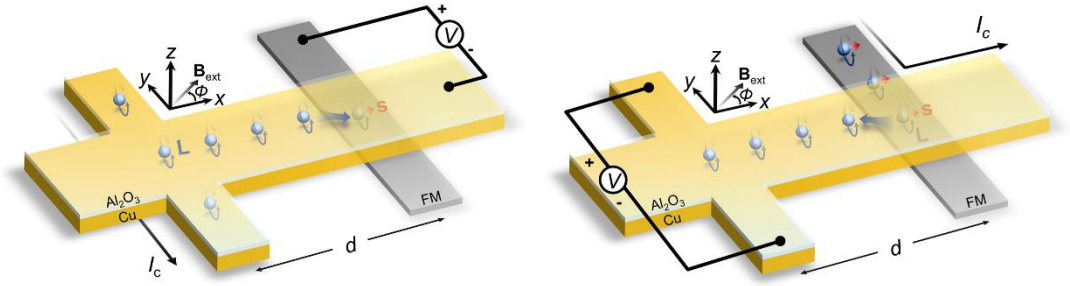

Fig. 1: *Left: The nonlocal measurement configuration to observe charge-to-orbital conversion (direct measurement). The nonequilibrium OAM are generated by charge current I_c at the Al_2O_3/Cu interface through charge-to-orbital conversion. The orbital accumulation then converts into spin via spin-orbit coupling in ferromagnets (FM) and induces a nonlocal response V. Right: The nonlocal measurement configuration to observe orbital-to-charge conversion (inverse measurement). Charge current extras nonequilibrium OAM from FMs. The orbital accumulation then converts to charge current at the Al_2O_3/Cu interface through orbital-to-charge conversion.*

Abstract ID: 30484

X-RAY DETECTION OF CURRENT-INDUCED ORBITAL ANGULAR MOMENTUM ACCUMULATION AT Cu/OXIDE INTERFACES

P. Pradeep[1], P. Olleros[2,3], A. Gudin[2], G. Orero-Gámez[1], H. Madathil[1], A. Guedeja-Marrón[4], M. A. Niño[5], M. Varela[4], F. Ajejas[2], M. Foerster[5], P. Perna[2], S. Vélez[1]

[1] *Spintronics and Nanodevices Laboratory, Universidad Autónoma de Madrid, E-28049 Madrid, SPAIN*
[2] *IMDEA Nanociencia, Campus de Cantoblanco, E-28049 Madrid, SPAIN*
[3] *CUNEF Universidad, Campus Almansa, E-28040 Madrid, SPAIN*
[4] *Departamento de Física de Materiales, Universidad Complutense de Madrid, E-28040 Madrid, SPAIN*
[5] *ALBA Synchrotron Light Facility, CELLS, E-08290 Bellaterra, SPAIN*

Orbital angular momentum currents generated from current flow in light materials and interfaces have emerged as a promising route for operating magneto-electronic devices. However, most experiments to date relied on indirect techniques based on orbit-to-spin conversion to investigate orbital phenomena. Here, we report the direct detection of orbital angular momentum accumulation driven by electric currents at Cu/oxide interfaces via x-ray circular dichroism (XMCD) experiments across the $L_{2,3}$ absorption edges of Cu [1]. Our experiments reveal a dominant orbital origin of the detected signals with an estimated average orbital momentum at the probing depth of the x-ray beam of $(-2.1 \pm 0.2) \times 10^{-12}$ and $(-0.84 \pm 0.36) \times 10^{-12}$ $\mu_B A^{-1} cm^2$ in Cu/CuO_x and Cu/AlO_x, respectively, per Cu atom. By considering the orbital diffusion length and relaxation time inferred from transport experiments in Cu, we estimate the charge-orbit conversion efficiency at the Cu/CuO_x interface to be ~5 times that of the effective charge-to-spin conversion efficiency in Pt. Our results are also consistent with spin-orbit torque measurements performed in Co/Pt/Cu(x)/oxide samples, showing that XMCD synchrotron techniques can be used to disentangle spin and orbit contributions and quantify charge-to-orbit conversion efficiencies.

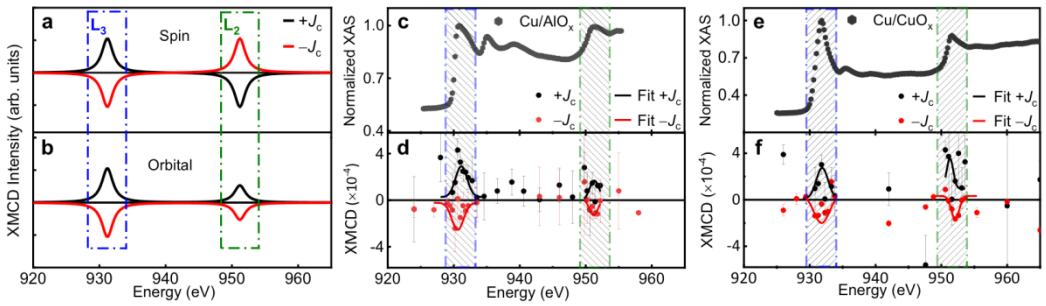

Fig. 1: *(a),(b) Expected XMCD signal for the detection of angular momentum of pure spin and orbital origin in a system with positive Rashba coefficient. (c),(e) X-ray absorption in Cu(10nm)/AlO_x and Cu(20nm)/CuO_x. (d),(f) XMCD spectra obtained at different current densities and current polarities in both Cu/AlO_x and Cu/CuO_x [$|J_c| = +4{,}5 \times 10^7$ Acm^{-2} in (d), and $|J_c| = +1{,}6 \times 10^7$ Acm^{-2} in (f)]. The lines are Gaussian fits to the data points at the L_3 and L_2 absorption edges (dashed regions). The error bars in (d), (f) are the uncertainty in the estimates of the XMCD signal from PEEM images (Figs. 1b,c).*

References

[1] P. Pradeep, *et al.*, submitted.

Abstract ID: 30528

ORBITRONICS WITH ORBITAL MAGNETS: MAGNETORESISTANCE, PUMPING AND BEYOND

S. Krishnia[1], C. Schmitt[1], O. Ledesma[1], D. Kumar[1], A. Do[1], E. Saitoh[2], O. Gomonay[1], G. Jakob[1], Y. Mokrousov[1], M. Kläui[1,3]

[1] *Institute of Physics, Johannes Gutenberg University Mainz, Mainz, GERMANY*
[2] *Department of Applied Physics, The University of Tokyo, Tokyo, JAPAN*
[3] *Center for Quantum Spintronics and Department of Physics, NTNU, Trondheim, NORWAY*

The Generation and transport of orbital angular momentum (OAM) current in solids have gained significant theoretical and experimental interest in recent years with the advent of a new research field called orbitronics [1–3]. Unlike spintronics, where the generation of spin current from charge current relies on relatively weak spin–orbit coupling (SOC) mechanisms (such as in Pt), OAM current can be directly generated from charge current because the crystal momentum of charge carriers (i.e., electrons) couples directly to their orbital angular momentum. This leads to a more robust and orders-of-magnitude larger current-induced OAM generation, even in light, abundant, inexpensive, and environmentally friendly materials (Cu, Al, Cr and Ti). These advantages position new emerging field of orbitronics as a promising platform for future energy-efficient information processing, storage, and neuromorphic technologies [3,4].

In this talk, I will present recent experimental results demonstrating a large enhancement of torques on 3d-ferromagnetic layers by employing various light elements. We utilize these orbital torques to reduce the switching power of magnetic memory bits by up to 50% [5,6]. Next, in non-local device geometries, we observe non-reciprocal transport behavior when using Ru as an OAM current source [7]. Going beyond the convential spin-based magnets, we have identified a new class of magnetic materials, including some oxides and rare-earth nitrides, in which the orbital angular momentum contributes significantly (and in some cases even dominates) to the net magnetization. In these materials the orbital moments provide a direct pathway for interaction between OAM current and static orbital magnetization, thereby eliminating the need for orbital-to-spin conversion and allowing to harness the full potential of orbitronics effects. By integrating such materials into all-orbitronic device, we demonstrate up to two orders of magnitude enhancement in orbitronic effects, paving the way for next-generation, energy efficient all-orbital green devices [8].

References

[1] D. Go, *et al.*, Phys. Rev. Lett., **121**, 086602 (2018).
[2] S. Ding, *et al.*, Phys. Rev. Lett., **125**, 177201 (2020).
[3] D. Go, *et al.*, EPL, **135**, 37001 (2021).
[4] G. Beneke, S. Krishnia, *et al.*, Nat. Commun. **15**, 8103 (2024).
[5] R. Gupta, *et al.*, Nat. Commun. **16**, 130 (2025).
[6] N. Sebe, S. Krishnia, *et al.*, arXiv:2512.18419 (2025).
[7] J. Ledesma, S. Krishnia, *et al.*, Nano Lett. **25**, 3247 (2025).
[8] C. Schmitt, S. Krishnia, *et al.*, under review.

Abstract ID: 30699

PHONON-DRIVEN MANIPULATION OF ORBITAL CURRENTS IN LIGHT TRANSITION METALS

M. Rovirola[1,2], J. Òdena[1,2], A. Castellví[1,2], Q. Badosa[1,2], J. M. Hernàndez[1,2], B. Casals[2,3], S. Vélez[4,5], F. Macià[1,2]

[1] *Dept. of Condensed Matter Physics, University of Barcelona, 08028 Barcelona, SPAIN*
[2] *Institute of Nanoscience and Nanotechnology (IN2UB), University of Barcelona, 08028 Barcelona, SPAIN*
[3] *Dept. of Applied Physics, University of Barcelona, 08028 Barcelona, SPAIN*
[4] *IFIMAC and Departamento de Física de la Materia Condensada, Universidad Autónoma de Madrid, 28049 Madrid, SPAIN*
[5] *Instituto Nicolás Cabrera, Universidad Autónoma de Madrid, 28049 Madrid, SPAIN*

Orbital angular momentum is a promising information carrier in solids, yet its coherent generation remains challenging in weak–spin–orbit systems. We demonstrate that chiral surface acoustic waves (SAWs) can efficiently generate and control orbital currents in ferromagnet | light-metal bilayers.

Using circularly polarized Rayleigh waves in Ni- and Co-based heterostructures with Cr, Ti, or Al caps, we identify two phonon-driven mechanisms: the acoustic orbital Hall effect (AOHE), originating from lattice vorticity, and acoustic pumping (AP) due to magnetoelastic coupling (see Fig 1). By decomposing the SAW-induced voltage into field-even and field-odd components, we can unambiguously separate these two contributions.

Strong orbital signals appear in Ni|Cr and Ni|Ti, while Ni|Al and Co-based bilayers show negligible response [1]. We further performed spin-torque ferromagnetic resonance and second-harmonic Hall measurements and found that electrically generated orbital currents are significantly weaker, demonstrating that phonons are far more efficient for orbital angular momentum manipulation than charge currents. These findings position SAWs as a powerful platform for orbitronics and phonon-controlled magnetism.

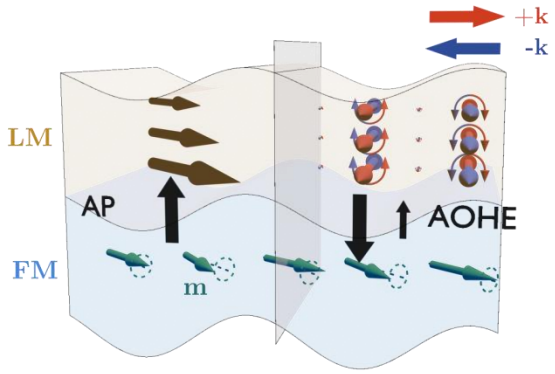

Fig. 1: *Schematics of AP (left side) and AOHE (right side).*

References

[1] M. Rovirola, *et al.*, arXiv: 2512.08385

Abstract ID: 30832

WHY ORBITAL CURRENTS APPEAR SHORT- OR LONG-RANGED: GENERALIZED ORBITAL DIFFUSION WITH MULTIPLE LENGTH SCALES

J. Sohn, S. Han, H.-W. Lee

Department of Physics, Pohang University of Science and Technology, Pohang, KOREA

The orbital angular momentum of an electron is attracting significant attention as a novel tool for energy-efficient information processing. Although numerous studies have investigated how long orbital angular momentum can survive in solids without being quenched, the measured relaxation lengths vary drastically, ranging from 1 nm to 70 nm. [1-3] This wide discrepancy makes it highly challenging to theoretically understand the underlying mechanisms of orbital propagation.

Using quantum transport simulations, we calculated the orbital relaxation lengths under two distinct conditions: generating an orbital current via an orbital magnetic field, and via the orbital Hall effect. We discovered that the orbital relaxation length significantly depends on the generation method. When the orbital current is driven by an orbital magnetic field, the relaxation length is exceptionally short, at approximately 1 nm. In contrast, when generated via the orbital Hall effect, it exhibits a much longer relaxation length of approximately 10 nm. Crucially, the long-range relaxation of the orbital current generated by the orbital Hall effect is not described by the conventionally expected diffusion of orbital angular momentum, but rather by the diffusion of "orbital angular position"—an orbital degree of freedom that has been largely overlooked until now.

Our findings not only provide a comprehensive framework to reconcile the conflicting results reported in various studies on orbital currents but also offer a fresh perspective on how to control and utilize them. Furthermore, because "orbital angular position" is a novel concept with no analogue in spin degrees of freedom, it is anticipated to give rise to uniquely orbital-driven transport phenomena that are fundamentally distinct from spin transport.

References

[1] Y. Choi, *et al.*, Nature, **619,** 52–56 (2023).
[2] T. Guan, *et al.*, Nat. Nano. (2026).
[3] M. Rang, *et al.*, Phys. Rev. B **109**, 214427 (2024).

Abstract ID: 30477

EFFICIENT MAGNETIC MANIPULATION VIA SUPERCONDUCTOR-ENHANCED SPIN-ORBIT TORQUES

R. Zhang[1], P. Li[2]

[1] *Huazhong University of Science and Technology, School of Integrated Chips, 430074, Wuhan, CHINA*
[2] *University of science and technology of China, School of Microelectronics, 230026, Hefei, CHINA*

The integration of non-volatile magnetic memory with superconducting logic is pivotal for the advancement of cryogenic computing and quantum information technologies. However, achieving efficient magnetic manipulation at liquid helium temperatures with a minimal thermal budget remains a formidable challenge. Here, we investigate the generation of spin-orbit torque in a superconductor/metal/ferromagnet heterostructure. By utilizing harmonic Hall measurements, we observe a distinct second-harmonic signal that reveals a dramatic enhancement of SOT efficiency as the system transitions into the superconducting state. We attribute this giant enhancement to a resonant skew-scattering mechanism: the interfacial inversion symmetry breaking at the superconductor/metal interface induces a static Rashba spin texture, while the divergence of the quasiparticle density of states at the superconducting coherence peaks acts as a spectral magnifier [1,2], resonantly increasing the scattering cross-section. Our findings provide a microscopic understanding of spin-charge conversion mediated by superconducting quasiparticles and offer a promising pathway for realizing ultra-low-power magnetic manipulation in future cryogenic spintronic architectures.

(a)

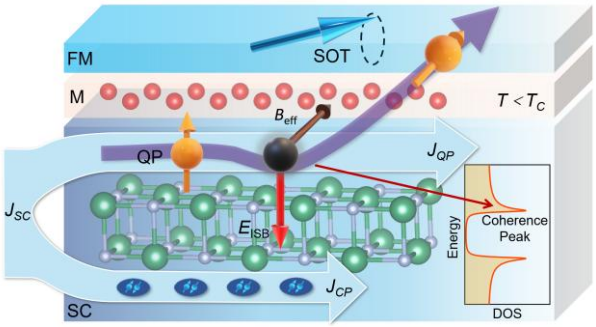

(b)

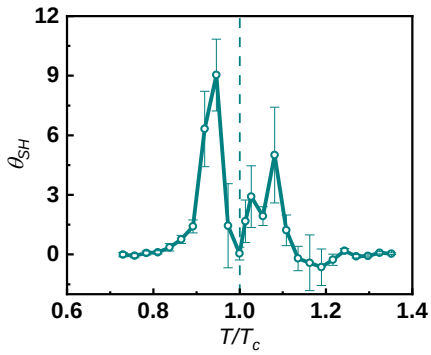

Fig. 1: *(a) Schematic illustration of the coherence-peak-assisted resonant SOT enhancement mechanism; (b) Giant SOT enhancement near T_c. The SOT efficiency shows a sharp increase below the transition temperature, peaking at 0.96 T_c, which indicates a resonant amplification of the spin-charge conversion process.*

References

[1] K.-R. Jeon et al., ACS Nano **14**, 15874 (2020).
[2] M. Inoue et al., Phys. Rev. B **96**, 024414 (2017).

Abstract ID: 30670

MAGNETIC ENGINEERING AND SPIN/ORBITAL TORQUE SWITCHING IN FERRIMAGNETIC GARNETS

C. O. Avci

Institut de Ciència de Materials de Barcelona, Campus de la UAB, Bellaterra, 08193, SPAIN

Spintronics—the use of the electron's spin as an active degree of freedom in electronic circuits—has grown into a vibrant, interdisciplinary field spanning condensed-matter physics, materials science, and nanotechnology. Rapid progress has been driven by advances in the understanding of spin transport and magnetic interactions, together with the discovery of new materials and experimental methods. A central theme in spintronics is the electrical control and detection of magnetization, which enables efficient and nonvolatile memory, logic, and signal-transmission technologies. Such capabilities not only enhance conventional CMOS architectures but also enable emerging beyond-CMOS device concepts with the potential to transform microelectronics [1]. Although early spintronic devices were largely based on metallic or semiconducting systems, magnetic insulators (MIs) have recently attracted significant interest due to their unique advantages [2]. These include tunable anisotropy, magnetization, and damping; highly ordered and chemically stable crystal structures; and, crucially, mechanisms that allow electrical manipulation and readout of their magnetic state.

In this talk, I will review recent progress in ferrimagnetic garnet–based spintronics, emphasizing materials engineering strategies and current-induced magnetization switching. In the first part, I will show how the magnetic properties of rare-earth iron garnets (REIGs)—in particular their magnetic compensation point—can be tuned via Al substitution, leading to striking exchange-bias effects in these systems [3]. I will also present recent efforts to integrate REIGs directly onto Si platforms, an essential step toward CMOS-compatible MI-based technologies [4]. In the second part, I will discuss how unconventional spin and orbital currents in ultrathin Pt layers, combined with light-metal capping, can efficiently switch magnetization in REIGs through spin- and orbital-Hall-effect mechanisms [5].

Together, these results illustrate the rapidly expanding opportunities offered by garnet-based magnetic insulators for next-generation spintronic devices.

References

[1] B. Dieny, *et al.*, Nat. Electron. 3, 446 (2020).
[2] C. O. Avci, J. Phys. Soc. Jpn. 90, 081007 (2021).
[3] T. Shiino, *et al.*, Adv. Mater. 38, no. 2, e10669 (2026).
[4] M. Fettizio *et al.*, submitted (2026).
[5] S. Fedel *et al.*, Comm. Phys. In press (2026).

44 - QUANTUM EMISSION AND DEFECTS IN SOLID STATE MATERIALS

Abstract ID: 30291

DEFECT ENGINEERING IN HEXAGONAL BORON NITRIDE FOR STABLE SINGLE-PHOTON EMISSION

H. Moon[1,2]

[1] *Center for Quantum Technology, Korea Institute of Science and Technology, Seoul 02792, REPUBLIC OF KOREA*
[2] *Nanoscience and Technology, KIST School, University of Science and Technology, Seoul 02792, REPUBLIC OF KOREA*

Quantum emitters in solid-state materials have attracted significant interest as key building blocks for quantum photonic technologies due to their compatibility with photonic integrated circuits. Two-dimensional (2D) layered materials offer additional advantages, including facile transfer onto various substrates and large-area, high-quality thin-film growth. In particular, defect centers in wide-bandgap hexagonal boron nitride (hBN) exhibit bright and stable single-photon emission at room temperature as well as spin-related properties for quantum information and sensing applications [1, 2]. Despite these advantages, hBN-based quantum emitters in the visible wavelength range often show a broad distribution of emission energies as well as pronounced spectral diffusion, which remain major obstacles to achieving uniform and stable quantum light sources [3, 4]. Here, we present an effective approach to generate hBN quantum emitters with highly stable and spectrally uniform optical emission. In addition, we demonstrate a one-step deterministic creation of nonclassical light sources in hBN [5]. The stable and reliable creation of quantum emitters in 2D material can open the possibility of scalable integrated quantum photonic devices.

References

[1] I. Aharonovich, *et al.*, Nat. Photonics, **10**, 631 (2016).

[2] A. Gottscholl, *et al.*, Nat. Comm. **12**, 4480 (2021).

[3] T. T. Tran, *et al.*, ACS Nano, **10**, 8, 7331 (2016).

[4] G. Grosso, *et al.*, ACS Photonics, **7**, 6, 1410 (2017).

[5] S. Karankova, *et al.*, Adv. Opt. Mat. (2025).

Abstract ID: 30376

THE BORON VACANCY IN hBN: FROM ELECTRONIC STRUCTURE THROUGH DECOHERENCE TO COHERENT NUCLEAR SPIN CONTROL

V. Ivády[1,2]

[1] *Eötvös Loránd University, Department of Physics of Complex Systems, Budapest, HUNGARY*
[2] *MTA-ELTE Lendület "Momentum" NewQubit Research Group, Budapest, HUNGARY*

This talk provides a perspective on the negatively charged boron vacancy (VB) center in hBN, progressing from fundamental microscopic theory to quantum control of nuclear spins. We first present an improved ab initio theory of the VB center's optical cycle, highlighting the role of static Jahn-Teller distortion and the sensitivity of intersystem crossing (ISC) rates to mechanical strain. The theoretical foundations facilitate a detailed analysis of the nuclear spin-mediated relaxation and decoherence limits that govern the center's spin lifetime within the spin-rich hBN host lattice. Finally, we demonstrate the coherent control of nitrogen nuclear spins mediated by the VB center, establishing it as a quantum memory for local spin registers. Collectively, these findings provide a comprehensive roadmap for utilizing VB centers as high-performance, strain-tunable quantum sensors in 2D architectures.

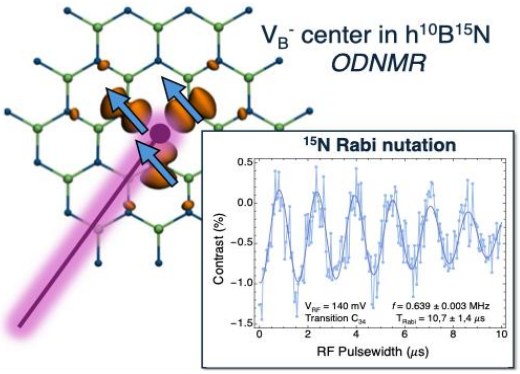

Fig. 1: *Schematic representation of nuclear spin control and Rabi drive of ^{15}N nuclear spins in hBN with a Rabi coherence time of ~11 μs.*

References

[1] Zs. Benedek, *et al.*, *An improved ab initio theory of the VB center in hBN: excited state fine structures, Jahn-Teller distortion, and strain-dependence of the optical cycle*, In preparation.

[2] A. Tárkányi, V. Ivády, *Understanding decoherence of the boron vacancy center in hexagonal boron nitride*, Advanced Functional Materials, e11300 (2025).

[3] C. Cholsuk, T. Vogl, V. Ivády, *Nuclear spin-mediated relaxation mechanisms of the VB center in hBN*, npj Computational Materials 11 (1), 344 (2025).

[4] A. Tibiássy, *et al.*, Coherent control of nitrogen nuclear spins via the V-center in hexagonal boron nitride, Advanced Functional Materials, **in press** (2026).

Abstract ID: 30443

ENGINEERING SINGLE SPIN DEFECTS IN HEXAGONAL BORON NITRIDE

M. Kianinia[1,2]

[1] *School of Mathematical and Physical Sciences, University of Technology Sydney, Ultimo, New South Wales 2007, AUSTRALIA*
[2] *ARC Centre of Excellence for Transformative Meta-Optical Systems, University of Technology Sydney, Ultimo, New South Wales 2007, AUSTRALIA*

The development of quantum light sources with addressable spin is essential for a plethora of applications in quantum technologies such as quantum computing, communication, and storage. Recently, hexagonal boron nitride (hBN) has emerged as a promising candidate to host spin active quantum emitters. However, on-demand generation of isolated single photon emitters with optically detectable spin transitions has remained challenging.

In this talk, our recent effort in engineering and the generation of such defects in high-quality hBN flakes will be presented. Notably, upon optimising the fabrication process, more than one quarter of the generated emitters display an unambiguous room-temperature optical spin readout, representing an improvement of approximately an order of magnitude compared to previously reported studies. The resulting spin defect complexes show both S=1 and S=1/2 transitions, which we attribute to charge transfer processes between strongly and weakly coupled spin pairs. These findings deepen our understanding of spin complexes in hexagonal boron nitride and open new opportunities for realizing single-spin–photon interfaces in layered van der Waals materials, with relevance for quantum sensing and quantum information technologies [1-3].

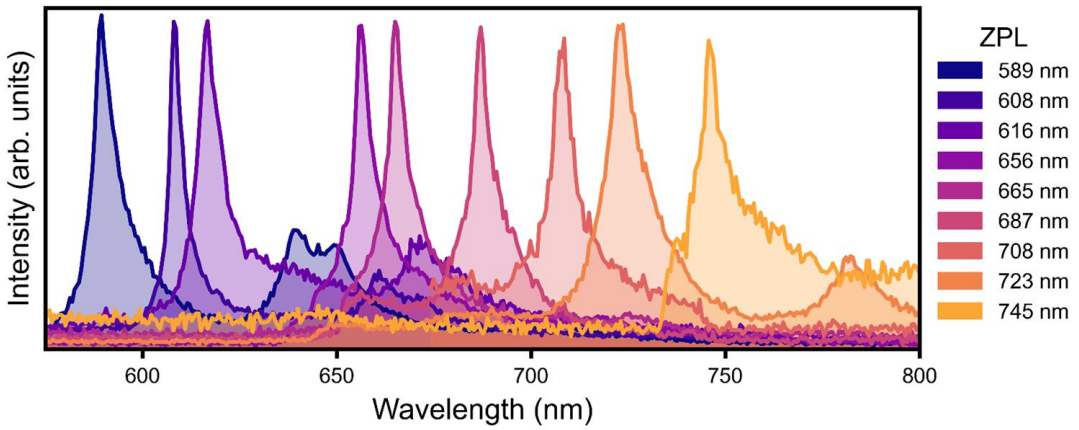

Fig. 1: *Engineering narrowband spin active quantum emitters in hexagonal boron nitride.*

References

[1] B. Whitefield, *et al.*, e-print arXiv:2501.15241V1 (2025).
[2] J. Liddle-Wesolowski, *et al.*, e-print arXiv:2601.03803 (2026).
[3] B. Whitefiled, *et al.*, e-print arXiv:2512.07067 (2025).

Abstract ID: 30463

QUANTUM EMISSION FROM COUPLED SPIN PAIRS IN HEXAGONAL BORON NITRIDE

S. Li[1], A. Pershin[1,2], A. Gali[1,2,3]

[1] HUN-REN Wigner Research Centre for Physics, P.O. Box 49, H-1525 Budapest, HUNGARY
[2] Department of Atomic Physics, Institute of Physics, Budapest University of Technology and Economics, Műegyetem rakpart 3., H-1111 Budapest, HUNGARY
[3] MTA–WFK Lendület "Momentum" Semiconductor Nanostructures Research Group, P.O. Box 49, H-1525 Budapest, HUNGARY

Optically addressable defect qubits in wide band gap materials are favorable candidates for room temperature quantum information processing. The two-dimensional (2D) hexagonal boron nitride (hBN) is an attractive solid state platform with a great potential for hosting bright quantum emitters with quantum memories with leveraging the potential of 2D materials for realizing scalable preparation of defect qubits. Although, room temperature bright defect qubits have been recently reported in hBN but their microscopic origin, the nature of the optical transition as well as the optically detected magnetic resonance (ODMR) have been remained elusive. Here we connect the variance in the optical spectra, optical lifetimes and spectral stability of quantum emitters to donor-acceptor pairs (DAP) in hBN by means of ab initio calculations. We find that DAPs can exhibit ODMR signal for the acceptor counterpart of the defect pair with S=1/2 ground state at non-zero magnetic fields depending on the donor partner. The donor-acceptor pair model and its transition mechanisms provide a recipe towards defect qubit identification and performance optimization in hBN for quantum applications.

This work was supported by the Cultural and Innovation Ministry of Hungary and the National Research, Development, and Innovation Office of Hungary (NKFIH) within Quantum Information National Laboratory (Grant No. 2022-2.1.1-NL-2022-00004) as well as the Horizon Europe EIC Pathfinder QuMicro project (grant no. 101046911).

11th International Conference on Superconductivity and Magnetism ICSM2026
4th International Conference on Quantum Materials and Technologies ICQMT2026
19th April to 26th April, 2026, Ölüdeniz – Fethiye/Muğla, Türkiye
https://icsmforever.org/

Abstract ID: 30575

ENHANCING SPIN-PHOTON INTERFACE SENSITIVITY THROUGH vdW ENGINEERING

E. Mayner[1], A. Radenovic[2]

[1] *Ecole Polytechnique Federale de Lausanne (EPFL), Institute of Biotechnology, 1015. Lausanne SWITZERLAND*
[2] *École Polytechnique Fédérale de Lausanne (EPFL), Institute of Physics, 1015, Lausanne, SWITZERLAND*

Spin defects in two-dimensional materials hold significant potential for quantum information technologies and sensing applications. The negatively charged boron vacancy (V_B^-) in hexagonal boron nitride (hBN) is one such defect that has attracted considerable attention due to its demonstrated sensitivity to temperature, magnetic fields, and pressure. The atomically flat nature of hBN enables its seamless integration into 2D electronics, imaging platforms, and integrated photonic circuits (IPCs). Although V_B^- centers can be reliably produced through ion bombardment or neutron irradiation, their applications are limited by an inherently low brightness. In this work, we demonstrate 5 to 45x enhancement of defect photoluminescence (PL) by making a van der Waals (vdW) heterostructure with a donor layer, lead iodide (PbI_2). The PbI_2 layer sensitizes the defect and enhances the PL intensity while maintaining compatibility with other heterostructures and vdW platforms. The heterojunction's type-I band alignment promotes efficient exciton migration while the large spectral overlap between the PbI_2 donor emission and the defect absorption facilitates fluorescence resonance energy transfer. We also show significant enhancement even with excitation energy below the PbI_2 band gap due to changes in the nonlinear susceptibility tensor of the defect. We observe the enhanced optically detected magnetic resonance (ODMR) signal and overall sensitivity and show the defects' use in sensing an external magnetic field. Ultimately, our results show that vdW heterostructures can effectively enhance V_B^- PL and improve its functionality as a 2D material-based quantum sensor with applications in vdW optoelectronics, IPCs, and widefield ODMR. Moreover, this work provides a pathway for amplifying weak defect signals in nanomaterials via structure coupling.

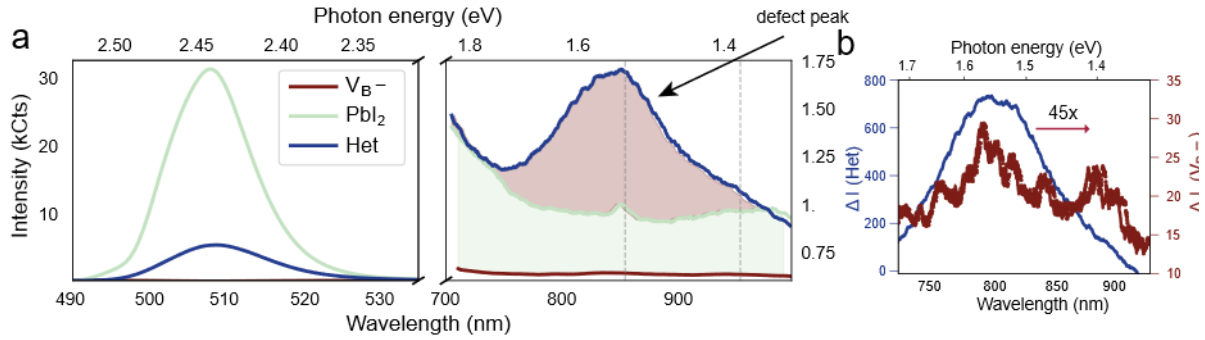

Fig. 1: *a) PL spectra e from different regions of the four-layer heterostructure. b) Differential PL of the heterostructure and the neutron irradiated "V_B^-" region, showing 45x enhancement of defect signal (heterostructure spectrum minus PbI_2 spectrum) compared to plain "V_B^-" region (V_B^- spectrum minus background spectrum).*

Abstract ID: 30719

HYBRID QUANTUM DEFECTS IN HEXAGONAL BORON NITRIDE AND THEIR ROLE IN SINGLE-PHOTON EMISSION

S. Amin[1], A. Jimenez[1], E. Mejia[1], Y. Cao[2], M. Silvetti[3], A. Biondini[3], M. Govoni[3], J. Pelliciari[2], G. Grosso[1]

[1] *Advanced Science Research Center, City University of New York, New York, NY, USA*
[2] *Brookhaven National Laboratory (BNL), USA*
[3] *University of Modena and Reggio Emilia (UNIMORE), ITALY*

Hexagonal boron nitride (hBN) has emerged as a promising material for quantum photonics due to its ability to host bright, stable single-photon emitters (SPEs) that operate at room temperature [1,2]. These emitters exhibit remarkable variability in spectral emission, lifetime, polarization, and spin structure [3]. Despite extensive studies, the microscopic origins of most SPEs remain elusive, limiting our understanding of their emission mechanisms and their integration into quantum technologies.

We present recent advances in elucidating the nature of SPEs in hBN and related nitrides through the combined use of resonant inelastic X-ray scattering (RIXS) and photoluminescence (PL) spectroscopy. RIXS measurements on defective hBN reveal a sequence of harmonic excitations that correlate with the emission energies of individual quantum emitters [4]. These excitations arise from nitrogen π^* anti-bonding orbitals and form a well-defined vibronic progression ascribable to molecular N_2-like defects. Complementary low-temperature PL measurements on the same samples confirm multiple, spectrally distinct SPEs. Analysis of these spectra using a donor–acceptor pair (DAP)-like nonlocal recombination model [5] uncovers a correlation between PL emission energies and the vibronic states of molecular defects, underscoring their central role in the emission process. Additional evidence from spectral instabilities supports that SPEs in hBN are governed by nonlocal recombination involving molecular-type centers.

These results establish a microscopic connection between single-photon emission and molecular defects in hBN, providing a predictive framework for spectral variability and tunability, and offering new strategies for engineering quantum light sources and solid-state spin qubits.

References

[1] T. T. Tran, *et al.*, Nat. Nanotechnol. **11**, 37 (2016).
[2] G. Grosso, *et al.*, Nat. Commun. **8**, 705 (2017).
[3] X. Gao, *et al.*, Nature **643**, 943 (2025).
[4] J. Pelliciari, *et al.*, Nat. Mater. **23**, 1230 (2024).
[5] E. Mejia, *et al.*, Opt. Mater. Express **14**, 2122 (2024).
[6] E. Mejia, *et al.*, J. Phys. Chem. C **29**, 2044 (2025).

Abstract ID: 30723

UNDERSTANDING THE ORIGIN OF DEFECT-BASED SINGLE-PHOTON EMISSION IN NITRIDE MATERIALS

A. Biondini[1], M. Silvetti[1], S. Amin[2], A. Jimenez[2], Y. Cao[3], J. Pelliciari[3], G. Grosso[2], M. Govoni[1]

[1] *Department of Physics, Computer Science and Mathematics, University of Modena and Reggio Emilia, Modena 41125, ITALY*

[2] *The Graduate School and University Center, City University of New York, New York, NY 10016, UNITED STATES*

[3] *National Synchrotron Light Source II, Brookhaven National Laboratory, Upton, NY 11973, UNITED STATES*

Wide-bandgap nitride materials host promising defect-based single-photon emitters, motivating efforts to clarify their microscopic origin and the role of vibronic effects. We investigate defect-driven single-photon emission in AlN, GaN, and hBN with the objective of identifying localized vibrational modes associated with defect states involving N_2 dimers and assessing their contribution to the vibronic fingerprints observed in photoluminescence (PL) and resonant inelastic X-ray scattering (RIXS) spectra. By combining first-principles molecular dynamics with many-body perturbation theory (GW-BSE), we explore a range of defect configurations and characterize their electronic and vibronic properties. Our results highlight specific defect-induced vibronic couplings involving donor–acceptor pairs that are common to AlN, GaN, and hBN, and may underpin robust solid-state single-photon emission in nitride-based platforms.

Abstract ID: 30273

QUANTUM EMISSION IN N-BASED MATERIALS: IMPORTANCE OF MOLECULAR-LIKE DEFECTS

J. Pelliciari

NSLS-II, Brookhaven National Laboratory, 11772, Upton, USA

Single photon emission is a phenomenon where upon proper excitations a system emits one photon at the time. This phenomenon is typical of color centers and localized defects, and it is intriguing for future technologies. Recently, single photon emission has been detected 2D materials and in N-based materials namely: hexagonal boron nitride (hBN) [1], GaN [2], and AlN [3]. Intriguingly these materials while different in terms of crystallographic and band structures display similar phenomena of single photon emission [1-4]. In detail, they display a richness and tunability in the photoluminescence peaks and a significant spectral wandering of the emitter lines. Using Resonant Inelastic X-Ray Scattering (RIXS) [5] we individuate a common defect structure in these materials. From the RIXS spectra we find a fundamental excitation at 285 meV which through a series of harmonics extends up to 3 eV. This harmonic series resembles what is observed by other RIXS measurements in molecular Nitrogen corroborating the presence of this thermodynamically stable defect across these N-based materials [6]. Using a donor acceptor pair model we also show how the RIXS spectral series correlates with the plethora of peaks observed in photoluminescence highlining a possible common mechanism leading to single photon emission in multiple N-based materials.

References

[1] T. T. Tran, K. Bray, M. J. Ford, M. Toth, I. Aharonovich, *Quantum Emission from Hexagonal Boron Nitride Monolayers*, *Nat. Nanotechnol.* Nat. Nanotechnol., **11(1)**, 37–41 (2016). https://doi.org/10.1038/nnano.2015.242.

[2] A. M. Berhane, K.-Y. Jeong, Z. Bodrog, S. Fiedler, T. Schröder, N. V. Triviño, T. Palacios, A. Gali, M. Toth, D. Englund, I. Aharonovich, *Bright Room-Temperature Single-Photon Emission from Defects in Gallium Nitride*, Adv. Mater., **29(12)**, 1605092 (2017). https://doi.org/10.1002/adma.201605092.

[3] S. G. Bishop, J. P. Hadden, F. D. Alzahrani, R. Hekmati, D. L. Huffaker, W. W. Langbein, A. J. Bennett, Room-Temperature Quantum Emitter in Aluminum Nitride, ACS Photonics, **7(7)**, 1636–1641 (2020). https://doi.org/10.1021/acsphotonics.0c00528.

[4] I. Aharonovich, D. Englund, M. Toth, *Solid-State Single-Photon Emitters*, Nat. Photonics, **10(10)**, 631–641 (2016). https://doi.org/10.1038/nphoton.2016.186.

[5] J. Pelliciari, E. Mejia, J. M. Woods, Y. Gu, J. Li, S. B. Chand, S. Fan, K. Watanabe, T. Taniguchi, V. Bisogni, G. Grosso, *Elementary Excitations of Single-Photon Emitters in Hexagonal Boron Nitride*, Nat. Mater., 1–7 (2024). https://doi.org/10.1038/s41563-024-01866-4.

[6] L. Kjellsson, V. Ekholm, M. Agåker, C. Såthe, A. Pietzsch, H. O. Karlsson, N. Jaouen, A. Nicolaou, M. Guarise, C. Hague, J. Lüning, S. G. Chiuzbăian, J.-E. Rubensson, *Resonant Inelastic X-Ray Scattering at the N 2 π * Resonance: Lifetime-Vibrational Interference*, Radiative Electron Rearrangement, and Wave-Function Imaging,. Phys. Rev. A, **103(2)**, 022812 (2021). https://doi.org/10.1103/PhysRevA.103.022812.

45 - QUANTUM FUNCTIONAL MATERIALS AND THEIR EMERGING TECHNOLOGIES

Abstract ID: 30346

PEROVSKITE PHOTONICS – HARNESSING NONLINEARITIES USING A FIBERIZED PLATFORM

N. Healy[1], L. Cording[1], C. Johnson-Richards[1], H.C.L. Tsui[1], P. Docampo[2]

[1] *School of Mathematics, Statistics and Physics, Newcastle University, NE1 7RU, Newcastle Upon Tyne, UNITED KINGDOM*
[2] *BCMaterials, IKERBASQUE. Basque Foundation for Science, Bilbao, 48009, SPAIN*

Recently, semiconductor optical fibers have emerged as an exciting platform for advanced photonic applications [1]. By combining the geometries of optical fibers with the properties of semiconductors, these devices achieve high optical nonlinearity, tight mode confinement, and broadband transparency, while simultaneously enabling optoelectronic integration with existing photonic architecture. While early research primarily targeted the unary semiconductors, such as silicon and germanium, current investigations are expanding the material scope of the platform. One developing material family is perovskites, which have high second- and third-order nonlinearities and can have wide bandgaps making them an exciting material for quantum optics applications [2,3].

In this talk, the perovskite optical fiber will be introduced with demonstrations of the exploitation of the second-order nonlinearity (via second-harmonic generation), the third-order nonlinearity (via self-phase modulation), and ion migration induced photorefraction (Fig 1.); all first examples in this platform.

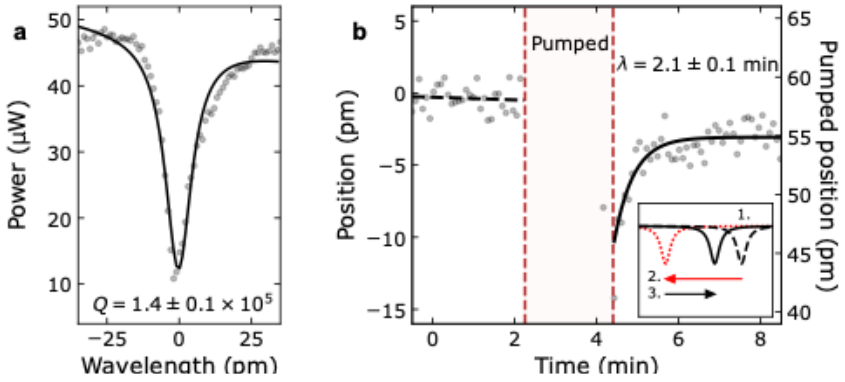

Fig. 1: *(a) Resonance used for monitoring the transmitted light as a function of wavelength. (b) Measurement of ion migration in a resonantly coupled optical fiber, showing the central wavelength of a resonant mode as a function of time. The measurement is divided into three regimes, described in the inset. (1) Initial stability over 2 minutes. (2) Pump-induced blue shift under high-energy pulsed excitation. (3) Exponential post-pump relaxation to a permanent blue-shifted offset relative to the initial position.*

References

[1] N. Healy, *et al.*, Semicond. Sci. Technol. **33**, 023001 (2018).
[2] H.C.L Tsui, *et al.*, APL Photonics **9**, no. 3 (2024).
[3] Y. Zhou, *et al.*, Science advances **8**, no. 38 (2022).

Abstract ID: 30480

PHOTON PAIRS, SQUEEZED LIGHT AND THE QUANTUM WAVE MIXING EFFECT IN A CASCADED QUBIT SYSTEM

R. D. Ivanovskikh[1], W. V. Pogosov[1,2,3], A. A. Elistratov[1], S. V. Remizov[1,4,5]

[1] *Dukhov Research Institute of Automatics (VNIIA), 127055 Moscow, RUSSIA*
[2] *Advanced Mesoscience and Nanotechnology Centre, Moscow Institute of Physics and Technology, Dolgoprudny, 141700, RUSSIA*
[3] *Institute for Theoretical and Applied Electrodynamics, Russian Academy of Sciences, Moscow, 125412, RUSSIA*
[4] *V. A. Kotel'nikov Institute of Radio Engineering and Electronics, Russian Academy of Sciences, Moscow 125009, RUSSIA*
[5] *HSE University, Moscow 109028, RUSSIA*

A cascaded system of two-level superconducting artificial atoms - a source and a probe - is an attractive platform for studying non-classical effects in quantum optics. Quantum wave mixing (QWM) [1] appears to be a promising tool for investigating such effects. It is shown that under strong drive the source atom emits correlated photon pairs or squeezed light. The QWM spectrum of the light emitted by the source and the coherent signal on the probe has been theoretically investigated. It is demonstrated that the equations of motion of the probe atom have the same form as the equations of motion of a qubit in the case of mixing squeezed light at the output of a degenerate parametric amplifier (DPA) with a coherent signal [2]. Numerical simulations were performed, which also confirm the presence of squeezed light in such a system for various ratios of the atoms' radiative constants. The QWM spectrum of the system is illustrated in Fig. 1 in comparison with the mixing spectrum of two coherent waves. The analysis of peak amplitudes can be used to probe photon statistics in the incoherent mode.

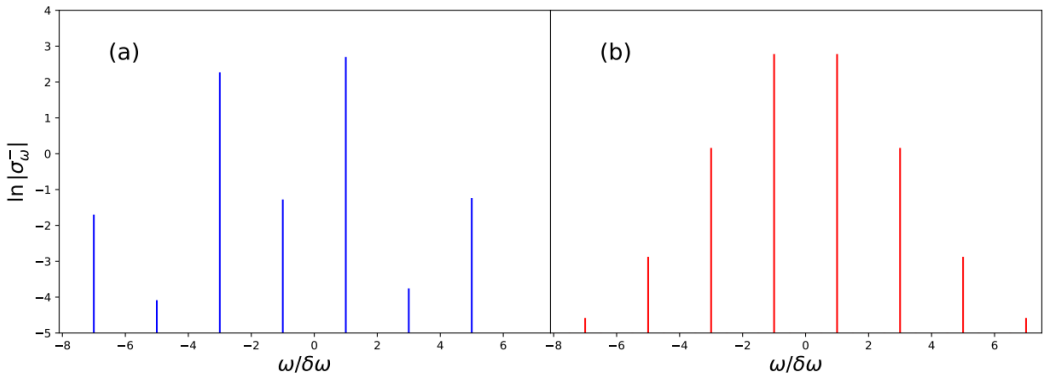

Fig. 1: *Spectral components of $\langle\sigma_-\rangle$ in the case of (a) qubit irradiation by a coherent wave together with the fluorescent light from the qubit-source, (b) of qubit irradiation by two coherent waves.*

References

[1] A. Y. Dmitriev, R. Shaikhaidarov, V. N. Antonov, T. Hönigl-Decrinis, and O. V. Astafiev, Nature Communications **8**, 1352 (2017).
[2] W. V. Pogosov, A. Y. Dmitriev, and O. V. Astafiev, Phys. Rev. A **104**, 023703 (2021).

Abstract ID: 30481

TOPOLOGICAL FUNCTIONALITY MEETS MODULAR GROWTH: A BOTTOM-UP APPROACH TO TI HETEROSTRUCTURES

K. Bandopadhyay, K. Markus, A. Materna, D. A. Pawlak

ENSEMBLE3 Centre of Excellence, Wolczynska 133, 01-919 Warsaw, POLAND

Three-dimensional (3D) topological insulators (TIs) are promising platforms for quantum computing, spintronics, and topological optoelectronics because of their topologically protected, gapless surface states [1]. However, their practical implementation is limited by environmental sensitivity, low surface-to-volume ratios, and the difficulty of fabricating high-quality heterojunctions with controlled interfaces. Overcoming these challenges requires scalable fabrication routes capable of preserving topological surface states while enabling functional integration with other materials.

Here, we demonstrate a simple, fast, and scalable bottom-up approach for fabricating 3D TI heterostructures based on single-step directional solidification [2]. This method produces eutectic composite materials in which two or more crystalline phases self-organize into ordered micro- and nanostructures with atomically smooth interfaces. Unlike conventional multi-step techniques such as molecular beam epitaxy or exfoliation-based assembly, directional solidification enables direct formation of high-quality heterostructures in a single growth process, ensuring excellent reproducibility and scalability. The resulting lamellar architectures preserve the intrinsic topological surface states of the TI phase while simultaneously enabling controlled interface engineering between TIs and adjacent functional materials, including semiconductors, metals, magnetic compounds, and superconductors.

A combination of spectroscopic, electronic, and transport measurements confirms the presence of Dirac-like surface states and the formation of built-in heterojunctions within the heterostructures [3]. In particular, for the Sb_2TeSe_2-Sb_2Se_3 composite, we observe topological surface states at the Fermi level in the Sb_2TeSe_2 phase, while THz and FTIR measurements reveal distinct optical and electronic contrasts between the two phases and across their interfaces. THz nanoscopy further resolves nanoscale variations in interfacial properties, highlighting the high quality and functional tunability of the heterojunctions. Additional eutectic systems - including Bi_2Te_3-Te, Sb_2Te_3-Te, Bi_2Te_3-BiTeI, Bi_2Te_3-Mn, SbTeI-Sb_2Te_3, and Fe_7Se_8-Bi_2Se_3 - demonstrate the versatility of this approach for tailoring electronic, magnetic, and topological interactions at interfaces.

By combining atomic-scale interface quality with large-scale manufacturability, this directional-solidification-based platform addresses key barriers in the integration of topological materials. It provides a robust route for exploring exotic interfacial phenomena such as topological superconductivity and magnetoelectric effects, and it establishes a scalable foundation for next-generation quantum and spintronic devices.

References

[1] D. Pesin, and A.H. MacDonald, Nat Mater, **11(5)**, p. 409–16 (2012).
[2] K. Bandopadhyay, *et al.*, Next Materials, **5**, p. 100252 (2024).
[3] F. Murakami, *et al.*, APL Materials, **11(3)**, p. 031102 (2023).

Abstract ID: 30595

SYNERGISTIC SILVER DOPING AND HALIDE PASSIVATION FOR STABLE, EFFICIENT $CsPbI_3$ QUANTUM DOTS FOR LED APPLICATIONS

P. Naziri[1,2], U. Aydemir[2,3]

[1] *Graduate School of Sciences and Engineering, Koç University, Istanbul 34450, TURKIYE*
[2] *Koç University Boron and Advanced Materials Application and Research Center (KUBAM), Istanbul 34450, TURKIYE*
[3] *Department of Chemistry, Koç University, Istanbul 34450, TURKIYE*

All-inorganic $CsPbI_3$ quantum dots (QDs) are highly attractive for next-generation light-emitting diodes (LEDs) due to their exceptional color purity, narrow emission bandwidth, and high photoluminescence efficiency. However, their long-term instability remains a major challenge for practical use[1,2]. In this study, we present a synergistic materials strategy that combines silver (Ag^+) substitution at the Pb site with dual-halide surface passivation (Cl^-/I^-) to simultaneously enhance structural integrity and optical stability. Ag^+ partially replaces Pb^{2+}, leading to slight lattice contraction and reduced defect density, while Cl^- ions preferentially occupy surface sites to passivate halide vacancies. Comprehensive structural and chemical analyses (XRD, HR-TEM/HR-STEM, XPS) confirm successful Ag^+ incorporation without secondary phase formation and reveal surface-localized Cl^- enrichment. The optimized composition, $CsPb_{0.95}Ag_{0.05}I_3$, obtained via mixed AgCl/AgI doping, maintains the cubic perovskite phase, achieves an outstanding PLQY of 96.6%, and exhibits significantly reduced nonradiative losses (time-resolved PL). Under continuous UV illumination (365 nm), the doped QDs retain ≈41% of their initial PLQY after 70 days, whereas undoped $CsPbI_3$ degrades below 10%. When applied as a red down-conversion layer on blue LED chips, the QDs deliver EQEs up to 36.8% with saturated emission and excellent operational stability. Overall, the combined Ag^+ doping and halide passivation approach offers a simple, scalable route to achieve durable, high-efficiency $CsPbI_3$ QDs for optoelectronic and LED applications.

References

[1] P. Naziri, A. Onal, P. Simon, *et al.*, ACS Appl. Nano Mater., **12**, 200 (2025).
[2] S. Lim, S. Han, D. Kim, J. Min, J. Choi, T. Park, Adv. Mater., **35 (4)**, 2203430 (2023).

Abstract ID: 30802

FAST-FORWARD ADIABATIC DYNAMICS: PRACTICAL ROUTES TO HIGH-FIDELITY STATE CONTROL

S. Ashirbekov, S. Matniyazov, A. Abdullayev, J. Matrasulov

Tashkent University of Information Technologies named after Muhammad al-Khwarizmi, Tashkent, UZBEKISTAN

We introduce a comprehensive framework that employs fast-forward (FF) protocols [1-3] to compress the inherently slow adiabatic evolution of complex systems into an ultrafast dynamical regime, seamlessly bridging quantum and classical domains. By carefully shaping quantum-state evolution, our approach enables controlled manipulation of a thermally isolated one-dimensional quantum gas confined in an expanding cavity, in which the usual equilibrium equation of state is effectively modified. In this regime, the force on the moving boundary admits a transparent decomposition into an adiabatic (equilibrium) contribution and a genuinely dynamical, nonadiabatic component whose magnitude and structure are governed by the wall's velocity and acceleration.

To broaden the scope of the fast-forward (FF) paradigm, we extend it to open quantum systems coupled to external reservoirs. By introducing systematically constructed nonadiabatic corrections to both the Hamiltonian and the dissipative (Lindblad) operators, we maintain the instantaneous Gibbs state even under rapid modulation of system parameters (e.g., the trap frequency). This generalizes the standard notion of detailed balance from a static equilibrium condition to a time-dependent, dynamically consistent form. The resulting framework sharpens control over nonequilibrium quantum dynamics while providing a robust route for implementing swift parameter changes in dissipative settings.

We further demonstrate the versatility of the FF strategy by translating it to classical transport: specifically, we accelerate solutions of the heat equation on a time-dependent domain. Through controlled modulation of temperature profiles and associated heat flux, the protocol enables tunable heat-transport dynamics and facilitates the engineering of targeted thermal response characteristics. Finally, we perform a quantitative assessment of the energetic cost of FF control. Under comparable operating conditions, we find that the FF protocol requires substantially less energy than conventional inverse-engineering approaches. Taken together, these results highlight fast-forward control as a broadly applicable route to ultrafast, energy-efficient manipulation—spanning quantum thermodynamics, classical heat transport, and the operation of nanoscale devices—while opening new directions for both fundamental studies and practical implementations.

References

[1] G. Babajanova, J. Matrasulov, K. Nakamura, *Quantum gas in the fast forward scheme of adiabatically expanding cavities: Force and equation of state*, Phys. Rev. E **97**, 042104 (2018).

[2] J. Matrasulov, J.R. Yusupov, A.A. Saidov, *Fast forward evolution in heat equation: Tunable heat transport in adiabatic regime*, Nanosystems: Phys. Chem. Math. **14(4)**, 421–427 (2023).

[3] J.D. Matrasulov, J.R. Yusupov, K.Sh. Matyokubov, *Fast forward problem for adiabatic quantum dynamics: Estimation of the energy cost*, Nanosystems: Phys. Chem. Math. **15(4)**, 457–464 (2024).

Abstract ID: 30806

MICROWAVE-TO-OPTICAL QUANTUM TRANSDUCTION WITH Er^{3+} IONS AND YIG

B. Rameev[1,2,3], M. Maksutoğlu[4], E. Demirci[1], S. Kazan[1], H. Pişkin[5]

[1] Physics Department, Gebze Technical University, Gebze/Kocaeli, 41400, TÜRKIYE
[2] Kazan State Power Engineering University, Kazan/Tatarstan, 420066, RUSSIAN FEDERATION
[3] Zavoisky Physical-Technical Institute – Subdivision of the Federal Research Center "Kazan Scientific Center of Russian Academy of Sciences", Kazan/Tatarstan, 420029, RUSSIAN FEDERATION
[4] Institute of Nanotechnology, Gebze Technical University, Gebze/Kocaeli, 41400, TÜRKIYE
[5] Department of Fundamental Sciences, Faculty of Engineering, Alanya Alaaddin Keykubat University, Alanya/Antalya, 07450, TÜRKIYE

Microwave-to-optical quantum transduction is an important challenge in quantum information and communication technologies. Hybrid quantum systems (HQS), formed by coupled interacting subsystems, have emerged as a promising platform for quantum frequency conversion [1]. Among the various HQS implementations, rare-earth-ion-doped crystals represent a potentially efficient approach for transferring quantum coherence between microwave and optical domains. The coupling between spin-flip transitions of RE ions in diluted crystals and microwave (MW) photons is usually weak. For that reason, it is very important to develop strategies to achieve strong-coupling regimes in these systems. Among rare-earth ions, Er^{3+} ions are particularly attractive due to optical transitions in the telecom range (~1.5 μm).

On the other hand, systems based on magnetically ordered (ferro- or ferri-magnetic) materials look promising because they enable the realization of an ultra-strong coupling regime between microwave photons and magnons, despite an intrinsically weak magnon-optical coupling [2]. Either approach has its own challenges to address to enable efficient quantum transduction. In addition to the constraints imposed by the basic physics of mediating substance, many parameters related to the engineering of optimal design are also extremely important. In this work, two approaches for quantum transduction based on magnon- and RE-based classes of materials are analyzed. Their specific features are reviewed, and the strengths and weaknesses of each material class are compared. The possibility of interfacing or combining these two approaches in a single device is also considered, along with the technical challenges of realizing such a hybrid system [3,4].

References

[1] G. Kurizki, *et al.*, *Quantum technologies with hybrid systems*, Proc. Natl. Acad. Sci. U.S.A. **112(13)**, 3866-3873 (2015).

[2] B. Bhoi, S.-K. Kim, *Roadmap for photon-magnon coupling and its applications*, Solid State Physics, **Vol.71** (Ed: R.L. Stamps), 39-71 (2020).

[3] T. Puel, A. Turflinger, S. Horvath, J. Thompson, M. Flatté, *Enhancement via the Kittel mode of a magnet of the microwave to optical quantum transduction in a rare-earth-doped crystal*, In: APS March Meeting Abstracts, **vol. 68(3)** (2023), Y67-003 (Las Vegas, Nevada, USA, March 5-10, 2023).

[4] T.O. Puel, A.T. Turflinger, S.P. Horvath, J. Thompson, M.E. Flatté, *Enhancement of microwave to optical spin-based quantum transduction via a magnon mode*, Proc. SPIE PC12911, Quantum Computing, Communication and Simulation IV, PC129110H (13 March 2024).

Abstract ID: 30807

GEOMAGNETIC ANOMALY MAPPING USING FLUXGATE MAGNETOMETERS

M. Maksutoğlu[1], N. G. Saribas[1], A. Demirtaş[1], H. Piskin[2], B. Rameev[3,4,5]

[1] *Institute of Nanotechnology, Gebze Technical University, Gebze, Kocaeli 41400, TURKIYE*
[2] *Department of Fundamental Sciences, Faculty of Engineering, Alanya Alaaddin Keykubat University, Antalya 07450, TURKIYE*
[3] *Physics Department, Gebze Technical University, Gebze, Kocaeli 41400, TURKIYE*
[4] *Zavoisky Physical-Technical Institute – Subdivision of the Federal Research Center "Kazan Scientific Center of Russian Academy of Sciences", Kazan/Tatarstan, RUSSIAN FEDERATION*
[5] *Kazan State Power Engineering University, Kazan/Tatarstan, RUSSIAN FEDERATION*

This study presents the design, implementation, and comparative performance analysis of two magnetic sensor systems developed for geomagnetic anomaly mapping under different operational conditions. The first system is a laboratory-based high-precision magnetometer configured for controlled environment measurements, while the second is a field-deployable system optimized for in-situ geomagnetic surveys under variable terrain conditions. Both systems are designed to measure magnetic field variations at the nT–μT level with high spatial resolution, targeting geophysical anomalies of interest. The laboratory system prioritizes maximum sensitivity and stability for reference measurements and controlled experiments, whereas the field system emphasizes robustness, portability, and reliable performance under challenging environmental conditions including temperature fluctuations, mechanical vibration, and limited power availability.

Comparative testing between the two configurations reveals the trade-offs inherent in translating laboratory-grade precision to field-deployable instrumentation. The laboratory system achieves superior signal-to-noise ratios under ideal conditions, while the field system demonstrates adequate sensitivity for practical anomaly mapping with the advantage of operational flexibility.

This work provides a systematic evaluation of both systems' performance characteristics, including sensitivity and environmental robustness. The results contribute to understanding how measurement objectives and operational constraints guide the development of specialized magnetic sensor systems for geophysical applications.

The work was supported by NATO Science for Peace and Security Programme (NATO SPS project No. G6063).

46 - QUANTUM INFORMATION TECHNOLOGY AND APPLICATIONS

Abstract ID: 30190

QUANTUM WAVE MIXING ON A SUPERCONDUCTING QUBIT AS A TOOL FOR STUDYING PHOTON STATISTICS

A. V. Vasenin[1,2], S. A. Gunin[1,2], A. Yu. Dmitriev[1], A. A. Elistratov[3], R. D. Ivanovskikh[3], S. V. Remizov[3,4], T. R. Sabirov[1,2], W. V. Pogosov[3,6,1], O. V. Astafiev[2,1]

[1] *Moscow Institute of Physics and Technology (MIPT), Institutsky Lane, 9, Dolgoprudny, 141700, Moscow Region, RUSSIA*
[2] *Skolkovo Institute of Science and Technology (Skoltech), Bolshoy Blvd, 30, 1, 121205, Moscow, RUSSIA*
[3] *Dukhov Research Institute of Automation, Sushchevskaya St., 22, 127055, Moscow, RUSSIA*
[4] *Kotelnikov Institute of Radio Engineering and Electronics, Russian Academy of Sciences, Mokhovaya St., 11-7, 125009, Moscow, RUSSIA*
[5] *National Research University Higher School of Economics, Myasnitskaya St., 20, 101000, Moscow, RUSSIA*
[6] *Institute of Theoretical and Applied Electrodynamics, Russian Academy of Sciences, Izhorskaya St., 13, 125412, Moscow, RUSSIA*

This work presents theoretical and partly experimental results on nonlinear optics at the level of a single two-level quantum system (qubit) and on the generation of non-classical light, in particular photon pairs, using a parametric amplifier and a strongly driven qubit-based quantum source. In the first approach, a degenerate parametric amplifier with a nonlinear medium, pumped by a strong classical field, produces squeezed vacuum containing correlated photon pairs with non-classical statistics. The interaction of this parametrically squeezed light with a qubit is described theoretically in a white-noise framework, and wave mixing of two frequencies (the pump and the probe) leads to characteristic sidebands in the qubit emission spectrum. Their structure, including missing lines, directly reflects the quantum properties and photon statistics of the squeezed field.

The second model considers a qubit under continuous excitation acting as a quantum source of antibunched single photons. When its radiation is mixed in frequency with a classical signal on a second qubit (two-frequency wave mixing), the resulting spectrum exhibits non-classical features, such as the suppression of high-order classical mixing lines and the dominance of multiphoton processes involving a single quantum photon. This enables the second qubit to function as a sensor of photon statistics.

Together, these approaches outline a route to photon-statistics sensors based on artificial quantum systems, where wave-mixing spectra of two-level systems replace direct correlation measurements, which is especially promising in the microwave domain.

References

[1] W. V. Pogosov, A. Yu. Dmitriev, O. V. Astafiev, Phys. Rev. **104**, 023703 (2021).

[2] A. Yu. Dmitriev, A. V. Vasenin, S. A. Gunin, S. V. Remizov, A. A. Elistratov, W. V. Pogosov, O. V. Astafiev, Phys. Rev. A. **111**, 043715 (2025).

Abstract ID: 30589

BOSE CONDENSATION AND BOGOLIUBOV EXCITATION IN RESONATOR-EMBEDDED SUPERCONDUCTING QUBIT NETWORK

P. Navez[1], V. Di Meo[2], B. Ruggiero[3], C. Gatti[4], F. Chiarello[5], A. D'Elia[4], A.Rettaroli[4], G. Brida[6], E. Enrico[6], L. Fasolo[6], M. Fistul[7], A. Zagoskin[8], P. Silvestrini[9], P. Vanacore[3], M. Lisitskiy[2]

[1] *Université de Montpellier, Laboratoire Charles Coulomb, Montpellier, FRANCE*
[2] *Institute for Superconductors, Innovative materials, and devices SPIN, CNR, Naples, ITALY*
[3] *Institute of Applied Science and Intelligent Systems - ISASI, CNR, Naples, ITALY*
[4] *National Laboratory of Frascati LNF, Rome, ITALY*
[5] *Institute for Photonics and Nanotechnologies, IFN CNR, Rome, ITALY*
[6] *National Institute of Metrological Research, INRIM, Turin, ITALY*
[7] *Ruhr University Bochum, Bochum, GERMANY*
[8] *Loughborough University, Loughborough, UNITED KINGDOM*
[9] *Università della Campania "Luigi Vanvitelli", Dipartimento di Matematica e Fisica, Caserta, ITALY*

Superconducting qubit networks (SQNs) embedded in a low-dissipative resonator is a promising device allowing one not only to establish the collective quantum dynamics on a macroscopic scale but also to greatly enhance the sensitivity of detectors of microwave photons. A quantum ac Stark effect provided by coupling between an SQN and microwave photons of a resonator, leads to a strong nonlinear interaction between photons. Here, we present a two-tone spectroscopy experiment in which a set of 10 superconducting flux qubits is coupled to the input R- resonator and the output T - transmission line. An external microwave pump field close to the resonance frequency populates macroscopically the resonator mode as a Bose-Einstein condensate, while a second probe beam scans the resonances referred also as Bogoliubov-like excitations. The corresponding excitation frequency measured from the transmission coefficient, $|S21(f)|$ displays an abrupt change of the resonant dip position once the power of the pump field overcomes a critical value Pcr . This sharp shift occurs in a narrow region of pump frequencies, and can be tuned by an applied magnetic field. It is a signature of bistability of the photon number inside the resonator, in agreement with theory.

Acknowledgements

Patrick Navez and Alexandre Zagoskin were supported by the European Union project: qrc-4-esp under grant agreement number 101129663

References

[1] P. Navez, A. G. Balanov, S. E. Savel'ev, A. M. Zagoskin, *Quantum electrodynamics of non-demolition detection of single microwave photon by superconducting qubit array*, J. Appl. Phys. **133**, 104401 (2023).

[2] C. Gatti, et al., *Coherent quantum network of superconducting qubits as a highly sensitive detector of microwave photons for searching of galactic axions*, IEEE Trans. Appl. Supercond. **33**, p. 1501705 (2023).

[3] P. Navez, V. Di Meo, B. Ruggiero, C. Gatti, F. Chiarello, A. D'Elia, A. Rettaroli, E. Enrico, L. Fasolo, M. Fistul, I. Eremin, A. Zagoskin, P. Vanacore, P. Silvestrini, M. Lisitskiy, *Bose condensation and Bogoliubov excitation in resonator-embedded superconducting qubit network*, https://arxiv.org/pdf/2601.15101

Abstract ID: 30631

QUANTUM IMPLICIT NEURAL REPRESENTED AUTOENCODER AND VARIATIONAL AUTOENCODER WITH MULTI-OBSERVABLE READOUTS

S. M. Eren

Department of Physics, Izmir Institute of Technology, Gülbahçe, Urla 35430, Izmir, TURKIYE

In this paper, we implement the Quantum Implicit Neural Representation (QINR) into the Autoencoder (AE) and Variational Autoencoder (VAE) in the field of image processing. In particular, we investigate the effects of multi-observable readouts on constructing and generating images when using QINR-AE/VAE for the MNIST, E-MNIST, and Fashion MNIST datasets. Our quantum-classical hybrid models consist of a classical Convolutional Neural Network (CNN) encoder and a QINR decoder with repeated data re-uploading and entangling layers. We test the models on noiseless simulations with a single-observable readout <Zi> and multi-observable readouts, i.e., <Zi>, <Xi>, <Yi>, <Zi Zi+1>. In order to make quantitative comparisons, we use the PSNR, SSIM, FID, and cosine similarity metrics and calculate the training losses. We find that the image quality improves as it goes from single readout to multi-basis readout since the system is sensitive to the phase information of the state. It also receives a correlation signal between the qubits.

Abstract ID: 30637

REAL-TIME DYNAMICS OF DOUBLE QUANTUM DOT ANDREEV MOLECULE

K. Wrześniewski, I. Weymann

ISQI, Faculty of Physics and Astronomy, Adam Mickiewicz University in Poznań, 61-614, Poznań, POLAND

We study a parallel double-quantum-dot Andreev molecule, in which two quantum dots are coupled to a common superconducting lead. Using the numerical renormalization group method, we determine the ground-state phase diagram as a function of key system parameters. Besides the conventional singlet and doublet phases, we identify a robust triplet ground state originating from strong lead-mediated interactions between the quantum dots [1]. Such a triplet state plays an important role in nonequilibrium regimes, where it can critically influence transport phenomena, for instance through the formation of Andreev blockade, and is also of interest for quantum information applications, as hybrid nanostructures are promising platforms for superconducting qubits.

Motivated by the importance of the triplet ground state in nonequilibrium regimes, we theoretically investigate the real-time dynamics of the Andreev double-quantum-dot molecule using the time-dependent numerical renormalization group (tdNRG) approach. The dynamics is induced by sudden quenches of the Hamiltonian parameters, in particular changes in the coupling of the dots to the superconducting electrode, shifts of the orbital level energies, and variations of the interdot hopping amplitude. The resulting nonequilibrium evolution exhibits the dynamical formation of the molecular state and a nontrivial time dependence reflecting the competition between superconducting correlations and local Coulomb interactions. Finally, we examine signatures of dynamical quantum phase transitions in this hybrid superconducting system.

Acknowledgments

We acknowledge support from the National Science Centre (Poland) through the Grant No. 2022/04/Y/ST3/00061. Computing time at the Poznań Supercomputing and Networking Center is also acknowledged.

References

[1] P. Zalom, K. Wrześniewski, T. Novotny, I. Weymann, *Double quantum dot Andreev molecules: Phase diagrams and critical evaluation of effective models*, Phys. Rev. B **110**, 134506 (2024).

Abstract ID: 30733

COMPARATIVE ANALYSIS OF QUANTUM ERROR CORRECTION APPROACHES WITH RANDOMLY COMPILED CIRCUITS

M. N. Akarsubaşı[1], M. Çolak[1], A. Bozbey[1], M. Ünlü[1], F. B. Atalay[2], B. Tavli

[1] *TOBB Economy and Technology University, Dept. of Electrical and Electronics Engineering, 06560, Ankara, TURKEY*
[2] *TOBB Economy and Technology University, Dept. of Computer Engineering, 06560, Ankara, TURKEY*

Quantum Error Correction (QEC) is essential for transitioning from the Noisy Intermediate-scale Quantum Computing (NISQ) to the fault-tolerant quantum computing era. While there are promising error correcting codes such as Surface and Heavy-Hex codes for reaching this goal, there are still issues with coherent errors and the threshold problem is yet be mitigated efficiently. There are various proposals in the literature for transforming coherent errors into Pauli noise. However, comparative performance evaluations of such solutions are missing, which is imperative in quantitatively assessing the characteristics of these solutions. To fill the gap in the literature, in this this study, we present a simulation-based performance analysis framework for the noisy circuits using the Pauli Twirling method, which enables us to characterize the performances of approaches for the conversion of coherent errors into Pauli noise and its effect on QEC codes.

Abstract ID: 30790

COMPARATIVE BENCHMARKING OF LEARNING BASED ERROR MITIGATION TECHNIQUES FOR NOISY QUANTUM COMPUTATION

M. Çolak[1], M. N. Akarsubaşı[1], A. Bozbey[1], M. Ünlü[1], F. B. Atalay[2], B. Tavlı[1]

[1] *TOBB Economy and Technology University, Dept. of Electrical and Electronics Engineering, 06560, Ankara, TURKEY*

[2] *TOBB Economy and Technology University, Dept. of Computer Engineering, 06560, Ankara, TURKEY*

Noisy intermediate-scale quantum (NISQ) devices suffer from errors such as decoherence, gate imperfections, measurement errors, and crosstalk, which significantly corrupt quantum state and measurement results. While quantum error correction remains the ultimate solution for fault-tolerant quantum computing, it is impractical for near-term devices due to reasons such as the high resource overhead, limited qubit counts, and error rates that exceed current correction capabilities. As a result, quantum error mitigation (QEM) techniques can be used for enhancing computational accuracy without requiring full fault tolerance. Among these, learning based error mitigation approaches have recently gained significant attention due to their adaptability, scalability, and error model free mitigation capabilities. In this work, we present a comparative study of learning based error mitigation techniques applied to noisy quantum circuits. More specifically, we provide quantitative comparative evaluations of a selected set of machine learning approaches with respect to their abilities to reconstruct ideal probability vectors and expectation values from noisy measurements. Furthermore, we analyze the aforementioned schemes by considering generalization, robustness to different noise channels, scalability, and computational cost aspects.

47 - QUANTUM TRANSPORT AND NOVEL BROKEN SYMMETRY GROUND STATES

Abstract ID: 30075

UNIFIED THEORY OF INTERACTING TWO-DIMENSIONAL DIRAC FERMIONS

I. F. Herbut

Department of Physics, Simon Fraser University, Burnaby, BC, V5A 1S6, CANADA

Dirac fermions appear as low-energy quasiparticle excitations in many condensed matter systems of current interest. They are often weakly interacting, as famously in graphene but at interactions of intermediate strength they can also exhibit many ordered ground states by going through phase transitions at which gapless Dirac fermions play a crucial role [1]. Prime example of such a transition occurs in the Hubbard model on honeycomb lattice at half filling, which has a Dirac semimetal - Mott insulator transition in the so-called Heisenberg-Gross-Neveu universality class. I will present a unified theory of order parameters for Dirac systems in two-dimensions, based on the hidden O(8) symmetry that emerges in the Majorana representation of Dirac fermions [2]. The interacting relativistic field theory with the full O(8) symmetry turns out to be nothing else but the celebrated Gross-Neveu model. I will argue, however, that this well-studied model has a novel phase transition at a strong interaction of previously unexplored sign, at which the O(8) becomes spontaneously broken [3]. The problem of the universality class of this transition, in which the order parameter is a symmetric second-rank tensor coupled to relativistic fermions, and the effect of a finite chemical potential on the phase diagram, will be also discussed [4,5].

References

[1] I. F. Herbut, Phys. Rev. Lett **97**, 146401 (2006).

[2] I. F. Herbut and S. Mandal, Phys. Rev. B **108**, L161108 (2023).

[3] S. Han and I. F. Herbut, Phys. Rev. D **109**, 096026 (2024).

[4] S. Han and I. F. Herbut, Phys. Rev. B **110**, 125131 (2024).

[5] S. Han and I. F. Herbut, Phys. Rev. B **112**, 155161 (2025).

Abstract ID: 30288

MODELING CHARGE DENSITY WAVE PHASE DIAGRAM AND ULTRAFAST DYNAMICS IN TRANSITION METAL DICHALCOGENIDES USING MACHINE-LEARNED ELECTRONIC FREE ENERGY

I. Lončarić

Rudjer Boskovic Institute , 10000 Zagreb, CROATIA

We present a machine learning approach to efficiently model the charge density wave (CDW) phase diagram of monolayer transition metal dichalcogenides. By learning the electronic density of states and zero-temperature interatomic potential, our model provides electronic free energy at orders of magnitude lower computational cost, decoupling electronic and ionic temperatures and enabling accurate simulations under thermal and laser-induced nonthermal conditions. Our results provide precise estimates of the CDW transition temperature and clarify the roles of hot electrons and phonons in the ultrafast, nonthermal melting of the CDW phase, see [1].

References

[1] L. Benic, F. Grasselli, C. Ben Mahmoud, D. Novko, I. Loncaric, Journal of chemical theory and computation, **21(16)**, 8130-8141 (2025).

Abstract ID: 30308

AN IMPURITY IN A HETERONUCLEAR TWO-COMPONENT BOSE MIXTURE

G. Bighin[1], A. Burchianti[2,3], F. Minardi[2,3,4], T. Macrì

[1] *Department of Physics, Faculty of Science, University of Zagreb, 10000 Zagreb, CROATIA*
[2] *CNR-INO, Istituto Nazionale di Ottica, 50019 Sesto Fiorentino, ITALY*
[3] *European Laboratory for Nonlinear Spectroscopy - LENS, 50019 Sesto Fiorentino, ITALY*
[4] *Dipartimento di Fisica e Astronomia, Università di Bologna, 40127 Bologna, ITALY*
[5] *Departamento de Física Teórica e Experimental and International Institute of Physics, Universidade Federal do Rio Grande do Norte, Natal-RN 59078-970, BRAZIL*

We study the fate of an impurity in an ultracold heteronuclear Bose mixture, focusing on the experimentally relevant case of a 41K-87Rb mixture, with the impurity in a 41K hyperfine state. Our work provides a comprehensive description of an impurity in a BEC mixture with contact interactions across its phase diagram. We present results for the miscible and immiscible regimes, as well as for the impurity in a self-bound quantum droplet. Here, varying the interactions, we find novel, exotic states where the impurity localizes either at the center or at the surface of the droplet, see the figure.

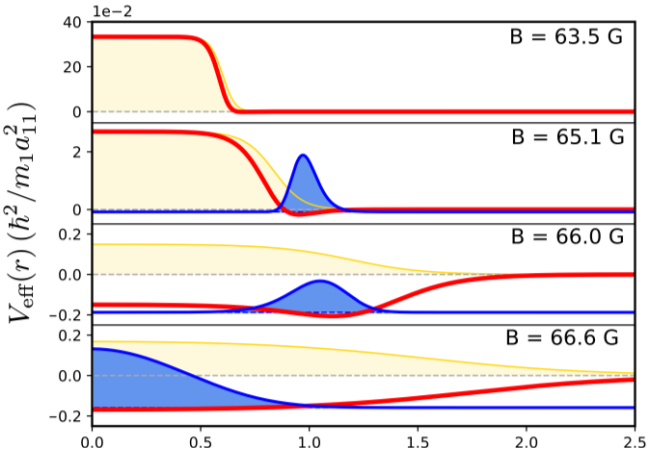

Fig. 1: *Effective radial impurity potential $V_{eff}(r)$ (red curves) for an impurity in a self-bound droplet (yellow shaded region). The impurity radial densities profiles (blue) are shown for several values of the magnetic field. From top to bottom, for B = 63.5 G the potential does not support bound states in three dimensions, for B = 65.1 G and B = 66.0 G the impurity is localized at the surface of the droplet at a distance r≈1μm from the center, for B = 66.6 G the impurity is centered in the self-bound droplet.*

References

[1] G. Bighin, A. Burchianti, F. Minardi, and T. Macrì, Phys. Rev. A **106**, 023301 (2022).

Abstract ID: 30372

NONRECIPROCAL TRANSPORT IN QUANTUM MATTER

R. Wang, B. Liu, W. Tian, P. Song

School of Electrical and Electronic Engineering, Nanyang Technological University, SINGAPORE

Nonreciprocal transport has emerged not only as an alternative approach to probe exotic physics in quantum materials, but also represents a new path to functional quantum electronic devices. In this talk, I will discuss our recent progress in both aspects. First, I will show that angle-resolved nonreciprocal transport, when combined with theoretical analysis, is particularly useful to decipher fine symmetry breaking. We demonstrated this with high temperature cuprate superconductor [1], where the symmetry breaking has been a key issue under debate. Second, I will discuss the electrical control of nonreciprocal transport, which is a key functionality for potential applications. While typically the nonreciprocity in quantum materials is fixed, we found that in a polar semimetal WTe_2, the rare coexistence of switchable ferroelectricity and nonreciprocal transport enables nonvolatile electrical switching of nonreciprocity [2]. Finally, I will also discuss the interplay between magnetism and nonreciprocity transport in van der Waals heterostructures.

References

[1] W. H. Tian, *et al.*, ACS Applied Materials & Interfaces, **17**, 68074-68082 (2025).
[2] R. H. Wang, *et al.*, Nature Communication, 11298 (2025).

Abstract ID: 30441

TOPOLOGY, NON-HERMITICITY, AND TOMOGRAPHY IN MULTI-TERMINAL ANDREEV CONTACTS

W. Belzig

Fachbereich Physik, Universität Konstanz, 78457 Konstanz, GERMANY

Hybrid multiterminal Josephson junctions (JJs) provide a versatile platform to engineer correlated superconducting transport and high-dimensional Andreev bound state (ABS) spectra with nontrivial topology. In junctions with four or more superconducting terminals, ABSs can depend on multiple independent superconducting phase differences, giving rise to synthetic band structures whose dimensionality exceeds real space. When at least three phases are involved, the resulting three-dimensional energy landscape can host zero-energy Weyl nodes and associated topological phases. Here we combine experiment and theory to investigate such phenomena in hybrid Al/InAs multiterminal JJs.[1] Tunneling spectroscopy of a four-terminal device reveals spectral signatures consistent with a tri-Andreev molecule, a bound state whose energy depends on three superconducting phases and enables topological ABSs. Numerical modeling reproduces the measured spectra and predicts the emergence of four Weyl nodes within an experimentally unresolved minigap, which remain stable over an extended and experimentally accessible parameter regime.

Beyond single-particle ABS physics, multiterminal junctions naturally support correlated multi-Cooper-pair tunneling processes without two-terminal analogs. We analyze quartets and sextets—processes involving two and three Cooper pairs, respectively—and demonstrate their intimate connection to ABS hybridization [2,3]. We show how these processes can be rigorously identified from current–phase relations and directly detected in ABS spectra, with application to recent three- and four-terminal Al/InAs devices. Finally, we extend these ideas to open multiterminal systems with controlled dissipation, predicting fragile and robust non-Hermitian topological phases driven by exceptional points. Together, these results establish multiterminal JJs as a powerful experimental framework for exploring correlated transport, non-Hermitian topology, and high-dimensional synthetic band structures in superconducting quantum systems.[4]

This presentation is in collaboration with all coauthors of the references.

References

[1] T. Antonelli, M. Coraiola, D. C. Ohnmacht, A. E. Svetogorov, D. Sabonis, S. C. ten Kate, E. Cheah, F. Krizek, R. Schott, J. C. Cuevas, W. Belzig, W. Wegscheider, F. Nichele, Phys. Rev. X **15**, 031066 (2025).

[2] D. C. Ohnmacht, M. Coraiola, J. J. García-Esteban, D. Sabonis, F. Nichele, W. Belzig, J. C. Cuevas, Phys. Rev. B **109**, L241407 (2024).

[3] M. R. Ebert, D. C. Ohnmacht, W. Belzig, J. C. Cuevas, Phys. Rev. B **112**, 195430 (2025); Editor's Suggestion & Physics Synopsis.

[4] D. C. Ohnmacht, V. Wilhelm, H. Weisbrich, W. Belzig, Phys. Rev. Lett. **134**, 156601 (2025).

Abstract ID: 30694

TRION STATE TRANSITIONS AND HYBRID BOUND STATES OF ELECTRON CHANNEL- QUANTUM DOT-TYPE STRUCTURE AT QUANTIZED MAGNETIC FIELDS

Z.-N. Wang[1], Y. Wang[1], F.-L. Song[1], S.-Y. Zheng[2], L. Lu[2], J. Zhang[1], C. Zhang[1]

[1] *Laboratory of Semiconductor Physics, Institute of Semiconductors, Chinese Academy of Science, Beijing, 100083, CHINA*
[2] *Institute of Physics, Chinese Academy of Sciences, Beijing 100190, CHINA*

We systematically investigate the transport and photoluminescence (PL) measurements of high mobility two-dimensional electron gas (2DEG) in a GaAs/AlGaAs quantum well (QW) at magnetic fields (B). By tuning the laser excitation power (P_{ex}), transitional patterns of the singlet and triplet (negative charged) trions occur at high B regime: the two branches of singlet trions (X^-_s) dominate at low P_{ex} (< 1 W/mm^2) and six more triplets (X^-_t) branches emerge at high Pex (~ 1−10 W/mm^2). At extremely high P_{ex} (> 100 W/mm^2) laser and at fixed B-fields, robust Fano resonance features are accompanied with the Gaussian resonance centered at X^-_s, which visualize the dark and bright trions. Therefore, the very high laser excitation (or EM-field) becomes an efficient tool to probe the dark trions. In addition, discontinuity and splitting features occur at the fillings of ν = 2, 4, 6, and the abrupt drops at high odd fillings factors (ν ~ 5, 7, 9, etc.) originate from spin resolved many-body interactions [1].

In the high-resolution PL study, we observe many-body bound states at even-number Landau level fillings in a high-mobility 2DEG. Our spatial-resolved photoluminescence (PL) reveals quantum dot (QD)-type emitters located at the barrier layer of QW. In the magneto-PL measurements, a set of four-fold sharp peaks occur at the precise integer filling of ν = 2, 4, 6. Our time-domain measurements illustrate the formation procedure of the hybrid states that involves intrinsically collective ultrafast dynamics. The trigger features at odd filling factors corresponds to the many-body states that involve quantum Hall states and (two-electron) spin-singlet and triplet states in heterostructures. The four-fold split peaks in PL energy stem from the correlation among electron states in QW and electron localized by QD-like potential in barrier. Our results demonstrate that the two-level quantum states in localized QD-like defect can be coupled to the high-mobility electron channel, and generate spin-split PL spectroscopy in the recombination of hybrid many-body bound states. Our experimental investigation provides a platform for potential quantum computation manipulations.

References

[1] Y. Wang, Z.-N. Wang, F.-L. Song, S.-Y. Zheng, L. Lu, K. Chang, J. Zhang, C. Zhang, Phys. Rev. B (accepted).

Abstract ID: 30830

GATE-TUNABLE POLARITY REVERSAL IN A SPIN-ORBIT JOSEPHSON DIODE

J. Shin[1], J.-H. Han[2,3], A. Rathore[4], J. S. Lee[4], S.-B. Shim[5], J. Cha[5], S. Park[3], J. Suh[1]

[1] *Department of Physics, Pohang University of Science and Technology (POSTECH), SOUTH KOREA*
[2] *Department of Physics, Korea Advanced Institute of Science and Technology (KAIST), SOUTH KOREA*
[3] *Center for Theoretical Physics of Complex Systems, Institute for Basic Science (IBS), SOUTH KOREA*
[4] *Department of Physics and Astronomy, University of Tennessee, USA*
[5] *Quantum Technology Institute, Korea Research Institute of Standards and Science (KRISS), SOUTH KOREA*

The Josephson diode effect is characterized by a unidirectional supercurrent across a Josephson junction [1]. Its behavior, including its polarity, is typically controlled by magnetic fields. Here, we report the Josephson diode effect in epitaxial Al-InAs planar Josephson junctions incorporated into a gate-tunable SQUID device. By controlling local gate voltages under in-plane magnetic fields, we observe a reversal of the diode polarity and analyze its evolution through SQUID oscillations and current-phase-relation analysis. The high-field diode response is strongly tunable by gate voltage, including a clear polarity reversal. Our theoretical model attributes the polarity reversal to the coherent interplay between finite Cooper-pair momentum arising from orbital effects and anisotropic spin-orbit coupling, including Rashba and Dresselhaus terms [2].

References

[1] M. Nadeem, M. S. Fuhrer, and X. Wang, Nat. Rev. Phys. **5**, 558 (2023).
[2] J. Shin, *et al.*, Phys. Rev. Applied **25**, 034070 (2026).

Abstract ID: 30429

MAGNETOTRANSPORT PROPERTIES AND GROUND STATE OF A TWO-DIMENSIONAL CONDUCTOR WITH THE ISOTROPIC FERMI SURFACE SUBJECTED TO THE BIAXIAL CHARGE DENSITY WAVE

B. Keran[1], A. M. Kadigrobov[1,2] D. Radić[1], Z. Rukelj[1]

[1] *University of Zagreb, Dept. of Physics, 10000, Zagreb, CROATIA*
[2] *Ruhr-Universität Bochum, Theoretische Physik III, D-44801, Bochum, GERMANY*

The study of charge density waves (CDWs) remains a central topic in condensed matter physics, with current focus on systems where CDW instabilities emerge without the, typically considered a paradigm, nesting property of the Fermi surface, i.e. in the absence of the Peierls mechanism. This behaviour is experimentally observed in materials such as high-temperature superconducting cuprates, intercalated graphite compounds, and transition-metal dichalcogenides. In this work, we introduce a minimal mean-field model at zero temperature for a biaxial CDW ground state in a two-dimensional metallic system with an initially circular Fermi surface and strong, momentum-dependent electron-phonon coupling, and explore its magnetotransport properties under conditions of magnetic breakdown in strong magnetic fields. The CDW ground state is stabilized through the Fermi surface reconstruction into a two-dimensional periodic network of diamond-shaped pockets, significantly altering the electronic band structure. In contrast to the nesting-driven systems, where the zero temperature CDW ordering is feasible for arbitrarily small coupling, here it appears in the Lifshitz type of transition, if the electron-phonon coupling is larger than the critical value determined by the properties of the electron band.

Exploring the properties of the system in a strong external magnetic field perpendicular to the conducting plane, special emphasis is placed on the role of a coherent magnetic breakdown (MB), treated within the semiclassical Lifshitz-Onsager formalism, for the first time formulated at the 2D MB network. MB is characterised by complex amplitudes of staying on the pocket and tunnelling to the adjacent one, depending on the magnetic field. The resulting spectrum consists of magnetic bands, with the width determined by the standard cyclotron energy and the product of the latter MB amplitudes, also exhibiting quantisation of magnetic flux, analogous to that of Zak/Hofstadter, but originating in the reciprocal space. This spectrum gives rise to three distinct magnetotransport regimes. The limit of narrow magnetic bands (effectively the Landau level limit), corresponding to weak or strong fields where one MB amplitude dominates, results in the standard hole-like or electron-like behaviour of magnetotransport, depending whether the semiclassical motion occurs along diamond-like (holes) or recreated circular (electrons) orbits, changing the sign of the Hall coefficient accordingly. In the intermediate regime of wide magnetic bands, with comparable MB amplitudes, semiclassical motion becomes diffusive-like and suppresses the Hall coefficient to zero. Fast quantum oscillations, periodic in inverse magnetic field with period determined by the area of the quasiparticle pocket in reciprocal space appear in diagonal components of the magnetoconductivity tensor in a similar manner as the standard Shubnikov-de Haas effect, but larger in amplitude since they appear as the result of the MB-induced interference.

References

[1] A. M. Kadigrobov, *et al.*, Phys. Rev. B **97**, 235439 (2018).
[2] B. Keran, *et al.*, Cond. Matt. **7**, 73 (2022).
[3] B. Keran, *et al.*, Phys. Rev. B **112**, 155116 (2025).

Abstract ID: 30453

DYNAMICAL CONDUCTIVITY OF A 3D DIRAC SYSTEM WITH HOLSTEIN-LIKE ELECTRON-PHONON COUPLING

P. Papac

Department of Physics, Faculty of Science, University of Zagreb, Bijenička 32, 10000, Zagreb, CROATIA

The zero-temperature electron-phonon memory function of a three-dimensional Dirac-like system with conical bands and with a Holstein-like electron-phonon coupling is investigated. The memory function is a complex function of the incoming photon energy and it describes the effect of electron-phonon scattering in the dynamical conductivity.

In the presented approach memory function is of the second order in electron-phonon interaction with the amplitude connected to the internal energy scales of the electron-phonon system and with imaginary and real parts being connected by Kramers-Kronig relations. A closed form expression is provided for the imaginary part of the memory function in the case when finite bandwidth, Fermi energy and optical phonon energy are comparable to one another, with several of its features closely investigated. Similarly, the properties of the real part of the memory function are given in a closed form, with its main features traced back to the properties of the imaginary part of the memory function.

Finally, the generalized frequency-dependent dynamical conductivity is calculated and analyzed. Fermi and optical phonon energy are determined from the conductivity curve.

Abstract ID: 30510

CHARGE DENSITY WAVE GROUND STATE IN THE INTERCALATED GRAPHITE CaC_6 AND ITS MAGNETOCONDUCTIVITY IN MAGNETIC BREAKDOWN CONDITIONS

P. Đ. Grozić[1], Z. Rukelj[1], B. Keran[1], A. M. Kadigrobov[2], D. Radić[1]

[1] *University of Zagreb, Faculty of Science, Physics Department, Bijenička 32, Zagreb, CROATIA*
[2] *Teoretische Physik III, Ruhr-Universitaet Bochum, Universit ̈atsstraße 150, Bochum D-44801, GERMANY*

The physics of intercalated graphite compounds (GIC), although these materials were synthesised quite long ago, is still in the focus of modern theoretical and experimental research. The interest of the scientific community is focused on GIC mostly due to the possibility of forming the unusual superconducting (SC) and charge density wave (CDW) ground states.

We focus on one of these materials, CaC_6, in which experiments demonstrate the existence of CDWs [1]. The very existence of the CDW is quite unusual due to the fact that the graphene Fermi surface (FS), chemically doped by calcium intercalates, shows no so-called "nesting property," i.e., no Peierls mechanism, which has been the paradigmatic mechanism leading to the CDW's instability since the 50s of the last century and was experimentally realised during the 80s in highly anisotropic materials with open Fermi surfaces [2].

We show that the CaC_6 Fermi surface undergoes a different CDW formation mechanism, based on the topological reconstruction (of the FS) and critical strength of the electron-phonon interaction. Such topological reconstruction, which transforms the set of closed Fermi pockets to the open Fermi sheets, has a profound effect on the transport and magnetotransport properties. We show the signature of the FS reconstruction by the CDW in the magnetotransport properties, taking into account magnetic breakdown, which shows characteristic quantum oscillations.

References

[1] K. Rahnejat, C. Howard, N. Shuttleworth, *et al.*, *Charge density waves in the graphene sheets of the superconductor CaC_6*, Nat. Commun. **2**, 558 (2011). https://doi.org/10.1038/ncomms1574

[2] R.E. Peierls, *Quantum Theory of Solids* (Clarendon Press, Oxford, 1955), pp. 108

48 - RECENT ADVANCES IN THERMOELECTRIC MATERIALS AND APPLICATIONS

Abstract ID: 30533

THERMOELECTRIC AND CHIRALITY DEPENDENT PROPERTIES OF *R*RhC$_2$ (R=La, Ce)

V. Levytskyi[1], U. Burkhardt[2], M. König[2], E. Svanidze[2], Yu. Grin[2], R. Gumeniuk[1]

[1] *Institut für Experimentelle Physik, TU Bergakademie Freiberg, 09599 Freiberg, GERMANY*
[2] *Max-Planck-Institut für Chemische Physik fester Stoffe, 01187 Dresden, GERMANY*

The phase LaRhC$_2$ and its magnetic counterpart CeRhC$_2$ with Ce^{3+} valence state are expected to exhibit attractive thermoelectric properties due to their chemical composition and semiconducting electrical conductivity. Furthermore, several closely related compounds RMC$_2$ (R = rare earth element, M = transition metal) have been identified as topological Weyl or Dirac (for GdRuC$_2$) semimetals [1]. At room temperature, however, the thermoelectric figure of merit values are small (LaRhC$_2$: zT(300 K) = 0.01 , CeRhC$_2$: zT(300 K) = 0.004), as their thermal conductivity $\varkappa$ is comparatively high and the thermopower S has low values (LaRhC$_2$: $\varkappa$ = 12 W/K m; S = -100 μV/K; CeRhC$_2$: $\varkappa$ = 10 W/K m; S = -40 μV/K). Our low-temperature conductivity and thermopower measurements on polycrystalline samples show that the band gap for the La and Ce compounds is approximately 30 meV and 10 meV, respectively. Hall effect measurements yield charge carrier concentrations n(300 K) ≈ 10^{20} cm^{-3} and 10^{21} cm^{-3} for the La and Ce compounds, respectively. Differences are evident in the thermal lattice conductivity and thermopower. The shorter relaxation time for Umklapp scattering scattering τ_u (CeRhC$_2$) << τ_u(LaRhC$_2$) leads to a significantly reduced thermal conductivity of the Ce compound at low temperatures. For the thermopower, CeRhC$_2$ shows an almost temperature-independent behavior between RT and 100 K (S(CeRhC$_2$) ≈ -40 μV/K), whereas LaRhC$_2$ a pronounced minimum at T = 77 K with S(LaRhC2) = -190 μV/K) is observed (Fig.1). The two phases are isotypic and crystallize in the chiral, tetragonal space groups $P4_1$ and $P4_3$. Our measurements on mono-chiral, single crystal samples (s. Fig.2) show significant differences in conductivity parallel and perpendicular to the tetragonal axis. The longitudinal magnetoresistance parallel to the screw axis shows a chirality dependence for the LaRhC$_2$ phase [2].

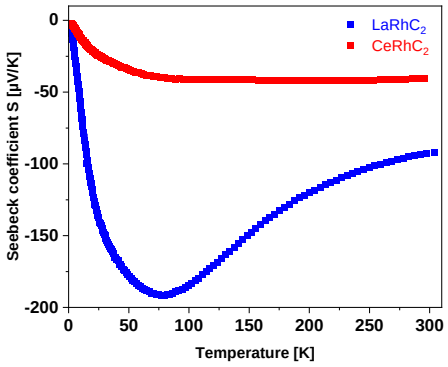

Fig.1: *Thermopower of polycrystalline material.*

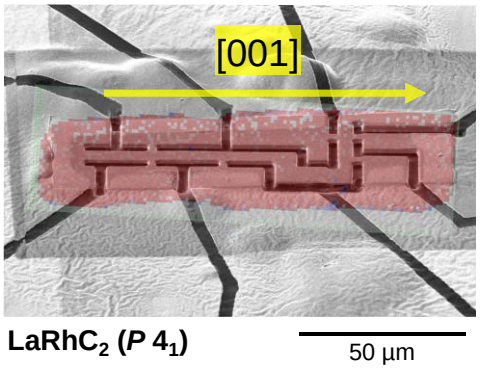

Fig. 2: *Monochiral, single crystalline microdevice of LaRhC$_2$ ($P4_1$).*

References

[1] R. Ray, B. Sadukhan, M. Richter, J. I. Facio, J. van den Brink; npj Quantum Materials **7**, 19 (2022).
[2] V. Levytskyi, U. Burkhardt, M. König, E. Svanidze, C. Hennig, Yu. Grin, R. Gumeniuk, submitted.

Abstract ID: 30534

EFFECTIVE MASS MODEL FOR THERMOELECTRICS

M. Heo[1,2], H.-S. Kim[2], G. J. Snyder[1]

[1] *Northwestern University, Dept. of Materials Science and Engineering, 60208, IL, UNITED STATES*
[2] *University of Seoul, Dept. of Materials Science and Engineering, 02504, Seoul, REPUBLIC OF KOREA*

Thermoelectric materials require precise doping to adjust the Fermi level in order to fully realize their thermoelectric potential. The effective mass (EM) model is commonly used to predict the maximum thermoelectric figure-of-merit (zT) and optimal carrier concentration [1,2], but its application is limited by the need for numerical Fermi integral solutions and Hall effect measurements. Since the thermopower (magnitude of the Seebeck coefficient, $|S|$) is effectively a measure of the Fermi level, it can be used as a direct descriptor of doping level in heavily doped semiconductors such as good thermoelectric materials. Here, we present a simple method to analyze thermoelectric transport using only the typical thermoelectric measurements: Seebeck coefficient, electrical conductivity and thermal conductivity. This enables evaluation of weighted mobility, quality factor (B), theoretical maximum zT, optimal thermopower, identification of anomalous scattering behavior; as well as a full prediction of zT, as a function of $|S|$ given by

$$zT = \frac{\left(\frac{|S|}{k_B/e}\right)^2}{\left(\frac{1}{B}\right)\left[\frac{\exp\left[\frac{|S|}{k_B/e} - 2\right]}{1 + \exp\left[-5\left(\frac{|S|}{k_B/e} - 1\right)\right]} + \frac{\frac{3}{\pi^2}\frac{|S|}{k_B/e}}{1 + \exp\left[5\left(\frac{|S|}{k_B/e} - 1\right)\right]}\right] + (1.34)\left[1.5 + \exp\left(-\frac{|S|}{116\ \mu V\ K^{-1}}\right)\right]}$$

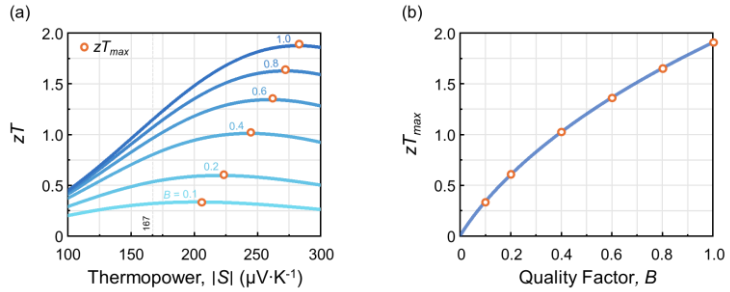

Fig. 1: *(a) Plot of zT as a function of $|S|$, (b) The zTmax values derived from different Bs in Fig. 1(a) are translated to a zTmax as function of B relationship.*

References

[1] X. Zhang, Z. Bu, X. Shi, Z. Chen, S. Lin, *et al.*, Sci. Adv. **6**, eabc0726 (2020).
[2] G. J. Snyder, A. H. Snyder, M. Wood, R. Gurunathan, B. H. Snyder, C. Niu, Adv. Mater. **32**, 2001537 (2020).

Abstract ID: 30747

ESSENTIAL ROLE OF TEMPERATURE-DEPENDENT BAND GAPS IN (p × n)-TYPE TRANSVERSE THERMOELECTRICS

Q. Shao[1], J. Li[1], X. Yan[1], B. Cui[1], X. Li[2], C. J. Zeman IV[1], M. A. Mosquera[1], L. O. Jones[1], G. C. Schatz[1], J. Yang[2], M. A. Grayson[1]

[1] *Northwestern University, 60208, Evanston, USA*
[2] *Materials Genome Institute, Shanghai University, 200444, Shanghai, CHINA*

Transverse thermoelectrics (TTE) have attracted attention as versatile energy materials where heat flows perpendicular to an applied electrical current due to structural asymmetry. Semiconductors and semimetals can exhibit TTE-behavior due to mixed conduction of anisotropic electron and hole dispersions with *p*- and *n*-type behavior in orthogonal crystal directions, hence (*p* × *n*)-type TTEs [1]. But despite a dozen such materials being discovered in the last decade, their experimental data still do not quantitatively fit a transport model across the measured temperature range *T*, partly because mixed anisotropic conduction is challenging to characterize. Here [2], a partial-gap analysis based on the Peltier conductivity is introduced which leverages the anisotropy of these materials to 'unmix' the electron-hole conduction and self-consistently extract the energy gap at each temperature, revealing a strong *T*-dependence that had been previously neglected. The method is demonstrated on independently measured datasets of differently doped Re_4Si_7. The analysis nonetheless provides nearly identical predictions for the *T*-dependent energy gap, decreasing by half over the measured thermal range. The results for Re_4Si_7 are also in quantitative agreement with electron–phonon renormalized density functional theory. This analysis establishes the importance of understanding T-dependent gaps in modeling TTE structure–property relationships.

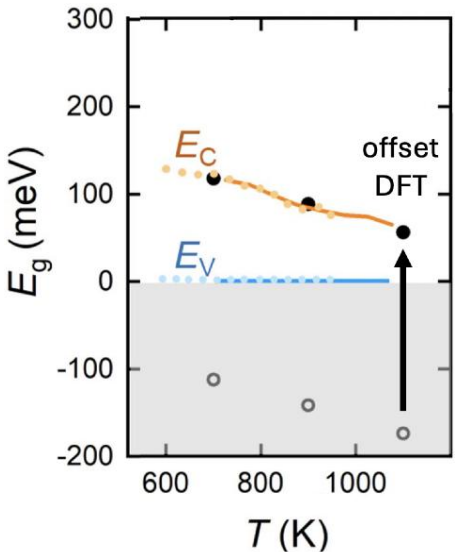

Fig. 1: *Energy gap of transverse thermoelectric Re_4Si_7 deduced from partial gap analysis introduced here (E_C = orange, E_V = blue). Experimental data from two different research groups [3,4] with differently doped samples results in identical measure of bandgap. Density functional theory prediction of temperature dependence also aligns with experimental data, after offset (black circles).*

References

[1] C. Zhou, S. Birner, Y. Tang, K. Heinselman and M. Grayson, Phys. Rev. Lett. **110**, 227701 (2013).
[2] Qing Shao, Juncen Li, X. Yan, Boya Cui, Xin Li, C. J. Zeman IV, M. A. Mosquera, L. O. Jones, G. C. Schatz, Jiong Yang and Matthew A. Grayson, J. Mater. Chem. A **14**, 4404 (2026).
[3] J.-J. Gu, M.-W. Oh, H. Inui and D. Zhang, Phys. Rev. B: Condens. Matter Mater. Phys. **71**, 113201 (2005).
[4] M. R. Scudder, B. He, Y. Wang, A. Rai, D. Cahill, W. Windl, J. P. Heremans and J. Goldberger, Energy Environ. Sci. 4009–4017 (2021).

Abstract ID: 30187

ACCELERATING DOUBLE HALF-HEUSLER THERMOELECTRIC SEARCH WITH MULTI-TASK ML

D. R. Baigutlin, V. V. Sokolovskiy, S. V. Taskaev

Chelyabinsk State University, Chelyabinsk, 454001, RUSSIAN FEDERATION

We present a transfer learning workflow that couples DFT simulations with a fine-tuned CHGNet surrogate, , a pretrained graph-neural-network interatomic potential, to accelerate the discovery of thermoelectric quantum materials in the double half-Heusler (DHH) family. DHH compounds offer a large, chemically diverse semiconductor space for thermoelectrics [1], but high-throughput screening is constrained by the hardest step to scale: lattice thermal conductivity κ_L. Predictive κ_L evaluation typically requires phonon Boltzmann-transport calculations built on second- and third-order interatomic force constants, or at minimum repeated strained DFT runs to obtain elastic tensors from stress-strain response.

To reduce this barrier, we have fine-tuned the pretrained CHGNet universal neural network potential on a curated DFT dataset of DHH structures labeled with energies, atomic forces, and full stress tensors. Stress targets are generated from homogeneous lattice deformations in a small strain window, enabling rapid ML-assisted stress-strain sweeps for elastic down-selection before running high-fidelity phonon transport. Because DHH are predominantly semiconductors, we generate the DFT labels at the r2SCAN meta-GGA level [2], which tends to improve band gaps relative to standard GGA baselines [3]. We benchmark pretrained versus fine-tuned models on a fixed train/validation/test split and report MAE for energies, forces, and stresses; the accompanying figure shows the fine-tuning learning curves and the pretrained-to-fine-tuned metric improvements. This E/F/σ surrogate enables fast relaxations and mechanically informed screening so that only the most promising candidates are forwarded to the most expensive phonon and κ_L calculations.

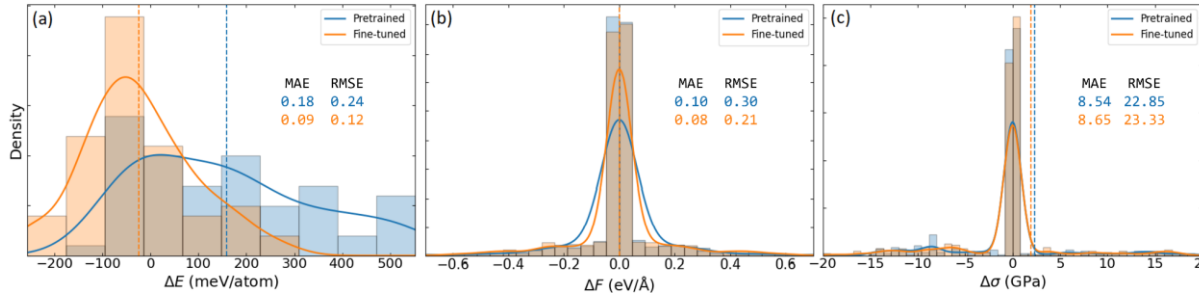

Fig. 1: *Test-set error distributions for the pretrained (blue) and fine-tuned (orange) models for (a) energy ⊿E, (b) forces ⊿F, and (c) stress ⊿σ. Dashed lines mark mean errors.*

The research was supported by the RSF - Russian Science Foundation project No. 24-12-20016.

References

[1] S. Anand, M. Wood, Y. Xia, C. Wolverton, and G. J. Snyder, Joule **3**, 1226–1238 (2019).

[2] J. W. Furness, A. D. Kaplan, J. Ning, J. P. Perdew, and J. Sun, J. Phys. Chem. Lett. **11**, 8208–8215 (2020).

[3] Z.H. Yang, H. Peng, J. Sun, and J. P. Perdew, Phys. Rev. B **93**, 205205 (2016).

Abstract ID: 30682

ENHANCING THE THERMOELECTRIC PERFORMANCE OF $Mg_3(Sb,Bi)_2$ VIA QUANTUM-DOT BOROPHENE INCORPORATION

S. S. Shahgoli[1,2], U. Aydemir[2,3]

[1] *Graduate School of Sciences and Engineering, Koç University, Istanbul, TURKEY*
[2] *Koç University Boron and Advanced Materials Application and Research Center (KUBAM), Istanbul, TURKEY*
[3] *Department of Chemistry, Koç University, Istanbul, TURKEY*

Zintl phases, have attracted significant interest for thermoelectric applications owing to their intrinsically low lattice thermal conductivity and highly tunable electronic transport properties.[1] Among them, $Mg_3(Sb,Bi)_2$-based compounds have emerged as promising n-type thermoelectrics for low- to mid-temperature cooling and energy-harvesting applications, owing to their earth-abundant, non-toxic constituent elements and excellent transport characteristics. o date, various strategies have been applied to enhance the thermoelectric efficiency of the $Mg_3(Sb,Bi)_2$ system, such as microstructure engineering, carrier concentration optimization, band structure modification, and thermal annealing.[2-4]

In this study, $Mg_{3.2}Sb_{1.5}Bi_{0.49}Te_{0.01}$ was synthesized and further modified by incorporating zero-dimensional quantum-dot borophene (QDB) to enhance thermoelectric performance. Samples with varying QDB contents were prepared via mechanical alloying followed by spark plasma sintering. The resulting $Mg_3(Sb,Bi)_2$-QDB heterostructure introduces dispersed particles, dislocations, and point defects within the matrix. These features collectively induce local lattice distortions, leading to enhanced multi-scale phonon scattering and a pronounced suppression of lattice thermal conductivity. Meanwhile, favorable Seebeck coefficients and electrical resistivity are largely preserved. As a result, a significant enhancement in the thermoelectric figure of merit (zT) is achieved, with an optimized composition exhibiting a maximum zT approaching ~2.0 at elevated temperatures. These results demonstrate that QDB incorporation is an effective strategy for improving the thermoelectric performance of $Mg_3(Sb,Bi)_2$-based materials, highlighting their strong potential as alternatives to conventional Bi_2Te_3-based thermoelectrics for low- to mid-temperature applications.

References

[1] G. Cordier, H. Schäfer, and M. Stelter, Z. Anorg. Allg. Chem. **519**, 183–188 (1984).
[2] M. Ozen, M. Yahyaoglu, C. Candolfi, I. Veremchuk, F. Kaiser, U. Burkhardt, G. Jeffrey Snyder, Y. Grin, and U. Aydemir, J. Mater. Chem. A **9**, 1733–1742 (2021).
[3] B.-Z. Tian, Y.-Y. Liao, F. Xu, X.-L. Qiu, F.-J. Zhang, and R. Ang, J. Mater. Chem. A **11**, 23319–23329 (2023).
[4] Y. Yan, S. Cao, X. Shi, W.Zhang, X. Wang, J. Liang, H. Kang, Z. Chen, E. Guo, R. Chen, and T. Wang, Acta Mater. **268**, 121394 (2025).

Abstract ID: 30571

BENCHTOP ROOM-TEMPERATURE SYNTHESIS OF HIGH PERFORMANCE THERMOELECTRICS

K. Kovnir[1,2]

[1] *Department of Chemistry, Iowa State University, Ames, Iowa 50011, USA*
[2] *Ames National Laboratory, U.S. Department of Energy, Ames, Iowa 50011, USA*

Se-containing materials are often synthesized from toxic and expensive organo-Se precursors. We are reporting a facile alternative utilizing elemental Se which is cheap and non-toxic. A process of elemental Se activation was developed resulting in stable solution of multiple Se species confirmed with ^{77}Se NMR studies, including Se in formal –1 oxidation states. The developed activated Se precursor allows us to produce and dope Ag_2Se-based materials at room temperature thus avoiding the high-temperature polymorphic phase transitions. Zn-doped Ag_2Se samples produced in the present work demonstrated remarkable thermoelectric performance with a maximum zT of 1.3 and averaged zT of 1.15 in 25-120 C range which outperforms all reported Ag_2Se materials and is on par with the best *n*-type Bi_2Te_3-based and Mg_3Bi_2-based materials. The latter materials require high-temperatures and complex synthetic modifications, while our synthesis employs a simple and sustainable benchtop chemistry to yield efficient room temperature thermoelectric materials.

49 - SPECIAL PANELS

Abstract ID: 30811

SPINAL EPIDURAL MAGNETIC FIELD CONTROLLED NANOPARTICLE SYSTEM FOR FERRITIN REGULATION: A NOVEL BIOPHYSICAL APPROACH FOR NEURODEGENERATIVE DISEASES

T. Yazar

Ankara University, Faculty of Medicine, 06100, Ankara, TURKEY

Neurodegenerative diseases, particularly Alzheimer's Disease, appear to be associated with an abnormal increase in the amount of iron metabolism and ferritin protein. Iron ions accumulating in brain tissue cause oxidative stress and damage. Currently, treatments for ferritin regulation rely on numerous pharmacological therapies. However, the target tissue dependence of the program and long-term control remain significant challenges.

This effective, novel biophysical model involves remote control of magnetic nanoparticles via an implant placed in the spinal epidural region. The system aims to modulate ferritin gain and iron metabolism with magnetic fields that control the lifespan of the spinal cord. The proposed model is theoretically based on electromagnetic field theory, nanoparticle physics, biofluid dynamics, and thermal safety analysis methods. The results demonstrate that the magnetic field generated by the epidural implant can direct nanoparticle movement while remaining within biological safety zones. Furthermore, the achieved thermal temperatures allow the tissue temperature increase to remain within the wireless safety boundary. This study proposes a novel therapeutic paradigm combining magnetic field-controlled neuromodulation and nanotechnology.

50 - SUPERCONDUCTING BASE ELEMENTS FOR SPINTRONICS AND NEURAL NETWORKS

Abstract ID: 30093

USING SPIN-ORBIT COUPLING TO GENERATE TRIPLET PAIRS IN HALFMETALLIC $La_{0.7}Sr_{0.3}MnO_3$

Y. Jungxiang[1], M. Cabero[2], J. Aarts[1]

[1] *Huygens-Kamerlingh Onnes Laboratory, University Leiden, PO Box 9504, 2300 RA Leiden, THE NETHERLANDS*
[2] *ICTS- Centro Nacional de Microscopía Electrónica, Universidad Complutense de Madrid, 28040 Madrid, SPAIN*

In earlier work, we reported on a method to fabricate bar-shaped lateral junctions consisting of the halfmetallic ferromagnetic manganite $La_{0.7}Sr_{0.3}MnO_3$ (LSMO) with superconducting NbTi contacts, where we demonstrated a Long-Range Proximity (LRP) effect with strong supercurrents over lengths up to 1.3 μm between the contacts [1]. However, in follow-up experiments, we found that, although supercurrents do exist even for longer junction lengths, the statistics of the critical current densities is still puzzling, since they do not show a simple monotonic decrease with the length between the contacts [2], pointing to limited control over the triplet generator that apparently resides at the LSMO/NbTi interface. This is a longer-standing issue. Since no magnetic inhomogeneity is purposely built in at the interface, the mechanism for triplet generation is not yet understood. The same is the case for LSMO in combination with $YBa_2Cu_3O_7$, where LRP effects are found as well [3]. In further experiments, we now separated the LSMO and the NbTi by a thin (5 nm) layer of Pt. Transmission Electron Microscopy showed the interface to be very smooth, with the Pt homogeneous and fully closed. We fabricated so-called 'full-film' devices, in which NbTi/Pt contacts are defined by lithography and Argon etching on a full film of LSMO, with a distance between contacts up to 2.1 μm. Again, we find strong supercurrents between the contacts, although in this geometry we cannot determine the critical current density. We draw two conclusions: it is not the specific combination of LSMO and NbTi that generates triplets; and a Pt interlayer appears to be very helpful in triplet generation. We will discuss how spin-orbit coupling in the Pt layer can be part of the triplet generation scenario.

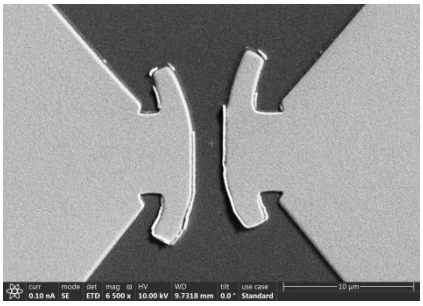

Fig. 1: *Electron Microscopy image of a NbTi/Pt contact structure (grey) on top of an LSMO thin film (black). The scalebar is 10 μm.*

References

[1] J. Yao and J. Aarts, Appl. Phys. Lett. **24**, 202601 (2024).

[2] J. Yao, J. van Doorn, M. Cabero and J. Aarts, in preparation.

[3] D. Sanchez-Manzano, *et al.*, Nature Mat. **21**, 188 (2022).

Abstract ID: 30116

FEATURES OF COHERENT TRANSPORT IN PLANAR JOSEPHSON SNS STRUCTURES WITH SPIN POLARIZATION IN THE BARRIER

T. E. Golikova[1], V. V. Ryazanov[2,1], I. A. Nazhestkin[2]

[1] *Institute of Solid State Physics, Russian Academy of Sciences, 142432, Chernogolovka, RUSSIA*
[2] *Moscow Institute of Physics and Technology, Dolgoprudny, 141700, RUSSIA*

We have studied the quasiparticle transport in planar submicron-size Josephson S-N/F-S (Al-Cu/Fe-Al) structures with Josephson barriers made of normal metal (N) and additional ferromagnetic sublayers (F) perpendicular to the N-barrier layer. Spin-split features were observed in the dependences of the differential resistance on voltage both near the $2\Delta/e$ and near the "gap" voltage. We attribute the origin of the observed subharmonic gap structure to multiple Andreev reflection in the presence of an induced effective exchange field in the N-barrier in contact with the ferromagnetic sublayer. Calculations show that the multiple Andreev reflection apparently involves the "mini-gaps" arising in the weak link due to a contact of the N-barrier with the superconducting banks. The splitting disappears in an external magnetic field applied in the plane of the structure at a value corresponding to the coercive field of the ferromagnetic nanostrip. The observed features of the coherent transport in planar hybrid Josephson nanostructures with ferromagnets in the presence of spin diffusion and spin injection into the N-barrier are discussed in terms of the approaches outlined in a recent review [1].

References

[1] V. V. Ryazanov, T. E. Golikova, V. V. Bol'ginov, I. V. Bobkova, A. M. Bobkov, Physics-Uspekhi, **68**, 717 (2025).

Abstract ID: 30727

SUPERCONDUCTING BASE ELEMENTS FOR BRAIN-INSPIRED NEURAL NETWORKS: SPINTRONIC INNOVATIONS FOR NEUROMORPHIC COMPUTER

A. Sidorenko[1,2]

[1] *TUM, Institute of Electronic Engineering and Nanotechnologies, MOLDOVA*
[2] *Moscow Institute of Physics and Technology, RUSSIA*

The development of two key elements for Artificial Neural Networks (ANN): Nonlinear switches (neurons) and linear connecting elements (synapses) rely on layered hybrid structures [1]. This design approach is becoming increasingly relevant due to advancements in technological capabilities and the ability to fine-tune the properties of nanostructures. A planar Josephson Junction is created by forming a multilayer superconducting heterostructure, typically comprising three functional layers in its simplest form.

The required properties of the Josephson Junction are determined during the formation of the superconducting SFS, SNINS and other heterostructures [2,3]. The intermediate or interlayer, positioned between two superconducting layers, governs the current transport mechanism and, consequently, the characteristics of the Josephson Junction. A highly effective technique for creating superconducting heterostructures is magnetron sputtering. When multiple magnetrons are used in a vacuum setup, this method enables the formation of the heterostructure within a single vacuum cycle, preventing contamination at the layer interfaces. Magnetron sputtering, with its relatively low energy, minimizes mutual diffusion, especially for refractory materials and ensures the atomic sharpness of boundaries during the formation of the superconducting heterostructure [4]. The developed basic elements, a superconducting neuron and superconducting synapse can be successfully applied for modeling of neural networks.

The study is supported by the Ministry of Science and Higher Education (project No 075-15-2025-010).

References

[1] S. Bakurskiy, M. Kupriyanov, N. Klenov, I. Soloviev, A. Schegolev, R. Morari, Yu. Khaydukov, A. Sidorenko, *Controlling the proximity effect in a Co/Nb multilayer: The properties of electronic transport*, Beilstein J. Nanotechnol., **11**, 1336–1345 (2020).

[2] A. A. Golubov, M. Yu. Kupriyanov, V. F. Lukichev, *Theory of the Josephson Junction in tunnel structures of SNINS and SNIS types*, – FNT, **vol. 10**, **No.8**, pp.799-811 (1984).

[3] T. Y. Karminskaya, A. A. Golubov, M. Y. Kupriyanov, A. S. Sidorenko, *Josephson effect in superconductor/ferromagnet-normal/superconductor structures*, Physical Review B, **79 (21)**, 214509 (2009).

[4] E. Antropov, M. S. Kalenkov, J. Kehrle, V. I. Zdravkov, R. Morari, A. Socrovisciuc, D. Lenk, S. Horn, L. R. Tagirov, A. D. Zaikin, A. S. Sidorenko, H. Hahn, R. Tidecks, *Experimental and theoretical analysis of the upper critical field in ferromagnet–superconductor–ferromagnet trilayers*, Superconductor Science and Technology, **26(8)**, 085003 (2013).

Abstract ID: 30746

CONTROLLING PROPERTIES OF PEROVSKITE THIN FILMS VIA STRAIN ENGINEERING (RESULTS OF THE PROJECT "INTERNATIONAL ACADEMIC COOPERATION" OF HSE UNIVERSITY)

M. R. Samatov, D. Liu, A. S. Vasenko

HSE University, 101000 Moscow, RUSSIA

Targeted modification of grain boundary (GB) properties is a critical challenge for enhancing the efficiency and stability of metal halide perovskite solar cells [1]. In this work, we employ a combination of *ab initio* and machine learning force field methods to investigate the dynamics and functional properties of GBs in $CsPbBr_3$ on nanosecond timescales [2]. Our simulations reveal that GBs exhibit significant lability, which is accompanied by the generation of transient trap states. Furthermore, GBs act as fast channels for Br^- ion migration. Most significantly, we demonstrate that both detrimental processes can be suppressed by applying uniaxial compressive strain. The applied strain stabilizes the GB structure, eliminating charge carrier traps, and induces lattice rearrangements that lead to the formation of dense, amorphous-like boundary phases, effectively blocking ionic transport, see Fig.1 [2,3]. These findings reveal the atomistic mechanisms of coupled ion and charge carrier dynamics at perovskite GBs and establish strain engineering as a viable physical strategy for controlling the functional properties of perovskite materials.

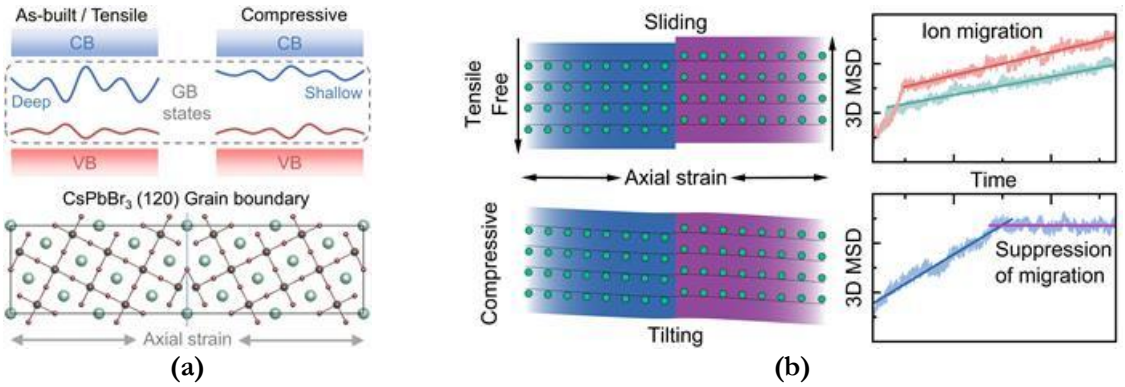

Fig. 1: *(a) Scheme of the impact of axial strain on the electronic structure of $CsPbBr_3$ GB; (b) compressive strain triggers lattice tilting within each grain and generates amorphous GB structures, blocking migration channels and ultimately quenching ion mobility.*

M.R.S. and A.S.V. acknowledge support from the project "International academic cooperation" of HSE University.

References

[1] R. Yin, Y. Wu, Z. Huang, A.S. Vasenko, S. Xu, H. Zhou, Adv. Funct. Mater. **35**, 2419184 (2025).
[2] D. Liu, Y. Wu, M.R. Samatov, A.S. Vasenko, E.V. Chulkov, O.V. Prezhdo, Chem. Mater. **36**, 2898–2906 (2024).
[3] M.R. Samatov, D. Liu, E.S. Amirov, M.A. Bubnova, A.E. Abrameshin, A.S. Kramarenko, P.A. Troshin, W. Chu, H. Zhou, O.V. Prezhdo, A.S. Vasenko, J. Phys. Chem. Lett. **16**, 13068–13074 (2025).

Abstract ID: 30770

JOSEPHSON EFFECT IN JUNCTIONS WITH BARRIERS BASED ON TOPOLOGICAL MATERIALS: THEORY AND EXPERIMENT

A. A. Golubov[1,2]

[1] *Moscow Institute of Physics and Technology, Dolgoprudny 141700, RUSSIA*
[2] *HSE University, Moscow 101000, RUSSIA*

Josephson junctions incorporating three-dimensional topological insulators (TIs) are promising platforms for realizing unconventional superconducting correlations and topological superconductivity. In particular, such junctions are expected to host low-energy Andreev bound states, potentially leading to nontrivial current–phase relations and anomalous dynamical responses. In this work, we present a unified study of Nb/$Bi_2Te_{2.3}Se_{0.7}$/Nb Josephson junctions operating in the ballistic regime, focusing on both microwave-induced Shapiro steps and magnetic-field-induced oscillations of the critical current. Under microwave irradiation, we observe a pronounced frequency-dependent suppression of the first Shapiro step below approximately 2 GHz. While such behavior is often discussed as a signature of a 4π-periodic current–phase relation associated with topological modes, a detailed analysis using a two-channel thermal resistively shunted junction (tRSJ) model demonstrates that overheating effects alone can quantitatively account for the missing odd-numbered Shapiro step, even in a ballistic junction. This highlights the necessity of careful thermal modeling when interpreting dynamical signatures of topology. At low temperatures (below 500 mK), the same junctions exhibit ultra-fine oscillations of the critical current in weak perpendicular magnetic fields, with a characteristic period on the order of 1 Oe, far smaller than expected from conventional flux quantization. We develop a theory of low-lying Andreev bound states formed at the superconductor–TI interfaces beyond the quasiclassical approximation and attribute these oscillations to resonant transmission of quasiparticles through these states. The inferred energy scale, in the μeV range, is consistent with the generation of a proximity-induced superconducting order parameter with unconventional symmetry in the TI and the presence of ballistic topological surface channels.

Taken together, our results demonstrate that Josephson junctions based on topological insulators exhibit a rich interplay between thermal effects, microwave response, and interface-bound Andreev physics. They also underscore that missing Shapiro steps do not constitute definitive evidence of topological superconductivity but must rather be interpreted within a comprehensive microscopic framework.

Acknowledgements

This work was supported by grant No.075-15-2025-010 from Russian Ministry of Education and Science and by the project "International academic cooperation" of HSE University.

Abstract ID: 30196

MULTIFUNCTIONAL LOGIC GATES FOR COMPACT SUPERCONDUCTING PROCESSORS

A. A. Maksimovskaya[1,2], V. I. Ruzhickiy[2], I. I. Soloviev[2], M. Yu. Kupriyanov[3], N. V. Klenov[1], S. V. Bakurskiy[3]

[1] *Lomonosov Moscow State University, Faculty of Physics, 119991, Moscow, RUSSIA*
[2] *Dukhov Research Institute of Automatics (VNIIA), 127030, Moscow, RUSSIA*
[3] *Lomonosov Moscow State University Skobeltsyn Institute of Nuclear Physics, 11999, Moscow, RUSSIA*

The key limitation for increasing the integration scale of traditional RSFQ logic is the size of geometric inductors. This work proposes a novel approach to the miniaturization of superconducting circuits, combining two key strategies: 1) a transition to inductor-free (all-JJ) logic, where Josephson junctions completely replace bulky geometric inductors [1], and 2) the introduction of a minimal number of elements with *controllable kinetic inductance* into key circuit nodes to enable functional reconfigurability.

We demonstrate the design of programmable splitters and tunable logic blocks, such as AND/OR and XOR/OR gates, where the same physical circuit can be dynamically switched between different logical functions. This programmability minimizes the total number of active components in complex circuits. Building upon these reconfigurable gates, we propose a novel architecture for a universal programmable logic cell. This architecture serves as an analogue of the Look-Up Table (LUT) used in FPGA designs. However, instead of storing pre-computed truth tables in memory, our approach implements a *programmable logic basis*, where the functionality is defined by the operational modes of the tunable logic gates, enabling true hardware-level dynamic reconfiguration.

Our circuit designs leverage inductor-free, junction-based approach within a reconfigurable architecture, demonstrating a path toward more compact and versatile superconductor computing systems. Furthermore, this methodology is exceptionally promising for neuromorphic systems, where the ability to dynamically alter the function of a cell significantly enhances the efficient implementation of plastic synaptic connections and adaptive network architectures, paving the way for next-generation, high-density, and energy-efficient superconducting processors.

References

[1] A.A. Maksimovskaya, V.I. Ruzhickiy, N.V. Klenov, S.V. Bakurskiy, M.Yu. Kupriyanov, and I.I. Soloviev, JETP Letters **115(12)**, 735 (2022).

Abstract ID: 30491

IMPURITY-ENHANCED DETECTION OF MAJORANA ZERO MODES IN VORTEX CORES

A. Vagov[1], V. D. Neverov[1], T. Karabassov[1], A. V. Krasavin[1], D. Roditchev[2], V. S. Stolyarov[2]

[1] *HSE University, 101000 Moscow, RUSSIA*
[2] *Institut des Nano-Sciences de Paris-Sorbonne Universite, Paris 75005, FRANCE*

The Majorana zero modes (MZMs) localized in vortex cores of topological superconductors are considered key elements for fault-tolerant quantum computation. Their experimental identification, however, is severely limited by the extremely small energy separation between the MZM and conventional Caroli–de Gennes–Matricon (CdGM) vortex states. In this work, we demonstrate that non-magnetic impurities can play a constructive role in resolving this long-standing challenge. Using a microscopic Bogoliubov–de Gennes approach applied to hybrid topological superconductors, we show that impurity-induced vortex pinning significantly increases the minigap between the MZM and other vortex-core excitations, while leaving the MZM itself intact due to its topological protection. As a result, a robust and well-isolated zero-bias peak emerges in the local density of states. Our findings overturn the conventional requirement of large Δ/E_F ratios for MZM detection and suggest an experimentally accessible strategy based on engineered non-magnetic pinning centers in conventional s-wave superconductors.

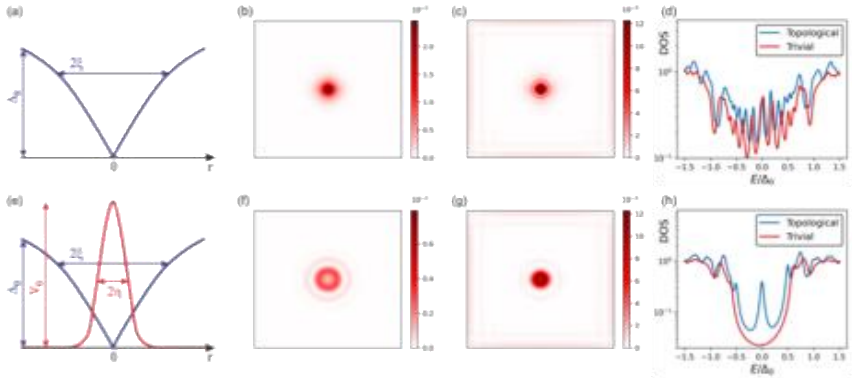

Fig. 1: Upper panels (clean system): *(a) Geometry and model parameters; the blue curve shows the vortex-core profile of the superconducting gap $|\Delta|$ with coherence length ξ and bulk value Δ_0. (b) Spatial profile of the lowest-energy CdGM state in a trivial superconductor. (c) Spatial profile of mue MZM in the topological phase. (d) Averaged vortex-core LDOS for topological (blue) and trivial (red) superconductors.* Lower panels (with pinning): *(e) Same geometry in the presence of a non-magnetic pinning potential (red curve) characterized by strength V_0 and width η. (f,g) Spatial profiles of the lowest CdGM state and the MZM, respectively. (h) Corresponding averaged vortex-core LDOS, demonstrating enhanced spectral separation of the MZM.*

References

[1] V.D. Neverov et al., Research, 2026, in print

Abstract ID: 30300

PHOTOGALVANIC PHENOMENA, VORTEX INTERACTION AND MAGNETOELECTRIC EFFECT IN SUPERCONDUCTORS SUPPORTING INTRINSIC DIODE EFFECT

A. Buzdin[1], S. Mironov[2], A. Melnikov[2], V. Plastovets[3] , A. Putilov[2]

[1] *University of Bordeaux, LOMA UMR-CNRS 5798, F-33405, FRANCE*
[2] *Institute for Physics of Microstructures, RAS, 603950 Nizhny Novgorod, RUSSIA*
[3] *University of Augsburg, 86135 Augsburg, GERMANY*

We develop a phenomenological theory of photogalvanic effects in superconducting materials and heterostructures characterized by an intrinsic diode effect. By employing a generalized London model that accounts for quadratic nonlinearities in the supercurrent-velocity relationship—corresponding to cubic gradient terms in the Ginzburg-Landau equations—we demonstrate that incident electromagnetic waves can induce a nontrivial superconducting phase difference across a sample [1]. When integrated into a superconducting loop, this "phase battery" generates a persistent circulating DC supercurrent. We show that increasing the radiation intensity can trigger transitions between loop states with distinct vorticities. Notably, this rectification mechanism is distinct from both the inverse Faraday effect, which necessitates circularly polarized light, and the photon drag effect in superconducting condensates [2].

Furthermore, we explore how these cubic gradient terms lead to a significant reshaping of Abrikosov vortices and the emergence of non-central interaction forces [3]. Finally, in superconductor/ferromagnet bilayers exhibiting an intrinsic diode effect, we demonstrate the ability to control magnetization via transport supercurrents in both DC and quasistatic AC regimes [4].

References

[1] S. V. Mironov, A.S. Melnikov, and A.I. Buzdin, Phys. Rev. B., **109**, L220503 (2024).

[2] S. V. Mironov, A.S. Melnikov, and A.I. Buzdin, Phys. Rev. Lett., **132**, 096001 (2024).

[3] A. V. Putilov, D. V. Zakharo, A. Kudluis, A.S. Melnikov, and A.I. Buzdin, Phys. Rev. B., **112**, 134507 (2025).

[4] V. Plastovets, and A. Buzdin, Phys. Rev. B., **110**, 144521 (2024).

Abstract ID: 30084

A FOUNDRY-READY TOP-DOWN EDA FLOW FOR ADIABATIC QUANTUM-FLUX-PARAMETRON LOGIC: FROM RTL TO GDSII

O. Chen

Faculty of Information Science and Electrical Engineering, Kyushu University, 819-039, Fukuoka JAPAN

Adiabatic Quantum-Flux-Parametron (AQFP) logic is a promising platform for ultra–energy-efficient computing. A key obstacle to moving AQFP circuits from laboratory prototypes to practical VLSI systems is the absence of a standardized physical design methodology. Unlike CMOS, where logic states are quasi-static, AQFP data propagates stage by stage under multi-phase AC excitation. This gives rise to a "phase-locking" constraint, in which the topology and physical length of each signal path must be tightly matched to the clock distribution network. Conventional design tools are not designed to capture the strong dependency of signal timing on logical topology and clock phase, so manual design quickly becomes unmanageable for complex arithmetic units.

We address this problem with a systematic, top-down EDA framework that implements a complete flow from register-transfer level (RTL) to design-rule-check (DRC)-clean GDSII layouts. The innovation of our approach lies in its distinct optimization strategies across design domains. In the logic domain, we employ an AQFP-specific majority-based synthesis algorithm. Unlike generic mapping, this engine explicitly targets the minimization of splitters (required for signal fan-out) and buffers (essential for phase synchronization), thereby significantly reducing the overall Josephson-junction count and circuit latency. In the physical domain, accounting for the strict constraints of current-based signal transmission, the framework performs topological re-optimization of the circuit graph. It seeks the most economical placement and routing solution that aligns logic depth with the multi-phase clock propagation, ensuring optimal signal integrity with minimal area overhead. Treating clock-phase synchronization as a first-class geometric constraint allows the flow to preserve data-path alignment across deep pipelines without manual layout edits.

We validate the methodology on an 8-bit Kogge–Stone adder (KSA) implemented in a standard-cell style and taped out in the AIST 10-kA/cm², four-layer planarized high-speed standard process (PHSTP). The circuit is synthesized, placed, and routed entirely within the proposed framework. Pre-tape-out signoff checks confirm that the generated layout satisfies all foundry design rules as well as the imposed AQFP phase-timing constraints, without hand-crafted Datapath layout. These results demonstrate the feasibility of organizing AQFP design as a standard-cell-based flow and suggest that the proposed approach can be extended to more complex superconducting VLSI systems.

Abstract ID: 30099

REINFORCEMENT LEARNING WITH SUPERCONDUCTING CIRCUITS

M. L. Schneider

National Institute of Standards and Technology, Applied Physics Division, 80305, Boulder, UNITED STATES

Superconducting circuits are an excellent bio-inspired computing technology. The basic building blocks that make up the brain and are used in modern AI neural networks are neurons (nodes) and synapses (weights.) In superconducting circuits, the Josephson junctions alone or few junction circuit can be used as the neurons (nodes) [1]. There are several potential small scale synaptic (weight) circuits, including a bipolar trainable synapse that we recently proposed [2]. Further, the near lossless transmission of spiking data on superconducting transmission lines is analogous to axons in the brains and offers a dramatic advantage for communications compared to many other technologies.

In this talk I will give a brief overview of bio-inspired superconducting circuits and describe SPICE simulations of a complete Josephson junction neural network that performs its own training via reinforcement learning. We find that we can implement the reinforcement learning weight updates using relatively standard SFQ logic gates resulting in a fully self-training hardware neural network without the need to explicitly program weight values or use any additional computation in the training loop. In addition, this hardware centered training method alleviates the need for relaying large amounts of global information that is typical in training algorithms like backpropagation.

Our SPICE simulations of a small deep neural network has a learning time of order one nanosecond per update and demonstrates robust learning of several different functions including the non-linearly separable XOR problem. Using the rules from these SPICE simulations, we extend the network in python simulations to one that can solve the MNIST benchmark with better than 90% accuracy. Because of the fast learning time and favorable scaling of these networks, our projection is that the complete training time for our network architecture to learn the MNIST benchmark would be about 100 ms. We will discuss the details of how we implement this network architecture in SPICE, its learning rules, and how such a network would scale to larger problems.

References

[1] P. Crotty, D. Schult, K. Segall, Phys. Rev. E **82.1**, 011914 (2010).

[2] M. L. Schneider, *et al.*, npj Unconventional Computing **2.1,** 5 (2025).

Abstract ID: 30100

REVISED RCLSJ MODEL WITH IMPROVED MODEL-TO-HARDWARE CORRELATION FOR SUPERCONDUCTING DIGITAL CIRCUIT SIMULATION

J. Ren[1,2], S. Wang[3], X. Gao[1,2]

[1] *State Key Laboratory of Materials for Integrated Circuits, Shanghai Institute of Microsystem and Information Technology, Chinese Academy of Sciences, 865 Changning Road, Shanghai 200050, P. R. CHINA*
[2] *University of Chinese Academy of Sciences (UCAS), Beijing 100049, P. R. CHINA*
[3] *Shanghai University, Shanghai 200444, P. R. CHINA*

The pursuit of high-speed response and precise phase reversal reconstruction in Josephson junctions (JJs) is core to device modeling for superconducting single-flux-quantum (SFQ) circuits, where accurate dynamic simulations are critical for performance optimization. The resistive-capacitive-inductive-shunted junction (RCLSJ) model, an extended RCSJ model with an additional shunt inductance, captures more detailed JJ current–voltage (I–V) characteristics than its predecessor. However, its effectiveness in dynamic simulations of practical digital SFQ circuits remains unsystematically validated.

Previously, we proposed a reliable process control monitor (PCM)-based method for RCLSJ parameter extraction. Here, we extend this method to digital SFQ circuit simulations. Leveraging the RCLSJ's strength in high-frequency response capture, we designed a simple D flip-flop (DFF) test structure to characterize bias margin variation over a broad frequency range. Post-simulations with the original RCLSJ model revealed noticeable mismatches with experimental data, especially above 60 GHz.

To resolve this, we developed a revised model (RCLSJv), reallocating junction parasitic inductance and introducing test-data-fitted correction coefficients. Its validity was thoroughly verified through comprehensive fitting of test results from multiple DFF configurations. Compared with the conventional RCSJ model, the RCLSJv model successfully confines the deviation between simulation and test results to within 3%. Notably, above 60 GHz, the matching degree is remarkably enhanced, with an improvement factor of 2–5 times. Additionally, when applied to low-frequency bias margin verification of multiple cells in an SFQ digital cell library, the RCLSJv model consistently outperforms the RCSJ model, demonstrating its reliability, accuracy, and versatility across both high- and low-frequency SFQ circuit simulations.

References

[1] Y. Gao, *et al.*, Physica C: Superconductivity and Its Applications,5**98,** 1354076 (2022).

[2] S. Wang, *et al.*, Supercond. Sci. Technol. **38**, 055011 (2025).

Abstract ID: 30108

SCANNED SQUID MICROSCOPY OF SUPERCONDUCTING DIGITAL LOGIC

I. W. Haygood[1], B. Xu[2,3], M. L. Schneider[1]

[1] *Nationial Institute of Standards and Technology, 80305, Boulder, USA*
[2] *Associate of NIST Spin Electronics Group, 80305, Boulder, USA*
[3] *University of Colorado – Denver, Physics Department, 80210, Denver, USA*

Trapped flux and the role of moats, or holes in the ground plane, have been theorized about and studied over the decades [1-4]. We report on the development of a scanned SQUID microscope for imaging of active superconducting digital logic circuits. The microscope utilizes planar gradiometric susceptometer/magnetometers with pickup loops as small as 500 nm in diameter which can simultaneously capture magnetic as well as susceptibility data at a sample temperature from 3.3 K – 40 K. System noise is 1.3 $\mu\Phi_0/\sqrt{\text{Hz}}$ at the system base temperature of 3.3 K. A cryogenic chip socket and silicon interposer can be installed in the system which can interface with a DUT with up to 40 RF lines. The approximate loss of the signal path is 15 dB at 20 GHz. This system has the capability to measure electrical performance and margins as well as determine and image the location of trapped flux in digital circuits and will hopefully facilitate the advancement of next generation superconducting digital log circuits.

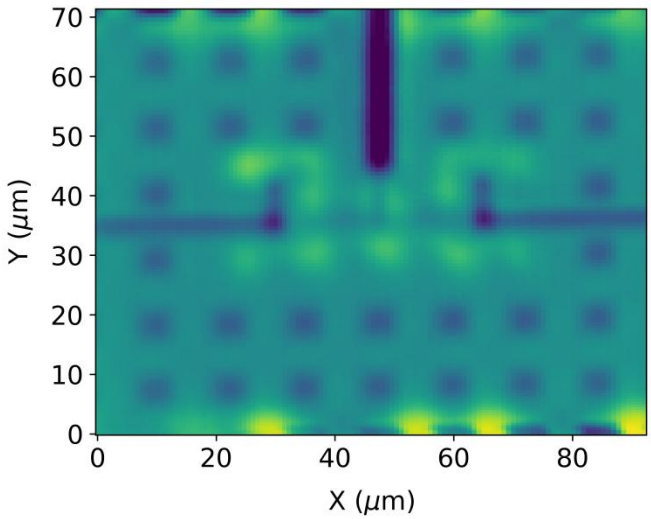

Fig. 1: *Image of a DC SQUID with an array of moats (yellow rectangles in the center of the image) surrounding the JJs and SQUID body. The niobium wiring layer appears in dark blue.*

References

[1] S. Bermon and T. Gheewala, IEEE Trans. on Magnetics, **19(3)**, 1160-1164, (1983).

[2] V. Semenov, M. Khapaev, IEEE Trans. on Applied Superconductivity, **26(3)**, 1300710 (2016).

[3] M. Jeffery et al., Applied Physics Letters, **67(12)**, 1769-1771, (1995).

[4] C. Fourie, K. Jackman, IEEE Trans. on Applied Superconductivity, **31(5)**, 1300507, (2021).

Abstract ID: 30124

DEVELOPMENT OF FABRICATION PROCESSES FOR HIGH-PERFORMANCE SUPERCONDUCTING ELECTRONIC DEVICES AND INTEGRATED DIGITAL CIRCUITS AT SIMIT

L. Ying, G. He, L. Ma, H. Xie, W. Shi, H. Li, J. Ren, Z. Lin, W. Peng, L. You, Z. Wang

Shanghai Institute of Microsystem and Information Technology (SIMIT), Chinese Academy of Sciences (CAS), Shanghai 200050, CHINA

The Superconducting Electronics Facility at SIMIT-Shanghai serves as a cutting-edge research and development platform dedicated to superconducting electronic devices and circuits. We have successfully developed a diverse array of fabrication technologies tailored for high-performance superconducting electronic devices and integrated circuits, meeting various application-specific requirements. The first standard fabrication process "SIMIT Nb03" with 10 mask levels includes 3 Nb superconducting layers and a Mo resistor layer. Based on our verified process "SIMIT Nb03", we added a Nb superconducting layer and developed the Nb03P process. Subsequently, by introducing CMP (Chemical Mechanical Polishing) technology, we have developed "SIMIT Nb04" fabrication technology for superconducting integrated circuits with Nb-based Josephson junctions. The "SIMIT Nb04" fabrication process using 19 mask levels includes 7 Nb superconducting layers and a Mo resistor layer. The device structure is composed of active layers including junctions at the bottom, two passive transmission line (PTL) layers in the middle and a DC power layer at the top. As a variant of the aforementioned processes, we have developed a superconducting quantum annealing process by utilizing CMP (Chemical Mechanical Polishing) technology and sub-micron Josephson junction fabrication techniques. A set of process control monitors (PCMs) for monitoring fabrication and design parameters was designed and tested to evaluate the process reliability and controllability. Feedback of the PCM results to the circuit design and fabrication parameters has efficiently improved the technology. Furthermore, a range of high-performance superconducting electronic devices and integrated circuits, including Superconducting Nanowire Single Photon Detectors (SNSPDs), Superconducting Quantum Interference Devices (SQUIDs), digital circuits, and qubits, have been successfully fabricated and rigorously tested, thereby validating the robust capability of our fabrication technology.

Abstract ID: 30143

THE INFLUENCE OF FLUX ON AQFP CIRCUITS FOR A DOUBLE-ACTIVE-LAYERED NIOBIUM FABRICATION PROCESS

L. Schindler[1,2], K. Jackman[1,2], N. Yoshikawa[3], C. J. Fourie[1,2]

[1] *Stellenbosch University, Dept. of Electrical and Electronic Engineering, 7600, Stellenbosch, SOUTH AFRICA*
[2] *SUN Magnetics, 7600, Stellenbosch, SOUTH AFRICA*
[3] *Institute of Advanced Sciences, Yokohama National University, 240-8501, Yokohama, JAPAN*

Adiabatic quantum-flux-parametron (AQFP) [1] is an ac-biased logic family noted for its extremely low switching energy of approximately 1.4 zJ per Josephson junction (JJ) at a clock frequency of 5 GHz. The AQFP logic family, therefore, offers a high-speed, ultra-low-energy alternative to CMOS technology. However, quantized flux trapped in the superconductor film can adversely affect circuit operation. A common solution to mitigate this issue is the introduction of low-potential holes, also known as moats, within the film. Quantized flux is statistically more likely to become trapped within these moats due to the lower energy potential compared to the surrounding film. Although basic guidelines have been derived from published circuits, no standard method currently exists for designing and analyzing moats for AQFP circuits. The Double Gate Process (DGP) [2], a double-active-layered niobium fabrication process, enables more compact circuit designs but also introduces new complexities regarding the behavior of flux across both active layers. We present measured results on how trapped flux influences the operation of fabricated AQFP cells and compare the efficiency of different moat structures with simulated results presented in [3].

References

[1] N. Takeuchi, *et al.*, SUST **26**, no. 3, 035010 (2013).

[2] T. Ando, *et al.*, SUST **30**, no. 7, 075003 (2017).

[3] L. Schindler, *et al.*, IEEE TAS **34**, no. 3, 1100908 (2024).

Abstract ID: 30155

THE EFFECT OF LAYOUT ON THE SENSITIVITY OF DIGITAL AQFP CIRCUIT MARGINS TO TRAPPED FLUX

C. J. Fourie[1,2]

[1] *Stellenbosch University, Dept. of Electrical and Electronic Engineering, 7600, Stellenbosch, SOUTH AFRICA*
[2] *SUN Magnetics, 7600, Stellenbosch, SOUTH AFRICA*

Experimental measurements and matching layout-extracted simulations of Adiabatic Quantum Flux Parametron (AQFP) logic cells confirm that both dc and ac operating margins are sensitive to trapped flux. This trapped flux may appear either as engineered fluxons in moats or as Pearl vortices pinned in superconducting ground planes.

This presentation discusses recent advances in mapping operating-margin dependence on fluxon position across a superconducting layout, with a particular focus on AQFP cells. A stepped-vortex scan method is demonstrated in which a pinned vortex is systematically moved across the layout. At each step, a high-fidelity model of vortex coupling—constructed using a fundamental inductor formulation [1]—is extracted and simulated using JoSIM [2] to determine the corresponding dc and ac margins. Results for control structures are compared directly with experimental data.

The method is then applied to a range of AQFP logic circuits with differing layout geometries. The results show how operating margins shift as a function of vortex position and can degrade to zero when vortices pin in locations that induce strong current-distribution asymmetry. The analysis further identifies favourable and unfavourable moat configurations, demonstrating that careful symmetry engineering between circuits and their moats can significantly reduce margin degradation caused by nearby trapped flux.

Finally, the study evaluates alternative layout and moat strategies to enhance robustness to trapped flux. The influence of sky planes in multilayer processes, vertical overlap in double-active-layer AQFP technologies, and chip stacking in future high-density implementations is analysed in terms of coupling strength and design viability.

The presentation concludes with guidelines for improved AQFP layout practices and an assessment of the prospects for multilayer and stacked-chip AQFP technologies.

References

[1] K. Jackman and C. J. Fourie, *Identification of Magnetic Couplings in Superconductor Circuits*, Supercond. Sci. Technol., accepted for publication.

[2] J. A. Delport, K. Jackman, P. Le Roux, and C. J. Fourie, *JoSIM—superconductor SPICE simulator*, IEEE Trans. Appl. Supercond., **29**, art. no. 1300905 (2019).

Abstract ID: 30166

LOW-POWER SUPERCONDUCTING CIRCUITS USING FERROMAGNETIC π-JUNCTIONS

M. Tanaka, S. Deguchi, K. Inagaki, K. Toyama, K. Suzuki, F. Li, A. Fujimaki

Nagoya University, 46408603, Nagoya, JAPAN

In this talk, we recent report progress of low-power superconducting circuits called half-flux-quantum (HFQ) circuits. In HFQ circuits, a superconducting quantum interference device (SQUID) containing a ferromagnetic junction is used as the switching element. Because of the assistance of the spontaneous current induced by the π phase shift in the ferromagnetic junction, the SQUID is easily switched by a weak driving force. This feature leads to significantly lowered the nominal critical current of the SQUID, and the HFQ circuits can be driven by small bias currents. We can also lower the bias voltages, thereby further reducing static and dynamic power consumption at junctions and bias-feeding resistors.

We use a "0-0-π SQUID" configuration composed of two conventional switching junctions and one non-switching π-junction [3]. The nominal critical current can be controlled by the loop inductance and the critical current switching junctions. We have designed, fabricated, and tested several basic elements of HFQ circuits, including wiring elements, flip-flops, interface circuits to SFQ circuits, by forming Nb/PdNi/Nb π-junctions on standard, Nb four-layer structure chips [4]. We have recently demonstrated a low-power shift register as a combination of HFQ circuit components [5], as shown in Fig. 1., and obtained the power consumption of 0.12–0.18 μW/bit, which was about 1/10 of the conventional, typical SFQ shift-register. We will also discuss the operation of HFQ circuits driven by ultra-low-bias currents to further reduce power consumption.

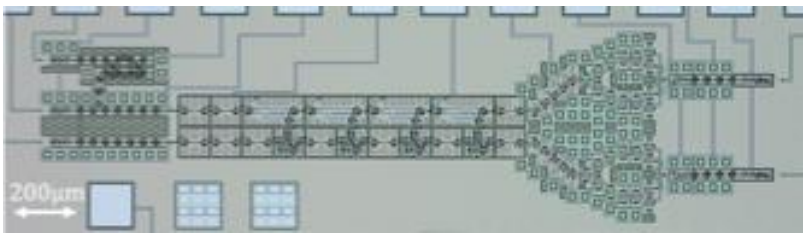

Fig. 1: *HFQ shift register fabricated with Nb/PdNi/Nb π-junctions [5].*

References

[1] T. Kamiya, *et al.*, *Energy/space-efficient rapid single-flux-quantum circuits by using π-shifted Josephson junctions*, IEICE Trans. Electron., **vol. E101-C**, pp. 385–390 (2018).

[2] F. Li, *et al.*, *Low-power high-speed half-flux-quantum circuits driven by low bias voltages*, Supercond. Sci. Technol., **vol. 34**, p. 025013 (2021).

[3] D. Hasegawa, *et al.*, *Demonstration of interface circuits between half- and single- flux- quantum circuits*, IEEE Trans. Appl. Supercond., **vol 31**, p. 1101504 (2021).

[4] A. Fujimaki, *et al.*, *Ferromagnetic π junctions on niobium four-layer structure for superconductor large-scale integrated circuits*, IEICE Trans. Electron., **vol. E108-C**, **no. 6**, pp. 348–353 (2025).

[5] M. Tanaka, *et al.*, *Demonstration of low-power shift-register based on half-flux-quantum logic*, IEICE Trans. Electron., **vol. E108-C**, **no. 6**, pp. 335–341 (2025).

Abstract ID: 30180

RECENT PROGRESS IN DUAL-RAIL DIRECT-COUPLED ADIABATIC QUANTUM-FLUX-PARAMETRON (D²AQFP) INTEGRATED CIRCUITS

N. Yoshikawa[1,2], Y. Hasegawa[2], Y, Hoshika[2], C. Ayala[1]

[1] *Institute of Advanced Sciences, Yokohama National University, 240-8501, Yokohama, JAPAN*
[2] *Graduate School of Engineering, Yokohama National University, 240-8501, Yokohama, JAPAN*

The adiabatic quantum-flux-parametron (AQFP) is an extremely energy-efficient superconducting logic family, owing to the adiabatic operation of flux-based logic circuits. One drawback of conventional AQFP logic is the use of superconducting transformers to propagate output signals to subsequent gates, which occupy a large circuit area. Furthermore, simple scaling laws for miniaturizing circuit size are not directly applicable to future submicron-scale AQFP circuits. To overcome these issues and increase the circuit density of AQFP logic, we are investigating dual-rail direct-coupled AQFP (D²AQFP) logic. D²AQFP uses dual-rail signal lines to represent positive and negative logic states and eliminates the superconducting transformers required for signal inversion in conventional AQFP circuits. Logic gates such as AND-OR and EXOR-AND gates can be implemented efficiently without increasing hardware cost compared with conventional AQFP logic. In this presentation, we report recent progress on D²AQFP, including the design and experimental demonstration of adder, multiplier, and decoder circuits. Their hardware costs and performance are evaluated and compared with those of circuits designed using conventional AQFP logic.

Abstract ID: 30183

THREE-DIMENSIONAL EXTRACTION OF PARASITIC INDUCTANCE AND CAPACITANCE IN LARGE SHUNT CAPACITORS FOR SUPERCONDUCTING QUBITS

K. Jackman[1], C. J. Fourie[1,2]

[1] *SUN Magnetics, Stellenbosch, 7600, SOUTH AFRICA*
[2] *Department of Electrical and Electronic Engineering, Stellenbosch University, Stellenbosch, 7600, SOUTH AFRICA*

Parasitic inductance and capacitance associated with the large shunt capacitors of superconducting qubits, such as transmon-type devices, play a critical role in defining their electromagnetic environment, mode structure, and integration density, especially in multilayer quantum integrated circuits. We present a numerical framework for accurately extracting three-dimensional inductance and capacitance of complex shunt-capacitor geometries used in superconducting qubit layouts, including the effects of multi-dielectric layering, superconducting film thickness, and kinetic inductance contributions. Particular emphasis is placed on the accurate evaluation of parasitic series and loop inductances arising from multilayer current-return paths and patterned superconducting films. We also address capacitance extraction in multilayer layouts with multiple dielectric layers, accounting for via structures, dielectric thickness variations, sharp layout corners, and fringing fields near ground-plane edges. Using a quasi-static three-dimensional field solver for multi-dielectric extraction, we analyse how geometric features such as interdigitated fingers and superconducting vias jointly contribute to unintended inductive loops and distributed capacitances. Our methodology provides compact, frequency-relevant parasitic models for qubit shunt capacitors and their current-return networks that can be directly incorporated into superconducting-qubit design flows without resorting to full qubit-level simulations. These insights offer practical guidelines for engineering shunt capacitors and interconnects with predictable inductive and capacitive parasitics, supporting scalable and robust superconducting qubit hardware.

Abstract ID: 30203

SFQ CONTROL OF A TRANSMON

A. Kirichenko, K. T. Tsai, A. Somoroff, C. Jordan, N. Shumiya, A. Weis, I. Vernik, R. Albu, S. J. Han

SEEQC Inc., Elmsford, NY 10523, USA

Superconducting single flux quantum (SFQ) electronics have some advantageous properties for controlling superconducting qubits in large scale quantum computers (QC). Operating at low temperature, they allow to step up the integration scale (i.e., the total number of qubits placeable in compact cryogenic environment) and to shorten the latency for control-readout cycle. The in-fridge digital control also results in much fewer RF cables needed to operate the QC, thus reducing the heat load. Each transmon needs a charge (XY) control and a flux (Z) control circuitry. In case of room-temperature control electronics this requires two RF cables for each qubit that amounts to hundreds of massive coaxial cables. The integrated SFQ digital approach would potentially need only a few RF cables for a hundreds-qubit system.

Here we present our all-digital transmon control system based on low-power ERSFQ digital circuits. The integration is achieved by placing qubit flip-chip on an active digital carrier, employing capacitive (XY) and magnetic (Z) coupling. We will describe the design and present the test results on the flux- and charge- control drivers.

Abstract ID: 30222

SUPERCONDUCTING QUANTUM CIRCUITS BASED ON NITRIDE SUPERCONDUCTORS

H. Terai[1], S. Kim[2], T. Fuse[2], S. Mima[1], D. Pham[1], S. Ashhab[2], K. Semba[2,3], T. Yamashita[4]

[1] *National Institute of Information and Communications Technology, Advanced ICT Research Institute, 6512492, Kobe, JAPAN*
[2] *National Institute of Information and Communications Technology, Advanced ICT Research Institute, 1848795, Koganei, JAPAN*
[3] *Institute for Photon Science and Technology, The University of Tokyo, 1130033, Tokyo, JAPAN*
[4] *Department of Applied Physics, Graduated School of Engineering, Tohoku University, 980857, Sendai, JAPAN*

Nitride superconductors such as NbN, NbTiN, and TiN have attracted attention as low-loss superconductors in superconducting quantum circuits. We successfully developed a technique for domain-matching epitaxy of TiN films on Si (100) substrates [1], which is being used in superconducting quantum processors under development in the Q-LEAP Flagship Project, a national project toward superconducting quantum computers in Japan [2]. We also developed NbN/AlN/NbN epitaxial junctions on Si (100) substrate with a TiN buffer layer, where the AlN tunnel barrier has a cubic structure. Considering that amorphous oxide tunnel barriers are a decoherence source in superconducting qubits, such crystallized AlN tunnel barriers could significantly improve the coherence time of superconducting qubits. The superconducting transition temperature T_C of NbN is also as high as 16 K, which is more than an order of magnitude higher than that of Al at 1 K. So superconducting qubits with NbN/AlN/NbN epitaxial junctions have the potential to operate at 1 K, which is never achievable with Al/AlO_X/Al junctions. We have established a fabrication technique for submicron NbN/AlN/NbN junctions epitaxially grown on Si (100) substrates [3], and fabricated C-shunt flux qubits based on these junctions, successfully observing an energy relaxation time T_1 of 16.3 ms and a spin-echo dephasing time T_{2E} of 21.5 ms [4]. We also successfully demonstrated the operation of C-shunt flux qubits at zero magnetic field with NbN/PdNi/NbN ferromagnetic junctions as p-phase shifters [5]. In this talk, we introduce recent progress in superconducting qubits based on nitride superconductors as a new material platform for future quantum technologies.

Acknowledgement

This work was partly supported by MEXT Q-LEAP (JPMXS0118068682, JPMXS0120319794), JST CREST (JPMJCR24I5, JPMJCR1775), JSPS Grant-in-Aid for Scientific Research (S) (25H00406) and Moonshot (JPMJM2067).

References

[1] R. Sun, *et al.*, IEEE Trans. on Appl. Supercond. **25**, 1101204 (2015).

[2] https://www.riken.jp/pr/news/2023/20230324_1/

[3] W. Qiu, *et al.*, Appl. Phys. Exp. **13**, 126501 (2020).

[4] S. Kim, *et al.*, Commun. Mater. **2**, 98 (2021).

[5] S. Kim, *et al.*, Commun. Mater. **5**, 216 (2024).

11th International Conference on Superconductivity and Magnetism ICSM2026
4th International Conference on Quantum Materials and Technologies ICQMT2026
19th April to 26th April, 2026, Ölüdeniz – Fethiye/Muğla, Türkiye
https://icsmforever.org/

Abstract ID: 30267

VORTEX MITIGATION STRATEGIES IN SUPERCONDUCTING MICROELECTRONIC DEVICES USING LARGE-SCALE SIMULATIONS

A. Glatz[1], D. Joseph[1], Z. Zhao[1], L. Cadorim[2], M. Milosevic[2] A. Koshelev[3], B. Janko[3]

[1] *Department of Physics, Northern Illinois University, DeKalb, IL 60115, USA*
[2] *Department of Physics, University of Antwerp, 2020 Antwerpen, BELGIUM*
[3] *Department of Physics & Astronomy, University of Notre Dame, South Bend, IN 46556, USA*

In superconducting electronic devices, trapped vortices/magnetic flux are a major obstacle to their intended operation. Therefore, appropriate mitigation strategies need to be developed. One possible option is to add anisotropically patterned superconducting layers to the circuits, which can be used to drive the flux out – which represents a geometrically realized superconducting diode. This can be achieved through nano-patterning, e.g., a "ratchet" pattern (see Fig. 1). Here we study such systems using the time-dependent Ginzburg-Landau (TDGL) equations, which are solved by a large-scale numerical solver [1]. We can use actual experimental patterned Niobium films as a template for the complex geometry of the simulated system.

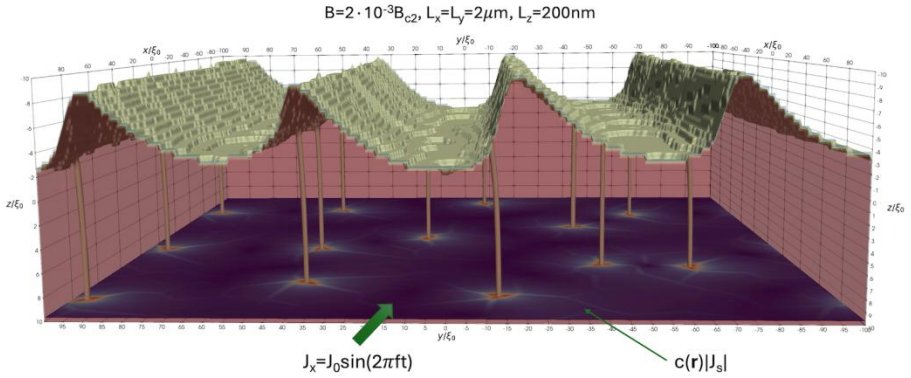

Fig. 1: *Simulation snapshot of an AC driven ratchet patterned Niobium film. For the ratchet structure an AFM height profile of a real ratchet with period of 500nm was used and the granular structure of the Niobium was approximated by a Voronoi modulation of the mean-free path. Shown is an isosurface of the superconducting order parameter amplitude and in the lower plane the supercurrent density multiplied by the inverse mean free path c(**r**).*

In this talk I will show that these structures can move flux in a particular direction using only an applied AC current, then show how these structures can be optimized for most efficient flux removal, and finally how these ratchets can be used to remove flux in adjacent circuit layers and Josephson junctions [2].

References

[1] I. A. Sadovskyy, *et al.*, Stable large-scale solver for Ginzburg-Landau equations for superconductors, J. of Comp. Phys. **294**, 639 (2015).
[2] A. Glatz, *et al.,* in preparation.

Abstract ID: 30362

A SUPERCONDUCTING ISING MACHINE BASED ON JOSEPHSON PARAMETRIC OSCILLATOR NETWORKS

B. Z. Ucpinar, S. Razmkhah, M. Pedram

University of Southern California, Ming Hsieh Dept. of Electrical Engineering, 90007, Los Angeles, CA, USA

Superconducting Ising machines have emerged as promising hardware accelerators for solving combinatorial optimization problems. In this work, we present the design and simulation of a superconducting Ising machine implemented using a network of Josephson Parametric Oscillators [1] within the Lechner–Hauke–Zoller (LHZ) architecture. NP-complete problems formulated in Quadratic Unconstrained Binary Optimization (QUBO) form are transformed into an equivalent Ising Hamiltonian using pairwise spin interactions and constraint-enforcing penalty terms. Both weighted and unweighted problems are supported. The solution is obtained through an annealing process, where the evolution of oscillator phases encodes the spin states of the Ising model. Key annealing parameters and operating regimes are investigated to optimize solution accuracy and convergence. To support rapid design exploration, an automated Python-based framework [2] is extended to enable problem mapping, netlist generation, and simulation using superconducting SPICE-based simulators. A complete superconducting hardware framework is developed, including the network of oscillator, control, and readout circuits [3], demonstrating the feasibility and compatibility of superconducting parametric oscillator networks for scalable Ising machine implementations.

References

[1] S. Razmkhah, M. Kamal, N. Yoshikawa and M. Pedram, *Josephson parametric oscillator based Ising machine*, American Physical Society (2024).
doi: 10.1103/PhysRevB.109.014511.

[2] B. Z. Ucpinar, S. Razmkhah, M. Kamal and M. Pedram, *Scalable Superconductor Ising Machine for Combinatorial Optimization Problems*, 2024 IEEE Computer Society Annual Symposium on VLSI (ISVLSI), Knoxville, TN, USA, pp. 565-570 (2024).
doi: 10.1109/ISVLSI61997.2024.00107.

[3] B. Z. Ucpinar, M. A. Karamuftuoglu, S. Razmkhah, M. Kamal and M. Pedram, *An On-Chip Control and Readout Circuit Design for an Ising Annealer*, in IEEE Transactions on Applied Superconductivity, **vol. 35**, **no. 5**, Art no. 1700906 (2025).
doi: 10.1109/TASC.2025.3540049.

Abstract ID: 30367

ADVANCING THE FRONTIERS OF ADIABATIC SUPERCONDUCTOR DIGITAL ELECTRONICS

C. L. Ayala

Yokohama National University, Institute of Advanced Sciences, 240-8501, Yokohama, JAPAN

As CMOS technology nears its physical limits, superconducting adiabatic quantum-flux-parametron (AQFP) logic arises as a transformative alternative for the energy-intensive demands of IoT and Big Data. Utilizing a 10 kA/cm² unshunted Nb/AlO_x/Nb Josephson junction process, AQFP circuits achieve sub-$50k_BT$ energy dissipation at 5 GHz. The landmark demonstration of the MANA microprocessor, integrating over 20,000 Josephson junctions (JJs), proved the feasibility of adiabatic computing showcasing the capability of the AQFP to perform both logic and memory [1]. However, it also highlighted critical scaling challenges, namely: lowering data propagation latency, reducing chip-scale clock skew, increasing circuit density, and improving signal integrity as well as resilience to unwanted flux trapping. This talk details our recent advancements in overcoming these bottlenecks to enable practical, feature-rich, high-performance applications. We present progress in microwave AC clocking networks [2] and data synchronization between clock domains [3] as well as heterogeneous superconductor logic architectures balancing ultra-low power with high-speed processing. Furthermore, we explore the evolution of AQFP-based SHA-3 cryptographic accelerators [4] with the latest iteration featuring a 3.5-GHz 200-bit state SHA-3 chip with over 70,000 JJs. These results position AQFP-based superconducting digital electronics as an emerging cryo-hardware platform for next generation computing.

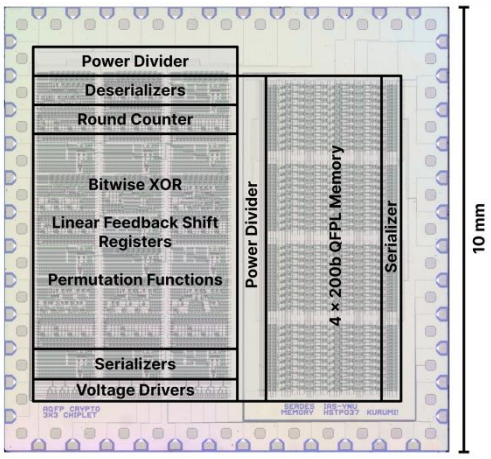

Fig. 1: *A 3.5 GHz 200-bit SHA-3 AQFP cryptographic accelerator chip comprising over 70k JJs.*

References

[1] C. L. Ayala, *et al.*, IEEE J. Solid-State Circuits, **vol. 56**, **no. 4**, pp. 1152–1165 (2021).
[2] Y. He, *et al.*, Supercond. Sci. Technol., **vol. 36**, **no. 1**, p. 015006 (2022).
[3] Y. He, *et al.*, Supercond. Sci. Technol., **vol. 38**, **no. 2**, pp. 1–8 (2024).
[4] C. L. Ayala et al., in 2024 IEEE Computer Society Annual Symposium on VLSI (ISVLSI), Knoxville, TN, USA, , pp. 557–564 (July 2024).

Abstract ID: 30384

INTEGRATED DIGITAL SYSTEM SOLUTION FOR SUPERCONDUCTING QUANTUM COMPUTING BASED ON mK-GENERATED SINGLE FLUX QUANTUM PULSE PATTERNS FOR MULTI-QUBIT CONTROL

Th. Ortlepp [1,2], A. Reinhardt[1], T. Haddad[1], M. Schmelz[3], N. Yoshikawa[2]

[1] *CiS Forschungsinstitut fuer Mikrosensorik GmbH, 99099 Erfurt, GERMANY*
[2] *Yokohama National University, Institute of Advanced Science, Yokohama, JAPAN*
[3] *Leibniz Institute for Photonic Technology IPHT Jena, 07745 Jena, GERMANY*

Quantum technologies are today regarded as one of the key technologies with huge implications to technological, economic and social developments in the next decades. Among the different platforms, superconducting implementations represent one of the most promising and are therefore pursued by several research institutions but also by numerous high-tech companies. Current research focusses e.g. on scaling towards a large number of qubits needed for practical implementations of this technology.

The realization of interface and control circuits represents an important key technology on the way to usable quantum computers but also complex quantum sensor systems. Due to the specific requirements on power consumption and technology compatibility, energy-efficient superconducting digital electronics can be considered as the most promising direct interface technology for superconducting quantum circuits. Amongst the various realizations, adiabatic quantum flux parametron (AQFP) circuits have shown lowest power dissipation reaching Landauer limit.

The operation of AQFP circuits down to mK temperature has been recently demonstrated. We will present a new concept for a digital control circuit based on the microwave pulse patters generated by single flux quantum circuits operating at mK temperatures. We discuss the circuit operation and the integration together with superconducting qubits to a compact and scalable approach for multi-Qubit control by digital pulse patterns.

Abstract ID: 30475

SFQ-BASED TDCS FOR SNSPDS

T. V. Filippov, D. E. Kirichenko

Hypres, 175 Clearbrook Rd., Elmsford, NY 10523, USA

Time-to-Digital converters (TDCs) for Superconducting Nanowire Single-Photon/Particle Detectors (SNSPDs) based on Single Flux Quantum (SFQ) logic families continue to attract attention because of their potentially high time resolution, high current sensitivity, low timing jitter, large dynamic range, scalability and their natural compatibility with cryogenic environment needed for detectors. Digitization performed close to a detector reduces requirements for output cables (heat load, extra timing jitter, etc.) and increases fidelity of upward datalink. The interest in superconducting TDCs is getting higher because superconducting nanowires are used to detect nowadays not only photons but particles of different types. In this paper we are trying to sort out existing architectures of SFQ-based TDCs, discussing their advantages and disadvantages, as well as their readiness for real applications. We group the known architectures based on 1) the target time resolution (clock or sub-clock period), 2) the type of clock source to be used (external clock generator or on-chip ring oscillators), 3) the mode of operation (continuous or event driven), and 4) the anticipated frequency of events (rare or multi-hit). We also discuss SFQ TDC architecture currently pursued by Hypres, Inc.

This work was supported in part by U.S. Department of Energy.

Abstract ID: 30136

SPATIALLY RESOLVED PHOTODOPING OF OXYGEN-DEFICIENT $YBa_2Cu_3O_{7-\delta}$ RESONATORS

N. Lejeune[1], L. Nulens[2], H. Li[3], T. Günkel[3], L. Fabrega[3], A. Palau[3], J. Van de Vondel[2], A. V. Silhanek[1]

[1] *Experimental Physics of Nanostructured Materials (EPNM), QMAT, Department of Physics, Université de Liège, Sart Tilman, BELGIUM*
[2] *Department of Physics and Astronomy, KU Leuven, Leuven, BELGIUM*
[3] *Institut de Ciència de Materials de Barcelona, ICMAB-CSIC, Bellaterra, SPAIN*

Oxygen-depleted $YBa_2Cu_3O_{7-\delta}$ exhibits a substantial drop in the normal-state resistivity and an increase in the superconducting critical temperature when illuminated with visible light. The photo-induced states are metastable, slowly decaying at high temperatures and essentially persistent at low temperatures. In this work, this effect is exploited to modify the response of half-wavelength $YBa_2Cu_3O_{7-\delta}$ resonators and simultaneously the high-sensitivity of the resonant circuit is used to investigate the persistent photodoping of this material. Under illumination, the bolometric effect and photodoping are clearly distinguished by the different time scales associated with each mechanism. Using a 60 μm-wide laser spot, the properties of the resonator are locally and reversibly modified, and the position-dependent sensitivity of the device is demonstrated. This enables the direct imaging of standing waves at both the fundamental resonance and the second harmonic.

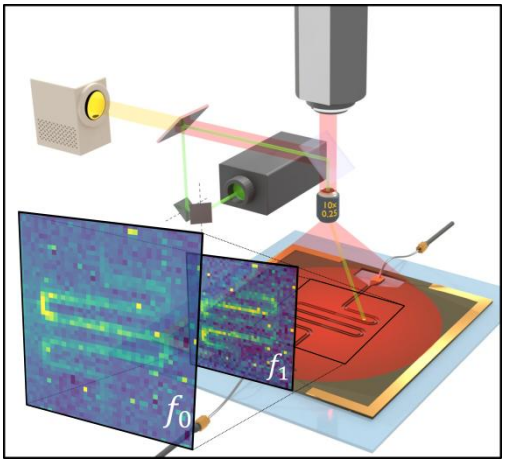

Fig. 1: ***Imaging Standing Waves via Photodoping****. A focused laser beam is used to induce local photodoping in oxygen-depleted $YBa_2Cu_3O_{7-\delta}$ resonators. This technique allows for the direct mapping of microwave current densities, clearly distinguishing the fundamental (f_0) and second harmonic (f_1) modes of the resonator, as shown in the inset data maps.*

References

[1] N. Lejeune, L. Nulens, H. Li, *et al.*, *Spatially Resolved Photodoping of Oxygen-Deficient $YBa_2Cu_3O_{7-\delta}$ Resonators,* Adv. Mater. Technol.: e01724. (2025).

Abstract ID: 30506

THE FLUXONICS MIXED-SIGNAL FABRICATION PROCESS BASED ON SUB-µm Nb/AlO_x/Nb CROSS-TYPE JOSEPHSON JUNCTIONS

M. Schmelz[1], J. Kunert[1,2], K. Peiselt[1,3], G. Oelsner[1], T. Ortlepp[4], R. Stolz[1,2,5]

[1] *Leibniz Institute of Photonic Technology, Albert-Einstein-Str. 9, 07745 Jena, GERMANY*
[2] *FLUXONICS - The European Foundry for Superconducting Electronics e.V., 38116 Braunschweig, GERMANY*
[3] *supracon AG, 07751 Jena, GERMANY*
[4] *CiS Forschungsinstitut für Mikrosensorik GmbH, 99099 Erfurt, GERMANY*
[5] *Technical University Ilmenau, Ehrenbergstr. 29, 98693 Ilmenau, GERMANY*

Superconducting quantum technologies are among the most promising platforms for realizing scalable quantum systems. As they are operated at very low temperatures down to few mK, the increase of circuit elements like qubit count, necessary for the development of practical quantum computers, typically comes along with the scale-up of the number of high-frequency address and readout lines. To overcome limitations due to available space and cooling power in cryogenic systems, mixed signal interface and control circuits have gained significant interest in recent years, accordingly. Access to those technologies is crucial, especially for start-ups and small and medium enterprises. The FLUXONICS foundry, thus, follows the mission to develop superconducting electronics in Europe and to provide and promote associated technological innovations for academic and industrial partners in the framework of the European FLUXONICS foundry.

We will present the development of the FLUXONICS mixed-signal foundry process based on sub-µm Nb/AlO_x/Nb cross-type Josephson junctions, enabling integration of superconducting analogue and digital circuits on the same chip. In our presentation, we will discuss the implementation of the technology and characterization of first circuits, like SQUIDs, RSFQ and AQFP circuits operated down to 30 mK. We will discuss their further implementation together with superconducting quantum circuits and quantum sensor systems.

This work was supported by the German BMBF projects QSolid (grant no. 13N15910), HiQuP (grant no. 13N15910), and SuperLSI (grant no. 13N16258).

Abstract ID: 30668

PROGRAMMABLE SUPERCONDUCTING NEURON WITH INTRINSIC IN-MEMORY SPIKING COMPUTATION AND DUAL-TIMESCALE PLASTICITY FOR ULTRA-EFFICIENT NEUROMORPHIC COMPUTING

M. Wang[1,2], S. Yang[1,2], J. Ren[1,2]

[1] *State Key Laboratory of Materials for Integrated Circuits, Shanghai Institute of Microsystem and Information Technology, Chinese Academy of Sciences, 200050, Shanghai, CHINA*
[2] *University of Chinese Academy of Sciences, 100049, Beijing, CHINA*

The escalating energy demands of artificial intelligence pose a critical challenge to conventional computing. Integrating the efficiency of event-driven, in-memory neuromorphic architectures with the ultra-high speed and low power dissipation of superconducting circuits offers a promising solution to energy efficient computation. However, the potential has yet to be released, due to the absence of the fundamental superconducting unit that unifies programmability, local memory, and multi-timescale plasticity. Here, we introduce a programmable Josephson-junction-based leaky integrate-and-fire (LIF) neuron that achieves intrinsic static memory and precise programmability by encoding somatic and synaptic parameters directly in bias currents. This neuron is capable of dual-timescale plasticity: picosecond-scale short-term modulation of spike transmission and long-term weight retention exceeding 10^4 seconds, facilitating both rapid temporal adaptation and robust weight storage. It operates at frequencies up to 45 GHz with femtojoule-level energy dissipation per spike, and supports 10 somatic threshold levels and 20 synaptic states. Furthermore, we demonstrate a crossbar-based spiking neural network (SNN) utilizing this neuron, which achieves outstanding performance across multiple tasks. By fusing computation, memory and plasticity into a single superconducting unit, our work paves the way for the next generation of ultrafast, energy-efficient neuromorphic computing.

Abstract ID: 30799

NOISE CHARACTERISTICS OF MgB_2 THERMAL KINETIC INDUCTANCE DETECTORS

T. Jabbari[1], A. Hawkins[2], A. Wandui[1], C. Frez[1], J. Greenfield[1,3], C. Roberson[3], M. J. Lee[3], P. Mauskopf[2,3], D. Cunnane[1]

[1] *Jet Propulsion Laboratory, California Institute of Technology, Pasadena, CA 91109 USA*
[2] *Department of Physics, Arizona State University, Tempe, AZ 85287 3 USA*
[3] *Earth and Space Exploration, Arizona State University, Tempe, AZ 85287 USA*

Thermal kinetic inductance detectors (TKIDs) enable scalability for large detector arrays in next-generation millimeter/sub-mm-wave instruments, maintaining the noise performance of traditional superconductive bolometers while utilizing a radio frequency multiplexing architecture. In this work, the design, fabrication, and characterization of magnesium diboride (MgB_2)-based TKIDs are presented, achieving phonon-noise-limited sensitivity within a novel temperature regime. The operating temperature range of MgB_2-based TKIDs enhance the potential applications of TKIDs, making them well-suited for high-background scientific studies, in certain cases, astrophysical hyperspectral imaging, atmospheric and surface temperature mapping of the planetary bodies (including earth).

In this work, the MgB_2 TKIDs are lumped-element resonators featuring a membrane-suspended inductor. The noise-equivalent power (NEP) is characterized internally using integrated on-membrane heaters. The detector architecture is intrinsically frequency agnostic and is compatible with a variety of optical coupling schemes, enabling practical implementations for remote sensing and imaging applications spanning millimeter-wave to far-infrared wavelengths. Phonon noise-limited performance is demonstrated over temperatures from 4-8 K even for a the fairly conservative bolometer design for these prototype devices. A comprehensive electrical, thermal, and noise characterization of the prototype devices is presented.

Abstract ID: 30800

ANALYSIS OF SQUIDS BASED ON NANO-JUNCTIONS

P. Febvre[1], U. Yilmaz[2], K. Jackman[3], C. Fourie[3]

[1] *University Savoie Mont Blanc, FRANCE*
[2] *IQM, GERMANY*
[3] *Stellenbosch University, SOUTH AFRICA*

Nano-SQUIDs, or SQUIDs based on nano-junctions, are useful sensors when ultimate sensitivity is needed, like for the detection of single magnetic particles or weak magnetic events for medical diagnostic or geophysics. The size of leads of such devices brings specific issues related to the relatively high kinetic inductance of the devices, especially when the geometry is different from the well mastered microstrip configurations. We have studied SQUIDs based on two different technologies, namely low-T_c Niobium-based SNIS junctions fabricated by Focused Ion Beam (FIB) technique, and high-T_c ion-irradiated YBCO films. The low-T_c SQUIDs present a full 3D geometry without any ground plane, while the high-T_c SQUIDs are planar but cannot have a ground plane due to technological limitations.

In both cases the configuration of currents within the circuit is associated with a high kinetic inductance and also to several magnetic couplings between different parts of the circuits surrounding the Josephson junctions. We used Inductex to evaluate the expected values of inductances and we compared them to experimental values obtained at different temperatures, as well as with simpler methods based on analytical approximations. From the comparison we can extract the influence of temperature on the kinetic inductance and investigate optimization regarding sensitivity and miniaturization.

Abstract ID: 30829

EXPERIMENTAL STUDY OF SUPERCONDUCTING SPIN VALVES

A. A. Kamashev[1], N. N. Garif'yanov[1], A. A. Validov[1], D. A. Arbuzov[1,2], V. Kataev[3], Ya. V. Fominov[4,5], A. S. Osin[4,5], I. A. Garifullin[1]

[1] *Zavoisky Physical-Technical Institute, FRC Kazan Scientific Center of RAS, 420029 Kazan, RUSSIA*
[2] *Kazan Federal University, 420008 Kazan, RUSSIA*
[3] *Leibniz Institute for Solid State and Materials Research, Helmholtzstrasse 20, D-01069 Dresden, GERMANY*
[4] *L. D. Landau Institute for Theoretical Physics RAS, 142432 Chernogolovka, RUSSIA*
[5] *Moscow Institute of Physics and Technology, 141701 Dolgoprudny, RUSSIA*

Modern microelectronics is approaching fundamental limitations in the functionality and miniaturization of devices, necessitating the search for alternative approaches. One promising area is superconducting spintronics, based on the control of the fundamental property of the electron - spin. Spin control occurs significantly faster than electron charge.

The relevance of this work is determined by the need to create next-generation energy-efficient and high-speed devices. Superconducting spin valves (SSVs), whose operating principle is based on the proximity effect of superconductor/ferromagnet and the control of the critical superconducting transition temperature, are considered as the basic elements of such systems.

This paper presents an experimental study of SSVs based on thin-film heterostructures using Heusler alloys ($Co_2Cr_{1-x}Fe_xAl_y$) and presents research results for structures with controlled transparencies of the superconductor/ferromagnet interfaces.

The main result is the achievement of a record-breaking operating temperature range for the superconducting spintronics (~ 0.6 K), significantly exceeding previously obtained values [1]. The implementation of superconducting spintronics with controlled transparencies at the superconductor/ferromagnet interface has also been achieved, enabling significant superconducting spintronics efficiency in low external magnetic fields [2, 3].

The practical significance of this work lies in the development of approaches to creating efficient superconducting spintronics elements applicable to quantum computing and high-speed electronics.

References

[1] A.A. Kamashev, N.N. Garif'yanov, A.A. Validov, *et al.*, Phys. Rev. B. **109**, 144517 (2024).
[2] A.A. Kamashev, N.N. Garif'yanov, A.A. Validov, *et al.*, Beilstein J. Nanotechnol. **15**, pp. 457-464 (2024).
[3] A.A. Kamashev, N.N. Garif'yanov, A.A. Validov, *et al.*, Phys. Rev. B. **112**, 134509 (2025).

52 - SUPERCONDUCTING MOTORS AND APPLICATIONS IN ELECTRICAL ENGINEERING

Abstract ID: 30009

STRATEGIES OF MODELING SUPERCONDUCTING MACHINES BY USING VOLUME INTEGRAL EQUATIONS

H. Menana

Université de Lorraine, GREEN, F-54000 Nancy, FRANCE

Superconducting electrical machines have reached a high level of maturation with a high potential of application in future energy conversion systems, such as renewable energies and electrical mobility. They offer the possibility to reduce volumes and weights up to 40% in the range of MW compared to conventional machines, while increasing the global efficiency [1].

Due to the strong dependency of the electromagnetic properties of superconducting materials to the magnetic field and temperature, the design of superconducting machines is mainly based on the evaluation of local quantities requiring numerical approaches. Presenting high scale effects and strong nonlinearities of the materials properties, differential methods such as finite element method struggle to provide accurate solutions in reasonable computation times. Being generally constituted of relatively large air regions, due to cryogenics, the volume integral (VI) approaches present an interesting alternative, allowing to restrict the discretization to the active parts of the modelled system [2]. In this context, we developed strategies of modeling superconducting electrical machines using VI equations, where each active part is treated as a source contributing to the creation of the magnetic field. 3D DC modeling is used for the design and optimization in a multi static approach, and the AC modeling is used for the AC losses evaluation. The developed strategies are highlighted thought some numerical examples, as shown in figure 1 describing a structure of an ironless axial flux high temperature superconducting (HTS) electrical machine subject to an optimization of the HTS tape length for a given torque, combining VI modeling and genetic algorithms. The use of VI modeling allows to reduce considerably the computation times.

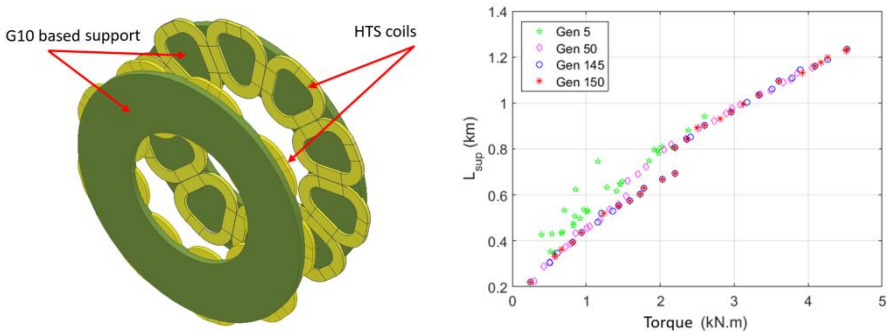

Fig. 1: *Ironless axial flux HTS machine structure and the minimal HTS wire length for each value of the developed torque. The external radius of the machine is Re=350mm, and the critical current density of the used HTS tape is 267.9 A/mm² @ 30K.*

References

[1] X. Song, *et al.*, IEEE Trans. on Energy Conversion, **vol. 35**, **no. 2**, pp. 757-764 (2020).

[2] Y. Statra, H. Menana, B. Douine, Physica C: Superconductivity and its Applications, **Vol.574**, p. 1353660 (2020).

Abstract ID: 30240

CHARACTERIZATION OF HTS COILS FOR SUPERCONDUCTING MOTOR APPLICATION

B. Douine

GREEN, Université de Lorraine, Nancy, FRANCE

High-Temperature Superconducting (HTS) coils used in superconducting motors are different depending if they are used in armature with AC current or inductor with DC current. Firstly, in armature windings, there are AC losses as AC hysteresis losses and AC eddy current losses. Secondly, in inductor with DC current, non-insulated (NI) HTS coils could be used to improve robustness of these coils. Due to these differences the characterization of these two kinds of HTS coils are different. For armatures windings the most important feature to study is the influence of frequency and amplitude of AC current on AC losses. This work presents measurement of AC losses for YBCO coils at liquid nitrogen temperature and for different frequency and different configurations. In another hand for inductor NI HTS coils it is crucial to know the critical current of this kind of coil and which criteria you have to use but also the behavior of t during the current ramp. So, this work presents the measurement of the critical current of NI HTS coil and the determination of parameters of lumped parameter model of this kind of coil. This study will be useful to correctly design future full HTS motors.

Abstract ID: 30345

BASIC OPERATIONAL CHARACTERISTICS OF A PARTIAL SUPERCONDUCTING SYNCHRONOUS MOTOR IMPREGNATED BY SOLID-NITROGEN REFRIGERANT

Y. Terao, T. Nakamura

Kyoto University, 615-8245, Kyoto-city, JAPAN

Electric motors have been introduced in many industries, transportation and energy sectors in the world. And these ten several years, superconducting (SC) motors have been studied for introducing liquid hydrogen pump systems [1, 2], electric aircraft [3, 4] and so on.

The cooling method of the SC part is one of the key technologies for development of SC motors. Following Iwasa's proposal [5], we have been studying the SC coil cooling method using solid nitrogen [6]. Solid nitrogen possesses the function of a heat bath, and is expected to serve as a fail-safe in the event of a failure in the SC motor's cooling system.

In this presentation, we report some basic characteristic results of a SC motor shown in Fig. 1 and Table I cooled by solid nitrogen.

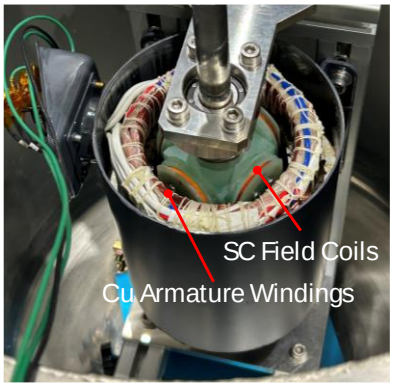

Fig. 1: *Photograph of a SC motor using YBCO field coils and copper armature windings.*

Table I. *Basic specifications of the SC motor.*

Voltage	200 V
Stator Innner Diameter	96.0 mm
Stator Outer Diameter	160.0 mm
Length	96.0 mm
Num. of Poles	4
Num. of Stator Slots	36
SC Field Coils	YBCO Wires
Armature Windings	Cu Wires

References

[1] TORISHIMA NEWS **228**, 13 (2024).

[2] Toyota Times News, URL: https://toyotatimes.jp/en/newscast/157.html (Accessed on Dec. 26, 2025).

[3] M. Yamamoto and T. Nakamura, Physica C, **632**, 1354690 (2025).

[4] Y. Terao, A. Seta, H. Ohsaki, H. Oyori and N. Morioka, IEEE Transactions on Applied Superconductivity, **29**, 5202305 (5pp) (2019).

[5] Y. Iwasa, R. Wheatley, J. Bascuñán, B. Haid and H. Lee, IEEE Transactions on Applied Superconductivity, **13**, 1636-1639 (2003).

[6] T. Nakamura, K. Higashikawa, I. Muta, A. Fujio, K. Okude and T. Hoshino, Physica C, **386**, 415-418 (2003).

Abstract ID: 30449

AC LOSS AND ELECTROTHERMAL STABILITY OF HIGH-TEMPERATURE SUPERCONDUCTING MOTORS FOR HYDROGEN-ELECTRIC AIRCRAFT PROPULSION

E. Pardo[1], A. Dadhich[1], A. Hussain[1], J. Šouc[1], J. Kováč[1], A. Colle[2], R. Dorget[2], M. E. Ahmed[2]

[1] *Institute of Electrical Engineering, Slovak Academy of Sciences (IEE SAS), Bratislava, SLOVAKIA*
[2] *Airbus UpNext, Toulouse, FRANCE*

Full superconducting motors are very promising for electric powertrains in hydrogen-electric aircraft, since liquid hydrogen can act as heat sink. Motors with REBCO stators enable high cryogenic flexibility because they can operate at a wide temperature range, from 20 to 50 K. However, AC loss in the stator needs to be kept as low as possible in order to increase efficiency, avoid electro-thermal quench due to self-heating, and simplify cryogenics. In this work, we made a systematic modelling study of the AC loss and electro-thermal stability in the stator REBCO coils in motor environment. We also measured the AC loss of downscaled test coils made of several tapes in parallel, at both liquid nitrogen and lower temperatures down to 20 K using a cryocooler-based set-up [1]. Modelling analyzed several aspects, such as the effect of several tapes in parallel forming a stack-based cable, finite resistance at the end of the stack connection, tape misalignment, and non-uniformity. For this study, IEE SAS used their own numerical method, based on the Minimum Electro-Magnetic Entropy Production (MEMEP) [2] for superconducting coils interacting with the rotor and iron yoke. We benchmarked the method with modelling by COMSOL in Airbus UpNext. For electro-thermal modelling, we couple MEMEP with IEE SAS own thermal modelling software [3]. We also compared modelling AC loss results with experiments on downscaled coils. Modelling results show that REBCO stators are promising for motors of 1 MW rating and above.

References

[1] J. Kováč, *et al.*, Scientific Reports **12.1**, 16454 (2022).
[2] E. Pardo and M. Kapolka, J. Comput. Phys. **344**, 339–363 (2017).
[3] A. Hussain, A. Dadhich, and E. Pardo, Supercond. Sci Technol. **38**, 105012 (2025).

Abstract ID: 30472

ELECTRO-THERMAL MODEL OF STATOR COILS IN SUPERCONDUCTING MOTORS UNDER AC AND DC VOLTAGES: PARALLEL TAPES AND INHOMOGENEITY

A. Hussain, A. Dadhich, E. Pardo

Institute of Electrical Engineering, Slovak Academy of Sciences, vvi, Dubravska Cesta 9, 841 04, Bratislava, SLOVAKIA

High-Temperature Superconducting (HTS) racetrack coils are ideal candidate for high-power-density and lightweight electric machines, particularly for next-generation aircraft propulsion systems. However, their operation is inherently constrained by thermal quench risks arising from self-heating under alternating-current (AC) excitation, transient overloads, or direct-current (DC) fault conditions. Accurate electrothermal modeling is therefore essential for the reliable design and protection of HTS motor coils [1-3]. In this work, we present an electrothermal modeling framework that couples the Minimum Electro-Magnetic Entropy Production (MEMEP) method with a Finite Difference Method (FDM) thermal solver to study quench initiation and thermal stability in HTS racetrack coils operating within a realistic motor environment (configuration for a motor of around 2 MW) for coils with multiple tapes in parallel. This modeling framework incorporates temperature-dependent electromagnetic and thermal properties, critical current density J_c, thermal conductivity κ, and volumetric heat capacity C_v, to accurately represent the coupled electromagnetic–thermal interactions. Critical current density also depends on the magnetic field and its orientation. In this study we investigate the response of HTS racetrack coils when subjected to either AC voltages or short-circuit DC voltages (1−1000 V), which represents the fault scenarios in voltage-driven HTS motors. The model is used to examine the influence of thermal boundary conditions ranging from adiabatic to realistically cooled configurations relevant to practical cryogenic motor environments. Particular attention is given to a damaged turn within the coil, modeled by reducing the local critical current density to a certain percentage of its nominal value (10 to 90%), in order to assess the impact of localized degradation on global coil stability. This study aims to clarify the role of fault voltage magnitude, cooling conditions, and local damage on electrothermal runaway, quench initiation, and stability margins in HTS racetrack coils. The outcomes are expected to provide valuable insights into the design and protection of HTS-based electric motors in high-performance and power applications.

References

[1] A. Hussain, A. Dadhich, and E. Pardo, *Thermal quench modeling of REBCO racetrack coils under conduction cooling at 30 K for aircraft electric propulsion motors*, Supercond. Sci. Technol. **38**, 105012 (2025).

[2] A. Hussain, A. Dadhich, and E. Pardo, *Thermal quench modeling of REBCO racetrack coils under either alternating current or short-circuit voltage*, Supercond. Sci. Technol. **37**, 115028 (2024).

[3] A. Dadhich, F. Grilli, L. Denis, B. Vanderheyden, C. Geuzaine, F. Trillaud, D. Sotnikov, T. Salmi, G. Hajiri, K. Berger, T. Benkel, G. dos Santos, B. M. O. Santos, F. G. R. Martins, A. Hussain, and E. Pardo, *Electromagnetic-thermal modeling of high-temperature superconducting coils with homogenized method and different formulations: A benchmark*, Supercond. Sci. Technol. **37**, 125006 (2024).

11th International Conference on Superconductivity and Magnetism ICSM2026
4th International Conference on Quantum Materials and Technologies ICQMT2026
19th April to 26th April, 2026, Ölüdeniz – Fethiye/Muğla, Türkiye
https://icsmforever.org/

Abstract ID: 30692

DESIGN STUDY OF DIRECT DRIVE MULTI-MW HTS GENERATORS FOR OFFSHORE WIND USING THE MODULAR AIR-CORED SUPERMACHINE TOPOLOGY

O. Keysan[1,2], S. You[1], A. Shah[1], H. Zhang[1], M. Mueller[1]

[1] *School of Engineering, University of Edinburgh, Edinburgh, UK*
[2] *Middle Eastern Technical University, Ankara, TURKEY*

Offshore wind turbine rating is increasing to 15-20 MW to accelerate installation and meet net-zero targets. Low speed high torque direct drive permanent magnet generators are the preferred choice for wind turbine manufacturers. Standard turbine designs have been produced by the IEA, which show that the active PM generator mass is in the range of 140 to 220 tons depending upon rating [1,2]. Shah et al provide a comprehensive review of HTS generator developments in wind [3], with limited advances in mass reduction. In the SuperMachine concept iron is eliminated by an array of air-cored coils to focus the magnetic field, to fully exploity HTS characteristics to produce a magnetic loading in the region of 2-3 T. Fig. 1 illustrates the SuperMachine topology – it is a modular axial flux machine with multiple layers each producing a conventional NSNS magnetic field pattern on the rotating field winding. SuperMachine has been demonstrated using a 20 turn per coil module tested in LN2, providing verification of design and modelling tools [4]. These tools have been used to optimize a SuperMachine HTS generator for comparison with IEA PM designs at 15MW, & 22MW. Results of active mass are shown in Table 1, and in all cases SuperMachine has lower mass and occupies a lower physical space. Estimates of the mass of the cooling system and cryostat structure are included in the active mass for SuperMachine. The presentation at the conference will include more information on the SuperMachine concept, a comparison with the 3.6 MW EcoSwing [5] and more details of the integrated design of the structure and cooling system.

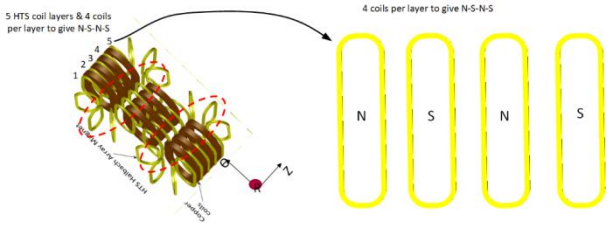

Fig. 1: *Modular SuperMachine Concept.*

	IEA Design	SuperMachine	IEA Design	SuperMachine
Rated Power	22 MW		15 MW	
Rated Speed	7 rpm		7.5 rpm	
Stator Outer Diameter	9759 mm	7983 mm	10516 mm	6930 mm
Airgap Diameter	**9524 mm**	**7000 mm**	**10160 mm**	**6000 mm**
Axial Length	2431 mm	540 mm	2170 mm	370 mm
Efficiency	95.40 %	96.00%	96.55 %	96.17%
Mechanical Airgap Length	7 mm	5 mm	10 mm	5 mm
Iron Lamination Mass	105.6 t	-	180.95 t	-
Magnet Mass	25.2 t	-	24.2 t	-
Copper Mass	17.1 t	30.15 t	9.01 t	18.77 t
HTS Mass	-	2.92 t (151.9 km)	-	2.36 t (123 km)
Cryostat & Cooling	-	40t	-	25t
Total Active Mass	**147.9 t**	**73.1 t**	**214.2t**	**46.1t**

Table 1: *Comparison SuperMachine with IEA Designs.*

References

[1] E. Gaertner, *et al.*, *IEA Wind TCP Task 37: Definition of the IEA 15-megawatt Offshore Reference Wind Turbine*, National Renewable Energy Lab (2020).

[2] F. Zahle *et al., Definition of the IEA Wind 22-Megawatt Offshore Reference Wind Turbine* National Renewable Energy Lab (2024).

[3] A. Shah, *et al.*, *Superconducting generators and cables for wind energy—A review,* Supercond. Sci. Technol. **38**, 093001 (2025).

[4] Q. Dong, *et al.*, *Design and Experimental Validation of an Air-cored Superconducting Generator Module*, IEEE Trans. Appl. Super., DOI: 10.1109/TASC.2026.3659456

[5] A. Bergen, *et al.*, *Design and in-field testing of the world's first ReBCO rotor for a 3.6 MW wind generator,* Supercond. Sci. Technol. **32**, 125006 (2019).

53 - SUPERCONDUCTING POWER APPLICATIONS FOR ENHANCED DATA CENTER EFFICIENCY

Abstract ID: 30382

SUPERCONDUCTING SOLUTIONS AS ENABLERS FOR HIGH POWER DENSITY DC DATA CENTERS

P. Corsaro[1,2], T. Botto[1], U. Melaccio[1]

[1] *ASG Superconductors SpA, Zip, Genoa, ITALY*
[2] *C&G Agency GmbH, 8004, Zurich, SWITZERLAND*

Superconducting cables are synonyms of high-power density, having as one of the main benefit the capability to carry high currents at low voltage with almost zero-losses and no voltage drop: typically, unrealistic to be obtained with conventional copper or aluminum conductors and bus bar. DC data centers mainly use standardized 48-54V and 380–400 V DC bus systems, with emerging interest in higher DC levels up to about 800 V as per latest by Nvidia and Hitachi that plan 1MW racks.

The equation is simple: if the rack requires more current at 48-54/12 V due to the increasing number of GPUs, the overall power is increased by increasing the voltage up to the rack to limit the cross section of conventional conductors.

This equation does not consider the development of superconducting materials and their capability to carry with a MgB_2 conductor with similar cross-section to a 2-euro coin, or a quarter of US dollar, 1 MW at 48-54V.

The paper will present this breakthrough solution and its potential in Data Centers.

Abstract ID: 30775

REVOLUTIONIZING DATA CENTER POWER DELIVERY WITH HIGH TEMPERATURE SUPERCONDUCTING CABLES

P. Feldman

QTD Systems, Inc., New York, NY, USA

Rapid growth in AI training, inference clusters, and emerging high-power computing facilities in the 500 MW to multi-GW range is driving data center electrical architectures toward unprecedented power density, higher current levels, and tighter efficiency demands. At the same time, operators are increasingly adopting mixed distribution strategies—combining high-voltage alternating current (HVAC), medium-voltage alternating current (MVAC), low-voltage alternating current (LVAC), and multiple direct current (HVDC and LVDC) buses—to support compute loads and unpredictable power demand curves. High Temperature Superconducting (HTS) power cables can serve as a unified distribution backbone for simultaneously delivering multiple voltage levels and both AC and DC power in large-scale AI and high-power data centers. We present an architecture in which a single, HTS corridor replaces multiple parallel copper feeders and conventional busway systems, enabling extremely high current density with zero resistive losses. In addition, HTS power equipment, such as Superconducting Magnetic Energy Storage (SMES), Superconducting Fault Current Limiters (SFCL), and superconducting transformers, can support high-demand power distribution and transport more efficiently at a reduced scale. The proposed approach enables direct delivery of optimized voltage levels to compute halls and power shelves, reducing or eliminating intermediate power-conversion stages. The resulting reduction in rectifiers, inverters, and step-down transformers produces measurable improvements in end-to-end electrical efficiency, floor-space utilization, thermal loading, and system reliability. HTS cables are ideal to support hybrid AC/HVDC/LVDC distribution topologies, fault-isolation strategies, and compatibility with modern power electronics and modular data-center layouts. We also discuss operational considerations, including cryogenic plant integration, maintenance boundaries, and scalability for future ultra-high-density facilities.

Abstract ID: 30596

MAGNETIZATION LOSSES AND NON-REDUCED THREE-DIMENSIONAL MODELLING OF HYBRID CORC-TSTC SUPERCONDUCTING CABLES

H. Alssalih[1], M. Clegg[1,3], A. Badia[2], H. S. Ruiz[1]

[1] *University of Leicester, Dept. of Engineering, LE1 7RH, Leicester, UK*
[2] *Dep. Física de la Materia Condensada, Universidad de Zaragoza, SPAIN*
[3] *UK Power Networks, London SE1 6NP, UK*

Hybrid superconducting cables combining Conductor-on-Round-Core (CORC) and Twisted Stacked-Tape Conductor (TSTC) architectures have recently been proposed as a route toward high-current, mechanically robust HTS conductors. While first experimental measurements of their magnetization losses have become available, a detailed physical understanding of the internal current dynamics governing these losses has remained incomplete. This is particularly true for hybrid conductors combining helically wound and twisted tape architectures, where reduced-dimensional modelling approaches may obscure key physical mechanisms. In this work, we present a fully three-dimensional electromagnetic study of magnetization losses in hybrid CORC-TSTC cables, based on a non-reduced H-formulation that explicitly retains the full thickness of the superconducting layers. Unlike reduced-order approaches, the model resolves current density profiles across the tape thickness and captures flux-free cores, internal shielding, and complex current loop closure mechanisms. Magneto-angular anisotropy of the critical current density is incorporated using experimentally informed material laws for REBCO tapes. The numerical framework is benchmarked against the first experimental magnetization-loss measurements of CORC-TSTC hybrid cables under transverse AC magnetic fields. Excellent quantitative agreement is obtained across a wide field range for hybrid configurations containing up to four stacked tapes in the TSTC core. Analysis of current density distributions reveals a clear separation of electrodynamic regimes: the outer CORC layers exhibit Bean-like magnetization patterns characteristic of cylindrical conductors under perpendicular fields, while the TSTC core behaves as a twisted thin-film system dominated by parallel-field shielding. The analysis reveals that magnetization losses are dominated by the outer CORC layers, while the TSTC core benefits from strong internal magnetic shielding and parallel-field current distributions. A systematic comparison with functionally equivalent single-layer and bi-layer CORC cables, as well as TSTC with identical tape counts, demonstrates that the hybrid architecture achieves a favourable balance between electromagnetic performance and structural complexity. In particular, hybrid cables exhibit lower losses than bi-layer CORC and comparable performance to pure TSTC designs, except at very low applied fields. These results demonstrate that fully 3D, non-reduced electromagnetic modelling is essential for capturing the true physics of magnetization in hybrid superconducting cables, establishing hybrid CORC-TSTC conductors as a physically well-understood and competitive option for AC-field-dominated superconducting applications.

References

[1] Y. D. Chung, *et al.*, IEEE Trans. Appl. Supercond., **34**, 3600205 (2024).
[2] H. N. H. Al-Ssalih, M. Clegg, A. Badía-Majós, H. S. Ruiz, IEEE Access, **13**, 186952 (2025).
[3] M. Clegg, H. N. H. Al-Ssalih, H. S. Ruiz, IEEE Access, **13**, 84013–84023 (2025).

54 - SUPERCONDUCTING THIN FILMS AND INTERFACE SUPERCONDUCTIVITY

Abstract ID: 30087

ELECTRON-PLASMON SCATTERING IN DOPED GRAPHENE

J. Jakovac

Institute of Physics, Bijenička 46, 10000 Zagreb, CROATIA

Decay mechanisms and plasmon satellites formed in the spectrum of a photo-excited hole in doped graphene is a phenomenon that has been investigated for a long time using angle resolved photoemission spectroscopy (ARPES) measurements [1,2,3]. I will present the *ab initio* simulation of photoemission spectra in electrostatically and chemically (KC_8) doped graphene in the framework of our recently developed *many body* RPA-G_0W_0 method [4].

The obtained results show that the decay width along the C (π^+/π^-) bands behaves according to the exponential law $\Gamma \sim |E_{\sigma,\pi\mathbf{K}}\text{-}E_F|^{\alpha}$, where $\alpha=3/2$ (**Fig. 1a**), which perfectly agrees with the previous experimental predictions [1,4] and deviates from the standard Fermi liquid behavior $\alpha=2$. At deeper energies (below the Fermi energy), the width of the π^+/π^- bands shows a peak that comes from the decay due to Dirac plasmon emission, also predicted experimentally [1]. I will also present the plasmonic satellites appearing in the spectrum (**Fig. 1b**), whose intensities are much lower than experimentally predicted [2,3]. Only in the frequency range $E_D<\omega<E_F$ stronger plasmon satellites appear. However, the relative Dirac plasmaron binding energy $\Delta_{DPS}/E_F=|E_{DPS}\text{-}E_D|\sim 0.5$eV is in excellent agreement with recent experiments [2,3]. Our simulations also predict a kink at the Fermi energy in highly doped graphene, due to the Fermi liquid theory (**Fig. 1b**).

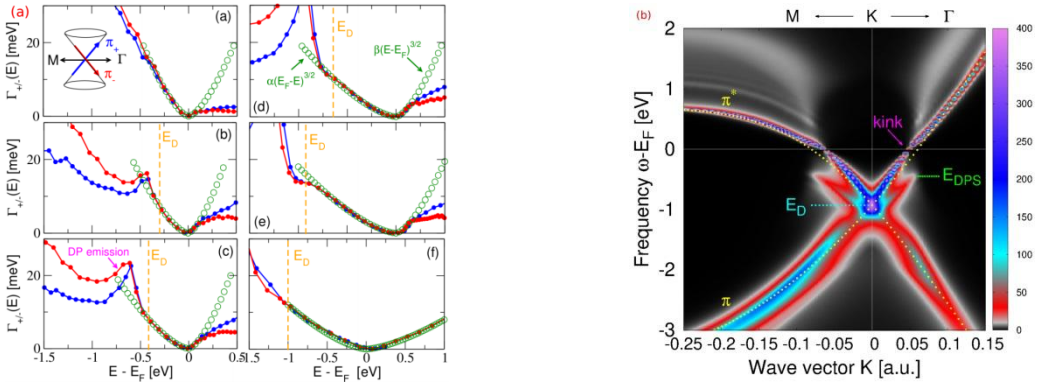

Fig. 1: *(a) The imaginary part of self-energy along π_+/π_- bands in electrostatically doped [concentrations increasing (a) → (e)] and chemically (f) doped (KC_8) graphene. (b) The simulation of spectral intensity along the high symmetry path (Γ-K-M-Γ) in electrostatically highly doped graphene (10^{14} cm^{-2}).*

References

[1] A. Bostwick, T. Ohta, T. Seyller, K. Horn and E. Rotenberg, Nature Phys. **3**, 36 (2007).

[2] H. Zhang, S. Wang, E. Wang, *et al.,* npj Quantum Mater. **6**, 83 (2021).

[3] A. Bostwick, F. Speck, T. Seyller, *et al.*, Science **328**, 999 (2010).

[4] J. Jakovac and V. Despoja, Phys. Rev. B **110**, 195425 (2024).

Abstract ID: 30090

PHENOMENOLOGY OF TWO-GAP SUPERCONDUCTOR HYDROGEN-INTERCALATED TITANIUM DISELENIDE EXPLAINED IN THE FRAMEWORK OF ELIASHBERG THEORY

G. A. Ummarino[1,2]

[1] *Dep. of Applied Science and Technology, Politecnico di Torino, Corso Duca degli Abruzzi 24, 10129 Torino, ITALY*
[2] *Dep. of Semiconductor Quantum Electronics, National Research Nuclear University MEPhI, Moscow Engineering Physics Institute, Kashira Hwy 31, 115409 Moskova, RUSSIA*

We have investigated the phenomenology of H-intercalated $TiSe_2$. Recent experiments have shed light on the symmetry of the wave parameter and the presence of multiple conduction bands [1].

All experimental data in the superconductive state (critical temperature, superconductive gaps upper critical fields etc have been explained in the framework of two-band s-wave Eliasherg theory with phononic mechanism. All data are in perfect agreement with the theory. We have also examined experimental data in normal state and also in this case the agreement with the theory is very good.

Although this material is certainly complicated and there are competent orders (superconductivity and charge density waves) we have shown that it is possible to explain the experimental data within a relatively simple conventional theory.

References

[1] E. Piatti, G. Gavello, G. A. Ummarino, F. Košuth, P. Szabó, P. Samuely, R. S. Gonnelli, D. Daghero, Materials Today Physics **59**, 101883 (2025).

Abstract ID: 30074

LASER STRATEGIES FOR THE FABRICATION OF Nb NITRIDES AND NbTi ALLOYS FOR SUPERCONDUCTING APPLICATIONS

J. Frechilla[1], A. Frechilla[1], G.F. de la Fuente[1], A. Larrea[1], C. Barreneche[2], S. Dosta[2], L.A. Angurel[1], E. Martinez[1]

[1] *Instituto de Nanociencia y Materiales de Aragón (INMA), CSIC-Universidad de Zaragoza, Zaragoza, SPAIN*
[2] *Dept. Ciència de Materials i Química Física, Universitat de Barcelona, Barcelona, SPAIN*

Niobium is a key material in superconducting and high-performance technological applications based on its combination of relatively high critical temperature for an elemental superconductor, excellent mechanical stability, and compatibility with thin-film processing routes. Its use in resonators, particle accelerators, microwave devices and emerging quantum technologies has stimulated intense research aimed at enhancing its superconducting properties while maintaining or improving its mechanical robustness. Several Nb compounds, nonetheless, exhibit even more attractive superconducting properties than elemental Nb and are subjected to further consideration in this study, based on advanced laser processing. Two promising strategies considered here include the generation of niobium nitride phases, which can exhibit significantly higher critical temperatures, and the formation of niobium–titanium alloys, widely used in superconducting magnets. Both approaches rely on controlled modification of Nb at the micro- and nano-scales and benefit from fast, localized, and contamination-resistant processing routes, making laser-assisted synthesis particularly attractive.

This work thus focuses first on the laser-induced nitridation of Nb using nanosecond IR laser irradiation under different N_2 pressures. By tuning the laser parameters, the formation of different nitride phases is induced. Systematic variation of laser conditions enables mapping the processing window leading to each nitride phase and its relative proportion. Extensive microstructural analyses reveal the thickness and properties of the different nitride layers formed during this process. Enhanced superconducting transition temperatures up to ~15 K and improved surface hardness are obtained under adequate laser irradiated conditions.

A second, complementary strategy, explores the laser-assisted formation of Nb-Ti superconducting alloys. Advantage is taken here of the rapid, localized laser processing to induce in-situ alloying in thin-film architectures. The precursor layers can be generated either by Pulsed Laser Deposition (PLD) or by cold plasma deposition of mixed-metal layers. The subsequent laser annealing acts as a fast mixing and alloying step, opening a versatile route to generate NbTi superconducting alloys with tunable composition.

Acknowledgments

The authors are grateful for funding from project PID2023-146041OB-C21 (funded by MICIU/AEI/10.13039/501100011033 and ERDF/EU) and from Gobierno de Aragón (Research Group T54_23R). The authors also thank the University of Zaragoza for the use of its Servicio General de Apoyo a la Investigación – SAI and the Spanish National Facility ELECMI ICTS, node Laboratorio de Microscopías Avanzadas (LMA). J. Frechilla acknowledges support from Gobierno de Aragón through a predoctoral contract.

55 - SUPERCONDUCTIVITY AND MAGNETISM IN HEAVY FERMION SYSTEMS

Abstract ID: 30244

QUANTUM ASPECTS OF HYPERBOLIC LATTICES

B. Roy

Department of Physics, Lehigh, Bethlehem, Pennsylvania, 18015, USA

Hyperbolic lattices constitute a unique platform to study various novel quantum phenomena on negatively curved space and identify the imprints of spatial curvatures therein. In this talk, first I will show a simple classification scheme on the family of two-dimensional bipartite hyperbolic lattices, resulting from simple but canonical spin-independent tight-binding model for free electrons, yielding three classes of ballistic quantum fluids on negatively curved space, namely Dirac liquids, Fermi liquids, and flat bands, that are, respectively, characterized by a vanishing, a finite, and a diverging density of states near the band center or zero-energy [1]. Next, I will show that such systems can be susceptible to different types of spontaneously ordered phases (such as the charge and spin density-waves) once Hubbard-like electronic interactions are considered, giving rise to dynamic mass generations in half-filled systems [2].

In the second half of the talk, I will exclusively focus on hyperbolic Dirac systems in which orderings can only take place beyond critical strengths of interactions via a quantum phase transition. I will propose two realistic approaches to trigger such dynamic mass generations on curved space Dirac liquids at sufficiently weak interactions. I show that (a) application of external magnetic fields [3, 4] and (b) rotational symmetric strain [5] give rise to a finite density of states near zero-energy in noninteracting systems, conducing various mass ordering at weak coupling.

Finally, I will discuss the role of disorder or impurities on hyperbolic Dirac liquids. I show that in contrary to our traditional wisdom, planar dirty hyperbolic Dirac liquids show two distinct quantum phase transitions as the disorder strength is gradually increased in the system. First the ballistic system undergoes a semimetal-to-metal transition at moderate disorder strength, which is subsequently followed by the Anderson metal-to-insulator transition, both being absent in two-dimensional Euclidean Dirac liquids, realizable on honeycomb lattices, for example [6].

I will close the talk with some possible future directions to further unfold unique quantum aspects of hyperbolic crystals.

References

[1] N. Gluscevich, A. Samanta, S. Manna, and B. Roy, Phys. Rev. B **111**, L121108 (2025).

[2] C. A. Leong and B. Roy, arXiv:2501.18591.

[3] B. Roy, Phys. Rev. B **110**, 245117 (2024).

[4] C. A. Leong, and B. Roy, arXiv:2510.02304

[5] C. A. Leong, and B. Roy, arXiv:2511.16667

[6] C. A. Leong, D. J. Salib, and B. Roy, arXiv:2512.05109

11th International Conference on Superconductivity and Magnetism ICSM2026
4th International Conference on Quantum Materials and Technologies ICQMT2026
19th April to 26th April, 2026, Ölüdeniz – Fethiye/Muğla, Türkiye
https://icsmforever.org/

Abstract ID: 30307

PROSPECTING FOR UNCONVENTIONAL SUPERCONDUCTING STATES IN HEAVY FERMION MATERIALS

F. M. Grosche

Cavendish Laboratory, University of Cambridge, Cambridge CB3 0HE, UK

Superconductivity without phonons [1] – tends to occur in materials tuned close to the threshold of magnetism, often under applied pressure. At such a magnetic quantum phase transition, magnetic excitations reach to low energies and mediate a long-ranged interaction which can stabilise superconductivity with an unconventional order parameter structure. This can produce superconducting domes that are surprisingly narrow, explaining why without a systematic search they could easily be missed.

Heavy fermion materials provide a fertile ground in the search for new unconventional superconductors, because these narrow-band systems tend to be close to the border of magnetism and have proven to be highly tuneable by applied pressure and magnetic field. The talk will focus on superconductivity and its interplay with strong applied magnetic fields in the new pressure-induced Ce-based superconductor $CeSb_2$ [2] and in the U-based superconductor UTe_2 [3]. The latter stands out because (i) it holds at least three distinct superconducting states, which can be selected by varying applied field, temperature and pressure, (ii) at least some of these are triplet pairing states, as demonstrated for instance by NMR measurements and by the unusual resilience of superconductivity to applied field of up to ≃ 60T in certain field directions, (iii) low temperature magnetic order identified at moderate pressure and strong magnetic fluctuations observed by neutron scattering at ambient pressure strongly suggest a central role for a magnetic pairing mechanism.

Although their transition temperatures are low, studying these and other heavy fermion systems can produce useful insights for finding and understanding unconventional superconductors more generally.

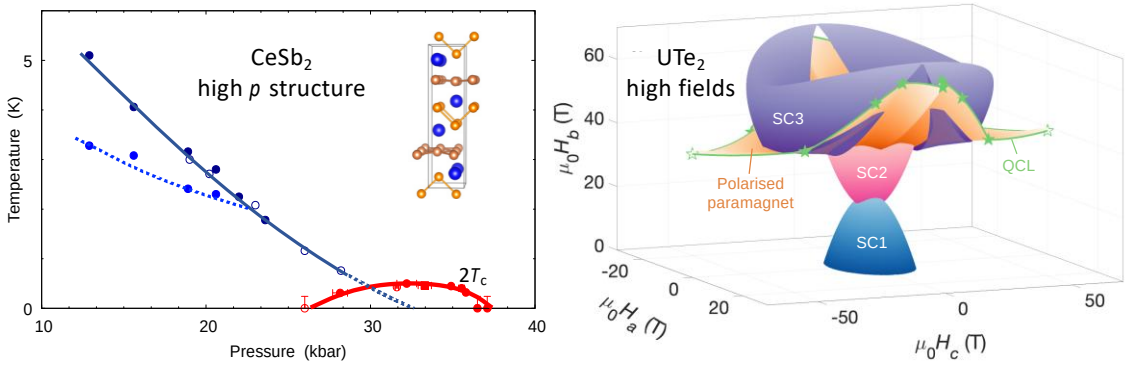

Fig. 1: *Pressure and field phase diagrams in the superconductors $CeSb_2$ and UTe_2*

References

[1] P. Monthoux, D. Pines, and G. G. Lonzarich, Nature **450**, 1177 (2007).

[2] O. P. Squire, *et al.*, Phys. Rev. Lett. **131**, 026001 (2023).

[3] Z. Wu, *et al.*, Phys. Rev. X **15**, 021019 (2025).

Abstract ID: 30586

SCREENED SUPEREXCHANGE MECHANISM FORSUPERCONDUCTIVITY APPLIED TO CUPRATES

P. Navez

Laboratoire Charles Coulomb UMR 5221 CNRS-Universit\'e de Montpellier, F-34095 Montpellier, FRANCE

Despite the repulsive Coulomb law and the Pauli statistics that do not favor bound states, attraction between electrons or holes is nevertheless possible in the context of many body interaction and of valley potential landscapes, reminiscent of exotic superconducting materials. In particular, in 1965, Kohn and Luttinger published a note revealing that the dynamical screening of the repulsive Coulomb interaction leads, under certain conditions, to an effective attraction necessary for the formation of Cooper pairs. We propose such a formalism adapted to the cuprates, where the screening arises from the superexchange dynamics of virtual holes in the oxygen orbitals of the CuO2 plane. Using an appropriate Schrieffer–Wolff transformation, the basic Hartree–Fock–Bogoliubov method, and the ab initio data on orbitals (energy, hopping, interaction), we derive some predictions for the temperature-doping phase diagram (pseudo-gap, strange metal, antiferromagnetism, superconducting, and normal states) and for the doping-dependent band energy spectrum in semi-quantitative agreement with observations.

References

[1] P. Navez, Low Temperature Physics **51**, 1606–1619 (2025).
[2] W. Kohn and J. M. Luttinger, Phys. Rev. Lett. **15**, 524 (1965).

Abstract ID: 30606

STRONGLY CORRELATION AND TOPOLOGY IN KONDO LATTICE SYSTEMS

S. Ran

Washington University in St. Louis, 63130, St Louis, USA

Quantum materials with both strong correlations and nontrivial band structure topology can have novel physics properties that do not exist in the non-correlated counterparts. Recent theoretical work has demonstrated that combination of Kondo physics and nonsymmorphic crystal symmetries can give rise to such strong correlated topological systems. In this talk, I will present our recent experimental exploration this direction. In one case, we found intrinsic anomalous Hall effect that seems to break the Fermi liquid scaling relation. In another case, we have discovered a candidate for topological Kondo insulator.

Abstract ID: 30630

INTERPLAY OF NAGAOKA FERROMAGNETISM, SUPERCONDUCTIVITY AND KONDO CORRELATIONS IN QUADRUPLE QUANTUM DOT ARRAY

E. Siuda, I. Weymann

Institute of Spintronics and Quantum Information, Faculty of Physics and Astronomy, Adam Mickiewicz University, Poznań, 61-614, POLAND

Quantum dot-based systems provide ideal platforms for studying electronic correlation effects, such as Nagaoka ferromagnetism [1], Majorana states in Kitaev chains [2], and superconductivity-induced bound states [3]. By carefully tuning the system parameters and selecting appropriate setups, it is possible to introduce multiple sources of correlations and study their interplay, revealing new physics arising from synergistic or competing interactions.

In this contribution, we investigate a quadruple quantum dot array coupled to an s-wave superconductor and a normal conductor. This system, when isolated, is known to exhibit Nagaoka ferromagnetism within certain ranges of the quantum dot energy levels. The presence of superconductor gives rise to a competition between magnetic and superconducting orders [1,4], affecting the phase diagram of the device. Here, with the aid of the numerical renormalization group method, we examine a setup, in which normal conductor is strongly coupled to one of the quantum dots, introducing Kondo correlations in the system. We calculate the system's ground state as a function of the dots' energy levels and the superconductor coupling strength. Four distinct phases are identified: one dominated by Kondo correlations, one dominated by Nagaoka ferromagnetism, and two other non-magnetic phases. Moreover, the corresponding spectral functions are computed in the Kondo and Nagaoka regimes, revealing the emergence of new correlations at the crossover between phases. These results provide deeper insight into strongly correlated systems and the interplay of magnetic, superconducting and Kondo correlations in coupled quantum dot devices.

This study was funded by the National Science Centre in Poland through the project No. 2022/45/B/ST3/02826.

References

[1] J. P. Dehollain, U. Mukhopadhyay, V. P. Michal, Y. Wang, B. Wunsch, C. Reichl, W. Wegscheider, M. S. Rudner, E. Demler, and L. M. K. Vandersypen, Nature **579**, 528 (2020).

[2] T. Dvir, G. Wang, N. van Loo, C.-X. Liu, G. P. Mazur, A. Bordin, S. L. D. ten Haaf, J.-Y. Wang, D. van Driel, F. Zatelli, X. Li, F. K. Malinowski, S. Gazibegovic, G. Badawy, E. P. A. M. Bakkers, M. Wimmer, and L. P. Kouwenhoven, Nature **614**, 445 (2023).

[3] L. Schneider, K. T. Ton, I. Ioannidis, J. Neuhaus-Steinmetz, T. Posske, R. Wiesendanger, and J. Wiebe, Nature **621**, 60 (2023).

[4] E. Siuda, and I. Weymann, Sci. Rep. **15**, 25349 (2025).

Abstract ID: 30677

HEAVY-FERMION QUANTUM CRITICALITY IN CeNiAsO: BEYOND LANDAU'S SCOPE

F. Lu, Z. Wang, Y. Luo

Wuhan National High Magnetic Field Center and School of Physics, Huazhong University of Science and Technology, Wuhan 430074, CHINA

The nature of quantum critical point (QCP) and its related emergent states pose fundamental but still not fully understood questions. The past decades have witnessed the accumulating examples that unconventional QCPs observed in heavy-fermion metals. Though theoretical models predicted that QCPs in these systems are beyond Landau's classic framework in that they include not only the well conceived spin degrees of freedom but also fermionic (charge) ones, yet straightforward experimental evidence for the latter from a local and microscopic perspective is still lacking. Here, on the example of pressure-tuned QCP in CeNi(As,P)O and by employing ^{75}As and ^{31}P nuclear magnetic resonance as local probes, the theoretically anticipated local-itinerant transition line separating the regimes with small and large Fermi surface is well determined experimentally and found to terminate at the QCP. Proliferation of charge fluctuations approaching QCP is also corroborated for the first time by spin-lattice relaxation measurements. Our results demonstrate the involvement and suggest the vital role of critical charge fluctuations in unconventional QCP that potentially bears serial ubiquitous consequences - e.g. strange metal and unconventional superconductivity - observed in heavy-fermion systems and many others.

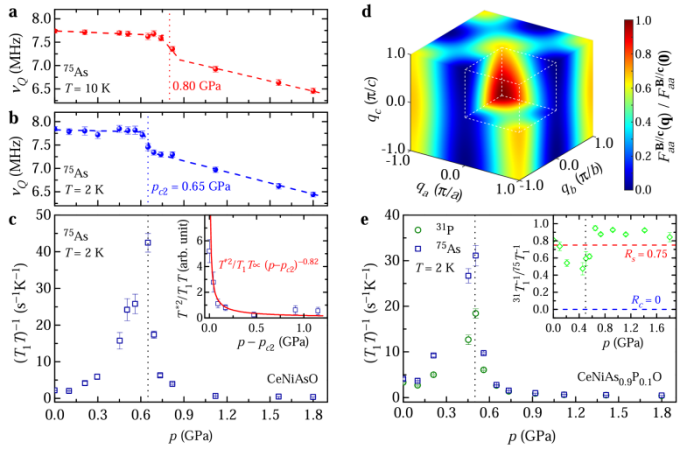

Fig. 1: *Pressure-dependent ν_Q and. a and b, Pressure dependen1/T_1T ce of ^{75}As ν_Q in CeNiAsO at 10K and 2 K, respectively. A jump in ν_Q is observed at ~ 0.80 Gpa for 10 K, and ~ 0.65 Gpa for 2 K. c, ^{75}As 1/T_1T as a function of p in CeNiAsO measured at 2 K. Near the QCP, 1/T_1T is significantly enhanced. The inset displays a fitting of T^{*2}/T_1T to $(p-p_{c2})^{-a}$. d, Distribution of hyperfine formfactor $F^{B//c}_{aa}(\mathbf{q})$ in momentum space. The results are presented afternormalized by the value at $\mathbf{q} = 0$. Note that $F^{B//c}_{aa}$ essentially vanishes near $\mathbf{q}_1$ and $\mathbf{q}_2$. e,Pressure dependencies of ^{75}As and ^{31}P 1/T_1T in $CeNiAs_{0.9}P_{0.1}O$. The inset shows the ratio $^{31}T^{-1}/^{75}T^{-1}$ vs p. Note that when approaching the QCP, the ratio remarkably deviates from Rs = 0.75, an expected value for spinfluctuations merely, suggesting the existence of charge fluctuations as well as spinfluctuations.*

References

[1] Y. Luo, *et al.*, *Heavy-fermion quantum criticality and destruction of the Kondo effect in a nickel oxypnictide*, Nat. Mater. **13**, 777-781 (2014).

[2] Y. Luo, *et al.*, *CeNiAsO: An antiferromagnetic dense Kondo lattice*, J. Phys. Condens. Matter **23**, 175701 (2011).

[3] F.Lu, *et al.*, *^{75}As NMR study of the antiferromagnetic Kondo lattice compound CeNiAsO*, Phys. Rev. B **107**, 045104 (2023).

56 - SUPERCONDUCTIVITY AND MAGNETISM UNDER PRESSURE AND STRAIN

Abstract ID: 30060

$LaCrGe_3$ UNDER PRESSURE: FROM FERROMAGNET WITH UNUSUAL COERCIVITY TO AVOIDED QUANTUM CRITICALITY

Sergey L. Bud'ko

Ames National Laboratory and Department of Physics and Astronomy, Iowa State University, Ames, IA 50011, USA

Studies of quantum phase transitions (QPTs) and quantum critical points (QCPs) in novel materials continue to be a flourishing direction in condensed matter physics. The fluctuations associated with QCPs, second order phase transitions at zero temperature, have been considered important for stabilization of superconductivity, non-Fermi liquid behavior, and other curious phenomena. Whereas for antiferromagnetic transitions, there are many experimental examples of QCPs, ferromagnetic (FM) transitions in clean, metallic magnetic systems are essentially different. [1] The QCP is avoided when a second-order paramagnetic (PM) - FM transition in such systems is suppressed to lower temperatures Instead, either (i) the PM-FM transition becomes a first-order QPT, or (ii) a new magnetic ground state emerges from the FM state.

One of relatively few materials where the second scenario was suggested to be realized under pressure is $LaCrGe_3$. In this talk ambient pressure properties of $LaCrGe_3$ will be briefly reviewed, followed by a discussion of the temperature – pressure – magnetic field phase diagram which is more complex than the four basic ones suggested for metallic ferromagnets. [1] The nature of the pressure – induced, non – FM phase in $LaCrGe_3$ was discussed in several publications [2,3] and still is ambiguous. Based on Hall effect measurements at ambient and high pressures, [4] a possible alternative interpretation for the nature of this phase will be discussed and H – T phase diagrams corresponding to a pressure - induced magnetic phase at several pressures will be presented.

This work was supported by US DOE, BES, under Contract No. DE-AC02-07CH11358.

References

[1] M. Brando, *et al.*, *Metallic quantum ferromagnets*, Rev. Mod. Phys. **88**, 025006 (2016).

[2] V. Taufour, *et al.*, *Ferromagnetic quantum critical point avoided by the appearance of another magnetic phase in $LaCrGe_3$ under pressure*, Phys. Rev. Lett. **117**, 037207 (2016).

[3] Elena Gati, *et al.*, *Formation of short-range magnetic order and avoided ferromagnetic quantum criticality in pressurized $LaCrGe_3$*, Phys. Rev. B **103**, 075111 (2021).

[4] S. L. Bud'ko, S. Huyan and P. C. Canfield, *Hall effect in $LaCrGe_3$ at ambient and $P < 24$ kbar pressure and a $H - T$ phase diagram of the pressure-induced magnetic phase*, under review (2025).

Abstract ID: 30221

DOPING AND PRESSURE EFFECTS ON THE SUPERCONDUCTING STATE OF CsV_3Sb_5 KAGOME

S. Sanna[1], A. Kataria[2], I. J. Onuorah [2], P. Bonfà[3], A. Capa Salinas[4], V. Mitrović[5], Z. Guguchia[6], R. Khasanov[6], S. D. Wilson[5]

[1] Univ of Bologna, Dep. of Physics and Astronomy, 40127, Bologna, ITALY
[2] Univ. Of Parma, Dep. of Math., Physical and Computer Sciences, 43124, Parma, ITALY
[3] Dipartimento di Fisica, Informatica e Matematica, Università di Modena e Reggio Emilia, Via Campi 213/a, I-41125 Modena, ITALY
[4] Materials Department and California Nanosystems Institute University of California Santa Barbara Santa Barbara California 93106 USA
[5] Department of Physics Brown University Providence Rhode Island 02912 USA
[6] PSI Center for Neutron and Muon Sciences CNM, Villigen PSI, SWITZERLAND

The two-dimensional kagome compounds AV_3Sb_5 (A = Cs, Rb, K) provide an ideal platform for investigating the interplay between competing electronic instabilities, charge-density-wave (CDW) order and superconductivity (SC), and for exploring the potential emergence of hidden chiral phases. Both CDW and SC are believed to originate from saddle points in the electronic band structure lying close to the Fermi level.

In this work, we tune the Fermi level by combining hole doping and pressure to study the effect on the superconducting state of the hole-doped $CsV_3Sb_{5-x}Sn_x$ system, studied via transverse-field muon-spin spectroscopy. As a function of hole doping, this material exhibits a reduction of the CDW coherence length [1] and a two-dome superconducting phase, with maxima at $T_c \approx 2.5$ K and ≈ 3.5 K for $x \approx 0.04$ and 0.35, respectively [2]. We investigate the pressure response of both compositions corresponding to the maxima of these domes. Our results show that the superconducting critical temperature increases under pressure for both samples, while maintaining an s-wave pairing character.

These findings illustrate how the superconducting symmetry parameter, the superconducting gap, and the superfluid stiffness evolve as a function of pressure [3], providing a novel phenomenological basis for understanding the complex behavior of superconductivity in 2D kagome materials.

References

[1] I. Nikolov, G. Allodi, A. Rosuel, G. Corsale, A. Kataria, P. Bonfà, R. De Renzi, A. Capa Salinas, S. Wilson, M.-H. Julien, S. Sanna, V. Mitrović, arXiv:2512.09256 (2025).

[2] Y. M. Oey, B. R. Ortiz, F. Kaboudvand, J. Frassineti, E. Garcia, R. Cong, S. Sanna, V. F. Mitrović, R. Seshadri, S. D. Wilson, Phys. Rev. Materials **6**, L041801 (2022).

[3] S.Sanna, *et al.*, paper in preparation

Abstract ID: 30355

PRESSURE CONTROL OF INTERTWINED QUANTUM ORDERS IN 6R-TaS_2

Z. Guguchia[1], V. Sazgari[1], J. Graham[1], S.S. Islam[1], P. Kral[1], A. Achari[2], O. Gerguri[1], J. Tangermann[3], G. Simutis[1], R. Khasanov[1], H. Luetkens[1], M. Janoschek[1], J. Yin[4], F.v. Rohr[3], R. Nair[2]

[1] *PSI Center for Neutron and Muon Sciences, 5232 Villigen PSI, SWITZERLAND*
[2] *Department of Chemical Engineering, University of Manchester, UNITED KINGDOM*
[3] *Department of Quantum Matter Physics, University of Geneva, SWITZERLAND*
[4] *Department of Physics, Southern University of Science and Technology, CHINA*

The transition metal dichalcogenide 6R-TaS_2 offers a natural platform for studying the interplay between charge density wave (CDW) order, superconductivity, and transport anomalies. Recent results show that, in the intermediate temperature range between charge order and superconductivity, an additional characteristic temperature scale emerges at T*=40 K, marked by pronounced magnetoresistance and an anomalous contribution to the Hall effect (ACH). However, the nature of the superconducting pairing, the origin of ACH, and their relationship with the CDW remain unclear. Using muon-spin rotation (μSR), magnetotransport, scanning tunnelling microscopy/spectroscopy (STM/STS) and hydrostatic pressure techniques, we identify a nodal superconducting state with low superfluid density at ambient pressure [1], with no spontaneous magnetic order detected below T*. This rules out magnetism as the origin of the ACH. Under pressures up to 2 GPa, the superfluid density rises markedly in correlation with the superconducting transition temperature, the nodal pairing shifts to a nodeless state, and the CDW onset is reduced by half. Notably, the ACH is fully suppressed and magnetoresistance drops by 50% within just 0.2 GPa, highlighting the fragility of the state with ACH. These results reveal an unconventional superconducting pairing in 6R-TaS_2, competing with both CDW and ACH through the weakened interlayer coupling and competition for the same electronic states. With this multifaceted approach, we establish a comprehensive phase diagram that reveals the intricate interplay and competition between the intertwined quantum orders in 6R-TaS_2.

Acknowledgement

Z.G. acknowledges support from the Swiss National Science Foundation (SNSF) through SNSF Starting Grant (No. TMSGI2_211750).

References

[1] V. Sazgari, *et. al.*, and Z. Guguchia, arXiv:2503.13944 (2025).

Abstract ID: 30603

ADVANCEMENTS IN HIGH-PRESSURE INSTRUMENTATION FOR STUDYING MAGNETIC PROPERTIES OF MATERIALS

K. V. Kamenev

The University of Edinburgh, Centre for Science at Extreme Conditions, School of Engineering, EH9 3FD, UNITED KINGDOM

High-pressure instrumentation is crucial for uncovering emergent magnetic and superconducting phases by tuning interatomic interactions far beyond ambient conditions. The approach to designing high-pressure cells (HPC) will be presented and illustrated with several examples of HPCs, covering different ranges of pressure, sample volume and sensitivity. The first class of HPCs enable sensitive magnetic measurements over a wide pressure range in commercial SQUID-based platforms [1]. These include several piston–cylinder cells operating up to 3 GPa, suitable for studying weakly magnetic samples. For measurements at up to 10 GPa and above, several miniature diamond anvil cells (DACs) were developed, including an entirely non-metallic diamond anvil cell for high pressure ac susceptibility, which reaches 5.6 GPa without magnetic screening from the cell body [2]. Finally, HPCs for direct probing of magnetic order using neutron scattering [3] and pressure tuned electronic transport. The performance of the cells will be illustrated with examples of experimental data collected to long range order transitions in Kagome antiferromagnets, Applications of these cells span pressure induced long-range antiferromagnetic ordering, spin liquid to long range order transitions in kagome antiferromagnets, and pressure tuned electronic transport in piezoelectronic materials [4]. The presented developments provide a coherent high-pressure toolkit that has significantly expanded the experimental phase space for magnetism and superconductivity under extreme conditions.

References

[1] X. Wang and K. V. Kamenev, Low Temperature Physics, **40**, 735 (2014).
[2] X. Wang, *et al.*, High Pressure Research, **34**, 371 (2014).
[3] M. G. Kibble, *et al.*, Journal of Neutron Research, **21**, 105 (2019).
[4] S. Afanasjevs, *et al.*, Advanced Electronic Materials, **10**, 2300680 (2024).

Abstract ID: 30824

HIGH TEMPERATURE SUPERCONDUCTIVITY WITH GIANT PRESSURE EFFECT IN 3D NETWORKS OF BORON DOPED ULTRA-THIN CARBON NANOTUBES IN THE PORES OF ZSM-5 ZEOLITE

T. H. Koo[1], Y. Wang[1], R. Huang[1], Y. H. Ng[1], T. T. Lortz[1], T. Zhang[1], W. M. Chan[1], Y. Hou[1], J. Pan[1], R. Lortz[2], N. Wang[1], P. Sheng[1,3]

[1] *Department of Physics, The Hong Kong University of Science and Technology, Kowloon, Hong Kong, CHINA*
[2] *Université Grenoble Alpes, INSA Toulouse, Université Toulouse Paul Sabatier, CNRS, LNCMI, Grenoble, FRANCE*
[3] *Clare Hall College, Cambridge University, Cambridge, THE UNITED KINGDOM*

We report the fabrication of three dimensional, interconnected networks of ultrathin carbon nanotubes (CNTs) embedded within the ~5 Å pores of zeolite ZSM 5 crystals using a controlled chemical vapour deposition (CVD) process. Confinement within these sub nanometre channels yields CNTs with strongly one-dimensional electronic characteristics, including pronounced van Hove singularities in the density of states. By introducing boron dopants during growth, we strategically tune the Fermi level toward a van Hove singularity, as supported by ab initio electronic structure calculations. This electronic tuning, combined with the intrinsic 3D connectivity of the CNT–zeolite framework, enables a dimensional crossover from 1D electronic states to a phase coherent, bulk superconducting state.

To establish the presence of superconductivity, we employ five complementary experimental probes—electrical resistivity, ac susceptibility, dc magnetization, specific heat, and point contact spectroscopy. All measurements consistently indicate a superconducting transition at ambient pressure with a critical temperature Tc in the range of 220–250 K. Simultaneous resistivity and ac susceptibility measurements reveal a three order of magnitude drop in resistance accompanied by the onset of a robust Meissner effect with nearly perfect diamagnetic screening. Point contact spectroscopy further uncovers a multigap superconducting state, with a dominant gap of approximately 30 meV, in reasonable agreement with expectations from Bardeen–Cooper–Schrieffer (BCS) theory. The differential conductance spectra exhibit clear particle–hole symmetry and evolve smoothly between the tunnelling and Andreev reflection regimes as the contact transparency is varied—behaviour uniquely characteristic of superconducting quasiparticles. Specific heat measurements show a distinct anomaly at the transition, reminiscent of signatures observed in high-Tc cuprate superconductors.

Finally, we find that the application of very modest external pressure further enhances the superconducting transition temperature, pushing Tc above ambient temperature and suggesting that the system remains far from its optimal tuning point. These results collectively point to a new pathway for achieving high temperature superconductivity in engineered low dimensional carbon-based materials.

57 - SUPERCONDUCTIVITY AND TOPOLOGY IN PTBI2

Abstract ID: 30454

QUASIPARTICLE INTERACTION IN 2H-TaS_2 REFLECTED BY POINT-CONTACT SPECTROSCOPY

O. Kvitnitskaya[1,2], M. Behnami[1], B. Büchner[1,3], Yu. Naidyuk[2]

[1] *Leibniz-Institute for Solid State and Materials Research, IFW-Dresden, 01069 Dresden, GERMANY*
[2] *B. Verkin Institute for Low Temperature Physics and Engineering of the National Academy of Sciences of Ukraine, Kharkiv 61103, UKRAINE*
[3] *Institute of Solid State and Materials Physics and Würzburg-Dresden Cluster of Excellence ct.qmat, Technische Universität Dresden, 01062 Dresden, GERMANY*

Among Ta-based dichalcogenides, metallic 2H-TaS_2 exhibits a range of physical properties 2H-TaS_2 which are highly sensitive to external conditions like pressure, doping, and structural imperfections. TaS_2 represents a classic example of a material in which charge density wave (CDW) order and superconductivity coexist and compete. Its superconducting transition temperature T_c can be enhanced by doping or applying pressure, while suppressing in the same time the competing CDW state. Point-contact (PC) spectroscopy is a direct method for measuring electron-phonon interactions and the superconducting gap [1]. Furthermore, PC measurements can be used to detect phase transitions that affect electron transport. In this report, we present the first PC study of 2H-TaS_2. At first, we observed that the superconducting critical temperature T_c in 2H-TaS_2 PCs is significantly increased up to 7 K, compared to its typical bulk value of about 0.8 K [2]. Simultaneously, the critical magnetic field reaches up to 5T at 2K. Nonlinear current-voltage characteristics I(V) of 2H-TaS_2 PCs also exhibit a feature, which is reflected in dV/dI as dips symmetrically placed versus zero-bias voltage. They bear a resemblance with resistivity and can be connected with the CDW transition. However, the temperature at which these features disappear is much higher than the T_{CDW} in the bulk and more consistent with that observed in degraded 20-30 nm thick flakes [3]. The specifics of electron-phonon interaction are still unresolved in PC spectra, probably due to dominating of electron-electron interactions as follows from the quadratic dependence of dV/dI (V) at low biases. These preliminary results are very intriguing and give impetus to their deeper investigation.

OK and YN acknowledge the funding of Alexander von Humboldt Foundation (Philipp Schwartz-Initiative and Research Group Linkage Programme) and the support by the National Academy of Sciences of Ukraine under project Ф19-5.

References

[1] Yu. G. Naidyuk and I. K. Yanson, Point-Contact Spectroscopy, Springer Series in Solid-State Sciences Vol. 145 (2005).
[2] A. H. Thompson, *et al.*, Phys. Rev. B, **5**, 2811 (1972).
[3] M. Lee, *et al.*, Appl. Phys. Lett. **118**, 193105 (2021).

Abstract ID: 30562

MECHANISM FOR NODAL TOPOLOGICAL SUPERCONDUCTIVITY ON $PtBi_2$ SURFACE

K. Mæland, G. Sangiovanni, B. Trauzettel

Institute for Theoretical Physics and Astrophysics and Würzburg-Dresden Cluster of Excellence ctd.qmat, University of Würzburg, D-97074 Würzburg, GERMANY

Experiments show that the Weyl semimetal $PtBi_2$ hosts unconventional superconductivity in its topological surface states. Hence, the material is a candidate for intrinsic topological superconductivity. Measurements indicate nodal gaps in the center of the Fermi arcs. We derive that anisotropic electron-phonon coupling on Weyl semimetal surfaces [1], combined with statically screened Coulomb repulsion, is a microscopic mechanism for this nodal pairing [2]. The dominant solution of the linearized gap equation shows nodal gaps when the surface state bandwidth is comparable to the maximum phonon energy, as is the case in $PtBi_2$. We further predict that if the screening of Coulomb interaction on the surface is enhanced by Coulomb engineering, the superconducting gap becomes nodeless, and the critical temperature increases.

References

[1] K. Mæland, M. Bahari, and B. Trauzettel, *Phonon-mediated intrinsic topological superconductivity in Fermi arcs*, Phys. Rev. B **112**, 104507 (2025).

[2] K. Mæland, G. Sangiovanni, and B. Trauzettel, *Mechanism for nodal topological superconductivity on $PtBi_2$ surface*, arXiv:2512.09994.

Abstract ID: 30574

TOPOLOGICAL SUPERCONDUCTIVITY ON THE SURFACE OF $PtBi_2$

C. Fulga

IFW Dresden, Helmholtzstraße 20, 01069 Dresden, GERMANY

By using angle-resolved photoemission spectroscopy, we have observed that the Weyl semimetal $PtBi_2$ harbors nodes in its superconducting gap, implying unconventional i-wave pairing symmetry. The existence of these nodes would mark the surface of this material as a naturally-occurring, or intrinsic topological superconductor. In this talk, I will address the nature of this potential state, discussing its various features such as surface Majorana cones, and zero-energy dispersionless Majorana flat bands located on hinges. I will explore how future measurements might be used to further confirm the existence of topological surface superconductivity, as well as how various perturbations may be used to alter its character.

Abstract ID: 30576

SURFACE-EXTENDED ANDREEV BOUND STATES EMERGING FROM INTRINSIC SURFACE SUPERCONDUCTIVITY OF $PtBi_2$

X. Huang[1], L. Zhao[2], S. Schimmel[3,4], J. Besproswanny[3,4], P. Härtl[1], C. Hess[3,4], B. Büchner[4,5], M. Bode[1,6]

[1] *Universität Würzburg, Experimentelle Physik 2, Physikalisches Institut, 97074, Würzburg, GERMANY*
[2] *Quantum Science Center of Guangdong-Hong Kong-Macao Greater Bay Area (Guangdong), 518045, Shenzhen, CHINA*
[3] *Bergische Universität Wuppertal, Fakultät für Mathematik und Naturwissenschaften, 42119, Wuppertal, GERMANY*
[4] *Leibniz-Institute for Solid State and Materials Research, 01069, Dresden, GERMAN*
[5] *Technische Universität Dresden, Dresden, Germany 01069, Dresden, GERMAN*
[6] *Universität Würzburg, Wilhelm Conrad Röntgen-Center for Complex Material Systems, 97074, Würzburg, GERMANY*

Intrinsic topological superconductivity remains a central question in condensed-matter physics. The three-dimensional Weyl semimetal $PtBi_2$ was recently shown by angle-resolved photoemission spectroscopy to host a superconducting gap that opens exclusively on its Fermi-arc surface states with a nodal structure, establishing it as a prime candidate for intrinsic topological superconductivity [1-3]. Using scanning tunneling microscopy and spectroscopy, we directly visualize surface-extended Andreev bound states (ABSs) across atomically pristine terraces within a sizable superconducting gap (Δ>10 meV) in $PtBi_2$. Quantitative analysis of the tunneling spectra within an anisotropic chiral pairing framework indicates that these states are compatible with a dispersive, Majorana cone-like quasiparticle band. Our results provide real-space spectroscopic insight into the unconventional superconducting state of $PtBi_2$ and highlight this material as a promising platform for exploring Majorana-related quasiparticle physics.

References

[1] A. Kuibarov, *et al.*, Nature **626**, 294 (2024).
[2] S. Schimmel, *et al.*, Nat. Commun. **15**, 9895 (2024).
[3] S. Changdar, *et al.*, Nature **647**, 613 (2025).

Abstract ID: 30616

UNCONVENTIONAL SURFACE SUPERCONDUCTIVITY OF t-$PtBi_2$

S. Schimmel[1,2], Julia Besproswanny[1,2], Y. Fasano[1,3], G. Shipunov[2], S. Aswartham[2], D. Baumann[2], B. Büchner[2], C. Hess[1,2]

[1] *Bergische Universität Wuppertal, 42119 Wuppertal, GERMANY*
[2] *Leibniz-Institute for Solid State and Materials Research (IFW-Dresden), 01069 Dresden, GERMANY*
[3] *Instituto de Nanociencia y Nanotecnologi□ a and Instituto Balseiro, CNEA – CONICET and Universidad Nacional de Cuyo, 8400 Bariloche, ARGENTINA*

The Weyl semimetal t-$PtBi_2$ (trigonal) recently emerged as an interesting host of unconventional and potentially topological superconductivity. Sizable superconducting gaps up to about 20 meV have been observed in scanning tunneling spectroscopy (STM/STS) [1] and ARPES [2,3]. The data suggest surface superconductivity emerging from the Weyl Fermi arc states while the bulk states remain normal. The order parameter has been reported to possess nodes, suggestive of topological *i-wave* superconductivity [3]. Here we present STM/STS data of the quasiparticle interference (QPI) in both the superconducting and the normal state as well as temperature dependent measurements of the superconducting gap. Our data clearly reveal that i) the states which are gapped out by superconductivity indeed are located at the Fermi arcs, and ii) the large superconducting gaps correspond to a high critical temperature T_c up to about 50 K. Thus $PtBi_2$ indeed qualifies as a truly unconventional and topological superconductor.

References

[1] S. Schimmel, *et al.*, Nature Communications **15**, 9895 (2024).
[2] A. Kuibarov, *et al.*, Nature **626**, 294 (2024).
[3] S. Changdar, *et al.*, Nature **647**, 613-618 (2025).

Abstract ID: 30619

GINZBURG–LANDAU THEORY FOR UNCONVENTIONAL SURFACE SUPERCONDUCTIVITY IN $PtBi_2$

H. Waje[1], F. Jakubczyk[1,2], J. van den Brink[1,2,3], C. Timm[1,2]

[1] *Institute of Theoretical Physics, Technische Universität Dresden, 01069 Dresden, GERMANY*
[2] *Würzburg-Dresden Cluster of Excellence ct.qmat, Technische Universität Dresden, 01062 Dresden, GERMANY*
[3] *Leibniz Institute for Solid State and Materials Research (IFW) Dresden, Helmholtzstrasse 20, 01069 Dresden, GERMANY*

Recent experimental evidence suggests the presence of an unconventional, nodal surface-superconducting state in trigonal $PtBi_2$. We construct a Ginzburg-Landau theory for the three superconducting order parameters, which correspond to the three irreducible representations of the point group C_{3v}. The irreducible representations A_1 and A_2 are the most likely. We develop a systematic method to determine the symmetry-allowed terms and apply it to derive all terms up to fourth order in the three order parameters. The Ginzburg-Landau functional also includes coupling to the magnetic field. The functional is employed to determine the effect of an applied uniform magnetic field on the nodal structure for A_1 and A_2 pairing. The results facilitate clear-cut experimental differentiation between these symmetries. We also predict field-induced helical superconductivity.

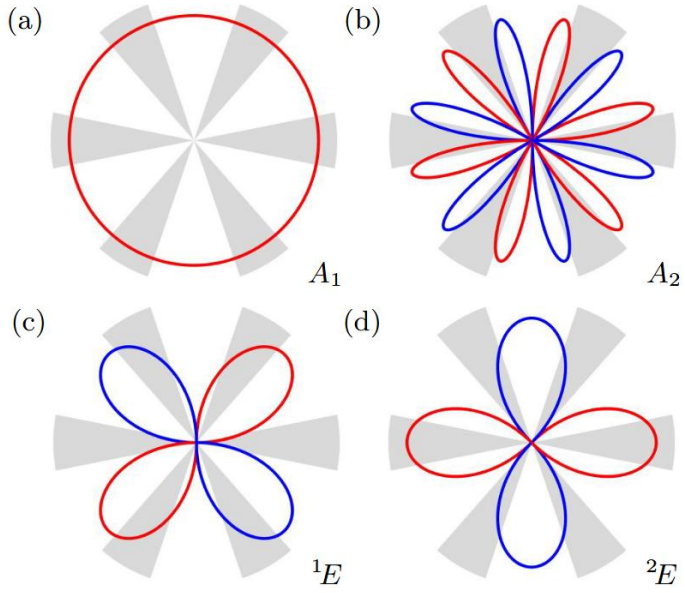

Fig. 1: *Polar plots of the lowest-order basis functions showing the symmetries of the superconducting pairing amplitudes of (a) A_1, (b) A_2, (c) ^1E, and (d) ^2E symmetry. Red and blue color refer to positive and negative sign, respectively. The angular ranges spanned by the Fermi arcs are sketched as gray sectors, which have been exaggerated for clarity.*

Abstract ID: 30649

ARPES EVIDENCE FOR UNCONVENTIONAL TOPOLOGICAL SUPERCONDUCTIVITY IN THE FERMI ARC STATES OF t-$PtBi_2$

S. Borisenko

IFW-Dresden, 01069, Dresden, GERMANY

Topological superconductivity is a key ingredient for realizing Majorana fermions, yet intrinsic material platforms remain scarce. Using angle-resolved photoemission spectroscopy (ARPES), we have recently demonstrated that the Weyl semimetal t-$PtBi_2$ hosts superconductivity confined to its topological surface states, the Fermi arcs [1]. This superconductivity is unconventional, with nodal i-wave symmetry and signatures of emergent Majorana modes [2], and can be robustly detected under both laser- and synchrotron-based ARPES conditions [3]. Moreover, t-$PtBi_2$ fulfills the canonical criteria favorable for high-T_c superconductivity, opening the door to tuning and optimizing this exotic state [4]. These findings establish t-$PtBi_2$ as a rare platform where ARPES directly reveals superconductivity of topological surface states, paving the way toward intrinsic realizations of Majorana physics.

References

[1] A. Kuibarov, *et al.*, *Evidence of superconducting Fermi arcs*, Nature **626**, 294 (2024).
[2] S. Changdar, *et al.*, *Topological nodal i-wave superconductivity in PtBi2*,Nature **647**, 613 (2025).
[3] A. Kuibarov, *et al.*, *Measuring superconducting arcs by ARPES*, Phys. Rev. B **112**, 144518 (2025).
[4] A. Kuibarov, *et al.*, *Three prerequisites for high-temperature superconductivity in t-PtBi2*, arXiv:2509.02178

58 - THE SPINTRONIC REVOLUTION IN NEUROMORPHIC COMPUTING

Abstract ID: 30055

PROBABILISTIC COMPUTING WITH DIGITAL CMOS INTEGRATED CIRCUITS AND VOLTAGE-CONTROLLED MAGNETIC TUNNEL JUNCTIONS

P. Khalili[1,2]

[1] *Department of Electrical and Computer Engineering, Northwestern University, Evanston, Illinois, USA*
[2] *Applied Physics Program, Northwestern University, Evanston, Illinois, USA*

The integration of magnetic tunnel junctions (MTJs) on CMOS semiconductor manufacturing technology provides exciting opportunities for the development of neuromorphic and probabilistic (p-) computing application-specific integrated circuits (ASICs). We discuss how appropriately designed voltage-controlled MTJs can serve as compact and high-throughput entropy sources for such hardware [1]. We discuss device/circuit interactions/trade-offs and show experimental results from a 130 nm ASIC interfaced with voltage-controlled MTJs [2], along with projections for more advanced technology nodes. We then discuss how appropriately designed extended probabilistic variables (termed probabilistic d-dimensional bits, or p-dits) can further accelerate the solution of various optimization problems [3]. Finally, we present the first experimental observation of the octupole-driven spin-transfer torque (OTT) effect [4], whereby all-antiferromagnetic tunnel junctions (ATJs) [4, 5] can be switched by direct tunneling current through the device in a two-terminal geometry. We discuss the potential of OTT-ATJs for p-bit implementation in p-computing applications, as well as for other physics-inspired computing approaches.

References

[1] Y. Shao, et al., Nanotechnology 34, 495203 (2023).

[2] C. Duffee, et al., Nature Electronics 8, 784–793 (2025).

[3] C. Duffee, et al., Physical Review Applied 24, 044077 (2025).

[4] J. Kang, et al., arxiv: 2509.03026 (2025).

[5] J. Shi, et al., Advanced Materials 36, 2312008 (2024).

Abstract ID: 30252

TOPOLOGICAL SPINTRONICS

Y. Zhou

School of Science and Engineering, The Chinese University of Hong Kong, Shenzhen 518172, PEOPLE'S REPUBLIC OF CHINA

Recently, tremendous attention has been focused on the continuous scaling of Moore's law as well as the advanced non-von Neumann computing architecture. Spintronics may go beyond classical electronics and offer low power logic/computing components to further increase the performance of modern information and communication technologies meanwhile reducing the energy consumption. In particular, magnetic skyrmions – topologically non-trivial spin nanostructures, have been endowed with great expectations as promising candidates for next-generation spintronic device applications [1]. However, there is a major roadblock for skyrmionics device applications – the skyrmion Hall effects, which may lead to skyrmions annihilation at the sample edge. In this talk, Dr. Yan Zhou will discuss his recent work of eliminating/suppressing the skyrmion Hall effects, which may overcome the main bottleneck of practical applications of skyrmionic racetrack memory and logic devices. In the last part of his talk, he will discuss some novel device concepts based on these intriguing topological spin textures (such as neuromorphic or skyrmionics computing etc).

References

[1] National Science Review, **vol. 6**, **No. 2**, pp 210-212 (2019).

Abstract ID: 30279

PROBABILISTIC COMPUTING WITH p-BITS: HARDWARE, OPTIMIZATION, AND GenAI

K. Y. Çamsarı

Department of Electrical and Computer Engineering, University of California, Santa Barbara, Santa Barbara, CA, 93106, USA

Probabilistic bits (p-bits) offer a hardware-native way to build large networks of stochastic binary units whose collective dynamics can be programmed to sample, infer, and optimize. In this invited talk, I will give a unified view of recent progress that connects spintronic p-bit hardware to two fast-moving application fronts: hard combinatorial optimization and efficient Transformer inference.

First, I will discuss a DAC-free, digital-input digital-output p-bit architecture that eliminates the analog bias bottleneck that has limited scalability of nanodevice p-bits. Using digital CMOS, we obtain robust sigmoidal control from roughly 50/50 entropy sources (e.g., sMTJs), while mitigating device variability via calibrated delay lines and whitening. This enables practical on-chip temperature control and asynchronous, conflict-resolving updates that naturally support parallelism.

Second, I will contrast probabilistic computers with quantum annealers by establishing a rigorous classical baseline for hard optimization. Using hardware-friendly Monte Carlo methods, including simulated quantum annealing and adaptive parallel tempering with non-local moves, we benchmark large 3D spin-glass instances showing scaling trends consistent with extreme value theory and regimes where adaptive tempering wins. I will briefly mention generalized PAOA as a variational umbrella that connects derivative-free updates to Markov-flow optimization and maps cleanly to Ising machines and FPGA-class probabilistic computers.

Finally, I will connect these ideas to generative AI through stochastic add-only attention (SANTA), a post-softmax sampling rule that replaces value-stage multiplications with sparse fetch-and-add operations plus a bitshift, yielding an unbiased estimator of dense attention and pointing toward fully multiplier-free Transformer inference when combined with modern quantization.

References

[1] K. Selcuk, N. Anjum Aadit, C. Delacour, J. Quintana Silva, N. Sanjay Singh, H. Kaneko, S. Kanai, Y.-J. Wu, Y.-H. Chen, Y.-S. Chen, Y. Ching Ong, K.-C. Huang, H. Chuang, H. Ohno, S. Fukami, K. Y. Camsari, *DAC-Free p-bits: Asynchronous Self-Coloring and On-Chip Annealing*, IEEE International Electron Devices Meeting (IEDM) (2025).

[2] S. Chowdhury, N. Anjum Aadit, A. Grimaldi, E. Raimondo, A. Raut, P. Aaron Lott, J. H. Mentink, M. M. Rams, F. Ricci-Tersenghi, M. Chiappini, L. S. Theogarajan, T. Srimani, G. Finocchio, M. Mohseni, K. Y. Camsari, *Pushing the Boundary of Quantum Advantage in Hard Combinatorial Optimization With Probabilistic Computers*, Nature Communications, (2025).

[3] A. S. Abdelrahman, S. Chowdhury, F. Morone, K. Y. Camsari, *Generalized Probabilistic Approximate Optimization Algorithm*, Nature Communications, (2025).

Abstract ID: 30485

STOCHASTIC MAGNETIC TUNNEL JUNCTIONS FOR PROBABILISTIC COMPUTING AND SOLVING COMBINATORIAL OPTIMIZATION PROBLEMS

A. D. Kent

Center for Quantum Phenomena, Department of Physics, New York University, USA

Magnetic tunnel junctions (MTJs) are widely used as nonvolatile memory elements, but they can also serve as controllable, high-rate sources of random bits [1]. In this talk, I will describe experimental studies of perpendicularly magnetized MTJs that are magnetically stable at room temperature [2,3]. Instead of relying on spontaneous thermal magnetization fluctuations (superparamagnetism), stochastic behavior is generated on demand by actuating the device with nanosecond electrical pulses in the ballistic spin-transfer regime. This approach enables precise control of the switching probability. I will present measurements showing high-rate (up to 100 MHz/MTJ), reproducible generation of random bit streams [4] and random telegraph noise [5]. By interfacing individual pMTJs with custom electronics and a field-programmable gate array (FPGA), we generate truly random numbers that pass the full NIST statistical test suite with no post-processing [6]. I will also show how such actuated stochastic MTJs (A-sMTJs) can be electrically connected in simple circuits to generate tunable, circuit-mediated interactions that map onto effective Ising couplings. Finally, I will discuss the potential of stochastic MTJs for physics-inspired computing systems, including their use for solving combinatorial optimization problems [7].

References

[1] For a recent review, see: J. Z. Sun, *et al.*, *Superparamagnetic and stochastic-write magnetic tunnel junctions for high-speed true random number generation in advanced computing*, J. Phys. D: Appl. Phys. **59**, 013002 (2026).

[2] L. Rehm, *et al.*, *Stochastic magnetic actuated random transducer devices based on perpendicular magnetic tunnel junctions*, Phys. Rev. Appl. **19**, 024035 (2023).

[3] L. Rehm, *et al.*, *Temperature-resilient true random number generation with stochastic actuated magnetic tunnel junction devices*, Appl. Phys. Lett. **124**, 052401 (2024).

[4] A. Sidi El Valli, *et al.*, *High-speed tunable generation of random number distributions using actuated perpendicular magnetic tunnel junctions*, Appl. Phys. Lett. **126**, 212403 (2025).

[5] A. Sidi El Valli, *et al.*, *Tunable random telegraph noise in stable perpendicular magnetic tunnel junctions for unconventional computing*, arXiv: 2509.13458 (to appear in PR Applied).

[6] T. Criss, *et al.*, *Magnetic tunnel junction as a real-time entropy source: Field-Programmable Gate Array-based random bit generation without post-processing*, J. Appl. Phys. **139**, 013903 (2026).

[7] Dairong Chen, Andrew D. Kent, Dries Sels, and Flaviano Morone, *Solving combinatorial optimization problems through stochastic Landau-Lifshitz-Gilbert dynamical systems*, Phys. Rev. Research **7**, 013129 (2025).

Abstract ID: 30797

ION-ENGINEERED MAGNETIC TUNNEL JUNCTIONS FOR MRAM, MAGNETIC SENSORS, AND NEUROMORPHIC COMPUTING

D. Ravelosona[1,2]

[1] *Spin-Ion Technologies, 91120 Palaiseau, FRANCE*
[2] *Centre de Nanosciences et de Nanotechnologies (C2N), CNRS, University of Paris-Saclay, 91120 Palaiseau, FRANCE*

We have developed a unique manufacturing process based on He+ ion irradiation to tailor the structural properties of ultra-thin magnetic films. The key feature of the technology is the post-growth control at atomic scale of magnetic properties. When realized through a mask this technology allows lateral modulation of magnetic properties without any physical etching.

In this talk, I will demonstrate that He+ ion irradiation can be used to enhance the performance of Magnetic Tunnel Junctions with perpendicular magnetic anisotropy for application to MRAM, magnetic sensors and neuromorphic computing. I will introduce the concept of light ion irradiation applied to complex heterostructures and illustrate a few examples of potential applications including neuromorphic chips that can address both ultra-low power inference and on-chip continual learning, hence greatly advancing the development of highly efficient, robust hardware amenable to neural applications on the edge.

59 - THEORY OF MAGNETISM

Abstract ID: 30053

A LANDAU PARADIGM FOR QUANTUM SPIN LIQUIDS: BEYOND GAUGE THEORY

Y. Zhou

Institute of Physics, Chinese Academy of Sciences, CHINA

We introduce a Landau-type effective theory as an alternative to the standard gauge-theoretic description of quantum spin liquids. The analysis of this framework reveals the nature of its quasiparticle excitations and collective modes, leading to testable physical predictions.

Abstract ID: 30150

MOLECULAR SPIN–ELECTRIC COUPLING IN NON-CENTROSYMMETRIC LANTHANIDE COMPLEXES: A COMPUTATIONAL STUDY

C. Bigelli[1], D. Sartini[1], L. Tacconi[1], M. Gakiya Teruya[2], A.Cini, L. Passerini, G. K. Gransbury[1], M. Fittipaldi[3], L. Sorace[1], M. Shatruk[2,3], M. Briganti[1], M. Perfetti[1]

[1] *University of Florence, Department of Chemistry, 50019, Sesto Fiorentino, ITALIA*
[2] *Florida State University, Department of Chemistry and Biochemistry, 32306, Thallahassee, UNITED STATES*
[3] *University of Florence, Department of Physics and Astronomy, 50019, Sesto Fiorentino, ITALIA*
[4] *National High Field Magnetic Laboratory, 32306, Thallahassee, UNITED STATES*

The interaction between magnetic materials and electric fields (magnetoelectric effect) enables the electric control of spin, offering advantages in speed, scalability, and energy efficiency[1]. While extensively studied in inorganic solids, the molecular counterpart remains less explored due to generally weak spin–electric coupling (SE). Here, we investigate by *ab initio* calculations the spin–electric behavior of the $[Ln(NSC)_3(OPPh_3)_3]$ (Ln = Dy, Er) series [2], chosen for their non-centrosymmetric trigonal crystal structure, which potentially enables first-order spin–electric effects. The unit cell contains two inequivalent molecules, 1a (with proper C_3 symmetry) and 1b (slightly distorted, lacking true C_3 symmetry). *Ab initio* calculations on equilibrium geometries show a strong symmetry dependence for Dy, while the Er complexes are much less sensitive to these symmetry variations [3].

The effect of external electric fields was first analyzed considering the electronic polarization: calculations indicate that 1a responds linearly only when the field aligns with the C_3 axis, while 1b shows a first-order response in all directions. To consider the field-induced distortions, we developed a MATLAB external code to analytically estimate field-induced displacements from frequency calculations. Preliminary results reveal that the response is dominated by field-induced geometric distortions while at lower fields electronic polarization seems to prevail.

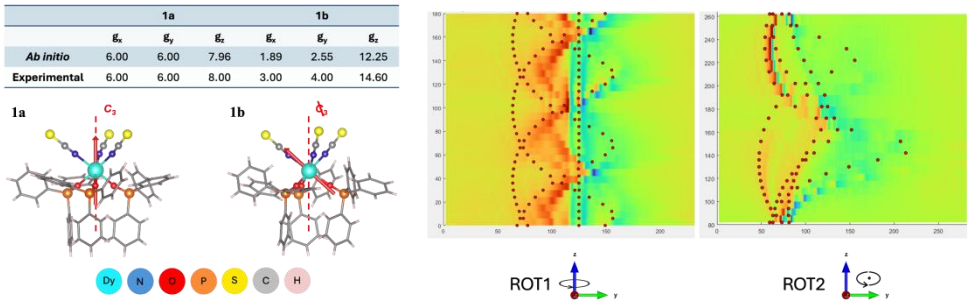

Fig. 1: ***Left****: molecular structure of* $[Dy(NSC)_3(OPPh_3)_3]$*. 1a is threefold symmetric; 1b lacks any formal symmetry. Dashed lines represent the C3 axis; red arrows represent the computed easy axis.* ***Right****: 2D experimental EPR spectra with the corresponding simulations overlaid as red dots.* ***Table****: computed vs experimental g-tensors components.*

References

[1] L. Tacconi et al., J. Am. Chem. Soc. 147, 33040-33051 (2025).

[2] S. Cotton et al., Coord. Chem. Rev. 340, 220-231 (2017).

[3] C. Bigelli et al., Manuscript in preparation.

Abstract ID: 30718

QUANTUM MONTE CARLO STUDY OF THE CYLINDRICAL BOUNDARY CONDITIONS IN THE TWO-DIMENSIONAL HUBBARD MODEL

N. Bulut

Department of Physics, Izmir Institute of Technology, 34530, Urla, Izmir, TURKEY

We use finite-temperature Quantum Monte Carlo (QMC) simulations to study the effects of the cylindrical boundary condition on the spin and charge correlations of the two-dimensional (2D) Hubbard model with nearest and next-nearest neighbor hopping parameters. In particular, we calculate the spin and charge correlation functions and susceptibilities in addition to the local electronic density on various 2D clusters, where in one direction open boundary conditions are used while the other direction has periodic boundary conditions. We present results on the doping, temperature and spatial dependence of the spin and charge correlations. These results give information on how the cylindrical boundary conditions influence the interplay of the spin and charge fluctuations in the 2D Hubbard model.

Abstract ID: 30836

EFFECT OF THE CRYSTAL LATTICE PARAMETER ON THE CRITICAL SUPERCONDUCTING TRANSITION TEMPERATURE IN Pd_2YSn: ab INITIO CALCULATIONS

M. Matyunina, V. Sokolovskiy, V. Buchelnikov

Chelyabinsk State University, 454001, Bratiev Kashirinykh 129, Chelyabinsk, RUSSIA

Based on experimental data on the lattice parameter (a^{exp}) and critical temperature (T_C) of the superconducting transition in the Pd_2YSn alloy [1-3], the electron–phonon interaction $\boldsymbol{\lambda}_{ep}$ was estimated using the McMillan equation [4]. The Debye temperature for various a^{exp} was obtained in the quasi-harmonic Debye approximation using density functional theory implemented in the VASP software package [5, 6]. The exchange-correlation interaction was taken into account in the meta-GGA – SCAN approximation [7]. The simulation was performed for an $L2_1$ (Fm-$3m$) crystal lattice.

Figure 1 shows that the electron–phonon interaction strengthens with increasing lattice parameter. For the theoretically estimated lattice parameter a^{theor}=6.78 Å, the critical temperature is 5.7 K. The obtained result shows that in order to increase the critical temperature in Pd_2YSn alloys, it is advisable to use alloying with atoms with a large radius or the creation of tensile mechanical stresses leading to an increase in the equilibrium lattice parameter.

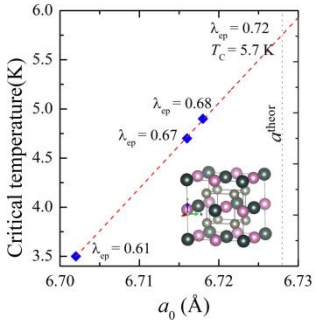

Fig. 1: *Dependence of critical temperature on lattice parameter. The electron-phonon coupling constant ($\boldsymbol{\lambda}_{ep}$) was calculated using the inverted McMillan formula [1].*

This work was supported by the Russian Science Foundation Project No. 25-19-20141 (https://rscf.ru/en/project/25-19-20141/).

References

[1] T. Klimczuk, C. H. Wang, K. Gofryk, *et al.*, Phys. Rev. B. **85 (17)**, 174505 (2012).
[2] J. H. Wernick, G. W. Hull, T. H. Geballe, *et al.*, Mater. Lett. **2 (2)**, 90-92 (1983).
[3] J. L. Jorda, M. Ishikawa, J. Muller. J Less-Common Met. **107,** 321- 330 (1985).
[4] W. L. McMillan, Phys. Rev. **167**, 331 (1968).
[5] G. Kresse, J. Furthmüller, Phys. Rev. B **54**, 11169 (1996).
[5] G. Kresse, D. Joubert. Phys Rev B, **59**, 1758-1775 (1999).
[7] J. Sun, A. Ruzsinszky, J. P. Perdew. Phys. Rev. Lett. **115**, 36402 (2015).

60 - THEORY OF SUPERCONDUCTIVITY

Abstract ID: 30012

PHASE-SPACE THEORY FOR FRACTIONAL ORBITALS AND FLAT BAND SUPERCONDUCTIVITY

T. Das, R. O. Sharma, Y. B. Yogendra

Department of Physics, Indian Institute of Science, Bangalore 560012, INDIA

Whether to be encouraged or not is a fair question: superconductivity has fascinated researchers for more than a century. Recent discoveries of two-dimensional superconductivity are particularly intriguing—not only because they defy traditional theories, but also because they reveal novel physics. Flat-band superconductivity is a striking addition to this landscape, where global condensation of Cooper pairs occurs without fully resembling real-space Bose–Einstein condensation. We develop a phase-space model for correlated electrons tailored for such flat bands, as well as for fractional particles such as Majorana fermions and anyons [1]. In a gauge-field-induced flat-band 2D superconductor with a square-octagon lattice (e.g., $Lu_2Fe_3Si_5$), we show that while superconductivity exhibits global coherence, the particle–hole entangled Bogoliubov orbital symmetry can be deduced from the pairing symmetry. Similarly, $IrTe_2$—a 2D centrosymmetric material with Ising spin–orbit coupling—presents an interesting case where a distinct non-centrosymmetric yet singlet multiband pairing emerges due to phase-space orbital symmetry [2]. If time permits, we will also discuss the application of this method to Majorana orbitals in a Kitaev spin model [3].

References

[1] R. O. Sharma, T. Das, Phys. Rev. B **111**, 214522 (2025).

[2] K. Dutta, R. O. Sharma, T. Das, I. Dasgupta, T. Saha-Dasgupta, Manuscript submitted (2025).

[3] K.B. Yogendra, G. Baskaran, T. Das, Phys Rev. X **15**, 031020 (2025).

Abstract ID: 30264

SUPERCONDUCTIVITY ON THE BRINK OF PHASE SEPARATION

A. Sinha, A. W. Max

Max Planck Institute for the Physics of Complex Systems, GERMANY

Doping a Mott antiferromagnet does not merely introduce carriers; it reorganizes the medium through which those carriers move. In the same parameter regime where superconducting correlations are strongest, the doped charge often refuses to remain uniform, forming stripes and fluctuating mesoscale charge clusters. This raises a mechanism question that is usually evaded rather than answered: when the doped holes self-organize into a nonuniform landscape, where does the macroscopic pairing weight actually live? Here we address this question in the square-lattice t-t'-J model on cylinders using minimally entangled typical thermal states. We diagnose superconductivity through the eigenstructure of a singlet pair reduced density matrix and characterize charge organization through snapshot-resolved hole-cluster statistics. We identify an extended intermediate-temperature regime of forestalled phase separation in which doped charge forms mesoscopic, fluctuating hole-rich backbones without macroscopic segregation. Pairing is strongly enhanced in this window, but not through a single channel: the leading pairing eigenvalues form a multiplet, indicating fragmentation originating at finite temperature. Snapshot eigenmodes and cluster-restricted spectra show that distinct macroscopic pairing channels preferentially reside on different hole-rich clusters, while the hole-poor antiferromagnetic background contributes only weakly. Upon further cooling, these channels progressively lock together as stripe order develops, yielding coherent d-wave superconductivity. Arrested phase separation thus emerges as an organizing principle for finite-temperature superconductivity in a prototypical doped Mott insulator!

Abstract ID: 30522

CHARGE-ENTROPY-STABILIZED SUPERCONDUCTOR (Ag,Sn)Se

M. Oudah

University of British Columbia, CANADA

Entropy in materials can play a role in stabilizing phases above a critical entropy threshold and enhancing material properties through configurational disorder [1,2]. Typically, the focus has been on the contribution of atomic species to the total entropy. Here, we extend this framework by introducing the concept of charge-entropy stabilization in the rocksalt superconductor (Ag,Sn)Se. We expect Sn to exist in a mixed-valent state, fluctuating between Sn^{2+}/Sn^{4+}, for the experimentally realized compositions [3]. We present spectroscopic evidence from HEXPES and Mössbauer measurements confirming the persistence of charge fluctuations down to 4 K, below the superconducting transition temperature [4]. We develop a model based on the mixed valence of Sn, considering the ionic species $Ag^{1+}/Sn^{2+}/Sn^{4+}$, that captures the observed phase stability region. This proposed model may allow for the synthesis of other superconducting rocksalt compounds containing valence-skipping elements.

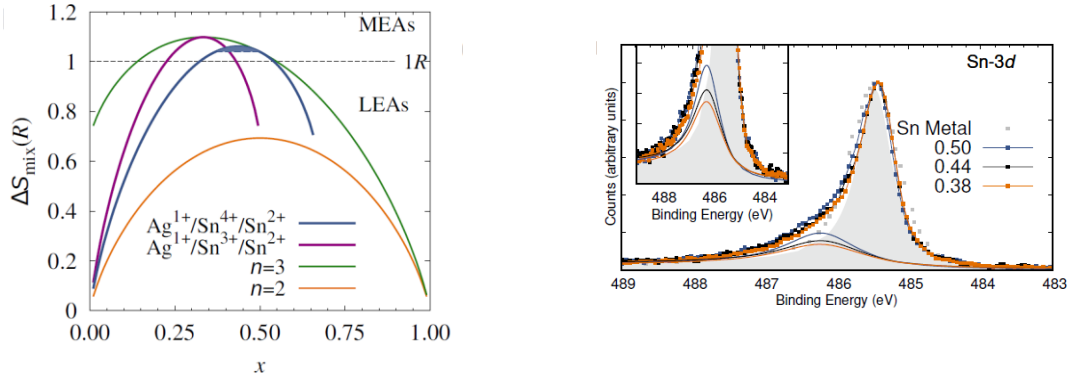

(a) **(b)**

Fig. 1: *(a) The entropy of mixing ΔS_{mix} for different numbers of components, n = 2, 3, sharing the same site as a function x for a single component with all other components being equal. The mixing ΔS_{mix} considering the charge entropy as a function of x for the case of $Sn^{2+}/Sn^{4+}/Ag^{+1}$ and $Sn^{2+}/Sn^{3+}/Ag^{+1}$ are shown for comparison. (b) The hard x-ray photoemission spectra of the Sn-3$d_{5/2}$ in $Ag_xSn_{1-x}Se$, highlighting a broad peak at higher energy.*

References

[1] S. Schweidler, *et al.*, Nat. Rev. Mater. **9**, 266-281 (2024).
[2] S. S. Aamlid, M. Oudah, *et al.*, JACS **145.11**, 5991-6006 (2023).
[3] A. Wold, and R. Brec., Mater. Res. Bull. **11**, 761 (1976).
[4] M. Oudah, *et al.*, Commun. Mater. **6.1**, 58 (2025).

Abstract ID: 30065

HOURGLASS STRUCTURE OF THE SPECTRAL WEIGHT OF THE MAGNON IN THE FL* APPROACH TO HOLE-DOPED CUPRATES

P.A. Marchetti[1,2]

[1] *Dipartimento di Fisica e Astronomia, Università di Padova, Padova, ITALY*
[2] *INFN, Sezione di Padova, Padova, ITALY*

Using the terminology of [1] we denote by FL* an exotic Fermi liquid that satisfies a version adapted to the topological order of Luttinger's theorem, in which, in addition to the standard electrons (or rather holes for hole-doped cuprates) carrying charge and spin, the excitations of the quasiparticles are the holons carrying only charge and the spinons carrying only spin. The hole and the magnon are then bound states, or in general resonances, consisting of a holon and a spinon the former and a spinon and an antispinon the latter. We apply the FL* formalism developed in ref. [2] based on a 2D *t-t'-J* model expressed in terms of gapped spinons (gap $m_s \approx J\,(1-2\delta)(\,\delta\,|Log\,\delta|)^{1/2}$) and gapless holons, to the superconducting region of the doping-temperature phase diagram below the "pseudogap phase" of hole-doped cuprates. There we show the appearance of the magnon as a spinon-antispinon resonance whose spectral weight exhibits an hourglass structure, qualitatively in agreement with neutron experiments [3], as a consequence of a finite density of RVB spinon pairs and a slave-particle gauge attraction between unpaired spinons and antispinons [4].

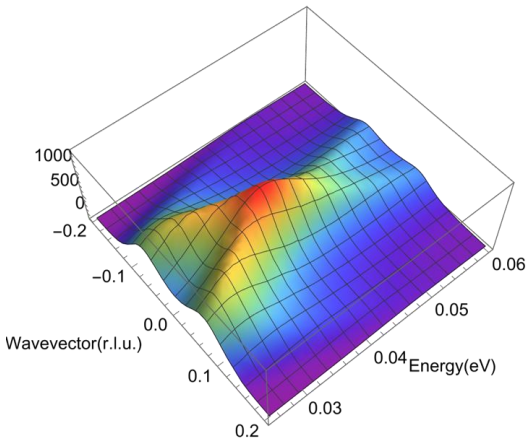

Fig. 1: *Calculated spectral weight of the magnon for doping δ=0.12 and T=5K; the wavevector is measured from the antiferromagnetic point.*

References

[1] T. Senthil, S. Sachdev and M. Vojta, Phys. Rev. Lett. **90**, 216403 (2003); A.Paramekanti and A.Vishwanath, Phys. Rev. B **70**, 245118 (2004).

[2] P.A. Marchetti, *et al.*, Phys. Rev. B **84**, 214525 (2011); **100**, 035103 (2019); P.A. Marchetti, Condens. Matter **5**, 12 (2020); **9**, 9 (2024).

[3] V. Hinkov, *et al.*, Nat. Phys. **3**, 780 (2007); B. Fauquè, *et al.*, Phys. Rev. B **76**, 214512 (2007); G. Xu, *et al.*, Nat. Phys. **5**, 642 (2009).

[4] P.A. Marchetti, paper submitted to J. Supercond. Nov. Magn. (2025).

Abstract ID: 30424

MASS OF POLARON IN Hg-1201 CUPRATE

G. G. Saburova, B. Ya. Yavidov

Nukus State Pedagogical Institute named after Ajiniyaz, 230105 Nukus, UZBEKISTAN

We have studied the dependence of the mass of charge carrier (CC) on the hole doping level (p) in Hg-1201 cuprate superconductor (SC). In doing so we rely on the bipolaronic mechanism (BpM) of HTSC [1]. BpM-HTSC has shown itself as a model capable of explaining various properties of HTSC [2] and there is much evidence showing that CC in the cuprates are (bi)polarons, too [3]. According to BpM-HTSC, the Bose-liquid of bipolarons undergoes superfluidity (and thus superconductivity) at some critical temperature (CT) T_s. (which is the CT of superconductivity, i.e. $T_c = T_s$). One can roughly estimate T_c putting it equal to Bose-Einstein condensation (BEC) temperature (T_{BEC}) of an ideal gas of bipolarons: $T_{BEC} = 3.31\hbar^2 n^{2/3}/2k_B m_p$, where m_p is three dimensional (3D) polaron's mass and n is density of bipolarons n which is expressed through the number of holes (p) per unit cell of YBCO as: $n = p/2V_a$, where V_a is a volume of unit cell of Hg-1201. Taking the experimental values of T_c and V_a at different p one can calculate the mass of 3D polaron. Further, we used the formulas $m_p = m_{p,ab}^{2/3} m_{p,c}^{1/3}$ and $\gamma_m = m_{p,c}/m_{p,ab}$ in order to extract CuO_2 or *ab*-plane polaron's mass $m_{p,ab}$ from m_p, taking into account the experimental mass anisotropy factor γ_m, which itself is p dependent. Calculated values of $m_{p,ab}$ is presented in Fig.1 as a function of p.

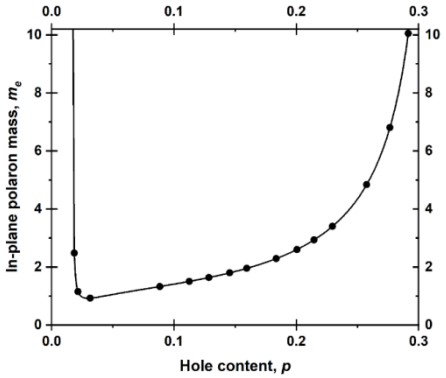

Fig. 1: *Doping dependence of $m_{p,ab}$ in Hg-1201 (in units of free electron mass, m_e).*

At present, a study is underway to compare theoretical results with experimental data.

References

[1] A.S. Alexandrov, Theory of Superconductivity (IOP Publishing Ltd., Bristol, 2003).
[2] A. Bussmann-Holder, H. Keller, Condens. Matter **7**, 10 (2022).
[3] K.A. Müller, J. Supercond. Novel Magn. **30**, 3007 (2017).

Abstract ID: 30435

A TWO-SCALE POLARONIC FRAMEWORK FOR THE MAGNETIC FIELD-DOPING PHASE DIAGRAM OF CUPRATES

O. K. Ganiev[1,2]

[1] *Institute of Nuclear Physics, 100214, Tashkent, UZBEKISTAN*
[2] *National University of Uzbekistan, 100174, Tashkent, UZBEKISTAN*

Despite decades of intensive research, the mechanism underlying high-temperature superconductivity in the cuprates remains one of the most significant and debated problems in condensed matter physics [1,2]. A central and enigmatic feature of these materials is the pseudogap (PG) phase, which coexists and competes with superconductivity in the underdoped region of the phase diagram [3]. While the temperature-doping ($T-p$) phase diagram is well-documented, the magnetic field-doping ($H-p$) plane offers crucial complementary insights into the fundamental energy scales governing the system. Experimental investigations of the $H-p$ phase diagram reveal a characteristic dome-shaped upper critical field, $H_{c2}(p)$, which peaks at a similar optimal doping level as the superconducting transition temperature, T_c [4,5]. Moreover, quasiparticle tunneling experiments have shown that a gap-like feature persists not only above T_c in the PG regime but also at low temperatures within the cores of magnetic vortices where superconductivity is locally suppressed [2,6]. This strongly suggests that the energy gap associated with pair formation is distinct from the energy scale for long-range phase coherence.

In this work, we present a theoretical framework for the magnetic field-hole doping ($H-p$) phase diagram of cuprate superconductors. The theory is based on a two-scale polaronic model that distinguishes the high-energy formation of polarons, which sets the pseudogap energy scale Δ_p, from the low-energy phase coherence of polaron pairs, which determines T_c. We show that these two distinct energy scales generate two fundamental, independent length scales that govern the response of the system to an applied magnetic field. Our framework quantitatively reproduces the characteristic dome of $H_{c2}(p)$ as a direct consequence of the doping-dependent phase coherence. Furthermore, we identify a significantly higher magnetic field, $H^*(p)$, corresponding to the breaking of pre-formed pairs. This upper field terminates at a pseudogap quantum critical point (QCP), where Coulomb repulsion ultimately unbinds the pairs. The theoretical predictions for both the superconducting coherence length $\xi_c(p)$ and the upper critical field $H_{c2}(p)$ show excellent quantitative agreement with experimental thermodynamic data for the $La_{2-x}Sr_xCuO_4$ system, without the need for any free fitting parameters.

References

[1] J. Tallon and J. Loram, Physica C: Superconductivity **349**, 53 (2001).
[2] O. Fischer, *et al.*, Rev. Mod. Phys. **79**, 353 (2007).
[3] M. Hashimoto, *et al.*, Nature Physics **10**, 483 (2014).
[4] G. Grissonnanche, *et al.*, Nat. Commun. **5**, 3280 (2014).
[5] Y. Wang and H.-H. Wen, Europhysics Letters **81**, 57007 (2008).
[6] S. H. Pan, *et al.*, Phys. Rev. Lett. **85**, 1536 (2000).

Abstract ID: 30462

A NEW VISION FOR THE THEORY OF SUPERCONDUCTIVITY (SC) AND PHASE DIAGRAM (PD) IN HTSC LBCO AND YBCO

Bassam M. Mustafa

Retired from Mosul University, IRAQ

The following topics are included in this study;

1.) The discovery of high-temperature superconductivity (HTSC) in 1986 in LBCO and YBCO and the opening a new era in the history of physics and science.

2.) Brief review of the efforts of the huge former researches and four decades of time with no consensus on a theoretical model to describe SC and PD in HTSC cuprates.

3.) Crystal structure of LBCO and YBCO and symmetry effects and the way for a new vision of a theory for SC in LBCO and YBCO.

4.) Abnormalities uncover secrets of HTSC.

5.) Formulations of theoretical models for application of symmetry principles on LBCO and YBCO: The statistical and the matrix models which leads to calculations of theoretical value of the coherence length CL in LBCO and YBCO starting from first essential elements of crystal structure to give a microscopic derivation of the essential parameter of SC that is the CL.

6.) Main features of theory of SC in LBCO and YBCO:

- **a)** SC will not started unless distance between dopants equals CL.
- **b)** Phase coherence (PC) linked with CL So PC controls start of superconductivity.
- **c)** SC includes three main stages: Parring of charge carriers during hole doping instant, condensation of charged pairs to low energy levels and phase coherence which occurs due to interaction between YBCO crystals doped with holes.
- **d)** Charge pairing and phase coherence are independent.
- **e)** Doping occurs in steps due to crystal symmetry effect and phase coherence this leads to formation of different phases in the phase diagram which represent the great puzzle for former theories of HTSC in cuprates.

7) On this basis builds: Models for phase diagram, charged strips, charge pairing which explains main features of HTSC in LBCO and YBCO cuprates.

Abstract ID: 30783

EXACT SOLUTION TO THE LINEAR GINZBURG--LANDAU EQUATION FOR A SINGLE-BAND TYPE-II SUPERCONDUCTOR CONFINED INTO THE THIN FILM STRUCTURE

E. I. Jafarov[1,2], A. M. Jafarova[1], I. N. Askerzade[1,3,4]

[1] Institute of Physics, Ministry of Science and Education, Javid av. 131, AZ1143, Baku, AZERBAIJAN
[2] Baku State University, Z. Khalilov str. 33, AZ1148, Baku, AZERBAIJAN
[3] Department of Computer Engineering and Center of Excellence of Superconductivity Research, Ankara University, Ankara, 06100, TURKEY
[4] Center for Theoretical Physics, Khazar University, 41 Mehseti Street, Baku, AZ1096, AZERBAIJAN

We solve exactly the linear Ginzburg-Landau equation for a single-band bulk superconductor confined to a thin film structure. In order to achieve a confinement effect, we replace the constant mass with an effective mass varying with position. We revisited a seminal problem of a model of the semi-infinite superconductor type-II with the vacuum or insulator if $x<0$, surface at the value of the position $x=0$, and superconductor if $x>0$ and managed to break the isotropic behavior of the bulk superconductor through the semiconfinement effect. We show that the obtained macroscopic order parameter of the type-II superconducting condensate is expressed via the Laguerre polynomials. Here, one observes first signatures of the anisotropy in y and z directions through the analytical expression of the quadratic Landau coefficient. Next, we restrict the superconductor from both sides to the symmetric thin film. The macroscopic order parameter is now expressed via the Jacobi polynomials. We also obtain a generalized symmetric expression of the quadratic Landau coefficient, which exhibits strong dependence on the kinetic energy y and z components. Finally, we break a symmetric confinement again and show that under such a generalized case, the quadratic Landau coefficient dependence on the kinetic energy y and z components drastically changes according to the sharply varying asymmetric confinement profile. We presented the relations, that connect the surface and bulk critical fields.

References

[1] D. Saint-James, P. G. Gennes, *Onset of superconductivity in decreasing fields*, Physics Letters **7**, 306-308 (1963).

Abstract ID: 30785

EXACT SOLUTION TO THE GINZBURG-LANDAU EQUATION FOR A SINGLE-BAND SUPERCONDUCTOR FULLY CONFINED INTO THE CYLINDRICAL THIN FILM STRUCTURE

A. M. Jafarova[1], E. I. Jafarov[1,2], I. N. Askerzade[1,3,4]

[1] Institute of Physics, Ministry of Science and Education, Javid av. 131, AZ1143, Baku, AZERBAIJAN
[2] Baku State University, Z. Khalilov str. 33, AZ1148, Baku, AZERBAIJAN
[3] Department of Computer Engineering and Center of Excellence of Superconductivity Research, Ankara University, Ankara, 06100, TURKEY
[4] Center for Theoretical Physics, Khazar University, 41 Mehseti Street, Baku, AZ1096, AZERBAIJAN

We generalized an exact solution of the linear Ginzburg-Landau equation for a single-band bulk superconductor to the case, when a superconductor becomes full confined to the cylindrical thin film structure with an anisotropic nature. In order to achieve a full radial confinement effect and anisotropic nature, we replaced the constant mass with an effective mass changing with position. We introduced a symmetric gauge in order to preserve exact result for case of the thin film of the cylindrical form. We show that the obtained macroscopic order parameter of the type-II superconducting condensate is expressed via the Laguerre polynomials. We presented some basic relations, which connect the surface and bulk critical fields under the change of the newly introduced anisotropy parameter. We also discussed some limit and special cases, when constructed cylindrical thin film recovers its bulk analogues.

61 - TOPOLOGICAL QUANTUM PHYSICS AND MATERIALS

Abstract ID: 30430

ANALYTICAL APPROACHES TO TIGHT-BINDING POLARONS IN FINITE-WIDTH CONDUCTION BANDS

S. N. Klimin[1], J. Tempere[1], M. Houtput[1], S. Ragni[2], T. Hahn[2], C. Franchini[2], A. S. Mishchenko[3]

[1] *Theorie van Kwantumsystemen en Complexe Systemen (TQC), Universiteit Antwerpen, BELGIUM*
[2] *Computational Materials Physics, University of Vienna, AUSTRIA*
[3] *Institute of Physics, Zagreb, CROATIA*

Polaron theory, initially of primarily mathematical interest [1], has since become relevant to a wide range of physically important problems, including superconductivity [2] and spintronics [3].

We study the polaron problem in a tight-binding conduction band with both linear and quadratic electron–phonon couplings, using several complementary analytical approaches [4, 5].

Approximations adapted to tight-binding polarons exhibit nontrivial and, in some cases, unexpected behavior compared to their continuum counterparts with parabolic dispersion. Notably, the Lee-Low-Pines canonical transformations method, originally formulated for the continuum Fröhlich polaron and commonly associated with weak coupling, provides an accurate description across the full range of coupling strengths in a finite-width conduction band, capturing both weak- and strong-coupling limits.

A central result of this work is the extension of the Feynman variational approach to polarons with non-parabolic dispersion in finite-width bands. The resulting theory shows excellent agreement with Diagrammatic Monte Carlo data [3, 6], with an accuracy comparable to – and in certain parameter regimes exceeding – that of the Momentum Average approximation and its systematic extensions [3].

The developed methods are applied to a single-band tight-binding polaron as well as to a polaron in the presence of Rashba spin-orbit coupling.

References

[1] R. P. Feynman, *Statistical Mechanics* (Reading, Mass., W. A. Benjamin, 1972).
[2] I. Zappacosta, M. Houtput, and J. Tempere, Phys. Rev. B **111**, 214525 (2025).
[3] L. Covaci, and M. Berciu, Phys. Rev. Lett. **102**, 186403 (2009).
[4] S. N. Klimin, J. Tempere, M. Houtput, S. Ragni, T. Hahn, C. Franchini, and A. S. Mishchenko, Phys. Rev. B **110**, 075107 (2024).
[5] S. N. Klimin, J. Tempere, M. Houtput, S. Ragni, T. Hahn, C. Franchini, and A. S. Mishchenko (*to be published*)
[6] M. Berciu, and G. L. Goodvin, Phys. Rev. B **76**, 165109 (2007).

Abstract ID: 30675

SUPERINSULATION, A NEW STATE OF MATTER REALIZING CONFINEMENT IN CONDENSED MATTER SYSTEMS

C. A. Trugenberger[1,2]

[1] *Division of Science, New Yok University, Abu Dhabi, UAE*
[2] *SwissScientific, rue du Rhone 59, CH-1204 Geneva, SWITZERLAND*

I will present the discovery on which I had the privilege to collaborate with Valerii Vinokur in the last ten years. His brilliance, insights and expertise will be thoroughly missed

Superinsulation is the realization of confinement in condensed matter systems, with Cooper pairs playing the role of quarks. It is the dual state to superconductivity, in which an infinite resistance (even at finite temperatures) is due to the formation of electric flux tubes between charges, which implies a linear confining potential giving rise to electric pions as fundamental excitations. I will review the theory and the numerous experimental measurements of this new state of matter.

Abstract ID: 30821

CONTROLLING AND SCALING-UP THE ENERGIES IN CUPRATE SUPERCONDUCTING QUANTUM TECHNOLOGIES

N. Poccia

Leibniz Institute for Solid State and Materials Research (IFW-Dresden), Dresden GERMANY

High temperature superconducting complex oxides ($La_{2-x}Sr_xCuO_4$, $YBa_2Cu_3O_{7-x}$, $Bi_2Sr_2CaCu_2O_{8+x}$) are complex quantum materials where dominant states are not spatially homogeneous [1]. The quantum state [2] lives in a heterogeneous landscape of "puddles" [3], correlated to a complex phase diagram [4]. Some of the interest in these materials now centers less on nitrogen-range T_c: and is progressively less motivated by achieving higher superconducting critical temperatures than before, but more on controlling this unparalleled and still-mysterious electronic state. Four decades of materials progress have clarified both limitations and enormous potential of these superconducting quantum materials, including their dominant d-wave order nature from grain-boundary junctions [5] and interference experiments [6], flourishing in an early attempt to demonstrate macroscopic quantum tunneling and energy level quantization in bicrystal grain-boundary $YBa_2Cu_3O_{7-x}$ junctions [7]. However, the characteristic voltage parameter of cuprate Josephson junctions, I_cR_n, remained for long-time in the low values of 0.5–2 mV, hindering their potential in the second quantum revolution. Based on recent material science breakthrough with cryogenic stacking technologies [8], it was measured a forward jump to 20–25 mV in a comparable twist-angle junction, using $Bi_2Sr_2CaCu_2O_{8+x}$ crystals and a wide d-wave angular dependence was observed. I will therefore discuss our understanding of the intrinsic fragility of these systems, the intrinsic new phenomenology discovered both electronically, optically, and the electrical engineering challenges that we are addressing [9] for potential superconducting quantum technologies [10].

References

[1] E. Dagotto,. *Complexity in Strongly Correlated Electronic Systems*, Science **309.5732**, 257-262 (2005).
[2] E. Fradkin, *et al.*, *Nematic Fermi Fluids in Condensed Matter Ph*ysics, Annu. Rev. Condens. Matter Phys. **1.1**, 153-178 (2010).
[3] M. Fratini, *et al.*, *Scale-Free Structural Organization of Oxygen Interstitials in La_2CuO_{4+y}*, Nature **466**, 841-844 (2010).
[4] B. Keimer, *et al.*, *From Quantum Matter to High-Temperature Superconductivity in Copper Oxides*, Nature **518.7538**, 179-186 (2015).
[5] H. Hilgenkamp, J. Mannhart, *Grain Boundaries in High-T_c Superconductors*, Reviews of Modern Physics **74.2**, 485 (2002).
[6] D. J. Van Harlingen, *Phase-Sensitive Tests of The Symmetry of The Pairing State in The High-Temperature Superconductors—Evidence for dx2− y2 Symmetry*, Reviews of Modern Physics **67.2**, 515 (1995).
[7] T. Bauch, *et al.*, *Quantum Dynamics of A d-Wave Josephson Junction*, Science **311.5757**, 57-60(2006).
[8] S. Y. F. Zhao, *et al.*, *Time-Reversal Symmetry Breaking Superconductivity Between Twisted Cuprate Superconductors*, Science **382**, 1422-1427 (2023).
[9] T. Confalone, *et al.*, *Preserving the Josephson Coupling of Twisted Cuprate Junctions via Tailored Silicon Nitride Circuits Boards*, Small (2025).
[10] T. Confalone, *et al.*, *Cuprate Twistronics for Quantum Hardware*, Advanced Quantum Technologies 2500203 (2025).

Abstract ID: 30823

PHOTOCURRENT AND PHOTOCONDUCTIVITY IN SUPERINSULATORS

A.Y. Mironov

A.V. Rzhanov Institute of Semiconductor Physics, 630090 Novosibirsk, RUSSIA

We present results of investigation of transport properties of NbTiN films and nanostructures 7-10 nm thick in presence of scattered visible light (with wavelengths from 457 to 850 nm). We found that this radiation leads to the appearance of measurable photocurrent both in superinsulating and insulating state. Also, the threshold voltage of superinsulating state decreases with increasing of light power. The increase in disorder degrees leads to a decrease in the observed photocurrent (see Fig. 1). We found that increasing the light power leads to a transition from non-ohmic to ohmic conductivity, like the Berezinskii–Kosterlitz–Thouless (BKT) transition. Unlike the temperature BKT transition, the photoinduced transition occurs at a nonzero threshold voltage, meaning it is not associated with direct heating of the structure by laser radiation. We note that irradiation of a three-dimensional superinsulators leads to an enhancement of the BKT transition, i.e., to an increase in the exponent of the current-voltage dependences. We attribute this behavior to a decrease in the effective thickness of the superinsulating region under the influence of radiation and, correspondingly, to a transition from a three-dimensional to a two-dimensional superinsulator.

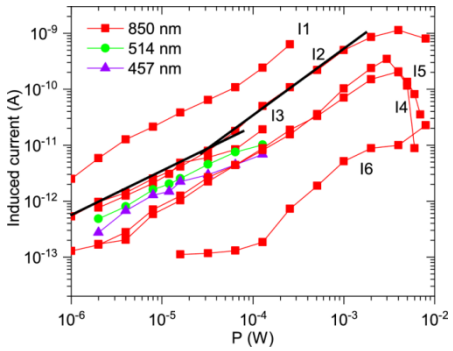

Fig. 1: *Evolution of the current induced by pulses of scattered visible laser radiation with increasing disorder from I1 to I6 [1].*

References

[1] A. Mironov, V. Vinokur, Sci. Rep. **15**, 41074 (2025).

Abstract ID: 30835

TYPE-III SUPERCONDUCTIVITY: VORTICES, TOPOLOGY AND QUANTUM MATTER

M. C. Diamantini[1], C. A. Trugenberger[2], V. M. Vinokur[3]

[1] *NiPS Laboratory, INFN and Dipartimento di Fisica e Geologia, University of Perugia, via A. Pascoli, I-06100 Perugia, ITALY*
[2] *SwissScientific Technologies SA, rue du Rhone 59, CH-1204 Geneva, SWITZERLAND*
[3] *Terra Quantum AG, Kornhausstrasse 25, CH-9000 St. Gallen, SWITZERLAND*

Superconductivity is conventionally understood in terms of symmetry breaking and the Anderson–Higgs mechanism. However, in strongly inhomogeneous systems this paradigm breaks down, and global superconductivity cannot be described by a local order parameter. In this talk demonstrate that novel type-III superconductivity, realized in granular media in any dimension, hosts a novel vortex physics.

Type-III superconductivity is characterized by coreless vortices, topological mass generation, and the absence of a conventional Higgs mechanism, and Ginzburg-Landau theory must be replaced by a topological gauge theory. The superconducting transition is driven by vortex proliferation rather than pair breaking, extending the Berezinskii–Kosterlitz–Thouless scenario to higher dimensions.

This perspective, developed in collaboration with Valerii Vinokur, emphasizes the central role of topology and vortex physics in shaping quantum phases of matter beyond the traditional paradigm.

References

[1] M. C. Diamantini, C. A. Trugenberger and V. M. Vinokur Frontiers in Physics 10:909310 (2022).

62 - UNCONVENTIONAL SUPERCONDUCTIVITY AND TUNABLE QUANTUM STATES

Abstract ID: 30106

FROM MONOLAYERS TO BULK: ISING SUPERCONDUCTIVITY IN LAYERED SYSTEMS

T. Samuely[1], M. Gmitra[1,2], P. Samuely[2]

[1] *Centre of Low Temperature Physics, Faculty of Science, Pavol Jozef Šafárik University in Košice, 04001 Košice, SLOVAKIA*
[2] *Centre of Low Temperature Physics, Institute of Experimental Physics, Slovak Academy of Sciences, 04001 Košice, SLOVAKIA*

Low-dimensional materials exhibit properties absent in bulk systems, such as Ising superconductivity in monolayer 1H-$NbSe_2$, where spin-orbit locking enables in-plane critical fields far beyond the Pauli limit. Ising superconductivity is particularly intriguing because it creates conditions for nontrivial band topology, offering a route to topological superconductivity. However, the instability of 2D materials limits practical use. We demonstrate that bulk heterostructures – $NbSe_2$ mono- and bilayers intercalated with spacer monolayers – preserve a 2D electronic structure and exhibit Ising superconductivity with in-plane critical fields up to ten times the Pauli limit [1]. Combining structural characterization, magnetotransport measurements, and ab initio calculations, we extract band parameters revealing reduced interlayer coupling and strong spin–orbit splitting, clarifying the microscopic origin of Ising superconductivity in bulk compounds [2]. Furthermore, using the 4Ha-$NbSe_2$ polytype as a case study, we show that broken inversion symmetry alone can sustain Ising protection in bulk without intercalation [3].

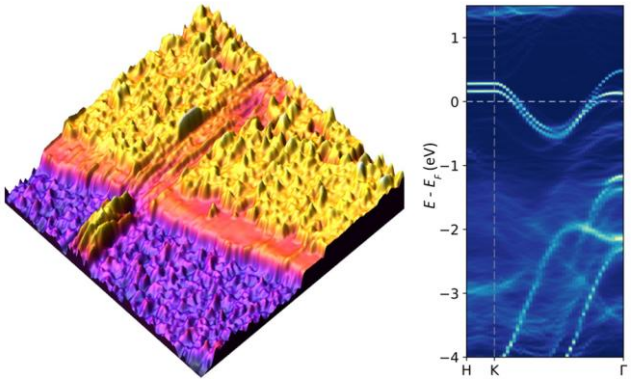

Fig. 1: *Left – Scanning tunneling micrograph (60 × 60 nm²) of atomic steps on the surface of $(LaSe)_{1.14}NbSe_2$. After cleavage, the surface is unstable due to strong bonding between the layers. Right – calculated band structure of $(LaSe)_{1.14}NbSe_2$ [2].*

References

[1] P. Samuely, *et al.*, Phys. Rev. B **104**, 224507 (2021).

[2] T. Samuely, *et al.*, Phys. Rev. B **108**, L220501 (2023).

[3] D. Volavka, *et al.*, e-print arXiv: 2501.08867 (2025).

Abstract ID: 30107

DISCOVERY OF NODAL-LINE SUPERCONDUCTIVITY IN CHIRAL CRYSTALS

T. Shiroka[1,2], J. Zhao[3], L.-H. Hu[4], K. Xia[5], M. O. Ajeesh[6], M. Nicklas[6], Y. Xu[5], Q. Zhan[5], D. J. Gawryluk[2], M. Shi[4], T. Shang[5]

[1] *Laboratorium für Festkörperphysik, ETH Zürich, 8093 Zurich, SWITZERLAND*
[2] *PSI Center for Neutron and Muon Sciences CNM, 5232 Villigen PSI, SWITZERLAND*
[3] *Department of Physics, School of Science, Tianjin University, Tianjin 300354, CHINA*
[4] *Center for Correlated Matter, Zhejiang University, Hangzhou 310058, CHINA*
[5] *School of Physics, East China Normal University, Shanghai 200241, CHINA*
[6] *Max Planck Institute for Chemical Physics of Solids, 01187 Dresden, GERMANY*

Structural handedness is a key feature of chiral crystals, known to host exotic quantum phenomena driven by the interplay of band topology, spin-orbit coupling (SOC), and electronic correlations. Due to the limited availability of suitable chiral-crystal materials, their unconventional superconductivity (SC) has remained mostly unexplored. Here, we report the discovery of unconventional SC in the La(Rh,Ir)Si family of materials by combining muon-spin spectroscopy, band-structure calculations, and perturbation theory. This family, characterized by a double-helix chiral structure, hosts exotic multifold fermions that are absent in other topological chiral crystals. While LaRhSi behaves as a fully gapped superconductor, the substitution of 4*d*-Rh by 5*d*-Ir significantly enhances the SOC and leads to the emergence of topological nodal-line SC in LaIrSi. Our newly developed model shows that the nodal-line SC arises from an isotropic SOC with a specific strength. Such an exotic mechanism extends our conventional understanding of material candidates for unconventional SC, which typically rely on a significantly anisotropic SOC to promote the triplet pairing. The current work establishes a new type of phase diagram, which provides a comprehensive roadmap for identifying and engineering unconventional superconductivity in chiral crystals.

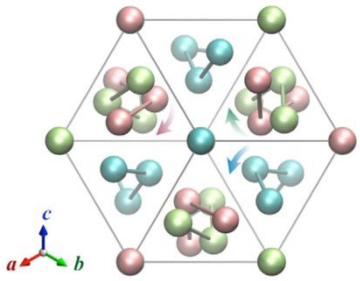

Fig. 1: *Illustration of the chiral crystal structure of La(Rh,Ir)Si. The double-helix arrangements are clearly visible in the top view along the [111]-direction.*

References

[1] P. Narang, C. A. C. Garcia, and C. Felser, Nat. Mater. **20**, 293 (2021).

[2] T. Shang et al., Adv. Matter e11385 (2025).

[3] T. Shang, T. Shiroka, Front. Phys. **9**, 270 (2021).

Abstract ID: 30605

IMPACT OF LOW-ENERGY SPIN FLUCTUATIONS ON THE STRANGE METAL IN A CUPRATE SUPERCONDUCTOR

D. J. Campbell[1], M. Frachet[1], V. Oliviero[1], T. Kurosawa[2], N. Momono[3], M. Oda[2], J. Chang[4], D. Vignolles[1], C. Proust[1], D. LeBoeuf[1]

[1] *Univ. Grenoble Alpes, INSA Toulouse, Univ. Toulouse Paul Sabatier, EMFL, CNRS, LNCMI, 38000 Grenoble, FRANCE*
[2] *Department of Physics, Hokkaido University, Sapporo 060-0810, JAPAN*
[3] *Muroran Institute of Technology, Muroran 050-8585, JAPAN*
[4] *Department of Physics, University of Zurich, CH-8057 Zurich, SWITZERLAND*

Strange metals – which exhibit unusual properties such as a resistivity that scales linearly with temperature – challenge our understanding of charge transport in metals. Here, we investigate how the strange metal phase of $La_{2-x}Sr_xCuO_4$ is impacted by a field-induced glassy antiferromagnetic state. Using magnetic fields above 80 T, we discover a strong enhancement of the normal state magnetoresistance when entering the antiferromagnetic glass phase. We demonstrate that the spin glass causes insulating-like upturns in the resistivity inside the pseudogap phase, which resolves the origin of the crossover from metal to insulator. In addition, the strange metal phase appears at low temperatures over an extended range of magnetic fields where magnetic moments fluctuate, and disappears when these moments freeze out. We conclude that the transport properties of the strange metal phase are closely linked to low energy magnetic fluctuations that persist at the lowest temperatures [1].

References

[1] D. J. Campbell, *et al.,* Nature Physics **21**, 1759–1764 (2025).

63 - UNCONVENTIONAL SUPERCONDUCTORS AND MAGNETS BASED ON LIGHT ELEMENTS

Abstract ID: 30003

PRESSURE SYNTHESIS OF NEW IMMISCIBLE MATERIALS

E. Svanidze

Max Planck Institute for Chemical Physics of Solids, Dresden, GERMANY

Uranium-based quantum materials have recently entered a renaissance era – evidence of correlated topological states, spin-liquid behavior, hidden order phases, and spin-triplet superconductivity proves that these materials are exceptionally interesting.[1,2] Because of their complex chemistry, many potentially fascinating uranium-based systems are currently entirely beyond the reach of conventional synthesis methods. I will discuss high-pressure, high-temperature synthesis coupled with micro-scale specimen isolation[3-5] – this method allows not only the creation of previously inaccessible materials but also the definitive determination of their crystal structure and physical properties. In particular, we targeted several compounds with structures similar to known uranium-based superconductors. By employing advanced synthesis and characterization techniques, we expand the family of uranium-based quantum systems and deepen our fundamental understanding of them. By characterizing these exceptional materials under extreme conditions, we gain further insights into synthesis optimization, helping to improve chemical composition and thus realize exotic chemistry and physics. To understand the underlying mechanisms of these intriguing phenomena, the nature of 5f-electrons (i.e., localized, itinerant, or both – the so-called "dual" nature) was investigated by applying a combination of experimental and theoretical tools.

References

[1] E. Svanidze, Handbook on the Physics and Chemistry of Rare Earths56, 163–201 (Elsevier B.V., 2019).

[2] E. Svanidze, *et al.*, Journal of the American Chemical Society, 147 (2, 39, 35809 025)

[3] A. Amon, *et al.*, Angew. Chemie -Int. Ed.58, 15928 (2019).

[4] I. Antonyshyn, *et al.*, Angew. Chemie -Int. Ed.59, 11136–11141 (2020).
Y. Shimizu, *et al.*, in preparation (2025)

Abstract ID: 30004

CONTROL OF SUPERCONDUCTIVITY IN UBe_{13} BY ATOMIC-SCALE IMPERFECTIONS

M. König

Max Planck Institute for Chemical Physics of Solids, 01187 Dresden, GERMANY

In many unconventional superconductors, the development of a comprehensive understanding is limited by the presence of imperfections. These can range from impurities on the macroscopic scale down to defects on the atomic level, and all of them can affect the observable physical properties very strongly. And the heavy-fermion superconductor UBe_{13} is no exception, despite it being one of the earliest ones being discovered and decades of intensive research.

We employ state-of-the-art tools to study UBe_{13} and resolve imperfections on the atomic scale. This microscopic investigation of UBe_{13} is complemented by transport studies on single-crystalline micron-scale specimen which were isolated from bulk samples synthesised by conventional methods. The results clearly demonstrate a connection between imperfections on the atomic scale and the emergence of superconductivity in this material. More specifically, we show that details of the defect configuration can significantly alter the superconducting state.

Abstract ID: 30112

ODD-PARITY-WAVE SPIN-POLARIZED MULTIFERROICS

J. Priessnitz[1], L. Šmejkal[1,2,3]

[1] *Max Planck Institute for the Physics of Complex Systems, 01187 Dresden, GERMANY*
[2] *Max Planck Institute for Chemical Physics of Solids, 01187 Dresden, GERMANY*
[3] *Institute of Physics, Czech Academy of Sciences, Cukrovarnická 10, 162 00 Praha 6, CZECH REPUBLIC*

Combining ferroelectricity with spin polarization in ferromagnets is difficult due to the poor compatibility of insulating band structures and ferromagnetism. Recently, an alternative strategy based on combining time-reversal-broken spin polarization in altermagnetic insulators and ferroelectricity into type-I multiferroics was suggested [1]. Here we propose a different strategy based on time-reversal-symmetric odd-parity-wave spin polarization, which we demonstrate in type-II multiferroics induced by noncollinear magnetism [2,3]. Via state-of-the-art spin group theory and first-principle calculations, we demonstrate the spin polarization in $GdMn_2O_5$, a type-II multiferroic material combining coplanar p-wave magnetic order with ferroelectric order. Furthermore, we propose the antialtermagnetoelectric effect - cross-coupling between ferroelectric and odd-parity-wave time-reversal-symmetric spin polarization, with the potential of controlling the spin polarization via electric field.U+0020

References

[1] L. Šmejkal, arXiv:2411.19928.

[2] A. Birk Hellenes, *et al.*, arXiv:2309.01607v3.

[3] A. Chakraborty, *et al.*, Nat Commun **16**, 7270 (2025).

Abstract ID: 30134

RECORD HIGH-TEMPERATURE SUPERCONDUCTIVITY IN HYDRIDES

S. Friedemann

HH Wills Physics Laboratory, University of Bristol, UK

Superconductivity is not restricted to low temperatures! Indeed, transition temperatures up to 260 K (-13 °C) have been demonstrated by multiple groups in H_3S, LaH_{10}, YH_9, at very high pressures [1–3]. This is a success story of both theory and experiment. Theory has mastered significant predictions of new superconductors and has been crucial to guide experimental efforts. Experiments have mastered many technical challenges. Together, these efforts open pathways to realise higher transition temperature at low pressures in the future.

I will present studies of hydride superconductors, where high-energy lattice phonons couple to hydrogen orbitals in structures stabilised at very high pressures only. We have developed methods for in situ synthesis and study of hydrides in diamond-anvil pressures cells at megabar pressures including thin-film methods for electrodes and superconducting samples. We have characterised the clean-limit superconductivity in H_3S and we have discovered the new superconductor La_4H_{23} [4]. We demonstrate superconductivity in thin films of LaH_{10} with a T_c=250 K consistent with bulk LaH_{10} [2,5]. We will present structural information from XRD and discuss stability of hydrides [6].

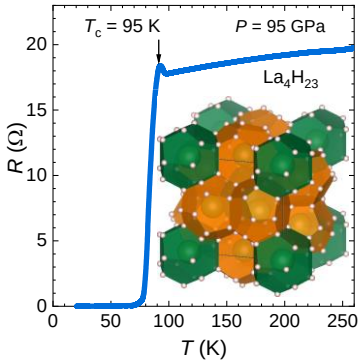

Fig. 1: *Discovery of Superconductivity in La_4H_{23}.*

References

[1] P. Kong, *et al.*, Nature Communications **12**, 5075 (2021).

[2] M. Somayazulu, *et al.*, Phys. Rev. Lett. **122**, 027001 (2019).

[3] A. P. Drozdov, *et al.*, Nature **525**, 73 (2015).

[4] S. Cross, *et al.*, Phys. Rev. B **109**, L020503 (2024).

[5] A. P. Drozdov, *et al.*, Nature **569**, 528–531 (2019).

[6] Y. Zhou, *et al.*, Nature Communications **16**, 1135 (2025).

11th International Conference on Superconductivity and Magnetism ICSM2026
4th International Conference on Quantum Materials and Technologies ICQMT2026
19th April to 26th April, 2026, Ölüdeniz – Fethiye/Muğla, Türkiye
https://icsmforever.org/

Abstract ID: 30216

UNIAXIAL-STRAIN TUNING OF THE METAL-INSULATOR TRANSITION IN κ-(BEDT-TTF)$_2$Cu[N(CN)$_2$]Br

P. Doležal[1,2], T. Pinter[1], K. Boniecki[1], A. Chen[1], R. Saito[3], A. Kawamoto[3], A. Pustogow[1]

[1] *TU Wien, Institute of Solid State Physics, 1040, Vienna, AUSTRIA*
[2] *Charles University, Dep. of Condensed Matter Physics, 121 16, Prague, CZECH REPUBLIC*
[3] *Hokkaido University, Dep. of Physics, Graduate School of Sci., 060-0810, Sapporo, JAPAN*

The organic charge transfer salts are intensely studied compounds for their unique physical properties, in particular the single-band Mott metal-insulator transition and frustrated magnetism. This is the reason why these compounds serve as an experimental playground for the theoretical investigation of Hubbard model on the half-filled triangular lattice of quantum-spin-liquid candidates [1]. The layers of cations and anions with weak bonding create the quasi-2D character and enable large compressibility which allows modification of their physical properties in a large area in the phase diagram. It can be realized by application of hydrostatic or uniaxial pressure or by chemical substitution. While these mechanical properties are advantageous for tuning the physical properties, on the other side the performance of such experiments is very challenging because these compounds are also very brittle. Only very recently the in situ uniaxial-strain tuning of correlations and frustration strength within a single crystal became accessible [2].

Here we report the first controlled tuning of the Mott transition via uniaxial strain on free-standing organic single crystals in a piezoelectric strain cell. This versatile tool enables us to tune through the metal-insulator transition in a quasi-continuous fashion at cryogenic temperatures, as shown in Fig. 1. Due to negative chemical pressure upon substitution of ^{1}H by ^{2}D this compound exhibits Mott-insulating behavior with an antiferromagnetic ground state at ambient pressure [3]. Here, we modified the strength of electronic correlations by uniaxial compression, yielding metallic and superconducting properties (Fig. 1a,b).

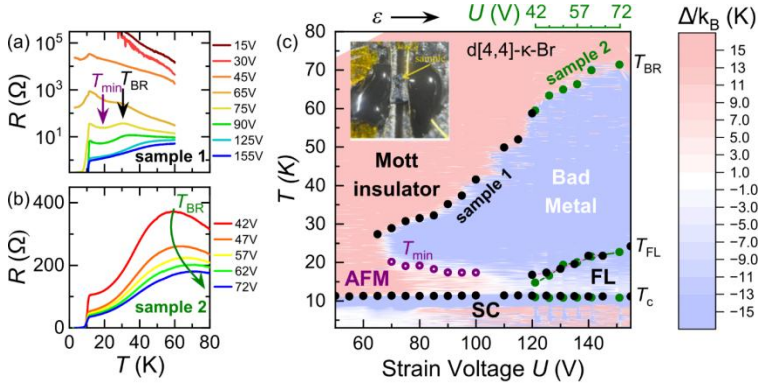

Fig. 1: *a), b) Electrical resistivity of d[4,4]-κ-Br under uniaxial strain. c) The resulting phase diagram.*

References

[1] A. Pustogow, *et al.*, Nat. Mater. **17**, 773-777 (2018).

[2] J. Wang, *et al.*, Phys. Rev. Lett. **131**, 256501 (2023).

[3] H. Ito, *et al.*, J. Phys. Soc. Jpn. **69**, 290-291 (2000).

Abstract ID: 30306

HYDROGEN ABSORPTION IN URANIUM: ACCESSING MAGNETISM VIA THIN-FILM SYNTHESIS

E. Tereshina-Chitrova[1], M. Paukov[2], L. Havela[3], L. Horak[3], F. Wilhelm[4], A. Rogalev[4], T. Gouder[5]

[1] Institute of Physics, Czech Academy of Sciences, Prague, CZECH REPUBLIC
2 Centrum výzkumu Řež, Husinec-Řež, CZECH REPUBLIC
3 Faculty of Mathematics and Physics, Charles University, Prague, CZECH REPUBLIC
4 European Synchrotron Radiation Facility (ESRF), Grenoble, FRANCE
5 European Commission, Joint Research Centre (JRC), Karlsruhe, GERMANY

Hydrogenation of nonmagnetic uranium induces the formation of pyrophoric hydrides such as UH_3, which form readily and host robust ferromagnetism with Curie temperatures (T_C) ~170 K [1,2]. In contrast, the stoichiometric UH_2 phase is metastable and cannot be obtained in bulk form, yet can be stabilized through thin-film growth [3,4]. By tuning the growth conditions, we can reproducibly stabilize different uranium hydride phases, providing controlled access to their structural and magnetic properties [2].

In this work we focus on the comprehensive magnetic characterization of UH_2 thin films prepared by reactive *dc* sputtering using different substrates. X-ray photoelectron spectroscopy confirmed complete hydrogenation. Magnetization and XMCD measurements show ferromagnetic ordering with T_C of 120-130 K and a uranium 5*f* moment of ≈ 0.9 μ_B/U, dominated by the orbital contribution ($\mu_L \approx 1.4\ \mu_B$, $\mu_S \approx -0.5\ \mu_B$), in a good agreement with GGA+U computations [5], which otherwise overestimate absolute values of the spin and orbital components. Our results demonstrate that thin-film synthesis opens pathways toward higher uranium hydrides and interface-engineered actinide systems.

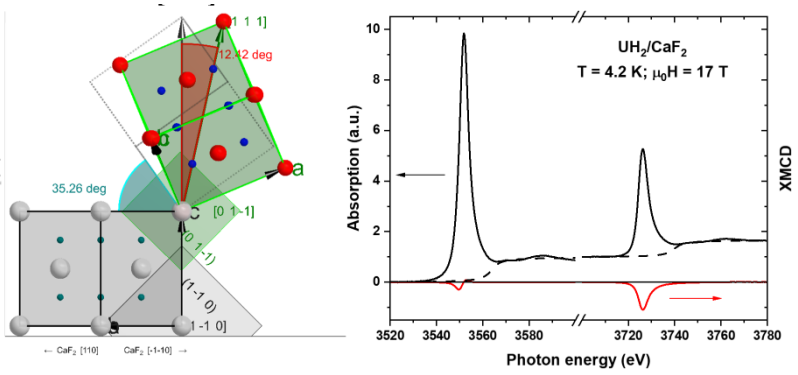

Fig. 1: *(Left) Stabilization of the metastable UH_2 phase on the CaF_2(001) substrate, forming four tilted [111] domains. (Right) XMCD signature of 5f magnetism in UH_2/CaF_2 thin films.*

References

[1] R. Troć, W. Suski, J. Alloys Compd, **219**, 1-5 (1995).

[2] E. Tereshina-Chitrova, *et al.*, Thin Solid Films **775**, 139860 (2023).

[3] L. Havela, *et al.*, Inorg. Chem. **57**, 15033–15043 (2018).

[4] E. Tereshina-Chitrova, *et al.*, arXiv preprint arXiv:2512.07183 (2025).

[5] L. Kyvala, *et al.*, Journal of Nuclear Materials, **567**, 153817 (2022).

Abstract ID: 30310

NODAL SUPERCONDUCTIVITY IN KAGOME FLAKES OBSERVED WITH HYBRID MICROWAVE CIRCUITS

U. Vool

Max Planck Institute for Chemical Physics of Solids, 01187, Dresden, GERMANY

Kagome superconductors have been recently discovered and their electronic structure provides a rich platform to study strongly correlated systems including superconductivity, charge density wave, pair density wave and time reversal symmetry broken states. Their electronic band structures include flat bands, van hove singularities, and Dirac fermions, which are of great importance in studying intriguing electronic properties. Measuring the superconducting pairing symmetry is crucial to understand the interplay between different quantum phases in these materials. Numerous experimental and theoretical attempts to discover the microscopic nature have been mostly conducted in bulk crystals, yet there is no consensus for the structure of the superconducting gap.

Exfoliated van der Waals Kagome flakes show a distinct phase from the bulk material, typically with significantly higher critical temperatures, and are difficult to probe with conventional techniques due to their small size and fragile nature. Superconducting microwave circuits are highly coherent and tunable devices for quantum technology, and in recent years are being used as sensitive probes of novel materials of microscopic size. Here, we investigate the pairing symmetry of van der Waals CsV3Sb5 superconducting flakes by incorporating them into a hybrid superconducting circuit made of thin Nb films. The superfluid density of the flake contributes to the inductive response of the circuit (kinetic inductance), and can be probed by tracking the circuit's resonance frequency. We find that the superfluid density in the material varies linearly with temperature, down to the milliKelvin temperature range, deviating significantly from a conventional fully gapped structure. This linear dependence is a signature of a nodal structure in the pairing symmetry, a hallmark of unconventional superconductivity. These results improve our understanding of the superconducting gap structure in these novel materials, and show that superconducting circuits are sensitive probes for material exploration. Additionally, it shows that quantum properties of unconventional superconductors remain when the material is incorporated in to a device, paving the way to utilizing quantum materials for technological applications.

Abstract ID: 30356

MAGNETIC AND STRUCTURAL PROPERTIES OF $Ce_5Fe_{18}B_{18}$: A PARAMAGNETIC RARE-EARTH IRON BORIDE WITH NON-MAGNETIC Fe

A. A. Aydın[1,2], Ö. Evren[3], M. Krnel[3], Y. Prots[3], E. Svanidze[3], G. J. Snyder[5], U. Aydemir[2,4]

[1] *Koç University, Graduate School of Sciences and Engineering, 34450, Istanbul, TÜRKIYE*
[2] *Koç University Boron and Advanced Materials Application and Research Center (KUBAM), 34450, Istanbul, TÜRKİYE*
[3] *Max-Planck Institute for Chemical Physics of Solids, 01187, Dresden, GERMANY*
[4] *Koç University, Department of Chemistry, 34450, Istanbul, TÜRKİYE*
[5] *Northwestern University, Department of Materials Science and Engineering, 60208, Evanston, Illinois, UNITED STATES*

The ternary Ce-Fe-B system remains vastly understudied compared to its Nd-Fe-B analogue, despite the technological importance of Ce as an abundant and inexpensive rare-earth substituent in permanent magnets. We report a comprehensive study of the $Ce_5Fe_{18}B_{18}$ phase, which has not been investigated since the work of Givord et al. over 40 years ago [1]. Understanding this phase is important since $Ce_5Fe_{18}B_{18}$ is a grain boundary phase in Ce-doped $Nd_2Fe_{14}B$ magnets, which can influence their coercivity and performance.

Polycrystalline $Ce_5Fe_{18}B_{18}$ samples were synthesized via arc melting and characterized using synchrotron X-ray diffraction, SQUID magnetometry (2-800 K) and transport (2-300 K) measurements. $Ce_5Fe_{18}B_{18}$ remains paramagnetic down to 1.8 K with no evidence of bulk magnetic ordering in contrast to isostructural $Nd_5Fe_{18}B_{18}$ which orders ferromagnetically at 14 K [2]. This finding is also confirmed by the absence of any anomaly in resistivity and heat capacity data which show conventional metallic behaviour. Curie-Weiss analysis yields an effective moment consistent with trivalent Ce^{3+}, and lattice parameters obtained from synchrotron XRD refinement follow the expected lanthanide contraction trend across the $RE_5Fe_{18}B_{18}$ series, further confirming the Ce^{3+} valence state. The absence of magnetic ordering despite the presence of magnetic Ce^{3+} ions indicates that Fe atoms in this boron-rich structure carry no moment which can be attributed to Fe 3d hybridization with B 2p states. The suppression of Fe magnetism by the high boron content (44 at.% B) demonstrates how light-element chemistry can fundamentally alter magnetic ground states in rare-earth intermetallics.

References

[1] D. Givord, P. Tenaud, J. M. Moreau, *Modulation of the Iron Tetrahedra Driven by Interactions with R Atoms in $R_{1+\epsilon}Fe_4B_4$ Compounds*, J. Less-Common Met., **115**, L7–L10 (1986).

[2] D. Givord, J. M. Moreau, P. Tenaud, *$Nd_5Fe_{18}B_{18}$ ($Nd_{1.11}Fe_4B_4$), A New Nowotny-Like Phase. Structural and Magnetic Properties*, Solid State Commun., **55**, 303–306 (1985).

Abstract ID: 30570

SYNTHESIS-ENABLED SEARCH FOR NOVEL BORIDE ALTERMAGNETS

K. Kovnir[1,2]

[1] *Department of Chemistry, Iowa State University, Ames, Iowa 50011, USA*
[2] *Ames National Laboratory, U.S. Department of Energy, Ames, Iowa 50011, USA*

Transition-metal borides exhibit rich structural chemistry and a wide range of physical properties. Owing to the chemical inertness of boron, these materials are typically synthesized using high-temperature techniques such as arc melting. Conventional synthesis routes have limited access to borides that undergo peritectic decomposition at moderate temperatures. To overcome these challenges, we developed an iodine-assisted synthesis approach in which boron is chemically activated through B–I bonding, enabling the formation of boride phases at reduced temperatures. This experimental strategy was combined with high-throughput computational screening of multiple boride structure types to identify candidate altermagnetic materials. Focusing on TM_2B_2 compounds (T = 3d and M = 4d/5d transition metals) crystallizing in the $FeMo_2B_2$ structure type, our screening identifies eleven altermagnets. In these materials, Fe or Mn atoms form parallel transition-metal chains with strong ferromagnetic intrachain coupling and antiferromagnetic interchain interactions. As a result, they exhibit momentum-dependent spin splitting of electronic bands characteristic of ferromagnets, while maintaining zero net magnetization, a hallmark of antiferromagnets. Four predicted altermagnets were successfully synthesized, and the magnetic ground-state structure of Mo_2FeB_2 was confirmed by neutron diffraction. Further exploration of metastable borides of refractory metals led to the discovery of a novel metallic d-wave boride altermagnet featuring zigzag Fe chains with ferromagnetic intrachain and antiferromagnetic interchain order. The synthesis, structural characterization, and magnetic properties of altermagnetic borides will be discussed in detail.

Abstract ID: 30752

WIDE-FIELD KERR MICROSCOPY AND MAGNETOMETRY: FROM MAGNETIC IMAGING TO LOCAL HYSTERESIS ANALYSIS

I. Soldatov

Leibniz Institute for Solid State and Materials Research IFW Dresden, Helmholtzstr. 20, 01069 Dresden, GERMANY

The study of magnetic domains is essential for understanding magnetization reversal from both fundamental and application perspectives. Since the 1980s, wide-field Kerr microscopy has become a highly effective tool for imaging magnetic microstructures from macro- down to the nanoscale [1,2]. Here, both fundamental and technical aspects of wide-field Kerr microscopy are considered: basics contrast formation, advanced techniques, including selective sensitivity and a number of *hands-on* examples. Additionally, we will consider the applicability of MOKE magnetometery. Kerr microscopy offers a distinct advantage over traditional focused-beam techniques [1,2]. By recording image intensity over a selected area, it acts as an optical magnetometer that correlates hysteresis loops directly with simultaneous domain imaging [3]. However, local MOKE loops require careful interpretation as they may not represent the bulk material. In soft magnetic in-plane materials, local coercivity varies significantly when the probe size is smaller than the domain size due to local internal fields [4]. Here we consider films with perpendicular anisotropy and we show that local coercivity can deviate by tens of percent from the global value (Fig. 1). Furthermore, we demonstrate the critical role of recording speed.

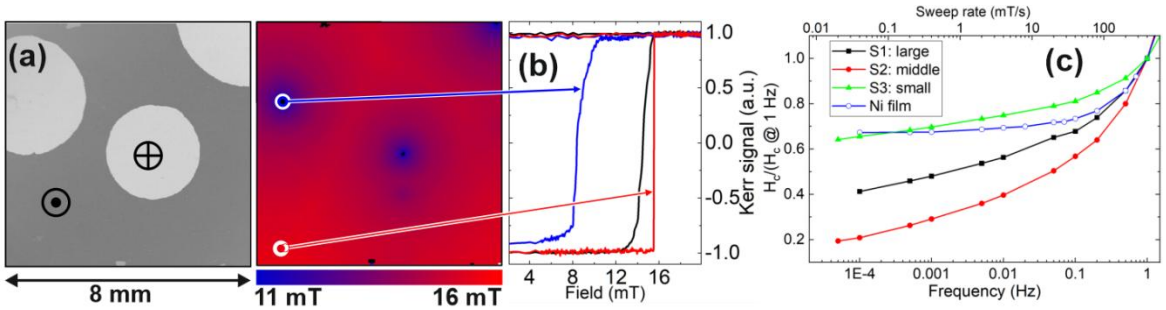

Fig. 1: *(a) Domains in a Co/Pt film during the magnetization reversal. Shown is the whole sample with three nucleation sides. (b) MOKE loops, measured on the whole specimen (black) and at two locations as indicated in the coercivity distribution. (d) The coercivity of the entire sample depends on the measurement speed without any signature of levelling off at very low frequency.*

References

[1] W. Kuch, R. Schäfer, P. Fischer and F. Hillebrecht, Magnetic Microscopy of Layered Structures, Berlin Heidelberg: Springer (2015).
[2] I. V. Soldatov and R. Schäfer, Rev. Scientifi c Instrum., **vol. 88**, **no. 7** (2017).
[3] I. Soldatov, P. Andrei and R. Schäfer, IEEE Magn. Lett., **11**, 1 (2020).
[4] I. Soldatov and R. Schäfer, J. Appl. Phys., **122**, 153906 (2017).

64 - VORTEX MATTER, DYNAMICS AND PINNING

Abstract ID: 30209

VORTEX DYNAMICS IN SUPERCONDUCTING MICROWAVE COPLANAR RESONATORS: ROLE OF NATIVE AND ARTIFICIAL PINNING CENTERS

G. Ghigo[1,2], M. Fracasso[1,2], R. Gerbaldo[1,2], L. Gozzelino[1,2], D. Torsello[1,2], C. Pira[3], M. Scuderi[4]

[1] *Department of Applied Science and Technology, Politecnico di Torino, ITALY*
[2] *Istituto Nazionale di Fisica Nucleare, Sezione di Torino, ITALY*
[3] *INFN Laboratori Nazionali di Legnaro, ITALY*
[4] *CNR-IMM, Catania, ITALY*

We report on vortex dynamics and microwave properties of superconducting films, investigated for both fundamental and application-oriented purposes by means of a coplanar waveguide resonator (CPWR) technique, with the CPWR obtained from the films themselves through suitable patterning [1].

In this presentation, an overview is given of recent results obtained by means of the CPWR technique, concerning the determination of the main high-frequency vortex parameters of NbTi [2,3], Nb_3Sn [4] and YBCO [4,5] films, in terms of depinning/crossover frequency, vortex viscosity, pinning constant and creep factor. The role of native and artificial pinning centers in determining and modifying the vortex dynamics was investigated. As for the artificial defects, we considered those produced by ion irradiation, ranging from 1.5 MeV protons to 250-MeV Au ions, to 1.2-GeV Pb ions, with the aim to investigate the role of the qualitatively different defects (as for dimensions and morphology) produced by these ions in modulating the behavior and the performance of superconducting materials.

A particular emphasis is given to the systematic investigation of the effects of heavy-ion-induced columnar defects in YBCO films [5]. The study encompasses their structural characterization and their impact on the vortex-pinning parameters. These parameters are analyzed and discussed within the theoretical frameworks proposed by Gittleman–Rosenblum, Coffey–Clem, and Blatter et al. Overall, columnar defects were found to enhance the pinning efficiency and, consequently, the critical current density j_c and its ratio to the depairing current density, j_c/j_0. To determine their absolute values, a comparative analysis was carried out by combining the results from different experimental techniques with a theoretical treatment of j_c/j_0 as a function of the column radius. All results converge into a consistent framework, yielding $j_c(5\ \mathrm{K}, 1\ \mathrm{T}) = 8.8 \cdot 10^{11}\ \mathrm{Am}^{-2}$ and $j_c/j_0 = 0.34$ for the YBCO film with irradiation-induced columnar defects.

Acknowledgements

This study was partially supported by INFN CSN5 under the experiments SAMARA and SuperMAD.

References

[1] G. Ghigo and D. Torsello, *Microwave Analysis of Unconventional Superconductors with Coplanar-Resonator Techniques*, Springer (2022).

[2] G. Ghigo, *et al.*, Sci. Rep. **13**, 9315 (2023).

[3] G. Ghigo, *et al.*, Results in Physics **57**, 107437 (2024).

[4] G. Ghigo, *et al.*, Superconductivity **13**, 100149 (2025).

[5] G. Ghigo, *et al.*, submitted.

Abstract ID: 30289

IRREVERSIBILITY FIELD REVISITED: WHEN STRUCTURAL INHOMOGENEITY, NOT VORTEX MELTING, SETS THE LIMIT

V. V. Guryev, S. V. Shavkin

NRC Kurchatov institute, 123182, Moscow, RUSSIA

The irreversibility field (Hirr) has long been interpreted as the boundary where thermal fluctuations destroy effective vortex pinning, causing the vortex matter to "melt" into a dissipative liquid. This vortex-centric view underpins most modern analyses of practical superconductors, especially high-temperature coated conductors. However, growing experimental evidence—particularly from two-dimensional current–voltage (2D-CVC) measurements [1]—challenges this paradigm.

In Nb-Ti and REBCO-based practical superconductors alike, the magnetic irreversibility field consistently falls well below the onset of resistive transition. So in commercial REBCO coated conductors magnetization hysteresis collapses at $\mu_0 H_{irr} \approx 2.7$ T (77 K, H ∥ n), while zero resistance persists up to ~ 6.4 T—a value that aligns with the suppression of diamagnetism and thus with the upper critical field (Hc2). This wide intermediate regime (2.7–6.4 T) exhibits zero resistance and diamagnetism, yet displays fully reversible magnetization, implying the absence of vortex pinning. Crucially, 2D-CVC data on Nb-Ti tapes reveal that above Hirr, the electric field is no longer orthogonal to the magnetic induction—a signature that the magnetic flux is no longer quantized into vortices.

These findings point toward a unified explanation based on macroscopic inhomogeneity rather than vortex dynamics [2]. In materials with $\delta\ell$-pinning (e.g., cold-worked Nb-Ti or REBCO tapes), regions with locally enhanced Hc2—such as grain boundaries or strain-induced defects—remain superconducting well above the average Hirr. The resistive onset thus reflects percolation through these pathways, not the loss of pinning.

We argue that the irreversibility field in practical superconductors should be reinterpreted not as a phase transition of vortex matter, but as the field above which macroscopic current-carrying homogeneity breaks down. This new interpretation resolves long-standing discrepancies between magnetic and transport characterizations and cautions against using resistive onset as a proxy for Hirr.

The study was supported by grant No. 25-72-10037 from the Russian Science Foundation.

References

[1] E.Y. Klimenko, S.V. Shavkin, P.V. Volkov Phys. Met. Metallogr., **92**, 6, 552-556 (2001).

[2] V.V. Guryev, S.V. Shavkin, V.S. Kruglov J. Phys.: Conf. Ser., **1697**, 012202 (2020).

Abstract ID: 30478

QUANTUM PRINTING AND OPTICALLY INDUCED VORTICITY IN SUPERCONDUCTORS

T.-T. Yeh[1], H. Yerzhakov[2], L. Bishop-Van Horn[3], S. Raghu[3], E. Wilson[1], M. Fogelström[2,4], A. Balatsky[1,2]

[1] *Department of Physics, University of Connecticut, Storrs, Connecticut 06269, USA*
[2] *Nordita, Stockholm University and KTH Royal Institute of Technology, SE-10691 Stockholm, SWEDEN*
[3] *Department of Physics, Stanford University, Stanford, California, USA*
[4] *Department of Microtechnology and Nanoscience MC2, Chalmers University of Technology, SE-41296 Goteborg, SWEDEN*

Questions of controlling quantum states of matter with light have been at the forefront of research on driven and nonequilibrium phases. In superconductors, vortices play a central role in determining macroscopic coherence and dissipation, yet their generation and dynamics are traditionally governed by thermal fluctuations or applied magnetic fields.

Here we introduce quantum printing, a framework in which structured light imprints optical quantum numbers and phase textures directly onto a superconducting condensate, enabling non-thermal and non-magnetic control of vortex matter [1-3]. Using Laguerre-Gaussian beams carrying orbital angular momentum, we demonstrate optical generation and steering of vortex-antivortex configurations from an initially homogeneous superconducting state. Beyond controlled imprinting, we show that light-induced vortex states exhibit current-assisted confinement-deconfinement dynamics, revealing a non-thermal two-dimensional vortex phase diagram [4].

Our results establish quantum printing as a versatile platform for engineering topological excitations and nonequilibrium phases in superconductors.

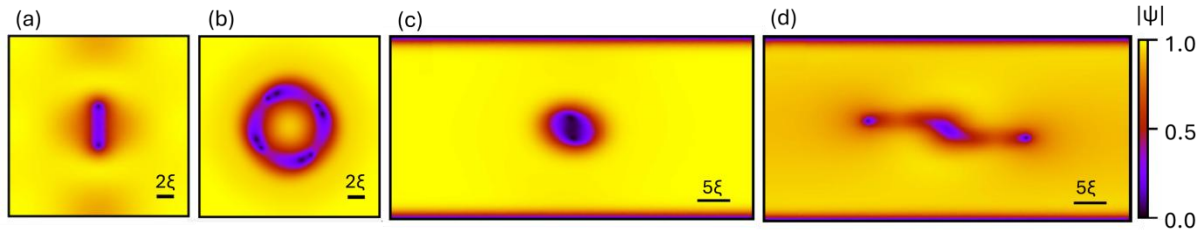

Fig. 1: *Snapshots of the superconducting order parameter showing vortices induced by (a) linearly polarized light and (b) an LG beam carrying spin and orbital angular momentum. (c,d) Vortex confinement–deconfinement states under varying optical fluence and applied current.*

References

[1] G. Aeppli, A. Balatsky, *et al.*, e-print arXiv: 2509.16792 (2025).
[2] T.-T. Yeh, H. Yerzhakov, *et al.*, Phys. Rev. Research **7**, 043111 (2025).
[3] T.-T. Yeh, H. Yerzhakov, *et al.*, Phys. Rev. Research **7**, 043112 (2025).
[4] T.-T. Yeh, E. Wilson, *et al.*, e-print arXiv: 2510.22645 (2025).

Abstract ID: 30563

VORTEX PHYSICS IN FeSe EXPLORED BY MEASUREMENTS OF THE MICROWAVE SURFACE IMPEDANCE, AND PERSPECTIVES FOR FeSe-COATED HALOSCOPES

A. Alimenti[1,2], G. Celentano[3], A. Magalotti[1,2], A. Mancini[3], A. Masi[3], N. Pompeo[1,2], E. Silva[1,2], K. Torokhtii[1], A. Vannozzi[3]

[1] *Dept. of Industrial, Electronic, Mechanical Engineering, University Roma Tre, Roma, ITALY*
[2] *INFN Sezione di Roma Tre, Roma, ITALY*
[3] *ENEA-Frascati, ITALY*

The search for cold intergalactic dark matter found important perspectives in the development of microwave haloscopes [1], basically microwave resonant cavities operating in high dc magnetic fields ($\mu_0 H$ ~ 10 T) to favor the interaction of an axion (dark matter particle) with virtual photons to generate a microwave photon [2]. Suitable superconductors are actively investigated to enhance the quality factor Q of haloscopes. FeSe is a potentially interesting candidate, in view of its simple phase and possible direct electrodeposition on large and curved internal walls of the haloscopes. However, little is known of its microwave surface impedance in dc magnetic fields (that dictates the losses, whence Q).

We present preliminary measurements of the microwave surface impedance $Z = R + iX$ in FeSe thin films [3]. Films of thickness ~80 nm were grown on CaF_2 substrates by Pulsed Laser Deposition. Structure and surface morphology were checked with X-ray diffraction and Atomic Force Microscopy.

We experimentally investigate the surface resistance R and reactance X at 8 GHz in magnetic fields up to 12 T of the obtained films, using a rutile-loaded dielectric resonator from 4.4 K up to T_c = 10 K. We estimate the main vortex parameters, such as the flux-flow resistivity ρ_{ff}, the pinning constant (Labusch parameter) k, and the characteristic frequency ν_c as a function of the applied magnetic field. By extracting the vortex viscosity, we also provide an estimate of the vortex core quasiparticles energy spectrum density, indicating a moderately clean regime.

Finally, with the measured vortex parameters, we give a broad estimate of the possible range for the main figures of merit (scan rate, power, signal-to-noise ratio) of a potential microwave haloscope [4], and we compare the results to previous estimates for other superconductors.

Work partially supported by MIUR-PRIN project IronMOON, Grant No.2022BPJL2L, and INFN-CSN5 project "SuperMAD".

References

[1] P. Sikivie, Phys. Rev. D **32**, 2988 (1985).
[2] Y. K. Semertzidis and S. Youn, Science Advances **8**, eabm9928 (2022).
[3] A. Magalotti, *et al.*, arXiv:2510.15537 [cond-mat.supr-con] (2025).
[4] A. Alimenti, *et al.*, Instruments **6**, 1 (2022).

Abstract ID: 30793

ANGULAR-DEPENDENT INTERTYPE DOMAIN IN ANISOTROPIC SUPERCONDUCTORS: FROM SCALING TRANSFORMATIONS TO EXPERIMENTAL SIGNATURES IN ZrB_{12}

T. T. Saraiva

Moscow Institute of Electronics and Mathematics, HSE University, 101000, Moscow, RUSSIA

The classification of superconductors into type-I and type-II, governed by the Ginzburg-Landau parameter $\kappa = \lambda/\xi$, becomes remarkably rich in the vicinity of the critical Bogomolnyi point $\kappa_0 = 1/\sqrt{2}$. Below the critical temperature, this point unfolds into a finite intertype (IT) domain where exotic vortex configurations and non-standard magnetic responses emerge, transcending the conventional dichotomy. While this scenario is well-established for isotropic materials, anisotropic superconductors present a fundamental challenge: the direction-dependent coherence and penetration lengths seemingly preclude the spatial matching required for self-duality.

In this work, we demonstrate that anisotropic superconductors nevertheless follow the same type-interchange scenario, governed by the Bogomolnyi point of an effective isotropic model obtained through a systematic scaling transformation. Extending the Klemm-Clem formalism, we develop a three-step transformation procedure that maps the anisotropic Extended Ginzburg-Landau free energy with an arbitrarily oriented magnetic field onto an isotropic form. The transformation comprises: (i) anisotropic coordinate scaling to eliminate mass anisotropy in gradient terms, (ii) a rotation aligning the scaled magnetic field with the principal axis, and (iii) a final isotropic scaling that yields an effective GL parameter $\tilde{\kappa}(\theta, \varphi) = \kappa_0 n(\theta, \varphi)$, where $n(\theta, \varphi)$ encapsulates the angular dependence through the effective mass tensor.

Using this mapping, we derive explicit expressions for the upper and lower boundaries of the IT domain for arbitrary field orientation:

$$\kappa^*_{min/max}(\theta, \varphi, T) = [1 + (A + B)\tau] / \left(\sqrt{2}\, n(\theta, \varphi)\right) \quad (1)$$

with universal constants $A = -0.407$, $B = 0.681$ and $\tau = 1 - T/T_c$. For uniaxial anisotropy $(m_x = m_y \neq m_z)$, $n(\theta) = \sqrt{(\sin^2\theta + \varepsilon \cos^2\theta)}$ with $\varepsilon = m_z/m_x$.

Our theoretical framework is applied to the cubic boride superconductor ZrB_{12} ($T_c \approx 5.85$ K, $\kappa_0 \approx 0.65$), recently identified as a promising IT candidate. Analysis of recent directional point-contact Andreev reflection spectroscopy and anisotropic susceptibility measurements [Datta et al., PRB 105, 094504 (2022)] reveals that the superconductivity type in ZrB_{12} is intrinsically angle-dependent: type-I behavior emerges for fields along the high-symmetry z-axis, while type-II characteristics appear for in-plane orientations. This angular dichotomy arises from the material's anisotropic effective masses ($\varepsilon \approx 0.8$–0.9), placing it near the IT boundary. The observed two-fold symmetry in angular-dependent susceptibility and the distinct vortex core signatures along different crystallographic directions are quantitatively reproduced by our model.

Our results establish that the intertype domain in anisotropic superconductors is not merely a temperature-dependent phenomenon but exhibits rich angular structure, offering new opportunities for controlled manipulation of vortex matter through field orientation. The scaling transformation approach provides a unified framework for predicting these effects in a wide class of anisotropic superconducting materials.

65 - POSTER SESSION

Abstract ID: 30000

TAILORING THE CONDUCTIVITY OF PARTICLE EMBEDDED NANOFIBERS FOR ENERGY STORAGE DEVICES

U. Fatima, W. Mehmood, M. Anis-ur-Rehman

Rawalpindi Women University, 6th Road Satellite Town Rawalpindi, PAKISTAN

Supercapacitors and other energy storage devices have garnered a lot of interest because of their high-power density, extended cycle life. The separator in the supercapacitor plays crucial part guarantees effective ion transport through the electrolyte in addition to preventing electrical short circuits between electrodes. For optimal device performance, a separator should have excellent electrolyte wettability, mechanical strength, and chemical stability. Electrospinning was used to create poly (vinylidene fluoride) (PVDF) nanofibers, and varying quantities of graphene oxide (GO) were added to the PVDF solution to adjust the separator properties. Structural and morphological characterizations were performed using X-ray diffraction (XRD) to investigate crystallinity, Fourier-transform infrared spectroscopy (FTIR) to establish chemical interactions and scanning electron microscopy (SEM) to assess fiber shape and GO dispersion. AC impedance analysis was used to assess electrochemical performance, namely dielectric characteristics, conductivity, and charge transfer resistance. The results showed that the addition of GO improved surface wettability, electrolyte absorption, and ionic conductivity. The modified PVDF/GO separator showed higher capacitance than pristine PVDF, indicating its potential for high-performance supercapacitor applications.

Abstract ID: 30006

NEW Ti-RICH HIGH-ENTROPY SUPERCONDUCTOR $Ti_{0.4}Zr_{0.2}(NbTaHf)_{0.4}$ WITH HIGH CRITICAL PARAMETERS

W. Idziak, P. Sobota

Institute of Experimental Physics, University of Wrocław, 50204, Wrocław, POLAND

High-entropy alloys (HEA) are the solid solutions of at least five elements mixed in non-negligible proportions, of more than 5 at.% of each element. They have recently gained significant attention in the field of material science and condensed matter physics, due to their unique mechanical properties, including well-defined structures, thermal stability, and potential in various applications, such as multifunctional superconducting wires.

Among the HEA superconductors the family of titanium rich materials shows great promise for the future applications as it exhibits high critical parameters - especially the upper critical field [1] comparable with those of commercial Nb-Ti binary alloys.

We present investigation into the superconductivity in new Ti-rich high-entropy alloy, $Ti_{0.4}Zr_{0.2}(NbTaHf)_{0.4}$. The sample was synthesized using conventional arc melting under Ti-gettered Ar atmosphere. Its crystal structure, morphology and compositional analysis were investigated by X-ray diffraction (XRD) and scanning electron microscopy combined with energy-dispersive X-ray spectroscopy (SEM-EDXS). The superconducting state was characterized by magnetic measurements (susceptibility, magnetization) as well as electrical resistivity and specific heat measurements down to 1.8 K. The results show that the alloy investigated has a critical temperature $T_c \sim 6$K and the value of the upper critical field is over 12 T.

References

[1] P. Sobota, *et al.*, Acta Materialia **Vol.285, 120666** (2024).

Abstract ID: 30030

DESIGN AND CHARACTERIZATION OF A HIGH-PERFORMANCE MAGNETIC TORQUE ROD WITH AN ANNEALED Ni-Fe ALLOY CORE

B. Tuncay[1,2], M. D. Topal[3], Y. E. Duran[4], Y. S. Çalışkan[4], Y. M. Demiral[4], K. A. Kardaş[4], M. A. Yiğit[4], F. Hıraman[4]

[1] TÜBİTAK National Metrology Institute (UME), 41470, Kocaeli, TÜRKIYE
[2] Yıldız Technical University, Dept. of Physics, 34220, Istanbul, TÜRKIYE
[3] Ankara Private Tevfik Fikret Schools, 06800 , Ankara , TÜRKIYE
[4] TÜBİTAK Science High School, 41400 , Kocaeli , TÜRKIYE

Magnetic torque rods are essential actuators used in satellite attitude control systems to counteract external torques affecting the orbit and to precisely control the spacecraft's position and orientation [1], [2]. Especially for systems with constrained size, weight, and power budgets, the magnetic moment to the current ratio of the actuator is critical importance. In the present work a high-permeability Nickel-Iron alloy was selected as the core material [3] to achieve the goals of targeted magnetic moment and low remanence (residual magnetism). Furthermore, the properties of the material were enhanced by annealing process at elevated temperatures as high as ~1000 °C to optimize its magnetic permeability and coercivity. The work also covers critical design approaches such as optimum coil geometry [4] and winding. Experimental results demonstrate that the prototype torque rod successfully generates the maximum magnetic moment under nominal operating conditions while consuming optimal power. These results confirm a remarkable performance increase, scaling the magnetic moment from a previous benchmark of 10 A.m² up to 300 A.m². The presented design and the obtained data show the suitability of special magnetic materials for satellite simulations

For future missions requiring high control authority, thus opening doors for new technological discoveries.

References

[1] J. R. Wertz, *Spacecraft Attitude Determination and Control* (Kluwer Academic Publishers, Dordrecht, 1978).

[2] B. J. Pokines and L. M. L. H. Slager, *A high-performance magnetic torque rod*, J. Spacecr. Rockets **34**, 2, pp. 200-205 (1997).

[3] R. M. Bozorth, *Ferromagnetism* (D. Van Nostrand, New York, 1951).

[4] M. Fakhari, M. N. Mirshams, and S. H. R. Haji, *Design and Manufacturing of a Research Magnetic Torquer Rod*, Contemporary Engineering Sciences **3**, 7, pp. 309 , (2010).

Abstract ID: 30054

SINGLE CRYSTAL GROWTH, MAGNETIC AND ELECTRIC PROPERTIES OF $Eu_5Sn_2As_6$

D. Kumar[1], R. Kalaivanan[2], R. Sankar[2], I. P. Muthuselvam[1,3]

[1] *Department of Physics, Banaras Hindu University, Uttar Pradesh-221005, INDIA*
[2] *Institute of Physics, Academia Sinica, Taipei 10617, TAIWAN*
[3] *Department of Physics & Astrophysics, University of Delhi, Delhi-110007, INDIA*

High-quality single crystal of $Eu_5Sn_2As_6$ were synthesized via the self-flux method, yielding a well-ordered orthorhombic crystal structure. Temperature-dependent magnetic susceptibility χ(T) measurements identify it as a canted antiferromagnet below 10.04 K. Both χ(T) and specific heat capacity CP(T) evident for two distinct phase transitions at low temperatures for magnetic fields (H) applied along H ‖ ac and H ‖ b. The Curie-Weiss analysis at a high-temperature paramagnetic range exhibits a positive Weiss constant, suggesting ferromagnetic interactions. The entropy and magnetic contributions are quantified from CP(T) data. Electrical resistivity ρ(T) measurement reveals a metal-to-insulator transition observed just below room temperature (RT) with a narrow activation energy of 66.2 meV. Further studies, including neutron scattering, magnetoresistance are suggested to examine the behavior of this complex two-phase magnetic system in greater detail.

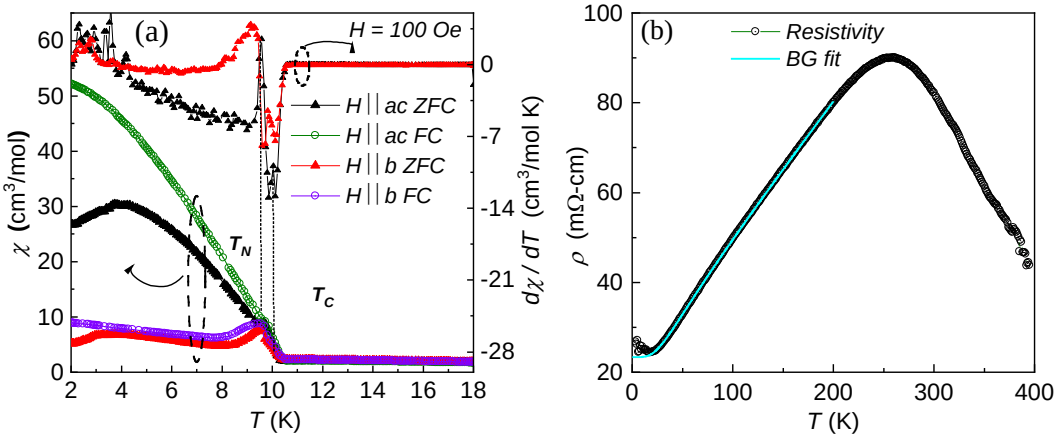

Fig. 1: *(a) Temperature-dependent magnetic susceptibility (χ) of $Eu_5Sn_2As_6$ at 100 Oe with Field-cool(FC) and Zero Field-cool(ZFC) data for both the direction H ‖ ac and H ‖ b including derivative of susceptibility (dχ/ dT) vs T on right y-axis, respectively. T_c and T_N represent the Curie Temperature and Neel Temperature. (b) Electrical resistivity (ρ) as a function of temperature at zero Field from 2 to 400 K, here, Bloch Gruneisen (BG) model(electron-phonon interaction) fitting is shown in metallic region (Cyan color).*

Abstract ID: 30057

HALL EFFECT IN $(MnSe)_{1-x}(Tm_{0.76}Se)_x$

A. M. Kharkov, D. A. Shakhbazian, R. V. Runov

Reshetnev Siberian State University of Science and Technology, Krasnoyarsk, RUSSIA

The Hall effect in nonstoichiometric compounds $(MnSe)_{1-x}(Tm_{0.76}Se)_x$ with concentrations x = 0.05, 0.1 and 0.2 in the temperature range of 100–500 K was studied. These compounds are of practical importance in the development of new materials for spintronics [1]. The temperature dependences of the electrical resistance (Fig. 1, a) and the Hall constant (Fig. 1, b) were constructed. The influence of nonstoichiometric conditions on the change in the sign of current carriers with temperature and concentration was established.

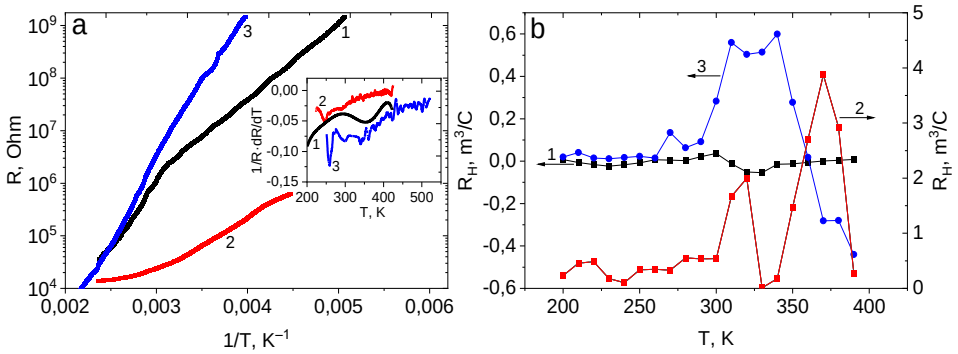

Fig. 1: *Temperature dependence of resistance (a) at H = 0 kOe and temperature dependence of the Hall constant (b) for $(MnSe)_{1-x}(Tm_{0.76}Se)_x$ with x = 0.05 (1), 0.1 (2), 0.2 (3). Inset: temperature coefficient of resistance 1/R·dR/dT for $(MnSe)_{1-x}(Tm_{0.76}Se)_x$ with x = 0.05 (1), 0.1 (2), 0.2 (3).*

In Fig. 1, a shows the temperature dependences of resistance for x = 0.05, it is described by a linear dependence with an activation energy of 0.28 eV below 330 K and 0.39 eV in the range of 375–420 K. The temperature coefficient of resistance 1/R·dR/dT (inset) has an extremum at T = 355 K. In the temperature ranges of 200–250 K and 310–370 K, the contribution of electrons to conductivity predominates, while in the range of 250–310 K and above 370 K, conductivity is due to holes.

For x = 0.1, the temperature dependence of resistance is not described by an exponential function. Resistance increases sharply at 248 K upon cooling, and 1/R·dR/dT has an extremum caused by the minimum mobility and maximum hole concentration. The current carriers are holes, since the Hall constant is positive.

As the thulium ion concentration increases, the resistance decreases upon heating for x = 0.2, and 1/R·dR/dT reaches an extreme value at 260 K, caused by a decrease in hole concentration and an order-of-magnitude increase in mobility. The Hall constant changes sign at 360 K. Nonstoichiometry results in multiple conduction channels with different types of current and energy carriers [2].

References

[1] S.S. Aplesnin, et. al., J. All. Comp. **1010**, 177925 (2025).

[2] S.S. Aplesnin, et. al., J. Sol. St. Chem. **346**, 125284 (2025).

Abstract ID: 30061

ENHANCING LEGAL INTERPRETATION THROUGH QUANTUM-INSPIRED PROBABILITY MODELING: A HYBRID LLM APPROACH

C. Aydın

Istanbul University, Management Information Systems, 34452, Istanbul, TURKEY

"Ontological indeterminacy," in which several legitimate interpretations of a statute or contract coexist until a judgment is issued, is a common occurrence in legal interpretation. Due to their reliance on deterministic probability distributions, classical large language models (LLMs) frequently fail to accurately capture this superposition of meanings, which causes them to prematurely collapse into a single output. In order to characterize and overcome such interpretive difficulties in computational law, this work presents a novel algorithmic framework influenced by quantum mechanics. Using complex probability amplitudes to encode evidentiary weight and the phase (φ) to encapsulate jurisprudential philosophies (e.g., Formalism vs. Purposivism), we represent competing legal interpretations as qubits in a superposition state $|\psi\rangle = \alpha|A\rangle + \beta\, e^{i\phi}\, |B\rangle$ [1].

The proposed framework integrates density matrix formalism and entanglement entropy to model non-local correlations between interconnected legal rules, treating them as entangled quantum systems [2]. We have developed a Python-based extraction and feedback architecture that utilizes amplitude amplification algorithms (Grover-like iterations) to refine LLM outputs. This quantum-probabilistic approach achieves a lower Von Neumann entropy compared to classical Shannon entropy ($S_{vN}<S_{Shannon}$), mathematically proving that the model captures the coherence between conflicting interpretations, according to preliminary experiments simulating ambiguous legal scenarios. By bridging the gap between natural language processing and quantum mechanical formalism, this hybrid architecture provides a reliable way to improve the accuracy and consistency of automated legal reasoning.

References

[1] N. Godfrey, *Toward a quantum-inspired framework for legal reasoning*, Quantum Economics and Finance, **1**, 138-187 (2024).

[2] N. Godfrey and T. Sichelman, *Legal entanglement*, SSRN Electronic Journal (2025).

Abstract ID: 30066

TUNING OF SECOND ORDER PHASE TRANSITION OF NiMnGa HEUSLER-TYPE GLASS-COATED MICROWIRES

C. Garcia[1], V. Zhukova[2], P. Corte-Leon[2], S. Shevyrtalov[3], A. Zhukov[4,5]

[1] *Universidad Técnica Federico Santa María, Dpto. de Física, 1680, Valparaiso, CHILE*
[2] *University of Basque Country (EHU), 20018, San Sebastian, SPAIN*
[3] *Immanuel Kant Baltic Federal University, 236041, Kaliningrad, RUSSIAN FEDERATION*
[4] *IKERBASQUE, Basque Foundation for Science, 48011, Bilbao, SPAIN*
[5] *University of Basque Country EIG, EHU, Dept. Appl. Phys., 20018, San Sebastian, SPAIN*

Various Heusler alloys can present magnetocaloric effect (MCE), ferromagnetic shape-memory effect, half-metallic behaviour, and even superconductivity [1]. The conventional preparation method of Heusler alloys is arc-melting, followed by long high temperature annealing [1,2]. However, the use of conventional methods for the preparation of thin Heusler-type materials is limited by poor mechanical properties and complex processing of Heusler alloys [2]. Therefore rapidly quenching technique opens a new opportunity for the preparation of low dimensional Heusler-type alloys, such as thin ribbons and wires [3]. The origin of high MCE effect of Heusler alloys is usually related to the first-order phase transition. Although the magnetization change is more abrupt for first-order phase transitions, the magnetic hysteresis that appears in some materials may reduce the actual efficiency of the cooling process. Therefore, studies of the materials exhibiting the second-order phase transitions with a broader peak in the magnetic entropy change have attracted attention [4]. Usually, the second-order phase transition temperature can be tailored by the chemical composition of the alloy [4]. We present our last results on the tuning of the second-order phase transitions in Heusler-type NiMnGa glass—coated microwires by annealing. NiMnGa glass-coated microwires, with a metallic nucleus diameter from 10 up to 21 μm, have been prepared using Taylor-Ulitovsky method [3]. We annealed the microwires at temperatures ranging from 550 up to 750 ^{o}C. Annealed samples present ferromagnetic behaviour and second-order phase transition at nearly room temperatures. Additionally, both temperature dependence of magnetization, *M(T)*, as well as the corresponding Curie temperature, T_c, are considerably affected by the annealing conditions (annealing temperature and duration). Mixing of glass-coated microwires annealed at different conditions allows tuning of *M(T)* dependence and hence obtain broader second-order phase transition. As discussed elsewhere [4] such expanding the temperature range over which a significant magnetic entropy change can be obtained is beneficial for the improvement of the refrigerant capacity.

References

[1] T. Graf, S.S.P. Parkin, C. Felser, IEEE Trans. Magn. **47**, 367–373 (2011).

[2] D.C. Dunand, P. Müllner, Adv. Mater., **23**, 216-232 (2011).

[3] A. Zhukov, C. Garcia, M. Ilyn, R. Varga, J.J. DelVal, A. Granovsky, V. Rodionova, M. Ipatov, V. Zhukova, J. Magn. Magn. Mater., **324**, 3558-3562 (2012).

[4] R. Caballero-Flores, V. Franco, A. Conde, K. E. Knipling, and M. A. Willard, Appl Phys. Lett. **98**, 102505 (2011).

Abstract ID: 30073

INFLUENCE OF ORGANIC COMPOUND ($C_{15}H_{12}O$) INCORPORATION ON THE MICROSTRUCTURAL AND SUPERCONDUCTING PROPERTIES OF IN-SITU SPS-PROCESSED MgB_2 BULK SUPERCONDUCTORS

H. Ağıl[1], A. A. Agil[1], E. Ayas[2]

[1] *Department of Material Science and Engineering, Faculty of Engineering, Hakkari University, 30000, Hakkari, TURKEY*

[2] *Department of Materials Science and Engineering, Eskişehir Technical University, Eskişehir, 26555, TURKEY*

In this study, pure and organic compound ($C_{15}H_{12}O$)-doped MgB_2 bulk superconductors were successfully produced in 20 mm graphite molds using the in-situ Spark Plasma Sintering (SPS) method at a temperature of 850 °C, a pressure of 50 MPa, and a 10-minute sintering time. The first stage aimed to produce high-density pure MgB_2 in a single step, starting from commercial magnesium and boron powders, and utilized the advantages of SPS, which provide rapid densification and energy efficiency. After obtaining pure MgB_2, the effects of organic compound doping on phase formation, densification behavior, and microstructural evolution were systematically investigated. Phase analyses were performed using X-ray diffraction (XRD), and density measurements were performed using the Archimedes principle. The effects of the dopants on grain morphology and microstructural organization were evaluated using scanning electron microscopy (SEM). Superconductor properties were characterized by temperature-dependent resistance (R–T) measurements and magnetization (M–H) analyses. The results show that organic compound doping significantly affects the microstructure and flux-stabilization properties of MgB_2, altering both the material's densification behavior and superconducting performance. This study demonstrates the potential of using organic additives to optimize functional properties in MgB_2 bulk superconductors produced by the SPS method.

Acknowledgment

This work was supported by the Research Fund of Hakkari University, Hakkari, Türkiye, under the project number FM24BAP7.

Abstract ID: 30077

MAPPING IN-PLANE MAGNETIZATION DYNAMICS WITH A HIGH RESOLUTION LASER SCANNING MOKE SYSTEM

B. Bozkurt[1], C. Rogenbuke[1], U. Topal[2]

[1] Saint Benoit Highschool, Science and Technology Dept., 34425, Istanbul, TURKEY
[2] TUBITAK National Metrology Institute (UME), Magnetics Laboratory, 41470, Kocaeli, TURKEY

This paper presents the development approach on a custom, low-cost laser scanning Kerr effect imaging system for visualizing magnetic domains of soft magnetic materials such as thin/thick films, ribbons, coated substrates, etc. The system will be capable of resolving information on in-plane magnetization profiles of the samples under study. Laser scanning approach will be utilized to provide high spatial resolution as high as 1.5 - 2 μm. The system will consist of a 650 nm laser diode as the illumination source and a 2 GHz cut-off range Avalanche Photodiode (APD) as the detector which will allow up to 1 GSPS data collection. The high sampling rate could be employed for fast time-resolved magnetometry applications such as analyzing nanosecond scale domain wall motion. In addition, a 50 nm step size 3-Axis motorized stage for precise laser rastering was used in the setup. The sample will be magnetized by a calibrated in-plane Helmholtz coil. Polarization vector rotation of the laser beam by magnetization will be filtered by a secondary linear polarizer (the analyzer). A 2D magnetization map of the desired sample region will be constructed using laser power intensity data from the APD. Initial testing will be performed on cobalt-based Metglas 2714A magnetic alloy ribbons.

References

[1] W. K. Hiebert, A. Stankiewicz and M. R. Freeman, Phys. Rev. Lett. **79**, 1134 (1997).

[2] A. Kirilyuk, A. V. Kimel and T. Rasing, Rev. Mod. Phys. **82**, 2731 (2010).

Abstract ID: 30101

3D MICROFLUIDIC SYNTHESIS OF MAGNETIC AEROGEL COMPOSITES: OPTIMIZATION, MORPHOSTRUCTURAL CONTROL, BIOEVALUATION, AND WATER DECONTAMINATION EVALUATION

D.-I. Tudorache (Trifa)[1], A. C. Bîrcă[1], A.-G. Niculescu[1,2], E.-T. Moldoveanu[1], A. Hudiță[2,3], M. S. Stan[3], A. C. Burdușel[1], B. Purcăreanu[1], T. Hadibarata[1,4], D. E. Mihaiescu[1], A. M. Grumezescu[1,2]

[1] *National University of Science and Technology Politehnica Bucharest, 011061 Bucharest, ROMANIA*
[2] *Research Institute of the University of Bucharest—ICUB, University of Bucharest, 050657 Bucharest, ROMANIA*
[3] *University of Bucharest, 050095 Bucharest, ROMANIA*
[4] *Curtin University Malaysia, CDT 250, Miri 98009, MALAYSIA*

Microfluidic synthesis enables precise control over nanoparticle nucleation, growth, and integration into multifunctional composite systems. In this study, we report the development of a 3D multilayered microfluidic platform designed for the on-chip fabrication of Fe_3O_4 nanoparticles functionalized with a salicylic acid (SA) shell and their subsequent incorporation into silica-based aerogel matrices via a controlled vortex-assisted synthesis. Process optimization was achieved by systematically tuning reagent concentrations to tailor nanoparticle size, crystallinity, and matrix embedding. The resulting nanocomposites were extensively characterized using X-ray diffraction (XRD), scanning electron microscopy (SEM), energy-dispersive X-ray spectroscopy (EDS), Brunauer–Emmett–Teller (BET) surface analysis, and Fourier-transform infrared spectroscopy (FTIR), confirming highly uniform porosity and homogeneous nanoparticle dispersion. Importantly, preliminary biocompatibility tests conducted on eukaryotic cell lines and microbiological assays demonstrated minimal cytotoxicity and significant antibacterial activity of selected formulations. Moreover, functional validation through preliminary pesticide adsorption tests (performed by Fourier Transform Ion Cyclotron Resonance Mass Spectrometry (FT-ICR-MS)) indicated enhanced removal efficiency for the optimized composite. These findings validate the proposed microfluidic-assisted strategy as an effective route for designing advanced magnetic aerogel-based nanocomposites with optimized morphostructural properties, enhanced biological safety, and excellent pesticide adsorption, paving the way for their application in environmental remediation and beyond.

Abstract ID: 30103

ENGINEERED MAGNETIC AEROGELS VIA MICROFLUIDIC PROCESSING - BRIDGING LABORATORY PERFORMANCE AND REAL-WORLD WATER REMEDIATION APPLICATIONS

E. C. Florea[1], D.-I. Tudorache (Trifa)[1], E.-T. Moldoveanu[1], A.-G. Niculescu[1,2], A. C. Bîrcă[1], D. A. Florea[1], A. C. Burdușel[1], R. D. Trușcă[1], T. Hadibarata[1,3], O. C. Pârvulescu[1], D. E. Mihaiescu[1], A. M. Grumezescu[1,2]

1 National University of Science and Technology Politehnica Bucharest, 011061 Bucharest, ROMANIA
2 Research Institute of the University of Bucharest—ICUB, University of Bucharest, 050657 Bucharest, ROMANIA
3 Curtin University Malaysia, CDT 250, Miri 98009, MALAYSIA

Pesticide contamination in aquatic environments remains a critical global challenge, demanding innovative and sustainable remediation strategies. In this work, we present the fabrication, multiscale characterization, and environmental evaluation of silica-based magnetic aerogel composites engineered for efficient pesticide adsorption. The composite materials were synthesized via a 3D microfluidic vortex-assisted platform, enabling precise integration of a silica aerogel matrix with Fe_3O_4 core–shell nanoparticles and magnesium ions to tailor porosity, morphology, and magnetic responsiveness. Comprehensive physicochemical analyses (SEM, EDS, FTIR, XRD) confirmed the intended structure and nanoparticle dispersion. Laboratory-scale decontamination assays performed in a controlled water tank containing 100 mg/L pesticide solutions demonstrated high removal efficiency, validated through high-resolution FT-ICR-MS. Building on these results, the aerogel-based composites were tested under field-relevant conditions using water collected from a botanical garden's artificial lake. The High-field SolariX 15T FT-ICR equipment enabled accurate detection of persistent organic pollutants, while iso-concentration maps generated using QGIS and Ocean Data View software revealed spatial variations in contaminant levels and confirmed substantial reductions after treatment. Together, the results highlight the strong adsorption performance, environmental compatibility, and scalable applicability of magnetic aerogel-based nanocomposites for advanced water decontamination. This study demonstrates the transition from controlled laboratory validation to field testing, underscoring the potential of microfluidically assisted magnetic aerogels as next-generation materials for aquatic remediation technologies.

Abstract ID: 30104

EVALUATING MAGNETIC AEROGELS IN A LABORATORY AQUATIC MODEL: WATER, FISH, AND PLANT RESPONSES TO DECONTAMINATION TREATMENTS

A.-G. Niculescu[1,2], A. C. Bîrcă[1], D.-I. Tudorache (Trifa)[1], E.-T. Moldoveanu[1], A. C. Burdușel[1], A. M. Croitoru[1], R. D. Trușcă[1], T. Hadibarata[1,3], A. Hudiță[2,4], M. S. Stan[4], D. E. Mihaiescu[1], A. M. Grumezescu[1,2]

[1] *National University of Science and Technology Politehnica Bucharest, 011061 Bucharest, ROMANIA*
[2] *Research Institute of the University of Bucharest—ICUB, University of Bucharest, 050657 Bucharest, ROMANIA*
[3] *Curtin University Malaysia, CDT 250, Miri 98009, MALAYSIA*
[4] *University of Bucharest, 050095 Bucharest, ROMANIA*

Advanced magnetic aerogel composites have emerged as promising candidates for aquatic remediation due to their high porosity, tunable surface chemistry, and efficient magnetic recovery. In this work, we report the synthesis, physicochemical characterization, and biological evaluation of a silica-based magnetic aerogel designed for the decontamination of pesticides and metal ions in controlled aquatic environments. The material was fabricated using an optimized microfluidic vortex-assisted platform and structurally characterized by XRD, FT-IR, SEM, EDS, DLS, and BET. To assess both decontamination efficiency and biological safety, a laboratory-built aquatic model was established comprising 10 water tanks, each containing *Carassius auratus* (3 individuals per tank) and an aquatic plant of the Cabomba genus, introduced as a biological buffer to support microbiological equilibrium and reduce initial organismal stress. Experimental conditions included aerogel + contaminants treatment, contaminants-only controls, and negative controls. Water decontamination performance was monitored through FT-ICR high-resolution mass spectrometry for pesticide identification and ICP-MS for elemental quantification in water, fish tissues, and plant biomass. The aerogel composite demonstrated efficient removal of selected organic pollutants and metal ions. At the same time, biochemical and ecotoxicological markers in *Carassius auratus* showed no indications of cytotoxicity or oxidative stress under environmentally relevant exposure levels, supporting the biological compatibility of the material. Overall, the results confirm that the engineered magnetic aerogel serves as an effective, biologically safe, and magnetically retrievable adsorbent suitable for integrated water decontamination systems. This study underscores its applicability as a next-generation platform for sustainable remediation strategies within controlled and potentially real-world aquatic ecosystems.

11th International Conference on Superconductivity and Magnetism ICSM2026
4th International Conference on Quantum Materials and Technologies ICQMT2026
19th April to 26th April, 2026, Ölüdeniz – Fethiye/Muğla, Türkiye
https://icsmforever.org/

Abstract ID: 30138

RESISTIVITY, DENSITY OF ELECTRONIC STATES, AND SUPERCONDUCTING TRANSITION TEMPERATURE IN DENSITY WAVE COMPOUNDS WITH IMPERFECT NESTING

A. V. Tsvetkova[1], Ya. I. Rodionov[2], P. D. Grigoriev[3]

[1] Dukhov All-Russia Research Institute of Automatics, Moscow, 127030, RUSSIA
[2] Institute for Theoretical and Applied Electrodynamics, Russian Academy of Sciences, Moscow 125412, RUSSIA
[3] L.D. Landau Institute for Theoretical Physics, RAS, Chernogolovka 142432, RUSSIA

In some quasi-2D compounds, due to peculiarity of electron-phonon interaction charge density wave (CDW) may be formed. The CDW creates a spatial modulation of the charge density of conducting electrons with the wave vector $\boldsymbol{Q}$ and opens a gap Δ at the Fermi level in the electronic spectrum, which reduces the electron energy. In our paper [1], we investigated a model describing such systems in a quasi-one-dimensional approximation. Nontrivial behavior of the electron density of states (DoS) was demonstrated: at two different energy values, $\varepsilon = \Delta_1 - \Delta$ and $\varepsilon = \Delta_1 + \Delta$, DoS exhibits a jump and logarithmic divergence respectively (Fig. 1). The magnitude of nesting violation is described by the antinesting term Δ_1. Based on this result, resistance of the compound was calculated numerically as a function of temperature. The obtained data qualitatively coincide with the experimental data from paper [2].

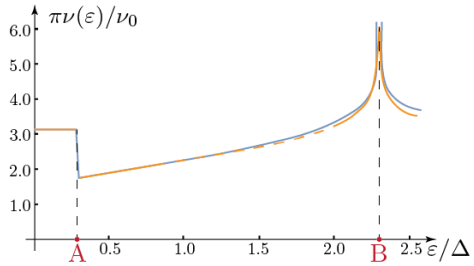

Fig. 1: *Comparison of the numerical DoS (blue curve) with analytical results (orange curve). We used the value ⊿1 = 1.3⊿. Here, $\nu_0 = [\pi v_F b]^{-1}$ is the DoS in the metallic state without CDW.*

It is known that a charge density wave can also arise in some high-temperature superconductors. Presence of the CDW cause to a renormalization of the superconductor's critical temperature:

$$T_c = \left(\frac{\Delta_1 - \Delta}{\omega_D}\right)^{\frac{\delta\nu}{\nu_0}} T_0, \; T_0 = \omega_D e^{\frac{-1}{\nu_0 g}}, \; \nu_0 = \frac{1}{\pi v_F b}, \; \delta\nu = \frac{1}{\pi v_F b}\sqrt{\frac{\Delta}{\Delta_1}}, \qquad (1)$$

where T_0 – BCS critical temperature without CDW; b– lattice constant, V_F – Fermi velocity. The results of this work clarify and generalize the conclusions of work [3].

References

[1] A. V. Tsvetkova, Ya I. Rodionov, and P. D. Grigoriev, Phys. Rev. B **111**, 205141 (2025).

[2] A. A. Sinchenko, *et al.*, Phys. Rev. Let. **112**, 036601 (2014).

[3] P. D. Grigoriev, Phys. Rev. B **77**, 224508, (2008).

Abstract ID: 30139

MAGNETIC LANDSCAPE OF NbTiN SUPERCONDUCTING RESONATORS UNDER RADIO-FREQUENCY EXCITATION

J. Baumgarten[1], N. Lejeune[1], L. Nulens[2] , J. Van de Vondel[2], A. V. Silhanek[1]

[1] *Experimental Physics of Nanostructured Materials (EPNM), QMAT, Université de Liège, Liège, BELGIUM*
[2] *Quantum Solid-State Physics, Department of Physics and Astronomy, KU Leuven, Celestijnenlaan 200D, Leuven, B-3001, BELGIUM*

Superconducting resonators are essential components in quantum circuits and highly sensitive sensors. However, their performance is often compromised by magnetic flux penetration, as the interaction of flux quanta and the induced radio-frequency (RF) currents in the superconducting thin film leads to significant energy dissipation. At low operating temperatures, this issue is aggravated as thermomagnetic instabilities can trigger the sudden propagation of magnetic flux avalanches [1]. An important open question is whether the RF excitation itself stimulates the nucleation and propagation of magnetic flux avalanches in the superconducting thin film. The literature remains inconclusive on this point, partly due to the lack of compelling evidence for this phenomenon. We address this issue by unprecedented direct visualization of magnetic flux penetration through Faraday rotation imaging under simultaneous RF excitation. We demonstrate that the avalanche activity exhibits a weak dependence on the RF intensity. However, magnetic flux bursts clearly influence the RF transmission properties of the device. Furthermore, we can unambiguously associate a particular avalanche event with a jump in resonance frequency. This enables us to identify the loci of most deleterious events and understand the distinct origins of upward and downward frequency shifts. These observations are supported by electromagnetic simulations in which local changes of the kinetic inductance mimic flux avalanches and confirm the invasive character of the MOI technique. The insights gained aim to contribute to the broader understanding of the magnetic resilience of superconducting resonators, with the goal of improving their efficiency and stability.

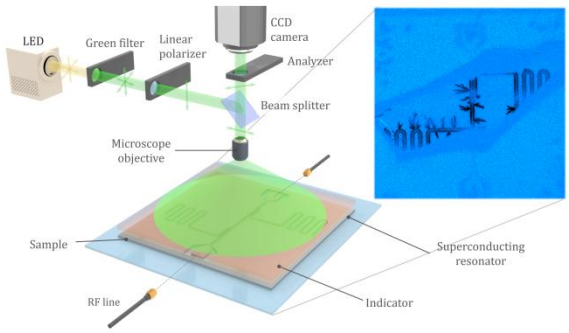

Fig. 1: *Experimental setup combining RF excitation of two resonators and simultaneous magneto-optical imaging of a fraction of the sample. The inset shows a magneto-optical image of the magnetic flux penetration depicting magnetic flux avalanches.*

References

[1] L. Nulens, N. Lejeune, *et al.*, Commun. Phys. **6**, 267 (2023).

Abstract ID: 30164

STATUS AND ON-SITE MAINTENANCE OF SCL2 CRYOGENIC PLANT FOR SUPERCONDUCTING LINAC OF RAON

H. C. Jo[1], M. K. Lee[1], I. Park[1], S. Kim[1], J. Kim[1], G. Lee[1], J. Han[1], Y. T. Choi[2], J. H. Shin[1]

[1] Institute for Basic Science(IBS), Institute for Rare Isotope Science(IRIS), 34000, Daejeon, REPUBLIC OF KOREA
[2] POSCO E&C, Nuclear Business Department, 22009, Incheon, REPUBLIC OF KOREA

Heavy ion accelerator, rare isotope Accelerator complex for ON-line experiments (RAON), at Institute for Rare Isotope Science (IRIS) consists of two superconducting linacs (SCLs): SCL3 and SCL2. For low energy experiments, SCL3 with cooling capacity of 4.5 kW has been in operation since 2022. The project of SCL2 composed of 24 (superconducting) cryomodules, 7 HTS magnets, and 13 LTS magnets for high energy experiments is underway. The SCL2 cryogenic plant that keeps these in a cryogenic state must provide cryogenic helium with 4.5K and 2K and have a total cooling capacity of 13.5 kW. In this paper, introduce and current status of SCL2 cryogenic plant are explained and several technical issues are discussed in the stage of commissioning.

Abstract ID: 30173

Ab INITIAL AUTOMATED PACKAGE FOR THERMOELECTRIC PROPERTIES ASSESSMENT AND CALCULATION

V. Buchelnikov, A. Enenko, V. Sokolovskiy

Chelyabinsk State University, Dept. of Cond. Matter Physics, 454001, Chelyabinsk, RUSSIA

Due to the intensive development of neural networks, the application of this technology for discovering and predicting promising thermoelectric materials has entered an active phase, relying on a limited volume of input data. However, the initial training of neural networks requires objective data, which is obtained through computational methods, including the application of density functional theory.

This paper presents a software package designed for the rapid assessment of the thermoelectric properties of various materials (including the lattice thermal conductivity and the thermoelectric figure of merit, ZT). The core of the package is implemented in Python, which forms a computational workflow using well-known third-party software. The DFT calculation is performed with VASP [1], the lattice thermal conductivity is calculated within the quasi-Debye approximation. Transport properties are calculated using the "BoltzTrap2" package [2] via Pymatgen interface. Phonon band is plotted using PhonoPy[3] within finite differences formalism. The use of specialized libraries such as "Fireworks" and "Automate" [4,5] achieves a high level of computational automation, freeing the operator from the need to perform additional manipulations with intermediate data. The scheme of calculations is presented in Figure 1.

Depending on the objectives, the package can be used to obtain either qualitative estimates with short computation times or more detailed dependencies of transport properties on temperature and carrier concentration for further analytical research.

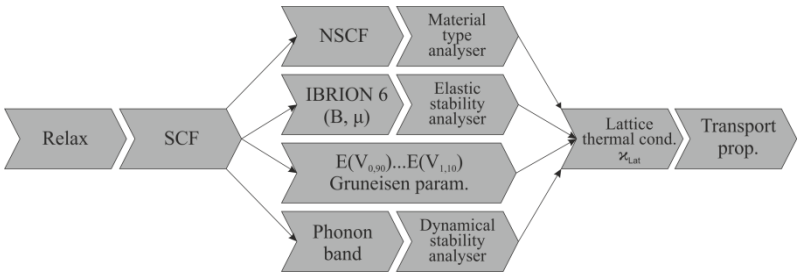

Fig. 1: *Calculation workflow.*

This work was supported by the Russian Science Foundation (project No. 24-12- 20016, https://rscf.ru/project/24-12- 20016/).

References

[1] G. Kresse, et al., Phys Rev. B, **54**, 11169 (1996).

[2] G. K. H. Madsen et al., Comp. Phys. Comm., **231**, 140 (2018).

[3] A. Togo et.al, J. Phys. Condens. Matter **35**, 353001 (2023).

[4] K. Mathew et al., Comp. Mat. Science, **139**, 140 (2017).

[5] A. Jain et al., Conc. and Comp., **27**, 5037 (2015).

Abstract ID: 30186

A REVIEW OF HIGH-PRESSURE GROWTH EFFECTS ON HIGH-T_c IRON-BASED SUPERCONDUCTORS

P. Singh, M. Azam, M. Manasa, S. J. Singh

Institute of High Pressure Physics (IHPP), Polish Academy of Sciences, Sokołowska 29/37, 01-142 Warsaw, POLAND

High-pressure growth remains a powerful technique for advancing high-T_c iron-based superconductors (FBS), enabling the stabilization of metastable phases and precise control of structural parameters that critically influence their electronic and magnetic behavior. In this work, we present a summary of our ongoing investigations across several FBS families synthesized using a high-gas-pressure and high-temperature method [1-7]. The synthesis employs a hot-isostatic pressing system capable of generating inert gas pressures up to 1.8 GPa within a cylindrical chamber and operating with a three-zone furnace reaching temperatures as high as 1700 °C [6]. A series of FBS bulk samples were fabricated under varying HP-HTS conditions and systematically examined using structural, magnetic, and transport measurements. Our results demonstrate that high-pressure growth significantly enhances superconducting performance, including increases in the transition temperature, critical current density, and vortex pinning force. High-pressure processing also improves sample densification and strengthens intergranular connectivity, leading to overall higher-quality superconducting bulks [2-7]. Furthermore, our comprehensive evaluation shows that an optimized pressure of approximately 0.5 GPa is sufficient to produce high-quality FBS bulks when combined with appropriate synthesis parameters. These findings highlight the effectiveness of HP-HTS as a robust route for tailoring and improving the superconducting properties of iron-based materials.

Acknowledgement

This research was supported by the National Science Centre (NCN), Poland through the SONATA-BIS 11 project (2021/42/E/ST5/00262). SJS acknowledges financial support from NCN Poland through Project number 2021/42/E/ST5/00262.

References

[1] P. Singh, *et al.*, Cryogenics **147**, 104028 (2025).

[2] S. J. Singh and M. I. Sturza, Crystals **12**, 20 (2022).

[3] M. Azam, *et al.*, IEEE Trans. Appl. Supercond. **34**, 7300205 (2023) and **34**, 7300405 (2023).

[4] S. J. Singh and A. Morawski, Jenny Stanford Publishing: New York, NY, USA, 2021; pp. 283–314.

[5] M. Manasa, *et al.*, IEEE Trans. Appl. Supercond. **34**, 7300605 (2023), J. Phys. Chem. Solids **190**, 111996 (2024).

[6] M. Azam, *et al.*, Crystals **13 (10)**, 1525 (2023).

[7] M. Manasa, *et al.*, Ceramics International **50 (1)**, 714-725 (2024) and Materials **16 (15)**, 5358 (2023).

Abstract ID: 30192

BIAS-PRESERVING ENTANGLEMENT OF KERR-CAT QUBITS WITH AN ATS COUPLER

K. Yurtseven[1,2], S. R. Jha[3,4], A. Limaye[5], R. Pokhrel[6], M. M. Kamelabad[7], M. W. Amin[8]

[1] *Department of Electrical and Electronics Engineering, Boğaziçi University, 34470, Istanbul, TURKEY*
[2] *Department of Physics, Boğaziçi University, 34470, Istanbul, TURKEY*
[3] *Research Laboratory of Electronics, Massachusetts Institute of Technology, 02139, Cambridge, Massachusetts, USA*
[4] *Department of Electrical Engineering and Computer Science, Massachusetts Institute of Technology, 02139, Cambridge, Massachusetts, USA*
[5] *Delft University of Technology, 2628, Delft, NETHERLANDS*
[6] *Pulchowk Campus, Institute of Engineering, Tribhuvan University, 44600, Lalitpur, NEPAL*
[7] *Faculty of Electrical and Electronics Engineering, Istanbul Technical University, 34485, Istanbul, TURKEY*
[8] *Quantum Science and Technology Group, Department of Physics and Applied Mathematics, Pakistan Institute of Engineering and Applied Sciences, 45650, Islamabad, PAKISTAN*

Kerr-cat qubits enable the autonomous and exponential suppression of bit-flip errors with only a linear increase in phase-flip errors. These residual phase-flip errors can be exponentially suppressed by concatenating these bosonic qubits into quantum Low-Density Parity-Check (LDPC) codes, such as the repetition code, offering a hardware-efficient path toward fault-tolerant quantum computing. To maintain this advantage, two-qubit gates must strictly preserve the high noise bias of the system. We propose using an asymmetrically threaded SQUID (ATS) parametric coupler to implement high-fidelity, bias-preserving entangling gates between Kerr-cat qubits. By driving the ATS, we activate a 400ns CX gate with fidelity exceeding 99.9% in simulation. Furthermore, we perform quantum process tomography simulations to characterize bias preservation during CX gate operation. Our results demonstrate a gate architecture that significantly outperforms non-bias-preserving alternatives while achieving bias comparable to the idling protection of each cat qubit.

Abstract ID: 30215

SYNTHESIS OF CURVED SUPERCONDUCTING NbN 3D STRUCTURES BY ATOMIC LAYER DEPOSITION

M. C. Mihaescu[1], D. Grundler[1,2]

[1] *Ecole Polytechnique Fédérale de Lausanne (EPFL), Institute of Materials, Laboratory of Nanoscale Magnetic Materials and Magnonics, 1015, Lausanne, SWITZERLAND*
[2] *EPFL, Institute of Electrical and Micro Engineering, 1015, Lausanne, SWITZERLAND*

Recent advances in nanofabrication have enabled three-dimensional nanoarchitectures for studying curvature-controlled superconductivity [1]. In this work, we investigate how curvature modifies the superconducting properties of thin-film NbN by combining two-photon lithography (TPL) and Plasma-Enhanced Atomic Layer Deposition (PEALD). Previously, this additive manufacturing strategy has been exploited for curved ferromagnetic structures [2,3]. Here, we apply it to superconducting NbN, enabling the systematic investigation of curvature-controlled superconducting properties. To assess the conformality of the PEALD process, bow-shaped structures were fabricated by TPL and subsequently coated with 30 nm of NbN by PEALD. The structures were then cross-sectioned using a xenon plasma focused ion beam. The scanning electron microscopy (SEM) images (Fig. 1a,b) reveal a conformal NbN coating beneath the bow, following the irregularities attributed to the stepwise TPL exposure of the polymeric resist.

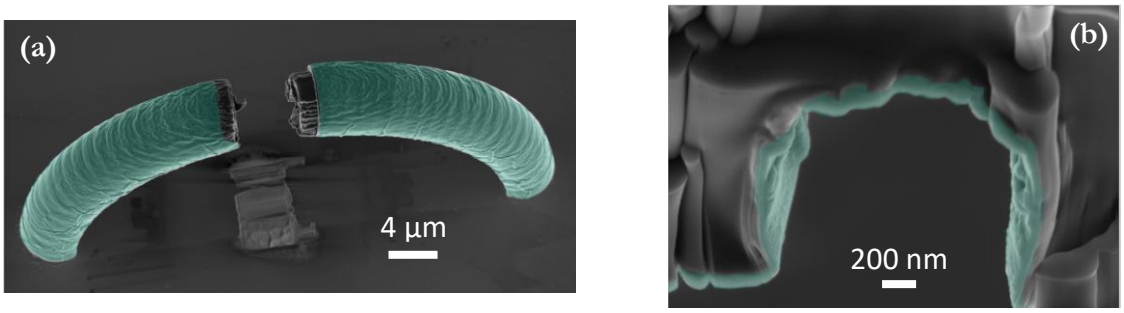

Fig. 1: *SEM images of (a) the bridge cross-sectioned at its center by focused ion beam (FIB) and (b) the left segment demonstrating conformal deposition of NbN (blue) beneath the bow.*

We explored the transport characteristics of ALD-grown NbN microbridges on planar substrates, stepped substrates and underneath the bow. The first two samples exhibited supercurrents below a critical temperature of about 13 K. For the bow, we found an onset of superconductivity at 11.4 K and a resistance drop of 1000 Ohm in a two-point measurement. For testing the zero-resistance state a 4-point measurement methodology is in progress. To conclude, we developed a scalable technology platform enabling systematic investigations on curvature-controlled superconductivity in 3D structures. Research supported by the Swiss National Science Foundation (Grant No. 10000845). Fabrication and SEM imaging were carried out at the Center of MicroNanoTechnology (CMi) of EPFL. FIB milling was performed at the Interdisciplinary Centre for Electron Microscopy (CIME) of EPFL.

References

[1] V. M. Fomin, and O. V. Dobrovolskiy, Appl. Phys. Lett. **120**, 090501 (2022).

[2] H. Guo, A. J. M. Deenen, M. Xu, M. Hamdi, and D. Grundler, Adv. Mater. **35**, 2303292 (2023).

[3] M. Xu, A. J. M. Deenen, H. Guo, P. Morales-Fernández, S. Wintz, E. Zhakina, M. Weigand, C. Donnelly, and D. Grundler, Nat. Nanotechn. **20**, 1258–1265 (2025).

Abstract ID: 30217

SUPERCURRENT IN A LATERAL S/F/S JOSEPHSON JUNCTION INCORPORATING NbTiN AND Ni GROWN BY ATOMIC LAYER DEPOSITION

F. Posva[1], D. Grundler[1,2]

[1] *Institute of Materials (IMX), School of Engineering (STI), Ecole Polytechnique Fédérale de Lausanne (EPFL), Lausanne 1015, SWITZERLAND*
[2] *Institute of Electrical and Micro Engineering, STI, EPFL, SWITZERLAND*

Superspintronics aims to manipulate spin-polarized supercurrents arising from the superconducting proximity effect in superconductor/ferromagnet (S/F) hybrid structures. They enable dissipationless spin transport and energy-efficient in-memory computing. Two materials are particularly studied for that purpose. The superconducting nitride NbTiN with its large superconducting gap and Ni with best supercurrent-carrying properties, long decay length and high I_cR_n product among all elemental ferromagnets [1]. Therefore, NbTiN/Ni-based junctions constitute a compelling platform for superspintronics.

We have optimized atomic layer deposition (ALD) of Ni (30-nm thick) that exhibits outstanding ferromagnetic and electrical properties, including a pronounced anisotropic magnetoresistance at 300 K [2] and low resistivity at cryogenic temperature (ϱ_{2K} = 1 μΩ·cm). We remove the native oxide of ALD-grown Ni with an Ar plasma before depositing 50-nm-thick NbTiN (T_c = 10.7 K, ΔT_c = 0.1 K) on Ni to create NbTiN/Ni/NbTiN junctions. The junction geometry is defined via an SF6-based dry etching process. DC transport measurements reveal a superconducting transition at Tc = 7.1 K for a Ni bridge length of 70±3 nm (Fig. 1A). Below Tc, we observe I-V-curves (Fig. 1B) characteristically dependent on the temperature. The critical current exhibits a Fraunhofer-like pattern with a modulation depth of about 10% of the maximum critical current (Fig. 1C). The results are interpreted in terms of an inhomogeneous supercurrent through the Ni microbridge. Combined with the conformal coating enabled by ALD, our approach offers a scalable route for free-form S/F hybrid structures on curved nanotemplates. Overall, our work paves the way for systematic studies of how curvature modifies supercurrent transport in 3D S/F/S geometries [3], opening exciting new opportunities for superspintronic device engineering.

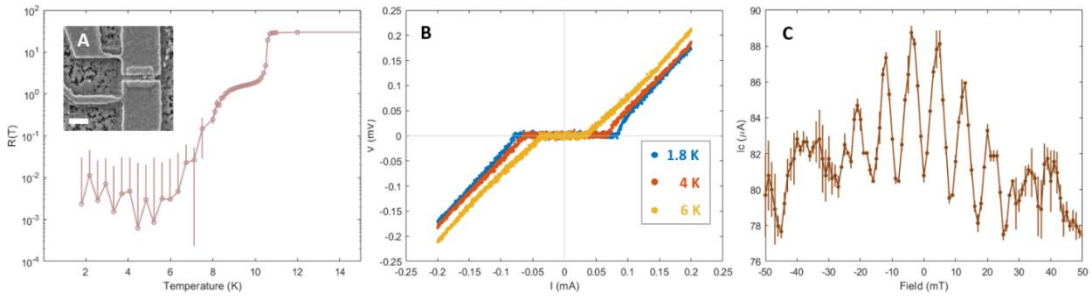

Fig.1: *(A) Resistance of the junction after lateral etching of the NbTiN. The inset shows a microscopy picture with a scale bar of 300 nm. (B) IV-curves at different temperatures. (C) Fraunhofer modulation of the critical current at 1.8 K. The field is applied perpendicular to the substrate.*

References

[1] N. O. Birge, *et al.*, APL Materials **12.4** (2024).

[2] M. C. Giordano, *et al.*, ACS applied materials & interfaces **12(36)**, 40443 (2020).

[3] A. J. Skarpeid, *et al.*, Journal of Physics: Condensed Matter **36(23)**, 235302 (2024).

Abstract ID: 30235

DEVELOPMENT OF SEARCH COIL MAGNETOMETER FOR DETECTION OF ULTRA LOW FREQUENCY (ULF) MAGNETIC FIELD VARIATIONS

A. E. Yıldırım[1], H. Can[1], U. Topal[1], M. A. Aksan[2], H. Sözeri[1]

[1] TUBITAK-UME, National Metrology Institute, PO Box 54, 41470, Gebze-Kocaeli, TURKEY
[2] Inönü University, Physics Department, 44100, Malatya, TURKEY

Search coil magnetometers (SCM), which measure time variation of magnetic flux density, can be used in detection of geomagnetic pulsations in ultra low frequency (ULF) ranges from 10 mHz to a few Hz. There are many reports in the literature stating that some anomalies were observed prior to earthquakes in ULF signals which may occur weeks or days before. The SCM in this work consists of 3 orthogonally aligned magnetic sensors to measure geomagnetic wave activities in directions of east-west, north-south and core-surface. The analog signals produced in the coils are first amplified, then send to band pass filters to observe the ULF emissions in various ranges. After this, the signal is digitized and processed in DAQ board. The search coils were precisely calibrated in Helmholtz coil and transfer functions together with noise values at 1 Hz were determined. In this paper, the construction, characterization and test procedures of SCM are discussed in details.

Acknowledgements

This study was supported by Scientific and Technological Research Council of Turkey (TUBITAK) under the Grant Number 123F249.

Abstract ID: 30238

BIOLOGICAL SOLITONS IN BIOMEMBRANES: ANALYTICAL SOLUTIONS OF A BOUSSINESQ-TYPE EQUATION WITH AMPLITUDE-DEPENDENT NONLINEARITY

S. A. Baloch

Department of Mathematics, University of Sargodha, PAKISTAN

Boussinesq-type equations play an important role in modeling nonlinear and dispersive wave phenomena in fluid mechanics, solid mechanics, and biological media. In particular, they provide an effective framework for describing longitudinal mechanical waves in lipid biomembranes, where amplitude-dependent nonlinear effects are essential for realistic nerve pulse propagation. In this work, we investigate a Boussinesq-type equation governing wave dynamics in biomembranes with amplitude-dependent nonlinearity. Exact analytical solutions are constructed using the Khater method and the Jacobi elliptic function method. A rich variety of nonlinear wave structures is obtained, including bell-shaped and anti-bell solitons, periodic waves, kink and anti-kink solutions. The influence of physical parameters on wave amplitude, width, and stability is analyzed in detail. Graphical representations in two-dimensional, three-dimensional, and contour plots are presented to illustrate key propagation characteristics of biological solitons. To the best of our knowledge, these biological soliton solutions for the considered biomembrane model have not been previously reported using the employed analytical approaches. The results provide new theoretical insights into nonlinear wave propagation in biomembranes and may contribute to the understanding of biological signal transmission and nonlinear phenomena in soft condensed matter systems.

Abstract ID: 30247

RAMAN SCATTERING FEATURES IN $MnSb_2Te_4$ MAGNETIC SEMICONDUCTORS

N. A. Abdullayev[1,2], Z. A. Jahangirli[1,2], Z. S. Aliev[2,1], I. R. Amiraslanov[1,2], N. T. Mamedov[1,2]

[1] *Institute of Physics, H. Javid av.,131, AZ1073, Baku, AZERBAIJAN*
[2] *Baku State University, Z. Xalilov str., 23, AZ1148, Baku, AZERBAIJAN*

Unlike the isostructural compound $MnBi_2Te_4$, which is an antiferromagnetic semiconductor [1], $MnSb_2Te_4$ compounds exhibit ferromagnetic ordering of the spins of magnetic atoms [2]. This is explained by the presence of a large number of defects, in particular antisite defects caused by the mutual substitution of the positions of Mn and Sb atoms. Our Raman scattering studies confirm the validity of this assumption. Four main differences between the Raman scattering in $MnSb_2Te_4$ and $MnBi_2Te_4$ are worth noting. First, since, according to theoretical calculations [3], Mn atoms are immobile in the displacements of the active Raman modes, the Raman spectra of $MnBi_2Te_4$ crystals are very similar to those for Bi_2Te_3 [3]. At the same time, the Raman spectra of $MnSb_2Te_4$ differ significantly from those of Sb_2Te_3 (Fig. 4(a)). Secondly, in the defect regions of two different Sb_2Te_3 samples (Fig. 4(b)) the spectra are very similar to those of $MnSb_2Te_4$ crystals (Fig. 1(a)), i.e., in the $MnSb_2Te_4$ crystal there are regions in which Mn is replaced by Sb. Thirdly, in contrast to the spectra of $MnBi_2Te_4$ (Fig. 4(c)), no polarization dependences are observed in the spectra of $MnSb_2Te_4$ (Fig. 4(d)) [4], which indicates a significantly higher defect content of $MnSb_2Te_4$ samples. Fourth, the theoretically calculated frequencies of the modes for $MnSb_2Te_4$ in ideal crystals are only partially observed, and the mode with a frequency of 263 cm^{-1} is far beyond the upper limit of possible frequencies for vibrational modes in $MnSb_2Te_4$.

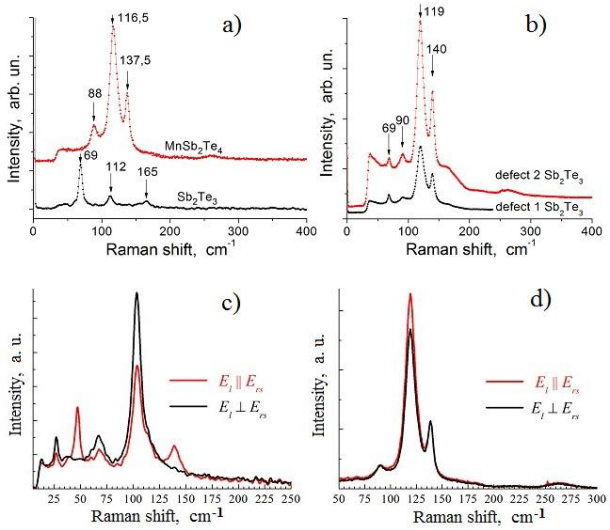

Fig. 1: *Raman scattering spectra of $MnSb_2Te_4$ and Sb_2Te_3 crystals.*

References

[1] M.M. Otrokov, I.I. Klimovskikh, *et al.*, Nature **576**, 416 (2019).

[2] V.N. Zverev, N.A. Abdullayev, *et al.*, JETP Letters **129 (1)**, (2026). (In print)

[3] I.R. Amiraslanov, Z.S. Aliev, *et al.*, Phys.Rev.B **106**, 184108 (2022).

[4] A.A. Maksimov, I.I. Tartakovskii, N.A. Abdullayev, *et al.*, JETP Letters **118**, 357 (2023).

Abstract ID: 30249

PHOTOLUMINESCENCE AND MAGNETIC PROPERTIES OF Nd-DOPED $ZnGa_2Se_4$

Z. A. Jahangirli[1,2], S. G. Asadullayeva[1,3,4]

[1] *1Institute of Physics, Ministry of Science and Education, Baku 1073, AZERBAIJAN*
[2] *Ministry of Science and Education, Baku State University, Baku 1073, AZERBAIJAN*
[3] *Azerbaijan State Oil and Industry University, 20 Azadliq Street, 1010 Baku, AZERBAIJAN*
[4] *Department of Physics and Electronics, Khazar University, Baku, AZERBAIJAN*

Wide band gap semiconductors with the general formula $A^2B^3{}_2X^6{}_4$, which crystallize in space groups $S^2{}_4$, exhibit significant potential for various applications. When doped with rare earth elements, these semiconductors exhibit significantly enhanced optical activity and photoluminescence properties, particularly in visible and near-infrared regions, rendering them suitable materials for advanced optoelectronic devices [1–3]. This study presents the first investigation of Nd-doped $ZnGa_2Se_4$, combining experimental analysis through photoluminescence spectroscopy with theoretical *ab*-Initio Density Functional Theory (DFT) calculations. Photoluminescence (PL) spectra in the infrared and visible region revealed high-intensity peaks associated with intra-center transitions of neodymium atoms. A comparison with the undoped compound demonstrated that the incorporation of neodymium significantly enhances the emission intensity within the host matrix. The observed spectral variations are primarily attributed to intracenter transitions of Nd ions, energy transfer from the host matrix to these transitions, and crystal field effect. DFT calculation results indicate that Nd preferentially occupies vacancy sites due to the lowest formation energy (− 0.95 eV), aligning with the minimal lattice distortion in this configuration. Total density of states (DOS) and atomic-projected DOS analyses reveal that $ZnGa_2Se_4$maintains its semiconducting nature with a bandgap of 2.65 eV, closely matching the experimental value of 2.6 eV. Notably, Nd doping induces magnetic behavior, evidenced by the non-equivalence of spin-up and spin-down states, resulting in a net magnetic moment of 3.79 μ_B, primarily from Nd-4f and Nd-4d orbitals.

References

[1] W. T. Kim, M. S. Jin, S. Hyeon, Y. K. Kim, B. S. Park, Solid State Commun. **74**, 123 (1990).

[2] J. Li, Y. Lin, M. Zhang, Y. Peng, X. Wei, Z. Wang, Z. Jiang, J. Appl. Phys. **133**, 105702 (2023).

[3] X. Jiang, W. R. L. Lambrecht, Phys. Rev. B **69**, 035201 (2004).

Abstract ID: 30323

EFFECT OF TWISTED SQUARE-LATTICE PINNING ARRAYS ON THE CRITICAL CURRENT DENSITY OF SUPERCONDUCTOR TAPES

Z. Owjifard, M. Hosseini

Department of physics, Shiraz University of Technology, Shiraz, 313-71555, IRAN

Artificial vortex pinning with various geometrical arrangements has attracted significant attention due to its potential to enhance the critical current [1-5]. Moiré patterns originate from interference effects produced when two identical lattices are superimposed, followed by a relative rotation or translational shift of one lattice [1-3]. The Langevin equations were solved under periodic boundary conditions for the vortices, and the vortex dynamics were computed using a molecular dynamics approach, allowing the critical current density to be determined [1,2].The effect of the twist angle θ between two square-lattice pinning arrays was investigated by varying θ. A range of twist angles and different values of the pinning force were considered, and specific angles were identified at which pronounced peaks correspond to an enhancement of the critical current density.

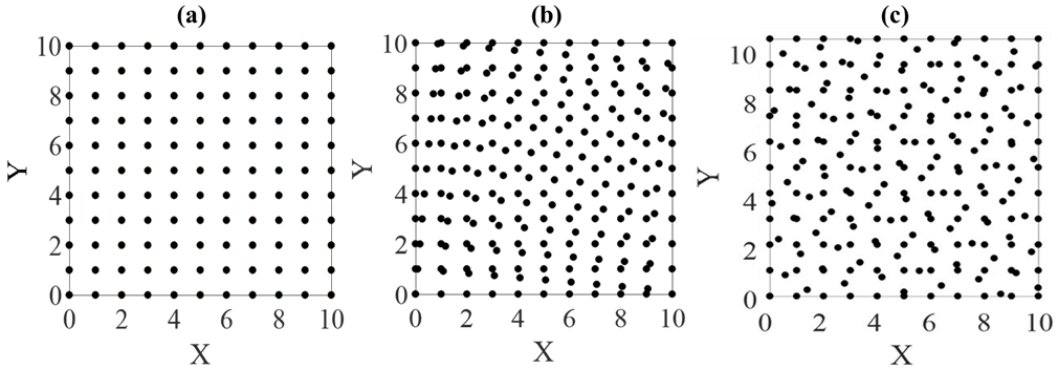

Fig. 1: *Normalized J_c versus Number of vortices for θ=0 ° (a), θ=5 ° (b) and θ=35°.*

References

[1] Z. Owjifard, A. Tavana, and M. Hosseini, AIP Adv. **15**, 025123 (2025).
[2] A. Zarei, M. Hosseini, Z. Owjifard, and A. Moftakharzadeh, J. Supercond. Novel Magn. **38**, 45 (2025).
[3] W. Li, C. J. O. Reichhardt, B. Jankó, and C. Reichhardt, Phys. Rev. B **104**, 024504 (2021).
[4] J. Wang, and E. Tosatti, Phys. Rev. B **112**, 155406 (2025).
[5] J. I. Martínez, P. Merino, A. L. Pinardi, O. I. Gonzalo, M. F. López, J. Méndez, and J. A. Martín-Gago, Sci. Rep. **6**, 20354 (2016).

Abstract ID: 30410

THE SURFACE TE-MAGNON-POLARITONS AT THE JUNCTION OF TWO MAGNONIC CRYSTALS WITH GRAPHENE SHEETS AT THE EACH INTERFACES

R. T. Askerbeyli[1,2], H. Elharkati[1], U. Kanbur[1]

[1] *Department of Physics, Karabuk University, TR78050, Karabuk, TURKEY*
[2] *Department of Business Administration, Karabuk University, Karabuk, TURKEY*

A theoretical analysis of surface transverse-electric (TE) magnon–polaritons supported at the junction of two magnonic crystals with graphene sheets deposited at the interfaces is presented. The system is modeled as a heterostructure composed of two semi-infinite antiferromagnetic superlattices separated by an intermediate slab that can be either magnetic or non-magnetic. The electromagnetic response is formulated within Maxwell's framework using the transfer-matrix approach, while the graphene layers are incorporated through their frequency-dependent surface conductivity.

Dispersion relations for localized surface and bulk magnon–polariton modes are derived from the electromagnetic boundary conditions and numerically evaluated for different values of the graphene Fermi energy. The results show that graphene strongly modifies the dispersion characteristics, confinement, and group velocities of the surface modes, with damping effects in the graphene layers playing a significant role. By tuning the graphene Fermi energy via electrostatic gating or doping, active control over the localization and propagation properties of the surface TE magnon–polaritons is achieved. These findings demonstrate the potential of antiferromagnet/graphene heterostructures as a versatile platform for tunable magnonic and terahertz applications.

References

[1] R. T. Tagiyeva (Askerbeyli) and M. Saglam, Solid State Commun. **122**, 413 (2002).
[2] M. S. Vasconcelos and M. G. Cottam, J. Phys. Appl. Phys. **52**, 285104 (2019).
[3] Y. V. Bludov, J. N. Gomes, G. A. Farias, J. Fernández-Rossier, M. I. Vasilevskiy and N. M. R. Peres, 2D Mater. **6**, 045003 (2019).
[4] R. T. Tagiyeva (Askerbeyli), M. Saglam and B. Boyacioglu, J. Phys. Chem. Solids **68**, 1296 (2007).
[5] R. T. Askerbeyli, J. Supercond. Nov. Magn. **30**, 1115 (2017).
[6] N. Tang, T. Tang, H. Pan, Y. Sun, J. Chen and Y. Du, in *Spintron. 2D Mater.* (Elsevier, 2020), pp. 137–161.
[7] C. H. Costa, M. S. Vasconcelos, U. L. Fulco and E. L. Albuquerque, Opt. Mater. **72**, 756 (2017).
[8] N.Raj and D.R. Tilley, Phys. Rev. B, **36**, 13 (1987).

Abstract ID: 30437

SINGLE-GAP VS TWO-GAP SCENARIOS IN UNCONVENTIONAL SUPERCONDUCTORS: AN ELECTRONIC SPECIFIC HEAT ANALYSIS

O. Ganiev[1,2], Z. Rakhmonov[3]

[1] *Institute of Nuclear Physics, Tashkent, UZBEKISTAN*
[2] *National University of Uzbekistan, Tashkent, UZBEKISTAN*
[3] *Engineering Physics Institute, Samarkand State University, Samarkand, UZBEKISTAN*

The electronic specific heat (C_{el}) serves as a fundamental probe for elucidating the pairing mechanism and gap structure in unconventional superconductors. While standard single-band BCS theory successfully describes conventional phonon-mediated superconductors, it fails to capture the complex thermodynamic response of multiband systems such as iron-based superconductors (FeSCs). In this work, we present a comparative theoretical analysis of the temperature-dependent specific heat in a diverse set of materials: the stoichiometric LiFeAs and FeSe, the electron-doped $Ba(Fe_{1-x}TM_x)_2As_2$ (TM = Co, Ni), and the non-centrosymmetric superconductor BeAu.

We model the experimental $C_{el}(T)$ data using two theoretical frameworks: the single-gap α-model and a self-consistent two-gap model. The single-gap α-model adjusts the BCS universal constant (1.764) to an effective coupling strength $\alpha = \Delta(0)/k_B T_c$ in an attempt to fit the anomaly at T_c. However, we demonstrate that this single-gap approach cannot simultaneously reproduce the jump at the transition temperature and the low-energy quasiparticle excitations observed in these materials.

In contrast, the two-gap model, which accounts for superconductivity on distinct Fermi surface sheets with gaps Δ_1 and Δ_2, yields excellent quantitative agreement with the experimental data. For the optimally doped $Ba(Fe_{1-x}TM_x)_2As_2$ systems, our two-band fitting parameters align with those reported in prior specific heat studies, accurately capturing the characteristic "shoulder" features in C_{el}/T. Similarly, we successfully model the thermodynamic behavior of BeAu, confirming that a multiband description is essential even in non-centrosymmetric systems. Our results validate the universality of the two-band picture for extracting reliable superconducting parameters (Δ_i, γ_i) and confirm the strong-coupling nature of the pairing interactions in these families of superconductors.

Abstract ID: 30455

CRYSTAL SYMMETRY EFFECT ON SUPERCONDUCTIVITY AND PHASE DIAGRAM IN 2212

B. M. Mustafa

Retired from Mosul University, IRAQ

2212 is one of the HTSC cuprates with T_c 110 ^oK which is mostly applicable as wires in modern advanced technology, its crystal structure its crystal structure is more complicated than LBCO and YBCO (1,2) which I studied formerly, considering crystal symmetry effect on superconductivity (SC) and phase diagram (PD) which introduce a new vision for their superconductive behavior, explains many of their abnormalities and unexplained behavior in SC and PD, considering the principles (1) crystal symmetry affects dopants distribution on lattice sites and (2) dopants affect lattice symmetry and superconductivity. In this research, the above principles for studying SC and PD will utilize the basic aspects of the new vision, which may lead to a shared insight into understanding 2212, ultimately improving its applications.

References

[1] B. M.: Mustafa, *The effect of Sr substitutions on the crystal symmetry and SC of the high temperature superconductor* $La_{2-x}Sr_xCuO_4$, J. Supcond. Nov. Mag. **38**, 55 (2025).

[2] B. M.: Mustafa, *Crystal Symmetry Effects on Oxygen Doping Distribution, SC, and Phase Diagram in* $YBa_2Cu_3O_7$, under review.

Abstract ID: 30490

INVESTIGATION OF STRUCTURE-RELATED CHANGES IN THE MAGNETIC PROPERTIES OF $SrFe_{12-x}Ni_xO_{19}$ (x = 0–0.3)

A. S. Abiyev, V. A. Turchenko

International Intergovernmental Organization Joint Institute for Nuclear Research, Dubna 141980, RUSSIA

M-type strontium hexaferrite ($SrFe_{12}O_{19}$) is widely used in low-cost permanent magnets and microwave components because it combines high chemical stability with strong uniaxial magnetocrystalline anisotropy, and **Ni substitution is one of the most popular, practical ways to tune its magnetic performance without changing the base hexaferrite framework.**

In this work, the results for $SrFe_{12-x}Ni_xO_{19}$ (x = 0.0–0.3) show that Ni doping is structurally conservative but magnetically consequential. Neutron diffraction and Rietveld refinement confirm that all compositions preserve the parent hexagonal M-type structure in the $P6_3/mmc$ space group, meaning that the applied Ni content does not trigger any structural phase transformation. Within this unchanged structural framework, Ni produces systematic lattice and microstructural responses. The refined unit-cell metrics reveal an overall contraction with increasing Ni content: the unit-cell volume decreases monotonically and the *a* parameter continuously decreases, while *c* displays a small increase at low substitution (x = 0.1) followed by a decrease at higher x; importantly, the contraction trend remains evident at x = 0.3. The refinement further indicates that Ni is incorporated predominantly at the Fe(12k) Wyckoff position, which is critical because 12k is the most populated Fe sublattice and strongly influences both the Fe–O coordination network and the magnetic exchange backbone of M-type hexaferrites.

Peak-broadening analysis provides an additional structural signature: the W(d) dependence becomes steeper with increasing x, evidencing a progressive rise in microstress as Ni content increases. This microstress growth supports the picture of enhanced lattice strain/disorder associated with substitution and is consistent with the refined atomic displacements. Local-structure parameters extracted from the refinement show that Ni introduction slightly modifies Fe–O bond geometry and affects the distortion of oxygen coordination polyhedra (S%), including the 12k-related environment where Ni preferentially resides. These subtle but systematic geometric changes are crucial for magnetism because the dominant interactions in hexaferrites are governed by Fe–O–Fe superexchange. Accordingly, the calculated Fe–O–Fe angles show composition-dependent trends in which several key angles decrease monotonically with Ni substitution (i.e., shift toward weaker-exchange geometries), while fewer angles increase and may locally enhance exchange; the net balance, however, favors an overall weakening of the exchange network as x increases.

The microstructure also evolves with Ni content. SEM-based particle analysis indicates a shift toward smaller characteristic size fractions as x increases, with the highly substituted sample (x = 0.3) showing a negligible contribution from larger (> ~2 μm) particles, consistent with a refinement tendency accompanying substitution. These structural and microstructural changes are reflected in the magnetic results. Analysis of hysteresis behavior (including the approach-to-saturation treatment used in the manuscript) indicates an overall tendency toward reduced saturation magnetization with increasing Ni concentration, consistent with substitution at the magnetically dominant 12k sublattice and the observed weakening of Fe–O–Fe exchange geometry. The decrease in exchange strength is most clearly verified by the Curie temperature, which drops from 678 K for x = 0.0 to 660 K for x = 0.3, demonstrating reduced thermal stability of ferrimagnetic ordering with Ni addition. Overall, the results support a single coherent mechanism: **preferential Ni occupation of Fe(12k) produces lattice contraction and higher microstress, slightly distorts oxygen polyhedra and shifts superexchange angles, and thereby reduces the net magnetic moment and Curie temperature, while the $P6_3/mmc$ hexaferrite framework remains intact.**

Abstract ID: 30495

EXPERIMENTAL TESTING OF A 10 kW-CLASS SCALED-DOWN HTS-ISM WITH SINUSOIDALLY DISTRIBUTED STATOR WINDING FOR PROPULSION MOTORS OF ELECTRIC AIRCRAFT SYSTEMS

M. Yamamoto, T. Nakamura

Kyoto University, Dept. of Electrical Engineering, 615-8245, Kyoto, JAPAN

With the increasing stringency of CO_2 emission regulations, electric aircraft incorporating superconducting technologies—characterized by extremely low electrical losses—have garnered significant attention. Within this context, the High Temperature Superconducting Induction/Synchronous Motor (HTS-ISM) [1] has emerged as a prominent candidate for aircraft propulsion, offering fail-safe functionality, high efficiency, and high power density. However, the total loss is dominated by the flux flow loss in the superconducting materials, which is generated by harmonics of magnetic flux density. A 20 MW-class HTS-ISM was previously prepared by using self-assembling design method for the stator winding. The self-assembling design method uniquely determines stator winding distribution based on sinusoidal spatial patterns, to reduce spatial harmonics. The reduced harmonics minimize flux flow losses in the superconductors and further enhance power density. The non-linear electromagnetic field analyses for the HTS-ISM have demonstrated superior performances with a maximum efficiency of 97.1 % and a maximum output of 33.4 kW/kg [2]. To validate these findings, a 10 kW-class HTS-ISM with sinusoidally distributed stator winding was designed and prototyped as a scaled-down model of the 20 MW-class HTS-ISM. This study provides a comparative analysis between the experimental results of the 10 kW-class HTS-ISM and the numerical results obtained through electromagnetic field analysis using the finite element method (FEM) of COMSOL Multiphysics®.

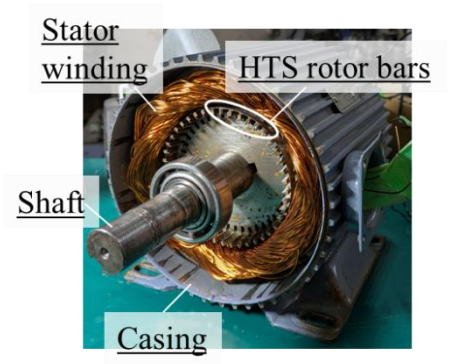

Fig. 1: *Fabricated 10 kW-class HTS-ISM.*

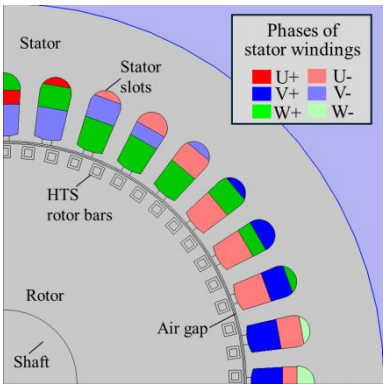

Fig. 2: *Simulation model of 10 kW-class HTS-ISM.*

References

[1] T. Nakamura, *et al.*, IEEE Trans. Appl. Supercond. **33(5)**, 5200205 (2023).
[2] M. Yamamoto and T. Nakamura, Phys. C Supercond. Appl. **632**, 1354690 (2025).

Abstract ID: 30498

TAILORING THE ELECTROCHEMICAL PERFORMANCE OF COBALT–MANGANESE PHOSPHATE ELECTRODES THROUGH SUBSTRATE ENGINEERING

H. Ali, M. Anis-ur-Rehman

Applied Thermal Physics Laboratory, Department of Physics, COMSATS University Islamabad, Islamabad 45550, PAKISTAN

The electrochemical performance of supercapacitor electrodes is governed not only by the intrinsic properties of active materials but also by the nature of the current collector. In this work, cobalt manganese phosphate (Co-Mn-PO_4) is employed as a model pseudocapacitive material to systematically investigate the effect of substrate engineering on electrochemical behavior. Identical Co-Mn-PO_4 electrodes were fabricated on nickel foam, carbon cloth, graphene sheet, fluorine-doped tin oxide (FTO) glass, and aluminum foil, while maintaining constant mass loading and electrode composition. Electrochemical measurements were carried out in a three-electrode configuration using 3.0 M KOH as the electrolyte. Pronounced variations in specific capacitance, charge-transfer resistance, rate capability, and cycling stability were observed as a function of substrate type. Nickel foam delivered the highest capacitance and fastest redox kinetics due to its three-dimensional porous architecture and superior electrical conductivity, whereas carbon cloth and graphene substrates exhibited enhanced cycling stability and reduced internal resistance. In contrast, planar substrates such as FTO glass and aluminum foil showed comparatively lower capacitance and higher interfacial resistance, highlighting the critical role of substrate–electrode interactions and ion transport pathways. This study demonstrates that substrate selection is a decisive parameter in unlocking the full electrochemical potential of cobalt–manganese phosphate electrodes and provides practical guidelines for optimizing current collectors in high-performance supercapacitor systems.

Abstract ID: 30499

DIELECTRIC BEHAVIOR OF RE-DOPED COBALT FERRITE ELECTROSPUN FIBERS

S. Gul-e-Rana, M. Anis-Ur-Rehman

Applied Thermal Physics Laboratory (ATPL), Department of Physics, COMSATS University Islamabad, 44000 PAKISTAN

The $CoFe_{2-2x}La_xSm_xO_2$ (x=0.0-0.1) fibers were effectively made by electrospinning method. Fourier transform infrared spectroscopy was observed to identify bond vibrations in particle-embedded fibers. The dielectric constant, tangent loss and ac conductivity were measured by LCR meter 6440B (frequency range 1kHz-3MHz). The prepared fiber $CoFe_{2-2x}La_xSm_xO_2$ (x=0.05) showed high dielectric constant among other composite fibers as shown in Fig.1. The Ac conductivity of $CoFe_{2-2x}La_xSm_xO_2$ (x=0.0, 0.05, 0.1) electrospun fibers increased with frequency. The $CoFe_{2-2x}La_xSm_xO_2$ (x=0.0) have less tangent loss value. These prepared materials are potential candidates for use in flexible electronic devices.

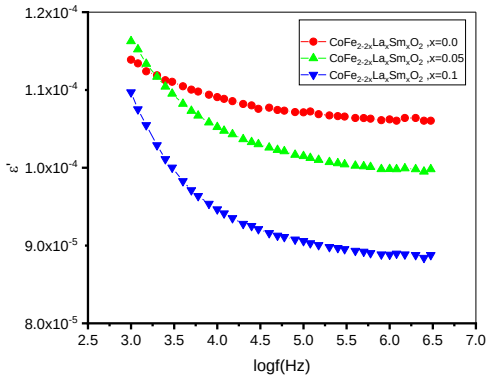

Fig. 1: *Dielectric constant (ε') of $CoFe_{2-2x}La_xSm_xO_2$ (x= 0.0, 0.05, 0.1) electrospun fibers as a function of frequency.*

Abstract ID: 30500

ROLE OF ELECTROLYTE SELECTION IN GOVERNING THE ELECTROCHEMICAL RESPONSE OF COBALT PHOSPHATE ELECTRODES

H. Ali, M. Anis-ur-Rehman

Applied Thermal Physics Laboratory, Department of Physics, COMSATS University Islamabad, Islamabad 45550, PAKISTAN

Electrolyte chemistry plays a crucial role in determining the electrochemical response of supercapacitor electrodes by influencing ionic conductivity, interfacial charge transfer, and redox activity. In this study, cobalt phosphate was employed as a pseudocapacitive electrode material and deposited onto nickel foam to evaluate the effect of electrolyte selection on electrochemical performance. The electrochemical behavior of the electrodes was systematically investigated in a three-electrode configuration using aqueous electrolytes, including 1.0 M KOH, 1.0 M NaOH, 1.0 M KCl, and 1.0 M Na_2SO_4, while maintaining identical electrode composition and mass loading. The results reveal a strong electrolyte-dependent performance, with alkaline electrolytes delivering significantly enhanced specific capacitance and faster redox kinetics compared to neutral electrolytes. Among the tested systems, 1.0 M KOH exhibited the highest capacitance and lowest charge-transfer resistance, followed by 1.0 M NaOH, whereas neutral electrolytes showed comparatively lower capacitance due to limited faradaic activity. These findings highlight the critical role of electrolyte–electrode synergy in optimizing the electrochemical performance of cobalt phosphate electrodes and provide practical insights for rational electrolyte selection in supercapacitor applications.

Abstract ID: 30504

CRITERION FOR SOFTENING THE PHONON SPECTRUM OF A CRYSTALLINE FILM WITH A TWO-DIMENSIONAL COATING

V. N. Kushnir[1,2], S. L. Prischepa[1]

[1] *Belarusian State University of Informatics and Radioelectronics, Dept. of Information Security, 220013, Minsk, BELARUS*
[2] *Belarusian State University, Dept. of Theor Phys. and Astrophysics, 220006, Minsk, BELARUS*

In [1], the stabilization of the critical temperature for the superconducting transition in a thin niobium film coated with two graphene layers was reported. The effect was interpreted using the concept of phonon-spectrum softening in the film (see Ref. [2]). This naturally raises the question of how the surface structure of the film influences the dynamics of its crystal lattice. Because this problem is technically challenging—its difficulties are reviewed in detail in [3] from the perspective of superconductivity theory—it is important to be able to estimate, in advance, the impact of different types of surface modification. For the purpose of enhancing superconductivity, a modification is considered beneficial if it increases the statistical weight of low-frequency modes in the phonon spectrum. As criteria for such a positive effect, one can use McMillan-type frequency averages [2]; for example, the second moment, $\langle\omega^2\rangle_M$, which in more traditional terms is simply the average frequency of the spectrum $\langle\omega\rangle$. We argue, however, that the trace criterion ($\langle\omega^3\rangle_M$ in McMillan's notation) is more effective. We define it as follows: surface modification leads to phonon-spectrum softening if the difference between the traces of the unperturbed and perturbed dynamical matrices (D_0 and D, respectively) is positive, $Crit \equiv \mathrm{Sp}(D_0) - \mathrm{Sp}(D) > 0$. In other words, we compare the sums of squared phonon frequencies. At first glance, this approach would not seem to offer an advantage if all phonon frequencies had to be computed explicitly. However, in our case, there exist rigorous theoretical methods that circumvent the need for full-spectrum calculation (see, e.g., [4]). Furthermore, we show that reasonable estimates of the criterion can be obtained using only minimal input data. As an illustration, we use a simple model from [1], for which the criterion can be determined exactly. The system is a classical one-dimensional chain of N identical atoms of mass M_0 connected by elastic bonds, to which a secondary chain of two atoms of mass M_1 is attached via an elastic bond. This setup mimics the Nb/G structure. It is straightforward to show that the criterion in this case is given by $Crit \equiv \omega_{max}^2 (1 - \alpha) - \omega_1^2$, where ω_{max} is the maximum eigenfrequency of the main chain, ω_1 is the eigenfrequency of the isolated attached link, and α is a dimensionless coupling constant. From this expression, we see that the condition for spectrum softening ($Crit > 0$) is satisfied only within a relatively narrow parameter range: the natural frequency of the additional chain must be within the frequency band of the main chain, and the coupling between the main and additional chains must be sufficiently weak and bounded. Explicit calculation of the phonon spectra for this elementary model fully supports these conclusions. Interestingly, analyzing a more complex system yields qualitatively similar results.

References

[1] S. L. Prischepa, *et al.*, Supercond. Sci. Technol., **34**, 115021 (2021).
[2] W. L. McMillan, Phys. Rev., **167**, 331 (1968).
[3] S. L. Prischepa and V. N. Kushnir, J. Phys.: Condens. Matter., **35**, 313003 (2023).
[4] I. M. Lifshitz, Adv. Phys., **13**, 483 (1964).

Abstract ID: 30508

CONTROLLED SPIKING BEHAVIOR OF A SUPERCONDUCTING NbTiN NEURON

Z. Alzoubi[1], K. Harrabi[1,2], L. R. Cadorim[3,4], A. Mekki[1,5], A. M. Aljalal[1], M. V. Milosevic[4]

[1] *Physics Department, King Fahd University of Petroleum and Minerals, 31261 Dhahran, SAUDI ARABIA*
[2] *Interdisciplinary Research Center (RC) for Intelligent Secure Systems, KFUPM, Dhahran 31261, SAUDI ARABIA*
[3] *Departamento de Fısica, Faculdade de Ciencias, Universidade Estadual Paulista (UNESP), Caixa Postal 473, 17033-360, Bauru-SP, BRAZIL*
[4] *Department of Physics, University of Antwerp, Groenenborgerlaan 171, B-2020 Antwerp, BELGIUM*
[5] *Center for Advanced Material, King Fahd University of Petroleum and Minerals, Dhahran 1261, SAUDI ARABIA*

We have investigated an artificial superconducting neuron composed of a superconducting NbTiN wire connected in parallel with a metallic resistor. When a voltage pulse is applied, the current initially flows through the superconducting wire due to its negligible resistance. As the current exceeds the critical value, a normal-state region (hot spot) forms, causing a significant increase in resistance and triggering a voltage spike that marks the neuron's "firing" event. This configuration mimics the behavior of biological neurons, where electrical pulses generate spiking activity. Following the formation of the hot spot, the current is redirected to the parallel resistor. The spiking frequency depends on the interplay between the wire's inductance, the resistance, and the applied current. We also studied the effect of temperature on spiking dynamics, observing that higher temperatures lead to increased spiking frequency. Additionally, we examined how variations in inductance affect the spike frequency, finding that higher inductance correlates with lower spiking rates. Our experimental results align well with simulations based on the time-dependent Ginzburg-Landau (TDGL) theory, confirming the model's accuracy in capturing the essential dynamics of artificial superconducting neurons. These findings contribute to the design and optimization of superconducting neuromorphic circuits, where precise control over spiking behavior is essential.

Abstract ID: 30518

SYNTHESIS AND CHARACTERIZATION OF (Mg-Co-Fe-O) PARTICLES FOR MEMORY DEVICE APPLICATIONS

M. Ammar Bin Masood, M. Anis-ur-Rehman

Applied Thermal Physics Laboratory, Department of Physics COMSATS University Islamabad, Islamabad 45550, PAKISTAN

The demand for advanced memory devices is continuously growing due to the rapid expansion of artificial intelligence. For that purpose, Ferrite based nanoparticles particular spinel ferrites have been used. Since magnesium ferrite is a soft semiconductor containing a normal spinel ferrite structure which makes it easy to study cations like (Co^{2+}) [1]. $Mg_{1-x}Co_xFe_2O_4$ (x=0.0, 0.2) was prepared by a sol-gel method in which cobalt was added as a dopant. The material was sintered at 730 °C for 3 h. To analyze the structural properties of the sample, x-ray diffraction (XRD) technique was used, which confirmed the spinel cubic structure. XRD data was used to analysis the crystallite size, lattice parameters, experimental and theoretical density and volume of samples. A precision component analyzer was used for dielectric study of the samples in the frequency range of 20 Hz to 3 MHz. AC conductivity increased at higher frequency. Impedance has progressively decreased at higher frequency. DC conductivity was measured using a two-probe method that showed a increasing trend with increasing temperature. The doped samples demonstrated highly improved structural and electrical properties as compared to those of the undoped sample.

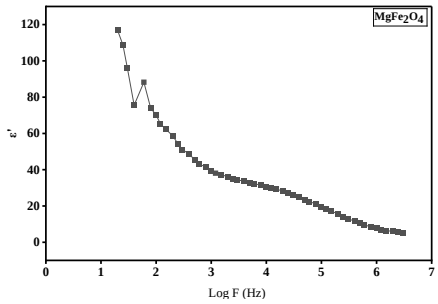

Fig. 3: *x=0.0*

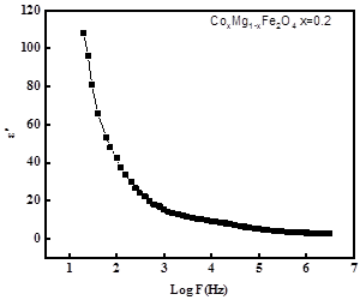

Fig. 2: *x=0.2*

References

[1] M. Kamran, M. Anis-ur-Rehman, *Enhanced transport properties in Ce doped cobalt ferrites nanoparticles for resistive RAM applications*, J. Alloy Compd., **822**, 153583 (2020).

Abstract ID: 30519

EFFICIENT ELECTRONIC STRUCTURE PREDICTION IN CARBON MATERIALS USING DFT-CALIBRATED EXTENDED HÜCKEL THEORY

G. S. Kupriyanova, I. G. Mershiev, V. V. Savin

Immanul Kant Baltic University, Institute of High Technology, 236041, Kaliningrad, RUSSIA

One of the central challenges in modern materials science is establishing quantitative relationships between atomic structure and electronic properties, thereby enabling the rational design of materials with tailored functionalities. In two-dimensional carbon-based systems, the π-electron network governs both electronic behavior and topological characteristics. While density functional theory (DFT) offers high accuracy in describing electronic structure, its computational cost restricts application to large or complex systems. This work presents a parameter-calibrated extended Hückel method (EHM) for efficiently computing electron densities in model carbon nanostructures—including coronene, corannulene, and graphene nanoribbons—using DFT results as a reference. The calibrated EHM not only reproduces key features of the electron density but also enables estimation of magnetic anisotropy and the nuclear chemical shift tensor (Fig. 1). For corannulene, EHM predictions are compared with benchmark DFT calculations. Despite its simplicity, the method yields electron density distributions in good agreement with DFT: the energy positions of corresponding density-of-states peaks differ by less than 1 eV. Both approaches reveal pronounced ring currents in corannulene [1], highlighting the potential of EHM as a computationally efficient tool for probing anomalous magnetic responses in curved and polycyclic carbon structurescan be used as a basis for studying the anomalous magnetic properties of complex carbon compounds.

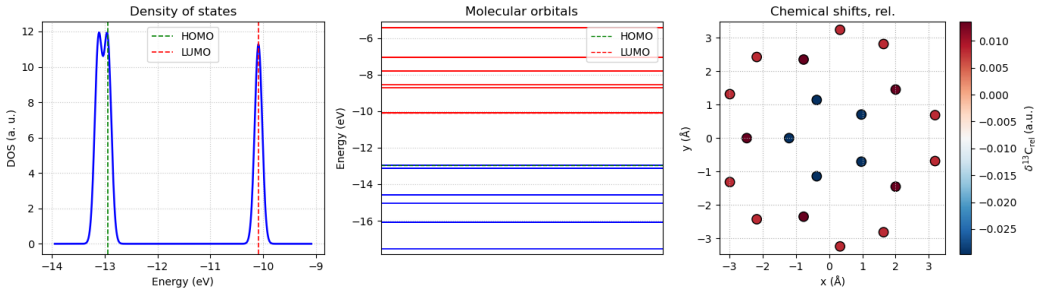

Fig. 1: *Density of states and chemical shifts calculations for an isolated corannulene molecule using Extended Hückel's method.*

This work was supported by grant No. 25-72-31032 from the Russian Science Foundation.

References

[1] E. Steiner, P. W. Fowler, L. W. Jenneskens *Counter-Rotating Ring Currents in Coronene and Corannulene // Angew*, Chem. Int. Ed. Wiley, T. 40, NO 2. C. 362–366 (2001).

11th International Conference on Superconductivity and Magnetism ICSM2026
4th International Conference on Quantum Materials and Technologies ICQMT2026
19th April to 26th April, 2026, Ölüdeniz – Fethiye/Muğla, Türkiye
https://icsmforever.org/

Abstract ID: 30525

ELECTROCHEMICAL STUDIES OF $NiMn_2O_4$–$NiFe_2O_4$/CNT COMPOSITES FOR ENERGY STORAGE APPLICATIONS

H. Sultan, H. Ali, M. Anis-ur-Rehman

Applied Thermal Physics Lab, Department of Physics, COMSATS University, Islamabad, 45550, PAKISTAN

Nickel manganite ($NiMn_2O_4$), nickel ferrite ($NiFe_2O_4$), and their composites with carbon nanotubes (CNTs) were successfully synthesized using a modified sol–gel (WOW) technique. X-ray diffraction (XRD) analysis confirmed the formation of a single-phase spinel structure in all synthesized samples, along with detailed evaluation of crystallite size, lattice parameters, and both experimental and theoretical densities. The electrochemical performance of the synthesized samples was further investigated by employing them as active electrode materials for supercapacitor applications in an aqueous KOH electrolyte. Cyclic voltammetry (CV), galvanostatic charge–discharge (GCD), and electrochemical impedance spectroscopy (EIS) were carried out to evaluate their charge storage capability, rate performance, and interfacial resistance. The results reveal that the incorporation of CNTs dramatically improves the electrical conductivity, charge transport pathways, and ion diffusion kinetics, leading to superior electrochemical activity. In particular, the CNT-based composites exhibit enhanced capacitance and stability, especially under high-frequency conditions, demonstrating their potential for precisely engineered ferrite–CNT hybrid materials in next-generation high-power energy storage and high-frequency electronic devices.

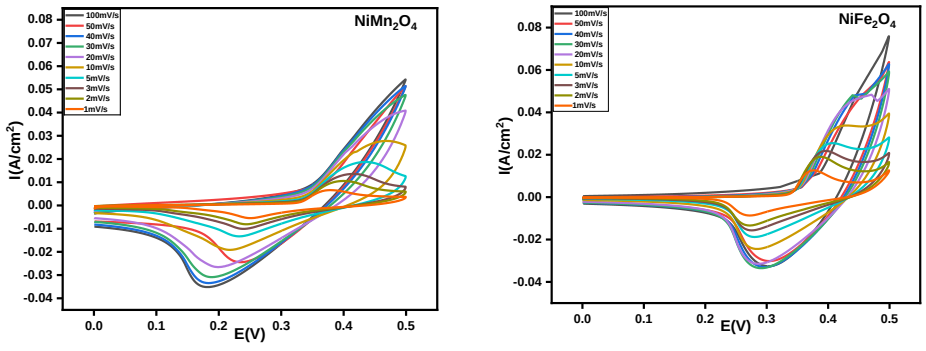

Abstract ID: 30538

THE PINNING ENERGY OF $Bi_2Sr_2Ca_{0.6}Zn_{0.4}Cu_2O_x$

S.S. Ragimov[1,2], I. N. Askerzade[3,4]

[1] *Baku State University, Institute for Physical Problems, AZ1148, Baku, AZERBAIJAN*
[2] *Institute of Physics of Azerbaijan Ministry of Science and Education, AZ-1143, Baku, AZERBAIJAN*
[3] *Computer Engineering Dept. of Ankara University, Ankara, TURKEY*
[4] *Center of Excellence of Superconductivity of Ankara University, Ankara, TURKEY*

As is known, one of the critical parameters of superconductivity is the critical current density. The value of the critical current depends on the synthesis regime of the superconductor. Moving vortices and pinning centers play a mainly role in forming the critical current density (J_c). The increasing of sample heterogeneity leads to rise of pinning flow. The impurities, super stoichiometric concentrations of elements, and phase boundaries may be plays as pinning centers.

This work is devoted to the experimental determination of the pinning energy of $Bi_2Sr_2Ca_{0.6}Zn_{0.4}Cu_2O_x$ superconducting sample.

It was sintered superconducting $Bi_2Sr_2Ca_{0.6}Zn_{0.4}Cu_2O_x$ and it's the room temperature phase purity analysis was performed by a Brucker D8 advance diffractometer.

The partial replacement of calcium by zinc in $Bi_2Sr_2Ca_{0.6}Zn_{0.4}Cu_2O_x$ the crystal structure is deformed and leads to the formation of defects. By increasing sample heterogeneity, the pinning flow is always enhanced. The small coherence length ξ leads to low energy U_p of the fluxoid and weak pinning energy.

The pinning energy was determined by considering upper critical magnetic fields and the coherence length. From the magnetic field dependence of resistance was determined the value of the upper critical magnetic fields. According to linear part of the dependence, $\ln(\rho/\rho_0) = f(1/T)$ was calculated the pinning energy U_p for fixed magnetic fields. It was observed that the value of U_0 is increased by Zn addition.

It is known that in HTSC materials there exist structural defects. These defects are an effective pinning center for magnetic flux lines. In this case the replacement of Ca with Zn leads to the formation of point defects and the presence of other phases. All this finally led to additional pinning centers and to increase of pinning energy U_p.

Abstract ID: 30557

EFFECT OF RARE EARTH DOPING ON ZINC COBALT FERRITE FOR RESISTIVE RANDOM ACCESS MEMORY

H. Mazhar, M. Anis-ur-Rehman

Applied Thermal Physics Laboratory, Department of physics, COMSATS University Islamabad,45550, PAKISTAN

Cutting edge science and technology needs high quality data storage devices for their applications in artificial intelligence and digital industries. Resistive random access memory (RRAM) is an emerging non-volatile memory used for recording and reproducing the digital information. Resistive Random-Access Memories (R-RAMs) have emerged as better alternatives for conventional charge-based flash memories due to their distinct features like high speed, ultra-low power consumption, simple structure, long retention [1]. In our work, rare earth doped zinc cobalt ferrite were synthesized by sol-gel method. X-ray diffraction (XRD) verified that single-phase spinel ferrites have formed. The following electrical characteristics were investigated between 20Hz-3MHz, such as, dielectric tangent loss, dielectric constant, dielectric loss, AC conductivity, and impedance. I–V measurements were carried out using a metal–insulator–metal (MIM) structure device consisting of an Ag top electrode and an FTO bottom electrode, with the ferrite layer spin-coated onto the pre-processed FTO substrate. In particular, rare earth doped zinc cobalt ferrite elements were frequently employed as insulator layers. The hysteresis behavior, as illustrated in Fig. 1 verified the presence of the resistive switching effect in zinc cobalt ferrite samples. The Co–Zn ferrite–based ReRAM devices demonstrate excellent resistive switching (RS) performance, characterized by long retention time, stable endurance over repeated switching cycles, and a relatively low forming voltage. This study illustrates an approach for developing resistive memory devices with improved performance for future non-volatile memory applications.

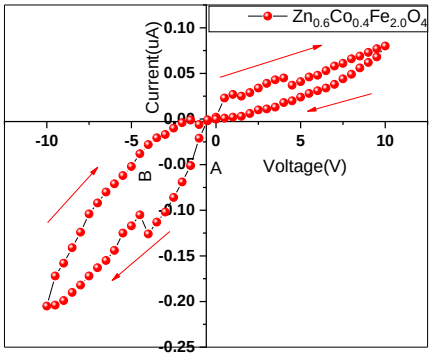

Fig.1: *I-V Hysteresis loop of $Zn_{0.6}Co_{0.4}Fe_2O_4$.*

References

[1] A. R. Patil, T. D. Dongale, R. K. Kamat, K. Y. Rajpure, *Binary metal oxide-based resistive switching memory devices: a status review*, Materials Today Communications **34**, 105356 (2023).

11th International Conference on Superconductivity and Magnetism ICSM2026
4th International Conference on Quantum Materials and Technologies ICQMT2026
19th April to 26th April, 2026, Ölüdeniz – Fethiye/Muğla, Türkiye
https://icsmforever.org/

Abstract ID: 30561

TAILORING THE ELECTRICAL PROPERTIES OF COBALT FERRITES THROUGH LITHIUM DOPING FOR RESISTIVE MEMORY DEVICES

Y. Iqbal, H. Mazhar, K. Naheed, M. Anis-ur-Rehman

Applied Thermal Physics Laboratory, Department of Physics, COMSATS University Islamabad, Islamabad 45550, PAKISTAN

Owing to their profound and inimitable electrical and structural properties cobalt ferrites have found applications in numerous disciplines such as solar cells, frequency devices and data storage devices [1]. Cobalt ferrites show hopping-based charge transport, which is useful for memory devices. In this work, lithium-doped cobalt ferrites with composition $CoFe_{2.5-x}Li_xO_{4-\delta}$ (x = 0.0, 0.1, 0.2, 0.3 and 0.4) were prepared. A simplified sol–gel method was used. These results are consistent with literature. For structural analysis, the phase formation and surface morphology were validated using FTIR spectroscopy and SEM. UV-Visible spectroscopy was used to study the variation of the energy band gap with cobalt concentration in cobalt ferrite and the energy bandgap of the material within the range of 2 electron volts as shown in Fig.1. The electrical properties including the dielectric constant (1.0×10^3), ac conductivity (5.0×10^{-4}) and impedance (3.0×10^6) and when doped with lithium ferrite at the concentration of x=0.2 the dielectric constant (2.5×10^3),ac conductivity (4.0×10^{-4}) and impedance (1.8×10^6) have been studied in the frequency range of 20 Hz to 3 MHz using precision analyzer. I–V characteristics were recorded at room temperature. DC conductivity increases with temperature and follows the Arrhenius relation as in Fig.2. This confirms thermally activated conduction. Charge transport occurs through small polaron hopping between Fe^{2+} and Fe^{3+} ions. The I–V curves show nearly linear behavior with slight hysteresis. Li-doped cobalt ferrites are suitable for ReRAM device application.

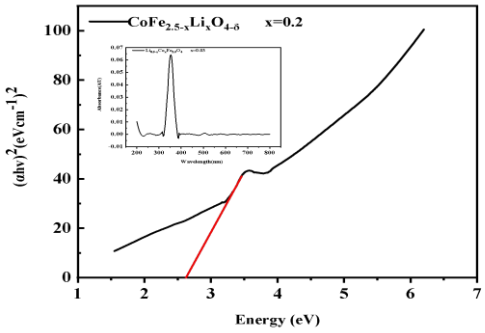

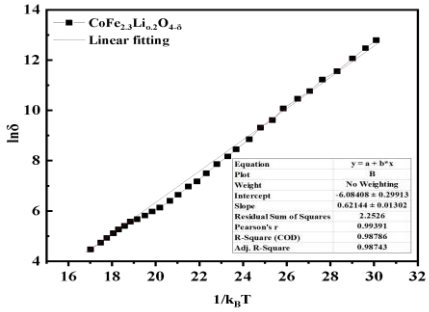

References

[1] K. O. Abdulwahab, M. M. Khan, J. R. Jennings, *Ferrites and ferrite-based composites for energy conversion and storage applications*, Critical Reviews in Solid State and Materials Sciences, **49(5)**, 807-855 (2024).

Abstract ID: 30582

DEVELOPMENT OF FOLATE RECEPTOR TARGETED AND LIPOIC ACID LOADED THERANOSTIC NANOPARTICLES

O. Gok[1,2], S. N. Ozkan[2], E. Ozkul[2], M. N. Atilmis[1], P. S. Unlu[1]

[1] *Acibadem University, Faculty of Engineering and Natural Sciences, Dept. of Biomedical Engineering, 34752, Istanbul, TURKEY*

[2] *Acibadem University, Graduate School of Natural and Applied Sciences, Biomedical Engineering Program, 34752, Istanbul, TURKEY*

DDS is an expression or device that facilitates the entry of a therapeutic agent into the body and improves efficacy and safety by controlling the rate, time and place of release of drugs in the body.[1] Targeted therapy approaches are among the innovative strategies that aim to enhance therapeutic efficacy while minimizing undesired effects in cancer treatment. Among the nano-sized nanocarriers, iron oxide nanoparticles (Fe-NPs) are used as MR contrast agents due to their superparamagnetic properties. They are known for their low toxicity and biocompatibility, together with large surface-to-volume ratio and need high surface energies.[2] Core-Shell nanoparticles enable the transportation of different therapeutic and imaging agents with their multilayered structures coated with PEG. Polyethylene glycol (PEG) is covalently bound to proteins. It is a water-soluble polymer that changes its properties to increase its potential uses.[3]

In this study, the nanoparticle surface of Fe-NPs, a powerful MR imaging agent, was coated with a biocompatible, biodegradable, and pH-sensitive Chitosan polymer, which was conjugated to PEG chains of 500 Da via amidation reaction. As a strong anti-oxidant drug molecule, Lipoic Acid (LA) was also attached to side chains of chitosan as the therapeutic agent with a yield of 90.32%. Prepared polymers were used to physically coat the surface of Fe-NPs and they were characterized for their size by DLS, chemical composition by FT-IR Spectroscopy, morphology by SEM and TEM. The size of nanoparticles was switched from 33 nm to a range of 90-150 nm. The drug release behavior from these nanoparticles concerning time were conducted by dialysis method and the collected samples were analyzed in LC-MS/MS instrument to show the system is pH-sensitive, with significantly higher drug release observed in acidic environments, typical of tumor microenvironments.[4] Their drug encapsulation efficiencies were calculated as 65-67%. A positive surface charge (+16.1 mV) indicates the successful coating of chitosan polymer on Fe-NPs. The nanoparticles were attached to Cy3 fluorescent dye for another imaging strategy (86.4 µg/mL) and folic acid as an active ligand on the surface (53.2 µg/mL) and, which converted the surface charge of NPs to negative (-29.5 and -16.4 mV). Also, the magnetic field response changes for polymer coated iron oxide nanoparticles were confirmed via a magnetometer yielding VSM measurements.

References

[1] S. A. Rizvi, A. M. Saleh, *Applications of nanoparticle systems in drug delivery technology*, Saudi pharmaceutical journal, **26(1)**, 64-70 (2018).

[2] B. Issa, I. M. Obaidat, *Magnetic nanoparticles as MRI contrast agents*, Magn. Reson. Imaging, **378**, 40 (2019).

[3] J. M. Harris, N. E. Martin, M. Modi, Pegylation. Clinical pharmacokinetics, **40(7)**, 539-551 (2001).

[4] L. R. Arcot, M. Lundahl, O. J. Rojas, J. Laine, *Asymmetric cellulose nanocrystals: thiolation of reducing end groups via NHS–EDC coupling* Cellulose, **21(6)**, 4209-4218 (2014).

[5]

Abstract ID: 30585

A BRIEF STUDY OF THE ENHANCED STRUCTURAL AND ELECTRICAL PROPERTIES OF SAMARIUM-DOPED COBALT FERRITE NANOPARTICLES FOR POTENTIAL RESISTIVE RAM APPLICATIONS

H. Ramzan, A. Saif, M. Anis-ur-Rehman

Applied Thermal Physics Laboratory, Department of Physics, COMSATS University Islamabad, PAKISTAN

Owing to their profound and inimitable electrical and structural properties cobalt ferrites have found applications in numerous disciplines such as solar cells, frequency devices and data storage devices. Rare earth doped spinel cobalt ferrite with the general formula CoFe(2-x)SmxO4 (with x = 0.00, 0.05 and 0.1) were synthesized via simplified sol-gel method. The prepared samples were calcined at 6000C and sintered at 6200C for 3 hours. The structural and electrical properties of the prepared samples were studied via different techniques. The spinel structure of all samples was confirmed by X-ray diffraction. XRD confirmed the lattice parameter of pure cobalt ferrite to be 8.391Å. The lattice parameter as well as the crystallite size decreased with increase in Samarium concentration. The electrical properties of the materials were analyzed across varying frequency and temperature. The dielectric constant (ε'), dielectric loss (tanδ), and impedance (Z) seemed to decrease as frequency varied from 100 Hz-3 MHz. DC conductivity was investigated across the temperature range of 300 K-700 K. The DC resistivity exhibited the decreasing trend as the temperature increased but it increased with increase in Samarium content. I-V analysis of all samples showed non-linear, hysteresis-type trend which indicates the resistance changing ability of samples. IV analysis hints that the investigated materials can potentially be used as insulators in metal-insulator-metal (MIM) resistive RAMs.

Abstract ID: 30608

CONTINUOUS AND TOPOLOGICAL PHASE TRANSITIONS IN THE JOSEPHSON MEDIUM OF GRANULAR HIGH-TEMPERATURE SUPERCONDUCTOR $DyBa_2Cu_3O_{7-\delta}$

T. V. Sukhareva

National scientific center "Kharkiv Institute of Physics and Technology," National Academy of Sciences of Ukraine, Akademichna st., 1, Kharkiv 61108, UKRAINE

For the first time, fundamental studies have been carried out on the nature and mechanisms of the influence of the filling of the electron shells of the central atoms in the crystal lattice of granular HTSCs of the 1:2:3 type on the course of continuous and topological phase transitions in a Josephson medium under the influence of an external magnetic field with a change in temperature using the example of $DyBa_2Cu_3O_{7-\delta}$. Based on the study of the influence of temperature and external magnetic field on the transport properties of granular HTSC $DyBa_2Cu_3O_{7-\delta}$, a phase *H-T* diagram was constructed (Fig. 1). It has been established that the presence of internal magnetic field sources in the structure of granular HTSC $DyBa_2Cu_3O_{7-\delta}$ leads to a significant expansion of the region of existence of the Josephson medium, thereby enhancing dissipation processes.

It is shown that the presence of magnetoactive REM atoms in the HTSC structure of the 1:2:3 type and a non-zero internal magnetic field H_{int} *does not affect the nature of the topological phase transitions*. BKT phase transitions occur exclusively in the region of existence of the Josephson medium resistivity, and their relative position on the temperature axis is determined by the nature of the vortex structure, the evolution of which can be controlled using temperature, magnetic field and/or transport current.

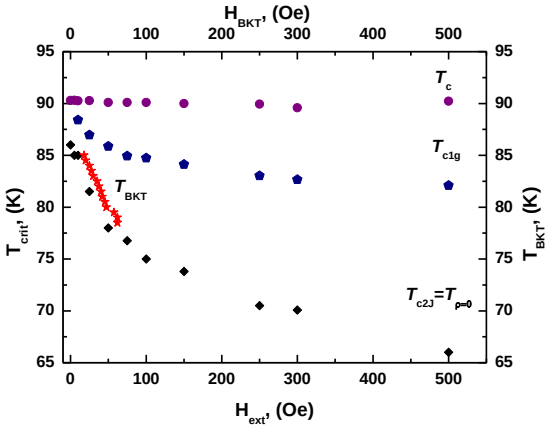

Fig. 1: *Dependences of critical temperatures $T_{c2J}(T_{\varrho=0})$, T_{BKT}, T_{c1g} and T_c of phase transitions of granular HTSC $DyBa_2Cu_3O_{7-\delta}$ on the strength of the external magnetic field.*

Abstract ID: 30613

THE PREPARATION OF HIGH CURRENT PERFORMANCE MgB_2 WIRES WITH CARBON COATED BORON

W. Yuan[1], Q. Guo[1], M. Wang[1], W. Xie[1], Q. Yu[1], Y. Zhu[1], B. Wu[1], Y. Shi[1], J. Li[2], X. Liu[1], Y. Feng[1], P. Zhang[1]

[1] *Western Superconducting Technologies (WST) Co. Ltd., Xi'an 710018, CHINA*
[2] *Superconducting Materials Center, Northwest Institute for Nonferrous Metal Research, Xi'an 710016, CHINA*

Due to the weak intrinsic flux pinning ability, the critical current density of MgB_2 superconductors decreases rapidly with the increase of magnetic field. This defect limits the application of MgB_2 superconductors in strong current transmission and strong magnetic field. According to the literature, carbon is the most effective doping source to improve the critical current density of MgB_2 in medium and high magnetic fields. The amorphous carbon, SiC and TiC three different carbon sources as dopants, the practical In-suit MgB_2 superconducting wire in the middle and high field Jc with the change of magnetic field was studied in this paper. The results showed amorphous carbon doped in MgB_2 wire has the highest Jc. Further, amorphous carbon was used as a dopant to mix with amorphous B powder to obtain uniform carbon-coated boron powder with carbon content of 0, 5~10 %, and 15~20 %, respectively. As a precursor powder, in-suit MgB_2 superconducting wire was prepared. The phase and microstructure differences of B powder with different carbon coating amounts were compared and analyzed by XRD and SEM characterization. The results show that uniform carbon coating on the surface of spherical B powder helps to improve the substitution efficiency of C and provide efficient flux pinning centers. The change of J_c of MgB_2 wires with different carbon coating amounts with the magnetic field was studied. It was found that the MgB_2 wire prepared without carbon-boron powder had higher J_c in the middle and low fields, and the MgB_2 wire prepared with C-boron powder had higher J_c in the high field. The high C doping amount helped to improve the H_{C2} of the wires in the high field. However, the T_c changes of the wires with different C contents were compared by R-T and n-B(T) curves. It was found that the T_c and n values of the wires decreased with the increase of C content.

Abstract ID: 30615

IMPACT OF LARGE-RADIUS IMPURITIES ON METAL/SUPERCONDUCTOR-INSULATOR TRANSITIONS AND SUPERCONDUCTIVITY ENHANCEMENT IN DOPED CUPRATES

S. Dzhumanov[1], U.T. Kurbanov[1,2]

[1] *Institute of Nuclear Physics, Uzbekistan Academy of Sciences, 100214, Tashkent, UZBEKISTAN*
[2] *Tashkent State Technical University, 100095, Tashkent, UZBEKISTAN*

In the high-doping regime, cuprate materials transition from pure insulators to a dual-phase state. This state comprises a metallic component with itinerant carriers and large polarons, alongside an insulating component where charge carriers remain localized. The classic one-electron band model and Wilson's band-filling rules [1] fail to explain the insulating state of undoped cuprates and various transition metal oxides possessing partially filled *d*-bands [2–7]. This limitation was overcome by Mott [3,5], who demonstrated that strong electron–electron correlations drive the metal–insulator transition. His established criterion for this transition in both doped and undoped systems has underpinned decades of intensive scientific inquiry.

In this paper, the possibility of hole localization and metal/superconductor–insulator transitions in large-radius impurity-doped La-cuprates is analyzed via the single-carrier model, leading to a refined understanding of these effects. The study further examines the interplay between superconductor–insulator transitions and different disorder mechanisms in the context of high-T_c enhancement in doped cuprates.

The work is financed by the state budget of the Republic of Uzbekistan.

References

[1] A.H. Wilson, Proc. R. Soc. Lond. A **133**, 458–491 (1931).
[2] J.H. de Boer, E.J.W. Verwey, Proc. Phys. Soc. **49**, 59 (1937).
[3] N.F. Mott, Proc. Phys. Soc. A **62**, 416 (1949).
[4] F.T. Walz, J. Phys.: Condens. Matter. **14**, R285 (2002).
[5] N.F. Mott, Metal-Insulator Transitions (Taylor and Francis, London, 1990).
[6] M. Imada, A. Fujimori, Y. Tokura, Rev. Modern Phys. **70**, 1039 (1998).
[7] S. Dzhumanov, Theory of Conventional and Unconventional Superconductivity in the High-T_c Cuprates and Other Systems (Nova Science Publishers, New York, 2013).

Abstract ID: 30624

THEORETICAL STUDY OF THE SEEBECK EFFECT IN DOPED HIGH-T_c CUPRATE SUPERCONDUCTORS USING THE HUBBARD MODEL

I. Sh. Kabulov[1], D. G'. Khajibaev[2], S. Dzhumanov[3], B. Ya. Yavidov[2], E. X. Karimbaev[1,3]

[1] *Institute of Fundamental and Applied Research, National Research University TIIAME, Kori Niyoziy 39, Tashkent 100000, UZBEKISTAN*
[2] *Nukus State Pedagogical Institute named after Ajiniyaz, 230105 Nukus, UZBEKISTAN*
[3] *Institute of Nuclear Physics, Academy of Sciences of the Republic of Uzbekistan, Ulugbek, 100214 Tashkent, UZBEKISTAN*

The Seebeck effect is a key probe for exploring charge transport and strong electronic correlations in high-T_c cuprate superconductors, which exhibit unconventional superconductivity and pseudogap behavior. While several experimental studies have reported temperature and doping-dependent thermoelectric responses in high-T_c cuprates [1–3], a unified theoretical description considering strong correlations and superconducting gap symmetry remains limited. Here, we present a **theoretical analysis** of the Seebeck effect in underdoped, optimally doped and overdoped high-T_c cuprates using the two-dimensional Hubbard model, incorporating on-site Coulomb repulsion and nearest-neighbor hopping. In the normal state, we study how hole doping and the pseudogap regime influence carrier asymmetry, entropy transport, and scattering mechanisms. Our results reproduce experimental trends [1–3] while providing microscopic insight into thermoelectric behavior. In the superconducting state, Cooper pair formation suppresses the Seebeck coefficient, but residual contributions arise from nodal quasiparticles in the d-wave gap. We analyze how electronic correlations, gap symmetry, and doping together determine the temperature dependence and magnitude of the thermoelectric response. Previous studies treated normal or superconducting transport separately [4–6], our approach **unifies both regimes** within a single Hubbard model framework, offering **novel insights** into correlated transport phenomena. Overall, this work demonstrates that Hubbard-model calculations, combined with experimental observations [1–3], provide a coherent framework for understanding thermoelectric response in doped high-T_c cuprates. The results highlight the value of Seebeck effect measurements as a sensitive tool to probe electronic correlations, pseudogap behavior, and unconventional superconducting mechanisms in strongly correlated materials.

References

[1] I. Terasaki, Y. Sasago, K. Uchinokura, *Large thermoelectric power in $NaCo_2O_4$ single crystals*, *Phys. Rev. B,* **46(19)**, 14514–14521 (1992).
[2] S. D. Obertelli, J. R. Cooper, J. L. Tallon, *Systematics in the thermoelectric power of high-T_c superconductors*, *Phys. Rev. B,* **46(22)**, 14928–14931 (1992).
[3] Y. Wang, L. Li, N. P. Ong, *Nernst effect in high-T_c superconductors*, *Phys. Rev. B,* **64(22)**, 224519 (2001).
[4] W. Koshibae, K. Tsutsui, S. Maekawa, *Thermopower in correlated systems: The effect of electron correlations*, *Phys. Rev. B,* **62(11)**, 6869–6872 (2000).
[5] C. Honerkamp, T. M. Rice, M. Sigrist, *Thermoelectric transport in unconventional superconductors*, *Phys. Rev. B,* **63(14)**, 140403 (2001).
[6] W. O. Putikka, M. U. Luchini, E. Dagotto, *Thermoelectric response of the 2D Hubbard model*, *Phys. Rev. Lett.,* **69(9)**, 2280–2283 (1992).

Abstract ID: 30625

RESEARCH ON PREPARATION OF HIGH CRITICAL CURRENT AND HIGH THERMAL STABILITY CABLE-IN-CHANNEL (CIC) SUPERCONDUCTING WIRES

J. Hu[1], Q. Guo[1,2], R. Wang[1,2], X. Liu[2], W. B. Jia[2], Y. W. Yang[1], Y. K. Fang[1]

[1] *Western Superconducting Technologies Co.,Ltd CHINA*
[2] *Xi'an Superconducting Wire Technologies Co., Ltd. CHINA*

With the continuous innovation of special superconducting magnet technology, the magnetic field requirements for superconducting magnets, their core components, are increasingly stringent, posing new demands for large copper ratio and large-size NbTi/Cu superconducting wires with high critical current and high thermal stability. Conventional Wire-in-Channel (WIC) NbTi/Cu superconducting wires have a maximum critical current of only 2000A at 4.2K and 4T, which fails to meet customer requirements.

In this paper, the Cable-in-Channel (CIC) process route was adopted to successfully prepare kilometer-grade high-performance NbTi/Cu superconducting wires with ten-thousand-ampere level, achieving a new breakthrough in the performance of NbTi/Cu superconducting wires. Firstly, 7 strands of NbTi/Cu wires were cabled, and the cabling pitch and tension were optimized to obtain kilometer-grade round cables. Then, the round cables were subjected to on-line tin plating, and tin-plated round cables were obtained by optimizing on-line tin plating parameters (temperature, speed, tension, etc.). Finally, the tin-plated round cables were embedded into large-size copper channel wires, and through optimizing key embedding and welding parameters (temperature, speed, processing rate, etc.), large-size kilometer-grade CIC superconducting cables with a width of up to 6mm were successfully prepared.

By optimizing the processing technology of large-size copper channel wires, the problems of uneven surface stress distribution, low residual resistance ratio (RRR) and high difficulty in long-length preparation of copper channel wires were solved, and large-size copper channel wires with high RRR were obtained. Through optimizing process parameters such as soldering temperature, speed and processing rate, an embedding and welding process with high RRR and CIC bare wires with good surface tin plating were achieved.

Meanwhile, the braided insulation process of large-size CIC cables was studied; by using different insulation materials, wire specifications and pitches, a stable braided insulation process with a stable voltage resistance of more than 500V was obtained. Comprehensive performance tests and evaluations of the CIC cables show that their critical current reaches 12kA at 4.2K and 4T, the RRR is as high as 200, and the dimensional accuracy of kilometer-grade cables is up to ±0.02mm, meeting the demands of special high-field superconducting magnets for wires with high critical current and high thermal stability.

Abstract ID: 30633

FORMATION OF MATTER-WAVE MODES IN BOSE-EINSTEIN CONDENSATES

O. Y. Otajonov[1], T. Iskandarov[2], E. X. Karimbaev[3,4]

[1] *New Uzbekistan University, Dept. of Physics, Tashkent city, Mirzo Ulugbek district, Movarounnahr street 1, 100007, UZBEKISTAN*
[2] *State Institution "Scientific and Technical Center for Radiation and Nuclear Safety", Khadra str, 100011 Tashkent, UZBEKISTAN*
[3] *Institute of Fundamental and Applied Research, National Research University TIIAME, Kori Niyoziy 39, Tashkent 100000, UZBEKISTAN*
[4] *Institute of Nuclear Physics, Academy of Sciences of the Republic of Uzbekistan, Ulugbek, 100214 Tashkent, UZBEKISTAN*

The formation of matter-wave modes in Bose-Einstein condensates (BECs) represents a fundamental manifestation of macroscopic quantum coherence and nonlinear dynamics in ultracold atomic systems [1,2]. Since the experimental realization of BECs in dilute atomic gases [1], extensive theoretical and experimental studies have focused on understanding how collective matter-wave patterns emerge and evolve under external confinement and interatomic interactions [2,3].

In this work, we present a theoretical study of matter-wave mode formation in BECs within the framework of the Gross-Pitaevskii equation (GPE), which is formally equivalent to a nonlinear Schrödinger equation describing the condensate wave function at ultralow temperatures [4,5]. The GPE incorporates kinetic energy, external trapping potential, and nonlinear atom-atom interactions originating from s-wave scattering. We analyze how the interplay between dispersion and nonlinearity governs the emergence of stationary and dynamical matter-wave modes.

Special attention is devoted to nonlinear effects leading to the excitation of higher-order modes, soliton-like structures, and collective oscillations in trapped condensates [6]. We further investigate the role of time-dependent modulation of the trapping potential and interaction strength as effective mechanisms for controlled generation of matter-wave modes [3,5]. The correspondence between the GPE and the general nonlinear Schrödinger equation is discussed, highlighting the universality of nonlinear wave phenomena in quantum fluids [6].

Our results demonstrate that matter-wave mode formation is strongly influenced by trap geometry, dimensionality, and interaction strength, reflecting a delicate balance between kinetic and nonlinear energies. These findings provide deeper insight into nonlinear quantum dynamics in BECs and are relevant for applications in atom interferometry, coherent matter-wave control, and precision quantum measurements [2,7].

References

[1] M. H. Anderson, *et al.*, Science **269**, 198–201 (1995).
[2] L. P. Pitaevskii, S. Stringari, Bose–Einstein Condensation. Oxford (2003).
[3] C. J. Pethick, H. Smith, BEC in Dilute Gases. Cambridge (2008).
[4] E. P. Gross, Nuovo Cimento **20**, 454–477 (1961).
[5] F. Dalfovo, *et al.*, Rev. Mod. Phys. **71**, 463–512 (1999).
[6] P. G. Kevrekidis, *et al.*, The Defocusing NLSE. SIAM (2015).
[7] L. Pitaevskii, Phys.-Usp. **59**, 109–128 (2016).

Abstract ID: 30642

INVESTIGATION OF ELECTRICAL TRANSPORT AND DIELECTRIC RESPONSE IN Zn–Mn–Co SPINEL FERRITES AS A FUNCTION OF TEMPERATURE

H. Mazhar, S. Kousar, M. Anis-ur-Rehman

Applied Thermal Physics Laboratory, Department of Physics COMSATS University Islamabad, Islamabad 45550, PAKISTAN

Ferrite materials are extensively investigated owing to their diverse applications in scientific and technological fields. Their unique combination of electrical, dielectric, and magnetic characteristics classifies them as a vital group within functional ceramic materials. In this work, pure and cobalt-doped manganese zinc samarium ferrites with the general formula $Zn_{0.6}Mn_{0.4-x}Co_xFe_{1.8}Sm_{0.2}O_4$ were successfully synthesized using a sol–gel method and sintered at 650 °C for 3 h. X-ray diffraction (XRD) confirmed the formation of a single-phase cubic spinel structure. The dielectric properties and AC conductivity were systematically investigated over a frequency range of 100 Hz–3MHz and a temperature range of 100–500°C. Temperature-dependent dielectric relaxation was analyzed by using Debye fitting. Jonscher's universal power law was employed to model the AC conductivity. The variation of the frequency exponent (n) with temperature indicated distinct conduction mechanisms: small polaron hopping (SPH) dominated. The compositions, $Zn_{0.6}Mn_{0.3}Co_{0.1}Fe_{1.8}Sm_{0.2}O_4$ exhibited improved electrical pathways, making it the most promising candidate for high-temperature applications, including capacitors and spintronic devices.

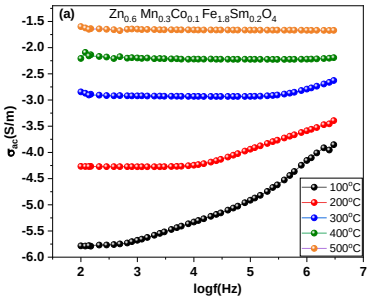

Fig.1: *AC conductivity of different temperature for $Zn_{0.6}Mn_{0.3}Co_{0.1}Fe_{1.8}Sm_{0.2}O_4$.*

References

[1] K. O. Abdulwahab, M. M. Khan, J. R. Jennings, *Ferrites and ferrite-based composites for energy conversion and storage applications*, Critical Reviews in Solid State and Materials Sciences **49**, **no. 5**, 807-855 (2024).

Abstract ID: 30646

FREQUENCY AND ELECTRIC FIELD-DEPENDENT CAPACITANCE BEHAVIOR IN BENZOIC ACID MODIFIED POLYURETHANE COMPOSITES

G. Sayın[1], S. Kurnaz[2], T. Seydioğlu[3], E. Aşıkuzun Tokeşer[4], Ö. Öztürk[1]

[1] *Kastamonu University, Department of Electrical & Electronics Engineering, Kastamonu, TÜRKIYE*
[2] *Kastamonu University, Central Research Laboratory, Kastamonu, TÜRKIYE*
[3] *Kastamonu University, Vocational School, Department of Electronics and Automation, Kastamonu, TÜRKIYE*
[4] *Kastamonu University, Department of Material Science and Engineering, Kastamonu, TÜRKIYE*

The addition of organic additives with polar groups to polymer matrices allows for the control of dielectric properties using frequency and electric fields. In this study, composite films were prepared by adding Benzoic Acid (BA) (0–10%) to a Thermoplastic Polyurethane (TPU) matrix. The dielectric behavior was analyzed in the frequency range of 1 kHz to 10 MHz under different electric field strengths (0, 4, 8, and 12 kV/cm). Fig. 1 shows that the capacitance decreases as the frequency increases. However, the capacitance values increase when an external electric field is applied. This enhancement indicates that BA strengthens the dipolar and interfacial polarization within the material. Consequently, the capacitance can be effectively controlled by adjusting the additive ratio, frequency, and electric field strength. This tunable behavior is advantageous for TPU-based applications, such as capacitive sensors, flexible electronic circuits, and dielectric layers.

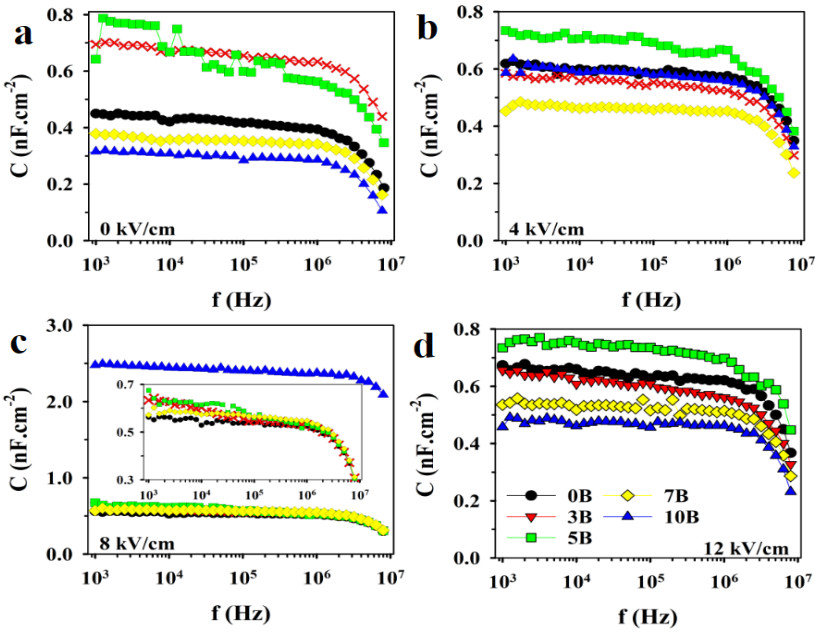

Fig. 1: *Frequency dependence of the dielectric properties for neat TPU and TPU/BA composites under various DC electric fields.*

This work was supported by Kastamonu University Scientific Research Projects Coordination Unit of Türkiye (KÜ-BAP01/2025-23).

Abstract ID: 30647

THE EFFECT OF EFFECT OF Co ON PARTICLE SIZE, MAGNETIC PROPERTIES AND MICROWAVE ABSORBANCE PROPERTIES OF Fe-25%Ni-5%Si-x%Co (x=0, 10, 15) NANO ALLOYS

H. Gungunes, S. Delice

Department of Physics, Hitit University, 19040 Çorum, TURKEY

In this study, the effect Co amount on the particle size, magnetic properties and microwave properties of bulk Fe-25%Ni-5%Si-x%Co (x=0, 10, 15) alloys after 75 h of milling by using SEM, VSM, Mössbauer Spectroscopy and VNA. The Average particle size for 0Co, 10Co and 15Co alloys was determined to be 140nm, 130nm and 55 nm, respectively. According to Mössbauer results, The Fe^{3+} was formed in the Fe-25%Ni-5%Si alloy while Fe^{3+} and Fe^{2+} formation were observed in the Fe-25%Ni-5%Si-10%Co and Fe-25%Ni-5%Si-15%Co alloys. The paramagnetic phase was formed only in Fe-25%Ni-5%Si and Fe-25%Ni-5%Si-15%Co alloys while ferromagnetic phase formed in the addition to the paramagnetic phase in the Fe-25%Ni-5%Si-10%Co alloy. The electromagnetic absorption behavior of nano alloys was evaluated in the frequency range of 8.2–12.4 GHz based on the calculated reflection loss (RL). The S_{11} parameters for 0Co, 10Co and 15Co alloys were determined to be -4.87dB, -5,43 dB and -4.89 dB respectively. However magnetization parameters such as M_s, M_r and H_c were determined by using VSM analysis.

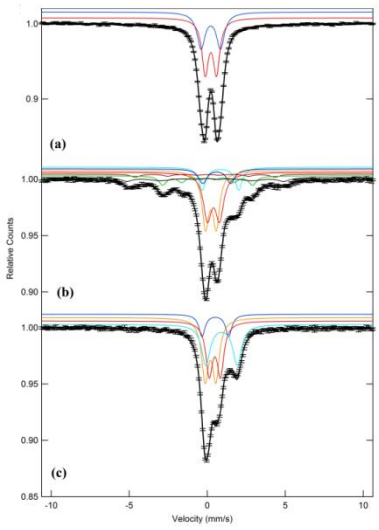

Fig. 1: *Room temperature Mössbauer spectra of Fe-28%Ni-5%Si-15%Co alloys.*

References

[1] S. Delice, U. Erdem, H. Gungunes, T. Kırındı, E. Aksu, U. Sarı, Mat. Chem and Phys. **352**, 132048 (2026).

[2] U. Erdem, K.A. Sarı, D.E. Dogan, H. Gungunes, G.O. Arıcan, U. Sarı, Journal of Alloys and Compounds **1036**, 181958 (2025).

Abstract ID: 30650

INFLUENCE OF A LOW-TEMPERATURE SN ACTIVATOR AND SINTERING CONDITIONS ON IMD-PROCESSED MgB_2 SUPERCONDUCTING WIRES

Y. Oznal[1,2], C. Guo[3], F. Almokdad[4], F. Ervüz[1], H. Koralay[5], S. Safran[1,6], S. Salahi[7], A. Seçkin[8], K. Sönmez[1,4], S. C. Taşkın[1], D. Wang[3], A. Gencer[1,6], Y. Ma[3]

[1] *Ankara University, Superconductor Technologies Application and Research Center, Ankara, TÜRKIYE*
[2] *Ankara University, Elmadag Vocational School, Electronics and Automation Department, Ankara, TÜRKIYE*
[3] *Chinese Academy of Sciences, Institute of Electrical Engineering, Key Laboratory of Applied Superconductivity, Beijing 100190, PEOPLES REPUBLIC OF CHINA*
[4] *Ankara University, Graduate School of Natural and Applied Sciences, Ankara, TÜRKIYE*
[5] *Gazi University, Science Faculty, Physics Department, Ankara, TÜRKIYE*
[6] *Ankara University, Science Faculty, Physics Department, Ankara, TÜRKIYE*
[7] *Gazi University, Department of Metallurgical and Materials Engineering, Ankara, TÜRKIYE*
[8] *Gazi University, Basic and Engineering Sciences Central Laboratory Application and Research Center (GUTMAM), Ankara, TÜRKIYE*

Magnesium diboride (MgB_2) superconducting wires continue to draw strong interest for intermediate-temperature applications, owing to their attractive balance of performance, material availability, and relatively affordable cooling requirements. To date, the incorporation of low-temperature activators in MgB_2 systems has been predominantly examined in Powder-in-Tube (PIT)-based fabrication schemes, with comparatively limited studies addressing their interaction with magnesium transport and phase evolution in IMD-processed filaments. Accordingly, in this work, MgB_2 wires are prepared using an Internal Magnesium Diffusion (IMD) method using carbon-doped boron powder precursors and a tin-coated magnesium rod. The study explores how the presence of a low-temperature Sn activator influences magnesium transport, phase formation, and the resulting filament structure during wire processing. Alongside the role of the Sn coating, the effects of sintering temperature and dwell time on both the microstructural and superconducting characteristics of the wires are examined. The superconducting transition behavior is evaluated through temperature-dependent resistivity (R-T) measurements under zero-field and applied magnetic field conditions. By linking processing parameters with structural properties and functional performance, this work seeks to provide insight into the design of IMD-processed MgB_2 wires suited for scalable fabrication and high-field superconducting applications.

Acknowledgment

This work has been supported by TÜBİTAK and the Chinese Academy of Sciences (CAS) through a Bilateral Cooperation program under Contract No. 123N624.

Abstract ID: 30651

SUPERCONDUCTING AND STRUCTURAL PROPERTIES OF Ag-COATED MgB_2 WIRES PRODUCED BY IMD METHOD

F. Ervüz[1] , S. C. Taşkın[1], C. Guo[3], F. Almokdad[4], H. Koralay[5], Y. Oznal[1,8], S. Safran[1,2], S. Salahi[6], A. Seçkin[7], K. Sönmez[1,4], D. Wang[3], A.Gencer[1,2], Y. Ma[3]

[1] *Ankara University, Superconductor Technologies Application and Research Center, Ankara, TÜRKIYE*
[2] *Ankara University, Science Faculty, Physics Department, Ankara, TÜRKIYE*
[3] *Chinese Academy of Sciences, Institute of Electrical Engineering, Key Laboratory of Applied Superconductivity, Beijing 100190, PEOPLES REPUBLIC OF CHINA*
[4] *Ankara University, Graduate School of Natural and Applied Sciences, Ankara, TÜRKIYE*
[5] *Gazi University, Science Faculty, Physics Department, Ankara, TÜRKIYE*
[6] *Gazi University, Department of Metallurgical and Materials Engineering, Ankara, TÜRKIYE*
[7] *Gazi University, Basic and Engineering Sciences Central Laboratory Application and Research Center (GUTMAM), Ankara, TÜRKIYE*
[8] *Ankara University, Elmadag Vocational School, Electronics and Automation Department, Ankara, TÜRKIYE*

This study presents the fabrication of magnesium diboride (MgB_2) superconducting wires using carbon-doped boron powders and silver-coated magnesium rods through the Internal Magnesium Diffusion (IMD) technique. Although numerous studies in the literature have examined Ag/MgB_2 wires primarily fabricated by the Powder-in-Tube (PIT) method, the influence of Ag on MgB_2 wires employing IMD techniques has remained comparatively less explored. In this work, Ag-coating deposited by a physical vapor deposition (PVD) method is introduced as an activator layer to examine its role during magnesium diffusion, phase formation, and microstructural development. The effects of Ag coating, as well as sintering temperature and sintering time, on the microstructural and superconducting properties of the prepared wires are systematically investigated. Temperature-dependent resistivity measurements under magnetic fields are employed to assess the superconducting transition behavior. This study aims to establish correlations between processing parameters, microstructural evolution, and superconducting performance in IMD-fabricated MgB_2 wires for high-field and scalable superconducting applications.

This work has been supported by TÜBİTAK and the Chinese Academy of Sciences (CAS) through a Bilateral Cooperation program under Contract No. 123N624.

Abstract ID: 30652

THE INFLUENCE OF Cu, Sn, AND Ag ACTIVATOR COATINGS ON THE SUPERCONDUCTING PERFORMANCE OF MgB_2 WIRES

S. Salahi[1], C. Guo[2], F. Almokdad[3], F. Ervüz[4], H. Koralay[5], S. Safran[4,6], Y. Oznal[4,7], A. Seçkin[8], K. Sönmez[3,4], S. C. Taşkın[4], A.Gencer[4,6], D. Wang[2], Y. Ma[2]

[1] *Gazi University, Department of Metallurgical and Materials Engineering, Ankara, TÜRKIYE*
[2] *Chinese Academy of Sciences, Institute of Electrical Engineering, Key Laboratory of Applied Superconductivity, Beijing 100190, PEOPLES REPUBLIC OF CHINA*
[3] *Ankara University, Graduate School of Natural and Applied Sciences, Ankara, TÜRKIYE*
[4] *Ankara University, Superconductor Technologies Application and Research Center, Ankara, TÜRKIYE*
[5] *Gazi University, Science Faculty, Physics Department, Ankara, TÜRKIYE*
[6] *Ankara University, Science Faculty, Physics Department, Ankara, TÜRKIYE*
[7] *Ankara University, Elmadag Vocational School, Electronics and Automation Department, Ankara, TÜRKIYE*
[8] *Gazi University, Basic and Engineering Sciences Central Laboratory Application and Research Center (GUTMAM), Ankara, TÜRKIYE*

Magnesium diboride (MgB_2), characterized by a superconducting transition temperature of approximately 39 K, has established itself as a highly promising material for practical superconducting applications operating near 20 K. Its intrinsic advantages, including strong superconducting performance, the abundance of constituent elements, and reduced cryogenic cost requirements, make MgB_2 particularly suitable for operation within the intermediate temperature range. Regarding preparation techniques, MgB_2 superconducting wires are predominantly produced using the Powder-in-Tube (PIT) and Internal Magnesium Diffusion (IMD) methods, as these approaches facilitate the formation of a dense MgB_2 microstructure with enhanced inter-granular connectivity, thereby leading to improved transport critical current density (J_c). Recently, IMD-fabricated MgB_2 wires have gained increasing attention due to research aimed at improving filament uniformity and superconducting filling factor. Although PIT processing has driven major advances over the past two decades, IMD has emerged as a strong alternative by enabling higher J_c and superior superconducting performance. The IMD method was employed in this work to manufacture continuous-length MgB_2 superconducting wires intended for high-field applications. The study provides a comparative evaluation of low-temperature activation strategies with Mg rods coated with copper (Cu), tin (Sn), and silver (Ag), while pure Mg rods were used as a reference. The influence of coating material and sintering parameters on superconducting behavior was examined through temperature-dependent resistivity measurements under applied magnetic fields. The experimental results demonstrate that coating of Mg rod with low temperature activators influences the microstructural characteristics and defect distributions and consequently the superconducting performance.

Acknowledgment

This work has been supported by TÜBİTAK and the Chinese Academy of Sciences (CAS) through a Bilateral Cooperation program under Contract No. 123N624.

Abstract ID: 30653

Cu-COATED IMD FABRICATION OF MULTIFILAMENT MgB_2 WIRES WITH ENHANCED SUPERCONDUCTING PROPERTIES

F. Al-Mokdad[1], K. Sönmez[1,2], C. Guo[3], F. Ervüz[2], S. Safran[2,4], H. Koralay[5], S. Salahi[6], S. C. Taşkın[2], A. Seçkin[7],Y. Oznal[2,8], D. Wang[3], A.Gencer[2,4], Y. Ma[3]

[1] *Ankara University, Graduate School of Natural and Applied Sciences, Ankara, TÜRKIYE*
[2] *Ankara University, Superconductor Technologies Application and Research Center, Ankara, TÜRKIYE*
[3] *Chinese Academy of Sciences, Institute of Electrical Engineering, Key Laboratory of Applied Superconductivity, Beijing 100190, PEOPLES REPUBLIC OF CHINA*
[4] *Ankara University, Science Faculty, Physics Department, Ankara, TÜRKIYE*
[5] *Gazi University, Science Faculty, Physics Department, Ankara, TÜRKIYE*
[6] *Gazi University, Department of Metallurgical and Materials Engineering, Ankara, TÜRKIYE*
[7] *Gazi University, Basic and Engineering Sciences Central Laboratory Application and Research Center (GUTMAM), Ankara, TÜRKIYE*
[8] *Ankara University, Elmadag Vocational School, Electronics and Automation Department, Ankara, TÜRKIYE*

Magnesium diboride (MgB_2) exhibits a superconducting transition temperature of approximately 39 K and presents a unique combination of high performance, abundant raw materials, and economic feasibility, thereby establishing itself as a highly promising material for superconducting applications in the intermediate cryogenic temperature range, even with liquid Hydrogen cooling to operate temperature around 20 K. In recent years, the Internal Magnesium Diffusion (IMD) technique has gained recognition as an advanced alternative to conventional Powder-in-Tube (PIT) processing, mainly because it enables the formation of a highly dense superconducting matrix characterized by improved grain connectivity and substantially enhanced transport critical current density (J_c). Furthermore, recent investigations on multifilament MgB_2 wires have demonstrated that the superconducting core with multiple fine filaments effectively enhances both operational stability and current-carrying performance at lower temperatures around 20 K. In the present work, seven-filament MgB_2 wires were produced via the IMD process employing C-coated boron powder and two distinct magnesium precursors: (I) Pure magnesium rods and (II) Cu-coated magnesium rods. The objective of this research is to enhance the superconducting properties of IMD-fabricated multifilament wires by facilitating more effective magnesium diffusion and inducing a refined microstructural development through Cu activation. The microstructural features were analyzed using scanning electron microscopy (SEM) and optical microscopy, whereas the superconducting performance was evaluated by J_c measurements under applied magnetic fields and temperature-dependent resistivity (R-T) measurements to identify the superconducting transition onset. The application of Cu-coated magnesium precursors produced a more uniform filament configuration and enhanced inter-granular connectivity, consequently achieving higher J_c values at 10 T. Resistivity measurements further suggested that the coating of Cu facilitates effective diffusion processes and leads to a sharper superconducting transition width. The results underscore the potential of Cu-assisted IMD processing as an effective strategy for advancing multifilament MgB_2 conductors, while highlighting the necessity for additional quantitative investigations into the fundamental diffusion and reaction mechanisms involved.

This work has been supported by TÜBİTAK and the Chinese Academy of Sciences (CAS) through a Bilateral Cooperation program under Contract No. 123N624.

Abstract ID: 30656

OVERVIEW OF MAGNETIC LEVITATION AND LATERAL FORCES IN MgB_2 BULKS WITH VARIOUS FABRICATION TECHNIQUES

B. Savaşkan[1], P. Badica[2], S. B. Güner[3]

[1] *Karadeniz Technical University, Faculty of Technology, Energy Systems Engineering, 61830, Trabzon, TÜRKIYE*
[2] *National Institute of Materials Physics, Bucharest, ROMANIA*
[3] *Recep Tayyip Erdogan University, Faculty of Arts and Sciences, Department of Physics, Rize, TÜRKIYE*

This study aims to investigate the relationship between the sintering mechanisms and the magnetic levitation performance of MgB_2 bulks produced by spark plasma sintering and conventional sintering methods. The conventional sintering method, *in-situ* and *ex-situ*, is the initial and most used method to prepare MgB_2 bulks [1]. In these methods, although the superconducting phase can be obtained with easily, the sintered bulk is generally only around 50% dense, due to formation of large pores. One of the most effective methods for producing high-density MgB_2 bulk is the use of high pressure. Spark plasma sintering (SPS) is one of the preferred techniques to prepare highly dense MgB_2 bulks. We investigated the magnetic levitation properties of MgB_2 disks produced using both conventional sintering and SPS at a temperature of 20 K. Vertical levitation force (F_z) and lateral force (F_x) measurements at 25 and 20 K were made under zero field cooling (ZFC) and field cooling (FC) conditions.

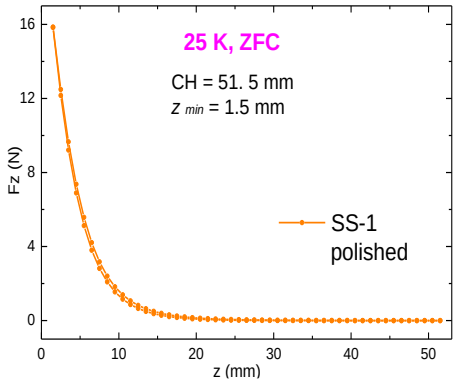

Fig. 1: *The levitation force (F_z) versus vertical distance (z) for SPS MgB_2 under ZFC regime at 25 K.*

References

[1] B. Savaskan, U. K. Ozturk, S. B. Guner c, M. Abdioglu, M. V. Bahadır, S. Acar, M. Somer, A. M. Ionescu, C. Locovei, M. Enculescu, P. Badica, , Journal of Alloys and Compounds **961**, 170893(2023).

Abstract ID: 30657

ECO-FRIENDLY MAGNETIC SILICA NANOCOMPOSITES: FROM RICE HUSK WASTE TO RAPID RECOVERY OF BRILLIANT BLUE R DYE

B. Akmeşe[1], Ç. Dönmez Güngüneş[2], V. Aliyev[3], İ. Tosun Satır[4]

[1] *Vocational School of Health Services/ Department of Pharmacy Services, Hitit University, 19030, TÜRKIYE*
[2] *Faculty of Health Sciences/ Department of Nutrition and Dietetics, Hitit University, 19200, TÜRKIYE*
[3] *Institute of Graduate Education, Hitit University, 19030, TÜRKIYE*
[4] *Faculty of Engineering and Natural Sciences/ Department of Chemistry, Hitit University, 19030, TÜRKIYE*

This study demonstrates the extraction of silica from rice husk, an agricultural byproduct, employing an environmentally sustainable method, and the successful synthesis of silica-based magnetic nanoparticles (Si-MNPs). The Si-MNPs were characterized using XRD, SEM, BET, FTIR, and Mössbauer spectroscopy, which confirmed the formation of the magnetic phase and the successful integration of silica. A key feature of these nanoparticles is their significant magnetic susceptibility, which enables rapid and efficient recovery from aqueous solutions via an external magnetic field, bypassing the need for traditional filtration or centrifugation. The adsorption capacity and efficiency of the synthesized Si-MNPs for removing Brilliant Blue R (BBR) dye were thoroughly evaluated. To optimize the process, the influence of variables such as pH, adsorbent dosage, contact time, temperature, and initial dye concentration was systematically investigated in a batch system. The results indicated that the highest adsorption capacity was achieved under acidic conditions (pH 2), with removal efficiency reaching equilibrium at an adsorbent mass of 0.08 g. Kinetic and temperature analyses demonstrated that the adsorption was initially rapid and that higher temperatures (20°C to 40°C) enhanced the process, yielding a maximum adsorption capacity of approximately 5.9 mg/g at 40°C. The adsorption data were further analyzed using kinetic models (pseudo-first-order, pseudo-second-order, and intraparticle diffusion) and isotherm models (Langmuir, Freundlich, and Dubinin-Radushkevich). This research highlights the potential of low-cost, waste-derived magnetic nanomaterials as highly efficient and easily separable adsorbents for environmental remediation.

Acknowledgements

This work was supported by the Hitit University Scientific Research Projects Coordination Unit (BAP) under grant number SHMYO19001.24.001.

References

[1] U. Fathanah, S. Muchtar, S. Aprilia, M.R. Lubis, S. Mulyati, M. Yusuf, *Unlocking synergies of $Mg(OH)_2$ and rice husk silica as dual additives for tailored pore properties, selectivity, and antifouling performances of PES membrane*, S. Afr. J. Chem. Eng. **48**, 22-29 (2024). https://doi.org/10.1016/j.sajce.2024.01.004.

[2] V Gargiulo, F.D. Natale, M. Alfe, *From agricultural wastes to advanced materials for environmental applications: Rice husk-derived adsorbents for heavy metals removal from wastewater*, J. Environ. Chem. Eng. **12**, 113497 (2024). https://doi.org/10.1016/j.jece.2024.113497.

Abstract ID: 30666

EFFECT OF Cu COATING THICKNESS ON MAGNESIUM DIFFUSION AND SUPERCONDUCTING PROPERTIES OF IMD-PROCESSED MgB_2 WIRES

K. Sönmez[1,4], C. Guo[3], F. Almokdad[4], F. Ervüz[1], H. Koralay[5], Y. Oznal[1,8], S. Safran[1,2], S. Salahi[6], A. Seçkin[7], S. C. Taşkın[1], D. Wang[3], A.Gencer[1,2], Y. Ma[3]

[1] *Ankara University, Superconductor Technologies Application and Research Center, Ankara, TÜRKIYE*
[2] *Ankara University, Science Faculty, Physics Department, Ankara, TÜRKIYE*
[3] *Chinese Academy of Sciences, Institute of Electrical Engineering, Key Laboratory of Applied Superconductivity, Beijing 100190, PEOPLES REPUBLIC OF CHINA*
[4] *Ankara University, Graduate School of Natural and Applied Sciences, Ankara, TÜRKIYE*
[5] *Gazi University, Science Faculty, Physics Department, Ankara, TÜRKIYE*
[6] *Gazi University, Department of Metallurgical and Materials Engineering, Ankara, TÜRKIYE*
[7] *Gazi University, Basic and Engineering Sciences Central Laboratory Application and Research Center (GUTMAM), Ankara, TÜRKIYE*
[8] *Ankara University, Elmadag Vocational School, Electronics and Automation Department, Ankara, TÜRKIYE*

Magnesium diboride (MgB_2) superconducting wires continue to be an important research topic for intermediate-temperature applications due to the favorable balance they offer between superconducting performance, raw material availability, and relatively low cooling costs. In MgB_2 studies, approaches aimed at improving reaction kinetics at low temperatures have mainly been addressed within the scope of bulk material production and Powder-in-Tube (PIT) based wire fabrication. In contrast, in wires produced by the Internal Magnesium Diffusion (IMD) method, the activation role of metallic coatings that can directly influence magnesium diffusion, as well as the effect of coating amount on phase formation processes, has been investigated in a relatively limited number of studies.

In this work, MgB_2 superconducting wires were fabricated by the IMD method using carbon-doped boron powder precursors and magnesium rods coated with copper layers of different thicknesses (approximately 200, 400, 600, and 800 nm). The effects of copper coating thickness on magnesium diffusion behavior, MgB_2 phase formation, and the resulting wire architecture were systematically investigated. In addition, the roles of sintering temperature and dwell time on the microstructural and superconducting properties of the wires were evaluated.

The superconducting transition behavior was characterized by temperature-dependent resistivity (R-T) measurements under both zero-field and applied magnetic field conditions. By establishing the relationship between processing parameters, microstructural evolution, and functional performance, insights were provided into the optimization of IMD-processed MgB_2 wires. In addition, based on the experimentally obtained superconducting properties, preliminary electromagnetic simulation studies were carried out to evaluate the potential of the developed wires for high-field and large-scale superconducting applications.

Acknowledgment

This work has been supported by TÜBİTAK and the Chinese Academy of Sciences (CAS) through a Bilateral Cooperation program under Contract No. 123N624.

Abstract ID: 30697

DETERMINATION OF THE OPTIMUM LEVITATION FORCE OF BULK YBCO USING IRON BLOCKS AND PMS OF DIFFERENT SIZES IN PMG THROUGH NUMERICAL MODELLING

İ. E. Gumrukcuoglu[1], U. K. Ozturk[1], O. Uzun[1], H. Mollahasanoglu[2]

[1] *Karadeniz Technical University, Dept. of Physics, 61080, Trabzon, TURKEY*
[2] *Recep Tayyip Erdogan University, Dept. of Electrical-Electronic Engineering, 53100, Rize, TURKEY*

In this study, the use of a permanent magnet guideway (PMG) incorporating NdFeB-based permanent magnets is investigated to enhance the levitation force of a bulk $YBa_2Cu_3O_{7-x}$ (YBCO) high-temperature superconductor. The numerical studies were performed considering liquid nitrogen temperature (77 K). The superconducting sample consists of a bulk YBCO with dimensions of 64 × 33 × 13 mm^3. The PMG configuration employs NdFeB permanent magnets with various geometries, including 20 × 20 × 40 mm^3, 30 × 30 × 40 mm^3, and 10 × 20 × 40 mm^3, providing surface magnetic flux densities in the range of 0.45–0.50 T. The effects of magnet size and orientation on the levitation force within the YBCO bulk were systematically examined. Numerical results demonstrate that both the geometry and alignment of the permanent magnets significantly influence the levitation force and spatial distribution of the trapped magnetic field in the superconductor.

Abstract ID: 30708

SURFACTANT-FREE SYNTHESIS OF MULTIFUNCTIONAL SPINEL FERRITE NANOPARTICLES: FROM FUNDAMENTAL TO PHOTOCATALYTIC PROPERTIES AND BIOMEDICAL APPLICATIONS

N. T. Mliki

Laboratory of Materials Organization and Properties (LMOP), Faculty of Science of Tunis, University of Tunis El Manar, Tunis 2092, TUNISIA

This work presents the design, synthesis, and characterization of spinel ferrite nanoparticles (MFe_2O_4, where M = Co, Ni, Mn, Zn) with controlled composition and size, aiming to achieve both fundamental understanding and practical applications. Using surfactant-free solvothermal and hydrothermal methods, we successfully synthesized phase-pure ferrites. We investigated their structural, magnetic, dielectric, and optical properties via XRD, TEM, Mössbauer spectroscopy, Raman spectroscopy, and UV-Vis spectroscopy.

Electrical analyses revealed interface polarization effects, mixed Debye and non-Debye relaxation behaviors, and hopping conduction mechanisms associated with cation distribution and oxygen vacancies. Manganese-substituted cobalt ferrites, for example, demonstrated enhanced photocatalytic activity and superparamagnetic behavior, while zeta potential measurements confirmed their colloidal stability in aqueous media.

Beyond their functional properties, biological evaluations revealed significant antibacterial activity in selected samples. Additionally, nickel ferrite nanoparticles were investigated for their anticancer potential using in-liquid Atomic Force Microscopy (AFM) under physiological conditions. Results indicated selective mechanical effects on MCF-7 breast cancer cells compared to healthy MCF-10 cells, suggesting their potential as biocompatible therapeutic agents.

This multidisciplinary study bridges nanomaterials science, physics, and biomedicine, and contributes to emerging applications in energy, environmental remediation, and healthcare.

Abstract ID: 30710

HIGH T_c OF $Tl_2Ba_2CaCu_2O_8$ SUPERCONDUCTOR

E. Yusrianto

Faculty of Education Sciences, Universitas Islam Negeri Imam Bonjol Padang, 25153 Padang, West Sumatera, INDONESIA

The $Tl_2Ba_2CaCu_2O_8$ superconductor was substituted and added with several materials to enhance the $T_{c\text{-}onset}$ [1,2]. But so far the maximum of $T_{c\text{-}onset}$ was around 110K [3,4]. Due to the interesting $T_{c\text{-}onset}$ of $Tl_2Ba_2CaCu_2O_8$ superconductor, several parameter such as paring interaction, lattice dynamics, microwave absorption, electron-density distribution, vortex matter properties, peak anomaly and irreversible magnetization of superconductor has been investigated [5-10]. The T_c of $Tl_2Ba_2CaCu_2O_8$ substitution with Cr was recorded at 157K (Fig.1). The sample still showed Tl-2212 as the major phase and $BaCO_3$, $BaCuO_2$ as the minor phases. This result may be due to the precursor process and heat treatment. According to Kirschner et al. [11], the high Tc superconductivity of Tl-Ba-Ca-Cu-O was depending on the heat treatment. Further studies are needed to evaluate precisely the phase composition of $Tl_2Ba_2CaCu_2O_8$ superconductor to get the correlation with high $T_{c\text{-}onset}$.

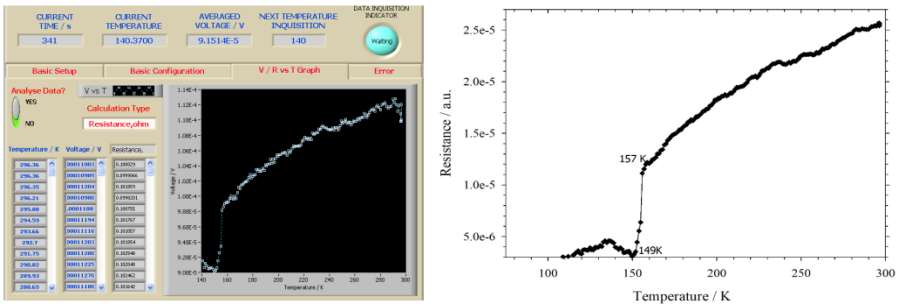

Fig. 1: *Electrical resistance versus temperature curves of $Tl_2Ba_2CaCu_2O_8$ with Cr 0.2 addition.*

References

[1] F. M. Salleh, A. K. Yahya, H. Imad and R. Abd-Shukor, Materials Science Eng. B **98**, pp. 17–20 (2003).
[2] A. I. Akimov, S. A. Lebedev and T. M. Tkachenko, Phys. Solid State. 49(**3**), pp. 413–419 (2007).
[3] V. N. Molchanov and V. I. Simonov, Acta Cryst. A **54**, pp. 905–913 (1998).
[4] A. M. Zibold, D. V. Tanner and H. Berger, Physica B **244**, pp. 27-32 (1998).
[5] W. A. Little, M. J. Holcomb, G. Ghiringhelli, L. Braicovich, C. Dallera, A. Piazzalunga, A. Tagliaferri and N. B. Brookes, Physica C **460–462**, pp. 40–43 (2007).
[6] C. S. Jia, P. Y. Lin, Y. Xiao, X. W. Jiang, X. Y. Gou, S. Huo, H. Li and Q. B. Yang, Physica C **268**, pp. 41-45 (1996).
[7] J. P. Joshi, A. Anand, S. V. Bhat, P. Chowdhury and S. N. Bhatia, Physica C **341–348**, pp. 1229–1230 (2000).
[8] S. Sasaki, T. Mori, K. Kawaguchi and M. Nakao, Physica C **247**, pp. 289–296 (1995).
[9] M. Pissas, D. Stamopoulos, y. C. Ma and N. L. Wang, Physica C **437–438**, pp. 267–269 (2006).
[10] P. Chowdhury, H. J. Kim, I. S. Jo and S. I. Lee, Physica C **384**, pp. 411–418 (2003).
[11] I. Kirschner, I. Halász, Cs. Sükösd, T. Porjesz, J. Kürti, Gy. Kovács, L. Korecz, T. Kárman, N.S. Rozlosnik, G. Zsolt and T. Träger, Phys. Letters A, **130(1)**, pp. 39–40 (1988).

Abstract ID: 30716

INFLUENCE OF MAGNETIC CORRELATIONS ON SCATTERING OF CARRIERS IN IRON ARSENIDES

D. E. Zhelezniakova, I. I. Gimazov, Y. I. Talanov

Kazan Physical-Technical Institute, FRC Kazan Scientific Center of RAS, 420029, Kazan, RUSSIA

This report presents the results of transport measurements of $Ba(Fe_{1-x}Co_x)_2As_2$ and $Ca(Fe_{1-x}Co_x)_2As_2$ crystals with varying concentrations of cobalt impurities. The data were obtained using direct current transport measurements (Fig.1) and high-frequency measurements (microwave absorption at 9.5 GHz). The contributions of different mechanisms to charge carrier scattering, including phonons, electron-electron interaction, spin fluctuations, and others, were analyzed. The influence of nematic fluctuations (anisotropic scattering due to magnetic fluctuations) on temperature dependence of resistivity was estimated.

Figure 1 shows the temperature dependence of the resistivity of $Ba(Fe_{1-x}Co_x)_2As_2$ crystals with different values of x. These dependencies reflect all phase transitions occurring in the crystal with decreasing temperature: structural transition from tetragonal to orthorhombic crystal lattice, antiferromagnetic ordering in the form of spin-density wave, and superconducting transition.

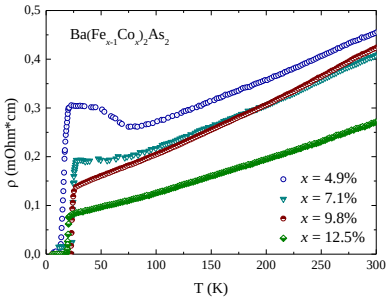

Fig. 1: *Temperature dependences of the resistivity of $Ba(Fe_{1-x}Co_x)_2As_2$ crystals.*

According to theoretical calculations [1], at high temperatures the resistivity exhibits a linear temperature dependence due to two-dimensional scattering of charge carriers by spin fluctuations. With decreasing temperature, fluctuations become three-dimensional, and the resistivity follows the relation $\rho(T) \propto T^{3/2}$. This change in dimensionality is due to an increase in correlation length of magnetic interactions and formation of exchange coupling between FeAs conducting planes.

The research was funded by the Russian Science Foundation (project No. 21-72-20153-P).

References

[1] R.M. Fernandes, E. Abrahams, J. Schmalian, Phys. Rev. Lett. **107**, 217002 (2011).

Abstract ID: 30717

ORIENTATION-DEPENDENT UPPER CRITICAL MAGNETIC FIELD AND DENSITY OF STATE FOR URANIUM DITELLURIDE

H. A. Muluneh

Dire Dawa University, Dept. of Physics, 1362, Dire Dawa, ETHIOPIA

The superconductor UTe_2 has garnered considerable attention due to its unique spin-triplet pairing and high upper critical magnetic field, making it a promising candidate for exploring unconventional superconductivity. This study presents a theoretical investigation into the angle dependence of the upper critical magnetic field HC_2 and the temperature-dependent density of states (DOS) within UTe_2. By employing anisotropic Ginzburg–Landau theory alongside microscopic modeling, the orientation-dependent behavior of HC_2 is analyzed along key crystallographic axes, particularly the a-, b- and c-axes, which demonstrate critical fields of ≈7, 15, and 11 T respectively. These results indicate a strong anisotropy in HC_2, with a peak along the b-axis, suggesting a profound alignment effect of the spin-triplet pairs with the magnetic field. Additionally, temperature-dependent DOS calculations reveal a pronounced increase in states near the Fermi level at lower temperatures, supporting the presence of unconventional pairing with potential nodal gaps. These findings suggest a complex interplay between spin fluctuations and electronic correlations, contributing to the robust superconducting phase in UTe_2 and also provide deeper insights into the mechanisms driving superconductivity in UTe_2 and highlight its potential for applications requiring high-field superconductors.

Abstract ID: 30722

FABRICATION OF 10-KILOMETER-CLASS MgB_2 WIRES BY THE INTERNAL-MAGNESIUM-DIFFUSION METHOD IN WST

W. Xie[1,2], Q. Yu[2], Q. Guo[1,2], M.-Wang[1], W. Yuan[1], Y. Zhu[1], B. Wu[2], Y. Shi[1,2], G. Yan[2], X. Liu[3], Y. Feng[1,2], J. Li[3], P. Zhang[3]

[1] *Xi'an Juneng Superconducting Wire Technologies Co., Ltd, 710018, Xi'an, PEOPLE'S REPUBLIC OF CHINA*
[2] *Western Superconducting Technologies Co., Ltd, 710018, Xi'an, PEOPLE'S REPUBLIC OF CHINA*
[3] *Northwest Institute for Non-ferrous Metal Research, 710016, Xi'an, PEOPLE'S REPUBLIC OF CHINA*

The internal-magnesium-diffusion (IMD) method is used to produce the high-performance MgB_2 superconducting wires. However, apart from the short samples, there are still technical obstacles in the IMD method that need to be overcome in the mass-manufacture of MgB_2 superconducting wires. In this work, we report the successful fabrication of the 10-kilometer-class 30-filament MgB_2 wire using the IMD method, which has length of 12 kilometers and is strikingly important in the development of IMD method. The obtained wire has diameter of 1.00mm and superconducting filling factor of 0.10. The superconducting current I_c at 4.2 K and 3 T reaches 575 A and the layer-superconducting current density J_c at 4.2K and 3T reaches 8.9×10^5 A cm^{-2}. The copper ration is around 0.25 in our wire which is related to the thermal stability. The scanning electron microscope and mechanical properties have also been analyzed. Above all, this is the first reported 10-kilometer-class IMD MgB_2 wire around the world.

Abstract ID: 30734

K-MAPPING: ADVANCED PHOTOLUMINESCENCE IMAGING METHOD FOR CHARACTERIZATION OF PEROVSKITE FILM QUALITY

M. Çoban

Middle East Technical University, Department of Physics, 06170, Ankara, TURKEY

Photoluminescence-based imaging methods are highly applicable in solar cell research, providing a contactless and rapid means to evaluate the quality of perovskite thin films. By utilizing the power-law relationship $I_{PL} \sim I_{exc}^{k}$ and performing a pixel-wise assignment of the proportionality constant k, it is possible to examine the dominant recombination-generation (R-G) mechanisms and assess the localized quality of the film. This parameter k, also known as the optical ideality factor [1], allows us to distinguish between the R-G processes of different regions within the solar cell. (Petermann et al) Specifically $k \approx 1$ signifies efficient radiative band-to-band recombination, while $k \approx 2$ indicates the dominance of Shockley-Read-Hall (SRH) traps. Benchmark results on doped glass showed that high radiative quality with k values between 1.03 and 1.06, whereas investigated perovskite samples exhibited k values between 1.71 and 1.74, indicating significant SRH recombination. These results demonstrate that k-mapping serves as a reliable tool for identifying localized defects and monitoring film quality in large-area photovoltaic research.

References

[1] J. Petermann, B. Hacene, M. Gholipoor, F. Laufer, R. Pesch, X. Liu, U. W. Paetzold, *Advanced Photoluminescence Imaging Method for Robust and Scalable Perovskite Quality Monitoring in Monolithic Tandem Solar Cells*, Solar RRL, **9(3)**, 2400571 (2025). https://doi.org/10.1002/solr.202400571.

Abstract ID: 30744

CYLINDRICAL VORTEX-TYPE MICROFLUIDIC DEVICE FOR ON-CHIP NANOMATERIAL SYNTHESIS TOWARD ADVANCED WATER TREATMENT TECHNOLOGIES

E.-T. Moldoveanu[1], D.-I. Tudorache (Trifa)[1], A.-G. Niculescu[1,2], A. C. Bîrcă[1], A. M. Croitoru[1], A. C. Burduşel[1], A. Hudiţă[2,3], T. Hadibarata[1,4], D. E. Mihaiescu[1], A. M. Grumezescu[1,2]

[1] *National University of Science and Technology Politehnica Bucharest, 011061 Bucharest, ROMANIA*
[2] *Research Institute of the University of Bucharest—ICUB, University of Bucharest, 050657 Bucharest, ROMANIA*
[3] *University of Bucharest, 050095 Bucharest, ROMANIA*
[4] *Curtin University Malaysia, CDT 250, Miri 98009, MALAYSIA*

Microfluidic engineering offers powerful opportunities for advancing environmental remediation technologies by enabling precise control over reaction conditions, mixing efficiency, and material morphology. In this study, we introduce a custom-designed cylindrical multilayered microfluidic device fabricated from PMMA sheets and tailored to generate vortex-based micromixing for rapid nanoparticle and aerogel precursor synthesis. The central architecture incorporates a dual-injection system in which one reagent flows axially into the reaction chamber, while the other is introduced tangentially, producing a controlled vortex that enhances mixing beyond that achievable with conventional planar microchips. The device was tested for the synthesis of Fe_3O_4–salicylic acid nanoparticles using two precursor solutions pumped in equal volumes via a classical osmosis-driven flow system. The resulting nanoparticles displayed uniform size distribution, magnetic separability, and excellent colloidal stability, enabling their subsequent integration into silica-based aerogel matrices. A microfluidic-assisted aerogel synthesis route was further developed by co-injecting a silica precursor/CTAB/alginic acid/magnetite suspension, along with a $CaCl_2$/NH_4Cl/acetic acid solution, into the same microfluidic platform. The vortex-driven environment enabled controlled nanoparticle incorporation and accelerated gelation, overcoming limitations of traditional sol–gel processes. After drying, the resulting magnetic aerogels exhibited high porosity, uniform morphology, and effective surface functionalization as confirmed by XRD, DLS, FT-IR, Raman spectroscopy, SEM/TEM, and BET analysis. To assess environmental applicability, the aerogels were tested as adsorbents for pesticide- and metal-contaminated water. Pollutant removal was evaluated using FT-ICR high-resolution mass spectrometry and ICP-MS, revealing substantial reductions in both organic contaminants and environmentally relevant trace metals. Overall, this work demonstrates an innovative vortex-based 3D microfluidic platform capable of producing high-performance magnetic nanomaterials and aerogels, with direct relevance to water remediation, and highlights a scalable route toward next-generation materials for sustainable pollutant removal.

Abstract ID: 30750

MAGNETIC PROPERTIES OF MAGNETIC NANOPARTICLE (Fe_3O_4)-FILLED POLYVINYLIDENE FLUORIDE NANOFIBERS

A. Demirtaş, M. Maksutoğlu

Institute of Nanotechnology, Gebze Technical University, Gebze, Kocaeli 41400, TURKIYE

Magnetic nanoparticles (NPs) are increasingly utilized to functionalize polymer nanocomposites due to their unique physical properties. Polyvinylidene fluoride (PVDF) is a leading piezoelectric polymer, prized for its flexibility, mechanical strength, and chemical stability, making it ideal for flexible electronics and energy devices. In this study, we embedded magnetic NPs (50–150 nm) into PVDF nanofibers (NFs) under varying stirring times to optimize their structure and performance

Fe_3O_4-dopped PVDF NFs were produced by electrospinning technique. The composite NFs were characterized via XRD, FTIR, and SEM to confirm phase composition and morphology. SEM images demonstrated how diameter of NPs (Fe_3O_4) changes, and how solution content stirring times affect the homogeneous distribution of NPs into composite NFs. Vibrating sample magnetometry (VSM) revealed key magnetic behaviors: (i) hysteresis loop squareness decreases near room temperature, and (ii) coercivity (H_C) declines with rising temperature. Importantly, the NPs enhanced the β-phase content of PVDF, critical for piezoelectricity. Fe_3O_4 NPs use their electrostatic property to help PVDF attract electrons in the case of Fe_3O_4 dopped-PVDF NFs dopped-PVDF NFs. These magnetic-PVDF NFs exhibit superior electromechanical coupling, enabling efficient mechanical energy harvesting and selfpowered sensing.

These magnetic NPs doped-PVDF NFs exhibit superior electromechanical coupling, enabling efficient mechanical energy harvesting and self-powered sensing. This work highlights the potential of magnetic PVDF NFs for wearable electronics (e.g., motion-sensing textiles and health-monitoring patches), biomechanical energy harvesters (cavenging energy from human motion), and smart textiles, advancing multifunctional nanocomposites for next-generation energy Technologies with embedded sensing capabilities. Furthermore, magnetoelastic coupling effecr of the NFs provides adjustable sensitivity in the presence of external magnetic fields, which makes them optimal for self-powered strain and pressure sensors that have a quick reaction time and exceptional endurance. The adoption of them in commercial applications is further supported by the cost-effective production ensured by the scalable electrospinning fabrication technology employed.

Acknowledgments

The authors gratefully acknowledge Prof. Dr. Fikret Yıldız and Prof. Dr. Mustafa Eginligil for their significant scientific contributions and fruitful discussions during the design, fabrication, and characterization of the nanocomposite structures used in this research. Also, this work was supported by Gebze Technical University, Research University Support Program (ADEP) under the Grant Number 2024-A-113-21.

Abstract ID: 30754

THE ONSET OF BULK SUPERCONDUCTIVITY AT + 39°C IN OXYGEN DOPED DELAFOSSITE $CuYO_{2.33}$

D. Djurek

Alessandro Volta Applied Ceramics (AVAC), 49247 Zlatar Bistrica, Augusta Šenoe 14. CROATIA

It was shown that delafossite $CuYO_2$, originally insulator, becomes highly conducting when doped by oxygen to molar 0.33. Unit formula $CuYO_{2.33}$ may be indexed in hexagonal lattice $Cu_6Y_6O_{14}$, indicated, by periodic arrangement of CuO planes sandwiched by YO_6 planes. The conductivity in CuO planes proceeds along CuO chains which in turn results in the superconductivity (SC) indicated by transition temperature + 39°C, previously spotted in the vacuum fired mixture Y-Ba-Cu-O [1]. SC state is further confirmed by the measurements of the electric resistivity in a magnetic field, while measurements of AC magnetic susceptibility reveal the onset of diamagnetism by cooling below transition temperature.

$CuYO_2$ exhibits the relativistic contraction [2] of Cu-Cu distance, when compared to that in the pure copper [3], which in turn may explain high transition temperature when considered by modern models of the topological superconductivity.

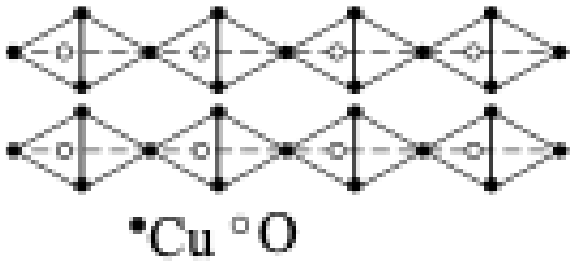

References

[1] D. Djurek, Condens. Matter. **9(1)**, 10 (2024). DOI: 10.3390/c
[2] P. Pyykko, Chem. Rev. **88**, 563-594 (1988).
[3] H. Ch. Kandpal and R. Seshadri, Solid State Sciences, **4**, 1045-1052 (2024).

Abstract ID: 30757

DECOUPLING BROWNIAN ALIGNMENT AND NEEL ROTATION IN SPIO TRACERS TO IMPROVE BIOMEDICAL MAGNETIC PARTICLE IMAGING PERFORMANCE

S. A. Shah[1,2], D. B. Reeves[1], R. M. Fergosun[1], K. M. Krishnan[1]

[1] *Materials Science and Engineering, University of Washington, Seattle, Washington, USA*
[2] *Department of Physics, Forman Christian College (University), Lahore, PAKISTAN*

Magnetic particle imaging (MPI) exploits the nonlinear ac magnetization of superparamagnetic iron oxide nanoparticles (SPIOs) to enable background-free, high-sensitivity biomedical imaging. However, tracer optimization is still often guided by equilibrium relaxation-time heuristics that can fail in realistic biofluids where internal Neel reversal and whole-particle Brownian rotation coexist. We present an experimentally validated framework that separates and quantifies these coupled mechanisms in PEG-coated magnetite SPIO suspensions driven by kHz fields. Magnetic particle spectroscopy is performed in liquid and in a reversibly immobilized state using a DMSO phase-change protocol, allowing the same nanoparticle ensemble to be measured with and without Brownian freedom. Immobilization produces marked changes in differential susceptibility and dynamic hysteresis that cannot be explained by the modest temperature shift alone. Field-freezing with weak static bias further imprints orientation-dependent signatures, while dilution studies remain linear, ruling out chain formation under our conditions.

To interpret these observations, we combine spectroscopy with stochastic Landau-Lifshitz-Gilbert simulations including thermal fields and log-normal distributions of particle size and effective anisotropy. Introducing partial Brownian alignment of an effective easy axis is sufficient to reproduce the liquid-versus-immobilized response and the bias-field orientation trends without invoking strong interparticle coupling. The key insight is that even when Neel rotation dominates the immobilized response, modest Brownian alignment in liquid can bias easy-axis populations and substantially steepen the nonlinear magnetization exploited by MPI. These results provide a practical route to environment-aware tracer characterization and design, improving prediction of harmonic content, sensitivity, and quantitative robustness for MPI and related magnetic biosensing and theranostic modalities in medicine [1,2].

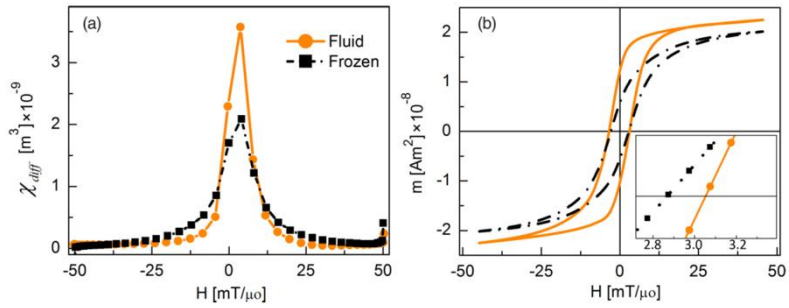

Fig. 1: *MPS comparison of the same SPIO sample in fluid (20 °C) and immobilized (frozen) states under 26 kHz, 50 mT/μ0 excitation: (a) differential susceptibility and (b) integrated m(H) curves.*

References

[1] S. A. Shah, D. B. Reeves, R. M. Ferguson, J. B. Weaver and K. M. Krishnan, Phys. Rev. B **92**, 094438 (2015).
[2] K. M. Krishnan, IEEE Trans. Magn. **46**, 2523 (2010).

Abstract ID: 30763

TIGHT BINDING MODEL AND BEYOND IN MODELING INTEGRATED SEMICONDUCTOR SINGLE AND FEW-ELECTRON DEVICES

K. Pomorski[1], E. Halubek[2], D. Górniak[3], F. Buchcic[4], M. Dolecki[5], A. Michalak[3], W. Nowakowski[5], P. Imiński[5], A. Żak[6]

[1] University of New Mexico & Quantum Hardware Software Systems LLC, USA
[2] Warsaw University of Technology & Institute of Physics, POLAND
[3] Warsaw University of Technology & Quantum Hardware Systems, POLAND
[4] VI Liceum Ogolnoksztalcace in Lodz, Poland & Quantum Hardware Systems, POLAND
[5] Lodz University of Technology & Quantum Hardware Software Systems LLC, USA
[6] Electronics Technical School,School Complex 1, Zgierz, Poland & Quantum Hardware Systems, POLAND

We present the methodology of modelling electrostatically interacting single-electron devices [1-2] using the concept of stochastic mechanics [3] and concept of quantum mechanics [4]. Very last is formulated by a tight-binding model of interacting particles and beyond as Schroedinger equations for many body interacting with spin. The obtained results are mapped into FPGA logical circuits [6], so new emulators of quantum systems can be implemented [5-6]. Various solutions for electrostatically interacting linear and roton circular position-based qubits with one and few electrons are given.

References

[1] T. Fujisawa, T. Hayashi, Y. Hirayama, H. D. Cheong, Y. H. Jeong, *Electron counting of single-electron tunneling current. Appl. Phys. Lett.,* **84**, 13 (2004). DOI: 10.1063/1.169149

[2] J. R. Petta, A. C. Johnson, C. M. Marcus, M. P. Hanson, A. C. Gossard, *Manipulation of a single charge in a double quantum dot*, Phys. Rev. Lett. , **93**, 18 (2004). DOI: 10.1103/PhysRevLett.93.186802

[3] E. Nelson, *Review of Stochastic Mechanics, J. Phys.: Conf. Ser.* **361**, 012011 (2012). **DOI:** 10.1088/1742-6596/361/1/012011

[4] K. Pomorski, E. Halubek, *CMOS-compatible electrostatic SWAP Gate in silicon quantum dots: justification of tight-binding model and going beyond*, ArXiv: 2311.04411 (2025).

[5] P. Foster, J. Huang, A. Serb, *et al., An FPGA-based system for generalised electron devices testing*, Sci Rep **12**, 13912 (2022). DOI: 10.1038/s41598-022-18100-3

[6] A. Michalak, *et al.*, *Room-Temperature Emulation of Single-Electron Devices*, IEEE Quantum Week 2025 Proceedings, DOI: 10.1109/QCE65121.2025.10472

Abstract ID: 30764

Cr-DRIVEN ELECTRONIC CONTROL OF MARTENSITIC TRANSFORMATION AND EXCHANGE BIAS IN Ni–Mn–Sb HEUSLER ALLOYS

M. Ayyıldız[1], G. Kırat[2], M. A. Aksan[1]

[1] *Inonu University, Department of Physics, 44200, Malatya, TÜRKIYE*
[2] *Inonu University, Scientific and Technological Research Center, 44200, Malatya, TÜRKIYE*

The influence of Cr substitution on structural stability, electronic structure, and magnetic phase transitions in $Ni_{50-y}Cr_yMn_{37}Sb_{13}+B_2$ (y = 0, 3, 5, 7) Heusler alloys is investigated through a combined experimental and multiscale theoretical approach. XRD and magnetization measurements reveal that increasing Cr content suppresses the martensitic transformation temperature (T_M) from 286 K to 204 K and stabilizes the cubic $L2_1$ austenite phase at room temperature. Density Functional Theory (DFT) calculations demonstrate that Cr substitution reduces the valence electron concentration (e/a), shifts the Fermi level from a high-density peak toward a pseudogap region, and weakens the band Jahn–Teller instability responsible for tetragonal distortion. Bain-path energy analysis confirms the progressive stabilization of the cubic phase with increasing Cr content. Magnetic exchange parameters derived from DFT were incorporated into a Heisenberg Monte Carlo framework to model temperature-dependent magnetic behavior. The simulations reveal the formation of nanoscale antiferromagnetic clusters within the ferromagnetic matrix, leading to a pronounced exchange bias effect at high Cr contents. Theoretical exchange fields are consistent with experimental observations. This integrated DFT–Monte Carlo approach provides a predictive framework for tailoring phase transformations and spintronic functionalities in multifunctional Heusler alloys.

Abstract ID: 30765

SYMMETRY-DRIVEN Nb-Sn STRUCTURAL MODELS WITH LONG-RANGE ORDER: PREDICTIVE DESIGN THROUGH THE INTERPLAY OF THEORETICAL MODELING AND ATOMIC SIMULATIONS

T. Priinits, A. Vargunin, A. Liivand

Institute of Physics, University of Tartu, Tartu, 51014 ESTONIA

As is well known, Nb_3Sn-based intermetallics play a crucial role in many scientific, industrial, and technological applications as superconducting systems with the A15 structure. However, there is one issue: although the theory is supported by well-understood principles of material chemistry, these compounds have not received much attention from crystallographic or crystal chemistry perspectives. Given the importance of technological applications, the proper theoretical modeling could be much more thorough and comprehensive. The situation becomes even worse when considering phenomenology because there is no experimental evidence indicating whether the Nb-Sn chemical interactions are strong or weak, or how well the Sn atoms will be accommodated in the Nb crystalline matrix. Adopting a crystal-chemical approach to structural design can resolve this issue. Our approach uses dimensional regularization based on crystallographic drivers of lattice geometry to predict and describe the pathways necessary for forming bonds between atoms. Our first major advance was developing a symmetry-guiding, crystal-chemistry-based framework for modeling various crystallization scenarios associated with the Nb-Sn binary intermetallic system. This framework employs density functional theory coupled with symmetry-determined predictors and theoretical group methods. In the context of retrosynthetic analysis, our study presents the theoretical prerequisites for forming long-range, ordered lattice patterns associated with Nb atoms. These patterns are integral to the cubic lattice of the A15 structure. Thus, our approach improves access to Nb_3Sn crystallization modeling, which is essential for understanding how the system may overcome the conventional morphological barrier and improve functionality through nano-reinforcement caused by the system's two-phase state. Many factors are at play, and we expect the experiment to corroborate our findings in the search for the two-phase state. Discovering this state will lead to extensive investigations into technological applications that can achieve advanced technological goals.

Abstract ID: 30769

PREPARATION OF THE hBN NANOCRYSTALS USING GREEN ROUTE

L. Bazgir[1], A. Bakoue[1], M. Sasani Ghamsari[2]

[1] *Department of Physics, Faculty of Basic Sciences, Tarbiat Modares University, 14115-111, Tehran, IRAN*
[2] *Photonics and Quantum Technologies Research School, NSTRI, 11155-3846, Tehran, IRAN*

Hexagonal boron nitride (h-BN) is a two-dimensional material known for its wide energy gap and excellent stability in terms of thermal, chemical, and electronic properties. In recent years, it has gained significant attention for advanced electronic and photonic applications. Over the past two decades, several methods have been developed for synthesizing this material [1]. One of the most common methods involves using ammonia gas as a nitrogen source and an oxygen scavenger. Alternatively, a more environmentally friendly approach combines nitrogen, hydrogen, and argon gases to completely eliminate ammonia during the synthesis process [2]. This approach not only reduces environmental risks but also enhances control over reaction conditions and improves the purity of the final product. This study investigates the synthesis of hexagonal boron nitride (h-BN) using an optimized and environmentally friendly method that eliminates the production of hydrogen gas. To achieve a pure crystalline phase and enhance structural quality, several synthesis routes were designed and evaluated, utilizing different starting materials and molar ratios. Among the tested compounds, the optimal ratio of urea to boric acid resulted in the formation of a dominant h-BN phase with excellent structural quality. Fourier transform infrared spectroscopy (FTIR) confirmed the presence of in-plane B–N tensile vibrational modes and out-of-plane B–N–B bending vibrational modes, indicating the successful formation of the hexagonal boron nitride (h-BN) network (Fig. 1a). X-ray diffraction (XRD) analysis also revealed the presence of a predominantly hexagonal layered structure with improved crystallinity and a reduction in secondary phases (Fig. 1b). These results suggest that careful control of the precursor ratio is crucial for achieving phase purity, minimizing secondary phases, and enhancing crystallinity. The results of this study demonstrate that the proposed method offers a stable, safe, and scalable approach for producing h-BN of sufficient quality for advanced applications in 2D materials and photonic systems. This method shows significant potential for use in next-generation 2D material platforms and advanced functional devices.

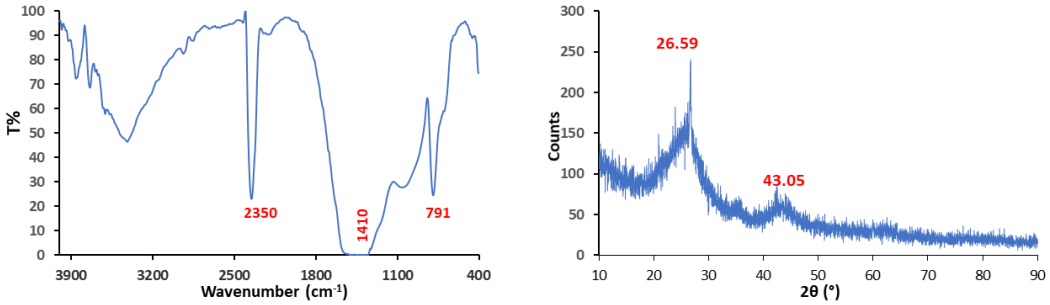

Fig. 1: *(a)FTIR spectrum and (b) XRD pattern of the prepared sample.*

References

[1] D. Yang, P. Dai, X. Jiang, S. M. Alshehri, T. Ahamad, T. Ahamad, Y. Bando, and X. Wang, Chem. Mater., **36**, 10008–10053(2024).
[2] Ö. Sen, M. Emanet, and M. Çulha, Front. Bioeng. Biotechnol. **6**, 83 (2018).

Abstract ID: 30771

MXene-BASED COMPOSITES FOR RENEWABLE ENERGY AND WASTE WATER TREATMENT

Z. N. Kayani, K. Javed

Lahore College for Women University, Lahore-54000, PAKISTAN

Two binary composites (Bi_2O_3/MXene), (Mxene/PPy) and three ternary composites Bi_2O_3/MXene/ PPy with varying PPy contents were synthesized by solution based and in-situ polymerization routes. XRD confirmed monoclinic phase of Bi_2O_3. SEM showed granular morphology. The band gap decreased with increase in PPy concentration while AC conductivity increased. Composites displayed ferromagnetism which increased with PPy concentration due to bound magnetic polarons. The photocatalytic activity was also enhanced. With high capacitance and dielectric constant, these materials were suitable for capacitors. They have high specific capacitance and the lowest charge transfer resistance and remarkable cycle life beneficial for electrode material for pseudo capacitors.

Abstract ID: 30773

ELECTRON SPIN RESONANCE AND MAGNETIC PROPERTIES OF COBALT SUBSTITUTED CHROMIUM NANOFERRITES

M. Sethosa[1], L. Kotsedi[2], T. Mokoena[3], T. Mokhena[4], A. Nhlapo[5]

[1] *Department of Physics, Sefako Makgatho Health Sciences University. P.O.Box 94, Medunsa 0204, SOUTH AFRICA*
[2] *iThemba LABS-National Research Foundation, Old Faure Road, Somerset West, 7129, SOUTH AFRICA*
[3] *Department of Physics, University of the Free State, P. Bag X13, Phuthaditjhaba 9866, SOUTH AFRICA*
[4] *DSI/Mintek-Nanotechnology Innovation Centre, Advanced Materials, Mintek, Randburg 2125, SOUTH AFRICA*
[5] *Department of Medical Physics, Sefako Makgatho Health Sciences University. P.O. Box 146, Medunsa 0204, SOUTH AFRICA*

Chromium-substituted cobalt ferrite nanoparticles $CoCr_xFe_{2-x}O_4$ ($0 \leq x \leq 2.0$) were successfully synthesized via the hydrothermal method. X-ray diffraction (XRD) patterns confirmed the formation of a single-phase cubic spinel structure [1-3]. Crystallite sizes ranged from 6.6 to 13.7 nm, while lattice parameters decreased from 8.2603 to 8.1974 Å with increasing chromium content. FTIR spectra exhibited characteristic metal–oxygen stretching vibrations at tetrahedral (615 cm^{-1}) and octahedral (468 cm^{-1}) sites, along with a weak Cr^{3+}–O^{2-} band at 499 cm^{-1}, confirming successful cation substitution and bond strengthening. The small remanent magnetization and coercive fields from *M-H* curves revealed superparamagnetic nature for all samples. The FC and ZFC measurements revealed the blocking temperature at 183K. The Electron spin resonance (ESR) spectra revealed composition-dependent variations in resonance field (H_{res}), g-values, and spin relaxation times. The *g*-value ranged from 4.49 ($x = 0$) to 2.04 ($x = 1.0$), indicating a transition toward a more symmetric crystal field and stronger Fe^{3+}–Cr^{3+} exchange coupling. These results demonstrate that controlled Cr^{3+} substitution effectively tunes the structural order, local bonding environment, and spin dynamics of cobalt ferrite nanomaterials, making them promising materials for magnetic, electronic, and biomedical applications [4,5].

References

[1] N. A. Spaldin, *Magnetic materials: Fundamentals and applications* (2010). https://doi.org/10.1017/CBO9780511781599.

[2] R. C. Pullar, *Hexagonal ferrites: A review of the synthesis, properties and applications of hexaferrite ceramics*, Prog. Mater. Sci. **57**, 1191-1334 (2012). https://doi.org/10.1016/j.pmatsci.2012.04.001.

[3] A.R. Shitre, V.B. Kawade, G.K. Bichile, K.M. Jadhav, X-ray diffraction and dielectric study of Co1-xCdxFe2-xCrxO4 ferrite system, Mater. Lett. **56**, 188–193 (2002). https://doi.org/10.1016/S0167-577X(02)00438-X.

[4] G.-S. Luo, Y.-H. Hong, W.-P Zhou, Z.-Z. Cheng, C.-C. Ma, Z.-K. Wu, H.-H. Huang, *Effect of chromium substitution on structural, electrical and magnetic properties of NiZn ferrites*, Trans. Nonferrous Met. Soc. China **30**, 1895–1903 (2020). https://doi.org/10.1016/S1003-6326(20)65348-1.

Abstract ID: 30774

INTERDISCIPLINARY INTEGRATION OF QUANTUM PHENOMENA FOR ADVANCING THE NEXT QUANTUM REVOLUTION

I. Ahmad[1,2]

[1] *Center for Computational Materials Science, University of Malakand, Chakdara, PAKISTAN*
[2] *Department of Physics, University of Malakand, Chakdara, PAKISTAN*

The next quantum revolution will be driven not only by advances in quantum physics, but also by the effective integration of quantum phenomena across multiple scientific and technological disciplines. This talk examines how foundational quantum behaviors, including entanglement, coherence, superposition, and tunneling, are emerging as powerful tools for innovation far beyond traditional physics. As fields such as computer science, mathematics, engineering, materials science, chemistry, biology, and medicine converge on quantum principles, a new interdisciplinary landscape is beginning to take shape. The central focus of the discussion will be the evolving role of physicists in this rapidly changing environment, highlighting the fundamental challenge they face: how to effectively communicate and translate quantum phenomena to scientists, engineers, and researchers working on next generation quantum technologies who may have little or no background in physics, particularly quantum mechanics. Addressing this challenge is crucial for enabling fruitful collaboration and ensuring that the interdisciplinary quantum workforce is equipped to contribute meaningfully to the next quantum revolution.

Abstract ID: 30776

EFFECTS OF DOPANT ON THE OPTOELECTRONICS PROPERTIES OF DOPED $LaAl_{1-x}Ga_xO_3$ NANO-PARTICLES

W. H. Shah

Department of Physics, Faculty of Science, Islamic International University, Islamabad, PAKISTAN

Perovskite oxides are an intriguing class of nanomaterials that have recently gained attention as catalysts due to their exceptional mechanical strength, high thermal and hydrothermal stability, and other notable qualities. In the present work, we employed the co-precipitation technique to fabricate the rare earth magnate perovskite oxide nano-particles of $LaAl_{1-x}Ga_xO_3$. Rare earth manganites have attracted significant attention due to their extraordinary sensitivity to small magnetic fields, tuning of the ban gap by doping divalent element. These materials belong to the class of strongly correlated electron systems, in which conventional theoretical approaches fail to adequately describe the many-body ground state. Intrinsic electronic inhomogeneities, involving ferromagnetic and antiferromagnetic clusters, are believed to play a crucial role in the large charge transport effects observed. Such nanoscale phase separation links manganites to other correlated systems, including cuprates. Overall, manganites provide an important platform for understanding complexity, tunability, high dielectric constant, high AC conductivity and emergent phenomena in doped rare-earth manganites perovskites.

We have evaluated the synthesized nanoparticles using an X-ray diffractometer (XRD), a scanning electron microscope (SEM), an energy dispersive X-ray spectrometer (EDX), Fourier transform infrared spectroscopy (FTIR), UV-visible absorption spectroscopy, dielectric properties, and ac conductivity. The XRD pattern confirmed the formation of the perovskite phase. According to the SEM micrographs, the surface morphology is porosity because of voids between the particles. We fabricate a tunable Mn^{4+}-doped $LaAl_{1-x}Ga_xO_3$ oxide phosphor with a perovskite structure. We used high-temperature solid-state methods to get around the problems of making cheap and effective narrow-band far-red emitting phosphors that can be used to make artificial white light for plant growth. We looked into how successfully replacing Ga^{3+} with Al^{3+} with larger ionic radii changes the photophysical characteristics. The host lattice of $LaAl_{1-x}Ga_xO_3$:0.001Mn^{4+} perovskite oxide phosphors expands, which changes the Stokes shift. This causes optical properties to change, such as blue shifting the emission spectrum from the near-infrared (NIR) to the far-red spectral region, as well as improving the brightness and thermal stability of the phosphors.

This work looks at how high-purity greenish-yellow $LaGaO_3$ phosphors doped with dysprosium ions Dy^{3+} change their structure and how they emit light. A high-temperature solid-state reaction approach was used to make the phosphors. X-ray diffraction (XRD) showed that a single-phase $LaGaO_3$:Dy^{3+} structure had formed, and scanning electron microscopy (SEM) showed that the particles were all the same size and shape. The phosphor may be easily stimulated by ultraviolet light at 350 nm, which gives out a greenish-yellow light with two strong peaks at 478 nm (cyan) and 572 nm (yellow). These peaks are due to the transitions of $^4F_{9/2} \rightarrow {}^6H_{15/2}$ and $^4F_{9/2} \rightarrow {}^6H_{13/2}$, respectively. The direct exchange interaction between activators is what causes the electronic transition mechanism, which leads to concentration quenching. The phosphor kept 67% of its brightness without changing color too much at temperatures between 25 °C and 150 °C. We figured out the CIE chromaticity coordinates of the light that was emitted and found that they were in the right greenish-yellow area. We used 365 nm LED chips to test the electroluminescence performance of the $LaGaO_3$:0.06Dy^{3+} phosphor to see if it could be used in white light-emitting diodes (WLEDs). The phosphors that were made showed that they could handle high temperatures, which makes them good for use in white LEDs. The study shows that $LaGaO_3$:Dy^{3+} phosphors could improve the color quality and efficiency of white LEDs.

Abstract ID: 30777

DEFECT-MEDIATED ROOM-TEMPERATURE FERROMAGNETISM IN Er-DOPED TiO_2 NANOSTRUCTURED THIN FILMS

S. Iram, Z. N. Kayani

Lahore College for Women University, Lahore, PAKISTAN

The induction of room-temperature ferromagnetism in wide bandgap oxides is critical for advancing spintronic and magneto-functional technologies. In this study, Er-doped TiO_2 nanostructured thin films (1–5 wt%) were synthesized via a sol–gel dip-coating technique and annealed at 500 °C. Rare-earth incorporation successfully transformed diamagnetic TiO_2 into a dilute magnetic semiconductor exhibiting stable ferromagnetic ordering.

X-ray diffraction confirmed retention of the anatase phase with a reduction in crystallite size from 7.96 nm to 5.62 nm as Er concentration increased, indicating lattice distortion and enhanced defect density. All doped films exhibited clear room-temperature ferromagnetism, with saturation magnetization increasing systematically with Er content. The magnetic behavior is attributed to defect-mediated exchange mechanisms, particularly oxygen-vacancy-induced F-center exchange and bound magnetic polaron (BMP) interactions facilitated by localized 4f electrons of Er^{3+} ions.

In addition to magnetic enhancement, Er doping modified the electronic structure, producing a blue shift in bandgap (3.39–3.69 eV) and altered dielectric response. The optimized 5 wt% Er-doped film demonstrated superior photocatalytic efficiency, achieving 84% degradation of indigo carmine under sunlight.

Abstract ID: 30778

CRITICAL CURRENT IN HIGH-T_c SUPERCONDUCTORS VIA HTS-PM INTERACTION USING THE BEAN MODEL

J. Rojas, A. Mariño

Universidad Nacional de Colombia, Grupo de Superconductividad y Nuevos Materiales, 111311, Bogotá, COLOMBIA

This work presents a numerical simulation of the attractive and repulsive forces between a high-T_c superconductor and a permanent magnet based on the Bean critical-state model, aimed at determining the critical current density (J_c). YBCO samples fabricated by melt-textured growth, sol-gel processing, and conventional sintering were evaluated under field-cooling (FC) and zero-field-cooling (ZFC) conditions. The modeled interaction forces enabled the estimation of J_c for each sample, revealing significant differences associated with the fabrication method and its influence on flux-pinning efficiency. Additionally, the simulation provides a clear visualization of magnetic flux penetration, improving the interpretation of the relationship between critical current density and magnetization hysteresis. Overall, this approach constitutes a rapid, reliable, and non-destructive method for the characterization of high-T_c superconducting materials.

Abstract ID: 30788

EFFECT OF ALKALI-METAL SUBSTITUTION IN TUNING BiCuSeO FOR HIGH-PERFORMANCE THERMOELECTRIC APPLICATIONS

T. Khalid, M. A. Rehman

Applied Thermal Physics Laboratory (ATPL), Department of Physics, COMSATS University Islamabad, Islamabad, 4550, PAKISTAN

Thermoelectric (TE) materials, which directly convert thermal gradients into electrical energy, offer promising solutions for sustainable energy in response to environmental and resource challenges [1]. Among metal oxides, BiCuSeO is distinguished by its favorable crystal structure, elemental abundance, low thermal conductivity, and thermal stability. However, its thermoelectric efficiency, governed by the figure of merit (ZT), is limited by suboptimal carrier concentration [2]. This study systematically investigates doping of an alkali metal sodium (x = 0.0–0.02) in polycrystalline $BiCu_{1-x}Na_xSeO$ synthesized via sol-gel method. Structural analysis confirmed a monoclinic phase (P21/c) with average crystallite sizes of 9–38 nm. Electrical conductivity measured using the two-probe method between 303–473 K, increased with sodium content, reaching 1.8×10^{-2} S/m at 473 K due to enhanced carrier concentration. The Seebeck coefficient, a critical parameter for TE efficiency, was maximized at 4.11×10^{-3} V/K for $BiCu_{0.98}Na_{0.02}SeO$, surpassing undoped samples. This optimal composition also exhibited reduced thermal conductivity (0.81 W/mK) and ohmic I–V behavior. These results demonstrate that sodium doping effectively enhances the power factor and thermoelectric performance of BiCuSeO, identifying $BiCu_{0.98}Na_{0.02}SeO$ as a promising candidate for moderate-temperature energy conversion applications.

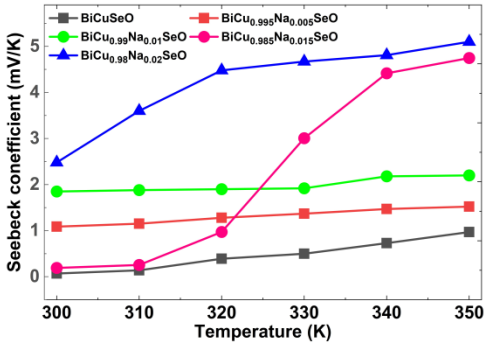

Fig. 1: *Seebeck coefficient of $BiCu_{1-x}Na_xSeO$ (x=0.0-0.02).*

References

[1] C. Zhao, T. Sun, H. Liu, Y. Wang, C. Chen, and L. Pan, J. Alloys Compd. **1038**, 182865 (2025).
[2] X. Huang, H. Wang, J. Jiang, L. Wang, S. Dong, and H. Ju, Ceram. Int. (2026).

11th International Conference on Superconductivity and Magnetism ICSM2026
4th International Conference on Quantum Materials and Technologies ICQMT2026
19th April to 26th April, 2026, Ölüdeniz – Fethiye/Muğla, Türkiye
https://icsmforever.org/

Abstract ID: 30801

INFLUENCE OF Fe INTERLAYERS ON PHONON AND CHARGE CARRIER DYNAMICS IN Bi_2Te_3 TOPOLOGICAL INSULATOR

Kh. V. Aliguliyeva[1], N. A. Abdullayev[2,3], S. Sh. Gahramanov[2]

[1] *Sumgait State University, 43th district, Baku str., 1, AZ5008, Sumgait, AZERBAIJAN*
[2] *Institute of Physics, H. Javid av.,131, AZ1073, Baku, AZERBAIJAN*
[3] *Baku State University, Z. Xalilov str., 23, AZ1148, Baku, AZERBAIJAN*

Interlayer bonds in bismuth chalcogenides are sensitive to changes in the value of interlayer interaction. The enhancement of the polarity of the bond and the redistribution of the electron density, depending on the broadening of the interlayer distance between quintets ...$Te^{(1)}$- -$Te^{(1)}$-Bi-$Te^{(2)}$-Bi-$Te^{(1)}$- -$Te^{(1)}$-Bi-$Te^{(2)}$-Bi-$Te^{(1)}$- -$Te^{(1)}$... (Fig. 1(a). We have established that iron atoms are intercalated between the cleavage planes of Bi_2Te_3 with van der Waals bonds, leading to increased chemical bonding between the quintets and strengthening of Bi_2Te_3<*Fe*>. This leads to the formation of interlayer nanostructures growing perpendicular to the (0001) surface of Bi_2Te_3<*Fe*>. Interlayer ferromagnetic iron nanostructures are most likely responsible for the transition to the ferromagnetic state and the anomalous Hall effect (and the increase in thermoelectric power) in $Bi_{2-x}Fe_xTe_3$ alloys. In alloys such as those $Bi_{2-x}Fe_xTe_3$ ($0 \le x \le 0.08$) with iron, a transition to a ferromagnetic state has been detected; an increase in thermoelectric power, an anomalous Hall effect, and a jump in resistance at $T=T_c$ are observed. The temperature of the transition to the ferromagnetic state T_c increases with increasing iron content, reaching 12 K at x = 0.08. The easy axis of magnetization is parallel to the crystallographic axis *C3* [1]. However, these studies do not focus on the formation of impurity fractal aggregates of *Fe* in the van der Waals gap and their influence on the properties of bismuth telluride. The magnetic properties of *Fe* change significantly with decreasing particle size from 5-10 nm. Interlayer nanoclusters exhibit a non-monotonic dependence of their properties on the cluster size [2], i.e., the number of atoms within it. A change in the interlayer interaction, leading to a redistribution of the electron density from the edges of the quintet to the inside of the layer, to a bond with the central chalcogen, changes the bond from a long-range resonant to a covalent form with a fraction of ionicity, and then to an ionic-covalent one, bringing the interatomic distances closer together as the nature of the bond changes. The shift of the charge towards the center of the quintet can lead to an increase in the degree of orbital overlap and an increase in the ionic component of the *Bi-Te*$^{(2)}$ bond, since this is energetically favorable, the spin-orbit interaction can also be enhanced - in an ion pair, the unpaired electron is partially delocalized on the cation and this leads to an increase in the spin-orbit interaction.

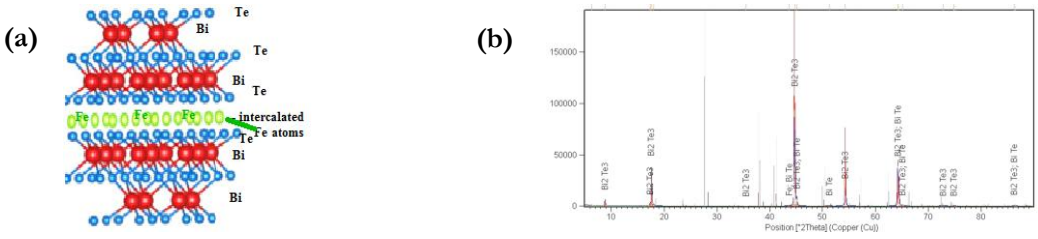

Fig. 1: *(a) Model of Bi_2Te_3 Fe intercalated and (b) Plane surface diffractogram.*

References

[1] S.S. Gahramanov, N.A. Abdullayev, *et al.*, Physics and Chemistry of Solid State **26(1)**,100-104 (2025).

[2] K.Sh. Gahramanov, N.A. Abdullaev, Kh.V. Aliguliyeva, *et al.*, Journal of Surface Investigation, **Vol. 15**, Suppl. 1, S98–S103 (2021).

Abstract ID: 30803

INVESTIGATION OF THE DEPENDENCE OF THE SPIN HALL ANGLE ON THE CONCENTRATION IN THE $L1_0$-Mn_xPt_{1-x} SYSTEM

A. Kh. Kadikova[1], I. V. Yanilkin[1], A. I. Gumarov[1], B. F. Gabbasov[1], D. G. Zverev[1], L. R. Tagirov[1,2], R. V. Yusupov[1]

[1] *Institute of Physics, Kazan Federal University, 420008, Kazan, RUSSIA*
[2] *Zavoisky Physical-Technical Institute, FRC Kazan Scientific Center of RAS, 42029, Kazan, RUSSIA*

Currently, antiferromagnetic materials are a relevant subject of research in spintronics due to the absence of net magnetization and a combination of their intriguing properties. For instance, antiferromagnetic magnons have frequencies in the terahertz and sub-terahertz ranges, which is promising for addressing the THz-gap problem.

Furthermore, antiferromagnetic materials are used as active elements for realizing spin-charge conversion. In heterostructures based on binary Mn_xMe_{1-x} alloys (Me = Pd, Ir, Pt), both the conventional and magnetic spin Hall effects have been demonstrated [1]. In addition, Mn_xMe_{1-x} alloys with an $L1_0$ structure possess a high Neel temperature.

In this work, we investigated spin-charge conversion in bilayer epitaxial $Ni_{80}Fe_{20}/Mn_xPt_{1-x}$ structures, where x = 49-61. The Mn_xPt_{1-x} alloy was chosen as the antiferromagnet because it exhibits the largest spin Hall angle among the series. Four heteroepitaxial $Ni_{80}Fe_{20}/Mn_xPt_{1-x}$ bilayers were synthesized on different substrates. The magnetoresonance properties and magnetocrystalline anisotropy of the samples were studied using ferromagnetic resonance (FMR) techniques in two configurations: in a cavity and through broadband measurements on a coplanar waveguide. Experiments to observe the inverse spin Hall effect were conducted under spin pumping conditions in an EPR spectrometer using cavity techniques. The dependence of the spin Hall angle on the platinum content in the layer was demonstrated, as well as the dependence of the observed transverse voltage signal on the crystallinity of the bilayer heterostructures.

References

[1] A. Hoffmann, W. Zhang, J. Magn. Magn. Mater. **553**, 169216, (2022).

Abstract ID: 30804

RAPID ADIABATIC CONTROL OF HEAT FLOW IN TRANSPARENT THERMAL NETWORKS

Y. Sattorov, M. Salohiddinov, D. Mardonov, J. Matrasulov

Tashkent University of Information Technologies named after Muhammad al-Khwarizmi, Tashkent, UZBEKISTAN

We investigate the fast-forward evolution of thermal processes governed by the heat equation in an adiabatically expanding time-dependent box. The study is motivated by the need to accelerate diffusive heat-transfer dynamics while preserving the essential features of adiabatic evolution. In conventional regimes, adiabatic changes of the system geometry require slow driving to avoid distortions of the temperature field, which limits the speed of thermal manipulation and control. To overcome this restriction, we explore the framework of shortcuts to adiabaticity and apply it to heat transport in expanding domains.

Our analysis focuses on the construction of fast-forward protocols that reproduce the final state of a slow adiabatic process within a significantly reduced evolution time. In this setting, the temperature distribution evolves under a suitably designed driving scheme that ensures rapid yet controlled thermal transport. We compare the standard adiabatic regime with the fast-forwarded one and identify the main differences in the transient and final behavior of the system. Particular attention is paid to the evolution of temperature profiles and heat flux, which provide direct insight into the efficiency and physical consequences of accelerated transport.

The results demonstrate that fast-forward strategies can substantially shorten the time required for adiabatic thermal processes while maintaining the desired spatial structure of the temperature field. At the same time, the accelerated regime exhibits distinctive intermediate dynamics, including modified heat-flux characteristics and nontrivial transient temperature deformations, which are absent or strongly suppressed in the standard slow protocol. These features highlight both the advantages and the physical cost of rapid thermal control.

The proposed approach extends shortcut-to-adiabaticity concepts beyond their usual applications in quantum and wave systems to the domain of diffusive heat transport. This opens new possibilities for the design of tunable thermal processes in time-dependent media and provides a theoretical framework for rapid heat-flow control in transparent thermal networks and related nonequilibrium thermal systems.

References

[1] G. Babajanova, J. Matrasulov, K. Nakamura, *Quantum gas in the fast forward scheme of adiabatically expanding cavities: Force and equation of state*, Phys. Rev. E **97**, 042104 (2018).

[2] J. Matrasulov, J.R. Yusupov, A.A. Saidov, *Fast forward evolution in heat equation: Tunable heat transport in adiabatic regime*, Nanosystems: Phys. Chem. Math. **14(4)**, 421–427 (2023).

[3] J.D. Matrasulov, J.R. Yusupov, K.Sh. Matyokubov, *Fast forward problem for adiabatic quantum dynamics: Estimation of the energy cost*, Nanosystems: Phys. Chem. Math. **15(4)**, 457–464 (2024).

[4] J. Matrasulov, K. Sabirov, *Fokker–Planck equation on metric graphs*, Physics A **608,** 128279 (2022).

Abstract ID: 30805

NEUTRON DIFFRACTION STUDY OF CRYSTALLINE AND MAGNETIC STRUCTURE OF $Sr_2FeMo_{1-x}V_xO_6$ (x= 0-0.25) AT ROOM TEMPERATURE

K. M. Hasanov[1,2], S. V. Sumnikov[2], V.G. Kostishin[3], M. Čebela[4], V. A. Turchenko[2,3]

[1] *Institute of Physics, Baku, AZERBAIJAN*
[2] *Joint Institute for Nuclear Research, Dubna, RUSSIA*
[3] *National University of Science and Technology "MISiS", Moscow, RUSSIA*
[4] *Institute of Nuclear Sciences Vinca, University of Belgrade, SERBIA*

Compounds with a double perovskite-like structure, denoted as $A_2BB'O_6$ (where A represents a rare earth or alkaline earth cation, while B and B' are transition metals), gain significant attention. These materials possess a distinctive crystal structure and remarkable properties, including excellent carrier transport capabilities, as well as magnetic, and optoelectronic characteristics. Such features make them highly suitable for a variety of technological applications [1-4].

The features of the crystalline and magnetic structure of double perovskite oxides, influenced by the degree of vanadium (V) ion substitution $Sr_2FeMo_{1-x}V_xO_6$ (x= 0 – 0.25), were investigated using neutron diffraction at room temperature on the HRFD neutron diffractometer. The diffraction data were analyzed using Rietveld refinement within the FullProf software package to achieve precise structural characterization.

The Rietveld refinement results indicate a systematic variation in lattice parameters with increasing vanadium content. The lattice parameter a decreases from 5.579 Å to 5.574 Å as concentration x increases from 0 to 0.1, but it slightly increases to 5.576 Å at x = 0.25. Also, the unit cell volume V contracts from 246.2 Å^3 (x = 0) to 245.5 Å^3 (x = 0.1) and expanding to 245.7 Å^3 (x = 0.25). This trend suggests that vanadium substitution leads to a slight lattice contraction, which can be attributed to the smaller ionic radius of V^{5+} (r = 0.54 Å) compared to Mo^{5+} (r = 0.61 Å). A notable decrease in magnetic moment per Fe atom is observed with increasing vanadium content. For undoped sample (x = 0) the magnetic moment per Fe atom is 2.39 μ_B/Fe, which diminishes to 1.15 μ_B/Fe for x = 0.25.

The neutron diffraction and Rietveld analysis of $Sr_2FeMo_{1-x}V_xO_6$ reveal that vanadium substitution leads to subtle structural modifications and a significant reduction of the magnetic moment. These findings contribute to the understanding of how B-site cation substitution influences the structural and magnetic properties of double perovskite oxides, providing insights for the design of materials with controlled functionalities.

References

[1] Z. Ghorbani,, M. H. Ehsani, *Synthesis and magnetic properties of $Ba_{2-x}Sm_xFeMoO_6$ ($0.0 \leq x \leq 0.1$) double perovskite*, Ceramics International **49(16)**, 27362-27372 (2023).

[2] J. Hwang, R. R. Rao, L. Giordano, Y. Katayama, Y. Yu, Y. Shao-Horn, *Perovskites in catalysis and electrocatalysis*, Science **358**, **6364**, 751-756 (2017).

[3] F. A. Najar, K. Sultan, *From halfmetallicity to dielectric tensor: Atomistic study of phase stability and optical spectrum of Sr_2FeMoO_6 double perovskite and its potential applications*, Journal of Physics and Chemistry of Solids **171**, 111039 (2022).

[4] A.S. Erchidi Elyacoubi, R. Masrour, A. Jabar, M. Ellouze, E.K. Hlil, *Magnetic properties and magnetocaloric effect in double Sr_2FeMoO_6 perovskites*, Materials Research Bulletin **99**, 132-135 (2018).

Abstract ID: 30808

A MULTI-SENSOR FLUXGATE SYSTEM WITH INTEGRATED DATA PROCESSING TECHNIQUES FOR HIGH-RESOLUTION MAGNETIC ANOMALY DETECTION

N. G. Saribas, A. Demirtaş, M. Maksutoğlu

Institute of Nanotechnology, Gebze Technical University, Gebze, Kocaeli 41400, TURKIYE

Magnetic anomaly detection (MAD) is widely used in mining, archaeology, and defense applications by measuring local perturbations in the Earth's magnetic field. This study presents a data acquisition system comprising four vector fluxgate sensors integrated with a moving-base DGNSS module providing centimeter-level positioning accuracy.

The data processing chain employs multiple complementary techniques: Kriging-based gridding for spatial interpolation, Euler deconvolution for source depth estimation, analytical signal amplitude (ASA) for edge detection, and median and Gaussian filtering for noise suppression. Integration of these methods yields a 12–15 dB improvement in signal-to-noise ratio (SNR) and enables detection of small buried targets at depths of up to 5 meters with 20% higher localization accuracy compared to conventional single-method approaches.

The system offers significant advantages for geophysical exploration and defense-related applications, combining high spatial resolution with robust performance under field conditions. This poster presents the system architecture, processing methodology, and validation results from controlled test sites.

The work was supported by NATO Science for Peace and Security Programme (NATO SPS project No. G6063).

Abstract ID: 30809

FIELD-DEPLOYABLE MAGNETIC ANOMALY DETECTION SYSTEM USING ORTHONORMAL BASIS FUNCTIONS DECOMPOSITION

E. Kaya[1], A. Demirtaş[2], N. G. Saribas[2], M. Maksutoğlu[2]

[1] *Department of Computer Engineering, Gebze Technical University, Kocaeli 41400, TURKIYE*
[2] *Institute of Nanotechnology, Gebze Technical University, Gebze, Kocaeli 41400, TURKIYE*

We present a field-deployable magnetic sensor system for geomagnetic anomaly mapping, integrated with an Orthonormal Basis Functions (OBF) decomposition algorithm for enhanced target detection. The system hardware is optimized for field robustness low-power operation. The OBF algorithm projects three-component fluxgate measurements onto orthonormal basis functions derived from the magnetic dipole model, enabling effective separation of target signatures from background variations. A normalized energy function is used as the detection statistic with adaptive thresholding for real-time anomaly identification. Field trials validate the system's performance under real environmental noise conditions. The OBF-processed energy signals exhibit clear monopulse characteristics at target locations with significantly reduced false alarm rates compared to raw amplitude-based detection.

This study presents the system architecture, algorithm implementation, and representative field results demonstrating the practical applicability of OBF-based methods for portable geomagnetic anomaly mapping.

The work was supported by NATO Science for Peace and Security Programme (NATO SPS project No. G6063).

Abstract ID: 30816

A COMPARISON BETWEEN THE NANOSTRUCTURE OF Y-123 AND Y-358 HIGH-TEMPERATURE SUPERCONDUCTOR

E. K. Al-Shakarchi[1], M. B. Abood[2]

[1] *Department of Medical Physics, College of Science, Dijlah University, Baghdad, IRAQ*
[2] *Department of Physics, College of Science, University of Baghdad, Baghdad, IRAQ*

Two high-temperature superconducting compounds, $YBa_2Cu_3O_{7-\delta}$ (Y123) and $Y_3Ba_5Cu_8O_{18}$ (Y358), were synthesized using the sol-gel auto-combustion technique. The precursors were dried at 250 °C for 1 hour to remove residual solvents, followed by a single calcination step at 750 °C for 12 hours. The powders were then compacted and sintered at 850 °C for 24 hours, with slow cooling to promote phase formation. X-ray diffraction (XRD) analysis confirmed the formation of orthorhombic crystal structures for both compounds, with well-matched lattice parameters obtained via CrystalDiffract simulation and the Open Crystallography Database. The Y358 sample exhibited sharper and narrower diffraction peaks, indicating improved crystallinity. Fourier-transform infrared spectroscopy (FTIR) analysis revealed distinct vibrational modes corresponding to Y-O, Ba-O, and Cu-O bonds in both samples. A stronger Cu–O absorption band in the Y358 spectrum suggested enhanced lattice stability and higher bonding energy. Transmission electron microscopy (TEM) images, analyzed using ImageJ, showed nearly spherical nanoparticles with average diameters of 35 nm for Y123 and 33 nm for Y358. The finer nanostructure of Y358 correlated with its superior superconducting performance. Electrical resistivity measurements revealed that the Y358 sample exhibited a higher superconducting transition temperature ($T_c \approx 150$ K) compared to Y123 ($T_c \approx 98$ K). This enhancement in T_c is likely associated with the optimized nanostructure, high crystalline quality, and nearly full oxygenation ($O \approx 7.92$) of the Y358 sample.

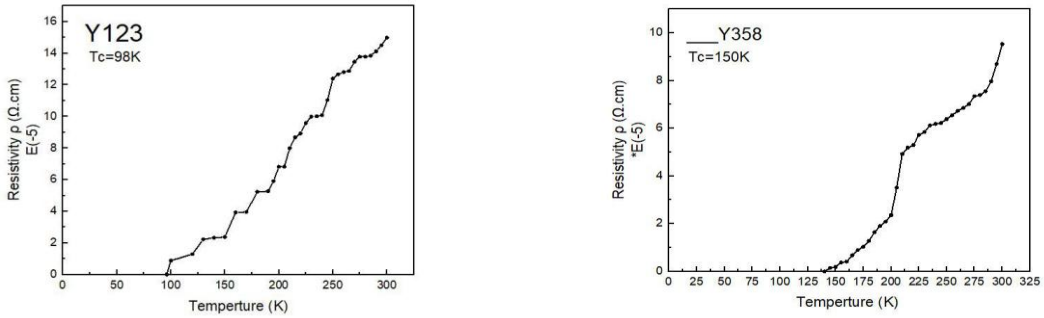

Fig. 1: *Resistivity curve of Y123, and Y358 superconductors.*

Abstract ID: 30819

MAGNETOCALORIC CHARACTERISTICS OF NiFeMnSnB SHAPE-MEMORY RIBBONS IN THE MARTENSITIC PHASE TRANSITION REGION

G. Kirat[1], M. Ayyildiz[2], M. A. Aksan2

[1] *Inonu Universitesi, Bilimsel ve Teknolojik Arastirma Merkezi, 44100 Malatya, TURKIYE*
[2] *Inonu Universitesi, Fen Edebiyat Fakultesi, Fizik Bolumu, 44100 Malatya, TURKIYE*

Fe-doped Ni-Mn-Sn-B shape memory ribbons were produced using the melt-spinning technique. The magnetocaloric properties of the ribbons were investigated under magnetic fields applied during heating and cooling. The magnetocaloric response was found to be closely related to the magnetostructural transition between the austenite and martensite phases. Near the transformation region, a negative magnetocaloric effect, arising from the difference in magnetization between the two phases, was observed. The results indicate that Fe doping alters both the magnitude and temperature range of the magnetic entropy change, leading to an expanded operating temperature range. Although a distinct magnetostructural coupling accompanies the phase transformation, the magnetocaloric performance shows a clear dependence on thermal hysteresis. These characteristics are critically important for evaluating the applicability of the ribbons in solid-state magnetic cooling. The present findings indicate that Fe-doped Ni-Mn-Sn-B shape memory ribbons provide a suitable approach for tuning the magnetocaloric behaviour in Heusler-type alloys.

Abstract ID: 30820

HIGH ENTROPY RARE-EARTH BORIDES: SYNTHESIS, CHARACTERIZATION AND POTENTIAL EVALUATION FOR SUPERCONDUCTORS

B. Boztemur, C. F. Arısoy, D. Ağaoğulları

Istanbul Technical University, Faculty of Chemical and Metallurgical Engineering, Department of Metallurgical and Materials Engineering, Particulate Materials Laboratories (PML), Graphene & 2D Materials Laboratory, 34469 Maslak, Istanbul, TÜRKIYE

Due to their excellent mechanical strength, melting point, corrosion resistance, wear resistance, and magnetic behavior, high entropy rare-earth borides have gained a lot of popularity in recent years. However, the production of these materials is very difficult. In this study, this can provide with mechanochemical synthesis (MCS) with high purity. The production of high entropy rare-earth boride (HEREB) nano-powders was reported in this study first time in the literature. 8 different compositions ((LaCeSm)B_6, (LaCeSmNd)B_6, (LaCeSmYb)B_6, (LaCeSmY)B_6, (LaCeSmYYb)B_6, (LaCeSmYNd)B_6, (LaCeSmYbNd)B_6 and (LaCeSmYYbNd)B_6) were synthesized in this study. Hardened steel vials (50 ml) were filled with prepared as-blended powders and hardened steel balls (ø = 6 mm). The ball to powder weight ratio (BPR) was maintained at 10:1. The vials containing the balls and powders were sealed in a glove box with an Argon atmosphere to occur reaction. Then, the vials were replaced to a high energy NanoMultiMix mill at 800 rpm for 5 h. The energy required to initiate the reaction was supplied by the high-energy impacts that mechanically deformed the powder particles. After this process, MgO and HEREB phases were observed. To remove MgO phase, the selective acid leaching (4 M HCl solution) was applied to powders. With a solid-to-liquid ratio of 1 g/10 cm^3, the leaching procedure was carried out for 15 min at 80 °C. Decantation, washing, and repeated centrifugation (8000 rpm, 30 min) were used to separate the residue from the leaching solution. The centrifugation was stopped when this pH value reached about 5, and the residue was dried in the air for 24 h at 100 °C on a stove. X-ray diffraction (XRD) was used to investigate the phase of nano-structured HEREB powders. Pycnometer density measurements and particle size analysis were conducted on the HEREB powders. The scanning electron microscope images with electron dispersive spectroscopy results and mapping images were taken for the powders. The homogeneity of elements distribution was detected, so it can be understood that the production was successful. The magnetism of HEREB powders was measured.

Acknowledgement

This project was supported by TUBITAK 1005 with 125M954 number and TUBITAK Directorate of Scientist Support Programs (BIDEB) 2211. Also, TENMAK 1981 project supported this study.

Abstract ID: 30825

LEVITATION FORCE RELAXATION ANALYSIS OF FLUX PINNING IN SINGLE-GRAIN YBCO

S. B. Guner[1,2,3], Z. Bekiryazıcı[4]

[1] *Department of Physics, Faculty of Science, Ankara University, 06170, Ankara, TURKIYE*
[2] *Center of Excellence for Superconductivity Research, Ankara University, 06500, Golbasi, Ankara, TURKIYE*
[3] *Department of Physics, Faculty of Arts and Sciences, Recep Tayyip Erdogan University, 53100 Rize, TURKIYE*
[4] *Department of Mathematics, Faculty of Arts and Sciences, Recep Tayyip Erdogan University, 53100 Rize, TURKIYE*

The temperature dependence of the magnetic levitation force in a single-grain Yttrium Barium Copper Oxide (YBCO) bulk superconductor (20 mm diameter, 9 mm thickness) fabricated by the top-seeded melt growth (TSMG) method using an Nd123 seed crystal was investigated. The superconducting properties were examined at low temperatures (37–77 K) using a Vibrating Sample Magnetometer (VSM) and a custom-built magnetic levitation force measurement system. For the first time, activation energy was determined from magnetic levitation force–time (relaxation) curves obtained at low temperatures. The calculated activation energies increase from 0.078 eV to 0.166 eV with increasing temperature, while the zero-field critical current density (J_c) decreases from 19.7×10^4 to 1.96×10^4 A/cm² over the same temperature range. These results demonstrate the strong influence of temperature on flux pinning and levitation performance, providing valuable insight for optimizing large-scale superconducting levitation applications.

Abstract ID: 30827

THE IMPACT OF Mn SUBSTITUTION ON THE STRUCTURAL AND MAGNETIC PROPERTIES OF HIGH-LAYER (m ≥ 5) AURIVILLIUS-PHASE MULTIFERROIC THIN FILMS

Y. Demirolmez[1], S. Conroy[2], L. Keeney[1]

[1] Tyndall National Institute, University College Cork, Cork, , T12 R5CP IRELAND
[2] Imperial College London Exhibition Rd, South Kensington, London SW7 2AZ, UNITED KINGDOM

Multiferroic materials that concurrently exhibit ferroelectric and ferrimagnetic characteristics present an intriguing potential for enhancing data storage capacity by up to as eight-fold. The limited availability of multiferroics exhibiting both functionalities at room temperature has impeded their widespread technological integration.

Our group has previously published a five-layered Aurivillius-phase multiferroic, $Bi_6Ti_xFe_yMn_zO_{18}$ (B6TFMO; m = 5), which distinctly demonstrates room-temperature ferroelectric and magnetic ordering, with saturation magnetisation and in-plane polarisation values in the range of hundreds, specifically 215 emu/cm³ and >26 μC/cm, respectively, along with reversible magnetoelectric switching at room temperature.

These materials possess significant possibilities for sensor, data storage, and spintronic devices [1-3].

This study investigates the synthesis and characterization of high-layer Aurivillius-phase thin films exhibiting enhanced magnetic functionality, focusing on six-layer $Bi_7Ti_xFe_yMn_zO_{21}$ (B7TFMO). The higher number of perovskite layers (m = 6) promotes increased incorporation of magnetic ions, particularly Mn. The films were deposited via Direct Liquid Injection Chemical Vapor Deposition (DLI-CVD).

Film morphology and crystallographic structure were characterised by atomic force microscopy (AFM) and X-ray diffraction (XRD). The macroscopic magnetic properties were determined using superconducting quantum interference device (SQUID) magnetometry. Nanoscale electrical and magnetic behaviour were examined through piezoresponse force microscopy (PFM) and magnetic force microscopy (MFM), respectively. Furthermore, high-resolution transmission electron microscopy (HRTEM) provided detailed insights into the local crystal structure and atomic-scale characteristics.

References

[1] L. Keeney, Z. Saghi, M. O'Sullivan, J. Alaria, M. Schmidt, and L. Colfer, *Persistence of ferroelectricity close to unit-cell thickness in structurally disordered aurivillius phases*, Chemistry of Materials, **vol. 32**, **no. 24**, pp. 10511–10523 (2020).

[2] A. Faraz, *et al.*, *Direct visualization of magnetic-field-induced magnetoelectric switching in multiferroic aurivillius phase thin films*, Journal of the American Ceramic Society, **vol. 100**, **no. 3**, pp. 975–987 (2017).

[3] L. Keeney, *et al.*, *Magnetic field-induced ferroelectric switching in multiferroic aurivillius phase thin films at room temperature*, Journal of the American Ceramic Society, **vol. 96**, **no. 8**, pp. 2339–2357 (2013).

INDEXES

A

Aarts J. 488
Abdioglu M. 282, 300, 660
Abdulkadirova N. Z. 237
Abdullayev A. 457, 626, 685
Abdullayev N. A. 626, 685
Abert C. 309, 316, 317, 351, 413
Abiyev A. S. 632
Abood M. B. 691
Abrahamsen A. B. 112
Achari A. 544
Adak A. 225
Affronte M. 320, 365
Ağaoğulları D. 693
Agero C. G. 392
Agil A. A. 611
Ağıl H. 611
Agostino A. 342
Ahmad H. G. 138
Ahmad I. 95, 680
Ahmed M. E. 523
Ahn C. H. 177
Ahn K. 106
Aichner B. 248
Ajayan A. 154
Ajeesh M. O. 584
Ajejas F. 437
Akarsubaşı M. N. 465, 466
Akashdeep[1] A. 105
Åkerman J. 315
Akin K. 102
Akmeşe B. 661
Aksan M. A. 624, 675, 692
Alatas A. 383
Albanesi M. 221
Albisetti E. 190, 193
Albrecht M. 136, 311, 409, 411
Albu R. 506
Alcalà J. 190
Alessio A. 342
Ali H. 95, 422, 634, 636, 641
Ali Q. 349
Aliev A. M. 237
Aliev Z. S. 626
Aliguliyeva Kh. V. 685
Alimenti A. 130, 601
Aliyev V. 661
Aljalal A. M. 638
Allan M. P. 157, 158
Almokdad F. 344, 656, 657, 658, 662
Al-Mokdad F. 659
Alocco A. 160
Al-Shakarchi E. K. 691
Alssalih H. 529
Altbir D. 135
Altena M. 157
Althammer M. 106
Álvarez-Alonso P. 292
Alvárez-Prado L. M. 421
Alvarruiz S. 189
Alzoubi Z. 638
Amaro N. 62
Amelichev V. A. 55
Amemiya N. 89
Ameziane M. 192, 204
Amin M. W. 621
Amin O. J. 94, 108, 110
Amin S. 449, 450
Amiraslanov I. R. 626
Amm K. M. 26
Anane A. 316, 347
Ando K. 124
Andres D. 73
Angurel L. A. 146, 154, 298, 533
Anis-ur-Rehman M. 297, 299, 604, 634, 636, 639, 641, 643, 644, 646, 653
Anis-Ur-Rehman M. 635
Annenkov D. 396
Ansaldo A. 343
Antoncik F. 112, 122, 123
Antonio G. N. 212
Aoki D. 25, 116
Aqeel A. 194
Arauzo A. 217, 218
Arauzo Ana 218
Arbuzov D. A. 518
Ari S. 102
Arısoy C. F. 693
Arita R. 188, 407
Armesto L. M. 200, 201
Aromí G. 364, 366
Arouca R. 213
Arredondo-López A. 199
Arregi J. A. 195
Arreguín-Hernández M. L. 292
Arsenin A. 100
Asadov A. G. 334
Asadullayeva S. G. 627
Ashhab S. 507
Ashirbekov S. 457
Askerbeyli R. T. 629
Askerzade I. 400, 401
Askerzade I. N. 574, 575, 642
Astafiev O. V. 454, 461
Aswartham S. 552
Atalay F. B. 465, 466
Athavale M. R. 101
Atilmis M. N. 645
Attanasio C. 149
Attané J. -P. 198
Ausanio G. 138
Avci C. O. 414, 442
Avci D. 336
Avella A. 180
Avitabile F. 149
Avsar A. 46
Ayala C. 504
Ayala C. L. 510
Ayas E. 611
Aydemir U. 42, 456, 483, 594
Aydın A. A. 594
Aydın C. 609
Ayyıldız M. 675
Azam M. 114, 620

Azarevich A. N. 301, 385

B

Baazizi Y. 67
Babij M. 119, 336
Bacani M. 73
Badia A. 529
Badía A. 146, 154, 298, 529
Badía-Majós A. 154, 298, 529
Badica P. 337, 660
Badosa Q. 439
Bag P. 296, 679
Bai P. 53
Baigutlin D. 232
Baigutlin D. R. 482
Bakoue A. 677
Bakurskiy S. V. 493
Balatsky A. 600
Ballarino A. 29
Ballestero C. G. 321
Baloch S. A. 625
Bandopadhyay K. 455
Banerjee N. 211
Barbour A. M. 182
Barišić N. 37
Barker J. 170
Barone P. 145, 189
Barreneche C. 533
Barrera A. 185
Barrera G. 191
Barrios L. A 364, 366
Barthélémy A. 198
Bartolomé E. 217, 218
Bartolomé Elena 218
Barts E. 189
Barucca G. 136
Bassi A. L. 193
Bateman R. 247, 269
Bauer G. E. W. 170
Baum A. 329
Baumann D. 552
Baumgarten J. 137, 146, 617
Bazgir L. 677
Bednorz A. 163
Begic K. 56
Behnami M. 548
Bekaert J. 329
Bekiryazıcı Z. 694
Belenli I. 336
Belogolovskii M. 342
Belojica T. 327, 328
Belzig W. 472
Benedicto A. 421
Berchialla L. 139, 147
Bertacco R. 193
Bertini V. 49
Besproswanny J. 20, 551
Besproswanny Julia 552
Bessas D. 404
Bestha K. 106
Bhandari H. 410
Bhartiya V. 171
Bhattacharya A. 98
Biancardi I. 190, 193
Bibes M. 198
Bicket I. C. 72
Bigelli C. 563
Bighin G. 470
Biondini A. 449, 450
Bîrcă A. C. 613, 614, 615, 670
Birch M. 291, 410
Birch M. T. 412
Bisogni V. 170, 171, 179, 451
Bittencourt G. H. R. 135
Black-Schaffer A. M. 213
Blagojević J. 327, 328
Blanco J. A. 292
Blatter G. 392, 395
Blom T. J. 157, 158
Bocklage L. 404
Bode M. 551
Bogach A. V. 262, 301, 385, 386
Böhm D. 352
Boltje D. B. 158
Bombardi A. 178
Bommanaboyena S. 106
Boneberg J. 311
Bonfà P. 543
Bonhommeau S. 225
Boniecki K. 591
Bonino V. 342
Bonizzoni C. 320, 365
Borisenko S. 554
Borisov A. 56
Borkovska L. 94
Borsari M. 358
Bort-Soldevila N. 120, 243
Botto T. 527
Bouchard B. 268
Boulle O. 190
Bouthillette A. 268
Boventer I. 198
Bozbey A. 39, 465, 466
Bozin E. 327
Bozin E. S. 326, 328
Božin E. S. 328
Bozkurt[1] B. 612
Božović I. 9, 10, 27
Boztemur B. 693
Braccini V. 130
Braithwaite D. 25, 369
Brandt C. 404
Brangi P. N. 214
Breitbach D. 193
Breth L. 349
Brida G. 462
Briganti M. 358, 563
Brink J. van den 31, 180, 479, 553
Brison J. -P. 25, 369
Bristow M. 129
Bruckner F. 309, 316, 318, 351, 413
Bruno A. 138
Bruscino C. 149
Buchanan K. S. 185
Buchcic F. 674
Buchelnikov V. 231, 232, 235, 424, 425, 565, 619
Büchner B. 48, 106, 141, 174, 548, 551, 552
Bud'ko Sergey L. 542
Buechner B. 20
Buffeteau T. 287
Bujault N. 387
Bulut N. 564

Burchianti A. 470
Burdușel A. C. 613, 614, 615, 670
Burghard M. 412
Burke M. D. 376
Burkhardt U. 479, 483
Burton J. 281
Buttiens T. 198
Buzdin A. 495
Buzzi M. 176

C

Cabala A. 371
Cabero M. 488
Cadorim L. 508
Cadorim L. R. 154, 638
Cai C. 54
Cai Y. Q. 380, 383
Calandra M. 214
Çalışkan Y. S. 606
Cambré S. 216
Camino F. 170, 171, 182, 258
Campbell D. J. 585
Campbell I. 290
Campion R. P. 108
Campo J. 294
Çamsarı K. Y. 558
Can H. 624
Cao Y. 393, 449, 450
Cao² S. 105
Carretta S. 221, 364
Carvalho-Santos V. L. 135
Casals B. 439
Castellví A. 439
Cavani M. 320
Cayao J. 399
Cazacu Maria 218
Čebela M. 688
Celegato F. 185, 191
Celentano G. 601
Celotto C. 160
Cha J. 81, 175, 474, 585
Chakraborty N. 224
Chan W. M. 546
Chang H-T. 411
Chang J. 585
Charvier A. 198
Chatterjee A. 281
Che P. 305, 316
Chen A. 433, 591
Chen G. T. 261
Chen J. 54, 86, 429, 432, 629
Chen O. 496
Chen Q. 412, 427, 432
Chen S. 53, 558
Chen Z. 394, 480, 483, 679
Cheong S. -W. 171, 173, 412
Cherednichenko K. A. 386
Chernenko V. 229, 230, 234
Chernoukhov I. V. 386
Chernyshev A. L. 377
Chi M. 358, 363, 410, 558
Chiarello F. 462
Chiesa M. 358, 363
Chiew Y. L. 407
Chiroli S. 143, 198
Chmaissem O. 125
Choi E. S. 423
Choi Y. T. 618
Chumak A. 309, 318, 351, 404
Chumakhov A. 404
Chung K. T. K. 376
Church S. 101
Cialone M. 130
Ciccarelli C. 212
Cincio L. 278
Cini A. 563
Ciria M. 298
Cirillo C. 149
Clegg M. 529
Clérac R. 220, 225, 358
Clermont G. 225
Cloos M. A. 276
Çoban M. 669
Cocconcelli M. 193
Coïsson M. 191
Çolak B. 74
Çolak M. 465, 466
Coldea A. I. 129
Colle A. 523
Coloma I. 287
Conder K. 251
Conroy S. 695
Cooper V. 171
Cording L. 453
Cornia A. 358
Corrielli G. 193
Corsaro P. 527
Corte-Leon P. 70, 610
Corte-León P. 70
Cortijo M. 287
Costilla J. I. 135
Courtois T. 210, 212
Crivillers N. 32, 216
Croitoru A. M. 615, 670
Croteau A. 268
Cudazzo P. 214
Cuello G. J. 292
Cui B. 433, 481
Cunill-Subiranas J. 120, 243
Cunnane D. 516
Cuocco M. 179
Cuoco M. 151, 182
Ćwik J. 228
Czaja P. 234
Czarnik P. 278
Czasch B. 72, 405
Czernuszewicz A. 228
Czujko T. 336

D

d'Aquino M. 150, 316, 347, 355
D'Elia A. 462
Dadhich A. 244, 523, 524
Dai C. 265
Daibo M. 57
Damascelli A. 78
Dannegger³ T. 105
Dao H. 56
Darwin E. 147
Das T. 567

Davídková K. 309, 312, 318
Davidson A. 271
Dean M. P. M. 171, 177, 179
Degtyarenko P. N. 55
Deguchi S. 503
Dekadjevi D. T. 200
Delfanazari K. 168
Delforge C. 92, 146, 298
Delice S. 655
Delport J. A. 156, 502
Del-Valle N. 120, 243
Demidov V. E. 308, 435
Demiral Y. M. 606
Demirci E. 458
Demirolmez Y. 695
Demirtaş A. 459, 671, 689, 690
Demokritov S. O. 150, 308
Denisov A. O. 392
Derlet P. M. 139
De-Santis M. 196
Devashibhai A. 331
Devred A. 265
Dhiman A. K. 348
Diamantini M. C. 581
Dias T. 199
Diego R. 225
Dijk B. v. 189
Dijken S. van 204
Dikarev E. V. 262
Diko P. 123
Din A. Dal 108
Ding H. 429
Dinh T. 393
Disa A. S. 177
Dissanayake C. 375
Djurek D. 672
Dmitriev[1] A. Yu. 461
Do A. 43, 438
Dobrovolskiy O. V. 143, 153, 622
Docampo P. 453
Doedes Y. C. 158
Dolecki M. 674
Doležal P. 591
Donnelly C. 317, 622
Dorget R. 523
Dorsch E. 162
Dosta S. 533
Douine B. 520, 521
Douveas I. 309
Dubs C. 313, 318
Dudziński M. 234
Dumesnil K. 210
Dunin-Borkowski R. 422
Duran Y. E. 606
Dzhumanov S. 649, 650

E

Eaton A. G. 371, 372
Edmonds K. W. 108
Edström A. 145
Egyenes F. 248
Elfimov I. 24
Elharkati H. 629
Elias M. 416
Elistratov A. A. 454, 461
Elistratov[3] A. A. 461
Ender M. 354
Enenko A. 231, 619
Engel-Herbert R. 198
Enrico E. 160, 462
Ensslin K. 392
Erager K. 232
Ercolano P. 149
Eren S. M. 463
Ervüz F. 344, 656, 657, 658, 659, 662
Eskadari-asl A. 180
Evren Ö. 594
Exl L. 350

F

Fabbris G. 177
Fabrega L. 513
Fagnard J. F. 113, 122
Fagnard J. -F. 112
Falus P. 387
Fan S. 171, 380, 383, 451
Fang Y. K. 651
Farjas J. 49
Farle M. 422
Fasano Y. 552
Fasolo L. 160, 462
Fatima U. 604
Faurie D. 143, 148
Fazlioglu Y. B. 198
Febvre P. 517
Fedotov A. K. 388
Fedotova J. 388
Feiguin A. E. 382
Feldman P. 528
Feng Y. 147, 341, 648, 668
Fennell T. 387
Fergosun R. M. 673
Fermin R. 158
Fernández-González C. 317
Fernández-Pacheco A. 22, 38, 317
Ferraiuolo R. 138
Ferreira L. 67
Feuchtwanger J. 230
Feuillet-Palma C. 159
Filippov T. V. 512
Finizio S. 317, 412
Fink J. 174
Firouzmandi R. 106
Fischbacher J. 349
Fischer J. 106
Fischer P. 22, 124, 596
Fistul M. 462
Fittipaldi M. 221, 563
Fittipaldi R. 179
Florea D. A. 614
Florea E. C. 614
Florio P. 190, 193
Foerster M. 185, 437
Fogelström M. 600
Fomin V. M. 35, 622
Fominov Ya. V. 518
Forte F. 182
Fourie C. 499, 517
Fourie C. J. 501, 502, 505
Fourneau E. 92, 154, 298

Foyevstova K. 24
Fracasso M. 113, 598
Frachet M. 585
Franchini C. 577
Francia E. Di 342
Frechilla A. 298, 533
Frechilla J. 146, 154, 298, 533
Fretto M. 342
Frez C. 516
Friedemann S. 590
Fuente G. F. de la 146, 154, 298, 533
Fuertes Sara 218
Fuhrmann[1] F. 105
Fujimaki A. 503
Fujita S. 57
Fukui D. 124
Fulga C. 550
Fuse T. 507

G

Gabbasov B. F. 686
Gabriele F. 182
Gaggioli F. 392, 394
Gaifullin M. 56
Gajda D. 228, 336
Gali A. 447, 451
Galindez-Ruales[1] E. 105
Galvano B. 160
Gamzatov A. 237
Ganiev O. 630
Ganiev O. K. 572
Ganss F. 306, 307
Gao L. 272
Gao S. 63, 90
Gao X. 449, 498
Gao Z. 53
Garcia C. 584, 610
Garcia D. 49
Garcia-Gassull L. 107
Gareeva Z. V. 197
Garg A. 357
Garif'yanov N. N. 518
Garifullin I. A. 518
Garlatti E. 221
Gas K. 109, 110
Gatta D. 138
Gatti C. 462
Gaulin B. D. 390
Gawryluk D. J. 76, 584
Gay F. 196
Gazzah M. El 410
Gen M. 150, 238
Gencer A. 6, 344, 400, 656, 657, 658, 659, 662
Genoni S. 193
Gentile P. 151
Geprägs S. 106
Gerbaldo R. 113, 598
Gerguri O. 259, 544
Geshkenbein V. 392
Geshkenbein V. B. 394, 395
Ghamsari M. Sasani 677
Ghiara E. 49
Ghigo G. 113, 598
Ghimire N. J. 410
Ghirri A. 320, 365
Ghosh A. K. 213
Ghosh S. K. 224
Giacco A. D. 193
Giaconi N. 287
Giannone V. 198
Gimazov I. I. 666
Gingras M. J. P. 376
Gippius A. A. 385
Girardi D. 190, 193
Giri S. 225
Glamsch S. 311
Glatz A. 508
Gloter A. 198
Glowacki B. A. 255, 345
Gmitra M. 583
Gnida D. 118
Godard P. 148
Godeke A. 66
Goennenwein S. T. B. 106
Goering E. 412
Gok O. 645
Gökçe S. 388
Gokita T. 409
Goksal I. 102
Golikova T. E. 489
Golubov A. A. 490, 492
Gómez-Coca S. 217
Gómez-Torres H. 199
Gomonay O. 438
Gong D. 131
Gonidec M. 225, 287
Gonzalez A. 70
Good J. 267
Goossens A. S. 198
Górniak D. 674
Górnicka K. 116
Gorria P. 292
Gotomyo T. 253
Gouder T. 592
Goueré D. 347
Gouéré D. 199
Goukassov A. 289
Govoni M. 449, 450
Goyal A. 7, 21
Gozzelino L. 113, 598
Graczyk P. 348
Gradauskaite E. 198
Graf D. E. 129
Graham J. 259, 544
Granata C. 138
Gransbury G. K. 563
Grasso G. 343
Grayson M. A. 481
Grebenchuk S. 394
Greenfield J. 516
Grigoriev P. D. 616
Grin Yu. 479
Grosche F. M. 371, 536
Gross B. 144
Grosso G. 444, 449, 450, 451
Grozić P. Đ. 477
Grumezescu A. M. 613, 614, 615, 670
Grundherr C. Kelvin von 73
Grundler D. 150, 323, 622, 623
Gruner M. E. 236
Gu Y. 170, 171, 204, 385, 433, 451
Gubbiotti G. 36, 143, 150, 319

Gudin A. 437
Guedeja-Marrón A. 437
Guguchia Z. 8, 259, 543, 544
Guidi T. 221
Gukasov A. 289, 379
Gul-e-Rana S. 635
Gumarov A. I. 686
Gumeniuk R. 479
Gumrukcuoglu İ. E. 663
Guner B. 123
Guner S. B. 660, 694
Güner S. B. 660
Güngüneş Ç. Dönmez 661
Gungunes H. 655
Gunin S. A. 461
Günkel T. 190, 513
Guo C. 340, 344, 656, 657, 658, 659, 662
Guo G. -Y. 407
Guo Q. 341, 648, 651, 668
Gupta K. 49
Guryev V. V. 599
Gusenbauer M. 349, 350
Gutierrez J. 48, 49
Gutmann M. 331
Gutmann M. J. 330

H

Haan J. D. de 158
Hachiya T. 280
Hackl R. 327, 328, 329
Haddad T. 511
Hadibarata T. 613, 614, 615, 670
Haghighirad A. A. 129
Hahn T. 577
Halder A. 44
Hałubek E. 674
Han J. 618
Han J. -H. 474
Han M. G. 182
Han S. 440, 456, 468
Han S. J. 506
Han Y. 132, 394
Hanzawa K. 127
Harrabi K. 638
Härtl P. 551
Hasanov K. M. 688
Hasegawa Y. 504
Haslinger P. 72, 405
Hassan M. 136
Hauet T. 210, 212
Haule K. 331
Havela L. 592
Hayami S. 291, 361, 408
Haygood I. W. 499
Hays M. 393
He G. 329, 500
He J. 241, 245
Healy N. 453
Heczko O. 233, 416
Hemmida M. 407
Heo M. 480
Herbut I. F. 468
Hernàndez J. M. 439
Herrero S. 287
Hertel R. 145, 150, 317, 355
Hess C. 551, 552
Heyderman L. J. 139, 192
Hierro-Rodríguez A. 317
Higashikawa K. 58, 61, 522
Hillard E. A. 287
Hioki T. 322
Hippalgaonkar K. 101
Hıraman F. 606
Hiramatsu H. 127
Hirata W. 57
Hirose H. 56
Hirose Y. 238
Hirschberger M. 85
Hirschmann E. 199
Hlasek T. 112, 122, 123
Hoffmann A. 378, 686
Hokuse Y. 238
Holleitner A. 412
Holzmann C. 311
Hong W. 90
Horak L. 592
Horide T. 280
Horio K. 280
Horn L. Bishop-Van 600
Hosoda H. 229, 234
Hosono H. 127
Hosseini M. 628
Hou Y. 546
Houtput M. 577
Hrabec A. 147, 192, 406
Hu B. 99, 134, 362
Hu F. -X. a 237
Hu J. 204, 394, 651, 674
Hu L. -H. 584
Hu S. 90, 412, 542, 665
Huang R. 54, 546
Huang W. 116, 373
Huang X. 20, 551, 684
Hübner R. 306, 307
Hudiță A. 613, 615, 670
Hug H. J. 147, 413
Hussain A. 523, 524
Hyvl M. 106

I

Ichino Y. 280
Ichinose A. 280
Idczak R. 117, 119
Idziak W. 117, 605
Iglesias L. 198
Ihn T. 392
Iijima Y. 57
Ikeda A. 238
Imatomi D. 238
Imiński P. 674
Imperato M. 358
Inagaki K. 503
Inanır F. 69
Inubushi Y. 238
Iqbal Y. 644
Iram S. 682
Ishii Y. 238
Ishizuka H. 285, 291
Iskandarov T. 652
Iskesen A. 102

Islam S. S. ... 259, 544
Ismail-Beigi S. ... 177
Itahashi Y. ... 398
Ito M. ... 124
IV C. J. Zeman ... 481
Ivády V. ... 445
Ivanovskikh R. D. ... 454, 461
Ivanovskikh[3] R. D. ... 461
Iwanaga R. ... 58
Iwasa Y. ... 398, 522

J

Jackman K. ... 499, 501, 502, 505, 517
Jafarov E. I. ... 574, 575
Jafarova A. M. ... 574, 575
Jahangirli Z. A. ... 626, 627
Jakob G. ... 105, 438
Jakob[1] G. ... 105
Jakovac J. ... 531
Jakubčin M. ... 418
Jakubczyk F. ... 553
Jamaluddin S. ... 410
Janičkovič D. ... 418
Janko B. ... 508
Janoschek M. ... 544
Janotová I. Gejdoš ... 418
Jarillo-Herrero P. ... 393
Jaroš A. ... 72, 405
Javed K. ... 678
Jay J. -P. ... 200
Jha S. R. ... 621
Ji Y. ... 319, 412, 433
Jia W. B. ... 651
Jiang G. ... 52
Jiang J. ... 177, 684
Jiang M. ... 24, 195
Jiang M. -C. ... 407
Jimenez A. ... 449, 450
Jo H. C. ... 618
Jobiliong E. ... 423
Johnson-Richards C. ... 453
Johnstone A. ... 266
Jones L. O. ... 481
Jones M. ... 273
Jordan C. ... 506
Joseph D. ... 508
Jungfleisch M. B. ... 319
Jungwirth T. ... 106, 110, 284
Jungxiang Y. ... 488

K

Kabanov V. V. ... 250
Kabulov I. Sh. ... 650
Kadigrobov A. M. ... 475, 477
Kadikova A. Kh. ... 686
Kadioğlu Y. K. ... 40
Kaffash M. T. ... 319
Kagawa F. ... 407
Kainuma R. ... 238
Kajikawa K. ... 254
Kakhaki Z. M. ... 149
Kakimoto K. ... 57
Kalaivanan R. ... 607
Kaleta A. ... 94
Kamashev A. A. ... 518
Kamelabad M. M. ... 621
Kamenev A. A. ... 55
Kamenev K. V. ... 545
Kanbur U. ... 629
Karabassov[1] T. ... 494
Karaboga F. ... 336
Karadeniz B. ... 363
Karakas V. ... 102
Karam R. ... 50
Karamat S. ... 45
Kardaş K. A. ... 606
Karimbaev E. X. ... 650, 652
Karpets M. ... 48
Karroum C. B. ... 200
Karube K. ... 407
Kastl C. ... 412
Kataev V. ... 134, 518
Kataria A. ... 543
Kato Y. ... 288, 291
Kawabata K. ... 280
Kawamoto A. ... 591
Kaya E. ... 690
Kayani Z. N. ... 678, 682
Kazan S. ... 74, 458
Keeney L. ... 695
Keller H. ... 251, 571
Keller L. ... 76, 407
Kent A. D. ... 55, 559
Keran B. ... 475, 477
Kern K. ... 412
Kethamkuzhi A. ... 48, 49
Keysan O. ... 525
Kézsmárki I. ... 407
Kfir O. ... 411
Khajibaev D. G'. ... 650
Khalaniya R. A. ... 262
Khalid T. ... 684
Khalili P. ... 556
Khaliullin G. ... 81
Kharkov A. M. ... 608
Khasanov R. ... 31, 76, 259, 543, 544
Khozhempo N. ... 56
Khrenov M. M. ... 164
Khymyn R. ... 315
Kianinia M. ... 446
Kichanov S. E. ... 334
Kihara T. ... 238
Kikkawa A. ... 410
Kikuchi A. ... 254, 339
Kikuchi K. ... 339
Kilic B. ... 189
Kim H. -S. ... 480
Kim J. ... 618, 665
Kim N. Y. ... 410
Kim S. ... 138, 383, 507, 618
Kim S. -W. ... 330, 331
Kim T. ... 171, 179, 627
Kim Y. -H. ... 410
Kinoshita Y. ... 238
Kintzel B. ... 221
Kırat G. ... 675
Kirichenko A. ... 506
Kirichenko D. E. ... 512
Kirsanova M. A. ... 301
Kiss T. ... 58, 61
Kisslinger K. ... 171

Kizilaslan O. 162
Kläui M. 105, 438
Kläui[1] M. 105
Kleiner R. 162
Klenov N. V. 493
Klíma J. 92, 318
Klimczuk T. 116, 565
Klimeczek A. 196
Klimin S. N. 577
Klimova L. 100
Klomp D. W. J. 275
Kluge R. 48
Knafo W. 129
Knebel G. 25, 369
Knöckl E. 412
Kobayashi H. 254
Kobialka A. 213
Kocaman B. 102
Kocsis V. 106
Kocyigit M. 102
Kodama M. 124
Koelle D. 162
Kohama Y. 127, 238
Köhler[1] J. 105
Kolli A. 316, 347
König M. 317, 479, 588
Konstantinos-Douveas I. 317
Koo T. H. 546
Koopmann P. 392
Kopasov A. A. 396
Koralay H. 344, 656, 657, 658, 659, 662
Koraltan S. 34, 38, 409
Koshkid`ko Y. 228
Kosogor A. 352
Kostishin V. G. 688
Kousar S. 653
Kováč J. 523
Kovacs A. 349, 422
Kovnir K. 484, 595
Kowalska M. 234
Kozachok M. 417
Kozlenko D. P. 334
Kozlov S. K. 159
Krajewska A. 286
Kral P. 544
Král P. 259
Krasavin A. V. 494
Kravchuk V. P. 135, 147, 150
Kriegner D. 106, 284
Krishnan K. M. 673
Krishnia S. 438
Krnel M. 594
Krstovska D. 423
Kruglov I. 100
Kuanr B. K. 263
Kubaščik P. 106
Kubota Y. 238
Kuchárová V. 123
Kulchu A. N. 262
Kumar D. 438, 607
Kumar M. 161
Kumarasinghe K. 375
Kunca B. 418, 419
Kundu[3] M. 105
Kunert J. 514
Kunitsyna E. I. 226
Kuo C. N. 261
Kuo C. -N. g. 296
Kuo C. -Y. 171
Kuo Y. -K. 296
Kupriyanov M. Yu. 490, 493
Kupriyanov P. 74
Kupriyanova G. 74
Kupriyanova G. S. 93, 640
Kurbanov U. T. 649
Kurnaz S. 654
Kurosawa T. 250, 585
Kushnir V. N. 637
Kvitnitskaya O. 548
Kwatek K. 114, 128

L

L'vov V. A. 352
Lahabi K. 157, 158
Lai C. -C. 296
Lake S. R. 308
Laliena V. 294
Lamirand A. 196
Lammel M. 106, 311
Lanceros-Mendes S. 229
Lang W. 248, 451
Lanza M. 365
Lapertot G. 25, 369
Larrea A. 533
Lasheras A. 420
Laureti S. 136
Lazarević N. 327, 328, 329
Lázpita P. 230
LeBoeuf D. 585
Lecis N. 193
Ledesma O. 438
Lee G. 618
Lee G. -H. 435
Lee H. -W. 440
Lee J. S. 474
Lee M. J. 516
Lee M. K. 618
Lee S. 56, 58, 171, 177, 186, 435
Lei N. 103, 104
Leiviskä M. 106
Lejeune N. 92, 137, 146, 154, 298, 513, 617
Lenz K. 150, 306, 307, 323
Leo N. 317
Leśniewski N. 348
Leupold O. 404
Levati V. 190, 193
Levchenko K. 318
Levchenko K. O. 312, 318
Levermore G. J. 64
Levytskyi V. 479
Lhotel E. 387, 390
Li C. 153, 157, 182, 384
Li D. 25, 48, 77, 83, 116, 235, 491
Li F. 32, 63, 79, 90, 503
Li H. 81, 90, 500, 513, 665, 684
Li J. 170, 171, 174, 221, 249, 258, 272, 301, 306, 307, 323, 341, 412, 432, 433, 446, 451, 481, 483, 627, 648, 668
Li P. 160, 384, 433, 441
Li P. L. 167
Li Q. 325, 430
Li S. 235, 385, 433, 447, 456, 480

Li X. 53, 104, 217, 283, 341, 412, 433, 481, 539, 648, 651, 668, 669
Li X. -B. 217
Li Y. 32, 37, 54, 121, 171, 176, 237, 258, 265, 276, 328, 329, 378, 433, 483, 627, 665
Liao L. 321, 436
Liao Y. -K. 358
Liedke M. O. 92, 199
Liivand A. 676
Limaye A. 621
Lin X. 53
Lin Y. 237, 627, 665
Lin Z. 174, 272, 283, 500
Lindner J. 306, 307, 323
Lindner M. 318
Liparo M. 200
Lisitskiy M. 462
Litvinenko A. 315
Liu B. 176, 432, 471
Liu C. 153, 182
Liu D. 491
Liu F. 63, 90
Liu G. T. 167
Liu H. 81, 90, 684
Liu X. 217, 341, 412, 539, 648, 651, 668, 669
Liu Y. 32, 171, 176, 258, 265, 328, 329, 433
Liu Z. 54, 82, 173, 235, 245, 412
Lizar Y. 121
Llamazares J. L. S. 292
Lohse L. M. 404
Lončarić I. 469
Longo D. 242
Lopeandia A. 199
Lopes A. C. 420
López-Pintó N. 205
Lortz R. 546
Lortz T. T. 546
Lou D. 225
Loubens G. de 347
Lovygin M. V. 55
Low A. K. 101
Lu F. 359, 363, 364, 490, 540
Lu J. 83, 217, 394
Lu L. 167, 473
Lu X. 373
Lu Y. 82, 195, 373, 540
Lue C. S. 261, 296
Luetkens H. 259, 544
Luis F. 359, 363, 364
Lukin E. V. 334
Luo Y. 195, 373, 540
Luzón J. 217
Lvov V. 229
Ly O. 202

M

Ma L. 201, 500
Ma Y. 126, 131, 340, 344, 656, 657, 658, 659, 662
Ma Z. 185, 195, 199, 200, 201, 205, 412
Ma² X. 105
Macauley G. M. 139
Macià F. 439
Macrì T. 470
Madami M. 193
Madathil H. 437
Mæland K. 549
Magalotti A. 130, 601
Magni A. 185, 191
Mahmoud H. Ben 148
Mailman A. 225
Maisuradze A. 251
Majcen F. 318
Makarov D. 141, 142, 143, 150, 151, 152
Maksimovskaya A. A. 493
Maksutoğlu M. 458, 459, 671, 689, 690
Małecka M. 228, 336
Mallik S. 198
Mamedov N. T. 626
Mammadov A. I. 334
Mamykin S. 94
Manasa M. 620
Mancini A. 601
Manfrinetti P. 130
Mangin S. 210, 212
Manna S. 263, 535
Mannini M. 287
Manuel P. 183
Marchetti P. A. 570
Marcin J. 418, 419
Mardonov D. 687
Mariño A. 683
Markus K. 455
Maroutian T. 198
Martella D. 191
Martemucci M. 198
Martín S. 154
Martinez E. 146, 533
Martínez E. 154, 298
Martínez-Criado G. 16
Martini F. 214
Maryasev I. G. 55
Masell J. 407
Masi A. 601
Masood M. Ammar Bin 639
Maspero F. 193
Masseboeuf A. 196
Mas-Torrent M. 32, 216
Matchonov K. 43
Materna A. 455
Mather P. 71
Mathonière C. 225
Matniyazov S. 457
Mato T. 279
Matrasulov D. 43, 457, 687
Matrasulov J. 457, 687
Matsuda Y. H. 238
Matsumoto J. 127
Matsumoto K. 280
Matyunina M. 231, 232, 235, 425, 565
Mauskopf P. 516
Mavilla L. C. 193
Max A. W. 568
Mayner E. 448
Mazhar H. 643, 644, 653
Mazin I. I. 31, 107
Mazzei F. 343
Mazzoli C. 177, 182
McClarty P. A. 289, 379
McKerns M. 278
Mehdiyeva R. Z. 334
Mehmood W. 299, 604
Meier G. 404

Mejia E. 449, 451
Mekki A. 638
Mel'nikov A. S. 165, 396
Melaccio U. 527
Melhem Z. 65
Melnikov A. 495
Melzer M. 152
Menana H. 520
Menéndez E. 199, 205
Meng G. 103
Mentink J. H. 353, 558
Meo V. Di 462
Merbouche H. 316, 347
Mershiev I. G. 93, 640
Mertelj T. 250
Mestres N. 190
Mestre-Torà A. 392
Meunier S. 67
Micaletti P. 319
Michalak A. 674
Mihaescu M. C. 622
Mihaiescu D. E. 613, 614, 615, 670
Mihailovic D. 250
Mihm M. 311
Mijin S. D. 328
Mijin S. Djurdjić 329
Mikailzade F. 388
Mila F. 389
Milkovic O. 416
Milosavljević A. 327, 328
Milosevic M. V. 154, 638
Milošević M. V. 329
Mima S. 507
Minardi F. 470
Minervini J. V. 60
Mironov A. V. 262, 301
Mironov A. Y. 580
Mironov S. 495
Mironova O. 358
Miroshkina O. 232, 236
Misawa R. 85
Mishchenko A. 98
Mishchenko A. S. 577
Mitrović V. 543
Mitsui K. 127
Miúdo L. 62
Miura M. 127
Miura T. 254
Miwa S. 188
Mliki N. T. 664
Mohapatra B. Das 308
Mokhena T. 679
Mokrousov Y. 438
Mola O. 49
Moldoveanu E. -T. 613, 614, 615, 670
Molina-Jirón C. 357
Mollahasanoglu H. 300, 663
Molodyk A. 55, 56, 57
Momono N. 585
Monserrat B. 330, 331
Monteblanco E. 199
Montemurro D. 138
Montoncello F. 319
Montoya E. A. 187
Moon H. 444
Morales A. 73
Morales R. 421
Morales-Fernández P. 317, 323, 622
Moreno-Pineda E. 357
Morgunov R. B. 226
Morineau F. 387
Moshchil V. 48
Mosquera M. A. 481
Motoki T. 122, 123
Motta M. 248
Moustafa H. 349
Mozzhukhin G. 74
Mozzhukhin G. V. 93
Mueller M. 525
Mugarza A. 222
Mühl T. 141
Müller C. 106
Muluneh H. A. 667
Munoz M. 347
Murta-Pina J. 62
Museur F. 139
Mustafa B. M. 631
Mustafa Bassam M. 573
Muthuselvam I. P. 607
Muto S. 57

N

Nadurata V. L. 225
Nádvorník L. 106
Nagamatsu J. 338, 339
Naheed K. 299, 644
Naidyuk Yu. 548
Naik A. 92, 298
Nair R. 544
Nakajima Y. 375
Nakamura N. 57
Nakamura T. 19, 188, 254, 522, 633
Nakao S. 280
Nakayama T. 339
Nandy S. 224
Nasriddinov K. 43
Navau C. 120, 243
Navez P. 462, 537
Nazhestkin I. A. 164, 489
Naziri P. 456
Negi A. 404
Nelson C. 383
Nelyubina Y. 366
Neto A. H. C. 394
Neu V. 141
Neverov[1] V. D. 494
Ney A. 306, 307
Ney V. 306, 307
Ng Y. H. 546
Nhlapo A. 679
Niapos E. 195
Nicklas M. 584
Nicolicea A. 152
Nicolini A. 358
Niculescu A. -G. 613, 614, 615, 670
Nidda H. -A. Krug von 407
Nie Y. 171
Nijhuis A. 265
Nikolaev K. O. 308
Nilsson S. 139, 192
Niño M. A. 437
Niu J. 158

Niu W. H. 104
Noda K. 238
Noguchi S. 279
Nogués J. 15, 205
Novikov V. 364, 366
Novokreshenov D. 232
Novoselov K. 100
Novoselov K. S. 394
Nowak W. 119, 674
Nowak[3] U. 105
Nowakowski W. 674
Nugteren B. van 247
Nulens L. 137, 513, 617

O

O'Leary T. 278
Obradors X. 48, 49, 58
Obuchi T. 253
Occhialini C. 179
Oda M. 250, 585
Òdena J. 439
Odobesko A. 207
Oelsner G. 514
Oezelt H. 349
Ogi K. 124
Ohsugi M. 57
Ohya M. 253
Okube M. 56
Okumura S. 291
Olejnik P. 118
Oliver W. D. 393
Oliviero V. 585
Olleros P. 437
Omori T. 238
Onuorah I. J. 543
Opačić M. 327
Opel M. 106
Orero-Gámez G. 437
Ortlepp T. 156, 514
Ortlepp Th. 511
Osellame R. 193
Osin A. S. 518
Otajonov O. Y. 652
Otani Y. 188, 321, 436
Otsubo M. 339
Otto A. 268
Otýpka M. 195
Oudah M. 569
Ovcharov R. 315
Owjifard Z. 628
Oyarzabal I. 225
Ozatay O. 102
Ozerov M. 381
Ozkan S. N. 645
Ozkat E. C. 282
Özkat E. C. 283
Ozkul E. 645
Oznal Y. 344, 656, 657, 658, 659, 662
Öztürk Ö. 654
Ozturk U. K. 282, 300, 660, 663
Öztürk U. K. 283

P

Pach E. 49
Padrón-Aleman K. 292
Pagliero M. C. 358
Palau A. 185, 190, 248, 513
Palumbo E. 160
Pamidi S. V. 88, 256
Pan J. 546
Pan W. 403
Panzeri M. 190, 193
Papac P. 476
Pardo E. 244, 523, 524
Park I. 618
Park J. -G. 171
Park S. 474, 627
Parkinson P. 101
Parlato L. 138, 149
Parmeggiani C. 191
Pârvulescu O. C. 614
Pascut G. L. 330, 331
Passerini L. 563
Pastor R. 62
Paukov M. 592
Paul S. 357
Pavlukhina O. 424
Pawlak D. A. 455
Peda M. 205
Pedersen K. S. 220
Pedram M. 509
Peiselt K. 514
Pelkner M. 152
Pellicer E. 201, 205
Pelliciari J. 77, 170, 171, 179, 449, 450, 451
Pellizzi N. 190, 193
Pelofske E. 278
Peluso M. 149
Peng L. C. 407
Peng W. 500
Pentz H. 98
Pepe G. P. 138, 149
Perego M. 392, 395
Peremadathil-Pradeep R. 147
Pérez-Checa A. 230
Perfetti M. 563
Peridon L. 210
Perlepe P. 225
Perna P. 437
Perna S. 316, 347
Pershin A. 447
Pešić J. 327, 328, 329
Petrovic C. 258, 327, 328, 329
Petrović C. 328
Petrykin V. 56, 58
Petti D. 190, 193
Pfaff C. 210, 212
Pham D. 507
Phulpin T. 67
Picozzi S. 145
Pientka F. 208, 402
Pinter T. 591
Piquer Cristina 218
Pira C. 598
Pirro P. 36, 153, 193, 354
Piskin H. 102, 459
Pişkin H. 458
Pizzini S. 196
Plakhotnyuk M. 99
Planas J. G. 217
Plass W. 221

Plastovets V. 495
Plazaola F. 230
Plechacek J. 112, 122
Plevachuk Yu. 418
Plokhikh I. 76
Poccia N. 579
Poggini L. 287
Poggio M. 144
Pogosov W. V. 454, 461
Pokhrel R. 621
Polevik A. O. 262
Pomjakushin V. 387
Pomjakushina E. 251
Pomorski K. 163, 674
Pompeo N. 130, 601
Ponomaryov S. 48
Pop C. 49
Popov A. A. 363
Popović Z. V. 328, 329
Porée V. 387
Porro J. M. 230
Porta-Velilla L. 146
Posva F. 623
Powalla L. 412
Powell A. K. 223
Pradeep P. 437
Prasad A. S. 141
Presniakov I. A. 301, 385
Priessnitz J. 589
Priessnitz T. 412
Priinits T. 676
Prikhna T. 48
Prischepa S. L. 637
Privitera S. 199
Pronto A. 62
Prots Y. 594
Proust C. 585
Ptok A. 260
Puebla-Hellmann G. 73
Puig T. 48, 49, 58
Purcăreanu B. 613
Pustogow A. 591
Putilov A. 495

Q

Qin J. 246, 265
Qiu Z. 394
Qu F. M. 167
Quaglio-Gomes C. C. 248
Quéval L. 67
Quintana A. 199, 200, 204, 205

R

Radenovic A. 448
Radić D. 475, 477
Radušovská M. 123
Raghu S. 600
Raghuvanshi P. R. 171
Ragimov S. S. 642
Ragni S. 577
Rahman AKM A. 375
Rahman M. U. 95
Raj A. 198
Raja E. 138
Rajnak M. 123
Rakhmanov S. 43
Rakhmonov Z. 630
Ramasamy P. 419
Rameev B. 74, 458, 459
Ramzan H. 646
Ran S. 378, 538
Ranieri A. 358
Ranno L. 196
Rasi S. 49
Rathore A. 474
Rau J. G. 289, 379
Ravelosona D. 199, 560
Ravishankar R. 141
Raza A. 358, 433
Razmkhah S. 509
Redondo C. 421
Reeves D. B. 673
Regmi R. B. 410
Regter R. Q. 157
Rehman M. A. 684
Reichlova H. 33, 106, 284
Reinhardt A. 511
Reiss P. 129
Remizov S. V. 454, 461
Ren J. 498, 500, 515
Renault P. -O. 148
Resare F. 243
Rettaroli A. 462
Reustlen D. 106
Rhensius J. 73
Ricart S. 49
Richert S. 32
Richter K. 417
Rinaldi C. 136
Río-López N. A. 230
Riordan E. 387
Roberson C. 516
Rodan-Legrain D. 393
Rodionov Ya. I. 616
Roditchev D. 159, 494
Rodríguez-Velamazán J. A. 230
Rog M. 157, 158
Rogal Ł. 234
Rogalev A. 225, 293, 307, 422, 592
Rogalev A. A. 220
Rogenbuke[1] C. 612
Röhlsberger R. 404
Rohr F. v. 544
Roik O. 418
Rojas J. 645, 683
Romanyuk V. 94
Romer F. 419
Romero S. B. 72
Romhanyi J. 376
Ropers C. 411
Rosa P. 287
Rossi L. 274
Rotheudt N. 112, 113, 122
Rothhardt D. 147
Roubeau O. 364, 366
Rouzieres M. 225
Rouzières M. 358
Rovatti L. 193
Rovirola M. 439
Roy B. 535
Ruben M. 357

Ruggiero B. 462
Ruiz E. 217
Ruiz H. S. 529
Ruiz-Gómez S. 185, 317
Rukelj Z. 475, 477
Runov R. V. 608
Rusin B. 119
Russo V. 193
Ruzhickiy V. I. 493
Ryazanov V. V. 489
Ryba T. 416
Rybakov F. N. 140

S

Sabirov T. R. 461
Saburova G. G. 571
Sachin S. 263
Sadashivaiah S. 404
Safeer C. K. 186
Safran S. 344, 656, 657, 658, 659, 662
Sagawa M. 11
Said A. 383, 457, 687
Saif A. 646
Sailler S. 106, 311
Saito R. 591
Saitoh E. 170, 322, 438
Sakakibara R. 279
Sakthivel S. 416
Salahi S. 344, 656, 657, 658, 659, 662
Salinas A. C. 259
Salinas A. Capa 543
Salinas A. N. Capa 157
Salohiddinov M. 687
Salterilli L. 49
Salvadori E. 358
Samarin A. N. 262
Samarth N. 12
Samatov M. R. 491
Samoilenkov S. 56
Samuely P. 398, 532, 583
Samuely T. 583
Sanchez D. 49, 488
Sandbaumhüter F. 141
Sangiovanni G. 549
Sankar R. 607
Sanna S. 543
Santos M. C. 351
Sanvito S. 23, 214
Saraiva T. T. 602
Saribas N. G. 459, 689, 690
Sarrat D. 120
Sartini D. 563
Sasun U. 102
Satariano R. 138
Satheesh S. 412
Satır İ. Tosun 661
Sato M. 399
Sattorov Y. 687
Savaşkan B. 660
Savero-Torres W. 198
Savin V. V. 640
Sawatzky G. 24, 181
Sawicki M. 109, 110
Sayın G. 654
Sazgari V. 544
Scagnoli V. 139
Schäfermeier C. 73
Schaffer S. 350
Schäfter D. 32, 216
Schatz G. C. 481
Scheufele M. 106
Schimmel S. 20, 551, 552
Schindler L. 501
Schlitz R. 311
Schmelz M. 511, 514
Schmidt G. 308
Schmidt T. 409, 411
Schmitt C. 105, 438
Schmitt[1] C. 105
Schneider M. L. 250, 497, 499
Schofield A. J. 129
Schrefl T. 349, 350, 352
Scuderi M. 598
Sechovsky V. 371
Seçkin A. 344, 656, 657, 658, 659, 662
Seguí C. 230
Seidel J. 182
Seifner M. S. 72
Seki K. 238
Selvamanickam V. 51
Semba K. 507
Semisalova A. 150, 422
Sensing Bosch Quantum 71
Sera S. 58
Serga A. A. 36, 310, 312
Sergeev I. 404
Serha R. 318, 321
Serha R. O. 310, 313
Serpico C. 150, 316, 347
Serpico G. 138
Sessoli R. 221, 223, 363, 364
Sethosa M. 679
Settele S. 216
Seydioğlu T. 203, 654
Seyfarth G. 25, 369
Seyidov M. H. Yu. 93
Sgarro P. 198
Shabani J. 402
Shah A. 303, 525
Shah S. A. 673
Shah W. H. 681
Shahgoli S. S. 483
Shahid A. 303
Shakhbazian D. A. 608
Shang T. 584
Shao Q. 481
Sharma A. 73
Sharma R. O. 567
Shatruk M. 290, 563
Shavkin S. V. 599
Sheng P. 546
Shengelaya A. 251
Shevelkov A. V. 262, 301, 385, 386
Shevyrtalov S. 610
Shi M. 188, 209, 368, 584
Shi W. 500
Shi Y. 25, 116, 124, 341, 587, 648, 668
Shim S. -B. 474
Shimada Y. 124
Shimizu M. 209, 368
Shimizu T. 250
Shin J. 208, 474

Shin J. H. 618
Shiohara K. 61
Shiotani S. 58
Shipunov G. 552
Shiroka T. 584
Shova Sergiu 218
Shukla K. M. S. 212
Shumiya N. 506
Sibille R. 387
Sidorenko A. 490
Silhanek A. 146
Silhanek A. V. 92, 137, 154, 248, 298, 513, 617
Silva E. 130, 601
Silvani R. 193
Silvestrini P. 462
Silvetti M. 449, 450
Simonelli L. 49
Simsek Y. 166
Simutis G. 544
Singh P. 128, 620
Singh S. 342
Singh S. J. 114, 128, 620
Sinha A. 568
Sinha I. 263
Sirenko A. 173
Siuda E. 539
Sivis M. 411
Skailand K. 192
Škorvánek I. 69, 418, 419
Slageren J. van 32, 216
Slavin A. 315
Sławińska J. 189
Šmejkal L. 94, 103, 105, 106, 107, 110, 589
Smolko R. 123
Smolyanyuk A. 107
Smortsova Y. 94
Snyder G. J. 480, 482, 594
Soban Z. 106
Sobolev A. V. 262, 301, 385
Soboleva I. S. 385
Sobota P. 117, 118, 119, 605
Sohn J. 440
Sokolovskiy V. 231, 232, 235, 424, 425, 565, 619
Sokolovskiy V. V. 482
Šolajić A. 327, 328
Solano E. 49
Soldatov I. 596
Soloviev I. I. 138, 164, 493
Solozabal I. 421
Somoroff A. 506
Song B. 53
Song F. -L. 473
Song P. 471
Sönmez A. 93
Sönmez K. 344, 656, 657, 658, 659, 662
Sorace L. 358, 363, 563
Sornborger A. T. 278
Sort J. 185, 199, 200, 201, 205
Šouc J. 244, 523
Sousa J. A. de 216
Sözeri H. 624
Spasojevic I. 185, 201, 205
Spasojević I. 185, 205
Spenato D. 200
Spina T. 343
Sr P. Švec 418
sr. P. Švec 419
Stachowiak P. 122
Stan M. S. 613, 615
Staňo M. 195
Stein D. 311
Stengel M. 145
Stepanova A. V. 301, 385
Stepien L. 163
Stern M. 260, 376
Stern R. 262
Steven E. 423
Stevenson P. 171
Stoffels D. 92, 248
Stolyarov V. S. 159, 494
Stolz R. 514
Straka L. 416
Su G. 86
Suarez D. 423
Sudbø A. 212
Suderow H. 13
Suess D. 309, 316, 317, 318, 351, 409, 413
Suh J. 474
Sukhareva T. V. 647
Sultan H. 641
Sultana R. 319
Sumnikov S. V. 688
Sun J. 10, 245, 409, 428, 432, 482, 565
Sun Q. 103
Sun Y. 263, 412, 629
Sunil A. 357
Sunny J. 409
Suturina E. A. 225
Suzuki H. 175, 249
Suzuki K. 419, 503
Svanidze E. 31, 479, 587, 594
Švec P. 69, 418, 419
Swain A. 289, 366
Szczerba M. J. 234
Szewczyk A. 128
Szewczyk D. 122
Szymanski D. 336
Szymański D. 228

T

Tacchi S. 193
Tacconi L. 563
Tafuri F. 138
Taga E. K. 102
Tagirov L. R. 490, 686
Taguchi Y. 407, 410
Takagi H. 286
Takahara Y. 127
Takayama T. 286
Takhsha M. 233
Talanov Y. I. 666
Tan H. 124, 179, 199, 200, 201
Tan H. H. 101
Tan Z. 205
Tanaka H. 124
Tanaka M. 393, 395, 503
Tangermann J. 544
Taniguchi T. 392, 393, 394, 451
Tarasov I. 422
Taskaev S. V. 482
Taşkın S. C. 344, 656, 657, 658, 659, 662
Tavli B. 465

Tavlı B. 466
Team all the Tesla Engineering Limited 271
Team Bosch Sensortec TMR 71
Team CRAFT TF 241
Teat S. J. 364, 366
Tempere J. 577
Temst K. 92
Terai H. 507
Terao Y. 112, 522
Tereshina-Chitrova E. 228, 592
Teruya M. Gakiya 563
Tesi L. 32, 216, 363
Thiaudière D. 148
Thielert P. 32
Tian W. 471
Tian W. S. 261
Tiberto P. 185, 191
Tigoianu Ionut-Radu 218
Timm C. 553
Tkachev A. V. 385
Tobise R. 250
Toda Y. 250
Tohyama T. 249
Tokeşer E. Aşıkuzun 654
Tokunaga Masashi 238
Tokura Y. 290, 407, 408, 649
Tomar R. 198
Tomlinson M. 375
Topal M. D. 606
Topal U. 69, 612, 624
Topal² U. 612
Torokhtii K. 130, 601
Torres C. 49
Torsello D. 598
Toyama K. 503
Toyfl J. 72, 405
Tran¹ D. M. 105
Trauzettel B. 549
Traverso A. 343
Trifa D. -I. Tudorache 613, 614, 615, 670
Trofimov I. 100
Tropeano M. 343
Truccato M. 342
Trugenberger C. A. 578, 581
Trușcă R. D. 614, 615
Tsai K. T. 506
Tsuchiya S. 250
Tsui H. C. L. 453
Tsvetkova A. V. 616
Tumino A. 343
Tuncay B. 69, 606
Turchenko V. A. 632, 688
Turnbull L. A. 317
Tyberkevych V. 315

U

Uchida M. 172
Ucpinar B. Z. 509
Uhlíř V. 195
Ukleev V. 407
Ullrich A. 136, 311
Ummarino G. A. 31, 532
Ünlü M. 465, 466
Unlu P. S. 645
Unterreiner A. -N. 32
Urabe Y. 238
Urbánek M. 142, 314, 318
Usami N. 97
Užarević K. 363
Uzun O. 663

V

Vagov A. 494
Valentí R. 107
Validov A. A. 518
Valikov R. 56
Valiska M. 371
Vanacore P. 462
Vanderbemden P. 112, 113, 122
Vannozzi A. 601
Varela M. 437
Varga. R. 416
Vargunin A. 676
Varignon J. 198
Varvaro G. 136
Vasenin A. V. 461
Vasenko A. S. 491
Vasiakin M. M. 165
Vasiliev A. L. 55
Vasina T. 25, 369
Vaskivskyi Y. 333
Vavrga M. 416
Vazquez E. 198
Vecchione A. 179
Veciana J. 32, 216
Vélez M. 421
Vélez S. 437, 439
Velten S. 404
Verba R. 36, 318
Verchenko V. Yu. 262, 301, 385, 386
Vereshchagin K. 56
Vernik I. 506
Veschunov I. 56
Vettoliere A. 138
Vicente-Arche L. M. 198
Vignolles D. 585
Vila L. 198
Vinokur V. M. 581
Višić B. 327, 328
Vitale B. 342
Vitali M. 190, 193
Vlad R. 48, 49
Vlaminck V. 318
Vocaturo R. 31
Voccio J. 268
Vogel J. 196
Vojta T. 129
Vojtková L. 123
Volkov O. 141, 142
Volkov V. 100, 599
Volochová D. 123
Vondel J. V. 92
Vondel J. Van de 137, 513, 617
Vool U. 593
Voronov A. 313, 351
Voulhoux M. 49
Vrcan H. 353
Vujević L. 363
Vyatkin V. 56

W

Wadley P. 108, 197, 284
Wagner A. 199
Waje H. 553
Walker F. J. 177
Wandui A. 516
Wang D. 340, 344, 375, 656, 657, 658, 659, 662
Wang J. 237, 432, 591, 628
Wang J. I-J. 393
Wang K. 330, 331, 412
Wang M. 76, 283, 341, 515, 648
-Wang M. 668
Wang N. 76, 546
Wang Q. 36, 80, 204, 262, 318, 351, 429
Wang R. 428, 432, 471, 651
Wang S. 370, 432, 433, 498, 531
Wang W. 246
Wang X. 53, 98, 290, 427, 432, 474, 483, 545, 677
Wang Y. 104, 177, 259, 412, 428, 473, 481, 539, 546, 572, 650, 684
Wang Y. -X. 290
Wang Z. 63, 283, 375, 403, 412, 432, 500, 540, 627
Wang Z. -N. 473
Watanabe K. 392, 393, 394, 451
Wei D. 103
Wei D. H. 104
Wei S. 272
Wei Y. 98, 232
Wei Z. 262
Weigand M. 317, 323, 412, 622
Weinberger T. I. 371
Weis A. 506
Weiss J. 50
Wen W. 241, 245
Werner J. 32
Wernsdorfer W. 223, 357
Weymann I. 464, 539
White J. S. 407
Wiebe J. 209, 539
Wieczorek W. 243
Wieland R. 162
Wiemeler J. 422
Wiersma D. S. 191
Wilhelm F. 220, 225, 307, 422, 592
Wilson E. 600
Wilson S. 259, 543
Wilson S. D. 157, 543
Wimbush S. C. 240
Wintz S. 34, 317, 323, 409, 412, 622
Wischnat J. 32, 216
Wojewoda O. 142, 314
Wolf D. 141, 174
Wolter A. U. B. 106
Wong W. W. 101
Wosnitza J. 17, 375
Wrześniewski K. 464
Wu B. 13, 341, 539, 648, 668
Wu H. 385, 433
Wu J. 9, 10, 27, 245, 558
Wu M. 394, 425
Wu Y. 241, 246, 265, 431, 432, 491
Wu Z. 58, 536
Wyrsta I. 50

X

Xia K. 427, 428, 432, 584
Xia X. 131
Xiao L. 18
Xie H. 326, 431, 432, 500
Xie W. 116, 341, 648, 668
Xu B. 499
Xu L. 167
Xu S. 52, 491
Xu X. 173, 238, 380, 433
Xu Y. 431, 584
Xu Z. 131

Y

Yabashi M. 238
Yadav R. L. 296
Yakovlev D. S. 159, 164
Yamamoto A. 124
Yamamoto M. 288, 522, 633
Yamashita M. 360, 363
Yamashita T. 507
Yan G. 668
Yan J. 173, 410, 481
Yan X. 432, 481
Yan Z. 245, 430
Yanase Y. 25, 368
Yanez R. 49
Yang F. 84, 86
Yang J. 173, 481
Yang L. 104, 385
Yang Q. 98
Yang S. 134, 515
Yang Y. 103, 431
Yang Y. M. 104
Yang Y. W. 651
Yang² W. 105
Yanilkin I. V. 686
Yao X. 84, 115
Yaresko A. 286
Yasin F. S. 410
Yastrubchak O. 94
Yavidov B. Ya. 571, 650
Yazar T. 486
Yeh T. -T. 600
Yemeli I. Ngouagnia 316, 347
Yerin Y. 400, 401, 403
Yerzhakov H. 600
Yetis H. 336
Yiğit M. A. 606
Yıldırım A. E. 624
Yildiz O. G. 42
Yilmaz U. 517
Yin J. 151, 544
Ying L. 500
Yogendra Y. B. 567
Yoshida T. 280
Yoshikawa N. 156, 501, 504, 509, 511
You L. 149, 500
You S. 525, 601
Yu Q. 341, 648, 668
Yu X. 410
Yu X. Z. 407, 410
Yuan H. 373
Yuan W. 341, 648, 668

Yurtseven K. 621
Yusrianto E. 121, 665
Yusupov H. 43
Yusupov R. V. 686
Yutronkie N. 225

Z

Zabala I. 230
Zabala-Lekuona A. 225
Zager B. 179
Zagoskin A. 462
Zagrebin M. 425
Zajarniuk T. 114, 128
Zajicek Z. 129
Żak A. 674
Zaleski A. 336
Zaltariov Mirela-Fernanda 218
Zaman S. 393
Zasada D. 336
Zaumseil J. 216
Zayko S. 411
Zelezny J. 106
Železný J. 111, 197
Zha Y. S. 408
Zhai Y. 427, 432
Zhakina E. 317, 323, 622
Zhan Q. 173, 219, 331, 431, 584
Zhang C. 9, 53, 473
Zhang C. J. 149
Zhang H. 301, 525, 531
Zhang J. 79, 433, 473, 483
Zhang N. 54
Zhang P. 341, 648, 668
Zhang Q. 173, 219, 331, 431
Zhang R. 412, 441
Zhang T. 430, 546
Zhang X. 90, 126, 384, 431, 433, 480
Zhang Y. 103, 104, 375, 385, 433
Zhao J. 394, 433, 584
Zhao L. 551
Zhao Y. 52
Zhao Z. 508
Zhelezniakova D. E. 666
Zhen S. 53
Zheng L. -M. 219
Zheng N. 171
Zheng S. -Y. 473
Zhou Y. 69, 283, 453, 557, 562, 590
Zhu J. 53, 235
Zhu L. 430, 432
Zhu Y. 80, 182, 258, 310, 341, 648, 668
Zhukov A. 70, 416, 417, 610
Zhukova V. 70, 416, 610
Zhurenko S. V. 385
Zighem F. 143, 148
Žilić D. 363
Zimmermann M. v. 332
Zmorayová K. 123
Zou S. 373
Zurbano R. 421
Zverev D. G. 686
Zvezdin A. K. 197
Zvyagin S. A. 375

SPONSORS

TURKISH AIRLINES


SuperMag

CryoPride PRIDe CRYOGENIC TECHNOLOGY

NanoSpek
www.nanospek.com.tr


phi
Quantum
Technologies


SHI
Cryogenics Group

ZENOTEK

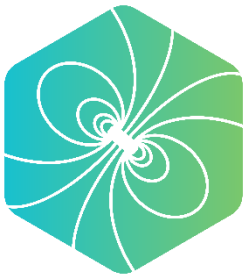

SUN Magnetics

Simulate with certainty. Build with confidence.

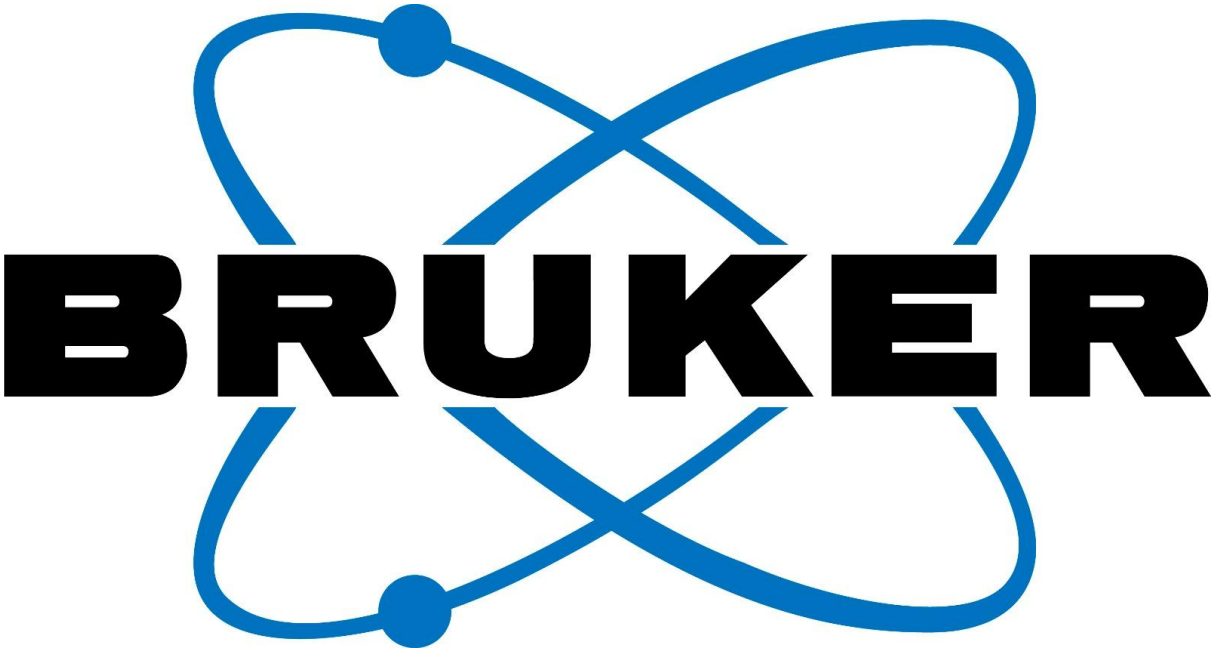
BRUKER



Western Superconducting Technologies Co.,Ltd.


Quantum Design
EUROPE

Sponsors

PLATINUM

SuperMag · phi Quantum Technologies · Turkish Airlines · SUNMagnetics · TİKA

GOLD

Quantum Design Europe · NanoSpek · Bruker

SILVER

SHI Cryogenics Group · Mtto · CryoPride · Western Superconducting Technologies Co.,Ltd. · ZENOTEK

Institutional Supporters

Ankara University · Abant İzzet Baysal University · Çukurova University · Gazi University · Hitit University · İnönü University · KTU · TOBB ETÜ · condensed matter · EMa The European Magnetism Association · Springer

